NASA Conference Publication 2238

Advances in Ultraviolet Astronomy:

Four Years of IUE Research

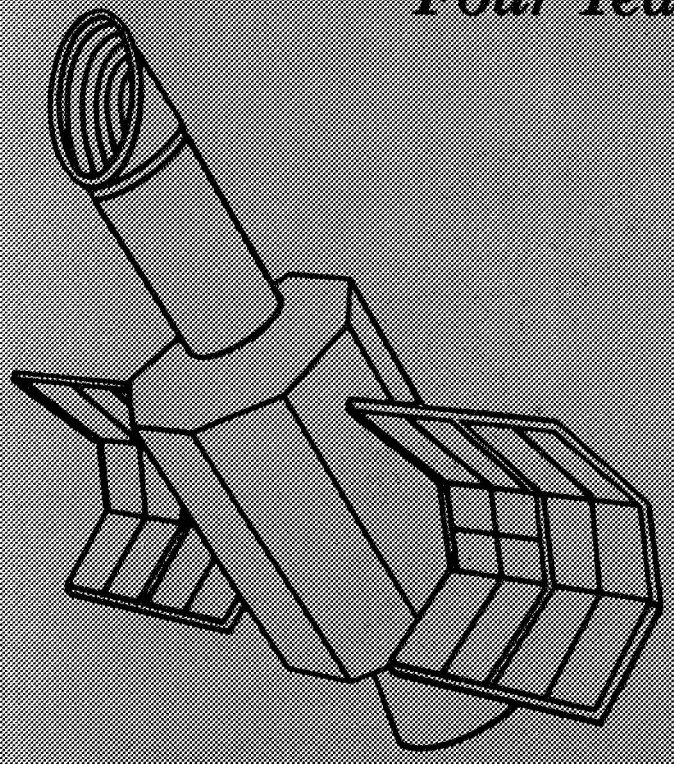

Proceedings of a symposium held at
NASA Goddard Space Flight Center
Greenbelt, Maryland
March 30 - April 1, 1982

NASA

NASA Conference Publication 2238

Advances in Ultraviolet Astronomy:

Four Years of IUE Research

Yoji Kondo, Jaylee M. Mead,
and Robert D. Chapman, *Editors*
NASA Goddard Space Flight Center
Greenbelt, Maryland

Proceedings of a symposium held at
NASA Goddard Space Flight Center
Greenbelt, Maryland
March 30 - April 1, 1982

NASA
National Aeronautics
and Space Administration

Scientific and Technical
Information Branch

1982

PREFACE

The present volume is the proceedings of the symposium entitled "Advances in Ultraviolet Astronomy: Four Years of IUE Research", held at the NASA-Goddard Space Flight Center on March 30 through April 1, 1982. It is based on the results obtained from the International Ultraviolet Explorer (IUE) satellite observatory. This is the second IUE symposium held here, the first of which took place in May 1980.

Twelve invited talks and 130 contributed papers were presented at the meeting. The current volume contains these papers and the discussions which followed each presentation, based on the question-and-answer forms filled out by the participants. Whenever these forms were returned to us, even without the written responses from the speakers, we have included them in the proceedings in an effort to preserve the flavor of the discussions.

In order to restrict the size of this publication, it was necessary to impose stringent page limitations on the participants. We appreciate the cooperation of the speakers, most of whom stayed within the guidelines. In order to publish as soon as possible after the meeting, all articles are being printed as they were submitted to us in the form of camera-ready sheets without any editorial changes or retyping, according to the procedures announced at the outset of the symposium.

We wish to express our appreciation to the members of the Scientific Organizing Committee and the Local Organizing Committee, without whose contributions this meeting would not have been such a success. Thanks are also due the personnel at the Goddard Space Flight Center, who provided competent support in conducting the 3-day conference, and to Ms. Sandra Kinnear and her staff at Dynatrend, who assisted so ably in the conference arrangements and compilation of the proceedings.

Proceedings Editors: Yoji Kondo, Jaylee M. Mead, Robert D. Chapman

IUE SYMPOSIUM PARTICIPANTS

Ahmed, I.D.
Aizenman, M.
Ake, T.B.
Albrecht, R.
Aller, L.H.
Ambruster, C.
Ameen, M.M.
Ayres, T.R.
Barker, P.K.
Baumert, J.H.
Bell, R.A.
Benvenuti, P.
Blades, J.C.
Blair, W.P.
Boeshaar, G.
Boggess, A.
Bohlin, R.C.
Bohm, K.-H.
Bohm-Vitense E.
Bregman, J.N.
Brown, D.N.
Brugel, E.W.
Bruhweiler, F.C.
Caldwell, J.
Canuto, V.M.
Caraveo, P.A.
Carruthers, G.R.
Cassatella, A.
Chanmugam, G.
Chapman, R.D.
Chen, K.-Y.
Currie, J.S.
Dean, C.A..
Devinney, E.J., Jr.
Doazan, V.
Dolan, J.F.
Donn, B.
Dorren, J.D.
Drake, S.A.
Dressel, L.
Drilling, J.S.
Dufour, R.J.
Dupree, A.K.
Durrance, S.T.
Eaton, J.A.
Ebbets, D.C.
Elvis, M.
Fabbiano, G.
Fahey, R.P.
Feibelman, W.A.
Feldman, P.D.
Felton, J.E.
Giampapa, M.S.
Glassgold, A.E.
Grady, C.
Grewing, M.
Guinan, E.F.
Gull, T.
Gursky, H.
Hack, M.
Hackney, K.R.H.
Hackney, R.L.
Hallam, K.
Hammer, R.
Hardorp, J.
Harrington, J.P.
Harris, A.W.
Harvel, C.A.
Heap, S.R.
Heckathorn, H.M.
Heckathorn, J.
Heckman, T.M.
Heidmann, J.
Helfer, H.L.
Henden, A.A.
Henry, R.C.
Henry, R.J.
Hodge, P.W.
Holm, A.V.
Hosach, B.
Huchra, J.
Hutter, D.J.

Imhoff, C.L.
Jenkins, E.B.
Jordan, S.
Jura, M.
Kafatos, M.
Kalinowski, J.K.
Kinney, A.L.
Kiplinger, A.L.
Koch, R. H.
Kondo, Y.
Lambert, D.L.
Landsman, W.
Leckrone, D.S.
Lesh, J.R.
Levine, J.
Linsky, J.L.
Locke, M.
Long, K.S.
Malkan, M.
Maran, S P.
Massa, D.
Matsui, Y.
Mattei, J.A.
Mattei, M.
McCluskey, G.E.
McCracken, C.W.
McKee, L.
Mead, J.M.
Michalitsianos, A.G.
Moos, H.W.
Morrison, N.D.
Mufson, S.L.
Mullan, D.J.
Mushotzky, R.
Nelson, R.M.
O'Brien, G.
Oke, J B.
Oliversen, N.
Parsons, S.B.
Penston, M.V.
Peters, G. J.
Pettini, M.
Plavec, M.J.
Polidan, R.S.
Ptak, R.
Rahe, J.
Reis, L.
Rocca-Volmerange, B.
Roman, N.D.
Sandford, M.C.W.
Sanyel, A.
Schiffer, F.H.
Sewall, J.R.
Shore, S.N.
Simon, T.
Sion, E.M.
Skinner, T E.
Slettebak, A.
Sonneborn, G.
Starrfield, S.G.
Stecher, T.P.
Stencel, R E.
Stoner, R.
Swank, J.W.
Szkody, P.
Thomas, R.N.
Turnrose, B.E.
Underhill, A.B.
Urry, M.
Wagener, R.
Walborn, N.R.
Waldron, W.L.
Walter, F.M.
Walter, S.
Wamsteker, W.
Weiler, E.J.
Welch, G.A.
Wilson, R.
Winkelstein, P.
Witt, A.N.
Worrall, D.M.
Wu, C.-C.
York, D. G.

TABLE OF CONTENTS

TABLE OF CONTENTS (Continued)

TABLE OF CONTENTS (Continued)

TABLE OF CONTENTS (Continued)

TABLE OF CONTENTS (Continued)

TABLE OF CONTENTS (Continued)

TABLE OF CONTENTS (Continued)

TABLE OF CONTENTS (Continued)

TABLE OF CONTENTS (Continued)

INVITED PAPERS

MASS LOSS FROM COOL STARS -- FACTS, FADS, AND FALLACIES

A. K. Dupree
Harvard-Smithsonian Center for Astrophysics
Cambridge, MA 02138

ABSTRACT

Sufficient observational material - ultraviolet spectroscopic measures, quantitative optical spectroscopy, and X-ray photometry - has accumulated to enable us to discern the presence and character of mass loss across the cool half of the H-R diagram and to establish constraints on theoretical models. Analogies with closed and open solar magnetic structures are found. Two determinants of atmospheric wind structure - temperature and gravity - may suffice in a most superficial way to define the wind and atmospheric structure in a star, however it is apparent that there is still a missing parameter which may stem from magnetic activity and its particular configuration. Theories that appear successful in reproducing observed line profiles, wind temperatures, and terminal velocities incorporate Alfven wave heating and momentum deposition. Successive observations of an active binary (λ And - G8III-IV) and a supergiant star, α Aqr (G2 Ib) have revealed that magnetic activity and perhaps mass loss occur on restricted regions of a stellar surface and that long-term structures are present in the wind. These phenomena are present in the solar atmosphere and wind and may be considered a general characteristic of stellar winds.

I. INTRODUCTION

During the last four years there has been a veritable Renaissance in the study of atmospheres and magnetic activity of cool stars, spurred on in a major way by results from the IUE satellite and photon-counting ground-based detectors and complemented by the X-ray measurements from the HEAO series of satellites. Much of the foundation for studies of cool stars is based on the knowledge gained from the physics of the Sun and the fruition of a decade or more of solar studies culminating in the SKYLAB experiments. It will be apparent that the fruits of solar research are necessary for the productive study of cool stars. Many research programs are flourishing in pursuit of the solar-stellar connection.

This invited contribution will begin with an overview of our understanding of the occurrence and character of mass loss and related atmospheric structure in the cool half of the H-R diagram. It is now possible for the first time to develop a comprehensive picture of cool stars with hot outer atmospheres. In Section III, we will discuss an example of a specific giant star - α TrA (K4 II) - a hybrid star representative of the critical link

between the winds of solar-type main sequence stars and those of the most luminous cool giant and supergiant stars. In Section IV pertinent results from solar physics are noted. Theoretical modeling of cool stellar winds and line profiles, apart from the solar case, is still in a rudimentary stage, but the most successful of these studies is noted in Section V.

The foregoing topics tacitly assume that a stellar atmosphere is homogeneous and that the mass loss occurs in a steady fashion. However, as we might foresee from the solar case, there are examples of variability which we discuss in Section VI. These topics and evidence can be considered as "facts" by any reasonable person. The "fads" and "fallacies" found in the literature - based on first glances, insufficient sampling, and shaky physics will be noted in passing.

II. ATMOSPHERIC EMISSIONS AND STELLAR WINDS

Frequently used spectroscopic signatures of mass loss are the asymmetry of an optically thick chromospheric emission line and/or the presence of narrow circumstellar absorption features. Figure 1 shows a typical set of Mg II and Ca II profiles and the presence of corresponding narrow absorption features is apparent in both profiles. The asymmetry of the emission peaks - in the sense, long wavelength peak > short wavelength peak or red > violet - and the accompanying blue-shifted line core (here distorted by the narrow absorption features) signal the presence of a massive stellar wind. It was the original suggestion of Hummer and Rybicki (1968) that a differentially expanding atmosphere could produce such a profile; this has been confirmed in simultaneous measurements of profiles and direct Doppler shifts in the Sun (Brueckner, Bartoe, and Van Hoosier 1977) and by theoretical calculation for the Sun (see Dupree 1981).

Observations such as these are used to identify stars undergoing mass loss and to measure the radial velocity of circumstellar absorption features. The highest outflow velocity is commonly identified as the terminal velocity of the wind (V_∞) and is taken as a constraint on wind theories. It is believed that such blue-shifted features result from recombination to Mg II and Ca II ions far out in the wind as it cools and flows into the interstellar medium. Corresponding features in both profiles support this empirical interpretation and as we shall see in Section V, detailed theoretical calculations offer confirmation.

The domain of mass loss in the H-R diagram was first established by Reimers (1977) from the presence of narrow circumstellar absorption features in the Ca II lines (see Figure 2). Additionally, blue and red Mg II and Ca II asymmetries occur systematically over a large region (Stencel 1978; Stencel and Mullan 1980). As a star's effective temperature and gravity decrease, first Mg II, then Ca II, and finally circumstellar absorption become noticeable. Moreover, the terminal velocity of the wind as inferred from the presence of narrow absorption features decreases in similar fashion. Supergiants such as β Aqr have a terminal velocity ~ 60 km s^{-1}, as seen from Figure 1; the cooler more luminous giants and supergiants exhibit absorption features indicating outflow of ~ 10 km s^{-1} (Reimers 1977).

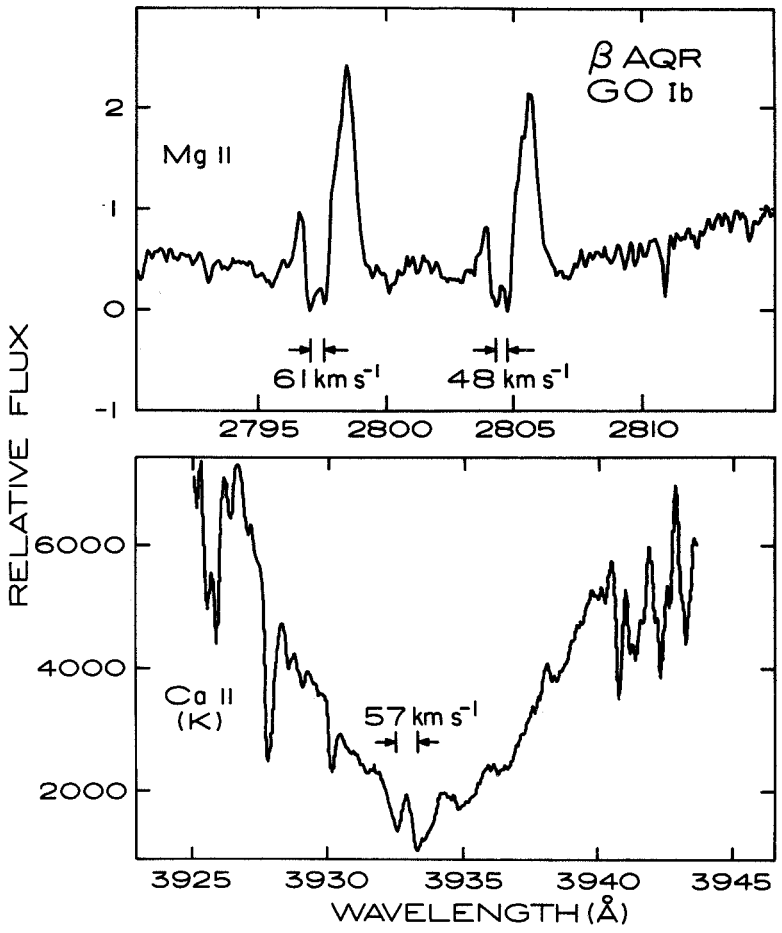

Figure 1. Profiles of the Mg II and Ca II chromospheric emission lines in the "hybrid" supergiant (Hartmann, Dupree, and Raymond 1980) β Aqr. Note the correspondence between the narrow absorption features in both profiles. The absorption component near the rest wavelength undoubtedly has an interstellar component. Mg II spectra were obtained with IUE; the Ca II spectra were taken with the echelle spectrograph and Reticon detector system at the F. L. Whipple Observatory (formerly the Mt. Hopkins Observatory). (Dupree 1980).

It is of interest to relate the domain of hot plasma to the presence of mass outflow. Figure 3 shows the presence of C IV emitting gas as a function of temperature and luminosity. Spectra of main sequence stars generally contain detectable C IV emission, whereas most cool luminous stars (spectral class M0-M3, luminosity class I-III) show no indication of C IV. A non-detection of C IV, if of sufficiently long exposure, results in upper limits

to the surface flux of 10^{-1} to 10^{-2} of the quiet Sun surface flux (see for instance Hartmann, Dupree and Raymond 1982). In the latter case these luminous stars possess strong winds as inferred from Figure 2. There is in addition a substantial intermediate region of stars showing both the presence of C IV emission and of low excitation features - the "hybrid" stars (Hartmann, Dupree, and Raymond 1980).

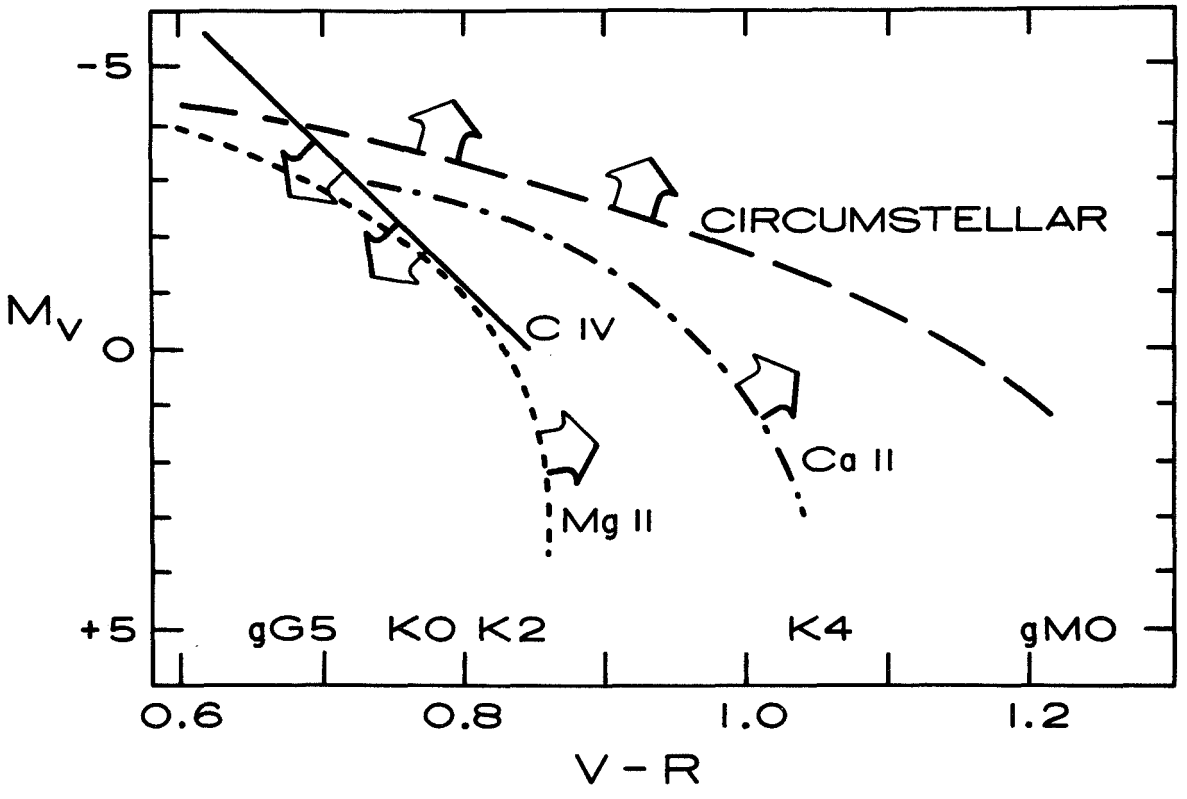

Figure 2. The appearance of various spectral features as a function of color and luminosity. C IV emission is prominent to the left of the solid line, the ratio of red:blue emission peaks for Mg II and Ca II is greater than 1 to the right of the appropriate broken lines (Stencel 1978; Stencel and Mullan 1980). Circumstellar Ca II features are found above the long broken line (Reimers 1977).

The X-ray surveys from HEAO-2 ("Einstein") made by the Center for Astrophysics and Columbia University groups (Vaiana et al. 1981; Helfand and Caillault 1982) support the C IV results in the extremes. X-rays are generally found in main sequence stars, but there is an absence of detectable X-ray emission in the luminous giant and supergiant stars - except for active binary systems.

It is important also to underscore the fact that through a broad region in the H-R diagram, the character of a star's atmosphere is not predicted by

two parameters. Moreover, hot plasma can coexist with massive winds as in the case of the hybrid stars.

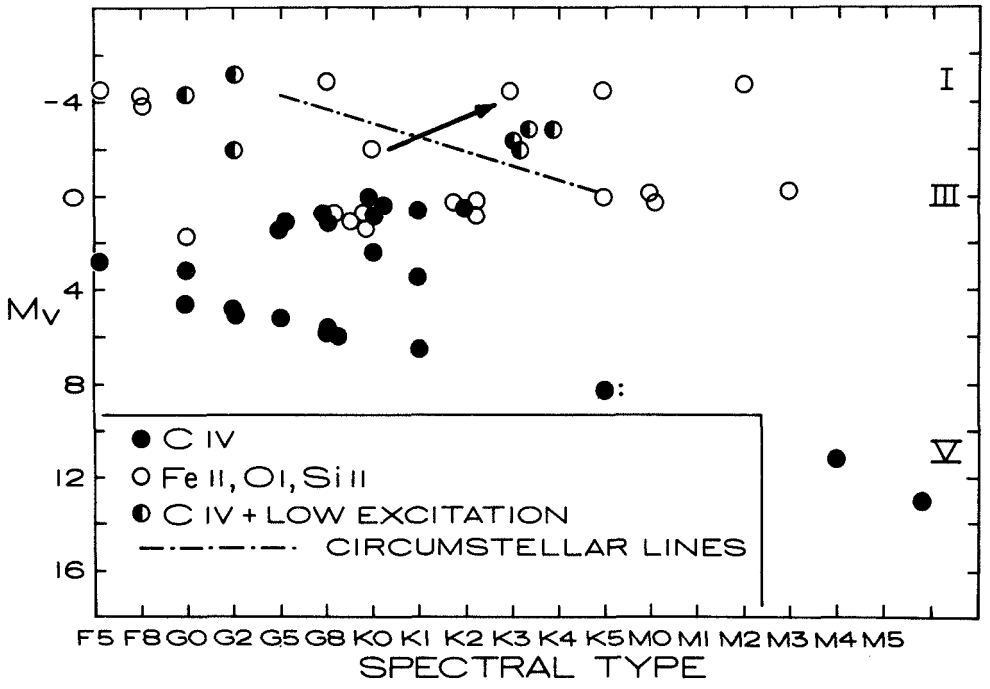

Figure 3. The presence of various spectral features in stars of different spectral types and luminosities. Stars exhibiting low and high excitation species are termed "hybrid" - and denoted by the half filled circles (Hartmann, Dupree, and Raymond 1980). The broken line denotes the high temperature boundary of the appearance of circumstellar lines in optical spectra (Reimers 1977).

Ultraviolet measurements of a few stars in the early days of IUE led Linsky and Haisch (1979) to claim that there were "two separate and distinct groups of [cool] stars" bisected in the H-R diagram by a "sharp dividing line". The overwhelming evidence does not support this simple phenomenology. Moreover, their scenario that the absence of hot material results from the onset of strong winds contradicts the evidence from the hybrid stars which possess both hot plasma and a massive wind.

III. THE HYBRID STARS

The hybrid stars - so defined because their ultraviolet spectra show the coexistence of hot plasma (C IV) and substantial amounts of low excitation material (Fe II, O I, and Si II) are a critical link between the winds of the dwarf star and those of the coolest giants and supergiants. High dispersion spectra of a bright example, α TrA, show the typical asymmetric chromospheric profiles with absorption features implying V $\sim$ -85. Most importantly broad line profiles are found. Not only are the resonance lines broad, but the in-

tersystem, C III transition at λ1909 displays a full width at half power of ~ 100 km s^{-1}. Since the line widths are commensurate with the terminal velocity, Hartmann et al. (1981) suggested that they were formed throughout the expanding atmosphere and signaled the presence of a warm wind. The temperature of this wind would be expected to be ~ 10^5 K.

The asymmetry of the chromospheric lines also provides a constraint for wind theory since these line profiles require the outflow to begin in the low chromosphere of the star. The expansion must begin at low temperatures.

It is important to note that higher temperature material, as indicated by soft X-rays, is strikingly absent (or weak) in these luminous stars. The surface flux of X-rays for a hybrid star, α_2Aqr, is lower than 10^{-3} of the value for the quiet Sun and a factor of 10^{-2} the value for a coronal hole (Rosner 1982). By contrast the surface flux of 10^5 K gas in α Aqr is ~ 2 to 3 times the quiet Sun surface flux (Hartmann, Dupree, and Raymond 1982). There may well be X-ray emitting material in small volumes in the atmosphere, but the emission measure of this volume is orders of magnitude below that of the material at 10^5 K.

IV. RESULTS FROM SOLAR PHYSICS

The SKYLAB decade since 1973 has left us with a legacy of unique, quantitative, and broad ranging solar measurements. Analysis of these has led to conclusions that are relevant to our understanding of mass loss and stellar activity. Possessing such a Rosetta Stone is invaluable since the direct resolution of stellar surface features is not now attainable.

Mere inspection of ultraviolet and X-ray images of the Sun (for an impressive collection see Eddy 1979) reveals the dominance and presence of magnetic fields in structuring the outer atmosphere. The resultant inhomogeneity of surface emissions is immediately apparent. And there is both short and long term variability in the proportion of open and closed magnetic regions of the Sun.

There are other more subtle results of use to us that derive from more detailed analysis (summaries are contained in Zirker 1977). The open field regions - so-called coronal holes because of lessened emission from high temperature material - are the source of high speed solar wind streams. And it is through these open field regions that a preponderance of the mass loss takes place. The energy requirements as measured by the observed and inferred losses may be the same for a coronal hole as for the quiet Sun (i.e. see Table in Withbroe and Noyes 1977). Although in a hole, the radiative and conductive losses are decreased from their values in the quiet Sun, the losses to the wind are increased. To maintain the observed density and temperature distinction in a coronal hole, extended mechanical heating will be needed - a requirement imposed from the very first spacecraft observations of the solar wind (Parker 1965).

We should emphasize that if the Sun were viewed as a star, direct spectroscopic evidence of mass loss would not be detectable. Chromospheric emission lines do not show evidence of circumstellar absorption; and the asym-

metries associated with mass outflow are only apparent - if at all - over restricted regions of the Sun. The presence of coronal holes would not be detectable in the strong chromospheric lines of Ca II and Mg II. This results from the relatively narrow formation region of the lines in a dwarf coupled with the fact that outward acceleration associated with eventual mass loss does not occur to a significant extent at low chromospheric levels in the Sun.

The analogy of stellar mass loss occurring through open field structures is an obvious one. The extrapolation of the energy and momentum deposition requirements from the Sun and coronal hole features to the stellar case will be considered in the following section.

We can also investigate the similarity between closed loop structures in the Sun and those found in the stars. If a standard loop model in hydrostatic equilibrium (Chiuderi 1981) is considered with both radiative and conductive losses, the relative amounts of plasma at two temperatures can be predicted by integration of the energy equation (see Hartmann et al. 1982). The ion N V is assumed to be formed at 2×10^5 K and the X-rays result from isothermal 10^7 K plasma. Figure 4 shows the predicted relation between the two emission measures and empirical results for many stars. The Sun, dwarf stars, and RS CVn stars fall on or near the theoretical relation; however giant stars, evolved contact binaries, supergiant stars, and T Tauri stars show a deficiency of high temperature (10^7 K) material relative to the plasma at 10^5 K. While there is a correlation between higher N V emission measure and increased X-ray emission measure, the relationship as defined by the dwarfs and active binaries is not followed. This deficiency is also a signature of coronal holes, and its occurrence in the luminous giants and evolved contact binaries is suggestive of a larger picture where winds develop as evolution proceeds. Boesgaard and Simon (1982) find additional evidence for the more rapid decay of material at 10^5 K relative to lower chromospheric emission in dwarfs.

Atmospheric structure appears to evolve in a way consistent with our understanding of the closed and open field structures found in the Sun. One should remember also that the onset of mass loss may not give a clear spectroscopic signature. Circumstellar envelopes have not developed and the first hint that mass loss is ongoing may be the decrease of high temperature material, the broadening of ultraviolet lines, followed by a developing line asymmetry as differential expansion becomes significant in the low chromosphere.

V. THEORETICAL MODELING

Our theoretical understanding of stellar winds is still in an elementary state, but there are promising directions. It is useful to summarize the constraints placed by these observations on a quantitative wind theory. Figure 5 gives an overview of these requirements. Our understanding of the behavior of winds from dwarf stars is based on measurements of the Sun and direct sampling of its wind in interplanetary space. To date there has been no spectroscopic detection of mass loss from a single, cool, dwarf star. For the more luminous stars, the circumstellar absorption features in Ca and/or Mg are identified with the terminal velocity of the winds. The wind temperatures are inferred

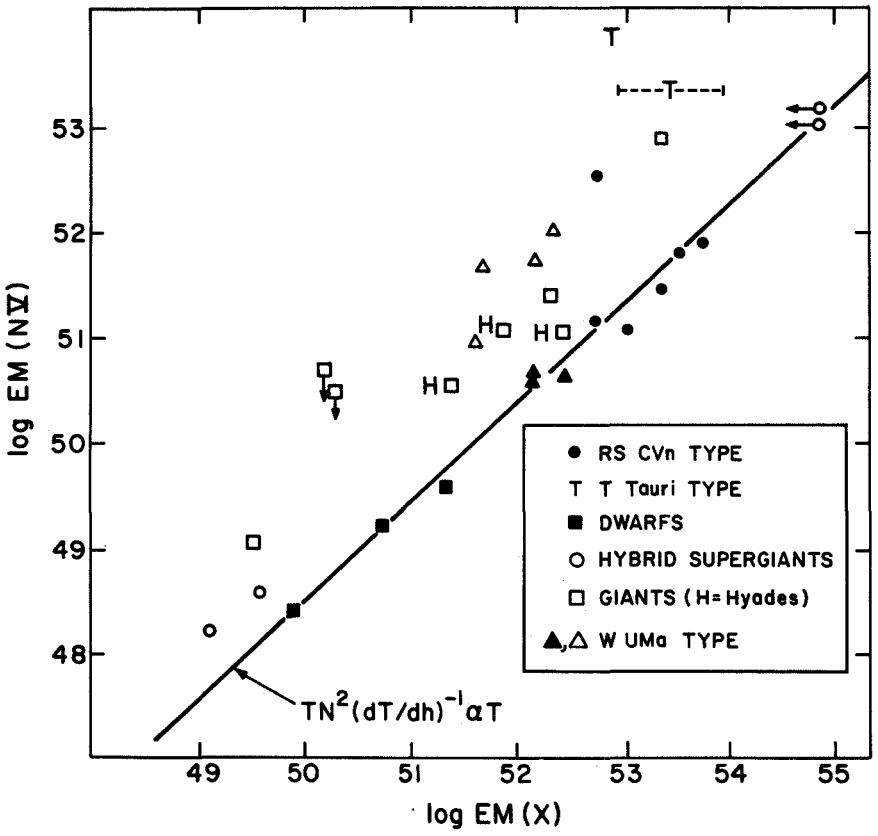

Figure 4. Observed relative emission measures for N V and X-rays (0.3-4 keV) for various stars as compared to a theoretical prediction for conductively dominated coronal loop structures. Data for RS CVn stars and the theoretical relation are from Hartmann, Dupree, and Raymond (1982). Fluxes for additional objects are from various authors: T Tauri type (Giampapa 1980; Sanders 1981); Dwarf stars (Ayres, Marstad, and Linsky 1981); Hybrid supergiants (Hartmann, Dupree, and Raymond 1981a; Ayres and Linsky 1980); W UMa type (Cruddace and Dupree 1982; Dupree and Dussault 1982). The Sun is indicated by a circle for both active and quiet state.

from the presence of ultraviolet emission lines and their profiles. The mass loss rates are more uncertain, and obtained by a variety of direct radio, infrared, and optical measures combined with modeling of line profiles where available. We believe that mass loss can result from a similar and continuous mechanism across the H-R diagram. For the most luminous stars, the acceleration begins in the chromosphere. The terminal velocity of the winds decreases as the effective temperature and gravity of a star decreases. Additionally, the electron temperature in the wind decreases as the effective temperature and/or gravity decrease.

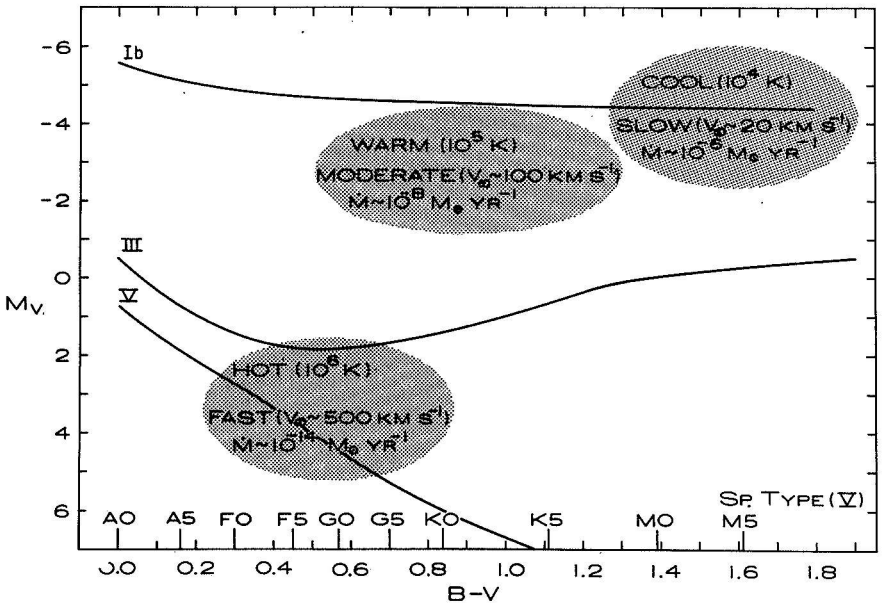

Figure 5. Characteristics of mass loss rates and winds in stars of various luminosities (from Dupree 1981).

From theoretical considerations, it had been suggested (Mullan 1978) that mass loss turns on abruptly as the sonic point is pushed below the coronal base and marks a supersonic transition locus - "STL". However, Holzer (1980) has emphasized that a smooth, continuous variation in mass loss occurs for thermally driven winds as the sonic point approaches the base of the corona. For lower penetration, the assumptions of an isothermal atmosphere no longer apply, and solution of the wind equations indicates that the sonic point remains at the coronal base until M_*/R_* is reduced by two orders of magnitude. Holzer remarks that this new position does not correspond at all with the locus of the proposed "STL" - and the concept has little significance.

If we consider pure thermally driven winds, it is not possible to have increased mass flux - by more than a factor of 10_8- in the most luminous stars. For instance, to produce the mass loss of $\approx 10^{-8}$ $M_\odot$ yr^{-1} as found by modeling the hybrid star α TrA, a temperature of greater than 5×10^5 K is required and then expansion will not be present in the chromosphere (Hartmann, Dupree, and Raymond 1981). Another force is required - one which offers large momentum input near the star to drive the mass flux and small momentum input far from the star to ensure low asymptotic flow speeds. A most attractive mechanism is offered if the mechanical flux is carried by Alfven waves. Such waves have been observed to be present in the solar wind at 1 AU (Belcher and Davis 1971) and theoretical models for the Sun reproduce the solar observations (Jacques 1978).

Hartmann and MacGregor (1980) have constructed a series of models by invoking a fixed magnetic field strength ($\simeq$10 gauss) and Alfven wave energy flux ($\simeq 3 \times 10^6$ erg cm^{-2} s^{-1}) and calculating the response of an atmosphere for stars of various masses and radii. The observational results outlined above are successfully reproduced by requiring Alfven wave dissipation which leads to mass loss and extended warm chromospheres in low-gravity cool stars. For stars with higher gravities, coronal heating results.

A model for such an extended atmosphere (Figure 6a) has been developed by

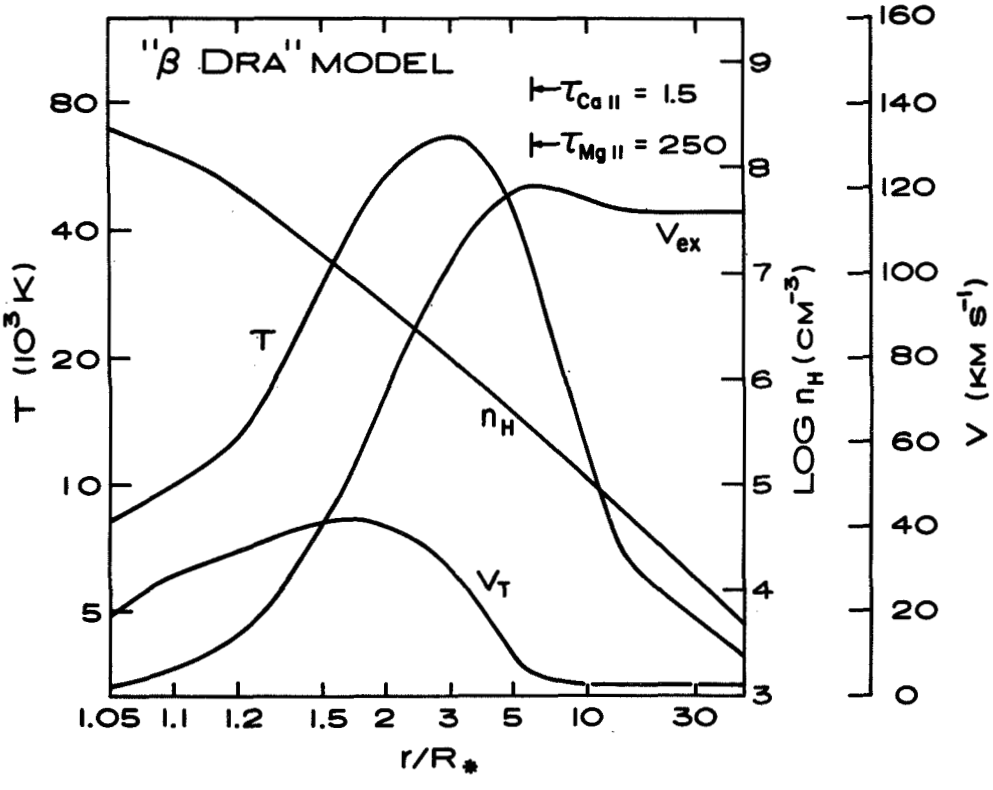

Figure 6a. Assumed model for an extended supergiant atmosphere. Note the substantial difference in optical depth between the Ca and Mg lines (Avrett, Dupree, and Hartmann 1982).

using the Hartmann-MacGregor (1980) theory to define the temperature, density, and velocity profiles in a luminous star with a wind (of spectral type approximately G2 II). This extended atmosphere was then joined with a static lower chromospheric model (Basri, Linsky, and Eriksson 1981). A solution of the complete non-LTE radiative transfer equations, including the effects of expansion and spherical geometry on the line source function as well as the emergent profiles was carried out by Avrett, Dupree, and Hartmann (1982) and the resultant line profiles (Figure 6b) show the same characteristics as the observations. Namely a circumstellar absorption feature at the asymptotic flow velocity and strong line asymmetry. It should be noted that a substantial difference in line optical depth between Mg II and Ca II occurs in the outermost parts of the atmosphere. This happens because Mg II and Ca III are the

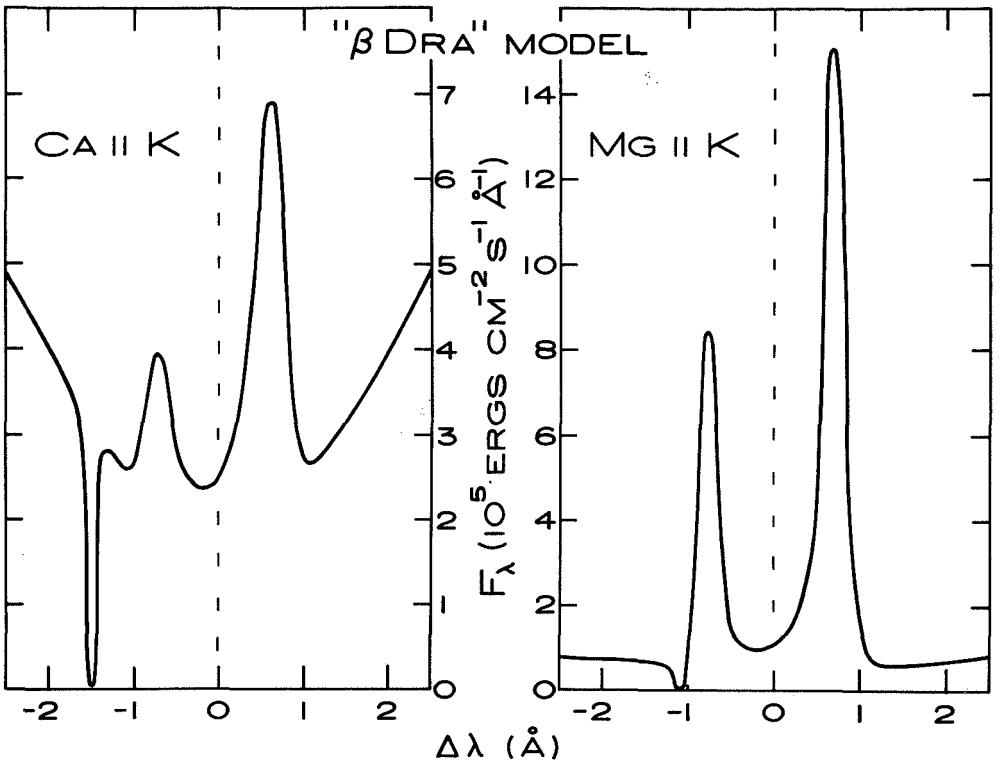

Figure 6b. Computed line profile of chromospheric Ca II and Mg II for an extended supergiant atmosphere (Avrett, Dupree, and Hartmann 1982).

dominant species in this outermost region - a fact that appears to result from the higher recombination rate of Mg III as compared to Ca III. Such different line forming properties can help to explain the independent variations observed in the Ca II profile as compared to the Mg II features. This is consistent with an earlier calculation for the Sun (see Dupree 1981) and the presence of a Mg II asymmetry in stars with higher gravities and temperature than found for Ca II (see Figure 2).

With such calculations, a promising start is under way to understand the mechanism of driving mass loss from stars.

VI. VARIABILITY

The previous discussion of stellar mass loss tacitly assumes that the atmosphere is homogeneous and that the mass loss occurs in a constant fashion. From the solar example we know that both inhomogeneity and variation are possible and accumulating observations indicate that variability occurs in stellar winds from many (if not all) cool stars. Two examples illustrate this variability: α Aqr (a hybrid supergiant) and λ And (an RS-CVn star).

The first star - α Aqr - was found (Dupree and Baliunas 1979) to undergo a substantial decrease in the blue peak of its Mg II emission over a period $\sim$ 1 year which corresponds to increased Mg II opacity in the high velocity part of the wind. During this time the Ca II (K) line varied in asymmetry on a time scale $\sim$ days (Dupree et al. 1982). The increased opacity appears to result from a long-lived phenomenon since the line profile has exhibited its new form for about two years.

The second system - an RS CVn binary with a $\sim$ 20 day orbital period, λ And, shows (Baliunas and Dupree 1982) distinctly different atmospheric structure depending on the presence or absence of spots as inferred from the optical photometric wave. When the optical light is at a minimum, spots are present and the line profiles of Mg II and Ca II are symmetric or asymmetric in the sense blue $>$ red. High temperature plasma lines are enhanced. When the optical light is at a maximum, the number of spots is greatly reduced or absent, the chromospheric lines are asymmetric in the sense red $>$ blue, and high temperature plasma lines are weakened. This behavior is strongly reminiscent of the Sun and the characteristics of active regions and coronal holes.

It is perhaps not too suprising that with selective observations, serendipity, and just plain more observing time that variability is beginning to be detectable in many systems.

One intriguing problem is the search for a quantitative understanding of the distribution of open and closed field structures in stars other than the Sun, and the physical mechanism responsible for the variability in the wind density and velocity profiles. To date, IUE has contributed in a major way by providing a unique instrument with which to probe stellar wind stratification and variability.

This work is supported in part by NASA Grants NAG5-87 and NAGW-100 to the Smithsonian Institution.

REFERENCES

Avrett, E. H., Dupree, A. K., and Hartmann, L., 1982, in preparation.

Ayres, T. R., and Linsky, J. L., 1980, Ap. J., 241, 279.

Ayres, T. R., Marstad, N. C., and Linsky, J. L., 1981, Ap. J., 247, 545.

Baliunas, S. L., and Dupree, A. K., 1982, Ap. J., 252, 668.

Baliunas, S. L., Hartmann, L., and Dupree, A. K., 1982, Ap. J., submitted.

Basri, G. S., Linsky, J. L., and Eriksson, K., 1981, Ap. J., 251, 162.

Belcher, J. W., and Davis, L. Jr., 1971, J. Geophys. Res., 76, 3534.

Boesgaard, A., and Simon, T., 1982, in Cool Stars Stellar Systems and the Sun, SAO Sp. Report No. 392, Volume II, p. 161.

Brueckner, G. E., Bartoe, J. D. F., and Van Hoosier, M. E., 1977, in "Proceedings of the November 7-10 1977 OSO-8 Workshop", (ed. E. Hansen and S. Schaffner), Lab. for Atmospheric and Space Physics, University of Colorado, Boulder, pp. 380-418.

Chiuderi, C., 1981, in Solar Phenomena in Stars and Stellar Systems, ed. R. M. Bonnet and A. K. Dupree, (Boston: D. Reidel), p. 269.

Cruddace, R., and Dupree, A. K., 1982, preprint.

Dupree, A. K., 1980 in Highlights of Astronomy, (ed. P. A. Wayman), 5, pp. 263-276.

Dupree, A. K., 1981, in Effects of Mass Loss on Stellar Evolution, (eds. C. Chiosi and R. Stalio), IAU Colloq. No. 59, D. Reidel, pp. 87-110.

Dupree, A. K., and Baliunas, S. L., 1979, IAU Circ. No. 3435.

Dupree, A. K., Baliunas, S. L., Hartmann, L., Bohm-Vitense, E., Mullan, D., Nicholas, K., and Stencel, R. E., 1982, in preparation.

Dupree, A. K., and Dussault, M., 1982, in preparation.

Eddy, J. A., 1979, A New Sun: The Solar Results from Skylab, NASA, Washington, D.C., SP-402.

Giampapa, M., 1981, private communication.

Hartmann, L., Dupree, A. K., and Raymond, J. C., 1980, Ap. J. (Letters), 236, L143.

Hartmann, L., Dupree, A. K., and Raymond, J. C., 1981, Ap. J., 246, 193.

Hartmann, L., Dupree, A. K., and Raymond, J. C., 1982, Ap. J., 252, 214.

Hartmann, L., and MacGregor, K. B., 1980, Ap. J., 242, 260.

Helfand, D. J., and Caillault, J. P., 1982, Ap. J., 253, 760.

Holzer, T. E., 1980, in Cool Stars, Stellar Systems and the Sun, (ed. A. K. Dupree), SAO Sp. Report No. 389, p. 153-181.

Hummer, D. G., and Rybicki, G. B., 1968, Ap. J. (Letters), 153, L107.

Jacques, S. A., 1978, Ap. J., 226, 632.

Linsky, J. L., and Haisch, B. M., 1979, Ap. J. (Letters), 229, L27.

Mullan, D. J., 1978, Ap. J., 226, 151.

Parker, E. N., 1965, Space Science Reviews, 4, 666.

Reimers, D., 1977, Astron. Astrophys., 57, 395.

Rosner, R., 1982, private communication.

Sanders, W., 1981, private communication.

Stencel, R. E., 1978, Ap. J. (Letters), 223, L37.

Stencel, R. E., and Mullan, D. J., 1980, Ap. J., 238, 221.

Stern, R. A., Zolcinski, M. C., Antiochos, S. K., and Underwood, J. H., 1981, Ap. J., 249, 647.

Vaiana, G. S., Cassinelli, J. P., Fabbiano, G., Giacconi, R., Golub, L., Gorenstein, P., Haisch, B. M., Harnden, F. R., Johnson, H. M., Linsky, J. L., Maxson, C. W., Mewe, R., Rosner, R., Seward, F., Topka, K., and Zwaan, C., 1981, Ap. J., 245, 163.

Withbroe, G. L., and Noyes, R. W., 1977, in Ann. Rev. Astron. and Astrophys., 15, 363.
Zirker, J. B., 1977, "Coronal Holes - An Overview", in Coronal Holes and High Speed Wind Streams, (ed. J. B. Zirker), Colorado Associated University Press, pp. 4-26.

THE STRUCTURE AND ENERGY BALANCE OF COOL STAR ATMOSPHERES

Jeffrey L. Linsky*
Joint Institute for Laboratory Astrophysics
National Bureau of Standards and University of Colorado
Boulder, Colorado 80309

ABSTRACT

A broad theme emerging from IUE observations of cool stars is that magnetic fields control the structure and energy balance of the outer atmospheres of these stars. For this review I summarize the phenomena associated with magnetic fields in the Sun and show that similar phenomena occur in cool stars. Gross atmospheric structures similar to the solar chromosphere and transition region occur in dwarf stars cooler than early F and perhaps in hotter stars. I will discuss the evidence for the weakening or disappearance of transition regions and coronae, together with the appearance of extended cool chromospheres with large mass loss, near V-R = 0.80 in the H-R diagram. Like the solar atmosphere, these atmospheres are not homogeneous and there is considerable evidence for plage regions with bright TR emission lines that overlie dark (presumably magnetic) star spots. The IUE observations are also providing important information on the energy balance in these atmospheres that should guide theoretical calculations of the nonradiative heating rate. Recent high dispersion spectra are providing unique information concerning which components of close binary systems are the dominant contributors to the observed emission, as well as estimates of densities and atmospheric extension. Emission line widths appear to increase with line formation temperature and luminosity, indicating properties of the random motions in these stars and that some resonance lines are opacity broadened. A recent unanticipated discovery is that the transition lines are redshifted (an antiwind) in β Dra (G2 Ib) and perhaps other stars, which I interpret as indicating downflows in closed magnetic flux tubes as are seen in the solar flux tubes above sunspots. Finally I classify the G and K giants and supergiants into three groups — active stars, quiet stars, and hybrid stars — depending on whether their atmospheres are dominated by closed magnetic flux tubes, open field geometries, or a predominately open geometry with a few closed flux tubes embedded.

I. INTRODUCTION

Looking back over the accomplishments of the first four years of IUE, I am struck by what we have learned about cool stars compared with how little we knew from ground-based observations and the Copernicus and balloon observations from space. Prior to IUE we were only able to study the chromospheric Mg II and Ca II resonance lines, He I λ10830, and several far ultraviolet

*Staff Member, Quantum Physics Division, National Bureau of Standards.

lines in only one star, Capella. IUE has truly opened up the ultraviolet for spectroscopic studies of the whole range of cool stars both at low dispersion and increasingly at high dispersion. This field has become too large to be surveyed in a short talk, so I must restrict myself to a few topics of current interest. For a more complete survey, I suggest the review papers by Ayres (1981), Dupree (1981a,b,1982), and Linsky (1980,1981a,b,c).

IUE is providing us with considerable evidence that changing magnetic fields are the cause of most phenomena observed in cool stars. I will therefore concentrate my attention on the consequences of magnetic fields in cool star atmospheres. The importance of magnetic fields should come as no surprise, however, as they lie at the basis of most solar phenomena, and the Sun is the best studied cool star (cf. Withbroe and Noyes 1977; Vaiana and Rosner 1978; Webb 1981). As a guide, I summarize below a few aspects of the solar magnetic field that should be applicable to a wider range of stars, and also list some factors which may produce magnetic fields in stars:

a) General properties of solar magnetic fields

(1) They are inhomogeneously distributed across the solar surface.

(2) They are variable on many time scales.

(3) Strong fields tend to clump into large groups of closed loop structures (active regions) or small groups (chromospheric network) at the edge of supergranule cells.

(4) Large regions of predominately weak fields with open topologies (coronal holes) exist at the poles and often at low latitudes.

b) Influence of closed magnetic loops on atmospheric structure

(1) Closed flux tubes are the dominant geometrical structures in the solar outer atmosphere.

(2) The nonradiative quasi-steady state heating rate, perhaps due to slow mode MHD waves, is enhanced in closed flux tubes. Rapid conversion of magnetic to thermal energy and energetic particles occurs during flares.

(3) Since strong, closed magnetic fields prevent flows across field lines, winds may occur only in open field geometries (coronal holes).

(4) Closed magnetic fields also restrict heat conduction across field lines, so that heat conduction to space is unimportant but heat conduction down to the chromosphere can be an important energy loss mechanism.

(5) The enhanced nonradiative heating rate and restricted loss of energy to space by outflow and thermal conduction together are responsible for the bright ultraviolet emission line spectra of typical magnetic flux tubes.

(6) Variability of the emission line flux from the Sun viewed as a point source is due to the rotational modulation of the few active regions present on the solar disk and to secular changes in the flux tubes.

(7) On the basis of the above properties, it is likely that the reason for the two order of magnitude spread in the ultraviolet emission line flux detected in stars lying in similar regions of the H-R diagram (Linsky and Ayres 1978; Basri and Linsky 1979), is in the number of magnetic flux tubes present in the outer atmospheres of different stars.

(8) Downflows with velocities of 10-20 km s^{-1} in the C IV and Si IV lines (Athay et al. 1982; Roussel-Dupre and Shine 1982) are commonly seen in magnetic flux tubes especially above sunspots.

c) Influence of open magnetic fields on atmospheric structure

(1) Since energy loss by outward thermal conduction and wind expansion is permitted in magnetically open regions, these regions tend to be cooler, of lower density, and be characterized by weaker ultraviolet emission lines than active regions. Coronal holes are the origins of high speed wind streams and perhaps most of the solar mass loss.

(2) Momentum deposition by MHD waves may be responsible for the acceleration of the solar wind in addition to the Parker-type thermal pressure gradient mechanism.

d) Origin of magnetic fields in stars

(1) In relatively young stars, remnant fields may exist from an earlier stage of evolution.

(2) Magnetic fields can be strengthened by dynamo processes from the interaction of convection and differential rotation. It is commonly assumed that dynamo processes are enhanced by rapid rotation and deep convection zones, but self-consistent calculations of internal rotation and field amplification are still in a primative state.

(3) Rapid rotation in cool stars could be a consequence either of youth, when the loss of angular momentum by the stellar wind has not yet slowed the rotation of the stellar envelope appreciably, or of tidally-induced synchronism for close binary systems such as the RS CVn, Algol, and W UMa systems.

II. GROSS ATMOSPHERIC STRUCTURE

In the Sun nonradiative heating processes produce a region called the chromosphere, extending typically over 6 pressure scale heights, where the temperature rises gradually from roughly 4200 K to 10,000 K. This region is easily detected by bright emission in the resonance lines of Ca II, Mg II, H I, C I, O I, and Si II. Chromospheric emission lines are detected in nearly all stars cooler than spectral type early F. Solar emission lines formed at temperatures above 10^4 K and below the corona ($T \gtrsim 10^6$ K) generally arise in an inhomogeneous yet geometrically narrow region, called the transition region (TR), where the temperature gradients are very steep. TR emission lines are typically seen in all dwarf stars cooler than spectral type early F, but the appearance or absence of these lines is a more complex phenomenon among the luminous stars.

The spectra of the Sun and two representative dwarf stars are compared in Figure 1 in terms of apparent line flux divided by the apparent bolometric luminosity. These spectra contain emission lines of C I, O I, Si II, Fe II, and other chromospheric species formed at temperatures cooler than 10^4 K, and lines of He II, C II, C III, C IV, N V, Si III, and Si IV formed at temperatures of $2 \times 10^4 - 2 \times 10^5$ K. On the basis of the presence of all these lines and the similar relative strengths compared to the Sun, we conclude that these stars and stars with similar spectra contain chromospheres and TRs, although the parameters characterizing these atmospheric regions may differ from those values for the Sun. There is an important difference, however, between the ultraviolet spectra of ξ Boo A and ε Eri compared to the Sun: the emission line fluxes (f_L/ℓ_{bol}) are roughly an order of magnitude larger (cf. Ayres, Marstad, and Linsky 1981b). All three stars have measured magnetic fields of several thousand gauss, but for the Sun these fields cover less than 1% of the photosphere whereas for ξ Boo A (cf. Robinson, Worden, and Harvey 1980) and presumably also ε Eri these fields cover roughly 30% of the stellar surface. These data suggest that the wide range in ultraviolet emission line surface flux and soft X-ray flux detected in cool stars of similar spectral-luminosity class (cf. Basri and Linsky 1979; Vaiana et al. 1981; Ayres et al. 1981a) is due to different fractional surface areas covered by strong magnetic fields.

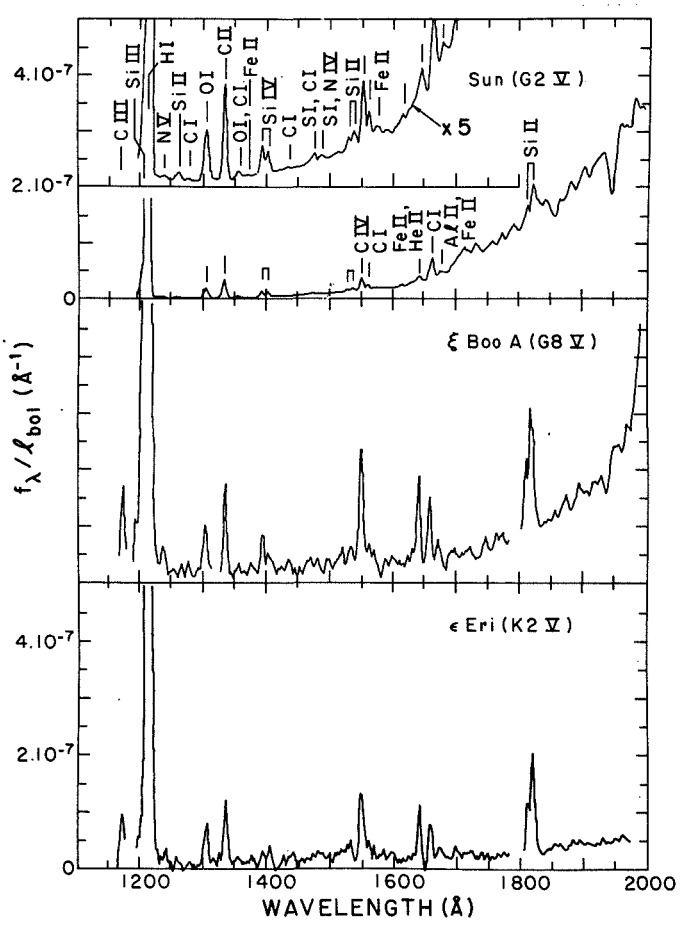

Fig. 1. SWP low dispersion spectra of ξ Boo A and ε Eri and the solar spectrum degraded to the IUE resolution (Ayres, Marstad and Linsky 1981b).

That is, stars with similar photospheres have bright chromospheres and TRs due to larger coverage by regions analogous to solar active regions (plages).

Böhm-Vitense and Dettmann (1980), and Linsky and Marstad (1981), among others, have noted the disappearance of chromospheric and TR emission lines as one goes to stars hotter than spectral type F0. While this could be due to the absence of these regions in the hotter stars as a consequence of weak convection, a more likely explanation is that the rapid increase in the photospheric ultraviolet continuum with increasing T_{eff} makes it difficult to measure the emission lines for lack of contrast (see discussion in Linsky 1981a). I believe this to be correct because some A stars like Vega (A0 V) and several A stars in the young Hyades cluster (Stern et al. 1981) exhibit coronal X-ray emission, and there must be layers with temperatures intermediate between the photosphere and corona in these stars. Since young A stars presumably have the largest magnetic fields, they should be searched carefully for ultraviolet emission lines.

As one proceeds down the main sequence, ultraviolet emission lines indicative of chromospheres and TRs are readily detected by IUE in stars as cool as UV Cet (M5.5e V) since the background continuum is very weak (see survey by Linsky et al. 1982). There are several dM dwarfs observed that do not show C IV emission at upper limits of 0.3 that of the quiet Sun, but weak TRs may exist on these stars as well. However, those stars that show indirect evidence of strong magnetic fields such as flares and photometric variability indicative of rotational modulation of dark star spots, invariably exhibit emission lines with surface fluxes 10-100 times that of the quiet Sun.

Near the beginning of IUE operations, Linsky and Haisch (1979) noted a trend in the ultraviolet spectra of cool giants and supergiants in which the warmer stars with V-R < 0.80 (the yellow giants) show emission lines formed at all temperatures up to 10^5 K, whereas the cooler stars with V-R > 0.80 (the red giants) show only chromospheric emission lines. On this basis they proposed a nearly vertical dividing line in the H-R diagram near V-R = 0.80 (see Fig. 2) separating the yellow giants that typically have TRs from the red giants that do not. Subsequently, Ayres et al. (1981a) showed that the Einstein soft X-ray observations are consistent with the typical presence of hot coronae in stars to the left of a similar boundary and the absence of coronae in single stars to the right (see Fig. 2). Also Stencel (1978), and Stencel and Mullan (1980a,b) presented evidence for the onset of massive cool winds in stars lying to the right of a similar boundary.

The idea of a boundary as proposed by Linsky and Haisch (1979) has been criticized on the basis of the few stars in the original data sample, the absence of detected TR emission lines in some yellow giants (Hartmann, Dupree and Raymond 1982), and the existence of some red giants, the so-called hybrid stars, that show evidence for massive winds and C IV emission lines (Hartmann, Dupree and Raymond 1980,1981; Reimers 1982). These valid criticisms led to a reexamination of the existence of a boundary by Simon, Linsky and Stencel (1982) on the basis of a much larger sample of 39 single stars and a smaller reverse bias sample. They found (see Fig. 2) that the yellow giants show a wide range of C IV fluxes (i.e. $f_{C\ IV}/\mathcal{L}_{bol}$), including stars with small upper limits, that they ascribed to a mixed evolutionary status of these stars.

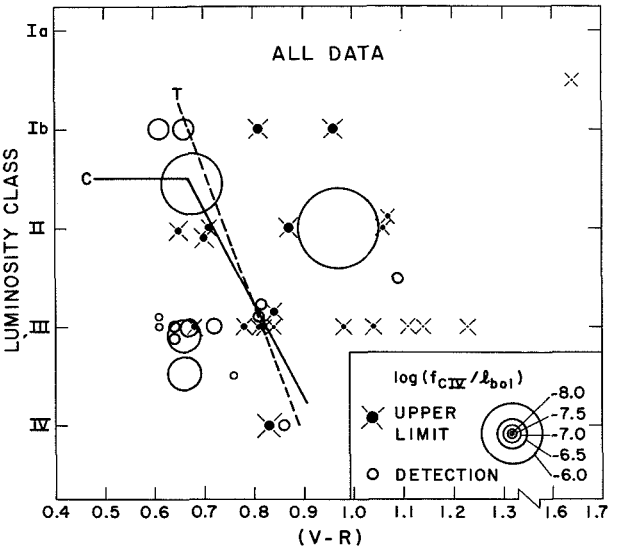

Fig. 2. Measured ratios of the C IV λ1550 flux to the apparent stellar bolometric luminosity from Simon, Linsky and Stencel (1982). Open circles are detections and filled circles are upper limits. The line marked T is that originally proposed by Linsky and Haisch (1979) to separate stars with (to the left) and without (to the right) 10^5 K plasma. The line marked C was proposed by Ayres et al. (1981a) to separate stars that generally show soft X-ray emission (to the left) from stars that generally do not (to the right). Two of the three detections to the right of the line marked T are previously unknown binary systems.

Some stars have just recently evolved from the upper main sequence and could be relatively rapid rotators with strong magnetic fields and bright emission lines, whereas some may be post-helium flash stars that are slow rotators. Among the 18 red giants in their sample, only three stars have detected C IV emission but two of these three show ultraviolet continuum emission indicative of previously unknown companions (56 Peg and α UMa) and the third is the hybrid star α TrA (Hartmann et al. 1981). Simon et al. (1982) therefore concluded that the boundary originally proposed by Linsky and Haisch is a real phenomenon in the sense that single stars to the right, with the exception of one hybrid star, contain significantly less 10^5 K plasma than typical single stars to the left of the boundary.

The question of a boundary remains open, however, for the following reasons. First, in the red giants, fluorescence in the fourth positive system of CO can produce emission features near the C IV 1550 Å and C II 1335 Å lines (Ayres, Moos and Linsky 1981c). Thus, high dispersion spectra are needed to reliably estimate upper limits for these TR emission line strengths. Second, the C IV emission lines detected in such hybrid stars as ι Aur (K3 II) and θ Her (K2 II) (cf. Reimers 1982) are so weak as to be at the level of some noise features. T. Simon recently reobserved θ Her with a 175 min SWP low-dispersion exposure (see Fig. 3), and saw no evidence for C IV emission. Thus

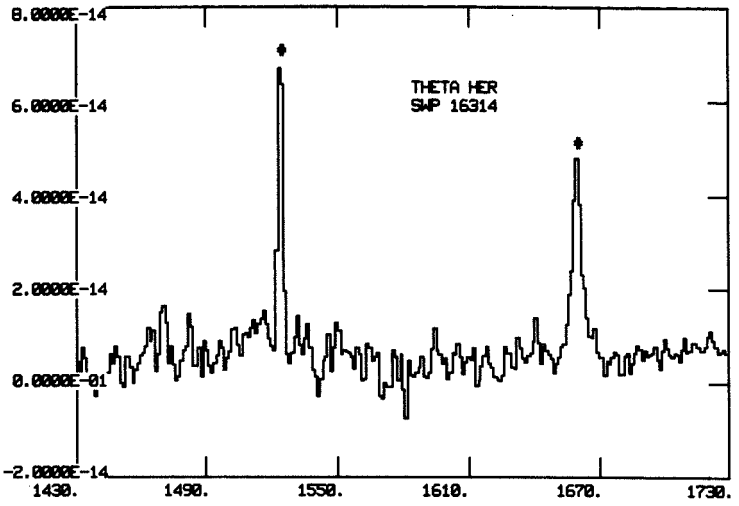

Fig. 3. A 175 minute SWP low dispersion spectrum of the hybrid star θ Her (K2 II) obtained by T. Simon. This long exposure shows no evidence of emission at the location of the C IV λ1550 feature. The two indicated features are radiation hits.

C IV emission in some of the hybrids is variable or not definitively detected. Third, the existence of a boundary demands a physically self-consistent explanation. I will return to these questions when I discuss high dispersion spectra at the end of this talk.

III. ATMOSPHERIC INHOMOGENEITY AND VARIABILITY

As mentioned in §I, magnetic fields produce inhomogeneity in the solar outer atmosphere by controlling the geometry and energy balance of closed flux tubes. A number of observing programs with IUE have confirmed that the outer atmospheres of cool stars are similarly inhomogeneous. Hallam and Wolff (1981), for example, have monitored the chromospheric emission line fluxes in three dwarf stars — 111 Tau (F8 V), ε Eri (K2 V), and 61 Cyg A (K5 V). They found that these fluxes vary sinusoidally with periods that are the likely rotational periods of the stars. These data provide evidence for the rotational modulation of an inhomogeneous distribution of bright emitting regions, presumably analogous to solar plages, across the surfaces of these stars. Several groups will be continuing such monitoring programs during the fifth year of IUE, in some cases with coordinated magnetic field observations to confirm the hypothesis that the plage regions have strong magnetic fields.

Close binary systems with cool components typically show bright ultraviolet emission lines and photometric variability indicative of rotational modulation of dark star spots (cf. Kunkel 1975; Hall 1981). One therefore expects that the ultraviolet emission line flux should vary with rotational phase such that emission line maximum corresponds to photometric minimum. Baliunas and Dupree (1982) have done this experiment on the long-period RS CVn system λ And (G8 III-IV + ?), confirming that the emission lines are strong at photometric minimum and weak at photometric maximum. Marstad et al. (1982) have monitored

three RS CVn systems (HR 1099, II Peg, AR Lac) and the prototype BY Dra system over at least one period for each system. Their work is described elsewhere in this volume, but they found clear variability in II Peg that is consistent with the presence of a relatively small plage region that is centered on the visible hemisphere at photometric minimum. They found that the plage and quiescent spectra differ, not only in the increased flux when the plage is on the disk, but also in the relative enhancement of high temperature lines in the plage spectrum, similar to what is seen in solar plage spectra.

Flares have also been detected in IUE spectra of the RS CVn system UX Ari (Simon, Linsky and Schiffer 1980) and in dMe flare stars (Butler et al. 1981; Haisch et al. 1982). Such flares are probably also magnetic in character with the dMe star flares similar to solar flares and the RS CVn flares perhaps involving reconnection between flux tubes of the two stars. One property seen in both the dMe and RS CVn flares is the relative enhancement of the high temperature (TR) lines compared to the chromospheric emission lines. This important property will be discussed next.

IV. ENERGY BALANCE AND NONRADIATIVE HEATING RATES

Since theoretical calculations of the nonradiative heating rates in stellar chromospheres and TRs have not proved useful in predicting the observed properties of cool star atmospheres, it is essential that empirical studies provide guidance for the theoreticians. IUE observations have provided four important pieces of information concerning nonradiative heating processes:

(1) Linsky and Ayres (1978) showed, on the basis of Mg II fluxes measured prior to IUE, that the chromospheric radiative loss rate per unit surface area of a star shows no dependence on stellar gravity. This implies that the heating rate is also independent of gravity, contrary to prior computations of heating due to the dissipation of shocks produced by purely acoustic waves, which imply a g^{-1} dependence and a T_{eff} dependence different than observed. This result was modified slightly by Stencel et al. (1980), who showed that IUE observations of cool supergiants are consistent with a small increase in the heating rate as the gravity decreases. Subsequently, Stein (1981) has proposed that slow mode MHD waves in magnetic flux tubes are a likely heating mechanism because they match the observed dependence of heating on g and T_{eff}, and these waves can produce the large heating rates observed in some young stars.

(2) Also using IUE observations of fluxes in the Mg II resonance lines, Basri and Linsky (1979) showed that there is a wide range in the chromospheric radiative loss rates and thus nonradiative heating rates in cool stars of similar effective temperature and luminosity (and thus gravity). Vaiana et al. (1981) and Ayres et al. (1981a) found a similar result for coronal X-ray emission. Thus the heating rate must depend on some parameter other than the values of T_{eff} and g that together determine where a star lies in the H-R diagram. The tight correlation of local nonradiative heating with magnetic field strength across the solar surface implies that the fractional coverage of a stellar surface by strong magnetic fields is the important missing parameter.

(3) Using SWP low dispersion observations of 28 cool stars, Ayres, Marstad and Linsky (1981b) showed that the emission line fluxes of chromospheric and TR lines are not linearly correlated (see Fig. 4). Instead, as one goes to stars with brighter chromospheric emission (i.e. $f_{Mg\ II}/\ell_{bol}$), the TR lines brighten even faster such that $(f_{C\ IV}/\ell_{bol}) \sim (f_{Mg\ II}/\ell_{bol})^{1.5}$. Walter, Basri and Laurent (1982) find a similar result using a different data sample. This phenomenon was previously noted in the comparison of the II Peg plage to quiescent spectra and the flare to quiescent spectra. It is also seen by comparing solar plage to quiescent spectra and thus must be a general property of stellar atmospheres. Elsewhere in this volume, Hammer, Linsky and Endler (1982) have proposed an explanation for this phenomenon.

(4) A general increase in chromospheric Ca II emission line flux with increasing stellar rotation rate and decreasing stellar age have been known since the 1950s from the work of Kraft, Wilson, Skumanich, and others, and had been explained as due to enhanced magnetic fields in the young rapidly rotating stars by dynamo processes. IUE and Einstein have extended this rotation-activity connection to TRs and coronae. For example, Stern et al. (1981) showed that the young Hyades stars have very large X-ray surface fluxes and Walter (1981), Walter and Bowyer (1981), and Walter, Basri and Laurent (1982) have proposed functional relations between X-ray or ultraviolet emission line fluxes and stellar angular velocity.

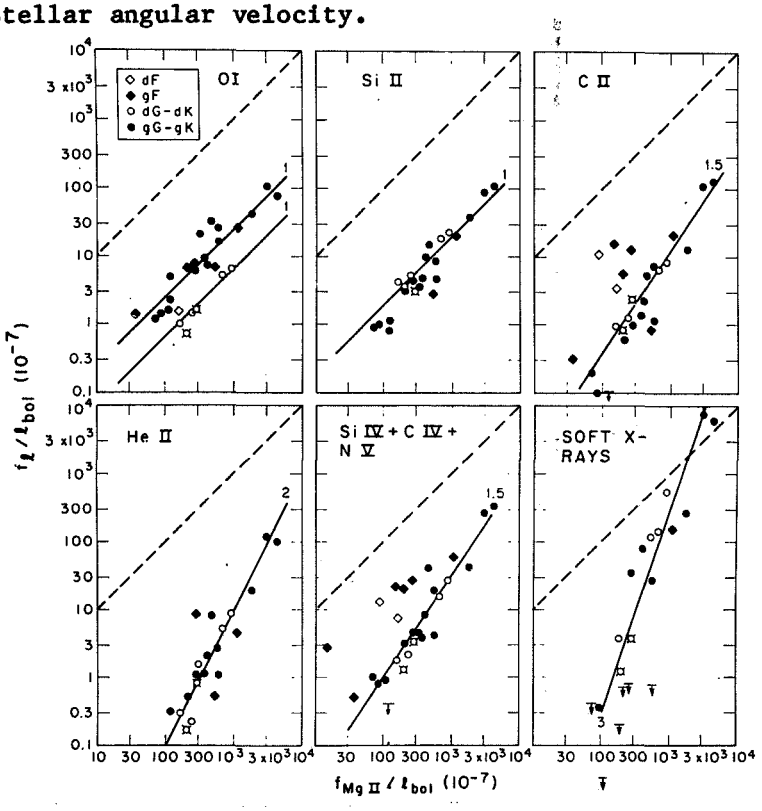

Fig. 4. Correlation plots of chromospheric, transition region, and coronal fluxes compared to the Mg II line relative flux (Ayres, Marstad and Linsky 1981b). The slope of 1.5 in the correlation plot for transition region lines (Si IV + C IV + N V) is an empirical result concerning the energy balance in stellar atmospheres.

V. NEW RESULTS ON COOL STAR ATMOSPHERES PROVIDED BY HIGH DISPERSION SPECTRA

Until now I have summarized some of the important results concerning cool stars that have been obtained by analyzing low dispersion SWP spectra, and high dispersion LWR spectra in the region of the Mg II resonance lines. High dispersion spectra, especially with the SWP camera, contain important new information that is only now beginning to be exploited. The reason for the few high dispersion SWP spectra of cool stars is that 16 hour observations are usually required even for second magnitude stars. Nevertheless, good exposures of several stars have been obtained with some unexpected results.

a) Spectral Line Identification

Line identification and line flux measurement is often difficult when several lines are likely to be present within a 6 Å spectral resolution element of the low dispersion format. For example, an emission feature in low dispersion at 1640 Å could contain lines of Fe II λ1640, He II λ1640, and O I λ1641, among others. High dispersion spectra show that for α Cen A (G2 V) the Fe II and He II lines have about equal flux and O I is absent, whereas for α Boo (K2 III) only the O I line is present (Ayres et al. 1982a,b). A determination of what fraction of the low dispersion 1640 Å emission flux is actually He II is important because the He II line may measure the soft X-ray flux (Zirin 1975; Hartmann et al. 1980). Another problem is to separate the C II λ1335 and C IV λ1550 features from the fluorescent CO bands at adjacent wavelengths (Ayres et al. 1981c). The high dispersion spectrum of α Boo shows no C II or C IV features present, which allowed Ayres et al. (1982b) to set surface flux upper limits 0.02 times those of the quiet Sun. Thus we can argue that this star has very little if any 10^5 K plasma.

b) Identification of Emission Components in Close Binary Systems

Since a spectral resolution element at high dispersion corresponds to roughly 30 km s^{-1}, IUE can determine from Doppler shift measurements which component in close binary systems is the dominant emitter in different lines, provided the maximum velocity separation is not too much smaller than 30 km s^{-1} and the signal-to-noise is adequate. In perhaps the first application of this technique to cool stars, Ayres and Linsky (1980) observed Capella (G6 III + F9 III) at conjunction (zero velocity separation) and one quadrature (maximum velocity separation) and found that the secondary star is responsible for essentially all of the TR emission line flux, whereas both stars contribute to the chromospheric emission line flux. Since the primary star had been previously assumed to be the dominant emitter in all lines, this result is important for understanding the system. Subsequently, Ayres and Linsky (1982) observed the RS CVn system HR 1099 (K0 IV + G5 V) at opposite quadratures. They found that the primary star is the dominant emitter as expected from previous optical studies, but that there are emission features at the G5 V star velocities in the Si II λ1808 and He II λ1640 lines. Another result of this study was evidence for a patchy distribution of emission across the surface of the K0 IV star as indicated by a factor of 1.5 enhancement of the TR line fluxes at phase 0.76 compared to phase 0.21 and a displacement of the emission centroid velocity at phase 0.76 consistent with emission from a plage region near the trailing limb of the K0 IV star, which faces toward the secondary star. Further studies of close binary systems are planned.

c) Densities and Atmospheric Extension

Measurements of integrated line fluxes can be converted to surface fluxes and volume emission measures (EM $\sim \int n_e^2 dV$), provided one can estimate the stellar angular diameter. Emission measures are important, but to determine the geometrical thickness of the emitting region, and thus whether it is thin or thick compared to the photospheric radius, one must measure the electron density separately. One important technique is to measure line ratios that are density-sensitive over the relevant range of densities. Stencel et al. (1981) have shown that ratios of lines in the UV 0.01 multiplet of C II at 2325 Å are sensitive to densities in the range 10^7-10^9 cm^{-3}, and that these emission lines are observed in high dispersion LWR spectra of cool giants and supergiants. These data and subsequent observations presented by Stencel and Carpenter (1982) indicate that the chromospheres of the yellow giants are geometrically thin, but those of the red giants and supergiants are extended with dimensions of several stellar radii. Also, upper limits to the C II λ1335/ C II λ2325 flux ratios in these stars indicate that the extended chromospheres are cool (T < 10,000 K).

Densities in stellar TRs at T ≈ 5 × 10^4 K can be derived using several line flux ratios available in the SWP data, including C III λ1909/Si IV λ1403, C III λ1909/O III λ1666, C III λ1909/Si III λ1892, C III λ1175/C III λ1909 (cf. Cook and Nicolas 1979; Doschek et al. 1978). Each of these line ratios has potential problems including line blending at low dispersion, but when they lead to consistent density estimates for a given star we should accept the resultant densities. These ratios have been used to estimate densities from low dispersion spectra for such systems as Capella, HR 1099, UX Ari, and β Dra. Recently, Stencel et al. (1982a,b) obtained a 1273 minute SWP high dispersion exposure of β Dra (G2 Ib). The line ratios in this spectrum are consistent with a previous low dispersion spectrum (Basri, Linsky and Eriksson 1981) and imply n_e = 2 × 10^{10} cm^{-3} and P = 0.3 dynes cm^{-2} for the emitting structures. This density and the measured TR line emission measures require that the TR in this star be geometrically thin like the Sun's despite the three order of magnitude difference in stellar gravities of the two stars.

d) Emission Line Widths

A comparison of line widths in five stars of similar effective temperature but different luminosity and gravity [α Cen B (K1 V), α Cen A (G2 V), λ And (G8 III-IV+?), α Aur Ab (F9 III), and β Dra (G2 Ib)] led Ayres et al. (1982a) to some interesting conclusions. First, they found that for all the stars the line widths (FWHM) increase with increasing temperature of formation. Second, there is a systematic trend of increasing line width with increasing stellar luminosity. A completely unexpected result, however, was the discovery that the widths of TR resonance lines (e.g. C II λ1336, Si IV λ1394, C IV λ1548) are twice as large as the widths of the TR intersystem lines (e.g. Si III λ1892, C III λ1909) formed at similar temperatures. The recent long exposure of β Dra confirms this result as the FWHM of the TR resonance lines is typically 150 km s^{-1}, whereas the FWHM of the TR intersystem lines is typically 80 km s^{-1} (see Fig. 5). Since none of these stars shows any evidence for winds, Ayres et al. (1982a) proposed that the lines are broadened by turbulence that increases with temperature and luminosity, and that the additional

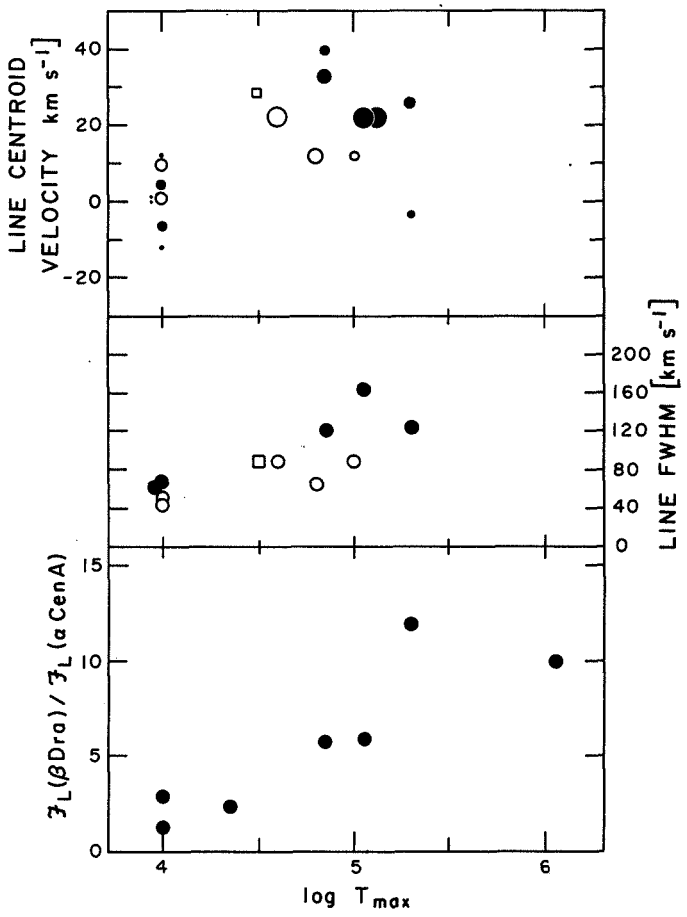

Fig. 5. Plots of the line centroid velocities, line widths, and relative surface fluxes as a function of line formation temperature for β Dra (G2 Ib) (Stencel et al. 1982b). In the top two panels resonance lines are indicated by filled circles and intersystem lines by open circles. In the top panel the size of the symbol indicates the relative line flux and thus its weight in determining the mean velocity for the low and high excitation lines.

factor of 2 in the line widths of the TR resonance lines in the luminous stars is due to opacity broadening of optically thick lines. Since the three luminous stars have TR line surface fluxes much larger than the quiet Sun, they are presumably covered by many magnetic flux tubes and the turbulent broadening could be due to upflows and downflows of plasma within these many flux tubes.

e) Properties of Stellar Winds

High dispersion IUE spectra will likely prove to be increasingly valuable in determining the properties of winds in cool luminous stars. Until now this work has primarily involved searching for blue-shifted circumstellar absorption components in the Mg II resonance lines that indicate cool outflowing gas. For example, Hartmann et al. (1980,1981) and Reimers (1982) have called attention to the hybrid stars which typically show Mg II absorption components both at low velocity and at roughly -100 km s^{-1}. Hartmann et al. (1981) also proposed that the 150-200 km s^{-1} FWHM of the C IV λ1548 line in the hybrid star α TrA (K4 II) is due to expansion of 10^5 K plasma from an extended region about the star. Hartmann and MacGregor (1980) have computed Alfven-wave driven wind models that predict a 10^5 K temperature maximum, ~100 km s^{-1} expansion velocities, and significant cool plasma outside of the 10^5 K material that may be observable as Mg II absorption components at -100 km s^{-1}.

It is important to test this hypothesis of 10^5 K winds in the hybrid stars observationally. One test is to search for stars with similar effective temperature and luminosity that have broad C IV lines yet no evidence of outflow of gas at any temperature. The star β Dra (G2 Ib) is an excellent test case because it is similar spectroscopically to the hybrid stars α Aqr (G2 Ib), β Aqr (G0 Ib), and α TrA (K4 II), yet it has broad lines and no evidence of a wind. On the basis of this test we conclude that broad C IV lines provide no unique evidence for a 10^5 K wind. A more conclusive test would be to directly measure the C IV line centroid velocity in the hybrid stars. Unless the TRs in these stars are extremely extended, the C IV lines should show a measurable blue shift. A 16 hour SWP high dispersion exposure recently obtained of α TrA may answer this question.

f) Systematic Flows of Transition Region Plasma

Perhaps the most exciting and unexpected discovery by IUE concerning cool stars is the very recent evidence for flows of the TR plasma. Stencel et al. (1982a) have measured line centroid velocities for 18 lines in the SWP high dispersion spectrum of β Dra by fitting least-squares Gaussians to the observed profiles. They estimate the velocity at the base of the chromosphere using eight subordinate or intersystem lines of C I, O I, S I, and Cℓ I. These low excitation lines have a mean velocity $\langle v_{LE} \rangle = 3 \pm 3$ km s^{-1}, where the error is the standard error of the flux-weighted mean. A similar measurement of the mean velocity of ten high excitation lines of He II, C III, C IV, N V, O III, Si III, and Si IV is $\langle v_{HE} \rangle = 23 \pm 3$ km s^{-1}. Thus the motion of the high excitation lines relative to the low excitation lines is $\langle v_{HE} \rangle - \langle v_{LE} \rangle = 20 \pm 4$ km s^{-1}. In other words, the TR plasma is flowing down into the star and we are observing a stellar antiwind. They believe that the possible alternative explanation (that the cool plasma is outflowing) is unlikely because the chromospheric lines chosen are not resonance lines and thus should be formed deep in the atmosphere. Also, the Mg II resonance lines show no evidence for outflow. Subsequently, T. Ayres has measured $\langle v_{HE} \rangle - \langle v_{LE} \rangle$ in a preliminary way using available spectra of nine other cool stars. He finds (see Fig. 6) that α Aur Ab, 56 Peg, and perhaps several dwarf stars appear to show redshifts, though with smaller amplitudes than β Dra.

At first sight the idea of an antiwind in a supergiant star seems preposterous, but upon reflection it should have been anticipated. At the beginning of this talk, I listed a number of properties of the solar magnetic field including the point (item b8) that downflows with velocities of 10-20 km s^{-1} are commonly seen in the C IV and Si IV lines in magnetic flux tubes above sunspots. I believe that the observed downflow of TR plasma in β Dra and perhaps other stars is merely one more piece of evidence that the phenomena in cool stars are largely controlled by magnetic fields.

VI. A PROPOSED EXPLANATION FOR THE OBSERVED SPECTRA OF COOL GIANTS AND SUPERGIANTS

In lieu of a summary, I would like to make two points. First, I believe that IUE is providing much evidence that magnetic fields play essential roles in determining the structure and energy balance of cool star atmospheres. As a result our explanations, models, and theoretical computations must take this

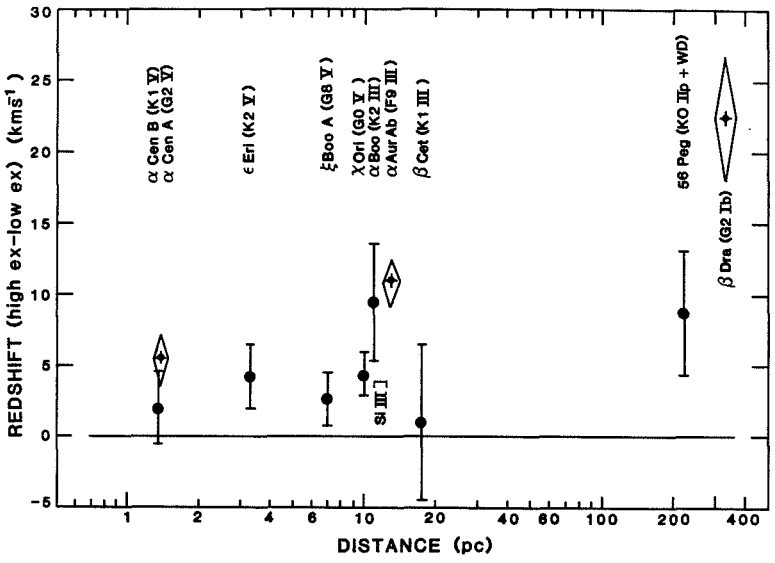

Fig. 6. The mean velocity difference for the high excitation lines compared to low excitation lines. These are preliminary results obtained by T. R. Ayres. Errors given are the standard errors of the flux-weighted means.

essential physics into account. Second, a clear picture appears to be emerging from the observations concerning the G and K giants and supergiants. I believe that three types of stars are present in this group.

(1) There are active stars, of which β Dra (G2 Ib) is a prototype, which show bright TR emission lines emitted by a geometrically thin region, bright X-ray emission, no evidence for any outflow of material, and redshifted TR emission lines. These are stars for which closed magnetic flux tubes dominate their outer atmospheres. These stars probably have large magnetic fields either because they have just recently evolved from the upper main sequence (β Dra may be an example) or because they are members of close binary systems that are forced to rotate synchronously (the cool components of RS CVn systems are examples).

(2) There are quiet stars, of which α Boo (K2 III) is a prototype, which show no evidence of TRs or hot coronae to very small upper limits, have cool winds with significant mass loss, and geometrically extended chromospheres. These stars probably have no, or very few, closed magnetic flux tubes but rather have outer atmospheres with magnetically open topologies like coronal holes, and little or no hot plasma. These are probably slow rotators. Precisely how the decay of magnetic fields can lead to a star changing from active to quiet remains to be worked out in detail.

(3) Finally, I believe that the hybrid stars, of which α TrA (K4 II) and α Aqr (G2 Ib) are prototypes, are hybrid but in a different sense than originally proposed. These stars show weak and likely variable TR emission lines,

no detected X-ray emission, and evidence for a cool wind. I believe that there is no real evidence for 10^5 K winds in these stars, but Doppler shift measurements are needed as previously described to help give a conclusive answer on this point. I would describe these stars as hybrid in the sense that their outer atmospheres contain mostly open field lines along which the cool wind flows, but they do contain a few closed magnetic flux tubes from which the TR lines are emitted. Rotational modulation of these few flux tubes could explain the variability. My guess is that these tubes also contain 10^6 K plasma emitting soft X-rays, but the X-rays are absorbed by the surrounding cool plasma.

This work was supported in part by NASA grants NAG5-82, NGL-06-003-057, and NAG5-199 through the University of Colorado. I would like to thank my colleagues T. R. Ayres, P. L. Bornmann, S. Drake, R. Hammer, N. C. Marstad, M. Schindler, T. Simon, R. E. Stencel, and F. M. Walter for stimulating discussions and for permission to describe unpublished work at this time.

REFERENCES

Athay, R. G., Gurman, J. B., Henze, W. and Shine, R. A. 1982, submitted to Ap. J.

Ayres, T.R. 1981, in The Universe at Ultraviolet Wavelengths: The First Two Years of IUE, ed. R. D. Chapman, NASA Conference Publication 2171, p. 237.

Ayres, T. R. and Linsky, J. L. 1980, Ap. J., 214, 410.

_____. 1982, Ap. J., in press.

Ayres, T. R., Linsky, J. L., Basri, G. S., Landsman, W., Henry, R. C., Moos, H. W. and Stencel, R. E. 1982a, Ap. J., in press.

Ayres, T. R., Linsky, J. L., Vaiana, G. S., Golub, L. and Rosner, R. 1981a, Ap. J., 250, 293.

Ayres, T. R., Marstad, N. C. and Linsky, J. L. 1981b, Ap. J., 247, 545.

Ayres, T. R., Moos, H. W. and Linsky, J. L. 1981c, Ap. J. (Letters), 248, L137.

Ayres, T. R., Simon, T. and Linsky, J. L. 1982b, submitted to Ap. J.

Baliunas, S. L. and Dupree, A. K. 1982, Ap. J., 252, 668.

Basri, G. S. and Linsky, J. L. 1979, Ap. J., 234, 1023.

Basri, G. S., Linsky, J. L. and Eriksson, K. 1981, Ap. J., 251, 162.

Böhm-Vitense, E. and Dettmann, T. 1980, Ap. J., 236, 560.

Butler, C. J., Byrne, P. B., Andrews, A. D. and Doyle, J. G. 1981, M.N.R.A.S., 197, 815.

Cook, J. W. and Nicolas, K. R. 1979, Ap. J., 229, 1163.

Doschek, G. A., Feldman, U., Bhatia, A. K. and Mason, H. E. 1978, Ap. J., 226, 1129.

Dupree, A. K. 1981a, in Solar Phenomena in Stars and Stellar Systems, eds. R. M. Bonnet and A. K. Dupree (Dordrecht: D. Reidel), p. 407.

_____. 1981b, in Effects of Mass Loss on Stellar Evolution, eds. C. Chiosi and R. Stalio (Dordrecht: D. Reidel), p. 87.

_____. 1982, this volume.

Haisch, B. M. et al. 1982, in preparation.

Hall, D. S. 1981, in Solar Phenomena in Stars and Stellar Systems, eds. R. M. Bonnet and A. K. Dupree (Dordrecht: D. Reidel), p. 431.

Hallam, K. L. and Wolff, C. L. 1981, Ap. J. (Letters), 248, L73.
Hammer, R., Linsky, J. L. and Endler, F. 1982, this volume.
Hartmann, L., Dupree, A. K. and Raymond, J. C. 1980, Ap. J. (Letters), 236, L143.
_____. 1981, Ap. J., 246, 193.
_____. 1982, Ap. J., 252, 214.
Hartmann, L. and MacGregor, K. B. 1980, Ap. J., 242, 260.
Kunkel, W. E. 1975, in Variable Stars and Stellar Evolution, eds. V. E. Sherwood and L. Plaut (Dordrecht: D. Reidel), p. 15.
Linsky, J. L. 1980, Ann. Rev. Astr. Ap., 18, 439.
_____. 1981a, in Solar Phenomena in Stars and Stellar Systems, eds. R. M. Bonnet and A. K. Dupree (Boston: Reidel), p. 99.
_____. 1981b, in Effects of Mass Loss on Stellar Evolution, eds. C. Chiosi and R. Stalio (Boston: Reidel), p. 187.
_____. 1981c, in Physical Processes in Red Giants, eds. I. Iben Jr. and A. Renzini (Dordrecht: D. Reidel), p. 247.
Linsky, J. L. and Ayres, T. R. 1978, Ap. J., 220, 619.
Linsky, J. L., Bornmann, P. L., Carpenter, K. G., Wing, R. F., Giampapa, M. S. and Worden, S. P. 1982, Ap. J., in press.
Linsky, J. L. and Haisch, B. M. 1979, Ap. J. (Letters), 229, L27.
Linsky, J. L. and Marstad, N. C. 1981, in The Universe at Ultraviolet Wavelengths: The First Two Years of IUE, ed. R. D. Chapman, NASA Conference Publication 2171, p. 287.
Marstad, N. et al. 1982, this volume.
Reimers, D. 1982, Astron. Ap., in press.
Robinson, R. D., Worden, S. P. and Harvey, J. W. 1980, Ap. J., 239, 961.
Roussel-Dupre, D. and Shine, R. A. 1982, Solar Phys., in press.
Simon, T., Linsky, J. L. and Schiffer, F. H. III 1980, Ap. J., 239, 911.
Simon, T., Linsky, J. L. and Stencel, R. E. 1982, Ap. J., in press.
Stein, R. F. 1981, Ap. J ., 246, 966.
Stencel, R. E. 1978, Ap. J. (Letters), 223, L37.
Stencel, R. E. and Carpenter, K. G. 1982, this volume.
Stencel, R. E., Linsky, J. L. and Ayres, T. R. 1982a, this volume.
Stencel, R. E., Linsky, J. L., Ayres, T. R., Jordan, C. and Brown, A. 1982b, submitted to Ap. J.
Stencel, R. E., Linsky, J. L., Brown, A., Jordan, C., Carpenter, K. G., Wing, R. F. and Czyzak, S. 1981, M.N.R.A.S., 196, 47P.
Stencel, R. E. and Mullan, D. J. 1980a, Ap. J., 238, 221.
_____. 1980b, Ap. J., 240, 718.
Stencel, R. E., Mullan, D. J., Linsky, J. L., Basri, G. S. and Worden, S. P. 1980, Ap. J. Suppl., 44, 383.
Stern, R. A., Zolcinski, M.-C., Antiochos, S. K. and Underwood, J. H. 1981, Ap. J., 249, 647.
Vaiana, G. S. and Rosner, R. 1978, Ann. Rev. Astr. Ap., 16, 393.
Vaiana, G. S. et al. 1981, Ap. J., 245, 163.
Walter, F.M. 1981, Ap. J., 245, 677.
Walter, F. M., Basri, G. S. and Laurent, R. 1982, this volume.
Walter, F. M. and Bowyer, S. 1981, Ap. J., 245, 671.
Webb, D. F. 1981, in Solar Active Regions, ed. F. Q. Orrall (Boulder: Colorado Associated University Press), p. 165.
Withbroe, G. L. and Noyes, R. W. 1977, Ann. Rev. Astr. Ap., 15, 363.
Zirin, H. 1975, Ap. J. (Letters), 199, L63.

IUE OBSERVATIONS OF SOLAR SYSTEM OBJECTS AND PROCESSES

Robert M. Nelson
Jet Propulsion Laboratory
California Institute of Technology
Pasadena, CA 91109

The IUE spacecraft has played a special and unique role in solar system studies because it is currently the chief means by which several areas of important research can be advanced; this, in spite of the fact that many solar system objects have been studied by flyby and/or orbiter missions. This uniqueness is due primarily to the following reasons:

(1) While spacecraft flyby missions provide information of high spatial resolution, the spectral resolution of the imaging systems is very low and the areal coverage of spectrometer systems has often been very limited. IUE, while having less spatial resolution, has very good spectral resolution.

(2) IUE is able to sample a spectral range that is at shorter wavelengths than the capability of most spacecraft imaging systems. For example, neither Voyager nor Galileo have imaging systems or spectrometers which cover IUE's spectral range.

(3) Instruments such as IUE allow for careful synoptic observations of phenomena over a variety of time scales not available to a flyby mission which, at best, can provide only a 'snapshot' view.

Observers have used IUE to identify previously undetected absorption features in planetary atmospheres, study spatial and temporal variations in planetary atmospheres and magnetospheres, and identify and map the distribution of constituents on the surfaces of solid bodies. In over four years of active research, the IUE spacecraft has observed 7 planets, 9 planetary satellites, 7 comets and 20 asteroids. In what follow is a brief review of some of the major findings of these research programs.

VENUS

Spectra of the Venus dayside and nightside have been obtained while the planet was near elongation. Conway et al. (1979) report absorption bands at 2080-2180 Å and identify these as being caused by SO_2 gas. They calculate a vertical SO_2 column density, which when combined with the column densities for SO_2 obtained by Pioneer Venus and from groundbased observations at 3000-3200 Å, provides a measure of the SO_2 mixing ratio with altitude and its variation on top of the cloud deck. Observations of Venus' darkside have led to the identification of the Venus nightglow. This phenomenon is caused by emission bands of nitric oxide. Because of the short lifetime of this species on the nightside, this finding implies the rapid (dayside - nightside) transport of material in the Cytherean atmosphere (Feldman, et al., 1979). Observations of the Venus dayside have lead to the discovery that the origin of the dayglow emission is carbon monoxide fluorescence; probably

due to fluorescent scattering of solar Lyman α radiation (Durrance, 1981).

MARS

Ozone has been detected over the southern region of Mars by Conway et al. (1980). They have shown that IUE can effectively monitor the seasonal variation of ozone on Mars, thereby allowing long term study of its abundance from earch orbit. Furthermore, their results for the southern hemisphere agree with the northern hemisphere ozone seasonal behavior reported by Mariner 9 thus giving a clue to the systematics in the variation of this species. In general, the ozone is in greatest abundance where the atmosphere is dry and cold.

JUPITER

The discovery of ultraviolet absorptions at 1775, 1755, 1735, and 1713 Å in Jupiter's atmosphere has led to the identification of acetylene. The mixing ratio for $[C_2H_2]/[H_2]$ has been calculated (Owen et al., 1980) and found to be 22×10^{-9}. Ammonia has also been detected and the mixing ratio is 5×10^{-8} $[NH_3]/[H_2] < 5 \times 10^{-7}$ (Combes et al., 1981). The observation of absorption features from these species from IUE indicates that they are present above the tropopause. Attempts to match the jovian spectral geometric albedo with model atmospheres of H_2, NH_3, C_2H_2, C_2H_6 indicate that other absorbers may be present (Winkelstein et al., 1982; Clarke et al., 1982). A search with IUE for CO absorption has detected none (Wagener et al., 1982). Emissions from the hydrogen Lyman α line (Hα) and molecular hydrogen Lyman and Werner bands have been spatially resolved on Jupiter. They are thought to be associated with polar auroral activity originating from particle impact excitation processes (Clarke et al., 1980). Synoptic observation of these emissions using IUE have shown that they are a periodic function of jovian System III longitude and therefore are associated with Jupiter's magnetospheric rotation and not its atmospheric rotation. Maximum emission occurs at $\lambda_{III} = 186^{o}$. No long term changes have been observed yet but peak to peak variations of up to a factor of 2 have been seen (Durrance et al., 1982).

Spatial maps of the Ly α emission line from the planet's disk have been constructed. It has been discovered that there exists an asymmetry in the Lα emission that resembles an equatorial bulge (Clarke et al., 1981). This feature has been observed for several years and it is now known that the maximum emission occurs at $\lambda_{III} = 90^{o}$. Furthermore it has been stable over this whole time period. It has been suggested that the cause of the "bulge" is related to an anomaly in the jovian magnetosphere (Skinner et al., 1982).

The search for and discovery of emissions in the vicinity of Jupiter's moon, Io, has led to the identification of several ionized species including SII, SIII and OIII (Moos et al., 1980). The abundances of the ionized species in the torus will provide a basis for a number of critical tests which must be passed by the various proposed mechanisms for the removal of material from Io (Matson et al., 1974).

SATURN

Absorption features discovered in the IUE spectra of Saturn near 1950 Å have been identified as being caused by acetylene (C_2H_2) in the upper atmosphere. Moos and Clarke (1979) calculate an upper limit of $7 \times 10^{17}/cm^2$ for the acetylene column density. Although C_2H_2 is a well known strong absorber in the UV, it alone cannot explain the low UV spectral geometric albedo of Saturn. Other absorbers have been searched for but to date, none can explain the apparent UV absorption. The species that have been searched for include PH_3, CH_4, C_2H_4, and NH_3 (Winkelstein et al, 1982).

North-South mapping studies of the Ly α emission across Saturn's disk have discovered pronounced spatial asymmetries in the emission and noted variations of a factor of 2 over several days. Observations of Titan during periods of enhanced Saturnian Ly α emission show no detectable excess emissions. Therefore, Titan has been dismissed as a possible source of hydrogen for Saturn's Ly α emission (Clarke et al., 1981b). It is interesting that observational studies of the Saturnian Lyman and Werner bands (molecular hydrogen) in the polar aurorae emissions, do not find any variation in intensity with Saturn's rotational period (Durrance, 1982). Thus, the important discovery that this emission on Saturn behaves differently from what was previously believed to be an analogous process with the jovian polar aurora emission.

URANUS AND NEPTUNE

Because these objects have much smaller angular sizes and are at much greater distance from the sun than Jupiter and Saturn, spatial imaging and high resolution spectroscopic studies are severely limited. In spite of this, encumberence, IUE observations have improved the spectral resolution in the 2000-3000 Å range by an order of magnitude. At 4 Å resolution no absorption features are found (at the 20% level) for Uranus and (at the 30% level) for Neptune. By binning their data into 50 Å intervals, Caldwell et al. (1981, 1982) have found that the continuum albedos are consistent with Rayleigh-Raman scattering models.

COMETS

Several spacecraft missions to the environs of a comet are being planned and IUE observations of comets will not only play a critical role in determining the instrument payload but will influence the planned observing sequences. Independent of these future possibilities, however, the results of comet observations with IUE have contributed much to the understanding of the physical processes that are operative on these objects. Recently these observations and interpretations been summarized by Weaver et al. (1981). The major species detected in IUE spectra of all comets are hydrogen, oxygen, and hydroxl. These are assumed to be the dissociation products of water. Minor species found in IUE spectra of some of the better studied comets are C, S, C_2, CS, CO_2^+. Because of the great compositional similarities in the ultraviolet spectra of comets, a common origin is implied. The development of water production models has progressed significantly based on

IUE data which moniters the strength of the H, O and OH emissions. Water production rates show variations between comets of an order of magnitude. Large variations in the dust to gas ratio of comets have also been found. Thus, IUE has played a significant role in furthering our understanding of these volatile members of the solar system.

ASTEROIDS

The asteorids are an important class of objects for study because their wide range of sizes, compositional variations, and spatial distribution. Because of their relatively small sizes, the asteroids are thought to contain significant amounts of pristine material and therefore, they may provide much information on questions regarding the origin and evolution of the solar system.

The spectra of 20 asteroids have been measured by IUE. In the case of brighter objects (e.g. 1 Ceres) the new IUE data have revised downward (by a factor of four) the albedos reported on the basis of earlier spaceborne ultraviolet observations. No pronounced UV absorption features have been identifed yet for any asteroid on the basis of IUE observations. However, this "apparent disaster" is very important because it significantly narrows the list of possible (solid state) mineral assemblages which otherwise could be present on asteroid surfaces (Veeder et al., 1980). Since asteroids are not particularly bright ultraviolet sources, most of the spectra obtained are noisy. Nevertheless, additional valuable information has been obtained by binning the IUE data into three bandpasses, each of which is ~ 200 Å wide. Ultraviolet color-color plots of these bands for asteroids show that S class asteroids, which group together on a classical B-V, U-B color-color diagram, scatter fairly widely on the IUE color-color diagram. This indicates that the asteroids classified as S are not compositionally similar as was previously believed.

PLANETARY SATELLITES

Ultraviolet spectra of 8 planetary satellites of Jupiter and Saturn have been obtained with IUE. This information has played a critical role in the detection and mapping of the solid state components on the surface of some of these objects. IUE studies of Titan, the only satellite with substantial atmosphere, have identified no new atmospheric species (Caldwell et al., 1981) but IUE obvservations have been very useful in eliminating Titan as the source for hydrogen needed to explain the Saturnian Lyman α emission (Clarke et al., 1981b).

The Galilean satellites of Jupiter have been the satellites most extensively observed with IUE. Spectra have been taken over a wide range of orbital phase angles. These observations have spanned the last 4 years. The two outermost Galilean satellites, Ganymede and Callisto, show no prominent absorption features. This is consistent with compositional hypotheses formed on the basis of groundbased visible and infrared spectral data. All of these observations are consistent with water ice as the primary surface species (Clark, 1980). Ultraviolet absorption features have

been discovered in IUE data for the two innermost Galilean satellites, Io and Europa. The absorption on Io has been attributed to frozen sulfur dioxide and this has been further supported by laboratory measurements (Nelson et al., 1980a; Nash et al., 1980). The absorption on Europa has been hypothesized to be due to energetic sulfur ions from the jovian magnetosphere which have embedded themselves in the ubiquitous water ice of this satellite's surface (Lane et al., 1981).

To improve signal to noise, the IUE spectral data have been binned into three ~ 200 Å wavelength bandpasses, and UV geometric albedos of Galilean satellites have been determined (Nelson et al., 1980b). These are presented in Table 1. Because of the variation in albedo of all four objects with orbital phase angle; the table divides the data into two separate orbital phase angle ranges 70-120° and 250 - 290°. We note that these albedos agree quite well with groundbased observations (Nelson and Hapke, 1978) in the wavelength region just longward of band #3. They also agree with the results reported by OAO-2 (Caldwell, 1975).

The strength of the ultraviolet absorption on Io is strongly dependent on orbital phase angle. This is known to be true at longer wavelengths also. The groundbased photometry (Morrison et al., 1974) show that Io's 'leading side' ($0<\theta<180$) is brighter than its 'trailing side' $180<\theta<360$. IUE has found that at wavelengths less than 3000 Å, the trailing side albedo is brighter than its leading side. No other solar system object yet observed exhibits this effect. Figure 1 demonstrates this dramatic albedo-wavelength orbital phase reversal on Io. This unusual behavior has been attributed to a variation in the longitudinal distribution of frozen sulfur dioxide (Nelson et al., 1980a). At visual wavelengths, laboratory spectra of frozen SO_2 show that it is strongly reflecting but below 3000 Å its spectrum is strongly absorbing (see Fig. 2). By measuring the variation in the strength of the ultraviolet absorption as a function of orbital phase angle, the abundance of frozen SO_2 relative to other surface materials has been determined as a function of longitude. The condensed SO_2 is present in greatest abundance at longitudes between 70° and 140°. It is least abundant at longitudes between 250° and 320° (Nelson et al., 1980a).

A careful search for the presence of SO_2 gas absorption on Io in the disk averaged IUE spectra has found none at abundances greater than the lower limit set at 0.008 cm.atm (Butterworth et al., 1980; Lane et al., 1979). Furthermore, this absence has been interpreted as meaning that SO_2 is not in equilibrium on Io's surface (Matson and Nash, 1982). Furthermore, a search of the Io spectra taken at different epochs does not reveal any major redistribution of observable condensates during four years of IUE observations. However, Io has long been suspected of exhibiting time variable albedo changes (Binder and Cruikshank, 1964; Nelson and Hapke, 1978b). This could be related to the demonstrated volcanic activity (Morabito et al., 1979).

The ultraviolet spectral absorption on Europa becomes evident when spectra of the satellite's trailing hemisphere are ratioed to spectra of its leading hemisphere (see Fig. 2). Lane et al. (1980) have suggested that

this feature is caused by an SO_2 absorption band. In this situation they suggest that the SO_2 is formed by the process of injection of magnetospheric sulfur ions into Europa's water ice surface. Because the jovian magnetosphere sweeps past Europa with a relative velocity exceeding 100 km/sec, it is expected that magnetospheric material should be deposited on Eurpoa's trailing side. The strength of the observed absorption when interpreted in the context of a steady state model implies a column abundance of $\sim 2 \times 10^{16}$ molecules per cm^2. When this value is combined with the observations of magnetospheric species by Voyager and laboratory data on sputtering of water ice, it allows for the calculation of erosion rates for satellite's surface (Eviatar et al., 1981).

Farther out in the solar system, number of spectra have recently been acquired of the Saturnian satellites Iapetus, Rhea and Dione. None of these spectra show pronounced absorption features but all of the satellites showed a marked decrease in albedo at shorter wavelengths. For Dione, no leading side data yet exist. For Rhea, the ratio of the trailing to leading side albedo increases toward shorter wavelength, from 1:1.25 at visual wavelengths to 1:3.8 at 2400-2700 Å. This effect indicates a change relative in slope of the spectral reflectance of the two hemispheres and limits the possible surface constituents. Iapetus has been known for centuries to have the greatest leading to trailing side asymmetry of any satellite in the solar system. At visual wavelengths the trailing side is five times brighter than the leading side. At ultraviolt wavelengths, this ratio increases further reach to 7:1! Table 2 lists the IUE spectral geometric albedos of the Saturnian satellites for three selected bands (Nelson et al., 1981). Until recently there have been little data on the Saturnian satellites. Accordingly, there has not been the requisite time to develop a complete theoretical structure within which these observations be further interpreted.

THE PAST AND THE FUTURE

IUE has provided significant and unique information on every solar system object it has observed. New atmospheric absorption features have been identified in the atmosphres of Venus, Mars, Jupiter and Saturn. Emission processes have also been studied and provided new insights into the physics of magnetosphere-atmosphere processes on Jupiter and Saturn. The comet studies have provided the basis for the development of coherent volatile evolution models. The possibility now exists for new classes of asteroids based on their ultraviolet albedos. New surface constituents have been identified on planetary satellites. Future observations over a longer baseline will allow for the study of time variable phenomena, and as signal to noise ratios improve with expanded data sets on the fainter objects, new species may yet be identified on the surfaces, in the atmospheres and in the magnetospheres of the planets.

ACKNOWLEDGEMENT

The author deeply appreciates the strong support given this effort by his co-workers, A.L. Lane, D.L. Matson, and G.J. Veeder. The assistance

given by S.W. Officer in manuscript preparation is gratefully acknowledged. A special note of thanks is due to the entire IUE staff, especially the resident astronomers and telescope operators who extended themselves considerably in order to accommodate the unique requirements of a planetary observing program IUE. This work represents one phase of research carried out at the Jet Propulsion Laboratory, California Institute of Technology under NASA contract NAS-700.

REFERENCES

Binder, A.B., Cruikshank, D.P. (1964). Evidence for an atmosphere on Io. Icarus, 3, 299-305.

Butterworth, P.S., Caldwell, J., Moore, V., Owen, T., Rivolo, A.R., Lane, A.L. (1980). An upper limit to the global SO_2 abundance on Io, Nature, 285, 308-309.

Caldwell, J. (1975). Ultraviolet observations of small bodies in the solar system by OAO-2. Icarus, 25, 384-346.

Caldwell, J., Owen, T., Rivolo, A.R., Moore, V., Hunt, G.E., Butterworth, P.S. (1981). Observations of Uranus, Neptune and Titan by the International Ultraviolet Explorer. Astron. Jour. 86, 298-305.

Caldwell, J., Winkelstein, P., Owen, T., Combes, M., Encrenaz, T., Hunt, G., Moore, V. (1982). Observations of Uranus and Neptune with the IUE. This symposium.

Clark, R.N. (1980). Ganymede, Europa, Callisto and Saturn's Rings: compositional analysis from reflectance spectroscopy. Icarus, 44, 388-409.

Clarke, J.T., Moos, H.W., Feldman, P.D. (1981a). IUE monitoring of the spatial distirbution of the H Lyα emission from Jupiter. Astrophys. J. 245, L127-L129.

Clarke, J.T., Moos, H.W., Atreya, S.K., and Lane, A.L. (1981b). IUE detection of bursts at H Lyα emission from Saturn. Nature, 290, 226-227.

Clarke, J.T., Moos, H.W., Feldman, P.D. (1982). The far ultraviolet spectra and geometric albedos of Jupiter and Saturn. This symposium.

Combes, M., Courtin, R., Caldwell, J., Encrenaz, Th., Fricke, K.H., Moore, V., Owen, T., Butterworth, P.S. (1981). Vertical distribution of NH_3 in the upper jovian atmosphere from IUE observations. Adv. Space. Res., 7, 169-175.

Conway, R.R., Durrance, S.T., Barth, C.A., Lane, A.L. (1980). Seasonal observations of Mars. Proceedings of the Symposium, 'The First Two Years of IUE', 33-37.

Conway, R.R., McCoy, R.P., Barth, C.A., Lane, A.L. (1979). IUE detection of sulfur dioxide in the atmosphere of Venus. Geophys. Res. Let. 6, 629-631.

Durrance, S.T. (1981). The carbon monoxide fourth positive bands in the Venus dayglow. Jour. Geophys. Res., 86, 9115-9124.

Durrance, S.T., Feldman, P.D., Moos, H.W. (1982). Ultraviolet spectroscopy of the Jovian and Saturnian aurorae. This symposium.

Eviatar, A., Siscoe, G.L., Johnson, T.V., Matson, D.L. (1981). Effects of Io ejecta on Europa. Icarus, 47, 75-83.

Feldman, P.D., Moos, H.W., Clarke, J.T., Lane, A.L. (1979). Identification of the UV nightglow from Venus. Nature 279, 221-222.

Lane, A.L., Nelson, R.M., Matson, D.L. (1981). Evidence for sulfur implantation in Europa's UV absorption band. NATURE, 292, 38-40.

Lane, A.L., Owen, T.C., Nelson, R.M., Mottler, F.C. (1979). Ultraviolet spectral variations on Io: An indicator of volcanic activity? Bull. Am. Ast. Soc., 11, 597.

Matson, D.L., Fanale, F.P., Johnson, T.V. (1974). Sodium D-line emission from Io: Sputtering and resonant scattering hypothesis. Astrophys. Jour. Let., 192, L43-L46.

Matson, D.L., Nash, D.B. (1981). Io's atmosphere: Pressure control by subsurface regolith coldtrapping. Lunar and Planetary Science Conf. Proceedings, March 1981.

Moos, H.W., Clarke, J.T. (1979). Detection of acetylene in the Saturnian atmosphere using the IUE satellite. Astrophys. Jour. 229, L107-L108.

Moos, H.W., Clarke, J.T., Atreya, S.K., Lane, A.L. Observations of the Io plasma torus (1980). In 'The Universe at Ultraviolet Wavelengths, The First Two Years of IUE'. 49-53.

Morabito, L.A., Synnott, S.P., Kupferman, P.N., Collins, S.A. (1979). Discovery of curently active extraterrestrial volcanism. SCIENCE, 204, 972.

Morrison, D., Morrison, N.D., Lazarewicz, A.R. (1974). Four color photometry of the Galilean Satellites. Icarus, 23, 399-416.

Nash, D.B., Fanale, F.P., Nelson, R.M. (1980). SO_2 frost: UV-visible reflectivity and Io surface coverage. Geophys. Res. Let., 1, 665-668.

Nelson, R.M. and Hapke, B.W. (1978a). Spectral reflectivities of the Galilean satellites and Titan, 0.32-0.86 micrometers. Icarus, 36, 304-329.

Nelson, R.M. and Hapke, B.W. (1978b). Possible correlation of Io's post-eclipse brightening with major solar flares. Icarus, 33, 203-209.

Nelson, R.M., Lane, A.L., Matson, D.L., Fanale, F.P., Nash, D.B., Johnson, T.V. (1980a). Io: Longitudinal distribution of sulfur dioxide frost. SCIENCE, 210, 784-786.

Nelson, R.M., Matson, D.L., Lane, A.L., Motteler, F.C., Ockert, M.E. (1980b). Ultraviolet albedos of the Galilean satellites with IUE. Bull. Am. Ast. Soc., 12, 713.

Nelson, R.M., Lane, A.L., Matson, D.L., Veeder, G.J. and Ockert, M.E. (1981). Ultraviolet spectral geometric albedos of selected Saturnian satellites, EOS. T. Am. Geophys. U., 62, 938.

Owen, T.B., Caldwell, J., Rivolo, A.R., Moore, V., Lane, A.L., Sagan, C., Hunt, G., Ponnamperuma, C. (1980). Observations of the spectrum of Jupiter from 1500 to 2000 Å with the IUE. Astrophys. J., 236, L39-L42, 1980.

Skinner, T.E., Durrance, S.T., Feldman, P.D., Moos, H.W. (1982). IUE observations of the Jovian HI Lyman α emission. This symposium.

Veeder, G.J., Matson, D.L., Nelson, R.M., Lane, A.L., Johnson, T.V., McCord, T.B., Gaffey, M.J. (1980). Observations of selected asteroids with IUE. Bull. Am. Ast. Soc. 12, 663.

Wagener, R., Owen, T., Caldwell, J., Winkelstein, P. (1982). High dispersion IUE Observations of Jupiter. This symposium.

Weaver, H.A., Feldman, P.D., Festou, M.D., A'Hearn, M.F., Keller, H.V. (1981). IUE observations of faint comets. Icarus, 47, 449-463.

TABLE 1

UV Albedos of the Galilean Satellites

	Band #1	Band #2	Band #3	Groundbased
Satellite	2400-2700Å	2800-3000Å	3000-3200Å	3200-3220Å
Io (70<θ<120)	0.013	0.015	0.033	0.068
Io (250<θ<290)	0.018	0.018	0.032	0.046
Europa (70<θ<120)	0.182	0.254	0.327	0.344
Europa (250<θ<290)	0.076	0.109	0.163	0.153
Ganymede (70<θ<120)	0.099	0.111	0.153	0.167
Ganymede (250<θ<290)	0.048	0.078	0.107	0.097
Callisto (70<θ<110)	0.036	0.042	0 049	*

* No suitable data available

TABLE II

UV Albedos of the Saturnian Satellites

	Band #1	Band #2	Band #3	V
Satellite	2400-2700Å	2800-3000Å	3000-3200Å	5600Å
Iapetus (0<θ<180)	0.024	0.032	0.037	0.092
Iapetus (180<θ<360)	0.19	0.24	0.25	0.46
Rhea (0<θ<180)	0.29	0.33	0.40	0.63
Rhea (180<θ<360)	0.07	0.10	0.11	0.50
Dione (180<θ<360)	0.23	0.27	0.31	

CAPTIONS TO FIGURES

Figure 1. Ultraviolet geometric albedo of the Galilean satellites as a function of rotational phase angle. The groundbased V and ubvy magnitudes are also shown. Of particular interest is Io's ultraviolet orbital phase curve which is in the opposite sense of its visible phase curve.

Figure 2. Left. Spectral geometric albedo of Io from IUE. The strong absorption shortward of 3200 Å is associated with condensed SO_2. A laboratory spectrum of SO_2 frost (Nash et al., 1980) is shown for comparison. The ultraviolet albedo variation with orbital phase angle is believed to be caused by a longitudinal variation in frozen SO_2 (Nelson et al., 1980).

Right. Top. SO_2 gas spectrum.
Mid. Ratio of IUE Europa trailing side spectrum to its leading side spectrum.
Bot. Ganymede comparison spectrum.

The ultraviolet absorption on Europa's trailing side is believed to be caused by sulfur ions from the jovian magnetosphere implanted in water ice on Io's surface (Lane et al., 1981).

IO (I.U.E.)

IO (Morrison et al. 1974)

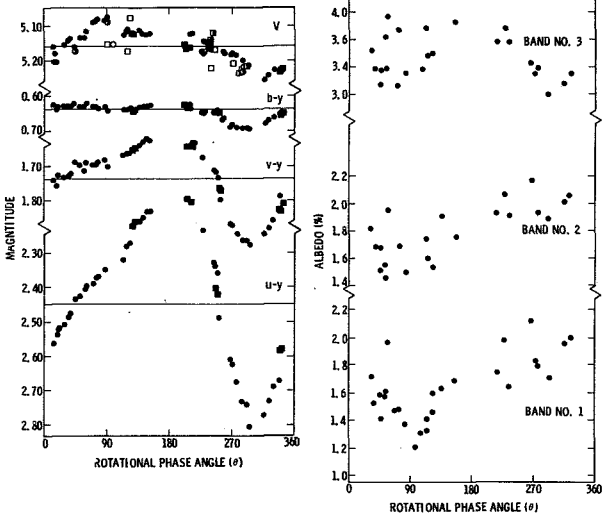

EUROPA (I.U.E.)

EUROPA (Morrison et al. 1974)

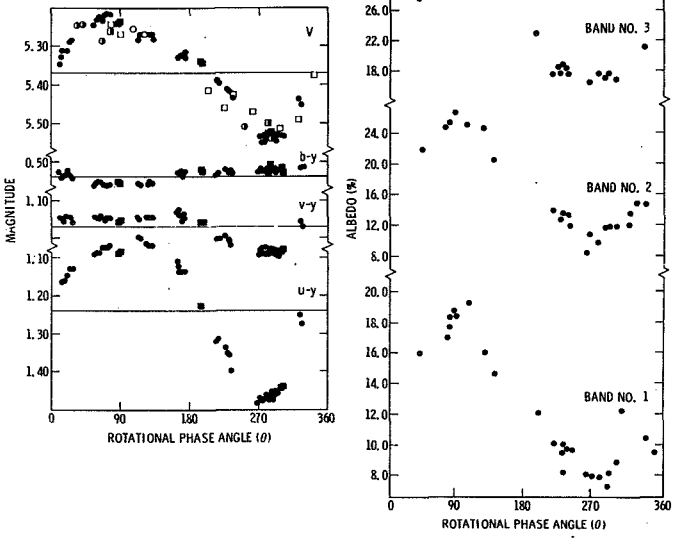

GANYMEDE (I.U.E.)

GANYMEDE (Morrison et al. 1974)

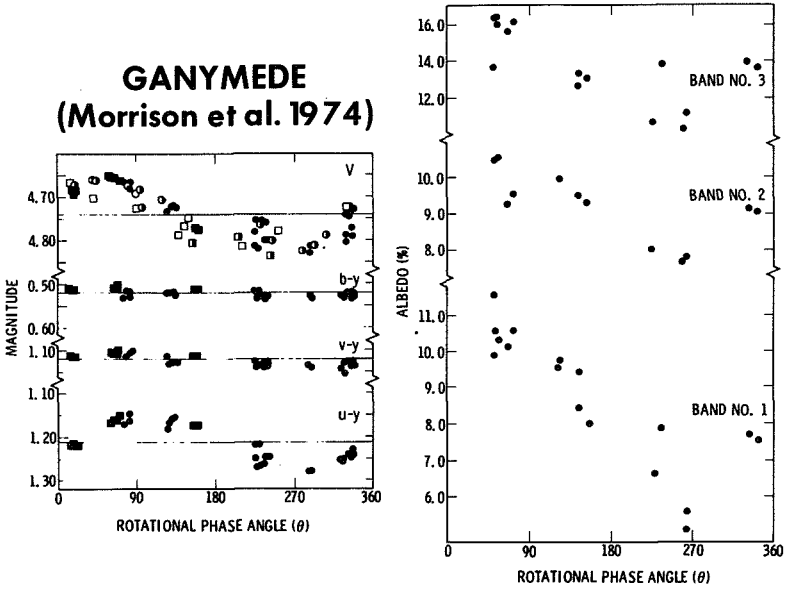

CALLISTO (I.U.E.)

CALLISTO (Morrison et al. 1974)

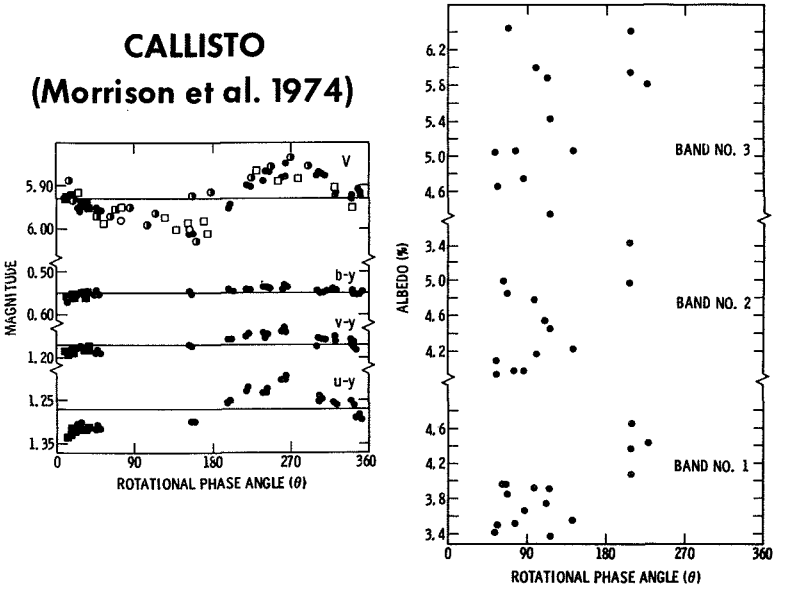

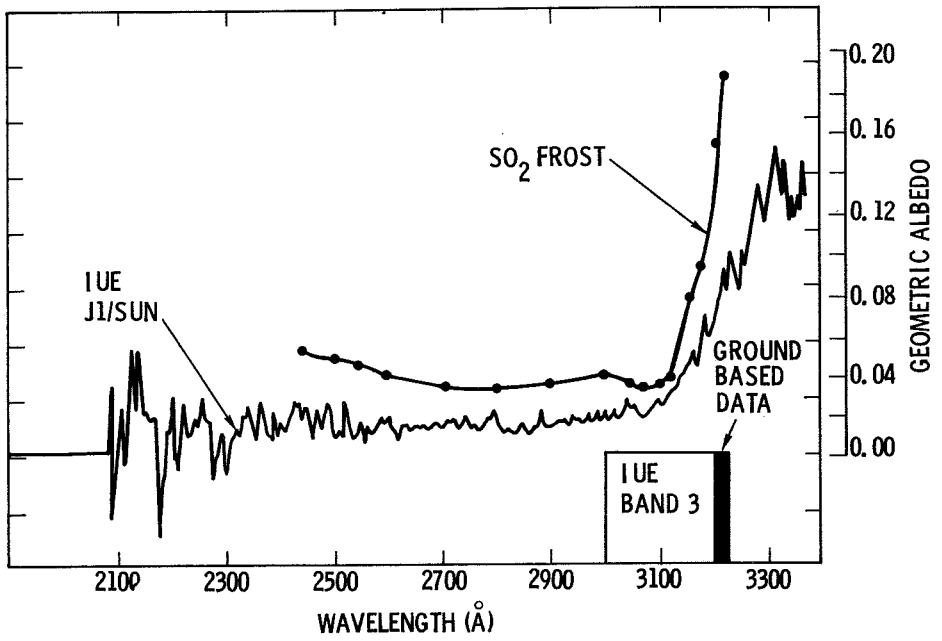
0.20
0.16
0.12
0.08
0.04
0.00
GEOMETRIC ALBEDO
SO_2 FROST
IUE
J1/SUN
GROUND
BASED
DATA
IUE
BAND 3
2100
2300
2500
2700
2900
3100
3300
WAVELENGTH (Å)

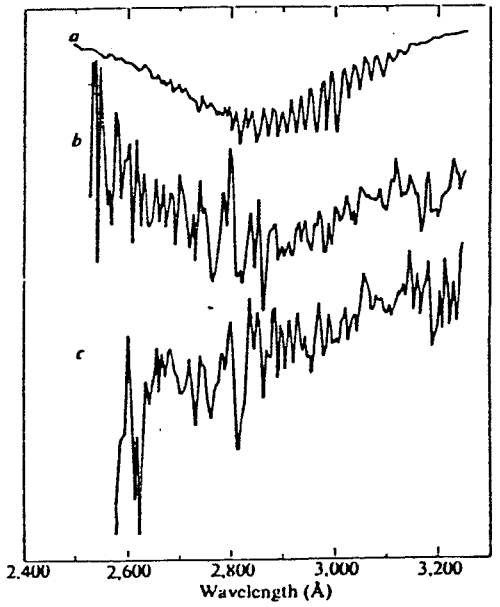
a
b
c
2,400
2,600
2,800
3,000
3,200
Wavelength (Å)

THE IMPACT OF IUE OBSERVATIONS ON OUR KNOWLEDGE ABOUT GALAXIES AND QUASARS

J. B. Oke
California Institute of Technology
Pasadena, CA 91125

ABSTRACT

In spite of the great difficulty in obtaining observations of extragalactic objects with IUE, many kinds of objects have been observed in at least modest numbers. Elliptical galaxies show the presence of very hot stars which are probably highly evolved horizontal-branch objects, although the observations are not adequate to rule out young OB stars. Spiral and irregular galaxies often show evidence of young OB stars although the nucleus of M31 is very similar to elliptical galaxies. Several narrow emission-line galaxies appear to have non-thermal continua. IUE observations of Seyfert galaxies permit detailed studies of the continua and line ratios such as Lα to Hβ to be made. Unlike quasars, there is evidence for dust based on the 2175 Å feature. The problem of understanding Seyfert galaxy spectra is no easier than that for quasars although observed variability in the broad lines may present useful clues. Observations of high-redshift quasars with IUE allow spectra to be obtained down to rest wavelengths of a few hundred Angstroms and provide information about the amount of ionizing flux. Observations of low-redshift quasars can be used to test whether the myriads of absorption lines seen below Lα in high-redshift quasars are indeed produced by intergalactic clouds and halos of intervening galaxies.

INTRODUCTION

In spite of the difficulty of making IUE observations of faint objects a large number of spectra have been obtained of many types of galaxies as well as quasars. In this paper many of the results obtained from studies of these spectra are summarized.

ELLIPTICAL GALAXIES AND EARLY SPIRALS

A number of elliptical galaxies, including the dwarf elliptical M32 (Johnson 1979), M87 (Bertola et al. 1980; Perola and Tarenghi 1980), NGC 3379 (Oke et al. 1981), NGC 4472 (Oke et al. 1981; Norgaard-Nielsen and Kjaergaard 1981), NGC 4649 (Bertola et al. 1982), and NGC 1052 (Fosburg et al. 1981) have now been observed with IUE. These observations confirm and greatly expand the earlier uv data obtained by OAO-2. Above about 2400 Å all the observations yield spectral energy distributions which appear to be uv extensions of the cool star dominated energy distributions in the visual. Spectral features such as Mg I λ2852 and Mg II λ2800 which are characteristic of cool stars (Morton et al. 1977) are clearly seen even at low resolution. In only

one of these objects, M87, is there evidence for an additional source of flux in this spectral range, and in this case the additional contribution can be traced up to 4000 Å; it may have something to do with the activity in the nuclear region.

Below 2400 Å a completely new source of radiation appears which has a blackbody color temperature of the order of 30,000 K. This new hot component is very strong in M87 and NGC 4649, at a modest level in NGC 3379, NGC 4472, and NGC 1052, and very weak at best in M32. Since this hot component is extended like the cool stars it is presumably stellar in nature and can be either hot horizontal-branch stars or young OB stars; in either case the number of stars is small. Because there is no evidence for recent star formation in these ellipticals it is probable that the stars are horizontal-branch stars. While attempts have been made to determine spectroscopically the nature of these hot stars, the observational material is not of high enough quality to make a decision. It may require the Space Telescope to solve the problem.

If this hot star component becomes even larger than in M87 and NGC 4649 it will begin to contribute in the visual and eventually will dilute the H and K lines of Ca II to the point where they are not seen. Such galaxies will appear to be blue and possibly may be identifiable with faint blue galaxies found in recent years.

A case has been made for emission lines in the ultraviolet of elliptical galaxies (Norgaard-Nielsen and Kjaergaard 1981), but in only one case, NGC 1052 (Fosburg et al. 1981) which has strong visual emission lines, is the evidence conclusive. In this object C III] λ1909 and C II] λ2326 are clearly seen and the emission is probably produced by shock waves.

Visual and ultraviolet energy distributions for the nuclear regions of M31 (Johnson 1979) and the two Sb galaxies NGC 4594 and NGC 3031 (Ellis et al. 1982) are all very similar to those of NGC 3379 and NGC 4472. They can be interpreted in the same way as the ellipticals although it should be noted that Ellis et al. have been able to model the energy distributions using main-sequence stars rather than by employing hot horizontal-branch stars.

EXTRAGALACTIC H II REGIONS

IUE observations of H II regions in other galaxies should isolate the radiation from hot OB exciting stars and the associated emission from the hot ionized gas from any background old-star population. D'Odorico et al. (1980) have analyzed a spectrum of N63 in the LMC. The continuum shows the presence of hot O stars. There are a number of absorption lines which are at least partly interstellar in origin. The only emission line clearly present is C III] λ1909. Observations of NGC 604 in M33 have been obtained by Rosa and discussed by Rosa (1980) and D'Odorico et al. (1980). Rosa as also studied NGC 5471 in M101. In both of these objects a hot stellar continuum is seen and strong P-Cygni profiles are observed particularly in NGC 604, indicating that the hot ionizing stars have high luminosities and rapid mass

loss. NGC 5471 shows the C III] emission line produced in the H II region.

Several dwarf galaxies which are H II regions have been observed by Barbieri and Kunth (1980). Again they show hot continua from O stars and absorption lines which are partly interstellar. Stellar C IV λ1550 and Si IV λ1400 absorption lines are seen in II Zw 70. Meier and Terlevich (1981) have observed H II region galaxies with redshifts large enough to separate Lα from the geo-coronal Lα line. In one object studied Lα is seen in emission; in the other three it is not, perhaps because of dust absorption. Stellar C IV and Si IV absorption lines may be present.

In general the spectra of extragalactic H II regions have the features which one would predict to be present, although the emission lines are surprisingly weak.

LATE-TYPE SPIRAL GALAXIES

IUE observations of the nuclear regions of late-type spirals would be expected to reflect a mixture of an old elliptical-galaxy-type population and superposed H II regions and OB stars. UV observations of the Sc galaxy NGC 4321 (Panagia et al. 1980) show a continuum dominated by stars with color temperatures of 15,000 to 20,000 K which are presumably OB stars. Interstellar absorption lines are also prominent. The irregular galaxy NGC 6052 (Benvenuti et al. 1979) which probably consists of clumps of very bright H II regions, also show a continuum and stellar features expected of O and B stars. Emission lines are absent.

Ultraviolet and visual energy distributions for NGC 3077, an irregular galaxy in the M81 group (Benacchio and Galletta 1981), and the Sbc or Sc galaxies M51 and NGC 4258 (Ellis et al.1982) are probably typical of normal late-type galaxies. At visual wavelengths the cool stars dominate while in the far ultraviolet hot stars contribute most of the light. Models for these energy distributions have been made using main-sequence O to G stars with M stars needed in some cases (Ellis et al. 1982). For these objects it is not possible to determine if an old elliptical-type population is present in addition to the young population.

NGC 4507 (a barred spiral), NGC 5508 (a late-type edge-on galaxy), and NGC 7582 (a barred spiral) are very different from the objects just discussed. The first two, narrow emission line high-excitation galaxies, have been observed and studied by Bergeron et al. (1981). The continuous energy distributions after correction for reddening are very reminiscent of power-law spectra seen in many Seyfert galaxies although a cool stellar component dominates in the visual. The uv shows no evidence for hot stars. In NGC 4507 the emission-line strengths are probably consistent with recombination theory. NGC 7582 (Clavel et al. 1980) has an ultraviolet continuum which is similar to that found in the other two objects. It differs markedly from NGC 4507 and NGC 5506 in the complete absence of ultraviolet emission lines. These three objects are X-ray sources.

There clearly is a need for many more observations of late-type galaxies, both those expected to be dominated by H II regions, and also those like NGC 4507 which differ from H II regions and Seyfert galaxies.

SEYFERT GALAXIES

A large effort has gone into the IUE study of Seyfert galaxies from the standpoints of the continuum, reddening, line ratios, line profiles, and variability. Part of the purpose has been to compare Seyferts and quasars, but particularly with respect to variability, Seyferts exhibit rapid changes which are not seen in quasars at least on time scales of months. Most observations have been of Type 1's because they have higher surface brightness and are more luminous than Type 2's in the uv.

The true shape of the continuum of Type 1 Seyfert's depends very much on the amount of reddening inferred either from the λ2175 interstellar absorption feature or from galactic latitude. Continuum energy distributions for instance for Markarian 9, 10, and 79 and 3C 120 (Oke and Zimmerman 1979; Oke and Goodrich 1981) show λ2175 absorption levels which are consistent with those expected from the Galaxy at their galactic latitudes. Wu et al. (1980) found evidence for λ2175 absorption in NGC 7469 and I Zw 1. After correction for interstellar reddening the Type 1 Seyferts have overall power-law slopes ranging from -0.5 to -2 with a tendency for the slope to be steeper in the visual and far red than in the ultraviolet. There is also usually evidence for a 3000 Å bump. The continuum properties of Type 1 Seyferts appear to be similar to those of quasars in the same spectral range.

Line ratios, in particular Lα/Hβ, have been measured by the authors listed above. Although the results depend on the reddening assumed, it is clear that the Lα/Hβ ratio is much smaller than predicted by recombination, a characteristic shared with quasars. Ferland et al. (1979) showed that the Lα/Hβ ratio was near the recombination value for the narrow-line components but much smaller for the broad-line components in 3C 390.3. This shows that reddening external to the line emitting region in the Seyfert or in the Galaxy is not responsible for the anomalous ratios.

Even in the IUE low-resolution mode it is possible to study line profiles to some extent. In the case of NGC 4151 a high-dispersion spectrum has been obtained and analyzed by Penston et al. (1979). It shows that Lα is much narrower than Hβ, while λ1550 of C IV is broad and λ1909 of C III] is intermediate in breadth. The strong absorption in C IV is between -100 and -1100 km s^{-1} and is so deep that absorbing material must cover the whole broad line emitting source. Wu et al. (1981) have measured C IV profiles in the low-resolution mode in several Type 1 Seyferts. The profiles are best matched by a ballistic outflow model such as that of Capriotti et al. (1980).

Variability in continua and emission lines of Type 1 Seyferts has been looked for by several people. Huchra et al. (1980) looked for variability in III Zw 2 and Markarian 509 but found none. In NGC 4593 Clavel et al. (1982) found in phase changes by factors of two in both continuum and line

intensities in an interval of 10 months. Changes in C IV in NGC 4151 are quite clearly visible in the sequence of observations of Penston et al. (1981). In NGC 5548 (Gregory et al. 1982) the emission-line profiles and intensities, and the Lα/C IV intensity ratio show changes in a few months.

It is crucial that continua, line profiles, and line intensities be monitored in the uv, since the observed changes provide important clues concerning the structure of the cloud regions and the mechanisms producing the lines.

The only Type 2 Seyfert studied in any detail is NGC 1068 (Neugebauer et al. 1980). If the reddening corresponds to $E_{B-V} = 0.40$, then the hydrogen and ionized helium line intensity ratios are consistent with recombination and the reddening sensitive forbidden line ratios are also correct. In spite of this strong evidence for reddening there is no signs of λ2175 interstellar absorption. A galaxy component dominates the visual spectrum while the uv is dominated by a non-stellar source. There is not enough predicted uv radiation to account for the observed infrared flux. The Lα/Hβ ratio in Markarian 78 is within a factor two of the recombination value (Wu et al. 1980).

QUASARS

IUE observations of quasars provide not only the possibility of studying these objects over a very wide wavelength range, but also the opportunity to compare quasars as they are now, and as they were early in the history of the Universe. Through absorption lines they also provide a way to explore intergalactic space.

Observations of very large redshift quasars have been obtained by Wilson et al. (1979) for Q2204-408 and by Green et al. (1980) for PG 1115+080. These reach rest wavelengths of a few hundred Angstroms and allow one to estimate the amount of uv ionizing radiation. The observations of PG 1115+080 suggest that power laws fitted to continua above Lα may seriously overestimate the uv ionizing flux in some cases. For Q2204-408 a power law $f_\nu \propto \nu^{-1.5}$ fits the far uv observations. If the ionizing flux is low the previous estimates of the covering factor may be too low.

Observations of quasars with redshifts of the order of 2 can be used to explore the optically observed absorption redshift systems in the neighborhood of the Lyman jump. In both 1101-264 (Boksenberg and Snijders 1981) and B21225+31 (Snijders et al. 1981) strong Lyman limit absorption is observed at the same redshifts as the prominent absorption line systems found for each object in the visual range. In B21225+31 the strong H I absorption occurs at nearly the same redshift as a strong metal-line absorption system which suggests that the H I absorption may be due to an extended halo around the galaxy which causes the metal-rich gas absorption.

Several quasars including 3C 273 (Boggess et al. 1979; Ulrich et al. 1980), PG 0026+129 (Baldwin et al. 1978) 3C 249.1, and 3C 232 (Dultzin-Hacyan et al. 1982) have been observed to measure continuum slopes and emission-line intensities. They show the well-known problem of the low

Lα/Hβ ratio. The spectral indices are typical of quasars in general. If the current view that the curtain of Lα absorption lines in large redshift quasars is due mainly to intergalactic clouds and halos of galaxies is correct, then these lines should disappear in low-redshift quasars. This question has still to be explored with IUE data.

A number of observations of BL Lacertae type objects have now been obtained with IUE, partly to look for spectral features and partly to study the continuum from X-ray to radio wavelengths. No features have been found in 0711+71 (Fricke et al. 1981) or in 2153-304 (Maraschi et al. 1980). On the other hand, Bregman et al. (1981) have found Lα and strong Lyman limit absorption in PKS 0735+178. Comparisons of X-ray, uv, optical and radio observations for some of the objects just mentioned and for Markarian 501 (Snijders et al. 1979; Kondo et al. 1981) suggest some continuity between the optical, uv, and X-ray fluxes, but the spectrum is usually flatter between the radio and optical region than in the visual to X-ray region. The interpretation is made more complicated because of the stellar contribution in the visual and near infrared seen in objects such as Markarian 501.

SUMMARY

(1) The ultraviolet spectra of elliptical and early-type spiral galaxies are dominated by hot stars which are probably horizontal-branch stars, although this still has not been proved.

(2) Late-type spirals show young O- and B-type stars in the uv. From the standpoint of the evolution of galaxies it is important to determine where the switch-over from horizontal branch to OB stars occurs.

(3) The relationship of the moderately narrow emission-line galaxies to ordinary and Seyfert galaxies should be explored further.

(4) Continued studies of extragalactic H II regions are needed with emphasis on the separation of interstellar from stellar absorption lines.

(5) Studies of ultraviolet continuum fluxes, emission-line intensities, and emission-line profiles in Seyfert galaxies, with particular emphasis on their changes with time, should yield important information about the structure and dynamics of the emission-line producing region. Similar studies are needed for quasars and BL Lacertae objects.

(6) Absorption features in low and moderate redshift quasars are needed to explore further the intergalactic medium.

REFERENCES

Baldwin, J. A., Rees, M. J., Longair, M. S., and Perryman, M. A. C. 1978, Ap. J. (Letters), 226, L57.
Barbieri, C., and Kunth, D. 1980, First ESO/ESA Workshop, Dwarf Galaxies, 113.
Benacchio, L., and Galletta, G. 1981, Ap. J. (Letters), 243, L65.

Benvenuti, P., Casini, C., and Heidmann, J. 1979, Nature, 282, 272.
Bergeron, J., Maccacaro, T., and Perolo, C. 1981, Astr. Ap., 97, 94.
Bertola, F., Capaccioli, M., Holm, A. V., and Oke, J. B. 1980, Ap. J. (Letters), 237, L65.
Bertola, F., Capaccioli, M., and Oke, J. B. 1982, Ap. J., in press.
Boggess, A. et al. 1979, Ap. J. (Letters), 230, L131.
Boksenberg, A., and Snijders, M. A. J. 1981, M.N.R.A.S., 194, 353.
Bregman, J. N., Glassgold, A. E., and Huggins, P. J. 1981, Ap. J., 249, 13.
Capriotti, E., Foltz, G., and Byard, P. 1980, Ap. J., 241, 903.
Clavel, J., Benvenuti, P., Cassatella, A., Heck, A., Penston, M. V., Selvelli, P. L., Beeckmans, F., and Macchetto, F. 1980, M.N.R.A.S., 192, 769.
Clavel, J., Joly, M., Bergeron, J., Collin-Souffrin, S., and Penston, M. V. 1982, preprint.
D'Odorico, S., Patriarchi, P., and Perinotto, M. 1980, First ESO/ESA Workshop, Dwarf Galaxies, 103.
Dultzin-Hacyan, D., Salas, L., and Daltabuit, E. 1982, preprint.
Ellis, R. S., Gondhalekar, P. M., and Efstathiou, G. 1982, preprint.
Ferland, G. J., Rees, M. J., Longair, M. S., and Perryman, M. A. C. 1979, M.N.R.A.S., 187, 65P.
Fosbury, R. A. E., Snijders, M. A. J., Boksenberg, A., and Penston, M. V. 1981, M.N.R.A.S., 197, 235.
Fricke, K. J., Kollatschny, W., and Schleicher, H. 1981, Astr. Ap., 100, 1.
Green, R. F., Pier, J. R., Schmidt, M., Estabrook, F. B., Lane, A. L., and Wahlquist, H. D. 1980, Ap. J., 239, 483.
Gregory, S., Ptak, R., and Stoner, R. 1982, preprint.
Huchra, J., Geller, M., and Morton, D. 1980, The Universe at Ultraviolet Wavelengths, NASA Conference Publication 2171, 743.
Johnson, H. M. 1979, Ap. J. (Letters), 230, L137.
Kondo, Y. et al. 1981, Ap. J., 243, 690.
Neugebauer, G. et al. 1980, Ap. J., 238, 502.
Maraschi, L., Tanzi, E. G., Tarenghi, M., and Treves, A. 1980, Nature, 285, 555.
Meier, D. L., and Terlevich, R. 1981, Ap. J. (Letters), 246, L109.
Morton, D. C., Spinrad, H., Bruzual, A. G., and Kurucz, R. L. 1977, Ap. J., 212, 438.
Nørgaard-Nielsen, H. U., and Kjaergaard, P. 1981, Astr. Ap., 93, 290.
Oke, J. B., and Zimmerman, B. 1979, Ap. J. (Letters), 231, L13.
Oke, J. B., Bertola, F., and Capaccioli, M. 1981, Ap. J., 243, 453.
Oke, J. B., and Goodrich, R. W. 1981, Ap. J., 243, 445.
Panagia, N., Vettolani, G., Palumbo, G. G. C., Benvenuti, P., and Macchetto, F. 1980, The Universe at Ultraviolet Wavelengths, NASA Conference Publication 2171, 725.
Perola, G. C., and Tarenghi, M. 1980, Ap. J., 240, 447.
Penston, M. V., Clavel, J., Snijders, M. A. J., Boksenberg, A., and Fosbury, R. A. E. 1979, M.N.R.A.S., 189, 45P.
Pentson, M. V. et al. 1981, M.N.R.A.S., 196, 857.
Rosa, M. 1980, Astr. Ap., 85, L21.
Snijders, M. A. J., Pettini, M., and Boksenberg, A. 1981, Ap. J., 245, 386.
Snijders, M. A. J., Boksenberg, A., Barr, P., Sanford, P. W., Ives, J. C., and Penston, M. V. 1979, M.N.R.A.S., 189, 873.

Ulrich, M. H. et al. 1980, M.N.R.A.S., 192, 561.
Wilson, R., Carnochan, D. J., and Gondhalekar, P. M. 1979, Nature, 277, 457.
Wu, C. C., Boggess, A., and Gull, T. R. 1980, Ap. J., 242, 14.
Wu, C. C., Boggess, A., and Gull, T. R. 1981, Ap. J., 247, 449.

ABUNDANCE FLUCTUATIONS IN THE INTERSTELLAR MEDIUM

Michael Jura
Department of Astronomy
University of California, Los Angeles

ABSTRACT

The determination of abundances within the interstellar medium is reviewed. It appears that interstellar abundances within 1 kpc of the sun are uniform to within a factor of two or three, but it is not yet possible to determine whether there are real fluctuations at this level except for deuterium for which the factor of two variations appear to be real. Establishing the level of local fluctuations in the abundances will be of considerable importance for understanding the history of nucleosynthesis in the solar neighborhood, the evolution of the interstellar medium and the formation of stars.

INTRODUCTION

Evolving stars eject matter into their surroundings and enrich the Galaxy in processed material. As a result, the study of the abundances in the interstellar medium provides an essential clue for understanding the history of nucleosynthesis in the Milky Way. Furthermore, the abundances in the interstellar medium play a key role in determining the microphysics of the material which ultimately controls the formation of new stars out of the gas.

For a number of years, the zero order approximation has been to assume that the interstellar abundances are characteristic of Population I in general and of the sun in particular. This hypothesis of "cosmic abundances" has been successful in understanding the relatively crudely determined abundances in stars, H II regions, diffuse interstellar clouds and the sun. However, much progress in the precision of measurements has been achieved, so that it is now possible to ask questions about the deviations from the mean of the "cosmic" abundances. That is, it is now possible to discuss sensibly such questions as the gradient of abundances within the Galaxy as a result of a different history of nucleosynthesis in different regions. It has even been suggested that the solar system does not have cosmic abundances (Olive and Schramm 1982). Here, I wish to specifically discuss the magnitude of the local fluctuations of abundances in the solar neighborhood and to consider how well mixed the solar neighborhood actually is. Different elements and isotopes are formed in different sorts of stars, and it is at least possible that interstellar clouds are not well mixed so that they have a wide range of abundances.

This discussion is restricted to abundances in cold clouds within 1 kpc of the sun that have been mainly determined by measuring ultraviolet absorption lines. Observationally, it is difficult to measure reasonably accurate abundances beyond this distance. Also, 1 kpc is characteristic of the extent of the epicyclic orbits around the Galaxy, and we might expect that abundance gradients are important at greater distances.

DUST TO GAS RATIO

Roughly half of all the elements in the interstellar medium heavier than helium are contained with solid grains (Aannestad and Purcell 1973, Spitzer 1978). As a result, one way to measure crudely the fluctuations of the local abundances is to measure the dust to gas ratio. By using Copernicus to measure H and H_2 but not H^+, Bohlin, Savage and Drake (1978) found that on the average that $N_H/E(B-V) = 5.8\ 10^{-22}$ mag cm^2 and that for $E(B-V) > 0.10$ almost all the lines of sight agreed with this value to within a factor of two. The most conspicuous deviation from the mean value of color excess to the amount of hydrogen is the measurement toward ρ Oph. In this direction, it is possible that grain coagulation has occurred so that the grains are unusual in the sense that E(B-V) is not a measure of the amount of dust (Jura 1980b). For stars with $E(B-V) < 0.10$, there are also some marked deviations from the mean value of $N_H/E(B-V)$. At the moment it is not clear whether these deviations arise because of the difficulties of determining small amounts of reddening or because the fractional fluctuations from the mean are greater in the smaller clouds.

Burstein and Heiles (1978) and Heiles, Stark and Kulkarni (1981) have argued from 21 cm measurements that at high galactic latitudes there is gas without dust. The column densities are sufficiently small that this does not obviously contradict the Copernicus results, but there is certainly some dust at high latitudes as is shown by the existence of interstellar polarization (Appenzeller 1975, Markannen 1979). Also, Knude (1978) has argued on the basis of very careful photometry that there is high latitude dust. The dust to gas ratio in directions where there is little gas remains somewhat uncertain.

VOLATILE ELEMENTS

Refractory elements such as calcium, iron and aluminum are mainly contained within the grains (Field 1974, Spitzer and Jenkins 1975). However, there are some volatiles that are found appreciably in the gas phase. By measuring the fluctuations in the amounts of these elements, it is possible to place limits on the fluctuations in the local abundances. However, since the abundance determinations in diffuse clouds relies upon understanding the curve of growth, there are often significant observational uncertainties.

Elements which may not be depleted in general by more than a factor of 3 in diffuse clouds are oxygen (de Boer 1979), phosphorus and chlorine (Jura and York 1978), nitrogen (Lugger et al. 1978), sulfur (Spitzer and Jenkins 1975), carbon (Jenkins and Shaya 1979, Hobbs et al. 1982) and zinc (Morton 1975, York and Jura 1982). To date, however, it has proven difficult to measure these abundances to much better than a factor of two because of the many different uncertainties. As a result, there is no conclusive evidence that there are real cloud-to-cloud variations. In general, it should be noted that the observed deviations from "cosmic" abundances are always low as would be expected if depletion onto grains dominates the departures from the average.

ISOTOPES -- DEUTERIUM

It is usually thought that measurements of the abundances of different isotopes may not be sensitive to depletion onto grains and they may serve to measure true variations of abundances. The measurement of the interstellar deuterium abundance (Rogerson and York 1973, York and Rogerson 1976) has received considerable attention and has been of considerable importance for cosmological models. The most straightforward but not conclusive interpretation of the observations is that the universe is open.

There is strong evidence for real variations in the local deuterium abundance in the sense that there appears to be at least a factor of 2 difference between the abundance toward ζ Pup and toward δ Ori (Laurent, Vidal-Madjar and York 1979). (There is also weak evidence that deuterium is variable from the interpretation of Lyman α emission line profiles from chromospheric emission from late type stars in the solar neighborhood, but these results are controversial [Dupree, Baliunas and Shipman 1977; McClintock et al. 1978]. Also, there is a possibility that D/H is correlated with the Zn/H ratio as might occur if deuterium is manufactured in stars rather than only in the Big Bang (York and Jura 1982). These observations therefore open the question of the cosmological interpretation of the observed deuterium abundance. Various models have been put forward to explain the observed deuterium abundance variations (Bruston et al. 1981), but none have been especially convincing. Here, I suggest that deuterium may be depleted onto grains.

It is usually tacitly assumed that deuterium like hydrogen, is mainly depleted; however, this may not be true. Unlike hydrogen, there is so little mass in deuterium that all of it could be depleted onto grains and it would not affect the dust. Here I outline an argument that deuterium depletion may be sustantial.

The widespread presence of H_2 in the interstellar medium means that the sticking probability of hydrogen onto grains is not far from unity (Jura 1975a,b; Spitzer 1978) in agreement with the theoretical prediction by Hollenbach and Salpeter (1970, 1971). The sticking probability of deuterium onto grains should also be high.

Once deuterium is attached to a grain, it need not behave on the surface as does hydrogen. First, the binding energy of deuterium is probably appreciably greater. That is, for adsorption, the binding energy is taken from the van der Waals attraction (the same for hydrogen and deuterium) minus the zero point energy in this potential. The zero point energies can be quite different between hydrogen and deuterium because of the factor of 2 difference in mass. Consequently, deuterium may be much more tightly bound to grains than is hydrogen. The exact magnitude of this effect depends upon the degree of localization of the wavefunction of the adsorbed species on the surface of the grains (see Hollenbach and Salpeter 1970, 1971), a quantity which is not very well

known. This uncertainty means that it is at least conceivable that deuterium behaves quite differently from hydrogen. Second, because deuterium is heavier than hydrogen, it cannot migrate on the surface of the grains by quantum mechanical tunneling to a site of enhanced molecule formation nearly as easily as does the hydrogen. As a result, it is by no means clear that deuterium should be able to come off the grains once it is attached.

Perhaps deuterium behaves on the surface of grains more like a heavy element like oxygen than like hydrogen. The depletion of oxygen onto interstellar grains is not particularly large (de Boer 1979). However, because deuterium is much lighter, it moves more rapidly through the gas than does atomic oxygen, and it is quite possible that the depletion of deuterium is larger. A depletion of deuterium by a factor of 2 or 3 seems possible.

If deuterium is depleted onto grains, it means that the Copernicus observations underestimated the amount of deuterium, so the universe is even more open than previously believed with the standard interpretation of this measurement. However, if depletion is important, it could explain the observed local variations of this species. Deuterium depletion onto grains may mean that it is extremely difficult to infer the gradient in the Milky Way of this species (Penzias 1979) since an unknown amount is undetectable.

OTHER ISOTOPES

The abundances of isotopes of elements other than hydrogen have been best studied by the radio astronomers (Penzias 1979, Wannier 1980) although some optical (Vanden Bout and Snell 1980) and ultraviolet (Wannier, Penzias and Jenkins 1982) work has been performed. Here, I add one point which means that it may be even more difficult to determine actual isotope ratios than previously believed. That is, it is well known that chemical fractionation can affect the isotope chemistry at low temperatures. What has been recently recognized is that the photodestruction of different molecules, paticularly CO, may be isotope sensitive. That is, the ultraviolet lines of ^{12}CO and ^{13}CO are typically separated by about 3 Å. If photodestruction occurs subsequent to absorption in one of these lines, the CO can be self-shielded and the different isotopes will have different destruction rates resulting in concentrations which do not truly reflect the $^{13}C/^{12}C$ isotope ratios. This phenomenon occurs both in diffuse interstellar clouds (Bally and Langer 1982) and in the circumstellar envelopes of mass-losing late type stars (Morris and Jura 1982). Evidently, it will be very difficult to measure abundances to better than a factor of two.

DISCUSSION

The best evidence for real fluctuations in the abundances in the interstellar medium is given by Copernicus measurements of D/H; a possible explanation is presented above. Here, I discuss the magnitude of possible abundance variations. One possibility is that mass loss from stars may eject material with deviant abundances; the other possibility is that some sort of separation occurs within the interstellar medium.

Besides supernovae, two well known examples of subsantial mass loss from stars which currently have nonsolar abundances are IRC +10216 and α Ori. IRC +10216, the brightest star in the sky at 5μ is a carbon star and shows distinctly nonsolar abundances. Furthermore, the dust to gas ratio is probably an order of magnitude below the "typical" interstellar value. That is, the dust mass loss rate is probably about 6 10^{-8} M_o yr^{-1} (Campbell et al. 1976, Fazio et al. 1980) while the gas mass rate is probably about 5 10^{-5} M_o yr^{-1} (Kwan and Linke 1982, Morris, Jura and Stark 1982). It seems that if this lost mass were to appear as an interstellar cloud it would show marked deviations from the "cosmic" abundances. In the case of α Ori, the abundances are apparently characteristic of CNO processing since carbon is low by about an order of magnitude (Jura and Morris 1981). Therefore, the ejecta from stars do exhibit distinctly nonsolar abundances.

Consider now the possibility that interstellar clouds "remember" such abundances. Let n be the number density and N the column density of an interstellar cloud. Unless the cloud is very flat and viewed face-on, its total mass is given approximately by its area $(N/n)^2$ times the mass per unit area, $N\mu$, or

$$M = \mu\ N^3/n^2 = 0.52\ N_{20}^3/n_{40}^2\ M_o \qquad (1)$$

where $N_{20} = 10^{-20}$ N and $n_{40} = n/40$ in cgs units. These densities are reasonable for diffuse clouds (Jura 1975a,b). Using the relationship between color excess and dust given by Bohlin, Savage and Drake (1978), this implies that

$$M = 0.52\ E_{0.017}^3/n_{40}^2 \qquad (2)$$

where $E_{0.017} = E(B-V)/0.017$. Most observed interstellar clouds have $E(B-V) > 0.05$ and masses greater than about 10 M_o. Therefore these clouds are presumably composed of mass loss from a number of different stars.

If the mass lost from an evolving star is underabundant in a particular species, then in a few cloud-cloud collision times, the fluctuations from "cosmic" abundances should be small, not more than, say, 25%, and not currently detectable. On the other hand, if the ejecta from a star is markedly overabundant by perhaps a factor of 100, the interstellar cloud into which this material is ejected may display "anomalous" abundances. However, in general, only underabundances are observed in cold clouds as would be expected if depletion onto grains is proceeding.

The time scale for cloud-cloud collisions is on the order of 10^7 years (Spitzer 1978). Since all clouds show some deuterium which presumably has survived for 10^{10} years, it seems that most interstellar matter has been present for a considerable time. It is therfore not surprising that striking abundance anomalies are not detected.

If there are real abundance variations, in almost all cases, they must result from processes that occur within the interstellar medium. Perhaps the best way to produce fluctuations in the abundances is to separate species which can behave very differently, the gas and the dust. The more comprehensive discussion to date of this process has been by Flannery and Krook (1978). Further observations to see if such separations occur seem appropriate.

This work has been partly supported by NASA and the NSF.

REFERENCES

Aannestad, P. A., and Purcell, E. M. 1973, Ann. Rev. Astron. and Ap., 11, 309.
Appenzeller, I. 1975, Astron. and Ap., 38, 313.
Bally, J., and Langer, W. D. 1982, preprint.
Bohlin, R. C., Savage, B. D., and Drake, J. F. 1978, Ap. J., 224, 132.
Burstein, D., and Heiles, C. 1978, Ap. J., 225, 40.
Campbell, M. F., Elias, J. H., Gezari, D. Y., Harvey, P. M., Hoffman, W. F., Hudson, H. S., Neugebauer, G., Soifer, B. Y., Werner, M. W., and Westbrook, W. S. 1976, Ap. J., 208, 396.
De Boer, K. S. 1979, Ap. J., 229, 132.
Dupree, A. K., Baliunas, S., and Shipman, H. L. 1977, Ap. J., 218, 361.
Fazio, G. G., McBreen, B., Steir, M. J., and Wright, E. L. 1980, Ap. J. (Letters), 237, L39.
Field, G. B. 1974, Ap. J., 187, 453.
Flannery, B. P., and Krook, M. 1978, Ap. J., 223, 447.
Heiles, C., Stark, A. A., and Kulkarni, S. 1981, Ap. J. (Letters), 247, L73.
Hobbs, L. M., York, D. G., Oegerle, W., and Cowan, R. 1982, Ap. J., in press.
Hollenbach, D. J., and Salpeter, E. E. 1970, J. Chem. Phys., 53, 79.
Hollenbach, D. J., and Salpeter, E. E. 1971, Ap. J., 163, 155.
Jenkins, E. B., and Shaya, E. J. 1979, Ap. J., 231, 55.
Jura, M. 1975a, Ap. J., 197, 575.
Jura, M. 1975b, Ap. J., 197, 581.
Jura, M. 1980a, in Highlights in Astronomy, P. A. Wayman ed., 5, 293.
Jura, M. 1980b, Ap. J., 235, 63.
Jura, M., and Morris, M. 1981, Ap. J., 251, 181.
Jura, M., and York, D. G. 1978, Ap. J., 219, 861.
Knude, J. 1978, in Astronomical Papers Dedicated to Bengt Stromgren (ed. A. Reiz and T. Anderson), Copenhagen.

Kwan, J., and Linke, R. 1982, Ap. J., in press.
Laurent, C., Vidal-Madjar, A., and York, D. G. 1979, Ap. J., 229, 923.
Lugger, P. M., York, D. G., Blanchard, T., and Morton, D. C. 1978, Ap. J., 224, 1059.
McClintock, W., Henry, R. c., Linsky, J. L., and Moos, H. W. 1978, Ap. J., 225, 465.
Markannen, T. 1979, Astron. and Ap., 74, 201.
Morris, M., and Jura, M. 1982, preprint.
Morton, D. C. 1975, Ap. J., 197, 85.
Olive, K., and Schramm, D. 1982, Ap. J., in press.
Penzias, A. A. 1979, Ap. J., 228, 430.
Rogerson, J. B., and York, D. G. 1973, Ap. J. (Letters), 186, L95.
Spitzer, L. 1978, Physical Processes in the Interstellar Medium (J. Wiley: New York).
Spitzer, L., and Jenkins, E., B. 1975, Ann. Rev. Astron. and Ap., 13, 133.
Vanden Bout, P. A., and Snell, R. 1980, Ap. J., 236, 460.
Wannier, P. G. 1979, Ann. Rev. Astron. and Ap., 18, 399.
Wannier, P. G., Penzias, A. A., and Jenkins, E. B. 1982, Ap. J., in press.
York, D. G., and Jura, M. 1982, Ap. J., in press.
York, D. G., and Rogerson, J. B. 1976, Ap. J., 203, 378.

AN ULTRAVIOLET VIEW OF Be STARS

Theodore P. Snow
Laboratory for Atmospheric and Space Physics
University of Colorado

ABSTRACT

Several types of ultraviolet observations of Be stars are briefly summarized, with a view towards identifying the characteristics, if any, that distinguish Be stars from other early-type objects. The present weight of the evidence is that, from the point of view of ultraviolet data, Be stars are nearly indistinguishable from normal B stars. Both groups have similar characteristics, with differences only in degree. Further comparative studies of Be and non-Be stars have the potential to reveal the causes of the Be phenomenon, and possibly also the origins of winds in early-type stars. Several areas for future ultraviolet research are suggested.

INTRODUCTION

In view of the recent IAU symposium devoted to the subject of Be stars, there is little need for a new comprehensive review of their ultraviolet properties. An excellent summary has been published with the proceedings of that symposium (Marlborough 1982a).

The present paper will briefly summarize the kinds of information that have been derived from ultraviolet observations of Be stars, and will suggest directions in which future UV studies might go. In the process, a few outstanding current problems will be stressed.

To set the context, particularly for the reader who is not familiar with Be star lore, the objects under discussion here are stars of spectral type (roughly) O9 through early A that show emission in certain lines, primarily the Balmer series of hydrogen. No doubt a variety of objects with rather different natures satisfy this criterion, and in an effort to distinguish among these (even in the absence of understanding what they are), astronomers speak of "classical Be stars", "Herbig Ae and Be stars", "P Cygni stars", and "peculiar Be stars". This paper is limited to the "classical Be stars", whatever they are. Generally, we define them by explaining what they are not: they are not pre-main sequence stars; they are not luminous B supergiants, and they are not B stars embedded in nebulosity which produces forbidden emission lines.

A "classical Be star" (hereafter referred to simply as a Be star) is on or near the main sequence, has an extended atmosphere, undergoes episodic behavior ranging from a complete absence of Be characteristics to having such a dense envelope that not only emission, but strong shell absorption lines are formed, may have an infrared excess, probably has intrinsic linear polarization, and, as discussed in the following, most likely has a stellar wind.

There are at least three or four alternative suggestions regarding their fundamental origin (Harmanec 1982), and such simple questions as whether or not the envelope is equatorially confined have so far defied unambiguous resolution. Probably even the so-called classical Be stars are a mixed lot, and no doubt with persistence at least one example could be found that would fit each of the diverse theories.

This paper will be addressed to questions of the intrinsic nature of the stars, and will seem myopic in some ways, as such phenomena as binary mass transfer are ignored. Instead, the emphasis will be on linking the Be stars to non-Be stars nearby in the H-R diagram, with the implicit assumption that the Be characteristics can be viewed as manifestations of processes that also occur in those other stars.

This work is therefore written with a theme in mind: how do the properties of Be stars, as manifested in ultraviolet observations, distinguish themselves from "normal" early-type stars? In the ultraviolet we probe directly the low-density gas that surrounds these stars. This gas must be related in some way to the circumstellar material that gives rise to the Be phenomenon, yet many hot stars not known as Be or shell stars show the same ultraviolet characteristics. Does this tell us that Be stars are not different in any essential way from their neighbors in the H-R diagram, except perhaps that they have slightly more extensive accumulations of material in their envelopes? The question of whether and how Be stars differ from non-Be stars will be addressed in the following survey of ultraviolet observations.

Since this is not intended to be an exhaustive review, no attempt has been made to ensure full coverage of the literature in the field. Where appropriate, the references that are cited are themselves reviews, and the reader is advised to seek them out if a comprehensive survey of the field is desired.

ULTRAVIOLET APPROACHES TO Be STAR PROPERTIES

Do Be Stars Have Emission Lines?

One of the first surprises for observers of high-resolution ultraviolet spectra of Be stars, obtained first with rockets and then Copernicus, and now IUE, was that they rarely show emission lines in this spectral region. The presence of visible-wavelength emission is, of course, the most obvious distinguishing characteristic of stars in this class, yet very few of them would ever be classified as Be stars on the basis of ultraviolet emission lines.

Emission does occur in some cases, most often with the appearance of the Mg II λ2800 doublet. Other resonance lines throughout the ultraviolet tend to be purely in absorption, although they are often affected by the presence of an extended atmosphere.

The lack of emission in ultraviolet resonance lines can be attributed to absorption in the intervening material between star and observer. Clearly Balmer-line emission leads to Lyman-line emission, but the interstellar medium consumes Lyman-line photons voraciously. The circumstellar environment also plays a role, for the complex profiles of ultraviolet resonance lines of highly-

ionized species are the result of a combination of emission and absorption, with the absorption dominant.

Ultraviolet Flux Distributions

A circumstellar envelope of any substance ought to cause some flux redistribution in the stellar continuum, and various studies (made mostly with instruments other than IUE, such as TD1 and ANS) have shown that this occurs in Be stars (e.g. Mendoza 1982, Zorec et al. 1982). There are few systematic trends, however, except that the stars with the densest or most extensive envelopes show the strongest effect, not a surprising result. The general tendency is for Be and shell stars to have ultraviolet flux deficiencies, with the missing photons shifted to infrared wavelengths by electron scattering. Thus, stars with subnormal ultraviolet continua tend to have infrared excesses.

Of all the ultraviolet diagnostics discussed here, this may be the one most reliably associated with Be stars, but it is not very sensitive. Many classical Be stars, with prominent visible-wavelength emission lines, have envelopes insufficiently dense or extensive to create an unambiguously detect able continuum redistribution. Observations of ultraviolet flux deficiencies are made intrinsically difficult, furthermore, by the large and non-uniform interstellar extinction in this spectral region.

Ultraviolet Line Widths

A particularly interesting characteristic of the ultraviolet spectra of many Be stars is the small width of the photospheric lines. The velocity widths of ultraviolet lines in a Be star spectrum can be substantially less than those of visible-wavelength lines in the same star. While this effect was first noticed in high-resolution data obtained by rocket (Morton et al. 1972; Heap 1976) for Be stars, it was soon recognized that it is a manifestation only of rapid rotation, and that it appears in Be and non-Be stars without discrimination.

The explanation was soon forthcoming (Hutchings 1976; Sonneborn and Collins 1977), and has been studied now in some detail (e.g. Sonneborn 1982; Ruusalepp 1982). Rotation causes equatorial gravity darkening, with the result that the ultraviolet flux comes predominantly from high latitudes on the solar disk. Hence the effective value of v sin i for the ultraviolet photospheric lines is lower than that for visible wavelength lines, which arise primarily in the equatorial zone. This effect, which means essentially that properties of the stellar atmosphere are latitude-dependent, greatly complicates the calculation of theoretical models for rotating stars. There is one outstanding motivation for attempting to fully analyze it, however; it might be possible, from comparisons of visible and ultraviolet line widths, to use such analyses to determine the inclination angles and the true rotational velocities of the stars. To do this for Be stars would help answer major questions about the geometry of the extended envelopes.

Stellar Winds, Anomalous Ionization, and Variability

Ultraviolet spectroscopy has revealed the presence of rapid stellar winds in a wide range of early-type stars, and the Be stars (as well as non-Be stars

of similar spectral type) lie just at the low-luminosity limit of the region in the H-R diagram where these winds occur. Hence it became an interesting question to ask whether Be stars have winds. The answer, based on data from rocket ultraviolet observations, Copernicus, and IUE, is that many, perhaps all, do.

The winds in Be stars are indistinguishable in general properties from those of non-be stars. The mass-loss rates (of order 10^{-11} to 10^{-9} solar masses per year; Snow 1981, 1982) appear to be simple extensions (to lower luminosity stars) of those found for O stars. The B main sequence is a borderline region for winds to be detectable, and therefore is a very important one to explore in seeking to understand the causes of the winds. The Be stars may be slightly more prone to having winds than the normal B stars, and there is some evidence (though not unambiguous) that rapid rotation is responsible for this.

An outstanding characteristic of many Be star winds is the presence of ions that are anomalous in the sense that they represent higher degrees of ionization than could be produced by radiative equilibrium with the stellar photosphere (see Marlborough 1982a,b). A second striking characteristic, often linked with the first, is the presence of transient narrow, high-velocity absorption components. These components, with velocities of hundreds of km s^{-1} in many cases, may appear only sporadically in the spectrum of a given star, and when present, often change their appearance and velocity in times of hours or days (Doazan et al. 1982). They have little respect for conventional geometrical wisdom about Be stars, appearing in "pole-on" Be stars and those with high vsini values alike (Peters 1982). One suggested explanation, apparently consistent with the observations, is that the high-velocity absorption components represent density enhancements flowing out through the wind (Henrichs 1982). Whatever they are, they probably also occur in the winds of more luminous stars; a recent survey has shown that most or all O stars with strong winds also have narrow components (Lamers et al. 1982), so again the Be stars are apparently distinguished only in degree from non-Be stars.

General Conclusion

If we lived in an ultraviolet world, and knew the heavens first and best in this wavelength band, we would scarcely recognize the existence of Be stars as a class. Winds and circumstellar envelopes in all early-type stars would be familiar, classical phenomena, and the Be stars might at most be known to us for having slight enhancements in these characteristics.

FUTURE ULTRAVIOLET OBSERVATIONS

Synoptic Multi-band Observations

It is of paramount importance to find unambiguous, model-independent ways of deducing the radial structure of the extended atmospheres of Be stars. It is difficult or impossible to decide, on the basis of present data, how the presence of stationary shell absorption lines is to be reconciled with the simultaneous presence of a high-velocity wind. We do not know how the shell

emission phases of these stars are related to the structure of the envelope or to the properties of the underlying star. We can speculate that the stellar wind plays some role in creating the regions that give rise to the stationary shell absorption and emission lines, but we haven't yet got a clear picture of the sequence of events. We do not know, for example, whether the winds are steady (with some fluctuating high-velocity components), filling a circumstellar region that occasionally disperses, or whether the winds themselves may come and go. We don't know the frequency of occurrence of episodes of rapidly-fluctuating high-velocity components, nor the relationships of these to the long-term development of Be and shell phases. We don't know exactly what the physical mechanism of these rapid fluctuations is, although there is evidence, described earlier, that they represent outflowing density enhancements.

All of these questions can be approached and potentially answered by making simultaneous observations of Be stars at as many wavelengths as possible with time coverage as complete as possible. The most broad-based such program to date has utilized IUE, Copernicus, Einstein (x-ray), and ground-based data, and has been in operation for several years (Doazan et al. 1981). It may take several more years to produce answers to the big questions that are asked, but it is worth the effort.

Synoptic monitoring programs will be enhanced considerably when the European EXOSAT spacecraft is in operation, for it will be the first instrument devoted primarily to monitoring soft x-ray fluxes and their variations. In view of the difficulties of obtaining true simultaneity in making observations with separate satellites as well as ground-based observations, such studies will be greatly improved when and if instruments designed to cover all wavelength bands are launched on a single spacecraft, an idea that has and will continue to be discussed.

The Link Between Be and Non-Be Stars

More work is needed to explore the region of the H-R diagram where the Be stars lie, and where stellar winds are apparently only marginally present. To do so holds great promise, both from the point of view of distinguishing what it is that makes B stars into Be stars, and for teaching us what the factors are that give rise to stellar winds.

The IUE can help in this, for its sensitivity allows a wide coverage of spectral type and stellar peculiarity. Work in this area is in progress. To detect and analyze extremely weak stellar winds, however, requires higher spectral resolution and better photometric accuracy than IUE provides, and some questions will remain until the High Resolution Spectrograph in the Space Telescope can be put into operation. As demonstrated by comparisons of Copernicus and IUE observations, very high-quality data are needed in order to distinguish subtle line asymmetries from line blends and detector noise.

Ultraviolet Line Widths

Detailed modeling of photospheric line profiles in the visible and ultraviolet wavelength regions can potentially provide unique information on the geometry of Be star envelopes by allowing the orientation and true rotational

velocity to be disentangled. Here further work is needed both in observational and theoretical areas. The theory of line formation is not yet sufficiently complete, and the observed profiles, at least in the ultraviolet, are not yet of sufficient quality. In this case there is little that IUE can do to help, and we must await future instruments such as the Space Telescope.

Further Exploration of the Spectrum

This last suggested area for further research really applies not only to the ultraviolet, but to the infrared and x-ray regions as well. Progress is being made in the infrared, but must await future instruments in the ultraviolet and x-ray wavelengths. Some Be star observations were made with Einstein, and we hope and expect that substantial work in this area will be done with EXOSAT. In the ultraviolet, both IUE and Space Telescope lack the coverage towards short wavelengths that Copernicus provided, and so we must be patient in awaiting data in far-ultraviolet and extreme ultraviolet spectra. The Extreme Ultraviolet Explorer will be capable of providing broad-band photometry in the extreme ultraviolet, but it is doubtful whether any Be stars will be detected through the highly opaque interstellar medium. The brightest hope for the future in this direction is the proposed Far Ultraviolet Spectroscopic Explorer, which is envisioned to have the capability for high-resolution spectroscopy down to the Lyman limit, and perhaps beyond. When such an instrument is available, it will be possible to better characterize the ionization balance in stellar winds for all early-type stars, and to further explore the ultraviolet signatures of extended envelopes in Be stars.

Preparation of this paper has been supported by NASA grant NSG-5300 with the University of Colorado.

REFERENCES

Doazan, V., Grady, C.A., Kuhi, L.V., Marlborough, J.M., Snow, T.P., and Thomas, R.N. 1982, IAU Symp. 98, Be Stars, ed. M. Jaschek and H.-G. Groth (Dordrecht: Reidel), p. 509.

Harmanec, P. 1982, IAU Symp. 98, Be Stars, ed. M. Jaschek and H.-G. Groth (Dordrecht: Reidel), p. 279.

Heap, S.R. 1976, IAU Symp. 76, Be and Shell Stars, ed. A. Slettebak (Dordrecht: Reidel), p. 315.

Henrichs, H.F. 1982, IAU Symp. 98, Be Stars, ed. M. Jaschek and H.-G. Groth (Dordrecht: Reidel), p. 431.

Hutchings, J.B. 1976, Pub. A.S.P., 85, 5.

Lamers, H.J.G.L.M., Gathier, R., and Snow, T.P. 1982, Ap. J., in press.

Marlborough, J.M. 1982a, IAU Symp. 98, Be Stars, ed. M. Jaschek and H.-G. Groth (Dordrecht: Reidel), p. 361.

Marlborough, J.M. 1982b, IAU Symp. 98, Be Stars, ed. M. Jaschek and H.-G. Groth (Dordrecht: Reidel), p. 387.

Mendoza, E. 1982, IAU Symp. 98, Be Stars, ed. M. Jaschek and H.-G. Groth (Dordrecht: Reidel), p. 3.

Morton, D.C., Jenkins, E.B., Matilsky, T.A., and York, D.G. 1972, Ap. J., 177, 219.

Peters, G.J. 1982, IAU Symp. 98, Be Stars, ed. M. Jaschek and H.-G. Groth (Dordrecht: Reidel), p. X.

Ruusalepp, M.K. 1982, IAU Symp. 98, Be Stars, ed. M. Jaschek and H.-G. Groth (Dordrecht: Reidel), p. 303.

Snow, T.P. 1981, Ap. J., 251, 139.

Snow, T.P. 1982, Ap. J. (Letters), 253, L39.

Sonneborn, G.H. 1982, IAU Symp. 98, Be Stars, ed. M. Jaschek and H.-G. Groth (Dordrecht: Reidel), p. 493.

Sonneborn, G.H., and Collins, G.W. 1977, Ap. J., 213, 787.

Zorec, J., Briot, D., and Divan, L., and Briot, D. 1982, IAU Symp. 98, Be Stars, ed. M. Jaschek and H.-G. Groth (Dordrecht: Reidel), p. 419.

ULTRAVIOLET OBSERVATIONS OF INTERSTELLAR DUST

Ralph Bohlin
Goddard Space Flight Center

ABSTRACT

A large fraction of astronomical observations in the UV are affected by extinction due to interstellar dust in the line of sight. The shape of the extinction curve varies markedly around the sky, especially in regions of nebulosity such as the Orion Nebula. The variations of the shape provide clues to the nature of the dust. Additional insight into the physical properties of dust can be obtained from reflected UV starlight as observed in NGC7023 by IUE and in the faint arms of M101 as photographed by a sounding rocket.

INTRODUCTION

The total mass in the interstellar medium is comparable to the mass of the stars in the Galaxy, but the total mass of the dust is less than one percent of the interstellar matter. Despite this low abundance, the dust contains about one half of the heavy elements in the interstellar medium that have been created by nucleosynthesis in the Galaxy. Dust is a site for molecule formation and is probably crucial in the overall process of cooling clouds that are contracting to form stars. The background sky brightness in the UV may be dominated by scattering off dust or may have cosmological significance. UV studies of extinction and scattering of starlight offer important clues to the nature of interstellar dust in relation to these important fields of study.

In addition, the extinction of light by interstellar dust is an important observational consideration. Except for the closest objects, UV flux distributions are usually affected significantly by wavelength dependent extinction by dust grains. Therefore, the magnitude of this problem and the accuracy of "standard" corrections for this interstellar reddening need to be explored.

EXTINCTION CURVES

A. Standard Stars

The loss of light through scattering and absorption by dust in the line of sight is studied by comparing a reddened stellar flux distribution with the intrinsic flux distribution from a star with the same spectral type. The first problem in deriving an interstellar extinction curve is to obtain the flux curve for an unreddened star with the same spectrum. A detailed discussion of typical errors involved in the process of finding standard spectra is given by Meyer and Savage (1981). In the case of IUE, the UV spectral atlas of Wu et al. (1982) is a tremendous aid in establishing a family of unreddened spectra. For some spectral types, unreddened stars are rare or nonexistent, forcing us to use standards that differ in their spectral classification or are somewhat reddened.

Figures 1-4 are useful in evaluating the errors in correcting for the small reddening of potential standards and in identifying standards with flux curves that agree with that expected from the neighboring prime standards. The prime standards shown in Figures 1-4 and identified in Table 1 have been selected from the IUE UV Spectral Atlas with a preference for low reddening and with the requirement that the flux curves define a family that is smooth as a function of spectral type. Each flux distribution in Figures 1-4 has been dereddened using the average extinction of Savage and Mathis (1979) and normalized to a visual magnitude V=0. Note that the giants and supergiants of different kinds differ considerably from each other and from the main sequence. The giant and supergiant standards are less satisfactory than main sequence standards, because the more luminous stars are more often reddened themselves, because there are fewer choices available, and because of the suspicion that the spectral type correlates worse with the intrinsic energy distribution. The Figures 1-4 illustrate the line strengths in IUE low dispersion data.

B. Comparison with Reddened Spectra

In addition to the spectral type, the line strengths in the reddened star help to establish the best standard to use in deriving the extinction curve. Figures 5-7 show extinction curves for 3 stars from an IUE program in collaboration with A. N. Witt and T. P. Stecher. The common interpretation is that the bump in the curve near 2200Å is caused by the material in the grains, often suggested to be graphite. The far UV rise from λ^{-1} about 6 to the limit of IUE coverage near 8 is attributed to a population of small grains. For this interpretation, the curves in Figures 5-7 would illustrate cases where the small grain population is near the average in Figure 5, while Figures 6-7 illustrate low and high populations, respectively.

The deviation from the average in Figures 6-7 is not unique and might be considered typical in estimating errors caused by using an average curve to correct arbitrary observations. For example, an error of 1 unit in $E(\lambda-V)/E(B-V)$ is a one magnitude error in a corrected flux distribution, when the color excess $E(B-V)=1$.

Figure 8 is the extinction curve for the Orion Trapezium star θ^1 Ori C, obtained from a recent IUE program in collaboration with T. A. Matilsky. The average Orion curve from Bohlin and Savage (1981) lies somewhat lower than the new data, primarily because of the improved standard star spectrum used here. Probably, Figure 8 is a better extinction curve for the Trapezium region than that of Bohlin and Savage (1981). Because of the great amount of activity and mass flow observed in Orion, the interstellar grains probably have been modified from the size and surface characteristics typical of a more quiescent cloud.

REFLECTION NEBULAE

Studies of grains in reflection nebulae can help define the physical properties of the dust beyond the restrictions found from extinction curves, if the geometry of the dust distribution can be understood. Visual and UV spectra, in conjunction with photometric images, have been used to investigate

the albedo, a, and phase function, ϕ, of the scattering off grains in the Orion Nebula and NGC7023.

A. Orion Nebula

Bohlin, et al. (1982) have photographed the Orion Nebula through 4 UV filters using a rocket borne telescope with 10 arcsec resolution. IUE spectra of points within the UV image provide the reference for the absolute calibration. Despite the fact that the Orion Nebula is primarily an emission line object in the visual, the UV data demonstrate that the prime source of the UV light is stellar continuum scattered from the dust. A significant fact, relevant to observations of other galactic and extragalactic HII regions, is that the total UV nebulosity is about 2.5 times the stellar flux as observed from the Trapezium stars.

In the case of Orion, uncertainties about the geometry limit the strength of any conclusions about the physical properties of the scattering dust. One picture of the inner Orion region is of stars approaching a dense cloud and carving out a bowl shaped region where the scattering could occur at large angles off the sides of the bowl. Another plausible geometry is the spherical shell model of Mathis et al. (1981). The two models imply opposite conclusions about the change of the phase function asymmetry factor, g, with wavelength.

B. NGC 7023

The inference of spherical symmetry of the reflecting dust in NGC 7023 is more likely than in Orion, because the single B3V star (HD200775) produces only a small HII region without the dramatic dynamics that affect the large-scale dust distribution near the Orion Trapezium. Witt et al. (1982) have used IUE, TD-1, visual, and IR observations to determine the dust albedo and phase function asymmetry, g. Our results are that the average grain albedo, a, remains high in the UV with a(1400)=0.6 and a(2200)=0.4 and that the scattering becomes more isotropic toward shorter wavelengths with g declining monotonically from 0.5 to 0.25 between 2500 and 1400Å.

EXTRAGALACTIC DUST IN M101

Dust in faint outer arms of M101 has been detected in UV images with an effective wavelength of 2250Å, a bandpass of 970Å, and 10 arcsec resolution (Stecher et al. 1982). The observed arms are unlikely to be stars, because the morphology is smooth, in contrast to the main arms with their abundance of HII regions. Therefore, any stellar contribution must be further restricted to the unlikely case of hot stars because the arms are not seen on typical visual photographs. Also, the dust is expected to lie far enough from the plane to be illuminated by the rest of the galaxy, because of likely warps and because the scale height is expected to be large. If this geometry is correct, the HI measurements at 21 cm by Allen and Goss (1979) imply that the dust in M101 has scattering properties and a gas-to-dust ratio similar to the dust in the solar neighborhood (Bohlin, Savage, and Drake 1978), suggesting that the metal content in these outer arms of M101 is similar to that of our Galaxy.

CONCLUSIONS

1. The importance of extinction in UV observations has been emphasized, and some typical examples of the uncertainties in standard corrections are given.

2. Progress has been made toward understanding the nature of dust, from a study of reflection nebulae. The grains in NGC7023 have a mean UV albedo of $\sim$0.5 with a phase function that becomes more isotropic toward shorter wavelengths.

3. A statistical approach to the solution of the geometry problem in reflection nebulae has been outlined. Plausible solutions with consistent grain properties have been found for the Orion Nebula, NGC7023, M101, and 3 Pleiades nebulae (Witt, Stecher, and Bohlin 1982). We plan to continue this study by analyzing IUE, TD-1, ANS, and ground based data for NGC2023 and other cases.

REFERENCES

Allen, R. J., and Goss, W. M. 1979, Astr. Ap. Suppl., 36, 135.
Bohlin, R. C., Harrington, J. P., and Stecher, T. P. 1982, Ap. J., 252, 635.
Bohlin, R. C., and Savage, B. D. 1981, Ap. J., 249, 109.
Bohlin, R. C., Hill J. K., Stecher, T. P. and Witt, A. N. 1982, Ap. J., 255 April 1.
Bohlin, R. C., Savage, B. D., and Drake, J. F. 1978, Ap. J., 224, 132.
Lesh, J. R. 1968, Ap. J. Suppl., 16, 371.
Lesh, J. R. 1972, Astron. Astrophys. Suppl., 5, 129.
Mathis, J. S., Perinotto, M., Patriarchi, P., and Shiffer, F. H. 1981, Ap. J., 249, 99.
Meyer, D. M., and Savage, B. D. 1981, Ap. J., 248, 545.
Stecher, T. P., Bohlin, R. C., Hill, J. K., and Jura, M. A. 1982, Ap. J. Letters, 255, April 15.
Savage, B. D., and Mathis, J. S. 1979, Ann. Rev. of Astron. Astrophys., 17, 73.
Witt, A. N., Walker, G. A. H., Bohlin, R. C., and Stecher, T. P. 1982, Ap. J., in press.
Witt, A. N., Stecher, T. P., and Bohlin, R. C. 1982, this conference.
Wu,C.-C., Boggess, A., Bohlin, R. C., Holm, A. V., Schiffer, F. H., and Turnrose, B. E. 1982, in preparation.

TABLE 1

PRIME IUE STANDARD STARS

HD	NAME	S.T.	V	B-V	E(B-V)	SWP	LWR
a	-	WD	13.43	-.34	.01	6159,10271-2	5324,8942
47839	15Mon	07V	4.65	-.25	.07	8146	7077
38666	μCol	09.5IV	5.16	-.29	.01	14340	10954
31726	-	B1V	6.15	-.21	.05	8165	7098
64802	-	B2V	5.49	-.20	.04	14308	10939
32630	ηAur	B3V	3.16	-.18	.02	8197	7125
147394	τHer	B5IV	3.88	-.15	.01	8194	7122
93222	-	07IIIf	8.11	.05	.37	11135	9805
63922	-	B0III	4.11	-.19	.09	9511	8237
79447	-	B3III	3.97	-.18	.01	14338	10952
83183	-	B5II	4.08	.00	.13	9512	8238
188209	-	09.5Ia	5.65	-.09	.21	8195	7123
150898	-	B0.5Ia	5.57	-.07	.18	10173	8837
91316[b]	ρ Leo	B1Iab	3.85	-.14	.08	8650,8652	7396
53138	o^{2}CMa	B3Ia	3.04	-.10	.04	8168	7102,7103
58350	ηCMa	B5Ia	2.46	-.08	.02	8199	7127
40111	139Tau	B1Ib	4.83	-.07	.15	8151	7081
165024	θAra	B2Ib	3.66	-.08	.10	10174	8838
86440	φVel	B5Ib	3.54	-.09	.01	9513	8239

a - The white dwarf central star of NGC7293 (Bohlin, Harrington and Stecher 1982).

b - Spectra obtained in the IUE program of Woodgate and Bohlin.

The photometry and spectral types have preferred sources of Lesh (1968) or Lesh (1972).

FIGURE CAPTIONS

1. Flux distribution for main sequence stars, dereddened by the average curve of Savage and Mathis (1979) and normalized to V=0.

2. Same as Fig. 1 for giants.

3. Same as Fig. 1 for luminosity class Ia.

4. Same as Fig. 1 for luminosity class Ib.

5. An interstellar extinction curve derived from IUE spectra binned in 5Å intervals and compared to the Savage and Mathis average (large open squares). The case illustrated is close to the average curve.

6. Same as Fig. 5 for a case of a low far UV extinction, generally attributed to a deficiency of small grains.

7. Same as Fig. 5 for a case with an excess of small grains.

8. Same as Fig. 5 for the anomalous case of the Orion Nebula.

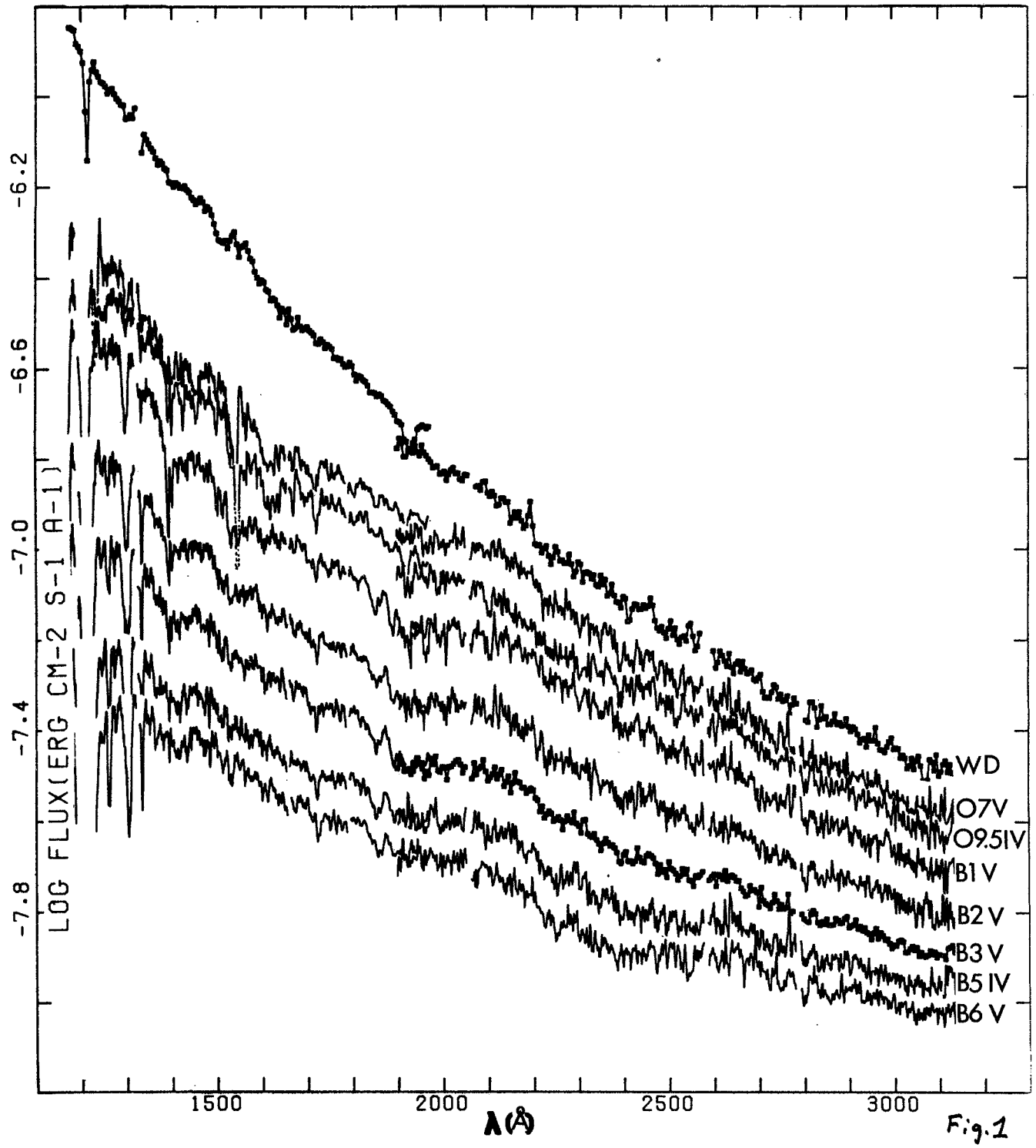
-6.2
-6.6
-7.0
-7.4
-7.8
LOG FLUX(ERG CM-2 S-1 A-1)
1500
2000
2500
3000
λ(Å)
WD
O7V
O9.5IV
B1 V
B2 V
B3 V
B5 IV
B6 V

Fig. 1

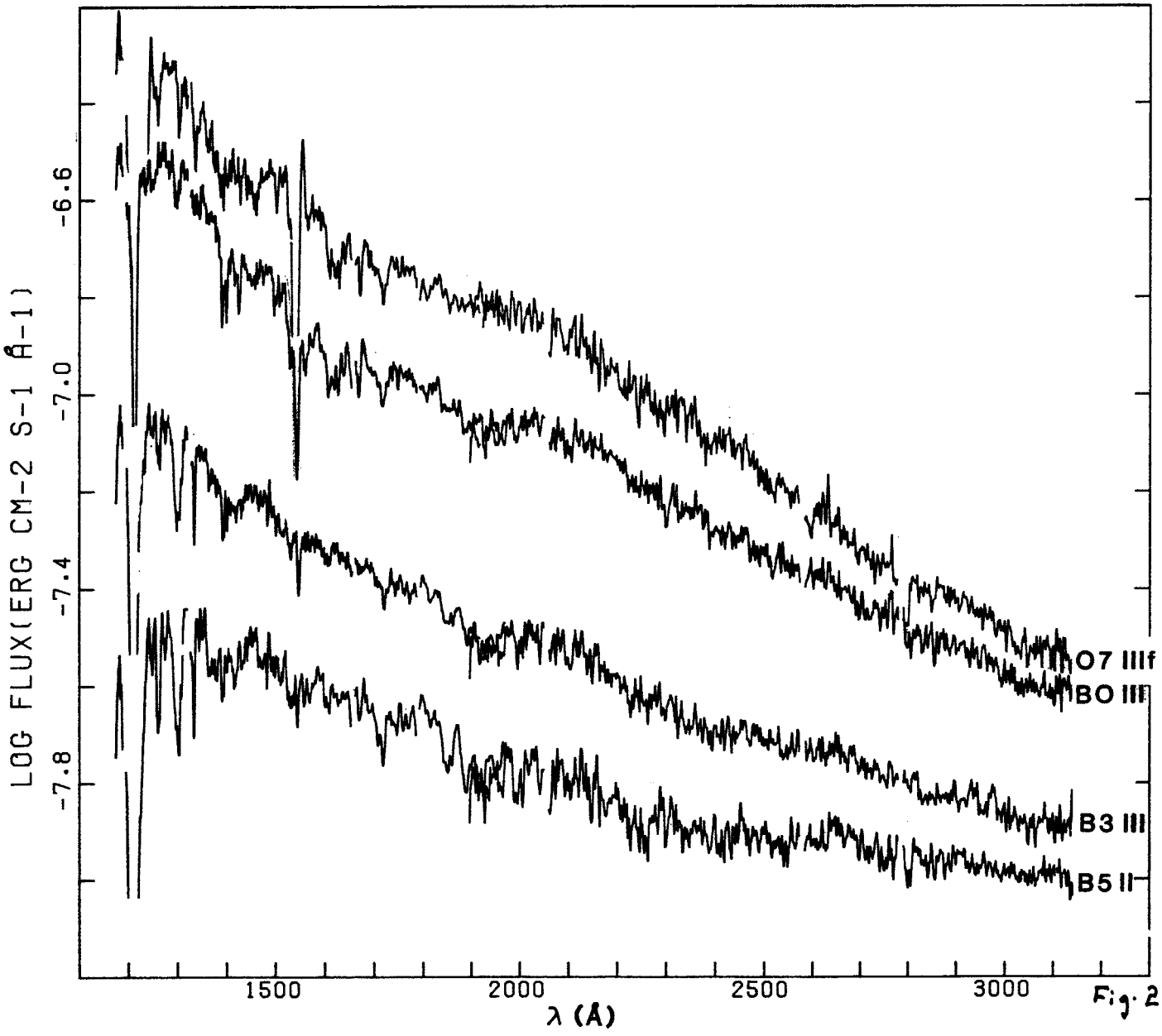
LOG FLUX(ERG CM-2 S-1 Å-1)
-6.6
-7.0
-7.4
-7.8
1500
2000
2500
3000
λ (Å)
O7 IIIf
BO III
B3 III
B5 II

Fig. 2

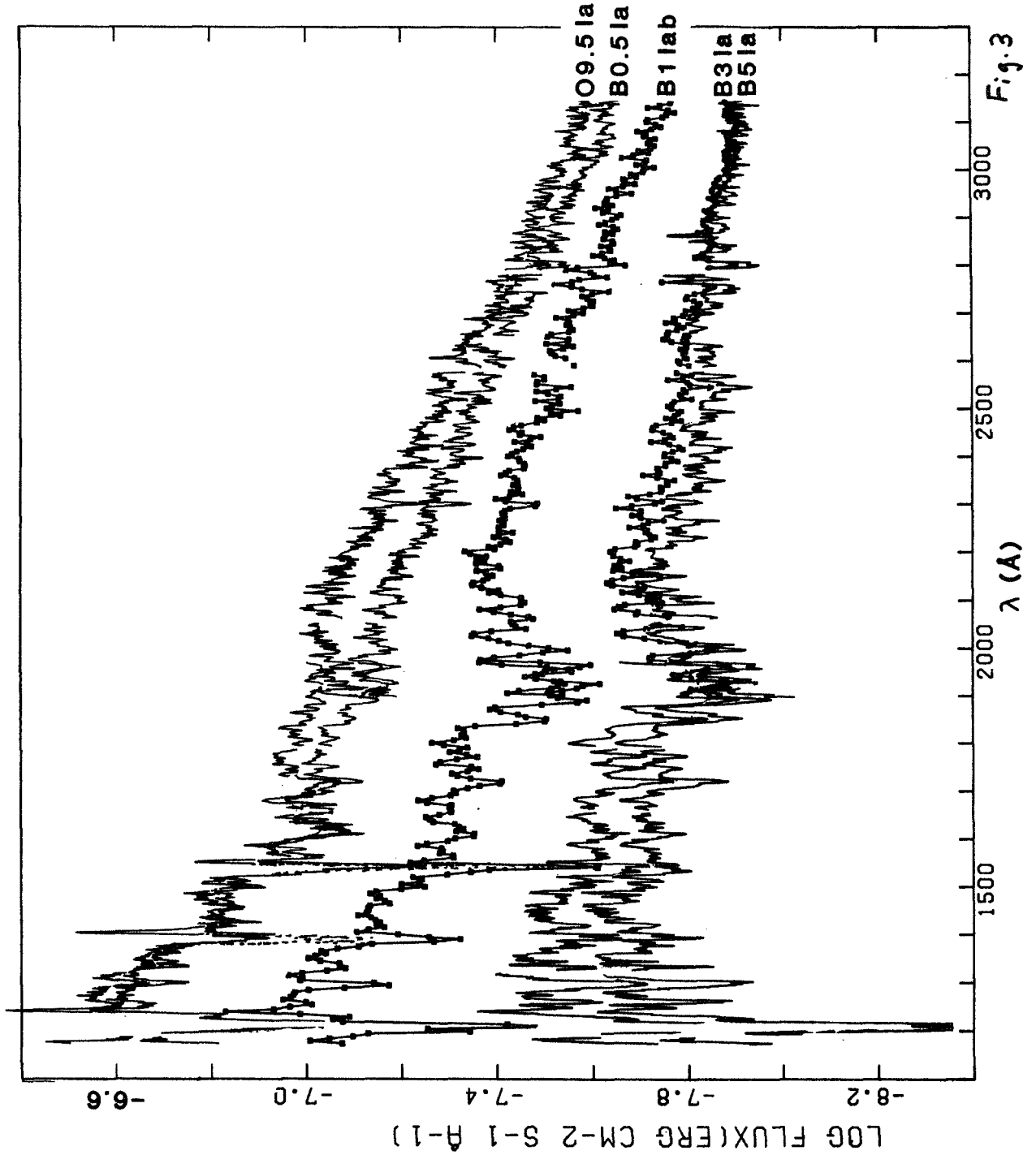
O9.5 Ia
B0.5 Ia
B1 Iab
B3 Ia
B5 Ia
LOG FLUX(ERG CM-2 S-1 Å-1)
-8.2
-7.8
-7.4
-7.0
-6.6
1500
2000
2500
3000
λ (Å)

Fig.3

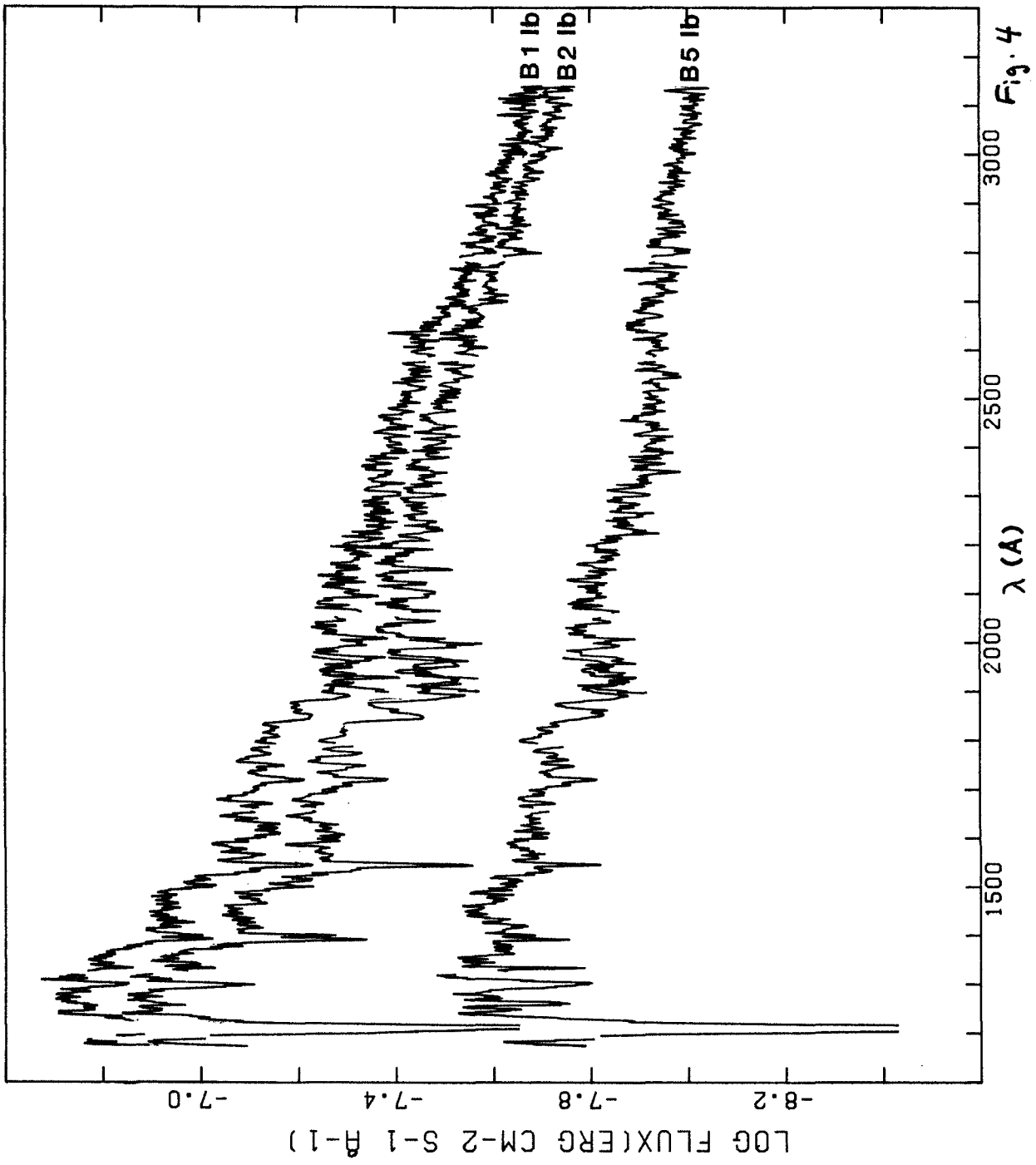
B1 Ib
B2 Ib
B5 Ib
LOG FLUX(ERG CM-2 S-1 Å-1)
-8.2
-7.8
-7.4
-7.0
1500
2000
2500
3000
λ (A)

Fig. 4

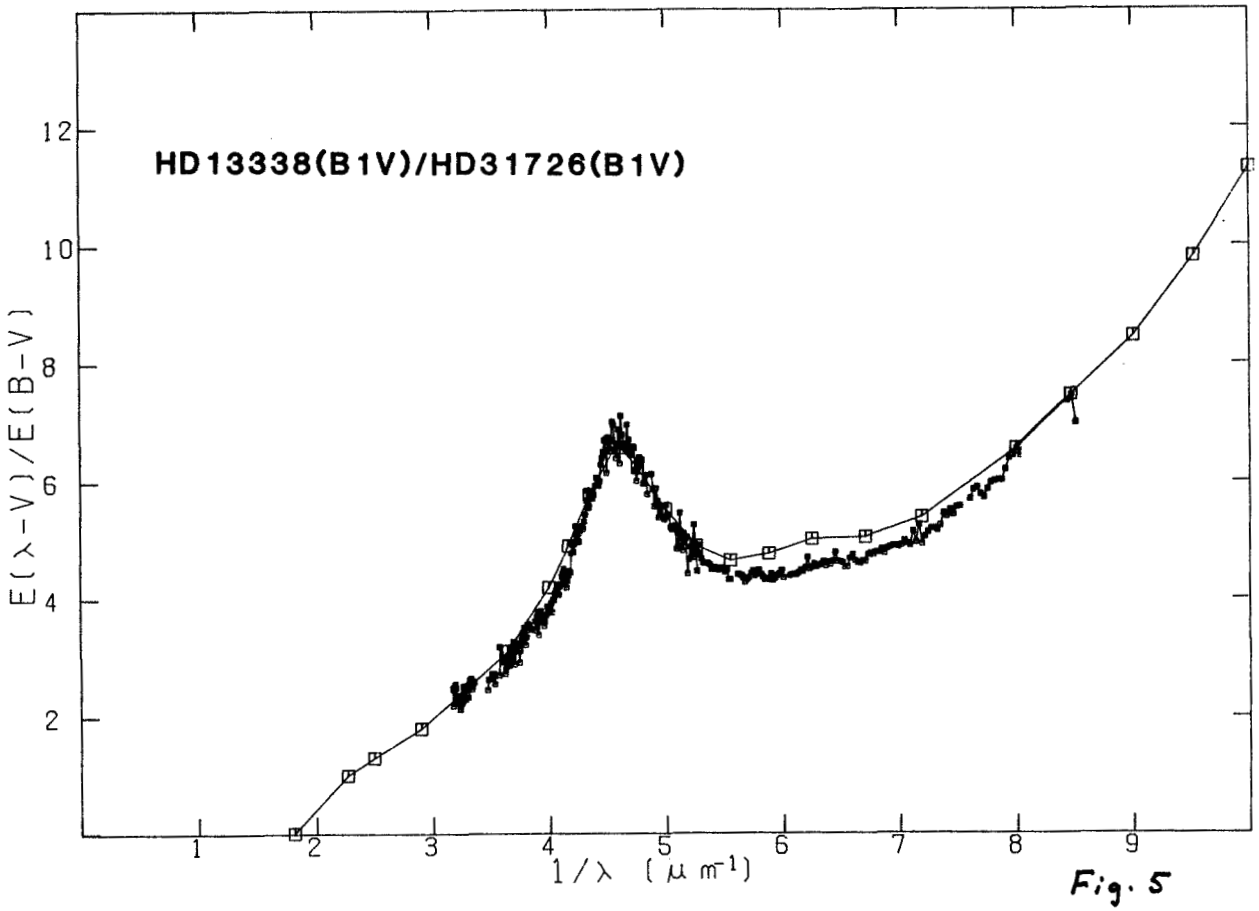
HD13338(B1V)/HD31726(B1V)
E(λ-V)/E(B-V)
1/λ (μm⁻¹)

Fig. 5

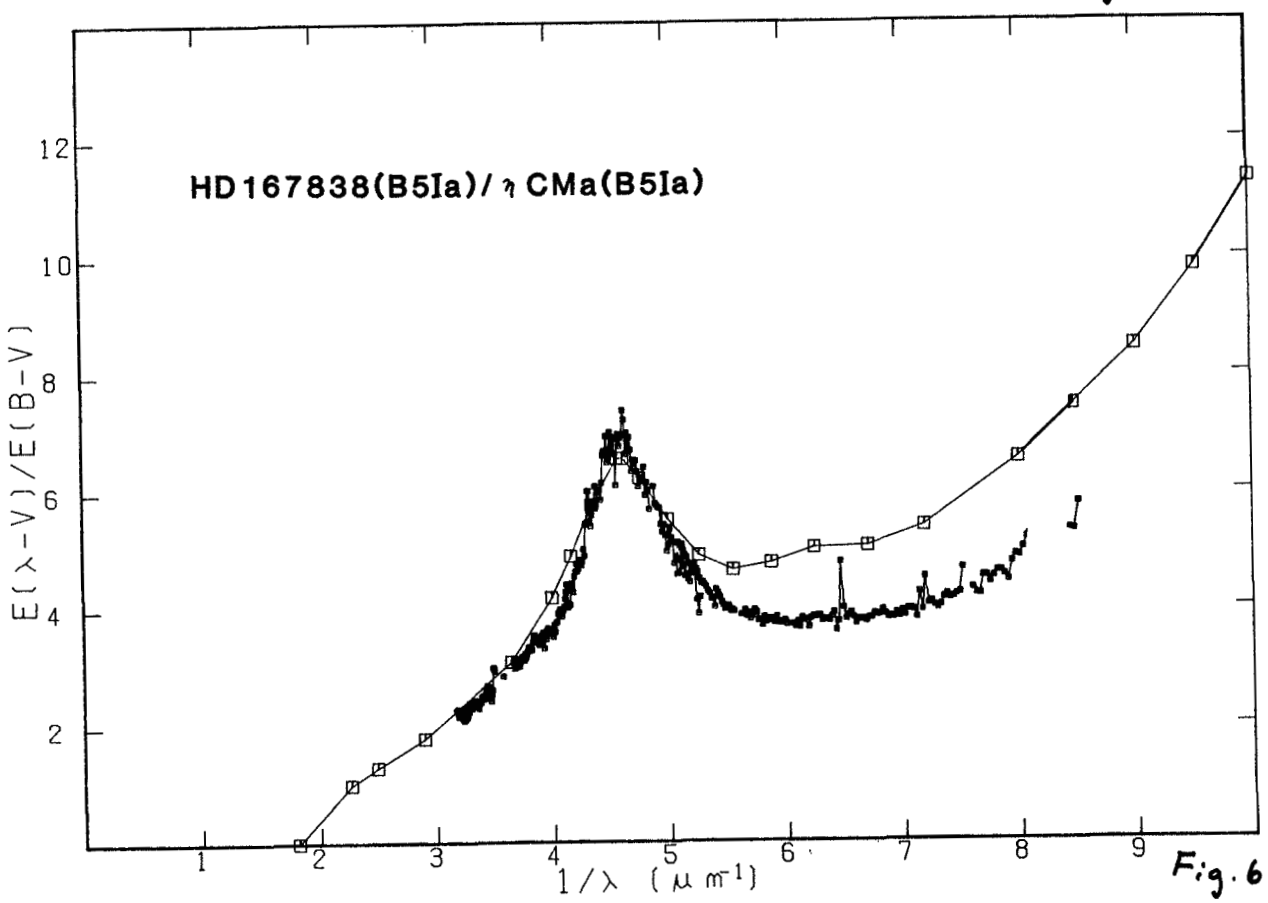
HD167838(B5Ia)/ηCMa(B5Ia)
E(λ-V)/E(B-V)
1/λ (μm⁻¹)

Fig. 6

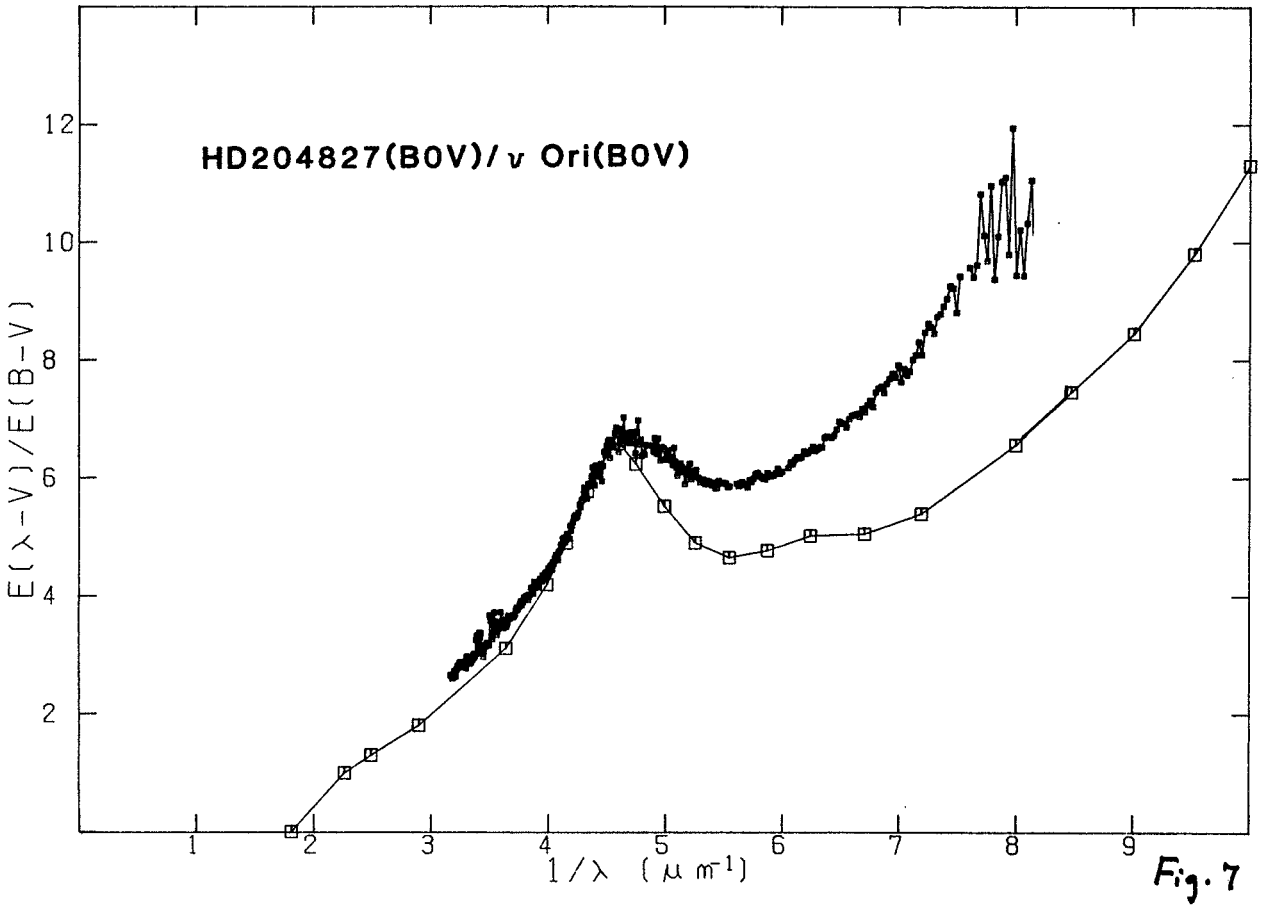
HD204827(B0V)/ν Ori(B0V)
E(λ-V)/E(B-V)
1/λ (μm⁻¹)

Fig. 7

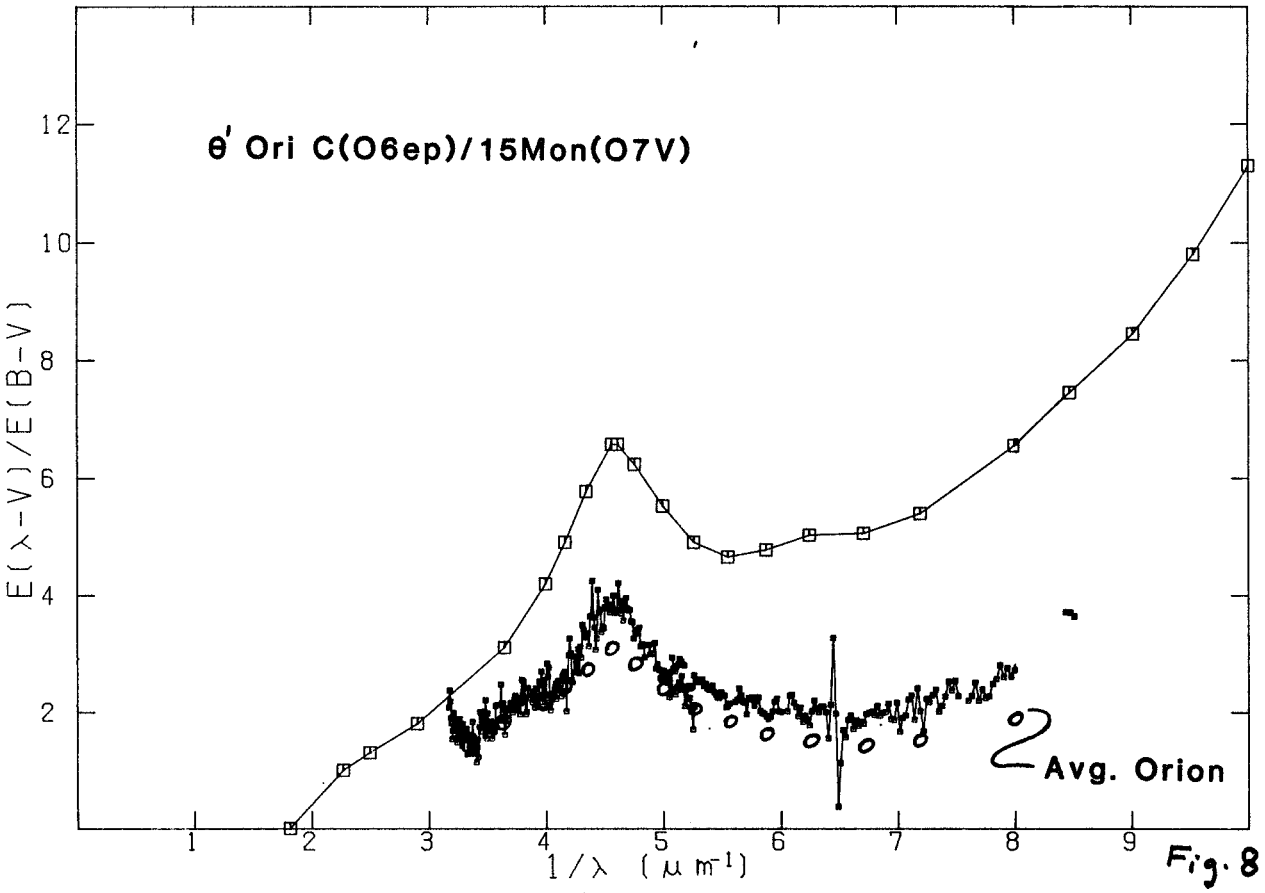
θ' Ori C(O6ep)/15Mon(O7V)
2 Avg. Orion
E(λ-V)/E(B-V)
1/λ (μm⁻¹)

Fig. 8

MORPHOLOGY OF GASEOUS HALOS OF GALAXIES

Donald G. York
Princeton University Observatory

ABSTRACT

Recent ultraviolet and optical observations of high latitude gas are reviewed. Hydrogen 21cm observations of high latitude gas and extended disks of spiral galaxies are used to formulate a picture of the gaseous halo which may be relevant to the origin of QSO absorption lines.

INTRODUCTION

Bahcall and Spitzer (1969) suggested that intervening gas associated with foreground galaxies could cause absorption lines with z(abs) << z(em) in QSO spectra. Bahcall (1978) reviewed recent data and concluded that intervening halos, protogalaxies, dead galaxies, discs of spiral galaxies and clusters of galaxies are all viable sources for some of the lines observed.

Recent observations of high latitude gas in our own galaxy and of HI in other galaxies can be used to assess the possibility that galactic halos are responsible for QSO absorption lines. We discuss in turn the near halo, the far halo, and the QSO lines, then synthesize the discussion and suggest new observations. A discussion of X-ray halos and cosmic ray (radio) halos is given by York (1982) who also gives more complete references for the material discussed here.

THE NEAR HALO

UV Data

Savage and de Boer (1979, 1981) first showed high resolution profiles of CIV and SiIV in possible halo gas. The lines appeared in spectra of distant LMC and SMC stars. Further work has strengthened their initial conclusion that CIV is not in the galactic disk generally but only arises at large z distances. Cowie et al (1980) and Laurent et al (1982) show that interstellar CIV lines are weak over long disk pathlengths (>2kpc) far from O star HII regions.

The ubiquity of CIV and SiIV in the near halo has been demonstrated by Pettini and West (1982) (summarized in this IUE Symposium volume). Based on CIV equivalent widths in stars within 10 kpc, most of the CIV seen toward the LMC could arise within 3 - 10 kpc of our galactic disk. The strong CIV lines are relatively narrow (< 60 km s^{-1} FWHM) and occur near zero velocity.

York et al (1982) discuss the general absence of high velocity gas in the halo (see Blades, this volume). (The CIV data are symbolically represented in Figure 2, to be discussed later.)

Optical Data

Interstellar NaI and CaII have been searched for in many high latitude distant stars, globular clusters and extragalactic sources (Songaila and York 1980, 1981; Blades and Morton 1982; Oort and Hulsbosch 1978). Given that lines near zero velocity are caused by nearly disk gas, little evidence for halo clouds is found. Excluding LMC/SMC lines of sight, an accumulated distance of 500 - 1000 kpc of high latitude space must be looked through to find a single cloud at $|v| > 60$ km s^{-1}, to a limit in W(CaII-K) of 30m Å. The few detections can usually be attributed to gas within 5 kpc of the disk, co-rotating with the galaxy.

In contrast, most stars in the LMC, SMC show CaII (and NaI, at better detection limits) at all velocities from 0 km s^{-1} to 250 km s^{-1} or more (the LMC velocity is v(LSR) $\sim$+280 km s^{-1}. Since this line of sight is peculiar in CaII, the UV lines of ions associated with CaII (SiII, CII, MgII) may not be representative of halo gas. Alternative views are given by de Boer and Savage (1981) and Songaila (1981).

HD93521

A study of UV and optical lines toward HD93521 (09.5) ($b = +63°$, $d = 750$ pc) has been completed by Caldwell (1979). Representative Copernicus profiles of interstellar lines are given in Figure 1. The blend near -55 km s^{-1} in ArI/SII can be associated with components at -48 km s^{-1} and -66 km s^{-1} seen by Meng and Kraus (1970) in the intermediate velocity cloud OLM 351 part of which lies within 1° of HD93521. The SiIII component near -80 km s^{-1} can be associated with the edges of the high velocity cloud MII, which includes gas from -70 to -105 within 2° of the star (Davies et al 1976). No CIV is detected for this line of sight and the OVI lines are at low velocity. Somehow this obviously turbulent region is shielded from whatever produces CIV at high latitude in other directions. Note the positive velocity HI gas not seen in UV absorption data which may be behind the star. It could be associated with side lobes as well (Giovanelli et al 1978).

THE FAR HALO

Above 3 kpc, we know of few probes of the halo, given the results for CaII noted above. We can only turn to 21cm high velocity clouds (HVC's), some of which may be at 70 kpc, and to observations of 21cm emission as far as 100 - 200 kpc from centers of spiral galaxies.

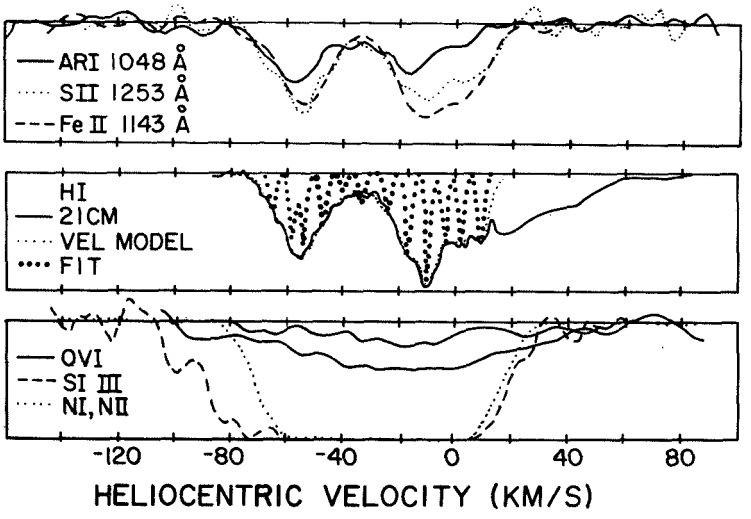

Figure 1: Copernicus spectra of interstellar lines in HD93521, a high latitude star behind several 21cm HVC's (-90, -66, -48 km s^{-1}).

High Velocity Clouds

Figures 2 and 3 show maps of 21cm HVC's, derived from the extended survey of Giovanelli (1980) or from maps given by Oort and Hulsbosch (1978). These references must be examined in detail to understand the limitations of the maps. The present contours show the maximum extent of clouds, to a limit of $N(HI) = 3 \times 10^{18} cm^{-2}$ above the -30° horizon line. Below that dashed line the data are imcomplete, and do not show the long stream of gas from the LMC to the SGP at $\ell = 290°$ (Mathewson et al 1974). The well-known fine structure as fine as 2' for cold clumps, is ignored in this discussion. HI within these large contours will consist mainly of profiles with FWHM > 20 km s^{-1} (Giovanelli et al 1973, Mirabel et al 1979).

Distances for specific features are reviewed by Oort and Hulsbosch (1978). They are however largely unknown. Lin and Lynden-Bell (1982) argue that the Magellanic Stream ($\ell = 80°$; $b < -40°$; $b = -90°$ to the LMC at $\ell = 290°$) arises beyond 50 kpc and mostly beyond 70 kpc. Watanabe (1981) used tidal disruption constraints to show that many HVC's can be 10 - 40 kpc away. Vershuur 1975 reviews assignment of some HVC's, particularly negative velocity gas from $\ell = 180°$, to gas associated with distant spiral arms, but as much as 5 kpc out of the plane. Oort and Hulsbosch (1978) summarize arguments that some clouds may be within 1 - 2 kpc of the Sun.

It thus appears that several clouds are well above the CIV layer of 3 - 10 kpc. They should in some way reflect the properties of the halo gas in which they must be embedded. Giovanelli and Brown (1973), for instance, discuss the possibility that detectable clouds are surrounded by invisible gas a $3 - 4 \times 10^5$°K, which however might be seen in absorption lines. We note the SiIII association with MII in the spectrum of HD93521 and the very

strong CIV, SiIV and NV lines seen toward a star near a cloud at $\ell = 310°$. $b = 15°$ of (West and Pettini 1982) (See Figure 2 and its caption).

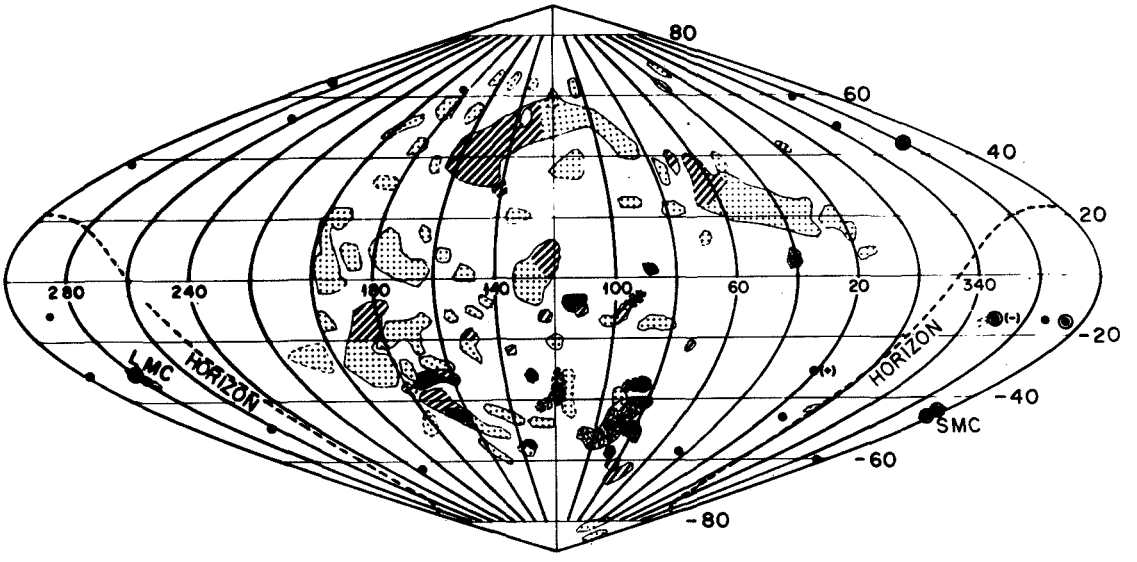

Figure 2: Maximum 21cm extent of negative LSR velocity HVC's. Shading denotes $50 < |v| < 150$, $150 < |v| < 250$, and $250 < v < 350$ km s^{-1} by dots, lines, and dense speckling. Isolated large dots represent stars where Pettini and West (1982) or Savage and de Boer (1981) observe interstellar CIV, always near zero velocity unless (-) or (+) appear. ●, $W\lambda(1548) < 100$ mÅ; ●, $200 < W\lambda < 300$ mÅ; ◉, $W\lambda > 400$ mÅ.

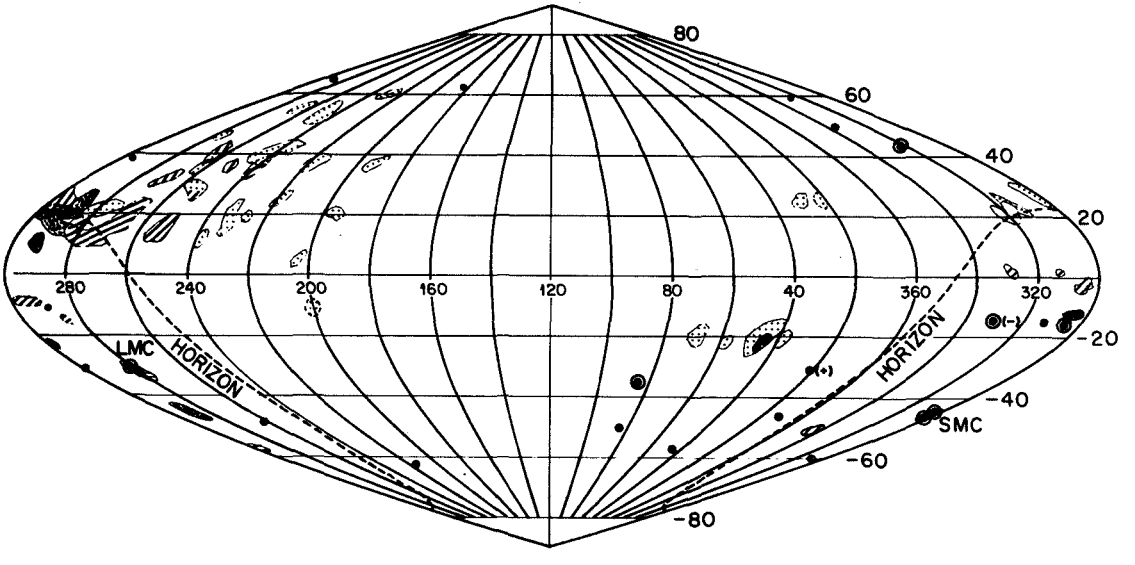

Figure 3: Negative LSR velocity 21cm clouds.

Extensions of Galaxies

Much work is now being done in mapping the outer parts of spiral galaxies in HI. Several galaxies M83, M101 extend to more than 3 Holmberg radii (Huchtmeier and Witzel 1979, Huchtmeier and Bohnenstengel 1981). Figure 4 shows 21cm contours superimposed on a picture of a Seyfert galaxy, MKN348 (Heckman et al 1982) as a perhaps somewhat extreme example. While not all galaxies show such extensions, they could show up as higher sensitivity becomes available: the best data are still limited to $N(HI) > 3\times10^{18} cm^{-2}$. A complete discussion is given by Sancisi (1981) on the general subject of 21cm extensions.

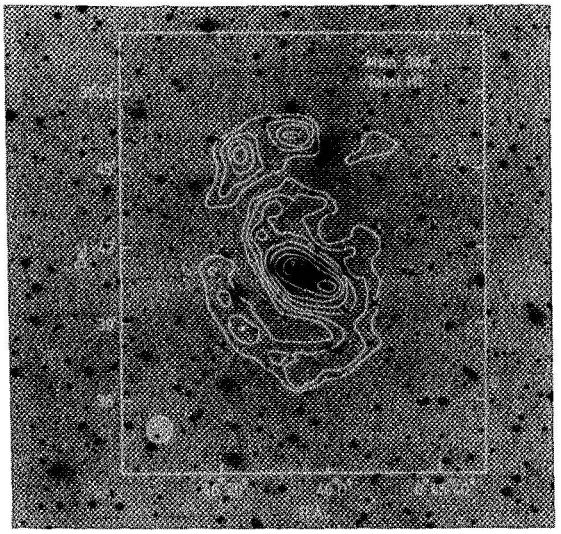

Figure 4: 21cm contours near MKN348 (Heckman et al 1982).

QSO ABSORPTION LINES

For purposes of this review, the low z absorption lines can be described by the following properties. They occur frequently enough that intervening galaxies must have extensions of 50 - 100 kpc to account for them. While some may arise near the QSO's themselves, many have such high velocities with respect to the QSO they are probably unrelated. The two point correlation function for lines in the same spectra show strong clustering over velocity intervals $\Delta v < 200$ km s^{-1}, and may show significant clustering for $\Delta v = 500 - 2000$ km s^{-1}. Most systems for which the apparent velocity with respect to the QSO is greater than 30000 km s^{-1} (and for which high resolution data are published in suitable form) show multicomponent profiles covering a range of > 150 km s^{-1}. Examples are given in Table 1. The QSO systems contain a wide range of ionization stages, CIV and Lyα being the most common lines identified. Photoionization is generally regarded as the ionization mechanism, but collisional ionization may have to be involved in some cases. All of these properties are described fully, with original references, by Weymann et al (1981) and York (1982).

Table 1

QSO absorption lines from Halos?

QSO	z(abs)	β**	Number of Components	Δv	Note
0119-046	0.6577	0.5	2	$<50 kms^{-1}$	1
0237-23	1.36-1.67	0.2-0.4	2-5 each	>150§	2, (3)
0421+019	1.6375	0.14	5	308	4
0735+178	0.474	?	>4	160	5
1225+31	1.624	0.2	3	250	6

* In general, the two point correlation suggests clustering on scales from 500 - 2000 km s^{-1} as well (Young et al 1982a).

** The apparent velocity of the cloud (ejection is plus) with respect to the QSO: $A = [1+z(em)]^2$, $B = [1+z(abs)]^2$, $B = (A-B)/(A+B)$

§ Typical component separations could be < 100 km s^{-1}. (Note 3)

Note: 1) Sargent et al 1982; 2) Boksenberg and Sargent 1975; 3) Bahcall 1975; 4) Young et al 1982b; 5) Boksenberg et al 1979; 6) Sargent 1977

SYNTHESIS

In light of the foregoing remarks, we can offer the following morphology for gaseous extensions of galaxies, commonly called halos. A schematic diagram is given in Figure 5. An edge-on spiral galaxy is shown. Several circles around the boundary of the galaxy represent the outer-most interstellar clouds of the disk and circles further away represent the high velocity 21cm clouds. Beyond the Holmberg radius (R_H) are clouds of 21cm gas, which lie close to the plane of the disk, but have a larger scale height than clouds in the stellar disk (Bergeron and Gunn 1977) and may be warped (Sancisi 1981). The length in this edge-on view is the size required to explain QSO absorption line ($\sqrt{2}\times$ the corresponding dimensions of a spherical halo model). UV radiation responsible for the QSO absorption line ionization comes from all directions, ionizing the edges of the 21cm clouds HVC's and the outer-most clouds in the disk. The main disk itself is not affected by this extragalactic UV radiation because the latter cannot penetrate very far through the mainly neutral gas in the disk. Likewise the outer-most clouds of the disk are shielded from stellar UV radiation in the disk by neutral gas.

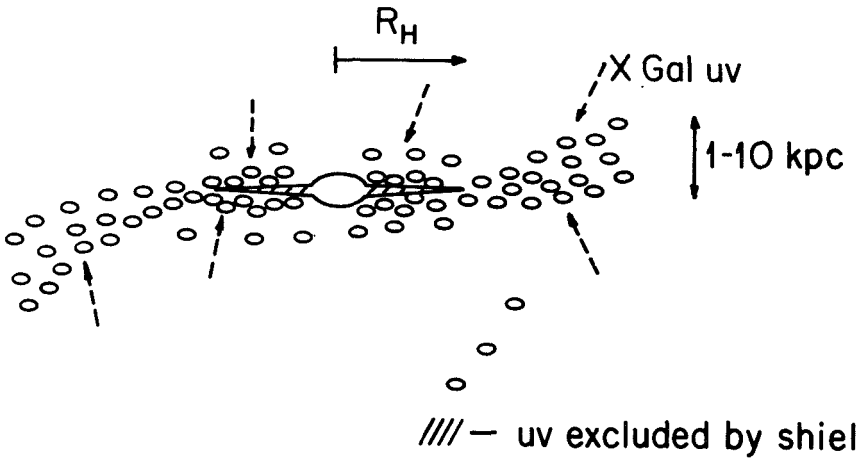

Figure 5: A sketch showing a possible configuration of a galactic halo, described in the text.

A distant observer looking at a QSO through any part of this galaxy would thus see an absorption spectrum including CIV, SiIV and (say) $3 \times 10^{18} cm^{-2}$ in HI Lyα. If this line of sight passed through the disk, many low ionization lines would be observed as well, along with much stronger Lyα and perhaps H_2. The lines could have widths of up to 40 km s^{-1} at 0.5 Å resolution (Cowie and York 1978), and would break into components at higher resolution. If the sight line included an HVC, at least three components could be seen: one from each side of the galaxy and one from the HVC. The total complex could be as much as 300 km s^{-1} wide. If a total hydrogen column density [N(HI) + N(HII)] > $6 \times 10^{18} cm^{-2}$ is encountered, the profiles of different ions (SiII, SiIII, SiIV) say, need not correspond exactly because of the shielding effects already noted.

This concept could explain all the current observations of high latitude gas in our galaxy and could in general explain the QSO lines.. A major difficulty given presently published data is the small filling factor of the high velocity clouds (Figures 2 and 3) as contrasted with the frequent occurance of broad line complexes in QSO spectra (Table 1). Perhaps they have a larger cross section in CIV absorption or are more numerous in typical galaxies. Furthermore, the clustering of galaxies such as the one shown would have to be arranged to produce the two point correlation function of the QSO absorption lines.

FUTURE OBSERVATIONS

One may hope in the near future to prove or disprove such a picture. For gas in our galaxy it is crucial to determine the densities of the CIV producing clouds and to obtain a reasonable estimate of the extragalactic UV flux. Then atomic and photon densities can be compared (McKee et al 1973) and the predicted ionization compared with observations. Such work should be rather straightforward with Space Telescope and may even be

possible with IUE, using fine structure lines of CII and SiII and the ratio MgI/MgII (York 1982 and references therein).

Note that while the expected extragalactic radiation field has been carefully computed by Sargent et al (1979), the numbers must be reevaluated to account for the attenuation of light from many QSO's at $z > 1.5$ by the continuous absorption at $\lambda < 912$ Å in intervening hydrogen systems (Snidjers 1980, Snidjers et al 1981, Bregman et al 1981).

Similar work should be done by studying distant objects behind outer edges of galaxies with known 21cm extensions such as M101 and M83. The densities, strengths of CIV, and velocity dispersion of the components are obvious quantities that need to be defined. More extensive discussions of relevant observations are given by Bahcall (1979) and York (1982).

It is a pleasure to acknowledge a series of discussions with C. Blades, M. Pettini, R. Sancisi and B. Savage and many other colleagues. This work is supported by NASA grants NAGW-10 and NAG5-48 and NASA contract NAS5-23576 to Princeton University. R. Giovanelli kindly provided his extended 21cm survey on magnetic tape.

REFERENCES

Bahcall, J.N. 1975, Ap. J. (Letters), 200, L1.
Bahcall, J.N. 1978, Physica Scripta, 17, 229.
Bahcall, J.N. 1979, Scientific Research with the Space Telescope, IAU Colloq. 54 ed. M.S. Longair, J.W. Warner (Washington DC: U.S. Government Printing Office), p. 215.
Bahcall, J.N. and Spitzer, L. 1969, Ap. J., 156, L63.
Bergeron, J. and Gunn, J. 1977, Ap. J., 217, 892.
Blades, J.C. and Morton, D.C. 1982, MNRAS, in press.
Boksenberg, A., Carswell, R.F. and Sargent, W.L.W. 1979, Ap. J., 227, 370.
Boksenberg, A. adn Sargent, W.L.W. 1975, Ap. J., 198, 31.
Bregman, J.N., Glassgold, A.E. and Huggins, P.J. 1981, Ap. J., 249, 13.
Caldwell, J. 1979, Ph.D. Dissertation, Princeton University Observatory.
Cowie, L.L., Taylor, W. and York, D.G. 1981, Ap. J., 248, 528.
Cowie, L.L. and York, D.G. 1978, Ap. J., 220, 129.
Davies, R.D., Buhl, D. and Jafolla, J. 1976, Astron. Astrophys. Suppl., 23, 181.
Giovanelli, R. 1980, Ap. J., 85, 1155.
Giovanelli, R. and Brown, R.L. 1973, Ap. J., 182, 755.
Giovanelli, R., Haynes, M.P., York, D.G. a d Shull, J.M. 1978, Ap. J., 219, 60.
Giovanelli, R., Vershuur, G.L. and Cram, T.R. 1973, Astron. Astrophys. Suppl. 12, 209.
Heckman, T., Sancisi, R., Balick, B. and Sullivan, W. 1982, MNRAS, in press.
Huchtmeier, W.K. and Bohnenstengel, H.D. 1981, Astron. Astrophys., 100, 72.
Huchtmeier, W.K. and Witzel, A. 1979, Astron. Astrophys., 74, 138.
Laurent, C., Paul, J. and Pettini, M. 1982, Ap. J., in press.
Lin, D.N.C. and Lynden-Bell, D. 1982, MNRAS, in press.

Mathewson, D.S., Cleary, M.N. and Murray, J.D. 1974, Ap. J., 190, 291.
McKee, C.F., Tarter, C.B. and Weisheit, J.C. 1973, Ap. Letters, 13, 13.
Meng, S.Y. and Kraus, J.D. 1970, Ap. J., 75, 535.
Mirabel, I.F., Cohen, R.J. and Davies, R.D. 1979, MNRAS, 186, 433.
Oort, J.H. and Hulsbosch, A.N.M. 1978, in Astronomical Papers Dedicated to Bengt Stromgren, ed. A. Reiz (Copenhagen: Copenhagen University Observatory), p. 409.
Pettini, M. and West, K.A. 1982, Ap. J., in press.
Sancisi, R. 1981, in Structure of Normal Galaxies, ed. S.M. Fall and D. Lynden-Bell (Cambridge, England: Cambridge University Press).
Sargent, W.L.W. 1977, in The Evolution of Galaxies and Stellar Populations, eds. B.M. Tinsley and R.B. Larson (New Haven: Yale University Observatory), p. 427.
Sargent, W.L.W., Young, P.J., Boksenberg, A., Carswell, R.F. and Whelan, J.A. 1979, Ap. J., 230, 49.
Sargent, W.L.W., Young, P.J. and Boksenberg, A. 1982, Ap. J., 252, 54.
Savage, B. and de Boer, K. 1979, Ap. J. (Letters), 230, L77.
Savage, B. and de Boer, K. 1981, Ap. J., 243, 460.
Songaila, A. 1981, Ap. J., 248, 945.
Songaila, A. and York, D.G. 1980, Ap. J., 242, 976.
Songaila, A. and York, D.G. 1981, Ap. J., 248, 956.
Snidjers, M.A.J. 1980, Proc. Second European IUE Conference, Tubingen, Germany, 1980 Mar 26 - 28 (ESA SP-157, 1980 April).
Snidjers, M.A.J., Pettini, M. and Boksenberg, A. 1981, Ap. J., 245, 386.
Vershuur, G.L. 1975, Ann. Rev. Astr. Ap., 13, 257.
Watanabe, T. 1981, Ap. J., 86, 30.
Weymann, R.J., Carswell, R.F. and Smith, M.G. 1982, Ann. Rev. Astr. Ap., 19, 41.
York, D.G. 1982, Ann. Rev. Astr. Ap., in press.
York, D.G., Blades, J.C., Cowie, L.L., Morton, D.C., Songaila, A. and Wu, C.C. 1982, Ap. J., 255, 467.
Young, P.J., Sargent, W.L.W. and Boksenberg, A. 1982b, Ap. J., 252, 10.
Young, P.J., Sargent, W.L.W. and Boksenberg, A. 1982a, Ap. J. Suppl., 48.

IUE OBSERVATIONS OF SYMBIOTIC STARS

M. Hack
Astronomical Observatory, Trieste (Italy)

ABSTRACT

The main photometric and spectroscopic characteristics in the ultraviolet and visual range of the most extensively studied symbiotic stars are reviewed. The main data obtained with IUE concern a) the determination of the shape of the UV continuum, which, in some cases, proves without doubt the presence of a hot companion; and the determination of the interstellar extinction by means of the λ 2200 feature: b) the measurement of emission lines, which enables us to derive the electron temperature and density of the circumstellar envelope, and, taken together with those lines observed in the visual, give more complete information on which spectroscopic mechanisms operate in the envelope; c) the observation of absorption lines in the UV, which are present in just a few cases.

INTRODUCTION

The symbiotic or "combination spectra" have been defined by Bidelman (1954) with the following sentence : "Stars with combination spectra show simultaneously very high excitation lines and low temperature absorption features, but cannot be considered certain binaries. Some or all may however be so. A number of these stars show nova-like variations". This definition is still valid and includes a variety of objects like very slow novae, recurrent novae, Mira variables, semiregular variables. Some of them are clearly binaries; the majority are not clearly so, although binariety is the most obvious explanation of their characteristics; a few could be red giants in the transition stage to planetary nebulae. Hence, rather than a homogeneous class of objects, we are considering a phenomenon- the symbiotic phenomenon- which occurs any time we have a red giant or supergiant producing an extended circumstellar envelope, and a source of energy able to ionize and excite the circumstellar gas. This source can either be a hot companion, or a source of mechanical or magnetic energy furnished by the red giant itself, or by a hypothetical companion.

The main results of ultraviolet observations of these objects (the majority of which are very faint, and none of which was observable before the IUE "era") are: a) the study of the continuous spectrum shows that in some cases it is very similar to that of dwarf novae, e.g. a combination of the emission from a very hot subdwarf (Rayleigh -Jeans tail of a black body -RJ BB- with

TABLE 1. MAIN PROPERTIES OF THE BEST STUDIED SYMBIOTIC STARS: OPTICAL OBSERVATIONS.

NAME Mag. and Sp-type	Photometric characteristics and variability	Optical emission spectrum	Notes and essential references
EG And 7.4–7.6 M2III (TiO)	Slow variations, P 470^d.	HI, [OII], [NeIII], no 4686 HeII. Weak Blue continuum.	Var. Magn. field? (1)
Z And 8–12.4 M6.5III (TiO)+Beq	Outbursts of 4mag. at intervals of 10–20yrs. Fluctuations with intervals between maxima ranging between 310 to 790 days.	PN-like [NeIII], [O III] [FeV, VI, VII], TiO bands in red.	At outburst: M spectrum not observable, veiled by blue continuum; P Cyg absorp.; excitation decreases (2)
R Aqr 5.8–11.5 M7e	Mira variable, P 386^d; variations of maxima and minima because of activity of a secondary? P_{orb}∿44 yrs?	HI, MgI, MnI, FeI, SiI, FeII, [FeII], [OII], [OIII], [NeIII], [FeXIII] λ 10747.	Blue continuum present in 1919–49; absent in 1964–65. (2,3)
T CrB 2.0–10.8 gM3+sdBe	Rec. Nova, outbursts at intervals∿80 yrs. Binary, P_{orb}= 227.6 d.	Hα, no HeI in 1936; [FeX, XIV] in 1946 during decline.	Excitation increases with declining light after outburst. (2)
CH Cyg 7.4–9.1 M6IIIe	Semiregular P∿700d. Activity phase not correlated with brightening. Binary ? P∿15 yrs ?	HI, CaII, MgI, HeI, FeII, [FeII], [OI], sometimes [OIII].	Typical M6III in quiet, blue cont. and emis. in activity phase. (4)
CI Cyg 10.7–13.1 M4III+Bep	Nova like outbursts + eclipse: P_{orb}∿855 d.	[OII], OIII, [OIII], [NII], NIII, FeII, [FeIII], V, VI, VII, X].	Slow spectral variability. (2,5)
V1016 Cyg 11.3–17.5	Slow Nova? Present in IR plates in 1947; Absent in blue plates before 1961. Brightening from B∿15 to B∿10 in 1966.	[OI], HeII, OIII, [OIII], NeIII, [NeIII, IV, V/, [ArIV], [FeVII].	Typical spectrum of PN with steadily increasing excitation after outburst. (6,7,8,9)
AG Dra 9.1–11.2 gKp	After outburst the G-K spectrum changes in a featureless blue continuum.	[FeVI] present, [FeVII] absent	(10)
YY Her 11.7–13.2 M2ep		Upper limit to ionization excitation of 30eV:	in conflict with UV observations or evidence of vast changes in thermal excitation. (11,12)
RW HYa 10.0–11.2 gM2ep	Slow variation, P∿370 d.	HI, HeI, HeII, [OIII], [NeIII] OIII.	(2,13)
BX Mon 9.5–13.4 gM4ep	Very LP variable, P=1374 d.	Broad Balmer emissions.	(12)
SY Mus 11.0–12.3 M3II–III	Semiregular variable P=623 d.	HI, HeI, HeII, SiII, CaII, FeII, [FeI], NIII, OIII, MgI, SiI.	At brightening the forbidden lines are very weak. (14,15,16)
AG Peg 6–9 M2III	Very slow nova (1840 V=9, 1870 V=6, 1980 V=8.3) Binary, P_{orb}=820 d. SR var. P∿600–700 d.	NII, NIII, [OIII] strong, CII, CIII weak, NIV, OI 8446.	Evidence of mass transfer from the hot to the cool component. (2,17,18)
RX Pup 11.1–14.1	Mira var. P=580 d.	In 1941: HeII, [NeV], [FeVII]; in 1968 low excitation; in 1979–80 [OIII], NIII, [FeII, III].	IR excess but no trace of TiO bands. (19,20,21)
CL Sco 11.2–13.9 Pec.		4686 HeII absent; Balmer series in emission.	(12)
τ^{4}Ser 7.5–8.9 M5IIb–IIIa	Slowly varying Irr. Var.	1972: no emission; 1978: strong Hα, Hβ emiss. with inverse P Cyg contour; eruptive event ?	(22,23)
HM Sge 11–16 IR excess	Brightening from B 15 to B 10 from April to Sept. 1975.	Early observ.: [FeII], [OI], [OIII], [NeIII]; in 1977 broad emissions, type WR star; 1979–80: increased excitation: [FeVI, VII] appear [FeII, III] decrease, but [OI], [N II] always present.	(7,24,25 26,27)
RR Tel 6.5–16.5 TiO bands in red	Very slow nova; 1928–1944: variation with P=386.73 d. Oct. 1944 outburst, 14m to 7m. At 7 m until 1949; in 1953 V=9.	[FeVII], [NiVI]; strong Balmer continuous emission.	(28,29)

REFERENCES: 1) Smith, 1980; 2) Swings, 1970; 3) Johnson, 1980; 4) Faraggiana, Hack, 1971; 5) Iijima, 1981; 6) Baratta, Cassatella, 1974; 7) Ciatti et al. 1978; 8) Flower et al., 1979; 9) Nussbaumer, Schild, 1981; 10) Smith, Bopp, 1981; 11) Allen, 1979; 12) Michalitsianos et al., 1982; 13) Merrill, Humason, 1931; 14) Henize, 1951; 15) Glass, Webster, 1973; 16) Feast et al., 1977; 17) Hutchings et al., 1975; 18) Szkody, 1977; 19) Swings, Struve, 1941; 20) Swings, Klutz, 1976; 21) Klutz et al., 1978; 22) Jennings, 1972; 23) Sato et al., 1978; 24) Ahern, 1975; 25) Stover, Sivertsen, 1977; 26) Thronson, 1981; 27) Blair et al., 1981; 28) Allen, 1980; 29) Raassen, Hansen, 1981.

TABLE 2. Main Properties of the ultraviolet spectrum of the best studied symbiotic stars.

NAME	Observation phase	Continuum	Emission Lines	Notes and references
EG And		No evidence.	HeII,CII,CIII]1909,CIV,NIII],IV],V, OIII],MgII,SiIII,IV.	No IR excess,BB for M-type $N_e \sim 3\ 10^9$ cm^{-3}. (1)
Z And	Quiescent	Fitted by BB at T = 43000K.	HeII,CIII]1909,CIV,FeII,III,OI,III[V], SIV,MgI,II[V],AlII,III,SiII,III,IV.	No IR excess,BB for T = 3050 K. $N_e \sim 10^{10}$ cm^{-3}. (2)
R Aqr	At V= 6.8 V=10.6 V=11.2	Flat(Balmer recombination + anomalous reddening?	HeII,OI,CIII]1909,CIV,NV,SiII,III,IV MgII.Some lines vary,some do not,but not in phase with the Mira light curve.	UV continuous flux almost constant, while V varies between 6.8 and 11.2.Radio-emitter. (3,4,5,6)
T CrB	Quiescent	Rather flat.It can be fitted by a model T_e11000K, log g=2.	HeII,CIV,NIII],OIII],NIV],SiIII], MgII.	MgII lines have P Cyg profiles similar to ζ Aur. (7,8)
CH Cyg	Activity started in 1977	Rather flat:Balmer recombination (weak emission at λ 3647) or A-F stellar continuum?	OI,SiII,III,CIII]1909,NI, FeII(mult.191) MgII:(P Cyg) FeII(LWR):inverse P Cyg.	Slight IR excess (silicate bump at 4.9 μ).Many strong absorption lines of once ionized metals are present in SWP and probably SiIV, CIV but no NV. N_e 10^9–10^{10} cm^{-3}. (9,10)
CI Cyg	During a full orbit (1979–81)	Weak Balmer recombination.	HeII,CIII],CIV,NIII],NIV],NV, OIII,OIII],SiIII],SiIV.	Overall decline in UV emission consistent with decline in optical emission following outburst of 1975.However HeII,CIV,NV appear to increase. (11,12)
V1016 Cyg		Flat Balmer,HeI,HeII recombination + hot star (160000K).	HeI,HeII,OI,CIII]1906,1909,CIV, NIII,IV,V,SiII,III,IV,[MgV],[NeV], [AV],FeII,MgII.Typical PN spectrum.	Strong IR excess, Variable radio emitter, X ray source. $N_e \sim 3\ 10^6$ cm^{-3}, $T_e \sim 16000$ K. (13)
AG Dra	Quiescent and outburst (Nov.1980)	Not compatible with BB, Faint continuum,SWP. Flux increases at outburst.	Variation depends upon ion:NIV 1486, NV 1240 ∿ constant,CIV,SiIV+OIV increase dramatically from June to Nov.1980. 1981:strong permitted and weak intercombination lines of OI, MgII,HeII,OV,SV,MgII:inverse P Cyg; NV:P Cyg with $v = -100$ Km s^{-1}.	X ray emitter. Absorption lines prominent in LWR. $N_e \sim 10^{10}$–10^{11} cm^{-3}. (14,15)
YY Her		Combination of RJ BB tail for T ∿ 10^5K + stellar cont. for T ∿ 10^4K + nebular recombination.	HeII,CIII,CIV,NIV,V,OI,OIII],OV], MgII,[MgV],SiIII],[NeV],MgII:[MgV]≪1 excitation in contrast with optical data (upper limit 30 eV).	Faint radio emitter.No IR excess M-type emission. (16)
RW Hya		Strong far UV rising toward short λλ.Hot star with T ∿ 10^5K; near UV:nebular recombination.	HeII,CIII,IV,NIII,IV,V,OI,III,IV, MgII,SiIII,[SV].	$10^8 < N_e < 10^9$ cm^{-3}. (17)
BX Mon		Similar to A5 star;it can be fitted with a Kurucz model.	CIII],IV,NIII],OIII,SiIII],SiIV.	No IR excess. In LWR strong absorptions of MgII,MnII,FeII compatible with A-type star. (16)
SY Mus	Quiescent until brightening of May–June 1981	Before brightening:nebular cont.no evidence of RJ BB tail; after: RJ BB tail for $T_e \sim 40000$ K.	HeII,CIV,NIII,OI,III,IV,[MgV], SiIV,SIV,FeII. Many emissions in LWR.	No IR excess,stellar M-type spectrum June 1981: $N_e \sim 10^8$ cm^{-3}. (16,18,19)
AG Peg		Evidence of hot star $T_e \sim 30000$ K.	HeII,CIV,NIV,NV,OIII,SiIV P Cyg absorptions are present: e.g. 1550 CIV.	Radio emitter, No strong IR excess. $N_e \gtrsim 10^{10}$ cm^{-3} (20)
RX Pup		Continuum mimics stellar spectrum later than A0.	HeII,CIII]1909,CIV,NIII];NIV],OI, OIII],OIV],SiII,III,SiIV,MgII. Line profiles are very complex,multi-components.	IR excess explicable by thermal radiation from dust at T ∿ 10^3K; radio emitter. N_e 10^9–10^{10} (21)
CL Sco		Continuum rises toward longer λλ.	Low excitation, no NV. CIII],CIV, NIII],SiIII],SiIV,OI,III].	BB IR for M star. (16)
τ ^{4}Ser		Continuum rises gradually toward longer λλ.	Low excitation, no emission except MgII.	MgII lines show strong absorption reversal. (22)
HM Sge		Very weak continuum.	HeII,NIV,V,CIII,IV,OIII,OIV,MgII, SiIII.	Variable radio emitter, Strong IR excess, X-ray source. $N_e \gtrsim 10^6$ cm^{-3} (23)
RR Tel		Complex continuum:nebular + A-type star + hot star.	HeI,II,CIII]1906,1909,CIV,OI,IV],V, MgII ,[MgV],SiII,III,IV,SiV,[NeIV], [NeV],[NaV],[AV],FeII,[FeIV],[FeVI], [CaV].	Radio emitter, Strong IR excess (CS dust), X-ray source. $N_e \sim 10^6$ cm^{-3} (24)

REFERENCES: 1) Stencel,1980;2) Altamore et al.,1981;3) Michalitsianos et al.,1980;4) Johnson,1980;5) Johnson,1981;6) Johnson,1982; 7) Stencel et al.,1981;8)Plavec,1981;9) Hack,Selvelli,1981;10) Hack, Selvelli,1982;11) Stencel et al.,1982;12) Michalitsianos et al.,1982,13) Nussbaumer,Schild,1981;14) J. Lutz, T. Lutz,1981;15) Fredjung,Viotti,1982;16)Michalitsianos et al.,1982;17) Kafatos et al.,1980;18) Michalitsianos et al.,1982;19) Michalitsianos et al.,1982;20) Keyes,Plavec,1980;21) Kafatos et al.,1982;22) Kafatos et al.,1981;23) Flower et al.,1979;24) Allen,1981.

$T \sim 10^5$ K, $F_\lambda \propto \lambda^{-4}$) and an accretion disk ($F_\lambda \propto \lambda^{-7/3}$); in some cases it is rather flat and can be explained by a stellar continuum for $T \sim 10^4$ K. In some cases it can be attributed to free-free and bound-free transitions. b) the LWR range of the spectrum permits us to obtain an independent determination of the interstellar extinction by means of the feature at λ 2200, to be compared with the determinations obtained in the visual or UV range, by comparison of the intensities of emission lines whose relative intensities are well known (on the hypothesis that they are formed in an optically thin layer). c) the emission line spectrum is often very similar to the spectra of young, relatively dense planetary nebulae. It can give information on the electron density and electron temperature of the CS envelope; on the various spectroscopic mechanisms producing the different lines, permitting to verify directly predictions made by means of the transitions observed in the optical or IR range ; and, by studying a larger range of excitation than that available from the optical spectrum only, to obtain more complete information on the stratification of the elements in the CS envelope, accretion disk, streams, and chromosphere and corona of the cool giant. For these purposes, atomic data like those provided by the work of Garstang (1981), and computations of line intensity dependence on T_e and N_e, made by Nussbaumer (1982) and collaborators, are greatly needed. d) stellar absorption lines are rarely present. In some cases the absorption line spectrum appears during the outburst phase, as occurs in envelopes of novae at maximum.

The conclusions we can draw from UV observations are that at least in some cases the shape of the continuum makes it possible to ascertain the presence of a hot subdwarf. Moreover, during the IUE age it has been possible to observe interesting phenomena like activity phases for AG Dra, SY Mus and CH Cyg, and eclipses for CI Cyg.

MAIN CHARACTERISTICS OF THE BEST STUDIED SYMBIOTIC STARS.

Table 1 summarizes the main properties of some well known symbiotic stars, as derived from optical studies, while Table 2 summarizes the results obtained using IUE observations. I will try to divide these stars into groups according to some common properties derived from the UV spectrum.

UV continuum: EG And, V1016 Cyg, HM Sge are characterized by a very faint continuum (practically absent in the case of EG And); Z And, YY Her, RW Hya, AG Peg have UV continua which clearly indicate the presence of a hot companion, with temperatures in the range of $3\ 10^4 - 10^5$ K (RJ tail of high temperature BB). In the case of YY Her and RW Hya also a flat continuum, due to Balmer recombination, is present. In the case R Aqr, BX Mon, T CrB, CH Cyg, CI Cyg, RX Pup, CH Sco, $\tau\ ^4$Ser, the continuum is rather flat or rises slowly toward larger $\lambda\lambda$, and can be explained by Balmer recombination, or also by a stellar continuum for temperatures ranging between $10^4 - 8\ 10^3$. Special cases are SY Mus and RR Tel. SY Mus has been observed in a quiescent state, and again, after a brightening occurred, between Sept.'80 and May'81. Before brightening

there was no evidence of a RJ tail of hot BB, while after brightening a RJ tail of a BB at T∿40 000 K was evident. The continuum of the very slow nova RR Tel is quite complex, and can be explained by the presence of a nebular continuum + A-type stellar continuum.

Emission line spectrum: the majority of the symbiotic stars studied with IUE have emission line spectra where very high to low excitation lines are present, typically emission lines of OI, MgII, FeII and HeII, CIV, NV are observed; in some cases (Z And, V1016 Cyg, AG Dra, YY Her, SY Mus and RR Tel) still higher excitations are present, and lines of OV, NeV, NaV, MgV, CaVI and FeVI (IP∿100 to 141 eV) are observed together with OI and MgII. Lower excitation spectra than the majority of SS are shown by CH Cyg, BX Mon, CL Sco, τ ^{4}Ser (this last one has very low excitation: only MgII lines are present). A loose correlation between excitation and type of continuous spectrum has been found (Table 3).

TABLE 3.

Correlation between excitation of the emission lines and shape of the continuum.

Excitation	Continuum		
	Hot RJ BB	Flat	A-F type
High	Z And, V1016 Cyg YY Her, SY Mus, AG Dra		
Average	RW Hyd, AG Peg	EG And, R Aqr, T CrB, CI Cyg RX Pup, HM Sge	
Low			CH Cyg, BX Mon, CL Sco, τ ^{4}Ser

In some cases there is some discrepancy between the degree of excitation observed in the UV and in the visual or IR spectrum. For instance, R Aqr presents an average degree of excitation both in the UV and visual range, but the presence of λ 10747 [FeXIII] has been reported (IP = 361 eV) by Zirin (1976); T CrB during decline in 1946 showed lines of FeX and FeXIV; CI Cyg in the optical range shows lines of FeV, VI, VII and X; visual observations indicate an upper limit of 30 eV for YY Her; SY Mus has a rather low excitation in the visual (up to HeII, OIII), while it shows MgV in the UV. Since almost all or probably all of these objects are variable it is impossible to say whether there is any real discrepancy between the degree of excitation in the IR, visual and UV ranges, or whether these discrepancies are only due to strong variations at different epochs of observation. This fact underlines the need for repeated simultaneous observations in UV, visual and IR.

Generally absorption lines are not prominent in the UV spectrum of SS. The few cases where they are present, escape any attempt at classification.

T CrB shows P Cyg profiles of MgII resonance lines; CH Cyg is a special case in that it presents numerous and strong absorption lines in the far UV; especially strong are all the ground level lines of NiII; complex absorption profiles of SiIV and CIV are present also, but no NV. In the near UV lines of ionized metals, FeII, MnII, CrII have inverse P Cyg profiles while MgII lines have direct P Cyg profiles with double absorptions. AG Dra also shows absorption lines in the near UV; in the far UV the NV lines have P Cyg profiles.
BX Mon, whose continuum suggests the presence of an A-type companion, also shows absorption lines of FeII, MnII, MgII, which are typical for an A-type spectrum.AG Peg shows P Cyg absorption at CIV lines. MgII lines in τ ^{4}Ser present a strong absorption reversal redshifted by 80 Km/s with respect to the emission contour.

Electron densities have been determined for several objects both from UV and from visual spectra. Where both measurements exist, we observe that electron densities derived from the optical spectrum are systematically lower by several orders of magnitude than those derived from the UV. Probably this is just evidence of the stratification effects in the CS envelope; actually lines generally used to derive the electron density in the optical range are forbidden lines, like the nebular lines and 4363 [OIII], while in the UV semiforbidden lines are used like CIII] 1909 and 1906 or 1892 SiIII].

Nineteen symbiotic stars have been observed by Allen (1981) with the Einstein Observatory, but only three of them have measurable X-ray flux:HM Sge, V1016 Cyg and RR Tel, in decreasing order of intensity. More recently also AG Dra has been detected in the X-ray range by Anderson et al. (1981). As remarked by Allen,"it might have been anticipated that the symbiotic stars with highest excitation would be the strongest X-ray sources. Instead this is not the case. The only correlation which appears to be present is between the X-ray flux and the type of variability: specifically stars which have undertaken slow nova outbursts in historic times are detectable X-ray sources." CH Cyg, which is an especially low excitation symbiotic, is possibly another X-ray source, at least during its activity phase, since it is situated in the error box of an X-ray source detected with Einstein (Marshall et al. 1979). We cannot rule out that soft X-ray emission is a common characteristic of symbiotic stars in their activity phase. Hence it is important to obtain simultaneous observations in UV and X. This is one of the programs proposed by a group of European astronomers for simultaneous observations with IUE and EXOSAT.

The stars observed in quiescent and activity phase in general show spectral variations recalling those of novae: the excitation increases with declining light; permitted lines decrease and forbidden lines increase. Most of them present emission lines in quiescent phase. A special case is CH Cyg, which shows a completely normal M6 III spectrum during its long periods of quiescent phase, and shows strong permitted and forbidden emission lines during its recurrent activity phases.

From what said above, it is not easy to classify SS. We will describe

more extensively at least a few objects which have been studied very recently: for instance, AG Dra; CH Cyg, one of the lowest excitation object; the Mira variable R Aqr and the eclipsing binary CI Cyg; SY Mus observed before and during brightening; RR Tel which is at the same time a typical SS and a very slow nova; V1016 Cyg and HM Sge which are probably very young PN rather than typical symbiotic stars with evidence of binariety.

The high velocity symbiotic star AG Dra just few months before IUE observations by Altamore et al. (1982), underwent a major luminosity increase followed by large spectral variations. In the UV the continuum and the emission lines have largely increased their intensity after the outburst while the IR photometry, made by C. Eiroa at Almeria, and by M. Ferrari-Toniolo and P. Persi at TIRGO seems to suggest that no variation occurred for the cool component of AG Dra.

A high excitation symbiotic, SY Mus, has been studied by Michalitsianos et al. (1982) at two different epochs, before brightening (Sept. 1980) and after (June 1981). The entire UV spectrum brightened between Sept. and June by a factor of 5, while the IUE FES magnitude brightened by only 0.3m. A very interesting variation is shown by the continuum energy distribution. In Sept. '80 the continuum had a complex shape suggesting a combination of a hot star emission plus nebular recombination emission. After brightening, on the contrary, the whole IUE range is closely fitted by a stellar continuum for T_e = 40000 K. All permitted and semiforbidden lines increase in intensity, while forbidden lines, like those of MgV and NeV, decrease after brightening. A similar behavior is observed in the optical range, which in May '81 is dominated by permitted emission lines.

High resolution observations of RX Pup have been made by Kafatos et al. (1982). This star, which at some epochs presents strong excitation lines (IP$\sim$100 eV, Swings and Struve, 1941), while at others it shows only a low excitation spectrum (Sanduleak and Stephenson,1973), does not show any clear evidence of the presence of an M type star, except for variability observed in the region 1-4μ (Feast et al. 1977) and for the detection of H_2O and CO absorption at 2μ (Barton et al. 1979). The high excitation lines of HeII, OIII], CIII], CIV, SiIII] show complex emission profiles with Doppler displaced multiple components and possible inverse P Cyg profiles in NIII] and NIV] , suggesting dynamic activity in the CS material.

CI Cyg, which is a well-ascertained eclipsing binary, has been observed with IUE during the course of nearly a full orbit (P = 855 d). Stencel et al. (1982) report that both secular and eclipse variations are observed: the unblended intercombination lines exhibit clear evidence of the eclipse, plus a secular decline inversely related to the excitation. The permitted lines of NV and HeII increase with time, while MgII decreases with time. Different lines show different eclipse depths, thus indicating that they are formed in different regions. While HeII shows a deep eclipse, as expected, indicating that it is formed near the hot companion, the NV lines are not eclipsed at all, thus

suggesting that they are formed far away from the hot component. Also the OIII lines at λ 2837 and λ 3130, fluorescently pumped by HeII λ 304 are not eclipsed. Instead semiforbidden lines have eclipse depths decreasing with decreasing IP, indicating, as expected, that they are formed at increasing distance from the hot star.

R Aqr has been studied by Michalitsianos et al. (1980) and by Johnson (1980, 1981, 1982) both in high and low resolution modes. Radio, optical and UV observations give evidence of the presence of a nebula with N_e included between 10^5 and 10^8 cm^{-3}, T_e between 10^4 and 3 10^4 K, and size between 10^{14} and 10^{15} cm. The M7 giant is a Mira variable with light variation, in a period of 387 days, similar to that of an ordinary Mira variable. The brightening observed in 1934 was probably an eruption event like a mild nova. Interesting results of the UV observations are: 1) the continuum flux intensities are practically constant while the visual magnitude varies between 11.2 and 6.8 (Johnson 1982); 2) the continuum between 1200 and 3100 A is remarkably flat; the absence of any detectable dip at λ2200 is incompatible with the color excess E_{B-V} = 0.67 derived by Wallerstein and Greenstein (1980) from the Hα/Hδ emission line ratio and confirmed by Kaler (1981). This flatness and the absence of the bump at λ2200 is explained by Johnson (1982) by suggesting that olivine is responsible for the extinction. Actually olivine is expected to condensate in the ejecta of oxygen-rich giants (Gilman 1969); 3) the asymmetry in the line profiles of the MgII doublet can be interpreted as due to mass ejection at 200 Km/s.

V1016 Cyg has an high excitation spectrum, both in the optical and in the ultraviolet range, very similar to that of planetary nebulae. The electron density is lower than that of the other CS envelopes of SS, as indicated by the presence of 1906 CIII] in its HR spectrum, while generally only λ1909 is present. An IR excess of 7 mag. and detectable radioemission (Purton et al. 1973) indicate the presence of a rather extended cool envelope, while the high excitation optical and UV emission lines, the UV continuum and the X-ray flux indicate the presence of a hot subdwarf with T = 160000 K, R = 0.06 R_o (Nussbaumer and Schild 1981).

Similar characteristics are shown by HM Sge, (Flower et al. 1979; Kindl and Nussbaumer, 1982). Both these objects can be interpreted as planetary nebulae in formation.

The very slow nova RR Tel has been studied in the high and low resolution modes (Penston et al. 1982). It has in common with V1016 Cyg and HM Sge the IR excess and the detectable radioemission, as well as detectable X-ray emission, and the relatively low density, indicated by the presence of 1906 CIII]. According to Penston et al. the energy distribution can be explained by several components, e.g.: 1) the nebular emission; 2) a hot source, necessary for explaining the high ionization of the envelope, but also suggested by the slow increase of the flux with decreasing wavelength, and by the ratio between the flux at λ<912 A (given by the total flux in the emission lines which presumably

originate from absorption by the gas of the stellar continuum shortward of the Lyman limit) and the flux in the IUE range (1200-3200 A); this ratio gives $T > 7\ 10^4$ K, and 3) a star of spectral type near A0, which is necessary to explain the decrease towards longer wavelengths, which is too slow to be explained by the two previous sources only. It is worth recalling that before the outburst of 1944 the spectrum, according to Henize and McLaughlin (1951) presented absorption features typical of an A-F star.

Diagnosis by means of the emission lines gives for the nebula a value of N_e included between 10^5 and $5\ 10^6$ cm^{-3} and T_e between 11600 and 19000 K.

CH Cyg (Hack and Selvelli, 1982a, 1982b) has been observed with IUE in 1978, 79, 80 and 81 both in the high and low resolution modes, and in the optical range from the start of its third observed outburst in 1977. The continuum derived from both high and low resolution spectra increases by a factor of 16 at λ1400 from Sept. 1979 to Dec. 1981, while the visual magnitude derived by the FES counts and using the values of B-V measured by Hopp and Witzigmann (1981) passes from 6.12 in 1979 to 5.3 in 1981. Fluctuations of 0.11 mag. in less than 40 min. were observed. The continuum is very flat from 1500 to 5500 A (V mag.) and decreases toward λλ shorter than 1500 A. It can be fitted very well with the Kurucz (1979) model for T_e = 8500 and log g = 1. Hence the continuum simulates the presence of a late A supergiant. If this were really there it would dominate the optical range, because its absolute visual magnitude would be at least 3 mag. brighter than that of the M6 III star. The line spectrum of CH Cyg indicates some interesting spectroscopic mechanisms: 1) for FeII we observe multiplet 191 at λ1785 in emission while multiplet 9, λ1260 as well as all the other FeII lines in the SWP range are in absorption. This indicates that a "closed circuit" scheme is working:

a^6 D ⟶ x^6 P^o (mult. 9, λ∿1260 in absorption)
x^6 P_o⟶ a^6 S (mult. 191, λ∿1785 in emission)
a^6 S ⟶ a^6 D (mult. 7F, visual range, in emission)

2) MgI, AlII and SiIII, together with MgII, AlIII and SiIV form two iso-electronic sequences. All the intersystem lines of the first sequences, 4571 MgI, 2669 AlII and 1892 SiIII, are present in emission: actually the low-lying metastable term is easily populated by collisions. On the contrary, only the resonance line of MgI 2852 is present because λ1670 AlII and λ1206 SiIII need higher electron energies to be populated. In the other sequence only MgII λ2800 is observed in emission, probably because the electron energy is not sufficient to populate the first excited level of AlIII and SiIV. 3) It is very interesting to note the presence of the OI triplet at λ∿1300 with an observed intensity ratio very different from the theoretical one, and the simultaneous presence of the semiforbidden line at λ1641. The same phenomenon is observable in several other stars (although in some cases λ1641 has been wrongly identified with λ1640 HeII): the symbiotics Z And, V1016 Cyg, RW Hya, RX Pup, RR Tel and the peculiar emission line star HD 45677. The anomalous ratio in the λλ1300 triplet

indicates that the physical conditions are far from the optically thin case. To explain the presence of λ 1641, which has the same upper level as λ 1300, Hack and Selvelli (1982a,b) have proposed the following picture: because of the large optical thickness the λ 1303 resonance photons will scatter many times before eventually escaping from the 0° region. These resonant photons can be considered as "trapped radiation". If the scattering number is very high, processes with a small probability per scattering of destroying resonance lines can become important (Hummer, 1968; Osterbrock, 1962). This fact will have two consequences:1) Anomalous line ratio. The 0.00 level is more populated and therefore after many scatterings, substantial reabsorption will occur mostly from this zero-volt level and the λ 1302 line will be weaker; the 0.04 level, on the contrary, is less populated and therefore the λ 1306 line will be less re-absorbed and will turn to be stronger. 2) There is a very small but finite chance that at each coherent resonance scattering, decay from the upper term $3s\ ^3S^\circ$ will occur through the λ 1641.3 intersystem emission line $3s\ ^3S^\circ \rightarrow 2p^4\ ^1D$ that shares the upper term with the λ 1303 lines. Unlike the λ 1303 photons that are trapped, the λ 1641.3 photons will leave the 0° region undisturbed. It is obvious that the more numerous the scattering processes, the stronger the λ 1641.3 intensity.

MODELS AND CONSTRAINTS POSED BY UV OBSERVATIONS.

The main question about symbiotic stars is: are they all binary systems or can some of them be explained by a single star model ? What new constraints and what proofs in favor of the one or the other class of models have been given by UV obsevations ? A very exhaustive and critical discussion of these problems was made by Friedjung at the IAU Colloquium on Symbiotic Stars held last summer in St. Michel (1982).

Those stars for which the IUE SWP range has made it possible to detect the RJ BB tail of a hot subdwarf and IR observations, on the other hand, have shown a BB IR continuum explicable with the presence of a cool giant, also when the M spectrum is not clearly detectable in the optical range, are clearly binary systems: however their radial velocity variations are generally not those expected from a simple non-interacting system. To complicate the problem further, the cool star is often a Mira or a SR variable and probably shows also radial velocity variations due to pulsation. Accretion from the cool star is thought to be very important in explaining many characteristics of the symbiotic stars; models analogous to those for dwarf novae have been computed by Bath and Pringle (1982), and are able to predict some features of the light curve, and to show that flickering with timescales of hours or days rather than seconds to minutes as in dwarf novae, is expected. However, in several symbiotic systems the red giant is not filling its Roche lobe. In these cases accretion may occur from stellar wind, but the line profiles generally do not indicate high expansion velocities. In some cases there is evidence of winds from the hot component too. Collision between winds from the two components may be important.

In several other cases the cool giant dominates the optical spectrum, while the hypothetical hot companion does not show up in the UV range, and the ultraviolet continuum can be explained by nebular recombination, or in other cases it may mimic an A-F type star. In the case of V1016 Cyg, HM Sge and RR Tel, the hot star continuum is weakly present. No trace of the cool giant is observable. Several authors have proposed a single star model for V1016 Cyg (Nussbaumer and Schild, 1981; Kwok, 1977; Ahern et al., 1977). It is possible that these three stars, which had a nova-like outburst in 1946 (RR Tel), 1963 (V1016 Cyg) and 1975 (HM Sge), were all cool giants on the asymptotic branch, and that they are now becoming very young planetary nebulae. Actually, of all the symbiotic stars studied in the HR mode, only V1016 Cyg and RR Tel show 1906 CIII] , although it is much weaker than that observed in the spectrum of planetary nebulae.

Single star models have been proposed also in the case where the M giant is clearly observable. High excitation emission lines such as those observed in symbiotic stars are actually present in the solar-type coronas, but with much lower intensity. Moreover they have not been observed in the UV spectra of later type giants. However, we cannot rule out that at least giants on the asymptotic branch may have an exceptional coronal activity, as a consequence of He-flashes. According to calculations by Wood (1974), internal instabilities can produce observable properties, resembling those of some symbiotic stars. According to recent calculations by Deupree and Cole (1981) the core He-flash can produce mass loss with velocity on the same order as that observed during the outburst of CH Cyg (about 150 Km s^{-1}).Moreover, calculations by Schönberner (1979) indicate that stars on the asymptotic branch, having core masses between 1 and 1.4 solar masses have very short interflash periods, on the order of 100 and 10 yrs respectively. Hence we suggest that stars like CH Cyg, for which there is no clear evidence of binariety, may be such objects, representing an earlier phase than that indicated by V1016 Cyg, on its way to become a planetary nebula.

It is a pleasure to thank all colleagues who made available to me their unpublished results. Especially I would like to thank Roberto Viotti who sent me the Proceedings of the IAU Colloquium No. 70 before publication. Many thanks are due to Ms. L. Canziani for typing the manuscript.

REFERENCES

Ahern, F.J. 1975, Ap. J., 197, 639.
Ahern, F.J., Fitzgerald, M.P., Marsh, K.A., Purton, C.R. 1977, Astr. Ap.,58,35.
Allen, D.A. 1979, in IAU Colloquium 46, Changing Trends in Variable Stars Research, ed. F.M. Bateson, J. Smak, I.H. Urch (Waikato University).
Allen, D.A. 1980, M.N.R.A.S., 192, 521.
Allen, D.A. 1981, M.N.R.A.S., 197, 739.
Altamore, A., Baratta, G.B., Cassatella, A., Friedjung, M., Giangrande, A., Ricciardi, O., Viotti, R. 1981, Ap. J., 245, 630.

Altamore, A., Baratta, G.B., Cassatella, A., Giangrande, A., Ponz, D., Ricciardi, O., Viotti, R. 1982, in IAU Colloquium 70, The Nature of Symbiotic Stars, ed. M. Friedjung and R. Viotti (Reidel Pub. Co., Dordrecht).
Anderson, C.M., Cassinelli, J.P., Sanders, W.T. 1981, Ap. J. (Letters), 247, L127.
Baratta, G.B. and Cassatella, A. 1974, Ap. J., 187, 651.
Barton, J.R., Phillips, B.A., Allen, D.A. 1979, M.N.R.A.S., 187, 813.
Bath, J.T. and Pringle, J.E. 1982, preprint.
Bidelman, W.P. 1954, Ap. J. Suppl., 1, 175.
Blair, W.P., Stencel, R.E., Shaviv, G., Feibelman, W.A. 1981, Astr. Ap., 99, 73.
Ciatti, F., Mammano, A., Vittone, A. 1978, Astr. Ap., 68, 251.
Deupree, R.C. and Cole, P.W. 1981, Ap. J. (Letters), 249, L35.
Faraggiana, R. and Hack, M. 1971, Astr. Ap., 15, 55.
Feast, M.W., Robertson, B.S.C., Catchpole, R.M. 1977, M.N.R.A.S., 179, 499.
Flower, D.R., Nussbaumer, H., Schild, H. 1979, Astr. Ap., 72, L1.
Friedjung, M. and Viotti, R. 1982, private communication.
Friedjung, M. 1982, in IAU Colloquium 70.
Garstang, R.H. 1981, in Proceedings North American Workshop on Symbiotic Stars, ed. R.E. Stencel (JILA - NBS - Univ. of Colorado).
Gilman, R.C. 1969, Ap. J. (Letters), 155, L185.
Glass, I.S. and Webster, B.L. 1973, M.N.R.A.S., 165, 77.
Hack, M. and Selvelli, P.L. 1982a, in IAU Colloquium 70.
Hack, M. and Selvelli, P.L. 1982b, Astr. Ap., in press.
Henize, K.G. 1951, Ap. J., 115, 133.
Henize, K.G. and McLaughlin, D.B. 1951, Ap. J., 114, 163.
Hopp, U. and Witzigmann, S. 1981, IBVS No 2048.
Hummer, D.G. 1968, in IAU Symposium 34, Planetary Nebulae, ed. D.E. Osterbrock and C.R. O'Dell (Reidel Pub. Co., Dordrecht).
Hutchings, J.B., Cowley, A.P., Redman, R.O. 1975, Ap. J., 201, 404.
Iijima, T. 1981, Astr. Ap., 94, 290.
Jennings, M.C. 1972, Ap. J., 177, 427.
Johnson, H.M. 1980, Ap. J., 237, 840.
Johnson, H.M. 1981, Ap. J., 244, 552.
Johnson, H.M. 1982, Ap. J., Febr. 1.
Kafatos, M., Michalitsianos, A.G., Feibelman, W.A. 1982, Ap. J., in press.
Kafatos, M., Michalitsianos, A.G., Feibelman, W.A., Hobbs, R.W. 1981, in Physical Processes in Red Giants, p. 263, ed. I. Iben, Jr., A. Renzini (Reidel Pub. Co., Dordrecht).
Kafatos, M., Michalitsianos, A.G., Hobbs, R.W. 1980, Ap. J., 240, 114.
Kaler, J.B. 1981, Ap J., 245, 568.
Keyes, C.D. and Plavec, M.J. 1980, in The Universe at Ultraviolet Wavelengths, p. 443, ed. R.D. Chapman (NASA, Goddard Space Flight Center).
Kindl, C. and Nussbaumer, H. 1982, in IAU Colloquium 70.
Klutz, M., Simonetto, O., Swings, J.P. 1978, Astr. Ap., 66, 283.

Kurucz, R.L. 1979, Ap. J. Suppl., 40, 1.
Kwok, S. 1977, Ap. J., 214, 437.
Lutz, J.H. and Lutz, T.E. 1981, in Proceedings North American Workshop on Symbiotic Stars.
Marshall, F.E., Boldt, E.A., Holt, S.S., Mushotzky, R.F., Pravdo, S.H., Rothschild, R.E., Serlemitsos, P.J. 1979, Ap. J. Suppl., 40, 657.
Merrill, P.W. and Humason, M.L. 1931, PASP, 44, 56.
Michalitsianos, A.G., Kafatos, M., Feibelman, W.A., Hobbs, R.W. 1982, Ap. J. Febr. 1.
Michalitsianos, A.G., Kafatos, M., Feibelman, W.A., Wallerstein, G.A. 1982, Astr. Ap., in press.
Michalitsianos, A.G., Kafatos, M., Hobbs, R.W. 1980, Ap. J., 237, 506.
Michalitsianos, A.G., Kafatos, M., Stencel, R.E., Boyarchuk, A.A. 1982, in IAU Colloquium 70.
Nussbaumer, H. 1982, in IAU Colloquium 70.
Nussbaumer, H. and Schild, H. 1981, Astr. Ap., 101, 118.
Osterbrock, D.E. 1962, Ap. J., 135, 195.
Penston, M.V., Benvenuti, P., Cassatella, A., Heck, A., Selvelli, P.L., Beeckmans, F., Macchetto, F., Ponz, D., Jordan, C., Manfroid, J. 1982, M.N.R.A.S., in press.
Plavec, M.J. 1981, in IAU Colloquium 70.
Purton, C.R., Feldman, P.A., Marsh, K.A. 1973, Nature Phys. Sci., 245, 5.
Raassen, A.J.J. and Hansen, J.E. 1981, Ap. J., 243, 217.
Sanduleak, N. and Stephenson, C.B. 1973, Ap. J., 185, 899.
Sato, K., Kizuchi, I., Yamashita, Y., Norimoto, Y. 1978, PASJ, 30, 557.
Schönberner, D. 1979, Astr. Ap., 79, 108.
Smith, S.E. 1980, Ap. J., 237, 831.
Smith, S.E. and Bopp, B.W. 1981, M.N.R.A.S., 195, 733.
Stencel, R.E. 1980, Ap. J., 238, 929.
Stencel, R.E., Michalitsianos, A.G., Kafatos, M. 1981, in Proceedings North American Workshop on Symbiotic Stars.
Stencel, R.E., Michalitsianos, A.G., Kafatos, M., Boyarchuk, A.A. 1982, Ap. J. Febr. 15.
Stover, R.J. and Sivertsen, S. 1977, Ap. J., 214, L33.
Swings, J.P. and Klutz, M. 1976, Astr. Ap., 46, 303.
Swings, P. 1970, in Spectroscopic Astrophysics, ed. G.H. Herbig (University of California press). p. 189.
Swings, P. and Struve, O. 1941, Ap. J., 94, 291.
Szkody, P. 1977, Ap. J., 217, 140.
Thronson, H.A., Jr., Harvey, P.M. 1981, Ap. J., 248, 584.
Wallerstein G. and Greenstein, J.L. 1980, PASP, 92, 275.
Wood, P.R. 1974, Ap. J., 190, 609.
Zirin, H. 1976, Nature, 259, 466.

IUE SPECTROSCOPIC INVESTIGATION OF

INTERACTING BINARY SYSTEMS

George E. McCluskey, Jr.
Division of Astronomy
Department of Mathematics, Lehigh University

ABSTRACT

The International Ultraviolet Explorer satellite (IUE) has provided us with a wealth of data on essentially every type of close binary system known to us. Both low and high dispersion spectra have provided us with new discoveries, verification of previous interpretations and, most of all, facts which will require modification or complete revision of some of our existing theories. This review will, due to the sheer volume of material already available, primarily limit itself to a discussion of binaries consisting of at least one early-type star, to the Algol systems and to W Serpentis systems.

The OB close binaries almost invariably show a stellar wind. The difference between an "unevolved" early-type system and a slightly "evolved" system is difficult to discern observationally and probably not meaningful in terms of Roche lobes. The ζ Aur stars show complex gas motions and shocks.

Many of the Algol systems show peculiarities in their ultraviolet continua and the resonance lines, particularly Si IV, are of abnormal and variable strength. Emission lines have been detected in several systems during the total eclipse.

The discovery by Plavec (1980) of a group of systems now known as W Ser stars characterized by numerous ultraviolet emission lines will provide much food for theoreticians.

1. INTRODUCTION

The manner in which mass is exchanged between the two components and lost from the system is of decisive importance to the evolution of close binaries. The last decade has seen much effort devoted to the observational and theoretical aspects of this problem. This is exemplified by the reviews of Plavec (1968), Kopal (1971), Paczynski (1971), Rees (1974), Kraft (1975), van den Heuvel (1976), Thomas (1977), and Paczynski (1980), among others.

The general picture of the evolution of close binaries is as follows for systems with initial primary masses greater than about 3-5 solar masses.

a. Detached phase. Both stars are main sequence stars. The more massive star begins to evolve and eventually reaches its critical Roche lobe. If either star is sufficiently luminous, mass may be lost in a stellar wind before the lobe is reached. This is quite effective for massive stars. In some cases, the system arrives (by unknown means) on the zero-age main sequence as a contact system. The subsequent evolution of such a system is also not well understood.

b. Rapid phase of mass loss. The primary component loses mass rapidly during a dynamic phase of mass exchange. The primary will lose a major portion of its mass, some of which leaves the system while the rest is collected by the secondary star. If the mass flow is rapid enough, the Roche lobe of the secondary fills and mass overflows both lobes enveloping the system in a common envelope. Loss of angular momentum and mass during this common envelope stage may drastically reduce the masses and separation of the system, particularly if the evolution takes place as case A (Plavec, 1973).

c. Slow phase of mass loss. The primary star is now less massive than its companion and continues to lose mass slowly. For massive systems, the evolved star becomes a Wolf-Rayet star in some cases. For lower masses, an Algol system apparently results. In this case, the evolved star is a sub-giant or giant with a main sequence companion.

d. Late stages of evolution. A variety of possible evolutionary scenarios may now occur depending on initial conditions and on the amount of mass and angular momentum lost to the system. The original primary may become a white dwarf or a helium burning star. It may then undergo a supernova explosion and become a neutron star or black hole. The now more massive primary will develop a stellar wind if of sufficient mass and with a neutron star or black hole companion, a massive X-ray binary phase may ensue. If the rate of mass loss becomes large, a second common envelope phase will develop and a number of possibilities exist, e.g., a low mass X-ray binary or a cataclysmic binary.

A good understanding of the late stages of close binary evolution will require much further observational and theoretical research. It is the purpose of this paper to discuss some of the contributions which IUE is making towards this goal. Several other invited speakers will discuss Be stars, cataclysmic binaries, symbiotic stars and topics dealing with cool stars in binary systems. Here, I will concentrate primarily on systems with at least one massive O- or B- star and on the Algol binaries.

2. OB BINARIES

Leung (1980) has summarized the observational results concerning early-type contact systems. Several of these have been observed with IUE.

The system AO Cas consisting of two O-type stars was observed with IUE at high resolution by McCluskey and Kondo (1981). A stellar wind with an average velocity of 1880 km s^{-1} originates from the hotter but probably

less massive star. The P Cygni features arising from the resonance lines of N V (1238, 1242 Å), Si IV (1393, 1402 Å) and C IV (1548, 1550 Å) in the stellar wind show narrow absorption features similar to those in single O-type star stellar winds noted by Snow (1979). A number of the primary's "photospheric" lines show non-orbital velocities. McCluskey and Kondo (1981) estimated a mass loss rate of 5×10^{-6} solar masses per year for AO Cas.

The O7f + OB binary UW CMa has been observed with Copernicus and IUE (McCluskey, Kondo and Morton, 1975; McCluskey and Kondo, 1976; Drechsel, et al., 1980, 1981, 1982). The O7f primary has a stellar wind with a mean terminal velocity of 1350 km s^{-1}. A mass loss rate of 2.3×10^{-6} solar mass per year has been derived by Drechsel (1978) who analysed the line profiles in detail. This is in good agreement with the value of 3×10^{-6} solar mass per year given earlier by McCluskey, Kondo and Morton (1975) based on the method of Morton (1967).

Koch, Siah and Fanelli (1979) obtained low resolution IUE spectra of the eclipsing binary V 382 Cyg consisting of an O6 or O7 star and a companion of one or two sub-types later. They found that C IV (1548, 1550 Å) has a P-Cygni profile with some emission. Si IV (1393, 1402 Å) has shortward shifted absorption. An expansion velocity of 2000-4000 km s^{-1} is indicated with a mass loss rate of $4\text{-}8 \times 10^{-5}$ solar mass per year.

Wilson and Starr (1976), using ground based data, investigated SV Cen (B1 V + B6 II-III) and came to the conclusion that the system is in a contact configuration with the secondary component being more massive but underluminous. They concluded that matter was flowing from the more massive to the less massive star at a rate of 4×10^{-4} solar mass per year. IUE spectra of SV Cen have been reported by Drechsel and Rahe (1982). They found that an expanding circumbinary envelope exists with velocities from 800 to 2000 km s^{-1}. No emission was observed. They estimate that 10^{-5} solar mass per year is lost to the system. Extensive optical and IUE observations of SV Cen reported on by Drechsel, Rahe, and Wargau (1982) indicate that the period decrease rate found for this system varies from 0 to -2.15×10^{-5} per year. The mass loss rate varies from 0 to 10^{-4} solar mass per year on a time scale of a few years. The ultraviolet resonance line profiles imply the occurrence of sudden shell ejections in addition to the stellar wind on a time scale of hours. The continuum indicates the existence of a small ($\lesssim$ 1% of the stellar projected areas) source at a temperature of about $2 \tilde{\times} 10^5$ K.

The above systems are all considered by some investigators to be contact systems. A number of other early type systems have been observed with IUE. I will discuss several of them here.

The eclipsing system δ Pic was observed by Kondo and McCluskey (Kondo, McCluskey, and Feibleman, 1980). This system consists of a B0.5 primary and a marginally detectable early B-type secondary. The primary may be of luminosity class III. If the detection of the secondary is correct (Thackeray, 1966) then the primary is the more massive star and the system

might be relatively unevolved.

The IUE high resolution far-ultraviolet spectrum shows that the metastable lines of C III (1175 A) and the resonance lines of Si IV (1393, 1402 A) show excess absorption and velocities as high as 600-700 km sec^{-1}. The phase coverage was not complete enough to decide if a wind or gas streaming is present. The origin of this gas is the primary star. Circumbinary gas with a temperature of about 10^4K and an expansion velocity of about 50 km s^{-1} may be present.

The system δ Cir (O7 + O) was also observed with IUE by Kondo and McCluskey. The spectral type of the primary star has been reported as O9 V, O8.5 V and O7.5 III f.

Ground-based spectroscopy of δ Cir by Thackeray and Emerson (1969) yielded a marginal detection of the secondary component which appears to be less massive than the primary. Minimum masses of 11.2 and 8.6 solar masses for the primary and secondary components, respectively, are derived.

The IUE spectra show the clear presence of a stellar wind. The Si IV resonance doublet shows no wind effect but the C IV doublet shows a strong P Cygni absorption with weak emission. Narrow absorption components also are present. The N V doublet also shows a strong P Cygni profile with moderate emission. Observations were made at only one orbital phase but in all probability we can conclude that the wind arises from the primary star and that the O7.5 III f classification is closest to the truth. The terminal velocity of the wind is 700 km s^{-1} for N V and 2330 km s^{-1} for C IV. The wind must be too hot for Si IV to appear. A mass loss rate of 3.6×10^{-7} solar mass per year was found by the method of Morton (1967).

Hutchings and van Heteren (1981) have discussed IUE observations of HD 149404 (O9+O7) and V 453 Sco (BO Ia+B1). HD 149404 appears to have a less massive primary with a stellar wind of mean velocity 1875 km s^{-1}. Weak Fe III lines appear at 1100 km s^{-1}. The authors found an expanding Fe III region in a number of early-type spectra. The stellar wind does not seem to show any strong phase dependence. V 453 Sco shows a wind velocity of about 450 km s^{-1} for Si IV and 670 km s^{-1} for C IV. Fe III lines appear with an expansion velocity of 170 km s^{-1}. The wind appears to be enhanced at photometric phase 0.35 which is at periastron although the eccentricity is small. The ultraviolet resonance lines of C IV, Si IV, and Mg II show emission only at phase 0.6 which is the same phase at which Balmer line emission is observed. An ultraviolet continuum temperature of about 14000 K is found. This is too low for a BO star, but this star has peculiar abundances and it may be misclassified.

Koch et al. (1981) analysed IUE spectra of the eclipsing binary V Pup (B1 V + B3). York et al. (1976) observed V Pup with Copernicus and noted that the system appears to be situated in an H II region with circumstellar lines of N II, Si II, Si III and Fe III clearly present. Koch et al. (1981) also detected narrow circumstellar lines. The system is semi-detached or contact with at least the cooler star at its Roche lobe.

There is evidence of gas streaming. There appears to be excess ultraviolet flux at wavelengths below 1600 A for an early B-star. The 1206 A line due to Si III appears to be about ten times weaker than expected. No stellar wind has been detected.

The binary V 861 Sco (BO I + B2 V) is an example of a system in which one component has evolved to the supergiant stage. This system has been investigated in great detail since it was once believed to be a massive X-ray binary. This is not the case. Major investigations based on high resolution IUE observations were done by Hutchings and Dupree (1980), Howarth et al. (1981), and Howarth (1981).

Hutchings and Dupree noted that the BO I star has a stellar wind of great complexity. They found wind velocities of 400 to 600 km s^{-1} which occur in sharp absorption components.

Howarth (1981) found that the ground based light curves could roughly be represented with a B2 V secondary. The primary has a mass of about 25 solar masses while the secondary's mass is about 8 solar masses. A mass ratio of 1/3 is unusual for early type binaries which seem to have mass ratios close to unity. The primary star may have already lost 10-20 solar masses. The stellar wind of V 861 Sco has a terminal velocity of 1600 km s^{-1}. A mass loss rate of 3×10^{-6} solar mass per year was derived. No significant variations of the stellar wind features occur with orbital phase but random variations occur on a time scale of a day or so. Line profile changes appear to be due to changes in the mass loss rate. A narrow absorption feature in the C II resonance lines appears at -620 km s^{-1} and is also seen in several other lines. The narrow feature is very stable with a variation of no more than 10 km s^{-1} over a period of several years.

Two systems with late B-type supergiants are μ Sgr and υ Sgr. Plavec (1981) and Plavec and Weiland (1980) discovered that the secondary component of μ Sgr is a BO V star. Duvignau et al. (1979) and Hack et al. (1980) discovered an O9 V companion to υ Sgr. The μ Sgr supergiant, of spectral type B8Ia, has a terminal wind velocity of 300 to 750 km s^{-1}. The B8Ia primary of υ Sgr is hydrogen poor (Hack and Pasinetti, 1963) and a stellar wind and gas flow of some complexity may originate from the O9V companion as well as from the supergiant.

3. W SERPENTIS BINARIES

Plavec (1980) has discovered a small group of interacting binaries with numerous strong emission lines in their ultraviolet spectra and has called this group W Serpentis stars. It appears that these systems may be related to β Lyrae as they seem to be in a phase of rapid mass transfer and their spectra show similarities to that of β Lyrae which has usually been considered as unique to our experience. Plavec et al. (1982) have studied the W Serpentis system SX Cas in some detail. The previously adopted spectral types of A6 III and G6 III are inadequate to explain the ultraviolet flux and they revise the spectral types to B7 + K3 III. A thick disk partially obscures the B-star. Further studies of this group of

objects should prove very interesting.

Hack et al. (1980) have discussed IUE observations of β Lyrae. The expanding gas in this system appears to be divided into two regions. A "chromospheric" region with $T \sim 10^4$K, $Ne \sim 10^{12}$ cm^{-3} which gives rise to the low ionization lines and a "coronal" region with $T \sim 10^5$ K, $Ne \sim 10^{10}$ cm^{-3} giving rise to the high ionization lines.

Plavec (1981) discusses the shallowness of the eclipses of β Lyrae in the λλ 1800-2200 region often attributed to the existence of numerous emission lines in this portion of the spectrum (Kondo et al., 1971; Hack et al., 1975, 1976, 1977). He suggests that the primary cause of the excess emission which fills in the eclipses is due to continuous hydrogen emission. Similar emission is apparently present in other W Serpentis stars.

4. WOLF-RAYET BINARIES

Numerous spacecraft have observed Wolf-Rayet stars and IUE is no exception. To mention only a few of the most recent IUE investigations, Willis (1982) has analysed high resolution spectra of ten of these stars covering essentially all WN and WC subtypes and Nussbaumer et al. (1982) have studied 15 WR stars at low resolution. In addition, Kondo and McCluskey have obtained high resolution IUE spectra of four WR binaries. Kondo et al. (1982) have reported on extensive IUE spectroscopy of γ^2 Vel. All of these investigations indicate that the massive stellar wind from a WR star is not strongly affected by the presence of a companion. The complexity of WR spectra are such that extensive observation and interpretation will be required to determine if and how the mass loss from a WR star is dependent on a companion.

5. MASSIVE X-RAY BINARIES

The systems HD 77581 and HD 153919 are bright and unreddened enough to study at high resolution with IUE. The strong stellar wind from the O7f primary of HD 153919 shows no phase dependent behavior in the ultraviolet (Dupree et al., 1978). On the other hand, the P Cygni profiles arising in the stellar wind from the B0.5 Ib component of HD 77581 do show a phase dependence which is probably caused by varying X-ray ionization effects as the positions of the X-ray source and supergiant change with respect to the observer. A similar effect is indicated in the low dispersion IUE spectra of Cyg X-1. Analysis of these effects can yield a better understanding of the X-ray emission and stellar winds in these systems.

6. ζ AURIGAE STARS

These systems have long periods and generally consist of a cool supergiant and a main sequence B-type star.

ζ Aur (K2 II + B8 V) has been observed using IUE by several investigators. Faraggiana and Hack (1980) noted complex absorption line profiles. They found that the K-star's chromosphere was very extended and contained clouds of material moving outward. Chapman (1980, 1981) and Stencel and Chapman (1981) detected the existence of several shock fronts in the system. A 100 km s^{-1} wind generated by the K-star creates a shock front near the B-star. In turn, the hemisphere of the K-star facing the B-star is heated and high speed flows and shocks are generated.

Stencel et al. (1979) analysed IUE spectra of 32 Cygni (K5 I+B5 V). Several P Cygni absorption components occur for a number of lines indicating velocities ranging from 200 to 400 km s^{-1}. A mass loss rate of 4×10^{-7} solar mass per year was derived for the K-star.

The much discussed peculiar binary ε Aur has been observed with IUE (Hack and Selvelli, 1979). The ultraviolet spectrum indicates the presence of a hot companion to the F0 I star. It is apparently a late B-star or B-type sub-dwarf. The problem of explaining just what eclipses the F-supergiant is still unresolved.

7. ALGOL SYSTEMS

Algol systems generally consist of a main sequence star of spectral type B or A and an evolved giant, usually of type F, G, or K but occasionally A, which is presumably at its Roche lobe and is often losing mass relatively slowly. These systems are often believed to have gone through Case B evolution and have finished with their first rapid stage of mass loss. Much evidence exists for the presence of gas streams, circumbinary material, rings or disks of gas, sudden "events" in which excess amounts of material may be ejected and other related phenomena (see Budding, 1981 and Plavec, 1981 for recent discussions and references).

One of the most intensively studied systems is U Cep (B7 V + G8 III). Extensive phase coverage has been obtained with IUE at high resolution by Kondo and McCluskey (Kondo et al., 1979, 1981). It was concluded that a stream of gas leaving the G-star circles around the primary star and leaves the binary system for the most part. The strength of the Si IV and C IV ultraviolet resonance lines indicates the existence of an extensive region, probably due to accretion by the B-star, with temperature corresponding to an early B-star. This system is subject to intervals of higher rates of mass flow (Olson, 1978), may have hot and/or cold spots on either star (Hall and Walter, 1974; Kondo et al., 1978) and a variable disk structure (Batten, 1974). Plavec et al. (1981) have noted the presence of ultraviolet emission lines of C IV, N V, Si IV, C II, Al III, Si II and Al II during the primary eclipse. No emission has been seen outside of eclipse by Kondo and McCluskey. This indicates either a hot region associated with the K-star or hot gas associated with the B-star but too spatially extensive to be eclipsed by the K-star which is about 1.6 times larger than the B-star. This eclipse is total.

Wilson and Caldwell (1978) have developed an interesting model for V 356 Sgr (B3 V + A2 II). This system shows a number of peculiarities and they suggest that a thick opaque disk with an equatorial temperature of 6000-7000 K circles the B-star's equator and hides about 1/3 of the star; we see the disk nearly edge-on. The origin of the material in this disk is presumably the A-star. It is suggested that the rapid phase of mass loss has just ended and that the B-star is gradually settling down as the disk is gradually accreted. The B-star is rotating near its limiting velocity.

Plavec (1982) has found the same emission lines, with somewhat different intensity ratios, in the primary eclipse spectrum of V 356 Sgr as discussed above for U Cep.

High resolution spectra of V 356 Sgr at phase 0.73 obtained by McCluskey and Kondo with IUE show that the far ultraviolet line spectrum is quite typical of a B3 V star with the exception that the Si IV and C IV resonance lines are a bit stronger than in B3 V standard stars. The mid-ultraviolet spectrum shows no indication of absorption lines except for a shallow broad absorption feature due to Mg II (2795, 2802 A) and a number of interstellar lines. The far-ultraviolet lines of the B3 V star are not indicative of rapid rotation which does not contradict the Wilson and Caldwell model since only the slowly rotating higher latitudes are not covered by the disk. The Mg II feature is certainly not typical of an A2 star. Perhaps it arises in the disk. Certainly, the B-star's continuum dominates the entire ultraviolet spectrum. No emission lines were seen at this phase.

The Algol system TT Hya (A2e + G5 III) displays strong phase dependent Hα emission indicative of a thin disk corotating around the primary star (Peters, 1980). Peters found a mass loss rate from the G-star of 2.5×10^{-8} solar mass per year. Peters and Polidan (1981) find a rich shell spectrum with mass flow indicated in the C II and Si II ultraviolet resonance lines.

Kondo et al. (1981) observed TT Hya with the Astronomical Netherlands Satellite (ANS) and found a large ultraviolet excess. Kondo, McCluskey and Wu observed TT Hya at high resolution with IUE. The far ultraviolet flux shortward of about 1600 A is primarily indicative of a B5 star. The Si IV and C IV resonance lines indicate an even hotter region. The spectrum "cools" longward of 1600 A and the mid-ultraviolet spectrum is close to A2 or A3 although shell lines are present and some line strength ratios appear anomalous. The Si IV and C IV lines vary in strength. No emission was detected outside of eclipse.

Another interesting system is U Sge (B8 V + G4 III). McNamara and Feltz (1976) found indications of the existence of a gas stream and/or a disk with a concentration of gas on the following hemisphere of the B-star. Naftilan (1976) noted abundance anomalies in the G-star spectrum. McCluskey and Kondo have obtained high resolution IUE spectra of U Sge at phases 0.26, 0.62 and 0.79. Many lines are weaker at phase 0.26. In particular, at phases 0.62 and 0.79 the Si IV and C IV resonance lines are

much too strong for the B8 spectral type.

8. R Arae

This single-lined spectroscopic binary which is eclipsing has a spectral type of B9p. Sahade (1952) discussed the variability and complexity of the optical spectrum. McCluskey and Kondo obtained high dispersion IUE spectra at phases 0.11, 0.26, 0.39 and 0.84. The ultraviolet spectrum is also variable and complex. Kondo, et al. (1981) found an ultraviolet excess and ultraviolet continuum variability. McCluskey and Kondo also detected X-rays from R Ara with the EINSTEIN X-ray satellite.

The complex ultraviolet variations are not described by simple temperature variations. At phase 0.39, the Si IV and Mg II resonance lines show a shortward displacement of 500 km s^{-1}. This was not seen at the other observed phases. The P Cygni emission is variable in strength and the strength of the Si IV and C IV features is too great for a B9 star. McCluskey and Kondo are obtaining detailed phase coverage of R Ara with IUE.

DISCUSSION

It is apparent that it is difficult to find a close binary consisting of two O-stars or an O-star and an early B-star in which no mass is being lost by means of a wind or some other mechanism. As has been discussed by several investigators (e.g., Schuerman, 1972; Kondo et al., 1972 and Vanbeveren, D., 1977, 1978), the geometry of the equipotential surfaces is altered if radiation pressure or any other effective force becomes important relative to the gravitational force. What should be emphasized and understood is that if these forces exceed gravity, then the conventional meaning given to the Roche lobes is meaningless! Any star with a stellar wind is in such a condition. If the Roche model is to be applied in order to give us information about the system, then a justification of this based on the physics of the problem must be given. This has not been done. The term 'early-type contact system' may be meaningless in its usual context. Since many investigators use the assumption of Roche lobe contact in deriving physical and orbital parameters of early-type binaries, the importance of a justification of such a model cannot be overemphasized.

The IUE observations of Algol systems by McCluskey and Kondo and other investigators discussed in this paper clearly indicate that many of these binaries are characterized by regions with temperatures significantly higher than the effective temperature of the early-type star as determined by ground-based studies. The Si IV resonance absorption lines and the ultraviolet emission lines, sometimes seen during primary eclipse, appear to be key indicators of Algol system activity. When considering absorption line asymmetries as indications of mass flow, great care must be taken as IUE high resolution spectra of sharp-lined B- and A-type stars show that line blending is complex and frequent in stars in this spectral range with

broader lines.

Kopal (1981) has made a number of very relevant comments concerning the problems of developing physical models for interacting binaries from observed photometric and spectroscopic phenomena. Let us continue to develop models of gas streams, disks, shells, rings, chromospheres, coronae, etc., but let us not become too enamored with our models or even with some of our basic "accepted facts".

I close by wholeheartedly agreeing with Professor Plavec (1981) that IUE has ushered in a new epoch of binary star research.

ACKNOWLEDGEMENTS

The author's research reported here has been partially supported by NASA grants. Thanks go to the U.S. IUE project team headed by Dr. A. Boggess for its competent assistance in obtaining the data.

REFERENCES

Batten, A. H. 1974, Pub. Dom. Ap. Obs., 11, 191.
Budding, E. 1981, Photometric and Spectroscopic Binary Systems, ed. E. B. Carling and Z. Kopal (Dordrecht: Reidel), p. 473.
Chapman, R. D. 1980, Nature, 286, 580.
_____. 1981, Ap. J., 248, 1043.
Drechsel, H. 1978, Ph.D. thesis, University of Erlangen-Nurnberg/FRG.
Drechsel, H. and Rahe, J. 1982, Astr. Ap., 106, 70.
Drechsel, H., Rahe, J., Kondo, Y., and McCluskey, G. E. 1980, Astr. Ap., 83, 363.
_____. 1981, Astr. Ap., 94, 285.
_____. 1982, Astr. Ap. Suppl., 45, 473.
Drechsel, H., Rahe, J., and Wargau, W. 1982, preprint.
Dupree, A. K., Hartman, L., Raymond, J. C., Faraggiana, R., and Hack, M. 1980, 2nd European IUE Conference, p. 223.
Dupree, A. K., et al. 1978, Nature, 275, 400.
Duvignau, H., Friedjung, M., and Hack, M. 1979, Astr. Ap., 71, 310.
Hack, M. 1981, Astr. Ap., 99, 185.
Hack, M., Flora, U., and Santin 1980, IAU Symposium No. 88, 271.
Hack, M., Hutchings, J. B., Kondo, Y., McCluskey, G. E., Plavec, M. J., and Polidan, R. S. 1975, Ap. J., 198, 453.
Hack, M., Hutchings, J. B., Kondo, Y., McCluskey, G. E., and Tulloch, M. K. 1976, Ap. J., 206, 777.
Hack, M., Hutchings, J. B., Kondo, Y., and McCluskey, G. E. 1977, Ap. J., Suppl., 34, 565.
Hack, M. and Pasinetti, L. 1963, Contr. Milano-Merate No. 215.
Hack, M. and Selvelli, P. L. 1979, Astr. Ap., 75, 316.
Hall, D. S. and Walter, K. 1974, Astr. Ap., 37, 263.
Howarth, I. D. 1981, Ph.D. thesis.
Howarth, I. D., et al. 1981, Astr. Ap., 93, 219.

Hutchings, J. B. and Dupree, A. K. 1980, Ap. J., 240, 161.
Hutchings, J. B. and van Heteren, J. 1981, Pub. A.S.P., 93, 626.
Koch, R. H., Bradstreet, D. H., Perry, P. M., and Pfeiffer, R. J. 1981, Pub. A.S.P., 93, 621.
Koch, R. H., Siah, M. J., and Fanelli, M. N. 1979, Pub. A.S.P., 91, 474.
Kondo, Y., Feibelman, W. A., and West, D. K. 1982, Ap. J., 252, 208.
Kondo, Y., McCluskey, G. E., and Feibelman, W. A. 1980, Pub. A.S.P., 92, 688.
Kondo, Y., McCluskey, G. E., and Gulden, S. L. 1976, Proc. Conf. on X-Ray Binaries, ed. E. Boldt and Y. Kondo (Washington, D. C.: NASA SP-389), p. 499.
Kondo, Y., McCluskey, G. E., and Harvel, C. A. 1981, Ap. J., 247, 202.
Kondo, Y., McCluskey, G. E., and Houck, T. E. 1971, IAU Colloquium No. 15, 309.
Kondo, Y., McCluskey, G. E., and Stencel, R. E. 1979, Ap. J., 233, 906.
Kondo, Y., McCluskey, G. E., and Wu, C.-C. 1981, Ap. J. Suppl., 47, 333.
Kopal, Z. 1971, Pub. A.S.P., 83, 521, 1971.
Kraft, R. P. 1975 in Neutron Stars, Black Holes and Binary X-Ray Sources, ed. H. Gursky and R. Ruffini (Dordrecht: Reidel), p. 235.
Leung, K. -C. 1980, IAU Symposium No. 88, 527.
McCluskey, G. E. and Kondo, Y. 1981, Ap. J., 246, 464.
McCluskey, G. E., Kondo, Y., and Morton, D. C. 1975, Ap. J., 201, 607.
McCluskey, G. E. and Kondo, Y. 1976, Ap. J., 208, 760.
McNamara, D. H. and Feltz, K. A., Jr. 1976, Pub. A.S.P., 88, 688.
Morton, D. C. 1967, Ap. J., 150, 535.
Naftilan, S. A. 1976, Ap. J., 206, 785.
Nussbaumer, H., Schmutz, W., Smith, L. J. and Willis, A. J. 1982, Astr. Ap. Suppl., 47, 257.
Olson, E. C. 1978, Ap. J., 219, 777.
Paczynski, B. 1971, Ann. Rev. Astr. Ap., 9, 183.
_____. 1980, Highlights of Astronomy, 5, 27.
Peters, G. J. 1980, IAU Symposium No. 88, 287.
Peters, G. J. and Polidan, R. S. 1982, IAU Symposium No. 98, 405.
Plavec, M. 1968, Adv. Astr. Ap., 6, 201.
_____. 1980, IAU Symposium No. 88, 251.
_____. 1981a, The Universe at Ultraviolet Wavelengths, NASA Conference Publ. 2171, ed. R. D. Chapman, p. 397.
_____. 1981b, Effects of Mass Loss on Stellar Evolution, ed. C. Chiosi and R. Stalio (Dordrecht: Reidel), p. 431.
_____. 1981c, preprint.
Plavec, M. J., Dobias, J. J., and Weiland, J. L. 1981, B.A.A.S., 13, 802.
Plavec, M. J. and Weiland, J. L. 1980, B.A.A.S., 12, 869.
Plavec, M. J. Weiland, J. L., and Koch, R. H. 1982, Ap. J., in press.
Rees, M. J. 1974, Highlights of Astronomy, 3, 89.
Sahade, J. 1952, Ap. J., 116, 27.
Schuerman, D. W. 1972, Ap. and Sp. Sci., 19, 351.
Snow, T. P. 1979, IAU Symposium No. 83, 65.
Stencel, R. E. and Chapman, R. D. 1981, Ap. J., 251, 597.
Stencel, R. E., Kondo, Y., Bernat, A. P., and McCluskey, G. E. 1979, Ap. J., 233, 621.
Thackeray, A. D. 1966, M.N.R.A.S., 131, 435.

Thackeray, A. D. and Emerson, B. 1969, M.N.R.A.S., 142, 429.
Thomas, H.-C. 1977, Ann. Rev. Astr. Ap., 15, 127.
Vanbeveren, D. 1977, Astr. Ap., 54, 877.
_____. 1978, Ap. and Sp. Sci., 57, 41.
Van den Heuvel, E. P. J., 1976, IAU Symposium No. 73, 35.
Willis, A. J. 1982, M.N.R.A.S., 198, 897.
Wilson, R. E. and Caldwell, C. N. 1978, Ap. J., 221, 917.
Wilson, R. E. and Starr, T. C. 1976, M.N.R.A.S., 176, 625.
York, D. G., Flannery, B., and Bahcall 1976, Ap. J., 210, 143.

BINARY STARS: MASS TRANSFER AND CHEMICAL COMPOSITION

David L. Lambert
Department of Astronomy, University of Texas at Austin

ABSTRACT

Mass exchange (and mass loss) within a binary system should produce observable changes in the surface chemical composition of both the mass-losing and mass-gaining stars as a stellar interior exposed to nucleosyntheses is uncovered. Three topics relating mass exchange and/or mass loss to nucleosynthesis are sketched: the chemical composition of Algol systems; the accretion disk of a cataclysmic variable fed by mass from a dwarf secondary star; and the hypothesis that classical Ba II giants result from mass transfer from a more evolved companion now present as a white dwarf.

NUCLEOSYNTHESIS REVEALED?

Along the evolutionary path connecting the main sequence star to the red giant, the stellar core where the severe, if simple, nucleosynthesis occurs is hidden from our view. At the base of the red giant branch, a developing convective envelope mixes out into the atmosphere regions formerly situated just outside the H-burning core. The resultant predicted and observed changes in surface chemical composition, which are reviewed by Lambert (1981), are restricted to the fragile light elements - Be, B and Li and perturbations of the CNO isotopes induced by the CNO tricycle. Very small and effectively unobservable changes in H and He including an increase in the ^{3}He abundance are also predicted. On the asymptotic red giant branch (AGB), theoretical calculations predict the conversion of the oxygen-rich red giant to a carbon star with enhanced abundances of the s-process elements. In a review of peculiar red giants with chemical composition changes attributable to the infusion of nucleosynthetic products, Scalo (1981) emphasizes the significant gaps in our theoretical understanding and suggests additional physical processes that might be included in interior calculations. The key problem is that the conversion to a carbon star is observed at luminosities and stellar masses substantially below the predicted limits for intermediate mass stars on the AGB. No imagination is needed to appreciate that the long, hard struggle to understand fully the chemical composition changes occurring during a star's life could be dramatically shortened if we were able to look directly at the interior. Spectroscopic examination of binary stars offers limited possibilities of performing this informative inspection of a stellar interior.

In a close binary system, mass exchange between the stars and mass loss from the system can have a cominating influence on the evolution of the stars. If the mass-losing star experiences a severe loss, it may be stripped down to the core and its spectrum should then betray the compositional changes arising from nucleosynthsis. If the mass-gaining star accepts the bulk of the mass lost by the other star, its photospheric spectrum will also be changed.

Often, the mass gathers in an accretion disk around the mass-gaining star. The emission line spectrum of gas within and around the disk can provide the composition of the layers most recently stripped from the mass-losing star.

In this talk, I shall sketch three topics whose common link is a spectroscopic examination of systems in which severe loss may be expected to uncover regions of a stellar interior. The reader is warned that our exploration of these topics is far from complete, our initial results may be revised before publication in a refereed journal and our initial hopes for a speedy, conclusive unravelling of the secrets of a stellar interior will surely dissipate as the theoretical and observational complexities are faced.

Three topics are sketched:

i) The chemical composition of Algol primary and secondary stars.
ii) The accretion disks of cataclysmic variables.
iii) Do Barium stars have white dwarf companions?

ALGOL SYSTEMS

The idea that the stars in an Algol system have exchanged a considerable amount of mass was first promoted by Crawford (1955). Simple arguments suggest that the former core of the mass-losing star may now be exposed to reveal an increase in He/H ratio and substantial changes in the relative abundances of CNO wrought by the CNO-tricycle. I select β Lyrae as an illustration of this point.

The B8 II primary is the mass-losing star with a mass estimated by Woolf (1965) to lie in the range 9.5 to 6.8 $\mathcal{M}_\odot$. The mass-gaining secondary with a mass between 21 and 17 $\mathcal{M}_\odot$ is substantially more massive. Plavec (1981) derived the ultraviolet spectrum of the secondary by differencing two spectra. The one taken during secondary eclipse providing a reference spectrum of the primary. This uv spectrum taken at low resolution showed no absorption lines. Their absence from the uv and optical spectra severely limits analysis of the secondary.

If we suppose that the mass transfer has been conservative (i.e. no mass is lost from the system), and has not occurred more than once, the initial mass of the primary must have exceeded one-half of the present total mass, i.e. $\mathcal{M}^0_{pr} \gtrsim 15$ to 21 $\mathcal{M}_\odot$ and the current mass represents a mass fraction $f = \mathcal{M}/\mathcal{M}^0_{pr} \sim 0.6$ of the initial star. On inspection of calculations describing the internal structure of a massive star at exhaustion of core H-burning (Iben 1966), we find that the H-burning shell lies close to $f \sim 0.23$. Carbon is depleted and converted to N over a mass fraction extending about 0.3 further out towards the surface. Convective overshoot should further broaden the mass fraction that has experienced nuclear processing. Backed by this expectation that the surface composition of the B8 II primary should reflect the nuclear processing, we began last summer to investigate the CNO abundances (Lambert, Parthasarathy and Tomkin 1982).

Initial observations uncovered the expected severe C deficiency. Figure

1 shows 4 C I lines in the spectrum of a standard B II star, γ Lyr and a quick check shows that the C abundance is near-solar. The C I lines are not present in the spectrum of β Lyr (upper part of Figure 1) taken at a phase $\phi = 0.5$ when emission lines are at minimum intensity. Similar observations of C I 8335 Å confirm the C deficiency. Carbon must be underabundant by at least a factor of 10. As expected for CNO tricycled material, the N I lines near 8690 and 7440 Å are enhanced. Our observations of O I are incomplete but seem to indicate a mild O deficiency. The γ Lyr spectra would seem to eliminate the possibility that non-LTE effects are responsible for the CNO changes seen in β Lyr. Several spectroscopists have shown that He is overabundant in the primary's atmosphere.

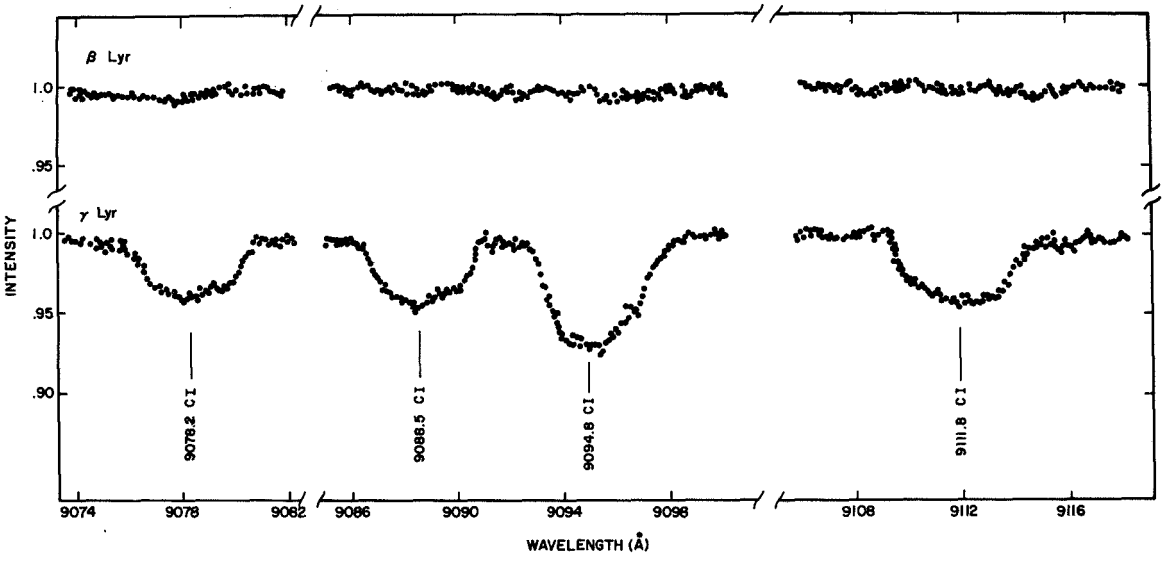

Fig. 1. Spectra of β Lyr and γ Lyr covering the C I lines 3s $^3P^0$ - 3p ^3P.

The CNO abundances resemble the composition of the H-burning shell in a star evolving off the main sequence. For example, Iben's (1966, Figure 6) calculations for a 15 $\mathcal{M}_\odot$ star give N/C ~ 20 and N/O ~ 1.3; the solar values are N/C ~ 0.2 and N/O ~ 0.1. If N/C ~ 20 in the atmosphere, the C I uv lines should be detectable on IUE spectra. The apparent discrepancy between the predicted He/H ~ 0.25 and the abundance analyses providing He > H might indicate a convective smearing of the predicted sharp boundary between the H-burning shell and the He-rich core. Of course, the evolution of the primary in a close binary may differ from that of a single star (tidal mixing?) so that this conjecture may not apply to the single stars modeled by Iben and others.

Many Algol systems should exhibit less dramatic changes in composition. U Cep is one such example. The primary is a B7 V star with $\mathcal{M}$ ~ 4.2 $\mathcal{M}_\odot$. The secondary, the mass-losing star, is a subgiant (B8 III-IV) with a mass $\mathcal{M}$ ~ 2.8 $\mathcal{M}_\odot$ (Tomkin 1981). In our analyses (Parthasarathy, Lambert and Tomkin 1979, 1982), we first check for abundance changes by comparing the secondaries of U Cep with κ Gem, a normal giant of similar effective temperature and

surface gravity. Spectrum synthesis is then used to calibrate the line intensity-abundance relation. Observations taken during the secondary eclipse showed that the secondary has a normal metal abundance (Parthasarathy, Lambert and Tomkin 1979) contrary to some earlier suggestions of a marked metal deficiency. We are now completing an analysis of the C and N abundances from Digicon spectra of the CN and CH bands in the blue. Figure 2 shows that the CH lines are weaker in U Cep. We find a C deficiency of 0.2 dex relative to κ Gem, a giant in which the deep convective envelope has mixed some CN-processed material to the surface (Lambert and Ries 1981). If prior to the onset of mass exchange the secondary evolved as theoretical models predict, the C deficiency suggests that the star has now been stripped down to a mass fraction f ~ 0.5 of the initial star so the initial mass was $\mathcal{M}^0_{sec} \sim 5.6\ \mathcal{M}_\odot$. If mass exchange were conservative, this estimate and the present total mass

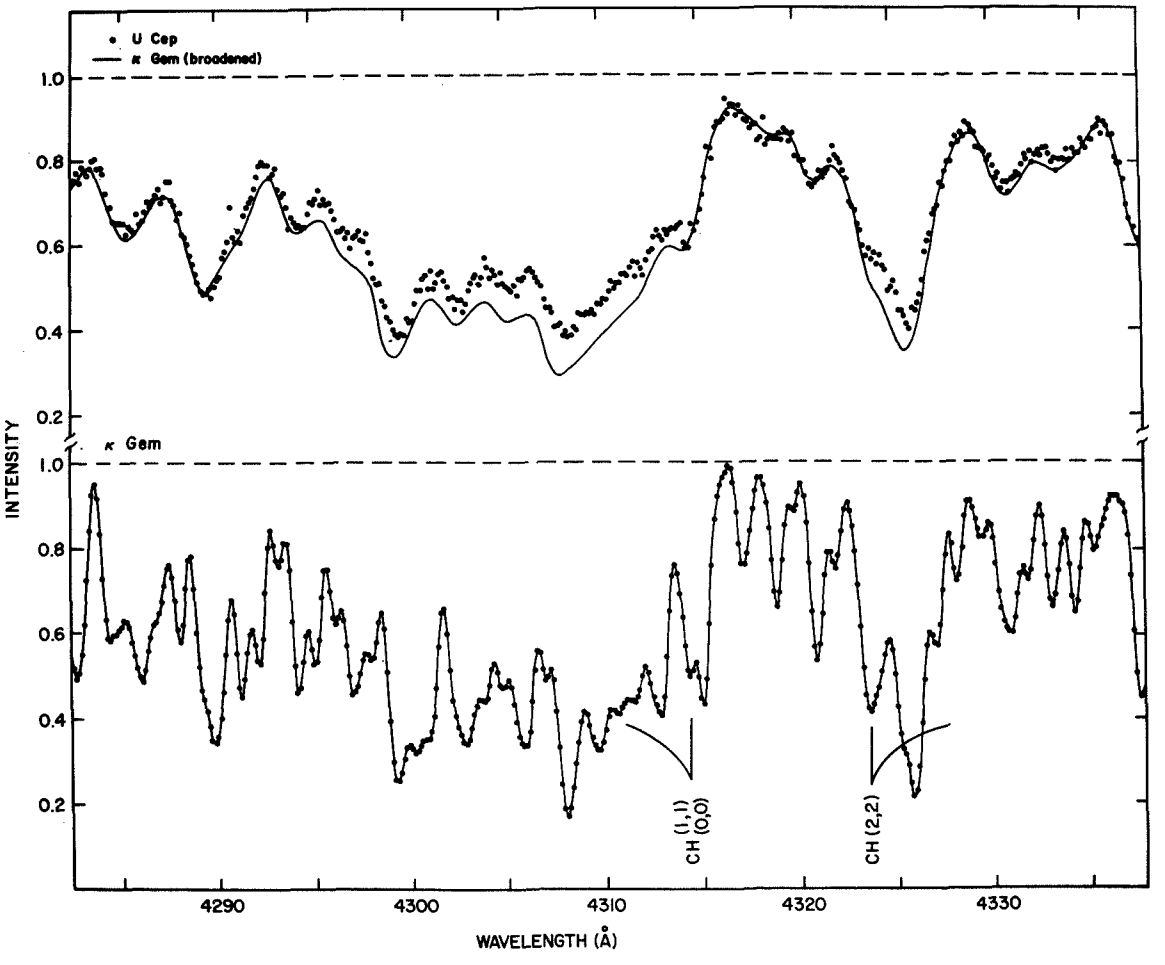

Fig. 2. Spectra near 4310 Å of U Cep and Kappa Gem. The lower panel shows a 0.2 Å resolution spectrum of κ Gem. After broadening to account for the higher rotational velocity of the secondary of U Cep, the κ Gem spectrum fits the secondary's spectrum except in regions where CH provides a major contribution -- see upper panel.

give $\mathcal{M}^0_{pr} \sim 1.4\ \mathcal{M}_\odot$ as a lower limit. The upper limit is $\mathcal{M}^0_{pr} \sim 4.2\ \mathcal{M}_\odot$ (the present mass) with $\mathcal{M}^0_{sec} \sim 5.6\ \mathcal{M}_\odot$ and mass loss from the system not mass exchange within the system. This latter condition cannot be excluded. Indeed, Kondo, McCluskey and Harvel (1981) note that the IUE spectra indicate that the bulk of the matter now being stripped from the secondary is leaving the system. Some information on the total mass transferred might be gleaned from a CNO analysis of the B7 V primary.

This modest overdeficiency of C for the secondary of U Cep is also present in U Sge, a rather similar system. One might expect outstanding abundance changes in the very low mass secondaries present in a few Algol systems. We selected S Cnc where the secondary mass $\mathcal{M}_{sec} \sim 0.2\ \mathcal{M}_\odot$ (Popper 1980) would seem to guarantee that we now see a stellar core. The minimum mass for the initial secondary was $\mathcal{M}^0_{sec} \sim 1.3$ or $f = \mathcal{M}_{sec}/\mathcal{M}^0_{sec} \lesssim 0.15$. Iben (1967)'s models for subgiant stars show that C is severely depleted inside $f \sim 0.4$ and H inside $f \sim 0.12$.

Our expectation, which seemed to conflict with published photometry and low-dispersion spectroscopy indicating a fairly normal spectrum, was upset by a recently acquired Digicon spectrum of the G-band region in the secondary. The CH bands give a C abundance only 0.5 dex below normal. This preliminary result assumes that H is not deficient. Nonetheless, this modest C deficiency would seem to be inconsistent with the idea that the low mass secondary is a naked He-rich stellar core. An initial reaction to the result is to suppose that the outer envelope of the star prior to mass loss was mixed such that C was not completely processed in any layer. Alternative explanations exist. Was some of the ejected mass recaptured to give the He-rich core a H-rich coating? Has the primary's envelope largely preserved its original composition because the mass exchange was non-conservative and, at a later stage, transferred mass to the secondary via a stellar wind?

Clearly, the chemical composition of the primary and secondary components of Algol systems would seem to contain answers to basic questions about their structure and evolution. Full definition of the compositions will call for spectroscopy across the electromegnetic spectrum from the ultraviolet to the infrared.

ACCRETION DISKS AND CATACLYSMIC VARIABLES

My discussion of the Algol systems focussed on the photospheric line spectra and the chemical composition of the stellar photospheres. The intrasystem and circumstellar gas provides emission and absorption lines from which to determine its chemical composition. This analysis is likely to be difficult. In the cataclysmic variables (CVs), the accretion disk around the degenerate star excites emission lines and so provides us with an opportunity to determine the chemical composition of the gas most recently lost by the secondary. The uv spectrum of the disk and its environs is crucial to a thorough analysis of CNO. Direct analysis of the degenerate star's atmosphere is seemingly impossible. A quantitative spectroscopic and photometric examination of the cool secondary star has not yet been attempted.

The mass-losing secondary fills its Roche lobe and feeds the accretion disk. Systems containing a low mass secondary ought to show an accretion disk overabundant in N and deficient in C. These and related changed in H, He and possibly O should be most evident in those systems with a very small secondary. I discuss here three CVs: V603 Aql with $\mathcal{M}_{sec} \sim 0.40\ \mathcal{M}_{\odot}$ (Warner 1976), AE Aqr with $\mathcal{M}_{sec} \sim 0.74\ \mathcal{M}_{\odot}$ (Patterson 1979) and G61-29 with $\mathcal{M}_{sec} \sim 0.02\ \mathcal{M}_{\odot}$ (Nather, Robinson and Stover 1981).

V603 Aql was Nova Aql 1918, the prototype of 'fast' novae. Our detailed analysis of the combined and optical spectrum is to be published elsewhere (Ferland et al. 1982). The continuous spectrum after correction for the estimated reddening of $E_{B-V} = 0^{m}.07$ is consistent with the flux distribution $f_{\nu} \propto \nu^{1/3}$ of a hot optically thick accretion disk. The Rayleigh-Jeans spectrum $f_{\nu} \propto \nu^{2}$ is not a good fit. Gas above the disk is considered to be photoionized by uv and x-ray radiation from the hot inner portions of the disk. Unfortunately, the far uv spectrum is not observable but the presence of strong C IV, 1550 Å lines and the absence of the N V 1240 Å doublet suggests that the $f_{\nu} \propto \nu^{1/3}$ spectrum turns over at $\lambda_{min} \sim 200$ Å or $T_{max} \sim 1.5 \times 10^{5}$ K

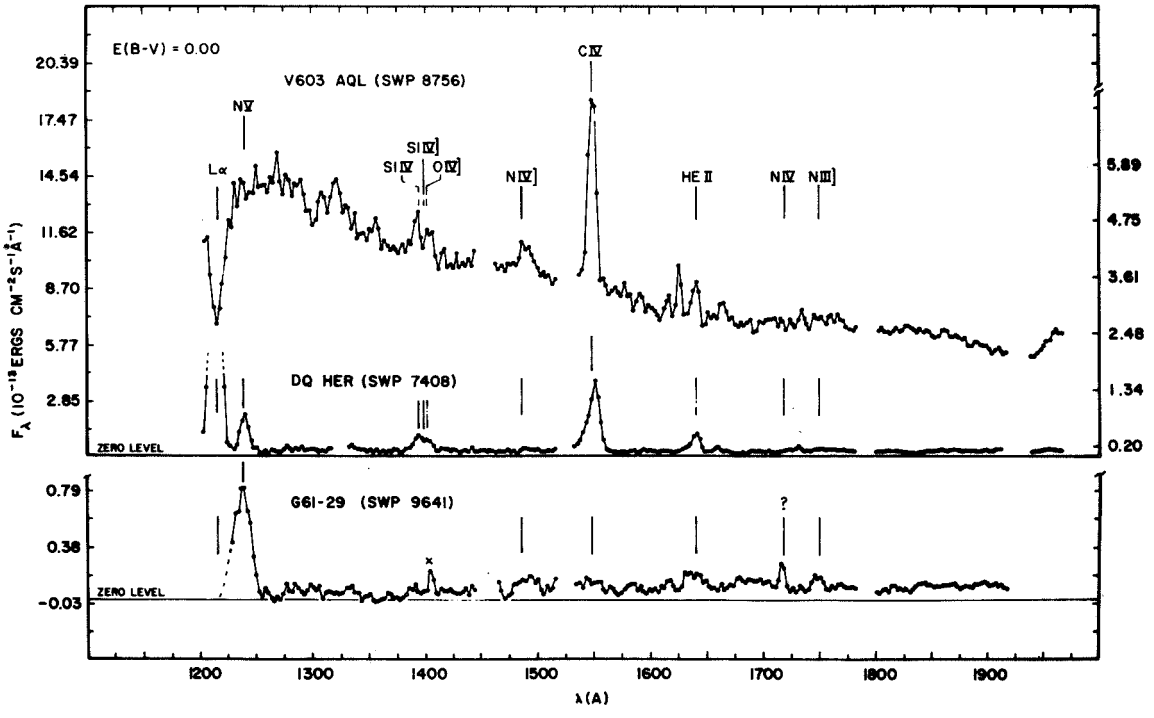

Fig. 3. Low-resolution SWP spectrum of G61-29, compared to similar spectra of the old novae V603 Aql and DQ Her. Absolute fluxes are plotted against wavelength. Scale on right (upper panel) is for DQ Her data. The gaps in the spectra indicate reseaux-contaminated regions. Strong Lα feature in DQ Her and G61-29 (not shown) are geocoronoal; Lα appears in absorption in V603 Aql. The (x) marks on ion "hit" on the G61-29 spectrum.

thanks to the exponential Wien tail of the blackbody emission from the hot inner disk. For λ_{min} = 200 Å, the total emission from the disk is $L_{tot} \sim 4 \times 10^{35}$ ergs s^{-1}. Stability arguments suggest that the outer radius of the disk cannot extend beyond about one-third of the binary separation of $R_{out} \sim 4 \times 10^{10}$ cm.

The emission lines (Figure 3) appear to come from a hot corona around the disk. The electron density in this corona, $N_e \sim 10^{10}$ cm^{-3} is estimated from the absence of the [O III] optical lines and the O III] 1666 Å line ($N_e \gtrsim 10^9$) and the presence of the N IV] 1486 Å ($N_e < 3 \times 10^{10}$). O^{++} should be abundant because the He I lines are strong. The Hβ flux with this density estimate gives the radius of the emitting volume (assumed cylindrical) $R \sim 6 \times 10^{11}$ cm which is the same order as the binary separation.

In our detailed analysis of optical and uv emission lines, we use a photoionization model characterized by the luminosity and character of the radiation field, the density and chemical composition of the coronal gas and the dimensions of the system (Ferland and Truran 1981). Application of statistical and thermal equilibrium then yields the temperature profile and the emission line fluxes. Although the chemical composition may be adjusted to bring predicted and observed line fluxes into agreement, the lack of specific information about some model parameters and uncertainties in the atomic data both suggest that enthusiasm be restrained when seeking evidence for nucleosynthesized material.

For V603 Aql, we considered three sources of ionizing radiation: the observed and (extrapolated) continuous spectrum of the accretion disk, the hard X-ray flux detected by Becker and Marshall (1981), and the X-ray radiation emitted from the boundary layer between the white dwarf and the accretion disk. The detected X-rays would appear to be optically thin bremmstrahlung from the corona. Accretion disk models predict the boundary layer to be hotter (x 5) than the disk and to emit with a luminosity equal to that of the disk. However, this predicted flux was not detected by the Einstein IPC (Becker and Marshall 1981). The reason for the suppression of the boundary layer flux is not understood. We ran models with and without it.

Our analysis provides weak evidence for the modest N enrichment expected in gas stripped from a main sequence remnant with $\mathcal{M} \sim 0.4\ \mathcal{M}_\odot$. The following table of relative line fluxes is abstracted from Ferland et al. (1982, Table 7).

These predictions are based on models in which the boundary layer was not a significant source of photoionizing radiation. The observed fluxes F_{OBS} are matched well by predictions F_{GIANT} which assume a C-poor, N-rich gas similar in composition to the outer envelope of a red giant (Lambert and Ries 1981). A solar composition - see F_{SOLAR} - leads to an underestimate of the N line fluxes. (See Ferland et al. for a discussion of the H line fluxes which are sensitive to radiative transfer effects.) Our conclusion that the accretion disk has a N/C ratio in excess of the solar value appears not to depend on most of the model's astrophysical and geometrical parameters; the key uncertainty is the flux and spectrum of ionizing photons from the boundary layer (or elsewhere) which could determine the ionic abundances of C and N. Abun-

dance conclusions do rely, of course, on physical parameters such as collision strengths.

Line		F_{OBS}	F_{GIANT}	F_{SOLAR}
He I	4471 Å	6	5	4
He II	1640 Å	142	141	143
C III]	1750 Å	< 40	19	18
C III	4650 Å	12	9	12
C IV	1549 Å	1000	1000	1000
N III]	1750 Å	< 60	11	2
N IV]	1487 Å	160	142	32
N V	1240 Å	< 100	107	46
O III]	1666 Å	< 70	45	26
O IV] Si IV	1397 Å	316	198	132

On cursory inspection, the IUE spectrum of AE Aqr with F(N V 1240)/F(C IV 1549) ≈ 6 (Jameson, King and Sherrington 1980) would seem to require a very N-rich composition for the gas now leaving the secondary and passing across to the accretion disk. Jameson et al. argue persuasively and correctly that the emission line fluxes arise in a photoionized corona around the disk but they do not present a detailed model. In fact, they adopt the implicit assumption that the CNO abundances are solar. It would be of interest to derive the abundance to check the suspicion that N is enhanced and C depleted.

V603 Aql and AE Aqr are nearly typical CVs. My third example is certainly an extreme case of mass transfer. G61-29 was shown by Nather, Robinson and Stover (1981) to consist of two white dwarfs with an orbital period of 46.5 minutes. The mass-losing star is a He white dwarf with a remarkably small mass $\mathcal{M} \sim 0.02\ \mathcal{M}_\odot$. No H lines are seen in the spectrum; the abundance is H/He < 0.008. Our IUE spectrum (Lambert and Slovak 1981) confirmed the extreme H deficiency (Ly α was absent), gave a marginal detection of He II 1640 Å and showed N V 1240 Å to be strong with no detectable flux in the C IV 1549 Å doublet (Figure 3). The ratio F(N V 1240)/F(1549) ≥ 14 is more extreme than that found for AE Aqr. On the crude assumption that the ionic and total abundance ratios are identical, we obtain N/C ≳ 18. Although models of the emitting region should be constructed, I suspect that the high N/C ratio for the gas and, hence, the mass-losing He white dwarf will be confirmed. Certainly, the ratio is most plausible as the He white dwarf surely experienced H burning and conversion of C to N. I conclude that mass transfer in G61-29 was initiated before the secondary reached the He-core burning stage. Spectra of higher quality, which will be obtainable with the Space Telescope, should provide emission lines of other ions including those of oxygen and several metals. Then, a more detailed analysis should provide estimates of the CNO relative abundances. Since the CNO equilibrium abundances for the CNO cycles depend on the core temperature, it should be possible to infer the initial mass of the secondary.

For the CVS, several of the links in the analytical chain connecting the emission line fluxes, the chemical composition of the accretion disk and adjacent gas, and the nucleosynthesis experienced by the mass-losing star are weak. For some stars out implicit assumption that the emitting gas and the current surface of the secondary have identical composition may be in doubt thanks to explosive ejection of processed material by the white dwarf in a nova event. (Our spectra of V603 Aql are of the stellar system not the expanding nebulosity.) Perhaps, the secondary acquires material just after a nova explosion and internal nucleosynthesis. The weakest link is most probably in the analysis of the emission lines. Improved spectra will be of assistance: e.g. the line profiles should betray the location of the emitting ions. Interesting tests of the coronal models are possible through time-resolved spectroscopy -- see Ferland et al. (1982) for a brief discussion.

DO BARIUM STARS HAVE WHITE DWARF COMPANIONS?

Classical Ba II giants apparently defy explanation by the standard calculations which predict a dredge-up of carbon and s-process elements to occur only for AGB stars of intermediate mass. Classical Ba II and other peculiar giants are found on the first giant branch at luminosities far below the AGB and with masses too small to be classified as intermediate mass stars. Scalo (1981) outlines potential additions to the physical processes employed in low mass models that might result in the production of a Ba II star. With their disvoery that all Ba II stars are binaries, McClure et al. (1980) recognized that the models of the intermediate mass AGB stars might yet account for the Ba II stars. If, in a binary system, the AGB star rich in C and s-process elements loses its envelope with the secondary capturing a significant fraction, the binary is transformed to a Ba II star accompanied by a white dwarf. The potential rôle of IUE in clarifying these ideas is obvious: detection of the ultraviolet continuum of a white dwarf in short wavelength exposures of Ba II giants would support the binary hypothesis advocated by McClure et al.

Supporting evidence was soon provided. Böhm-Vitense (1980) found a hot white dwarf to accompany the luminous classical Ba II star ζ Cap (spectral type G5p). She also claimed a tentative identification of a cooler white dwarf for ζ Cyg, a mild Barium star of spectral type G8 II. A third identification involving another mild Barium star, 56 Peg, was described by Schindler et al. (1981). I discuss below the significance of these detections involving luminosity class II stars to the binary hypothesis of the classical Ba II stars which are overwhelmingly of luminosity class III.

In the last year, we have obtained long exposures of two Ba II stars, the R star HD 156074 and the mild Ba star ζ Cyg. Our spectrum of ζ Cyg confirms that a white dwarf is present. A full discussion will be given elsewhere (Dominy and Lambert 1982). I give here a preliminary analysis of our SWP exposures of the Ba II stars 16 Ser and HR 4862. The trigonometrical parallax and the Ca II K line width (Wilson 1976) both indicate that 16 Ser is at a distance of only about 50 pc; note that ζ Cap is at a distance of about 220 pc. Then, our non-detection of a uv excess in a 4-hour exposure sets an interesting limit on the bolometric magnitude of a white dwarf companion. We find that it must fall in a HR diagram at or below the locus corresponding to

a cooling line of 10^9 yrs for C/O white dwarfs (Weidemann 1968). Since the post-main-sequence lifetime as a subgiant and giant is 0.8×10^9 yrs for $\mathcal{M} \sim 1\ \mathcal{M}_\odot$ decreasing to 0.5×10^9 yrs for $\mathcal{M} \sim 1.5\ \mathcal{M}_\odot$, our non-detection of a white dwarf accompanying two classical Ba II stars (and the R star HD 156074) would suggest one or two direct conclusions:

i) Membership in a binary system is not a necessary condition for evolution to a Ba II giant. Obviously this statement is stronger than is warranted by our failure to detect white dwarfs accompanying 16 Ser and HR 4862. Re-examination of these and other Ba II stars with the Space Telescope will certainly test this conclusion. Other arguments lend some support to the idea that the binary hypothesis is not yet unassailable. Culver and Ianna (1980) argue that McClure et al.'s separation of stars into the categories 'mild' and 'Ba II' is largely responsible for the conclusion that all Ba II stars are binaries. Culver and Ianna remark that published classifications of the Ba-richness by experienced spectroscopists indicate that some reassignment between McClure et al.'s two groups is appropriate. Recently, Lü (1982) has given a photometric classification of McClure et al.'s Ba II stars and finds that 3 stars should belong to the 'mild' group. Culver and Ianna note that if the 'mild' and 'Ba II' samples are merged, significant radial velocity variations were found by McClure et al. in 9 of the 17 stars with a similar statistic for the normal GK giant sample (possibly 7 out of 20).

ii) Ba II stars do result from transfer of nuclear processed material as the original primary sheds its envelope and evolves to a white dwarf. Although our analysis remains to be completed, the IUE spectra appear to require that the white dwarf be not younger than about 10^9 yrs. Since the Ba II giants appear to have a mass $\mathcal{M} \geq 1\ \mathcal{M}_\odot$, the mass transfer should have occurred before the secondary had evolved significantly from the main sequence and so raises the question 'Where are the Ba rich main sequence stars?' Bond's (1974) subgiant CH stars are candidates but, as Luck and Bond (1982) note, it is difficult to understand why the Ba enriched stars should be concentrated so in the narrow spectral type interval occupied by these subgiants. The apparent absence of Ba rich main sequence stars is a troubling one.

The discovery of white dwarf companions to ζ Cap, ζ Cyg and 56 Peg cannot be construed as decisive evidence for the binary hypothesis. Neither ζ Cyg nor 56 Peg is truly a barium star. They are mild barium stars or even normal supergiants. Sneden, Lambert and Pilachowski (1981) obtained a small s-process abundance [s/Fe] = +0.17 for ζ Cyg. Identification of 56 Peg as a barium star appears to rest largely on a narrow-band photometric study (Warren and Williams 1970) which reported both 56 Peg and ε Peg to be barium stars. However, Hyland and Mould (1974)'s abundance analysis failed to confirm the Ba overabundance in ε Peg. I suspect that 56 Peg is not terribly Ba-rich.

The association of a white dwarf with the supergiants ζ Cap, ζ Cyg and 56 Peg is most probably a reflection of a GK supergiant's short lifetime, i.e. main sequence stars with $\mathcal{M} \geq 3\ \mathcal{M}_\odot$ can evolve up to a supergiant before the white dwarf produced by an initially more massive companion has cooled significantly. The association of the white dwarf with a Ba enhancement in the supergiant is unproven.

I thank my colleagues J. F. Dominy, M. Parthasarathy and J. Tomkin for their contributions to the research discussed in this talk. My research in ultraviolet stellar spectroscopy is supported in part by the National Aeronautics and Space Administration (contracts NSG-5379 and NAS 8-32905), the National Science Foundation (AST 81-17485), and the Robert A. Welch Foundation.

REFERENCES

Becker, R.H., and Marshall, F.E. 1981, Ap. J. (Letters), 244, L93.
Böhm-Vitense, E. 1980, Ap. J. (Letters), 239, L79.
Bond, H.E. 1974, Ap. J., 194, 95.
Crawford, J.A. 1955, Ap. J., 121, 71.
Culver, R.B., and Ianna, P.A. 1980, P.A.S.P., 92, 829.
Dominy, J.F., and Lambert, D.L. 1982, in preparation.
Ferland, G.J., Lambert, D.L., McCall, M.J., Shields, G.A., and Slovak, M.H. 1982, Ap. J., in press.
Ferland, G.J., and Truran, J. 1981, Ap. J., 244, 1022.
Hyland, A.R., and Mould, J.R. 1974, Ap. J., 187, 277.
Iben, I., Jr. 1966, Ap. J., 143, 516.
_____ 1967, Ap. J., 147, 624.
Jameson, R.F., King, A.R., and Sherrington, M.R. 1980, M.N.R.A.S., 191, 559.
Kondo, Y., McCluskey, G.E., Jr., and Harvel, C.A. 1981, Ap. J., 247, 202.
Lambert, D.L. 1981, in Physical Processes in Red Giants, eds. I. Iben, Jr., and A. Renzini, Reidel Pub. Co., Dordrecht, p. 115.
Lambert, D.L., Parthasarathy, M., and Tomkin, J. 1982, in preparation.
Lambert, D.L., and Ries, L.M. 1981, Ap. J., 248, 228.
Lambert, D.L., and Slovak, M.H. 1981, P.A.S.P., 93, 477.
Lü, P.K. 1982, preprint.
Luck, R.E., and Bond, H.E. 1982, preprint.
McClure, R.D., Fletcher, J.M., and Nemec, J.M. 1980, Ap. J. (Letters), 238, L35.
Nather, R.E., Robinson, E.L., and Stover, R.J. 1981, Ap. J., 244, 269.
Parthasarathy, M., Lambert, D.L., and Tomkin, J. 1979, M.N.R.A.S., 186, 391.
Patterson, J. 1979, Ap. J., 234, 978.
Plavec, M.J. 1981, in The Universe at Ultraviolet Wavelengths: The First Two Years of IUE, NASA Conf. Rep. 2171, Washington, p. 397.
Popper, D.M. 1980, Ann. Rev. Ast. Ap., 18, 115.
Scalo, J.M. 1981, in Physical Processes in Red Giants, eds. I. Iben, Jr., and A. Renzini, Reidel Pub. Col, Dordrecht, p. 77.
Schrindler, M., Stencel, R.E., Linsky, J.L., and Basri, E. 1981, preprint.
Sneden, C., Lambert, D.L., and Pilachowski, C.A. 1981, Ap. J., 249, 1052.
Tomkin, J. 1981, Ap. J., 244, 546.
Warner, B. 1976, in Structure and Evolution of Close Binary Systems, IAU Symp. No. 73, p. 85.
Warren, P.R., and Williams, P.M. 1970, Observatory, 90, 115.
Weidemann, V. 1968, Ann. Rev. Astr. Ap., 6, 351.
Wilson, O.C. 1976, Ap. J., 205, 823.
Woolf, N.J. 1965, Ap. J., 141, 155.

The Distribution of Interstellar Gas within 50pc of the Sun

Frederick C. Bruhweiler
Astronomy Department
Computer Sciences Corporation

ABSTRACT

Previous Copernicus determinations of H I column densities in nearby stars (d~5pc) are reviewed. These results are compared with recent ultraviolet (IUE), data and data acquired at other wavelengths. From this combined data set a coherent picture for the distribution of neutral hydrogen within 50pc of the Sun emerges. For directions away from the galactic center, the total H I column density for a 50pc line of sight is typically $\sim 10^{18} cm^{-2}$, while toward the galactic center it may be $1\text{-}2 \times 10^{19} cm^{-2}$ or higher. A tentative model is proposed which suggests that the bulk of the H I resides in a cloud in a direction toward $\ell^{II} \sim 0^0$. The data are consistent with the Sun being embedded, but near the edge of the cloud.

I. INTRODUCTION - THE IMPORTANCE OF UNDERSTANDING THE LOCAL ISM

Our knowledge of the interstellar medium (ISM) in the vicinity of the Sun, within about 50pc, has been quite limited. Only recently has one been able to obtain a coherent picture of the physical conditions of the ISM in the proximity to the Sun. We shall, here, concentrate upon reviewing recent interstellar absorption line data for lines of sight $\lesssim$50pc acquired with IUE and then compare those results with data obtained through other means. The goal is to sketch out a coherent physical picture for the distribution of neutral hydrogen within 50pc of the Sun.

One might ask, "why the local ISM is so important?" Typically, in interstellar line studies, one probes the gas in the interstellar medium (ISM) against the backdrop of the spectral continuum of luminous early-type stars. Generally, these objects are distant and various clouds along the line of sight are contributing to the observed interstellar spectral features making a unique analysis incomplete. Therefore, it is important to study and understand the physical conditions in much shorter lines of sight before attempting to completely unravel and interpret longer lines of sight. Furthermore, long lines-of-sight, also sample the extensive high density H I and H II regions normally associated with O and B stars. Thus, these lines-of-sight most certainly do not reflect the average physical conditions of the "typical" volume element in the ISM. Only by sampling short lines of sight can we hope to sample the so called "intercloud medium" (ICM) and avoid contamination by large cloud complexes. Observations using the Copernicus satellite have revealed the ubiquitous presence of interstellar O VI toward many O and B stars. (Jenkins and Meloy, 1974) Of the stars yielding positive detections, four are on the order of 100pc or less from the Sun. These observations have been interpreted as evidence from a pervasive, hot, ($T = 10^5\text{-}10^6 K$), low density

($n = 10^{-2}$-10 cm^{-3}) component to the ISM. Either supernovae (Cox and Smith 1974; McKee and Ostriker 1977), or the combined effects of supernova and winds from massive stars (Bruhweiler et al. 1980; Kafatos et al. 1980; Weaver et al. 1977) are believed responsible for supplying the energetics to support this component.

Finally, studies are now being made for future UV and Extreme-UV astronomical experiments. Specifically, discussions have centered around a follow-on experiment to the current IUE, the Far Ultraviolet Space Explore (FUSE). This experiment may have detection capabilities extending into the Extreme-UV. The distribution of neutral hydrogen in the ISM will play a very fundamental role in determining the ultimate utility of any EUV experiment.

So far, the studies of gas in the solar neighborhood have provided very intriguing results. The Copernicus satellite has been utilized to study interstellar Lα and Mg II h (2802Å) and k (2795Å) in selected objects closer than 50pc. The Lα features were observed as central reversals of emission profiles in late-type stars (Anderson et al. 1978; McClintock et al. 1978), while the narrow absorption lines of Mg II were observed in the broad troughs of stellar features of nearby A and B stars. (Kondo et al., 1978). These results consistently indicate that the immediate vicinity of the Sun (3.5pc) is a region which is typified by a neutral hydrogen number density ($n_{HI} \sim 0.1$ cm^{-3}) while there is some evidence that the region beyond is typified by much lower values of n_{HI} (McClintock et al., Anderson and Weiler, 1978). We shall further discuss these and other data in Section IV.

II. RECENT IUE OBSERVATIONS OF WHITE DWARFS

Within the past year a serious attempt has been made toward studying and understanding the local ISM within 50pc of the Sun. High dispersion IUE data principally of hot white dwarfs were obtained (Bruhweiler and Kondo 1981, 1982), although a few B stars and one A star have very recently been studied. (Bruhweiler and Kondo 1982b).

So far, five hot dwarfs ranging in distance from 48pc, G192-B2B, to 2.7pc Sirius B have been studied (See Table 1.).

TABLE 1

WHITE DWARF DATA CURRENTLY ANALYZED

WD	d(pc)	T(x10^3K)	ℓ^{II}	b^{II}
G191-B2B	48	55-60	156	+7
W1346	15	21	67	-9
Sirius B	2.7	26	227	-9
HD 149499B	34	55-85	330	-7
40 ERI B	5	17	201	-38

Distances (d), approximate effective temperatures (T), and galactic coordinates (ℓ^{II}, b^{II}) are given.

The interstellar species detected in the white dwarf IUE spectra include C II, N I, O I, Si II, Fe II, Mg II, and likely Si III. Since data acquired using the LWR camera were somewhat noisy, only ions with multiple interstellar features in the SWP camera, N I and Si II, could be used to define an interstellar curve of growth. The details of the analysis for these objects can be found in Bruhweiler and Kondo (1982a).

Even though we cannot directly measure neutral hydrogen number densities from our data, a good determination of the actual H I column density can be derived from the N I column density. This can be done since N I is neutral with an ionization potential (14.5eV) not too different from hydrogen, and is relatively undepleted in the interstellar medium. A review of Copernicus data by Ferlet (1981) shows that N I is typically depleted by 0.15 dex and the average logarithmic value of N(N I)/N(H I + 2N(H_2) is -4.21. Using this relation, the total column density [N(H I)] and average particle density ($\bar{n}_{H\ I}$) of neutral hydrogen were estimated and given in Table 2.

The data clearly show that the longer lines of sight yield lower values of $n_{H\ I}$. The results for G191-B2B are extremely low giving $\bar{n}_{H\ I} = 6 \times 10^{-3} cm^{-3}$.

TABLE 2

INTERSTELLAR NEUTRAL HYDROGEN TOWARD NEARBY WHITE DWARFS

	G191-B2B	HD 149499 B	W1346	Sirius B
d(pc)	48	34	13	2.7
log N(H I) cm^{-2}	17.92	18.09	18.04	17.93(?)
$n_{H\ I}(cm^{-3})$	0.006	0.012	0.024	0.087(?)

(?) Indicates N I data not available, value deduced from average of Mg II and Si II.

III. COMPARISON WITH OTHER RESULTS

One might ask how the results presented here compare with previous Copernicus observations of the local ISM. Previous Copernicus measurements have been made for stars with distances ~5pc from the Sun from interstellar absorption superimposed on chromospheric H I Lα emission of nearby late type stars. Estimates of hydrogen column density and average hydrogen number density come from a variety of sources (cf. Anderson and Weiler, 1978; McClintock et al., 1976; Anderson, Henry, and Moos, 1978). The stars sampled range in distance from 1.33 pc for α Cen A to 33pc for HR1099. The average neutral hydrogen number density, $\bar{n}_{H\ I}$, is found to be close to 0.1 in most cases, although the most distant objects HR1099 (Anderson and Weiler, 1978) and α Aurigae (14 pc) yields $\bar{n}_H$ = 0.005 and 0.04 - 0.05 cm^{-3} (McClintock et al., 1978).

The recent Extreme-UV observations obtained by the UVS aboard the Voyager A and B spacecraft also provide estimates of the H I column density toward 2 nearby white dwarfs. (Holberg et al. 1980, 1981) Based upon little or no detectable hydrogen continuum absorption shortward of 912Å, the Extreme-UV observations of HZ43 (d = 62pc) indicate a low neutral hydrogen number density of $\bar{n}_{H\ I} = 0.002 \pm 0.001\ cm^{-3}$, while an upper limit of $\bar{n}_{H\ I} \leq 0.01\ cm^{-3}$ is derived for G191-B2B. The upper limit for G191-B2B is consistent with the $\bar{n}_{H\ I} = 0.006\ cm^{-3}$ found from IUE data.

In an effort to visually display how the previous Copernicus, EUV, and recent IUE results compare, we have attempted to construct a picture which we hope will provide information (Figure 1) about the distribution of gas in the local ISM within 50 parsecs of the Sun. We have included all the H I results as described on the works mentioned above.

Several important aspects are immediately apparent. First, the deduced values of $\bar{n}_H$ from the three different methods mesh quite well and present a coherent picture for the distribution of H I gas. The IUE results for Sirius B definitely support a local interstellar hydrogen density of $\bar{n}_H \sim 0.1\ cm^{-3}$ at distances up to 3-4 pc in that direction. More importantly, the derived values of $\bar{n}_{H\ I}$ in the direction of α Aur and HR1099 which indicated a drop off in density at distances larger than 3-4 pc is substantiated by observations at even larger distances by Voyager and IUE. The large drop off in $n_{H\ I}$ at larger distances strongly suggests the interstellar H I is concentrated in a small region about the Sun.

There is some indication from the H I distribution in Figure 1 that the density toward $\ell \sim 135\text{-}180^0$ may be lower than in other directions, or alternatively one might place the Sun near the edge of the diffuse H I cloud. The deduced values of $\bar{n}_{H\ I}$ for G191-B2B, HR1099, and HZ43 would place the boundary of a uniform density ($\bar{n}_{H\ I} = 0.1\ cm^{-3}$) hypothetical cloud within 2 pc of the Sun. The data as presented indicate this cloud does not extend beyond 4 to 5 parsecs in most directions. Beyond that distance one breaks out of the diffuse H I cloud into a region of extremely low $\bar{n}_{H\ I}$. This region most likely is the permeating sea of hot interstellar "coronal" gas (10^5 - 10^6 K), in which the local diffuse H I cloud is embedded.

This coronal gas is also an emitter of soft X-ray radiation. The diffuse soft X-ray results (Fried et al. 1980) between 0.1 and 2 Kev (especially their lowest energy bands) indicate that the X-ray emission originates locally in a 10^6 K plasma closer than the nearest $5 \times 10^{19}\ cm^{-2}$ of absorbing neutral or lowly-ionized gas. Otherwords, there is no evidence of shadows cast by X-ray absorbing cloudlets like that predicted by McKee and Ostriker (1977); which have total column densities for lines of sight intersecting their cores of $28 \times 10^{19}\ cm^{-2}$.

The IUE observations, combined with the soft X-ray EUV, and Copernicus results strongly indicate that beyond the local cloud in which the Sun is embedded, is a region of extreme low density, identifiable with the coronal hot interstellar component, with no evidence of additional clouds out to $d \simeq 50$pc.

IV. THE DISTRIBUTION OF INTERSTELLAR Mg II

We have attempted to determine the distribution of gas within the local cloud. The uncertainties in the derived H I column densities for nearby late-type stars from Copernicus necessitate using other data. The only other ion studied at distances $\leq$ 25pc is Mg II. An examination of the local distribution of Mg II in this region is quite revealing. There have been several studies of the local ISM where interstellar Mg II data have been presented. (Bohm-Vitense 1980; Kondo et al. 1978; Oegerle et al 1982; Morgan et al. 1978; Frisch 1981; Bruhweiler and Kondo 1981, 1982a, 1982b). From these works and recent IUE observations we have culled-out those observations of highest quality where individual observations pose definite constraints upon the distribution of interstellar Mg II. This is important since the doublet ratio defines the Mg II curve of growth and the Mg II lines in some lines of sight are approaching saturation. These culled data, which appear in Figure 2 come from Kondo et al. 1978, Bruhweiler and Kondo 1982b, plus recently reduced IUE data. These data clearly indicate that the Mg II distribution about the Sun is not uniform. In particular, the Mg II column density, N(Mg II) = 2.3×10^{12} cm^{-2}, toward α Leo (d = 25pc) is an order of magnitude less than those objects in the opposite direction from the Sun, but are also closer to the Sun. This variation does appear real, and suggests a Mg II density gradient toward $\ell^{II} \sim 0^0$.

V. INTERSTELLAR POLARIZATION

Recently extremely accurate polarization measurements of stars in the local ISM have become available. Tinbergen (1982) in a study of stars within 35pc of the Sun finds that the visual extinction over 35pc is extremely low or non-existent being $A_V \leq 0.002$ mag corresponding to N (H I) $\leq 5 \times 10^{18}$ cm^{-2}. One exception is an anomalous region centered near $\ell = 5^0$, $b = -20^0$ with angular extent 30^0 to 60^0. This area or "patch" of higher dust content with ($A_V \approx$ 0.01) corresponds to a H I column density of 1-2 x 10^{19} cm^{-2} when the relation of Knude (1979) N(H I) = 7.5×10^{21} E(B-V) is used. This patch appears to extend no further than a distance of 20pc. This patch is in the general direction of increased Mg II density and the line of sight toward α PsA, where C I has been detected (Bruhweiler and Kondo 1982b). Thus, we tentatively suggest that this patch lies in the general direction of the core of the local cloud.

VI. OTHER EVIDENCE FOR THE LOCAL CLOUD

Neutral hydrogen column densities are available for two early type stars with $d \lesssim 50$pc observed by Copernicus (York 1976). Although these lines of sight have not been studied in detail, York found from S II, N(H I) = 7×10^{17} cm^{-2} for η UMa (50pc) and (.8 - 1.6) x 10^{19} cm^{-2} for α Gru (20pc).

The line-of-sight toward α Gru is toward the suggested local cloud center and the deduced H I column density agrees with the implied H I column density for that direction from the polarization results. In addition, the data for η UMa (ℓ^{II} =101^0, b^{II} = +67^0) directly supports the, with $\bar{n}_{HI}$ = 0.005 cm^{-3}, the low values deduced from IUE and EUV data in the direction away from the local cloud.

Recently, we have acquired multiple high dispersion IUE exposures for the stars η UMa and σ Sgr. Both of these stars are B3V stars with distances of 50-55pc. The star σ Sgr (ℓ^{II} = 10^0, b^{II} = -12^0) is toward the interstellar polarization patch. The interstellar spectra in these stars are radically different, and show conclusively that the interstellar medium is not homogeneous on distance scales $\lesssim$ 50pc. The interstellar N I is extremely weak and at the detection limit in stacked, well exposed spectra of η UMa, while it is definitely saturated in σ Sgr. From a preliminary analysis, the N I implies a H I column density for η UMa slightly lower, but still in good agreement with that of York based upon S II. However, the N I toward σ Sgr implies N(H I)$\geq$ 10^{19} cm^{-2}. These results further support the interpretation presented here.

VII. SUMMARY

When the ultraviolet data, both IUE and Copernicus, are combined with recent EUV diffuse soft X-ray, He I backscattering, and visual polarization data, a single coherent picture of the interstellar medium within 50pc of the Sun begins to emerge. Although many aspects of the local ISM remain unresolved, it is worthwhile to review the important points, and by so doing sketch out a coherent picture for the local ISM.

The important characteristics are as follows:

(a) The Sun appears to be embedded in a low density region of cloud with the local H I number density ~0.1 cm^{-3}.

(b) The gas is not homogeneously distributed among the Sun. Lower density is likely the case toward α Leo, which may be in the anti-center direction of the local cloud as possibly defined by the polarization "patch".

(c) The local cloud is surrounded by the pervasive low density, (10^{-2} -10^{-3} cm^{-3}) high temperature (10^5-10^{6}K) component. There is no evidence for any other clouds out to distances of 50pc.

(d) If the local ISM is typical, present observations; EUV, UV, interstellar polarization, and soft X-rays, argue that the interstellar material is confined to larger clumps (or cloudlets), which are more sparsely spaced than originally envisioned by McKee and Ostriker. Specifically, with a predicted cloudlet mean free path of 12pc for any line of sight, one should expect to intersect 4 and 5 clouds respectively for G191-B2B and HZ 43. The general picture outlined by McKee and Ostriker may be still valid, but should be modified to include larger, more sparsely spaced cloudlets.

There are many aspects of the local ISM that we have not discussed, such as the interstellar wind, ionization, depletion, and observations for much longer lines of sight. Certainly, these other aspects are equally exciting as those discussed here. In any event our samples are small and more data are needed to adequately map out the distribution and physical conditions of the gas in the local ISM. Clearly, such an effort would only increase our knowledge of not only the local ISM, but also our understanding of physical processes in the general ISM.

REFERENCES

Anderson, R.C., Henry, R.C., Moos, H.W., and Linsky, J.L. 1978, Ap.J., 226, 883.

Anderson, R.C., and Weiler, E.J. 1978, Ap.J., 224, 143.

Bertaux, J.L., Blamont, J.E., Tabarie, N., Kurt, W.G., Bowgin, M.D., Smirnov, A.S., and Dementeva, N.N., 1976, Astr. Ap., 46, 16.

Böhm-Vitense, E. 1981, Ap.J. 244, 504.

Bruhweiler, F.C. and Kondo, Y. 1982a, Ap.J., In Press.

_____. 1982b, Ap.J., (Letters), Submitted

_____. 1981, Ap.J. (Letters), 248, L123.

Bruhweiler, F., Gull, T., Kafatos, M., and Sofia S. 1980, Ap.J. (Letters), 238, L27.

Ferlet, R. 1981, Astr. Ap., 98, L1.

Fried, P.M., Nousek, J.A., Sanders, W.T., and Kraushaar, W.L. 1980, Ap.J., 242, 987.

Frisch, P. 1981, Nature, 293, 318.

Holberg, J.B., Sandel, B.R., Forrester, W.T., Broadfoot, A.L., Chipman, H.L., and Barry, D.C., Ap.J., 242, L119.

_____. 1981, Bull. A.A.S., 12, 872.

Kafatos, M., Sofia, S., Bruhweiler, F., and Gull, T. 1980, Ap.J. 242, 294.

Kondo, Y. Talent, D.L., Barker, E.S., Dufour, R.J., and Modisette, J.L. 1978, Ap.J., 220, L97.

Knude, J. 1979, Astr. Ap. 71, 344.

McClintock, W., Henry, R.C., Linsky, J.L., and Moos, H.W. 1978, Ap.J., 225, 465.

McKee, C.F., and Ostriker, J.P. 1977, Ap.J., 218, 148.

Oegerle, W.R., Kondo, Y., Stencel, R.E., and Weiler, E.J. 1981, Ap.J. 252, 302.

Tinbergen, J. 1982, Astr. Ap. 105, 53.

Weaver, R., McCray, R., Castor, J., Shapiro, P., and Moos, R. 1977, Ap.J., 218, 377.

Weller, C.S. and Meier, R.R. 1981, Ap.J., 246, 386.

York, D.G. 1976, Ap.J., 204, 750.

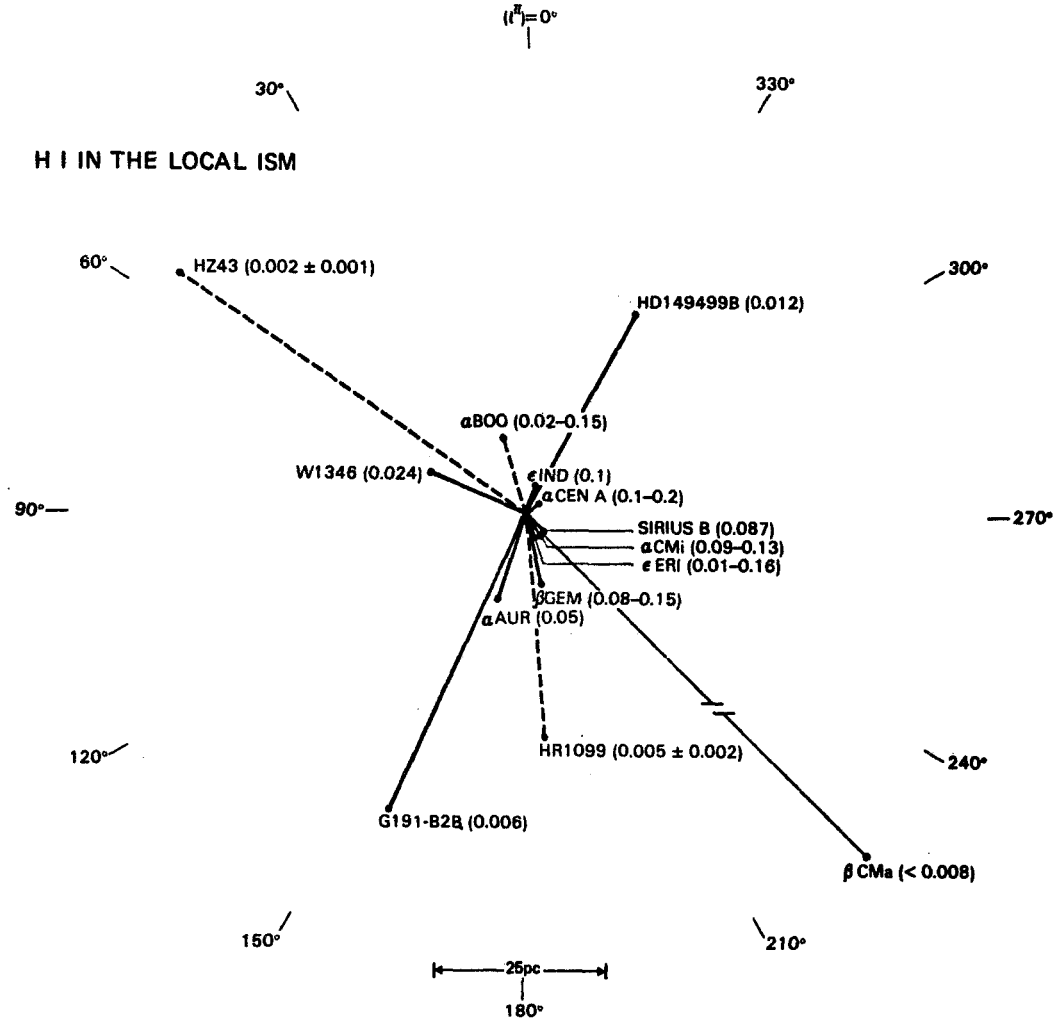
H I IN THE LOCAL ISM
(l^II)=0°
30°
330°
60°
300°
90°
270°
120°
240°
150°
210°
180°
HZ43 (0.002 ± 0.001)
HD149499B (0.012)
αBOO (0.02–0.15)
W1346 (0.024)
εIND (0.1)
αCEN A (0.1–0.2)
SIRIUS B (0.087)
αCMi (0.09–0.13)
εERI (0.01–0.16)
βGEM (0.08–0.15)
αAUR (0.05)
HR1099 (0.005 ± 0.002)
G191-B2B (0.006)
βCMa (< 0.008)
25pc

Figure 1

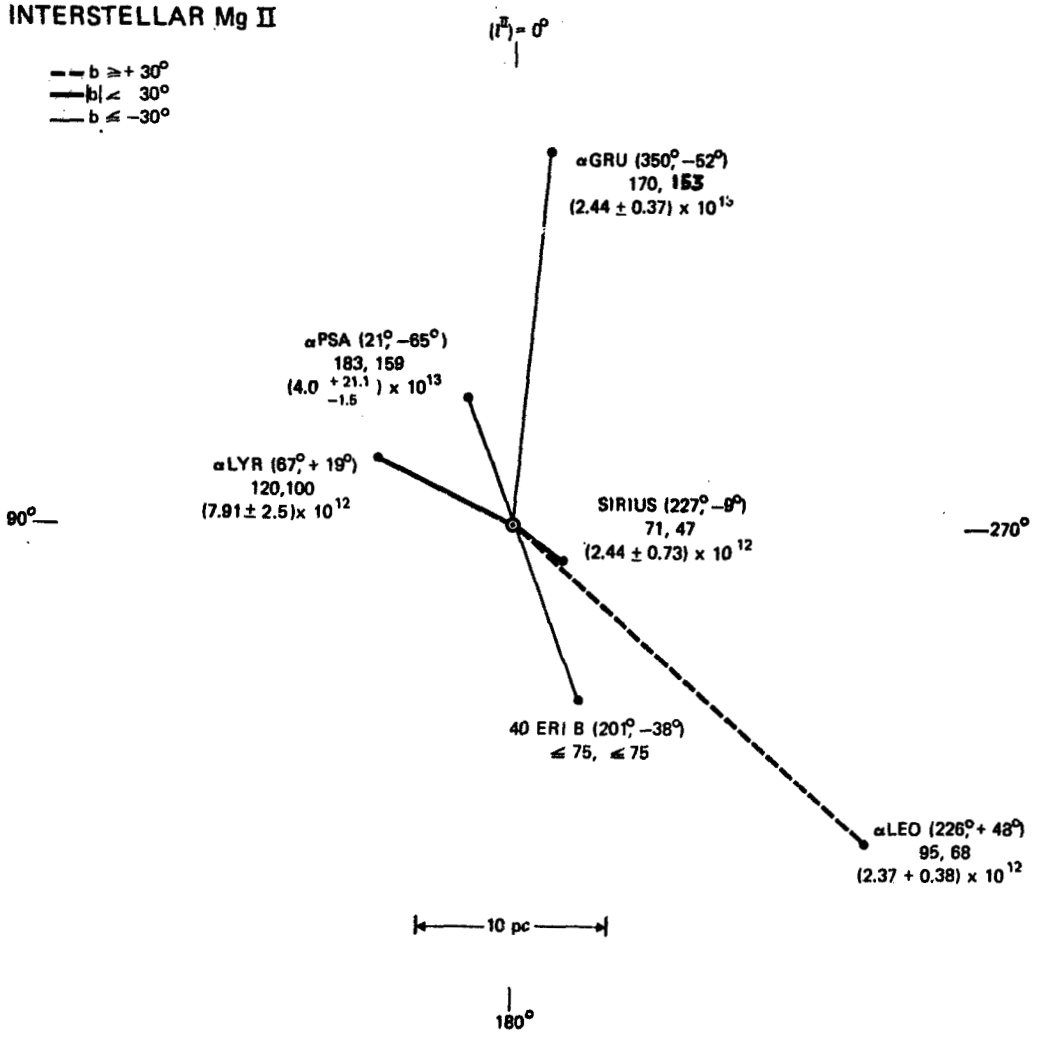
INTERSTELLAR Mg II
$(l^{II}) = 0^{\circ}$
$b \geq +30^{\circ}$
$|b| < 30^{\circ}$
$b \leq -30^{\circ}$
αGRU (350°, −52°)
170, 153
(2.44 ± 0.37) x 10^13
αPSA (21°, −65°)
183, 159
(4.0 +21.1 −1.5) x 10^13
αLYR (67°, +19°)
120,100
(7.91 ± 2.5) x 10^12
90°
SIRIUS (227°, −8°)
71, 47
(2.44 ± 0.73) x 10^12
270°
40 ERI B (201°, −38°)
≤ 75, ≤ 75
αLEO (226°, +48°)
95, 68
(2.37 + 0.38) x 10^12
10 pc
180°

Figure 2

Mullan: Mass loss requires magnetic field lines to be open. However, field lines are always created in closed form. Thus, an essential ingredient in driving mass loss must be some kind of process to either open up the field lines or disconnect them from the surface of the star. What this process is has so far not been determined in detail.(For a possible suggestion, see Mullan, D. J. "Physical Processes in Red Giants", ed. I. Iben and A. Renzini, 1981, p. 355.) But in any case, the process must involve tapping a significant source of energy. (Reconnection provides a possible source of energy.) If this source of energy can be identified, one will have gone a long way to identifying the true source of energy which drives mass loss. Other sources of energy may also contribute, such as Alfven waves, but since Alfven waves need straight open field lines to be useful in driving a wind, one is again forced back to the fundamental requirement: what opens up the field lines in the first place?

Dupree: (No reply necessary.)

Harris: Zn is apparently undepleted in the local interstellar medium. Is there any evidence that this is true also over distances greater than ~1 kpc?

Jura: No.

Doazan: I would like to summarize the situation of Be stars by emphasizing two paradoxical pictures that emerge from a superficial analysis of visual and UV data. From visual data, the existence of a mass flux is inferred in Be stars from the presence of emission lines. From UV data, both B and Be stars exhibit a mass flux which seems to be statistically of the same order of magnitude. Thus these new UV data do not seem to help in answering the fundamental question: how do B and Be stars differ? An answer to this question comes from our systematic simultaneous observations, in the UV and in the visual, of individual stars that we made since 1978. These show that Be stars are characterized by large variations of the superionized lines and of the mass flux at certain epochs of variation, whereas this variability and enhanced-mass flux epochs do not seem to occur in normal B stars.

Underhill: The difference in spectrum between B and Be stars at any wavelength range, visible, infrared, or ultraviolet, tells about the visibility of the mantle of the star at those wavelengths. Rather cool regions of the mantle are seen in the visible and infrared; rather hot regions are seen most easily by means of the ultraviolet resonance lines. How the mantle modifies the stellar spectrum depends on the physical state of the mantle, its geometry, and how these vary. To understand these factors and their changes it is essential to make models

using the physics of gas and radiation and the equations derivable from the conservation equations. One of the most important next steps in studying Be stars is to do some modeling of appropriate sort. It is necessary to consider departures from spherical geometry. Inhomogeneities of the atmosphere are probably very important. A geometric pattern of closed magnetic loops and open lines of force is one picture which needs exploring. Making plans for some systematic attacks on the problem of modeling the mantles of Be stars is more essential at this time than further acquisition of observations. It is almost certain, from present knowledge, that old observations and new ones will not repeat exactly. We need to concentrate on obtaining an improved theoretical representation of what we are seeing, a representation based on use of realistic physics.

Holm: I want to add to Blair Savage's caveat regarding derivation of extinction from the 2200 Å feature. If a system contains circumstellar dust, then, as shown by Blair and his graduate students, by Greenstein, and by me and my colleagues, the effects can be very different than with interstellar dust.

Helfer: (1) What is the uncertainty in g at the short wavelength region? (2) What is the contribution of gaseous emission to the total lightobserved?

Bohlin: (1) g~0 to .45 (2) It turns out to be ignorable. We even looked for H_2 flourescence at ~1700 Å and did not find any.

Penston: Are there any variations in the dust properties across the face of M101 related to the abundance gradients usually seen in this sort of galaxy?

Bohlin: See Stecher, Bohlin, et al., 1982, Ap. J. Lett, 255, April 15 and references therein.

Rocca: You present various extinction curves with spectral types. Do you agree with the idea that variations are also possible due to metallicity variation in the interstellar medium due to the grain size?

Bohlin: Certainly. Extinction can vary with grain composition and with grain size distribution.

Underhill: When matching the apparent continua of B5 to B8 supergiants, you should fit the two energy distributions together shortward of 2500 Å. This is because these stars show an infrared excess which extends

extends into the visible spectral range and Balmer continuum excess radiation. (See my paper given at the previous IUE Symposium held at GSFC.) The Ia supergiants have stronger f-f and Balmer continuum excesses than do the Ib supergiants.

Bohlin: For the purposes of deriving extinction curves, this consideration is not relevant. The only thing that matters is that the standard star intrinsic flux distribution matches the intrinsic flux distribution of the reddened star. I agree that the supergiants are more difficult to work with because of the difficulty of confirming that all intrinsic flux distributions are the same for a given spectral type.

Dufour: (1) Do you notice any radial gradients in the dust-to-gas ratio in M101? (2) Will the radial gradient in metallicity across the disk of M101 and its effects on the UV opacities and consequently fluxes of OB stars affect your derivations of dust-to-gas ratios?

Bohlin: (1) We have measured the dust only in the outer arms of M101. The surprising thing is that the dust seems more normal but that the oxygen has been measured to be most depleted in the outer parts. As a speculation, the dust could be mostly carbon from low mass stars and the oxygen could be from nucleosynthesis in more massive stars, which might be rarer. See Stecher, et al., 1982, Ap. J. Lett, 255, April 15 and references therein. (2) No, we expect warps and/or a large scale height in the outer parts of M101 so that the dust you see is illuminated directly by the galaxy without extinction by dust in the plane.

Bregman: Doesn't the maximum observed velocity toward F9, corrected for latitude effects, violate the velocities expected from a corotating halo?

York: My statements were to the effect that the data were consistent with, but did not prove, a picture of corotating gas near the disk. I have tried to correct for latitude effects. In addition, peculiar velocities of as much as ± 40 km s^{-1} are found in the disk and these could also occur at high latitudes.

Starrfield: RR Tel shows a cool continuum characteristic of a red companion. It is a binary. In addition, Dupree and Cole (1981) may have some problems. It is not the last word on PN ejection.

Plavec: What is the optical thickness of the scattering envelope needed to produce the anomalous O I multiplet ratios?

Hack: According to Osterbrock (1967, Ap. J. 135, 195) the number of scattering $\langle N \rangle \simeq 3\tau_o/\pi \ln\tau_o$ If $\langle N \rangle$ is very high, e.g., $\sim 10^5$ - 10^6, process with small probability can become important. The number of scattering at

λ1300 will be roughly 10^3 times larger than these at λ1641 (A_{21} 1300/A_{21} 1641~10^5). For $\tau(1641) \sim 2$, $N_{1641} \sim 10$, $N_{1300} \sim 10^6$.

Aizenman: What fraction of the symbiotic stars are best explained by assuming they are binaries. What fraction are best explained by a single star hypothesis?

Hack: About 40% of symbiotic stars are probably binaries, (the continuum of a hot star is observed in the UV, and the continuum of a cool star is observed in the IR, a few are eclipsing binaries). Less than 30% can be explained by both hypotheses.

Aller: The idea that symbiotic stars are transitive stages from red giants to planetaries was already proposed by Menzel in 1946 and adopted by a number of us as a working hypothesis, although we realized some objects must be binaries. In the early fifties I applied the Zanstra method to derive the temperature of the hot components of Z And, BF Cygni and CI Cygni and tried to set lower limits on N_e in BF Cygni from time changes in spectrum. It is interesting to see how T [Zanstra]'s have been substantiated by IUE observations of the continuum. Some of the puzzles about these systems (in particular unambiguous discrimination between binaries and single stars) are still unresolved.

Blair: (1) I was interested to see that the UV continua of HM Sge and V1016 Cygni are classified differently, yet their optical spectra are very similar. Since V1016 Cygni underwent its outburst about a decade earlier, the possibility of an evolutionary trend may be indicated. To what extent are variations in the UV continua of individual objects observed?

Hack: Considerable variations have been seen in the UV continua of some objects; some have been observed to change classes (e.g., SY Mus, EG And). However, evolutionary trends cannot be elucidated at this time.

Blair: The proto-planetary nebula interpretation for HM Sge and V1016 Cygni run into problems. People have estimated the amount of mass ejected in the recent outbursts of these stars and they are way below PN mass estimates.

Penston: Well, I agree with the comment that there is still strong evidence of a cool component in RR Tel. But in addition I am not convinced about the presence of λ1641 of OI] in this star. The He II is present and very strong and there is evidence it is self-absorbed both from the ratios to other He II lines and from the shift in the λ1640 line. Thus, the putative OI] line may merely be part of the He II profile. This is also consistent with the Balmer line profiles.

Hack: From the identification list of RR Tel (Selvelli, personal communication) and from the general appearance of the spectrum, I think that λ1641 is correctly identified with OI. Actually, all the outer He II lines, and especially λ3203 show no evidence of self absorption.

Kondo: The recent data obtained by Chapman, Stencel and myself indicate that the far-ultraviolet spectrum of Epsilon Aur is consistent with that of a late A supergiant; there is no apparent evidence of a hot companion. The C IV and Si IV absorption lines observed in late B to early A components in Algol type binaries may indicate the presence of hot spot(s) resulting from mass accretion. The primary uncertainty in classifying Plavec's W Ser type binaries in the same category as βLyr is the lack of high-resolution ultraviolet spectra for those relatively faint binaries.

McCluskey: If the Si IV and C IV arose in a wind, we might expect to have some emission. Also, the Si IV and C IV do appear to follow the orbital motion to a fair degree in Algol systems. In essence, we can only say that hot regions are present and seem to be associated with the primary star although association with the secondary may also occur.

Plavec: When observed at totality, U Cephei and V 356 Sagittarii display an emission spectrum of the W Serpentis - βLyrae type. Only the emission lines are much weaker compared to the out-of-eclipse continuum. It seems that the "W Ser" phenomenon begins in some active Algols of short period, and is fully developed in longer period/more active systems.

McCluskey: I consider the discovery of these lines as quite important. If this is a stage occurring just after a W Serpentis stage, it should provide useful information in a "simpler" situation. It is important to find out which systems do or do not show these lines and, of course, whence they arise.

Helfer: In using these "core" models for interpreting the spectra, has "restratification" of the atmosphere of the stripped star been built into the analysis?

Lambert: We hope to. There are other more critical problems.

Aller: The spectrum of the alleged planetary NGC 6302 shows an enhanced N, depleted C and slightly depleted O. It differs from conventional, often C-enriched planetaries, that presumably eject shells on asymptotic giant branch and has a composition recalling the stripped core of β Lyrae. Some planetaries are binaries. If it was a close binary, precursors of NGC 6302 may never have evolved as a normal planetary nebula progenitor, but it was a massive object whose envelope got stripped off before it had a chance to evolve on asymptotic giant branch.

Linsky: I would like to point out that the IUE spectrum of the mild Barium star 56 Pegasi (Stencel et al., Ap.J., in press) provides some important information on the system. The low dispersion SWP spectrum indicates a T≈30,000K white dwarf. Einstein observations indicate that 56 Peg is a bright X-ray source. This can be interpreted as due to accretion of matter from the primary onto the white dwarf for mass loss rates of 10^{-8} to 10^{-9} solar mass per year. Finally, the bright emission lines seen in the SWP low dispersion spectrum with excitation up to N V could be explained by recombination of the X-ray photoionized plasma about the white dwarf.

Walborn: There is growing observational and theoretical evidence for mixing and mass-loss effects in massive stars which are not included in the Iben models, and which can produce observable composition anomalies even in single stars. However, some of the most extreme OBN objects are also binaries; HD 163181 is an eclipsing system which has been analyzed quantitatively.

Aizenman: Following up on Walborn's comment, if one accepts Maeder's models of convective overshooting, it is possible that you would be able to match the composition (in the βLyr system) without having to go as deep as as a mass fraction of 0.3 to 0.5.

Starrfield: U Sco is a recurrent nova transferring He and carbon. Its current secondary must be the remains of a massive star. In G61-29 the lack of carbon suggests that the star was very low mass.

Slovak: G61-29 apparently shows some nebulosity surrounding the system, yet no outburst has been recorded for the system. Thus, the mass transfer may be non-conservative and could affect the abundance determinations.

Chanmugam: For V603 Aql, is the short wavelength continuum a Rayleigh-Jeans spectrum?

Lambert: No. The continuous spectrum after correction for a slight amount of reddening is close to the $f_\mu \propto \mu^{1/3}$ spectrum of an optically thick accretion disk.

Shore: A naive comment. If the MS mass gainers are the ones which have cool WD's, shouldn't these be in general the mildest Ba stars? One might think that turbulent mixing post-MS would dilute the S-process abundances somewhat. Isn't this possibly orthogonal to the detection results for WD's in Ba II stars?

Lambert: If Ba-rich and C-rich main sequence stars are produced with a relatively thin layer of processed material atop a normal composition envelope, the convective envelope that develops as a star ascends the giant branch will mix the thin layer with the envelope. The S-process abundances will decline through dilution. Carbon will decline by a larger amount because the deeper parts of the main sequence envelope were depleted in C-poor. Then, the star might be a mild Barium star which according to Sneden, Lambert and Pilachowski (1981) have slight S-process enhancements without detectable C enhancements. In our paper, we ascribed the mild Ba stars to the result of fluctuations in the D-process abundances in interstellar clouds. Your comment suggests an alternative idea.

Hack: Do you have recent determinations of the ratio N/C for U Sgr? I found 20 years ago, by curve of growth method, N/C $\sim$20, which is just what we expect from CNO cycle.

Lambert: Dr. Parthasarathy and I are currently obtaining CNO for υ Sgr. In a discussion of their CNO abundances for HD30353, a star quite similar to υSgr, Wallerstein, Greene, and Tomley (Ap. J., 150, 245, 1967) proposed that the CNO-cycles operated in two steps. After high temperature processing ($T\sim25\times10^6$K), severe mass loss led to a drop in the central temperature to $T=10\text{-}15\times10^6$K with CN cycling continuing but the O abundance frozen at this lower temperature.

Peters: Particularly interesting are the Algol binaries with low mass ratios (0.1 - 0.3). Ron Polidan and I have observed a number of these systems with IUE and ground-based telescopes. We have analyzed absorption lines formed both in gas stream and the primary's photosphere and find, although the analysis is still incomplete, we do not note any striking abundance peculiarities; N and C appear to be normal. This has been puzzling to us.

Lambert: Our observations of S Cnc show a mild C deficiency in contrast to the severe deficiency expected from simple stellar models. Perhaps, the outer envelopes are mixed to create mild C deficiencies over the whole envelope.

Plavec: We should not say that the secondary star in βLyrae is invisible. Its continuous radiation is visible and is that of a disk (no unique effective temperature). Both components are immersed in a luminous hydrogen cloud, which will veil the aborption lines and must be taken into account in abundance analyses. However, your case for the absence of the C I IR lines remains quite convincing.

Shore: Both a question and a comment. What is the velocity of the cloud relative to the LSR? You might now think of applying this observation to the Milankovitch cycle for ISM cloud-induced ice ages. Your IS bugger appears far too optically thin to be useful and should militate against the mechanism.

Bruhweiler: The He I 584 Å backscattering data of Weller and Meier (1981) suggest a value $\sim$22-28 km s^{-1}. You are absolutely right. This is not the type of cloud as proposed by Vidal-Madjar. I might also emphasize that this cloud shows no suggestion of being part of a shell centered upon the Sco-Cen association as suggested by some in the literature.

Linsky: ηUMa is at high galactic latitude. Could the low hydrogen column density to this star indicate that the low column densities are due to high galactic latitude and not due to the line of sight being away from the galactic longitude.

Bruhweiler: The distances to ηUMa (50pc) and also HZ43 (62pc) are still much smaller than the characteristic scale height of the HI gas. Also, there is evidence of patchy clouds at higher Z distances. I also point out the G191-B2B (48pc) lies only 10° out of the plane and also shows very low values of N HI.

GALAXIES

IUE and Einstein Observations of NGC5204

G. Fabbiano[1] and N. Panagia[2]

(1) Harvard-Smithsonian Center for Astrophysics, Cambridge, Mass.
(2) Istituto di Radioastronomia del CNR, Bologna, Italy.

I. Introduction

NGC5204 was observed in X-rays with the Einstein satellite (Giacconi et al. 1979) as part of a program to study blue irregular galaxies in the M101 group (Fabbiano and Panagia, in preparation), and was detected at a $L_x \sim 4.2 \times 10^{39}$ erg s^{-1}. The ratio of the X-ray to the blue flux (f_x/f_B) for this galaxy is exceptionally high, comparable with the highest values found in an X-ray survey of peculiar late type galaxies (Fabbiano, Feigelson, and Zamorani 1982)(Figure 1). The X-ray source associated with NGC5204 appears extended in the IPC, suggesting either a region of diffuse emission or the integrated output of a number of point sources. Given the X-ray luminosity of NGC5204, between ~400(10^{37} erg s^{-1}) and ~40(10^{38} erg s^{-1}) binary X-ray sources could be present in it. We would then expect $\sim 10^4$-10^5 OB stars to be present in this galaxy (Fabbiano, Feigelson, and Zamorani 1982). To test this prediction, we observed NGC5204 with IUE (Boggess et al. 1978). In the following we report the results of this observation and discuss their implications.

II. IUE Observations and Data Analysis

An IUE 200 min short wavelength low dispersion exposure of NGC5204 was taken on December 10, 1980 (SWP10847). The spectrum (Figure 2) show a rising continuum at the short wavelengths and a complex series of absorption features. The main features, that persist also when the data are smoothed (by averaging over 3 and 5 points) are a complex absorption band centered at ~1300 Å, a SiIV doublet blueshifted by ~2 Å, a CIV line blueshifted by ~10 Å and a broad deep band centered at ~1650 Å. No SiIV and CIV emission lines are visible in the spectrum. Figure 2 shows an enlargement of the regions around the SiIV and CIV lines. The spectrum here has been averaged over three points to reduce some of the noise. Unfortunately this has also the effect of making the SiIV and CIV lines look less deep. The IUE image also appears rather spread ortogonal to the spectral dispersion, suggesting an extended emission region.

III. Discussion

We can try to get an estimate of the early star content of NGC5204 from the IUE spectrum by comparison with similar spectra of stars (IUE spectral Atlas, Wu et al. 1981). Since the spectrum of NGC5204 rises at the short wavelengths the UV emission is clearly dominated by early type stars. The two broad absorption bands at ~1300 Å and ~1650 Å (Figure 2) suggest that the UV emitting stellar population must contain a significant number of supergiants, because these wavelength regions in main sequence stars do not show such pronounced absorption features. To fit the NGC5204 spectrum in term of early type stars, we tried to match the continuum as well as the

equivalent widths of the absorption features. The main uncertainty is of course due to the unknown internal reddening in NGC5204. We, therefore, considered in our analysis a range of E_{B-V} going from 0.0 to 0.3. For our fit we chose to use the ratios between the continuum fluxes at 1300 Å, 1600 Å, and 1900 Å so as to have a broad baseline over all the IUE spectrum.

From the IUE spectral Atlas (Wu et al. 1981) we choose five early type stars that showed the absorption features present in the spectrum of NGC5204 and we attempted to fit in terms of these stars. They are HD303308 (O3V), HD188209 (O9.5Ia), HD53138 (B3Ia), HD58350 (B5Ia) and HD104035 (A0Ia). The presence of A0I stars seems at a first glance attractive because of the broad 1650 A absorption band and of CIV redshifted in absorption (all the other stars show a certain amount of CIV redshifted in emission). However, considering the spectral slopes between 1300 Å and 1600 Å and between 1600 Å and 1900 Å, it appears that the presence of a significant component of A0Ia stars in the spectrum will not give the expected continuum. We estimate that the percentage of A0 stars must be <10% because a model consisting of 10% A0 stars + 90% O stars already barely fits the continuum slope. We therefore tried a mixture of O and B stars. B stars must be present in the spectrum because of the absorption lines at 1200-1300 Å. We find that a satisfactory fit is given by 10% O3 + 30% O9.5 + 30% B3 + 30% B5 stars. Less than 50% O type stars are required, otherwise the equivalent width of the CIV absorption line would be significantly larger than observed. A greater amount of stars of later type than early O stars are needed to produce a large enough SiIV absorption line. The B stars could also account for the ~1300 Å and ~1650 Å absorption bands.

Using the spectra in the IUE Atlas we can also estimate the number of OB stars responsible for the NGC5204 emission. After correcting for reddening the spectra used for our fit and estimating the distance to the stars by comparison with the H-R diagram, we derive that an OB star representative of the NGC5204 spectrum will have a flux of $\sim 3.7 \times 10^{-14}$ erg cm^{-2} s^{-1} between 1300 Å and 1900 Å. Comparing this to the corresponding flux from NGC5204 (after correcting for reddening), we obtain a number of OB stars between 140 and 1460 (for $E_{B-V} = 0.0$ to $E_{B-V} = 0.3$). Since the IUE aperture is 20" x 10" and the UV emitting region is likely to be ~1'.5 x 1'.5 (the approximate size of the X-ray emitting region), this number of stars should be multiplied by a factor of ~40, giving N(OB stars) $\sim 6 \times 10^{3}$-6×10^{4}. This is compatible with what was expected based on the X-ray luminosity of NGC5204.

Lequeux et al. (1981) comparing IUE spectra of extragalactic HII regions with theoretical predictions conclude that most likely these HII regions experience only a short burst of star formation. Using their method we can derive the age of the burst and the total mass of stars formed. We can estimate the UV monochromatic luminosity at 1600 Å from our data. We obtain $L_{1600} \sim 1.1 \times 10^{38}$ erg s^{-1} A^{-1} ($E_{B-V} = 0.1$) or $\sim 2.3 \times 10^{38}$ erg s^{-1} A^{-1} ($E_{B-V} = 0.2$). We multiply L_{1600} by a factor of ~40 to take into account the size of NGC5204 versus the IUE aperture. The number of Lyman continuum photons is evaluated using the equation (10) of Lequeux et al. (1981), for a radio flux density of 25 mJy at 10.7 GHz (Gioia, Gregorini, and Klein 1982) and assuming an electron temperature ~40,000 °K. From

these quantities we derive a time since the occurrence of the burst of star formation of ~3 x 10^6 yrs and a mass ~3-4 x 10^6 $M_\odot$ for the total mass of formed stars. Since we could be seeing as much as ~10^5 OB stars in NGC5204, the total mass of star formed is compatible with the observations, although suggesting the presence of fairly massive stars.

IV. Conclusions

The Einstein and IUE observations of NGC5204 have given us an unique opportunity to test some of the hypothesis put forward as a result of an X-ray survey of blue peculiar late type galaxies (Fabbiano, Feigelson, and Zamorani 1982). In particular the hypothesis that binary X-ray sources of Pop I progenitors are responsible for most of the X-ray emission, is strengthened by the IUE short wavelength spectrum of NGC5204. This spectrum suggests a number of OB stars in agreement with the one inferred from the X-ray luminosity. It also shows an ultraviolet excess in agreement with the large f_x/f_B ratio. We think that the results reported in this paper clearly show the potential of coordinated IUE/X-ray observations of galaxies. A careful study of the stellar population of NGC5204 will need IUE long wavelength data and good optical spectrophotometry, both to measure the extinction and to give informations on the later type stellar component.

Acknowledgements

We acknowledge the help of J. Patterson in obtaining the IUE spectrum and of T. Varner in the data analysis. We thank A. Boggess who made it possible for us to observe NGC5204 with IUE.

References

Boggess, A. et al. 1979, Nature, 275, 377.
Fabbiano, G., Feigelson, E., and Zamorani G. 1982, in press.
Giacconi, R. et al. 1979, Ap.J., 230, 540.
Gioia, I., Gregorini, L., and Klein, U. 1982, submitted.
Lequeux, J., Maucherat-Joubert, M., Deharverg, J.M., and Kunth, D. 1981, A.A. 103, 305.
Wu, C.-C., Boggess, A., Holm, A.V., Schiffer, F.H.,III, and Turnrose, B.E. 1981, IUE Ultraviolet Spectral Atlas (Greenbelt: GSFC), preliminary edition.

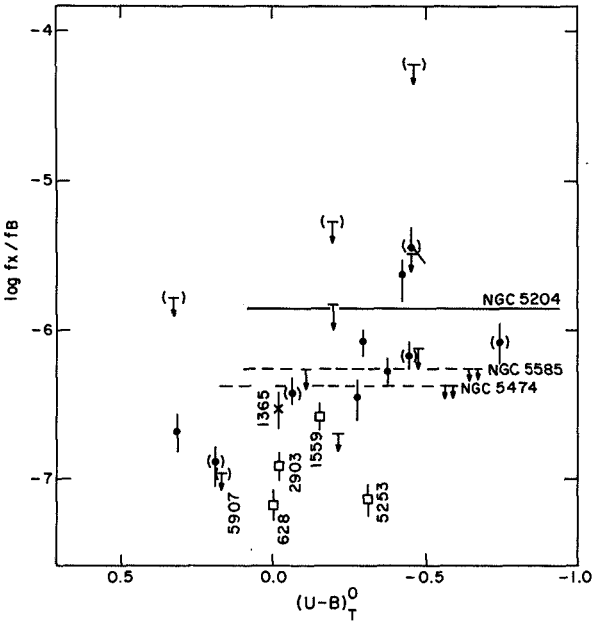

Figure 1. The log of the ratio of 2 keV monochromatic X-ray flux to the blue flux (f_x/f_B) is plotted versus U-B for a sample of peculiar late type galaxies (the dots) and more "normal" late type spirals (the squares).

NGC5204 has a f_x/f_B ratio comparable to the highest ones found for the peculiar irregular galaxies.

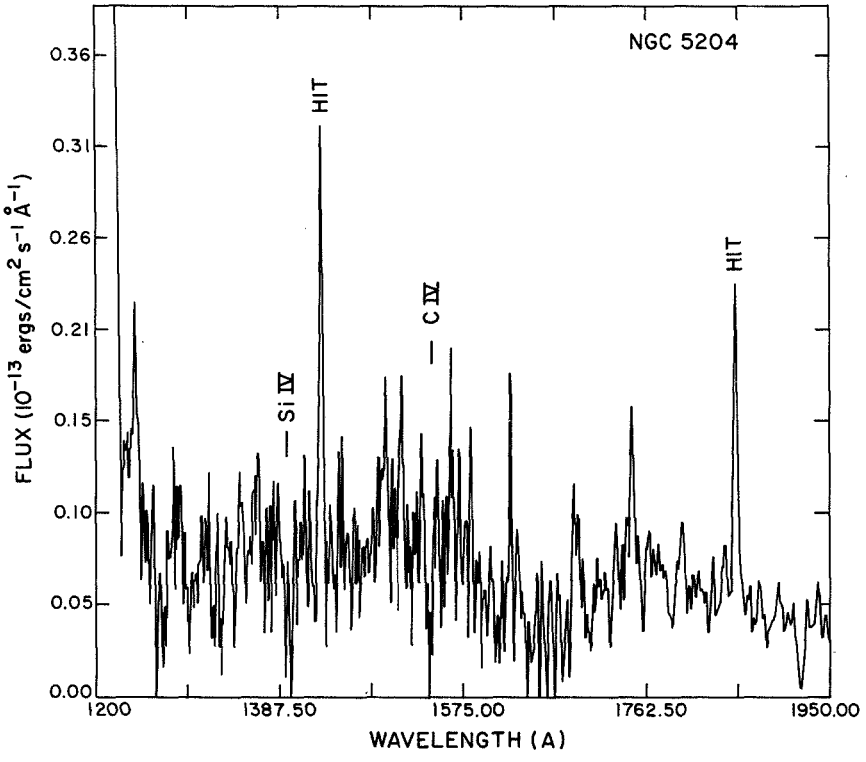

Figure 2. Short wavelengths low dispersion IUE spectrum of NGC 5204.

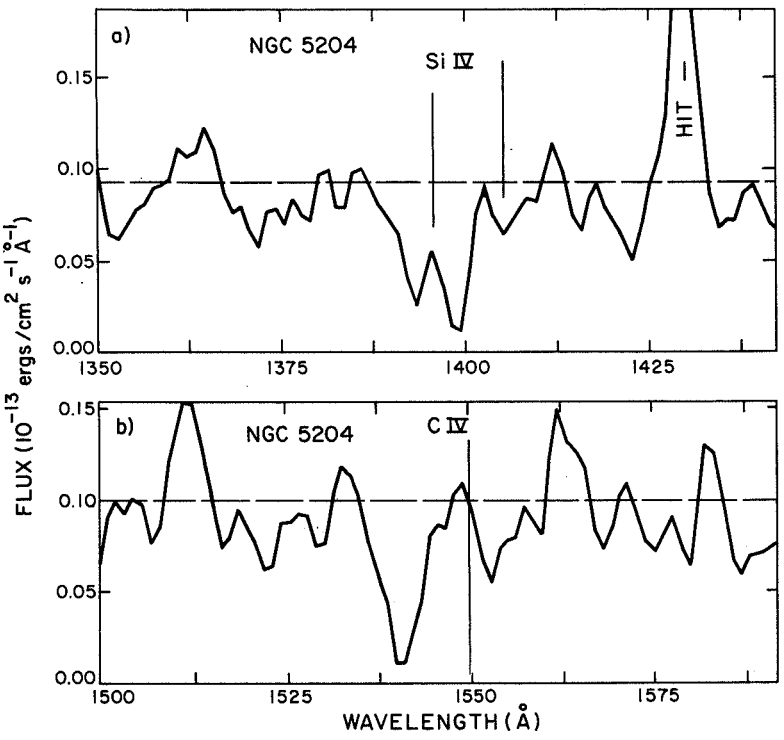

Figure 3. Three points smoothed spectra at the wavelengths of CIV and SiIV.

THE IUE LOW-DISPERSION SPECTRUM OF THE CENTER OF M31

Gary A. Welch, Saint Mary's University
Halifax, Nova Scotia

A total of twelve long exposure low resolution IUE images have been used to study the spectrum and surface brightness distribution of the ultraviolet radiation within the central 50 parsecs of M31. The presence of weak absorption features near 1300 Angstroms demonstrates that the radiation of the well-known spectral upturn below 2000 Angstroms does not originate in young metal-rich stars. The energy distribution is bluer than that measured by experiments with larger entrance apertures, and below 2000 Angstroms the surface brightness gradient near the nucleus increases. These findings indicate that the blue stars are more centrally concentrated within the bulge of M31 than the more metal-rich red giants. The energy distribution measured by IUE appears to be much bluer at short wavelengths than that of the metal-rich globular cluster 47 Tucanae, yet it also differs from those of clusters having more populous blue horizontal branches.

MARKARIAN 36: A YOUNG GALAXY!? *

John Huchra and Margaret Geller
Harvard-Smithsonian Center for Astrophysics
Diedre Hunter and Jay Gallagher
University of Illinois at Urbana-Chambaign

ABSTRACT

The optical spectrum of Markarian 36, a dwarf galaxy, is dominated by strong emission lines. The UV spectrum however shows no strong emission lines, only weak CIV and Si absorption and a strong blue continuum that is still rising shortward of Lyman alpha. Combined UV, optical and IR observations show that the continuum is nearly Rayleigh-Jeans from 1100 Å to 2.2 microns, with a slight excess in the optical due to free-free emission and recombination lines. This galaxy has few, if any, red stars. Combined with its low metal content, this lack of red stars is a very strong indication that this galaxy has only recently begun to form stars.

In the last few decades a population of very blue galaxies has been identified by such astronomers as Haro, Markarian and Zwicky. These objects have optical integrated properties similar to well known Magellanic irregular galaxies and to individual HII regions in irregular and late type spiral galaxies. These very blue galaxies appear to be forming stars at prodigious rates everywhere. We have started to study these "hot" blue galaxies with IUE. The star formation history and current population are dependent on the initial mass function (IMF), the star formation rate, the age and the metallicity. Earlier studies based only on optical data miss the dominant populations in objects with high star formation rates - the hot OB stars and the red supergiants. Both ultraviolet and infra-red observations are necessary if we hope to constrain models of the stellar and gaseous content.

Here we report UV, optical and IR observations of three galaxies - NGC 4214, NGC4670 = Haro 9, and Markarian 36. The ultraviolet observations were made with the SWP camera on IUE in the low dispersion mode. Exposures of 180m, 180m, and 310m respectively were obtained after carefully offsetting from bright stars to accurately measured galaxy positions. Infrared (JHK) observations were obtained for Mk 36 with the MMT and for N4670 and N4214 at Kitt Peak and Steward Observatories. Optical spectra were obtained at Mt. Hopkins and optical (UBVR) photometry from Huchra (1977a) and deVaucouleurs (1961).

The UV spectra of N4670 and N4214 are remarkably similar both in spectral shape and features. There are a number of prominent absorption lines characteristic of hot stars and the CIV line shows the P-Cygni profile associated with mass loss. There are no other strong emission lines (Lyman alpha is not visible due to the geocorona), although the optical spectra show strong sharp recombination lines. A composite spectrum of these two

galaxies is shown in Figure 1(a). The spectra of these galaxies are hotter than those of "starburst" nuclei such as N7714 (Weedman et al. 1981) and N3310, which we also have observed. The latter galaxies are more luminous and also probably more highly reddened.

The UV spectrum of Mk 36 is quite distinct from the other galaxies. It rises very steeply towards short wavelengths and shows only weak absorption lines. [CIII] 1909Å is seen weakly in emission, indicating an electron temperature > 20,000K. The UV spectrum is shown in Figure 1(b), and the optical spectrum is shown in Figure 2. The optical continuum is nearly flat and the spectrum is dominated by sharp recombination lines of large equivalent width. The [OIII] lines are very strong and the [NII] lines are virtually nonexistent, indicative of very low metallicity. Table 1 summarizes some of the observed properties for N4670, N4214 and Mk36. The 21cm observations come from Heckman et al. (1978), Allsopp (1979), and Gordon and Gottesman (1981). The metallicities come from Alloin et al. (1979), and indicate that the metallicity for Mk 36 is lower than for the other galaxies. Note also that the relative HI content as measured by M_H/L_B is nearly the same for all three galaxies.

Simple models for the stellar energy distributions from the UV to IR have been constructed as in Huchra (1977b). These models are at present limited to solar metallicity both in the evolutionary tracks and the color-effective-temperature conversion, however we can make qualitative estimates of the effects of metallicity by examination of the stellar models of Brunish and Truran (1981). N4670 and N4214 are easily fit by models with nearly normal (Salpeter) IMF's and with a high present rate of star formation relative to their integrated star formation history. MK 36, on the other hand, is best fit by a very "young" model with an age of only ten million years and a power law IMF with slope between 2.35 and 1.35 (the Salpeter slope is 2.35 in mass). There is no room in the energy distribution for many red supergiants: V-K is only 0.7. There must be less than one M supergiant for every hundred early O stars and the galaxy contains at most a few hundred O stars. The presence of any stars later than O limits the number of red supergiants even more strongly.

The age could be longer than ten million years if the low metallicity were properly taken into account. Low metal stellar models are hotter and do not produce red supergiants before carbon ignition for masses > 15 solar. The age can not be greater than 50 million years for near normal IMF's or the intermediate mass stars will populate the red giant region. The IMF cannot be much flatter than Salpeter, however, without violating the observed H beta equivalent width (which is reddening independent). Although it is possible to construct models with constant star formation rates and large ages if evolutionary tracks with no red supergiants are used, these are inconsistent with the very low observed present metallicity. It is hard to escape the conclusion that this galaxy is young!

We would like to acknowledge S. Willner, L. Hartmann and J. Raymond for data and useful discussions. Research reported here used the Multiple Mirror Telescope Observatory, a joint facility of the University of Arizona and the Smithsonian Institution.

REFERENCES

Alloin, D., Collin-Souffrin, S., Joly, M. and Vigroux, L. 1979, Astron. and Ap. 78, 200.
Allsopp, N. 1979, M.N.R.A.S. 188, 765.
Brunish, W. and Truran, J. 1981, preprint.
de Vaucouleurs, G. 1961, Ap. J. Suppl 5, 233.
Gordon, D. and Gottesman, S. 1981, A. J. 86, 161.
Heckman, T., Balick, B. and Sullivan, W. 1978, Ap. J. 224, 745.
Huchra, J. 1977a, Ap. J. Supp. 35, 171.
Huchra, J. 1977b, Ap. J. 217, 928.
Neugebauer, G., Becklin, E., Oke, J. and Searle, L. 1976, Ap. J. 205, 29.
Weedman, D., Feldman, F., Balzano, V., Ramsey, L., Sramek, R. and Wu, C-C. 1981, Ap. J. 248, 105.

Table 1 Galaxy Properties

	N4670	N4214	Mk36
V (km/s)	1050	288	640
D (Mpc)	15	7	10
M_V	-17.68	-15.99	-14.49
M_{HI}/L	0.33	0.30	0.33
V	13.20	13.24	15.51
B-V	0.38	0.33	0.31
U-B	-0.54	-0.39	-0.70
J	12.10	11.50	15.40
H	11.47	11.00	14.99
K	11.28	10.80	14.49
W(Hβ)	-21	-26	-66
W(λ5007)	-55	-78	-307
W(Hα)	-101	-194	-256
W(λ6583)	-9	-19	-4
W(λ6717)	-11	-23	-16
W(λ5876)	-6	-6	-13
[O/H]	-0.22		-0.94
[N/H]	-0.89		<-1.16

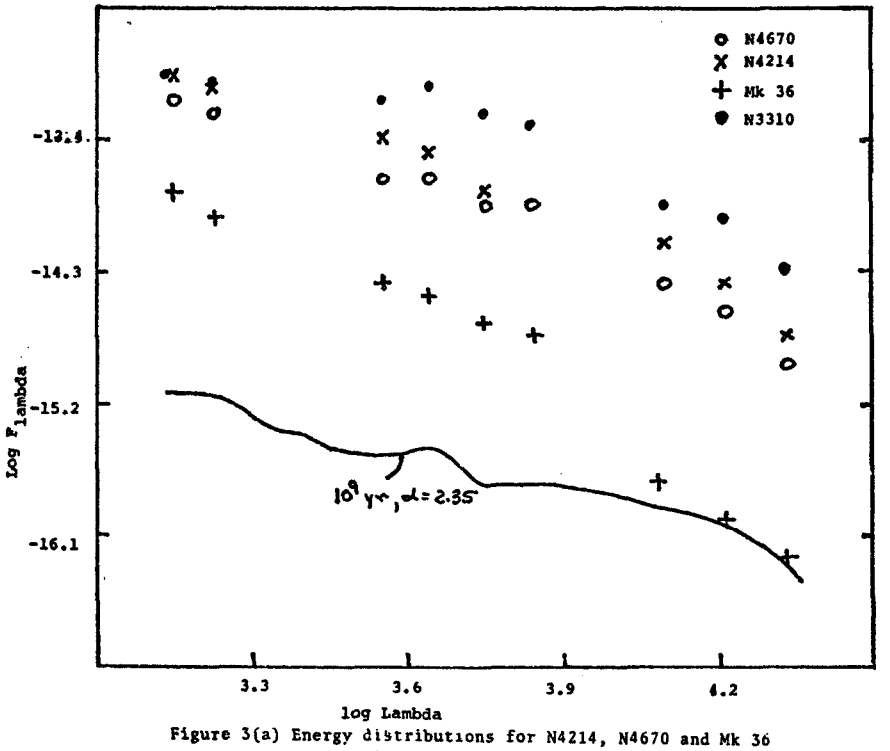

Figure 3(a) Energy distributions for N4214, N4670 and Mk 36

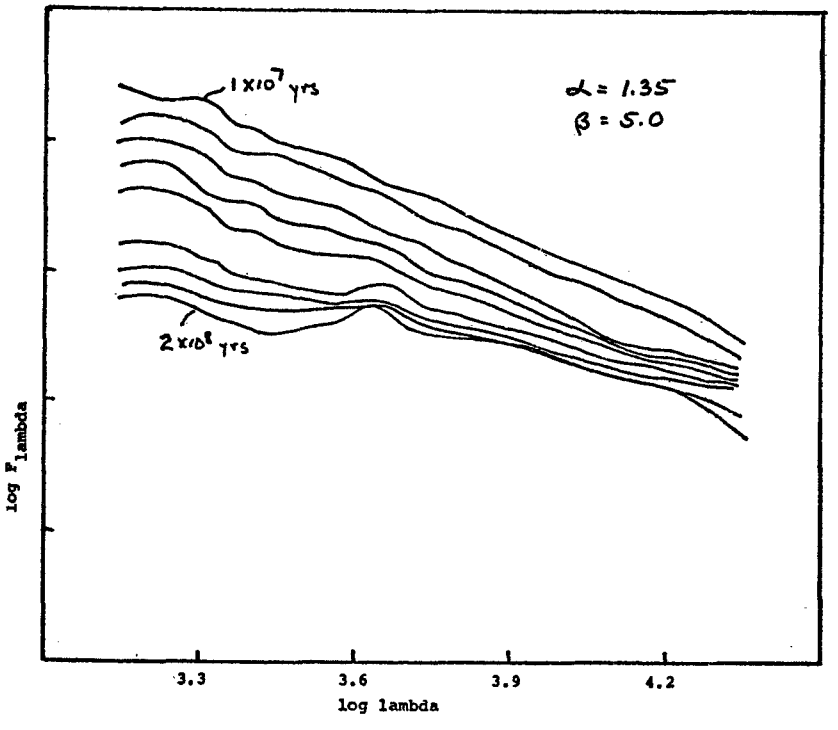

Figure 3(b) Energy distributions for a sequence of models

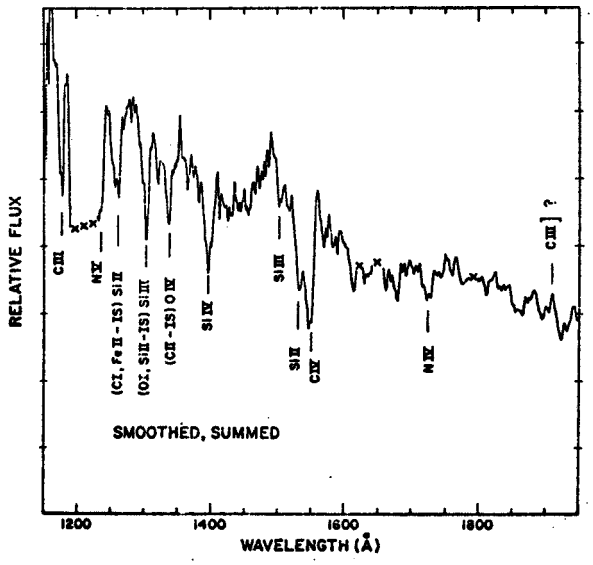

Figure 1(a) UV spectra of NGC 4214 • NGC 4670

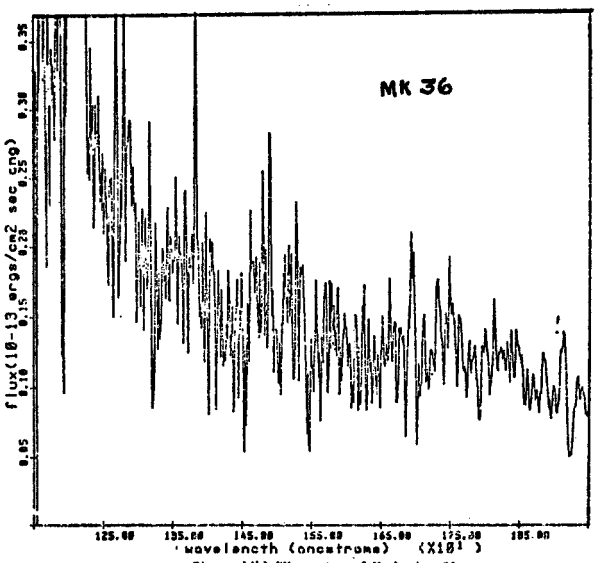

Figure 1(b) UV spectra of Markarian 36

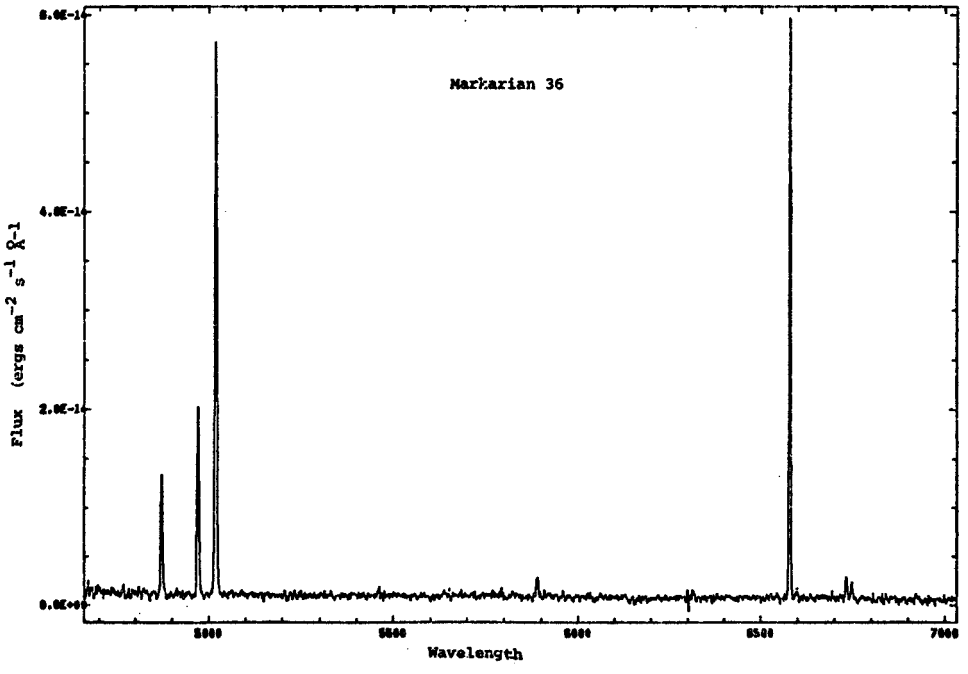

Figure 2 Optical spectrum of Mk 36 in ergs/cm^{-2}/s/Å

FOUR YEARS OF IUE RESEARCH ON CLUMPY IRREGULAR GALAXIES

P. Benvenuti - ESA IUE Satellite Tracking Station, Madrid
C. Casini - Istituti di Astronomia e di Fisica, Milano
J. Heidmann - Observatoire de Paris, Paris

INTRODUCTION

First hand information about large scale star formation in galaxies may be obtained from investigation of giant clumpy irregular galaxies in which bursts of star formation of exceptional magnitude are taking place.

Clumpy irregular galaxies were initially identified mainly by morphological criteria: 5-10 high surface brightness clumps loosely scattered in a common envelope. Later work showed that each clump is on average equivalent, in total mass and optical luminosity, to 100 giant H II regions like 30 Doradus (Casini and Heidmann, 1976; Heidmann, 1979; Casini et al., 1979).

During the first four years of IUE operations 7 shifts were used to observe 4 clumpy irregular galaxies: Markarian 7, 8, 297 and 325. All spectra were obtained at low resolution in both short and long wavelength, with exposure time ranging from half to a full shift.

Crucial results were obtained from the first IUE spectra:

i) on the average one clump radiates intrinsecally 100 times more than 30 Doradus at 1550 Å.
ii) absorption lines typical of early O, B type stars are present with indication of supergiant stars.
iii) the continuum could be accounted for by the radiation of a mixture of 70,000 stars of type O8 V and B8 I for one average clump (Benvenuti et al. 1979, 1982).

CONTINUUM DATA

In Table 1 we present a summary of the previous and new IUE results on the global properties of the continuum emission as measured at 1550 and 2500 Å, taking into account the presence of absorption lines. F_{obs} is the observed flux density in erg cm^{-2} s^{-1} $Å^{-1}$. A_B is the B absorption in our Galaxy from de Vaucouleurs et al. (1976). G_{corr} is the flux density in mJy corrected for the above absorption using Seaton's (1979) extinction curve and Code et al. (1976) differential galactic absorption 4.04. D is the distance in Mpc obtained from radial velocities reduced to the Local Group and using a Hubble constant of 75 Km s^{-1} Mpc^{-1}. L is the intrinsic UV luminosity in erg s^{-1} Hz^{-1}.

It should be noted that the UV luminosities reach very high values, though they refer only to that part of the clumpy galaxies that fall inside the IUE large aperture. Table 1 gives also the number of clumps included into the slit and the mean UV luminosity of these clumps. As a comparison, the giant H II region 30 Doradus value is $L_{1550} = 1.8 \times 10^{25}$ erg s^{-1} Hz^{-1} (Israel and

Koorneef, 1979), i.e. 100 times less than the mean UV luminosity L_{1550} = 1.8 x 10^{27} erg s^{-1} Hz^{-1} obtained for one clump from the data in Table 1.

The last line in the Table gives the spectral index α of the UV continuum ($G \propto \alpha$). The mean value is $\alpha = -1.4$, with some dispersion, the spectra of Mkn 7 and 325 being flatter than the ones of Mkn 8 and 297. We should note that the position angles of the slit for the short and long wavelength observations were not always equal and a scaling factor might therefore exist.

SYNTETIC FIT

Recently we made an attempt to fit the spectrum of Mkn 325 with a syntetic spectrum of standard stars extracted from the IUE Spectral Atlas by C.C.Wu (1981). Although a final fit has not yet been obtained, a first result which is reported in Fig. 1, is very promising: not only the continuum can be satisfactorily fitted but also the equivalent width of the stellar absorption lines are reproduced. The fit shown in Fig. 1 has been obtained from a mixture of O8 V, B5 Ia, B7 III and A0 V stars and provide a good match for Si II 1257, Si III 1300, C II 1335, Si IV 1400, CIV 1550 and for the broad absorption features of Al III, Fe III at $\sim$ 1600 Å, and Si III, Fe III at $\sim$ 1850 Å. Discrepancies still exist at $\sim$ 1700, 1900, 2220, 2470 and 3150 Å. Internal absorption and/or gas emission can modify these results: future work will tend to identify and match only those features which can be considered uncontaminated by the interstellar medium, in an attempt to reconstruct the Initial Mass Function in a clump.

CONCLUSIONS

IUE spectra of clumpy irregular galaxies have shown that the clumps contain a very large number of early O and B type stars, with a large number of supergiants with respect to the main sequence stars - a fact which is not understood. Possibly WR stars and massive object of the type of R 136a could also contribute to the clump luminosity. On the average, each clump radiates in the UV 100 times more than 30 Dor. On the other end the linear dimension of a clump is not much larger than the one of 30 Dor (Coupinot et al., 1982). This should lead to quite interesting physical conditions and the IUE data will be very important for the investigation of the Initial Mass Function of the gigantic bursts of stars formation in ralation with centimetric radio VLA maps via young supernovae and X-ray observations via supernova remnants.

REFERENCES

Benvenuti, P., Casini, C., Heidmann, J. 1979, Nature, 282, 272
" " " 1982, M.N.R.A.S., in press
Casini, C., Heidmann, J. 1976, Astron. Astrophys., 47, 371
Casini, C., Heidmann, J., Tarenghi, M. 1979, Astron. Astrophys. 73, 216
Code, A.D., Davis, J., Bless, R.C., Hanbury Brown, R. 1976, Ap.J. 203, 417
Coupinot, G., Hecquet, J., Heidmann, J. 1982, M.N.R.A.S., in press
de Vaucouleurs, G., de Vaucouleurs, A., Corwin, H.J.Jr. 1976, Second Reference Catalogue of Bright Galaxies, Univ. of Texas Press.
Heidmann, J. 1979, Ann. Phys. Fr. 4, 205
Israël, F.P., Koorneef, J. 1979, Ap.J. 230, 390

Seaton, M.J. 1979, M.N.R.A.S. 187, 73p
Wu, C.C., Boggess, A., Holm, A.V., Schiffer, F.H. III, Turnrose, B. 1981, IUE NASA Newsletter #14, pag. 2

TABLE 1

MKN	7	8	297	325	
F OBS 1550	1.1	.6	1.2	2.1	E-14
2550	.6	.6	1.0	1.2	E-14
ABS(B)	.41	.41	.31	.31	
DIST	43	50	63	49	Mpc
G CORR 1550	1.9	1.0	1.7	3.0	mJy
2550	2.5	2.3	3.5	4.2	mJy
INTRINSIC L 1550	4.1	3.0	8.2	8.6	E+27
2550	5.5	7.0	16	12	E+27
# CLUMPS IN SLIT	2.5	2.5	4	4	
MEAN L 1550 (1 CLUMP)	1.6	1.2	2.0	2.1	E+27
SP. INDEX	- .6	-1.7	-1.5	- .7	

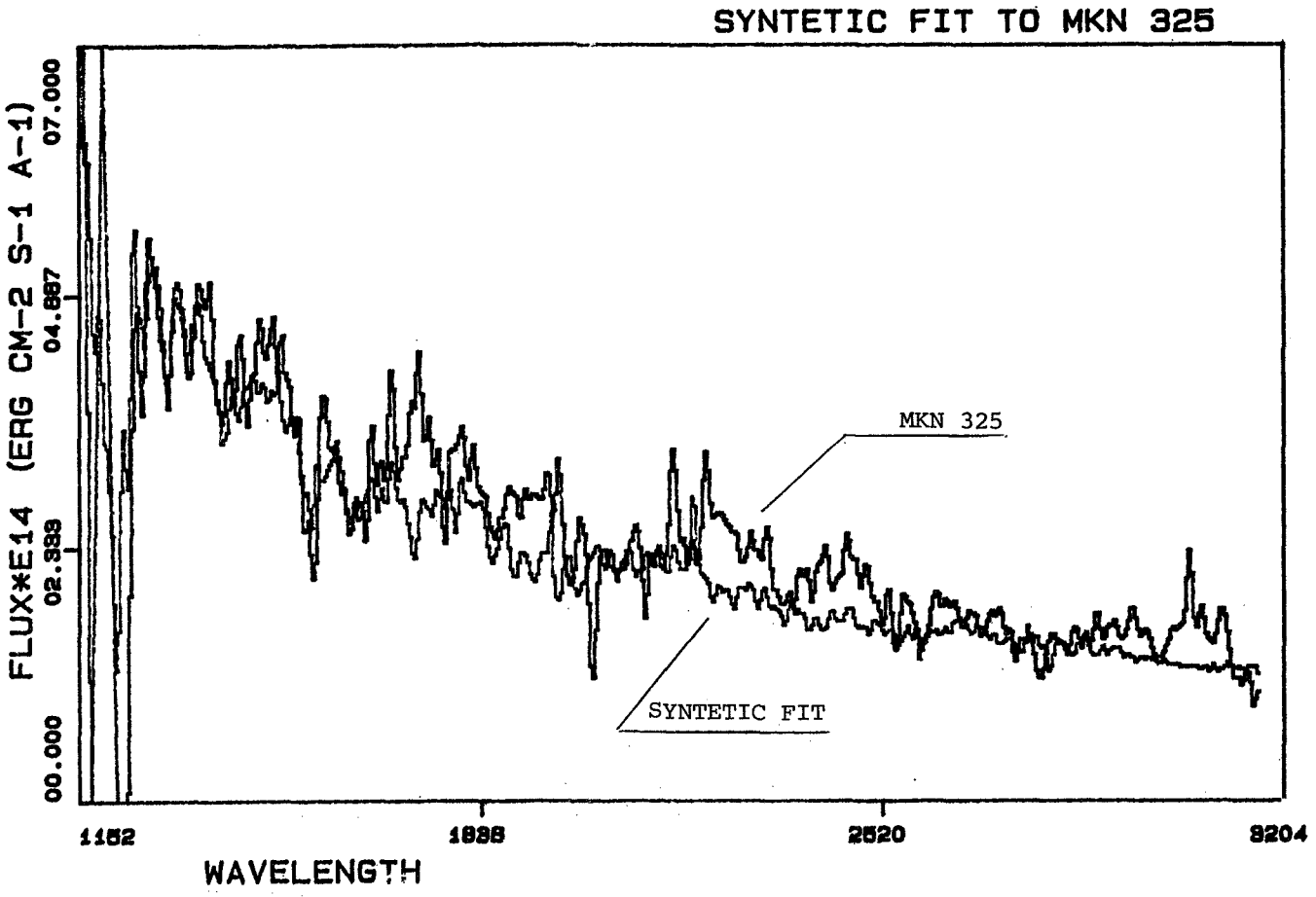

FIGURE 1 - Syntetic Fit to MKN 325

A COMPARISON OF THE EMISSION LINE PROPERTIES BETWEEN QUASARS AND TYPE 1 SEYFERT GALAXIES

Chi-Chao Wu
Computer Sciences Corporation

and

Albert Boggess and Theodore R. Gull
Laboratory for Astronomy and Solar Physics
NASA/Goddard Space Flight Center

ABSTRACT

For quasars and Seyfert galaxies, the equivalent width of C IV λ1550 increases as the continuum luminosity of an object decreases. A reasonable interpretation is that the covering factor increases as luminosity decreases. This is consistent with the fact that the Lα and C IV equivalent widths for Seyferts are a factor of 2 larger than those for high redshift quasars. The C IV/C III] ratio, which is a sensitive indicator of the ionization parameter, is about 5 for many Seyferts while it is about 2 for high redshift quasars.

INTRODUCTION

IUE low dispersion observations have produced a homogeneous volume of data for Seyfert galaxies. There are several sets of data on high z quasars measured in a consistent manner with ground based instruments (e.g. Baldwin 1977; and Osmer and Smith 1980), hence, meaningful comparisons can be made between the emission line properties of high z quasars and type 1 Seyfert galaxies.

RESULTS

The Log L_ν (1450) and Log EW (C IV) Correlation

In Figure 1 we plot the data for high redshift quasars (Baldwin 1977), Seyfert galaxies (Wu, Boggess and Gull) and low redshift quasars 3C 273 (Boggess et al. 1979), Mrk 205 and MR 2251-178 (Wu, Boggess and Gull 1982), PKS 0405-123 and PG 0953+415 (Green et al. 1980). The increase in the C IV equivalent width towards lower luminosity is quite obvious. One reasonable interpretation is that the lower luminosity objects have higher covering factor, therefore, a larger fraction of the ionizing photons are absorbed and eventually coverted into emission line photons. There are several lines of evidence which support this interpretation: (1) As will be shown later, the

equivalent widths of Lα and C IV for Seyferts are a factor of 2 larger than those of high z quasars; (2) As already pointed out in Peterson et al. (1982), the Mg II λ2800 absorption observed in high z QSOs occurs at wavelengths well removed from the Mg II emission of the QSOs. Therefore, intergalactic clouds or intervening galaxies, but not the broad line clouds (BLC) of the QSOs, are responsible for the absorption. For Seyfert 1s on the other hand, Mg II absorption several angstroms shortward of the emission line peak is observed in Mrk 279, NGC 5548 and NGC 7469. Strong Mg II absorption is also observed in the low luminosity objects NGC 3783, 4151 and probably NGC 4593. In the case of NGC 3783, however, a good fraction of the Mg II absorption originates in our own Galaxy because strong absorption lines of OI λ1304, C II λ1335 and Mg I λ2852 are detected near zero redshift; and (3) X-ray absorption increases with decreasing luminosity of the active galaxies (Mushotzky 1982).

Figure 1 seems to suggest that for low luminosity Seyferts, their covering factor is near unity and the C IV equivalent width approaches an upper limit. Another interesting point in Figure 1 is that the region occupied by the QSOs and broad line radio galaxies is above that for Seyfert 1s. In other words, for the same luminosity the QSOs and BLRGs have larger C IV equivalent widths. This is also true for other emission lines. Maybe radio emission is a manifestation of conditions in some active galactive nuclei which also provide additional heating (e.g. high energy particles).

The Lα and C IV Equivalent Widths

Figure 2 gives the histograms for the distribution of the Lα and C IV λ1550 equivalent widths for quasars and type 1 Seyfert galaxies. The observational data for quasars are from Osmer and Smith (1980) and the data for Seyfert 1s are given by Wu, Boggess and Gull (1982). The equivalent widths have been corrected for redshift. It is obvious that on the average, the Lα and C IV equivalent widths for type 1 Seyferts are a factor of 2 larger than those for high redshift quasars. As discussed earlier, a reasonable interpretation for this phenomenon is that the covering factor is higher for low luminosity objects.

The C IV/C III] Ratio

Figure 3 shows the distribution of the I(C IV λ1550)/ I(C III] λ1909) ratio for high z quasars (Osmer and Smith 1980) and Seyfert 1s (Wu, Boggess and Gull 1982). Quasars have C IV/ C III] ∿2 while a large fraction of the Seyferts have C IV/ C III] ratio clusters around 5. This ratio is very sensitive to the ionization parameter U_1 (Davidson 1977), the observed C IV/ C III] values correspond to $U_1 \sim 10^8$ and 4×10^8 cm s^{-1} respectively for high z quasars and type 1 Seyferts.

Some Seyferts have a C IV/C III] ratio comparable to that for quasars. I Zw 1, Mrk 478, II Zw 136, NGC 1566 and 7213 belong to this group. The first three of these objects have very strong Fe II emission (Phillips 1977; Osterbrock 1977). The low luminosity Seyferts NGC 4151, Mrk 279 and NGC 3783 are the objects which have high C IV/C III] ratio.

This research is supported by the IUE research contract NAS5-25774.

REFERENCES

Baldwin, J.A. 1977, Ap. J., 214, 679.
Boggess, A., et al. 1979, Ap.J. (Letters), 230, L131.
Davidson, K. 1977, Ap.J., 218, 20.
Green, R.F., Pier, J.R., Schmidt, M., Estabrook, F.B., Lane, A.L., and Wahlquist, H.D. 1980, Ap.J., 239, 483.
Mushotzky, R.F. 1982, preprint.
Osmer, P.S., and Smith, M.G. 1980, Ap.J.Suppl., 42, 333.
Osterbrock, D.E. 1977, Ap.J., 215, 733.
Peterson, B.M., Foltz, C.B., Capriotti, E.R., and Wu, C.-C. 1982 preprint
Phillips, M.M. 1977, Ap. J., 215, 746.
Wu, C.-C., Boggess, A., and Gull, T.R. 1982, preprint.

FIGURE CAPTIONS

Fig. 1. - The correlation between the continuum luminosity at 1450 Å and the equivalent width of C IV λ1550. The filled triangles are quasars, those without numbers are the high redshift objects observed by Baldwin (1977); the low redshift quasars are observed by the IUE: A: PKS 0405-123; B: PG 0953+415; C: Mrk 205; D: 3C 273; 28: MR 2251-178. The open triangles are broad line radio galaxies, 8: 3C 120; 22: 3C 390.3. The filled circles are type 1 Seyfert galaxies, 1: Mrk 335; 2: III Zw 2; 3: I Zw 1; 4: F9; 5: NGC 985; 9: Akn 120; 11: Mrk 9; 13: Mrk 79; 14: Mrk 10; 15: NGC 3783; 16: NGC 4151; 17: NGC 4593; 19: Mrk 279; 20: NGC 5548; 21: Mrk 478; 23: ESO 141-G55; 24: Mrk 509; 25: II Zw 136; 26: NGC 7213; 27: NGC 7469; 29: MCG-2-58-22.

Fig. 2. - The distribution of the Lα and C IV λ1550 equivalent widths for high redshift quasars (solid line) and type 1 Seyferts (dashed line).

Fig. 3 - The distribution of the C IV λ1550/C III] λ1909 ratio for high redshift quasars and type 1 Seyferts.

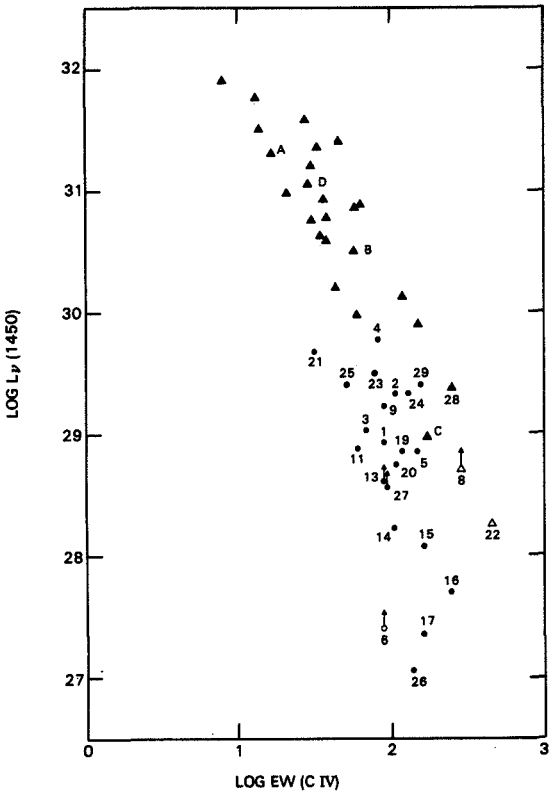
LOG L_ν (1450)
LOG EW (C IV)
32
31
30
29
28
27
0
1
2
3
A
B
C
D
1
2
3
4
5
6
8
9
11
13
14
15
16
17
19
20
21
22
23
24
25
26
27
28
29

Figure 1

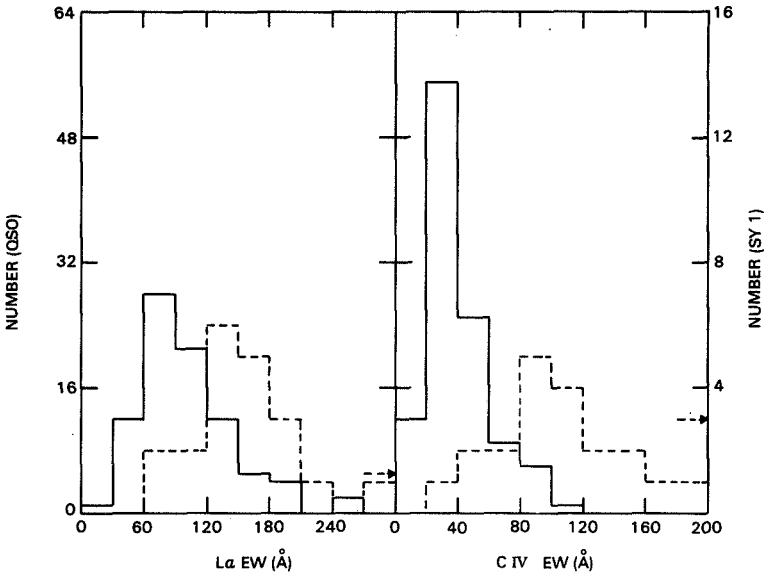

Figure 2

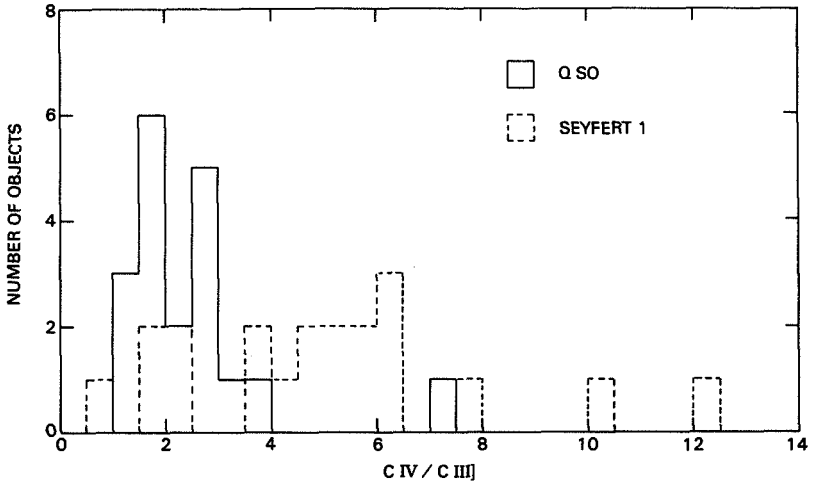

Figure 3

COORDINATED OBSERVATIONS OF SEYFERT I GALAXIES+

W. Wamsteker, P. Benvenuti
C. Cacciari, A. Cassatella,
L. Bianchi, P. Patriarchi

Astronomy Division
ESA-ESTEC, C/O ESA-VILSPA
P.O. Box 54065, Madrid,
Spain

J. Blades

IUE Observatory
Rutherford &
Chilton, United
Kingdom

A.C. Danks

ESO-Chile
La Silla Observatory
Stgo., Chile

INTRODUCTION

The variability of Seyfert I nuclei in all observable wavelength regions is a, by now, well established fact. These variations seem to show time-scales ranging from days, in X-rays, to months, at larger wavelengths. In addition to these continuum variations also line shape and intensity variations have been observed for various Seyfert galaxies. Unfortunately most observations are normally made at different wavelengths regions at different times. This is one of the main reasons why cause and effect relations in Seyfert nuclei variations have not really been established. Elaborate models have been calculated by various authors (e.g. Kwan and Krolik , 1981) but in view of the complexity of the models, observations covering a larger wavelength interval then is usually available, would be needed to make a valid test of such models. To remedy this unfortunate situation we are trying to coordinate the observations at various wavelengths made of some bright Seyfert I galaxies. This would seem the more desirable since the next few years will give us the unique opportunity of having available, apart from the IUE observatory, also the European X-ray satellite EXOSAT. To obtain simultaneous observations from the X-ray to the IR and maybe extending into the radio wavelengths, we have started a program of observations of a small number bright Seyfert I galaxies regularly with IUE. We attempt to support these observations by ground-based spectroscopy and IR photometry. We invite others who are interested in such observations to contact us, then we can attempt to obtain simultaneous ground-based observations. Our priority objects are ESO 113-IG45, NGC 3783, NGC 5548, ESO 141-G55, NGC 7469 and AKN 120. We will here present some preliminary results of our first observations for the Seyfert I galaxies ESO 113-IG45 (Fairall-9) and AKN 120.

ESO 113-IG45 (F-9)

The spectrum of F-9 as observed on 27 Dec 1981 is shown in figure 1b. Optical spectra were made at the 1.5m telescope at La Silla with the IDS. Both high resolution spectra (res$\sim$2A) of the Hβ,|OIII| profiles were made as well as low resolution spectra to obtain the continuum energy distribution. For comparison we show in figure 1a the UV spectrum, obtained from the IUE Database, taken on 3 Aug 1978 by Snijders. Optical spectra at more or less the same time are also available, however only at low resolution.

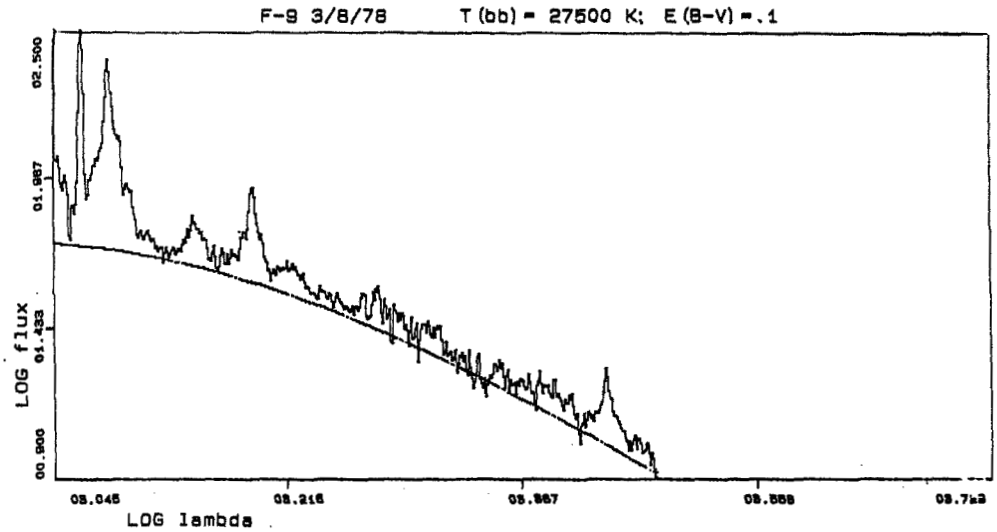

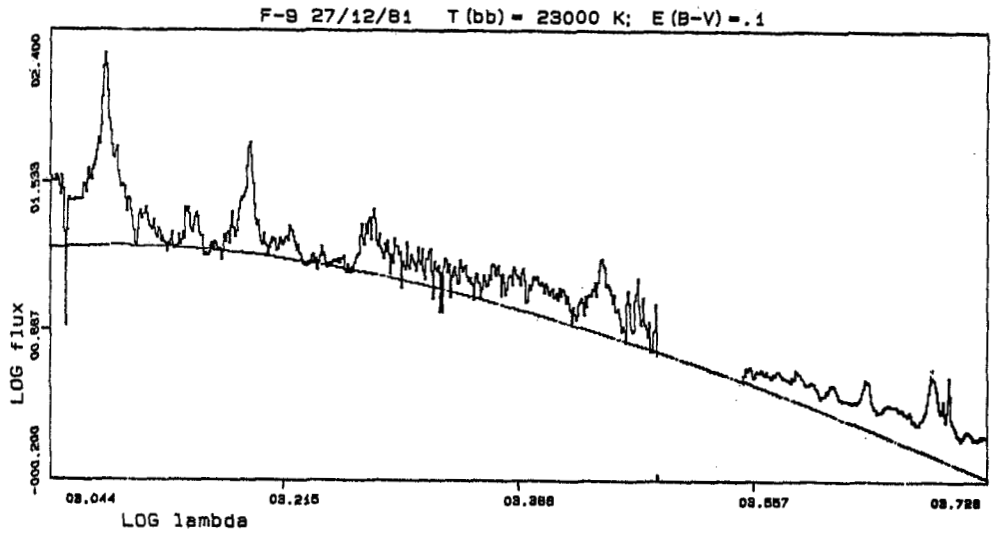

Figure 1a and 1b. Log F_λ (ergs $sec^{-1}cm^{-2}A^{-1}*10^{-14}$) vs log λ for ESO113-IG45 (F-9) for the two indicated dates of observation.For the 1981 spectrum(fig.1b) part of the optical spectrum is shown.The gap between 3000A and 3600A is a consequence of the instrumental sensitivity. The smooth drawn lines represent the best,single temperature black-body,fits to the overall appearance of the UV part of the spectra.Both spectra are corrected for reddening as indicated and for redshift(see text).The temperature for the black bodies is indicated in the captions.Note also the drastic changes in the emission line spectrum between the two epochs.The continuum brightness ratio between 1981 and 1978 is about 4 in the UV.

AkN 120

The UV variability of AkN 120 was first reported by Kollatschny et al. (1981). We also observed this galaxy in December both with IUE and ground based spectra. Our results do not shown the large jump between the UV and visual reported by Kollatschny et al. (1981).

DISCUSSION

The present discussion will mainly be oriented towards the continuum flux distribution in the UV for the two above mentioned galaxies. Various causes for the UV variability have been suggested, such as variations in power law spectra (Perola et al., 1982) and (Barr et al. 1982). Extinction is a serious problem in the interpretation of the continua of these galaxies. Although considerable amounts of dust are suggested to be present by Rieke (1978), direct evidence of internal obscuration in the Seyfert nucleus itself is not available. For AkN 120 an estimate of the interstellar absorption can be obtained from the strength of the NaD lines of A_V = 0.15-0.20 (Blades, prv. comm.) The higher limit of this range is in good agreement with the strength of the 2200 feature in the UV spectra. For F-9 no such indepedent information is available, therefore we have applied to the F-9 spectra normal cosec b^{II} absorption, amounting to (E(B-V)=0.1) Seaton (1979) extinction law was applied to the UV and Whitford extinction law for the visual part of the spectrum. The contribution to UV and visual spectra by various components as f-f and b-f continuum, two foton continuum, stellar continuum cannot be evaluated until a more detailed line analysis has been finished. However the overall shape of UV continuum for both epochs in F-9 shown in figure 1, appears surprisingly, quite well represented by a single temperature black body distribution. In figure 1 we have drawn the best fitting black body, corrected for Z = 0.0463, the redshift of F-9 as determined from the narrow component in the |OIII| lines. For both epochs, which show a UV flux difference of a factor of $\sim$ 4, quite different temperatures are required. When the galaxy is bright (figure 1a) we find T_{BB} = 27500 K, when it is faint (figure 1b) a temperature T_{BB}=23000 K, is required. For AkN 120, we find a similarly good fit a T = 24000 K, correcting similarly for a redshift Z = 0.0330.

These results indicate that the temperature variations of these blackbody, which could represent dense clouds, may be responsible for the large UV flux variations. In that case we can obtain a size estimate of these clouds from the observed continuum flux. We find (H = 55 Mpc/kmsec^{-1}) the following results:

F-9 1978 : R_{bb} = 75 AU

F-9 1981 : R_{bb} = 60 AU

AkN 120 1981 : R_{bb} = 70 AU.

Such size would put the shortest possible time scale for variation in the UV flux of these objects at approximately 1 day. This is not inconsistent with the observed variations. With respect to the line variations we can not say much at this stage. It is interesting however to point out that for

the |OIII| λ5007, we find for both objects that the line is composed of a narrow (FWHM $\leqslant$ 200 km sec^{-1}) and a broad component (FWHM = 750 km sec^{-1}). For both AkN 120 and F-9 the broad component is blue-shifted with respect to the narrow one by resp $\sim$ 100 km sec^{-1} and $\sim$ 75 km sec^{-1}. A similar behaviour seems to occur in many Seyfert I galaxies (Pelat and Alloin, 1982). A similar behaviour is indicated in NGC 3393, a Seyfert II galaxy (Danks and Wamsteker, unpublished), although there the relative strengths of the broad component is much less then in the Seyfert I galaxies. Also we would like to mention the presence of apparently unresolved ($\Delta\lambda$ < 3 A) components possibly to be identified with multiplets 36 and 42 of Fe II in the wings of λ5007.

References:

Barr,P.,Willis,A.J.,Wilson,R.,1982,preprint
Kollatschny,W.,Fricke,K.J.,Sschleicher,H.,Yorke,H.W.,1981,Astron. Astrophys.,102,L23.
Kwan,J.,Krolik,J.H.,1981,Astrophys.J.,250,478.
Pelat,D.,Alloin,D.,1982,Astron.Astrophys.,105,335
Perola,G.C.,Boksenberg,A.,Bromage,G.E.,Clavel,J.,Elvis,M.,Elvius,A.,Gondhalekar,P.M.,Lind,J.,Lloyd,C.,Penston,M.V.,Pettini,M.,Snijders,M.A.J.,Tanzi,E.G. Tarenghi,M.,Ulrich,M.H.,Warwick,R.S.,1982,preprint,Univ.di Roma,1982/1.
Rieke,G.,1978,Astrophys.J.,226,550.
Seaton,M.J.,1979,M.N.R.A.S.,187,73P.

+) Based on observations made with IUE at the ESA Villafranca Tracking Staion in Madrid,Spain and on observations made at the European Southern Observatory,La Silla,Chile.

ULTRAVIOLET VARIATIONS OF NGC 4151

A. Boksenberg[1], G.E. Bromage[2], J. Clavel[3], A. Elvius[4], M.V. Penston[1], G.C. Perola[5], M. Pettini[1], M.A.J. Snijders[6], E.G. Tanzi[7], M. Tarenghi[8] and M.H. Ulrich[8] (The "European Extragalactic Collaboration")

After the initial six epochs of IUE observation revealed 8 different variable components in the low dispersion spectra, now, from data at 31 epochs, the systematics have become clearer.

The continuum is described by 3 parameters, the slope and intensity of a power law that fits well in the region 2000 - 3000 Å and an excess seen at shorter wavelengths, 1000 - 2000 Å. The power law component steepens as it fades. The short wavelength excess is however not simply correlated with the power law component. It is generally constant but becomes fainter at a few "anomalous" epochs.

The high ionization absorption lines, as well, are found to be correlated with the power law component and therefore it is concluded that this is again the dominant source of ionization near 300 Å. This implies that the "short wavelength excess" must turn down exponentially between 1000 and 300 Å in a way similar to that of a thermal source with $T \sim 30\,000$K. Thus the short wavelength excess may represent thermal radiation from an accretion disk. The low ionization absorption lines, by contrast, are anticorrelated with the continuum.

The strong emission lines each show different widths, in contrast to the common situation in quasars, except at anomalous epochs when all emission lines are relatively narrow (8000 km s^{-1}). The CIV intensities are well correlated with the continuum but there is some hysteresis associated with a lag of 15-20 days. This delay is caused by light travel times in the CIV emitting region. The MgII emission region seems to be bigger perhaps 80 light days in diameter - so that the continuum variations are somewhat smeared out - whereas the lack of variation in CIII] suggests an emission region larger than a light year.

Key to Institutions

1 = Royal Greenwich Observatory, Hailsham, UK
2 = Rutherford & Appleton Laboratory, Didcot, UK
3 = Observatoire de Meudon, Meudon, France
4 = Stockholm Observatorium, Saltsjobaden, Sweden
5 = Istituto Astronomica dell'Universitá, Rome, Italy
6 = University College London, UK
7 = Istituto di Fisica Cosmica, Milano, Italy
8 = European Southern Observatory, Garching, Germany

Time Variations In CIV λ1550 and Lyα Emission Lines In NGC5548

Roger Ptak and Ronald Stoner
Physics and Astronomy, Bowling Green State University

ABSTRACT

We have obtained two short-wavelength images of NGC5548 separated by a three month interval. Combining this data with that obtained by Wu et al. (1981) one year prior to our first image, we have discovered time variations in the CIV λ1550 and Lyα profiles as well as in the intensity ratio. In our image obtained in November, 1980, the CIV profile is essentially the same as that of Wu et al. in December, 1979. However, our Lyα profile is substantially narrower and the Lyα to CIV intensity ratio is reduced by roughly a factor of 2. In our February, 1981 image, the CIV profile is narrowed by approximately a factor of 2 compared with the other two observations, while the Lyα profile and Lyα to CIV ratio is essentially the same as in November. We have also obtained an excellent short-wavelength image of the very bright Seyfert galaxy Fairall 9, and we find that the CIV and Lyα lines in this object have essentially identical profiles.

INTRODUCTION

Although the Lyα and CIV λ1550 lines for high redshift quasars have been investigated for some time, these lines were not studied in Seyfert galaxies until the IUE became operational. CIV profiles in four Seyfert 1 galaxies, including NGC5548, have been reported by Wu et al. (1981). Using a pseudo-trailing technique, they obtained profiles with a sufficient signal-to-noise ratio for testing theoretical models. We have obtained a short-wavelength image of NGC5548 using the same technique, and we have obtained a single-exposure image of this object three months after our first image. Here we report the differences seen in the Lyα and CIV lines in NGC5548 when these three images are compared.

We have also obtained an excellent image of Fairall 9 (F9), a very luminous Seyfert 1 galaxy with a redshift large enough so that the Lyα line is completely distinct from the geocoronal emission. Thus, it is possible in this object to make a meaningful comparison of the Lyα and CIV profiles.

RESULTS AND DISCUSSION

All of our observations were made with the short wavelength prime (SWP) camera aboard the IUE satellite. Our first image of NGC5548 was obtained in November, 1980. In February, 1981, we obtained our second image of NGC5548

as well as the image of F9. Wu et al. (1981) observed NGC5548 in December, 1979.

When we compare the December and November images of NGC5548, we find that the CIV profiles and line intensities are essentially the same. However, the Lyα lines appear to be substantially different, although blending with geocoronal Lyα and with NV λ1240 make these lines much less well determined than the CIV. As seen in the table, the Lyα intensity is about 40% less in November than it was in December, and the November Lyα full-width-at-half-maximum (FWHM) as well as the Lyα to CIV intensity ratio are only about one-half as large as the values for the previous December.

In comparing the November and February images of NGC5548, we find that the Lyα lines have a similar profile although there is an intensity change. However, the CIV profiles are decidedly different. As can be seen in the table, the FWHM of the February image is smaller than that in November by roughly a factor of 2. Furthermore, the comparison of the two profiles in the figure shows that the narrowing is similar on both sides of the line center. (In the figure, the broken curve is the CIV profile for February 23, 1981 and the solid curve is that for November 27, 1980.) We also see that the data are consistent with only a small change or no change at all in the Lyα to CIV ratio between these two observations.

The time variation we have found for the CIV line in NGC5548 provides a strong test for theoretical models of the broad line emitting region of this object. If the broad lines were produced by radially moving photo-ionized clouds, one would expect to see time variations in such a line propagate from one side of the line to the other. Of course, we have only two glimpses of the spectrum separated by 3 months. and it is possible that we missed this propagation. If the observed variation occurred because the higher velocity clouds turned off for some reason, then the diameter of the entire broad line emitting region must be less than 3 light-months to be consistent with our observations.

Our SWP image of F9 is a psuedo-trailed and well exposed spectrum. Since the redshift of this galaxy is 0.048, there is insignificant blending of the geocoronal emission with the Lyα line, and a comparison of the Lyα and CIV profiles can be made directly. We show such a comparison in the figure. The two lines are shown with the same velocity scale and with the continuum subtracted. The solid curve is the CIV profile and the broken curve is that of Lyα plus NV λ1240. The differences in the red wing are mostly due to the NV line.

REFERENCES

Wu, C., Boggess, A., and Gull, T. R. 1981, Ap. J., 247, 449.

Comparison Of Three Images Of NGC5548

	Dec. 1979 (Wu et al. 1981)	Nov. 1980	Feb. 1981
Intensity of CIV (10^{-12} erg/cm^2 sec)	6.1 ± 0.2	7.0 ± 0.2	3.2 ± 0.2
CIV FWHM (10^3 km/sec)	4.4	4.6	1.8
Intensity of Lyα (10^{-12} erg/cm^2 sec)	7.8 ± 1.7	4.8 ± 0.9	2.8 ± 0.6
$\frac{\text{Ly}\alpha}{\text{CIV}}$ intensity ratio	1.3 ± 0.3	0.7 ± 0.2	0.9 ± 0.3
Lyα FWHM (10^3 km/sec)	4.2	2.2	2.0

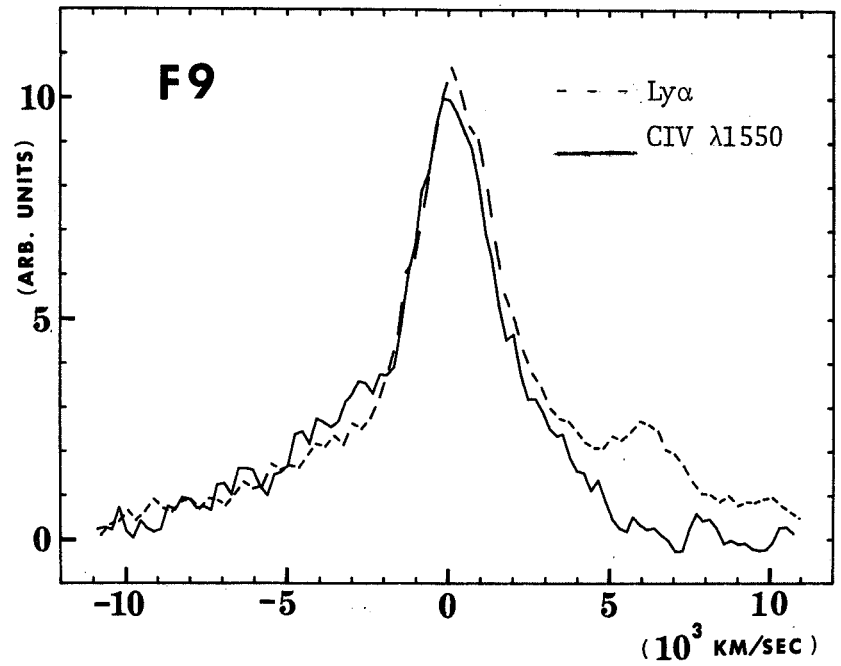
F9
Lyα
CIV λ1550
(ARB. UNITS)
10
5
0
-10
-5
0
5
10
(10³ KM/SEC)

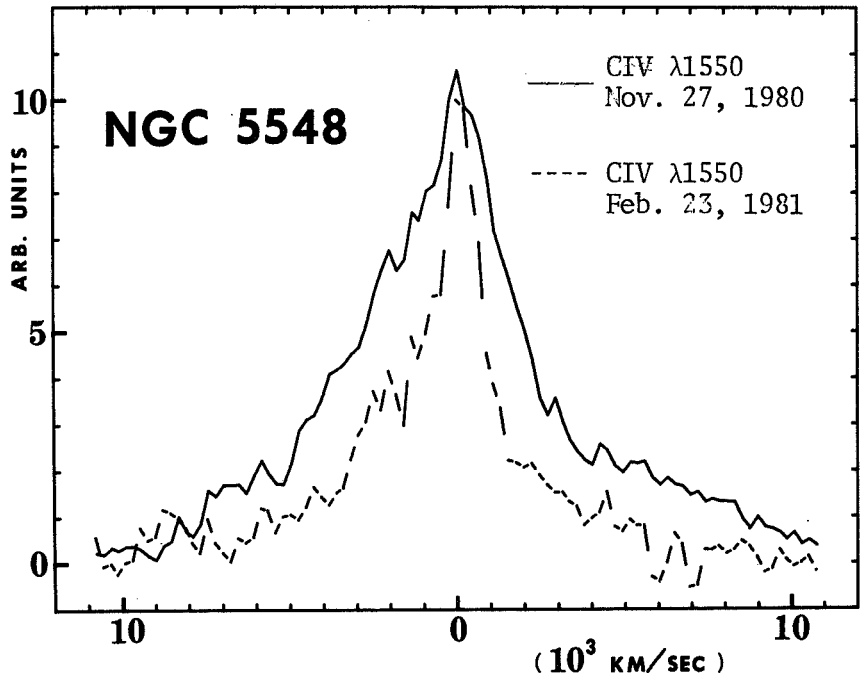
NGC 5548
CIV λ1550
Nov. 27, 1980
CIV λ1550
Feb. 23, 1981
ARB. UNITS
10
5
0
10
0
10
(10³ KM/SEC)

IUE OBSERVATIONS OF MARKARIAN 3 AND 6

Matthew A. Malkan and J. B. Oke
California Institute of Technology

We have obtained IUE spectra to study the infrared/optical/ultraviolet continua of the Seyfert 2 galaxy Markarian 3 and the Seyfert 1.5, Markarian 6. Their starlight is reddened by 0.18 and 0.06 mag. in E_{B-V}, respectively; the forbidden line emission of both galaxies is reddened by 0.27 mag. Unless the permitted hydrogen lines in these galaxies are more obscured than the forbidden lines, the intrinsic Hα/Lyα and Hα/Hβ ratios are almost twice those predicted by Case B recombination.

Starlight contributes 80±10 and 70±10 % of the visual flux in Mrk 3 and 6, in a 14 arc second aperture. The spectrum of the non-stellar light appears to be a power-law with slopes -1.35±0.2 and -1.2±0.15. Other spectral shapes are also possible, but they must include a significant contribution in the near infrared, and in the far ultraviolet. Mrk 3 differs from Seyfert 1 galaxies in having a 50% smaller Balmer continuum/Hα ratio, a 100% larger C III] /C IV ratio, and an emission-line covering factor near unity.

FIGURES

Figure 1 shows the infrared/optical/ultraviolet spectra of Mrk 3 and 6, in a 14 arc second aperture. The lines represent fits to the spectra which combine galactic starlight with three possible non-stellar components. The solid line includes a power-law, while the dot-dash line has an exponential component with $f_\nu \propto \exp(-h\nu/k \cdot 25{,}000)$. The dashed line is a fit with a 20,000 K blackbody. The lower dashed line through Mrk 3's spectrum has only starlight and recombination emission.

Figure 2 is a blow-up of the optical portion of the spectra in Figure 1. The same fitted lines from Figure 1 are plotted here, but they are almost indistinguishable from one another at optical wavelengths.

A more complete discussion of this work will be submitted to the Astrophysical Journal.

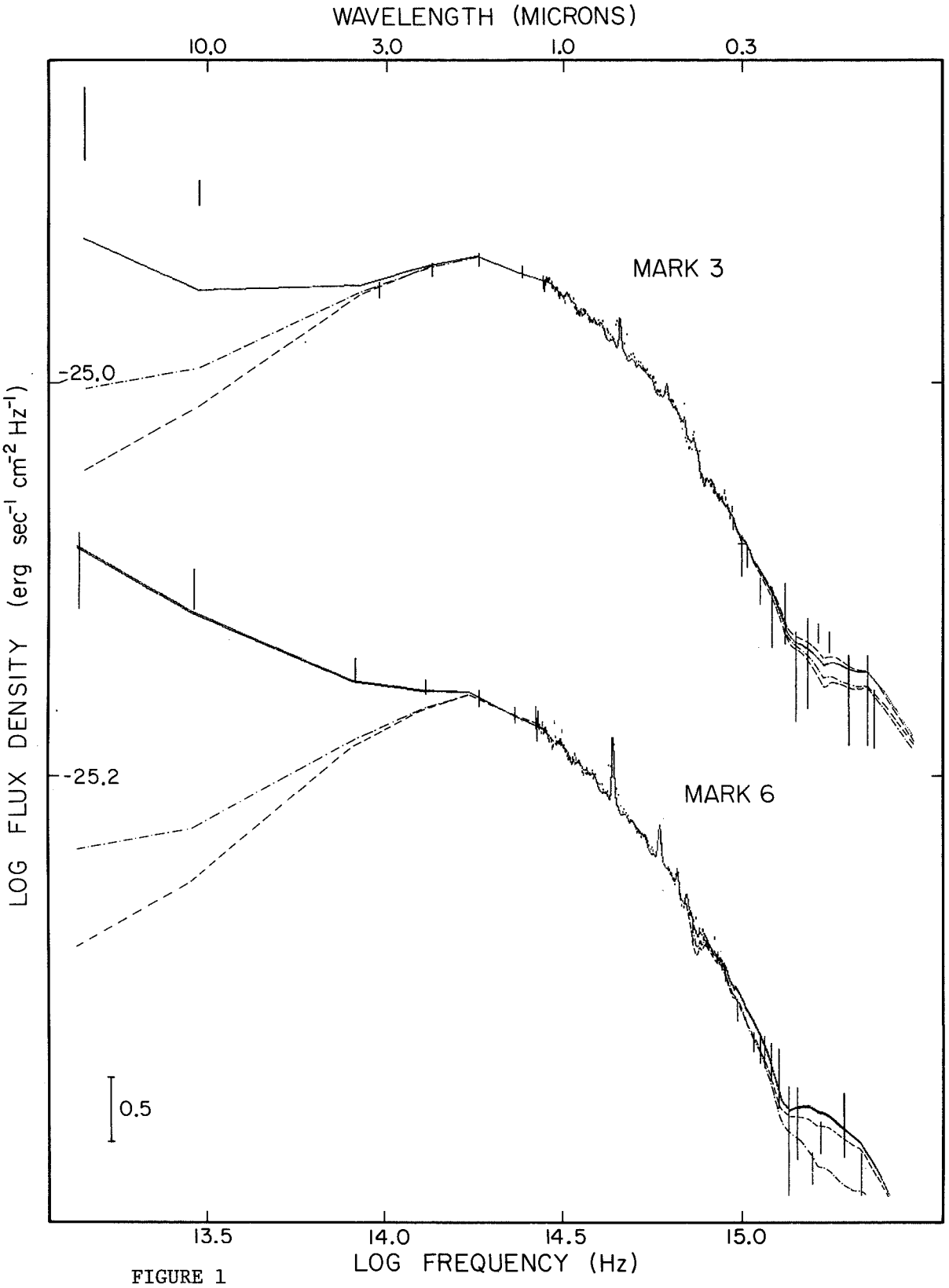
WAVELENGTH (MICRONS)
10.0
3.0
1.0
0.3
MARK 3
-25.0
MARK 6
-25.2
0.5
LOG FLUX DENSITY (erg sec^{-1} cm^{-2} Hz^{-1})
13.5
14.0
14.5
15.0
LOG FREQUENCY (Hz)

FIGURE 1

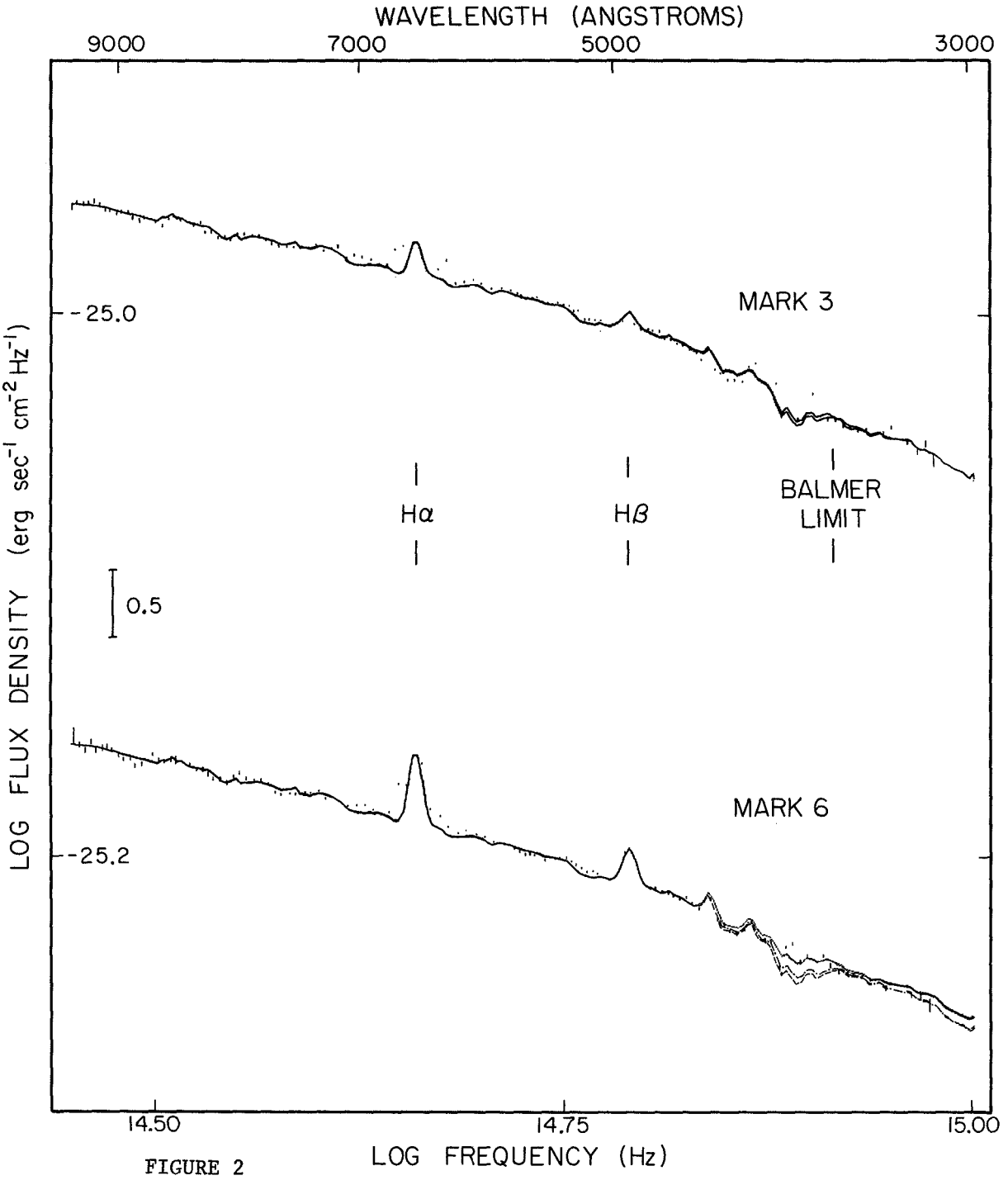
WAVELENGTH (ANGSTROMS)
9000
7000
5000
3000
MARK 3
-25.0
Hα
Hβ
BALMER
LIMIT
0.5
MARK 6
-25.2
LOG FLUX DENSITY (erg sec^{-1} cm^{-2} Hz^{-1})
14.50
14.75
15.00
LOG FREQUENCY (Hz)

FIGURE 2

SPECTROSCOPY OF TWO BL LACERTAE OBJECTS

M. Urry*, S. Holt**, Y. Kondo***, R. Mushotzky**
NASA Goddard Space Flight Center

K. Hackney and R. Hackney
Department of Physics and Astronomy
Western Kentucky University

ABSTRACT

As part of a continuing program of observations of BL Lac objects, we have used the IUE SWP and LWR cameras to look at PKS 0548-322 and PKS 2155-304. The spectra obtained are well-described by power laws with $\alpha \sim 0.8$ in each case. For each object, one set of simultaneous X-ray data was obtained using the Solid State Spectrometer (SSS) on the Einstein Observatory. These data show that the power law extends from ultraviolet frequencies into the X-ray regime, although it steepens slightly for PKS 2155-304. Both objects are variable in the ultraviolet and/or X-ray; in neither case does the small spectral variability appear to correlate with the intensity variability. The overall spectrum of these objects is interpreted in light of a synchrotron self-Compton model with relativistic beaming.

OBSERVATIONS

The BL Lac object PKS 0548-322 is one of the faintest objects which has been observed with IUE (its apparent visual magnitude is 15.5), and because of the long exposure times necessary for reasonable spectra, we have only two SWP images, taken about a year apart. In constrast, PKS 2155-304 is the brightest BL Lac object known in the ultraviolet, and high quality spectra are relatively easy to obtain. We present here the results of 11 short wavelength and 11 long wavelength observations of this object. Table 1 summarizes the observations. The analysis of the IUE images was fairly standard: spectra were assembled from the line-by-line files of the GO tapes, following recommended procedures (Bohlin and Holm 1980, Cassatella et al. 1980, Holm and Schiffer 1980, Turnrose and Harvel 1980), with modifications indicated by the study of Hackney and Hackney (1981). Similarly, the SSS analysis followed standard procedures, which are described in Holt et al. (1979) and Becker et al. (1979). Details of the analysis of both the IUE and SSS data for PKS 0548-322 may be found in Urry et al. (1982); the analysis of PKS 2155-304 was essentially the same, except that the IUE data have much better signal-to-noise because the source is so much brighter.

*Also Johns Hopkins University and LHEA
**Also Laboratory for High Energy Astrophysics (LHEA)
***Also Laboratory for Astronomy and Solar Physics

RESULTS

We have three important results. First, we see no lines in the ultraviolet or X-ray spectra of either object. Second, all spectra are well-described by power law models. Third, both objects exhibit variability, but intensity changes and spectral changes are not correlated. A discussion of each of these points follows.

We have looked carefully at our IUE and SSS data for evidence of line emission or absorption. While we see no lines in the spectra of either object, both the IUE and the SSS spectra of PKS 2155-304 are of higher statistical quality, so our discussion will focus on that object. Maraschi et al. (1981) have reported weak, variable absorption and emission features in the ultraviolet spectra of PKS 2155-304, using some of the same IUE images that we present here. We cannot affirm the presence of these features. The reported features are mostly in absorption, but they are so weak that it is unclear whether they should be identified as an absorption feature at a certain wavelength or an emission feature in the adjacent bins. Many of the features are not reproduced from one image to the next, and it is unlikely that they are sometimes swamped by a bright continuum. Two more criticisms must be mentioned. One concerns the possibility of spurious emission features due to fixed pattern camera noise. (See Hackney, Hackney, and Kondo 1982.) The other problem concerns unidentified features. The identified lines are so weak that one would like to be convinced by a consistent set of spectral lines (i.e., all at one redshift) which explains all of the principal features in the spectrum. However, in addition to the lines identified by Maraschi et al. (1981), there are several features of comparable or even greater significance which remain unidentified. Almost all features in a given image are 1.5σ or less from the mean, and in an average of five images, only one feature persists, a possible absorption near 1280 Å, where one might expect a spurious emission feature (Hackney, Hackney, and Kondo 1982).

In the X-ray band, the results are the same: no lines. The SSS is sensitive from 0.8 to 4.5 keV (corresponding to 3 Å to 16 Å), with an average energy resolution of about 160 eV FWHM. For PKS 0548-322, the equivalent width of a silicon line at 1.8 keV is less than 50 eV and the equivalent width of a sulfur line at 2.5 keV is less than 85 eV (at 99% confidence). For PKS 2155-304, the analysis is complicated by the fact that the redshift is uncertain; these upper limits will be discussed in Urry et al. (1982b).

The ultraviolet and X-ray continua of both BL Lac objects are well-fit by power laws of the form $F_\nu \sim \nu^{-\alpha}$, with $\alpha \sim 0.8$ and $\alpha \sim 1.2$ respectively. For PKS 0548-322, a single power law with $\alpha \sim 0.9$ connects the UV and X-ray, but PKS 2155-304 is flatter in the UV than in the X-ray band, and smooth connection of the two requires a gradually steepening power law. The composite spectrum of this object is shown in Fig. 1. With the exception of the two black bands, which represent our IUE and SSS observations of 5/15/79, all of the data in this figure have been previously published (see Urry and Mushotzky 1982, and references therein). This spectrum serves to illustrate both the variability of the source,

which will be discussed below, and the synchrotron-like power law form of the emission. We apply a simple model: a homogeneous blob of relativistic electrons in a uniform magnetic field, radiating isotropically in its rest frame, but possibly moving along the line-of-sight at relativistic speed. Details of this analysis are given in Urry et al. (1982a) and Urry and Mushotzky (1982), but the result is that the composite spectra of PKS 0548-322 and PKS 2155-304 can be explained if the Doppler factors for the bulk relativistic motion are $\delta \gtrsim 7$ and $\delta \gtrsim 5$, respectively.

Finally, we have seen significant variability in both objects. We have only two ultraviolet spectra of PKS 0548-322, and only two SSS observations of each of the objects, so we concentrate here on the 22 IUE observations of PKS 2155-304. A light curve is shown in Fig. 2. LWR fluxes are indicated with dots, and SWP fluxes by crosses. There was a sharp decrease of >30% in the flux in both bands during the one month interval between October and November 1979. Even more striking is the decrease of about 10% in the SWP flux between 13 and 14 October 1979 (see Maraschi et al. 1980). Since two SWP spectra were taken on each of these days, we are confident that this intensity change is real. This timescale ($t_\nu = d\ \ln F_\nu / dt = 10$ days) is comparable to that previously reported in the visible (Greenstein, Oke and Wade 1979) and in the X-ray (Snyder et al. 1980, Urry and Mushotzky 1982). Although our coverage in 1980 was less complete, we do see a distinct brightening trend, such that both SWP and LWR fluxes have almost doubled during that year. As inspection of Table 1 will show, there have been small changes in spectral index (the combined spectral index varies between 0.68 and 1.02) but these changes are uncorrelated with flux changes.

REFERENCES

Becker, R.H., Holt, S.S., Smith, B.W., White, N.E., Boldt, E.A., Mushotzky, R.F., and Serlemitsos, P.J. 1979, Ap.J.(Lett.), 234, L73.

Bohlin, R.C. and Holm, A.V. 1980, IUE NASA Newsletter, 10, 37.

Cassatella, A., Holm, A., Ponz, D., and Schiffer, F.H. 1980, IUE NASA Newsletter, 8, 1.

Greenstein, J.L., Oke, J.B. and Wade, R.A. 1979, IAU Circ.No.3324.

Hackney, R.L. and Hackney, K.R. 1981, B. A. A. S., 13, 532.

Hackney, R.L., Hackney, K.R., and Kondo, Y. 1982, this volume.

Holm, A.V. and Schiffer, F.H. 1980, IUE NASA Newsletter, 8, 45.

Holt, S.S., White, N.E., Becker, R.H., Boldt, E.A., Mushotzky, R.F., Serlemitsos, P.J., and Smith, B.W. 1979, Ap.J.(Lett.) 234, L65.

Maraschi, L., Tanzi, E., Tarenghi, M., and Treves, A.1980, Nature, 285,555.

Maraschi, L., Tanzi, E.G., Tarenghi, M., and Treves, A. 1981, Space Sci.Rev., 30, 129.

Snyder, W.A., et al. 1980, Ap.J.(Lett.), 237, L11.

Turnrose, B.E. and Harvel, C.A. 1980, IUE Image Processing Information Manual, Version 1.0, 6-6.

Urry, C.M. and Mushotzky, R.F. 1982, Ap.J., 253, 38.

Urry, C.M., Hackney, K., Hackney, R., Kondo, Y., and Mushotzky, R.F. 1982a, to be published in Ap.J.

Urry, et al.1982b, in preparation.

Table 1. ULTRAVIOLET DATA (IUE)

Date	Image	Length of Observation (min)	Ave. Flux (mJy)	Spectral Index, α	
0548-322					
4/6/79	SWP 4874*	372	0.34	0.84±0.39	
4/1/80	SWP 8625	400	0.32	0.76±0.48	
PKS 2155-304					
5/15/79	SWP 5238*	180	10.3±0.3	0.65±0.13	0.71±0.02
	LWR 4522*	50	13.8±0.5	0.86±0.09	0.70±0.02
	SWP 5239*	120	10.6±0.3	0.78±0.06	
8/19/79	LWR 5397	50	13.8±0.4	0.81±0.11	0.75±0.03
	SWP 6221	90	10.0±0.4	0.84±0.06	
	LWR 5398	50	14.4±0.4	0.81±0.10	0.72±0.02
	SWP 6222	77	10.6±0.4	0.76±0.06	
10/13/79	LWR 5828	30	15.3±0.4	0.56±0.13	0.78±0.03
	SWP 6856	40	10.7±0.4	0.85±0.06	0.83±0.04
	LWR 5829	21	15.8±0.4	0.52±0.16	0.98±0.04
10/14/79	SWP 6867	48	9.7±0.1	0.84±0.07	
	SWP 6868	48	9.6±0.1	1.00±0.07	1.02±0.04
11/2/79	LWR 6009	90	12.6±0.5	0.82±0.08	
	LWR 6010	50	13.4±0.5	0.50±0.10	
11/13/79	SWP 7139	120	7.4±0.1	0.75±0.06	0.71±0.03
	LWR 6135	75	10.1±0.3	0.68±0.09	
	SWP 7140	120	7.5±0.1	0.62±0.05	0.75±0.03
	LWR 6136	60	10.5±0.3	0.80±0.11	
5/22/80	LWR 7813	60	11.6±0.5	0.79±0.12	0.79±0.03
	SWP 9066	120	8.2±0.4	0.77±0.05	
12/12/80	SWP 10799	40	12.4±0.4	0.75±0.07	0.68±0.03
	LWR 9476	40	16.8±0.4	0.65±0.10	
Average Values±Std. Dev.		SWP	9.7±1.5	0.78±0.10	0.79±0.11
		LWR	13.5±2.1	0.71±0.13	

*Simultaneous SSS observation

Table 2. X-RAY DATA (SSS)

Date	Length of Observation (min)	Flux at at 3 keV (μJy)	Spectral Index, α
PKS 0548-322			
3/10/79	44	3.8 ± 0.7	1.2 ± 0.3
4/6/79	54	2.9 ± 0.5	1.1 ± 0.3
PKS 2155-203			
5/15/79	88	2.5 ± 0.6	1.2 ± 0.5
5/26/79	88	4.5 ± 0.6	1.2 ± 0.2

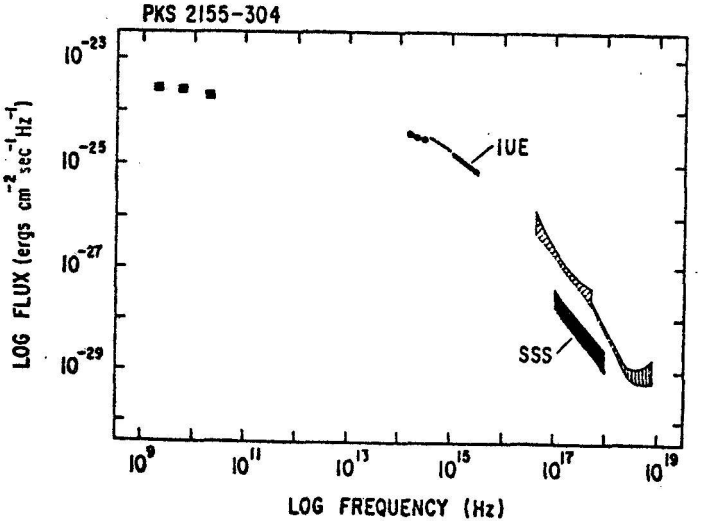

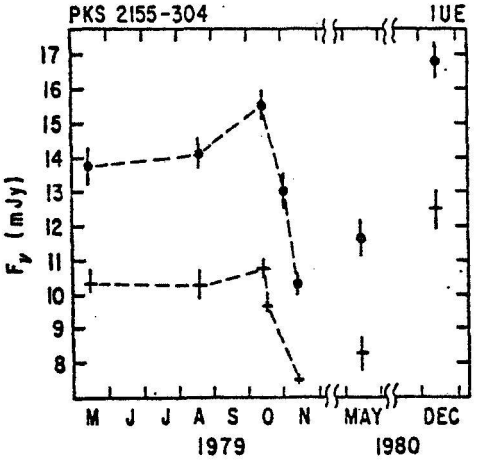

IUE OBSERVATIONS OF FOUR BL LACERTAE-TYPE OBJECTS

D.M. Worrall
Center for Astrophysics and Space Sciences
University of California at San Diego
F.C. Bruhweiler
Computer Sciences Corporation, Silver Spring, Maryland

Abstract

We present spectral fits to IUE observations of four BL Lacertae-type objects. Combined with near-simultaneous measurements at longer wavelengths, we find positive spectral curvature within the infrared to ultraviolet energy range. We show that the data provide strong evidence for relativistic beaming in the sources. We discuss Lyman α emission and possible CIV and NV absorption features in the spectrum of 3C 371.

Observations.

Low resolution large aperture-mode observations were made as given in table 1. The objects were relatively faint (M_v = 15.6-14.5) and we used an entire 8-hour observing shift for all exposures except 6 and 7. We improved upon the signal-to-noise ratio of the IUE Standard Image Processing System spectrum by manually selecting a narrower extraction slit and thus including only those "line-by-line" data sets with measureable source contribution. For both the on-source and background accumulations we selected data sets least contaminated by radiation hits on the SEC-Vidicon camera face. We derived absolute fluxes using the Fahey-Klinglesmith FORTH software at GSFC. Extinction corrections for OJ 287 and 3C 371 used the wavelength dependence given by Savage and Mathis (1979), and values of A_v which we derived using the method of Burstein and Heiles (1978).

Table 1.
IUE continuum fits to $f_\nu(Jy)=K\ \nu_{15}^{-\alpha}$

Object	A_v	Date(U.T.)	Camera*	χ^2	d.o.f.	K(10^{-3})	α (2σ error)
1 OJ 287	0.06	1980 Oct 24,25	SWP+LWR	74	23	1.41	1.58(+0.04,-0.04)
2 OJ 287	0.06	1980 Dec 15	SWP	153	30	0.79	1.39(+0.12,-0.14)
3 OJ 287	0.06	1980 Dec 17	LWR	83	31	0.94	1.48(+0.20,-0.20)
4 OQ 530	0.0	1980 Dec 13,14	SWP+LWR	72	23	0.73	1.79(+0.09,-0.08)
5 ON 325	0.0	1981 May 2	SWP+LWR	61	12	1.01	0.89(+0.11,-0.12)
6 3C 371	0.13	1981 May 1	SWP	244	30	1.76	1.50(+0.12,-0.11)
7 3C 371	0.13	1981 May 1	LWR	42	18	2.37	1.76(+0.27,-0.27)
8 3C 371	0.13	1981 Aug 3	SWP	98	16	1.34	1.60(+0.15,-0.15)

* Frequency ranges: SWP: ν=1.54-2.5 10^{15} Hz; LWR: ν=0.94-1.54 10^{15} Hz.

We tested the data with single power-law fits. The noise level renders unacceptable values for χ^2. Since the observations are close to the IUE detection limit, they are dominated by systematic effects. Additional fluctuations may be introduced by weak unresolved emission and absorption features and, possibly, continuum variability on a time scale shorter than 8

hours. The observations 2,3 and 6,7 are not consistent with single power-law components through the SWP and LWR ranges. In the former pair, OJ 287, this implies either positive spectral curvature or variability of ≃16% on a time scale of two days or less. For the 3C 371 observations, we consider that the quoted statistical error for the SWP slope is an underestimate of the true uncertainty, due to the line features and greater level of noise in the spectra (see later). We consider the range α=1.7-2.0 to be a more accurate description.

The Synchrotron self-Compton Model.

For each epoch, near-simultaneous measurements were made at radio, infrared and optical wavelengths. Each source shows positive spectral curvature within the infrared to ultraviolet energy range, although for OJ 287 the evidence is weak. We have fit a synchrotron self-Compton emission model to the observations (see equations in e.g. Marscher *et al.* 1979). Two important parameters, the self-absorption frequency of the synchrotron source, ν_m, and the source size at this frequency (or variability time scale,t) are highly uncertain. We therefore assumed no relativistic beaming (i.e. δ=1) and fit our measurements to solve for acceptable values of ν_m and t. The curves in figure 1 correspond to situations in which the predicted Compton flux equals the measurement or upper limit of the X-ray flux, as determined with an experiment on board the Einstein or HEAO 1 satellite. Regions above a curve are permitted if the Compton contribution to the X-ray flux is lower. A reduction by an order of magnitude increases t by roughly a factor of 1.3. For OQ 530 and ON 325, we assume a range of values for z. The electron lifetime (hrs) against synchrotron losses is given at intervals along each curve. We see that for the typical source variability time of a few hours to a few days measured in the radio and optical energy bands, the synchroton lifetime is generally shorter than t. This

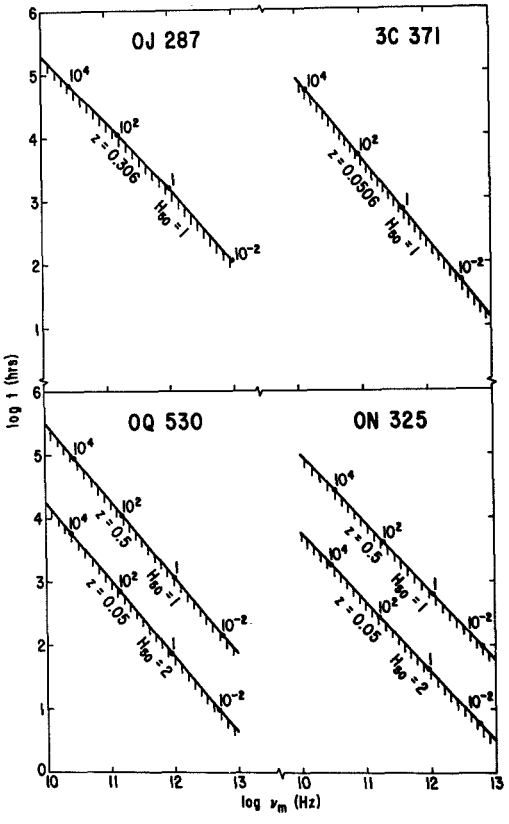

Figure 1.

Logarithmic plots of the self-absorption frequency versus the variability time scale at that frequency. Plots assume no relativistic beaming (δ=1). Values above the curves are allowed, and depend on the precise level of X-ray emission. However, the numbers along the curves represent the electron lifetime against synchrotron radiation in hours. If this is less than t, reacceleration would be necessary, or we must assume that relativistic beaming (δ>1) is present and the curves should be lowered.

would imply that either some reacceleration mechanism must be considered, or that relativistic beaming is required to lower the curves of figure 1 (i.e. $\delta>1$). A detailed treatment for OJ 287 gives $\delta \geq 20$ (Worrall *et al.* 1982). We note that the parameters fit by Bregman *et al.*(1982) for IZw 187 ($\delta=1$) imply an electron lifetime shorter than their assumed value for the source variability timescale.

3C 371.

3C 371 was the only object of the four to show significant line features in the ultraviolet. Both the May and August 1981 spectra exhibit emission at ~1280A, corresponding to Lyman α at a redshift of z=0.0520+/-0.0017. This agrees with the redshift of z=0.0506+/-0.009 determined from the visually observed emission lines (Sandage 1966; Miller 1975). The line fluxes for May and August are in good agreement and average 1.0 10^{-13} ergs cm^{-2} s^{-1}. The level of noise in the underlying continuum emission would imply that this flux value is accurate to about 30%. In the May 1981 spectrum (fig. 2) we also identify absorption lines of CIV (λ1550) and NV (λ1240) at redshifts of 0.0506+/-0.0016 and 0.0491+/-0.0013 respectively. The significance of these features is clearly in question, considering the level of continuum noise. However, they were noticed when the SWP image was read down from the IUE and viewed on the RAMTEC display unit. They are also seen on the IUE Observatory furnished "photowrite". We estimate equivalent widths for the carbon and nitrogen lines of 6.1+/-1.0A and 3.5+/-1.0A respectively. In August 1981, 3C 371 was at 70% of its May flux level (table 1) and the NV feature was not detected. Unfortunately a radiation "hit" in the vicinity of redshifted CIV renders the August spectrum useless for confirmation of this absorption line.

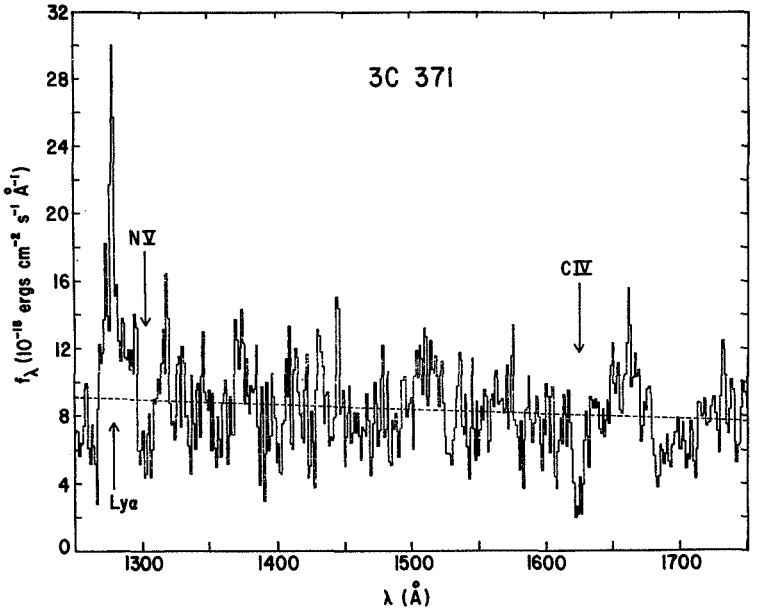

Figure 2.

May 1, 1981 1250-1750A spectrum of 3C 371 after deredenning using $A_V = 0.13$. The dashed line representing the continuum level is the best fit to the complete SWP data: $f_\nu = 1.76\ 10^{-3}\ \nu_{15}^{-1.5}$ Jy. The bin width is ~20% of the instrumental resolution.

Miller (1975) compares the optical emission line spectrum of 3C 371 with that of the elliptical galaxy NGC 1052. This in turn can be described by a shock-heating model with a shock velocity of ~130 km s^{-1} (Fosbury *et al.* 1978). From Cox (1972), (see also review of McKee and Hollenbach (1980)), the emission lines should correspond to gas which is photoionized by hot gas just behind the shock front and the Lα/Hβ ratio should be close to its recombination value of $\simeq$

33. We find $L\alpha/H\beta \simeq 63$ when we combine our $L\alpha$ flux with the $H\beta$ value of Miller, French and Hawley (1978). However, the uncertainty in the $H\beta$ measurement is at least 50% and we cannot claim significant deviation from the recombination value. The optical emission lines are all weak and precise flux measurement is subject to the modeling of the continuum galaxy component, which was ~50% of the nuclear component at 5000A when the $H\beta$ flux was derived. In contrast, at the IUE wavelengths the galaxy contribution is negligible.

We deduce lower limits to the column density by assuming that the measurements fall on the linear part of the curve of growth: $N(CIV) > 7.6\ 10^{14}$ atoms cm^{-2} and $N(NV) > 2.7\ 10^{14}$ atoms cm^{-2}. The absence of SiIV (λ1394) and CII (λ1335) absorption in the IUE spectrum, and the relative strength of NV(pending confirmation), would imply a slightly hotter temperature ($\geq 3\ 10^{5}$ K) than for the gas in our galaxy halo (as detected in absorption against continuum emission from 3C 273 by Ulrich *et al.* 1980), but possibly a similar column density. The heating of such a gas may result from a wind in the elliptical galaxy (Mathews and Baker 1971) or may be cosmic ray-induced, as modeled for our galaxy by Weisheit and Collins (1976). We note in regard to the latter, the presence of extended 1425 MHz continuum radio emission (Fomalont and Moffet 1971), which suggests cosmic ray electron containment in a region of size at least ~40 kpc.

A number of observers were involved in the collaborative program of multifrequency measurements. In particular we acknowledge the contributions of M.Aller, H.Aller, F.Cordova, P.Hodge, B.Jones, W.Ku, K.Mason, K.Matthews, H.Miller, G.Neugebauer,J.Puschell, R.Rudy, M.Sitko, T.Soifer, W.Stein, and W.Wisniewski. We thank Drs.A.P.Marscher, H.E.Smith and J.J.Puschell for invaluable discussions and Dr.D.Klinglesmith for making available the Fahey-Klinglesmith software package. The IUE observations were supported by NASA grant NAG 5-63.

Bregman,J.N. *et al.*, 1982, Ap.J., *253*, 19.
Burstein,D., and Heiles,C., 1978, Ap.J., *225*, 40.
Cox,D.P., 1972, Ap. J., *178*, 143.
Fomalont,E.B. and Moffet,A.T., 1971, A.J., *76*, 5.
Fosbury,R.A.E., Mebold,U., Goss,W.M., and Dopita,M.A., 1978, M.N.R.A.S., *183*, 549.
Marscher,A.P., Marshall,F.E., Mushotzky,R.F., Dent,W.A., Balonek,T.J. and Hartman,M.F., 1979, Ap.J., *233*, 498.
Mathews,W.G. and Baker,J.C., 1971, Ap. J., *170*, 241.
McKee,C.F. and Hollenbach,D.J., 1980, Ann. Rev. Astron.Astrophys.,*18*, 219.
Miller,J.S., 1975, Ap. J. Lett., *200*, L55.
Miller,J.S., French,H.B., and Hawley,S.A., 1978, Proc. Pittsburgh Conf. on BL Lac Object, ed.A.M.Wolfe, Univ.Pittsburgh Press, p312.
Sandage,A., 1966, Ap. J., *145*, 1.
Savage,B.D. and Matthis,J.S., 1979, Ann. Rev. Astron.Astrophys.,*17*, 73.
Ulrich,M.H. *et al.*, 1980, M.N.R.A.S., *192*, 561.
Weisheit,J.C. and Collins,L.A., 1976, Ap.J., *210*, 299.
Worrall,D.M. et al., 1982, submitted to Ap. J.

COORDINATED OBSERVATIONS OF MARKARIAN 180 AT ULTRAVIOLET, X-RAY, OPTICAL, AND RADIO WAVELENGTHS

S.L. Mufson[1], D.J. Hutter[1], K.R. Hackney[2], R.L. Hackney[2], Y. Kondo[3], R.F. Mushotzky[3], C.M. Urry[3], W.Z. Wisniewski[4], M.F. Aller[5], H.D. Aller[5], and P.E. Hodge[5]

INTRODUCTION

We present here the results of multifrequency observations of Mrk 180 = 1133+704, a BL Lac object embedded in a giant elliptical galaxy (Mufson and Hutter 1981), obtained during the period November-December 1980. The importance of Mrk 180 derives mostly from its association of a quasar-like object with a galaxy whose absorption-line redshift ($z = 0.046$; Ulrich 1978) unambiguously determines its distance. This implies that physical conditions within this local quasar can be discussed without the confusion introduced by distance uncertainties.

OBSERVATIONS

In fig. 1 we have plotted the data we obtained from our multifrequency observations.

The ultraviolet data shown here were obtained by the LWR on IUE on 10 November 1980. The parameters of the power law spectrum ($S \sim \nu^{\alpha}$) which best fit the ultraviolet data are $\alpha = -1.73 \pm 0.37$ and $\log S_{\nu}(\mathrm{Jy}) = -3.11 \pm 0.05$ at $\log \nu(\mathrm{Hz}) = 15.1$ (errors are 95% confidence limits). Since Mrk 180 is at a galactic latitude of 70°, there were no corrections made for galactic extinction (Burstein and Heiles 1978).

The BVR photometry was obtained on 30 December 1980 with the 1 m telescope of the Lunar and Planetary Laboratory on Mt. Lemmon, AZ. These observations were made with an aperture of 46". Extinction and transformation coefficients were determined from observations of the Johnson et al. (1966)

[1] Astronomy Department, Indiana University

[2] Department of Physics and Astronomy, Western Kentucky University

[3] NASA Goddard Space Flight Center

[4] Lunar and Planetary Laboratory, University of Arizona

[5] Radio Astronomy Observatory, University of Michigan

primary UBVRI standards. The BVR magnitudes of Mrk 180, corrected for the star offset 7".2 from the galactic nucleus (Mufson and Hutter 1981), are B = 15.78 ± 0.06, V = 14.95 ± 0.06, and R = 14.20 ± 0.06 (errors are 95% confidence limits). There were again no corrections made for galactic extinction.

The x-ray observations were made by the IPC aboard HEAO-2 on 28 December 1980. The parameters of the power law spectrum with a low energy cutoff that best fit the x-ray data are α = -0.67 ± 0.6, log S_ν(Jy) = -5.36 ± 0.07 at log ν(Hz) = 17.4, and a hydrogen column density $N_H = (0.4(+4,-0.4))\times10^{20}$ cm^{-2} (errors are 99% confidence limits).

The radio observations represent flux density measurements at 8.0 and 14.5 GHz made between 4 - 30 November 1980 using the 26 m paraboloid of the University of Michigan Radio Astronomy Observatory. The weighted mean values of the flux density during this period are $\bar{S}_8$(Jy) = 0.54 ± 0.10 and $\bar{S}_{14.5}$ = 0.39 ± 0.16 (errors are 95% confidence limits).

MODEL

The data were fit using a relativistic beam model in which a freely expanding, constant velocity jet of relativistic particles emits radiation by the synchrotron-self Compton process. Such a model can naturally explain many aspects of the BL Lac phenomenon, including the observed radio spectra, rapid flux variations, and changes in polarization. A beam model can also greatly reduce the rest frame energy requirements of the source, as compared with an isotropic emitter. In our models the synchrotron spectrum was calculated using the relations given in Königl (1981). These expressions assume continuous reacceleration of the relativistic electron population. The self Compton spectrum was calculated by the method of Baylis, Schmid, and Lüscher (1967). Both the magnetic field and particle densities were assumed to have a power law variation with radial distance along the jet axis. In the model calculation, the radio spectrum was assumed to have a spectral index of α_{s1} = 0, and a low frequency cutoff $\nu_{sm} = 1.0\times10^8$ Hz. The optical-ultraviolet slope was defined by the IUE observation.

Best fits to our data were obtained using a chi-square minimazation technique. The best fit model yields a chi-square per degree of freedom χ^2_ν = 1.09 for 3 degrees of freedom. The values of the model parameters are: angle between the jet axis and the line of sight θ = 6°.3; opening angle of the jet ϕ = 5°.7; the radio-infrared break frequency $\nu_{sM} = 9.2\times10^{12}$ Hz; the flux density at the break $S(\nu_{sM})$ = 0.545 Jy; the average spectral index of the optical-ultraviolet spectrum α_{s2} = 1.6; and the ratio of the flux density of the nonthermal emission to that of the galaxy in the V bandpass $[S_\nu(\text{nonthermal})/S_\nu(\text{galaxy})]_V$ = 1.7.

In fig. 1 we show this best fit model superimposed on the observations. The insert shows the decomposition of the optical data into the galaxy and nonthermal components. (The horizontal bars indicate the model's prediction of the total flux in each bandpass.) Note particularly that the x-ray flux in this model is primarily due to Compton scattering. This results from the

dual requirements of fitting the very steep optical-ultraviolet spectrum and the relatively high level of x-ray emission.

The best fit model yields the following values for the physical parameters of the jet: index m = 1.35, and normalization B1 = 1.5×10^{-3} G of the magnetic field variation with radius ($B = B1 \cdot r^{-m}$, r in pc); index n = 1.35, and normalization K1 = 6.59×10^{5} cm^{-3} of the particle density variation with radius ($K = K1 \cdot r^{-n}$, r in pc); and the inner radius of the optically thin portion of the jet $r_{min} = 9.0 \times 10^{-4}$ pc. For these parameter values, the jet flow is particle dominated (particle energy density $\gg$ magnetic field energy density) at all radii. This result is similar to that found for a beam model of the BL Lac object PKS 2155-304 by Urry and Mushotzky (1982).

This work was partially supported by NASA contracts NAG 8831 and NAG-5-198.

REFERENCES

Baylis, W.E., Schmid, W.M., and Lüscher, E. 1967, Zeitschrift für Astrophysik, 66, 271.

Burstein, D., and Heiles, C. 1978, Ap.J., 225, 40.

Johnson, H.L., Mitchell, R.I., Iriarte, B., and Wisniewski, W.Z. 1966, Communications of the Lunar and Planetary Laboratory, 4, 99.

Königl, A. 1981, Ap.J., 243, 700.

Mufson, S.L., and Hutter, D.J. 1981, Ap.J. (Letters), 248, L61.

Ulrich, M.-H. 1978, Ap.J. (Letters), 222, L3.

Urry, C.M., and Mushotzky, R.F. 1982, Ap.J., 253, 38.

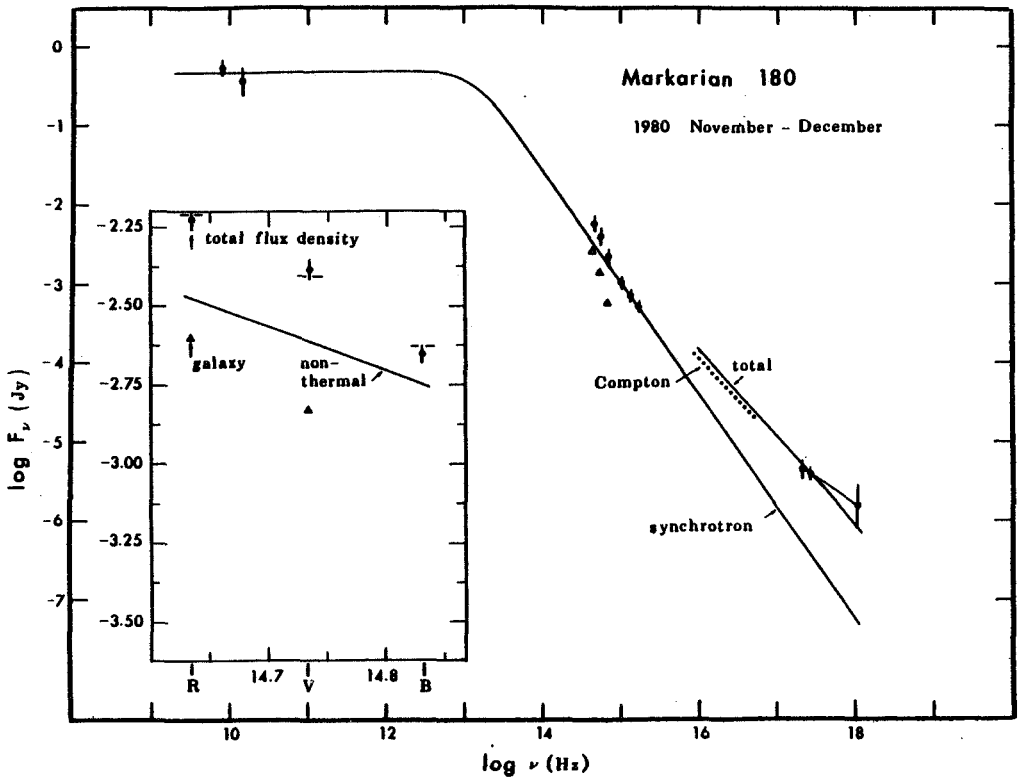
Markarian 180
1980 November - December
total flux density
galaxy
non-
thermal
Compton
total
synchrotron
R
V
B
14.7
14.8
-2.25
-2.50
-2.75
-3.00
-3.25
-3.50
0
-1
-2
-3
-4
-5
-6
-7
10
12
14
16
18
log F$_\nu$ (Jy)
log ν (Hz)

Fig. 1

COORDINATED OBSERVATIONS OF MARKARIAN 501 AT ULTRAVIOLET, X-RAY, OPTICAL, AND RADIO WAVELENGTHS

D.J. Hutter[1], S.L. Mufson[1], K.R. Hackney[2], R.L. Hackney[2], Y. Kondo[3], R.F. Mushotzky[3], C.M. Urry[3], W.Z. Wisniewski[4], M.F. Aller[5], H.D. Aller[5], and P.E. Hodge[5]

INTRODUCTION

We present here the results of multifrequency observations of Mrk 501 = B2 1652+39, a BL Lac object embedded in a giant elliptical galaxy (Ulrich et al. 1975), obtained during the period August 1980 - March 1981. We argue that Mrk 501 varies sufficiently slowly at ultraviolet, optical and radio wavelengths on time scales of months that our data are representative of a spectrum obtained at a single epoch. The importance of Mrk 501 derives mostly from its association of a quasar-like object with a galaxy whose absorption-line redshift ($z = 0.034$; Ulrich et al. 1975) unambiguously determines its distance. This implies that physical conditions within this local quasar can be discussed without the confusion introduced by distance uncertainties.

OBSERVATIONS

In fig. 1 we present the data we obtained from our multifrequency observations.

The ultraviolet data were obtained by the SWP on IUE on 7 March 1981. The parameters of the power law spectrum ($S_\nu \sim \nu^\alpha$) which best fit the ultraviolet data are $\alpha = -0.79 \pm 0.08$ and $\log S_\nu(\mathrm{Jy}) = -2.88 \pm 0.01$ at $\log\nu(\mathrm{Hz}) = 15.3$ (errors are 95% confidence limits). There were no corrections made to these data for the effects of galactic extinction (Burstein and Heiles, 1978). Comparison of these spectral parameters with the parameters reported by Kondo et al. (1981) for IUE observations made in 1978 show that only marginal variations have occurred in this 2 - 3 year period.

[1] Astronomy Department, Indiana University

[2] Department of Physics and Astronomy, Western Kentucky University

[3] NASA Goddard Space Flight Center

[4] Lunar and Planetary Laboratory, University of Arizona

[5] Radio Astronomy Observatory, University of Michigan

The BVR photometry was obtained on 31 August 1980 with the 1.5 m telescope of the Lunar and Planetary Laboratory on Mt. Lemmon, AZ. These observations were made with an aperture of 12".3. Extinction and transformation coefficients were determined from observations of the Johnson et al. (1966) primary UBVRI standards. The BVR magnitudes are B = 14.70 ± 0.04, V = 13.95 ± 0.04, and R = 13.03 ± 0.04 (errors are 95% confidence limits). Comparison of the magnitudes reported here with those found in Kondo et al. (1981) shows that the optical spectrum of Mrk 501 has remained relatively unchanged for the past several years.

The x-ray observations were made by the IPC aboard HEAO-2 on 15 August 1980. The parameters of the power law spectra with a low energy cutoff that best fit the x-ray data are α = -0.8 ± 0.5, log S_ν(Jy) = -4.78 ± 0.06 at log ν(Hz) = 17.4, and a hydrogen column density $N_H = (1.9(+2,-1))\times10^{20}$ cm^{-2} (errors are 99% confidence limits).

The radio observations represent flux density measurements at 8.0 and 14.5 GHz made in March - April 1981. The weighted mean values of the flux density during this period are $\bar{S}_8$(Jy) = 1.28 ± 0.04 and $\bar{S}_{14.5}$(Jy) = 1.11 ± 0.04 (errors are 95% confidence limits). Archival measurements have shown that the radio spectrum of Mrk 501 varies slowly on a time scale of years (Aller, Aller, and Hodge 1982). Additional data on fig. 1 have been obtained from Allen (1976), Colla et al. (1975), Ghigo and Owen (1973), Joyce and Simon (1976), Owen et al. (1978), Owen et al. (1980), Sulentic (1976), and Ulrich et al. (1975).

MODEL

See Mufson et al. (previous paper) for a description of the relativistic beam model. In fitting our data for Mrk 501 the radio spectrum was assumed to have a spectral index of α_{s1} = 0.238, and a low frequency cutoff at $\nu_{sm} = 1.19\times10^6$ Hz. The optical-ultraviolet slope was defined by the IUE observation. The best fit model yields a chi-square per degree of freedom χ^2_ν = 0.803 for 4 degrees of freedom. The values of the variable parameters for this best fit model are as follows: angle between the jet axis and the line of sight θ = 14°.3; opening angle of the jet ϕ = 5°.7; the radio-infrared break frequency $\nu_{sM} = 3.48\times10^{11}$ Hz; the flux density at the break $S(\nu_{sM})$ = 0.62 Jy; the average spectral index of the optical-ultraviolet spectrum α_{s2} = 0.76; and the ratio of the flux density of the nonthermal source to that of the galaxy in the V bandpass $\left[S_\nu(\text{nonthermal})/S_\nu(\text{galaxy})\right]_V$ = 0.49.

In fig. 1 we show this best fit model superimposed on the data. The insert shows the decomposition of the optical data into the galaxy and nonthermal components. (The horizontal bars indicate the model's prediction of the total flux in each bandpass.) Note that a far greater percentage of the optical-ultraviolet flux is due to the galaxy in Mrk 501 than was the case for Mrk 180 (previous paper). In this model, the x-ray emission is a high frequency extension of the optical-ultraviolet synchrotron spectrum.

The best fit model yields the following values for the physical parameters of the jet: index m = 0.98, and normalization B1 = 0.0905 G of

the power law variation of the magnetic field with radius ($B = B1 \cdot r^{-m}$, r in pc); index n = 1.77, and normalization K1 = 11.7 of the power law variation of the particle density with radius ($K = K1 \cdot r^{-n}$, r in pc); and the inner radius of the optically thin portion of the jet $r_{min} = 0.0102$ pc.

For these values of the jet magnetic field and particle density, the jet flow is not particle dominated as was the case for Mrk 180. This is to be expected, as the values of the indices m and n are near their equipartition values (m = 1, n = 2; Blandford and Königl, 1979).

This work was partially supported by NASA contracts NAG 8831 and NAG-5-198.

REFERENCES

Allen, D.A. 1976, Ap.J., 207, 367.

Aller, M.F., Aller, H.D., and Hodge, P.E. 1982, A.J., submitted.

Blandford, R.D., and Königl, A. 1979, Ap.J., 232, 34.

Burstein, D., and Heiles, C. 1978, Ap.J., 225, 40.

Colla, G., Fanti, C., Fanti, R., Gioia, I., Lari, C., Lequeux, J., Lucas, R., and Ulrich, M.-H. 1975, Astr. Ap. (Suppl.), 20, 1.

Ghigo, F.D., and Owen, F.N. 1973, A.J., 78, 848.

Johnson, H.L., Mitchell, R.I., Iriarte, B., and Wisniewski, W.Z. 1966, Communications of the Lunar and Planetary Laboratory, 4, 99.

Joyce, R.R., and Simon, M. 1976, P.A.S.P., 88, 870.

Kondo, Y., Worrall, D.M., Mushotzky, R.F., Hackney, R.L., Hackney, K.R.H., Oke, J.B., Yee, H.K.C., Neugebauer, G., Matthews, K., Feldman, P.A., and Brown, R.L. 1981, Ap.J., 243, 690.

Owen, F.N., Porcas, R.W., Mufson, S.L., and Moffett, T.J. 1978, A.J., 83, 685.

Owen, F.N., Spangler, S.R., and Cotton, W.D. 1980, A.J., 85, 351.

Sulentic, J.W. 1976, A.J., 81, 582.

Ulrich, M.-H., Kinman, T.D., Lynds, C.R., Rieke, G.H., and Ekers, R.D. 1975, Ap.J., 198, 261.

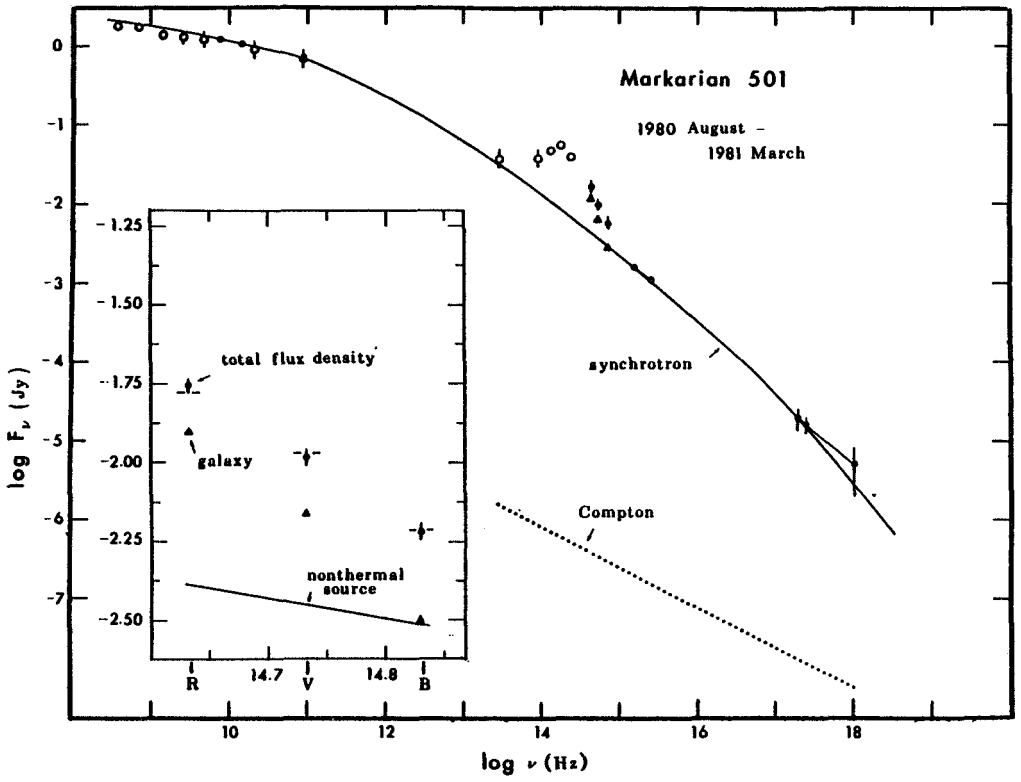
Markarian 501
1980 August -
1981 March
synchrotron
Compton
total flux density
galaxy
nonthermal
source
R
V
B
14.7
14.8
log F$_\nu$ (Jy)
log ν (Hz)

fig. 1

THE ULTRAVIOLET SPECTRUM OF THE HIGH REDSHIFT BL LAC OBJECT 0215+015

J.C. Blades[1], M. Pettini[2], R.W. Hunstead[3] & H.S. Murdoch[3]

[1]Rutherford Appleton Laboratory, UK
[2]Royal Greenwich Observatory, UK
[3]School of Physics, University of Sydney, Australia

ABSTRACT

The object 0215+015 is highly variable, with a range in the optical band of more than 4 magnitudes, and exhibits rapidly variable polarization. At optical wavelengths it shows no emission lines but has a rich absorption spectrum with at least six, separate redshift systems. We have combined 3 LWP low-dispersion images of the object to produce a high signal-to-noise spectrum between 2400 - 3200 Å which we use to study the hydrogen Lyman lines of the various redshift systems.

INTRODUCTION

The six, separate redshift systems in the BL Lac 0215+015 occur at z_a = 1.254, 1.345, 1.491, 1.549, 1.649 and 1.686. The z_a = 1.345 system exhibits a strong, mixed-ionization spectrum whilst the other five are predominantly C IV systems. At high-resolution most of the absorption systems show complex sub-structure, especially the C IV systems at z_a = 1.549 and 1.649 (Blades *et al*, 1982).

Four of the absorption systems have their hydrogen Lyman α line within the range of the long-wavelength camera of IUE. Because this line, in conjunction with our optical spectra, allows determination of abundances in the various redshift systems, we have secured three, long-wavelength, low-resolution IUE spectra of 0215+015. We present here preliminary results from this work, including an analysis of the abundances in the z_a = 1.345 system.

ULTRAVIOLET OBSERVATIONS LWP or LWR?

Over the wavelength region of interest - expected to be from 3200 Å to the Lyman limit of the z_a=1.649 system ($\sim$2416 Å) - it has been shown by Settle *et al* (1981) that the long wavelength prime (LWP) camera is more sensitive than the redundant camera and has improved signal-to-noise characteristics, see Figure 1a & b. Additionally, there is evidence that the LWP is less sensitive to the radiation background, and it does not suffer from the narrow band of microphonic-type distortion prevalent in the LWR camera. An ITF table has recently been determined for the LWP camera, and the original problem in reading the camera, which arose

shortly after launch of IUE, can be circumvented. Clearly, with these advantages we had no alternative but to use the LWP and the results vindicate our choice. We obtained 3 LWP spectra of 0215+015 in 1981 Sept 12.8 (duration 233 min) and in 1982 Feb 15.3 (322 min) and Feb 23.3 (305 min).

RESULTS

Individual LWP spectra were extracted from the line-by-line file using a slit height of 3 pixels, so as not to degrade the signal-to-noise, the background being assessed from both sides of the spectrum. The net spectra were then aligned, using prominent absorption lines as a guide, and co-added.

The co-added, rectified spectrum is shown in Figure 3. Its most striking aspect is the richness of its absorption spectrum. We identify Lyman α lines from four of the redshift systems and in the $z_a = 1.649$ system, Lyman β, γ, δ, possibly ϵ, and the series limit. Also present are features we attribute to zero-redshift, galactic Mg II and Fe II. The improvement obtained with the LWP is well shown in the comparison of the spectral region near Lyα in the $z_a = 1.345$ system with the two cameras (the LWR data being from the archive). The hydrogen line is virtually black in the LWP spectrum, whereas it is only $\sim$70% deep in the LWR spectrum - see Figure 2. Improvements in S/N and resolution are also present.

Column densities were derived for six ionic species in the $z_a = 1.345$ system by Blades *et al* (1982), and a comparison of these values with those derived by Savage & Jeske (1981) for halo, galactic gas in an LMC sightline showed remarkable agreement. Hence the $z_a = 1.345$ system plausibly arises in an intervening galaxy in the line of sight to 0215+015. The strength of Lyα corresponds to $N(H\ I) = 7.2\ (+2.3, -1.9) \times 10^{19}\ cm^{-2}$, assuming a pure damping profile. With the ion column densities in Blades *et al* we find the elements Mg, Fe, Si & Al are depleted by between 4 - 10 times their solar values. Numerous uncertainties plague abundance determinations: Lyα may not have a pure damping profile, or not all of it may be associated with the metal lines; the model used to determine the ion densities may be unrealistic, and there could be large contributions from unseen ionization levels. These uncertainties give rise to overestimates in the H I and underestimates in the ion column densities. However, these may be real depletions in the (postulated) intervening galaxy, hence future observations of Zn II (normally undepleted) and the λ2175 extinction feature (reddening indicator) will be important. Another possibility is that we are observing gas that has undergone less nuclear processing than solar-type material.

REFERENCES

Blades, J.C., Hunstead, R.W., Murdoch, H.S. & Pettini, M. 1982, M.N.R.A.S. accepted.

Savage, B.D. & Jeske, N.A. 1981, Ap. J., 244, 768.

Settle, J., Shuttleworth, T. & Sandford, M.C.W. 1981, LWP Users' Guide.

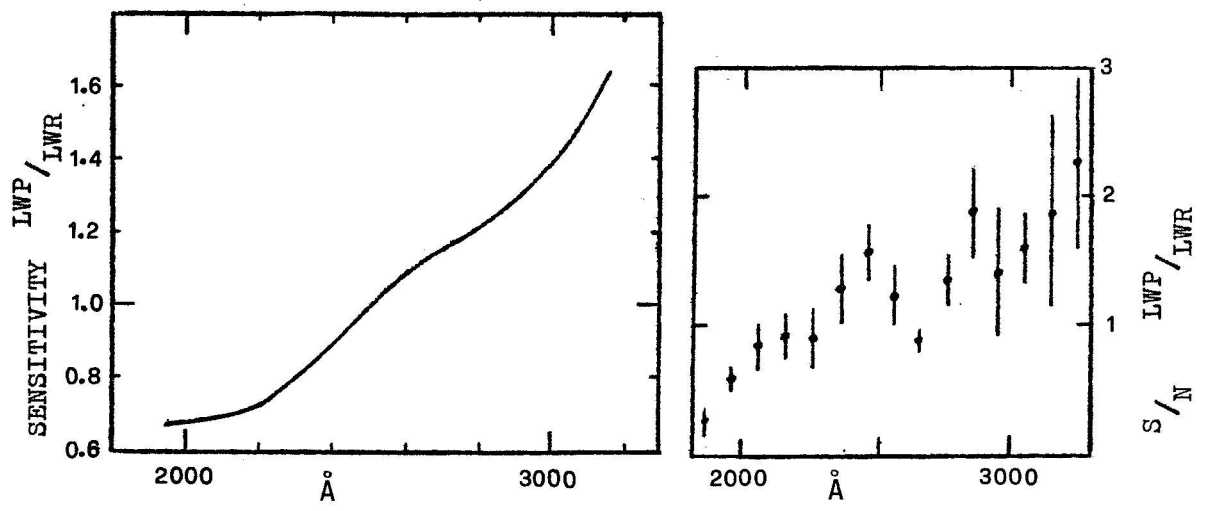

Figure 1a & b. A comparison of the sensitivity and signal-to-noise characteristics of the LWP and LWR cameras, adopted from Settle et al (1981).

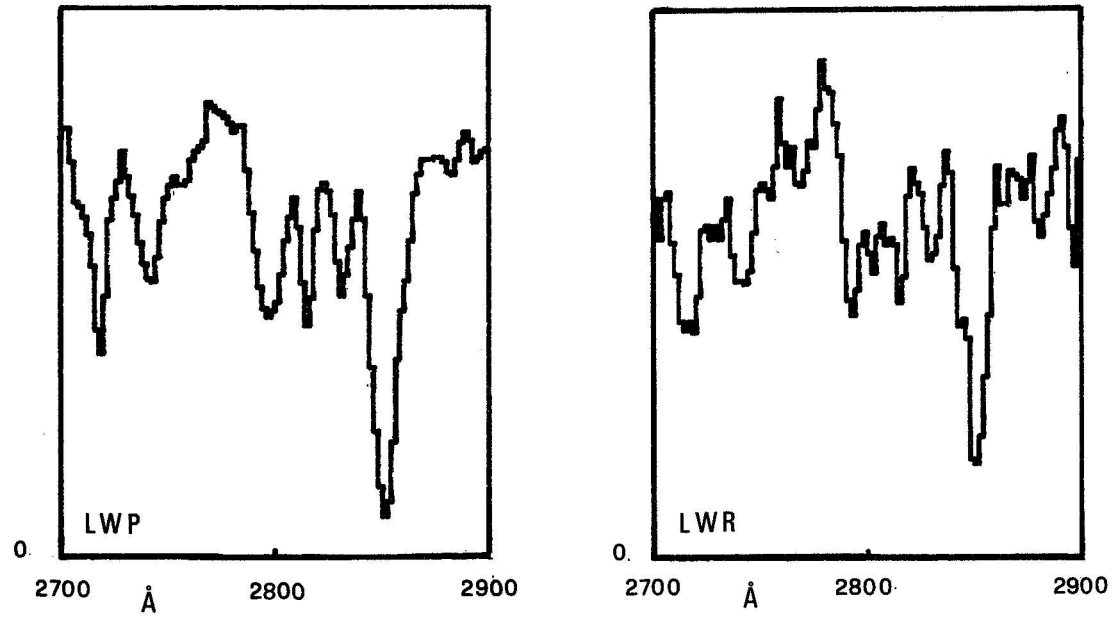

Figure 2. Part of the 0215+015 spectrum near Lyman α in the 1.345 absorption system. Note how this line is deeper in the LWP spectrum, the other lines also are better resolved.

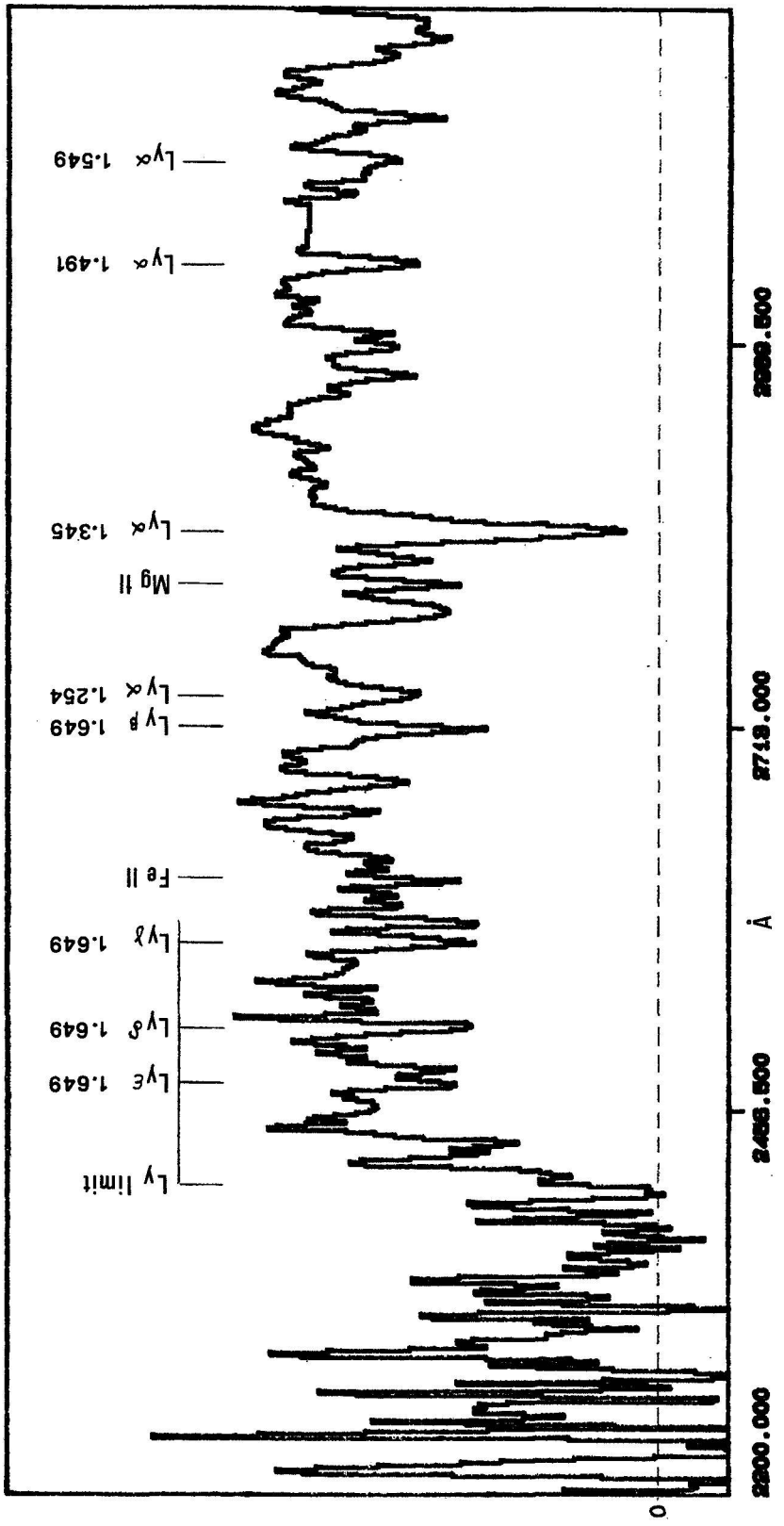

Figure 3. The co-added, low resolution, LWP spectrum of 0215+015

SIMULTANEOUS MULTIFREQUENCY OBSERVATIONS OF BL Lac OBJECTS AND VIOLENTLY VARIABLE QUASARS

J.N. Bregman, A.E. Glassgold, and P.J. Huggins
Physics Department, New York University

Abstract

Ultraviolet spectra simultaneous with radio, infrared, optical, and X-ray measurements were obtained for three BL Lac objects and one violently variable quasar during several epochs (0735+178, BL Lac, IZw-187, and 3C446). A feature common to these objects is that the radio-mm continuum must steepen in the far-infrared region in order to connect smoothly to the IR-UV continuum. This indicates that synchrotron emission becomes optically thick in the mm or far-infrared region. The continuum of 3C446 and BL Lac steepen quite rapidly between the IR and UV regions, unlike 0735+178 and IZw-187, which have single power-law IR-UV spectra with slopes near unity. The X-ray emission in BL Lac, 3C446, and 0735+178 has a different origin from the IR-UV radiation, probably from the inverse Compton process. However, the synchrotron radiation is the probable source of X-ray emission in the X-ray bright BL Lac object IZw-187. In IZw-187, most of the energy emerges in the UV - X-ray region, while for the other sources, most of the energy emerges in the far infrared region.

Introduction

Simultaneous multifrequency spectra are powerful tools for studying the nonthermal continuum in violently variable quasars and BL Lac objects. Such spectra allow one to study the connection between the various spectral regions (radio, IR-UV, X-ray), to determine the important emission processes, and to calculate the physical conditions within the emitting region. As part of our IUE program, we have obtained ultraviolet spectra and coordinated the acquisition of multifrequency observations of several BL Lac objects and violently variable quasars. Here we present a study of four such objects: BL Lac, 0735+178, IZw-187, and 3C446.

Results

Each of our objects was detected in the radio region ($<10^{11}$Hz), the IR-optical-UV region (10^{14}-2×10^{15}Hz), and the X-ray region (10^{17}-10^{18}Hz). Because of the limited frequency response of current instruments, participation by at least seven different observers were needed to obtain multifrequency spectra of each object. Our collaborators are listed in Table 1. The IR-UV data were generally obtained within a day of the X-ray data and most of the radio data were obtained within a few days of the other observations.

The resulting multifrequency spectra, corrected for the effects of absorption within our galaxy, are given in Figure 1. Reddening corrections for IZw-187, 0735+178 and 3C446 of E(B-V) = 0.025, 0.05, and 0.05 were calculated from the reddening law of Burstein and Heiles (1978). A reddening correction for BL Lac of 0.31, taken from the work of Du Puy et al. (1969), is in agreement with that derived by other methods (Burstein and Heiles 1978, Hackney and Hackney 1982). These multifrequency spectra were used to (1) examine the connection between emission from the three spectal region (radio, IR-UV, X-rays), (2) determine the frequency region in which most of the energy emerges, and (3) calculate the physical properties in the emitting region.

A common characteristic of each spectra is that when the IR-UV continuum is extrapolated to radio frequencies, it does not connect smoothly onto the radio data. In order for a smooth connection to be made, the slope of the extrapolated IR-UV continuum must decrease (flatten) in the $10^{11.5}$-10^{13} Hz region. If the radio and the IR-UV emission arises from the synchrotron process (argued for by Kellermann and Pauliny-Toth 1981, Angel and Stockman 1980), then the flattening of the spectrum may be interpretated as due to the source becoming optically thick at low frequencies.

These objects display two kinds of IR-UV continua. In IZw-187 and 0735+178, the continua are simple power laws with slopes close to unity (0.9 and 1.1 respectively). In contrast, the IR-UV continua in 3C446 and BL Lac, which are nearly identical, steepen from a slope of 1.4 in the infrared to >3 in the ultraviolet region. In these two objects, the ultraviolet continua, when exrapolated to higher frequencies, passes far below the X-ray observations. We view this as strong evidence that the X-ray emission has a different origin from the IR-UV emission and that the X-rays arise from Compton scattering of low energy photons by the relativistic electrons. In IZw-187, the extrapolated ultraviolet power-law passes through the X-ray observations, indicating that in this object, the IR-UV and the X-ray emission may share a common origin in synchrotron radiation. This interpretation is supported by variability data (Bregman et al. 1982). 0735+178 differs from the other objects because the extrapolated IR-UV spectra passes well above the X-ray data. Without variability data (below) it is impossible to determine whether the X-rays are synchrotron or inverse Compton in origin.

Multifrequency spectra of 0735+178 were obtained at three epochs between October 1979 and March 1981. Although the UV-IR continuum was approximately four times brighter in October 1980 than in October 1979, a comparable flux increase was not seen in the X-ray region. The X-ray emission again remained nearly unchanged as the UV-IR flux decreased by 50% between October 1980 and March 1981. This evidence favors an inverse Compton origin rather than a synchrotron origin for the X-ray radiation.

The multifrequency spectra allow us to locate the

frequency region where most of the radiated energy emerges. In IZw-187, most of the energy emerges in the X-ray region, while in 0735+178, BL Lac, and 3C446, most of the energy emerges in the far infrared region ($10^{11.5}$-10^{13} Hz) where the continuum reaches a slope of unity.

The physical condition in the continuum emitting region can be calculated with the use of a radiation model, such as the synchrotron-self-Compton model (e.g. Jones, O'Dell, and Stein 1974). We summarize here the results of the modeling, the details of which will be reported in the Astrophysical Journal. We find that the size of the optically thin emitting region is between a light week and a few light months, in contrast to the radio emission region, which comes from a larger region. The magnetic fields that we calculate are in excess of one Gauss, and except for IZw-187, the emitting region may exhibit relativistic beaming (Lorentz factor for the motion of 1.5-7).

References

Angel, J.R.P., and Stockman, H.S. 1980, Ann. Rev. Ast. Ap., 18, 321.

Bregman, J.B., et al. 1982, Ap.J., 253, 19.

Burstein, D., and Heiles, C. 1978, Ap.J., 225, 40.

DuPuy , J., et al. 1969, Ap.J., 156, L135.

Hackney, R., and Hackney, K. 1982, in preparation.

Jones, T.W., O'Dell, S.L., and Stein, W.A. 1974, Ap.J., 192, 261.

Kellermann, K.I., and Pauliny-Toth, I.I.K. 1981, Ann. Rev. Astr. Ap., 19, 269.

Figure Caption

Multifrequency spectra of IZw-187 (8/80), 3C446 (6/80; shifted down by 2 in log F), BL Lac (6/80; shifted down by 3.5 in log F), and 0735+178 (10/80; shifted down by 4.5 in log F).

Table 1. Collaborating Observers

Name	Institution	Wavelength Region
Dent, Balonek	U. Mass.	2.7 - 90 GHz
H. Aller, M. Aller, and P. Hodge	U. Michigan	4.8 - 14.5 GHz
Rieke, Lebofsky, and Rudy	Steward Obs.	1 - 10 μm
Impey, Brand, and Williams	UKIRT	1 - 2.2 μm
Neugebauer	Palomar Obs.	1 - 2.2 μm
Miller	Lick Obs.	.35 - .7 μm
Smith, Pica, Pollock, and Webb	U. Florida	.36 - .7 μm
Bregman, Glassgold, and Huggins	New York Univ.	.12 - .32 μm
Ku and Helfand	Columbia Univ.	.25 - 3.5 keV *
Tananbaum and Schwartz	Center for Astro.	.25 - 3.5 keV *

* Einstein Observatory data

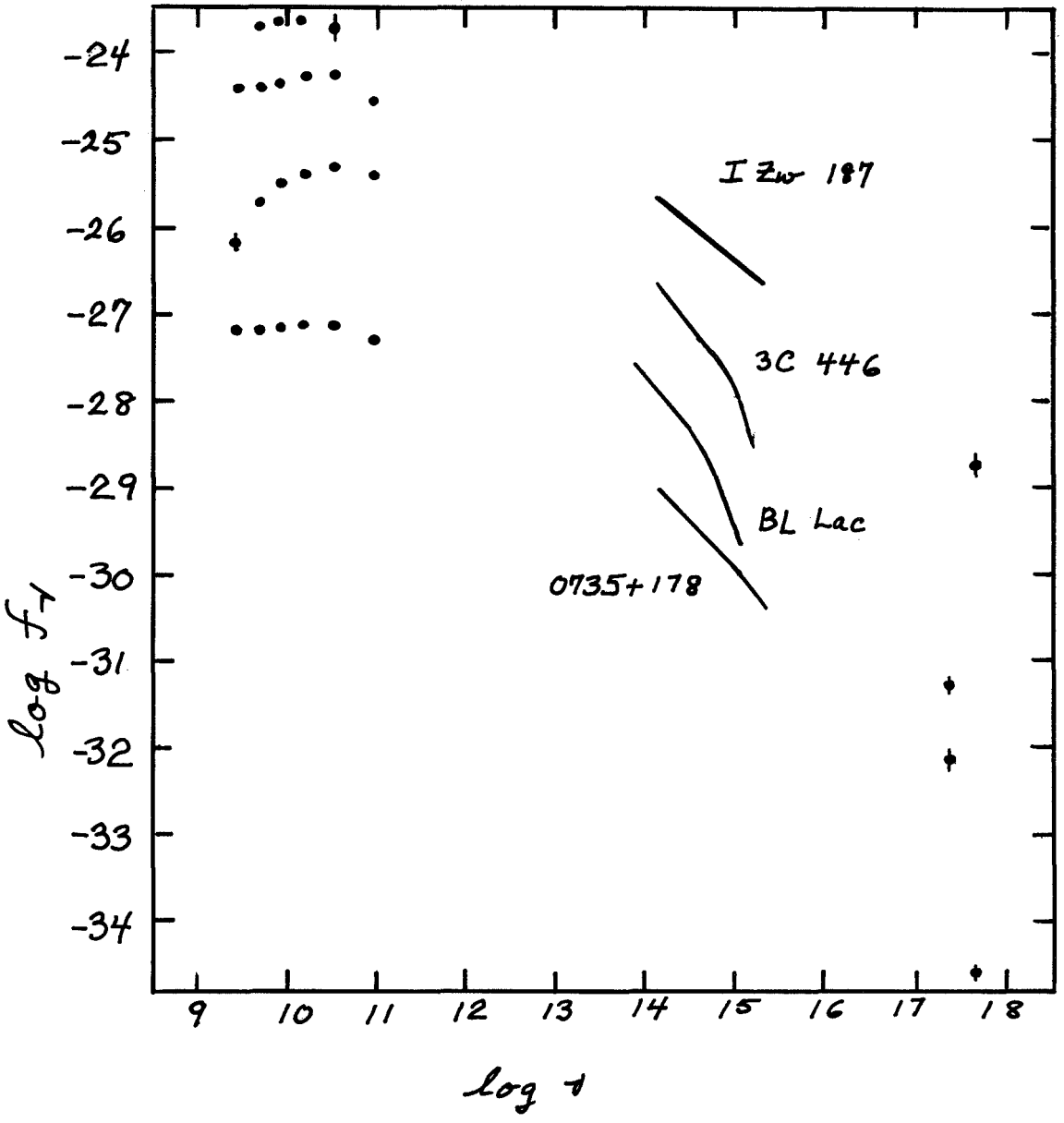
-24
-25
-26
-27
-28
-29
-30
-31
-32
-33
-34
log f_ν
9
10
11
12
13
14
15
16
17
18
log ν
I Zw 187
3C 446
BL Lac
0735+178

Multifrequency Observations of the Quasar 1156+295

A.E. Glassgold, J.N. Bregman, and P.J. Huggins
Physics Department, New York University

Abstract

The recent outburst in the quasar 1156+295 was discovered in the course of optical monitoring made in preparation for IUE observations in April 1981. We obtained short and long wavelength spectra on three occasions when the object was very bright, and which were separated in time by intervals of 4 and 60 days. The UV continuum in all cases is a steeply falling power law, with slope close to -2.0. No spectral features are apparent in the UV. Closely simultaneous observations were made by our collaborators at radio, infrared, and optical frequencies. The continuum is less steep at optical and infrared frequencies, and the overall spectra show little change in shape with time.

Introduction

The quasar 1156+295 has been a target in our program to carry out simultaneous, multifrequency observations of rapidly varying quasars and BL Lac objects. (It was also listed as a 3rd year target to detect a Lyman discontinuity; at a redshift of 0.73 the Lyman edge is at 1580 A.) Stockman (1978) classified this object as an optically violent variable quasar on the basis of its large, variable polarization. Because most of our objects of interest are usually faint, a number are always measured photometrically (B filter) by A. Smith's group of the University of Florida just prior to our IUE observing runs. On April 4, 1981, it was discovered that 1156+295 had brightened so dramatically that it had become one of the most luminous of all quasars. We obtained simultaneous multifrequency spectra shortly after this date and again two months later. Here we present a preliminary report of these data. Additional observers were notified by J. Pollock of U. Florida and one of us (J.N.B.) in order to insure maximal coverage. A report of these other observations is in preparation (Wills et al. 1982).

Results

The IUE observations were analyzed by techniques previously described (Bregman et al. 1981, 1982). The short and long wavelength spectra were then averaged in 50 A bins. The combined spectra for each date are shown in Figure 1, and some information about the observations are given in Table 1. No reddening corrections were applied because standard considerations (Heiles 1976, Burstein and Heiles 1978) give $E(B-V) = 0.00 \pm 0.03$ for this direction. The statistical errors

in the average data points in Figure 1 are much smaller than the photometric accuracy. We estimate the latter as approximately 10% from the ripples in the curves. The best fit slopes are α = -1.94, -1.90, and -1.79 for April 4, 8, and June 5, 1981. These power law spectra are most easily interpreted as optically thin synchrotron radiation.

Figure 2 shows IR and optical photometry and optical spectrophotometry. The slope is considerably smaller than at UV wavelengths. There appears to be little change in the overall shape of the IR-optical-UV spectra with time, although the closely simultaneous data are complete only for April 8, 1981. The IR-optical slope on this date is -0.90.

The radio frequency observations (not shown in Fig. 2) are flatter, and can not be obtained by a simple extrapolation of the IR-optical spectrum. In other words, the spectrum turns over in going from 10^{13} to 10^{11} Hz, suggestive of optically thick synchrotron radiation.

During the period of our UV observations, the Mg II line was observed by our collaborators at optical frequencies at the redshift of 0.73. Its equivalent width remained fixed to within experimental error. The optical polarization was also measured to be very large during the outburst.

Most of the energy we have measured from the flaring quasar is in the optical region from 3000-9000 A (90% of the total). The luminosity of 1156+295 on April 4, 1981, when we first observed it with IUE, was in excess of 10^{48} ergs/s, making it one of the most luminous objects in the sky.

References

Bregman, J.N., Glassgold, A.E., and Huggins, P.J. 1981, Ap.J., 249, 13.

Bregman, J.N., Glassgold, A.E., Huggins, P.J., et al. 1982, Ap.J., 253, 19.

Burstein, D., and Heiles, C. 1978, Ap.J., 225, 40.

Heiles, C. 1976, Ap.J., 204, 379.

Stockman, H. 1978, in Pittsburgh Conference on BL Lac Objects, Ed. A.M. Wolfe, p. 149.

Wills, B. et al. 1982, in preparation.

Table 1
IUE Observations of Quasar 1156+295 (4C 29.45, Ton 599)

Date (U.T.)		Image	Exposure (min)	B^1	B^2
10:54	4 4 81	L10283	60	14.0	13.7
12:03	4 4 81	S13653	180	14.0	13.7
9:52	4 8 81	S13679	120	14.6	14.5
11:50	4 8 81	L10312	60	14.6	14.5
6:33	6 5 81	L10785	105		15.6
8:23	6 5 81	L14191	327		15.6

1. J. Pollock, Univ. of Florida
2. IUE; estimated uncertainty of 0.2 mag.

Figure Captions

1. Composite UV spectra based on 50 A averages for 1156+295 on April 4, 8, and June 5, 1981, in sequence with April 4 at the top.
2. Optical to UV spectra for 1156+295 based on power law fits to the UV spectra in Fig. 1 and (a) IR photometry by C. Impey (solid points); (b) UBVRI photometry by W. Wisniewski; (c) B magnitudes by J. Pollock for April 4 and 8, 1981 (crosses); and spectrophotometry on April 4 by H. Jeske and H. Spinrad and on June 5 by J. Miller.

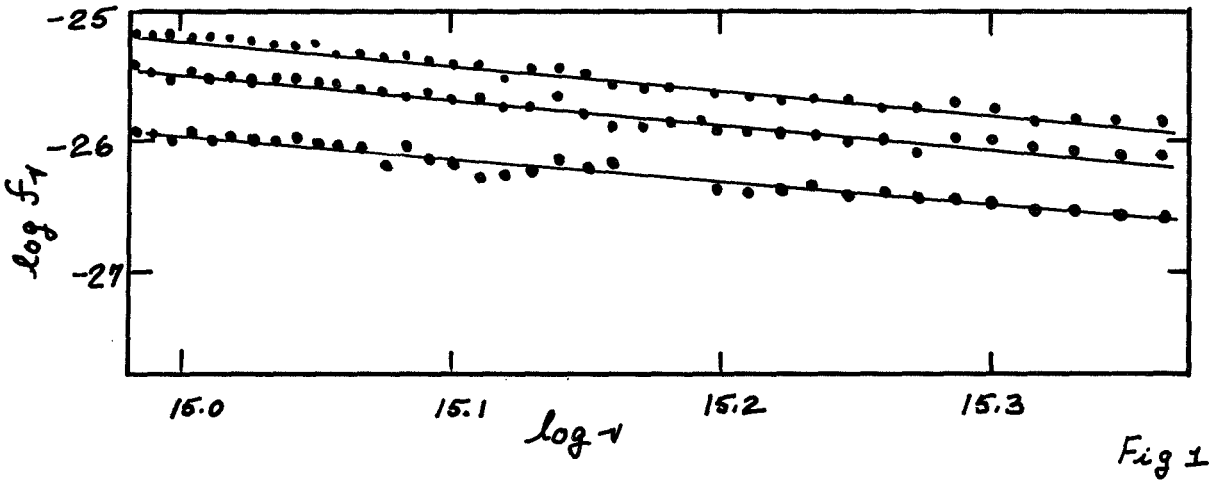
-25
-26
-27
log f_ν
15.0
15.1
15.2
15.3
log ν

Fig 1

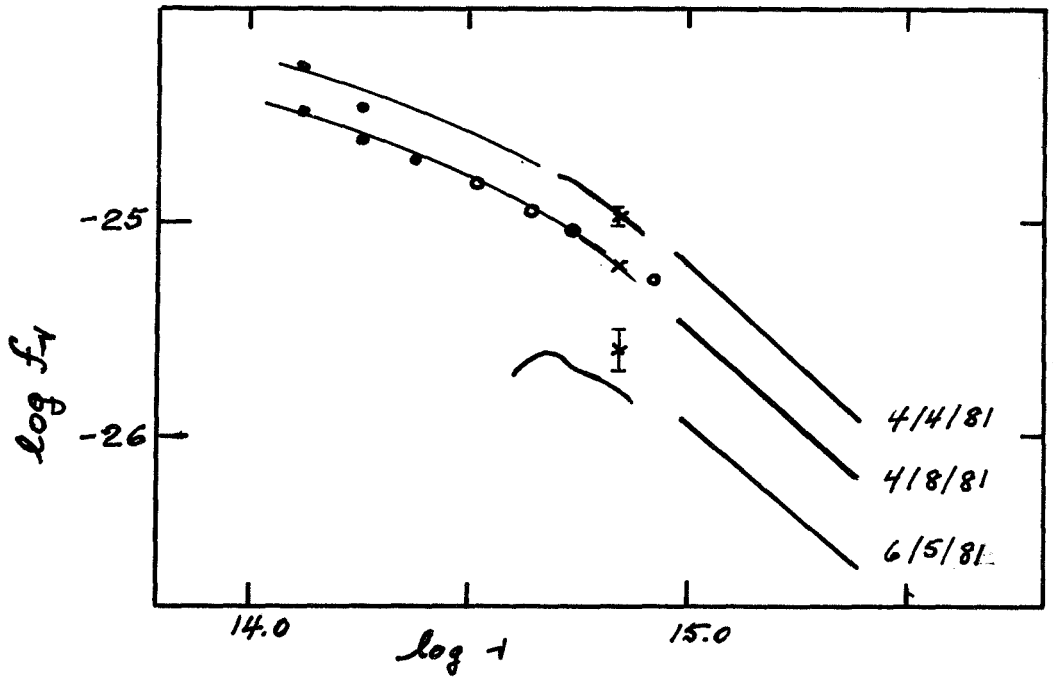
-25
-26
log f_ν
14.0
15.0
log ν
4/4/81
4/8/81
6/5/81

Fig 2

X-RAY AND UV SPECTRA OF TWO QUASARS:

PKS0637-75 and PKS1004+13 (4C13.41)

Martin Elvis and G. Fabbiano
Harvard-Smithsonian Center for Astrophysics

ABSTRACT

We observed the two quasars 4C13.41 (1004+13, V~15.2, z = 0.140) and PKS0637-75 (V = 15.75, z = 0.651) in December 1980 with IUE. Both were detected in the short wavelength region. 4C13.41 has the lowest L_x/L_{opt} measured in quasars. PKS0637-75 was observed quasi-simultaneously with the Einstein Observatory and a spectrum obtained with the IPC. The UV and soft X-ray spectra have been combined and are discussed together with the optical and infrared data for both objects.

INTRODUCTION

Only one decade of frequency separates the softest X-rays and the shortest wavelength UV seen by the Einstein and IUE satellites. This unobserved region is very important to our understanding of active galaxies and quasars since it is here that the bulk of the ionizing flux exists that produces the strong optical emission lines.

Towards the untimely end of the Einstein Observatory (Giacconi et al. 1979) mission we initiated a program of quasi-simultaneous X-ray and UV measurements of quasars to put the best possible constraints on this ionizing continuum. The quasars needed to be both optically bright and have a high X-ray count rate which limited the available targets. Two quasars were successfully observed with IUE and for one of them a nearly simultaneous X-ray spectrum was obtained. The results are reported here.

PKS0637-75

A radio-loud, flat spectrum, quasar at moderate redshift (Z = 0.651, Hunstead, Murdoch, and Shobbrook 1978) this object seemed a good candidate for simultaneous IUE and Einstein observations. It had an IPC count rate of 0.25 ct s^{-1} (Zamorani et al. 1981) and an accessible magnitude of V = 15.75 (Adam 1978).

Our IUE data (Table 1, Figure 1) show a clear continuum with no strong lines and no strong reduction shortwards of λ_{em} = 912 Å. A low line of sight covering factor is thus implied. When plotted together with the UBV data of Adam (1978) and J,K magnitudes of Hyland and Allen (1982) no discontinuities are seen (Figure 2). The IUE spectrum shows a downward curve greater than 0.5 at ν_{em} ~15.5. A similar down turn has been seen in a number of other quasars (Green et al. 1980) at ν_{em} ~15.4. If the optical continuum is synchrotron we may be seeing the turnover particle energy distribution.

The IPC spectrum shown in Figure 2 is a PROVISIONAL best fit at nominal gain (BAL = 14.0). The overall flux level is undoubtedly correct but the details of the slope and cut-off are not yet well determined. We expect this difficulty to be solved in the coming months. Clearly the addition of X-ray spectra will add a new dimension to quasar study. There are of order 20 quasars in the Einstein data base with sufficient counts to give a good spectrum eventually.

PKS1004+13 (4C13.41)

This nearby quasar ($z = 0.24$) is notable for having an optical to X-ray slope $\alpha_{ox} > 1.82$ (2500 Å–2 keV) which is the largest value of all the 107 quasars in Zamorani et al. (1981). A spectral break somewhere in the UV or extreme UV seems to be implied when the flatter optical slope is considered. We therefore obtained a short wavelength IUE spectrum in an attempt to constrain this break. We also report an improved X-ray upper limit.

Details of the Einstein and IUE observations are given in Table 2a,b. Problems with the Einstein spacecraft prevented us from obtaining simultaneous observations in this case. Fortunately PKS1004+13 is not a strong variable. The largest magnitude change observed has been ~0.8 (Pica et al. 1980). Also it is one of the objects regularly monitored by the University of Florida group and their photometry for the relevant dates is given in Table 2c (A. Smith, private communication). The IUE spectrum is shown in Figure 3. Although the signal to noise is low, continuum can be seen as can emission at Lyα. A possible emission feature is also seen at NV. Flux values for the continuum derived by summing the data into approximate 200 A wide bins are given in Table 2b.

We have plotted the infrared through soft X-ray spectrum of PKS1004+13 in Figure 4. The new IPC observation yields $\alpha_{ox} > 2.01$. Comparison with PKS0637-75 (Figure 2) shows how extremely low this L_x/L_{opt} ratio is. The steep slope and low fluxes of the IUE data suggest that the sought for break in the spectrum occurs in the UV. α(1250 Å–2 keV) has to be greater than 1.8. This can be compared with the power law slopes derived from the UBV colors of 0.42(U-B) and 0.15(B-V) and with the 0.3-2 μm slope of ~0.4 found by Neugebauer et al. (1979).

Malkan and Sargent (1982) have found, for a sample of 8 active galaxies and quasars, that a uniform underlying power law of slope 1.1±0.1 can be fit from 10 μm through to the UV when emission lines, including Balmer continuum emission, and a 20-30,000K black body are included. For PKS1004+13 a slope of 1.1 can also plausibly be drawn between the 10 μm (Neugebauer et al. 1979) and our 0.13 μm points. This would seem to imply a relatively weak 'blackbody' component in this object. Clearly a thorough analysis in these terms should be performed. A long wavelength IUE spectrum would help this analysis greatly. If a Malkan and Sargent-like slope is present then our 'detection' of a spectral break is artificial and the 1.1 slope must break to >1.8 between ~1250 Å and ~40 Å (0.3 keV).

We can use our Lyα flux to compare with the Hα and Hβ fluxes given by Baldwin (1975) and Neugebauer et al. (1979). The two Hβ fluxes agree well with each other (2.1 and 2.74 x 10^{43} erg s^{-1} respectively). We find Lyα/Hβ = 0.7 and Hα/Hβ =4.6. This is comparable to values seen for other, normal α_{ox}, active objects (e.g., MKN79, Wu, Boggess, and Gull 1980). These ratios are consistent with Case B values reddened by E(B-V) ~0.4. Although this should not be viewed as other than coincidental given the great bulk of evidence against such a situation in most quasars (e.g., Wu, Boggess, and Gull 1980; Puetter et al. 1981) a search for the λ2200 Å dust absorbtion feature would be valuable.

We wish to thank J. Patterson and G. Zamorani for assistance in making these observations, A.G. Smith for providing the optical photometry on PKS1004+13, and A. Boggess for making available two discretionary IUE shifts. This work was carried out under NASA Contract NAS8-30751.

References

Adam, G. 1978, Astr. and Astrophys. Suppl., 31, 151.
Baldwin, J.A. 1975, Ap.J., 201, 26.
Bolton, J.G., Kinman, T.D., and Wall, J.V. 1968, Ap.J., 154, L105.
Giacconi, R., et al. 1979, Ap.J., 230, 540.
Green, R.F., Pier, J.R., Schmidt, M., Estabrook, F.B., Lane, A.L., and Wahlquist, H.D. 1980, Ap.J., 239, 483.
Hunstead, R.W., Murdoch, H.S., and Shobbrock, R.R. 1978, MNRAS, 185, 149.
Hyland, A.R. and Allen, D.A. 1982, MNRAS, in press.
Malkan, M.A. and Sargent W.L.W. 1982, Ap.J., 254, 22.
Neugebauer,G., Oke,J.B., Becklin,E.E., and Mathews,K. 1979, Ap.J.,230, 79.
Pica, A.J., Pollock, J.T., Smith, A.G., Leacock, R.J., Edwards, P.L., and Scott, R.L. 1980, Astron.J., 85, 1442.
Puetter,R.C., Smith,H.E., Willner,S.P., and Pipher,J.L. 1981, Ap.J.,243, 345.
Wu, C-C., Boggess, A., and Gull, T.R. 1980, Ap.J., 242, 14.
Zamorani, G. et al. 1981, Ap.J., 245, 357.

Table 1

Observations of PKS0637-75

m_v = 15.75; Z = 0.651

(a) Einstein IPC

Date: 14 December 80
Seq.No.: 8494
Effective exposure: 6512 sec

(b) IUE

Date: 18 December 80
Image Seq.No.: SWP10832
Exposure: 416 min

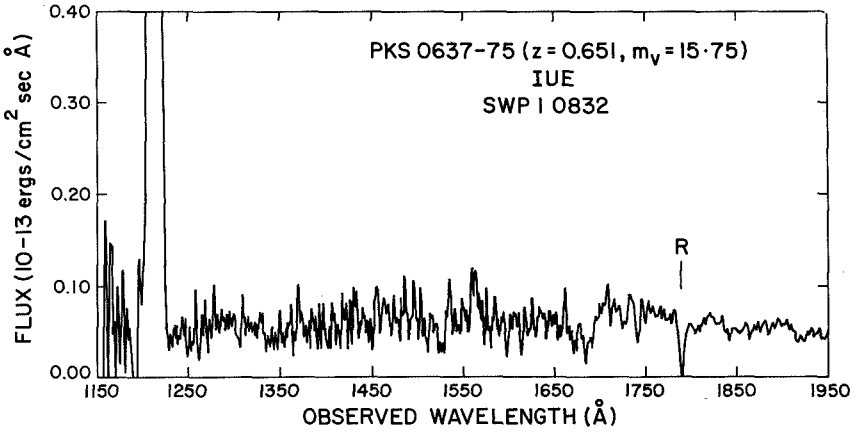

Figure 1: IUE SWP spectrum of PKS0637-75.

Table 2

Observations of PKS1004+13 (4C13.41)

M_V ~15, Z = 0.241

(a) Einstein IPC

Date: 9 May 1980
Seq.No.: 563
Effective exposure: 8366 sec
F_X <1.4 x 10^{-13} erg $cm^{-2}s^{-1}$
(3σ, 0.5-4.5 keV)

(b) IUE

Date: 22 December 1980
Image Seq.No.: SWP10850
Exposure: 32 min
F_ν(.129-.148μm) = 4.23 x 10^{-4} Jy
F_ν(.164-.184μm) = 6.5 x 10^{-4} Jy
α_{UV} = 1.8
F(Lyα) = 2.6 x 10^{-13} erg $cm^{-2}s^{-1}$

(c) Optical Photometry
(A. Smith, private communication)

Date	m_{pg}
6/7 May 80 (1)	14.93
10/11 May 80 (2)	14.49
11/12 May 80	14.80
5/6 Dec. 80 (3)	14.63

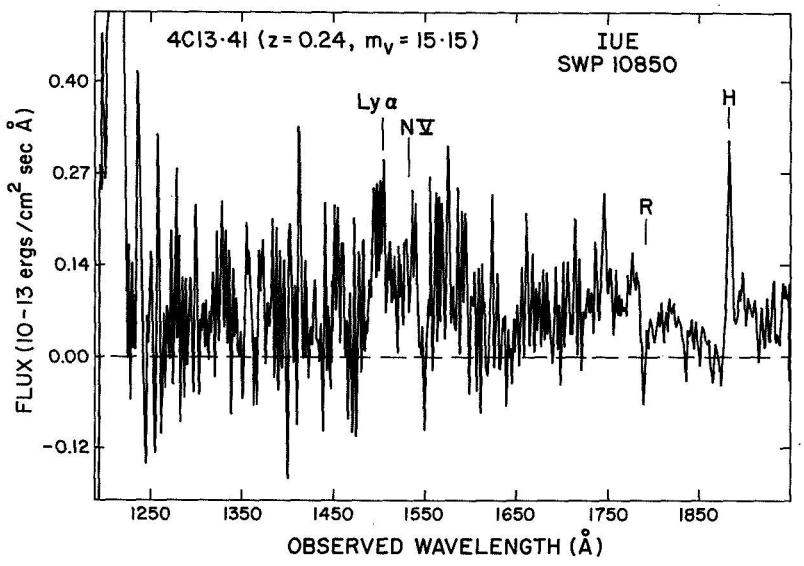

Figure 3: IUE SWP Spectrum of PKS1004+13.

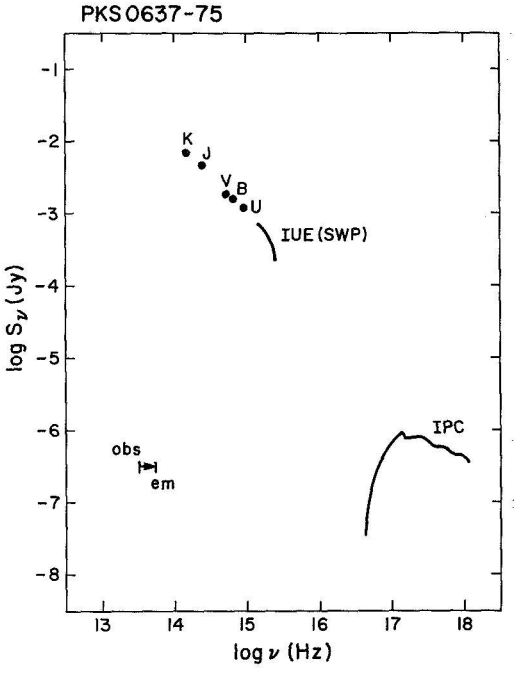

Figure 2: Infrared-Soft X-ray Spectrum of PK0637-75. The IPC spectrum is only PROVISIONAL.

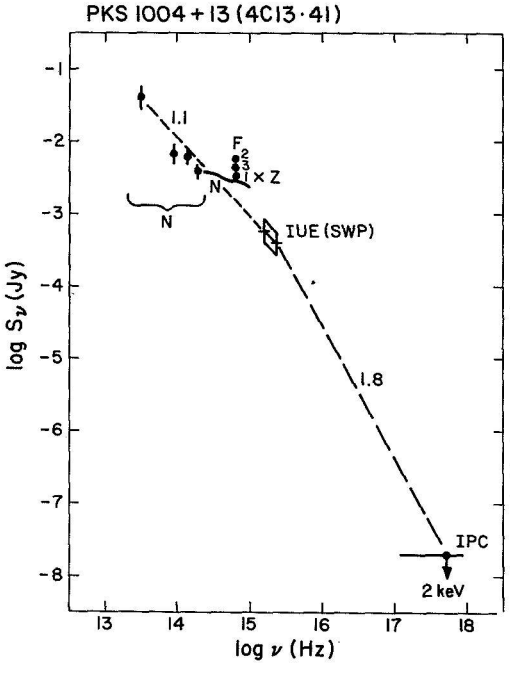

Figure 4: Infrared-soft X-ray spectrum of PKS1004+13. A nominal uncertainty of a factor 2 in the IUE fluxes is indicated by the parallelogram. The points 'F' '1,2,3' are the Florida photometry values corrected by -0.4 to give approximate B magnitudes. The numbers (1)-(3) refers to those in Table 2c. They indicate the range of the possible errors due to optical variability. The point 'Z' is the assumed 2500 Å flux density derived from the UBV photometry of Bolton, Kinman, and Wall (1968) by the standard procedure of Zamorani et al. (1981).

DISCUSSION - GALAXIES

Blades: Could the C IV and Si IV absorption lines that you find in the SWP spectrum be due to interstellar gas situated in our Galaxy or NGC 5204?

Fabbiano: (Reply unavailable.)

Helfer: Can you place any limits on interstellar absorption in the center region by looking at the depth of the 2200 Å feature?

Welch: I haven't examined this because of the high noise level in this portion of the LWR.

Rocca: Do you agree with the superior limit of star formation rate proposed recently by Deharveng et al.?

Welch: I can't say, since I haven't looked into the matter.

R. Hackney: I also believe that the absorption features at 1260, 1302, and 1335 Å are instrumental effects. We see them even in null spectra, i.e., exposures of blank fields. They are probably due to what has been called "fixed-pattern noise" in IUE spectral extractions. I'd be happy to show you the null-image plots.

Welch: Thanks. I'd be interested.

Carruthers: How can you distinguish between the explanation of the M31 spectrum as due to (a) metal-rich, young stars or (b) metal-poor, horizontal branch stars with interstellar absorption features? (The comparison galactic B2V and B7V star spectra seemed to have about the same strength of 1300 Å absorption as the M31 spectrum.) Have you made comparisons with interstellar extinction/interstellar line correlations for galactic stars?

Welch: Even without any correction for interstellar absorption, the equivalent width of the 1302 feature in M31 is a factor of 3 less than in mid-B stars near the sun. Despite the uncertainties due to low signal-to-noise, I think this is a significant difference; and I believe that it rules out young metal-rich stars. Corrections for interstellar absorption just make the case stronger. I'm not aware of an established correlation between visual absorption and the strength of interstellar

1302, and so have used typical values taken from the work of deBoer and Savage for the direction toward the Magellanic Clouds. They find that the interstellar absorption in this region is very patchy, and therefore this approach clearly has large uncertainties. Furthermore, there is the possibility of additional interstellar absorption within M31. As a result I really havae a very poor understanding of the size of the interstellar contribution to the 1302 feature. It is possible that most of the observed absorption is interstellar, in which case the stars in the nucleus must be extremely weak-lined.

Huchra: Can you rule out a burst of star formation with an age of 4 or 5 billion years (a la O'Connell) for the change in color near the nucleus?

Welch: I have not looked into that question. However, I would expect stars formed that recently to be relatively metal-rich. The weak-lined nature of the spectrum would then argue against this possibility.

Bregman: If you remove the instrumental feature at 1280 Å, do the absorption lines near 1280 Å still persist in the spectrum?

Welch: Although I have not tried it, I believe that the lines would be virtually unaffected. This is based on the narrowness of the feature in the unsmoothed spectrum.

Mushotsky: Does this object look like other "young" objects (such as Orion)? What is the lower limit on the temperature?

Huchra: Yes, this looks like "young" H II regions in nearby galaxies. Lower limit on electron temperature is ~22,000°K.

Aller: If this galaxy is very young, where did the S and O come from? You emphasized the low abundance of nitrogen as indicative of a small amount of element building. Yet O and S (which require some vigorous stellar element building) are present. If Mark. 36 is young, the material of which it is made must have involved some previous history of element building in massive stars, where products of the C-N cycle were not preserved.

Huchra: This is true; there are some metals but at levels like those in globular clusters. Whatever the case may be, the metallicity is so low that there could have been only a small amount of processing in the past. This object cannot have had star formation proceeding anywhere near the rate it is now.

Rocca: In your infrared models, did you include the metallicity effect?

Huchra: The models do not include the effect of metallicity on the stellar evolutionary track. Low metal stars will tend to produce few if any red supergiants and this is definitely part of the effect we see in Mk 36. A full set of models, including a stellar atmospheres calibration for low metal stars would be useful.

Blades: I would like to comment that on the basis of our knowledge of the interstellar medium of our Galaxy and the Magellanic clouds, I would have expected very strong C IV and Si IV absorption lines associated with the H II regions. It is surprising how weak these lines actually are - once you have accounted for the probable stellar contribution.

Benvenuti: Certainly the gas emission could be important. In the future we plan to use also spectra of extragalactic H II regions attempting to improve the fit and eventually estimate the amount of gas.

Aller: It would appear that the UV spectra of these objects are pretty well represented by stellar spectra. Can we assess the amount of gas present? Perhaps one could construct synthetic spectra of the galaxies (as you have done) using observed profiles of C III, C IV, etc., then from the amount of filling in of absorption line profiles, deduce the amount of gas involved.

Benvenuti: Certainly the gas emission could be important. In the future we plan to use also spectra of extragalactic H II regions attempting to improve the fit and eventually estimate the amount of gas.

Aller: Do you feel that you have enough data to construct fairly detailed models or do you need additional information?

Wamsteker: I think that with the UV, optical, and IR data we have obtained, we should be able to contruct fairly complete snapshots of the conditions in these nuclei. Of course if the size arguments for the black body can be applied, we are getting close to the size of the structures seen in the VLBI radio observations; we also hope to obtain similar simultaneous observations with EXOSAT when it starts operation.

Helfer: How good is the 30-50 km/s velocity dispersion?

Penston: Very good. However, data showed this morning indicated that Ca II shows 15 km/s structure.

Malkan: A lot of the 3100 Å flux in 4151 (possibly most of it) probably comes from Balmer continuum emission, which is strongly variable. So it is dangerous to just draw straight lines through this part of the spectrum. How would your conclusions change if you took the Balmer continuum emission into account?

Penston: I am very interested in what you say and obviously this must give us some problems. However, maybe this is not too disastrous. To some extent at least, the Balmer continuum emission may vary with the long wavelength source although as discussed in the paper there is considerable smearing in the response of, say, the Mg II region to the continuum.

Wamsteker: Do you have any optical data available, after so much IUE data, that would give support to the picture you present here? I feel very reluctant to have only the UV data which really have too low a resolution for a proper analysis.

Penston: Since the line profiles are seen not to be all the same, I am not convinced by what you say. However, the optical data since 1975-76 have shown that the HeI lines were broader than the Balmer lines and hinted that their widths were variable. Unfortunately, during the period of the data I presented today, we had not organized any optical spectroscopic back-up. However, our current program is supported in this way.

Mushotsky: The UV spectrum rolls over at ~400 Å and so the IR-UV continuum, while it may predict the X-ray, does not extend smoothly into the X-ray.

Malkan: Yes, there is a sharp high-frequency cut-off at wavelengths less than ~1000 Å, but it is due to the exponential drop in the 20-30,000°K thermal component. It is the infrared power-law, not the ultraviolet continuum, which is a good predictor of the X-rays. We do not yet know how far into the ultraviolet this power-law extends. IUE observations of high redshift quasars we are doing will tell us whether or not the power-law extends down to 400 Å (at this wavelength the thermal emission is negligible). But I agree with you that the power-law probably does not extend all the way to the X-rays, since they have a flatter slope. But the intimate relation between the IR power-law and the X-ray flux is the sort of thing you might expect if the X-rays were, for example, Comptonized infrared photons.

Penston: Before we push the analogy with NGC 1052 too far, can you tell us the line widths in 3C371, including the optical lines?

Worrall: From Lick Observatory work of J. Miller and colleagues, the 3C 371 H β line is weaker than in NGC 1052 and its flux is uncertain by ~50%. The H$_\alpha$ line is more poorly determined, since this lies on an atmospheric absorption band. I have not seen any published line widths. Clearly, these would be important measurements. The upper limit to velocity broadening in our IUE (low resolution) Lyα emission line measurements is not inconsistent with the value one might predict through analogy with NGC 1052.

Malkan: Is there any λ2175 absorption in OJ 287, and is it consistent with the expected foreground reddening?

Worrall: Yes, the values are consistent. Our non-detection of an absorption feature at 2175Å supports $A_V \leq 0.24$. We have derived and used $A_V = 0.06$, from the method of Burstein and Heiles. I think that the Sandage reddening law gives $A_V \simeq 0.12$

Worrall: I believe that Mk 501 does not show large radio variability, but how about Mk 180? Is there coverage over an extended frequency band, in particular, out to millimeter wavelengths? If so, what is known about correlated variations with frequency?

Hutter: Mk 501 does not show any large radio variability. Our observations show Mk 180 has varied by perhaps 50% or so from the mean flux density of the known archival measurements. The range of frequencies over which Mk 180 has been measured is not large; in particular, no 90GHz measurements have been made to the best of our knowledge. In the range of radio frequencies over which it has been observed (1-20 GHz) the spectrum is flat ($\alpha \approx 0$).

Felten: Your spectral calculation presumably requires a double integral over the distributions of relativistic particles and nonthermal photons. But it is not clear to me how many free parameters there are in the source model. Specifically, is it assumed that the fast-electron spectrum is the same at each point in the source, despite the fact that B is a function of position? Also, is your approach completely new, or is it based on some theoretical work already in the literature?

Hutter: With regard to the number of free parameters in the sources model, there are six in the case of Mk 180 and five in the case of Mk 501. The relativistic electron population at a given radius is a function of a quantity raised to the power of another quantity. The first quantity varies with position but the expression for the power is independent of position and is determined from the observed spectrum indices (see Konigl).

As indicated in our paper, the synchrotron spectrum was calculated by Konigl's (1981) relations. We do not, however, use the 8-function approximation in calculating the Compton spectrum, as did Konigl.

Helfer: To expand on that last question, does your beam model consider magnetic flux conservation?

Hutter: No, magnetic flux conservation is not specifically required in the model.

Helfer: In your table of abundances [X/H] are the figures for Si II, Fe II based on assuming these are the only ionic species present?

Blades: Yes, we have done some modeling and if corrections for other stages of ionization are made, we suspect these abundances will be nearly solar.

Mushotsky: What is the origin of the five velocity structures in C IV absorption lines?

Blades: Multiple absorption clouds in a single galaxy seem ruled out. Could be due to ejection and/or accretion as in model of Dyson et al.

Chanmugam: What is the electron density in your model?

Bregman: About 10^3 if you assume that the minimum energy electrons have an energy of thirty times their rest mass energy.

Worrall: Since BL Lac is at relatively low galactic latitude, did you measure 2170 Å absorption?

Bregman: No, but Richard and Karen Hackney have measured the 2200 Å feature in their very good spectra of BL Lac. They measured absorption that corresponds to $E(B-V) \cong 0.37$, which is consistent with what optical workers have measured.

Mushotzky: What lines were observed to determine He redshift and did their EW change with time?

Glassgold: MgII λ2798 and CIII] lines. Mg II very weak during outburst (~ 5 Å) but had been stronger in past. IUE did not detect Lyα or C IV lines.

Heckman: Could the anomalously low X-ray luminosity in 4C 13.41 be due to a large column of "cool" gas along the line of sight? One might expect a small minority of quasars to have cloud(s) from the broad line region in front of the continuum.

Elvis: True. To produce the factor 30 or so reduction over the expected IPC flux would need a fairly large column of 5-10 x 10^{22} atom cm^{-2}. However, in Seyfert galaxies such an absorbing column is usually accompanied by strong reddening. Since our (broad) $L\alpha$: $H\alpha$: $H\beta$ ratios allow only $E(B-V) \sim 0.4$ (even if case B is assumed), we should see an N_H of $\sim 3 \times 10^{21}$ atom cm^{-2}. Sometimes larger x-ray N_H's are found than the line ratios predict, but not by the factor 20 or so needed here.

COOL STARS

CHANGES IN THE UV SPECTRUM OF HD 4174

Robert E. Stencel
Joint Institute for Labortory Astrophysics, University of Colorado
and National Bureau of Standards, Boulder, CO 80309

ABSTRACT

The symbiotic-like object HD 4174 (EG And) exhibits the optical spectrum of an M2 giant star, but also shows Balmer and nebular line emission. The first UV spectrum showed an intense far UV emission line spectrum typical of many symbiotic stars. Smith has proposed a 470 day binary or pulsation period for this system, based on the changing strength and velocity of the Hα emission. I have examined three years of IUE data on this object and searched for trends correlated with his ephemeris. Preliminary indications are that the Hα and far UV continuum are eclipsed near phase 0.6 (at maximum Hα redshift), but that the correlation for the emission lines remains unclear and requires additional observations. These issues can be clarified with careful coverage of the next eclipse, predicted for 1982 December.

INTRODUCTION

The M2ep III star HD 4174 (EG And) has been discussed for decades in the literature because of its peculiar optical spectrum (Wilson 1950) and possible 3kG magnetic field (Babcock 1950; Slovak 1978). Photometric variations of 0.07 magnitudes were reported on a 40 day period (Jarzebowski 1964), but more recently, Smith (1980) has discussed spectroscopic Hα observations which indicate a pronounced 470 day period in changes of the equivalent width, profile, and velocity of the Hα emission, with the ephemeris:

$$\text{Phase (Max. H}\alpha\text{ E.W.)} = \text{J.D. } 2{,}443{,}200.5 + 470^{d}\ E.$$

In light of the possibility of this ephemeris representing a binary star orbital period, and considering that several single star models have been promoted for this object (see Smith 1980), the availability of UV data could provide a key test for these considerations. Further, if HD 4174 is a symbiotic binary system, its apparent brightness makes it one of the most accessible of its class for multiwavelength studies.

DATA

Combining observations obtained during 1981 under program ZADRS with archival data from 1978-1980, HD 4174 can be studied in parts of over three cycles of its 470 day period. Some of the early spectra were obtained by Jorge Sahade and Mark Slovak. Figure 1a shows the 1175-1425 Å segment of the low dispersion SWP spectrum of HD 4174, and illustrates a key result: at certain phases, the continuum (blackbody temperature in excess of 30,000 K before dereddening) essentially vanishes. It is simpler to comprehend this as an eclipse phenomenon rather than as an effect of stellar pulsation. This is plausible if one considers the changes in what appears to be Lyα absorption

Table 1

Ultraviolet Spectra of HD 4174 (EG And)

	SWP 3753L	SWP 5834L	SWP 9644L	SWP 14753L	SWP 15271L
Obs. Date	30.xii.78	19.vii.79	30.vii.80	14.viii.81	16.x.81
J.D.-2,440,000	3,873	4,074	4,451	4,831	4,894
Hα phase	0.43	0.85	0.66	0.47	0.60

Feature:		f_L	f_c	f_L	f_c	f_L	f_c	f_L	f_c	f_L	f_c
1240Å	N V	2.5[a]		1.2[a]		0.5[a]		---[a]		<.3[a]	
1250	Cont.		3.6[b]		4.0[b]		<.1[b]		4.5:[b]		<.1[b]
1350	Cont.		3.1		3.8		2.0		4.0		<.1
1400	Si IV & O IV]	6.2		5.5		7.7		15.5:[c]		7.2	
1450	Cont.		2.8		3.2		2.1		3.3		<.1
1485	N IV]	5.2		5.3		4.5		8.1		1.5	
1500	Cont.		2.8		2.9		1.9		3.0		<.1
1550	C IV	29:[c]		21:[c]		61:[c]		58:[c]		29:[c]	
1600	Cont.		2.2		2.1		1.6		2.3		<.1
1640	He II	2.5		5.7		3.9		5.8		<.5	
1663	O III	25.3		12.6		10.3		20:[c]		6.4	
1700	Cont.		2.0		1.6		1.1		1.7		<.1
1720	N IV]	0.5		2.8		0.5:		1.3		<.2	
1750	N III]	2.6		5.6		2.7		5.0		2.7	
1850	Cont.		1.9		1.4		1.0		1.6		<.1
1892	Si III]	2.5		5.1		1.5		3.9		2.1	
1909	C III]	7.3		10.3		5.5		10.7:[c]		6.9	
1950	Cont.		1.8		1.0		1.1		1.5		<.1

[a]Integrated line flux, in units of 10^{-12} ergs cm^{-2} sec^{-1}.

[b]Continuum monochromatic flux, in units of 10^{-13} ergs cm^{-2} sec^{-1} $Å^{-1}$.

[c]Saturated pixels.

strength between phases 0.47 and 0.85 in Fig. 1a, because this could be construed to be due to a larger absorption column through the red giant atmosphere as eclipse of the hot continuum source approaches.

The variations in continuum strength can be correlated with the Hα phase, as is shown in Fig. 1b. The difference between observations made at phases 0.60 and 0.66 is striking in this regard because while the 1250 Å continuum is depressed in both, the 1350 Å continuum is only depressed in the former (see Table 1). This can delimit the semi-duration of the continuum eclipse. Variations in the line emission strengths are roughly correlated with the Hα ephemeris, in the sense that near phases 0.60-0.66 the lines are generally fainter than at phases 0.47 and 0.85. However, the behavior at phase 0.43 (1978 observation) is at odds with this trend. This older observation may represent conditions at variance with the more recent spectra obtained one to two periods later. Thus, it is critical to monitor line changes in a synoptic manner, particularly during the eclipse intervals.

Profiles of the C IV lines obtained in a 360 minute exposure at phase 0.60 in 1981 show an interesting red asymmetry extending out to nearly 200 km s^{-1}. These particular data were obtained during minimum continuum level and also correspond to minimum Hα emission strength and maximum redshift of the Hα emission. Thus, we can speculate that material involved in the hot star in EG And is directed in a flow moving away from the center of mass of the binary, perhaps in a manner analogous to the accretion shock proposed for Zeta Aur by Chapman (1981).

INTERPRETATION

The data, although sparse in phase coverage, argue for eclipse phenomena in the symbiotic star HD 4174, and suggest a binarity may be the key to understanding its spectrum. The pattern of increasing absorption of the far UV continuum suggests that continuum eclipse duration is ±30-60 days, judging from spectra obtained 60 days apart (see Fig. 1a and Table 1). The Hα ephemeris predicts an eclipse for early December 1982, and on the basis of the ultraviolet spectra, it would be prudent to obtain spectra on a monthly basis starting in late summer 1982, in order to properly gauge the eclipse effects.

ACKNOWLEDGMENTS

I wish to thank NASA and the staff of the IUE observatory for assistance in obtaining these data.

REFERENCES

Babcock, H. 1950, P.A.S.P., 62, 277.
Chapman, R. 1981, Ap. J., 248, 103.
Jarzebowski, T. 1964, Acta Astron., 14, 77.
Slovak, M. 1978, B.A.A.S., 10, 609.
Smith, S. 1980, Ap. J., 237, 831.
Wilson, R. 1950, P.A.S.P., 62, 74.

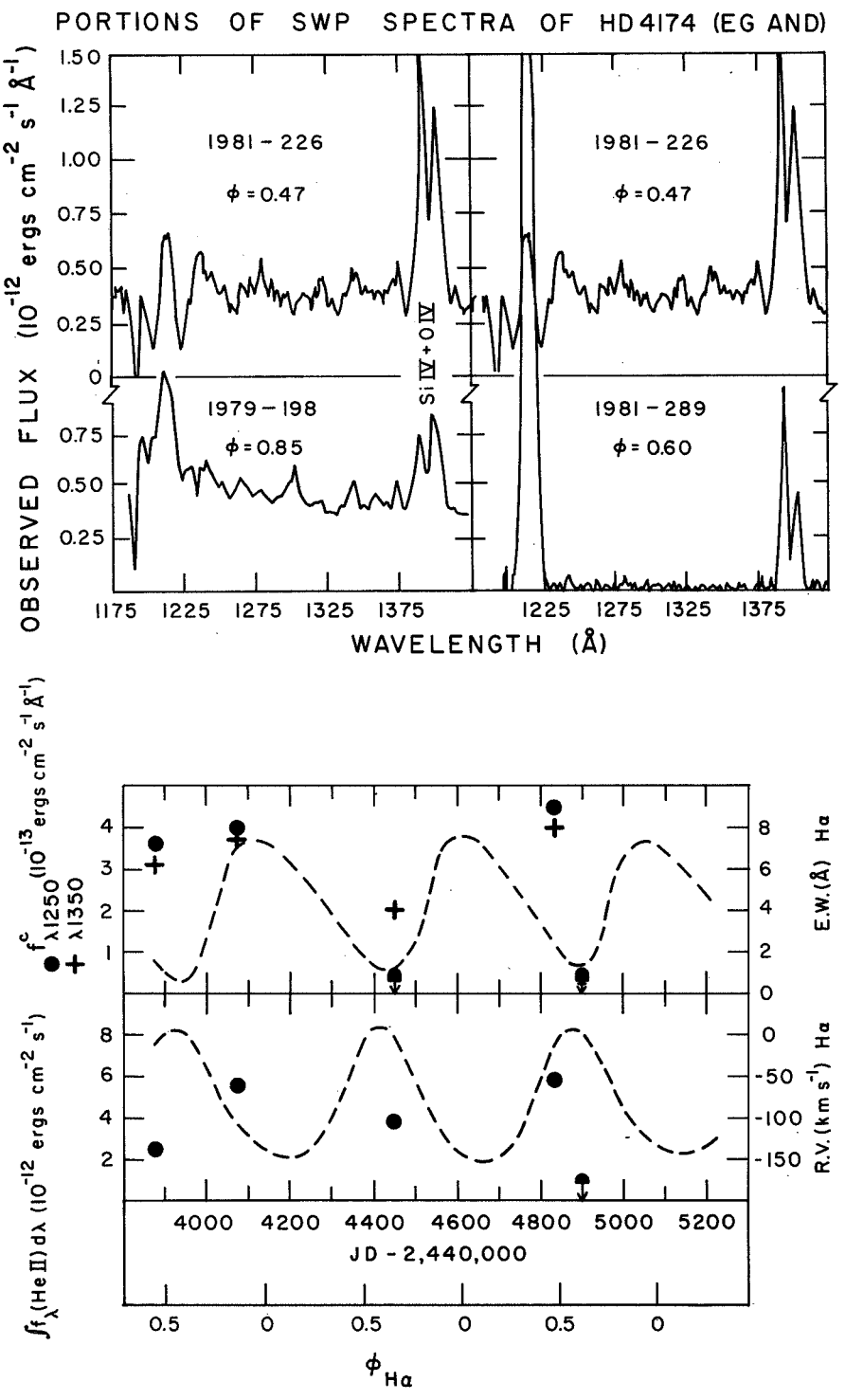

Fig. 1. Upper panel shows changes in the SWP spectrum; lower panel shows phase variations of continuum and line fluxes versus H-alpha variations (dashed lines).

ULTRAVIOLET SPECTRA OF HERBIG-HARO OBJECTS AND OF THE ENVIRONMENT OF THE COHEN-SCHWARTZ STAR

K. H. Böhm, E. Böhm-Vitense and J. A. Cardelli
Astronomy Department, University of Washington

ABSTRACT

Observations in both spectral regions have been used in order to determine the continuous energy distribution and the emission line fluxes for H-H 2. The continuous spectrum is similar to that in H-H 1 and F_λ increases rapidly towards shorter wavelengths. We find this statement qualitatively correct for all obvious choices of the ultraviolet extinction curve if we use the E(B-V) value determined by the use of the [S II] method. The origin of the continuum remains enigmatic.-The emission line spectrum of H-H 2 shows an even somewhat higher degree of ionization than the spectrum of H-H 1, indicating an even larger discrepancy between ionization information from optical data and that contained in the uv spectra.

The immediate environment of the Cohen-Schwartz star emits a continuous spectrum similar to that of a H-H-object but increasing even more steeply towards shorter wavelengths. If we accept Cohen's and Schwartz' E(B-V) value and use Seaton's extinction curve we get approximately $F_\lambda \alpha \lambda^{-10}$ for this continuum.

INTRODUCTION

Herbig-Haro (H-H) objects are small relatively dense nebulae which usually have rather high velocities and which seem to have been ejected from the immediate environment of certain T Tauri and Herbig Ae stars (Herbig and Jones 1981, Jones and Herbig 1982). The formation of the H-H emission line spectra in the optical range can be attributed to the recombination regions of shock waves (Schwartz 1975, Dopita 1978a,b, Raymond 1979). Other observational facts, however, could not yet be explained so convincingly. Some intriguing difficulties have become apparent especially through the study of the ultraviolet continua and emission lines of the brighter H-H objects with IUE.

The first ultraviolet spectra of the (visually) brightest H-H object H-H 1 (see Herbig's 1974 catalogue) were obtained by Ortolani and d'Odorico (1980) and by Böhm, Böhm-Vitense and Brugel (1981). The fact that this object could be detected with IUE using moderate integration times was a surprise since 1) it has a visual magnitude which is only slightly brighter than 16, and 2) it shows moderate reddening with E(B-V) = 0.47 (Brugel, Böhm and Mannery 1981b). The spectra showed a strong continuum and emission lines from surprisingly high ionization stages.

We have now obtained ultraviolet observations of two other H-H objects, namely H-H 2 and H-H 32. We have also determined the energy distribution of the ultraviolet radiation coming from the immediate environment of the Cohen-Schwartz (1979) star, the object from which H-H 1 and H-H 2 move radially away (Herbig and Jones 1981).

The following discussion will be restricted mostly to the ultraviolet spectrum of H-H 2 and the environment of the Cohen-Schwartz star and to a comparison of the H-H 2 and H-H 1 spectra.

OBSERVATIONS AND REDUCTIONS

We have obtained a total of 3 LWR and of 2 SWP spectra of H-H 2 between September 25, 1980 and April 27, 1981. Exposure times for the LWR spectra range from 150 to 380 minutes, those for the SWP spectra from 270 to 290 minutes. For the study of the environment of the Cohen-Schwartz star we have obtained one 300 minute SWP spectrum on April 28, 1982. The large aperture has been used for all our observations.

Obviously the energy distribution in the ultraviolet will depend on the extinction corrections which we apply. Consequently it is important to try out different assumptions about the extinction. We have always used E(B-V) = 0.34 for H-H 2H (Brugel, Böhm and Mannery 1981b) which follows from an application of the [S II] method (Miller 1968). We consider this determination as very reliable. As extinction curve A_λ for the ultraviolet λ-range we have used the following three different alternatives: 1) Seaton's (1979) extinction curve (which may be considered as an "average" galactic A_λ), 2) Seaton's extinction curve with the λ2200 feature removed (which may simulate the A_λ in some star-forming regions, cf. Snow and Seab 1980), 3) the θ Ori extinction curve as determined by Bohlin and Savage (1981). Qualitative properties which remain unchanged for all three extinction curves are of course of special interest.

The extinction correction for the radiation from the "environment" of the C-S star poses special problems since we cannot be certain that the extinction of the diffuse region emitting uv radiation and the C-S star is really the same. In fact the A_V found by Cohen and Schwartz (1979) for the C-S star is so high that an application of the corresponding extinction curve in the uv leads to somewhat implausible results for the observed diffuse radiation. We have consequently made an additional reduction for the C-S star environment with E(B-V) = 0.47 (as determined for H-H 1).

RESULTS

The observations of H-H 2 show apparently larger uv fluxes for this object than for H-H 1. This is understandable as a consequence of the somewhat lower reddening of H-H 2 (E(B-V)$\sim$.34 vs. .47 for H-H 1). After correction for reddening we obtain the averaged continuous energy distribution which is compared to that of H-H 1 in fiture 1. We see that (after the

reddening correction) the uv flux of H-H 2 is indeed somewhat smaller than the uv flux of H-H 1 in agreement with the properties in the optical range. In its relative distribution the continuous F_λ of H-H 2 is very similar to that of H-H 1. Both show a rather enigmatic steep rise towards shorter wavelengths which is a continuation of the trend of the (very faint) continuum in the optical range (see also Brugel, Böhm and Mannery 1981a). Figure 1 shows F_λ reddening corrected with Seaton's (1979) extinction curve with the λ2200 feature eliminated.

Using the Θ Orionis extinction curve (Bohlin and Savage 1981) instead we find qualitatively similar F_λ curves though F_λ now rises by "only" a factor of 4 from 3000Å to 1300Å (compared to a factor $\sim$12 for Seaton's curve.

The emission line fluxes in H-H 2 are also similar to those of H-H 1 except that they seem to indicate an even somewhat higher ionization. The fluxes of the four strongest lines C IV 1548/51, C III] 1909, C II] 2326 and Mg II 2796/2803 agree to within 15% (if measured with respect to Hβ in both cases) with those observed in H-H 1. On the other hand, Si IV 1394/1403 and N III] 1747/1754 seem to be definitely fainter in H-H 2 than in H-H 1. It is intriguing to note that [Ne V] 1575 is present in H-H 2 with moderate strength. This result makes even more obvious the large discrepancy with the optical spectrum which indicates e.g. a ratio of O II to O III particles of 0.48/0.06 and shows no indication of any ionization stage above O III. (Brugel, Böhm and Mannery 1981b).

Our observations of the environment of the Cohen-Schwartz star show a pure continuum which is similar to that of an H-H object but which seems to increase even more steeply towards shorter wavelengths. This is especially true if we assume that it has the same reddening as the C-S star itself for which Cohen and Schwartz (1979) give $E(B-V)\sim1.7$ and if we combine this with the Seaton (1979) extinction curve. In this case the continuum varies approximately like λ^{-10}. Even if we assume the same reddening as for H-H 1 we obtain a considerably steeper rise towards shorter wavelength than in H-H 1 and H-H 2.

REFERENCES

Bohlin, R. C. and Savage, B. D. 1981, Ap.J. 249, 109.
Böhm, K. H., Böhm-Vitense, E. and Brugel, E. W. 1981, Ap.J. (Lett.) 245, L113.
Brugel, E. W., Böhm, K. H. and Mannery, E. 1981a, Ap.J. 243, 847.
Brugel, E. W., Böhm, K. H. and Mannery, E. 1981b, Ap.J. Suppl. 47, 117.
Dopita, M. A. 1978a, Astr. Ap. 63, 237.
Dopita, M. A. 1978b, Ap.J. Suppl. 37, 117.
Herbig, G. H. 1974, Lick Obs. Bull., No. 658.
Herbig, G. H. and Jones, B. F. 1981, A.J. 86, 1232.
Jones, B. F. and Herbig, G. H. 1982, preprint.
Miller, J. S. 1968, Ap.J. (Lett.) 154, L57.
Ortolani, S. and D'Odorico, S. 1980, Astr. Ap. 83, L8.
Raymond, J. 1979, Ap.J. Suppl. 39, 1.
Schwartz, R. D. 1975, Ap.J. 195, 631.
Seaton, M. J. 1979, M.N.R.A.S. 187, 73p.
Snow, T. P. and Seab, C. G. 1980, Ap.J. (Lett.) 242, L83.

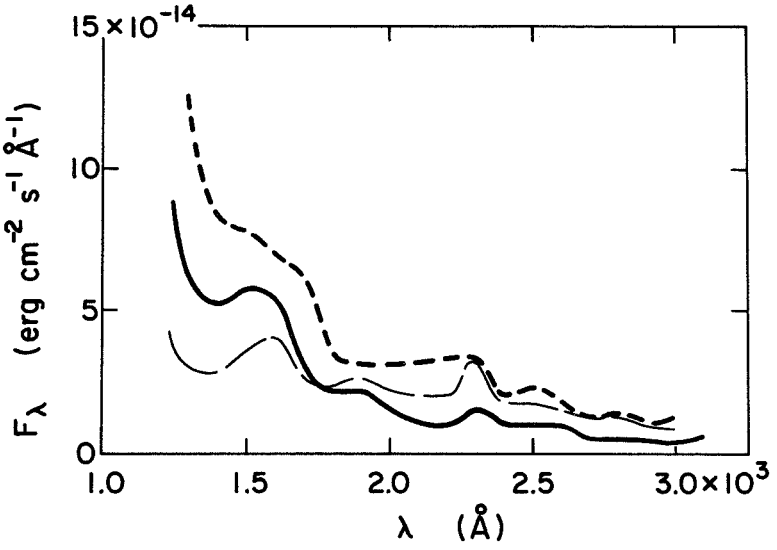

Figure 1. The continuous energy distribution in the range 1270Å$\lesssim\lambda\lesssim$3000Å for H-H 2 (solid curve), H-H 1 (short dashes) both reduced with Seaton's (1979) extinction curve. Also shown is the continuum for H-H 2 reduced with the Bohlin-Savage (1981) average θ Ori extinction curve (long dashes).

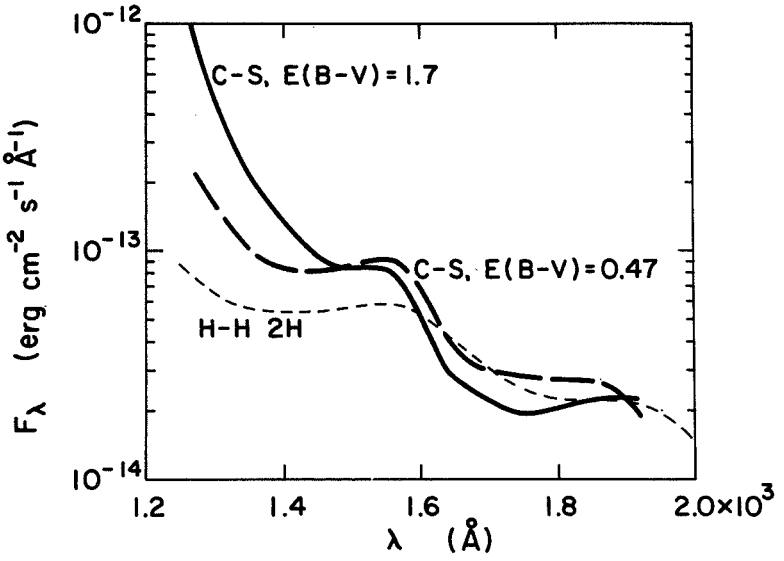

Figure 2. The continuous ultraviolet radiation from the environment of the Cohen-Schwartz star. Extinction corrections are based on the Seaton curve with an E(B-V) = 1.7 (see Cohen and Schwartz 1979, solid curve) and with an E(B-V) = 0.47 (which is the same as for H-H 1, Brugel, Böhm and Mannery 1981b, long dashes). The energy distribution for H-H 2H is shown for comparison. The curve for E(B-V) = 1.7 is shifted downward by 4 powers of ten in order to put it on the same diagram.

SYNOPTIC STUDIES OF CHROMOSPHERIC VARIABILITY IN F - K DWARFS WITH THE IUE

Kenneth L. Hallam
Laboratory for Astronomy and Solar Physics
NASA/Goddard Space Flight Center

Charles L. Wolff
Laboratory for Planetary Atmospheres
NASA/Goddard Space Flight Center

James R. Sewall
Applied Research Corporation

ABSTRACT

Time-sequential series of IUE spectra for ten F, G and K dwarfs were obtained in 1980 and 1981 to study the rotational dependence of chromospheric flux in the ultraviolet. An interactive computational method using unbiased estimators was developed to measure emission line fluxes free of arbitrary judjement concerning the behavior of the underlying spectrum and shapes of the line profiles. Due to the limited number of observational samples per star, we have used special techniques to analyze the sparsely and anharmonically sampled emission line flux data. Two different autocorrelation measures were computed for each emission line as a function of temporal frequency. Examples and results of this analysis now in progress are given for several stars.

INTRODUCTION

We are attempting to determine for several stars with the IUE how the rotationally modulated flux of various ionic emission lines differ in shape, amplitude and period. With sufficient IUE longevity, we also hope to determine the nature of their longer term changes, analogous to the 11-year solar cycle variations. In addition, these synoptic observations provide us with an abundance of data which can be examined in greater detail for evidence of other temporal changes in the spectra of the chromospheres of these stars, some of which may be relatable to the rotational period.

OBSERVATIONAL METHODS

Over the past two years, we have obtained one or two series of 6 to 12 SWP and LWR spectra for each of 9 F - K luminosity class V stars. The observing epochs were anharmonically spaced to reduce aliasing of the data in the periodic analysis. We optimized the low resolution SWP exposures for Ly α 1216 A. The LWR exposures were optimized for Mg II 2800 A, either in high resolution for stars G5 or earlier, or in low resolution for later types. A constant exposure time was maintained for each star and camera throughout the series to minimize errors due to uncertainties in the

calibration of the IUE system response.

For a given emission line and star, the integral flux was interactively measured using Interactive Data Language (IDL) procedures for all epochs in a precisely defined and repeatable manner. This method has now been applied in the reduction and analysis of all our 1980 and 1981 spectral data. Our goal is to establish internally consistent sets of unbiased flux estimates for each line and star. In the case of Lyα 1216Å, the spectra were reduced line-by-line in order to remove the geocoronal contribution.

FLUX VARIABILITY

All nine stars of our program are found to exhibit flux variability of about 10 percent in Mg II and several times more in Lyα. Final values for specific stars await further refining of our flux measurement and periodic analysis techniques. There is also an abundance of information concerning the behavior of the individual spectral line characteristics which we wish to examine in greater detail. For instance, in the case of the K2 V star ϵ Eri, the modulation depth in Mg II 2795Å calculated from the measured values alone is 0.09. But we find that the emission component of the observed line profile does not sensibly change over all 11 observational epochs, or ten rotational cycles, if based on the mean UV period of 12.2 days reported earlier (Hallam and Wolff 1981). Apparently all the flux variability is due to changes in the amount of the central absorption feature, which is sufficiently narrow not to affect the major portion of the emission component profile. This would seem to imply that all or most of the variability in the Mg II flux is occurring only in the upper gaseous layers contributing to that line.

PERIODIC ANALYSIS

According to reasonably simple functional model assumptions which we have discussed elsewhere (Hallam and Wolff 1981), a minimum of eight flux samples distributed over all phases are required to uniquely determine the modulation period for any emission line. In practice, we have found that even with as many as 12 samples, it is not always possible to arrive at an unambiguous solution for the period. We are now using even more samples per observational series for a given star and emission line. When data is available from more than one line for a given star, only those rotational periods in near-coincidence are allowable in common.

To illustrate our periodic analysis procedure, we have chosen our data set for the Mg II 2800Å doublet flux for the K5 V star 61 Cyg A. It consists of 10 LWR samples taken over a total span of 122 days. It is obvious from the flux verus time plot in Figure 1 that it is not easy to discern in this manner what the actual nature of the variability might be, due to the low density of points. It is necessary to replot the flux data as a function of phase for different trial periods in order to select those that are most consistent with a periodic interpretation. The sample span must cover a minimal time of 1-1/2 to 2 cycles to establish repetition.

The number of possible trial periods which must be examined depends upon the ratio of the total span to the shortest interval, and upon the number of samples. For our data sets, it may amount to several thousand. It is clear that some screening method to sort out the most likely candidates for detailed examination is required. We have found two auto-correlation procedures which have been extremely useful. The first was developed by Lafler and Kinman (1964) for a similar application to Cepheid variable data. For each trial rotational frequency, it calculates the rms dispersion from all neighboring-phase flux pairs. The minima of the resultant flux correlation spectrum occur for periods where the phase plots have maximum near-neighbor coherence. We have developed another auto-correlation function, which calculates the total length of all the point-to-point line segments of the phase plots for each rotational frequency. Unlike the Lafler-Kinman function, it also includes phase information, so that it is more sensitive to skewness in the shape of the trial variability function.

In Figure 2 we illustrate the auto-correlation spectra of the 61 Cyg A Mg II data for both of these functions. Greater correlation corresponds to smaller numerical values in each case, and the preferred values of rotational frequency are indicated by the upright arrows at 33.2 or 34.4 days. If the star's flux variation is under-sampled, then the auto-correlation spectra will produce multiple major minima indicating that several possible periods could fit the data. More data samples would then have been required to eliminate all but the actual period. The flux data are plotted as a function of phase for the 34.4 day solution in Figure 3. This period is consistent with that of 36.7 days found by Stimets and Giles (1980) from O. C. Wilson's Ca II H, K data obtained over a period of more than ten years total, and also with the 37 day Ca II H, K period found by Vaughan et al., 1980.

The error in the estimate for a period depends upon the stability of the chromosphere throughout the observational time span, and flux measurement errors. It is not possible to assess the former without a more extensive series of observations. We have developed only a limited amount of data ourselves by which to specifically determine measurement errors. Nevertheless, based on the few cases where we obtained redundant observations, on the behavior of our entire mass of data, and upon other IUE observational results, we believe the relative repeatability error of a single measurement is about a few percent.

REFERENCES

1. Hallam, K. L. and Wolff, C. L. 1981, Ap. J. 248, L73.

2. Lafler, J. and Kinman, T. D. 1964, Ap. J. Suppl. 11, 216.

3. Stimets, R. W. and Giles, R. H. 1980, Ap. J. (Letters) 242, L37.

4. Vaughan, A. H., et al. 1981, Ap. J. 250, 276.

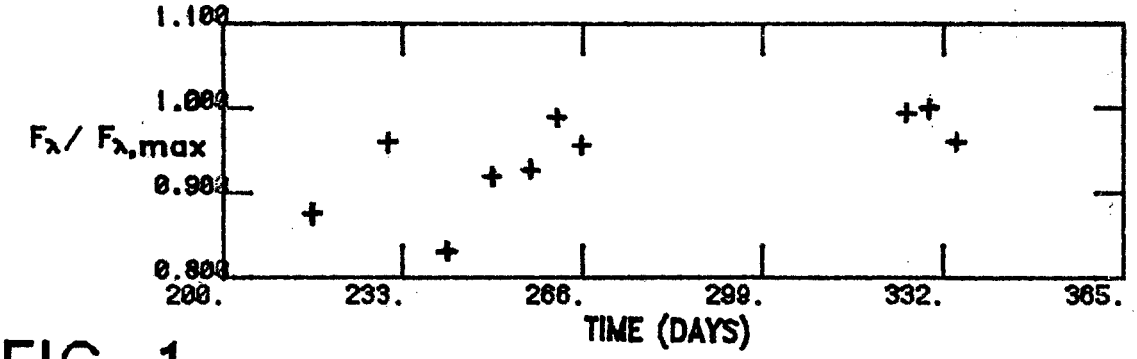

FIG. 1

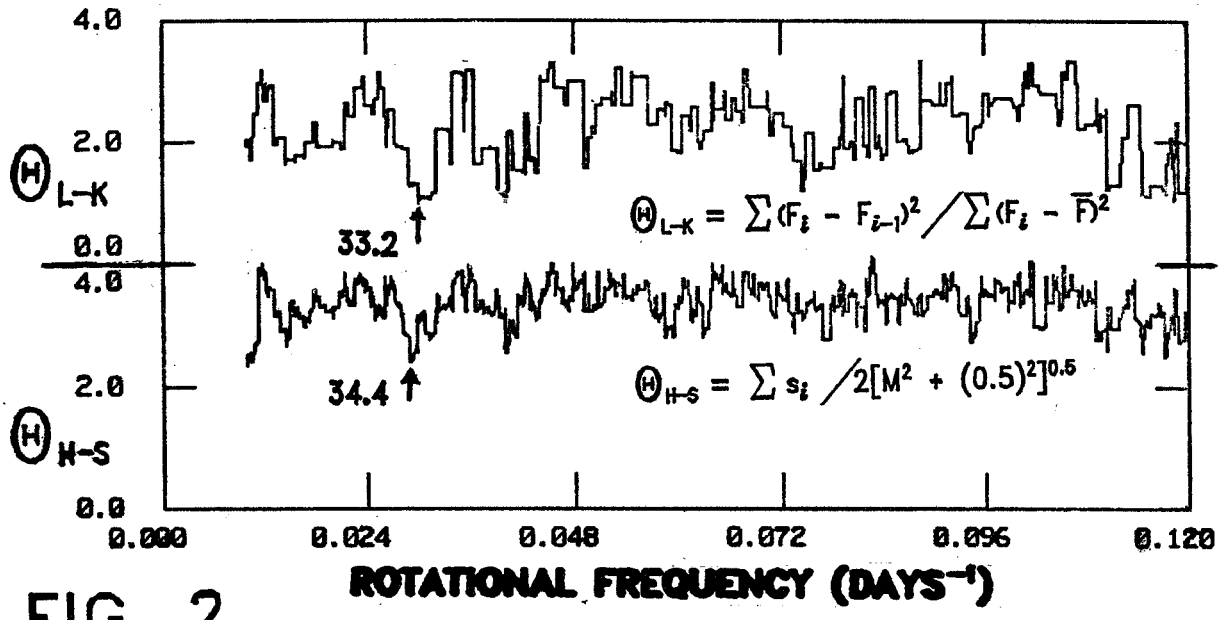

FIG. 2

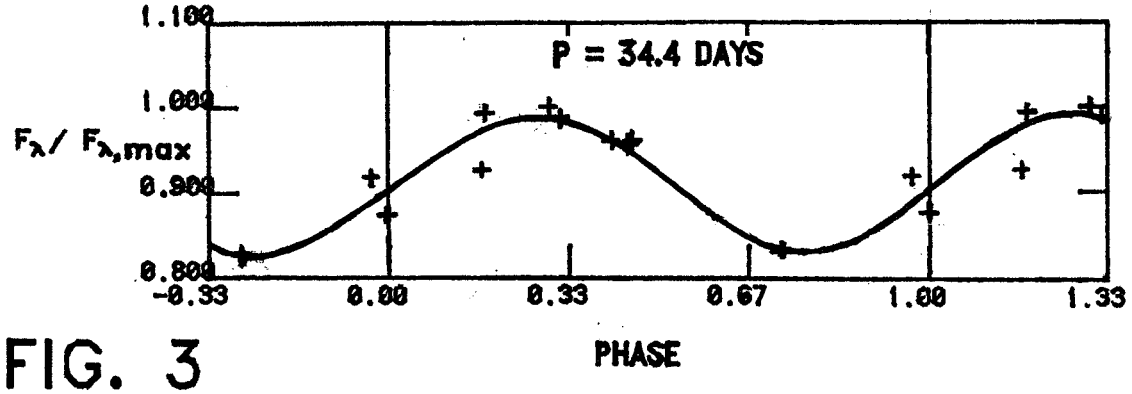

FIG. 3

CHROMOSPHERIC, TRANSITION LAYER AND CORONAL EMISSION OF METAL DEFICIENT STARS

Erika Böhm-Vitense
Astronomy Department, University of Washington

ABSTRACT

We show that while MgII k line emission decreases for metal deficient stars, the Lyα emission increases. The sum of chromospheric hydrogen and metallic emission appears to be independent of metal abundances. The total chromospheric energy loss is estimated to be $4 \cdot 10^{-5} \cdot F_{bol}$. The chromospheric energy input does not seem to decrease for increasing age if the age is larger than $\sim 2 \cdot 10^9$ years. The transition layer emission is reduced for metal deficient stars, but we cannot say whether the reduction is larger than can be explained by curve of growth effects only. Coronal X-ray emission was measured for 4 metal deficient stars. Within a 12 limit it could still be consistent with the emission of solar abundance stars.

INTRODUCTION

Earlier studies by Wilson (1970) and Skumanich (1972) had shown that the CaII K emission for stars in the Pleiades, Hyades and Ursa Major stream decreases with increasing age of the stars. Our studies of the MgII k (Böhm-Vitense 1982) and the Lyα emission (Böhm-Vitense and Wood 1982) also showed enhanced emission for Hyades stars and also for close binaries. In order to study the age dependence of chromospheric emission for much larger ages of the stars we have studied chromospheric emission for metal poor stars which are supposedly very old. We have to keep in mind that the reduced metal abundance in itself leads to a reduced emission due to curve of growth effects. In our previous study of the MgII k emission we found reduced chromospheric emission for metal deficient stars but we were unable to decide whether this was merely a curve of growth effect or whether it indicated reduced energy input into the chromospheres of these stars.

CHROMOSPHERIC ENERGY LOSS

If the chromospheric energy input were actually reduced then the total radiative losses due to H, H^- and metallic line and continua emission should be reduced. We have therefore in collaboration with Jack Woods attempted to determine Lyα emission fluxes from low resolution short wavelength spectra. The measured fluxes were corrected for the geocoronal contribution and for stellar continuum and scattered radiation. We estimated that the measured fluxes should be multiplied by roughly a factor of 2 for all stars in order to correct for the effects of interstellar Lyα absorption. Since the column densities $N(H) \cdot \ell$ appear to be nearly the same for stars with distances d between 3 and 50 pc (Bruhweiler and Kondo 1982) the correction should be nearly the same for all our stars.

In Figure 1 we show the Lyα emission line fluxes divided by the bolometric fluxes f_{bol} for all non-Hyades and non-binary stars (except for the metal deficient binaries δ Tri, ζ Her and perhaps γ Ser) as a function of metal abundances. We see that the Lyα fluxes increase with decreasing metal abundances. Presumably the chromospheric structure changes in such a way that the energy loss which cannot be accommodated any more by metallic line emission will now be made up for by additional radiation in the Lyman lines and the hydrogen and H^- continua. If the total hydrogen related energy loss can be estimated to be 4 times the measured Lyα flux (twice the stellar Lyα flux) plus 4 times the MgII k line flux (MgII k + h, CaII K+H) then the sum of the Lyα flux and the MgII k line flux should show the dependence of the total chromospheric energy loss on the metal abundance and therefore on age for old stars. Figure 2 shows that the sum of these fluxes divided by the bolometric flux is independent of metal abundance and therefore presumably of age. For stars older than about $2 \cdot 10^9$ years the chromospheric energy input appears to be independent of metal abundance and therefore presumably age and comes out to be roughly $4 \cdot 10^{-5} \cdot F_{bol} = 4 \cdot 10^{-5} \cdot \sigma T_{eff}^4$.

TRANSITION LAYER ENERGY LOSS

Does this also apply to the transition layer and corona emission for which the heating mechanism may be more dependent on the magnetic field? We have measured the emission line fluxes in the OI, CII, CIV and SiIV emission lines for stars with different metal abundances.

The OI line emission is independent of B-V and metal abundances.

For the SiIV lines at 1400Å we do not find any systematic dependence of line intensities on metal abundances. These lines may be a blend of several lines of different elements, however.

Figure 3 shows the results for the CII and CIV lines. The bottom figures show the "standard" dependence on B-V as determined from the four slowly rotating, single, solar abundance stars. The top figures show the reduction factors with respect to this standard relation as a function of metal abundances. δ Tri, a metal deficient, short period binary always shows enhanced emission, while γ Pav shows overly reduced emission as observed already for the MgII k line, so does β Hyi, a peculiar star who shows variable chromospheric emission. Luminosity class IV stars also show reduced ratios of emission line intensities to bolometric luminosity L_{bol} due to their larger L_{bol}. Apart from these exceptions we find no reduction of emission line intensities in excess of what is to be expected from the reduced abundances, at least for reductions by less than a factor of 10. For larger reductions our upper limits are too high to permit definite conclusions, however the star HR 3578 shows normal CII emission on both of our images. For these metal poor stars the observational limit was actually set by the continuum radiation which is higher for the metal deficient stars. The upper limits given may be somewhat too large since they were estimated from the fluctuations observed in the continuum, which are probably mainly due to absorption lines in the stellar continuum.

CORONAL EMISSION

If coronal X-ray emission is mainly due to free-free transitions it should for equal T and n_e be independent of metal abundances. The Einstein Observatory observed 4 metal deficient stars for us, the giant HD 122563

(log $Z/Z_\odot$ = -2.5), and the dwarfs HD 140283 (log $Z/Z_\odot$ = -2.3), HR 3578 (log $Z/Z_\odot$ = -1.1) and 72 Her (log $Z/Z_\odot$ = -0.3). Charles Proffitt collaborated with the reductions. The three stars with large deficiencies actually gave negative counts after background subtraction. This prevails at the 1σ level if we combine the measurements for the three stars. At the 2σ level the upper limits fall within the measured fluxes for solar metal abundance stars. Since astronomers at the Einstein Observatory estimate the uncertainty to be larger than 3σ we feel we cannot draw any firm conclusions unless we could find a way to reduce the error limits, though we suspect that metal poor stars are weak or zero X-ray emitters.

REFERENCES

Böhm-Vitense, E. 1982, Ap.J. in press.
Böhm-Vitense, E. and Woods, J. 1982, Ap.J. submitted for publication.
Bruhweiler, F., and Kondo, Y. 1982, preprint.
Skumanich, A. 1972, Ap.J. 171, 565.
Wilson, R. 1970, Ap.J. 160, 225.

FIGURES

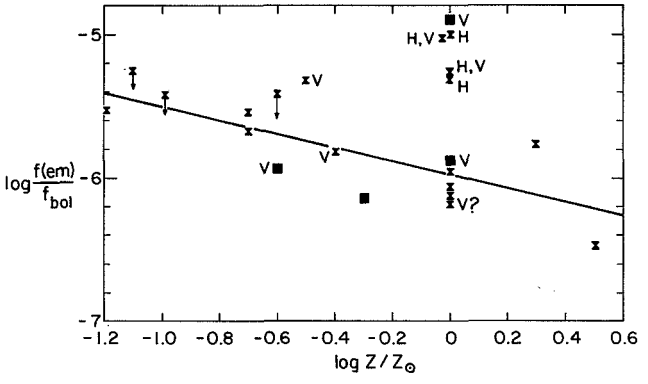

Figure 1. The observed Lyα emission line fluxes divided by the bolometric fluxes f_{bol} as a function of metal abundance. The different symbols indicate different luminosity classes. The V or V? indicate stars with variable or possibly variable radial velocity. H indicates Hyades stars. The short period binary δ Tri shows enhanced emission. The straight line gives the least squares fit to the points without the stars with a V or V? or H.

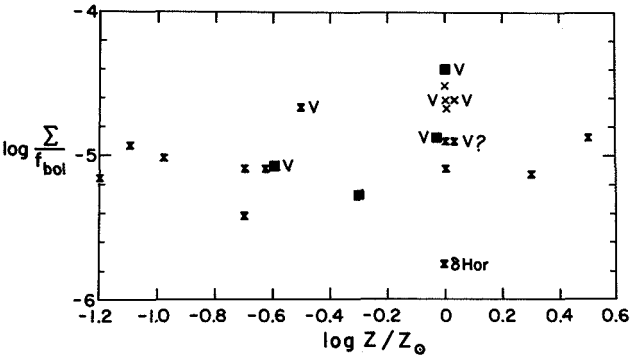

Figure 2. The sum of the measured Lyα flux (uncorrected for interstellar absorption and MgII k line emission) divided by the bolometric flux f_{bol} as a function of metal abundance in the stars. The chromospheric energy loss is estimated to be 4 times this sum. It appears to be independent of metal abundance and therefore presumably independent of age for these old stars.

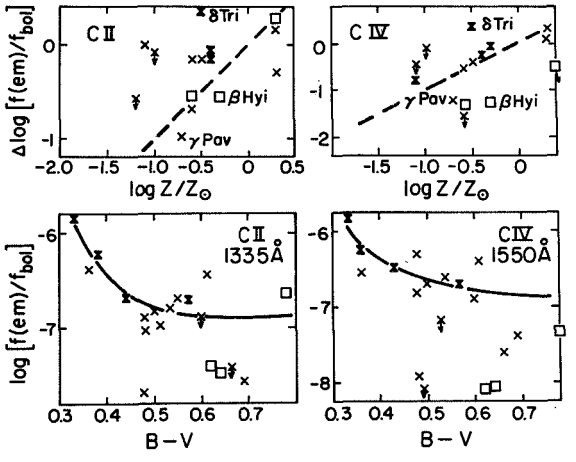

Figure 3. The CII and CIV line-emission divided by the bolometric flux f_{bol} for stars with different metal abundances. Filled symbols indicate stars with variable radial velocities. X, ⧗ luminosity class V stars, □ , ■ luminosity class IV. Downward arrows indicate upper limits. The transition layer emission is reduced for metal deficient stars, but the upper limits for the emission line fluxes in very metal poor stars are too high to decide whether the reduction is larger than expected from curve of growth effects due to the reduction of available metallic ions.

"DISCREPANT ASYMMETRY" STARS: THE ROLE OF UNSTEADY MAGNETIC FLUX LOOPS IN THE ATMOSPHERES OF LATE-TYPE GIANT STARS

D. J. Mullan
Bartol Research Foundation, University of Delaware

R. E. Stencel
J.I.L.A., University of Colorado

ABSTRACT

We draw attention to a number of spectroscopic peculiarities of K giants and other stars which lie in a "wedge" in the HR diagram. These peculiarities can be understood in terms of unsteady magnetic flux loops emerging into the stellar atmosphere from beneath the surface.

INTRODUCTION

We have surveyed mass loss in cool giants using IUE profiles of Mg II h and k emission. As a mass loss signature, we use S/L (= intensity ratio of shortward/longward emission peaks; see Stencel and Mullan, 1980 (SM)). We have identified a boundary (labelled Mg in Fig. 1) above which S/L becomes less than unity, implying rapid mass loss. Previously, Stencel (1978), using CaII K emission, discovered a similar boundary, but in a different position (Ca in Fig. 1). Stars which lie either below the Mg boundary or above the Ca boundary agree in the sense of their S/L asymmetries, both being either <1 or >1. However in the "wedge" between the Mg and Ca boundaries, Mg shows mass loss (S/L <1) while Ca does not (S/L>1). We call these "discrepant asymmetry stars" (Fig. 2). Among ∿100 cool giants, none shows the discrepancy in the opposite sense (i.e. S/L <1 in Ca, but >1 in Mg). High resolution solar studies also show no features where S/L >1 in Mg and S/L <1 in Ca (Bonnet, 1981).

PROPERTIES OF STARS IN THE "DISCREPANT ASYMMETRY WEDGE"

(i) Weak X-ray and TR emission. Along the left-hand edge of the "wedge", both transition region (TR) lines and X-rays become weak (Simon et al., 1982; Ayres et al., 1981) (see Fig. 1). However, chromospheric emission intensity does not vary sensibly across this boundary (Mullan and Stencel, 1982 (MS)).

(ii) "Hybrid" stars. A few exceptions to the general properties in (i) exist, the so-called "hybrid" stars (Hartmann et al., 1980; Reimers, 1981). If these are single stars, then the boundaries in Fig. 1 may not be perfectly sharp. In some hybrids, TR line intensities may vary. At least two hybrids (θ Her and ι Aur) have undergone several discrete mass loss episodes in ∿10 years (Zirin, 1982). There is not one-to-one correspondence between hybrid and discrepant asymmetry stars: Arcturus, the archetypal discrepant asymmetry star, is not a hybrid.

(iii) Variable Mg and Ca profiles. Variability is a prominent feature of stars in the wedge (Reimers, 1977; MS). In some "wedge" stars, Mg emission flux can vary at levels of 10^{31} erg/s on time scales of 10^{6-8} s. Variable mass loss rates appear as varying S/L values, and as variations in strength and velocity of circumstellar (CS) lines ($v \sim$ 10-100 km/s).

(iv) Behavior of He I 10830 Å line. In the wedge, the 10830 line is strong and variable (O'Brien, 1980; Zirin, 1982). Among G-M giants, the line strength and variability are greatest at K3 (Zirin, 1982). Coronal X-rays can be important for 10830 excitation (Zirin, 1975). This makes excitation in cool non-coronal giants puzzling (Simon et al., 1982). Emission in 10830 requires a CS shell. Among G stars, 10830 strength (i.e. coronal emission measure) correlates with Ca K emission strength (i.e. chromospheric) (Zirin, 1982): this is consistent with solar data. However, in K stars, the correlation between Ca K strength and 10830 strength breaks down. Zirin (1982) interprets this to mean that although active regions may be prominent on a star's surface, the star "cannot keep the corona from flying away in the stellar wind".

(v) Extended chromospheres and coronae. Stars in the wedge appear to have extended chromospheres (Stencel, 1982). A single example which suggests similar coronal behavior may be AR Lac: the corona is compact around the G star but extended around the K star (Walter et al., 1981).

(vi) C-13 enrichment. Stellar atmospheres apparently become enriched in the C-13 isotope when stars evolve across the Mg boundary (Fig. 1). In the stars studied by Lambert and Ries (1981) for C-13 content, 18 overlap with the SM data. Of 11 stars with normal C-13, we find 9 with S/L >1, while of 7 stars with high C-13 we find 5 with S/L < 1, and 2 with S/L $\gtrsim$ 1.

(vii) Large macroturbulence. Photospheric macroturbulence becomes large rather abruptly among K giants brighter than $M_V \gtrsim -1$ (Smith and Dominy, 1979), i.e. for K giants in the wedge. Chromospheric macroturbulence may also be large in stars in the wedge (e.g. Mullan and Cram, 1982).

THE ROLE OF UNSTEADY MAGNETIC FLUX LOOPS IN COOL GIANTS

In the solar atmosphere, helmet streamers are features with closed field lines near the base, and open field lines surrounding them. These cannot exist in static equilibrium if thermal pressure becomes too high (Pneuman, 1968), or if gravity becomes too weak. To find where in the HR diagram static equilibrium is possible, a semi-empirical technique has been used (Mullan, 1982). It is found that static helmet streamers exist only below a boundary in the HR diagram which coincides with the Mg boundary (Fig. 1). Hence, in solar-like stars, closed static flux loops can exist in the atmosphere, showing good correlation between chromospheric and coronal emission, and the closed loops will impede mass loss. However, above the boundary, magnetic flux loops emerging into the atmosphere from beneath the surface of the star may not be able to find static equilibrium. If that happens, we expect that as soon as the loop appears in the atmosphere, it will be in a phase of dynamical evolution. The ultimate evolution of a dynamically evolving loop in a cool giant atmosphere has so far not been solved in detail. However, rapid upward distension is expected to occur (Low, 1981). Reconnection near the base of a greatly distended loop may serve to eject material from the star (Mullan, 1981). In such stars, mass loss would contain a pronounced episodic component, individual episodes corresponding to emergence of individual flux loops into the atmosphere from below, and there would be no analogs of the "building blocks" (i.e. long-lived closed loops) which characterize the solar corona. As a result, coronal and chromospheric emissions need not be closely coupled (see (iv) above).

We suggest that the properties of stars in the "wedge" can be understood in terms of magnetic loops changing from steady and closed in solar-like stars to unsteady (and eventually open) in non-solar-like stars. As regards (i), disappearance of closed loops allows mass loss to become rapid, but also removes the major sources of steady X-rays (the "building blocks"). This is relevant in connection with a problem raised by Castor (1981), viz. closed field regions need to become cool just when the stellar wind becomes strong.

As regards (ii), discrete mass loss episodes can be understood, provided that individual magnetic loops disconnect from the star as a well-defined "event". If the event involves reconnection, the energy released in the reconnection is expected to create transient hot material in stars with rapid mass loss, thereby accounting for highly variable TR emission in hybrids. Reconnection also alters the chemical composition (Mullan and Levine, 1981): Mg can be enriched relative to Ca, and so Mg line profiles may be formed farther out in the wind than Ca, thereby making the mass loss signature more pronounced in Mg than in Ca. Transient X-ray emission from reconnection will cause 10830 excitation to be highly variable: the greater the magnetic activity, the more X-ray flux, and the stronger 10830 will be (see (iv)).

Unsteady distended loops are clearly relevant for (v), and their motions are relevant for (vii). As for (vi), unstable loops emerging from deep within a cool giant provide an efficient dredge-up mechanism for processed material, including C-13. Isotopic enhancement is seen as one further piece of evidence that the atmospheres of cool giants are in a state of continual magnetic upheaval.

REFERENCES

Ayres, T. R., et al., 1981, Ap. J. 247 545.
Bonnet, R. M., 1981, Space Sci. Rev. 29, 131.
Castor, J., in "Physical Processes in Red Giants", p. 295.
Hartman, L., et al., 1980, Ap. J. 236, L143.
Lambert D. L. and Ries, L. M. 1981, Ap. J. 248, 228.
Low, B. C., 1981, Ap. J. 251, 352.
Mullan, D. J., 1981, in "Physical Processes in Red Giants", p. 355.
Mullan, D. J., and Levine, R. H., 1981, Ap. J. Suppl. 47, 87.
Mullan, D. J., 1982, Astron. and Ap. (in press).
Mullan, D. J. and Cram, L. E., 1982, Astron. and Ap. (in press).
Mullan, D. J. and Stencel, R. E., 1982, Ap. J. 252 (in press). (MS)
O'Brien, G., 1980, thesis, Univ. of Texas, Austin.
Pneuman, G. W., 1968, Solar Phys. 3, 578.
Reimers, D., 1981, in "Physical Processes in Red Giants", p. 269.
Reimers, D., 1977, Astron. and Ap. 57, 295.
Simon, T., Linsky, J. L. and Stencel, R. E., 1982, Ap. J. (in press).
Smith, M. A. and Dominy, J. F., 1979, Ap. J. 231, 477.
Stencel, R. E., 1978, Ap. J. 223, L37.
Stencel, R. E. and Mullan, D. J., 1980, Ap. J. 238, 221; ibid. 240, 718.(SM)
Stencel, R. E., 1982, SAO Spec. Rep. (in press).
Walter, F. M., Gibson, D. and Basri, G., 1981, Bull. AAS 13, 833.
Zirin, H., 1975, Ap. J., 199, L163.
Zirin, H. 1982, Big Bear Solar Observ. Preprint #0207.

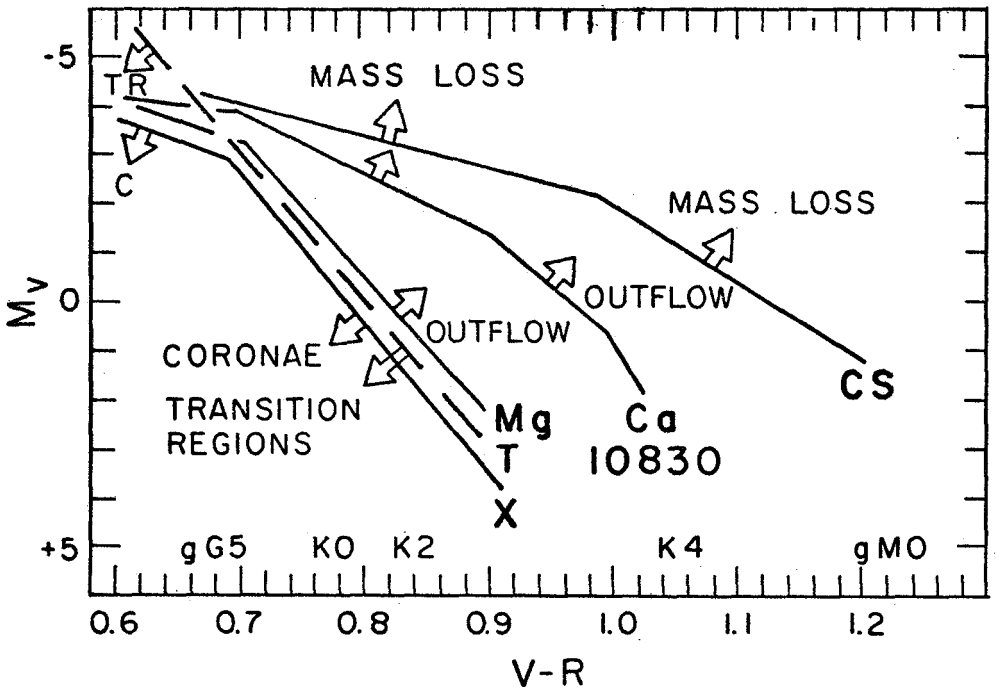

Fig. 1. Boundary lines in the HR diagram

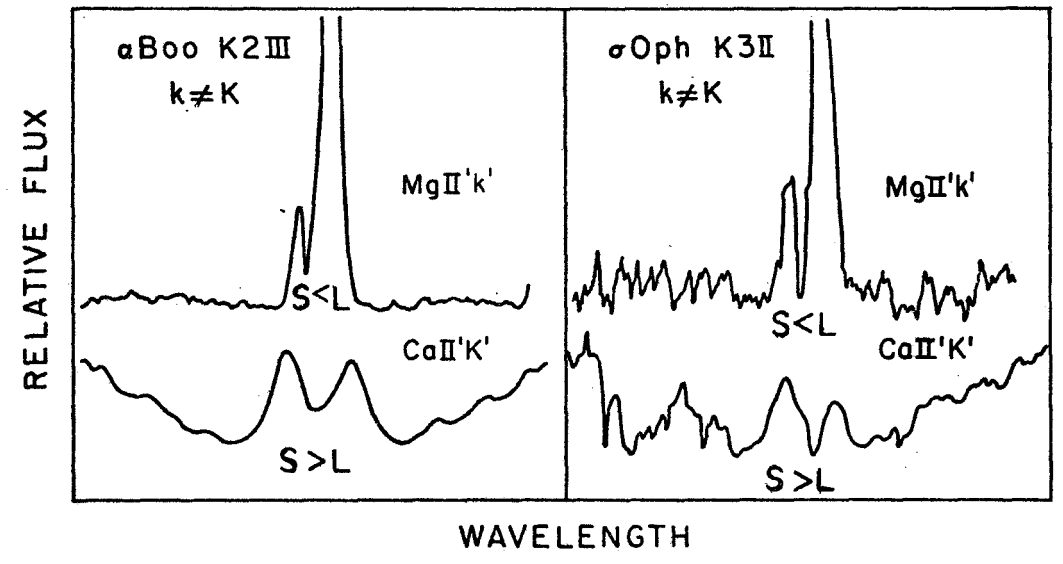

Fig. 2 Examples of discrepant asymmetries

ACKNOWLEDGEMENT This work was supported in part by NASA Grants NAGW-5 and NAS5-26595.

PROGRESS REPORT OF AN IUE SURVEY OF THE HYADES STAR CLUSTER

M-C.Zolcinski(1),L.Kay(2),S.Antiochos(2),R.Stern(3),A.B.C.Walker(2)
(1)Physics dept.,Univ. of New Hampshire,Durham,NH 03824
(2)Inst. for Plasma Research,Stanford Univ.,Stanford,CA 94305
(3)Jet Propulsion Lab.,Pasadena,CA 91109

ABSTRACT

To date 11 of the brightest X-Ray stars (F-K dwarfs) in the Hyades have been observed with the IUE satellite with the short wavelength spectrograph.Combining the IUE results with the X-Ray observations from the Hyades survey with the Einstein Observatory (Stern et al,1981) we estimate the differential emission measure function for each of the 7 stars which show evidence of emission lines. We derive constraints on stellar atmospheric parameters (chromospheric pressure, coronal temperature and "filling factor") and discuss the implications of our results in the contextof loop models for the corona and transition region (TR) of these stars.

I-INTRODUCTION AND MODEL

Stern et al (1981) have demonstrated that typical dwarfs in the Hyades have X-Ray luminosities $L_x \sim 30$ times more than solar.However the X-Ray spectra can only be roughly determined at this time from the Einstein IPC data. Far ultraviolet observations of TR lines in conjunction with the X-Ray measurements can be used to constrain stellar parameters, since the TR line fluxes have been found to correlate well with X-Ray fluxes (Ayres,Marstad,Linsky,1981).In this paper we will assume that the TR plasma and the coronal plasma are confined in coronal loops covering a fraction Σ of the stellar surface such as the loops in solar active regions.We will assume that the loop plasma is static and that isobaricity prevails in the TR as in the Sun.Furthermore we will assume that in the TR radiative losses dissipate the conductive flux from the corona as it is postulated for the Sun.

II-OBSERVATIONS AND ANALYSIS

The 11 selected stars from the Einstein Hyades survey were observed with the short wavelength prime camera on IUE at low dispersion (see Boggess et al(1978a, b) for IUE description).We estimated the accuracy of the line fluxes (NV 1240Å, CII 1335Å,SiIV 1397Å,CIV 1550Å) to be better than a factor of 2 for the 7 stars (F-K dwarfs) which show evidence of emission lines.With the assumptions stated in §I one may derive an expression for the product of the TR pressure P_o and Σ, at the temperature T_λ at which the excitation function for the (optically thin collisionally excited) line λ peaks (Zolcinski et al,1982a):

$$(P_o.\Sigma)_\lambda = 2.76\times10^{-13}\ (2\pi R^2)^{-1}\ T_\lambda^{-3/4}\ \Lambda(T_\lambda)^{1/2}\ EM_\lambda \qquad (1)$$

where R is the stellar radius,$\Lambda(T)$ is the radiative loss function for optically thin emission (Cox,Tucker,1969,Raymond,Cox,Smith,1976) and EM_λ is the effective emission measure at T_λ derived from the intensity of the line λ.Assuming constant

loop cross-section from the TR through the base of the corona we have:

$$(P_o.\Sigma)_{CIV} \simeq (P_o.\Sigma)_{NV} \simeq (P_o.\Sigma)_{cor} \qquad (2)$$

The temperature at the base of the corona can then be derived:

$$G_x(T_{cor})\ T_{cor}^{3/4}\ \Lambda^{-1/2}(T_{cor}) = 2.76\times10^{-13}(L_x/2\pi R^2)\ (P_o.\Sigma)_{cor}^{-1} \qquad (3)$$

where $(L_x/2\pi R^2)$ is the X-Ray surface flux, G_x is the emissivity of the plasma in the X-Ray band observed. Because the temperature size scale of the coronal emission must be less or of the order of the gravitational scale height we may derive an upper limit on Σ:

$$\Sigma \leq \Sigma_{max} = 3\times10^{26}\ T_{cor}^{-7/4}\ \Lambda(T_{cor})^{1/2}\ (P_o.\Sigma)_{cor}\ g^{-1} \qquad (4)$$

where g is the stellar surface gravity. We have performed the above analysis for the 7 stars as well as the Sun (as a check). Table 1 lists the values of the stellar parameters thus obtained. We also estimated the differential emission measure function for these stars and normalized them by their respective emission measure at $T=10^5$K, namely EM_{CIV}. The results are plotted in figure 1. For static isobaric loops with constant cross-section, the form of the differential emission measure function is:

$$EM(T) \propto T^{\delta} \qquad (5)$$

where $\delta \leq 1$ allows the contribution of cool loops (Antiochos, 1980).

III-RESULTS AND CONCLUSION

The errors on the results listed in table 1 are probably quite large, at least a factor of 2, due to the many uncertainties in the data and the model, however they do provide a critical test of the hypothesis that the emission from these stars is due to a solar-like corona and TR. The two F dwarfs tend to have similar characteristics: cooler coronae, larger coverage and hence smaller densities than the G dwarfs. Except for BD+14°693 the G dwarfs have similar characteristics to those of the active Sun. However BD+14°693, which has been observed twice with both IUE and Einstein has a very hot corona ($T>10^7$ K) and a very small coverage ($\sim$0.2%) leading to high densities especially in the TR. Such a small coverage would be appropriate for a star in a flaring state however neither the X-Ray observations (Zolcinski et al, 1982b) nor the ultraviolet observations show any time variability which could be associated with a flare or even a single rotating active region.

The first striking feature that can be seen in figure 1 is that $EM(T=10^5K)$ is minimum in all stars and that in fact, while the absolute value of the emission measure may change for different stars (by a factor of 30 or more) the shape of the emission measure for $3\times10^4 K<T<10^5 K$ seems to be the same for the Sun and the Hyades stars. Doschek et al (1978) have obtained similar results for αAur, HR 1099, λAnd and εEri. Below 10^5K the form of EM(T) is $\simeq T^{-2}$, which implies that the static model fails in this temperature range for all these stars as in the Sun. While below 10^5K the derivation of EM is model independent the calculation of the coronal emission involves the knowledge of T_{cor}. Therefore if one allows the contribution to the emission from cool loops our estimate of T_{cor} is only a lower limit (equation (5)).

REFERENCES

Antiochos,S.K.,1980,Ap.J.,241,385.
Ayres,T.R.,Marstad,N.C.,Linsky,J.L.,1981,Ap.J.545.
Boggess,A.,et al,1978a,Nature,275,372.
Boggess,A.,et al,1978b,Nature,275,377.
Cox,D.P.,Tucker,W.H.,1969,Ap.J.,157,1157.
Doschek,G.A.,Feldman,U.,Mariska,J.T.,Linsky,J.L.,1978,Ap.J.,226,L35.
Raymond,J.C.,Cox,D.P.,Smith,B.W.,1976,Ap.J.,204,290.
Stern,R.A.,Zolcinski,M-C.,Antiochos,S.K.,Underwood,J.H.,1981,Ap.J.,244,647.
Zolcinski,M-C.,Antiochos,S.,Stern,R.A.,Walker,A.B.C.,1982a,to appear in Ap.J. (July 1)
Zolcinski,M.C.,Stern,R.A.,Antiochos,S.,1982b,in preparation.

TABLE 1- Stellar parameters (n is the density and H_o the temperature scale height)

Star	T_{cor} (K)	Σ_{max}	$P_{o\ min}$ (dynes/cm^2)	$n_{o\ min}$ at T=10^5K, cm^{-3}	$n_{cor,min}$ at T=Tcor, cm^{-3}	$H_{o max}$ (cm)
BD+15°640 F2 V	9.7 (5)	1	1.3	4.7 (10)	4.8 (9)	3.8 (9)
70 TAU F8 V	1.9 (6)	1	0.9	3.3 (10)	1.7 (9)	1.1 (11)
BD+16°592 G1 V	4.3 (6)	0.13	5.0	1.8 (11)	4.2 (9)	8.6 (10)
BD+14°693 1 G0 V	4.6 (7)	2.3(-3)	435.	1.6 (13)	3.4 (10)	2.8 (11)
BD+14°693 2 G0 V	6.1 (7)	1.1(-3)	692.	2.5 (13)	4.1 (10)	2.0 (11)
BD+17°731 G0 V	4.9 (6)	0.11	6.4	2.3 (11)	4.8 (9)	1.6 (11)
BD+16°577 G5 V	3.7 (6)	0.18	4.5	1.6 (11)	4.4 (9)	9.7 (9)
BD+14°690 double G0 V	5.3 (6)	0.10	7.6	2.8 (11)	5.2 (9)	1.7 (10)
Quiet Sun	1.6 (6)	0.05	0.2	7.2 (9)	4.5 (8)	1.3 (10)
Moderately active Sun	3.0 (6)	0.02	2.5	9.0 (10)	3.0 (9)	9.9 (9)

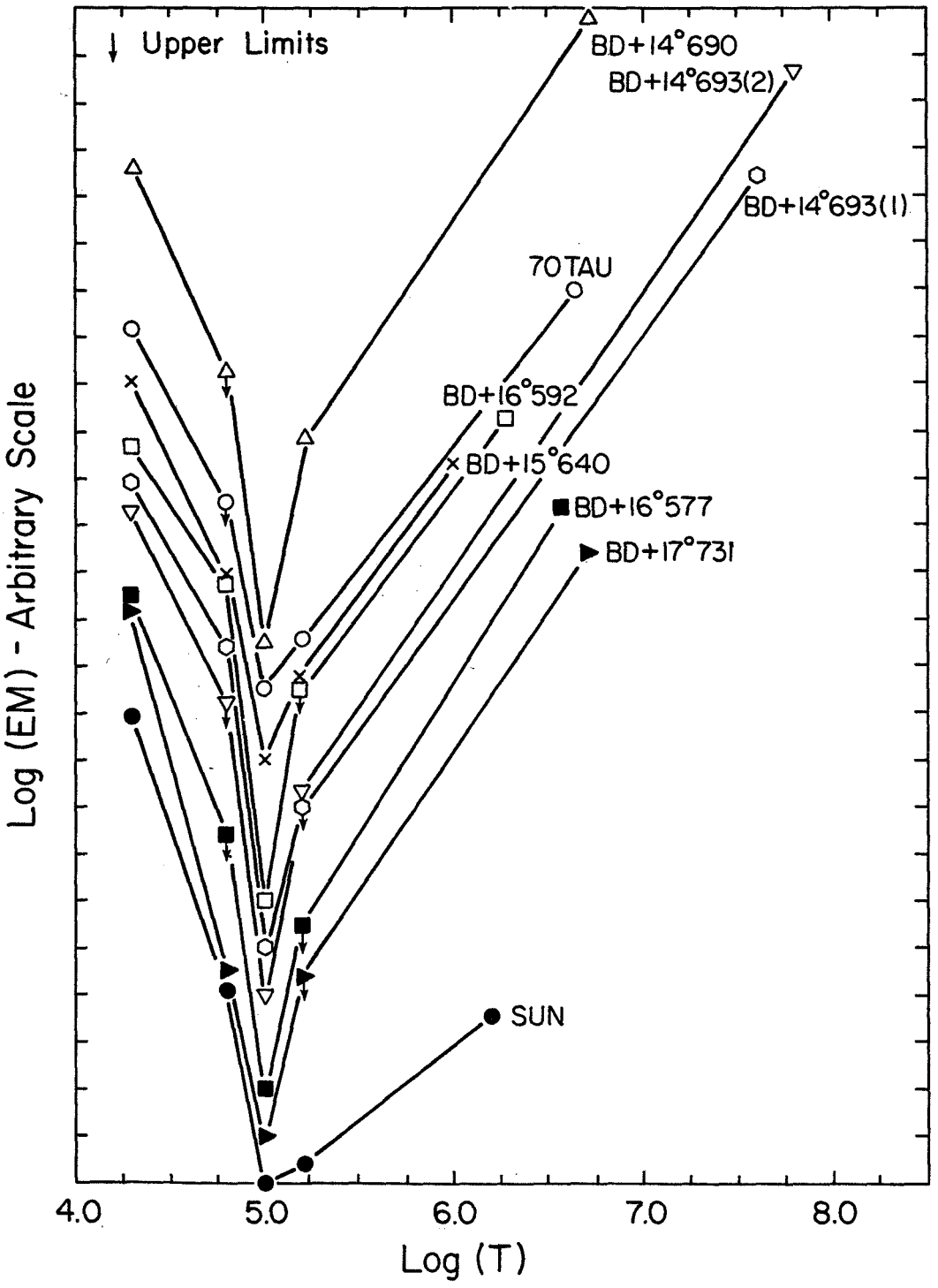

FIGURE 1 - Differential emission measure for seven Hyades stars and the quiet Sun in units of EM_{CIV} (emission measure at $T = 10^5$ K). Time between observations (1) and (2) ~1 year.

DENSITY SENSITIVE C II LINES IN COOL GIANT STARS

Robert E. Stencel
Joint Institute for Laboratory Astrophysics, University of Colorado and
National Bureau of Standards, Boulder, CO 80309

and

Kenneth G. Carpenter
Department of Astronomy, Ohio State University
Columbus, OH 43210

ABSTRACT

The density sensitivity of the emission lines within the UV 0.01 multiplet of C II near 2325 Å has been examined in additional late type giants and supergiants with deep LWR high dispersion exposures. The new data support the original contention based on these lines that noncoronal red giants possess geometrically extended chromospheres.

INTRODUCTION

Given the complexity of the spectra of late type post main sequence stars, it is crucial that spectroscopic methods be established which can unambiguously determine basic atmospheric parameters, such as the electron density. One such density diagnostic involves the mid-UV intercombination lines of C II, multiplet UV 0.01 near 2325 Å (Stencel et al. 1981). By iterating between three observed line ratios within the multiplet and atomic theory, a self-consistent set of atomic parameters which fit the observations was derived. These lines exhibit a density sensitivity between 10^7-10^9 cm^{-3}. In that study, except for the solar chromosphere which provided the high density limit, all of the stars considered were late K and M giants and supergiants which are inferred to lack solar-like corona on the basis of their low upper limits of soft X-ray emission (Ayres et al. 1981a).

We have endeavored during the fourth year of IUE operations to extend the observational sample across the cool half of the H-R diagram, particularly to explore the so-called Linsky and Haisch (1979) division between giant stars with and without transition regions (TR) and coronae. To this end, we have observed three coronal type stars: Beta Dra (G2 Ib-II), Beta Gem (K0 III) and 56 Peg (K0 IIp + wd). The latter is an interacting binary and must be cautiously compared with single stars (cf. Schindler et al. 1982). In addition, we have observed Epsilon Gem (G8 Ib) and Epsilon Peg (K2 Ib) to extend the survey of C II] in the spectra of noncoronal stars.

OBSERVATIONS

Figure 1 displays the 2320-2330 Å region of spectrum in the five new observations, plus a comparison with the previously observed, high signal-to-noise (S/N), strong C II lines in Alpha Ori (M2 Iab). The figure also indicates the exposure times used for these LWR echelle mode observations during 1981. The wavelength scales are those provided by the IUESIPS, and given the small range of THDA (13±1°C), suggest real velocity shifts. The primary member of the multiplet, near 2325.4 Å appears to have been detected in each case, except perhaps in Beta Dra where a strong continuum has swamped much of the emission. The ratio of 2325.4 Å/2328.1 Å (R_1) theoretically decreases with increasing electron density, while the ratios 2325.4 Å/2326.9 Å (R_2) and 2324.7 Å/2326.9 Å (R_3) both increase with increasing electron density. On this basis we can derive some preliminary density estimates, limited largely by the low S/N:

Star	Spectral Type	Radial Velocity	C II] Ratios			Log $\bar{N}_e$
			R_1	R_2	R_3	
β Dra	G2 Ib-II	−20 km s^{-1}	1.8	2.3	1.5	8.3 ± 1.0
β Gem	K0 III	+3	2.2	4.8	2.0	8.7 ± 0.3
56 Peg	K0 IIp+wd	−24	3.0	2.5	1.3	8.0 ± 0.5
ε Gem	G8 Ib	+11	3.2	2.3	0.9	7.8 ± 0.6
ε Peg	K2 Ib	+5	2.5	2.7	1.2	8.0 ± 0.8

Improvements in the use of the C II ratios for accurate density determinations must await more accurate atomic parameters for C II, as well as higher S/N observations which will become possible with the High Resolution Spectrograph on the Space Telescope in the mid-1980s.

INFERENCES

The ratios of the 1335 Å resonance lines of C II to the intercombination lines is sensitive to T_{exc}. Among coronal type giants like Beta Dra and Beta Gem, the lines of C II near 1335 Å are clearly present. Among the noncoronal giants, the resonance lines of C II are much weaker and often blended with fluoresced CO emission (Ayres et al. 1981b). These resonance lines are computed to form in the lower TR in the Sun ($\lesssim$20,000 K), but our calculations for giant stars suggest significant contribution to the line flux from the chromospheres. We are typically finding upper limits to the T_{exc} for noncoronal giant stars, of 5000-7000 K. Physically, the emission measure suggests that in order to obtain significant flux from the intercombination lines when the resonance lines are weak or absent (low T_{exc}), formation in an extended chromosphere is required. Solving for the line emissivity of C II UV 0.01 requires an accurate ionization equilibrium, which is difficult to compute in the turbulent and partially-ionized chromospheres of red giants. However,

because the C II UV 0.01 lines are not self-reversed, we can adopt an optically thin approximation, and the emitting layer thickness (cm) can be expressed as a function of the observed flux, distance factors and the ionization-excitation populations which involve an exponential of inverse T_{exc}. Thus, coronal type giants like Beta Dra and Beta Gem which have solar like T_{exc} are deduced to have thin C II emitting layers ($r \ll R_*$). The noncoronal giants with low T_{exc} are deduced to have very large C II emitting layers ($r > R_*$). Although the calculations require improvements and generalization, it is encouraging that this evidence concurs with parallel data from radio and narrow band speckle interferometry observations which also point to extended chromospheres among noncoronal giants and supergiants (cf. Stencel 1982). The evidence for a discontinuous change in chromospheric extent between coronal and noncoronal giants must be a crucial clue to the mechanism of rapid mass loss (cf. Mullan and Stencel — this volume).

LINES OF Si II UV 0.01

Multiplet UV 0.01 of Si II which occurs between 2330-2350 Å also appears in emission in the spectra of our observed stars. We have examined line ratios in this multiplet to look for any correlation they may exhibit against the C II derived densities, and find little evidence for such. Presumably chromospheres can easily populate the upper level of UV multiplet 1 of Si II (which is only 1.5 eV above the upper level of UV 0.01), in contrast to populating the upper levels of UV 1 of C II, which are 4.0 eV above UV 0.01.

ACKNOWLEDGMENTS

We wish to thank R. F. Wing, J. L. Linsky and C. Jordan for useful discussions, along with the staff of the IUE Observatory for their generous assistance. This work was supported in part by NASA grant No. NAG5-82 for which we are grateful.

REFERENCES

Ayres, T., Linsky, J., Vaiana, G., Golub, L., and Rosner, R. 1981a, Ap. J., 250, 293.

Ayres, T., Moos, H., and Linsky, J. 1981b, Ap. J., 248, L137.

Linsky, J., and Haisch, B. 1979, Ap. J., 229, L27.

Schindler, M., Stencel, R., Linsky, J., Basri, G., and Helfand, D. 1982, Ap. J., submitted.

Stencel, R., Linsky, J., Jordan, C., Brown, A., Carpenter, K., Wing, R., and Czyzak, S. 1981, M.N.R.A.S., 196, 47p.

Stencel, R. 1982, in Proceedings, Second Cambridge Workshop on Cool Stars, ed. M. S. Giampapa, S.A.O. Spec. Report, in press.

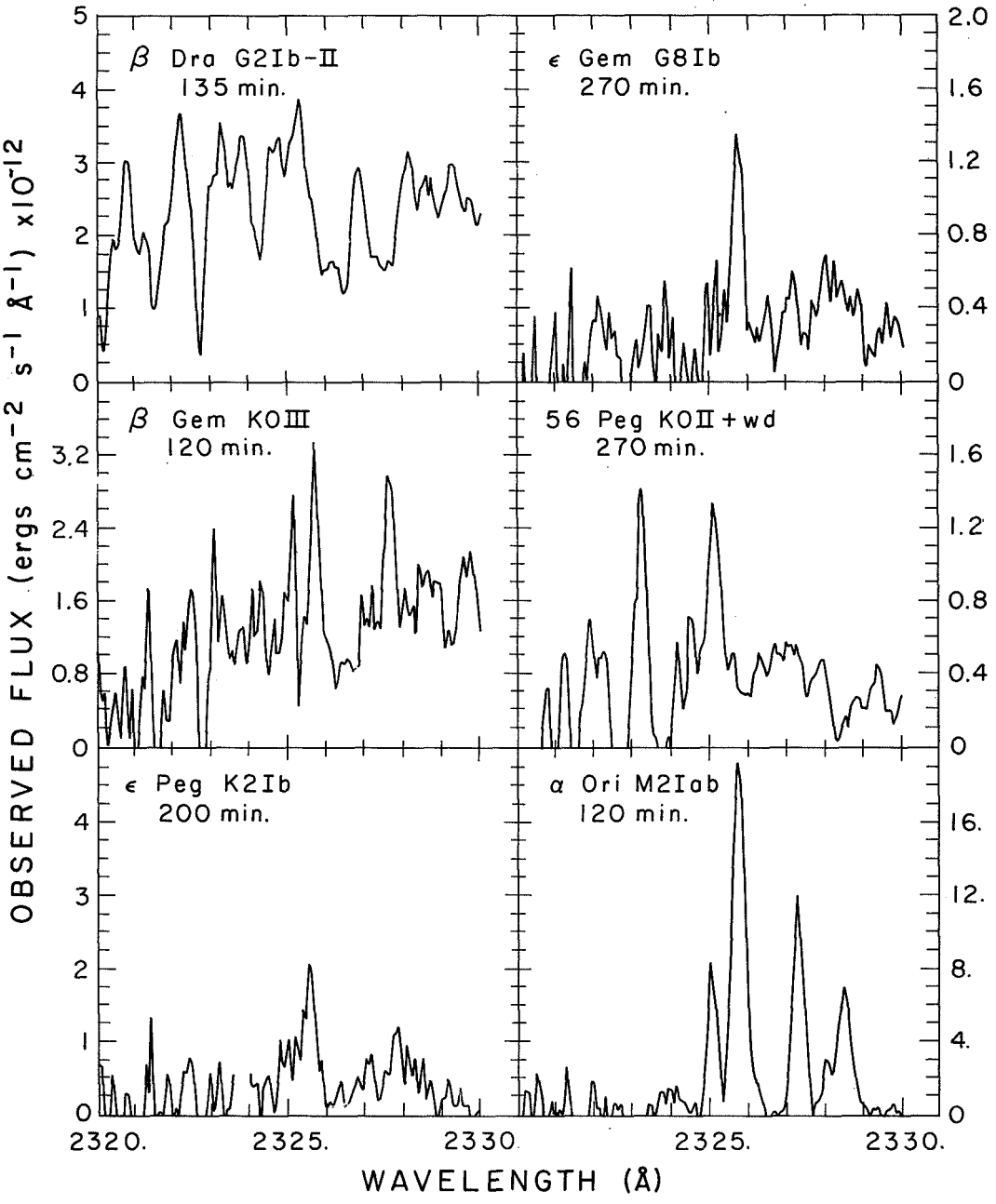

Figure 1. The C II intersystem lines in several late-type stars.

CHROMOSPHERIC, TRANSITION LAYER AND X-RAY EMISSION FOR STARS WITH DIFFERENT ROTATIONAL VELOCITIES

Erika Böhm-Vitense
Astronomy Department, University of Washington

ABSTRACT

In agreement with our previous findings for the MgII k line emission in F stars we do not find an increase of Lyα and transition layer emission with increasing v_r sin i, if v_r sin i > 30 km/sec. For v_r sin i ≤ 30 km/sec. The measured line intensities are consistent with an increase in emission with increasing v_r sin i. Such a relation between emission and rotation for single stars is also in agreement with X-ray observations. For the young F stars in the Hyades we find generally enhanced emission independently of rotational velocities. The enhancement is most pronounced for low excitation lines.

INTRODUCTION

In our study of MgII k line emission for F stars with different rotational velocities (Böhm-Vitense 1982) we found that for the non-Hyades and single stars the emission does not increase with increasing rotational velocities, contrary to expectations. Studies by Wilson (1970), Kraft (1967) and Skumanich (1972) and others seemed to indicate increasing CaII K line emission with increasing rotational velocities v_r sin i. For binaries increasing emission for decreasing orbital periods was found for instance by Glebocki and Stawikowski (1975). Middelkoop and Zwaan (1981) also found that emission increased with decreasing orbital periods which they interpreted as showing increased emission for increasing rotational velocities. Ayres and Linsky (1980) find increasing X-ray emission with increasing v_r sin i for G star binaries and Walter (1981) found increasing X-ray emission for RS CVn stars of decreasing period lengths again interpreting this as showing increasing X-ray emission with increasing rotational velocities. Pallavicini et al. (1981) also find a positive correlation between X-ray emission in F and G stars with v_r sin i. Since our observations of the MgII k line emission for single stars did not confirm a positive correlation between chromospheric emission and v_r sin i, we may wonder whether the rotational broadening might cause our MgII k emission line measurements to be in error. Measurements of the short wavelength emission lines on low resolution IUE spectra will avoid this difficulty. It will also be interesting to see whether the dependence on v_r sin i might change for higher excitation lines, which presumably may depend more strongly on the magnetic field which supposedly increases with increasing rotation.

CHROMOSPHERIC AND TRANSITION LAYER EMISSION LINE INTENSITIES

In Figure 1 we have plotted the emission line intensities for F stars with 0.3 < B-V < 0.4 as a function of their rotational velocities v_r sin i.

(We have chosen a narrow range in B-V such that a T_{eff} dependence of the emission will be unimportant.)

Hyades stars and stars with variable or possibly variable radial velocities are indicated by filled or half filled symbols respectively. For all low excitation lines the stars with filled symbols show enhanced emission as compared to the other stars. The differences decrease for increasing excitation of the lines. β Cae does not seem to be a close binary.

For the other stars, i.e. non-binaries and non-Hyades stars we generally find somewhat decreasing emission for increasing rotational velocities except for stars with $v_r \sin i < 30$ km/sec. For small rotational velocities our observations are consistent with an increasing emission with increasing $v_r \sin i$.

This is important when we compare our results with those of previous investigators. The studies of the CaII K line emissions all refer to stars with $v_r \sin i < 30$ km/sec or to close binaries which should however be considered separately since they show generally enhanced emission, and the enhancement may be due to gravitational interaction.

COMPARISON WITH X-RAY OBSERVATIONS FOR EARLY STARS

If there is indeed a different dependence of emission on $v_r \sin i$ for small and large $v_r \sin i$ one might wonder, whether the same trend can be observed for the X-ray emission. No F and G stars with large $v_r \sin i$ were included in the Einstein observations published by Vaiana et al. (1981), but high rotation O, B and A stars were studied. Pallavicini et al. (1981) consider this whole group together and do not find any dependence on $v_r \sin i$. In our Figure 2 we have replotted their data considering the different spectral types separately. They are indicated by alternating open and filled symbols. Different luminosity classes are also indicated by different symbols. Concentrating on each spectral class separately, I think it is clear that for early spectral types and $v_r \sin i > 80$ km/sec we generally find decreasing X-ray emission for increasing $v_r \sin i$. For small $v_r \sin i$ the observations are consistent with increasing emission for increasing $v_r \sin i$. The velocity for which the emission starts to decrease increases for earlier spectral types. Presumably the X-ray emission in early type stars has a different origin than in F stars. Nevertheless it is interesting to see that a similar correlation exists between X-ray emission and $v_r \sin i$ for these two types of coronae.

It is also interesting to note that α^2CVn, the only star in the sample, known to have a strong magnetic field, apparently shows quite normal X-ray emission and no enhancement.

X-RAY EMISSION IN F STARS

In Figure 3 we have replotted the curve shown for A stars in Figure 2. We have also plotted the X-ray fluxes measured for F stars and cooler stars.

The F stars have enhanced X-ray emission as compared to A stars as pointed out by Pallavicini et al. (1981), presumably due to the onset of efficient convection. For these stars the correlation between X-ray flux and v_r sin i is surprisingly tight showing that not only v_r but also sin i must be important. This, I think, can only mean that the equators emit more X-rays than do the poles. We are reminded of the coronal holes observed at the solar poles. For larger v_r sin i the X-ray emission does not increase any more.

SUMMARY

Chromospheric and transition layer emission lines show no increase, if anything they show somewhat decreasing intensities for increasing rotational velocities if v_r sin i > 30 km/sec. For smaller v_r sin i the line intensities probably increase with increasing v_r sin i. If this increase is due to increasing magnetic field strengths, we have to explain why the magnetic star α^2CVn does not show abnormally strong X-ray emission.

The slightly decreasing emission line intensities for increasing v_r sin i for large rotational velocities do not contradict other observations for single stars. They are in fact similar to the decrease in X-ray emission with increasing v_r sin i found for early type stars.

The transition layer emission lines of F dwarfs show the least dependence on other stellar properties like age or binary nature. This may be understood qualitatively if we remember that the temperature gradient in this layer is determined mainly by conductive energy flux. The higher the temperature in the corona the larger the conductive temperature gradient and the smaller the height of the region which can contribute to the emission of a given line. An increase in coronal heating will therefore lead to a lesser increase in transition layer emission.

REFERENCES

Ayres, T., and Linsky, J. 1980, Ap.J. 235, 76.
Böhm-Vitense, E. 1982, Ap.J. in press.
Glebocki, R., and Stawikowski, A. 1977, Acta Astronomica 27, 225.
Kraft, R. 1967, Ap.J. 150, 551.
Middelkoop, F. and Zwaan, C. 1981, Astron. Astrophys. 101, 26.
Pallavicini, R., Golub, L., Rosner, R., Vaiana, G. S., Ayres, T. and Linsky, J. L. 1981, Ap.J. 248, 279.
Skumanich, A. 1972, Ap.J. 171, 565.
Vaiana, G. S., Cassinelli, J. P., Fabbiano, G., Giacconi, R., Golub, L., Gorenstein, P., Haisch, B. M., Harnden, Jr., F. R., Johnson, M., Linsky, J. L., Maxson, C. W., Mewe, R., Rosner, R., Seward, F., Topka, K., and Zwaan, C. 1981, Ap.J. 245, 163.
Walter, F. M., and Bowyer, S. 1981, Ap.J. 245, 671.
Wilson, O. C. 1970, Ap.J. 160, 225.

FIGURES

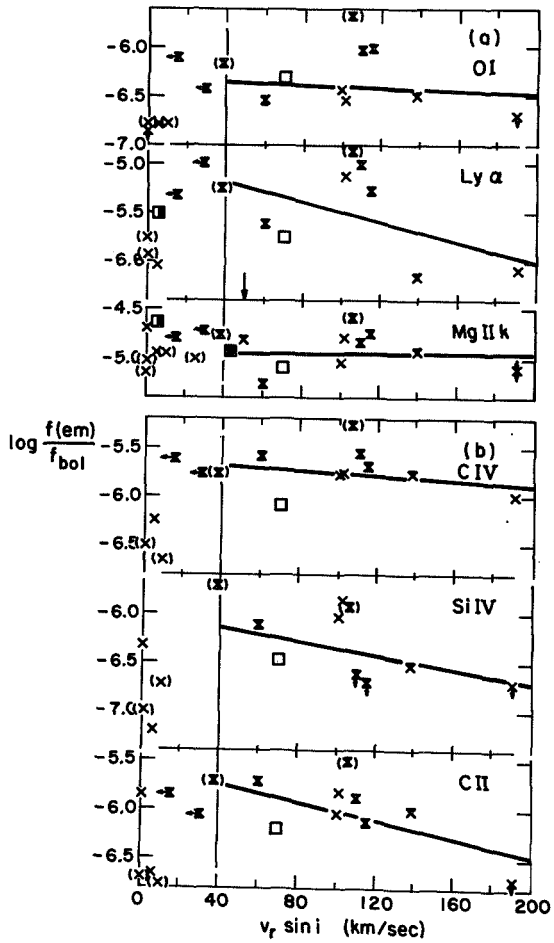

Figure 1a. Chromospheric emission line intensities for F dwarfs as a function of rotational velocities v_r sin i. Hyades stars and stars with variable or possibly variable radial velocities are indicated by filled or half filled symbols respectively.

Figure 1b. Same as figure 1a but for transition layer emission lines.

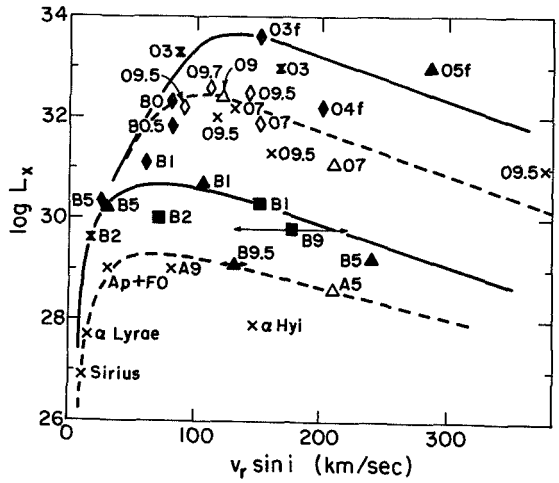

Figure 2. X-ray emission for early type stars as a function of v_r sin i. Different spectral classes are differentiated by alternating open and closed symbols as well as dashed and solid lines. Different luminosity classes are indicated by different symbols (x, ⧗→V, ▣■→IV, Δ, ▲→III, ○ ● →II and I). The solid and dashed lines are the eye fitted lines to the points for the different spectral classes.

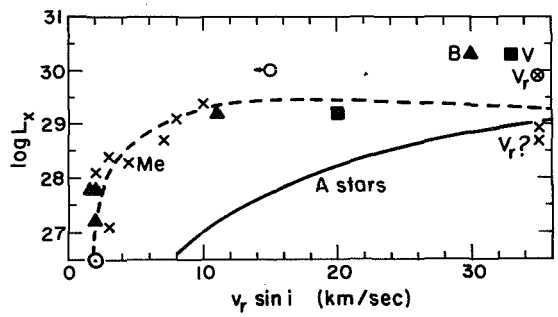

Figure 3. Correlation between X-ray emission and v_r sin i for F + G stars. The correlation is surprisingly tight, showing that sin i must also be important for the emission. V = variable star, B = binary, V_r = variable radial velocity. Symbols as in Figure 1.

CAPELLA REVISITED

Thomas R. Ayres
Laboratory for Atmospheric and Space Physics
University of Colorado, Boulder

ABSTRACT. I summarize the highlights of two IUE programs to study the active chromosphere binary, Capella (α Aurigae A: G6 III + F9 III).

INTRODUCTION. One of the more puzzling stellar systems in the solar neighborhood is the spectroscopic binary Capella (d $\cong$ 13 pc). Both components are nearly identical in mass, temperature, luminosity and age, but visible and ultraviolet spectra of the pair are remarkably different. For example, the optical spectrum of the primary is sharp-lined while that of the secondary is diffuse and difficult to identify (Wright 1954), aside from an unusually strong Li I λ6708 absorption (Wallerstein 1966). In the ultraviolet, on the other hand, the chromospheric emission spectrum of the secondary is quite prominent, while that of the primary star is difficult to detect (Ayres and Linsky 1980).

Iben (1965) offered a solution to the lithium richness and spectral diffuseness of the secondary spectrum. He proposed that the primary is a slowly rotating post helium flash giant, while the secondary is crossing the Hertzsprung gap for the first time. Accordingly, the F giant is still shedding the angular momentum inherited from its rapidly rotating early-type progenitor, and still burning off its surface primordial lithium by deep mixing. The enhanced ultraviolet emission of the Capella secondary likely also can be traced to its recent incursion into the yellow giant region. In particular, stellar chromospheres and coronae are thought to derive from magnetic activity (Vaiana and Rosner 1978), and fast rotating convective stars likely manufacture more magnetic flux than slow rotators (Parker 1970).

From the standpoints of stellar evolution, the origin of magnetic activity, and the development of chromospheres and coronae, the Capella system clearly provides an important prototype. Here, I present the highlights of two studies of Capella undertaken during the third and fourth years of IUE. The first program consists of high dispersion spectroscopy at critical phases of the Capella orbit, and will be published in more detail elsewhere (Ayres, Schiffer and Linsky 1982). The second program is a two month monitoring effort to search for ultraviolet modulations induced by the rotation of magnetic active regions onto and off of the visible hemisphere of the Capella secondary.

OBSERVATIONS. In the study of Capella at critical orbital phases, entire NASA #2 shifts were devoted to sequential exposures alternating between the long wavelength and short wavelength echelles, with typical exposure times of 1 minute and 30 minutes, respectively. The multiple exposures improve S/N by co-addition, provide an empirical assessment of spectrum reproducibility, and can reveal short term ($\cong$hours) fluctuations in emission line strengths. In the rotational modulation program, 10 NASA #2 shifts were split into 22 observing opportunities, each typically consisting of four echelle exposures: 2 LWRs of 1 minute and 2 SWPs, one of 10 minutes and the other of up to 60 minutes. A description of the high dispersion reduction procedures and the results of

an echelle mode calibration study undertaken during the monitoring effort can be found in Ayres (1982a).

For this presentation, I analyzed in detail the fluxes of three features--the C IV λλ1548,1551 doublet, Si II λ1808 and Mg II λ2796--from both programs. I normalized the Si II and Mg II line emission to "continuum" fluxes measured in bands well separated from the line cores to minimize systematic errors owing to mispositioning of the target in the large slot and the thermal sensitivity of the image converters. I corrected the raw wavelength scales provided by the IUE SIPS for the telluric component, the radial velocity of Capella, and a temperature dependent term having a slope of 5.2 km $s^{-1}C^{-1}$ for LWR and 2.4 km $s^{-1}C^{-1}$ for SWP, with a zero offset of 13 km s^{-1} for THDA(LWR) = 13°C and THDA(SWP) = 8°C (see Ayres 1982b). Finally, I adjusted the C IV absolute fluxes by 0.8% C^{-1} x [THDA - 8°C] (Bohlin et al. 1980).

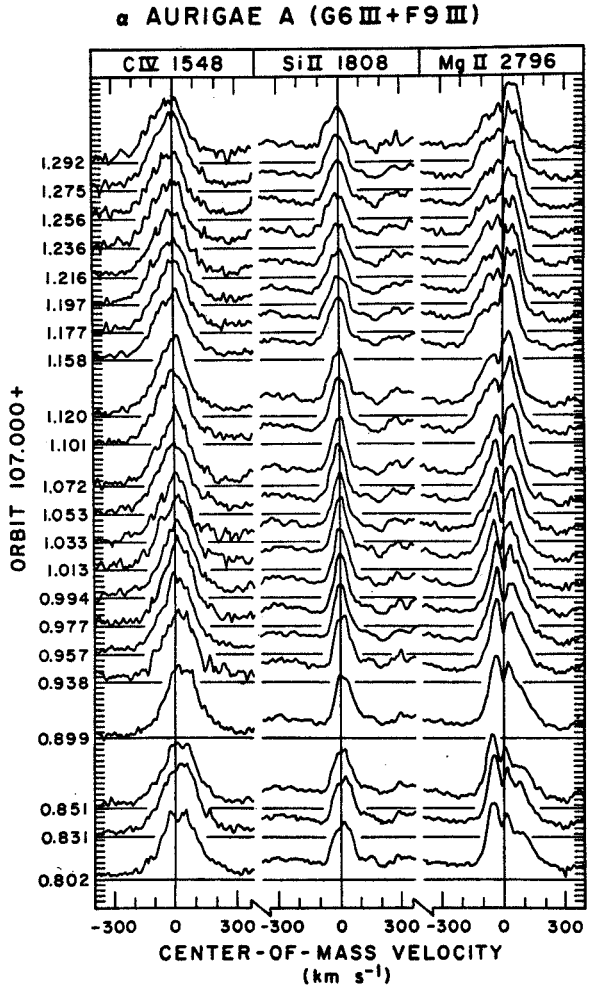

ANALYSIS. Figure 1 depicts profiles of C IV λ1548, Si II λ1808 and Mg II λ2796 from the monitoring program. The ordinate of the figure is a relative intensity scale with the Mg II feature reduced by a factor of 25. For each profile set, the horizontal line denotes the zero intensity level which is displaced upwards in proportion to the temporal separation between observing opportunities. Orbital phases are from the Heintz (1975) ephemeris. For reference, at the phase 0.75 quadrature, the primary and secondary are at -27 km s^{-1} and +27 km s^{-1}, respectively; at the phase 0.25 quadrature, the component radial velocities are reversed; while at the phase 0 conjunction the giants have the same radial velocity and the spectrum is single lined.

The secondary is quite prominent in the Mg II k line, which is formed at about 6000 K in the stellar chromosphere. The weaker primary star contribution can be seen clearly near the quadratures, although the interstellar feature at -8 km s^{-1} obscures it somewhat near the phase 0 conjunction. The primary probably accounts for no more than 30% of the total Mg II emission. The secondary also is prominent in Si II λ1808, which is formed at about 10^4 K in the upper chromosphere. A moderate (≤30%) contribution by the primary is indicated by the increase in FWHM from the conjunction towards

either quadrature. Note that the Si II emission envelope is symmetric about zero velocity (vertical line) near the conjunction. In C IV λ1548, formed at about 10^5 K, the influence of the secondary is dominant, and the contribution of the primary is difficult to assess. The line width and profile shape do not change as dramatically as those of the lower excitation features, and the C IV emission appears to shift bodily from one quadrature to the other. The primary contribution is no more than 10%. Finally, near the conjunction, when the spectrum is single lined, C IV λ1548 appears to be redshifted relative to Si II λ1808 by roughly 10 km s^{-1}, reminiscent of the downflows observed over solar magnetic active regions in high excitation lines (Athay 1981). A similar redshift phenomenon has been reported by Stencel et al. (1982), who analyzed a long SWP echelle exposure of the early G supergiant β Draconis.

Figure 2 summarizes the results of the timing program, including fluxes from the critical orbital phase study. The line fluxes or flux ratios are normalized to the mean value for the 1981.19-1981.33 period (stippled box). The error bars on the values from the critical orbital phase study (1980 through early 1981) refer to the dispersion of the individual fluxes from the mean of the multiple exposure sequences. I adopt that dispersion to characterize the error associated with single flux measurements, as well as an upper limit on short term fluctuations of the Capella emission. The vertical extent of the stippled box represents the dispersion of the individual fluxes of the timing sequence about the mean value. Statistically significant modulations appear in each diagnostic, particularly Mg II for which the S/N is quite good. The major fluctuations are compatible with a rotation period of ≅10 days, consistent with the v sin i ≅ 30 km s^{-1} derived from the width of Li I λ6708 (Ayres and Linsky 1980). Despite the existence of fluctuations in all three diagnostics, the most remarkable result of the timing study is the steadiness of the Capella ultraviolet emission. In particular, the system has exhibited a dispersion in its ultraviolet line output of only ±6% (1σ) in C IV and ±3% (1σ) in Si II λ1808 and Mg II λ2796 over the 1980-1981 period.

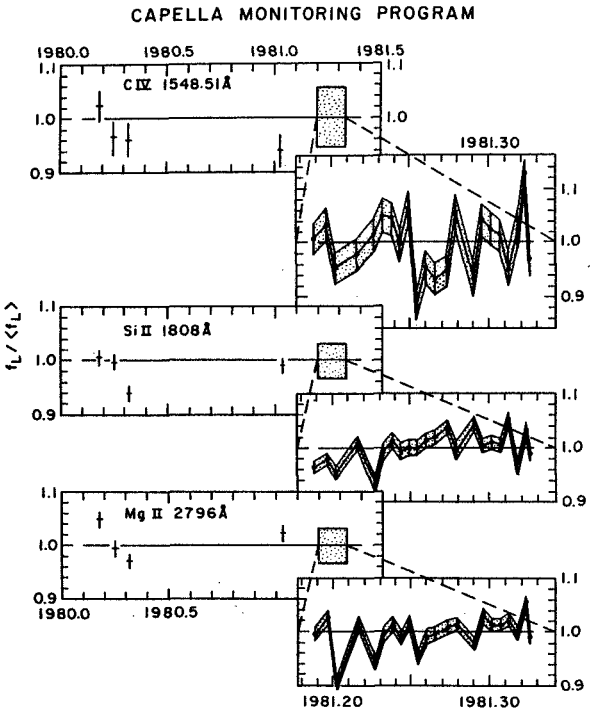

DISCUSSION. The observations of Capella at critical orbital phases confirm that the fast rotating secondary star is responsible for the bulk of the ultraviolet line emission from the system, particularly in the high excitation C IV doublet. The emission dichotomy between the otherwise similar giants implies that the spindown of single stars evolving across the Hertzsprung gap

must be very rapid, particularly if both the Capella giants are in their first crossing as suggested by Boesgaard (1971). Accordingly, the majority of the single yellow giants, which are post helium flash, should be slow rotators and comparatively inactive like the Capella primary (cf., Simon, Linsky, and Stencel 1982). Only the relatively rare first crossers should be fast rotators with active chromospheres and coronae like the Capella secondary.

Finally, the ultraviolet steadiness of the Capella secondary is remarkable in light of the large fluctuations typical of active dwarf stars (Hallam and Wolff 1981) and the K subgiant components of tidally synchronized RS CVn-type binaries (Simon and Linsky 1980). Among these cooler stars, factor of 2 fluctuations in C IV are not uncommon (Boesgaard and Simon 1981; Ayres and Linsky 1982). The steadiness of the Capella secondary suggests a nearly homogeneous organization of its surface magnetic field. In contrast, the emitting regions on the cooler stars appear to be spatially concentrated. For example, the starspots of the RS CVn subgiants are large enough to produce optical photometric modulations (Hall 1978). Small decaying spots which are dark in Mg II may well be responsible for the quasi-periodic dips in the Capella timing record. If so, the spots probably are located in the northern hemisphere of the secondary since the dips are comparatively narrow (Note: $i = 135°$). Nevertheless, the Capella secondary must be covered almost uniformly with bright regions analogous to solar plages in order to produce the steady emission behavior. I speculate that the shallowness of the F giant convective envelope is responsible for the lack of large scale spatial structure in its surface magnetic active regions. Only when the convective envelope becomes deep can dynamo action (Parker 1970) impress the large scale spatial coherence on the subsurface field required to produce large "spotted" areas on the stellar disk.

ACKNOWLEDGEMENTS

I thank the staff of the IUE Observatory and the many Guest Investigators with whom I timetraded for their help in acquiring the Capella exposures. This work was supported by NASA grant NAG5-199 to the University of Colorado.

REFERENCES

Athay, R.G. 1981, in "Solar Active Regions", ed. F.Q. Orrall, Boulder: Colorado Associated University Press), p. 83.
Ayres, T.R. 1982a, IUE Newsletter (submitted).
Ayres, T.R. and Linsky, J.L. 1980, Ap. J., 241, 279.
Ayres, T.R. and Linsky, J.L. 1982, Ap. J. (in press, March 1).
Ayres, T.R., Schiffer, F.H., 3rd, and Linsky, J.L. 1982 (in preparation).
Boesgaard, A.M. 1971, Ap. J., 167, 511.
Boesgaard, A.M. and Simon, T. 1981, in "Second Workshop on Cool Stars, Stellar Systems and the Sun", ed. M.S. Giampapa and L. Golub, (in press).
Bohlin, R.C., Holm, A.V., Savage, B.D., Snijders, M.A.J., and Sparks, W.M. 1980, Astr. Ap., 85, 1.
Hall, D.S. 1978, A.J., 83, 1469.
Hallam, K.L., and Wolff, C.L. 1981 Ap. J. (Letters), 248, L73.
Heintz, W.D. 1975, Ap. J., 195, 411.
Iben, I., Jr. 1975, Ap. J., 142, 1447.
Parker, E.N. 1970, Ann. Rev. Astr. Ap., 8, 1.
Simon, T. and Linsky, J.L. 1980, Ap. J., 241, 759.
Simon, T., Linsky, J.L., and Stencel, R.E. 1982, Ap. J. (in press).
Stencel, R.E., Linsky, J.L., Ayres, T.R., Jordan, C., and Brown, A. 1982, Ap. J. (submitted). (See also these proceedings.)
Vaiana, G.S., and Rosner, R. 1978, Ann. Rev. Astr. Ap., 16, 393.
Wallerstein, G. 1966, Ap. J., 143, 823.
Wright, K.O. 1954, Ap. J., 119, 471

The Ultraviolet Spectra of R and N Type Stars

George T. O'Brien and Hollis R. Johnson
Astronomy Department, Indiana University

INTRODUCTION

Progress in our understanding of the structure of the outer atmospheres of carbon stars has been hampered by several factors. The warmer, R-type stars have effective temperatures similar to those of G and K stars, but they are quite faint, with V > 7-8 mag. Consequently, the high dispersion observations needed to study chromospheric line-cores and possible circumstellar features are difficult to obtain. The cooler N-type stars are much brighter but they are quite cool (Teff ~ 2000-3500 K); moreover, the spectral region below about 4200 Å is very heavily blanketed by an opacity source of uncertain origin.

Attempts have previously been made to obtain IUE spectra of N stars, but the objects selected were so heavily blanketed that no light was obtained in exposure times of two and four hours. Not all N stars are so heavily obscured, however. The unknown opacity source is not as effective in blanketing the late R and early N stars, and we suspected that if the target list were prepared with these objects in mind, IUE spectra could be obtained. Such spectra would be useful for several reasons. Ultraviolet observations could provide information on the nature of chromospheric activity in these evolved objects. Carbon stars are most likely in a post-helium burning stage (Scalo 1976; Iben 1981) and thus represent stars which are generally more evolved than the bulk of the K and M giants and supergiants. The continuous flux distribution itself should provide clues into the nature and wavelength dependence of the unknown opacity. Finally, the relative strengths of the chromospheric emission lines on the one hand, and the photospheric flux on the other, might indicate whether the ultraviolet obscuration is located in the photosphere (as suggested for gaseous C_3) or in the circumstellar shell (in the form of SiC grains). Ground-based observations of the violet spectral region generally favor a photospheric origin for the opacity.

We have successfully obtained low dispersion LWR spectra of three early N-type carbon stars (BL Orionis, TX Piscium and T Indi) on March 20 and October 26, 1981 with the IUE satellite. Observations of several R-type stars were also obtained on the same dates. The observations span the range of subtypes within the R-star classification: HD 182040 (R0), HD 16115 and HD 137613 (R3), HD 52432 (R5) and HD 37212 (R8). A high dispersion spectrum of HD 182040 was obtained, but the other R stars were observed in the low dispersion (6 Å resolution) mode. In Figure 1 we illustrate three representative spectra of M, R and N stars.

RESULTS

The Photospheric Spectrum

Comparison of the N-star spectra with IUE observations of late M-type stars (our own observations, as well as those obtained from the IUE archives) reveals several differences. The photospheric flux-distribution shows a more rapid fall-off with decreasing wavelength in the N stars than in the M stars. This is to be expected because, in general, the N stars are much cooler. In a recent determination of N-star effective temperatures, Tsuji (1981) derives Teff = 3420 K for BL Ori. Although such a value makes BL Ori one of the

warmer N stars, such a Teff corresponds to a spectral type of about M3.

Moreover, the absorption-line spectrum of the N stars is richer than that of the M stars. There are several absorption features in common -- for example, low excitation lines of Fe I, Ni I, Ti I -- but there are a number of striking differences as well. The deep, broad absorption around 3150 A in the N stars arises (at least in part) from the (0, 0) and (1, 1) bandheads of the 3143 A system of CH ($C^2\ \Sigma^+ - X^2\Pi$). The absence of this feature in the M-star spectra (see Figure 1) is a consequence of their oxygen-rich composition. CO consumes most of the carbon in M stars and so there is little free carbon left over to form carbon-bearing molecules. The reverse is true in carbon stars. The oxygen is tied-up in CO and hence there is little free oxygen available to form oxides. Consequently the N star spectra do not reveal the presence of the bandheads of OH at $\lambda\lambda$ 2811, 3064 that can be seen in M stars. Several features in the N-star spectra are still unidentified however. Many of these probably arise from electronic transitions in carbon-containing molecules. However, assignment of a given absorption feature with a particular molecular band is difficult because of the low resolution and the crowded spectra.

The CH feature at 3143 Å weakens in the R stars, but is visible as early as R3. Not surprisingly, it is not seen in HD 182040, a well-known hydrogen-deficient carbon star (Warner 1967). Mg I λ 2852 appears as a strong absorption line in K and M stars. It is strong in the R stars as well. There is no strong feature at this wavelength in the N stars which could be interpreted as either an absorption or an emission line.

The Chromospheric Spectrum

A few chromospheric emission lines are visible in the IUE spectra, most notably Mg II and C II. Because of the heavy blanketing in the violet of N stars the chromospheric emission cores of Ca II H and K have not yet been observed. Consequently the Mg II and C II emission lines reported here represent the first convincing detection of a 10,000-20,000 K chromosphere in the N stars. The fluxes in the Mg II and C II lines are presented in Table 1 for a selection of the R, N and M stars. It can be seen that the fluxes are quite low, especially for the N stars, with the ratios of f(Mg II)/f(bol) ranging from one to two orders of magnitude smaller than in M stars.

If energy losses by conduction and mass flow can be neglected, the radiative losses in the chromospheric emission lines must balance the non-radiative energy input which heats the chromosphere. Ayres and Linsky (1978) concluded that the Mg II lines dominate these radiative losses. Consequently, the Mg II fluxes measured here would suggest that chromospheric heating has weakened appreciably in the evolved carbon stars. Before accepting such a conclusion, however, the complicating effects of the unknown opacity source must be considered.

The early N stars were selected for observation because they are expected to be much less heavily obscured than the later N stars. That they are not entirely free of this obscuration is evidenced simply by a comparison of exposure times for N and M stars of similar brightness. Nevertheless, there is no strong evidence that the LWR spectra are seriously mutilated by the ultraviolet opacity. Moreover, as noted earlier, the bulk of the evidence from visual and near ultraviolet spectra favor a photospheric origin for the opacity. If this is the case, the chromospheric features will clearly be

unaffected by the obscuration. Hence the fluxes tabulated below should represent an intrinsic weakening of chromospheric activity with age in the evolved carbon stars. Such an effect is only statistical in nature however. The metal deficient α Boo is a member of the old disk population and may well be one of the most evolved stars in the table. Nevertheless it has relatively intense Mg II emission. We also note that, in contrast to M supergiants, these N stars are not surrounded by extensive envelopes of dust and gas. Consequently, their chromospheric Mg II fluxes should not be appreciably weakened by absorption from the cool shell.

Finally, we note the smaller ratio of f(Mg II)/f(C II) in the N stars compared to the M stars. In TX Psc at least, carbon is enhanced by less than a factor of 2 over its solar value (Johnson, O'Brien and Climenhaga 1982) so the strength of the C II feature is not solely an abundance effect. High-resolution LWR spectra of the C II multiplet have yielded electron densities and chromospheric scale heights for bright M stars, but these N stars are, unfortunately, much too faint for such an analysis.

Table 1
Carbon II and Magnesium II Emission-Line Fluxes

Star	Spectral Type	$\frac{10^8 f(Mg)}{f(bol)}$	$\frac{10^8 f(c)}{f(bol)}$	$\frac{f(Mg)}{f(C)}$
TX Psc	N	10	5	2
T Ind	N	22	6	3.5
BL Ori	N	5	8	0.7
HD 37212	R8	< 140	< 240	--
HD 52432	R5	< 210	< 175	--
α Her	M5 II	130	--	--
72 Leo	M3 III	670	--	--
β Peg	M2 II-III	360	--	--
α Ori	M2 Iab	320	20	28
α Tau	K5 III	280	19	14
α Boo	K2 III	950	19	51

REFERENCES

Ayres, T. R., and Linsky, J. L., 1978, Ap. J. 220, 619.
Iben, I., 1981, Ap. J. 246, 278.
Johnson, H. R., O'Brien, G. T. and Climenhaga, J., 1982, Ap. J. 254, in press.
Scalo, J. M., 1976, Ap. J., 206, 474.
Tsuji, T., 1981, preprint.
Warner, B., 1967, M.N.R.A.S. 137, 119.

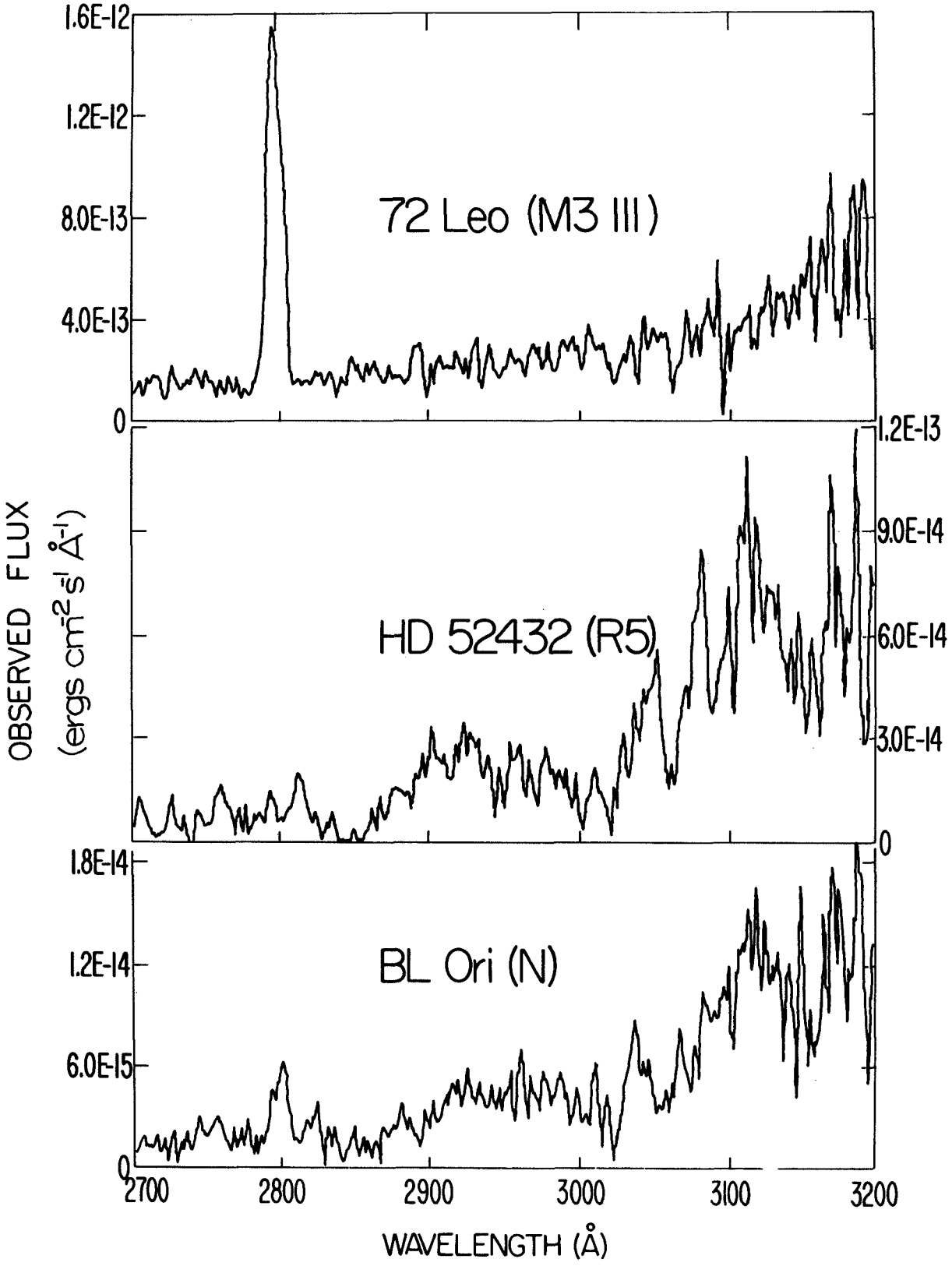
1.6E-12
1.2E-12
8.0E-13
4.0E-13
0
72 Leo (M3 III)
1.2E-13
9.0E-14
6.0E-14
3.0E-14
0
HD 52432 (R5)
1.8E-14
1.2E-14
6.0E-15
0
BL Ori (N)
OBSERVED FLUX
(ergs cm⁻² s⁻¹ Å⁻¹)
2700
2800
2900
3000
3100
3200
WAVELENGTH (Å)

HIGH DISPERSION FAR ULTRAVIOLET SPECTRA OF COOL STARS

Robert E. Stencel, Jeffrey L. Linsky,* Thomas R. Ayres†: Joint Institute for Laboratory Astrophysics, Univ. of Colorado and National Bureau of Standards

Carole Jordan, Alexander Brown‡: Oxford University

Oddbjorn Engvold: University of Oslo

ABSTRACT

We discuss recent far UV high dispersion spectra of two cool supergiant stars, Beta Dra (G2 Ib) and Alpha Ori (M2 Iab), which are examined in the context of current questions regarding stellar chromospheres, coronae and mass loss. These stars show very different outer atmosphere structure. Beta Dra has a geometrically thin transition region with bright emission lines of 10^5 K plasma that are red-shifted, indicating downflow in magnetic flux tubes. By contrast, Alpha Ori has a cool extended chromosphere and circumstellar envelope with large mass loss.

I. THE IMPORTANCE OF FAR UV HIGH DISPERSION SPECTRA

Unsolved problems concerning the winds of late-type stars include the geometry of the regions in which the flow occurs, the flow velocities, wind generation mechanisms, and mass loss rates. The cool supergiants are interesting in this regard, because some of these stars, the so-called "hybrids" possess both hot plasma comparable to the solar transition region (TR), and cooler outflowing gas at substantial terminal velocities (cf. Hartmann et al. 1980). Although these data might imply a continuous variation in outer atmospheric properties between late type stars of decreasing surface gravity, there is also considerable evidence that a discontinuous change occurs, separating the solar-like stars with hot, multi-million degree coronae and apparently small mass loss rates, from the noncoronal red giants and supergiants (see the invited papers by Dupree and Linsky in this volume, and references therein).

High resolution spectra of far ultraviolet emission lines in cool stars can provide key information in solving some of these problems. Such spectra which can be obtained only for the brightest cool stars with the IUE, permit measurements of spectral line shape parameters. These can be used to infer properties of the emitting plasma, such as the electron density, emitting volume and flow velocities.

II. THE OBSERVATIONS

These data were obtained with the IUE in its echelle mode of operation, as an international collaboration involving the Universities of Colorado, Oxford, and Oslo. For each spectrum, two or three consecutive eight hour shifts of IUE time were used to obtain the lengthy exposures. In some instances, the frequently noisy US2 shift was particularly quiet, permitting a 1273 min (21.2 hour) exposure of Beta Dra (SWP 15293).

---

*Staff Member, Quantum Physics Division, National Bureau of Standards.
†Laboratory for Atmospheric and Space Physics.
‡Department of Physics, Queen Mary College London.

In addition to the spectra of Beta Dra and Alpha Ori that are discussed below, we also obtained useful exposures of Beta Cet (K1 III, 795 minutes, SWP 14786) and 56 Peg (K0 IIp + wd, 1040 minutes, SWP 15283). Beta Cet is the coolest giant known to emit soft X-rays, and Eriksson et al. (1982) have computed a model chromosphere/TR that successfully matches the observed line profiles. 56 Peg is an interacting binary which has been analyzed by Schindler et al. (1982) in the context of "barium" binaries that contain cool giants and white dwarfs.

III. BETA DRACONIS

Beta Dra (HD 159181) is a G2 Ib star that lies in the Cepheid instability strip. Our 1273 minute echelle mode exposure (SWP 15293) shows emission features from a wide range of temperatures, from O I and Si II (8000 K) to C IV, Si IV and N V (150,000 K). Narrow intercombination lines of C I, O I, O III, Si III and C III were also detected. A photospheric continuum, appropriate for the 5700 K effective temperature, rises steeply toward the longwave end of the spectrum.

We have measured the line shape parameters for the emission features with a least-squares gaussian fitting procedure that yields line centroids, FWHM, and integrated fluxes. Using a flux-weighted average of the narrowest chromospheric lines to determine the stellar velocity scale, we find that the high temperature resonance lines are red-shifted by $+20\pm4$ km s^{-1}, suggesting systematic downflows in the TR gas relative to the chromosphere in Beta Dra (see Fig. 1). This result is similar to that seen in solar transition region lines, where the emission lines are formed mainly in downflowing gas in closed magnetic flux loops. Accordingly, the portions of the Beta Dra transition region that are bright in C IV and N V do not likely participate in any wind expansion, but instead should be formed in the infalling component of a circulation pattern.

Because the high temperature resonance lines probably do not participate in any wind expansion, their widths can be interpreted to be due to local Doppler motions. This concept is supported by the narrower intercombination lines of O III, Si III, C III that are formed at comparable temperatures. Furthermore, the lines of O I and Si II are of sufficient breadth as to be opacity broadened, and we propose this may also be the case in the high temperature lines.

As shown in Fig. 1c, a comparison of the surface flux ratios between Beta Dra and G2 V solar-like star Alpha Cen A (Ayres et al. 1982), indicates increasing relative emission measure with increasing temperature of formation. To estimate the geometrical thickness of the Beta Dra transition region, we derive the emission measure distribution by multiplying the solar distribution by the surface flux ratios in Fig. 1c and estimate $n_e = 2 \times 10^{10}$ cm^{-3} at $T = 5 \times 10^4$ K using four density sensitive line ratios. From these data we conclude that the transition region is geometrically thin like the Sun even if the emitting regions cover only a small fraction of the stellar surface. The corona, on the other hand, would be 0.01 stellar radii thick if the X-ray emission is uniform across the surface or perhaps extended if the emission is only from small regions.

Beta Dra is a close neighbor in the H-R diagram to the so-called "hybrid" stars Alpha Aqr (G2 Ib) and Beta Aqr (G0 Ib). Unlike the hybrids, Beta Dra

exhibits soft X-ray emission and lacks circumstellar absorption features. These data combined with the previous analysis lead us to suspect a discontinuous change in the outer atmospheric properties between solar like and nonsolar like stars, in the sense first argued by Linsky and Haisch (1979). There is sufficient indication to further hypothesize that magnetic topology is the controlling factor (see Mullan and Stencel, this volume).

IV. ALPHA ORIONIS

Alpha Ori (HD 39801) is the brightest M2 Iab supergiant visible from Earth. Consistent with its lack of soft X-ray emission (f_x/ℓ_{bol} less than 3×10^{-9}), our 930 minute echelle mode exposure (SWP 14775) lacks any trace of high temperature lines associated with transition regions. The observed emission features can be identified with O I, S I, Si II and Fe II. Comparison of high and low dispersion spectra of Alpha Ori indicates that bright low dispersion emission features which are not seen in high dispersion may in many cases be diffuse atomic or molecular bands, such as 1541Å CO emission (Ayres et al. 1981). In high dispersion, the lines of S I appear doubly reversed, suggesting very high opacity. The total lack of the O I 1300Å and S I 1295Å fluorescent lines also argues for considerable circumstellar absorption. This level of absorption is consistent with the arguments for an extended cool chromosphere surrounding such noncoronal giants and supergiants (cf. Stencel 1982).

An interesting result of this exposure, not detected in previous shorter echelle mode observations, is the appearance of the Fe II (UV 191) mutiplet in emission near 1785 Å. These lines are seen prominently in emission in the spectra of the late type supergiant eclipsing binaries like Zeta Aur, 32 Cyg and VV Cep. In those cases the continuum of the hot dwarf companion can populate the 10 eV upper state via Fe II UV9 lines near 1270Å (see Stalio and Selvelli 1981). However, such pumping seemingly should not occur for Alpha Ori given its lack of a hot companion or high temperature material in its outer atmosphere. The high excitation Fe II emission may represent a preferred deexcitation channel for Fe II excited by free electrons or multiply scattered Lyman photons in the vast chromosphere of Betelgeuse.

We wish to thank the resident astronomers and telescope operators for their invaluable assistance in making these exceptional observations. We also thank NASA, SRC and ESA for their support.

REFERENCES

Ayres, T.R., Moos, H.W. and Linsky, J.L. 1981, Ap J., 248, L137.
Ayres, T.R., Simon, T. and Linsky, J.L. 1982, in preparation.
Eriksson, K., Linsky, J.L., and Simon, T. 1982, in preparation.
Hartmann, L., Dupree, A.K. and Raymond, J. 1980, Ap. J., 236, L143.
Linsky, J.L. and Hasich, B.M. 1979, Ap. J., 229, L27.
Raymond, J.C. and Smith, B.W. 1977, Ap. J. Suppl., 35, 419.
Raymond, J.C. and Doyle, J.G. 1981, Ap. J., 247, 686.
Schindler, M., Stencel, R.E., Basri, G.S. Linsky, J.L. and Helfand, D.J. 1982, Ap. J., in press.
Stalio, R. and Selvelli, P.L. 1981 The Universe in UV Wavelengths, ed. R. Chapman, NASA CP-2171, p. 201.
Stencel, R.E. 1982, in Proceedings of the Second Cambridge Workshop on Cool Stars, ed. M. S. Giampapa, SAO Spec. Report, in press.

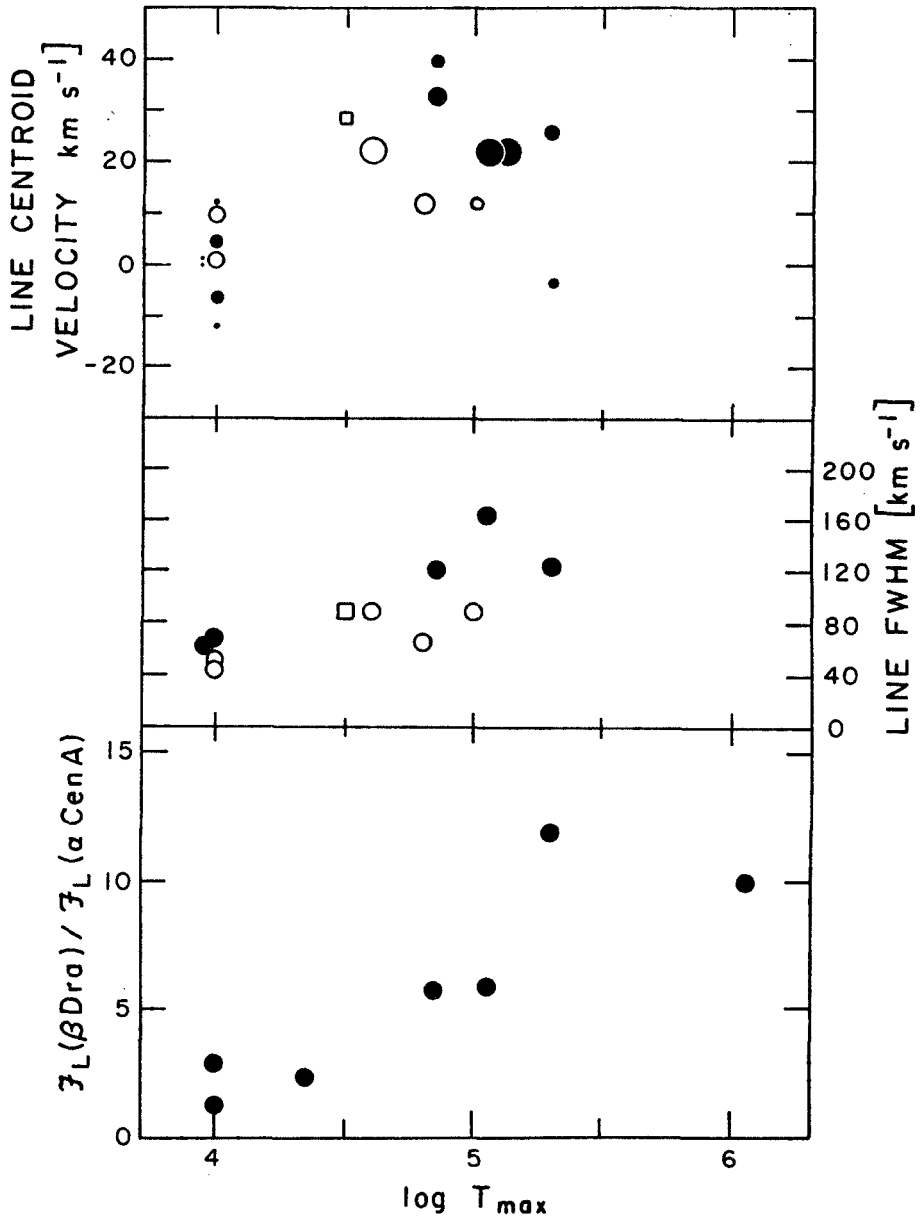

Fig. 1. The top panel shows emission line centroid velocities for emission lines in Beta Dra, with symbol size proportional to flux. The open circles are intercombination lines, filled circles are resonance lines and the square is He II 1640 Å. The middle panel shows the FWHM of these features. The bottom panel shows a comparison of surface fluxes of lines in the spectra of Beta Dra and Alpha Cen A. For each line the corresponding volume emission measures should be proportional to the surface fluxes.

UV EMISSION FROM THE M1 SUPERGIANT TV GEM

by

A.G. Michalitsianos

and

M. Kafatos*

Laboratory for Astronomy and Solar Physics

NASA Goddard Space Flight Center

Greenbelt, Maryland

ABSTRACT

Low and high dispersion ultraviolet spectra were obtained of the M1 supergiant TV Gem with IUE. Previous IUE observations of this late type supergiant revealed unexpected UV continuum emission, perhaps arising from an early B companion. Low resolution spectra obtained approximately one year apart suggest that the strong Si III in combination perhaps with O I at wavelengths $\sim$ λ1300 A varies considerably with time. Large variation in the column density is required to explain these changes. Sporadic mass expulsion with mass loss rates $dM/dt \sim 10^{-5}\ M_{\odot}\ yr^{-1}$ from the M supergiant could lead to a dense circumstellar wind near the hot early companion, and thus could account for these observed variations in equivalent width. The high resolution spectrum in the λ2000 to 3200 A wavelength range is characterized by narrow absorption lines primarily due to Fe II, Mn II and Mg II (h and k), which are skewed in profile with an extended red wing. We tentatively attribute this profile structure to interstellar absorption and an intervening differentially moving cloud in the direction of Gem OB1, of which TV Gem is a known association member.

INTRODUCTION

The late type supergiant TV Gem = HD 42475 (M1 Iab) that was found to exhibit strong UV continuum (Michalitsianos, Kafatos and Hobbs 1980) has been re-investigated with IUE. A comparison of low dispersion spectra obtained in the SWP wavelength range approximately one year later suggests that a few of the strong absorption features attributed to S II?, Si III and C II vary with time. Previously we have applied an interstellar correction to the UV continuum of E(B-V)=0.4, consistent with early estimates for reddening obtained in the visual by Crawford et al. (1955) and Eggen (1967). However, this extinction correction did not fully correct for the strong λ2200 A feature which is clearly present in our LWR (λ2000 to 3200 A) spectra. Rather, more recent estimates of E(B-V)=0.65 (A_V = 2.16) of Humphreys (1978) agrees more closely with the strength of the λ2200 A feature observed with IUE. We adopt an E(B-V)=0.65 and show the de-reddened spectra for different observing epochs in Figure 1.

*on leave spring semester from George Mason University

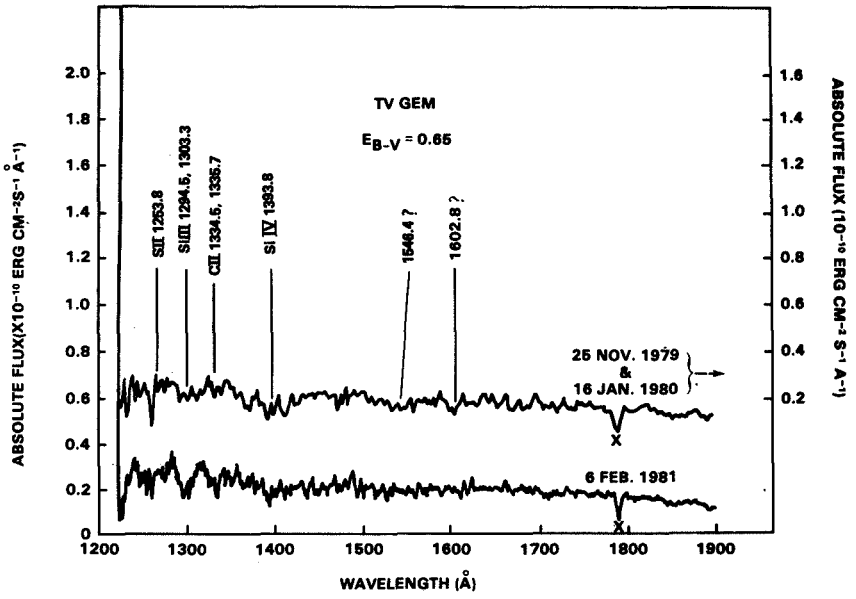

Figure 1

The continuum distribution in the SWP (λ1200 - 2000 A) wavelength range corrected with E(B-V)=0.65 is best approximated by an early B type companion. The presence of Si III, Si IV and possibly S II is consistent with absorption features that characterize UV spectra of early type stars, although variations in the absorption strengths of these features suggests somewhat more complicated processes are present. This follows because considerable variations in column densities are required to produce the observed changes. Possibly, sporadic mass ejection in the wind of the M supergiant results in large variations in column density along the line-of-sight with $\rho \sim 10^{13}$ cm^{-3}. Such high values in wind density are unusual, but are required to explain the changes in equivalent widths for Si III and/or O I.

Additionally, high resolution spectra obtained in the LWR wavelength range (λ2000 - 3200 A) reveal narrow absorption lines which are attributed to interstellar Mn II, Fe II and Mg II (h and k). The strong h and k lines of Mg II (λλ2795, 2802 A) centered at their rest wavelengths appear skewed in profile in the sense of an extended red wing. Skewed profiles of interstellar Mg II also characterize the line profiles of Mn II, but are not as clearly evident in Fe II. This skewness is possibly explained by an intervening differentially moving cloud ($\sim$+20 km s^{-1}) in the direction of Gem OB1, of which TV Gem is a known association member, and which is estimated to be $\sim$1400 pc (Crawford et al. 1955). Our observing program and analysis of data follows. The apparent magnitude corrected for extinction is m_V = 6.58.

OBSERVING PROGRAM

In Figure 1 the SWP spectra for 25 November 1979 and 16 January 1980 (10 minute exposures each) have been averaged together in order to reduce the relative noise in the data. Inspection of the individual spectra for each of these dates indicates that the absorption features present did not

change. A 40-minute SWP spectrum on 6 Feb. 1981, however, clearly indicates significant increases in absorption strength at λλ1256, 1300 and 1334 A. Sufficient signal was not obtained that absorption features could be discerned with an 8-hour SWP exposure.

Table 1

Ion	Multiplet	λIUE(A)	λLaboratory(A)
S II?	1	1259.8	1253.8
Si III	4	1295.5	1294.5-1303.3(6 lines)
O I?	2	1301.0	1302.2
C II	1	1333.0	1334.5,1335.7
Si IV	1	1393.4	1393.8
C IV?	1	1546.4?	1548.2,1550.7
Fe II?		1435.6	1434.9
Fe II?	193	1473.4	1473.8
Fe II?	38	1708.6	1708.6
Fe II?	397	1844.4	1844.6
Fe II?	65	1853.8	1852.4

A number of ions indicated with ? in Table1 are tentatively shown. In Table 2 absorption lines detected with the high dispersion LWR camera are given, that are corrected for Earth and satellite motion (+22.5 km s^{-1})

In Figure 2 the Mg II (h&k) lines are shown at their measured wavelengths, which is very close to the rest wavelengths. Two unidentified lines are present, where the feature at λ2798.9 A should not be confused with the subordinate line Mg II mul. (3) λ2797.9 A. Its associated line at λ2790.8 A is not present. The unidentified feature at λ2800.5 A appears real and may be a blend of high order multiplets of Mn II (6), (7), (20), (21) and (22). Figure 3 shows the strongest Mn II (1) line which exhibits similar structure as Mg II (h & k).

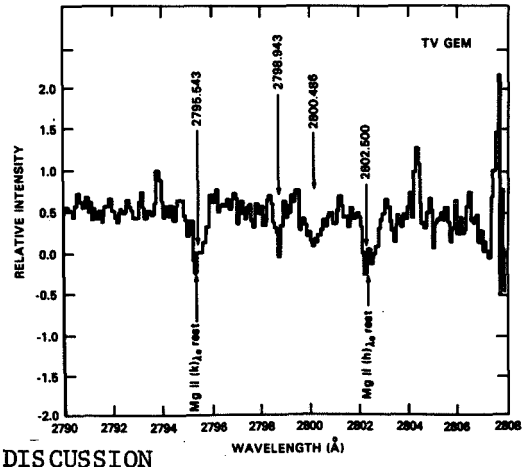

Figure 2

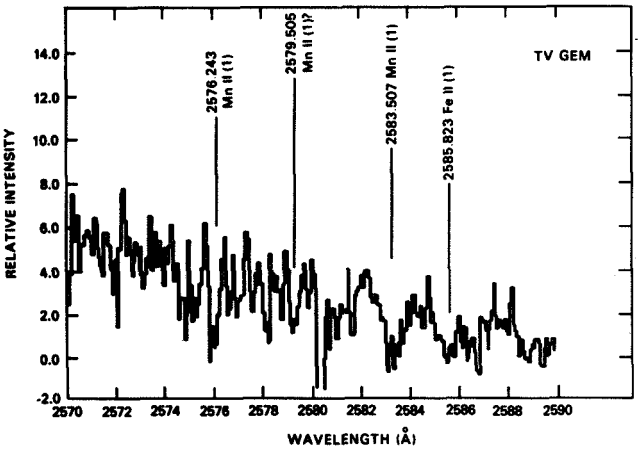

Figure 3

DISCUSSION

The average UV continuum flux observed throughout the entire sensitivity range of IUE is $F_\lambda \sim 2 \times 10^{-11}$ erg cm^{-2} s^{-1} A^{-1}, after applying an interstellar extinction correction E(B-V)=0.65 to the observations. The relative apparent visual magnitudes between primary and secondary stars can be obtained by extrapolating the corrected UV continuum to the visual. The bolometric magnitude is derived that corresponds to a distance d ∿ 1400 pc for which $M_{bol} \sim -3.0$. This value of M_{bol} lies well within the range of a B5 to B0 star (Allen 1973) if the secondary is a main sequence type companion. For a B5 star, $M_V = -1.1$ and $m_V \sim 11.8$, and correspondingly for a B0 star, $M_V = -4.1$ and $m_V \sim 8.8$. The relative magnitude differences between primary

Table 2

High Dispersion LWR Spectrum

Ion	Multiplet	λ IUE (A)	λ Laboratory (A)
Fe II	3	2343.5	2343.495
Fe II	2	2373.8	2373.733
Fe II	2	2382.2	2382.034
Mn II		2492.9	2492.716
Mn II	1	2576.2	2576.107
Fe II		2579.5	2579.406
Mn II	1	2583.5	2583.538
Fe II	1	2585.8	2585.876
Mn II	1	2593.8	2593.731
?		2599.3	
Mn II	1	2605.7	2605.697
Mn II		2617.3	2616.934
Mn II	19	2618.5	2618.145
Fe I		2738.0	2732.832
Mn I		2738.9	2738.861
Mn II		2740.4	2740.161
Mg II (k)	1	2795.5	2795.523
?		2798.9	
?		2800.5	
Mg II (h)	1	2802.5	2802.697
Fe II	255	2826.3	2826.024
Fe I		2827.9	2827.670
Mn II	2865	2865.7	2865.600

and secondary, respectively are $\Delta m_V \sim 5.2$ and 2.2, a sufficiently large difference that the secondary can remain undetected in the visual. As found by Michalitsianos et al. (1980) the companion dominates the integrated light at wavelengths $\lambda < 3600$ A.

The Si III $^3P^o$–^3P multiplet has an equivalent width of ∿6100 mA in Feb. 1981 (for all 6 lines), and if compared to our previous low resolution spectra has attainted this width over a period 1 year. Using the "square root" portion of the curve of growth curve we find column densities $n(\text{Si III}, ^3P^o)L \sim 3.5 \times 10^{23}$ cm^{-2}, which corresponds to atomic parameters for this multiplet of Weise, Smith and Glennon (1966), where $n(\text{Si III}, ^3P^o)$ is the number density of Si III ions in $^3P^o$ (lower level of $^3P^o$–^3P). Because $^3P^o$ levels are metastable to the ^1S level, the population of the $^3P^o$ levels builds up collisions from the ground state. Writing the equilibrium equation for the three lowest levels for Si III, namely ^1S (ground state), $^3P^o$ (6.6 eV above ground) and the $^7P^o$ (10.3 eV above ground), we find that the relative abundance of the $^3P^o$ levels is

$$N(^3P^o) \sim \omega_1 e^{-E_{21}/kT} / [\omega_1 (\tfrac{\omega_2}{\omega_1} e^{-E_{21}/kT} + 1) + \omega_1 e^{-E_{32}/kT}] , \quad (1)$$

where "1", "2" and "3" refer to the ^1S, $^3P^o$ and $^1P^o$ states, respectively. It follows that if $T \sim 17{,}000$K appropriate for a B star (B3), then $N(^3P^o) \sim 0.1$, $N(^1S) \sim 0.9$ and $N(^1P^o) \ll N(^3P^o)$, $N(^1S)$. It follows from equation (1) that the lower limit to column hydrogen density (assuming cosmic abundances) is $nL \sim 4 \times 10^{24}$ cm^{-2}, where n is the hydrogen density and L the pathlength through the region.

If we use the wind equation $\dot{M} = 4\pi R^2 m_H v$ and use $R \sim L/2$ appropriate for a B3 star ($R \sim 5.2 R_\odot$) and $v \sim 700$ km s^{-1} (B3 star of $7M_\odot$), we find that $\dot{M} \gtrsim$ 1.6×10^{-5} $M_\odot$ yr^{-1}. We note that the mean laboratory wavelength for transition λ1298.9 A is ∿2 A redward of the observed feature, indicating possibly mass motion ∿450 km s^{-1}. Had we used the wind equation appropriate to a red supergiant, i.e. $v \sim 100$ km s^{-1} and $R \sim 600 R_\odot$ we would find (assuming a $T \sim 10^4$K shell around the supergiant) that $\dot{M} \gtrsim 6 \times 10^{-3}$ $M_\odot$ yr^{-1}, which would be reflected in

in changes of zero volt lines such as O I λ1302.2 A. If most of the changes in equivalent width around λ1300 A is attributed to Si III, the absorbing region would have to be located near the B star. At present it is not clear as to which of the two stars this large value of $\dot{M} \sim 10^{-5}$ $M_\odot$ yr^{-1} actually refers. Unfortunately, the present low dispersion spectra cannot provide unambiguous information regarding the velocity profiles of these observed features. Mass loss rates $\sim 10^{-5}$ $M_\odot$ yr^{-1} are substantially large compared to typical values associated with either early B stars (cf. Cassinelli 1979), or late type supergiants (cf. Goldberg 1979). If, however, material is expelled from the cool M supergiant in sporadic bursts, the presence of dense material in the direction of the B companion could provide spectroscopic indications of the total mass loss from the supergiant, in a manner similar to that found for α Sco by van der Hucht et al., (1980) who suggest a large extended dusty region for this star. TV Gem is likely another example of such systems, where UV continuum arising from the early companion enables us to obtain additional spectroscopic methods of examining mass loss from late type supergiants. Further UV-satellite observations could resolve this question if high dispersion spectra were feasible in the λ1200-2000 A wavelength range. Perhaps Space Telescope will provide the clues?

REFERENCES

Allen, C.W. 1973, Astrophysical Quantities (3d ed.; London:Athlone Press).
Cassinelli, J.P. 1979, Ann. Rev. Astr. and Astrophys., 17, 275.
Crawford, C., Limber, D.N., Mendoza, V., Schulte, S., Steinman, H. and Swihart, T. 1955, Astrophys. J., 121, 24.
Eggen, O.J. 1967, Astrophys. J., 14, 307.
Goldberg, L. 1979, Q. Jl. Roy. Ast. Soc., 20, 361.
Humphreys, R. 1978, Astrophys. J. Supp., 38, 309.
Michalitsianos, A.G., Kafatos, M. and Hobbs, R.W. 1980, Astrophys. J., 241, 774.
van der Hucht, K.A., Bernat, A.P. and Kondo, Y. 1980, Astron. and Astrophys., 82, 14.
Weise, W.L., Smith, M.W. and Glennon, B.M. 1966, Atomic Transition Probabilities, vol. II (NSRDS-NBS 4).

On the Correlation Between Chromospheric and Coronal Emission

R. Hammer and J. L. Linsky*
Joint Institute for Laboratory Astrophysics, University of Colorado and
National Bureau of Standards, Boulder, Colorado 80309 U.S.A

and

F. Endler
Institut für Astronomie und Astrophysik, Am Hubland, D-8700 Würzburg, FRG

ABSTRACT

According to empirical chromospheric models, the mechanical (magnetic and non-magnetic) energy flux F_M decreases over large parts of the solar chromosphere less rapidly than the pressure p ($d \log F_M / d \log p < 1$). The total energy loss F_{Loss} of the transition region and corona, on the other hand, increases faster than the pressure, p_{TR}, of the transition region ($d \log F_{Loss} / d \log p_{TR} > 1$), as is indicated by theoretical models of coronal loops and open coronal regions as well as by semiempirical studies. Therefore, the relation $d \log F_M / d \log p < d \log F_{Loss} / d \log p_{TR}$ appears to be generally valid. In the present study we discuss the implications of this relation. We show that it explains qualitatively the recent observational result of Ayres, Marstad and Linsky (1981) that with increasing stellar activity the emission of the transition region and corona increases faster than the emission of the chromosphere. It also explains why the pressure of the transition region increases with increasing stellar activity. Further, we show that this relation is a necessary requirement for the global stability of the chromosphere/transition region/corona system.

INTRODUCTION

Systematic studies based on IUE observations (Ayres, Marstad and Linsky 1981, Walter 1982) show that with increasing stellar activity the emission of the transition region and corona increases faster than the chromospheric emission. Further, it is known (cf. Linsky 1980) that the pressure of the transition region increases with increasing chromospheric activity. Similar correlations between chromospheric and coronal energy losses and the pressure of the transition region exist for regions of varying activity on the Sun. In the present study we want to explain these observed trends. Obviously, such an explanation necessitates the combination of chromospheric and coronal models. Since, however, the detailed physics of chromospheric and coronal heating is presently unknown, it is not possible to derive the observed correlations quantitatively. Nevertheless, we want to point out that all existing chromospheric and coronal models (both for magnetically closed and open coronal regions) fulfill a requirement that suffices to explain the observed trends qualitatively.

*Staff Member, Quantum Physics Division, National Bureau of Standards.

COMBINING CHROMOSPHERIC AND CORONAL MODELS

The energy losses of a chromosphere and corona are balanced by the mechanical energy flux, which presumably includes various kinds of mechanisms, like hydrodynamic and magnetohydrodynamic waves, flux tube twisting, etc. Owing to the chromospheric radiative losses, the total mechanical energy flux F_M decreases in the chromosphere with increasing height and thus decreasing pressure p (see Fig. 1). The transition region is situated at a certain pressure p_{TR}. The remaining mechanical energy flux F_{TR} at this point balances the total radiative energy losses of the transition region and corona; in magnetically open coronal regions it also accounts for the energy losses due to stellar wind and outward thermal conduction (cf. Hammer 1982a,b).

In order to illustrate the chromospheric decrease of F_M with decreasing pressure, we have integrated (see Fig. 1) the radiative losses ($-\nabla \cdot F_M$) of the chromospheric models A, C, and F of Vernazza, Avrett and Loeser (1981 — hereafter VAL; see also Avrett 1981). The integration was performed in the inward direction, starting at the point where the temperature of the models reaches 2×10^4 K. We have identified this point with the base of the transition region ($p = p_{TR}$, $F_M = F_{TR}$). To obtain the integration constant, we have assumed that the remaining energy flux F_{TR} balances the energy losses of a coronal loop of pressure p_{TR} and semilength $S = 5 \times 10^9$ cm, of the type discussed by Rosner, Tucker and Vaiana (1978 — RTV; see their eq. [4.4]),

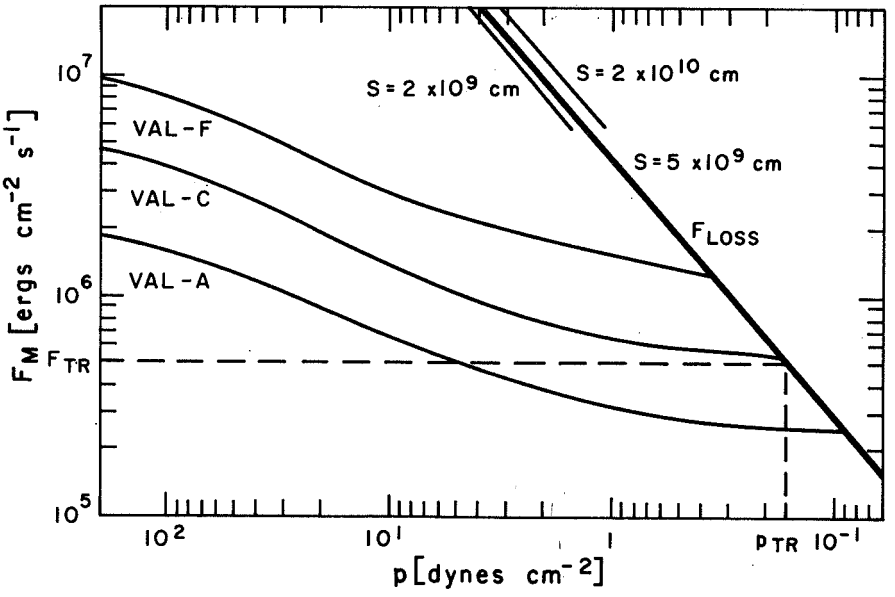

Fig. 1. Total mechanical energy flux F_M as a function of the pressure p for the chromospheric models A, C, and F of Vernazza, Avrett and Loeser (1981). The transition region lies at the intersection point with a curve (drawn heavy) that gives the total energy losses F_{Loss} of the transition region and corona as a function of the base pressure and the semilength S of the coronal loops (cf. eq. [1]).

$$F_{TR} = F_{Loss} = 9.8 \times 10^4 \, p_{TR}^{7/6} S^{1/6} \qquad (1)$$

Since F_{Loss} depends only very weakly on S, as is shown in the upper part of Figure 1, the special choice of the loop length does not affect our general arguments. Further, we want to note that scaling laws of this kind are known to be very insensitive to the details of the coronal heating law, the loop geometry, and the boundary conditions (cf. Pallavicini et al. 1981 and references cited therein).

Model A of VAL refers to a dark point (in the EUV continuum) on the Sun, model C to the average solar chromosphere, and model F to a very bright network element. Therefore, the sequence A-C-F illustrates the effects of increasing chromospheric emission and increasing average magnetic field strength. Obviously with increasing activity the chromospheric curve log F_M (log p) is shifted upward in Figure 1, with largely unchanged slope. Therefore, the intersection point with the coronal curve log F_{Loss} (log p_{TR}), which defines the pressure and energy flux at the base of the transition region, is shifted toward the upper left in the diagram. This explains the observed trends that with increasing chromospheric activity the pressure of the transition region and the total energy losses of the transition region and corona increase and that the coronal losses increase stronger than the chromospheric losses. This explanation remains valid if with changing activity the geometry of the coronal loops or the details of coronal heating change, because F_{Loss} (p_{TR}) depends only weakly on these parameters.

Moreoever, our explanation does not depend on any particular property of the chromosphere models of VAL and the coronal loop models of RTV. The single requirement that must be met in order to explain the observed correlations is that the slope of the chromospheric curves is smaller than the slope of the coronal curve,

$$\frac{d \log F_M}{d \log p} < \frac{d \log F_{Loss}}{d \log p_{TR}} \qquad (2)$$

Over large parts of the solar chromosphere the average value of d log (dF_M/dr)/d log p is about 0.7 in the VAL models. However, since the integration constant F_{TR} is always positive, the slope of the integrated radiative losses is smaller. From Figure 1 we find d log F_M/d log p $\lesssim$ 0.5. In any case, even if the VAL models are modified in the future, it is safe to assume that the slope of the chromospheric curves is everywhere smaller than 1. On the other hand, the slope (d log F_{Loss}/d log p_{TR}) of the coronal curve is larger than 1. This is not only true for the loop models of RTV, but also for other published models of coronal loops and open coronal regions (cf. Hammer 1982b, Fig. 2). Further, it has also been confirmed by semiempirical studies (Jordan 1980, Fig. 4). Consequently, relation (2) appears to be generally valid, irrespective of the underlying chromospheric and coronal models. In the following we show that this relation is also a necessary requirement for the global stability of the whole outer atmosphere.

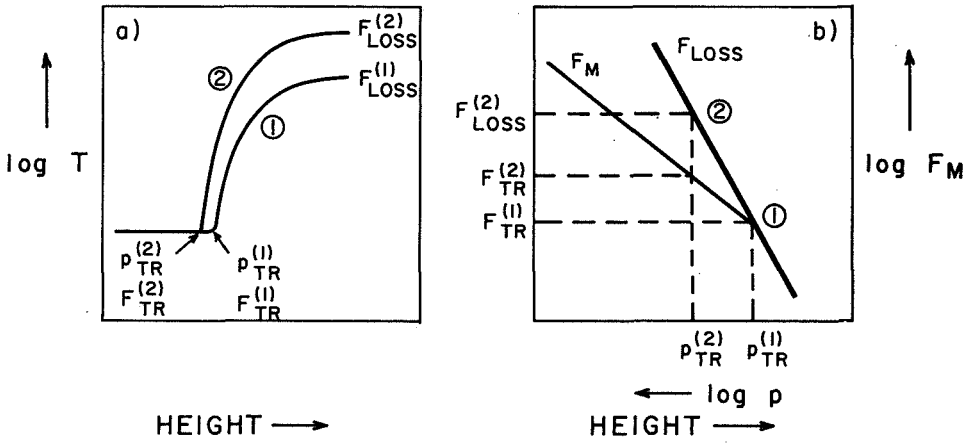

Fig. 2. Global stability of the system chromosphere/transition region/corona (schematic). Left Panel: The equilibrium model (index 1) is perturbed to a state with larger coronal pressure, temperature, and energy losses (index 2). Right Panel: Schematic energy flux vs. pressure diagram (cf. Fig. 1). If the coronal curve (F_{Loss}, drawn heavy) is steeper than the chromospheric curve (F_M), the perturbed corona receives less energy ($F^{(2)}_{TR}$) than it loses ($F^{(2)}_{Loss}$); hence, it cools and moves back toward the initial state.

STABILITY

Let us consider an equilibrium model of the chromosphere/transition region/corona system. The temperature as a function of height for such a model is schematically shown in Figure 2a (index 1). For this equilibrium model the pressure $p^{(1)}_{TR}$ and energy flux $F^{(1)}_{TR}$ at the base of the transition region are determined by the intersection of the chromospheric curve $F_M(p)$ and the coronal curve $F_{Loss}(p_{TR})$ in Figure 2b, as we have discussed before.

We now investigate the effects of a special perturbation of the transition region and corona, during which the coronal boundary conditions remain roughly valid. We assume that the corona is perturbed from a valid steady-state model (index 1) to another valid steady-state model (index 2). For this kind of perturbation the relation between the base pressure and the total energy losses of the transition region and corona is described by the coronal curve $F_{Loss}(p_{TR})$ in Figure 2b. If the total energy losses increase from the equilibrium value $F^{(1)}_{Loss} = F^{(1)}_{TR}$ to $F^{(2)}_{Loss}$, the base pressure increases from $p^{(1)}_{TR}$ to $p^{(2)}_{TR}$. Therefore, the transition region is shifted towards the photosphere, and the thickness of the chromosphere as well as the chromospheric radiative losses are reduced. Consequently, the mechanical energy flux at the base of the transition region increases from $F^{(1)}_{TR}$ to $F^{(2)}_{TR}$ according to the chromospheric curve $F_M(p)$ in Figure 2b. If, as shown in Figure 2b, the coronal curve is steeper than the chromospheric curve, the energy losses, $F^{(2)}_{Loss}$, of the perturbed transition region and corona are larger than the available mechanical energy flux $F^{(2)}_{TR}$. Consequently, the corona tends to reduce the energy losses, and the system evolves back towards the initial state. (The

details of this time-dependent process depend on the geometry, boundary conditions, and heating law of the coronal model. For an estimate of the relevant time scales see Eqs. [1]-[3] of van Tend [1979].) Therefore, the system is stable against this kind of perturbation. On the other hand, if the coronal curve would be less steep than the chromospheric curve, then the system would be instable. The present argument corresponds essentially to the classical concept of thermal stability; however, we have not used this concept as a local criterion, but we have applied it to the complete chromosphere/transition region/corona system.

FINAL REMARKS

To summarize, we have shown that the observed correlations between chromospheric and coronal emission and the pressure of the transition region may be explained by the fact that existing models of chromosphere and corona fulfill relation (2); and that this relation is a necessary requirement for stability.

In Figure 1 we have fitted the chromospheric and coronal models at 2×10^4 K because this is the temperature at the base point of the RTV models. However, this method probably underestimates the Lα losses at the foot of the transition region. Therefore, we have also investigated the possibility of significantly enhanced Lα losses, which may be supplied either from above or below, so that either the coronal or the chromospheric curve in Figure 1 must be modified. Further, we have investigated the possibility that p_{TR} is not determined by the coronal energy requirements, as was assumed in the present discussion, but that p_{TR} and the ratios of Lα to coronal losses are determined solely by the chromospheric physics. We have investigated all of these possibilities; this discussion will be published elsewhere (in preparation). This added complexity does not change our present arguments in general, but only in detail. In all cases the observed correlations appear to be qualitatively a natural consequence of the underlying physics of chromosphere, transition region, and corona. Hopefully, the quantitative correlations will help us to understand more of this physics.

REFERENCES

Avrett, E. H. 1981, in Solar Phenomena in Stars and Stellar Systems, eds. R. M. Bonnet, A. K. Dupree (Dordrecht: D. Reidel), p. 173.

Ayres, T. R., Marstad, N. and Linsky, J. L. 1981, Ap. J., 247, 545.

Hammer, R. 1982a, Ap. J., in press (August 15).

Hammer, R. 1982b, Ap. J., in press (August 15).

Jordan, C. 1980, Astron. Ap., 86, 355.

Linsky, J. L. 1980, in Stellar Turbulence, Proceedings of the IAU Colloq. No. 51, eds. D. F. Gray and J. L. Linsky, p. 248.

Pallavicini, R., Peres, G., Serio, S., Vaiana, G. S., Golub, L., Rosner, R. 1981, Ap. J., 247, 692.

Rosner, R., Tucker, W. H., Vaiana, G. S. 1978, Ap. J., 220, 643.

van Tend, W. 1979, Solar Phys., 64, 229.

Vernazza, J. E., Avrett, E. H., Loeser, R. 1981, Ap. J. Suppl., 45, 635.

Walter, F. M. 1982, this volume.

ULTRAVIOLET OBSERVATIONS OF YELLOW GIANT STARS

Theodore Simon
Institute for Astronomy, University of Hawaii
Jeffrey L. Linsky*
Joint Institute for Laboratory Astrophysics
National Bureau of Standards and University of Colorado

ABSTRACT

Low-dispersion spectra of 18 yellow giant stars of spectral types G4-K0 were obtained with the short wavelength camera of IUE. Using the emission strength of the C IV 1550 Å multiplet as a measure of high temperature 10^5 K plasma, we find that the normalized C IV flux, $f_{C\ IV}/\ell_{bol}$, where ℓ_{bol} is the apparent stellar bolometric flux, is typically 10^{-7} or smaller, indicating very feeble stellar transition regions. By combining these results with earlier data from IUE, we show that there is nearly a two orders of magnitude spread in $f_{C\ IV}/\ell_{bol}$ among the yellow giants. Several likely reasons for the observed range in high-temperature emission line strengths are discussed; the more likely appears to be that the majority of the yellow giant stars observed are slow rotators evolving across the Hertzsprung Gap for the second time along a blue loop.

INTRODUCTION

Among single late-type giants and supergiants, strong UV emission from 10^5 K plasma and strong X-ray emission from 10^6-10^7 K plasma are often detected from high luminosity G-K stars having V-R $\lesssim$ 0.8 (Linsky and Haisch 1979; Simon et al. 1982; Ayres et al. 1981). Cooler high-luminosity stars, the red giants and supergiants, generally show evidence for much weaker transition region (TR) and coronal emission, in some cases with very low upper limits. This observed dichotomy in the detection of stellar TRs and coronae has led to speculation that the apparent weakness, or perhaps disappearance, of high temperature plasma among the late K-M giants and supergiants may be due to the onset of massive cool winds (cf. Linsky and Haisch 1979).

X-ray surveys with the Einstein (HEAO-2) Observatory of luminous G stars, on the other hand, show a wide range of coronal emission measures of more than three orders of magnitude (Ayres et al. 1981). This paper briefly summarizes the findings of two IUE Guest Observer programs involving yellow giant stars (V-R $\lesssim$ 0.8). In parallel with the large spread in coronal emission, we have observed a range in the brightness of UV emission lines from 10^5 K plasma of more than a factor of 20.

---

*Staff Member, Quantum Physics Division, National Bureau of Standards.

OBSERVATIONS

IUE spectra of 18 G4-K0 giants and bright giants (luminosity class III or II) have been obtained in low dispersion with the SWP camera and in high dispersion with the LWR camera. In the short wavelength region, exposure times of 2-3 hours were needed to determine fluxes, or flux upper limits, for weak emission lines of N V, C II, Si IV, and C IV. We measured emission strengths for all of these ions, but here we discuss only the C IV data as representative of the high temperature lines. The LWR spectra are all well exposed at the 2800 Å Mg II h-k emission lines, which are representative of 10^4 K chromospheric emission.

The C IV data are presented in a pseudo-HR diagram in Fig. 1. The size of an open circle indicates the strength of a detected C IV emission feature, and the closed circles denote corresponding upper limits. The measured line

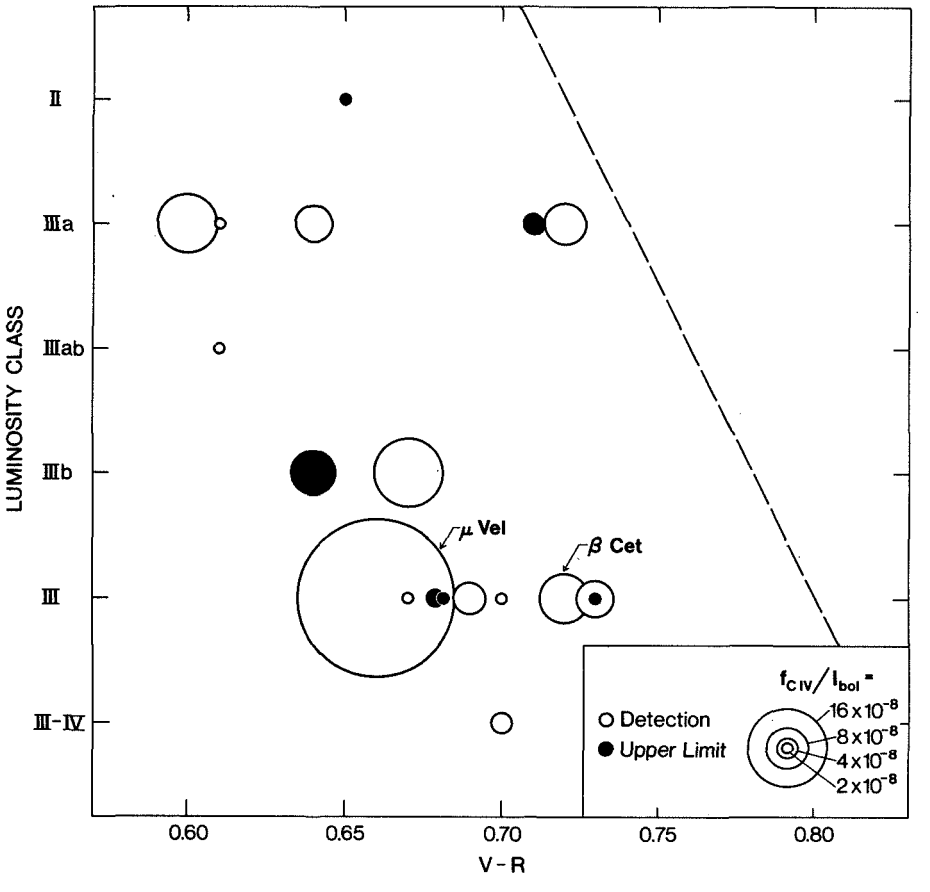

Fig. 1. Ratios of the C IV 1550 Å flux to the apparent bolometric luminosity are plotted for the G4-K0 giants in our sample as open circles (detections) or closed circles (upper limits). The dashed line is the dividing line between regions of the HR diagram containing stars generally with or without evidence for 10^5 K plasma as proposed by Linsky and Haisch (1979).

strengths are plotted as normalized flux ratios $f_{C\ IV}/\ell_{bol}$, where $f_{C\ IV}$ is the observed line flux and ℓ_{bol} the apparent stellar bolometric luminosity. For comparison we also plot μ Vel and β Cet, two stars observed by Linsky and Haisch (1979). In Fig. 1 there appears to be no obvious trend either with V-R (T_{eff}) or luminosity, although luminosity subclasses are currently available for fewer than half of the stars.

In Fig. 2 we plot the C IV:Mg II flux ratio against color index, V-R. The line ratio $f_{C\ IV}/f_{Mg\ II}$ measures the differential emission measure of 10^5 K plasma and 10^4 K plasma. Again, no obvious trends are apparent.

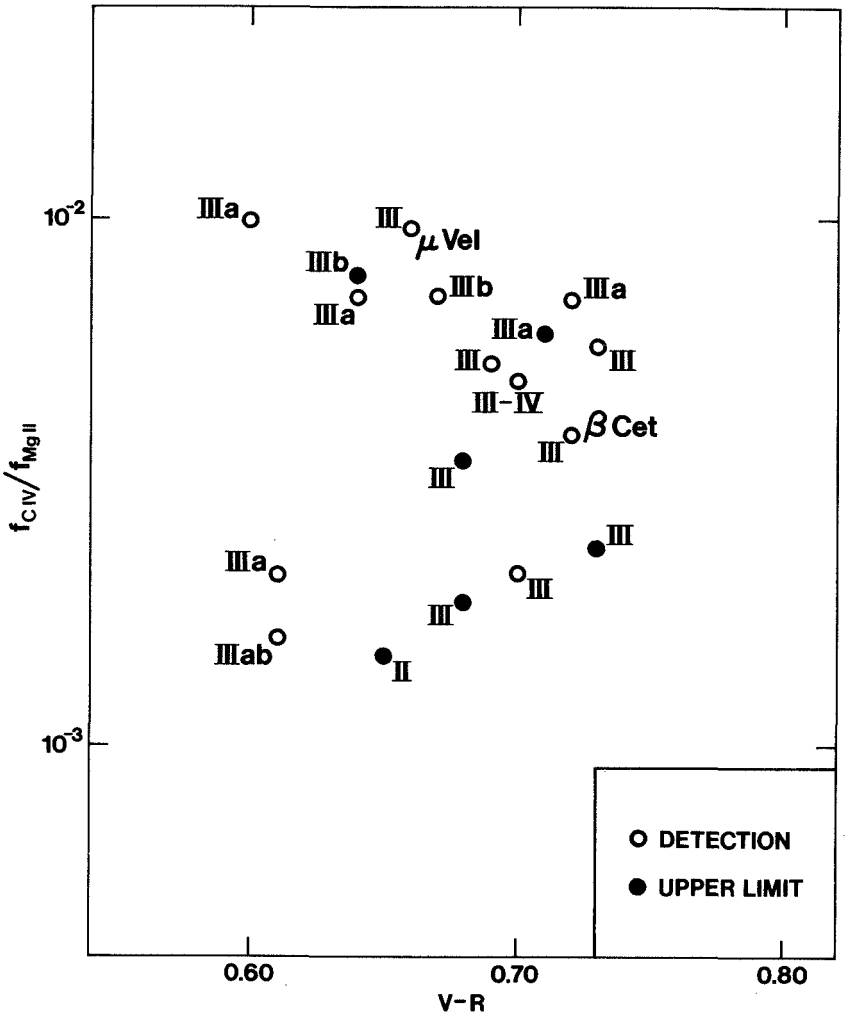

Fig. 2. Ratios of the C IV 1550 Å flux to the Mg II 2796, 2803 Å flux for the G4-K0 giants in our sample. Stellar luminosity classes are indicated.

DISCUSSION

The observed range in C IV normalized flux among the yellow giants is more than a factor of 20. This apparent spread in UV emission line brightness might be attributable to stellar activity cycles; for example, the bright line giants may be at the peaks of their cycles or the faint emission line stars may have been observed at quiescent phases in their activity cycles. This possibility remains only a speculation since none of these stars has been monitored extensively in the UV or at the Ca II H-K lines.

Alternatively, the observed range in UV and X-ray brightness may signify a difference in the intensity of stellar hydromagnetic dynamos, with the strong emitters being rapid rotators having strong dynamos and the weak emitters being relatively slow rotators with feeble dynamos. Several explanations can be offered for the implied spread in axial rotation. It is possible that the yellow giants with weak TRs and coronae evolved from slowly rotating main sequence progenitors of mass $1.5 \lesssim M/M_{\odot} \lesssim 4.0$. If these stars evolved from rapid rotators and are crossing the HR diagram for the first time from left to right, then magnetic braking in the Hertzsprung Gap must be very efficient for some stars. However, unlike the weak line red giants, whose asymmetric Mg II and Ca II profiles indicate massive cool winds, the UV spectra of the G giants show no evidence for mass loss. Thus, cool winds cannot account for the weak emission observed among the yellow giants.

The weak line yellow giants may be crossing the Hertzsprung Gap for the second time, as post-red giants. According to evolutionary models for low mass stars (Iben 1967), evolution along blue loops through the G giant region takes roughly an order of magnitude longer than the first crossing of the Hertzsprung Gap. We therefore expect that the majority of yellow giants are evolved "second-crossers." As red giants, these stars may have lost considerable angular momentum. A minority of yellow giants, e.g., μ Vel or the hybrid stars (α Aqr and β Aqr), may be in their initial crossing, prior to the red giant stage. As relatively rapid rotators, they would be expected to have intense dynamos and strong TRs and coronae.

A choice among the alternative explanations offered here awaits further information on stellar rotation and evolutionary status of the yellow giant stars. Stellar rotation velocities, now being obtained for these stars, will be discussed along with the ultraviolet data at a later date.

We thank Dr. A. Boggess and the staff of the IUE Observatory for their assistance in the acquisition and reduction of these data. We acknowledge support of NASA grants NAG 5-146 to the University of Hawaii and NAG 5-82 to the University of Colorado.

REFERENCES

Ayres, T. R., Linsky, J. L., Vaiana, G. S., Golub, L., and Rosner, R. 1981, Ap. J., 250, 293.
Iben, I., Jr. 1967, Ann. Rev. Astr. Ap., 5, 571.
Linsky, J. L. and Haisch, B. M. 1979, Ap. J. (Letters), 229, L27.
Simon, T., Linsky, J. L., and Stencel, R. E. 1982, Ap. J., in press.

SOLAR ANALOGS IN THE 2600 to 3200 Å REGION

Johannes Hardorp, John Caldwell, and Richard Wagener
Astronomy Program, State University of New York
at Stony Brook, NY 11794

ABSTRACT

No new criteria for the selection of solar analogs are found. At low dispersion, the spectra of 16 Cyg A, 16 Cyg B, 18 Sco and α Cen A look identical to each other and to sunlight reflected from Galilean satellites with the possible exception of Mg II λ 2800 being stronger in the stars. The use of α Cen A or 16 Cyg B as solar substitutes for planetary photometry is expected to be far superior to using published solar irradiances.

INTRODUCTION

The idea of solar analogs, namely replacing the unobservable solar spectrum by that of a suitable star when reducing planetary observations, should be valid down to at least 2000 Å, above which limit the solar spectrum seems to be non-variable within a percent or so (Brueckner 1981).

In the visible region, 16 Cyg B (G5V) seems to be the best solar analog. It shares the solar energy distribution and violet absorption spectrum (Hardorp 1980, 1982). Perrin and Spite (1981) found no difference whatsoever between the solar spectrum from 4300 to 6000 Å and that of 16 Cyg B at high dispersion. Branch et al. (1980) found 16 Cyg B only 30 K cooler than the sun from high precision Hα profiles. Keenan (1981) has recently reclassified this star as G2.5V, with the sun at G2V and 16 Cyg A at G1.5V.

The question posed here is whether the same choice holds for the far ultraviolet. Garrison (1979) has claimed to see differences between 16 Cyg A and B in IUE spectra, preferring A as analog.

28 and 50 Å BINNING

At Stony Brook we developed reduction programs that allow us to calibrate, match, shift, coadd and ratio IUE spectra. We first looked at all LWR low dispersion spectra of near solar type stars released before December 1980. We were unable to see any significant differences to the Broadfoot (1972) spectrum of the Sun with 28 Å bins. Obviously the noise present in one or two well exposed spectra makes all solar type stars look alike. In January 1982 we then spent an entire IUE shift each on 16 Cyg A, B and 18 Sco, the star used by Savage et al. (1980) for reducing their Uranus and Neptune data. This is about the best one can reasonably do with IUE. We obtained between 8 and 11 trailed spectra per star, coadded them and compared them to published spectra of the Sun (Mount and Rottman 1981) and to the sum of 21 spectra of Galilean satellites. We discuss here only the large aperture exposures, since the small aperture spectra, being noisier, add very little information.

Fig. 1 shows an attempt of using IUE for photometric purposes. The ratio 16 Cyg A/B (50 Å bins) fits extremely well onto the values in the visible

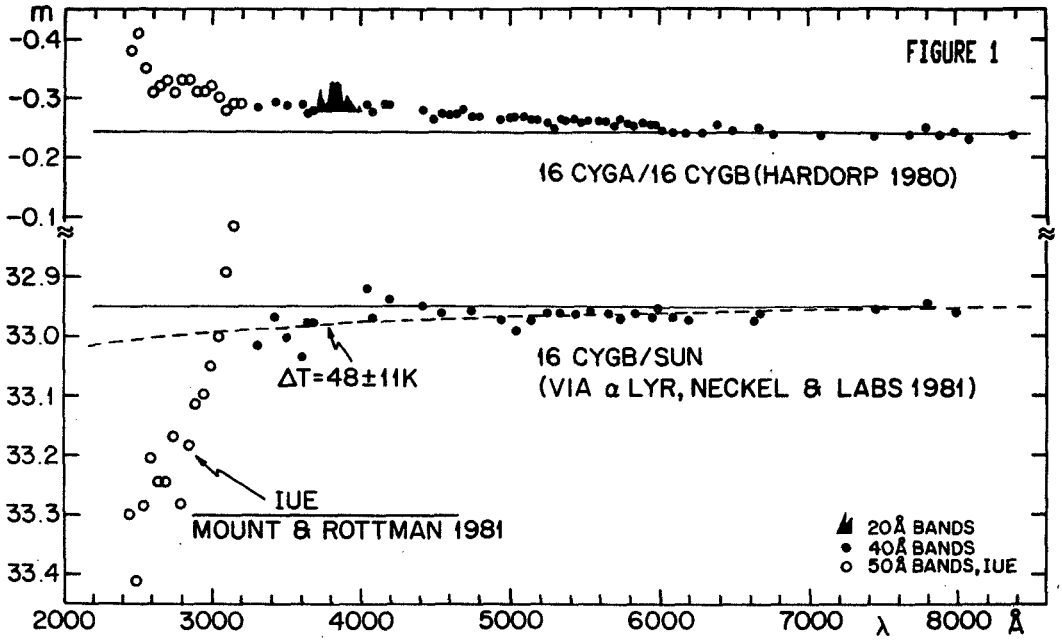
m
-0.4
-0.3
-0.2
-0.1
32.9
33.0
33.1
33.2
33.3
33.4
FIGURE 1
16 CYGA/16 CYGB (HARDORP 1980)
16 CYGB/SUN
(VIA α LYR, NECKEL & LABS 1981)
ΔT=48±11K
IUE
MOUNT & ROTTMAN 1981
20Å BANDS
40Å BANDS
50Å BANDS, IUE
2000
3000
4000
5000
6000
7000
λ
8000 Å

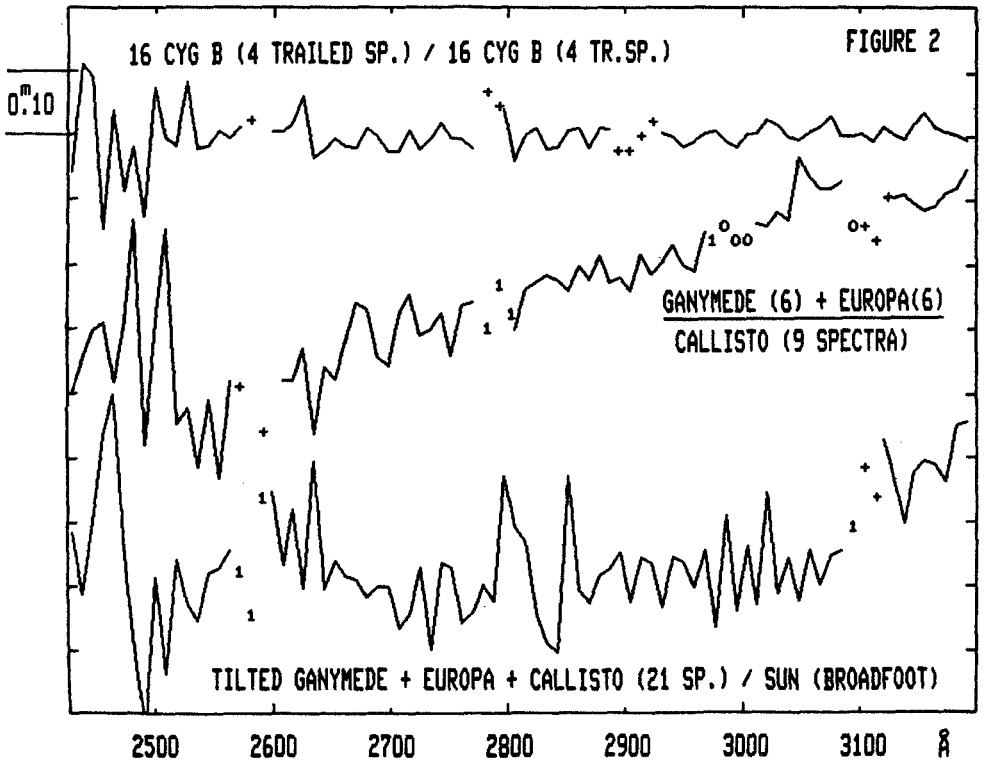
16 CYG B (4 TRAILED SP.) / 16 CYG B (4 TR.SP.)
FIGURE 2
0.m10
GANYMEDE (6) + EUROPA(6)
CALLISTO (9 SPECTRA)
TILTED GANYMEDE + EUROPA + CALLISTO (21 SP.) / SUN (BROADFOOT)
2500
2600
2700
2800
2900
3000
3100
Å

region. The internal accuracy is on the order of one or two percent! 16 Cyg A is about 60 K hotter than 16 Cyg B. In comparing stars with the Sun we are not so fortunate: the energy distribution of 16 Cyg B (and of any solar type star we have looked at) falls off much more steeply than that of the Sun below 3200 Å. This is most likely unreal, because stars just do not compare that way, as the upper graph shows. It must be an artifact due to errors in calibration of either IUE or the rocket observations by Mount and Rottman (1981) or both. The Broadfoot (1972) Sun yields a similar slope but is half a magnitude dimmer. Thus, at the present time, energy distributions cannot be used as a criterion for or against solar analogs in the ultraviolet. This magnifies the importance of solar analogs for deriving planetary albedos.

9 Å BINNING

The accuracy of spectroscopic comparisons at 9 Å resolution can be judged from Fig. 2, where all spectral features seen must be artifacts. The top graph compares the first four with the last four trailed spectra of January 24,1982. From the lower graph it is clear that IUE spectra of stars should be compared to IUE spectra of Galilean satellites rather than to published solar spectra.

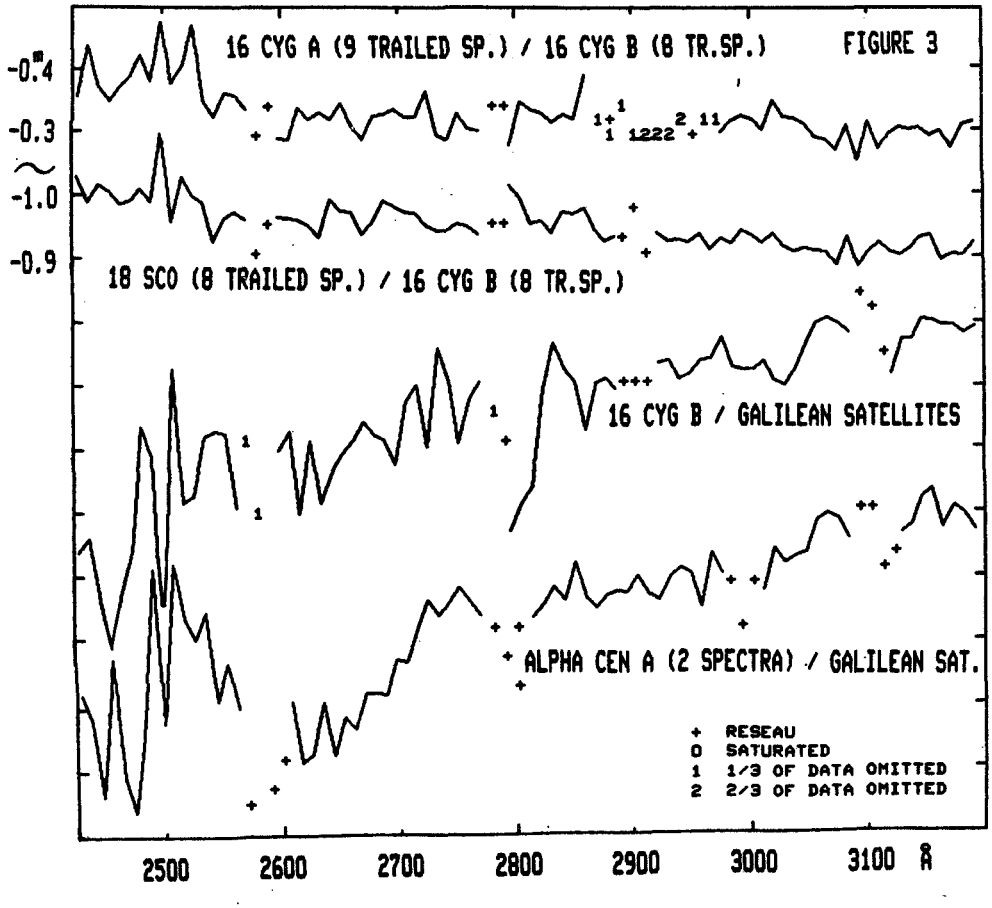

More spurious spectral features show up at this resolution when spectra are not carefully aligned in wavelength before coadding or ratioing. The large scatter below 2600 Å is due to low count rates.

In Fig. 3 no spectroscopic differences can be seen between the spectra of 18 Sco, 16 Cyg A and 16 Cyg B at 9 Å binning, only the slopes of the continua look slightly different. We also looked at the photowrites, as Garrison (1979) has done when he did see differences between 16 Cyg A and B. We couldn't see any. The differences between 16 Cyg B and the Galilean satellites are hardly beyond the noise, with the possible exception of a deeper Mg II 2800 absorption line in 16 Cyg B. This much difference would be seen if 16 Cyg B had no emission cores at all in Mg II 2800. The spectrum of α Cen A agrees also well with that of the Galilean satellites.

CONCLUSIONS

IUE spectra of solar type stars do not add any criteria for the selection of solar analogs. One can therefore follow one of two procedures: Since the choice of a solar substitute star seems not to be critical for spectroscopic work in the far ultraviolet, take α Cen A as a solar analog. The other approach would be to rely on the selection done with criteria in the visible region. Then 16 Cyg B should be used. This month we spent another two shifts on this star alone, extending the coverage down to 1700 Å at low dispersion.

ACKNOWLEDGEMENTS

We thank Vivian Moore, Peter Winkelstein and James Scott for help with the data reductions. This research is supported by NASA grant NSG 5250.

REFERENCES

Branch, D., Lambert, D. L., Tomkin, J.: 1980, Astrophys. J. 241, L83.
Broadfoot, A. L.: 1972, Astrophys. J. 173, 681.
Brueckner, G. E.: 1981, Adv. Space Res. 1, 101.
Garrison, R. F.: 1979, Bull. Amer. Astron. Soc. 11, 647.
Hardorp, J.: 1980, Astron. Astrophys. 91, 221.
Hardorp, J.: 1982, Astron. Astrophys. 105, 120.
Keenan, P. C.: 1981 (private communication).
Mount, G. H., Rottman, G. J.: 1981, J. Geophys. Res. 86, 9193.
Neckel, H., Labs, D.: 1981, Solar Phys. 74, 231.
Perrin, M. N., Spite, M.: 1981, Astron. Astrophys. 94, 207.
Savage, B. D., Cochran, W. D., Wesselius, P. R.: 1980, Astrophys. J. 237, 627.

HIGH DISPERSION IUE SPECTRA OF ACTIVE CHROMOSPHERE G AND K DWARFS

Thomas R. Ayres
LASP, University of Colorado

Jeffrey L. Linsky†
JILA, University of Colorado and NBS

Alex Brown and Carole Jordan
Department of Theoretical Physics, University of Oxford

Theodore Simon
Institute for Astronomy, University of Hawaii

ABSTRACT. We analyze IUE far ultraviolet echelle spectra of three active chromosphere dwarf stars: χ^1 Orionis (G0 V), ξ Boötis A (G8 V), and ε Eridani (K2 V), utilizing spectra of α Cen A (G2 V) and α Cen B (K1 V) as quiet chromosphere comparisons.

INTRODUCTION. The advent of IUE has permitted the beginnings of detailed far ultraviolet studies of nearby late-type dwarf stars similar to our Sun. Despite our inability to observe the surfaces of such stars directly, we can utilize the high dispersion capability of the IUE echelles to obtain surrogate information concerning the spatial organization of dwarf star chromospheres ($T \cong 6000$ K) and higher temperature layers analogous to the solar transition region ($T \cong 10^5$ K) and corona ($T \cong 10^6$ K). Such information is valuable for elucidating the surface magnetic properties of dwarf stars, since the high temperature plasma of the solar outer atmosphere is known to be intimately associated with compact, bipolar magnetic structures that are distributed inhomogeneously across the solar disk (Vaiana and Rosner 1978). Here, we report a spectroscopic comparison of five dwarf stars that span a wide range of chromospheric activity.

OBSERVATIONS. We have obtained IUE echelle spectra of five representative dwarf stars with SWP exposure times ranging from 120 minutes to 952 minutes, and LWR exposures of 1 to 60 minutes. The SWP and LWR images were reduced as outlined by Ayres (1982), incorporating the provisional echelle mode calibration of Cassatella, Ponz and Selvelli (1981). Line centroid velocities, integrated fluxes and FWHMs were determined by least squares Gaussian fits to the observed emission profiles. Each image was registered to the flux-weighted mean velocity of the strongest features.

Figure 1 compares profiles of the 2800 Å Mg II doublet in the active and quiet dwarfs. The ordinate of the figure is the monochromatic flux measured at Earth divided by the stellar bolometric flux, with units commensurate to the segmented velocity scale of the abscissa. The area under the doublet profiles is the fraction of the stellar bolometric luminosity provided by Mg II emission, which in turn is a measure of the chromospheric heating rate (e.g. Linsky and Ayres 1978).

†Staff member, Quantum Physics Division, National Bureau of Standards

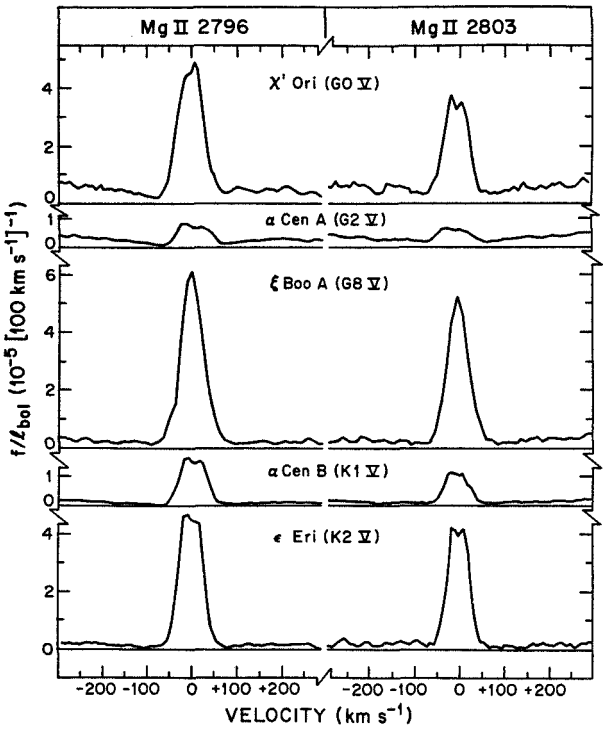

Note that the Mg II profiles of the active stars, aside from their obvious flux enhancement, tend to be narrower at the peaks but broader at the bases than those of the quiet chromosphere comparison stars, although the FWHMs are nearly the same. Such behavior is typical of Mg II and Ca II profiles in solar magnetic active regions (plages) and has been interpreted in the context of schematic chromosphere models by Ayres (1979).

Figure 2 depicts selected bright lines from the far ultraviolet spectra of the five dwarfs, plotted in the same way as Figure 1. In addition, crosshatching indicates saturated pixels (or reseau marks); "#" symbols denote prominent particle radiation hits; and "⊕" or "sa" designates geocoronal Lyα emission.

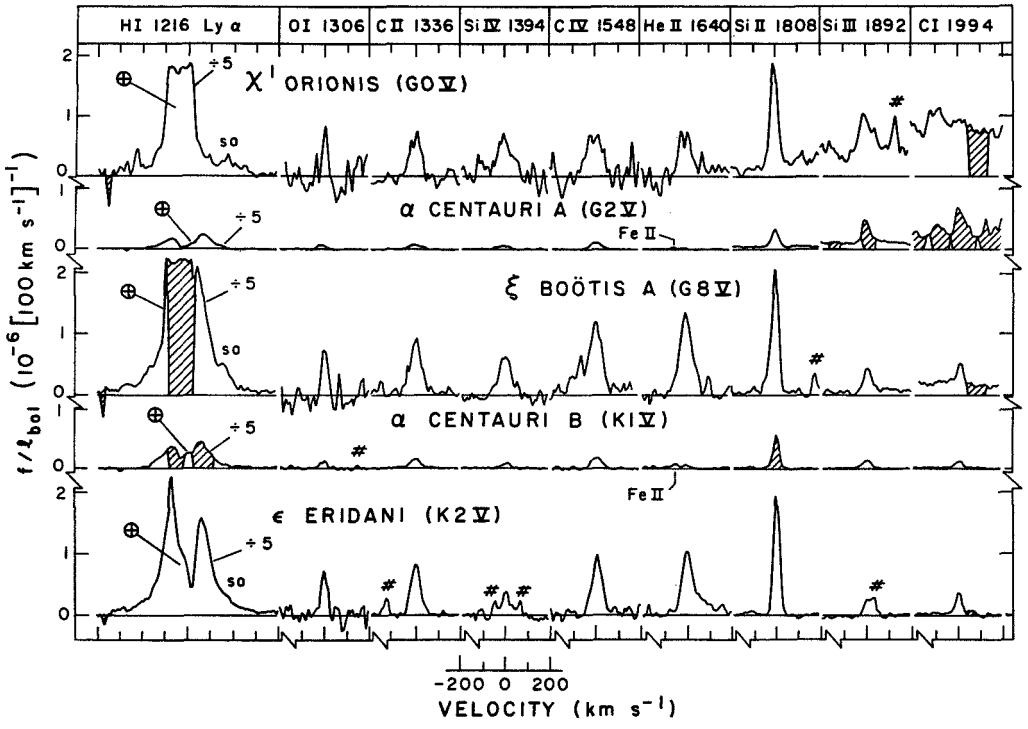

ANALYSIS. Despite the order of magnitude increase in line emission strengths of the active dwarfs compared with the quiet chromosphere stars, the FWHMs of low excitation features like Si II λ1808 and high excitation features like C IV λ1548 are very similar between the two classes. In fact, the only feature that behaves anomalously with respect to both strength and width between the active and quiet dwarfs is the λ1640 Balmer α line of He II. (The utility of high dispersion observations is clear in this case, since the weak He II emission of the quiet dwarfs is blended partially with an Fe II feature of comparable or greater strength.) However, it is believed that the He II emission is produced largely by an XUV photoionization-recombination mechanism (e.g. Avrett, Vernazza and Linsky 1976). Consequently the He II intensity may be a proxy diagnostic for coronal radiation fields. To test this possibility, we have compared in the left hand panel of Figure 3 He II λ1640 flux ratios measured here to soft x-ray flux ratios derived from the detections reported by Golub et al. (1982), Walter et al. (1980), and Johnson (1981). The linear correlation of He II with soft x-rays is apparent. The power law plotted in the figure is the relationship predicted by Hartmann, Dupree and Raymond (1980) using a model based largely on solar considerations.

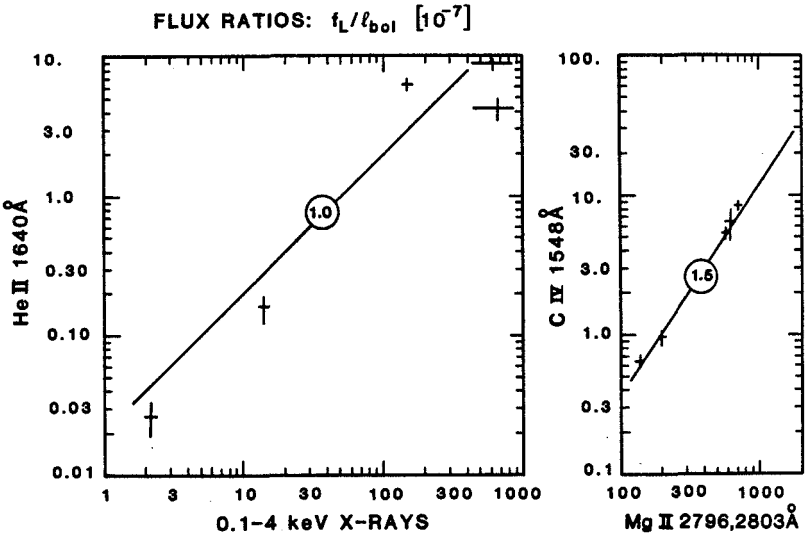

Although the "low excitation" He II emission appears to be simply proportional to the "high excitation" coronal x-ray flux, a similar purely linear relation does not hold between chromospheric and transition region emission. The right hand panel of Figure 3 compares C IV λ1548 flux ratios with those of the Mg II doublet. A power law slope of 1.5 appears to fit quite well, as might have been anticipated from the results reported in the low dispersion survey by Ayres, Marstad and Linsky (1981).

Finally, note that the range in Mg II flux ratios between the active and quiet dwarfs is only about 0.7 dex, while the range of soft x-ray flux ratios is nearly 2.5 dex. Chromospheric flux modulation periods available from Stimets and Giles (1980) and Hallam and Wolff (1981) indicate a range in equatorial rotational velocities of 0.9 dex or more. Accordingly, the dependence of chromospheric emission on stellar rotation could be nearly linear for these stars (c.f. Skumanich 1972), while the x-ray rotation-activity connection

must be described by a steeper power law (e.g. Ayres and Linsky 1980). However, our results also are entirely consistent with a sharp break in the rotation-activity relation near P ≅ 10 days, as proposed by Walter (1981), and discussed recently by Durney, Mihalas and Robinson (1981) in the context of mode switching by the stellar magnetic dynamo.

CONCLUSIONS. The ultraviolet spectra of active chromosphere dwarfs presented here are morphologically similar to chromospheric and transition region spectra of solar plages. The fact that the emission line FWHMs do not broaden substantially with increasing activity suggests that the major difference between active and quiet dwarfs occurs in the surface coverage of magnetic regions, rather than a gross physical change in the stellar "transition region" itself. In particular, if the emitting structures simply were becoming optically thicker in the active stars, rather than spatially more pervasive, we would expect opacity broadening to increase the FWHMs of lines like C IV λ1548 which are strong enough in the Sun to begin to exhibit optical depth effects. In short, the active dwarfs probably are largely covered by solar-like plage. Accordingly, the solar analogy appears to be viable, at least in the narrow context of late-type dwarf stars of near-solar temperature. Finally, the comparatively shallow dependence of chromospheric emission on stellar rotation, but the rather steep x-ray rotation-activity relation suggests that the heating of the multi-million degree corona is far more sensitive to the details of the magnetic flux production and spatial organization mechanisms than is that of the underlying chromosphere.

We acknowledge support by NASA through grants NAG5-199, NAG5-82 and NGL-06-003-057 to the University of Colorado and NAG 5-146 to the University of Hawaii, and thank the staff of the IUE Observatory for their assistance in the acquisition and reduction of the stellar spectra reported here.

REFERENCES

Avrett, E.H., Vernazza, J.E., and Linsky, J.L. 1976, Ap. J., 207, L199.
Ayres, T.R. 1979, Ap. J., 228, 509.
Ayres, T.R. 1982, IUE Newsletter (submitted).
Ayres, T.R. and Linsky, J.L. 1980, Ap. J., 241, 279.
Ayres, T.R. Marstad, N.C., and Linsky, J.L. 1981, Ap. J., 247, 585.
Cassatella, A., Ponz, D., Selvelli, R.L. 1981, IUE Newsletter No. 14, p. 270.
Durney, B.R., Mihalas, D., and Robinson, R.D. 1981, P.A.S.P., 93, 537.
Golub, L., Harnden, F.R., Jr., Pallavicini, R., Rosner, R., and Vaiana, G.S. 1982, Ap. J. (in press).
Hallam, K.L. and Wolff, C.L. 1981, Ap. J., 248, L73.
Hartmann, L., Dupree, A.K., and Raymond, J.C. 1980, Ap. J., 236, L143.
Johnson, H.M. 1981, Ap. J., 243, 234.
Linsky, J.L., and Ayres, T.R. 1978, Ap. J., 220, 619.
Skumanich, A. 1972, Ap. J., 171, 565.
Stimets, R.W., and Giles, R.H., 1980, Ap. J., 242, L37.
Vaiana, G.S., and Rosner, R. 1978, Ann. Rev. Astr. Ap., 16, 393.
Walter, F. 1981, Ap. J., 245, 677.

DISCUSSION - COOL STARS

Simon: What temperatures were used to calculate the envelope radii from the C II lines, and what would be the effect of reducing these values to one-half of your derived values?

Stencel: Excitation temperatures were inferred from the ratio of the fluxes in the 1335 Å resonance lines of C^+ to the intersystem lines (at 2325 Å). For Arcturus and Betelgeuse only upper limits to T_{exc} are available, 9300 K and about 5000 K, respectively. Neglecting changes in ionization balance, reducing these temperatures would imply larger chromospheric thickness.

Simon: What are the implications (if any) of your IUE observations for Canto's H-H model of a focused, self-shocked wind?

Böhm: As far as we can see, the present spectroscopic predictions for Canto's model are not yet detailed enough to show whether the apparent contradiction between optical and UV emission line results can be resolved by this model. We feel that the interpretation of the strong UV continuum is presently more dependent on the correct identification of the relevant radiation or scattering process than on the structure of the model. Radial velocity and proper motion studies are probably a better means to test the validity of Canto's model than are UV observations.

Holm: Bohlin has shown that there may be errors in high dispersion fluxes of the order of 15%. Have you measured the continuum near the Mg II lines to check whether the variability you find is instrumental?

Hallam: We understand that the type of error referred to here is a systematic securlarly decreasing change in the sensitivity of a particular localized region of the detector, which has been confirmed only in the last year. The maximum value quoted does not occur in the vicinity of the Mg II lines, where the corresponding value is much less, and is not nearly so well determined. Yes, we have made numerous measurements of the integral flux of nearby continuum comparison bands, and we are continuously looking for better ways to analyze the data in order to identify and compensate for systematic errors, and to reduce the effects of random measurement errors. We have certainly never seen evidence for residual systematic errors in our data as large as 15%. Such a large error would be very disturbing indeed, especially if it were random. But as I stated previously in the talk, our best assessment of all errors in the entire mass of data suggests that the total residual error in repeatability per measurement is a few percent, under our controlled exposure conditions.

Underhill: The phenomena which you are analyzing, i.e., X-ray intensity, strengths of emission lines from low ions and from high ions, reflect the

physical conditions in the mantle of the star. Therefore, they give a measurement of the effect of the disposition of non-radiative energy and momentum in the outer atmosphere of the star. The sources for these non-radiative factors are not direct functions of the effective temperature and radius of the star, which are the factors underlying the ordering of stars in the HR diagram. I see little purpose in drawing lines in the HR diagram where some excitation parameter has a certain level unless you make a direct coupling to the mechanism by which energy and momentum form its storage form (magnetic fields in your case) is released in the mantle. No evolutionary trends can be deduced until one has a theory of how the mechanism which releases non-radiative energy and momentum is related in an unambigous way to the stage of evolution of the star.

Simon: Originally, you proposed the magnetic bubble model to explain mass loss in late-type stars, including those which in the HR diagram lie to the right of the wedge-shaped region occupied by the discrepant asymmetry stars. Are you now modifying this proposal, or should we still expect to find transient X-ray and transition-region emission among these somewhat cooler stars?

Mullan: I am not modifying the earlier proposal. The purpose of the present work has been to concentrate on a subset of stars (the discrepant asymmetry stars) in which we believe we can discuss several different lines of argument, on the basis of several different kinds of observational data, pointing towards the idea of transient mass loss episodes. I still believe that transient mass loss, with transient X-rays and transient transition region emission, is a general characteristic of all cool giant stars lying above the Mg mass loss dividing line as defined by Stencel and Mullan (1980, Ap.J. 240, 718). These observational data can be interpreted, in our opinion, as evidence for unsteady magnetic field behavior in essentially all cool giant stars. It may be that stars which have the observational characteristics to place them in the "discrepant asymmetry wedge" in the HR diagram have stronger magnetic fields than stars further towards the upper right hand corner of the HR diagram. These stronger fields then simply serve to enhance the detectability of activity (in all its forms). From an evolutionary point of view, stars evolving into the "wedge" for the first time may be expected to have stronger dynamos than those which have already spent some time in giant evolution. Further enhancements in sensitivity of both X-ray and UV line detectors are required to test the hypothesis for stars in which the magnetic fields are weak.

Walter: To amplify Dr. Dupree's comment on the X-ray flux from α Aur, HEAO I observations seem to show the X-ray flux varying significantly, by up to nearly a factor of two, on timescales of a few hours. However, the mean between two observations separated by six months appears constant.

Mullan: It is interesting that He II 1640 Å in cool dwarfs can be interpreted in terms of a solar analogy, whereas in giants of late type, analogs of solar behavior may be of little assistance in interpreting the

data. This stands as a caution against applying solar analogs indiscriminately in the HR diagram. Solar analogs may be useful in stars where longlived closed loops can persist, just as they are known to exist in the solar corona. Stars in which solar analogs may be of little use are those in which long-lived, static closed loops do not exist. In such stars, the atmosphere is in a state of continued magnetic upheaval, and there are no analogs of the "building blocks" which characterize the solar conona (i.e., closed loops).

Stencel: Have you considered the effect on the 2325 Å C II] flux from the interstellar/circumstellar extinction/blanketing?

O'Brien: No, we have not. Most of the evidence from the visible spectral region suggests that the ultraviolet opacity has a photospheric origin. Consequently, the chromospheric emission features would not be affected. The three N-stars discussed here are not known to have extensive circumstellar envelopes. Finally, Eggen's values of E(B-V) suggest that interstellar reddening may not be significant.

Slovak: What are the photometric variations exhibited by TV Gem and were the FES magnitudes similar for your exposures?

Michalitsianos: There were no significant changes in FES magnitudes between the observing dates for TV Gem. If any changes did occur, they would be on the order of 0.1 magnitude in the visual. The UV continuum for both dates essentially maintained a constant level as measured from our low resolution IUE data in the SWP wavelength range.

Ake: (1) Can you derive a luminosity for the secondary? (2) Is that from the lines or the continuum?

Michalitsianos: (1) It's about a main sequence type star which is based on relative magnitude arguments between primary and secondary in the system at its known distance of 1400 pc, consistent with the UV flux corrected for extinction E(B-V) = 0.65, which we conclude arises wholly from the hot companion. (2) It's from arguments about the distance and observed flux of the continuum of a B3-5, class III-V star.

Shore: Considering that the Rosner et al. loss rates depend on the loop scale length, is it really kosher to assert that a global analysis is possible? What loop size could you tolerate before the analysis, and loop, becomes unstable? Admittedly, S is a weak parameter but it does affect the heating and cooling rates.

Endler: (Reply unavailable.)

Underhill: The spectroscopic features which you are observing give information about the physical state in the mantles of late-type stars, that is in parts of the atmosphere where the deposition of non-radiative energy and momentum is important. It will be possible to relate the physical state of the mantle to the stage of evolution of the star only after you have determined a mechanism for controlling how much non-radiative energy and momentum is deposited in the mantle, and have been able to show how the action of this mechanism is related to the stage of evolution of a star in an unambiguous way.

Simon: Semi-empirical modeling does provide some understanding of the structure of the outer atmospheres of cool stars, for example, the sun. We agree that it would be more satisfying to have a better understanding of the physical processes responsible for stellar chromospheres and coronae, that is, a model with predictive capabilities. Observational studies, perhaps similar to the one described here, and semi-empirical modeling may help us to achieve that level of understanding.

Stencel: Can you comment on the ratio of C IV detections/non-detections compared with the ratio of the timescales for "first crossers"/"blue loop" ($\sim$0.1)?

Simon: Your question raises several important points. Observationally, we cannot be sure that the sample of stars included in our magnitude-limited survey is statistically unbiased. At the same time, evolutionary models in the most appropriate mass range, between approximately 1.2$M_\odot$ and 3$M_\odot$, are lacking. Such calculations would need to include a proper stellar wind model in order to address your question. All that we can do at this point is to make reasonable speculations about the relative evolutionary time scales (for first- and second-crossing cool giants) and the relative intensities of stellar dynamos.

Roman: In view of the albedo differences between Io and the other Galilean satellites, do you assume Europa, Callisto, and Ganymede are gray bodies?

Hardorp: No, they definitely are not gray. But since they have no atmospheres, their reflectivities can be assumed to be smooth functions of wavelength. Thus, for spectroscopic purposes, they do show the solar spectrum. You can not use them to derive albedos of planets on an absolute scale, though. It is here that you need solar analogs.

Wamsteker: Just as a matter of interest I would like to mention that in a high resolution study of the 3200-2500 Å region for 16 Cyg A and 16 Cyg B, Dr. Greve (MPI) and myself find that, although the optically determined temperatures (Spite and Ferrin) are quite different, no difference exists. The spectra are essentially identical at the high resolution mobe of IUE.

SOLAR SYSTEM

THE RELEVANCE OF THE IUE RESULTS ON YOUNG STARS FOR EARTH'S PALEOATMOSPHERE

V. M. Canuto
NASA, Goddard Institute for Space Studies, New York, N.Y. 10025
J. S. Levine and T. R. Augustsson
NASA, Langley Research Center, Hampton, VA 23365
C. L. Imhoff*
Computer Sciences Corporation, Silver Spring, MD 20910
M. S. Giampapa*
Harvard-Smithsonian Center for Astrophysics

ABSTRACT

In constructing a scenario for the composition of the Earth's early atmosphere and its chemical evolution over geological time, a basic problem concerns the quantification of the amounts of O_2 and O_3 present. An accurate quantification of the amount of atmospheric oxygen requires information on the UV flux emitted by the young Sun and a detailed description of the photochemical (e.g. the photolysis of H_2O and CO_2) and chemical processes (e.g. the chemistry leading to the production of O_2 and O_3) in the paleoatmosphere. Using the latest IUE results for seven T Tauri stars, which are believed to represent the young Sun and a detailed photochemical/chemical model of the paleoatmosphere, we have calculated the vertical distribution of O_2 and O_3 in the early atmosphere. The calculations indicate that the surface O_2 mixing ratio is as much as six orders of magnitude larger than previously estimated, but appears low enough for the formation of amino acids via the Urey-Miller type of experiments. We believe that the quantification of the O_2 level in the Earth's paleoatmosphere presented in this paper can reconcile the demands of both biological and geological considerations.

INTRODUCTION

Indirect evidence concerning the oxygen content of the Earth's paleoatmosphere has been sought in a variety of ways. Biochemists performing laboratory simulations on the production of amino acids have precluded the presence of significant levels of oxygen in the early atmosphere. Geologists however require some oxygen to explain the oxidation state of the oldest rocks. We have taken another approach in determining the amount of O_2 in the prebiologic paleoatmosphere. Using a detailed photochemical model of the paleoatmosphere, we are able to quantify the oxygen and ozone in the early atmosphere. (Ozone is particularly important for an understanding of the evolution of primitive biological organisms.) Two of the important parameters needed for these calculations are the ultraviolet radiation from the young Sun and the early carbon dioxide abundance. IUE observations have been used to obtain estimates of the UV flux from the early Sun and paleoclimatogical considerations have been used to estimate CO_2 levels in the early atmosphere.

*Guest Observer, International Ultraviolet Explorer

IUE AND THE YOUNG SUN

In the past it has commonly been assumed that the ultraviolet radiation from the Sun should be scaled to its luminosity, which may have been as much as 30% lower than present values (Sagan and Mullen, 1972). However, IUE observations of T Tauri stars and young solar-type main sequence stars indicate that the UV flux from the young Sun was considerably enhanced due to chromospheric activity.

The T Tauri stars are generally thought to resemble the Sun at an age of a few million years. These stars emit strongly in the ultraviolet, primarily in the MgII h and k and the far-ultraviolet chromospheric and transition-region lines. The surface fluxes of the stronger lines are typically 10^6 to 10^7 erg cm^{-2} s^{-1}, or some 100 to 5000 times the present solar values (Imhoff and Giampapa 1982). In addition, these contracting protostars have larger surface areas than the Sun by a factor of $(R_*/R_\odot)^2$. We find that the total enhancement of the UV flux from the T Tauri stars is thus 10^3 to 10^4 times the present solar value (Canuto et al., 1982).

The UV flux emitted by young stars continues at high levels relative to the present Sun. Recently Boesgaard and Simon (1982) have shown that the UV chromospheric emission-line surface fluxes decrease with age approximately as $t^{-0.5}$. The higher temperature transition-region lines fall more rapidly, as $t^{-0.9}$.

We have computed the enhancement of early solar UV flux over present levels as a function of age using the observational relation given by Boesgaard and Simon (1982). As before, the total fluxes must include a factor to account for the changing radius of the Sun as it contracts to the main sequence. Radii at specific ages for solar-mass stars were estimated from temperatures and luminosities taken from the theoretical diagrams of Iben (1965) and Cohen and Kuhi(1979). The results are given in Table 1. We find that even after the Sun reaches the main sequence (5×10^7 years), the UV flux is enhanced by a factor of about 100 over present levels.

THE PHOTOCHEMISTRY OF OXYGEN AND OZONE IN THE EARTH'S PALEOATMOSPHERE

The photochemical reactions leading to the production of oxygen and ozone are critically dependent on the solar UV flux and the atmospheric carbon dioxide abundance. The CO_2 abundance may have been enhanced by as much as 10^3 over pre-industrial levels (Owen et al., 1979). A greatly enhanced level of CO_2 in the paleoatmosphere is necessary to have kept the Earth's oceans from freezing. Stellar evolutionary theory suggests that the Sun was about 30% less luminous than it is now. This would have resulted in a temperature of 238°K at the Earth's surface, without the "greenhouse effect" of the enhanced CO_2.

To study the effects of enhanced solar UV flux and enhanced levels of atmospheric CO_2 on the photochemistry of the early atmosphere, calculations were performed using the photochemical model of the paleoatmosphere of Levine et al. (1981). The model includes 31 chemically-active species, 25 photochemical processes, and 77 chemical reactions, as described in Canuto et al. (1982).

The O_2 mixing ratio has been calculated as a function of height above the Earth's surface. The larger UV flux together with the enhancement of carbon dioxide produces an increase as large as 10^6 in the oxygen content

of the atmosphere near the surface, i.e. the O_2 mixing ratio increases from 10^{-15} to 10^{-9} (see Table 2). We have also computed the column density of ozone for various levels of enhanced solar UV flux and atmospheric CO_2. The results are also given in Table 2. It may be seen that the O_3 column density may be increased by as much as a factor of 10^3 due to the increased levels of UV flux and CO_2. (A column density of 10^{19} cm^{-2} is required for biologically effective screening of UV radiation.)

CONCLUSIONS

We have computed the levels of oxygen and ozone in the Earth's paleoatmosphere as functions of the early Sun's UV flux as indicated by IUE observations and of the CO_2 level determined by paleoclimatological considerations. The values we have calculated are high enough to allow the observed state of oxidation and reduction in early rocks but small enough to allow chemical evolution of amino acids. We note that the values of the O_2 mixing ratio found here fall within the range of 10^{-13} to 10^{-3} required to explain the simultaneous existence of oxidized iron and reduced uranium in the early rocks (Klein and Bricker, 1977; Grandstaff, 1980; Towe, 1978). Thus observations with the IUE satellite have contributed to reconciling a long-standing debate over the amount of oxygen in the Earth's paleoatmosphere.

REFERENCES

Ackermann, M. 1971, in Mesospheric Models and Related Experiments (ed. G. Fiocco), p. 149.

Boesgaard, A. M., and Simon, T. 1982, in Proceedings of the Second Cambridge Workshop on Cool Stars, Stellar Systems, and the Sun (ed. M. S. Giampapa) in press.

Canuto, V. M., Levine, J. S., Augustsson, T. R., and Imhoff, C. L. 1982, Nature, in press.

Cohen, M., and Kuhi, L. V. 1979, Ap. J. Suppl., 41, 743.

Grandstaff, D. E. 1980, Precambrian Research, 13,1.

Iben, I. 1965, Ap. J., 141, 993.

Imhoff, C. L., and Giampapa, M. S. 1982, this volume.

Klein, C., and Bricker, O. P. 1977, Economic Geology, 72, 1457.

Levine, J. S., Augustsson, T. R., Boughner, R. E., Natarajan, M., and Sacks, L. J. 1981, in Comets and the Origin of Life (ed. C. Ponnamperuma), p. 161.

Owen, T., Cess, R. D., and Ramanathan, V. 1979, Nature, 277,640.

Sagan, C., and Mullen, G. 1972, Science, 177, 52.

Towe, K. M. 1978, Nature, 274, 657.

Table 1
Stellar UV Flux as a Function of Age

Age (years)	UV Enhancement
10^6	10^4
10^7	500
5×10^7	100
10^8	32
5×10^8	8
10^9	4
5×10^9	1

Table 2

Surface Mixing Ratio of Oxygen (O_2) and Column Density of Ozone (O_3) in the Prebiological Paleoatmosphere for Various Combinations of Atmospheric CO_2 and Solar Ultraviolet Flux

Solar UV Flux	CO_2	O_2 Surface Mixing Ratio	O_3 Column Density (cm^{-2})
1[a]	1[b]	3.18(-15)[c]	1.72(12)
	10	1.12(-13)	2.49(14)
	100	1.37(-12)	1.38(15)
10	1	9.63(-14)	3.94(13)
	10	6.66(-12)	5.36(14)
	100	2.24(-11)	1.95(15)
30	1	2.85(-13)	1.50(14)
	10	1.29(-11)	7.81(14)
	100	7.33(-11)	2.06(15)
100	1	2.44(-12)	1.76(14)
	10	4.73(-11)	8.15(14)
	100	2.75(-10)	2.04(15)
300	1	8.53(-12)	1.52(14)
	10	1.46(-10)	9.41(14)
	100	1.10(-9)	2.19(15)

[a]Present level of solar UV flux (Ackermann, 1971) and multiples.
[b]Pre-industrial level of CO_2 (ppmv); other values are multiples of this value.
[c]3.18(-15) is read as 3.18×10^{-15}.

IUE OBSERVATIONS OF THE JOVIAN HI LYMAN α EMISSION (1979-1982)

T. E. Skinner, S. T. Durrance, P. D. Feldman, and H. W. Moos
Physics Department, Johns Hopkins University, Baltimore, Md. 21218

ABSTRACT

Observations of the Jovian HI Lyman-α emission made with the IUE observatory beginning in December 1978 just before the time of the Voyager encounters and extending through January 1982 are presented. A constant disk center brightness of about 8 kR is observed for the central meridian longitude range $\lambda_{III} \simeq 200°$ to 360° and a variable brightness 9-15 kR is found for the range $\lambda_{III} \simeq 50°$ to 150°. These brightness values have persisted throughout the three years of observation. The hydrogen bulge near $\lambda_{III} \simeq 100°$ appears to be a permanent feature of the Jovian atmosphere, and no long term change of the planetary Lyman-α emission is seen. Since the early IUE observations were made near the two Voyager encounters, this indicates that no substantial changes in the atomic hydrogen concentration or the average atmospheric conditions have taken place between then and now.

INTRODUCTION

Measurements made over the past 15 years (Moos *et al.*1969; Carlson and Judge 1974; Bertaux *et al.* 1980; Clarke *et al.* 1981; Broadfoot *et al.* 1979) show that the Lα brightness of Jupiter increased considerably in the period prior to the Voyager encounter in 1979. It is of interest to know whether this quantity has continued to change, either upward or downward, due to influences such as changes in the Jovian magnetosphere or solar conditions. The data presented here have the advantage that they were obtained in a consistent manner using a single instrument, the short wavelength spectrograph of the IUE, the sensitivity of which is stable to better than 5% (Bohlin *et al.* 1980). The uncertainties introduced by comparing data obtained with instruments possibly having different sensitivity calibrations is thus eliminated.

OBSERVATIONS

Beginning 1978 December 2 and extending through 1982 January 12, 24 measurements were made of the Jovian disc-center Lα emission brightness (1200-1230 Å) averaged over the $10'' \times 20''$ solid angle of the instrument aperture. From these values were subtracted the intensity of scattered light from the planet in a 30 Å interval (1230-1260 Å), and the geocoronal-interplanetary Lα emission taken from measurements $40''$-$60''$ away from the planet. During a 16 hour period in December 1981, the geocorona was observed to vary between a maximum value of 9 kR when the earth passed between Jupiter and the satellite and a constant value of 1.6 kR approximately 6 hours after maximum. The same trend was observed in the 6 hours before maximum, leading to the inference that the measured geocoronal intensity is constant during the 12 hours the earth is behind the satellite, rising to a maximum and then falling again as the earth passes between the satellite and the planet.

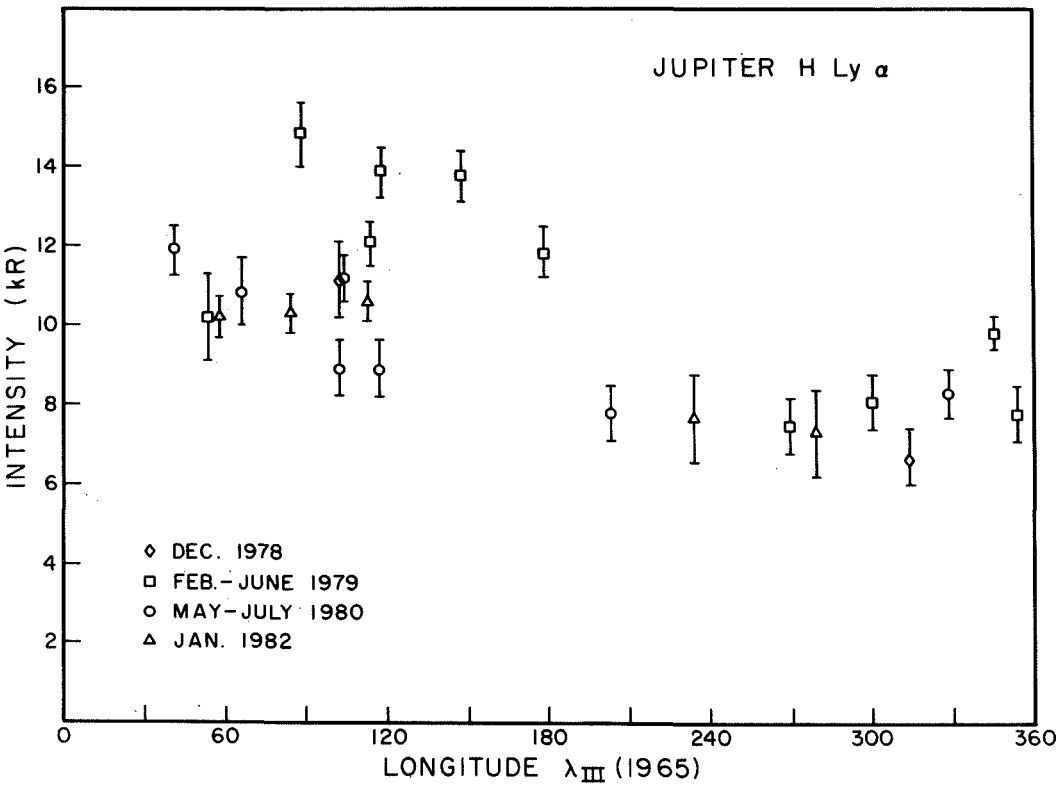

Fig. 1. Jovian disc-center emission brightness plotted vs. magnetic longitude.

Of the 24 observations, 16 occurred more than 6 hours after the expected maximum in geocoronal intensity, as determined from sky maps provided by the IUE staff for each observation. In these cases, either the background measured during the same shift was subtracted, or, in the 8 cases where no background was available, the entire range of intensities observed at minimum during the 3 year period was used (1.3 - 2.5 kR), thus introducing an uncertainty of ± 0.6 kR into these values. The remaining 8 observations occurred during periods of geocoronal enhancement, and it was necessary to fit the backgrounds, half of which were measured and half of which were estimated as above, to the curve describing this variation. In addition, an uncertainty in placing the time of maximum geocoronal brightness of each observation and a maximum possible 60% error in background measurements taken before 1979 July have been included. All of the uncertainties discussed here are indicated by the vertical error bars in Figure 1. Not shown is the ±10% uncertainty in the absolute calibration of the SWP camera since the comparison is between data taken with the same instrument.

DISCUSSION

The final values obtained are presented in Figure 1, plotted vs. magnetic longitude. A maximum spread of approximately ±25° for each observation due to the 10" width of the slit, a 2" uncertainty in pointing

accuracy, and the 4.5° the planet rotates in each 15 minute exposure has been suppressed. Despite over-estimating the error, the data separate into 2 distinct regions: one, centered about 100°, of enhanced and variable intensity (9 - 15 kR) associated with the known hydrogen bulge and another around 200° - 360° of constant intensity (8 kR).

These results argue strongly that the hydrogen bulge has been a permanent, though variable, feature of the Jovian atmosphere for the 3 year period covered. Moreover, the equatorial region of the planet away from the bulge has shown a remarkable consistency in Lα brightness over this same period. Since this is the only long-term study of this feature undertaken using an instrument of stable sensitivity, the implication of this result is that no significant change in the atomic hydrogen abundance in the Jovian upper atmosphere has occurred between the time of the Voyager encounters and now. Further work in the next few years will indicate whether this constancy in Jovian Lα emission brightness persists or is a 3 year pause in a longer term variation.

This work was supported by NASA grant NSG-5393.

REFERENCES

Bertaux, J. L., Festou, M., Barker, E., and Jenkins, E. 1980, *Ap.J.* 238, 1152.
Bohlin, R. C., Holm, A. V., Savage, B. D., Snijders, M. A. J., and Sparks, W. M. 1980, *Astr. Ap.* 85, 1.
Broadfoot *et al.* 1979, *Science* 284, 979.
Clarke, J. T., Moos, H. W. and Feldman, P. D. 1981, *Ap.J. (Letters)* 245, L127.
Carlson, R. W. and Judge, D. L. 1974, *J. Geophys. Res.* 79, 2623.
Moos, H. W., Fastie, W. G. and Bottema, M. 1969 *Ap.J.* 155, 887.

INVESTIGATIONS OF THE ULTRAVIOLET ALBEDO OF JUPITER AND SATURN

Peter Winkelstein, John Caldwell, Tobias Owen
E.S.S. Dept. SUNY at Stony Brook, N.Y. 11794

Michel Combes, Therese Enerenaz
Observatoire de Paris, Meudon 92190, FRANCE

Garry Hunt, Vivien Moore
Dept. of Phys. and Ast., UCL, London WC1E 6BT ENGLAND

We have taken several low dispersion spectra of both Jupiter and Saturn and have combined them to cover the range 1500 Å to 3000 Å with a good signal-to-noise ratio. These spectra were ratioed to a solar spectrum (Mount, et al. 1980) to obtain albedo curves. The resulting albedos show that the two planets differ significantly in composition.

Using a multilayer inhomogeneous model, we have computed the albedos of Jupiter and Saturn. We find that the albedo of Jupiter can generally be matched well by a hydrogen atmosphere with absorptions by the minor species ammonia, acetylene and ethane. However, this model atmosphere is too bright in the region around 1600 Å and we have not identified any species that will reduce it. The albedo of Saturn clearly shows absorption bands of acetylene but not ammonia. A model with only hydrogen and acetylene cannot match the Saturn data. The Voyager IRIS model for Saturn (Courtin, et al., 1981) cannot match the ultraviolet observations because it predicts too much absorption by phosphine.

This research has been supported by NASA Grant NSG 5250 in Stony Brook. We thank Darell Judge for communicating his results on phosphine absorption coefficients, and William Cochran for his assistance with the computing codes.

References:

R. Courtin, D. Gautier, A. Marten and W. Maguire, B.A.A.S. 13, 722, 1981

George H. Mount, Gary J. Rottman and J. Gethyn Timothy, JGR 83, 4271, 1980.

ULTRAVIOLET SPECTROSCOPY OF THE JOVIAN AND SATURNIAN AURORAE

S. T. Durrance, P. D. Feldman, and H. W. Moos
Physics Department, Johns Hopkins University, Baltimore, Maryland 21218

ABSTRACT

Auroral activity in the polar regions of Jupiter and Saturn can be monitored through ultraviolet emissions of the H_2 Lyman- and Werner-bands and an enhancement of Lyman-α. Using the IUE short wavelength spectrograph, spatially resolved spectra of both planets have been obtained periodically from early 1979 to the present. Many of these spectra contain auroral emissions seen to be localized near the poles. In the Jovian case, sequential exposures of the north polar region show the auroral intensity to increase and decrease in a periodic way as the planet rotates with a maximum occuring at $\lambda_{III} \simeq 186°$. Variations in the maximum intensity of about a factor of two have been observed to occur between one rotation and the next, but there appears to be no long term change in the auroral activity. Using three of the spectra nearest one of the observed maxima, a composite spectrum of the aurora is obtained with high signal-to-noise ratio, and many of the H_2 Lyman- and Werner-bands in this spectral region (1150-1700 Å) are identified. A comparison between this spectrum and an H_2 laboratory spectrum sets upper limits on the column abundances of CH_2 and C_2H_2 above the auroral emissions. In the Saturnian observations, the first indication of auroral activity was in the polar enhancements of the H Lyman-α emission. No simple periodicity in the auroral intensity related to the rotation of the planet has been observed. From the most recent observations, a spectrum of the aurora is obtained, and many of the H_2 Lyman- and Werner-bands are identified. This spectrum is compared with both the Jovian aurora and the H_2 laboratory spectrum.

INTRODUCTION

For Jupiter we present the results of a series of IUE observations of the north polar aurora obtained during a substantial fraction of one complete rotation. From these data a spectrum of the aurora with high signal-to-noise ratio, and a resolution of about 8 Å is obtained, making possible the identification of many H_2 Lyman- and Werner-bands. The spectrum is of sufficient quality to provide reliable quantative data for a comparison with the model atmosphere calculations. The lack of an observable absorption signature makes it possible to set an upper limit on the column density of CH_4 and C_2H_6 above the auroral emissions and hence an upper limit on the primary particle energies. A comparison of this spectrum with a laboratory spectrum of discharge-excited H_2 shows a remarkable similarity.

For Saturn we present the results of several IUE observations of the full disk. The exposures were of approximately 2 hours each, and the H_2 Lyman- and Werner-bands were observed near the north pole in two of them.

OBSERVATIONS

A series of observations of the north polar region of Jupiter was made using the short-wavelength spectrograph of the IUE satellite in January 1981. Exposures of 15 minutes each were made at regular intervals of about 45

minutes around the time when the tilt of the north magnetic pole was toward the Earth. The large aperture was used throughout and its orientation with respect to the disk of Jupiter is shown in the upper portion of Figure 1. The rotational position of Jupiter is indicated for four of the observations in the series. The projected auroral zone, assumed to be a mapping of magnetic field lines that intersect the Io torus, is shown as the dashed line. The portion of the auroral oval accepted by the entrance aperture can be seen to vary from a significant fraction ($\sim$ 1/3) to almost zero as the planet rotates.

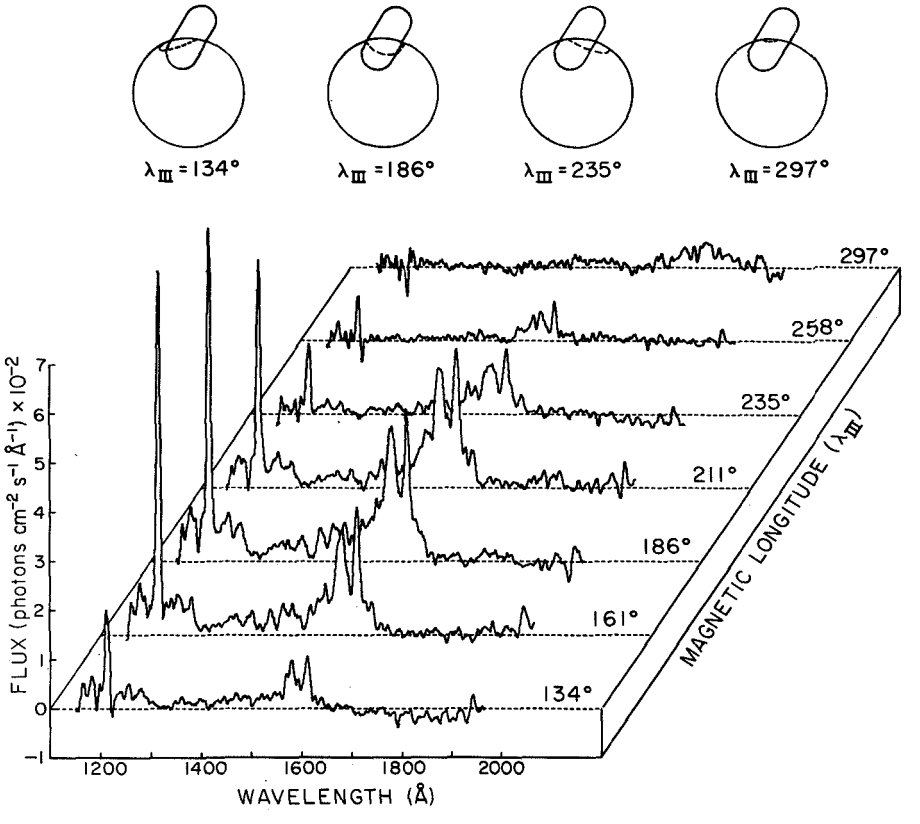

Fig. 1 Spectra of the Jovian aurora as a function of magnetic longitude (λ_{III}).

The resolution of the IUE instrument is about 6$\hat{''}$, making it possible to resolve the auroral emissions near the north pole, the disk of the planet at lower latitudes and, in the case of Lyman-α, the non-Jovian component of this signal present in the aperture above the planet. Only the auroral emissions are of interest here. Spectra were formed by combining data from the central portion of the aperture, including all of the auroral emissions but excluding any of the planetary signal from lower latitudes. A background spectrum was formed by combining three observations made the following day under nearly identical observing conditions, with the exception that the rotational position of Jupiter was such that the projected auroral zone was approximately zero. The same portion of the aperture was used. The amount of non-Jovian Lyman-α present in each spectrum was taken as the measured Lyman-α-signal in

the portion of the aperture off the planet. Uncertainties contributed by the subtraction of non Jovian Lyman-α are typically less than 15% of the Jovian signal; those contributed by the subtraction of non auroral planetary light are typically less than 10%.

The auroral spectra for each of the seven observations in this series are shown in the lower portion of Figure 1. The right hand scale gives the longitude of the central meridian in $\lambda_{III}(1965)$ coordinates at the midpoint of each exposure. The auroral emissions from H Lyman-α and the H_2 Lyman- and Werner-bands are well resolved. Their variation in intensity is roughly symmetric about $\lambda_{III} \sim 185°$.

RESULTS AND DISCUSSION

A spectrum of the Jovian aurora with high signal-to-noise ratio, obtained by combining the three spectra nearest the observed maximum, is shown as the upper spectrum in Figure 2. It was plotted here to emphasize the molecular band emissions so the Lyman-α signal is off scale. The full width at half maximum of the Lyman-α line, which should be indicative of the instrumental resolution, is ~ 8 Å. The data have been smoothed with a running mean over the instrumental bandwidth. There is a blemish in the spectrum at ~ 1195 Å due to a detector reseau mark.

Molecular hydrogen is the dominant constituent in the upper atmosphere of Jupiter. Its electron impact spectrum in this wavelength range consists of the Lyman bands ($B\ ^1\Sigma_u^+ - X\ ^1\Sigma_g^+$), the Lyman dissociative continuum, the Werner bands ($C\ ^1\Pi_u - X\ ^1\Sigma_g^+$), and H Lyman-α produced by dissociative excitation. The relative intensities from direct electron impact excitation and wavelength positions of the stronger Lyman- and Werner-bands are displayed above the auroral spectrum. The H_2 spectrum is somewhat more complicated than this. About 20% of the B state population decays to the Lyman dissociative continuum [Dalgarno, Herzberg and Stevens, 1970], and there is a substantial contribution to the B state population via cascading, down from higher states [Heaps, Bass and Green, 1973]. Also there is some confusion in the literature about the total electron impact excitation cross section of the C state, as pointed out by Yung et al. [1981].

For comparison, a laboratory spectrum of discharge-excited H_2 is plotted on the same scale in the lower portion of Figure 2. It was obtained using a spectrograph with ~ 13 Å resolution, similar to that of the IUE spectrograph, and a water cooled hollow cathode discharge lamp [Paresce, Kumar and Bowyer, 1971]. It has been suggested that the ratio of long- to short-wavelength emissions in this spectral range may provide information about the amount of hydrocarbon absorption present in the Jovian auroral spectrum [Clarke et al., 1980], and Yung et al. give a detailed model calculation relating this ratio to the primary particle energies. We found with the laboratory spectrum that it was possible to vary the long- to short-wavelength emission ratio by about a factor of two as the operating pressure in the lamp was varied. The spectrum shown here is for a lamp pressure of $\sim 130\mu$ and was chosen because it best matched the Jovian spectrum. The agreement between these two spectra is excellent. It leaves little doubt that the dominant emissions in the Jovian aurora are from electron impact excited H_2. The only substantial difference is a 60% more intense Lyman α emission in the auroral spectrum.

To assess the effects of hydrocarbon absorption on the auroral emissions,

the CH_4 and C_2H_6 photoabsorption cross sections [Mount and Moos, 1978; Mount et al., 1977] are plotted above the laboratory spectrum in Figure 2. It is clear from this that if there were any substantial absorption present, it would produce an observable signature in the spectrum. It would appear in emissions from the Lyman band system alone, and thus this determination is independent of the ratio of Lyman- to Werner-bands. By comparing these cross sectional data, and the laboratory H_2 spectrum, with the Jovian auroral spectrum it is possible to set a model independent upper limit of $\sim 2 \times 10^{17} cm^{-2}$ on the slant column densities of CH_4 and C_2H_6 above the auroral emissions. Assuming an emission angle of $\sim 60°$ and the equatoral model atmosphere of Festou et al. [1981], deduced from the Voyager 1 stellar occultation experiment, this places the auroral emissions near or above an altitude of about 330 km (referenced to the cloud tops).

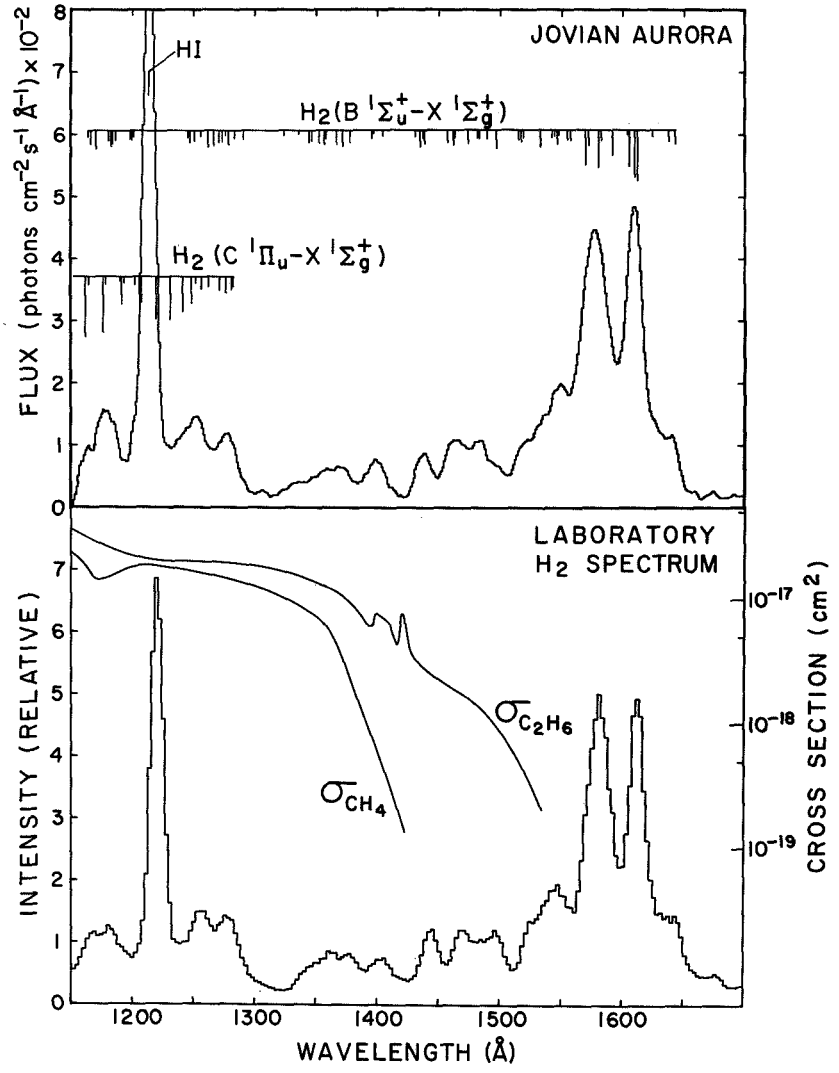

Fig. 2 Comparison of the Jovian auroral spectrum with a laboratory spectrum of discharge-excited H_2.

The spectrum of the Saturnian aurora shows emissions from the H_2 Lyman- and Werner-bands very similar to the Jovian aurora, but the lower signal-to-noise ratio does not allow a definitive upper limit to be set on the hydrocarbon column density above the auroral emissions. One obvious difference is the strong CI 1657 Å emission line in the Saturnian spectrum. With the present observations it is not possible to determine if this is associated with the aurora or if it is an albedo feature. More observations should be able to resolve this.

This work is supported by NASA Grant NSG 5393.

REFERENCES

Clarke, J. T., Moos, H. W., Atreya, S. K., and Lane, A. L., 1980, *Ap.J. (Letters)* **241**, L179.

Dalgarno, A., Herzberg, G. and Stephens, T. L. 1970, *Ap.J. (Letters)* **162**,L49.

Festou, M. C., Atreya, S. K., Donahue, T. M., Sandel, B. R., Shemansky, D. E. and Broadfoot, A. L. 1981, *J. Geophys. Res.* **86**, 5715.

Mount, G. H. and Moos, H. W. 1978, *Ap.J. (Letters)* **224**, L35.

Paresce, F., Kumar, S. and Bowyer, C. S. 1971, *Appl. Opt.* 10, 1904.

Yung, Y. L., Gladstone, G. R., Chang, K. M., Ajello, J. K. and Srivastava, S. K. 1982, *Ap.J. (Letters)*, in press.

OBSERVATIONS OF URANUS AND NEPTUNE WITH THE IUE

John Caldwell, Peter Winkelstein, Tobias Owen
E.S.S. Dept., S.U.N.Y. at Stony Brook, N.Y. 11794

Michel Combes, Therese Encrenaz
Observatoire de Paris, Meudon 92190, FRANCE

Garry Hunt, Vivien Moore
Dept. of Phys. and Ast., UCL, London WC1E 6BT, ENGLAND

The differing infrared properties of Uranus and Neptune[1] could be due to different thermal structures in their atmospheres or to different abundances of such trace constituents as acetylene (C_2H_2). Because C_2H_2 has a strong characteristic ultraviolet absorption, which strongly influences the albedos of Jupiter and Saturn between 170 and 190nm[2,3], we have attempted to resolve the Uranus/Neptune infrared difference with IUE observations of the region below 200nm, where the albedo is not directly sensitive to temperature. We present new observations of both planets, consisting of fifteen hour exposures obtained in consecutive shifts with international cooperation. Because of previously conflicting reports[4,5] we have emphasized the investigation of possible systematic errors, including solar variability[6] and scattered light within the IUE SWP. The latter work includes IUE observations of G stars, some of which were scheduled after this abstract was written.

This research is supported by NASA grant NSG 5250 at Stony Brook.

References:

1) Gillett, F. C. and Rieke, G. H. (1977) Ap. J. 218, L41.

2) Moos, H. W., and Clarke, J. T. (1979) Ap. J. 229, L107.

3) Owen, T. et al. (1980) Ap. J. 236, L39.

4) Savage, B. D., Cochran, W. D., and Wesselius, P. R. (1980) Ap. J. 237, 627.

5) Caldwell, J. et al. (1981) A. J. 86, 298.

6) Brueckner, G. E. (1981) Adv. Space Research 1, 101.

THE ULTRAVIOLET SPECTRUM OF PERIODIC COMET ENCKE

P. D. Feldman and H. A. Weaver
Physics Department, Johns Hopkins University, Baltimore, Md. 21218

M. C. Festou
Service d'Aéronomie du CNRS, Verrières-le-Buisson, France

H. U. Keller
Max-Planck-Institut für Aeronomie, Katlenburg-Lindau, FRG

ABSTRACT

A comparison of the ultraviolet spectrum of periodic comet Encke, recorded by the IUE between 1980 October 24 and November 5, with similar spectra of short and long-period comets shows the gaseous composition of P/Encke to be virtually identical to that of the other comets. If P/Encke is indeed the remains of a once giant comet, this similarity implies a homogeneous structure for the cometary ice nucleus. The OH brightness distribution shows a spatial variation similar to the visible fan-shaped image of the comet. The total derived water production rate is a factor of five higher than that derived from HI Lyman-α observations during the 1970 apparition and shows a variation with heliocentric distance (r) as $r^{-3.3}$ over the range from 0.81 to 1.02 AU.

OBSERVATIONS

Periodic comet Encke (1980 XI) was observed with IUE on 24 October 1980 and from 3 November 1980 to 5 November 1980. During this time the comet moved towards the sun with heliocentric distance (r) ranging from 1.014 to 0.81 AU. The geocentric distance (Δ) remained essentially constant at 0.3 AU. Figure 1 shows a composite spectrum of comet Encke from four IUE images taken when r = 0.82 AU with the center of brightness of the comet centered in the large aperture. The H Lyα line at 1216 Å and the OH(0,0) band at 3085 Å are the strongest emissions. H and OH are photodissociation products of H_2O and are expected to be the most abundant species in the coma if H_2O is the primary constituent of the nucleus. Oxygen is also a photodissociation product of H_2O and OH and is detected by its emission in the (unresolved) triplet at 1304 Å. Minor species detected in comet Encke are C, S, CS, and CO_2^+.

DISCUSSION

Figure 1 can be compared to a similar composite spectrum for comet Bradfield (1979 X), which was observed early in 1980 with IUE. Comets P/Tuttle (1980 XIII), P/Stephan-Oterma (1980 X), Meier (1980 XII), P/Borrelly (1980i), and Panther (1980u) were also observed with IUE. A comparative analysis of all of these comets (Weaver et al. 1981a) demonstrates that not only are the same coma species common to all of these comets but the relative abundances of these species also appear to be roughly the same. Since comet Encke has probably made thousands of passages through the inner solar system, each time losing more and more of its nucleus to sublimation, it is likely the remains of a once giant comet. The similarity of its UV spectrum to those of the long-period comets (which have made far fewer trips through the inner solar system) implies a homogeneous structure for the cometary ice.

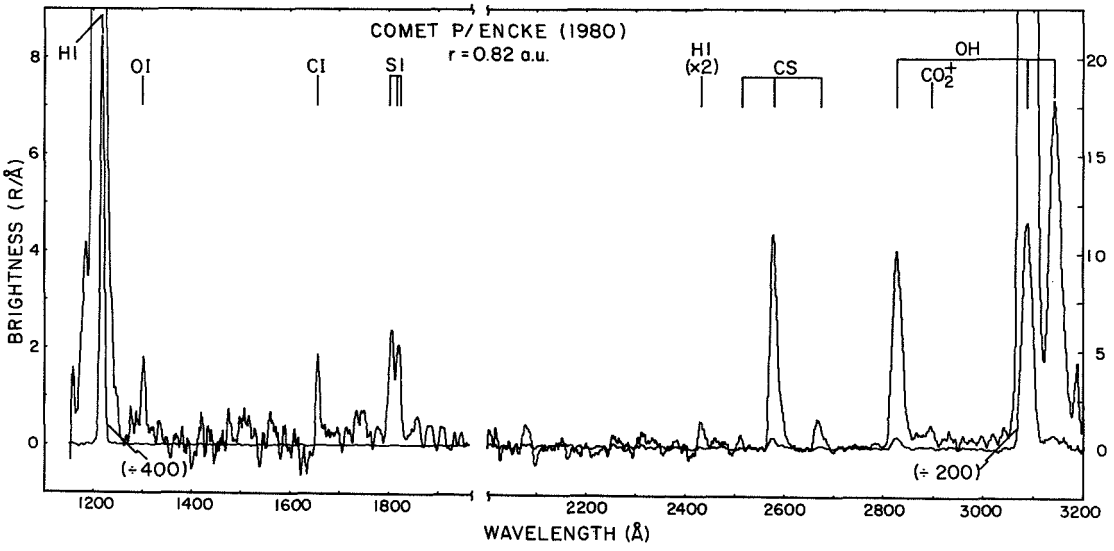

Fig. 1. Composite spectrum of comet Encke.

Table 1 gives surface brightness and wavelengths for the species which have been positively identified. These data represent average surface brightnesses over a 10" x 15" portion of the IUE aperture when the aperture was centered on the center of brightness of the comet. Visible images of comet Encke show an apparent asymmetrical gas production, the brightness of the visible coma being concentrated into a sunward "fan". The OH(0,0) band brightness of comet Encke was mapped with IUE and shows a spatial brightness distribution similar to that of the visible coma. The geometry of the IUE observations is indicated in figure 2. The data in Table 2 show that there is indeed an asymmetry in the OH brightness distribution and that for both the visible and ultraviolet observations, the hemisphere towards the sun is brighter than the hemisphere away from the sun.

The OH spatial brightness profile can be used to derive an OH lifetime for comet Encke. The OH lifetime is a function of heliocentric velocity and thus varies from comet to comet (Jackson 1980). Figure 3 shows this profile along with a Haser model prediction for the brightness distribution. The data are taken from Table 2 and are shown as boxes. The horizontal size of the box represents 15" projected onto the comet. The vertical size of the

TABLE 1. AVERAGE BRIGHTNESS OF SPECTRAL FEATURES

Species	Wavelength (Å)	Brightness (R)
H	1216	28,100
O	1304	15
C	1657	15
S	1807-1826	50
CS (1,0)	2507	20
(0,0)	2576	410
(0,1)	2662	60
OH (1,0)	2825	460
(0,0)	3085	11,600
(1,1)	3144	600
CO_2^+	2890	25

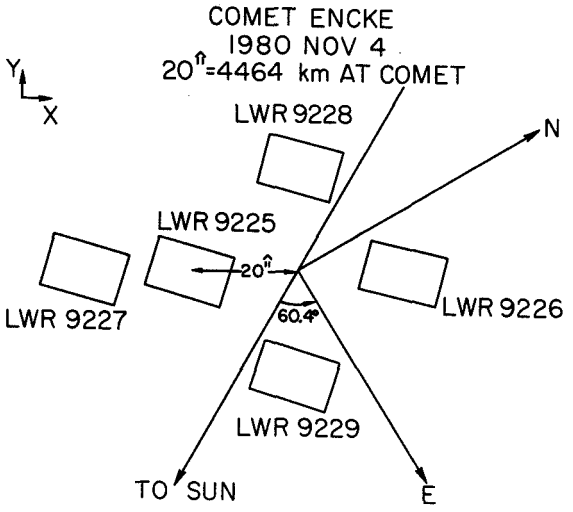

Fig. 2. Geometry of IUE observations for mapping of the OH coma.

TABLE 2. OH(0,0) BAND SPATIAL BRIGHTNESS PROFILE

Image	$B_{OH}(0,0)$ (kR)
LWR 9224 (center)	10.3
LWR 9225	6.9
LWR 9226	5.0
LWR 9227	4.5
LWR 9228	4.2
LWR 9229	6.7

boxes represents only the relative measurement uncertainty ($\pm 2\sigma$), and does not include the ±10% uncertainty in the absolute calibration, so as to emphasize that the brightness asymmetry measured for the OH coma is real. In the model calculation photodissociation of water is assumed to be the only source of OH. The H_2O scalelength and OH velocity used are 8.2×10^4 km and 1.15 km s^{-1}, respectively (Festou 1981). The OH coma is optically thin and an excitation factor for the OH(0,0) band of 4.4×10^{-4} photons s^{-1} mol^{-1} (Schleicher and A'Hearn 1982) is used to relate the predicted column density to surface brightness. Since the Haser model is spherically symmetric, it cannot explain the OH brightness asymmetry measured at ~4500 km from the nucleus. However, it does produce a satisfactory fit to the measured profile for the brighter hemisphere (the hemisphere facing the sun). The derived OH lifetime is 5×10^4 s, very close to the value derived from comet Bradfield. The derived water production rate at 0.83 AU is 1.8×10^{28} mol s^{-1}. This value may be a little high for a production rate averaged over all solid angles, since this is the value required to match the brightness profile for the brighter hemisphere.

From the OH(0,0) band brightnesses at the center of brightness of the comet, water production rates have been derived for the entire period of our IUE observations and are plotted in figure 4. The heliocentric variation in the water production rate for comet Encke varies as $r^{-3.3}$ for $0.81 \leq r \leq 1.014$ AU. This is to be compared to a variation of Q_{H_2O} as $r^{-3.7}$ for comet Bradfield (1979 X) over the range $0.71 \text{ AU} \leq r \leq 1.55$ AU (Weaver et al. 1981b). It appears that the heliocentric distance dependence of water production varies significantly from comet to comet and simple vaporization equilibrium models of the nucleus cannot explain this heliocentric variation.

Comet Encke was observed in HI Lyman-α during its 1970 apparition by the OGO-5 satellite. Bertaux et al. (1973) used the Lyα isophotes obtained during these observations to derive a hydrogen atom production rate of 6×10^{27} atoms s^{-1} for r = 0.715 AU and Δ = 0.438 AU. Assuming that $Q_{H_2O} = Q_H$, since they observed essentially only one of the two hydrogen

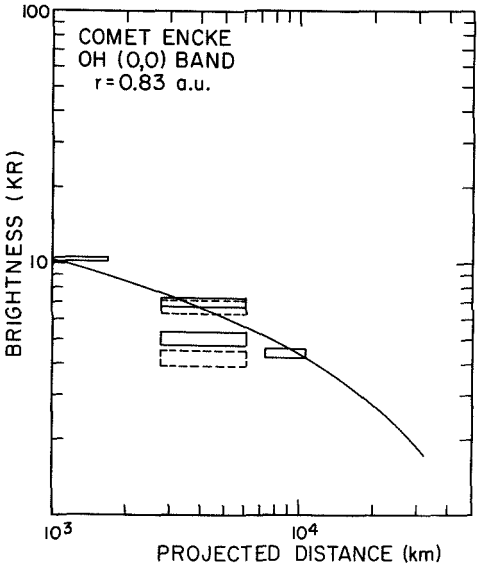

Fig. 3. Comparison of OH(0,0) band brightness profile with a Haser model. See text for details.

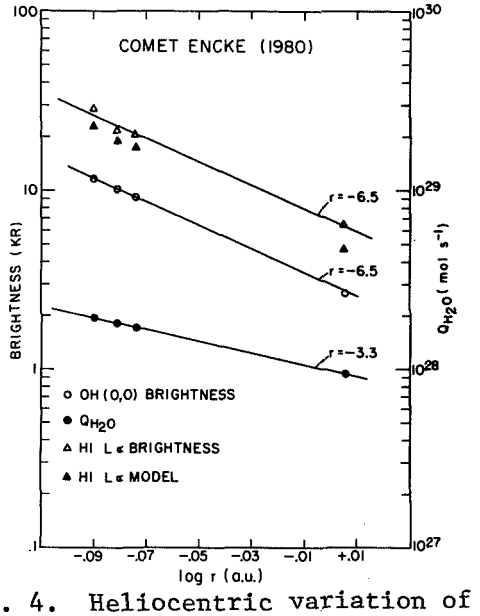

Fig. 4. Heliocentric variation of the OH and Lyman-α brightnesses and the derived water production rate.

components, this translates into a water production rate approximately a factor of five less than that reported here (extrapolating the IUE results for Q_{H_2O} to r = 0.715 AU assuming a heliocentric variation of $r^{-3.3}$). However, extreme caution must be exercised in comparing the results at these different heliocentric distances as the pre-perihelion visual light curve of P/Encke is known to exhibit an abrupt change in slope at r ≈ 0.8 AU with no further increase in brightness at smaller values of heliocentric distance. Moreover, during the 1980 apparition ground-based observations of A'Hearn and Millis (private communication, 1982) found the OH production rate to decrease as the comet moved from ≈ 0.79 AU to 0.75 AU by approximately a factor of five. Thus, the difference between the H_2O production rate derived from the IUE and OGO-5 data is not likely due to a change in the comet's activity between the 1970 and 1980 apparitions but rather to an anomalous gas production variation at r < 0.8 AU.

A full description of these results will be given elsewhere. This work was supported by NASA grant NSG-5393.

REFERENCES

Bertaux, J. L., Blamont, J. E. and Festou, M. 1973, Astr. Ap. 25, 415.

Festou, M. 1981, Astr. Ap., 95, 69.

Jackson, W. M. 1980, Icarus, 41, 147.

Schleicher, D. G. and A'Hearn, M. F. 1982, Ap. J., in press.

Weaver, H. A., Feldman, P. D., Festou, M. C. and A'Hearn, M. F. and Keller, H. U. 1981a, Icarus, 47, 449.

Weaver, H. A., Feldman, P. D., Festou, M. C. and A'Hearn, M. F. 1981b, Ap. J. 251, 809.

HIGH DISPERSION IUE-OBSERVATIONS OF JUPITER

R. Wagener, T. Owen, J. Caldwell, P. Winkelstein
E.S.S. Dept., SUNY, Stony Brook, N.Y. 11794

Four LWR and four SWP high dispersion IUE-exposures of Jupiter (center of the disk) have been combined to obtain a high resolution Jupiter spectrum with good signal-to-noise ratio in the wavelength range from 180 nm to 230 nm. This wavelength region is of particular interest for Jupiter, because of the already detected absorptions of Acetylene (Owen et al., 1980) and Ammonia (Combes et al. 1981) and potential absorbers like CO, PH_3 or CH_3.

As both the solar flux and the albedo of Jupiter decrease rapidly towards shorter wavelengths, it is impossible even with the longest exposure times of about 12 hours to obtain a good signal-to-noise ratio below 180 nm , where the strongest absorption bands of C_2H_2 are.

The spectra have been examined for CO absorptions at around 206 nm , but none have been detected thus far.

This research is supported by NASA grant NSG 5250 at Stony Brook.

References:

Combes, M., Courtin, R., Caldwell, J., Encrenaz, Th., Fricke, K.H., Moore, V., Owen, T., Butterworth, P.S., 1981, Adv. Space Res. Vol. 1, 169-175.

Owen, T., Caldwell, J., Rivolo, A.R., Moore, V., Lane, A. L., Sagan, C., Hunt, G., Ponnamperuma, C., 1980, Ap.J., 236, L39-42.

DATA REDUCTION

OSCILLATOR STRENGTHS AND COLLISION STRENGTHS FOR SOME IONS OF OXYGEN AND SULPHUR

Y. K. Ho and Ronald J. W. Henry
Department of Physics and Astronomy, Louisiana State University

ABSTRACT

Collision strengths for electron impact excitation of the O II, O III, S II and S III for some transitions in the ultraviolet of the type $ns^2\ np^q \rightarrow ns\ np^{q+1}$, $ns^2\ np^q \rightarrow ns^2\ np^{q-1}\ (n+1)s$ and $3s^2 3p^q \rightarrow 3s^2 3p^{q-1}\ 3d$ are calculated in a close-coupling approximation for an energy rate up to 10^6 K. Configuration interaction target wave functions which give oscillator strengths accurate to 10% for O II and O III, and 20-30% for S II and S III, are used in the expansion. Accurate knowledge of the electron impact excitation cross sections is particularly significant for a proper interpretation of the combined ultraviolet observations of the Voyager UVS and IUE results on properties of the Io plasma torus.

INTRODUCTION

Moos and Clarke (1981) used the short wavelength spectrograph of the International Ultraviolet Explorer (IUE) Satellite to obtain spectra of the torus of Io. These spectra show emissions of S II λ 1256, S III λ 1199, O III λ 1664, and S IV λ 1406. Observations of the extreme-ultraviolet spectrum of the Jupiter planetary system during the Voyager 1 and 2 encounters revealed bright emission lines of O II, O III, O IV, S II, S III, S IV, S V, and K III ions (Broadfoot et al. 1979, 1981; Shemansky 1980; Strobel and Davis 1980; Shemansky and Smith 1981). Interpretation of those lines has been uncertain due to a lack of accurate atomic data. For example, to date there is no consistent model of a plasma torus which simultaneously predicts intensities for the observed lines using ground-based measurements, IUE data, and Voyager data. The atomic collision data used is inaccurate since no allowance was made for considerable configuration mixing in previous calculations.

RESULTS

Wave functions for a given LS state of an ion are represented by a configuration-interaction (CI) expansion. The configuration weights, eigenenergies and the oscillator strengths in the dipole length (f_ℓ) and dipole velocity (f_v) approximations are obtained with program CIV3 of Hibbert (1975).

Configuration interaction effects are very important, particularly for transitions of the type $3s^2 3p^n \rightarrow 3s3p^{n+1}$. Table 1 gives oscillator strengths for these types of transitions in S II and S III. When the ground and

excited states are represented by single configurations (Hartree-Fock approximation, column HF), we obtain 0.78 and 0.39 for $3s3p^3\ ^4S^o$ - $3s3p^4\ ^4P$ in S II and $3s^23p^2\ ^3P$ - $3s3p^3\ ^3D^o$ in S III, respectively. At a similar level of approximation, Strobel and Davis (1980) obtained 0.71 and 0.39, respectively. These are contrasted with our C I results of 0.029 and 0.022 and similar values from experiments of Wiese, Smith, and Miles (1971) and Berry et al. (1970). Note also that agreement between f_ℓ and f_v may be necessary but it is not sufficient as an indicator of the reliability of a calculation. The oscillator strengths calculated in C I are probably accurate to 10%. Addition of configurations other than those used to obtain the given results did not significantly change the values.

We used the wave functions which give reasonably accurate oscillator strengths in a two-state close-coupling approximation calculation to obtain collision strengths. The collision strengths for the dipole allowed transitions are fitted to a simple functional form

$$\Omega(x) = c_o + c_1 x^{-1} + c_2 \ln x + c_3 x^{-2}$$

where $x = k_i^2/\Delta E_{ij}$, k_i^2 is the energy of the incident electron relative to the lowest state i, and ΔE_{ij} is the energy difference between states i and j.

Oscillator strengths and collision strengths have been calculated for the lines listed in Table 2. In addition, calculations of oscillator strengths have been made for some uv lines of O II which have lower states $2p^3\ ^2D^o$ or $2p^3\ ^2P^o$ (Ho and Henry 1982a); of S II which have lower states $3p^3\ ^2D^o$ or $3p^3\ ^2P^o$ (Ho and Henry 1982b); and of S III which have lower states $3p^2\ ^1D$ and $3p^2\ ^1S$ (Ho and Henry 1982c).

We conclude that use of elaborate C I wave functions is probably more important than the choice of scattering approximation in determining accurate collision strengths. Oscillator strengths obtained with the same target wave function as collision strengths probably provide a figure of merit for the latter.

Research was supported in part by NASA grant NAGW-48.

REFERENCES

Berry, H. G. et al. 1970, J. Opt. Soc. Am., 60, 335.

Bhadra, K. and Henry R. J. W. 1980, Astrophys. J., 240, 368.

Broadfoot, A. L. et al. 1979, Science, 204, 979.

Broadfoot, A. L. et al. 1981, J. Geophys. Res., 86, 8259.

Hibbert, A. 1975, Comput. Phys. Commun., 9, 141.

Ho, Y. K. and Henry, R. J. W. 1982a, submitted to Astrophys. J.

Ho, Y. K. and Henry, R. J. W. 1982b, in preparation.

Ho, Y. K. and Henry, R. J. W. 1982c, in preparation.

Moos, H. W. and Clarke, J. T. 1981, Astrophys. J., 247, 354.

Shemansky, D. E. 1980, Astrophys. J., 236, 1043.

Shemansky, D. E. and Smith, G. R. 1981, J. Geophys. Res., 86, 9179.

Strobel, D. F. and Davis, J. 1980, Astrophys. J. 238, L49.

VanWyngaarden, W. L. and Henry, R. J. W. 1981, Astrophys. J., 246, 1040.

Wiese, W. L., Smith, M. W., and Miles, B. M. 1969, NSRDS-NBS 22, Vol. 2.

Table 1

Oscillator Strengths

Ion	λ(nm)		HF	CI	EXP
S II	125.6	f_ℓ	0.78	0.029	0.028[a]
		f_v	0.79	0.030	
S III	119.9	f_ℓ	0.39	0.022	0.023 ± 0.001[b]
		f_v	0.46	0.025	

REFERENCES: [a]Wiese, Smith, and Miles (1971).

[b]Berry et al. (1970).

Table 2

Calculations of Collision Strengths

Ion	Transition Wavelengths λ(nm)	Ref
O II	83.4 , 53.9	1
O III	83.5 , 70.3 , 50.8	1
S II	125.6 , 91.0 , 76.5	2
S III	119.9 ,101.8 , 72.6 , 70.1 , 68.3 , 68.0	3
S IV	140.6 ,107.3 , 81.6 , 75.3	4
S V	119.3 , 78.6 , 51.9 , 49.8 , 42.6 , 32.1	5

REFERENCES:
1. Ho and Henry (1982a).
2. Ho and Henry (1982b).
3. Ho and Henry (1982c).
4. Bhadra and Henry (1980).
5. VanWyngaarden and Henry (1981).

THE IUE ECHELLE BLAZE FUNCTION

Thomas B. Ake

Computer Sciences Corporation

Abstract

An improved form for the echelle blaze function derived by Ake (1981) has been used to study the apparent variation of grating constant K with order m for the long and short wavelength spectrographs. For the LWR camera, early images indicate that K should vary linearly with order. It is suggested that this represents a rotation of the observed blaze centers on the camera compared to a constant $K=m\lambda$ line. In four years of use, changes in sensitivity across the camera has changed the observed blaze function, inducing a curvature in the K versus m relation. This curvature varies in time with variations in camera response. The SWP camera shows these effects to a lesser degree.

The Blaze Function

Ahmad (1981) has suggested and Ake (1981) has derived a correction for the echelle blaze of the form $\mathrm{sinc}^2(\pi\alpha X)$, $X=m(\lambda/\lambda_c-1)$ where m is the order number, a is a constant dependent upon the grating profile, and λ_c, the wavelength at the blaze peak, is given by the grating constant K divided by m. By using least squares techniques to optimize the α and K constants for well-exposed continuous sources, they found that α (which sets the blaze width) is constant ($\cong 0.85$ for SWP, $\cong 0.89$ for LWR), but that K varies with order number. When correcting the observations using these parameters, each order can be flattened independently of the others, but Ake demonstrated that fluxes in regions of order overlap will not agree unless each order is adjusted by a scaling constant. Furthermore, when the observed blaze centers are plotted as they appear on the camera faceplate, the locus is curved rather than linear as the $K=m\lambda_c$ relation implies.

The cause of these problems lies with the fact that the wavelength sensitivities of the cameras has not been explicitly taken into account. To do this we note that the observed flux is the convolution of the stellar flux with the instrument transmission function:

$$FN(\lambda,m) = \int_0^\infty F_*(\lambda')\ P(\lambda-\lambda')\ B(\lambda'-K/m)\ S(\lambda')\ d\lambda'$$

where FN is the IUE flux number, F_* the stellar flux, P the high dispersion point spread function, B the echelle blaze function, and S the response of the rest of the system. For continuous sources we let $P = \delta(\lambda-\lambda')$, and since the only difference between the echelle setup and the low dispersion mode is the use of a plane mirror in front of the echelle grating, we let $S(\lambda)$ be the calibrated low dispersion sensitivity (Bohlin and Holm 1980). We then try to optimize the blaze function K and α parameters so $B = FN/F_*/S_{low}$. For the LWR, we must also transform the IUE wavelengths from air back to vacuum values before performing the computations.

The resultant α values are found to be virtually unchanged from the previous analyses by Ahmad and Ake, and although the derived K values are found still to vary with order, the location of the blaze wavelengths are linearized on the camera faceplate (figures 1 and 2). Moreover fluxes in the order overlap regions are found to agree. However, when examining images taken for calibration purposes since the IUE commissioning phase, it became apparent that while the SWP parameters were constant with time, those for the LWR were changing secularly: for $m > 95$, the observed blaze center was shifted towards shorter wavelengths and the shape was becoming narrower.

Apparent Sensitivity Changes

Such changes for the LWR are consistent with non-uniform changes occurring in the camera response. Schiffer (1982) summarizes sensitivity variations seen in the low dispersion mode for the LWR and SWP. For high dispersion, observations of the IUE standard η U Ma have been taken periodically since launch, although not as often as the low dispersion standards. Only 15 LWR and 16 SWP useable large aperture spectra are available, and for this study, all were re-processed with the new high dispersion software.

Nine areas on the camera, located along the nominal peak and half-power points of the blaze and centered on orders 82, 97 and 112, were examined (figures 1 and 2). Linear rates of change in sensitivity were calculated for each area (table I), although Schiffer has found that each camera has had periods of both stability and greater change. For the LWR, a differential degradation is found, increasing towards higher orders on the long wavelength side of the blaze peak. This alters the observed blaze shape, shifting the observed peak towards shorter wavelengths, decreasing the width, and lowering the total flux in the order.

Results for the SWP are consistent with little change occurring, and indeed the observed blaze function parameters are quite steady.

References

Ahmad, I. A. 1981, IUE NASA Newsletter, No. 14, p. 129.

Ake, T. B. 1981, IUE NASA Newsletter, No. 15, p. 60.

Bohlin, R. and Holm, A. V. 1980, IUE NASA Newsletter, No. 10, p. 37.

Schiffer, F. H. III 1982, Report to the Three-Agency Meeting, March 1982.

Table I. Gross Camera Sensitivity Changes (% Change per year)

Area	LWR	SWP	Area	LWR	SWP
1	-1.43 $\pm$ 0.71	-1.34 $\pm$0.59	6	-3.61	+0.19
2	-1.31	-0.65	7	-2.42	+0.24
3	-1.73	-0.27	8	-2.42	-0.10
4	-1.60	-0.74	9	-5.59	+1.06
5	-2.81	-0.73			

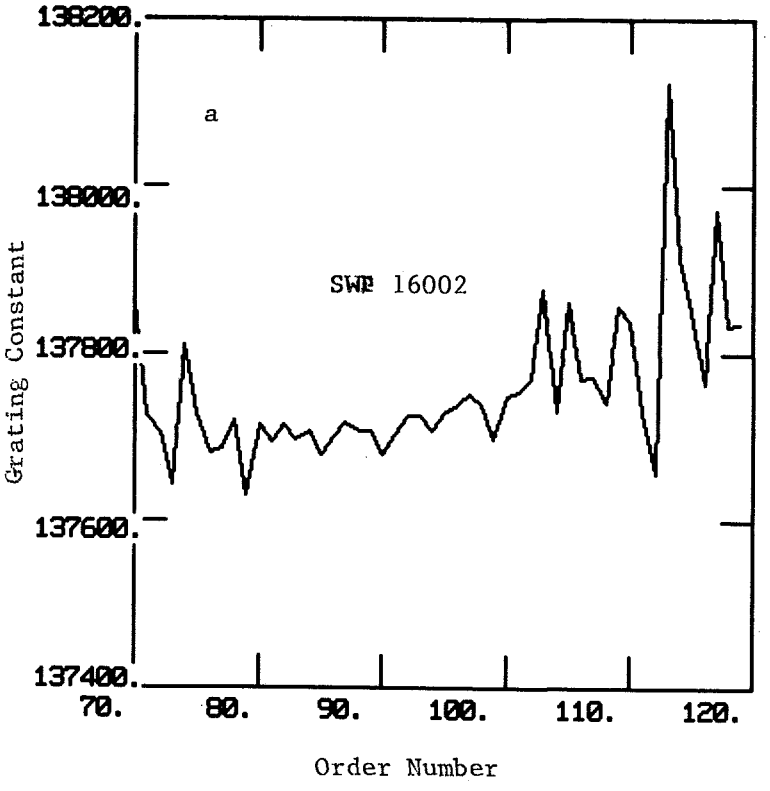

Figure 1. a. Variation of grating constant K with order for η U Ma, SWP 16002 taken January 1982.

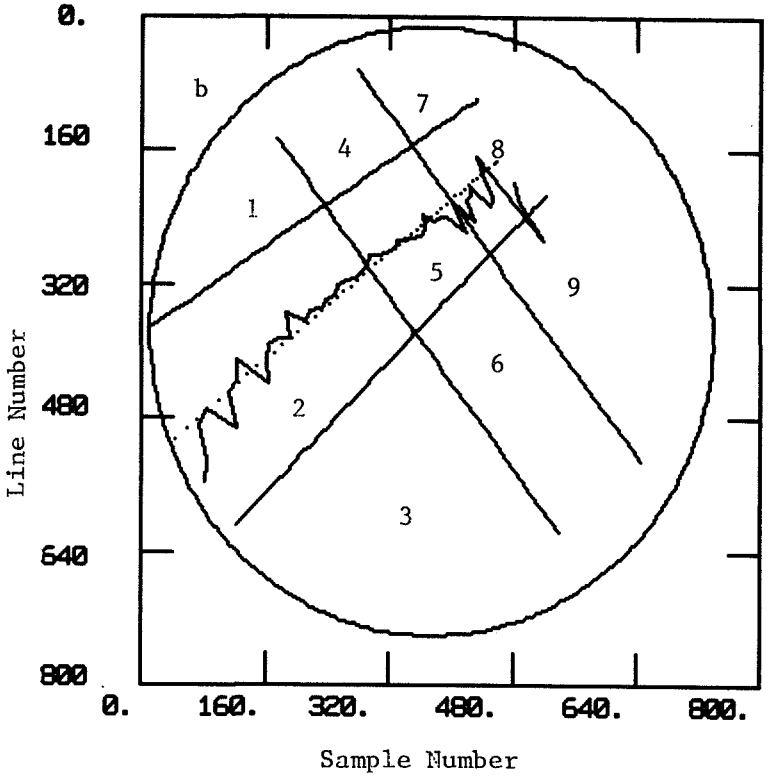

b. Location of observed blaze centers on camera (line) compared to λ_c = 137725/m (dots). Regions in table I used to study sensitivity changes are shown.

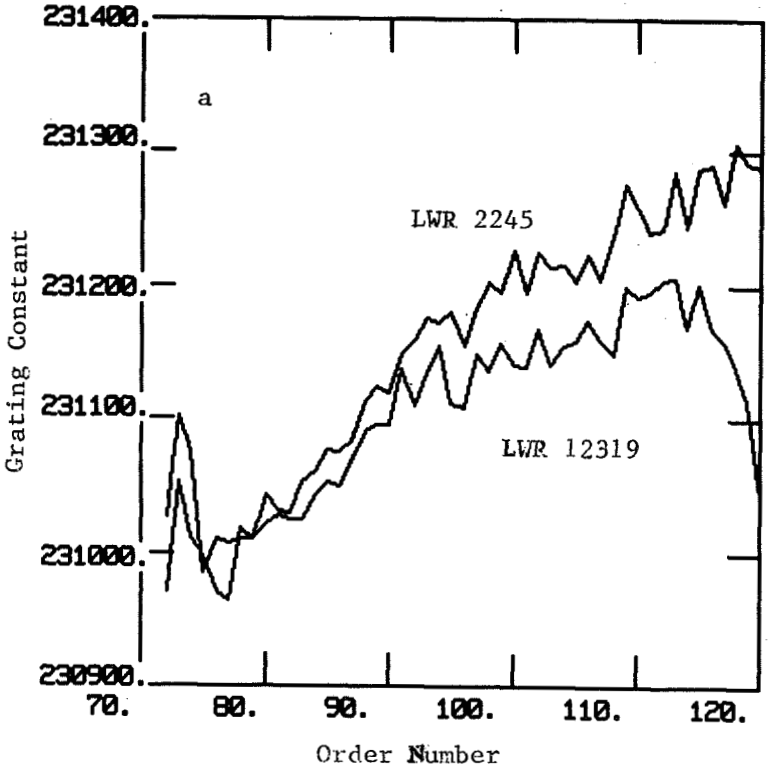

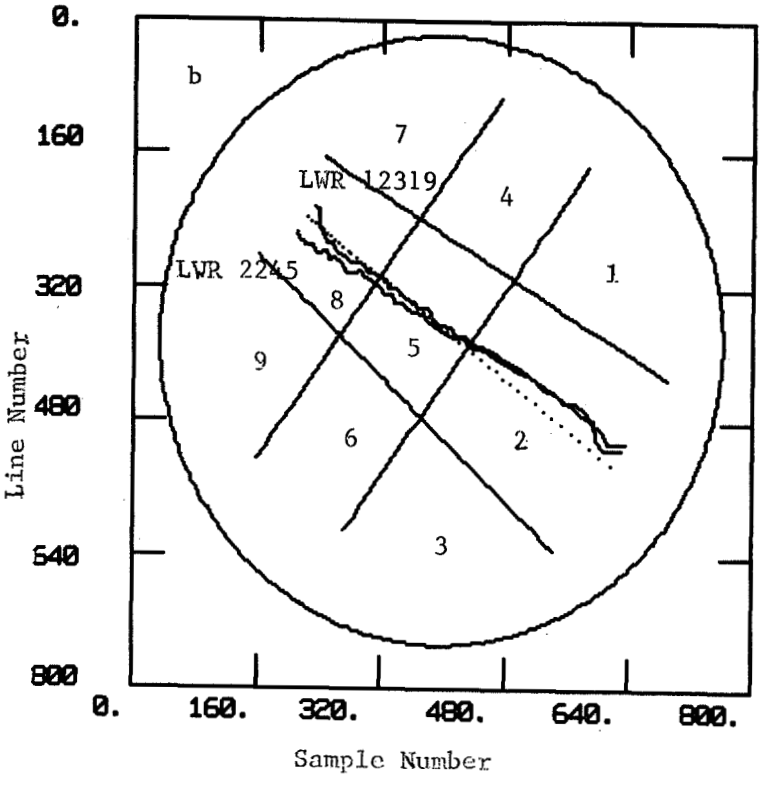

Figure 2. a. Variation of grating constant K with order for η U Ma, LWR 2245 taken September 1978 and LWR 12319 taken January 1982. K values are for vacuum wavelengths, not air.

b. Location of observed blaze centers on camera (lines) compared to λ_c = 231150./m (dots). Regions in table I used to study sensitivity changes are shown.

BIBLIOGRAPHICAL INDEX OF OBJECTS OBSERVED BY IUE

Jaylee M. Mead and Albert Boggess

Laboratory for Astronomy and Solar Physics
Goddard Space Flight Center

ABSTRACT: We have searched six astronomical journals and identified 343 papers describing studies using data obtained with the International Ultraviolet Explorer (IUE) satellite. From a review of these papers, we have recorded the names of the astronomical objects discussed. These objects have been compiled into a list of 2460 entries, along with each reference, and sorted by object name or catalogue number. This index enables a user to tell immediately where to find published papers describing IUE observations of the objects of interest to him.

* * * * *

Four years of observations with the International Ultraviolet Explorer (IUE) satellite have yielded approximately 23,000 spectra of many diverse astronomical objects. Most of this data is now in the public domain and can be obtained for further analysis upon request to the National Space Science Data Center or through the IUE Regional Data Analysis Facility at the Goddard Space Flight Center.

The purpose of this paper is to provide the prospective user of IUE data with a bibliographic index to the literature which describes observations made with or related to IUE. We have searched six journals (Astrophys. J., Astron. & Astrophys., Mon. Not. Roy. Astron. Soc., Astron. J., Nature, and Publ. Astron. Soc. Pacific) covering 1978 through 1981 to identify papers describing observations made using the IUE satellite. These 343 papers have been reviewed in order to record the names of the objects discussed by these authors. This data has been sorted by object name or catalogue number for convenient use, and the bibliographical information retained for each entry.

Although some journals do provide bibliographic indices by object name, they usually record only those names which are explicitly given in the title. Many papers report data for a group of stars or galaxies; objects in such lists would be omitted from the usual index. An additional advantage of a merged index for these six journals is that it is neccesary for one to review only one source.

One of the earliest developments in the area of bibliographic data archival was led by Cayrel et al. (1974). His group compiled the Bibliographical Star Index (BSI), a machine-readable data file of stellar references covering twelve periodicals from 1950-72 and more than 30 since then. Updated versions of the BSI are released periodically by the Centre de Données Stellaires (CDS) at Strasbourg. The major difference between the BSI and the IUE Bibliographical Index is that the latter is restricted to IUE observations and its coverage ranges from the solar system to extragalactic objects. Because it is a smaller data set, it can be produced on a more current basis in an easily distributable format.

The following criteria were used in deciding which objects, in addition to the primary ones covered in the paper, should be retained in the final index: did the author provide additional data or comments about the object, and should this paper be consulted if one were using IUE to study this object? In cases where an author states only that a certain object was observed by another worker, the object's name is not recorded unless the author used the object for comparison or included additional data or comments about the object. In cases where multiple identifications of an object were given, all of the names were entered in our listing. The index of 2460 entries is ordered alphabetically by astronomical object name.

Table 1 shows the first page from the 19-page Object Index. The double-columned listing gives the object's name or catalogue number, the journal, volume, page, year, and the author(s). Because there are few standardized nomenclature practices for most of the objects included in this list, there is little uniformity in the entry of the names. It is our hope that compilations such as this may be useful in pointing out some of the ambiguous designations currently used in the naming of stellar and extragalactic objects.

The complete reference, including the title of the paper, is given in the 15-page Author Index, as illustrated in Table 2. Table 3 gives a breakdown of the number of IUE papers by journal covered in this survey.

It is hoped that this Bibliographical Index will help the prospective user of IUE data to locate the papers describing the objects of interest to him. In this way he may be led to useful sources in the literature which he might otherwise overlook.

Future plans include expanding the number of journals covered, especially for solar system objects. We are also considering the possibility of incorporating the IUE Merged Observing Log in order to provide positions and information on the types of objects observed.

We welcome any comments and recommendations which will help us to make this a more useful reference tool. We thank Gilbert Mead for writing the programs to sort the data and generate Table 1 on a TRS-80 computer. Table 2 was prepared by AB on an Apple computer. Copies of the index may be obtained from J. Mead, Code 680, GSFC.

REFERENCE: Cayrel, R., J. Jung, and A. Valbousquet. CDS Inform. Bull. 6, 24 (1974).

Table 1 - OBJECT INDEX

OBJECT	JOUR	VOL	PG	YR	AUTHOR(S)
0115+61	PASP	93	486	81	Hutchings & Crampton
0716+71	A&A	100	1	81	Fricke et al.
2A 0311-227	Nat	290	119	81	Coe & Wickramasinghe
2A 0526-328	Nat	290	119	81	Coe & Wickramasinghe
2A 0620-00	MN	195	61	81	Barlow et al.
2A 2315-428	MN	192	769	80	Clavel et al.
2A0311-23	A&A	102	31	81	Mouchet et al.
2A0526-33	A&A	102	31	81	Mouchet et al.
3C 58	MN	192	861	80	Panagia et al.
3C 120	ApJ	231	L13	79	Oke & Zimmerman
3C 120	ApJ	242	14	80	Wu et al.
3C 120	ApJ	243	445	81	Oke & Goodrich
3C 120	A&A	97	94	81	Bergeron et al.
3C 232	Nat	275	404	78	Boksenberg et al.
3C 273	ApJ	226	L57	78	Baldwin et al.
3C 273	ApJ	230	L131	79	Boggess et al.
3C 273	ApJ	242	14	80	Wu et al.
3C 273	A&A	97	94	81	Bergeron et al.
3C 273	A&A	102	321	81	Joly
3C 273	MN	187	65p	79	Ferland et al.
3C 273	MN	192	561	80	Ulrich et al.
3C 273	Nat	275	377	78	Boggess et al.
3C 273	Nat	275	404	78	Boksenberg et al.
3C 274	Nat	275	404	78	Boksenberg et al.
3C 351	ApJ	239	483	80	Green et al.
3C 390.3	ApJ	242	14	80	Wu et al.
3C 390.3	ApJ	243	445	81	Oke & Goodrich
3C 390.3	MN	187	65p	79	Ferland et al.
3U 1700-37	Nat	275	394	78	Grewing et al.
4U 0352+30	A&A	94	345	81	Bernacca & Bianchi
4U 0352-130	A&A	85	119	80	Hammerschlag-Hensbg.etal
4U 0900-40	ApJ	238	969	80	Dupree et al.
4U 1145-61	A&A	85	119	80	Hammerschlag-Hensbg.etal
4U 1145-61	A&A	89	214	80	Bianchi & Bernacca
4U 1145-61	A&A	104	150	81	De Loore et al.
4U 1651+39	MN	189	873	79	Snijders et al.
4U 1656+35	Nat	275	400	78	Dupree et al.
4U 1700-37	ApJ	237	19	80	Bruhweiler et al.
4U 1700-37	ApJ	240	161	80	Hutchings & Dupree
4U 1700-37	Nat	275	400	78	Dupree et al.
4U 1908+00	MN	195	61	81	Barlow et al.
4U 1956+35	Nat	275	400	78	Dupree et al.
AS 205	ApJ	251	113	81	Giampapa et al.
AS 205	A&A	90	184	80	Appenzeller et al.
AS 374	MN	196	101	81	Barlow et al.
AS 422	MN	196	101	81	Barlow et al.
Abell 30	ApJ	245	124	81	Greenstein
Ak 120	A&A	102	321	81	Joly
Akn 120	A&A	102	L23	81	Kollatschny et al.
Akn 120	A&A	104	198	81	Kollatschny et al.
And 51	ApJ	234	1023	79	Basri & Linsky
And 51	ApJ	238	221	80	Stencel & Mullan
And 51	ApJS	44	383	80	Stencel et al.
And Beta	ApJ	234	1023	79	Basri & Linsky
And EG	ApJ	238	929	80	Stencel & Sahade
And Lambda	ApJ	226	L35	78	Doschek et al.
And Lambda	ApJ	229	L27	79	Linsky & Haisch
And Lambda	ApJ	234	1023	79	Basri & Linsky
And Lambda	ApJ	247	545	81	Ayres et al.
And Lambda	ApJ	251	113	81	Giampapa et al.
And Lambda	A&A	102	207	81	De Castro et al.
And Lambda	A&A	104	240	81	Saxner
And Lambda	Nat	275	389	78	Linsky et al.
And Mu	ApJ	244	938	81	Bohm-Vitense
And RX	ApJ	247	577	81	Szkody
And Z	ApJ	245	630	81	Altamore et al.
And Zeta	A&A	102	207	81	De Castro et al.
And Zeta	A&A	104	240	81	Saxner
Aps Gamma	ApJ	238	221	80	Stencel & Mullan
Aps Gamma	ApJS	44	383	80	Stencel et al.
Aps Gamma	ApJ	244	504	81	Bohm-Vitense
Aql 31	ApJ	244	504	81	Bohm-Vitense
Aql Alpha	ApJ	236	560	80	Bohm-Vitense & Dettmann
Aql Alpha	ApJ	244	938	81	Bohm-Vitense
Aql Alpha	A&A	93	412	81	Mundt et al.
Aql Eta	ApJ	238	L87	80	Mariska et al.
Aql Gamma	ApJ	234	1023	79	Basri & Linsky
Aql R	A&A	92	320	80	Kafatos et al.
Aql V603	ApJ	248	1059	81	Slovak
Aql V603	A&A	88	L9	80	Rahe et al.
Aql V603	A&A	99	166	81	Drechsel et al.
Aql V603	A&A	102	337	81	Krautter et al.
Aql V603	PASP	93	477	81	Lambert & Slovak
Aql X-1	MN	195	61	81	Barlow et al.
Aql Zeta	ApJ	244	199	81	Witt et al.
Aqr 88	ApJ	234	1023	79	Basri & Linsky
Aqr AE	ApJ	247	577	81	Szkody
Aqr AE	MN	191	559	80	Jameson et al.
Aqr Alpha	ApJ	236	L143	80	Hartmann et al.
Aqr Alpha	ApJ	236	560	80	Bohm-Vitense & Dettmann
Aqr Alpha	ApJ	238	221	80	Stencel & Mullan
Aqr Alpha	ApJ	239	555	80	Parsons
Aqr Alpha	ApJS	44	383	80	Stencel et al.
Aqr Alpha	ApJ	244	504	81	Bohm-Vitense
Aqr Alpha	ApJ	244	552	81	Johnson
Aqr Alpha	ApJ	246	193	81	Hartmann et al.
Aqr Alpha	ApJ	251	162	81	Basri et al.
Aqr Alpha	A&A	104	240	81	Saxner
Aqr Beta	ApJ	234	1023	79	Basri & Linsky
Aqr Beta	ApJ	236	L143	80	Hartmann et al.
Aqr Beta	ApJ	236	560	80	Bohm-Vitense & Dettmann
Aqr Beta	ApJ	238	221	80	Stencel & Mullan
Aqr Beta	ApJ	239	555	80	Parsons
Aqr Beta	ApJS	44	383	80	Stencel et al.
Aqr Beta	ApJ	244	504	81	Bohm-Vitense
Aqr Beta	ApJ	244	552	81	Johnson
Aqr Beta	ApJ	251	162	81	Basri et al.
Aqr Beta	A&A	104	240	81	Saxner
Aqr Pi	ApJ	239	502	80	Black et al.
Aqr Pi	A&A	100	79	81	Ringuelet et al.
Aqr R	ApJ	237	506	80	Michalitsianos et al.
Aqr R	ApJ	237	840	80	Johnson
Aqr R	ApJ	244	552	81	Johnson
Aqr R	Nat	284	148	80	Michalitsianos et al.
Ara Gamma	ApJ	245	201	81	Parsons
Ara OBla	ApJ	248	528	81	Cowie et al.
Ara OBla	ApJ	250	L25	81	Cowie et al.
Ara OBlb	ApJ	248	528	81	Cowie et al.
Ara OBlb	ApJ	250	L25	81	Cowie et al.
Arcturus	ApJ	235	519	80	Haisch et al.
Arcturus	ApJ	247	545	81	Ayres et al.
Arcturus	ApJ	248	L137	81	Ayres et al.
Arcturus	A&A	99	120	81	Nesci
Arcturus	A&A	103	L11	81	Spite et al.
Ari Alpha	ApJ	234	1023	79	Basri & Linsky
Ari Alpha	ApJS	44	383	80	Stencel et al.
Ari TT	A&A	98	27	81	Krautter et al.
Ari TT	A&A	102	337	81	Krautter et al.
Ari UX	ApJ	229	L27	79	Linsky & Haisch
Ari UX	ApJ	234	1023	79	Basri & Linsky
Ari UX	ApJ	239	911	80	Simon et al.
Ari UX	ApJ	241	279	80	Ayres & Linsky
Ari UX	ApJ	241	759	80	Simon & Linsky
Ari UX	ApJ	247	L131	81	Bopp & Stencel
Ari UX	ApJ	251	113	81	Giampapa et al.
Ari UX	A&A	104	240	81	Saxner

Table 2 - AUTHOR INDEX

Table 3 - JOURNALS SEARCHED FOR IUE BIBLIOGRAPHICAL INDEX AND NUMBER OF IUE PAPERS BY JOURNAL

	'78	'79	'80	'81	Totals
Astrophys. Journ.	2	18	59	68	147
Astron. & Astrophys.	2	18	25	50	95
Mon. Not. Roy. Astron. Soc.	-	5	22	26	53
Nature	10	7	8	5	30
Publ. Astron. Soc. Pacific	-	3	3	9	15
Astron. Journ.	-	-	-	3	3
Totals	14	51	117	161	343

IUE DATA REDUCTION: WAVELENGTH DETERMINATIONS AND LINE IDENTIFICATIONS USING A VAX/750 COMPUTER

J.P. Davidson
Department of Physics and Astronomy, University of Kansas

and

D.J. Bord
Department of Physics, Benedictine College

ABSTRACT

A fully automated, interactive system for determining the wavelengths of features in extracted IUE spectra using a VAX/750 computer is described. Wavelengths are recorded from video displays of expanded plots of individual orders using a movable cursor, and then corrected for IUE wavelength scale errors. The estimated accuracy of an individual wavelength in the final tabulation is 0.050 Å. Such lists are ideally suited for line identification work using the method of wavelength coincidence statistics (WCS), and we present the results of WCS studies of the ultraviolet spectra of the chemically peculiar (CP) stars ι CrB and κ Cnc. Aside from confirming a number of previously reported aspects of the abundance patterns in these stars, our searches have produced some interesting, new discoveries, notably the presence of Hf in the spectrum of κ Cnc. The implications of this work for theories designed to account for anomalous abundances in chemically peculiar stars will be briefly discussed.

INTRODUCTION

The method of wavelength coincidence statistics (WCS) has been shown to be a useful ancillary tool for line identifications in stars in the visual region of the spectrum (Hartoog, Cowley, and Cowley 1973; Cowley, Hartoog, and Cowley 1974). More recently, it has been demonstrated that this method can also be effectively used in the ultraviolet region of the spectrum (Bord and Davidson 1982; Davidson and Bord 1982). The ultimate success of this method depends in part on the ability to rapidly and accurately assemble lists of wavelengths of features judged to be real in displays of the stellar spectra. In the visual, stellar line lists can be prepared in the usual fashion from plate material using Grant measuring engines. In the ultraviolet, using high dispersion data returned by the IUE spacecraft, other methods must be found to display and record the wavelengths of the stellar lines.

VAX/750 ANALYSIS SYSTEM

Within the last year, we have developed an interactive system designed for use with extracted IUE spectra which runs on a VAX/750 computer supported by a Tektronix 4020A color graphics terminal in FORTRAN. The system

capabilities are similar to those described by Klinglesmith and Faney (1980) in that one can display single order plots or expanded plots of parts of one order, and determine the wavelengths of features in each. Other analysis routines involving the determination of equivalent widths and central depths for individual lines, and the filtering and/or averaging of multiple spectra are currently being perfected, but are not required for use with the WCS methodology.

At the present time, we display a fraction of an order on the video monitor at a scale of ~1 Å/inch and record the wavelengths of all features judged to be real using a movable cursor. The measured wavelengths are stored in order of increasing wavelength in an order-by-order fashion and then corrected for IUE wavelength scale errors in a semi-automated version of the technique described by Leckrone (1980). The resulting lists are automatically purged of reseaux marks and duplicate lines from adjacent orders, and then merged to form one master list of stellar wavelengths whose estimated accuracy per line is ~0.050 Å. To assemble a list of this type by hand using CalComp plots drawn to the same scale originally required ~100 man-hours of effort; with the current system, the process requires substantially less than 1/2 of that amount of time.

RESULTS

κ Cancri

This sharp-lined, Hg-Mn star has been extensively studied since 1960 when Bidelman described its remarkable spectrum (see Bord and Davidson 1982 and the references cited therein). Our interest in this star originally derived from the report by Leckrone and Heacox (1979) of 27 short wavelength IUE features which they attributed to Au III. We undertook a search for gold and other heavy elements in the long wavelength IUE spectrum of this star using the method of WCS, but have now expanded our element search to include the first three ionization states of nearly every species in the periodic table from lithium through uranium. The stellar line list for this star, established in the manner described in the previous section, comprised 2524 lines spanning the interval 1969.202 to 3227.429 Å. Laboratory wavelengths were taken mainly from the list of Kurucz and Peytremann (1975), but were supplemented where necessary from the tabulations of Kelly (1979), and Reader and Corliss (1980). To achieve some degree of compatibility between the strengths of the weakest lines taken from each of these sources and those of the measured lines, we compiled only those features having log $gf \geq -1.50$ from the Kurucz-Peytremann list. The details of the application of the WCS method in the ultraviolet are given elsewhere (Bord and Davidson 1982); we present in Table 1. the results of our survey for those atoms/ions likely to be present with 95% confidence or greater.

Based on the criteria adopted in our previous work, we see from Table 1. that there is "good" statistical evidence to support the identification of Ca II, Mn II, Fe II, and Cd II since these species all have S>3. Aside from the cadmium identification, these results are not surprising given previous investigations of this star. Moreover, we are disposed to believe the identification of cadmium in this star despite the small number of lines in the

wavelength range searched since an examination of the spectral tracings reveals moderately strong lines at the correct wavelengths (λλ2144.38, 2265.02, 2312.84, and 2572.93) for which no better, alternative identification(s) could be found. This is, to our knowledge, the first reported observation of cadmium in κ Cnc.

The remaining identifications given in Table 1. have S<3 but $f \leq 0.05$, and belong to the category of "possibly present" elements. We have estimated the number of marginal events to be expected from our analysis using the technique developed by Cowley and Hensberge (1981) and find that the number of chance identifications in a search for 105 uncorrelated atomic species not known to be definitely present beforehand is 3, assuming $\Omega \approx 0.03$. The fact that 13 such cases have been found indicates that the vast majority of these identifications are real. Careful scrutiny of the spectral tracings has produced evidence to corroborate the identifications of Mg II, Si II, Cl II, Cr II, Ni II, Sr II, Zr II, and Os II (Bord and Davidson 1982; Davidson and Bord 1982). Of the remaining elements, N II, P I, Ti III, In I, and Hf II, the most likely candidates for chance identifications are P I, In I, Ti III, and/or N II given their ionization potentials and the temperature of the star (T_e = 13,500 K). In view of this, the likelihood of hafnium being present in κ Cnc is enhanced, in which case κ Cnc joins HR 465 as showing evidence of this rare earth element (Hartoog, Cowley, and Cowley 1973).

ι Coronae Borealis

Similar analyses of the Hg-Mn star ι CrB were undertaken using short wavelength IUE data spanning the interval 1233.967-2124.700 Å. The stellar line list contained 4071 features, and coincidences were sought between these lines and laboratory line lists for some 104 species. Although we have yet to carry out a careful line-by-line search to substantiate the results of our statistical survey, there appears to be marginal evidence to support the first-time identification of the following ions in this star: W II (at the 99.5% confidence level), Co II (at the 98.5% confidence level), and Mo II (at the 96% confidence level). With regard to the latter two species, it is of interest to note that Hartoog, Cowley, and Cowley (1973) have reported "good" evidence of their existence in the spectrum of the Ap star HR 465.

DISCUSSION

The preceding results, though in need of confirmation in several instances, demonstrate the value of the WCS method as a tool for rapidly identifying trace elements in stellar spectra. They also point out the gains which stand to be made in establishing abundance patterns in CP stars from studies in the ultraviolet. For example, the emerging similarities between the Hg-Mn stars κ Cnc and ι CrB and the Cr-Eu Ap star HR 465 as regards their heavy element abundances leads one to wonder, with Hartoog, Cowley and Cowley (1973), whether there may be some relationship between these two types of peculiar stars. The identification of such relationships between differing groups of CP stars would be yet another step toward enabling definitive statements to be made about the mechanism(s) responsible for CP star phenomena.

REFERENCES

Bidelman, W.P. 1960, Pub. A.S.P., 72, 471.

Bord, D.J., and Davidson, J.P. 1982, Ap. J., in press.

Cowley, C.R., Hartoog, M.R., and Cowley, A.P. 1974, Ap. J., 194, 343.

Cowley, C.R., and Hensberge, H. 1981, Ap. J., 244, 252.

Davidson, J.P., and Bord, D.J. 1982, Astron. Astrophys., in press.

Hartoog, M.R., Cowley, C.R., and Cowley, A.P. 1973, Ap. J., 182, 847.

Kelly, R.L. 1979, Atomic Emission Lines in the Near Ultraviolet: Hydrogen Through Krypton, NASA Technical Mem. 80268.

Klinglesmith, D.A., and Faney, R.P. 1980, IUE NASA Newsletter No. 8, p. 39.

Kurucz, R.L., and Peytremann, E. 1975, Smithsonian Astrophys. Obs. Special Report No. 362.

Leckrone, D.S. 1980, IUE NASA Newsletter No. 10, p. 25.

Leckrone, D.S., and Heacox, W.P. 1979, Pub. A.S.P., 90, 492.

Reader, J., and Corliss, C.H. 1980, Wavelengths and Transition Probabilities for Atoms and Atomic Ions, Part I: Wavelengths, NSRDS-NBS 68.

Table 1. WCS Results for κ Cancri

Atom-Ion	Z	N[a]	H[b]	$\langle H_{200} \rangle$[c]	S[d]	f[d]
N II	7	99	26	14.65	1.887	0.025
Mg II	12	18	8	2.96	2.716	0.02
Si II	14	75	22	2.69	2.029	0.02
P I[e]	15	26	14	6.32	2.031	0.03
Cl II	17	73	19	10.63	1.985	0.03
Ca II	20	8	5	1.33	3.280	0.005
Ti III	22	29	12	5.51	2.746	0.005
Cr II	24	731	191	110.77	2.561	0.0
Mn II	25	1224	483	197.48	4.891	0.0
Fe II	26	736	319	123.40	5.165	0.0
Ni II	28	667	233	140.76	1.719	0.0
Sr II	38	8	5	1.63	2.539	0.035
Zr II	40	135	26	15.98	2.327	0.015
Cd II	48	4	4	0.76	3.776	0.0
In I	49	11	4	1.18	2.775	0.03
Hf II	72	175	42	25.46	2.308	0.01
Os II[f]	76	37	13	6.32	2.692	0.005

[a]N = Number of laboratory lines in the spectral range investigated.

[b]H = Number of coincidences or "hits" on the laboratory wavelengths.

[c]$\langle H_{200} \rangle$ = Average number of "hits" on 200 sets of random control wavelengths.

[d]S, f = Significance parameters for the WCS methodology; definitions and interpretations of these quantities may be found in Hartoog, Cowley, and Cowley (1973), and Cowley, Hartoog, and Cowley (1974).

[e]Laboratory wavelengths for this species were taken from Kelly (1979).

[f]Laboratory wavelengths for this species were taken from Reader and Corliss (1980).

FAINT OBJECT STUDIES WITH IUE

Theodore R. Gull
Laboratory for Astronomy and Solar Physics
NASA/Goddard Space Flight Center

To push IUE to the limit on faint sources, it is necessary to establish detector background contributions from the night sky, energetic particle events, detector flaws and calibration errors. A recent study of the Crab Nebula (K. Davidson, T.R. Gull, S.P. Maran, T.P. Stecher, R.A. Fesen, R.A. Parise, C.A. Harvel, M. Kafatos, and V.L. Trimble, 1982, Ap.J. 253, 696) intercompared multiple spectra of faint nebular filaments with multiple spectra of sky background. Radiation hits dominate the background of any long exposure spectrum but bright spots of the detector can be misconstrued to be radiation hits, or spectral information. The spectra were normalized and then, on a pixel-by-pixel basis, average and median spectra were constructed. Four data sets (six SWP nebular, six SWP sky, six LWR nebular, and six LWR sky) were processed in parallel. A number of bright and faint background features remain, especially for SWP images. Several features could be misconstrued to be emission from a faint object.

A systematic study is now being done (1) to establish stability of these features over the lifetime of IUE and, (2) to separate possible sky background contributions from instrumental contributions. Progress on this study will be reported through the IUE Newsletter.

Fig. 1 (p. 2). Six long (~300 minutes each) low dispersion SWP exposures of a filament in the Crab Nebula are displayed as the top six spectra. Many radiation hits and bright spots are noticeable both on the spectrum and on the detector background. The bottom two spectra, processed pixel-by-pixel, are an average and a median of the six target spectra. Note many bright spots remain in both spectra, but that the median image has rejected radiation hits.

Fig. 2 (p. 3). The four low dispersion SWP spectra are each the results of combining multiple spectra. The top two spectra are reproduced from Figure 1, being the average and the median of six individual spectra. The third frame is a median of six "blank field" images recorded during long LWR exposures of extragalactic objects. Many bright spots reproduce in the first three frames. The fourth spectrum is a subtraction of the median "blank field" spectrum from the median target spectrum. While the target spectra were obtained during a nine day period under very similar conditions, the "blank field" spectra were obtained over an eighteen month period under very diverse conditions. A two-pixel running average was passed through the "target minus blank field" spectrum to cut down on granularity.

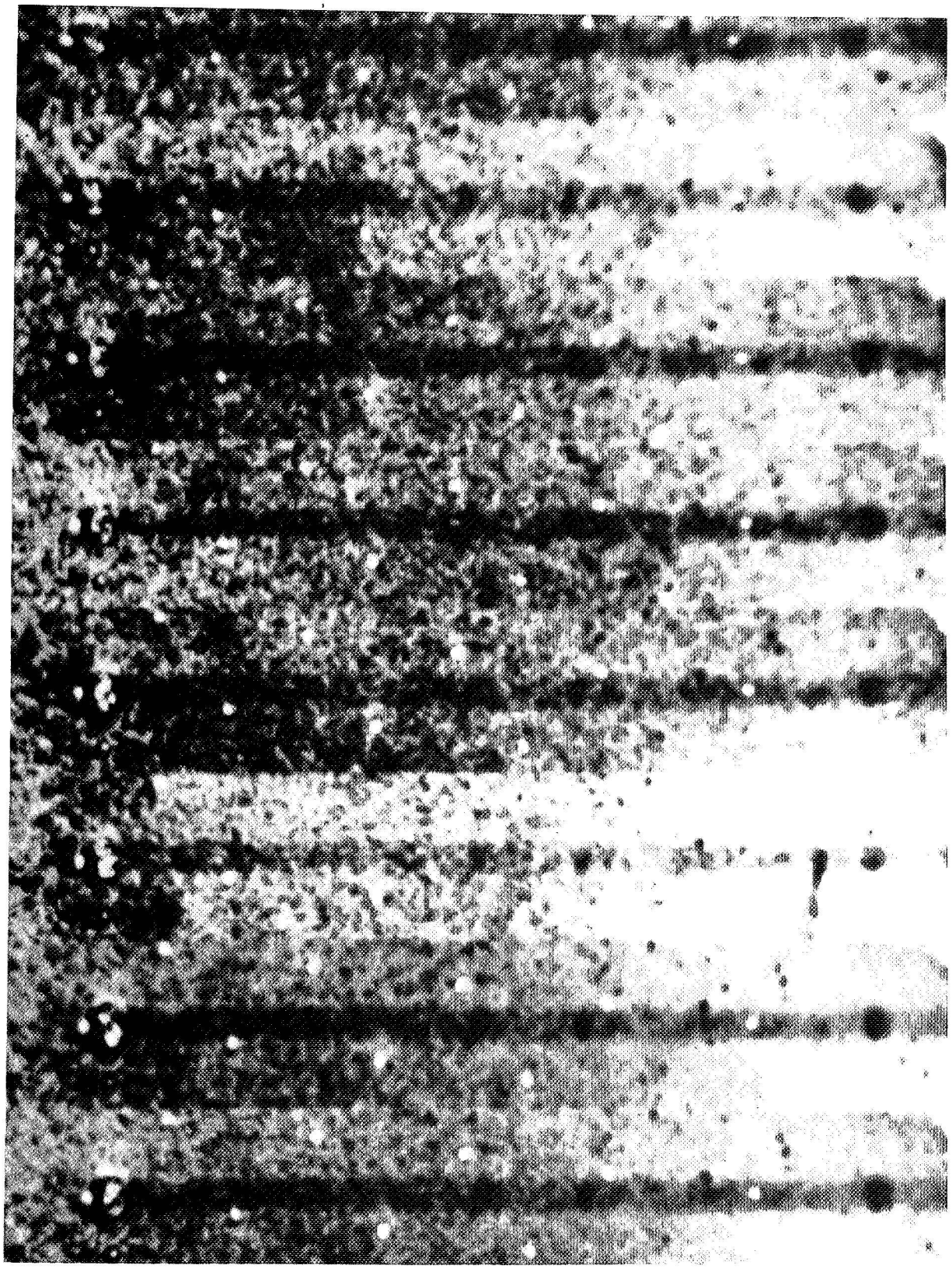

Figure 1

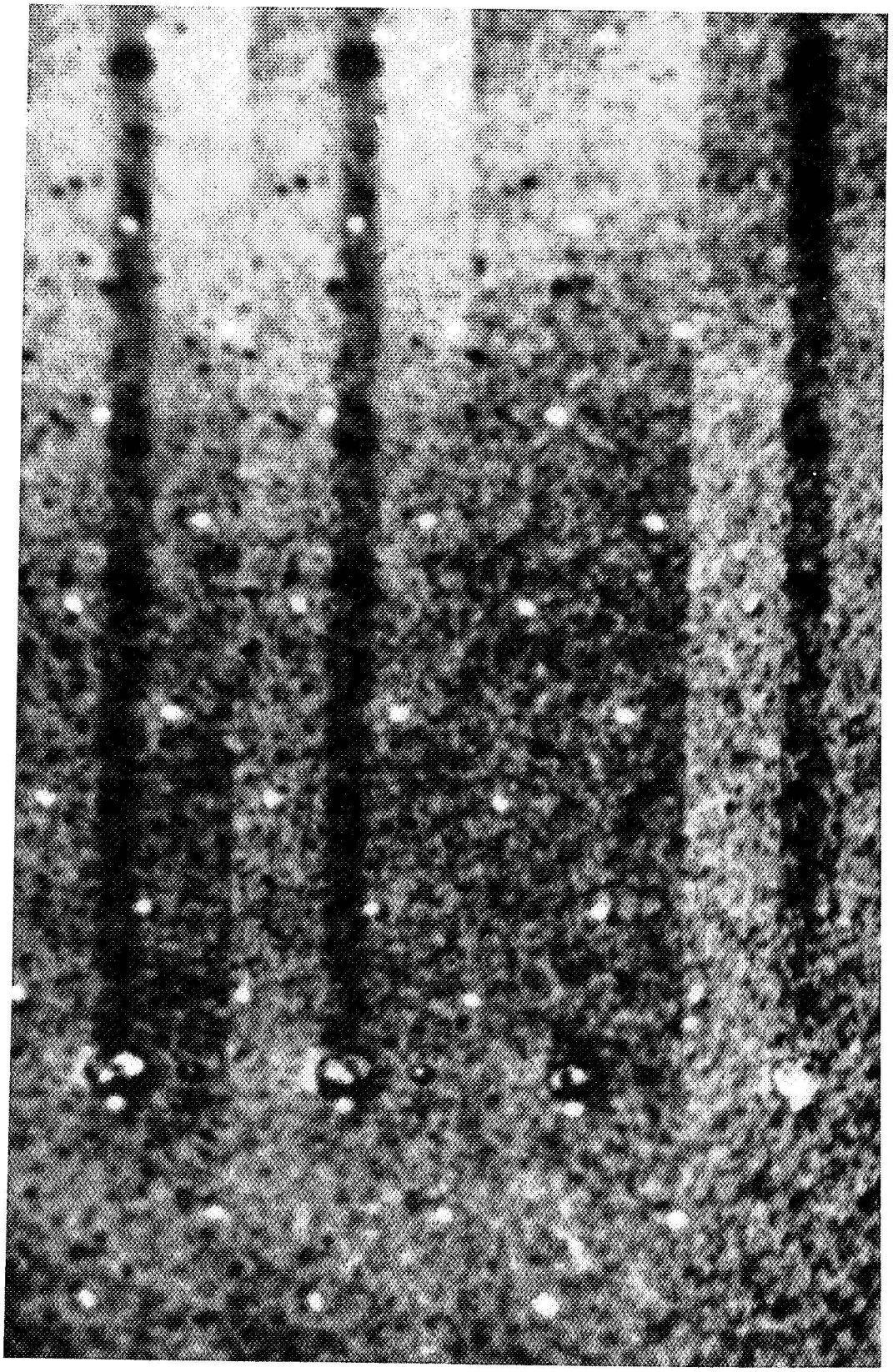

Figure 2

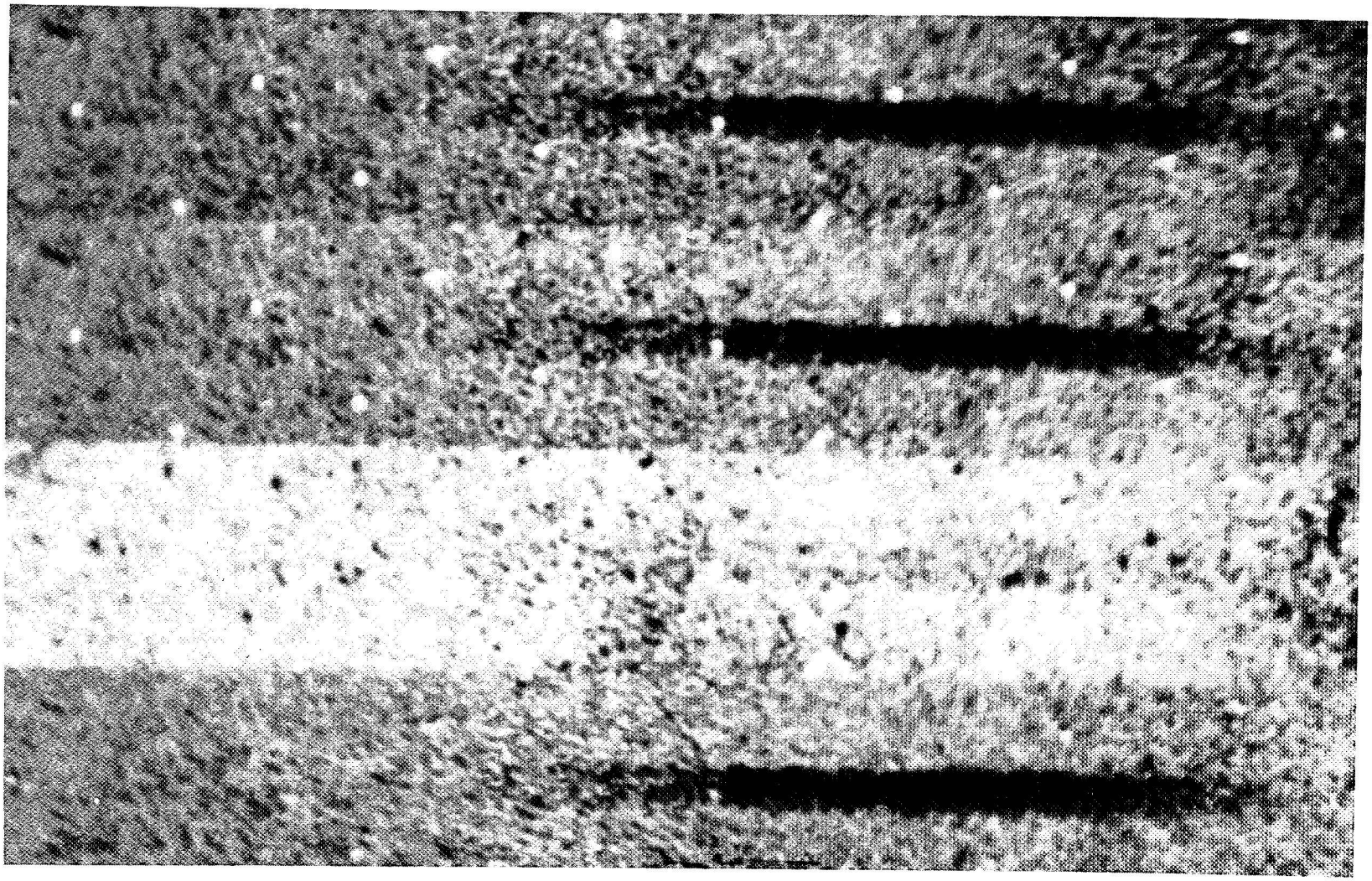

Fig. 3. Four low-dispersion LWR spectra processed from six target and six "blank field" exposures as for SWP in Fig. 2. The effects, so easily noted for SWP, are less pronounced for LWR.

SPECTRAL ANOMALIES IN LOW-DISPERSION SWP IMAGES

Richard L. Hackney and Karen R. H. Hackney
Department of Physics and Astronomy
Western Kentucky University

Yoji Kondo
Laboratory for Astronomy and Solar Physics
Goddard Space Flight Center

ABSTRACT

Physical interpretation of *IUE* spectra obtained with the SWP camera may be significantly affected by artificial spectral features of several types. In low-dispersion large-aperture SWP exposures of sources with nominally featureless spectra, we identify: a spectral imprint which alters the shape of the continuum, several spurious "emission features" which recur at fixed locations on the camera target, and fixed-pattern noise which can result in illusory emission and absorption features. The anomalies appear in spectra extracted from line-by-line files generated by IUESIPS at all epochs, regardless of the ITF or rectification scheme used for processing.

OBSERVATIONS AND REDUCTION

The effects to be reported are inferred from low-dispersion large-aperture SWP observations of BL Lac objects and of the sky in exposures ranging from 1 to 8 hours during low-noise shifts. All spectra were assembled from the line-by-line files of the GO tapes, using the IUESIPS standard slit parameters for point-source extractions. Background smoothing was performed using a 21-point median filter followed by a 7-point running average. The resulting net spectra were calibrated using the 1980 May version of the sensitivity function (Bohlin and Holm 1980) and were corrected for reddening. Each fully resolved spectrum (S/N $\sim$ 5-20) was averaged in 50-Å bins prior to obtaining a least-squares power-law fit as a first approximation to the continuum in the SWP spectral window. Comparison of the resolved spectra to the power-law approximations revealed deviations which commonly occur at fixed wavelengths in the observer's frame for sources with different redshifts and for sources in different physical classes. We distinguish apparent artifacts which have distinctly different spatial frequencies in the spectral plots: (1) a slowly varying function of wavelength which distorts continuum shape, and (2) narrow fixed-pattern features which simulate spectral lines.

CONTINUUM DISTORTION

Many calibrated SWP spectra are found to bear a common imprint, as seen in Figure 1, illustrating for 3 BL Lac objects the wavelength dependence of the ratio between observed flux and a fitted power law. The spectra have been smoothed with a 15-point median filter, eliminating features narrower than about 15 Å. The multiple-image averages shown for the BL Lac objects PKS 2155-304 (5 images, z = 0.17), MK 421 (7 images, z = 0.031), and MK 501 (4 images, z = 0.034) have remarkably similar deviations from power-law behavior at the same observed wavelengths. The composite average for 16 images of the 3 BL Lac objects shows a residual 10% flux deficit near 1650 Å and an

excess near 1500 Å, superimposed on a rising trend between 1650 and 1300 Å. Similar deviations are evident in the spectrum of the subdwarf O star BD+28°4211 when SWP data from Bohlin and Holm (1980) are compared to a power-law approximation (Fig. 1) or to a model atmosphere (Holm 1981).

A modification of the calibration suggested by the composite residuals for the BL Lac objects is shown in Figure 2. Application of the modified calibration to the spectrum of BD+28°4211 (Fig. 2) reduces apparent errors in continuum shape such as the depression near 1600 Å, although errors in slope and level may remain. The modification also reduces the similar errors in continuum shape noted by Greenstein and Oke (1979) in *IUE* observations of white dwarf stars. However, the spectral imprint is not simply a calibration effect, as its amplitude depends on target flux, becoming noticeable for fluxes $\lesssim 10^{-23}$erg cm^{-2}s^{-1}Hz^{-1}. Figure 3 compares -- in terms of indicated energy in the exposure -- binned spectra of 3 BL Lac objects (1980 May calibration) with binned spectra for the faint galaxies M87 and NGC 4472 (processed with the similarly-shaped calibration function given by Bohlin and Snijders [1978]). Similar trends are seen in all of the spectra, and the amplitude of the imprint seems to increase for fainter sources. The comparison suggests there may be camera-intrinsic features (e. g., near 1750 Å) which underlie all exposures and become more conspicuous for fainter targets.

FIXED-PATTERN FEATURES

Several spurious "emission features" are, in fact, found to recur at fixed wavelengths even in long-duration sky or null exposures of the SWP camera. Figure 4 compares 3 calibrated null images (1 to 4.5 hours exposure), including both a fully resolved composite average and the average smoothed by a 3-point box filter. Approximate wavelengths are indicated for features which occur in all three images and which have amplitude $\geq$0.5 mJy in at least one image. The most prominent feature occurs near 1750 Å, with other notable features near 1890, 1870, 1660, 1570, 1480, and 1280 Å. For the range of exposures studied, most of the noted features are essentially constant in F_ν, with amplitudes as large as 2 mJy. In retrospect, the same features can be identified in the fully resolved spectrum of M87 (Bertola *et al.* 1980) which corresponds to the binned spectrum of M87 in Figure 3. Binned null images are also found to resemble the shapes of the fainter spectra in Figure 3.

Examination of the separate orders in line-by-line files reveals that some intensity spikes are associated with fixed locations on the camera target. Figure 5 depicts the flux in the central 9 orders of the line-by-line file used for extraction of the gross flux for the 4.5-hour null exposure SWP 3181. Boxes indicate intensity spikes in individual orders which are seen at the same location in 3 or more images (in a set of 5). Reseaux (R) and isolated spikes (I) are also indicated. Features such as those at 1750 Å in orders 96-98 of SWP 3181 have adequate contrast for detection by comparison with a running standard deviation of the samples. However, Figure 5 also shows that similar features in orders 96-98 of the 3-hour null exposure SWP 3166 are nearly hidden by greater noise in this image. The only distinctive difference in the exposure conditions for these two images is in camera preparation, with the S-prep apparently resulting in greater noise in the orders than with the X-prep sequence. It appears that routine flagging of radiation events and fixed-pattern spikes within the line-by-line orders is useful but not sufficient; it is still necessary to examine the line-by-line files for possibly spurious origins of apparent features in the spectra.

In addition to the major spikes in Figure 5, there are small-scale noise patterns which persist in the same orders from image to image. Fixed-pattern runs of several points above or below the local median level can simulate emission and absorption features which recur from image to image and from target to target. The absolute amplitude of the noise (including random and fixed-pattern components) increases with increased exposure to target flux as seen in Figure 6, which compares line-by-line orders 97-100 for image SWP 5189 exposed on the target MK 421. The noise is greatest in the central order (100), which receives the greatest exposure. In the sensitive region between 1250 and 1450 Å, images of various BL Lac objects show similar alternating "emission and absorption features" (short runs of alternating polarity) which may be due to fixed-pattern noise. Averaging of images reinforces the fixed-pattern features, and features seen in the averaged spectra of various BL Lac objects do not differ significantly from those seen in averaged null spectra. Most of the points involved deviate from the local median by less than 2 standard deviations, defined locally by at least 21 contiguous points.

Figure 6 reveals another effect which may be related to the previously discussed spectral imprint. If the central order exactly follows the dispersion line, adjacent orders should mimic the shape of the central-order flux distribution but with reduced amplitude. However, excess flux appears in orders 99 and 98 at wavelengths near 1450 and 1800 Å. Corresponding depressions (not shown) occur in orders on the other side of the center, indicating deviation of the center of light with respect to the central order. The effect is evaluated as a function of wavelength in the upper panel of Figure 6, showing the center-of-light deviation from the central order averaged for 4 images of MK 421. The similarity between this deviation function and the previously discussed spectral imprint may be coincidental, but it suggests an area for further investigation.

CONCLUSIONS

The effects which have been discussed appear in images processed with either the old or the new ITF and in images processed with or without the resampling for geometric correction prior to photometric correction. The spectral imprint seen in sources with fluxes $\lesssim 10^{-23}$erg cm^{-2}s^{-1}Hz^{-1} may be related to the other anomalies. The effects of the fixed-pattern spikes may be reduced by filtering in the line-by-line file, if the noise level is sufficiently low. Features with amplitudes less than about 2 mJy should always be regarded skeptically; their origins should be examined in the line-by-line file and they should be compared with the local fixed-pattern noise. A study of the origins of fixed-pattern noise and possible means of reducing it might significantly improve the limits of detection of discrete features as well as continuum definition in *IUE* spectral images.

REFERENCES

Bertola, F., Capaccioli, M., Holm, A. V., and Oke, J. B. 1980, *Ap. J. (Letters)*, 237, L65.

Bohlin, R. C., and Snijders, M. A. J. 1978, *IUE Newsletter*, No. 2.

Bohlin, R. C., and Holm, A. V. 1980, *IUE Newsletter*, No. 10, 37.

Greenstein, J. L., and Oke, J. B. 1979, *Ap. J. (Letters)*, 229, L141.

Holm, A. V. 1981, private communication.

Oke, J. B., Bertola, F., and Capaccioli, M. 1981, *Ap. J.*, 243, 453.

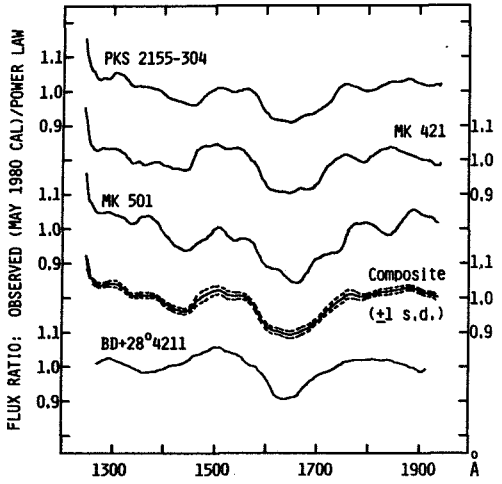

FIG. 1 -- Systematic departures from fitted power laws seen in various sources processed with calibration of May 1980; and 16-image composite of 3 BL Lac objects.

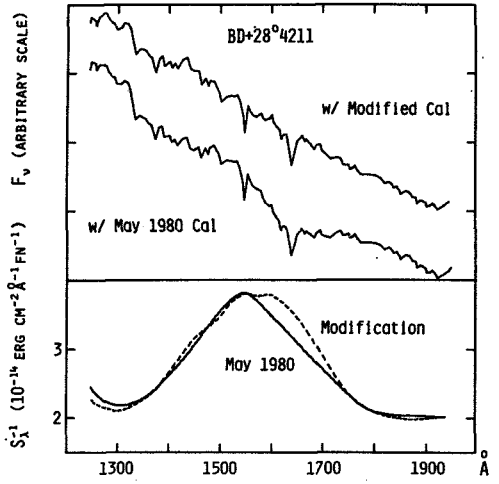

FIG. 2 -- SWP May 1980 calibration and modification (lower panel); and effect on spectrum of BD+28°4211 (upper panel, different treatments offset vertically).

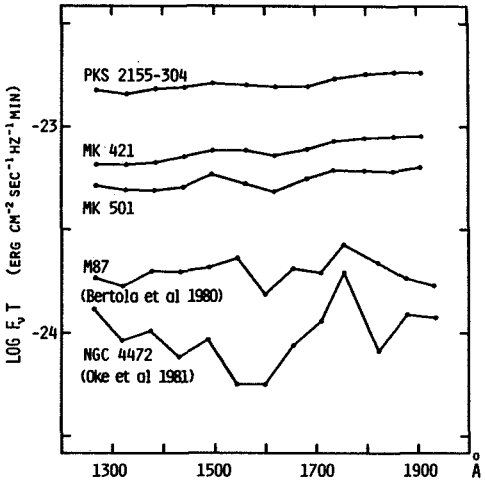

FIG. 3 -- SWP low-dispersion spectra at various levels of effective exposure energy (F_ν times exposure time). Points are binned data, connected to indicate trends.

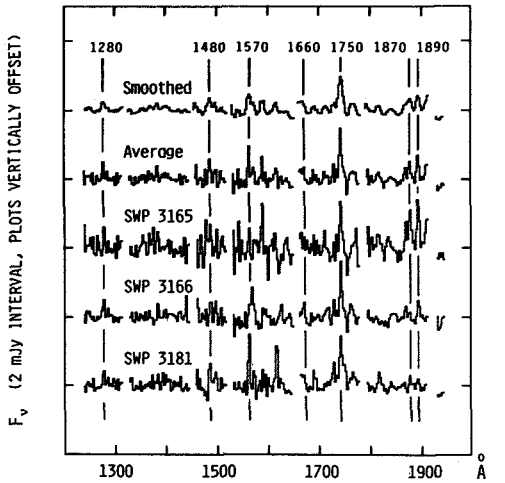

FIG. 4 -- Recurrent features in null-exposure images. Calibrated extractions from SWP large-aperture line-by-line files (with average and smoothed average).

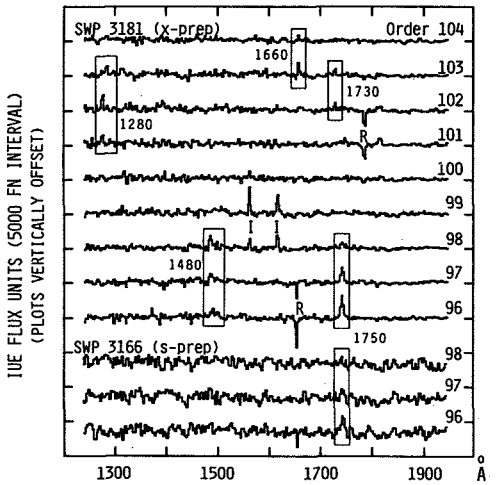

FIG. 5 -- Null-image flux in low-dispersion "orders" near center of SWP large aperture. Boxed features are seen at the same location in 3 or more null images.

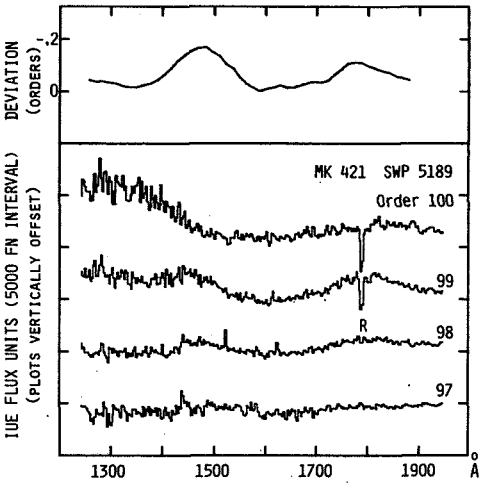

FIG. 6 -- Line-by-line orders 97-100 in large-aperture low-dispersion image SWP 5189; and the center-of-light deviation from central order (averaged for 4 images).

THE PHOTOMETRIC PERFORMANCE OF THE IUE

Albert V. Holm
Computer Sciences Corporation

ABSTRACT

Analysis of low dispersion spectra shows that there are systematic photometric errors which are a function of exposure level. These errors are referred to as linearity errors. Spectra from both the Long Wavelength Redundant (LWR) camera and the Short Wavelength Prime (SWP) camera show linearity errors. Examples of these errors are shown. Their stability in time is examined. Some data concerning their spatial uniformity on the cameras' image area is discussed.

INTRODUCTION

Figures 1 and 2 illustrate what is meant by linearity errors. Figure 1 shows the ratio of fluxes from pairs of identical, optimally-exposed trailed spectra of HD 60753, a sixth magnitude B3 IV star. Ideally, this ratio should be identically unity. The deviations of 2 to 3 percent from unity represent the reproducibility limits of the IUE detectors. Figure 2 shows the significantly larger errors that appear when the ratioed fluxes are derived from spectra that were exposed to different exposure levels. In this case, fluxes from spectra exposed to only 30 percent of the optimum level are compared with fluxes from optimally-exposed spectra. The type of error illustrated in Figure 2 is systematic with the exposure level and is called the linearity error.

It must be noted that the wavelength dependence of the errors shown in Figure 2 represent this example only and will change with changes in the wavelength dependence of the exposure level, with changes in the background level, and with a change from trailed spectra to point source spectra.

STABILITY IN TIME

Figures 3 and 4 illustrate the stability of the linearity errors. In both figures, the linearity error as a function of IUE Flux Number (FN) was defined by a sequence of low dispersion spectra taken with varying exposure levels during a single observing shift. In all cases, the spectra were trailed. The test FN were extracted in 100 Å intervals from the middle three orders of the spatially-resolved spectral file. This extraction provided a data set where each point represented a reasonably well-determined position in the Intensity Transfer Function (Bohlin et al. 1980). The linearity errors were determined by comparing the measured FN with the FN predicted from a reference level using the ratio of exposure times and the difference in background levels.

Such sequences having identical exposures for 4 of the spectra were observed for the LWR in 1978 November, 1981 February, and 1981 December.

For the SWP, the sequences were repeated in 1978 November and 1981 July. The results of these tests are plotted in Figure 3 for the LWR and Figure 4 for the SWP. These plots show no changes that can not be explained by the reproducibility errors shown in Figure 1.

SPATIAL UNIFORMITY

An important question is whether the linearity errors are the same function of FN for all wavelengths in both low and high dispersion spectra. Since the spectra are spread across the image area of the cameras this question is equivalent to asking whether the errors as a function of FN are spatially uniform.

Figure 5 shows that the linearity errors do extend over most of the LWR. This plot was generated from selected orders of three high dispersion spectra observed with different exposure times. The spectra were trailed perpendicular to the dispersion for exposures of 6, 12, and 18 seconds. The spectra were extracted from the central portions of the widened orders using a point source extraction slit height in order to get a more nearly uniform level for each sample. The 12 second exposure was chosen as the reference spectrum and errors at each sample of the other two spectra were calculated relative to it. These errors were then plotted against the summed FN in the sample. Thus Figure 5 does not represent the linearity errors relative to a single FN value as do Figures 3 and 4, but it does show that linearity errors are present throughout the region covered by high dispersion spectra.

For comparison, Figure 6 shows the linearity errors at 2700 Å from all the available low dispersion spectra obtained for checking linearity. Qualitatively the shapes of the curves in Figure 5 and in Figure 6 are similar but the high dispersion results show greater scatter. Unfortunately that scatter appears to be caused by a real variation of the functional dependence of the linearity error on FN over the camera's area. Analyses of flood lamp exposures confirm that there are spatial variations, especially toward the lower left portion of the image. However, much of the region where the low dispersion spectra are integrated has a fairly uniform error.

No similar analysis has yet been done for the SWP camera.

CONCLUSIONS

Linearity errors may be significant for many IUE spectra. They are especially likely for spectra exposed to different levels than the optimally exposed hot star spectra used to calibrate the instrument and for spectra with non-zero background levels. They also affect high dispersion spectra. The presence of linearity errors can sometimes be recognized from a discontinuity between fluxes from the SWP and fluxes from the LWR. At the present there is no evidence for major changes in the error between late 1978 and 1981. The whole of the LWR image area is affected by linearity errors but they are not spatially uniform.

Work is now in progress to derive empirical corrections for LWR Flux Numbers to correct the linearity error for low dispersion spectra. This

work will be published in the IUE Newsletter along with a more complete version of the present report.

REFERENCE

Bohlin, R.C., Holm, A.V., Savage, B.D., Snijders, M.A.J., and Sparks, W.M. 1980, Astron. Astrophys., 85, 1.

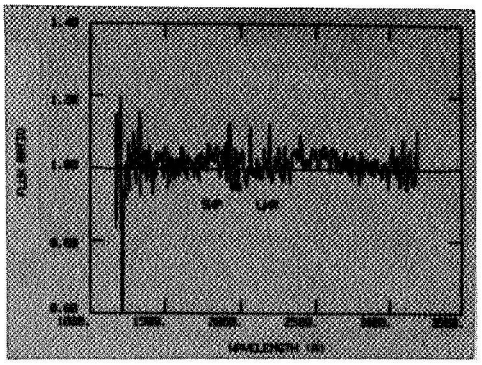

Fig. 1- An example of the reproducibility of IUE spectra.

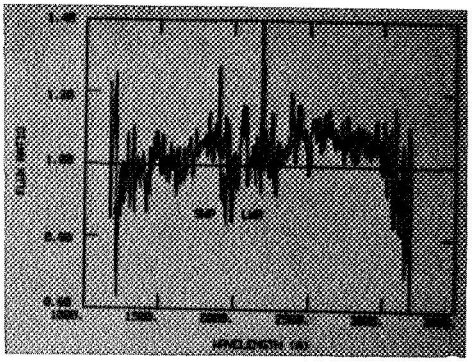

Fig. 2- An example of the linearity errors for underexposed spectra.

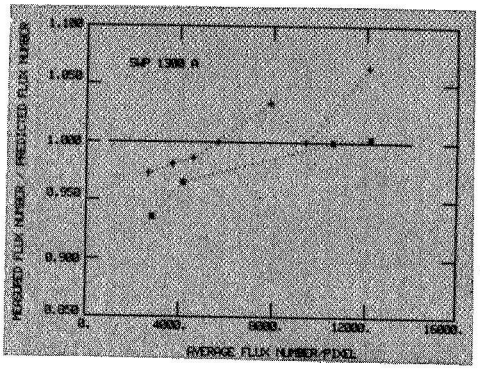

Fig. 3- The stability of SWP linearity errors using spectra from 1978 Nov (crosses) and 1981 July (asterisks).

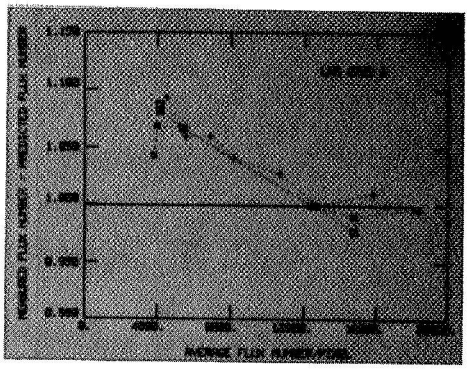

Fig. 4- The stability of LWR linearity errors using spectra from 1978 Nov (crosses), 1981 Feb (boxes), and 1981 Dec (asterisks).

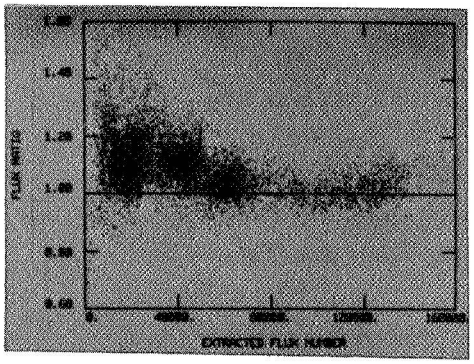

Fig. 5- LWR errors from high dispersion spectra.

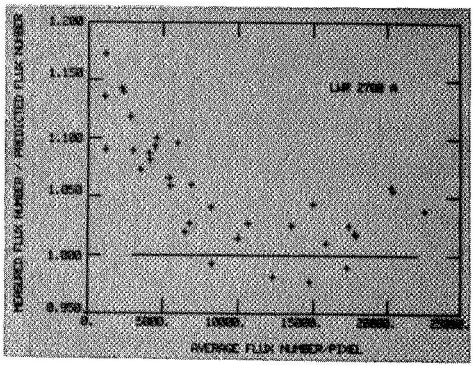

Fig. 6- LWR errors from trailed, low dispersion spectra.

POSSIBLE IUE FOLLOW-ON MISSIONS: FUSE AND MAGELLAN

THE FAR ULTRAVIOLET SPECTROSCOPIC EXPLORER

Albert Boggess

Laboratory for Astronomy and Solar Physics
NASA/Goddard Space Flight Center

NASA is beginning to define in some detail the scientific objectives and performance characteristics of a new astronomy mission referred to as the Far Ultraviolet Spectroscopic Explorer, or FUSE. The broad outlines of this mission have been discussed by NASA's various science advisory committees, which have all given it strong endorsement. The next step has been to form an ad hoc Science Definition Team involving people experienced in instrumentation, observations and theory in order to develop mission and instrumental requirements that best meet the scientific needs. This team, whose membership is shown in the attached table, has had one meeting so far. It is intended to have a lifetime of about one year, ending with the submission of a report to NASA which could be used as the basis for an engineering design study.

The principal objective of FUSE is to obtain astronomical spectra at wavelengths shorter than is possible with the Space Telescope. For most practical purposes, ST is insensitive shorter than 1200Å and thus cannot be used for many important interstellar, stellar and extra-galactic programs. Wavelengths between 1200 and 900 Angstroms were first explored by Copernicus, but that satellite was restricted to observing bright stars. Even so, its contributions to our understanding of interstellar gas and the physics of hot stellar atmospheres have been enormous. The need to extend these observations to fainter objects provides the main motivation for FUSE. During the first meeting of the FUSE definition team, the scientific objectives were discussed in some detail, along with the various instrumental designs that could be used to obtain the observations. We realized that several instrumental concepts might be suitable for the region between 900 and 1200 Angstroms, but that the choice would be reduced considerably if we attempted to use the same equipment for other spectral regions.

Discussion of what other spectral regions should be emphasized have quickly centered on the shorter EUV wavelengths, for rather obvious reasons. Space Telescope can observe down to 1200Å and FUSE should not duplicate this capability other than providing enough spectral overlap to allow cross-calibrations, etc. At wavelengths shorter than the Lyman limit, the opacity of interstellar hydrogen overwhelmingly dominates any consideration of what can be observed. It appears that column densities in the range 10^{18}–10^{20} can be expected within 100 pc of the Sun, and under these conditions it may be feasible to do spectroscopy with a FUSE-class instrument at wavelengths below about 500Å. It may even be possible to find some directions at high latitudes where the total column density out of the galaxy is within this range; if so, an exciting number of extra-galactic observations would become feasible.

The instrumental concept, then, becomes similar to IUE in the sense that the telescope would feed two spectrographs - long wavelength and short wavelength - packaged side-by-side. However, in the case of FUSE the two spectrographs probably would be quite dissimilar, one optimized in the range from 1200Å to 900Å and the second optimized from about 500Å to about 100Å. The shorter wavelength spectrograph would certainly require grazing-incidence optics and would necessitate the use of a grazing-incidence telescope. Various designs for such instrumentation are already being developed, notably by Webster Cash. The task of the FUSE definition team during the next several months will be to review the various scientific objectives in the context of what is possible instrumentally in order to end up with a set of realistic performance requirements that can result in an observatory with outstanding scientific potential.

A second task for the definition team will be to discuss possible operational concepts. FUSE is to be a national facility (like the IUE), with all of its observing time allocated on the basis of competitive proposals. One of the aspects of the IUE that contributes in a major way to its success is the real time operations. If possible, FUSE should adopt this same approach, but that does not necessarily mean that it must be in a 24-hour geostationary orbit. Other possibilities include a low orbit (perhaps on a space platform) with communications through the Tracking and Data Relay Satellite, or a highly elliptical orbit that would allow real time communications through most of the orbit away from perigee. The merits and disadvantages of these various operational approaches must be evaluated in terms of their impact on the scientific objectives in order to help determine the final nature of the mission.

TABLE

Membership of the FUSE Science Definition Team

A. Boggess, Chairman
C. S. Bowyer
J. J. Caldwell
J. G. Cohen
A. K. Dupree
R. F. Green
M. A. Jura
D. S. Leckrone
J. L. Linsky
H. W. Moos
B. D. Savage
H. L. Shipman
T. P. Snow
E. J. Weiler, Co-chairman
D. G. York

MAGELLAN: HIGH RESOLUTION SPECTROSCOPY AT FUV AND EUV WAVELENGTHS

presented by

M. Grewing
Astronomisches Institut der Universität Tübingen

on behalf of the MAGELLAN Science Team of ESA:

S. di Serego Alighieri
ESA Space Science Department, ESTEC, Noordwijk

W. Burton
Rutherford and Appleton Laboratories, Chilton

C.I. Coleman
Marconi Space and Defence Systems, Stanmore

M. Grewing
Astronomisches Institut der Universität Tübingen

R. Hoekstra
Laboratorium voor Ruimte-Onderzoek, Utrecht

C. Jamar
Institut d'Astrophysique, Liège

A. Labeque, C. Laurent & A. Vidal-Madjar
Laboratoire de Physique Stellaire et Planétaire, Verrières-le-Buisson

P. Rafanelli
Osservatorio Astronomico, Padova

ABSTRACT

The aim of the MAGELLAN mission is to provide high resolution spectra of celestial sources down to sixteenth magnitude over the extreme ultraviolet wavelength range (between 50 and 140 nm). This region of the electromagnetic spectrum contains the majority of the resonance lines of the most abundant atoms, ions and molecules and is of fundamental importance in the study of a variety of astrophysical objects. The range extends from studies of interstellar matter in the disc and halo of our and other galaxies, to stellar envelopes, hot and evolved stars, clusters, intergalactic matter, nuclei of galaxies, quasars, and, finally planets and satellites.

The instrument has a non-conventional optical design using only one reflecting surface: a high groove density concave grating collects the star light, diffracts it and focusses its spectrum into a bi-dimensional windowless detector operated in a photon counting mode. The slitless configuration will provide the spectra of all the sources (point-like and extended) in the field of view of the grating. This field of view is limited by a grid collimator to reduce the diffuse background, the stray light and the probability of over-

lapping spectra in crowded fields. The present instrument design will allow observation of a 16 magnitude unreddened 09 star at a resolution of 0.003 nm with a signal-to-noise ratio of 10 in a 10-hour exposure ($\sim$ 100 times more sensitive than IUE). A low resolution (0.05 nm) mode is being investigated to allow observation of fainter objects, covering about 30 nm simultaneously.

MAGELLAN is planned as an observatory, operating with real time interaction with the observer, and is intended to be used in a similar way to IUE by astronomers whose observing proposals have been accepted by a selection committee.

INTRODUCTION

The European Space Agency is presently undertaking a Phase A study of the ultraviolet spectroscopy mission called MAGELLAN. Analogous studies are being made for an X-ray spectroscopy/timing and transient mission called X-80, an infrared space observatory, ISO, a mass geophysical orbiter, named Kepler, and the solar physics mission called DISCO. All of these aim to be ready for the next project selection that is expected to occur at the end of this year or early in 1983. The one mission that will be chosen will then fly in 1987 at the earliest.

BROAD SCIENTIFIC AIM

MAGELLAN is primarily aiming at very high resolution spectroscopy ($\lambda/\Delta\lambda \geq 2.5 \times 10^4$) at far ultraviolet (900 - 1550 Ångstrom) and at extreme ultraviolet wavelengths (500 - 900 Ånstrom) of faint galactic and extragalactic objects ($V \lesssim 16^m$). The first priority is assigned to the FUV range. The very high spectral resolution is particularly needed for studies of the interstellar gas in our own and in external galaxies, it is foreseen, however, that MAGELLAN will also provide a so-called low resolution mode ($\lambda/\Delta\lambda \approx 10^3$) which will allow extremely efficient FUV and EUV studies of stellar atmospheres, galaxies and QSO's with visual magnitudes as faint as 18^m or even 19^m.

With these capabilities MAGELLAN will in some sense be a follow up of both the NASA OAO-3 "COPERNICUS" mission, and of IUE. At the same time this mission will be complementary to the Space Telescope Project in a very important spectral band as witnessed in Figure 1 where the wavelength positions are given for all the resonance lines that arise from the astrophysically most important atoms and ions.

BASIC MISSION CONCEPT

The reason why neither IUE nor ST are entering into the MAGELLAN wavelength bands, is of technical nature. No mirror coating material is known that will give the same high efficiency at $\lambda < 1200$ Å as at $\lambda > 1200$ Å, i.e. normal incidence optics can not simultaneously be optimized for wavelengths shortward and longward of 1200 Å. For IUE and ST the choice has been made for the wavelength band $\lambda > 1200$ Å. In contrast, MAGELLAN will be optimized for the 900 - 1200 Å band.

In principle the reflectivity problem at FUV and EUV wavelengths can be

circumvented by going from normal to grazing incidence optics. This solution has previously been considered by ESA in its EXUV mission study and is presently contemplated by NASA for the FUSE mission. As the reflectivity problem increases dramatically with the number of reflecting surfaces, one is indeed immediately driven for a spectroscopic experiment into the alternative of either minimizing the number of surfaces to one (concave objective grating), or adopting a totally non-conventional, all-grazing-incidence optical concept. The MAGELLAN study explores the first, the FUSE study will probably explore the second of these alternatives.

The key elements of the MAGELLAN payload design are sketched in Figure 2 where the concave 40 cm diameter objective grating, the mechanical collimator and the focal plane detector are shown. The instrument characteristics for the high resolution mode are shown in some more detail in Table 1.

TABLE I

MAGELLAN INSTRUMENT CHARACTERISTICS

Grating diameter		400 mm	
Grating focal length		1700 mm at 1000 Å	
Groove density		3600 gr/mm (baseline)	5000 gr/mm (option)
Dispersion		1.6 Å/mm	1.2 Å/mm
Total wavelength range		≲ 584 - 1550 Å	500 - 1400
Instantaneous spectral coverage		66 Å	47 Å
Collimator field of view		15 arc min x 1°	
Scale		82 μm/arcsec	
Pixel size		13 μm	
Pointing stability (2σ)		1.5 arcsec	
Spectral resolution	on axis	25 - 25 mÅ	20 - 30 mÅ
	± 10Å off axis	55 - 70 mÅ	55 - 75 mÅ
S/N for a 16^m unreddened 09 star		10 in (10h exposure)	

As shown in Table 1, the field of view of the collimator will be 15 arcmin in the dispersion direction and 1° in the orthogonal direction. From this entire field of view the detector will receive diffuse background photons originating in the Earth's geocorona. The largest photon flux is in the hydrogen Lyman-alpha line at 1215 Ångstrom, which will lead to roughly 250 counts $pixel^{-1}h^{-1}$ in the ± 8 Å band around Lyman-alpha. Correspondingly, the geocoronal Lyman-beta emission will produce roughly 2 counts $pixel^{-1}h^{-1}$ in the ± 8 Å band centered at λ 1025 Å, the exact numbers in either case depending on the orbit conditions and the viewing directions. Whereas inside these ± 8 Å bands the background radiation is a severe limitation, in particular in the case of Lyman-alpha, outside these bands no problems are foreseen, the expected background count rates being roughly 0.025 counts $pixel^{-1}h^{-1}$. This corresponds to the counts from an unreddened 09 star of $V = 22^m$.

Another problem which could arise from the fairly large field of view of the mechanical collimator is the crowding of targets producing spectral over-

lap. Crowding would occur if there is a second source within the 5 arcsec x 15 arcmin box centered on the actual source of interest. One can easily demonstrate that this situation is very unlikely to occur except e.g. in the densest regions of the Magellanic clouds.

CURRENT MISSION OUTLINE

From the Assessment Study and the partial Phase A Study that have been undertaken so far (the Phase A Study is still continuing) we have derived at the mission outline summarized in Table II.

TABLE II

MAGELLAN: SYSTEM REQUIREMENTS

Orbit:	- To provide 'observatory type' operation - Stay outside main radiation belts for most of the orbit
Lifetime:	- 2 years
Launcher:	- ARIANE 2/3 in the dual launch configuration
Ground Station:	- VILLAFRANCA and/or CARNARVON
Operations:	- Continuous real time while spacecraft is visible.

MAGELLAN: MASS AND POWER BUDGETS

	MASS (KG)	POWER (W)
Structure	80	-
Thermal	15	25
AMCS	105	51
Data Handling	14	12
Communications	12	26
Power	86	100
Harness	30	-
Balance	5	-
Total Spacecraft	347	214
Payload	200	100
Fuel	85	-
15% Contingency	95	-
TOTAL	727 KG	314 W
MARGIN	Dependent on 2nd passenger*	70**W

* ARIANE 2 places 1883 KG in GTO with SYLDA 3990
** With 3 ECS type panels

A possible spacecraft/instrument configuration for MAGELLAN which would be compatible with an Ariane launch and which would also make maximum use of existing satellite components is sketched in Figure 3.

REFERENCE

ESA-SCI(81)4. "MAGELLAN Assessment Study".

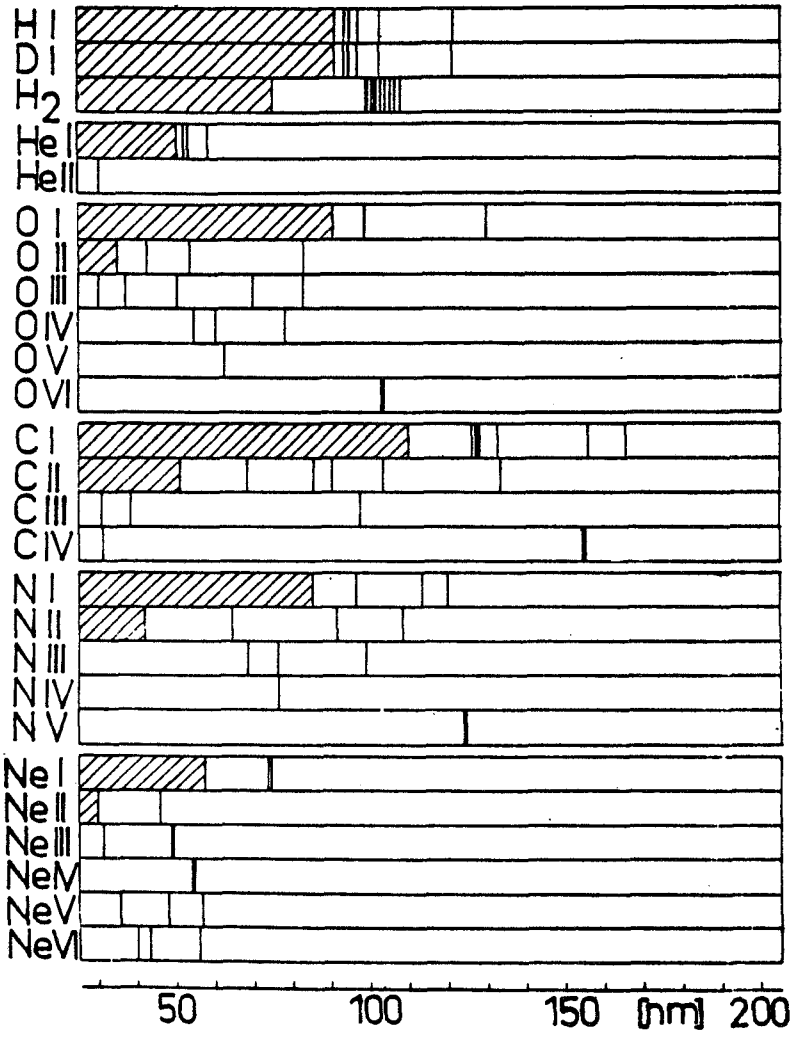

Figure 1 Wavelength of interstellar resonance lines of H,D,H_2,He,O,C,N,Ne in their most interesting stages of ionization. The hatched areas correspond to the ionization limit.

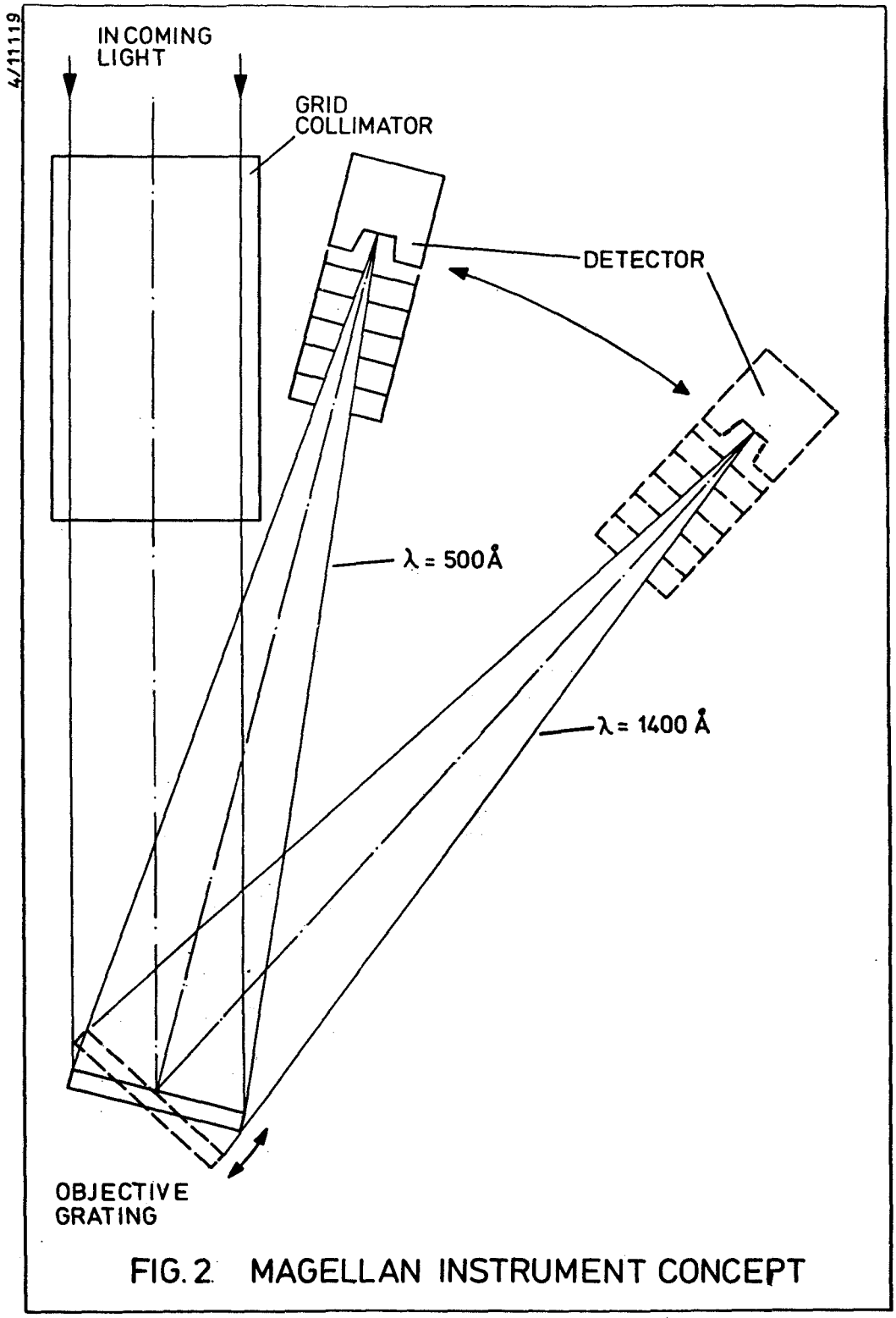

FIG. 2 MAGELLAN INSTRUMENT CONCEPT

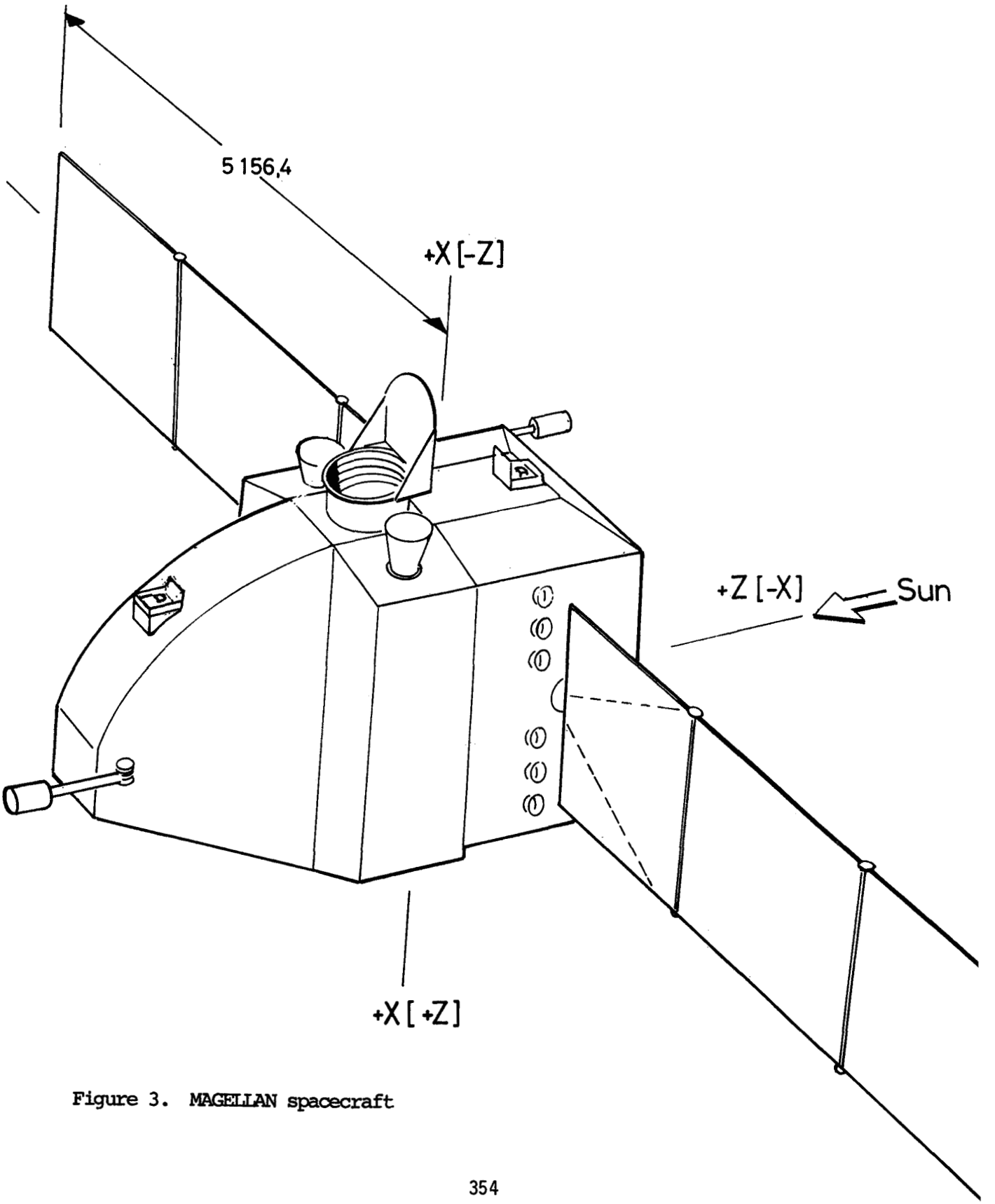

Figure 3. MAGELLAN spacecraft

DISCUSSION - FUSE AND MAGELLAN

Carruthers: Has any consideration been given to spatial resolution and angular size of the spectrograph entrance aperture? This is important for such studies as those of hot white dwarfs in close binary systems.

Boggess: Spatial resolution will be a problem, particularly if it is necessary to use grazing incidence optics which usually suffer from very narrow fields-of-view. If good imagery cannot be achieved, then good resolution could be obtained at the expense of observing efficiency by use of a very small entrance aperture.

Roman: Do you plan to put FUSE in synchronous orbit? If not, how do you expect to get real time operation?

Boggess: Various possibilities will be considered. Synchronous orbit provides the maximum flexibility. Highly eccentric orbits can also be designed to permit long periods of real time operation. Low orbits with communication via TDRS are also possible. Each alternative has good and bad features which we must compare before making a recommendation.

Linsky: IUE has benefitted greatly both scientifically and technologically from European collaboration. I would hope that FUSE would similarly benefit from European collaboration.

Boggess: I agree wholeheartedly. Both European and Canadian astronomers have been invited to attend meetings of the Definition Team in order to promote the possibilities for collaboration.

Elvis: The "low" resolution (1 Å) mode proposed for FUSE sounds very high to those of us who study quasars. Has consideration been given to 10, 20 or 50 Å systems with high throughput? For instance a 2-dimensional imaging camera with a simple filter wheel would be a very powerful tool.

Boggess: Lower resolution modes will be considered. At the very least they can be achieved through proper binning of data from the pulse counting detector.

Elvis: What is the feature of ST that prevents it covering the 900-1200 Å region?

Boggess: The telescope mirrors will have magnesium fluoride interference coatings designed to provide high reflectivities at wavelengths longer than 1200 Å. These coatings are very inefficient shortward of about 1150 Å.

Snow: Would you comment further on the detector that is envisioned for use on Magellan?

Grewing: As a baseline concept we are looking at microchannel plates fiber-optic-coupled to CCD's. Centroiding techniques will be used to get event positions accurate to 10-15 μm. It is indeed the effective pixel size which is our chief concern at this time, and we feel confident that, based on the experience gained from current detector development like that for the ST-FOC, we shall achieve a pixel size of 13 μm, which in combination with a 3600l/mm grating would give us the desired on-axis spectral resolution of 0.02 Å.

Jenkins: How much of the incoming beam will be diffracted by the grids in the mechanical collimator?

Grewing: I am unable to give a quantitative answer at this time as both the theoretical and experimental studies are still underway. We are, however, aware of the problems and try to optimize the exact layout of the individual collimator grids as well as the baffling precautions. As a last resort we plan to deconvolve the spectral images for those ghost-images which will result from the diffraction.

Linsky: We know that the interstellar medium is highly inhomogenous, but the 500-912 Å spectral region is close to the Lyman edge where the interstellar absorption will be large. Could you comment on the numbers of different types of astronomical sources that will likely be detected by Magellan?

Grewing: We realize the problem, of course, and I am afraid that I shall not have a quantitative answer to your question. We tried to estimate the number of objects of different catagories (e.g., late type stars, nuclei of planetary nebulae, hot white dwarfs, neutron stars, etc.), that might be observable, but as you know, the answer depends critically on both the assumed space density of those objects and the actual amount of absorption due to neutral interstellar hydrogen in a given direction.

INTERSTELLAR MEDIUM

DISTRIBUTION OF GAS IN THE HALO OF THE GALAXY

J.C. Blades[1], L.L. Cowie[2], D.C. Morton[3], D.G. York[4] & C-C. Wu[5]

[1]Rutherford Appleton Laboratory
[2]Physics Department, M.I.T.
[3]Anglo-Australian Observatory
[4]Princeton University Observatory
[5]Computer Sciences Corporation

ABSTRACT

Results are presented from a high-resolution, ultraviolet study of interstellar gas situated away from the plane of our Galaxy, using the nuclei of Seyfert galaxies Mkn 509 and F9 as background probes. In these directions we detect low-velocity, galactic gas as well as two extragalactic clouds, one probably associated with the Magellanic Stream and the other with Mkn 509.

These data are combined with results from other lines of sight to show that the ultraviolet species extend about 10 kpc from the plane, assuming the the high-latitude gas corotates with the galactic disk.

Complimentary observations of the optical Ca II and Na I species suggests that these do not extend as far - perhaps 2 to 3 kpc from the plane. Further, the exceedingly complex velocity structure found only in Magellanic Cloud directions suggests that these sight-lines are not typical of high-latitude gas in general.

INTRODUCTION

The International Ultraviolet Explorer with its high resolution spectrograph and sophisticated guidance system provides the capability to search for gas clouds beyond the Galactic disk but in the neighborhood of our own and other low redshift galaxies. The brightest extragalactic objects which may be observed are the O and B supergiants in the Magellanic Clouds where Savage & de Boer (1979,1981) have suggested that both absorption from our Galactic halo and that of the Clouds may be seen along the line of sight.

Other directions are more difficult to observe since the next brightest extragalactic targets are close to the detection limit of the IUE in its

high-dispersion mode. However, the strongest emission lines in these objects serve as suitable continua, and useful observations may be obtained with a few 14-hour exposures. This procedure of studying specific, galactic interstellar absorption lines superimposed on red-shifted emission lines extends the range of the IUE to about a dozen Seyferts & QSOs. In addition, by combining the IUE observations with high-resolution observations of optical species Ca II & Na I, a detailed picture of the gas distribution can be constructed. We have been involved in such a programme over the last few years, and present here some of the results. Full details are contained in York et al (1982).

OBSERVATIONS

High-dispersion, SWP, observations were made of Mkn 509 & F9. The exposures were started at the ESA Tracking Station and read down at NASA, Goddard. In this way, advantage was taken of the low particle radiation encountered by the satellite during this part of its orbit. The spectra were reduced with the standard point-source extraction schemes. For Mkn 509 three spectra were co-added. High-resolution observations of Na I & Ca II were obtained with the 3.9-m Anglo-Australian Telescope at a dispersion of 5 Å/mm for Ca II and 10 Å/mm for Na I. These data were reduced in the standard manner.

RESULTS

In Mkn 509 we detect interstellar absorption lines belonging to Fe II, Si II & S II near zero redshift as well as Lyα and probably C IV at a redshift of 0.0354. After allowance for the instrumental width, the mean velocity of the Si II and Fe II lines is from -65 to +75 km/s. In the weaker optical lines we detect two components with LSR velocities of +5.9 and +62.4 km/s.

In F9 we detect Si II which shows two velocity components, with an overall FWHM extending from -45 to +220 km/s. We attribute the lower velocity component to gas in our Galaxy; the higher velocity component, which extends from about +100 km/s to 220 km/s may be associated with the Magellanic Stream or be an outer halo component of the SMC.

Interestingly, an absorption line system may be seen at a redshift of 0.0354 in the Lyα and C IV absorption lines of Mkn 509; this is close to the redshift (0.0344) of Mkn 509. The absorption may be associated with the Seyfert or it could be truly intergalactic.

In the enclosed figure we show the velocity profiles of the galactic absorption lines of Si II, Fe II, Ca II and Na I in the direction of Mkn 509. We have calculated the velocity difference owing to rotation as a function of height from the plane of the observed gas, assuming that

the halo corotates with the disk. The resulting velocity profile for Mkn 509 is shown in the adjacent figure where we have also indicated the velocity ranges of the UV and optical lines. Clearly, the data are consistent with a corotating halo. If this is the case then the height of gas producing the ultraviolet lines is about 10 kpc, or less, whilst the optical species probably originate within a few kpc of the plane. A similar result was found for the ultraviolet lines in the 1981 supernova in NGC 6946. However, the supernova occurred at a very low galactic latitude (b=+12) in a sight-line near both the local and Perseus spiral arms. Hence the interstellar absorption may be quite local.

Finally, we remark that the absorption line strength of Ca II in Mkn 509 and F9 is within the range of strengths seen towards other high-latitude, extragalactic background sources as well as halo B stars (for a review of the data see Blades & Morton, 1982). The implication is that most of the low-velocity absorption seen in high-latitude background sources originates within local material (1 - 2 kpc of the solar neighborhood). Interestingly, there is growing evidence from these optical measures that the Magellanic Cloud sight-lines may not be typical of halo gas. As a general rule, high-velocity interstellar components, which occur frequently in LMC directions, are only rarely seen in other sight-lines penetrating the entire halo. This reinforces the urgent need to sample in the ultraviolet other extragalactic lines of sight.

REFERENCES

Blades, J.C., and Morton, D.C. 1982, M.N.R.A.S., submitted.

Pettini, M., Benvenuti, P., Blades, J.C., Boggess, A., Boksenberg, A., Grewing, M., Holm, A., King, D.L., Panagia, N., Penston, M.V., Savage, B.D., Wamsteker, W., and Wu, C-C. 1982, M.N.R.A.S., in press.

Savage, B.D., and de Boer, K.S. 1979, Ap. J. (Letters), 230, L77.

_____. 1981, Ap. J., 243, 460.

York, D.G., Blades, J.C., Cowie, L.L., Morton, D.C., Songaila, A., and Wu, C-C. 1982, Ap J., in press.

FIGURE CAPTIONS

Figure 1 LSR velocity profiles of the galactic absorption lines Na I D2, Ca II K, Fe II λ1608.5 and Si II λ1260.4 in the direction of Mkn 509.

Figure 2 Plot of LSR velocity due to galactic rotation as a function of distance from the plane for Mkn 509. The horizontal bars show the velocity ranges of the interstellar absorption lines. Their vertical position shows the distance from the galactic plane where these lines could originate according to the corotating model.

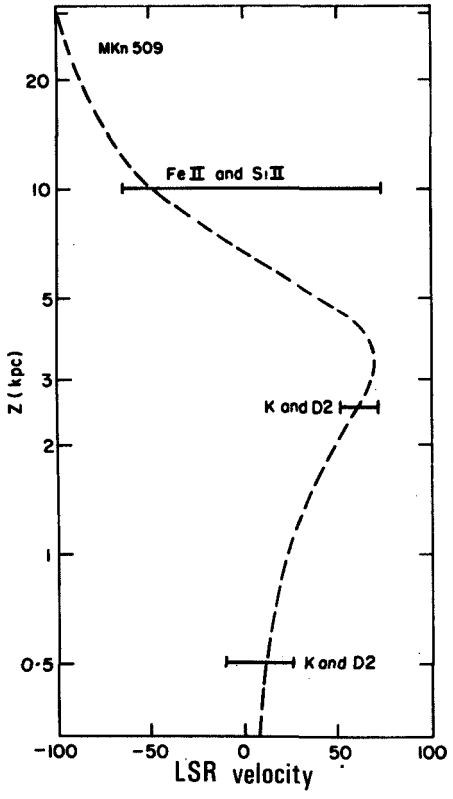
MKn 509
Fe II and Si II
K and D2
K and D2
Z (kpc)
20
10
5
3
2
1
0·5
-100
-50
0
50
100
LSR velocity

Fig 2

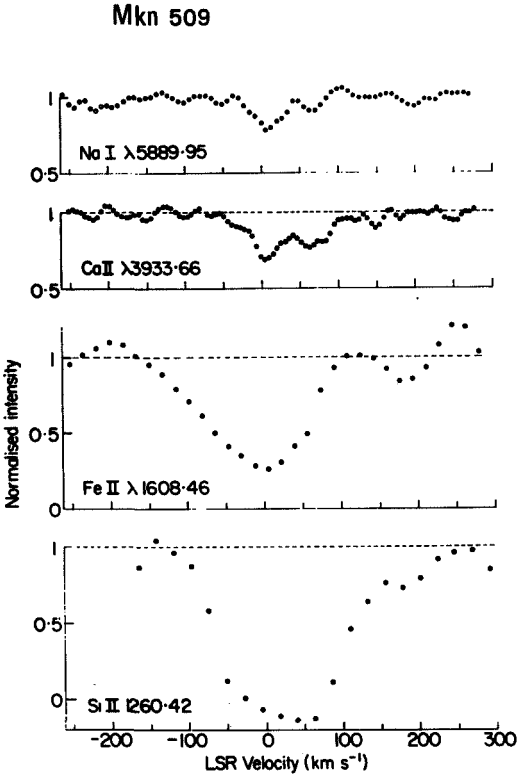
Mkn 509
Na I λ5889·95
Ca II λ3933·66
Fe II λ1608·46
Si II 1260·42
Normalised intensity
1
0·5
0
-200
-100
0
100
200
300
LSR Velocity (km s⁻¹)

Fig 1

HIGHLY IONIZED GAS IN THE GALACTIC HALO

Max Pettini[1] and Kym A. West[2]

[1] *Royal Greenwich Observatory, U.K.*
[2] *Department of Physics and Astronomy*
University College London, U.K.

INTRODUCTION

The study of the interstellar medium in the Galactic halo received a strong impetus with the launch of the IUE satellite. The early observations by Savage and de Boer (1981) of stars in the Magellanic Clouds showed that in these directions absorption is found at velocities expected for distant material distributed along the line of sight. If this gas corotates with the disk, the velocity range of the lines implies that the halo may extend up to 10-15 kpc below the plane of the Galaxy. Absorption lines of CIV and SiIV are very much in evidence in halo gas. The discovery of significant amounts of these highly ionized species away from the disk has been interpreted as evidence for a medium at $T \sim 10^5$ K, with properties similar to those of the Galactic corona originally proposed by Spitzer (1956).

Although it is obviously important to extend this work to other directions in the halo, progress has been slow, owing to the paucity of extragalactic sources sufficiently bright to be observed at high resolution with IUE. At present only early-type stars at high Galactic latitudes offer the possibility of carrying out a large-scale study of interstellar absorption in the inner regions of the halo. During the past decade spectrophotometric surveys of faint blue objects at high latitudes have consistently revealed a small but significant number of apparently normal OB stars at distances of up to a few kpc from the plane. Although their origin is not well understood, recent detailed studies have confirmed that many of these stars have atmospheric parameters and chemical composition typical of Population I stars.

In this presentation we summarise the major results of a study of interstellar absorption in the halo which makes use primarily of IUE observations of a sample of 24 OB stars at z distances between 0.5 and ~ 3 kpc. These data, which cover a wide range of directions, are analysed together with other available results in order to investigate the distribution and physical conditions of highly ionized gas in the halo. A more detailed account of the work is given in an article to be published in the Astrophysical Journal (Pettini and West 1982).

INTERSTELLAR LINES IN THE HALO.

In our analysis we concentrated on interstellar lines of the highly ionized species accessible with IUE: CIV, SiIV and NV; for comparison we also included measurements of FeII λ1608.456, a convenient tracer of gas in a lower state of ionization. Most of the background stars observed are early B. Often in these the interstellar CIV and SiIV lines are hidden in the cores of their

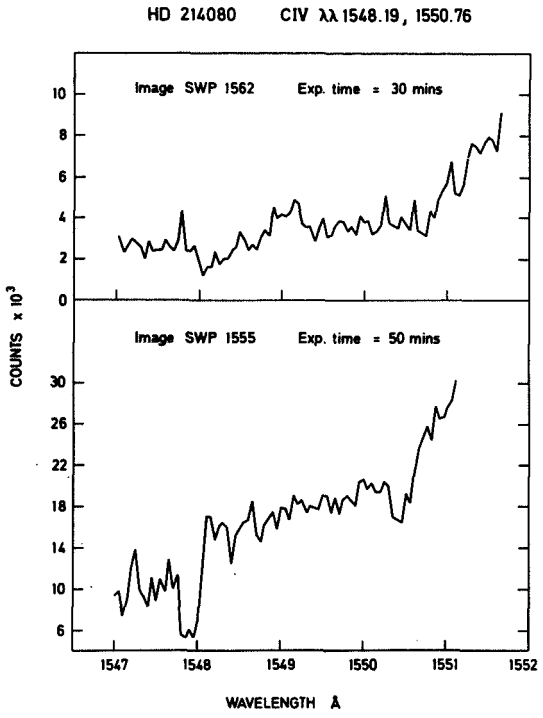

Figure 1

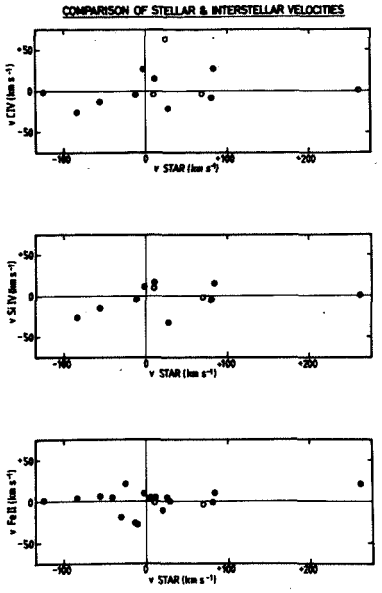

Figure 2

stellar counterparts (Figure 1, top) and it is necessary to overexpose most of the stellar continuum in order to detect the interstellar lines at all (Figure 1, bottom). We found that for single IUE images an equivalent width $W_\lambda \sim 60\text{-}70$mÅ is a typical threshold for the detection of interstellar CIV and SiIV. Above this limit, about two thirds of the stars observed show absorption by these ions, reaching $W_\lambda \sim 200\text{-}300$mÅ in the stronger line of each doublet. In contrast NV is detected only in two directions, where all interstellar lines are exceptionally strong; a typical upper limit is $W_\lambda \lesssim 50$mÅ.

Before proceeding further, it is important to consider whether the lines observed are indeed formed in the diffuse interstellar medium in line to the stars or are attributable primarily to circumstellar material. In Figure 2 the velocities of the interstellar lines are plotted versus those of the background stars. It is evident that the gas observed is not dynamically associated with the stars, since the interstellar velocities are scattered about zero, rather than about a line of unit slope, and span a much smaller range than the stellar velocities. Statistical tests showed the two samples to be uncorrelated. A circumstellar origin for the lines observed also seems excluded by consideration of the line strengths. Model HII region calculations, which reproduce well the observations of CIV and SiIV lines in the spectra of disk stars, predict negligible absorption by these ions in the Stromgren spheres of the late O and early B stars which constitute our sample. On the other hand, on the basis of their widths and velocities, the lines are most naturally interpreted as arising in the intervening halo gas.

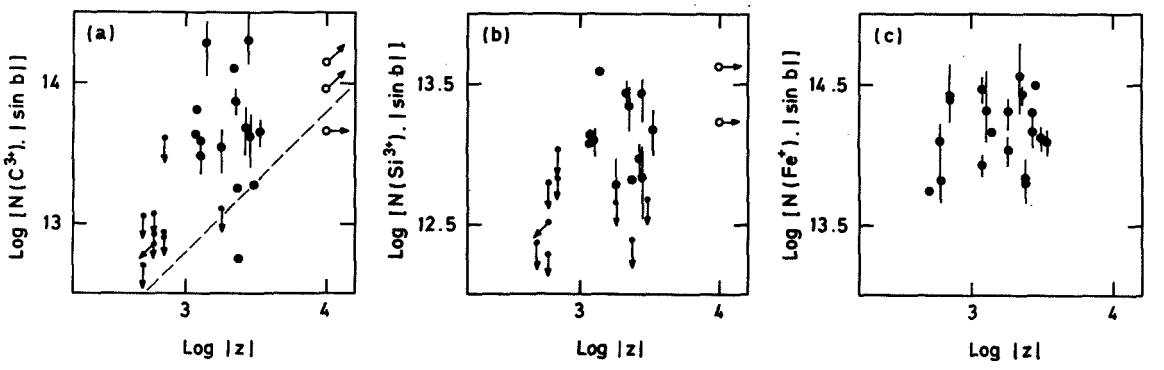

Figure 3

DISTRIBUTION OF HALO GAS.

In Figure 3 the column densities of C^{3+}, Si^{3+} and Fe^{+}, resolved along the $\underline{z}$ direction, are plotted against the stellar distances from the plane. (Ion column densities N were derived by fitting the corresponding absorption lines with theoretical profiles computed with the largest values of ion velocity dispersion compatible with the observed line widths. For the strongest lines the corresponding values of N may be lower limits). If the distribution of the ions in Figure 3 were plane parallel and the density profile with $|\underline{z}|$ Gaussian or exponential, we would expect the quantity $N.|\sin b|$ to increase linearly with $|\underline{z}|$ for $|\underline{z}| \lesssim h$ (the scale height of the gas) and to flatten off for $|\underline{z}| > h$, tending to a limiting value determined by h and the density at $\underline{z} = 0$. Thus, the lack of any clear correlation between $N(Fe^{+}).|\sin b|$ and $|\underline{z}|$ in Figure 3c may indicate that the scale height of Fe^{+} is less than ~ 500 pc, as found for HI (Bohlin, Savage and Drake 1978). Alternatively, it may be due to the fact that, at the IUE resolution, Fe II halo absorption could by masked by that due to foreground disk gas.

On the other hand, C^{3+} and Si^{3+} are clearly distributed differently from Fe^{+}. Although the points in Figures 3a and 3b show considerable scatter, it is noteworthy that: (a) none of the stars within 1 kpc from the plane show CIV or SiIV absorption; (b) between $\underline{z}$ = 1 and 3 kpc C^{3+} and Si^{3+} are detected in most cases, although there appear to be large differences in the column densities measured at the same distance $\underline{z}$; (c) in the few cases where observations referring to the whole extent of the halo are available, the column densities of C^{3+} and Si^{3+} are not significantly greater than those for stars 2-3 kpc from the plane. The implied steep increase in the density of highly ionized gas between $\underline{z}$ = 0.5 and 3 kpc is consistent with the earlier suggestion by Savage and de Boer (1981), based on different arguments, of the existence of a Galactic transition layer between cooler gas in the plane and outer halo regions at $T \sim 10^6$ K. If such a transition region exists, our results show it to be a widespread phenomenon and to occur nearer the plane than could be deduced from observations of extragalactic sources alone. In any case it appears that the amounts of C^{3+} and Si^{3+} present in the diffuse ISM in the disk are insufficient to account for the observed column densities of these ions in the halo. The broken line in Figure 3a shows the column density of C^{3+} which would be expected

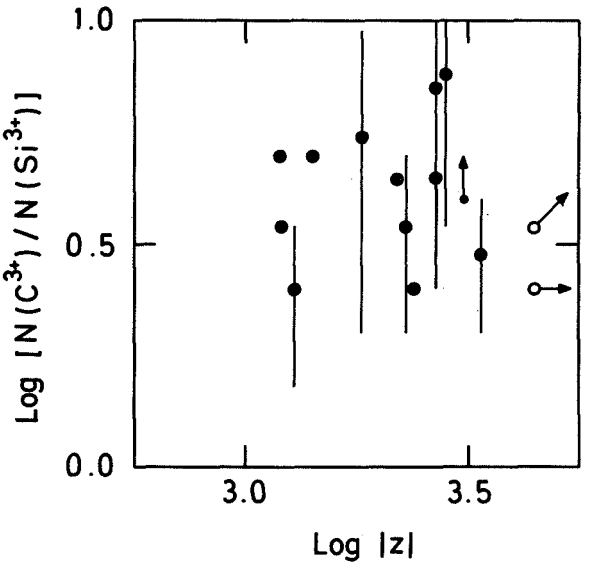

Figure 4

if the average $n(C^{3+}) \simeq 2 \times 10^{-9}$ cm^{-3} in the disk (Cowie, Taylor and York 1981; Laurent, Paul and Pettini 1982) extended into the halo with infinite scale height.

ION FRACTIONS

From Figure 4 it is evident that the ratio $N(C^{3+})/N(Si^{3+})$ is independent of z and shows a remarkably small scatter about the mean value $N(C^{3+})/N(Si^{3+}) = 4.5 \pm 1.5$ (1σ), suggesting large scale uniformity in the mechanisms producing these ions. The most stringent limit we can place on the relative proportions of C^{3+} and N^{4+} is $N(C^{3+})/N(N^{4+}) > 7$. The measured value of the C^{3+}/Si^{3+} ratio clearly differentiates halo gas from the circumstellar H II regions primarily responsible for the CIV and SiIV observed in the disk since, for the stars in our sample, HII region calculations predict $N(C^{3+})/N(Si^{3+}) < 0.1$. Thus, if these ions are produced by photoionization in the halo, we require a harder ionizing flux than that due to OB stars. An additional constraint is that the ionizing photons be confined at a few kpc from the plane, in order to explain the enchancement in the density of highly ionized species in the halo. York (1982) pointed out that the integrated QSO Lyman continuum is sufficient to account for the observed C^{3+} and Si^{3+} for reasonable values of particle density.

Alternatively, the highly ionized species may be formed in a hot gas by collisional ionization balanced by recombination processes. In this case the C^{3+}/Si^{3+} ratio fixes the temperature to a narrow range: $T = 8.0 \pm 0.3 \times 10^4$ K, at which value essentially no NV should be present. This would require a heating mechanism favouring this particular temperature, since in this domain the cooling curve is a slowly changing monotonic function of T. Alternatively, it is possible that gas in the corona is distributed over a wide range of temperatures and that in the CIV and SiIV lines we isolate material at the temperature favouring these ions. Cooling gas in a galactic fountain model (Bregman 1980) may be the site of the observed absorption. At present a comparison of the measured ion fractions with predictions from time-dependent ionization models is not very instructive, since available calculations (eg. Shapiro and Moore 1976) do not include the effects of change-transfer reactions which could alter the ionization balance considerably. However, we note that for gas cooling from high temperatures significant fractions of NV are expected, corresponding to column densities within the observing capabilities of IUE.

REFERENCES

Bohlin, R.C., Savage, B.D., and Drake, J.F. 1978, *Ap.J.*, 224, 132.
Bregman, J.N. 1980, *Ap.J.*, 236, 577.
Cowie, L.L., Taylor, W., and York, D.G. 1981, *Ap.J.*, 248, 528.
Laurent, C. Paul, J., and Pettini, M. 1982, *Ap.J.*, in press.
Pettini, M., and West, K.A., *Ap.J.*, in press.
Savage, B.D., and de Boer, K.S. 1981, *Ap.J.*, 243, 460.
Shapiro, P.R., and Moore, R.T. 1976, *Ap.J.*, 207, 460.
Spitzer, L. 1956, *Ap.J.*, 124, 20.
York, D.G. 1982 *Ann. Rev. Astr. Ap.* in press.

ABUNDANCES IN THE MAGELLANIC STREAM

M.V. Penston, P. Pettini, A. Boksenberg
Royal Greenwich Observatory, Hailsham, UK
T.R. Gull
Laboratory for Astronomy and Solar Physics, Code 683, Goddard Space Flight Center
M.A.J. Snijders
University College London, UK

ABSTRACT

The bright southern Seyfert 1 galaxy ESO 113-IG45 (Fairall 9) lies behind a dense portion of the Magellanic Stream. AAT and IUE observations at resolutions ~ 10^4 show 12 interstellar lines (at +195km/s) representing HI, CII, CIV, OI, MgII, SiII, CaII and FeII in the Stream and confirming the original detection of CaII K by York and Songaila. The velocity dispersion b = 30 to 50 km/s can be deduced as well as abundances of the Stream material. The presence of metals in the Stream show it is not composed of primordial matter. The deduced abundances may be a little less than solar and are broadly consistent with those in the Magellanic Clouds.

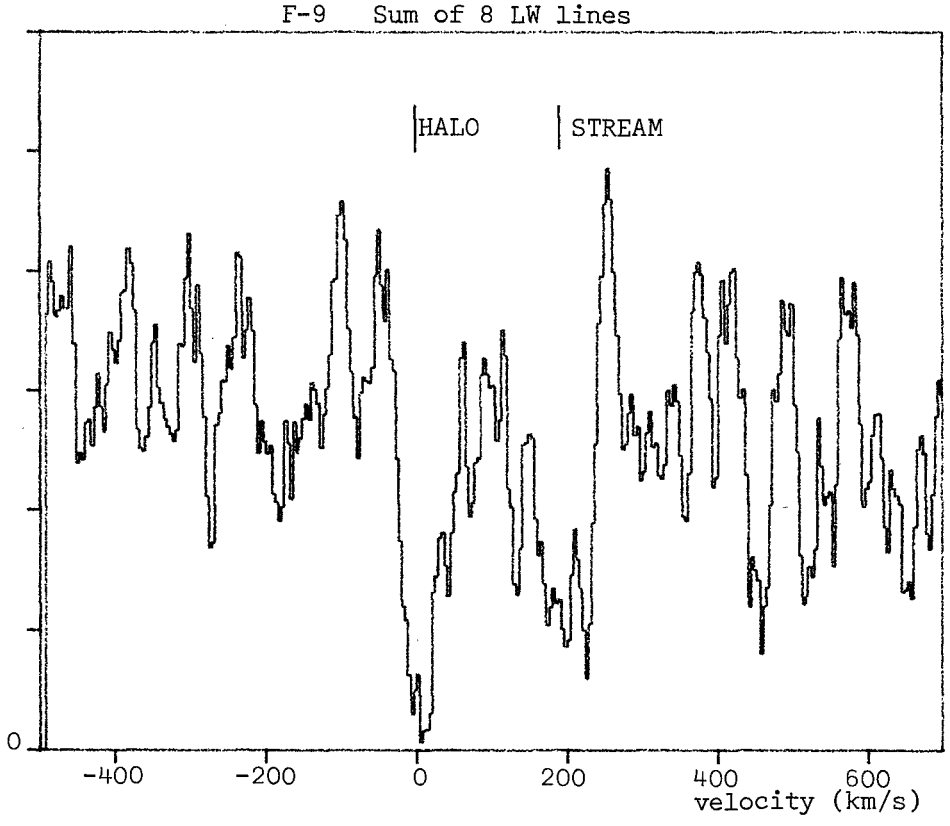

KINEMATICS OF GAS IN THE VELA SUPERNOVA REMNANT

George Wallerstein, University of Washington
Edward B. Jenkins, Princeton University and
Joseph Silk, University of California, Berkeley

High resolution, short wavelength, spectra of 46 stars in the general field of the Vela supernova remnant have been obtained with IUE. Radial velocities and equivalent widths for all measurable interstellar absorption features have been tabulated. Thirty-one components with velocities greater than 20 km s^{-1} with respect to the local standard of rest have been isolated. If low velocity components are present it is difficult to identify a high velocity component unless $|V| \gtrsim 50$ km s^{-1}. Hence components in the range of 20-50 km s^{-1} are seen only in SiIV and especially CIV for which frequently no low velocity component is seen. The highest measured velocity is -175 km s^{-1} in HD 74455. Nine stars that are clearly outside the nebula or in front of it show no high velocity gas confirming that the high velocity components are associated with the supernova remnant and not the large B association in which it is immersed.

High velocity CI is never seen and high velocity OI is seen in only two stars. High velocity CII, SiII and FeII are most commonly seen in stars that are members of IC 2395 which is located behind and just within the southern edge of the remnant. SiIV and especially CIV are seen much more often at high velocities than are singly ionized species. This indicates that the acceleration and ionization of clouds correlate; presumably a shock wave is responsible for both. High velocity gas is never seen in AlIII, which may indicate that this normally highly depleted species recombines on a time scale which is shorter than the time scale for grain disruption. When the stars are divided into four distance bins: 300-499 pc., 500-799 pc., 800-1199 pc., and greater than 1200 pc; we find that the percentage of stars showing high velocity components is constant (within the small number statistics). Hence it seems likely that the Vela remnant is at a distance of 400±100 parsecs. The small size of the remnant, about 40 parsecs diameter, as compared to the depth of the B association, explains why we see about an equal number of positive and negative high velocity clouds. Evidently only a few of our stars are actually immersed in the remnant.

New high resolution CaII and NaI data obtained for us by E. Hu and N. Walborn for 6 stars show a number of new components including six components in HD 72089. The various components in that star show an extremely strong Spitzer-Routly effect with the logarithmic ratio of CaII/NaI column density ranging from < -0.8 for the lowest velocity component to > 1.2 for one high velocity component.

SMALL SCALE STRUCTURE IN THE INTERSTELLAR MEDIUM: ORION'S THREADBARE CLOAK

Steven N. Shore
Warner and Swasey Observatory
Case Western Reserve University

ABSTRACT

The interstellar medium in the central portion of the Orion Cloak dynamical feature has been examined for evidence of fine structure. Four stars in the Ori OB I association, HD 37017, 37468, 37479, and 37776 bracket the stars in the lower belt region that have been studied previously. Two are members of the σ Ori subcluster. A lower limit to the scale of inhomogeneity can be set using these at 0.1 pc, while on a scale of about 10 pc, the high velocity component of the second spectrum ions shows optical depth variation of more than a factor of 5. Neutral lines do not display the high velocity component. Some preliminary abundances are also given.

INTRODUCTION

As part of a survey of helium rich spectrum variables in the Orion Association, HD 37479, 37017 and 37776, spectra were obtained of the brightest member of the σ Ori subcluster, HD 37468, in order to remove the interstellar contribution to several line profiles. In the tradition of Messier, it has turned out that one of the most interesting uses of this program is that for which it was intended to be a cure -- the structure of the interstellar diffuse component across the Ori OB I B and C groups (see Warren and Hesser 1977). This region has been previously examined by Cowie, Songaila and York (1979) with COPERNICUS. Our program stars bracket ζ Ori and allow for a very fine structure study of the Orion Cloak dynamical feature that they report on. Since three of our program stars are spectrum variables, it is possible to minimize the effects of photospheric contamination to the IS lines by chosing phases of He I maximum (Shore and Adelman 1981). This note presents some preliminary results. A more detailed study is under way.

OBSERVATIONS

All spectra used in this study were obtained between 3 Jan. and 8 Jan. 1980, using both the SWP and LWR of the International Ultraviolet Explorer Satellite. For HD 37468, only one SWP and one LWR spectrum was obtained; for all others, the quoted values in Tables I and II for the equivalent widths are averages of two. A more detailed discussion of the observations is given in Shore and Adelman (1981, 1982).

RESULTS

The measured equivalent widths for all relevent lines are listed in Tables I and II. Lines of the neutral species N I and Mg I are at the rest wavelength found by Cowie *et al.* (1979)(CSY). Since we share HD 37468 in common, it has been used as a wavelength standard for comparison of data.

In particular, for both HD 37479 and 37468, the Si III 1206 line, which in the former is heavily "contaminated" by the photospheric line, shows a velocity separation between the low and high velocity components in agreement with the COPERNICUS data (- 93 km s^{-1}). This also agrees with the velocity separation (- 93 $\pm$ 2) derived from the C II doublet. In addition, all strong lines of Si II, S II, Fe II, Mn II, and Mg II are doubled, with the low velocity component generally being broader than that for the neutral species. For instance, the FWHM for N I is 25 km s^{-1}, which is about half that of C II for both HD 37468 and 37479. Examples of the line profiles used are in figures 1 and 2.

One of the most striking features of the inner portion of the Orion Cloak feature is the scale of its inhomogeneity. Moving north from the σ Ori subcluster, the high velocity feature on the C II lines disappears. Between HD 37468 and 37776, the change in optical depth is at least an order of magnitude. Moving south to HD 37017, a similar result holds. It therefore appears that HD 37468 and 37479 are sitting behind a local flocule in the expanding shell, having an angular extent of only some 4 degrees, at most. The results derived from this study for the high velocity component abundance of C II is $(4\pm2)\times10^{14}$ cm^{-2} assuming that b = 8 $\pm$ 2 km s^{-1}, from both HD 37479 and 37468. Since the line profiles obtained from IUE are not resolved to the degree that the COPERNICUS data are, this is probably an underestimate of the error; it is, however, in qualitative agreement with the results presented by CSY using the CIIλ1036 line. Line profiles of both C II and Mg II, and of Si III show that the region is uniform at least across the face of the σ Ori group (40 arcsec) so that on a scale of 0.1 pc the medium is uniform. The fact that the three variables in this sample are all within the same portion of the association, and all magnetic, suggests that some of the fine structure in this region might be connected with magnetic fields, as well as instabilities in the expanding front.

An additional by-product of this study has been the determination of the FeII abundance toward HD 37468. Using the low velocity components of FeII 2586 and 2599, and oscillator strengths from Kurucz (1981), ϵ (FeII) = 10.0 ($\pm$ 0.5), again in qualitative agreement with other determinations which show an Fe depletion in the diffuse ISM. Using the value for CII derived from the resonance doublet, Fe appears underabundant by about 100x. That the high velocity lines appear on both Mn II and Fe II lines may allow for a determination of the rate of grain sputtering in the shock expanding about Orion.

I wish to thank the staff of the IUE observatory for their kindness during this program, and especially Dr. A. Boggess, who permitted a last minute change in the program which made these observations possible. I also thank Dr. Saul J. Adelman for help in obtaining these observations as part of our spectrum variables program.

REFERENCES

Cowie, L.L., Songaila,A., and York,D.G. 1979, Ap.J., 230, 469.
Shore, S.N. and Adelman, S.J. 1981, 23rd Liege Symposium, p. 429.
———————————. 1982, in preparation.
Warren, W. H. and Hesser,J.E. 1977, Ap.J.Suppl., 34, 115.

TABLE I

PROGRAM STAR EQUIVALENT WIDTHS (A)

λ	Ion	HD 37017	37468	37479	37776
1190	S III,Si II	0.64	0.77	0.74	0.56
1193	Si II	0.63	0.89	0.69	——
1199	N I	0.40	0.49	0.41	0.43
1200	N I	0.27	0.33	0.29	0.27
1201	N I	0.31	0.29	0.33	0.31
1251	S II	——	0.26	0.30	——
1254	S II	0.35	0.29	0.26	0.40
1259	S II	0.34	0.29	0.28	0.47
1260	Si II	0.69	0.54	0.57	(R)
1277	C I	——	0.12	0.13	——
1304	Si II	0.38	0.35	0.42	0.35
1526	Si II	0.56	0.47	0.50	0.45
1608	Fe II	——	0.16	(0.30)	——
1808	Si II	0.14	0.14	0.14	0.11
2344	Fe II	0.64	0.53	0.52	0.64
2384	Fe II	0.68	0.70	0.81	0.68
2576	Mn II	0.24	0.25	0.19	0.22
2586	Fe II	0.46	0.41	0.55	0.49
2594	Mn II	0.15	0.21	0.14	0.19
2599	Fe II	0.67	0.68	0.77	0.70
2795	Mg II	1.04	0.99	1.03	1.11
2802	Mg II	0.85	0.92	0.90	0.86
2853	Mg I	0.46	0.37	0.41	0.39

TABLE II

HIGH VELOCITY COMPONENTS: W_λ (A)

λ	Ion	HD 37468	HD 37479
1251	S II	0.18	——
1260	Si II	0.16	0.23

TABLE II (Continued)

λ	Ion	HD 37468	HD 37479	
1334	C II	0.51	——	low v comp.= 0.62
1335	C II	0.08	——	low v comp.= 0.46
2344	Fe II	0.08	——	
2586	Fe II	0.05	——	
2795	Mg II	0.23	0.20	
2802	Mg II	——	0.06	

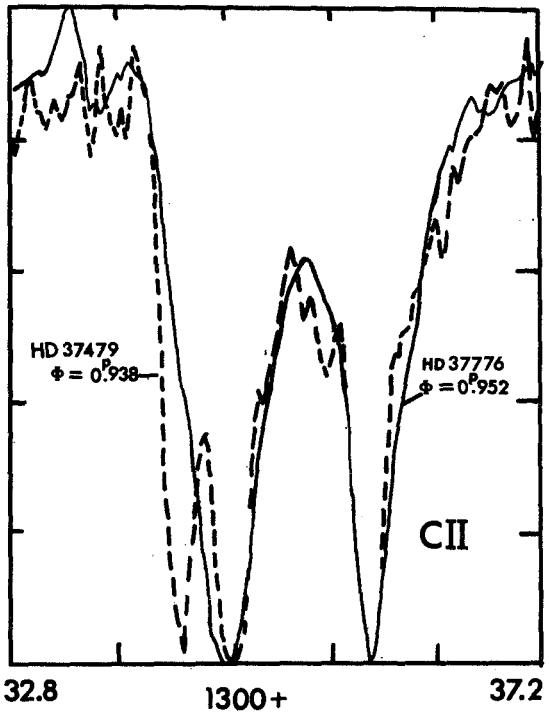

Fig. 1. Sample CII profiles for two spectrum variables near HeI strong phases. HD 37479 is line 37468, HD 37776 shows a CII like 37017. An optimal three point filter has been used.

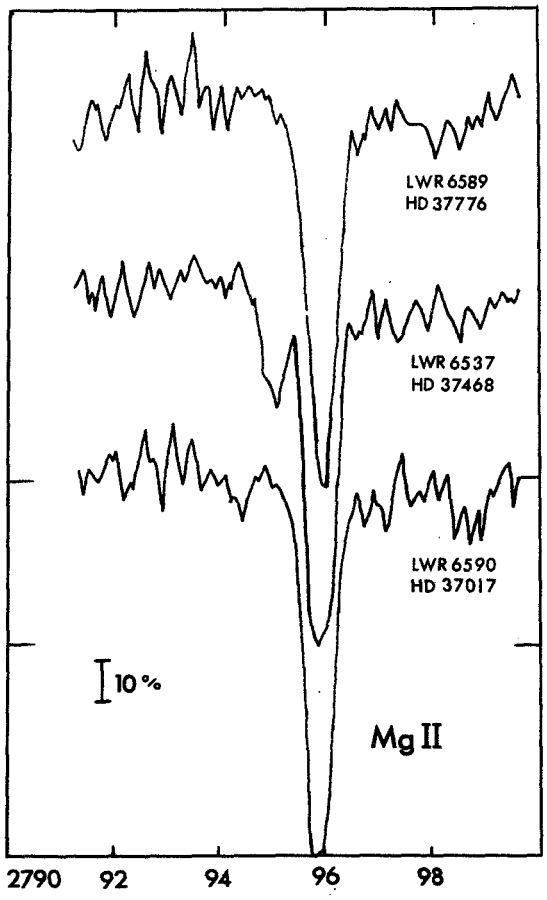

Fig.2. Sample MgII 2795 profiles for HD 37468 (like 37479), 37017, and 37776. Ordinate marks the zero intensity level. Unsmoothed data.

HIGH DISPERSION OBSERVATIONS OF SELECTED REGIONS IN THE ORION NEBULA

G.O. Boeshaar and C.A. Harvel
Astronomy Department, Computer Sciences Corporation
and Space Telescope Science Institute

A.D. Mallama, P.M. Perry, R.W. Thompson, and B. Turnrose
Astronomy Department, Computer Sciences Corporation

ABSTRACT

High resolution spectral observations were made of several regions of the Orion Nebula near θ^2 Ori A using the IUE. The positions were selected using a moderate spatial resolution map from a previous low dispersion IUE survey of this section of the nebula. Using the SWP and LWR cameras, 28 spectra were obtained of the bright bar, three Taylor-Münch cloudlets, and several surrounding locations. Emission lines of He, C, N, O, Mg, and Si allow a characterization of these cloudlets and of the gas in and around the bar. Small aperture observations provide radial velocity information for the ultraviolet emission of these features. These data show ionization variations from region to region and are suggestive of stellar wind interactions between the cloudlets and θ^2 Ori A.

INTRODUCTION

Studies of giant H II regions such as 30 Doradus in the LMC show extreme structural, spectral, and kinematic complexities,[1,2]. Yet such objects are of critical importance to our understanding of interstellar abundances, star-formation dynamics, and stellar wind/interstellar gas interactions. Of comparatively modest dimensions, the nearby Orion nebula is a simpler, spatially-resolved example for which elemental abundances[3] and a global structural model[4] already exist. The central region of Orion provides case studies of relatively isolated features that have a bearing on the analysis of more complex nebulae. Southeast of the Trapezium stars, the bright bar represents an ionization front due to the UV flux of θ^1 Ori C[5] and the Taylor-Münch cloudlets are thought to be shock fronts produced by the stellar wind from θ^2 Ori A.[6,7]

OBSERVATIONS

An IUE map of the bright bar region in Orion[8] was used to select the most promising positions for spectral observations. With the high dispersion large and small aperture modes of the SWP and LWR cameras, 60- to 385-minute exposures were obtained

for the points shown in Figure 1. Here BB refers to the bright bar; A, B, and C, to the three Taylor-Münch cloudlets; N, to a region north of the bar; and S, to a selection of positions southeast of the bar. Using the Tololo-Vienna image processing system on the Space Telescope Science Institute computer system, a preliminary analysis of the ripple-corrected spectra was performed providing feature identifications, relative emission line strengths, and some radial velocity information. The results for multiple spectra from the same position were averaged, normalized to the strength of the [O II] λ2470 line, and combined for the two wavelength ranges on the basis of the C III] λλ1907, 1909 line strengths observed with both the SWP and LWR cameras. The high dispersion mode both decreased the contamination of emission lines by the continuum and allowed (for the small aperture observations) radial velocity details to be seen.

SPECTRAL CHARACTERISTICS

Table 1 presents preliminary spectral results for six nebular regions. While uncorrected for interstellar reddening, the line strengths indicate a wide variety of emission characteristics in this section of Orion. Several general traits are worth noting. While O I and O II lines are well observed, no emission from O III and O IV is detectable, even though Si IV and C IV features are evident. The ionization extremes are illustrated by the presence of both Mg I and Mg V, with the latter strong at the sites of ionization and shock fronts. Finally, nitrogen lines are effectively absent with only a marginal detection of N III at λ1747 occurring for the two deepest exposures.

KINEMATIC FEATURES

The complexities of geometry and kinematics for the comparitively simple Orion H II region are depicted in Figure 2. The upper panels show the Mg II λ2798 observations for regions A and N. For cloudlet A, the nebular emission line lies to the blueward side of the absorption line (due to scattered starlight[9]), while the nebular emission is to the redward side for region N. The complicating nature of the scattered stellar continuum is further shown for the Si IV line in the lower left of this figure. A particularly spectacular velocity feature is seen in the lower right of Figure 2. For these two distinct sets of the C III] λλ1907, 1909 doublet, the separation of $\sim$1 Å implies a redshifted component moving at 150 km/sec with respect to the systemic velocity of the Orion nebula. This is an unusually high positive velocity for this section of Orion, although such a value is consistent with θ^2 Ori A wind predictions.[7]

The authors gratefully acknowledge the support of the IUE Observatory and RDAF, the resident astronomers, C.C. Wu, and A. Boggess. In addition, appreciation is due to the Space Telescope Science Institute for providing the computer facilities, to Rudy Albrecht for assistance with the TV image processing system, D.E. Osterbrock for valuable line-identification materials, and to Karen Myers for manuscript typing.

REFERENCES

1. Boeshaar, G.O., Boeshaar, P.C., Czyzak, S.J., Aller, L.H., and Lasker, B.M. 1980, Ap. Space Sci., 68, 335.

2. Balick, B., Boeshaar, G.O., and Gull, T.R. 1980, Ap. J., 242, 584.

3. Torres-Peimbert, S., Peimbert, M., and Daltabuit, E. 1980, Ap. J., 238, 133.

4. Balick, B., Gammon, R.H., and Hjellming, R.M. 1974, P.A.S.P., 86, 616.

5. Balick, B., Gull, T.R., and Smith, M.G. 1980, P.A.S.P., 92, 22.

6. Münch, G., and Taylor, K. 1974, Ap. J. (Letters), 192, L93.

7. Taylor, K., and Münch, G. 1978, Astr. Ap., 70, 359.

8. Turnrose, B.E., Perry, P.M., Harvel, C.A., Thompson, R.W., and Mallama, A.D. 1980, S.P.I.E., 264, 257.

9. Perinotto, M., and Patriarchi, P. 1980, Ap. J., 238, 614.

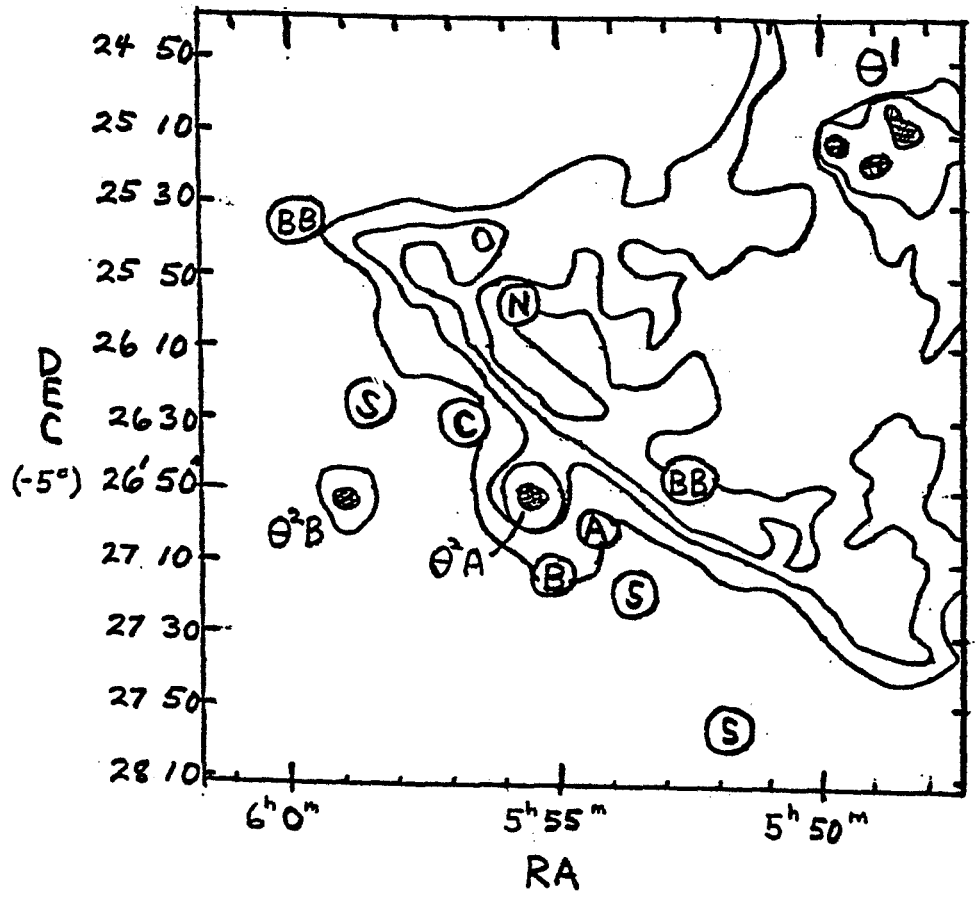

Figure 1. Isophotal map (red light) of the central section of the Orion showing the regions sampled spectroscopically for this study. The bright bar is the ridge running from northeast to southwest and the locator circles are approximately the projected size of the IUE large aperture.

Figure 2 (next page). Samples of the high dispersion data: upper left, the Mg II 2798 feature for cloudlet A; upper right, the Mg II 2798 feature for region N; lower left, the Si IV 1394 feature for cloudlet B; lower right, the C III] 1907, 1909 features for region N.

TABLE 1

RELATIVE LINE STRENGTHS FOR ORION ([O II] = 100)

Lines	Bright Bar	Cloudlet C	North of Bar	Cloudlet A	Cloudlet B	South of Bar
1305/6·OI		14.9	3.14		1.43	
1305·Si II		1.27	0.12		0.36	
1334/6 C II		14.0	12.9			
1394/1403·Si IV		4.27	1.73	2.92	6.42	3.17
1533·Si II		1.75	3.06	0.68	1.62	6.98
1549/51·C IV	5.38	0.92	2.29		2.32	3.40
1760·C II ?			2.23		1.18	
1817·Si II + [Ne III]			2.69	1.44	0.39	
1882/92·Si III		1.65	3.41	0.84	1.74	
1907/9· C III]	35.7	15.3	10.8	5.44	11.5	24.6
2324/9·C II] +[O III]						
2470·[O II]	100.0	100.0	100.0	100.0	100.0	100.0
2764·He I	18.0	18.3	15.9	23.0		12.6
2784· [Mg V]	30.6		6.61	20.9		
2798/2803·Mg II		3.72	11.0	135.0	70.0	8.31
2829·He I	15.3	23.5	33.6	37.8	30.5	24.0
2852·Mg I		6.99	15.3	22.5	3.55	9.98
3067·O VI	78.2	23.8	21.5	61.2	19.4	9.32

THE VIOLENT INTERSTELLAR MEDIUM ASSOCIATED WITH THE CARINA NEBULA.

Max Pettini[1], Claudine Laurent[2] and Jacques A. Paul[3]
[1] *Royal Greenwich Observatory, U.K.*
[2] *Laboratoire de Physique Stellaire et Planétaire, France.*
[3] *Section d'Astrophysique, Centre d'Etudes Nucléaires de Saclay, France.*

Introduction

The Great Carina Nebula (GCN) and its surroundings constitute the most remarkable aggregate of young star clusters in the Galaxy and are the site of some of the most conspicuous manifestations of the interaction between young, massive stars and the ambient interstellar medium. The Nebula is a copious source of X-rays and of high energy γ radiation, which have been interpreted as a global consequence of the large amounts of mechanical energy released by the numerous mass-losing stars (Montmerle, Cassé and Paul 1981, Seward and Chlebowski 1982). The process of star formation is propagating through the region at the unusually high speed of 30 km s^{-1} (Turner et al 1980). Radio and optical emission line observations (Huchtmeier and Day 1975, Deharveng and Maucherat 1975) have shown that the central portions of the Nebula are expanding at $\sim$ 20 km s^{-1}, the expansion being centred on the two young clusters Tr14 and Tr16. Interstellar line surveys in the visible and ultraviolet (Walborn and Hesser 1975, 1982) have revealed an exceedingly complex structure of the local interstellar medium, with many discrete components spanning a wide velocity range of up to 550 km s^{-1}. These are the highest velocities known for galactic interstellar gas, attesting to the extreme physical conditions prevailing in the Nebula. In this presentation we summarise the main results of a detailed study of the interstellar spectrum of HD 93205, an O3V star in the cluster Tr16, located inside the most active part of the GCN. This work is described more extensively in a forthcoming article (Laurent, Paul and Pettini 1982).

Interstellar Absorption Lines

In order to exploit fully the resolution capabilities of IUE, we extracted the data directly from the raw images, using a specially developed extraction procedure described elsewhere (Laurent, Paul and Vidal-Madjar 1981). From the analysis of 67 lines of 25 atoms, ions and molecules we identified up to six discrete absorption components spanning a maximum velocity range of $\sim$ 375 km s^{-1}. Table 1 summarises the component structure for different species. In Figure 1 we have reproduced sample absorption lines, indicating at the top the positions of the six components, labelled A to F. Ion column densities appropriate to each component which can be resolved in at least one line were derived by constructing empirical curves of growth and by fitting the observations with corresponding theoretical absorption line profiles. We now discuss in turn the most important results concerning each component.

TABLE 1
ULTRAVIOLET COMPONENT PATTERN

Components Velocity (km s^{-1})	A -275	B -134	C - 89	D - 29	E + 4	F + 102
Minor HI region species						
CI					Y	
MgI			Y	Y	Y	
ClI					Y	
Major HI region species						
CII		(Y)	Y	Y	Y	Y
OI	Y	(Y)	Y	Y	Y	Y
MgII		(Y)	Y	Y	Y	Y
AlII			Y	Y	Y	Y
SiII		(Y)	Y	Y	Y	Y
SII			Y	Y	Y	
CrII				Y	Y	
MnII			Y	Y	Y	
FeII			Y	Y	Y	
NiII					Y	
CuII					Y	
ZnII				Y	Y	
Metastable levels						
CI*					Y	
CII*			Y	Y	Y	Y
OI*				Y		
OI**				Y		
SiII*			Y	Y		
Higher ions						
CIV			Y	Y	Y	Y
AlIII			Y	Y	Y	
SiIV			Y	Y	Y	

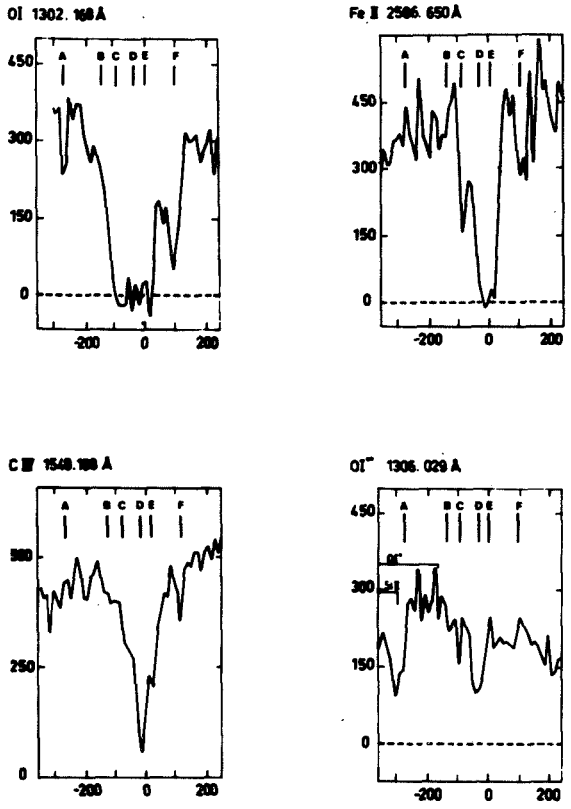

Figure 1

Component E: $v_{LSR} = -8$ *km* s^{-1}

This is most naturally interpreted as arising in the intervening ISM between the Sun and the GCN. It is noteworthy that, using our improved extraction method, we are able to resolve weak interstellar lines of highly ionized species (CIV, SiIV, AlIII), free from contamination by circumstellar HII regions which normally affects measurements of these lines in disk stars. The equivalent widths of CIV and SiIV measured in component E are very much smaller than those observed in IUE spectra of O stars (Black et al. 1980; Cowie, Taylor and York 1981) and Wolf-Rayets (Smith, Willis and Wilson 1980). This provides observational evidence in support of the view that, in the disk, the CIV and SiIV lines are formed primarily in ionized nebulae associated with early-type stars. The origin the smaller amounts of CIV and SiIV present in the diffuse ISM is still to be established. These species may occur at the conductive interfaces between cool clouds and coronal gas at a few million degrees, in analogy with current ideas for the origin of OVI absorption. Our data support this interpretation on the basis of two considerations. Firstly, no systematic velocity difference could be found in component E between the highly ionized species and neutral atoms such as CI and ClI. Secondly, the measured average density of CIV, $n(CIV) \simeq 3 \times 10^{-9}$ cm^{-3}, is in good agreement with the value predicted by ionization fraction calculations appropriate to conductive interfaces, (Weaver et al., 1977) assuming that the average value of the OVI density in

the disk applies to the line of sight to HD 93205.

Component D: $v_{LSR} = -41$ *km* s^{-1}

This component can be readily identified with the approaching portion of the ionized nebula around the Carina OB associations, thus establishing that HD 93205 is inside the expanding bubble. The velocity of the UV feature agrees well with that of the blue-shifted component of the radio and optical emission lines. These are split into two components, separated by ~ 45 km s^{-1}, over a region 25' in diameter (Huchtmeier and Day 1975), indicating a diameter ~ 20 pc (at a distance of ~ 2.7 kpc) for the inner cavity of the expanding shell. In component D absorption lines characteristic of a dense HII region are in evidence: we detect strong absorption by the highly ionized species AlIII, SiIV and CIV and lines arising from metastable levels of SiII and OI which are normally too sparsely populated to be detected in the quiescent interstellar medium. In principle, these lines are diagnostic of the temperature and density of the gas, since the relative populations of the fine-structure levels of the ground state are determined primarily by particle collisions. In the case under study, however, we are unable to carry out a quantitative analysis of the physical conditions from the UV lines since the available transitions from the corresponding ground state of SiII and OI are all strong and intrinsically blended with absorption due to other components at nearby velocities. Nevertheless, analysis of the radio recombination lines (Smith, Bierman and Mezger 1978) gives electron densities in the range n(e) = 80 - 230 cm^{-3} for the expanding HII region.

Clearly it is of interest to determine the likely source of the the observed expansion. Given the relatively small age of the inner associations ($\sim 1 \times 10^6$ years), the expansion is more likely to be driven by the energetic stellar winds than by successive supernova explosions, since the evolutionary time of supernova progenitors is $\sim 3 \times 10^6$ years. In the framework of the stellar wind-bubble model proposed by Castor, McCray and Weaver (1975), the mechanical power L_W (erg s^{-1}) required to sustain the expansion of a spherical bubble of diameter D(t) (pc) moving with velocity v(t) (km s^{-1}) after t years, is given by

$$L_W = 9.5 \times 10^{17}\ n_o\ v(t)^5\ t^2 \qquad (1)$$

where n_o is the density (cm^{-3}) of the medium in which the shell is expanding and

$$D(t) = 3.5 \times 10^{-6}\ v(t)t \qquad (2)$$

Adopting $n_o = 100$ cm^{-3}, $D(t) = 20$ pc, and $v(t) = 20$ km s^{-1}, we obtain $T \simeq 3 \times 10^5$ years and $L_W = 2.5 \times 10^{37}$ erg s^{-1}. Using recent estimates of mass-loss rates and terminal velocities appropriate to the early-type stars in Carina, Montmerle, Casse and Paul (1981) estimated that $L_W \simeq 6.5 \times 10^{37}$ erg s^{-1} is available from the stellar winds of the O stars and $L_W \simeq 2 \times 10^{38}$ erg s^{-1} from the 3 Wolf-Rayets in this region. Thus, it appears that sufficient kinetic energy is released by the stars in the inner Carina associations to drive the observed expansion of the nebula.

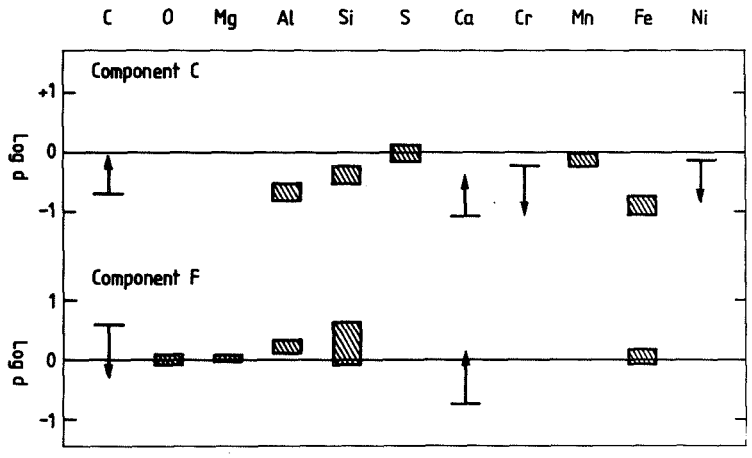

Figure 2

High velocity gas

Four high velocity components are detected in the IUE spectra of HD 93205. Components C (v_{LSR} = -101 km s^{-1}) and component F (v_{LSR} = + 90 km s^{-1}) are particularly well observed, being resolved in several lines of atoms and ions in different stages of ionization (see Table 1). Moreover, in these components ion column densities can be determined with a reasonable degree of confidence, since most lines are only weakly saturated and the respective curves of growth are well defined by the observed transitions. Interstellar line surveys of the GCN have shown that high velocity components are detected only in front of stars in the inner OB associations and indeed components C and F in HD 93205 are observed only in the spectra of a few neighbouring stars. This suggests that they are located *inside* the 20 pc cavity swept up by the expanding shell, implying in turn a lifetime of less than 2 x 10^5 years, assuming a velocity of 100 km s^{-1}. Their mass is likely to be less than ~ 0.3 $M_\odot$, on the basis of the observed angular size and the hydrogen column densities indicated by UV lines. Thus, the power required to accelerate this parcels of gas to the observed high velocities is significantly smaller than that necessary to drive the expansion of the whole nebula and is well within the energy budget from the stellar winds.
Figure 2 shows the abundance of elements observed in components C and F relative to the solar values, given by the lines at log d = 0. Abundances are plotted relative to observed species which are normally undepleted in the ISM: O in component F and S in component C. It is noteworthy that the two components apparently exhibit differences in their chemical composition. Most likely, abundances are solar in component F, since elements which are normally depleted by largely different factors in the ISM, (eg Al and O) are found in component F in solar relative proportions. This result can be understood as being due to efficient grain destruction in the high velocity shock. On the other hand, some residual depletions appear to be present in component C. The abundance pattern deduced cannot be readily explained by assuming that the yield of the on-going grain destruction processs is not yet complete, or that gas with typical interstellar depletions is mixed with solar composition material ejected by the stars. An interesting possibility to be tested with future observations is that the puzzling chemical composition of component C results from mixing with freshly synthesized material produced in a recent supernova explosion. The presence of a supernova remnant in Carina has been suggested but not yet firmly established (see Montmerle, Cassé and Paul 1981).

References

Black, J.H., Dupree, A.K., Hartmann, L.W., and Raymond, J.C. 1980, *Ap.J.*, 239, 502.

Castor, J., McCray, R., and Weaver, R. 1975, *Ap.J.*, (Letters), 200, L107.

Cowie, L.L., Taylor, W., and York, D.G. 1981 *Ap.J.*, 248, 528.

Deharveng, L., and Maucherat, M. 1975 *Astr. Ap.*, 41,27.

Huchtmeier, W.K., and Day, G.A. 1975, *Astr. Ap.*, 41. 153.

Laurent, C., Paul, J.A., and Pettini, M. 1982, *Ap.J.*, in press.

Laurent, C., Paul, J.A., and Vidal-Madjar, A. 1981, Proceedings of the Wien Workshop on IUE data reduction, p. 169.

Montmerle, T., Cassé, M., and Paul, J.A. 1981 *Ap.J.*, in press.

Seward, F.D., and Chlebowski, T. 1982, *Ap.J.*, in press.

Smith, L.F., Biermann, P., and Mezger, P.G. 1978, *Astr. Ap.*, 66, 65.

Smith, L.J., Willis, A.J., and Wilson, R. 1980, *M.N.R.A.S.*, 191, 339.

Turner, D.G., Grieve, G.R., Herbst, W., and Harris, W.E. 1980, *Astr. J.*, 85, 1193.

Walborn, N.R., and Hesser, J.E. 1975, *Ap.J.*, 199, 535.

Walborn, N.R., and Hesser, J.E. 1982, *Ap.J.*, 252, 156.

Weaver, R. McCray, R., Castor, J., Shapiro, P., and Moore R., 1977, *Ap.J.*, 218, 377.

CNO ABUNDANCES IN H II REGIONS OF THE MAGELLANIC CLOUDS AND THE GALAXY WITH IMPLICATIONS REGARDING THE NUCLEOSYNTHESIS OF THE CNO ELEMENT GROUP

Reginald J. Dufour, Rice University

and

Gregory A. Shields, University of Texas at Austin

INTRODUCTION

This report summarizes the results of IUE observations of the UV spectra of three H II regions in the Small Magellanic Cloud (SMC) and four H II regions in the Large Magellanic Cloud (LMC). Full details of the investigation have recently appeared in the 15 January 1982 issue of the Astrophysical Journal (Dufour, Shields, and Talbot, 1982); here we will present only the final abundance results and concentrate our discussion on the implications that the results have on the nucleosynthesis of the CNO group elements and the chemical evolution of galaxies.

OBSERVATIONS, ANALYSIS, AND RESULTS

Low dispersion SWP and LWR spectra of the SMC H II regions N66A, N66 (Northwest lobe), N81, and the LMC H II regions N4A, N79A, N157 (30 Doradus Nebula), and N159 (where the designations are those of Henize 1956) were obtained in which the absolute flux of the blended λ1909 C III] lines were measured in each nebula. These (along with a few other UV lines detected in some of the spectra) were corrected for reddening and combined with ground-based photoelectric scanner observations of emission-line strengths in the nebulae. Nebular models were then constructed in order to assess the physical conditions and derive abundances of elements with one or more ions showing observable lines in the spectra. Similar analyses were performed on the UV-optical spectra of two areas in the Orion Nebula using IUE and ground-based data from Torres-Peimbert, Peimbert, and Daltabuit (1980).

In this manner the relative gaseous-phase abundances of H, He, C, N, O, Ne, Ar, and S were derived for each H II region. Table 1 gives the average abundances found for the three SMC H II regions, the four LMC H II regions, and the two areas in Orion. The errors quoted represent the statistical standard deviations from the mean abundances for the three groups of nebulae. It is apparent from Table 1 that the statistical errors for C/H are comparable to those for O/H and N/H. This suggests that the errors in scaling the UV lines to the ground-based data on the basis of absolute flux do not vary significantly from nebula to nebula. The C/O ratios among the nebulae in the SMC and LMC (Table 1) show less statistical variation than the C/H ratios; possibly because C/O is less sensitive to errors in the derived (from the observed [O III] λλ5007/4363 ratio) electron temperatures for each nebula. For one SMC H II region, N81, the O III] λ1663 lines were observed in the IUE spectra and permitted direct calculation of the C/O ratio independent of absolute flux. The result (log C/O = -0.94) is in excellent agreement with the ratio (-0.91)

based on absolute flux and the mean ratio (-0.89) for the three SMC nebulae. This suggests that any systematic errors in the carbon abundances due to observational errors are small.

Therefore, the errors in the average abundances are probably mostly due to analytical factors such as ionization corrections and atomic parameters used in the models. We estimate that the effective errors in the abundances are ± 0.03 dex for He; ± 0.10 dex for C, O, and Ne; and ± 0.20 dex for N, S, and Ar.

DISCUSSION -- CNO NUCLEOSYNTHESIS

The major new result evident from this study is the prominent deficiency of carbon in the Magellanic Clouds relative to most of the other elements studied. This is shown in the right side of Table 1 where we present the logarithmic differences between the abundances found in the SMC and LMC relative to the Orion Nebula (which we will assume to be representative of the local galactic ISM). The C/H abundances in the SMC and LMC are lower than found in Orion by factors of 20 and 4, respectively. The C/H deficiency in the SMC is (marginally) greater in magnitude than even the N/H deficiency when compared to Orion or solar abundances.

The results of this investigation now permits one to study the nucleosynthesis of the interesting CNO element group using data on the average gaseous-phase abundances of the interstellar medium of three galaxies with significantly different metallicity. Recent studies (Lequeux et al. 1979; Talent 1980) of the chemical composition of H II regions in gassy irregular and late-type spiral galaxies show that the abundances of primary nucleosynthesis elements such as oxygen and neon general satisfy the predictions of the simple "closed box" model (no infall, instantaneous recycling) of galactic chemical evolution. In Figure 1 we show a plot of C/H and O/H versus $\ln\mu$, where μ is the astration parameter ($\mu \equiv M_{gas}/M_{tot}$). In the simple model the abundance of a primary element Z is related to the astration by the relation $Z = -y \ln\mu$, where y is the "yield" of the primary element. Inspection of Figure 1 shows that while O/H for the Clouds and our galaxy, shows a linear increase with $-\ln\mu$ (this relation is more clearly evident when data on other galaxies are included), C/H increases more rapidly than expected. This can be accounted for if the nucleosynthetic origins of carbon and oxygen are different, such that the oxygen enrichment arises from stars greater than 10 $M_\odot$, while the carbon enrichment arises from stars over a larger mass range extending downwards to that of planetary nebulae and novae progenitors ($\sim$ 1-3 $M_\odot$). The larger C/H ratio for the Galaxy compared to the Clouds expected from the simple model could then be attributed to the additional production of carbon by less massive stars from an older stellar population in the Galaxy that has no equivalent counterpart in the Clouds.

From the data in Table 1 and Figure 1 it is possible to calculate the yields of carbon and oxygen in the Magellanic Clouds and compare with the predictions of galactic chemical evolution models such as those by Arnett (1978) and by Chiosi and Caimmi (1979). The yields derived in this study: $y(C) = 6.3 \times 10^{-4}$ and $y(O) = 1.6 \times 10^{-3}$, agree best with Arnett's yields for

an IMF exponent of $\alpha = 10/3$ or with Chiosi and Caimmi's yields for $7/3 < \alpha < 10/3$ for models without mass loss, or with the yields for $4/3 < \alpha < 7/3$ with mass loss. Consequently, our results for carbon and oxygen are consistent with the theoretical models of bulk nucleosynthesis in massive stars for reasonable IMF's.

Our data also permits one to evaluate the nucleosynthetic origin of nitrogen as being predominantly a secondary element produced from carbon as its seed. For such a situation the simple model (c.f. Talbot and Arnett 1973) predicts that $N/C \propto C/H$. However, Tinsley (1979) has shown that this relation would hold only for low C/H values in extreme infall models and that N/C would initially lag behind C/H during the early phases of galactic chemical evolution if the secondary progenitor stars have relatively long lifetimes.

In Figure 2 we plot log N/C versus log C/H using the data in this study and mean abundances for planetary nebulae from Aller and Keyes (1980) and solar abundances given in Shields et al. (1981). From the figure we find the rather unexpected result that log N/C decreases with log C/H over the SMC-LMC-Orion range. This relationship could be due to a variety of factors, including (1) an increase in the primary yield of nitrogen relative to carbon with increasing stellar mass coupled with IMF variations; (2) a time delay in the production of carbon relative to nitrogen due to most of the carbon being produced in intermediate mass stars (e.g., $10 \lesssim M_{\odot} \lesssim 4$), while most of the nitrogen is produced in massive ($> 10\ M_{\odot}$) stars; and (3) infall effects which would tend to decrease N/C if nitrogen is predominantly produced in more massive stars than carbon. Recent studies of unevolved field stars by Sneden, Lambert, and Whitaker (1979) which found that $[C/Fe] = 0.0 \pm 0.3$ in stars for which $-2.3 \lesssim [Fe/H] \lesssim \pm 0.3$ suggest that the dominant stellar sources of iron and carbon are similar. This, coupled with the arguments of Tinsley (1979) that most of the iron enrichment arises from SNI stars in the $4 \lesssim M_{\odot} \lesssim 6.5$ mass range, and the scenario that significant primary nitrogen is released from stars $> 10\ M_{\odot}$, makes the variation of N/C with C/H found between the Clouds and the Galaxy accountable without the need to invoke significant differences in the IMF or infall rate between the three galaxies.

REFERENCES

Aller, L. H., and Keyes, C. D. 1980, Proc. Nat. Acad. Sci., 77, 1231.
Arnett, W. D. 1978, Ap. J., 219, 1008.
Chiosi, C., and Caimmi, R. 1979, Astr. Ap., 80, 234.
Dufour, R. J., Shields, G. A., and Talbot, R. J. 1982, Ap. J., 252, 461.
Henize, K. G. 1956, Ap. J. Suppl., 2, 315.
Lequeux, J., Peimbert, M., Rayo, J. F., Serrano, A., and Torres-Peimbert, S. 1979, Astr. Ap, 80, 155.
Shields, G. A., Aller, L. H., Keyes, C. D., and Czyzak, S. J. 1981, Ap. J., 248, 569.
Sneden, C., Lambert, D. L., and Whitaker, R. W. 1979, Ap. J., 234, 964.
Talbot, R. J., Jr., and Arnett, W. D. 1973. Ap. J., 186, 51.
Talent, D. L. 1980, Ph. D. thesis, Rice University.
Torres-Peimbert, S. Peimbert, M., and Daltabuit, E. 1980, Ap. J., 238, 133
Tinsley, B. M. 1979, Ap. J., 229, 1046.

TABLE 1
ABUNDANCES

Element	12 + log N(x)/N(H) ± σ* SMC	LMC	ORI	SMC/ORI	LMC/ORI
He	10.92±.02	10.92±.02	10.98±.01	-0.06	-0.06
C	7.16±.04	7.90±.15	8.46±.07	-1.49	-0.75
N	6.60±.12	6.94±.10	7.48±.06	-1.36	-1.02
O	8.05±.06	8.38±.12	8.60±.01	-0.82	-0.49
Ne	7.34±.01	7.68±.07	7.79±.01	-0.71	-0.37
S	6.61±.10	7.01±.12	7.12±.06	-0.38	-0.22
Ar	5.77±.09	6.10±.04	6.27±.01	-0.80	-0.47
C/O	-0.89±.03	-0.48±.06	-0.14±.08	-0.67	-0.26
C/N	0.56±.08	0.96±.11	0.98±.02	-0.13	0.27
N/O	-1.45±.07	-1.44±.07	-1.12±.07	-0.54	-0.53

*Errors are statistical rms standard deviations between abundances for the H II regions observed in each galaxy (3 in SMC, 4 in LMC, 2 areas in the Orion Nebula); they do not indicate systematic errors in line strength, atomic data, or ionization corrections for unobservable ions. Actual uncertainties are estimated to be ±0.03 dex for He; ±0.1 dex for C, O, and Ne; and ±0.2 dex for N, S, and Ar.

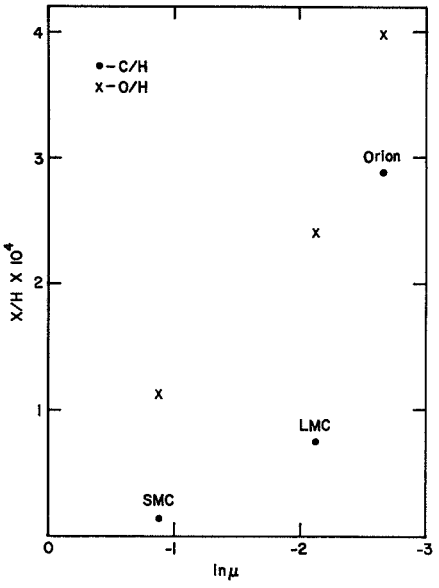

FIG. 1.—The variation C/H (*filled circles*) and O/H (*crosses*) with $\ln \mu$ ($\mu \equiv M_{gas}/M_{tot}$) for H II regions in the SMC, LMC, and the Orion Nebula.

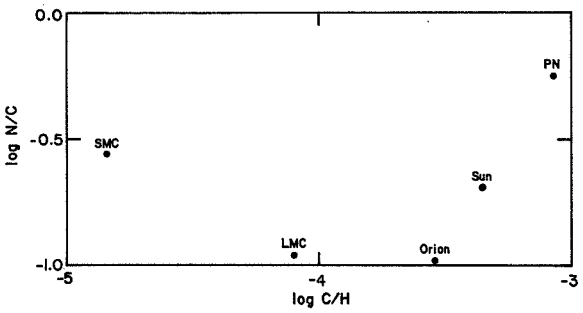

FIG. 2.—The variation of log N/C with log C/H for H II regions in the SMC and LMC, the Orion Nebula, the Sun, and planetary nebulae.

THE UV EMISSION LINE SPECTRUM OF NGC 6572

M.Grewing, G.Krämer, P.R.Preussner, E.Schulz-Lüpertz
Astronomisches Institut der Universität Tübingen (AIT)

ABSTRACT

Ultraviolet spectra of the medium excitation planetary nebula NGC 6572 have been obtained with IUE both in the low and in the high resolution mode. These spectra reveal a superposition of emission lines arising in the expanding atmosphere of the central star, evidenced e.g. by their P Cygni profiles, and features arising in the planetary nebula proper. The latter have been analysed in order to determine C,N,O abundances.

INTRODUCTION

The medium excitation planetary nebula NGC 6572 has been well studied at optical wavelengths (see e.g. Aller and Walker (1970), Peimbert and Torres-Peimbert (1971), Torres-Peimbert and Peimbert (1977)). One of the most recent studies is that of Aller and Czyzak (1979). These authors list the intensities of 96 optical emission lines derived from measurements made with the Robinson-Wampler image tube scanner, supplemented by electronic camera observations and photographic data. An entrance aperture of 2arcsecx2arcsec was generally used in these observations, and this must be kept in mind when the optical results are compared to the measurements made with IUE , using its large 10arcsec x 20arcsec oval shaped aperture which covers essentially the entire nebula.

Observations of NGC 6572 at ultraviolet wavelengths have first been made by Pottasch et al.(1978) who obtained the broad band fluxes at 3300, 2500, 2200, and 1500 Ångstrom. Pottasch (1980) has later used the measurements at 2200 Ångstrom to re-determine the extinction and from this the distance to NGC 6572. His value of 520pc is considerably smaller than other values quoted in the literature (e.g. Acker 1978).

Previous IUE-observations of NGC 6572 have been reported by Boggess et al. (1980), Feibelman (1980), and Flower and Penn (1981). Boggess et al. have listed the absolute fluxes of 16 emission lines from low-resolution spectra observed with cameras 2 (LWR) and 3 (SWP) through the large entrance apertures. Flower and Penn have used IUE in the same mode and report the absolute fluxes for 7 emission features, 6 of which are in common with the list by Boggess et al. . The results of these two groups agree extremely well in three cases, and differ significantly in the remaining three.-In the third paper quoted, Feibelman has analysed the C III] - intercombination lines which are resolved in the high resolution spectrum of NGC 6572. He obtained I(1907)/I(1909)=0.80, and from this $N_e = 3 \cdot 10^4$ cm^{-3} . This value for the electron density in NGC 6572 is somewhat larger than that derived from the optical data (e.g. Aller and Walker 1970).

In the following two sections we summarize our own observations of NGC 6572 and briefly discuss some of their implications.

THE OBSERVATIONS

In addition to a number of low resolution spectra we obtained four high resolution spectra : LWR 4946 (90 min.), LWR 11481 (145 min.), SWP 5717 (70 min.), and SWP 14919 (121 min.). All four spectra were aquired at the ESA Satellite Tracking Station at Villafranca.

These spectra have been analysed in Tübingen with an interactive image display and analysis system having a 1 Megabyte refresh memory linked to a PDP 11/34 host computer and an array processor FPS100 in which the image extraction is performed.

We found it particularly useful in the case of this extended object to have the image display capability as we see a large number of emission lines some of which exhibit a very complex structure due to the superposition of emission arising in the atmosphere of the central star, the extended expanding atmosphere surrounding this object, and in the nebula proper. We see some of the latter components (e.g. C III]) to be clearly more extended in the slit direction than the stellar features (e.g. N V).

In Table 1 we list the stronger of the emission features seen in the high-resolution spectra of NGC 6572.

Table 1

UV EMISSION LINES IDENTIFIED IN THE IUE SPECTRA OF NGC 6572

Ion	Wavelength Å	Ion	Wavelength Å	Ion	Wavelength Å
He I	2945.2	C II]	2328.1	N III	1885.8
	2829.1		2326.9	N V	1240
	2763.8		2325.4	O II	2887.9
	2723.2		2324.7	[O II]	2470.4
	2696.1		2323.5	O III	3132.3
	2677.1	C III	2296.6		3047.1
	2663.3	C III]	1908.7		1872.8
He II	2652.9		1906.7		1760.4
He II	3203.1	C IV	1550.8	O III]	2321.0
	2733.3		1548.2	O IV	1604.9
	2511.2	N II	2142.8	Mg II	2802.7
	1640.5	N III]	1753.8		2795.5
C II	2992.6		1752.0	Si III]	1892.0
	2837.6		1749.5	[Ar III]	3109.0
	2836.7		1748.5	[Ar IV]	2853.6
	1760.4		1746.7		

ABSOLUTE EMISSION LINE INTENSITIES FOR He-,C-,N-,AND O-LINES

Some of the emission line profiles extracted from the geometrically and photometrically corrected IUE-images are shown in Fig.1. These spectra have been used to determine the emission line fluxes compiled in Table 2.

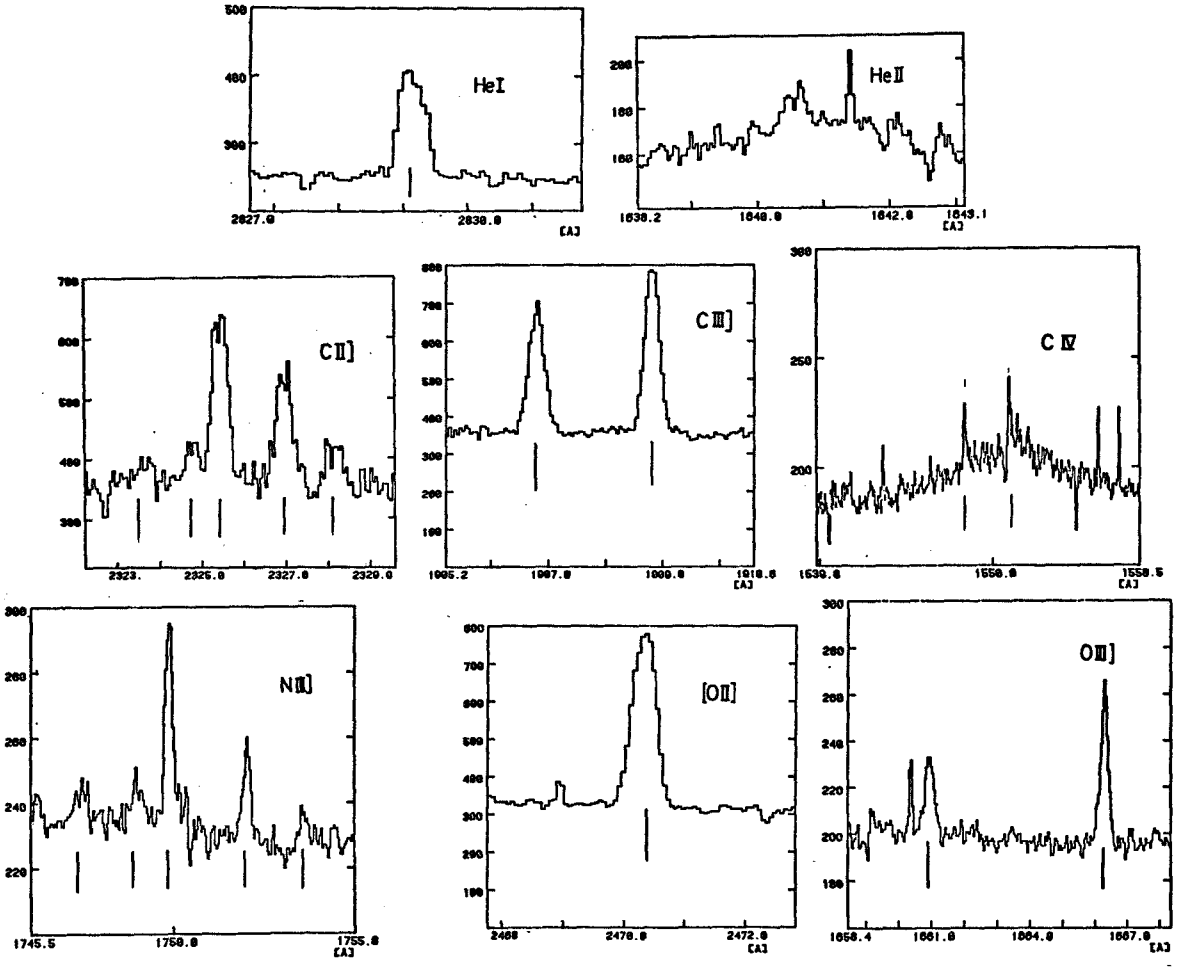

Fig.1: He-,C-,N-,and O-emission lines seen in the high resolution spectra of NGC 6572. Note that there is an offset in the wavelength scale. The intensity scale corresponds to IUE-FN/256, uncorrected for the Echelle ripple.

Absolute intensities were calculated from these spectra using the method of Cassatella et al.(1981), and also by comparing the results to the absolutely calibrated low resolution spectra of NGC 6572. Both methods produced very nearly the same results.

The intensity ratios of the intercombination lines of C III] I(1907)/I(1909) and O III] I(2321)/I(1661) , I(2321)/I(1666) can be used to re-determine the electron density and -temperature in NGC 6572. We find $N_e=3\cdot10^4$ cm^{-3} , in full agreement with Feibelman (loc.cit.), and $T_e=1.02\cdot10^4$ K (cf. Fig.2).

Table 2

ABSOLUTE EMISSION LINE INTENSITIES FOR NGC 6572, CORRECTED FOR EXTINCTION

Ion	Wavelength Å	Intensity erg $cm^{-2}s^{-1}$		Ion	Wavelength Å	Intensity erg $cm^{-2}s^{-1}$	
He I	2829.1	6. (-12)		N II]	2141.8	7. (-12)	
	2763.9	2. (-12)		N III]	1746.7	1.8 (-12)	
He II	1640.5	2.0 (-12)	neb.		1748.5	1.8 (-12)	
		19. (-12)	st.		1749.5	7.9 (-12)	
C II]	2323.5	11.3 (-12)			1752.0	5.8 (-12)	
	2324.7	14.9 (-12)			1753.8	2.4 (-12)	
	2325.4	73.5 (-12)		N V	1240	63. (-12)	st.
	2326.9	48.5 (-12)		[O II]	2470.3	46. (-12)	
	2328.1	18.2 (-12)		O III]	1660.9	8.5 (-12)	
C III]	1906.7	368. (-12)			1666.2	17.3 (-12)	
	1908.7	469. (-12)			2321.1	13. (-12)	
C IV	1550	57. (-12)	st.				
	1548.2	4. (-12)	neb.				
	1550.8	6. (-12)	neb.				

From these line intensities we derive the following ionic abundances : $N(He\ III)/N(H\ II)=3.5\cdot10^{-5}$ for the nebular component, $N(C\ II)/N(H\ II)=1.1\cdot10^{-4}$, $N(C\ III)/N(H\ II)=4.0\cdot10^{-4}$, $N(C\ IV)/N(H\ II)=6.2\cdot10^{-6}$ for the nebular component, $N(N\ III)/N(H\ II)=1.1\cdot10^{-4}$, $N(O\ II)/N(H\ II)=1.3\cdot10^{-4}$, and $N(O\ III)/N(H\ II)=3.0\cdot10^{-4}$. We must be careful in converting these numbers into total element abundances without knowing the density- and ionisation-structure of NGC 6572 in detail but it seems as if the C,N,O-abundances in this object differ from normal galactic abundances in that carbon is as abundant or even slightly more abundant than oxygen.

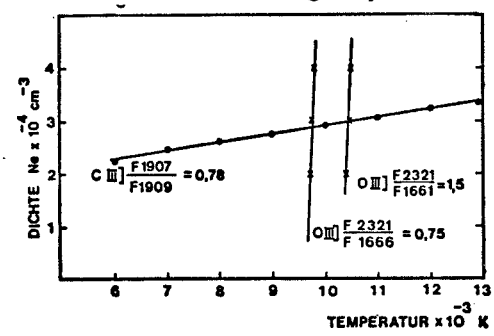

Fig.2: The density-temperature relations implied by the C III] - and O III] - intercombination line strengths observed in NGC 6572.

REFERENCES

Acker,A.:1978,Astron.Astrophys.Suppl. 33,367
Aller,L.H.,and Walker,M.F.:1970,Astrophys.J. 161,917
Aller,L.H.,and Czyzak,S.J.:1979,Astrophys.Space Sci. 62,397
Boggess,A.,Feibelman,W.A.,McCracken,C.W.:1980,NASA Conf.Publ. 2171,663
Cassatella,A.,Ponz,D.,Selvelli,P.L.:1981, ESA IUE-Newsletter 10,31
Feibelman,W.A.:1980,NASA Conf.Publ. 2171,613
Flower,D.R.,and Penn,C.J.:1981,Mon.Not.R.astr.Soc. 194,13P
Peimbert,M.,Torres-Peimbert,S.:1971,Bol.Obs.Tonantzintla y Tacubaya 6,21
Pottasch,S.R. et al.:1978,Astron.Astrophys. 62,95
Pottasch,S.R.:1980,Astron.Astrophys. 89,336
Torres-Peimbert,S.,Peimbert,M.:1977,Rev.Mex.Astr.Astrofis. 2,181

STRATIFICATION EFFECTS AND IUE SPECTRA OF HIGH EXCITATION PLANETARIES

Walter Feibelman, NASA Goddard Space Flight Center, and
Lawrence H. Aller, University of California, Los Angeles

ABSTRACT

Individual strips across IUE low resolution images of a number of high excitation planetaries with appreciable angular disks (including NGC 2452, 3242, 6818, and IC 1297) are analyzed to assess stratification effects. The familiar enhancement of high excitation lines toward the center is well exhibited, but some unexpected structural features are found in NGC 2452 where C IV shows a single central maximum, but C III, [Ne IV], and He II seem to have a central dip. The new IUE data permit improved chemical composition estimates for several planetaries previously analyzed by Aller and Czyzak.

FLUX PROFILES

Observations with the IUE permit one to study not only the integrated fluxes from the nebular images, but also the intensity distribution across any particular one. Figure 1 shows the relative brightness found in successive strips (lines) across images of NGC 2452 and NGC 6818. NGC 2452 has the appearance of a "Z" or, more accurately, two approximately 90° segments of a broken ring on opposite sides of a nucleus with a diagonal bridge connecting the E edge of the N ring segment with the W edge of the S ring segment (Curtis 1918). Optical spectrophotometric measurements have been made by the Peimberts (1977) and by Aller and Czyzak (1979). The former measured the integrated nebular light, the latter the emission at the center, and at the eastern ends of the N and S ring segments. Line intensities of C III] λ1909 and He II λ 1640 but not [Ne IV] in the central IUE scans may be affected by the central star. We conclude that [Ne IV] and perhaps also C III] and He II show a reduced emissivity near the central star where C IV λ1550 is enhanced. Possibly near the central region, neon is mostly Ne V and carbon exists as C IV. In order to account for the reduced emissivity in He II while C IV is greater, we may suppose that the electron temperature is higher in the central region. The C IV feature may come partly from the central star.

Scans taken across the central star for NGC 6818 suggest a shell-like concentration of ions such as Si III, Si IV, N III, N IV, and Ne IV. In IC 1297, strong enhancements of C II λ1335, N V λ1240 and OV λ1371, towards the center may reflect an influence of the central star. In IC 351, C III λ1909, C IV λ 1550, and He II λ1640 show pronounced peaks. The identification of λ1575 with [Ne V] is uncertain; e.g., its observed intensity in NGC 6818 with respect to the nebular-type transitions λ3346 and λ3426 is much too high. Detailed comparisons with theoretical models will be made as soon as a set of new calculations can be completed.

RESULTS

NGC 6818 and Hu 1-2 (86-8°1) show the richest spectra of objects studied in present programs (see Table 1). Successive columns give the wavelength,

the ion deemed responsible, and for each nebula the line flux F (in units of 10^{-12} ergs cm^{-2} sec^{-1}) and the logarithm of the intensity, I_n, corrected for interstellar extinction and normalized as described below. We derived extinction factors C = log I(Hβ)/F(Hβ) as 0.15, 0.5, and 0.76 for NGC 6818, NGC 2452, and Hu 1-2, respectively. These objects were larger than the slot size, so we normalized the intensities to that of λ1640, using the theoretical 1640/4686 ratio by Seaton (1978) and observed 4686/Hβ ratios (Aller and Czyzak 1979). We derived I_n = 479, 493 and 627 for NGC 6818, 2452, and Hu 1-2, respectively, on the scale I(Hβ) = 100 and corrected the UV fluxes with the aid of the Seaton extinction function. Basic plasma diagnostics (N_ε, T_ε) are obtained mostly from optical region data. We take T = 12,500°K, $x = 0.01\ N_\varepsilon/\sqrt{T_\varepsilon} = 0.25$ (NGC 6818); T_ε = 12,000°K, x ≅ 0.2 (NGC 2452), and T_ε = 16,000°K, x = 0.80 (Hu 1-2). These T_ε values apply mostly to O III and for the inner zones we must use results from theoretical models. Successive columns of Table 2 give the wavelength, the ion responsible, and then for each nebula; $t = T_\varepsilon/10{,}000°K$ (adopted from diagnostics or theoretical model, the logarithm of the ionic concentration, log $N(X_i)$ for each ion X_i, the logarithm of the sum of the $N(X_i)$ values for each element, and then in ( ), the value of the ionization correction factor (ICF) derived from theoretical models (Aller 1982). Table 3 compares derived abundances of C, N, O, and Ne denoted as (FA), with previous nebular values (AC) by Aller and Czyzak (1981) and solar values as quoted therein. For NGC 6818 a theoretical model gave a good representation of the observed intensities with log N(C) = 8.67, log N(N) = 8.32, log N(O) = 8.72, and log N(Ne) = 8.06. NGC 2452 was represented approximately by a model for IC 2165, but Hu 1-2 cannot be represented by any simple model, so the ionization correction factors are somewhat uncertain. The new abundances do not differ much from those obtained by Aller and Czyzak who used IUE intensities by Boggess, Feibelman, and McCracken (1981). All objects appear to be nitrogen rich compared with the sun. Presumably, these nebulae show the effects of operation of the C-N cycle with subsequent mixing of the reaction products to the surface. O, C, and Ne are depleted in Hu 1-2. See also Marionni and Harrington (1981).

This program was supported in part by NASA grant NSG 5358 to UCLA.

REFERENCES

Aller, L.H. 1982, Astrophys. and Sp. Sci. (in press).
Aller, L.H. and Czyzak, S.J. 1979, Astrophys. and Sp. Sci., 62, 397.
_____. 1981, Proc. Natl. Acad. Sci. USA, 78, 5266 (for logN(C) in Hu 1-2 read 8.09).
_____. 1982, preprint, UCLA.
Boggess, A., Feibelman, W.A., and McCracken, C.W. 1981, NASA Conf. Publ. 2171, The Universe at Ultraviolet Wavelengths, R. Chapman, ed., p. 663.
Curtis, H.C. 1918, Publ. Lick Obs., 13, 57 (Fig. 20).
Marionni, P.A. and Harrington, J.P. 1981, NASA Conf. Publ. 2171, p. 639.
Seaton, M.J. 1978, Mon. Not. Roy. Astr. Soc., 185, 5P.
_____. 1979, Mon. Not. Roy. Astr. Soc., 187, 73P.
Torres-Peimbert, S. and Peimbert, M. 1977, Rev. Mex. Astr. Ap., 2, 181.

Table 1. Observed Data

λ	Ion λ	NGC 6818 F_λ	NGC 6818 log I_n	NGC 2452 F	NGC 2452 log I_n	Hu 1-2 F_λ	Hu 1-2 log I_n
1239/41	N V	(0.51)	1.33	0.066	1.595	1.00	2.47
1390	Si III	1.28	1.68	0.073	1.45	0.63	2.02
1401	O IV						
1487	N IV	1.25	1.65	0.176	1.79	1.85	2.43
1549	C III	4.85	2.24	0.186	1.79	5.58	2.87
1575	[Ne V]?	0.10	0.56:			0.09	1.07
1601	[Ne IV]?	0.30	1.02:			0.05	0.80
1640	He II	13.7	2.68	1.60	2.69	5.10	2.80
1663	O III	1.43	1.70	0.092	1.45	0.36	1.64
1750	N III	1.26	1.64	0.132	1.605	1.15	2.14
1892	Si III	0.49	1.24	0.061	1.32	0.14	1.29
1908	C III	19.3	2.84	1.06	2.57	3.50	2.70
2327	C II/C III	1.74	1.8:			0.41	
2424	[Ne IV]	4.74	2.22	0.383	2.065	1.90	2.35
2511	He II	0.42	1.14:			0.24	
2734	He II	0.85	1.40:	0.154		0.41	
2784	[Mg V]	0.30	0.93			0.31	1.21
2830	He I					0.10	
2855	Ar IV					0.10	
2929	[Mg V]					0.104	0.67
3024	O III	0.45	1.10	0.24			
3047	O III	1.05	1.47	0.558		0.11	0.64
3133	O III	6.19	2.23	0.84		1.02	1.58

Table 2. Nebular Diagnostics and Ionic Concentrations

λ	Ion	NGC 6818 t	NGC 6818 log N_i	NGC 6818 log Σ (ICF)	NGC 2452 t	NGC 2452 log N_i	NGC 2452 log Σ (ICF)	Hu 1-2 t	Hu 1-2 log N_i	Hu 1-2 log Σ (ICF)
4267	C III	1.25	8.69:						(8.5)	
1908	C III	1.25	8.36	8.41	1.2	8.19	8.23	1.6	7.66	7.92
1549	C IV	1.4	8.44	(1.5)	1.4	7.05		1.7	7.57	(1.3)
6563	N II	1.25	6.61		1.2	7.42			7.49	
1747	N III	1.25	8.01	8.24	1.2	8.16	8.53	1.6	7.89	7.375
1487	N IV	1.35	7.79	(1.07)	1.3	8.11	(1.0)	1.7	7.94	(1.22)
1239	N V	1.6	6.81		1.4	7.59		1.8	7.62	
3727	O II	1.25	7.075		1.2	7.27		1.6	6.99	
5007	O III	1.25	8.46	8.48	1.2	8.40	8.65	1.6	7.83	7.88
1663	O III	1.25	8.50	(1.87)	1.2	8.24	(1.0)	1.6	7.80	(1.45)
3863	Ne III	1.25	7.67		1.2	7.69		1.6	7.27	
4725	Ne IV	1.5	7.74	8.08			8.03	1.7	7.34	7.87
2423	Ne IV	1.5	7.72	(1.0)	1.4	7.69	(1.0)	1.7	7.60	(1.0)
3426	Ne V	1.6	7.26		1.5	7.00		1.8	7.28	

Table 3. Logarithms of Derived Abundances; logN(H) = 12.00

	Carbon FA	Carbon AC	Nitrogen FA	Nitrogen AC	Oxygen FA	Oxygen AC	Neon FA	Neon AC
6818	8.59	8.64	8.27	8.14	8.75	8.74	8.075	8.11
2452	8.3	----	8.53	8.66	8.65	8.59	8.03	7.95
Hu 1-2	8.09	8.08	8.51	8.50	8.045	8.10	7.86	7.83
Solar	8.65		7.96		8.87		8.05	

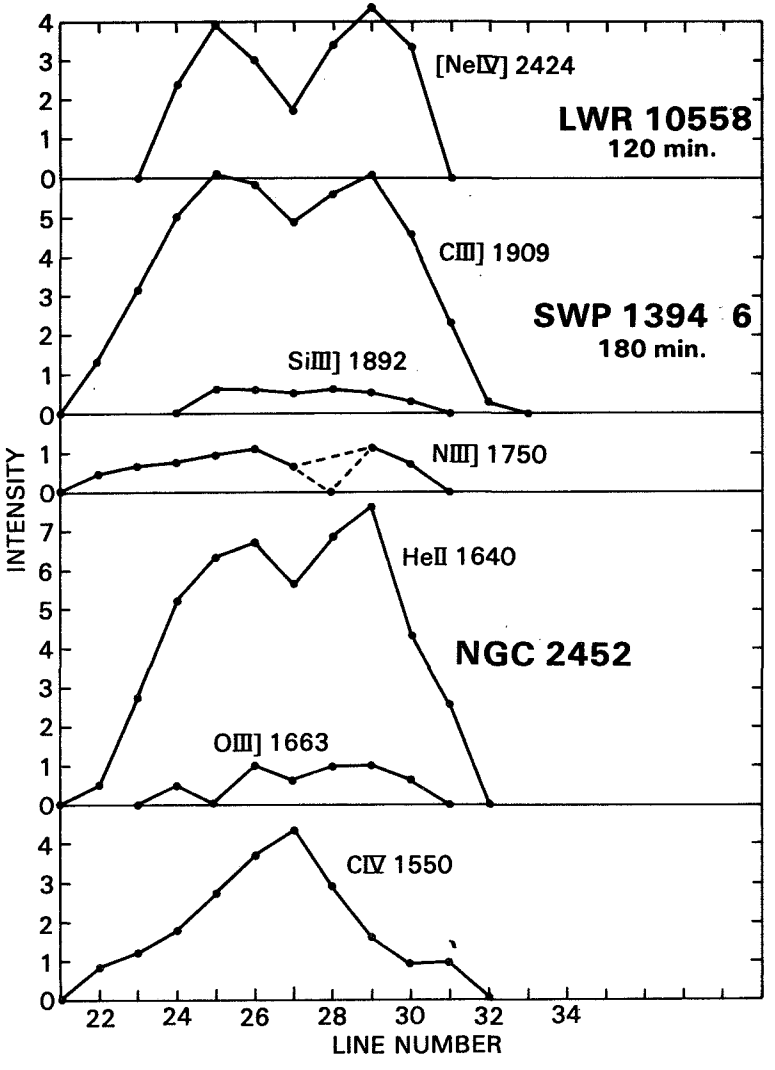
[NeIV] 2424
LWR 10558
120 min.
CIII] 1909
SWP 1394 6
180 min.
SiIII] 1892
NIII] 1750
HeII 1640
NGC 2452
OIII] 1663
CIV 1550
INTENSITY
LINE NUMBER

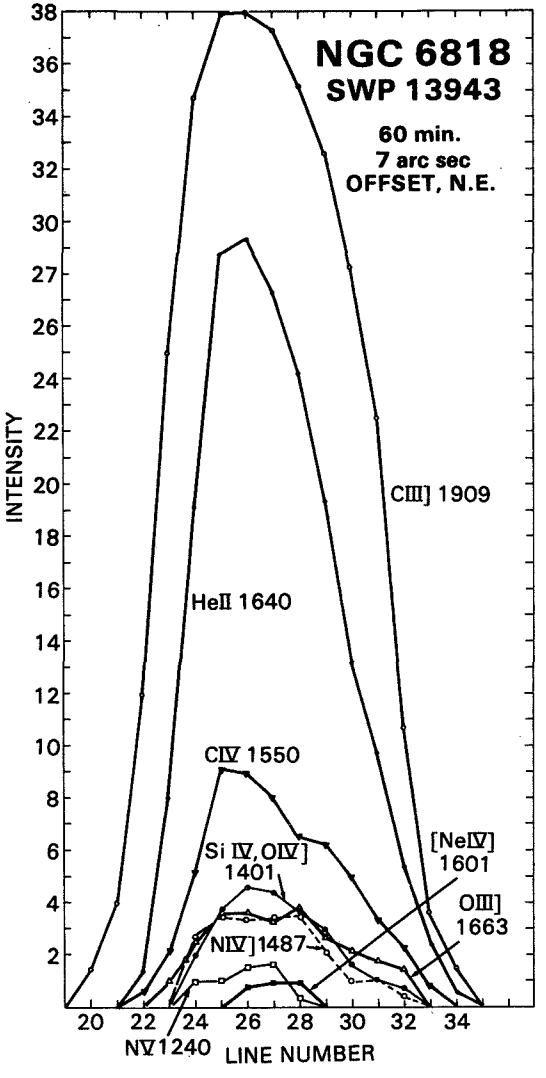
NGC 6818
SWP 13943
60 min.
7 arc sec
OFFSET, N.E.
CIII] 1909
HeII 1640
CIV 1550
Si IV,OIV]
1401
[NeIV]
1601
OIII]
1663
NIV]1487
NV1240
INTENSITY
LINE NUMBER

IUE OBSERVATIONS OF PLANETARY NEBULAE AND THEIR CENTRAL STARS IN THE MAGELLANIC CLOUDS

Stephen P. Maran, Theodore P. Stecher, Theodore R. Gull
Laboratory for Astronomy and Solar Physics
NASA-Goddard Space Flight Center

Lawrence H. Aller
Department of Astronomy
University of California, Los Angeles

Malcolm P. Savedoff
Department of Physics and Astronomy
University of Rochester

ABSTRACT

The planetary nebulae LMC P40, SMC N2, and SMC N5 and their central stars were observed with IUE. The C abundances in the nebulae, compared with those in galactic planetaries, indicate that convective dredgeup of locally nucleosynthesized C has occurred. The progenitors of the nebulae were C stars at the theoretical upper luminosity threshold, thus such stars do occur as predicted, although none so bright have been found in the Clouds. The central stars of the nebulae have masses $\sim 1\ M_\odot$, luminosities $\sim 4 \times 10^4\ L_\odot$, and radii $\sim 0.7\ R_\odot$; they have probably not yet reached their maximum luminosities. With m_v 19.1-19.8, they may be the visually faintest stars yet observed by UV spectroscopy. Clearly, it is not true that planetary nebulae nuclei all have masses $M = (0.6 \pm 0.1)\ M_\odot$.

INTRODUCTION

This work is being published in full elsewhere: Maran et al. (1982) report results on the nebular composition and convective dredgeup; Stecher et al. (1982) describe the central stars and the relationship to the theory of C stars and the formation of planetary nebulae (PN).

RESULTS

The spectra were obtained during three low-radiation IUE shifts in May 1981. Short wavelength, low dispersion spectra were made for all three targets, using coordinates measured by Gull. Emission lines were easily detected; exposure times as short as 45 min were satisfactory. In addition, continua were weakly detected; they are dominated by the stars at the shortest wavelengths and by the nebulae at the longest wavelengths. A long wavelength, low dispersion spectrum also was made for LMC P40; it shows nebular continuum and the $\lambda 2422$ [Ne IV] line. Calibrated groundbased spectrometry was obtained for each nebula from prior work of

Aller and associates. Observational data on emission lines are tabulated in Maran et al.; sample spectra appear here in Figure 1.

Nebular ionization models, ionization correction factors, and chemical abundances were calculated with existing computer codes at UCLA. Results on chemical composition are reproduced in Table 1. Note that the C/O abundance ratio is about 2 in each of the targets, which means that the progenitors were C stars. In Table 1, the abundances are compared with similar data for two samples of galactic PN. The compositions of the interstellar media (ISM) of the Clouds also are shown. There is much less C in the LMC ISM than in the Galaxy, and much less in the SMC ISM than in the LMC ISM. Yet, the PN in the Galaxy, the LMC, and the SMC all have comparable C abundances much larger than those in the corresponding ISM. This is convincing evidence that the envelopes of the progenitors, which were ejected to form the PN, were enriched by C dredged from the stellar cores where it was synthesized.

Interstellar extinction for each PN was determined by Maran et al. from the He II lines; refined values found by Stecher et al. are listed here in Table 2. The observed continua were corrected for these extinctions, using the appropriate extinction laws for the Clouds. Then, nebular continua consisting of H^0 two-photon and H Balmer contributions, scaled to the observed Hβ fluxes, were subtracted to yield the stellar continua. Figure 2 shows an example. Blackbody fits yield $T_{eff} \sim 100{,}000$ K; a similar result for the He II Zanstra temperature is obtained from the emission line and stellar continuum fluxes at λ1640.

The distances of the Clouds are well determined; we adopt Crampton's (1979, 1982) distance moduli: 18.63 for the LMC and 19.1 for the SMC. The stellar continua in absolute units at the earth were found by the above procedure; computed model atmospheres for planetary nebulae nuclei, which predict emergent flux intensities, are also available. The luminosities and radii of the central stars are readily calculated. The results (Table 2) are preliminary, but the general conclusion that these are very large and luminous central stars is beyond doubt. This explains why the nebulae and their nuclei were detected so readily with IUE. Masses computed from Iben's (1981) M-L relation are $\sim 1\ M_\odot$ for each of the stars; the progenitors had $\sim 4\ M_\odot$ according to the theory of Renzini and Voli (1981). Thus, $\sim 3\ M_\odot$ must have been lost in winds.

CONCLUSIONS

Convective dredgeup must have occurred in the nebular progenitors, which were C stars with $M_{bol} \sim -6.8$, near Iben's (1981) theoretical upper luminosity threshold. The brightest C stars in the Clouds have only $M_{bol} = -6.0$. Perhaps, as Iben suggested, the most luminous C stars veil themselves with C grains of their own making. Radiation pressure on grains may then provide a mechanism for PN ejection (Krishna Swamy and Stecher 1969). The suggestion that virtually all PN central stars have masses $M = (0.6 \pm 0.1)\ M_\odot$ (Weidemann 1977, Schönberner and Weidemann 1981) appears to be wrong. The observed luminosities of the stars studied here are above the Eddington luminosity for an $0.6\ M_\odot$ star.

REFERENCES

Due to space limitations, we refer readers to our papers, which list all other work cited above. Preprints and reprints are available.

Maran, S. P., Aller, L. H., Gull, T. R., and Stecher, T. P. 1982, Ap.J. (Letters), 253, L43.
Stecher, T. P., Maran, S. P., Gull, T. R., Aller, L. H., and Savedoff, M. P. 1982, in preparation (to be submitted to Ap.J.).

Table 1: Composition of the Magellanic Planetaries

Element	P40	N2	N5	Galactic Planetaries		Interstellar Media LMC	SMC	Sun
(1)	(2)	(3)	(4)	(5)	(6)	(7)	(8)	(9)
He	11.02	11.03	11.05	11.04	11.02	10.92	10.92	11.03
C	8.70	8.60	8.87	8.89	8.8:	7.90	7.16	8.65
N	7.5:	7.42	7.60	8.39	7.97	6.94	6.60	7.96
O	8.33	8.30	8.36	8.66	8.66	8.38	8.05	8.87
Ne	7.62	7.53	7.79	8.02	8.02	7.68	7.34	8.05
S	6.42	6.26	----	7.03	6.98	7.01	6.61	7.23
Ar	6.19	6.04	6.02	6.48	6.38	6.10	5.77	6.57

After Maran et al. The tabulated quantity equals 12 + log N(X)/N(H).
Sources: Col. 5, Aller and Czyzak 1981; Col. 6, Aller 1978; Cols. 7, 8, Dufour et al. 1982; Col. 9, Ross and Aller 1976, Lambert 1978, Aller 1980.

Table 2: Derived Properties of Planetary Nebula Central Stars

	LMC P40	SMC N2	SMC N5	Dimensions
Log extinction at Hβ	0.19	0.10	0.23	
Log nebular F(Hβ)	-12.79	-12.67	-12.81	ergs/cm^2 s
Log nebular F(λ1640 He II)*	-12.00	-11.84	-12.09	ergs/cm^2 s
Log stellar continuum F(λ1640)*	-14.40	-14.10	-14.22	ergs/cm^2 s Å
Zanstra temperature	1.0	0.95	1.0	10^5 K
Stellar mass	1.2	0.90	1.1	$M_\odot$
Stellar radius	0.70	0.67	0.67	$R_\odot$
Apparent visual magnitude	19.76	19.55	19.09	
Log surface gravity	4.84	4.74	4.84	cm/s^2
Stellar luminosity	4.47	3.30	4.10	10^4 $L_\odot$
Absolute bolometric magnitude	-6.88	-6.55	-6.79	

Table after Stecher et al. 1982.
*Flux at the earth, with interstellar reddening removed.

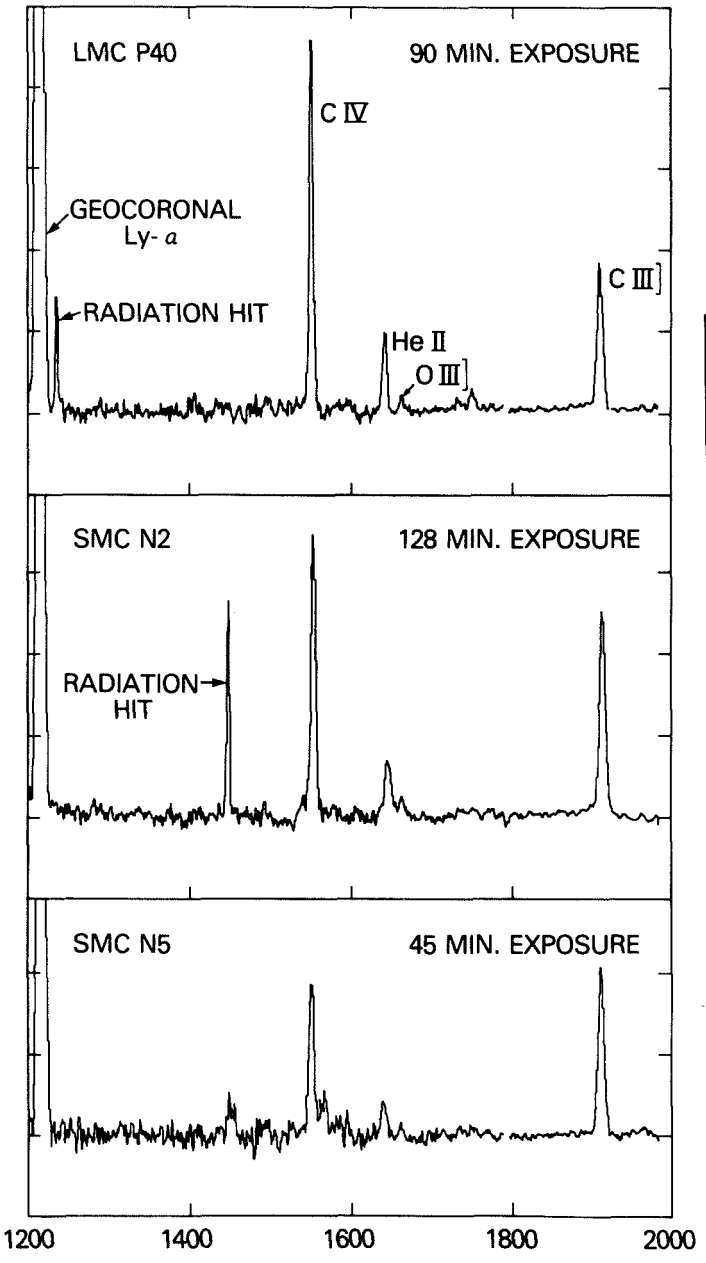

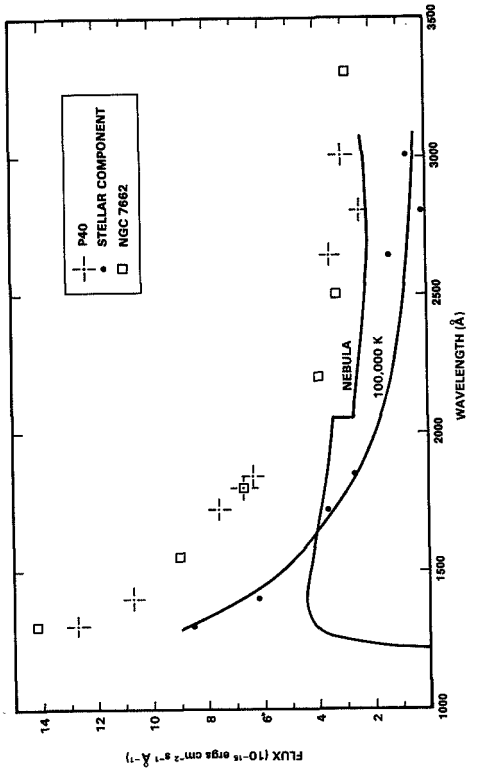

Figure 1. (Left, above) Low-dispersion, short wavelength IUE spectra of planetary nebulae LMC P40, SMC N2, and SMC N5. Exposure times, wavelengths (Å), and line identifications are indicated. Continua are not distinguished in this presentation.

Figure 2. (Right, above) Separation of the observed short and long wavelength continua of LMC P40 into stellar and nebular components.

IUE OBSERVATIONS OF REFLECTION NEBULAE

A. N. Witt
The University of Toledo

R. C. Bohlin and T. P. Stecher
Goddard Space Flight Center

ABSTRACT

Low-resolution IUE spectra in the SWP and LWR ranges have been obtained of several reflection nebulae in the vicinity of their respective illuminating stars. New data for NGC 7023 (HD200775), NGC 1435 (Merope, 23 Tau), NGC 1432 (Maia, 20 Tau) and the Electra (17 Tau) nebula have been found to display significant differences in the shape of their normalized nebular spectra. If the dust in these nebulae is similar from one object to the next, these differences can be most readily explained by differences in the line-of-sight dust distribution, coupled with a wavelength-dependent phase function, changing from a strongly forward throwing form ($g = 0.6$-0.7) in the visible to a more nearly isotropic shape ($g \approx 0.25$) at 1400 Å.

INTRODUCTION

As systems where the scattering of starlight off interstellar grains may be observed, reflection nebulae offer particular advantages. The geometric relationship between source of illumination and scatterers in them is constant with wavelength, because ideally only a single illuminating star is present, and the nebular surface brightness is about two orders of magnitude higher than is the case in other instances of interstellar scattering. As a consequence, even the relatively small 10" x 20" IUE entrance apertures will admit measurable fluxes from such nebulae, thus allowing the study of scattered light spectra with an unprecendented angular resolution. Combining this condition with the wavelength independent geometry provides the opportunity for obtaining information about the wavelength dependence of the scattering phase function of interstellar grains.

OBSERVATIONS

Low-resolution spectra with both the LWR and the SWP cameras of IUE have been obtained of NGC 7023 (HD200775), NGC 1435 (23 Tau), NGC 1432 (20 Tau), and the Electra (17 Tau) nebula. The offset range covered extended from 15" to 60" in radial distance from the illuminating stars in the different cases, and exposure times from one hour to four hours were typical. Instrumentally scattered light originating from the image of the illuminating star was the principal source of contamination for the nebular spectra. A determination of the necessary correction was made by measuring the instrumentally scattered light produced by placing η UMa at a range of offsets (10" to 40") and at several position angles with respect to the large IUE entrance apertures. The resulting corrections for the reflection nebula spectra range typically

from 10% to 50% of the total recorded signal. Details of our investigation of instrumentally scattered light in IUE will be published in a future IUE NASA Newsletter.

Using the IUE photometric calibration of Bohlin and Holm (1980) and the aperture sizes from Bohlin et al. (1980) the measured nebular fluxes were converted into intensities and were expressed in units of the flux from the illuminating star, per steradian of solid angle.

RESULTS

An assessment of the relative quality of our IUE data was made by comparing them in the case of the Merope nebula (NGC 1435) to existing UV observations obtained with ANS at larger offset angles (Andriesse, Piersma, and Witt 1977), or in the case of NGC 7023 to observations at the same offset at longer wavelengths (Witt et al. 1982). In both instances a high degreee of consistency between new and existing data was found, demonstrating the power of IUE of significantly extending the offset range and the wavelength range available for reflection nebula observations.

Among our targets, NGC 7023 was chosen as a bright reflection nebula with a deeply embedded star. Observation at small offset angles (~20") made it likely that the scattered flux would be dominated by scattering at small angles. Thus, the wavelength dependence of the forward half of the phase function can be probed. The Pleiades nebulae are examples of nebulae where large-angle scattering predominates (Witt 1977), and where only minor foreground reddening exists. Here the behavior of the scattering phase function in the range of scattering angles $60^{o} < \alpha < 120^{o}$ is the likely subject of exploration.

Table 1 contains four examples of nebular spectra normalized to the 2900-3100 Å region, as well as information about the reddening of the illuminating stars. The quantity S is the nebular intensity, F is the stellar flux observed by IUE at the same wavelengths. The wavelength dependence of extinction in the UV applicable to these four objects has been determined previously by Walker et al. (1980) and by Witt, Bohlin and Stecher (1981), and has been found to be very similar in these cases.

The factors influencing the shape of the normalized nebular spectra to first order are the wavelength dependence of the optical depth, the wavelength dependence of the albedo, and the wavelength dependence of the phase function coupled with the distribution of dust along the line-of-sight, fixing the range of dominant scattering angles. If the dust in these four nebulae is of a similar nature, it is mainly the last factor, a wavelength dependent phase function, which can explain the significant differences found in the spectra in Table 1. The flat UV spectrum of the forward scattering NGC 7023 and the remarkable increases in nebular brightness towards shorter wavelengths observed in the Pleiades (23 Tau, 20 Tau, 17 Tau), where large angle scattering prevails, can occur for similar grains only if the phase function undergoes a drastic change from a strongly forward throwing form

($g = 0.6$-0.7) in the visible to a more nearly isotropic form ($g \simeq 0.25$) in the far UV.

A detailed analysis of our data supporting this conclusion will be published in the Astrophysical Journal. This research has been supported through NASA grants NSG 5388, NSG 7620 and NAGW-89.

REFERENCES

Andriesse, C. C., Piersma, Th. R. and Witt, A. N. 1977, Astr. Ap., 54, 841.

Bohlin, R. C. and Holm, A. V. 1980, IUE NASA Newsletter No. 10, p. 37.

Bohlin, R. C., Holm, A. V., Savage, B. D., Snijders, M. A. J., and Sparks, W. M. 1980, Astr. Ap., 85, 1.

Walker, G. A. H., Yang, S., Fahlmann, G. G., and Witt, A. N. 1980, Pub. Astr. Soc. Pac., 92, 411.

Witt, A. N. 1977, Pub. Astr. Soc. Pac., 89, 750.

Witt, A. N., Bohlin, R. C., and Stecher, T. P. 1981, Ap. J., 244, 199.

Witt, A. N., Walker, G. A. H., Bohlin, R. C. and Stecher, T. P. 1982, Ap.J., (in press).

Table 1

Normalized Nebular Spectra

Nebula:	NGC 7023	NGC 1435	NGC 1432	Electra
Star:	HD200775	23 Tau	20 Tau	17 Tau
E(B-V):	0.44	0.083	0.047	0.029
Offset:	22".5	60"	40"	40"
λ(Å)	$\log (S/F)_\lambda - \log \langle S/F \rangle_{2900-3100}$			
3000	+0.02	-0.03	+0.01	-0.02
2900	0.00	-0.01	-0.01	+0.10
2800	+0.03	+0.04	+0.05	+0.22
2700	+0.02	+0.04	+0.05	+0.22
2600	+0.01	+0.04	+0.09	+0.28
2500	-0.02	+0.06	+0.14	+0.23
2400	+0.02	+0.10	+0.32	+0.41
2300	0.00	+0.11	+0.21	+0.33
2200	-0.01	+0.18	+0.22	+0.28
2100	-0.01	+0.18	+0.17	+0.34
2000	-0.06	+0.19	+0.27	+0.38
1900	-0.03	+0.29	+0.27	+0.47
1800	-0.01	+0.27	+0.22	+0.47
1700	+0.12	+0.32	+0.26	+0.51
1600	+0.16	+0.35	+0.27	+0.73
1500	+0.07	+0.35	+0.24	+0.61
1400	+0.09	+0.38	+0.30	+0.68
1300	+0.13	+0.44	+0.31	+0.73

IUE OBSERVATIONS OF DUST ALBEDO IN NEBULAE

J. Wolf, H. L. Helfer, J. L. Pipher, T. L. Herter*
University of Rochester
*Presently at Cornell University

IUE observations were obtained with the low dispersion spectrographs, for four positions in M8, near Herschel 36, and for the outer regions of several planetaries in order to determine: 1) what fraction of the observed light is due to dust scattering; and 2) whether variations in the wavelength dependence of the dust albedo could be determined. Perinotto and Patriarchi (1980) and Mathis et al. (1981) have previously discussed IUE data for Orion.

The IUE observations were corrected for absorption, using the standard absorption law of Bless and Savage (1972). The dust continuum is obtained from the corrected observations by subtracting out the computed continuous emission of the gas component, (c.f. Brown and Mathews (1970)), once a value of the gas emission at a particular wavelength is known.

The gas emission at e.g. 1600 Å was determined from high resolution radio measurements at ~ 5 GHz (c.f. Turner et al. (1974) for M8; Terzian et al. (1974) for several planetaries) using the emissivity calculations. We also determined the dust contribution by looking at the strength of a stellar spectral feature in the nebula's reflected star light. [For M8 we used the strength of the characteristic break in the spectra of early type stars in going from ~ 1450 Å to 1600 Å. For NGC6543, the strength of the P-Cygni absorption edge CIV1550 was used.]

For M8, spacially resolved data taken at 3 positions (2.7"W, 15.5"N), (15.0"E, 8.4S), and (24.6"E, 2.9"N) of Herschel 36, the exciting star, have been analyzed. At each position, data for 3 successive pseudo-orders have been added giving 9 effective collecting areas ea.~65 square seconds of arc. Foreground extinction, corresponding to $E(BV) \cong 0.33$ (c.f. Walker 1957; Johnson 1967) was corrected for. In addition part of the peculiar extinction around Herschel 36 (Hecht et al. 1982), corresponding to EBV=0.22, was assumed to be between the star and the nebula. [This assumption is necessary in order to avoid getting very large effective albedoes at very long wavelengths $\geq$2500 Å, or getting very low albedoes in a narrow wavelength interval around 2200 Å.]

For 6 of the 9 M-8 areas, we have adequate signal to noise, and the gas emission constitutes 10%-20% of the nebula continuum at 1600 Å. The ratio of the dust contribution, I^d, to the stellar flux, I^*, (normalized for convenience to 0.5 at 1600 Å) gives the wavelength dependence of the albedo, γ_R, if the scattering region is optically thin and extensive. Other models are possible. An extreme model results from assuming the scattering is optically thick and so situated that only forward scattering occurs. Then, $I^d/I^* \propto \gamma_R P_o$ where P_o is the value of the phase function for $\Theta \cong o°$ (normally given by $P_o \cong (1+g)/(1-g)^2$). While the I^d/I^b observations in M8 show considerable variation from one spot to another their values generally seen bounded by the γ_R and $\gamma_R P_o$ values predicted for the mixture proposed by Mathis et al. 1977 (MRN), though g (3000A) ~0.4 rather than ~0.5 appears more appropriate.

Values of g>0.8 in the interval λ1750-2250 seem inapplicable for M8 (c f. Lillie and Witt (1976)). The recently derived optical parameters for Orion are not as suitable for M8 as those proposed by MRN because some nebula positions clearly require an effective albedo increasing with wavelength for λ≳~2000 Å. At least half of the M8 I^d/I^* vs λ curves seem to indicate strong forward scattering effects.

Some planetaries have also been examined. NGC6543, noted for having a large IR excess and $E_{(B-V)} \simeq 0.0$, shows UV scattering, the P-Cyg. profile of CIV 1550 clearly appearing 15" away from the light center. Two different large aperature exposures were made: one 15", the other 8" away from the center star. At 1500 Å, gas emission provides 18% (40%) of the total nebular light for the 1st (2nd) position. While both numbers are somewhat uncertain because of instrumental scattering, the gas fraction at 1600 Å at the first position must be less than ~40% because the nebula is quite deficient in light at λ≳2500 A. The I^d/I^* data for position 1 favors models with strong forward scattering (using MRN optical data) and the 2nd position data suggests that the albedo at λ≳2700 is appreciably greater than that found in the region λ≲1800-2000.

REFERENCES

Bless, R. C. and Savage, R. D. 1972, Ap. J 171, 293.
Brown, R. L. and Mathews, W. G. 1970, Ap. J 160, 939.
Hecht, J., Helfer, H. L., Wolf, J., Donn, R., and Pipher, J. L. 1982. This proceedings. also: Ap. J Letters (submitted).
Johnson, H. L. 1967, Ap. J 147, 912.
Lillie, C. F. and Witt, A. N., 1976. Ap. J 208, 64.
Mathis, J. S., Rumple, W., and Nordsieck, K. H. 1977, Ap. J 217, 425.
Mathis, J. S., Perinotto, M., Patriarchi, P., and Schiffer III, F. H., 1981, Ap. J 249, 99.
Perinotto, M., and Patriarchi, P. D., 1980, Ap. J 238, 614.
Terzian, Y., Balick, B., and Bignell, C. (1974) Ap. J 188, 257.
Turner, B. E., Balick, R., Cudaback, D. D., Heiles, C., and Boyle, R. J. 1974, Ap. J 194, 279.
Walker, M. F., 1957, Ap. J 125, 636.

Figs. 1, 2 Representative plots of I^{dust}/I^*, Normalized to 0.5 at 1600A for two different positions (given in text) in M8.

ABSTRACT

The wavelength dependence of the effective albedo of the dust at several positions near the Hourglass region of M8 has been determined. Accurate estimates of the contribution of the continuous gas emission can be made using the region 1400-1600A. The main uncertainty results from the peculiar extinction of the exciting star, Herschel 36, and the possibility that extinction between the star and the reflecting portions of the nebula exists and needs to be corrected for. The albedo for some planetaries such as NGC 6543 has also been investigated. The main uncertainty here is estimating instrumental contributions to the scattering in observing these small objects.

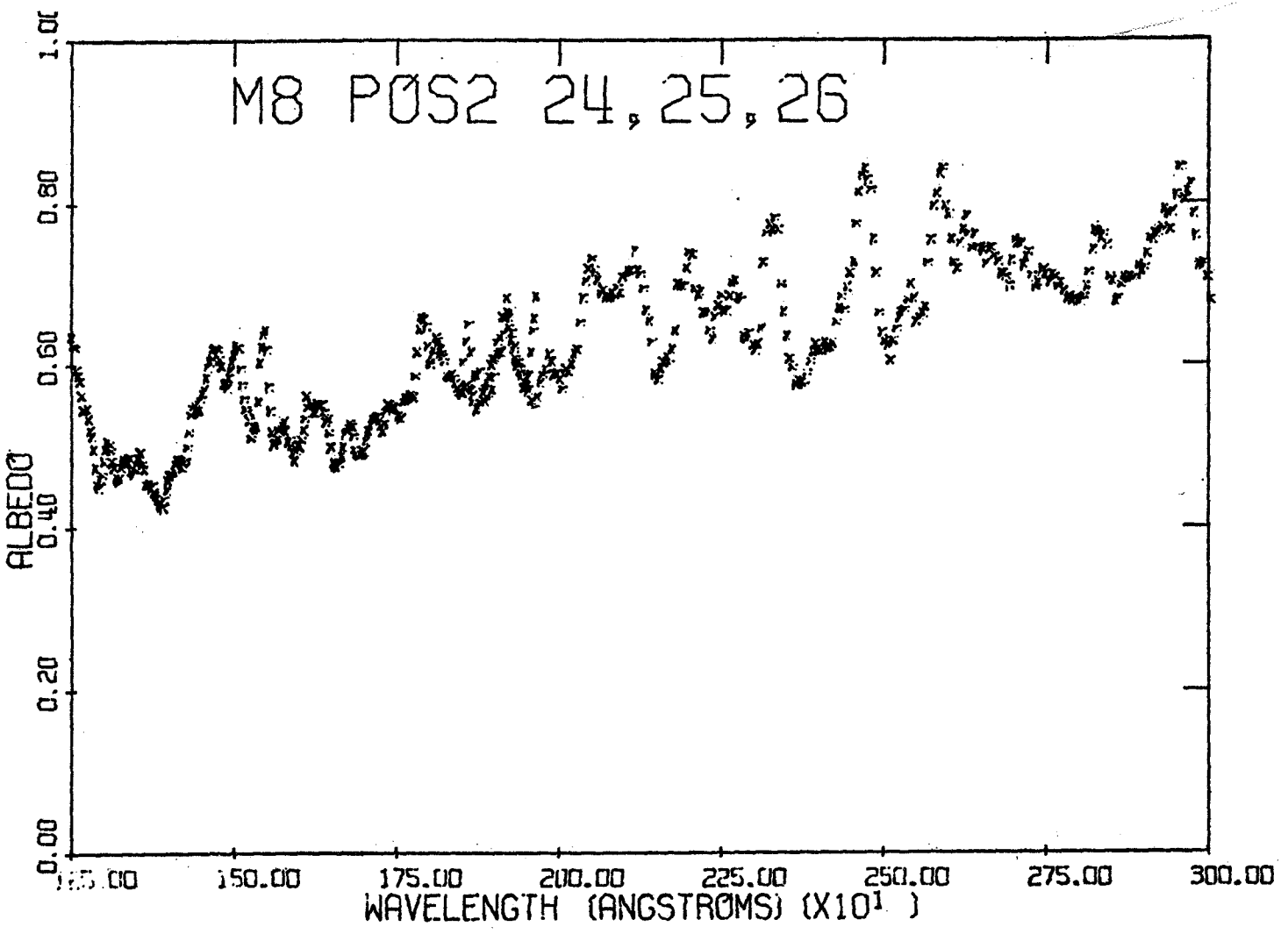
M8 POS2 24, 25, 26
ALBEDO
1.00
0.80
0.60
0.40
0.20
0.00
150.00
175.00
200.00
225.00
250.00
275.00
300.00
WAVELENGTH (ANGSTROMS) (X10[1])

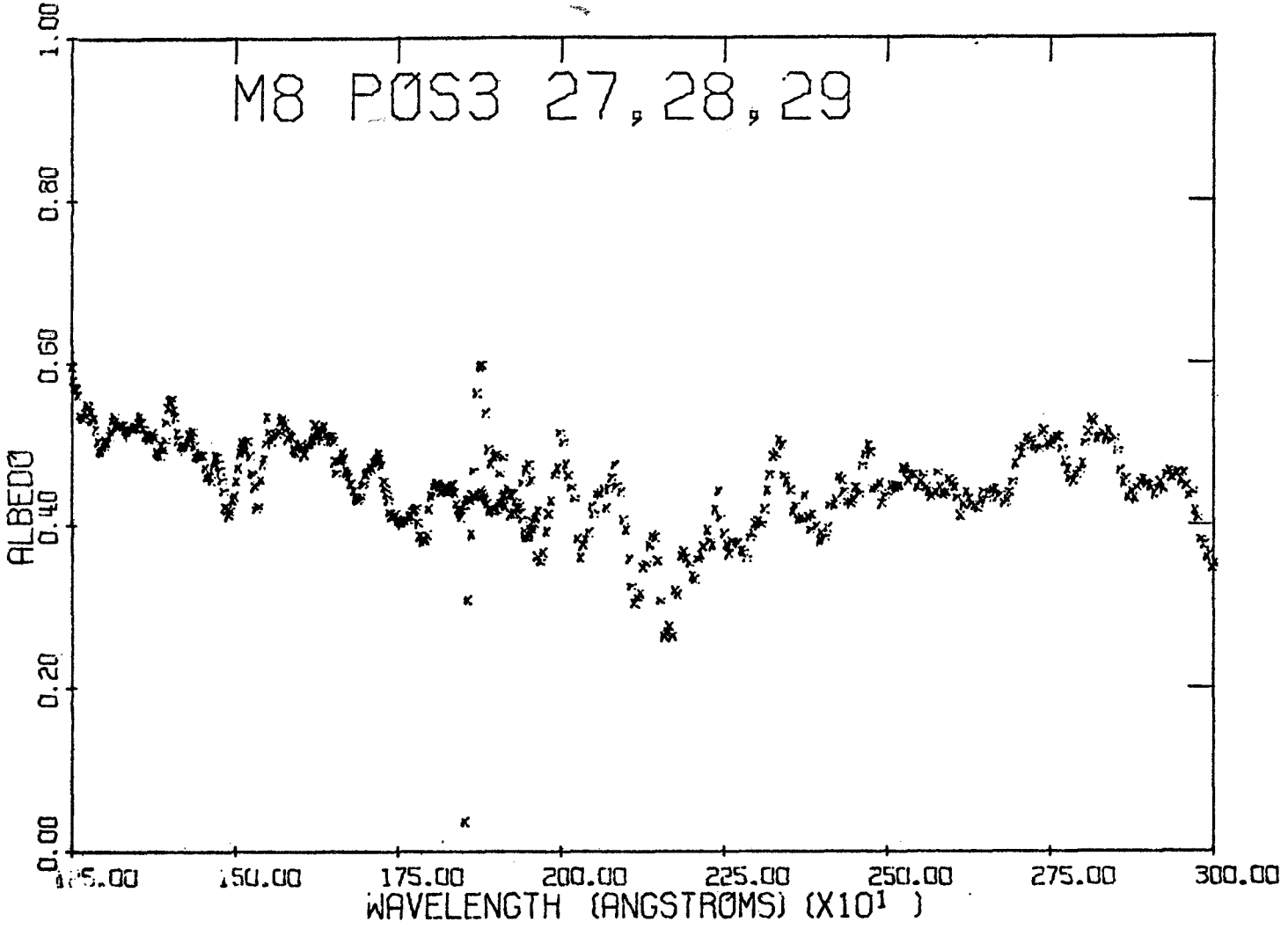
M8 P0S3 27, 28, 29
ALBEDO
1.00
0.80
0.60
0.40
0.20
0.00
125.00
150.00
175.00
200.00
225.00
250.00
275.00
300.00
WAVELENGTH (ANGSTROMS) (X10¹)

IUE OBSERVATIONS OF LINES OF SIGHT WITH PECULIAR ULTRAVIOLET EXTINCTION

Derck Massa, Edward L. Fitzpatrick, and Blair D. Savage
University of Wisconsin-Madison

ABSTRACT

Low resolution IUE data were used to derive UV extinction curves for a group of stars known to have peculiar extinction parameters from ANS data. The resulting curves have a wide range of appearances. Although the ratio E(BUMP)/E(B-V) differs by a factor of three in the extreme cases, the wavelength of maximum absorption does not appear to change. No evidence for new fine structure in UV extinction has been found. The structure near 6.2 μm^{-1} in the existing mean extinction curves appears to be the result of luminosity mismatch errors. The new extinction curves have shapes that separate into two distinct classes; those associated with clear field extinction and those associated with extinction in dense nebular environments. The range of variation in the curves is so large, the common practice of "ironing out the bump" can produce enormous errors in the resultant UV energy distributions when $E(B-V) > 0.3$.

INTRODUCTION

The study of peculiar UV extinction is important in two respects. First, in order to deredden a star with an unknown energy distribution one must be able to identify what form of extinction is affecting it. The study of peculiar extinction may reveal the means to accomplish this. Second, it is of interest to determine new information about the chemical and physical nature of the dust. A study of peculiar extinction may provide important clues about dust composition, particle sizes, and the modification of these properties in a variety of interstellar environments.

Meyer and Savage (1981, MS hereafter) used ANS satellite data to locate stars affected by apparently peculiar extinction. We selected 12 stars from this sample in order to verify the MS results and to examine the extinction in detail using IUE observations. Our selection differs from previous ones which have been based on either stars associated with nebular regions where extinction is expected to be anomalous or stars known to have abnormalities in other extinction parameters such as the wavelength of maximum visual polarization or diffuse interstellar band strengths. While such studies can demonstrate that peculiar infrared or visual extinction parameters imply peculiar UV extinction, our survey is capable of testing the converse of this statement.

RESULTS

Of the 12 stars in the sample, 8 were verified to have peculiar UV extinction, while the anomalous ANS curves for the others were found to be due to observational errors or stellar peculiarities. The extinction curves were derived by comparing the program stars to lightly reddened stars given by Wu et al. (1981), once the latter were dereddened with the Galactic Mean Curve (Savage and Mathis 1979). One exception is the pair HD

37903 and HD 37744 which was observed by K. S. de Boer specifically to isolate the local extinction of HD 37903. Table 1 lists the data used to construct the curves shown in Figure 1. The expected errors for the curves are less than 0.5 for the main sequence stars and become progressively larger for the more luminous stars. The details of the error analysis and the derivation of the curves will be reported elsewhere.

DISCUSSION

Our results verify that most of the scatter in the MS color excess plots is indeed caused by variations in the wavelength dependence of extinction. This result implies that peculiar extinction is very common. When the curves shown in Figure 1 are supplemented with the IUE curves for θ Ori and HD 147889 (Bohlin and Savage 1981), it becomes evident that a very wide range of extinction curve morphology is possible. Curves can display extinction that is normal, weak, or strong at λ2200 and normal, weak, or strong in the far UV in almost any combination. These descriptions depend critically upon the choice of normalization.

Since UV extinction is sensitive to so many factors, any interpretative simplification is desirable. A natural simplification is to select curves which arise from a single type of environment. There are two primary classes of these. First, curves derived from stars situated in clear fields, free of obvious dark clouds or nebulosity. These curves are probably the result of dust coexisting with relatively low density gas. Second, curves derived from stars whose extinction is primarily due to dust in a localized high density region. Figure 2a and b show curves derived from IUE data for these two groups. These curves are normalized to E(BUMP) = 1.0 where E(BUMP) is defined as the extinction at λ^{-1} = 4.62 μm^{-1} with respect to a linear "background extinction" intersecting the curve at λ^{-1} = 3.5 μm^{-1} and 5.75 μm^{-1}. Curves normalized to equal bump strength display the amount of extinction at a given wavelength relative to that caused by the material responsible for the bump. The RMS variance for each group is also shown. This is a measure of the "background extinction". Values of E(BUMP)/E(B-V) are listed in Table 1.

The curves shown in Figure 2 form two well defined groups throughout the UV and the apparent progression extends to the visual for the clear field cases. The major morphological difference between the UV portions of the two sets of curves is that the far UV portion ($\lambda^{-1} \geq 6.0\ \mu m^{-1}$) of the nebular extinction exhibits more curvature. Since both variances are very similar, the additional curvature may be related to the bump.

We have examined our curves for changes in the wavelength structure of the bump. The only case which may deviate is the curve for HD 210072. However, the UV spectrum of this star clearly shows that it is a luminous object so its extinction curve is of low weight. Furthermore, Bohlin (1982) has derived a very simliar curve from the BOV star HD 204827 which is only 1.6° away from HD 210072 in galactic longitude and its curve shows no evidence of a change in bump structure. Thus, we have not detected any conclusive variability in the bump position within the accuracy of our data. The implications of this lack of variation in the bump position are discussed in Savage (1975) and Mathis and Wallenhorst (1981).

The curves were also examined for broad and narrow band structure. With the exception of the curvature in the far UV mentioned above, no convincing evidence of either ledges or broad band absorption features

which are characteristic of materials thought to be possible consitutents of the interstellar dust could be found. The background extinction is apparently very smooth as can be seen in the variance shown in Figure 2b which is derived from curves with much better signal to noise ratios than those in Figure 2a. In fact, the weak feature near $\lambda^{-1} = 6.2\ \mu m^{-1}$ in the average curve shown in Figure 1 which traces back to the Nandy et al. (1976) mean curve does not appear in any of our curves. This feature in the mean curve is probably the result of stellar mismatch error arising from the fact that the most reddened star of a given spectral type in a magnitude limited survey will tend to be the most luminous star of that type and luminous O stars have strong P Cygni absorption in C IV λ1550. Thus, the recent identification of the $6.2\ \mu m^{-1}$ feature as evidence for interstellar MgO grains by MacLean and Duley (1982) is questionable.

ACKNOWLEDGEMENTS

Special thanks go to the IUE observatory staff for their help in acquiring and processing the data presented in this paper. Marilyn R. Meade from the University of Wisconsin provided valuable assistance with the IUE data processing. We thank R. C. Bohlin and K. S. de Boer for providing prior to publication IUE extinction data. This research has been supported by NASA through grant NAG 5-186.

REFERENCES

Bohlin, R.C. 1982, This volume.
Bohlin, R.C. and Savage, B.D. 1981, **Ap.J.**, 249, 109.
MacLean, S. and Duley, W.W. 1982, **Ap.J.Letters**, 252, L25.
Mathis, J.S. and Wallenhorst, S.G. 1981, **Ap.J.**, 244, 483.
Meyer, D.M. and Savage, B.D. 1981, **Ap.J.**, 248, 545.
Nandy, K., Thompson, G.I., Jamar, C., Monfils, A., and Wilson, R. 1976, **Astr.Ap.**, 51, 63.
Savage, B.D. 1975, **Ap.J.**, 199, 92.
Savage, B.D. and Mathis, J.S. 1979, **Ann.Rev.Astr.Ap.**, 17, 73.
Wu, C.-C., Boggess, A., Bohlin, R.C., Holm, A.V., Schiffer, F.H., and Turnrose, B.E. 1981, **IUE Spectral Atlas**, (in preparation).

TABLE 1

Reddened Star	Sp.Ty.	Comparison Star	Sp.Ty.	E(B-V)	E(BUMP)/E(B-V)
HD 24432	B3II	HD 83183	B5II	0.70	3.05
HD 37367	B2V	HD 64802	B2V	0.38	4.15
HD 37903	B1.5V	HD 37744	B1V	0.31	1.93
HD 73882	O8V	15 Mon	O7V	0.71	1.80
HD 193682	O5	15 Mon	O7V	0.82	4.08
HD 207198	O9I	HD 188209	O9.5Ia	0.53	2.74
HD 210072	B3III	HD 83183	B5II	0.46	2.12
HDE 251204	BOIV	HD 63922	BOIII	0.71	3.17
HDE 252325	B1V	υ Ori	BOV	0.85	2.66
Ori mean	See Bohlin and Savage (1981)				1.37
HD 147889	See Bohlin and Savage (1981)				3.24
Galactic Mean Curve	See Savage and Mathis (1979)				2.74

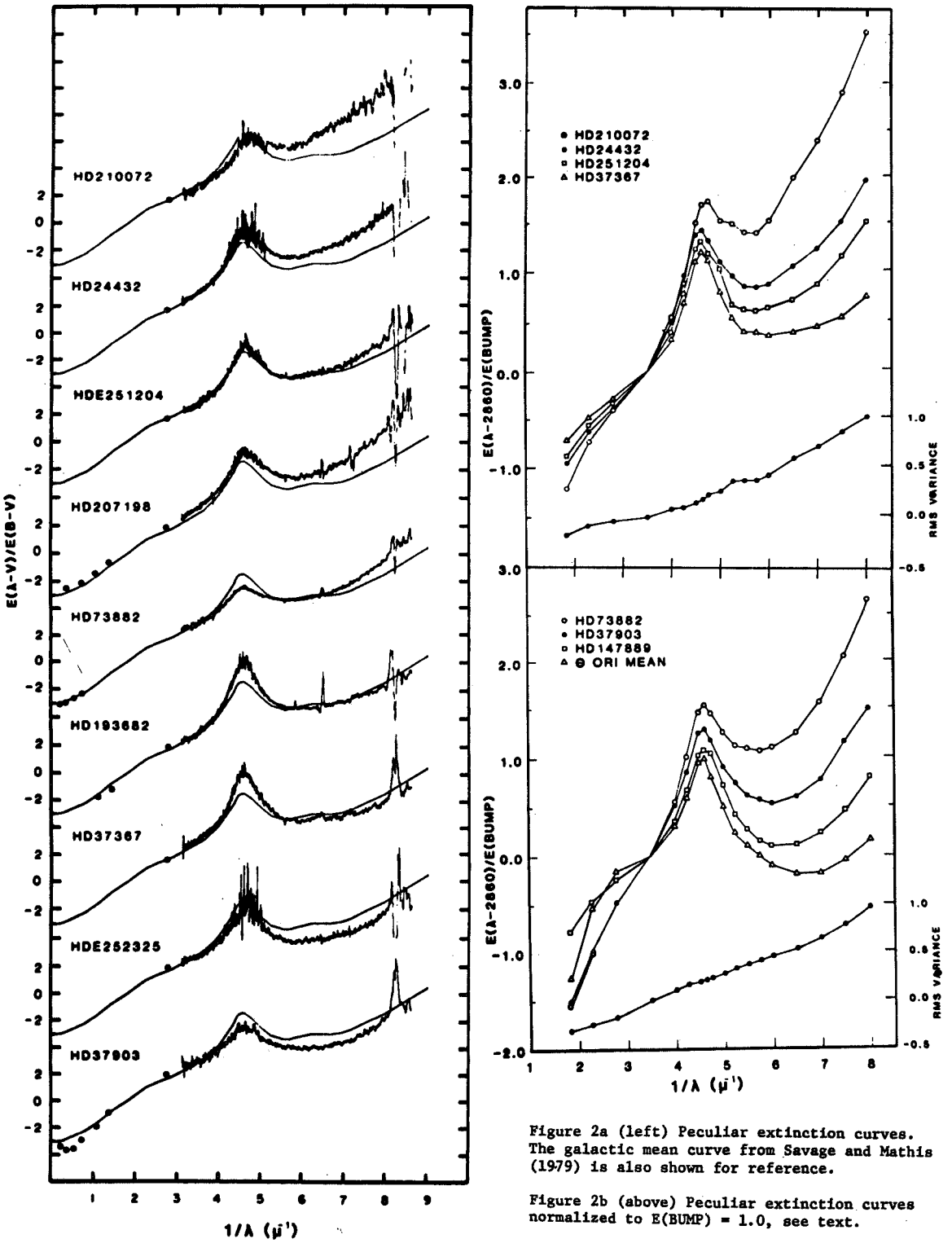

Figure 2a (left) Peculiar extinction curves. The galactic mean curve from Savage and Mathis (1979) is also shown for reference.

Figure 2b (above) Peculiar extinction curves normalized to E(BUMP) = 1.0, see text.

THE PECULIAR UV EXTINCTION OF HERSCHEL 36

J. Hecht, [1,2,4] H. L. Helfer, [3] J. Wolf, [3] Bertram Donn, [2] & J. L. Pipher [3]

1. NAS/NRC Resident Research Associate
2. Laboratory for Extraterrestrial Physics, NASA/Goddard Space Flight Center, Greenbelt, Maryland 20771
3. Department of Physics and Astronomy, University of Rochester, Rochester, New York 14627
4. Presently at Aerospace Corp.

The O star, Herschel 36, probably excites part of the M8 complex near the Hourglass (Thackeray 1950, Woolf 1962). Johnson (1967) showed that the UBVRIJKL photometry of the star was similar to that found in the Orion Trapesium stars. While Her 36 may be a member of NGC6530, the young cluster associated with M8, it is 4.36 visual magnitudes fainter than 9 Sgr, another O star member, and has E(B-V)=0.88, compared to E(B-V)=0.33 for 9 Sgr and the other cluster members. Her 36 therefore seems buried in dust and it is of interest to see if the dust around it possesses the same peculiar extinction characteristics that the Trapesium stars have (Bohlin and Savage (1981)).

The differential extinction curve was calculated using 15 Mon as a comparison star. (λOri and 10Lac were also used without altering the results). The curve is quite unusual, characterized by a distinct 2200Å peak with a very low fat blue end at 5 to $7\mu^{-1}$, the curve does resemble that obtained for θ^1C Ori. We find R~5.6 for the residual extinction of the dust cloud around Her 36, after subtracting out the foreground extinction.

Analysis of the extinction indicates that the absorbing graphite and silicate grains are somewhat larger than those usually found in the interstellar medium. Further the cloud around Her 36 seems to be predominately graphite. The decrease in extinction at 1500 Å to a value $E(\lambda-V)/E(B-V)\sim0.9$ for the residual extinction is probably caused by multiple scattering effects. Details of this argument will be published elsewhere.

Bohlin, R. C., and Savage, B. D. 1981, Ap. J 249, 109.
Johnson, H. L. 1967, Ap. J 147, 912.
Thackeray, A. D. 1950, MNRAS 110, 343.
Woolf, N. J. 1962, PASP 73, 206.

Fig. 1. Extinction vs wavelength. The shortest wavelength shown is 1260 Å.
- a. Normal interstellar extinction curve.
- b. Herschel 36 measured total extinction.
- c. Herschel 36, with foreground extinction corresponding to E(B-V)=0.33 removed.

ABSTRACT

The differential extinction curve of Herschel 36 has been determined from IUE data. It is quite unusual, characterized by a distinct 2200A peak with a very low far blue end at 5 - $7\mu^{-1}$. The star appears to be an extreme

member of the group Savage drew attention to, previously consisting only of Θ Ori, NU Ori, σ Sco, and ρ Oph. It appears that multiple scattering effects are needed to explain the observations.

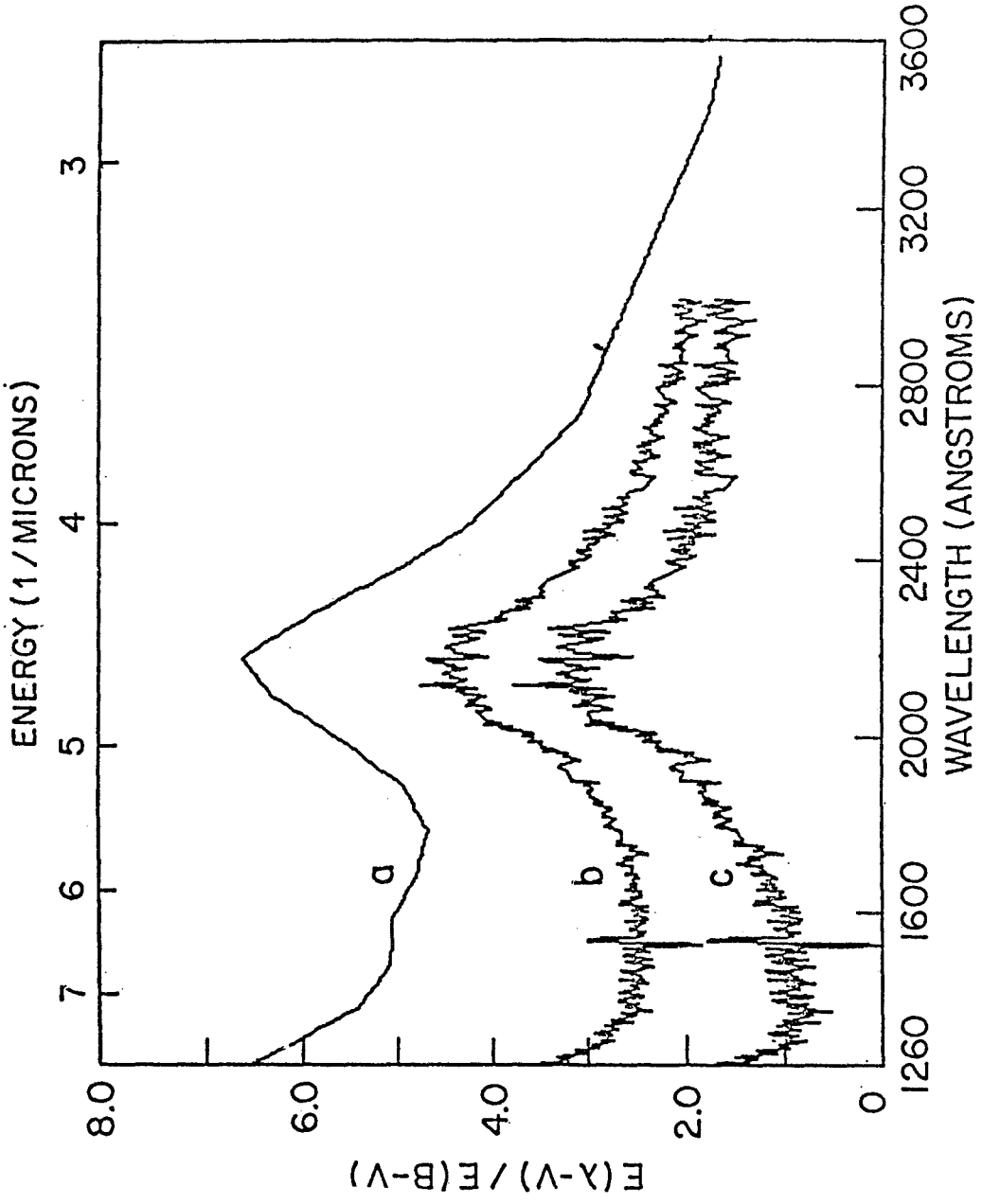
ENERGY (1/MICRONS)
7
6
5
4
3
8.0
6.0
4.0
2.0
0
E(λ-V) / E(B-V)
a
b
c
1260
1600
2000
2400
2800
3200
3600
WAVELENGTH (ANGSTROMS)

RECENT RESULTS ON EXTINCTION IN THE SMALL MAGELLANIC CLOUD

L. Prévot[1],[4] M.L. Prévot[1], J. Lequeux[2], B. Rocca-Volmerange[3]
E. Mauricen[4]

1 : Observatoire de Marseille, France
2 : Observatoire de Meudon, France
3 : Institut d'Astrophysique, Paris
4 ; European Southern Observatory, La Silla, Chile

Twelve SMC early type supergiants have been observed with IUE in order to determine the interstellar extinction curve in the wavelength range 1200-3000 A. All stars have been observed with both cameras in the low resolution mode and through the large aperture. The objects have been selected especially for this purpose and we use the classical method which consists in comparing the spectra of reddened and unreddened stars of the same type. The present results use two comparison stars (Sk 82 : B 1 Ia, E(B-V) = 0.06 and Sk 85 : B 1.5 Ia, E(B-V) = 0.08) and four reddened stars (Sk 191 : B 1.5 Ia, E(B-V) = 0.16 ; Sk 124 : B 1.5 Ia, E(B-V) = 0.17 ; Sk 13 : B 2 - B 2.5 I, E(B-V) = 0.21 - 0.19 and Sk 143 : B 1.5, E(B-V) = 0.30). Stars Sk 191, Sk 124 and Sk 13 give extinction curves in good agreement with each other, which also agree with the first curve already published (Rocca-Volmerange et al., 1981, in Astron. Astrophys., 99,L5), and presented on the Figure :

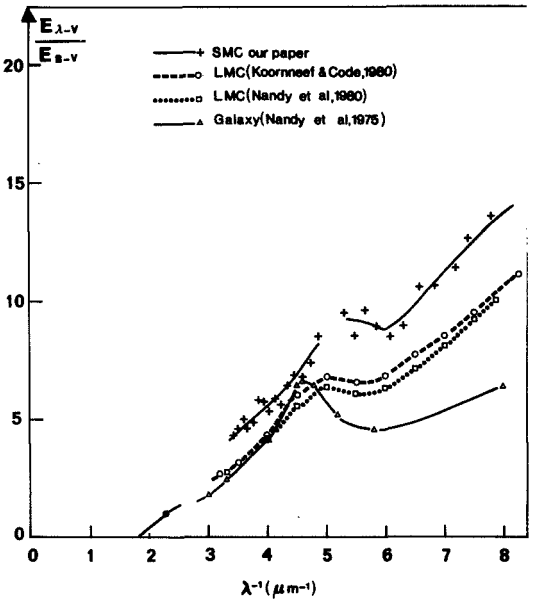

The SMC UV extinction curve does not exhibit the 2200 A feature typical of the galactic extinction and it rises well above the galactic curve and even above the LMC one. A bump around $^{-1}$ = 5.2 corresponds probably to uncompletely removed effects of blanketing by Fe III lines. The heavily reddened star Sk 143 shows a completely different behaviour ; the extinction curve in its direction is similar to the average galactic one ; a strong 2200 A feature is very conspicuous in the IUE spectrum of this star. Moreover, the H I column density NH, as derived from a preliminary examination of the Lyman alpha interstellar profile in the IUE spectrum of Sk 143, is such that NH/E(B-V) has the galactic value while all other observed SMC stars show a considerably larger gas-to-dust ratio. The situation of Sk 143 is reminiscent of the case of the unique star Sk -69° 108 in the LMC (Nandy Morgan, 1978, Nature, 276,478). High latitude clumps of galactic matter might be responsible for the extinction in both cases. Further studies of these stars are in progress.

DISCUSSION - INTERSTELLAR MEDIUM

Blades: Do you find component structure in C IV and Si IV, or any evidence for high velocity components? Secondly, how do your profiles compare with those found in Magellanic cloud supergiants?

Pettini: Generally, the C IV and Si IV lines we observe do not show complex component structure, but tend to be broad and shallow. The profiles are not so complex as those in the Magellanic Clouds possibly because we are sampling observable shorter path lengths. Exceptions to this general pattern do exist, however.

Blair: I am interested in the lack of detection of N V. Were your spectra optimized to the C IV region, and, if so, how much is this responsible for the lack of detection of N V?

Pettini: The sensitivity of IUE is such that we can place reasonable upper limits on the strength of [N V]. Its absence in the halo is not well understood, but it may be that there is a paucity of gas at the proper temperature to produce N V. The ratio of C IV/Si IV can be used with models to predict the expected strength of N V, and some of these estimates are at just about the level of upper limits. Greater sensitivity is needed, in general, to detect N V.

Bruhweiler: If I remember correctly, the cooling curves of Shapiro and Moore indicate that a hot gas is cooling quite rapidly and would be unstable at 8×10^4K. Can you comment?

Pettini: Indeed, if the corona were isothermal at $T = 8 \times 10^4$K, we would require a heating mechanism favoring this temperature, since the cooling curve is a smooth function of T in this domain. Recently T. Hartquist at UCL has considered heating of the corona by magnetohydrodynamic waves and put forward arguments favoring $T = 8 \times 10^4$K. However, photoionization of gas by the integrated QSO radiation field remains an attractive explanation for the presence of significant amount of C IV and Si IV in the halo.

Harrington: I am also surprised by the presence of that Mg V line. You do see it in some planetary nebulae, but it requires very high excitation. It is harder to produce than lines of Ne V. To produce much Mg^{+4} in models you need stellar temperatures of over 100,000K.

York: Could you comment on the absorption lines spectrum? Is it in the telescope or grain scattering? I was intrigued by the absence of a broad Si IV emission in the scattered spectrum.

Boeshaar: The light is scattered light of θ Ori. We still need to check that the IUE large aperture was not including part of the stellar image. Part of the apparent modular emission could be from scattered light.

Savage: Would you comment on the possible origin of the Mg V emission?

Boeshaar: The [Mg V] λ2784 feature is unlikely to be produced as a result of photoionization. The clearest detections of this line correspond to the position of shock and ionization fronts and may indicate collisional effects contributing at these points.

Carruthers: In our sounding rocket flight of 3/12/82, we observed θ Ori with an objective grating spectrograph. The Si IV feature shows a definite P-Cygni profile. Have any high-resolution IUE spectra been taken of θ^1, θ^2 Ori including the 1400 Å Si IV doublet, for comparison with the nebular spectra?

Boeshaar: The Si IV 1394 emission feature shown was superimposed on an absorption feature with no P-Cygni emission component on the red side. This observation is for a region on the opposite side of the bright bar from θ^1 Ori C and may be shielded from its radiation. We have observations of both θ^1 Ori C and θ Ori^2 A which may clarify this point.

Shore: Do you detect, and do you have any evidence for a variation of the Si III] 1895/C III] 1908 or 1909 ratio with position in the nebula?

Boeshaar: The Si III] 1895 is seen in only some of our spectra and does not provide enough statistically significant information for us to address that point.

Aller: Two comments: (1) Use of theoretical models seems to be very much preferable to other methods for getting abundances of Ne, S and Ar even though there are some limitations in theoretical models, at least that is what Keyes, Czyzak, and I concluded from our models for SMC and LMC H II regions in 1978. (2) O, Ne, S and Ar seem to go together in many H II regions (in LMC, SMC, M33, M101, and planetaries). Thus, these elements must have been manufactured together at an early stage in an epoch of massive star formation. Building of C and N, as you have emphasized, must come from other processes. I happen to think planetaries are good factories for making both C and N.

Shore: I would just caution against the use of such simple one zone models for the nucleosynthesis. A model including the effects of non-linear star-to-gas and induced-star formation conversion processes leads

to bursts, which represent rapid enhancement of Z. In these cases, the time scale for ΔZ may be short compared with the mixing timescale. Although you obtain qualitative agreement, it might be premature to draw any sweeping conclusions. By the way, this result for bursts is not the result of a variable IMF.

Savage: Geocoronal Lyman β emission appears to be a major problem when observing the 1032 A line of O VI. Just how serious is this problem?

Grewing: Within a ± 8 Å band around Lyman we must expect a count rate of roughly 2 counts/pixel-hr from geocoronal Lyman β. Obviously, the actual number will depend on the final choice of the orbit and the instantaneous viewing direction.

Aller: (1) How do UV region diagnostics agree with those found from visual region data? (2) A slitless spectrogram secured by O.C. Wilson in the late forties with the Mt. Wilson 2.5^m telescope under conditions of exquisite seeing showed NGC6572 to be a ring structure with an outer amorphous-like structure. Some radiations of high excitation showed a strong concentration to the central star. (Tracings are given in my article in Sky & Telescope, 1969-1970).

Grewing: (1) For several ionic species we find very good agreement with earlier abundance determinations based on optical data. In a few cases, however, there are striking differences, one example for this being He II for which we determine a considerably lower abundance than suggested by optical measurements. (2) Our spatial resolution is clearly insufficient to check on stratification effects, and we are aware of the uncertainties that result from this fact. In some of the spectral features I showed, we actually can separate the emission arising in the extended atmosphere from that arising in the nebula proper.

Dufour: Do you have any data on line ratios from a single ion which span a significant range of wavelength in the UV that could be used to study internal dust amounts and spatial distribution?

Feibelman: The spatial distribution of He II 2734 is the same as that of He II 1640, though the intensity is smaller. These lines, and possibly some of the O III lines could be used, but we have not yet done this.

Witt: Have corrections been made for sensitivity profile along the IUE slit?

Feibelman: No. Only information in central orders is considered where such corrections are small.

Dufour: Have you observed any lines of silicon and/or magnesium in the planetary nebula spectra?

Maran: No.

Aller: What happens if you take a simplistic approach, assuming you can use the Mie theory? What conclusions can you draw concerning the size distribution function of the dust; can the same particles work for both visual and ultraviolet?

Witt: If the same particles responsible for the strongly forward-directed scattering in the visual were also to dominate the scattering in the UV, the Mie theory would require that the UV scattering would be even more asymmetric than the visual. Consequently, our results require that there is at least one second component, particles small compared to UV wavelengths, which is responsible for the scattering in the UV. These particles would also need to have a high UV albedo, because the overall albedo in the UV is about 0.5 and the larger particles causing scattering and polarization in the visual contribute very little to scattering in the UV.

Carruthers: If you use the dust reflection curve for the Electra nebula to represent the intrinsic properties of the dust (optically thin limit) can you work back to determine the dust extinction between the star and nebula (and between nebula and observer) in the other cases you showed (Pleiades and NGC 7023), which had much flatter reflection curves?

Witt: The very steep reflection spectrum of the Electra nebula appears to be primarily the consequence of quite large scattering angles ($\sim 100°$) coupled with the wavelength dependent phase function. This interpretation is supported by the surface brightness of this nebula in the visual which is only about 40% of that of the Merope Nebula (23 Tau) and the Maia Nebula (20 Tau) at corresponding offset distances. It is important that the spectra of all three nebulae as well as that of NGC 7023 can be reproduced using the same wavelength dependence of the optical depth and the identical phase function variation, if one takes the differences in geometry into account. If the phase function were constant with wavelength, however, all these nebulae would have essentially identical spectra despite their different geometries.

Aller: What is the fraction of continuum light in NGC 6543 to be attributed to dust?

Helfer: 20-40% of the light at 1600 Å is attributed to gas. (The spectrum falls so steeply in intensity with increasing wavelength that one cannot use > 60% gas emission at 1600 Å without predicting more radiation at $\lambda > 2800$ Å than is observed.)

Witt: What are the extinction characteristics of the dust in your nebula, i.e., of Herschel 36?

Helfer: We do not know the extinction characteristics of the dust along the line of sight into the nebula. We assumed we could correct the nebula light with a standard extinction curve using the foreground field value E(B-V) = 0.33. For Herschel 36 itself, the story is more complicated (see text and second paper after this). Essentially we removed foreground extinction and about two-thirds of the remaining peculiar extinction around Herschel 36. (Removing substantially more or less, resulted in very peculiar extinction curves, e.g., with a strong decrease in a narrow band around 2200 Å.)

Underhill: When interstellar extinction curves are determined, it is essential to know that the two stars being compared have the same intrinsic energy distribution. What criteria did you use to ensure that this condition was met? My experience with O and B stars indicates that you should try to restrict your program stars to main sequence stars (luminosity classes IV and V), and spectral types B3, B2, and possibly B1.

Massa: I agree that compact early B stars are the best to use. Of the curves shown in Figure 2, only one (HD 73882) is derived from an O star and this is an O8 V. We were dubious of our curve for HD 210072 (B5 II) for the very reasons you suggest and it was not until we saw Bohlin's nearly identical curve for the nearby B0 V star HD 204827 (this volume) that we were convinced of the reality of our curve for HD 210072. HD 204827 has an $E(B-V) \cong 1.0$ mag and deviates from the mean curve by more than four units at $\lambda 1250$. For this difference to arise from stellar mismatch, m ($\lambda 1250$)-V for HD 204827 would have to be four mag fainter than μOri and I find this hard to believe.

Witt: If multiple scattering is required to explain the peculiar extinction at $\lambda < 2000$ Å, why is this not a significant effect at 2200 Å where, in light of your earlier paper, the albedo is also high?

Helfer: Multiple scattering is needed for the entire UV wavelength interval observed. I noted, in passing, that at 2200, τ extinction >4; certainly multiple scattering must be considered at the extinction peak. The point I was making was that to get $E(\lambda-V)/E(R-V) < 1$ at $\sim$1300, with theoretical grain distributions, one had to include multiple scattering at this wavelength.

Underhill: I notice that you are determining extinction laws from stars classified as B1 supergiants. This is very dangerous because the B1 supergiants appear to be a very heterogeneous group of stars with widely differing effective temperatures and for UV line blanketing. Consequently their true far-ultraviolet continua may not be the same. In addition it is difficult to be sure that you are determining the same "continuum" in each case.

VARIABLE STARS

SHORT-TERM UV LINE PROFILE VARIATION IN 59 CYG

C.A. Grady, V. Doazan, G.J. Peters, A. Willis, T.P. Snow, D. Aitken, P.K. Barker, C.T. Bolton, H. Henrichs, C.R. Kitchen, L.V. Kuhi, J.M. Marlborough, P. Meikle, J. Mendzies, W. Oegerle, R.S. Polidan, R. Rosner, P. Selvelli, R. Stalio, R.N. Thomas, G. Vaiana, P. Whitelock, R. Wilson and C. Wu

ABSTRACT: IUE high dispersion spectra of 59 Cyg obtained as part of the long term monitoring program have shown that noticeable variation can occur in C IV and N V on timescales 3 hours < t < 24-28 hours. In order to begin to resolve whether these changes occur continuously or sporadically, 48 hours were devoted to monitoring this star in January 1982. The January spectra show no short term variation which may be consistent with sporadic rather than continuous variation.

OBSERVATIONS: 59 Cyg (B1.5 IVe) has been extensively monitored in the ultraviolet, primarily with IUE, since the end of 1978. The most striking aspect of this star's ultraviolet spectrum is spectacular variation in the resonance lines of C IV and N V (Doazan et al. 1980a,b; Doazan et al. 1981). Since a number of physical mechanisms could potentially be responsible for this variation, it is important to establish the timescale of the variation.

59 Cyg has been observed at intervals of a few days on several occasions in the course of an ongoing monitoring program. Observations made in December 1978, December 1980, and January 1981 (Figure 1) suggested that significant, but relatively minor line profile variation could occur on intervals of 1-3 days. Further observations made in April 1981 at approximately 48-hour intervals suggested that these minor variations in the C IV profile structure could occur in less than 2 days, but larger changes in the profile structure were less frequent (Figure 2). Similar results were observed in N V. Most of the variation in the pairs of spectra taken within a few days of each other is not in equivalent width, but in the radial velocity of the strongest absorption component(s) (Table 1). The short term variations appear to be of relatively small amplitude of the order 3 to 5σ above the noise.

Table 1.
59 CYGNI

Date	CIV Equivalent Width (A)		CIV Major Velocity Components V_{cen} (km s^{-1})	FWHM (km s^{-1})
1978 354 16	2.69	± .36	800	240
1978 355 17	2.68	± .04	800	50
			700	300
1980 355 03	3.37	± .05	650	150
1980 357 06	3.19	± .05	800	250
1981 23 16	2.90	± .08	800	300
1981 27 00	2.85	± .08	870	240
1981 106 00	3.17	± .08	700	400
1981 108 01	2.97	± .10	745	340
1981 109 20	3.15	± .04	969	50
			846	150
			660	50
1981 111 19	3.11	± .06	845	230
1981 115 19	2.64	± .04	950	100
			840	100
1982 27-28 (avg)	1.143	± .26	1000	100
			0	200

48 hours of continuous IUE time was devoted to monitoring 59 Cyg and one other Be star, γ Cas (B0 IVe) in January 1982. At that epoch, the Si IV profiles of both stars were similar in

having weak high velocity absorption components in addition to the normal low velocity absorption profiles. The same is true in C IV, with the low velocity component in 59 Cyg being weaker than γ Cas. N V in both stars showed substantial absorption at high velocities.

During the 48-hour observing period, no variation greater than 1σ was observed in either star (10% in flux). This has permitted careful stacking, using a software developed by Seab, of a number of spectra (10 for 59 Cyg, 9 for γ Cas) to produce a higher signal-to-noise profile in C IV, Si IV, and N V (Figure 3).

This lack of variation has a number of interesting implications. First, no modulation of the profiles was observed with any periodicity. Since these absorption profiles perferentially sample material in the direct line of sight to the star, this implies that the wind acceleration zone was stable through greater than one rotation cycle for both stars. This rules out the presence, at that epoch, of azimuthally localized features in the wind and implies at least cylindrical symmetry, if not spherical symmetry in the wind. Secondly, the wind appears to have been quite stable during the 48 hours with no velocity components moving across the profile (as has been suggested for a puff moving through a monotonic acceleration zone) or appearing at high velocities as has been suggested for the high velocity components in γ Cas (Henrichs, 1980) and ζ Oph (Willis, private communication, 1982). Coupled with previous observations of variation on intervals of 1-2 days, this suggests that the variation in the wind conditions which we observe as line profile variation is sporadic.

SUMMARY: The observations of short timescale line profile variability in 59 Cyg suggests that major changes in the wind occur on timescales larger than 1-2 days. The short term variability which has been observed is smaller in amplitude and similar in timescale (order 1-2 days) to the small amplitude, short term variability already known to exist in Be stars from visible spectra, but is not always present.

We wish to thank T. Ayres, J.M. Shull, and C.G. Seab for help in obtaining these spectra. We also wish to thank E.W. Brugel and T. Armitage for help with software used in this project. Data reduction was performed at the IUE Regional Data Analysis Facility at the University of Colorado. Data reduction for this project was supported by NASA grant NAS5-26409.

REFERENCES

Doazan, V. Kuhi, L.V. and Thomas, R.N., 1980a, Ap. J. 235, L17.
Doazan, V., Kuhi, L.V., Marlborough, J.M. Snow, T.P. and Thomas, R.N., 1980b, The Second IUE Conference, ESA-SP-157, p. 151.

Doazan, V., Grady, C., Kuhi, L.V., Marlborough, J.M., Snow, T.P. and Thomas, R.N., 1981, "The Active UV Phase of 59 Cyg", J. Jaschek and H.G. Groth (eds), Be Stars, IAU Symp, Munich, pp. 415-418.

Henrichs, H.F., 1981, "UV Observations of γ Cas: Intermittent Mass-Loss Enhancement", M. Jaschek and H.G. Groth (eds), Be Stars, IAU Symp., Munich.

Willis, A., 1982, private communication.

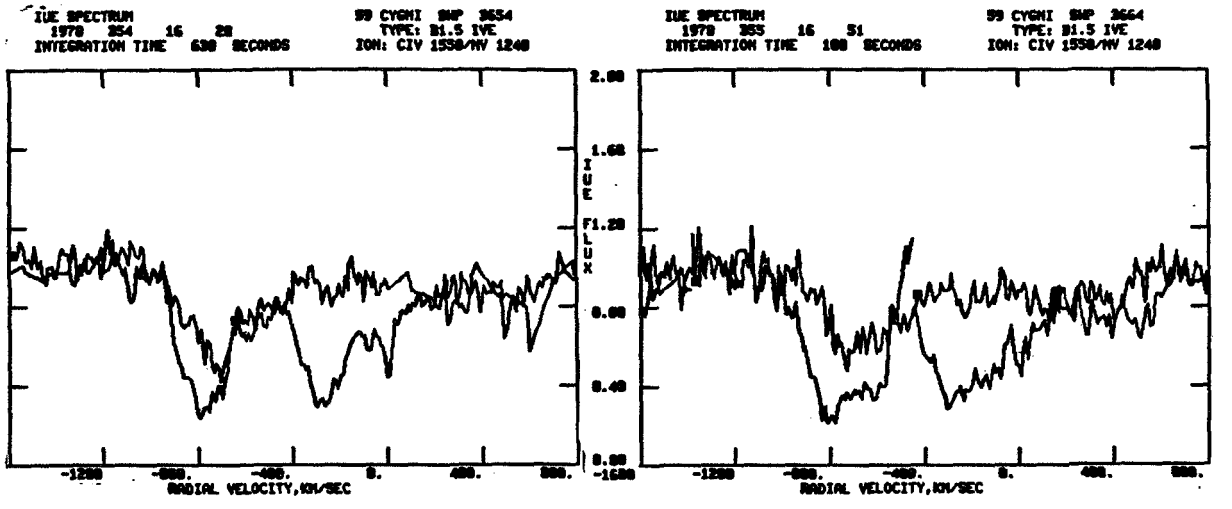

Figure 1. (a) N V (upper tracing) and C IV (lower tracing) for Day 354, 1978.
(b) N V and C IV, 24.5 hours after (a).

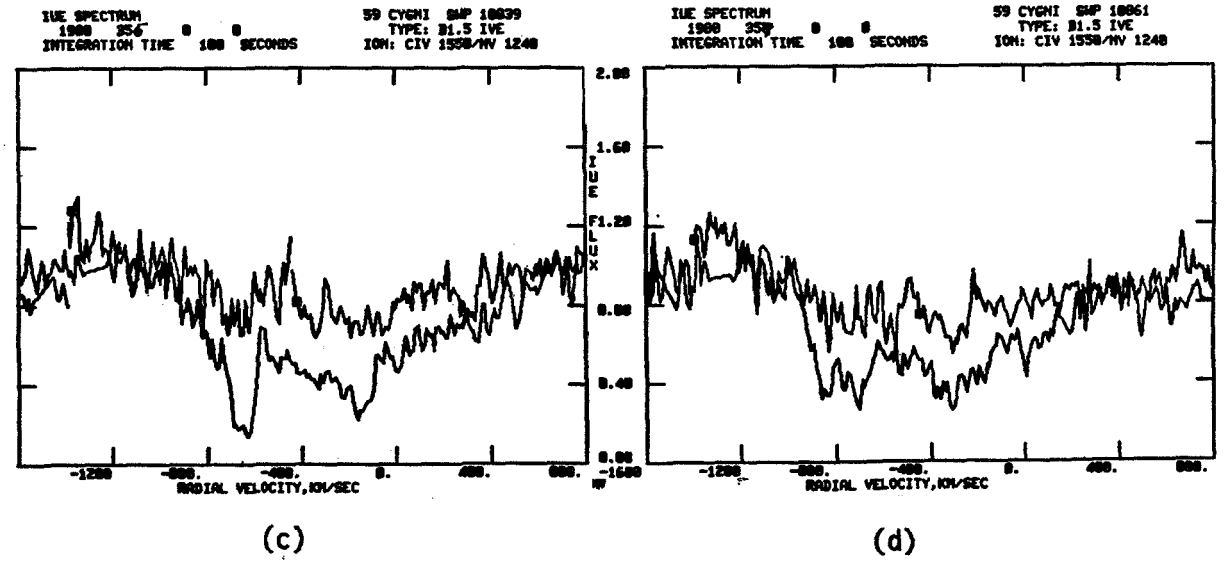

Figure 1. (c) N V and C IV for Day 355, 1980.
(d) N V and C IV 51 hours after (c).

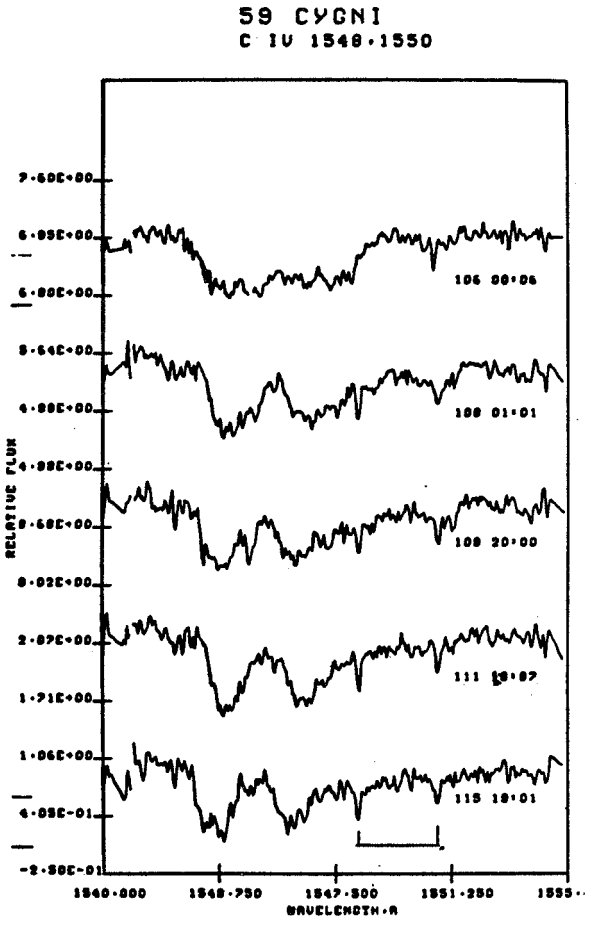

Figure 2. C IV profiles for April 1981.

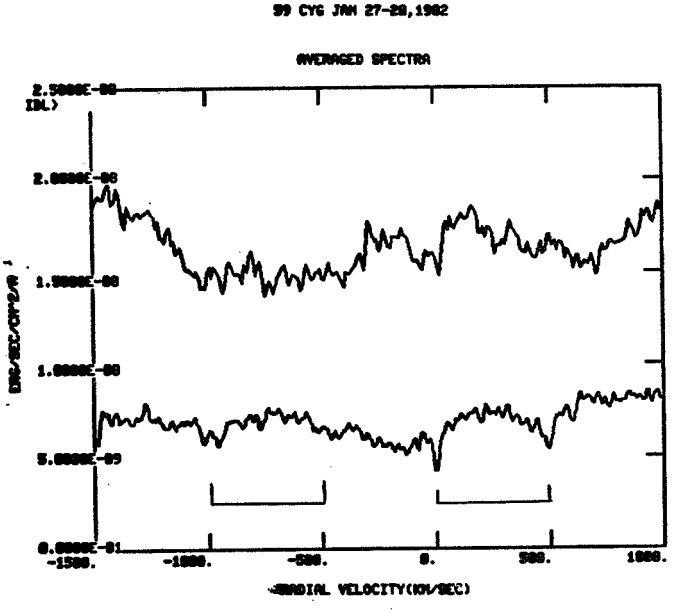

Figure 3.

N V (upper tracing) and C IV for 59 Cyg in January 1982. 10 spectra were averaged to produce these profiles. The interstellar C IV lines at 0 and 500 km s^{-1} and high velocity C IV stellar components are indicated by the vertical lines.

ULTRAVIOLET SPECTRA OF R CORONAE BOREALIS STARS

Albert V. Holm and Chi-Chao Wu
Computer Sciences Corporation

ABSTRACT

We have obtained IUE spectra of the R CrB-type variables R CrB, RY Sgr, XX Cam, and MV Sgr. Our analysis of these spectra suggests that: 1) it should be possible to construct useful models for the atmospheres of these hydrogen-deficient, carbon-rich stars if present standards of metallic line blanketing are used; and 2) the observed wavelength dependence of the circumstellar extinction is primarily due to circumstellar grains.

INTRODUCTION

The R CrB-type variables are astrophysically interesting because of their hydrogen-deficient, carbon-rich atmospheres, because of their occasional visible light declines of 5 to 10 magnitudes, and because of their pulsational variation. In late 1978, we began an IUE observing program to determine the wavelength dependence of the flux changes of these stars during the visible light minima. This program also has produced information on the ultraviolet spectra of these stars at maximum light. In this paper we present examples of these spectra and discuss some implications.

THE SPECTRA AT MAXIMUM LIGHT

The atmospheres of R CrB, RY Sgr, and XX Cam are under abundant in hydrogen by a factor of about 1.0E-5 and over abundant in carbon by a factor of about 30 (Schonberner 1975). Thus their energy distributions and spectral features can provide data for tests of the state of the art in model atmosphere calculation.

In Figure 1, we show IUE low dispersion spectra of these three stars in comparison with the normal F8 Ib star γ Cygni. All four spectra show strong absorption features which we have identified with Mg II, Fe II, Mn II, and Al I. The identifications of the Mg II doublet at 2800 A in the spectrum of R CrB is confirmed by high dispersion spectra (Fig. 3). The identification of the Fe II and Mn II lines near 2600 A is also confirmed by the high dispersion spectrum of R CrB. The identification of the features at shorter wavelengths and all the features in the spectra of RY Sgr and of XX Cam is based on wavelength coincidence with features in the spectra of brighter stars. In addition to the absorption features, the spectra of R CrB and RY Sgr show C II λ1335 in emission. The emission fluxes are 8.6E-14 ergs/cm^2/s for R CrB on 1978 Dec 25 and 2.0E-14 ergs/cm^2/s for RY Sgr on 1981 Sept 24 .

Figure 1 shows that the ultraviolet spectra and energy distributions of R CrB and RY Sgr mimic the appearance of those of γ Cygni. This is not the case in the visual where, for example, the Balmer jump of γ Cygni is

considerably larger than that of R CrB. In the ultraviolet, line blanketing by the metals contributes much of the atmospheric opacity (e.g. Kurucz 1979) in normal stars. The similarity in the spectra of R CrB, RY Sgr, and γ Cygni suggests that hydrogen-deficient model atmospheres using the line list of Kurucz and Peytremann (1975) would be successful in predicting the energy distributions of R CrB and RY Sgr.

The spectrum of XX Cam differs somewhat from those of the other stars. Qualitatively, this difference may be caused by a slightly higher effective temperature and by some modification by interstellar extinction. Lacking suitable models, we have not yet tried to quantify this estimate.

If we use a bolometric correction appropriate for F-type supergiants with normal abundances, then we find that the C II emission fluxes are 7E-7 of the stellar luminosity for R CrB and about 4E-7 of the stellar luminosity for RY Sgr. If we assume the light of RY Sgr to be reddened by an amount corresponding to E(B-V)=0.1, then the corrected C II emission flux is about 7E-7 of the stellar luminosity. These fluxes are within the range seen for other stars (Bohm-Vitense 1981).

SPECTRAL CHANGES IN MINIMUM

Holm et al. (1982) have shown that the change in the energy distribution of RY Sgr during its recovery from the 1977/78 minimum is consistent with variable circumstellar extinction by graphite grains with radii of 0.043 microns or by amorphous carbon smoke grains. However, they could not rule out the possibility that blended line features from a hypothetical dense circumstellar gas cloud distorted the observed ultraviolet extinction curve. In this paper, we use high dispersion spectra of R CrB to show that changes in line features are negligible compared with the extinction at some wavelengths.

Figure 2 shows an average extinction curve for RY Sgr and an extinction curve for R CrB during its minor minimum of 1980 September. The generation of the RY Sgr curve is discussed in Holm et al. (1982). The R CrB extinction curve was formed by ratioing fluxes measured on 1980 September 18 to fluxes measured on 1980 April 30. Using Fernie's (1982) mean pulsational period of 46 days, the difference in pulsational phase for these two measurements was 0.06. The difference in the Fine Error Sensor magnitude (Holm and Rice 1981) of R CrB was 0.72.

The circumstellar extinction for both RY Sgr and R CrB show broad maxima in this wavelength range. That of RY Sgr occurs near 2500 A; that of R CrB occurs near 2400 A. This difference may be real or it may be caused by irregularities in R CrB's pulsation (Fernie 1982). Regardless of this difference, both extinction curves differ considerably from the mean interstellar extinction curve which shows a strong maximum at 2200 A (e.g. Savage and Mathis 1979).

High dispersion spectra of R CrB were obtained on both dates. Figure 3 shows the Mg II and Mg I resonance lines from the spectrum obtained on 1980

April 30 (LWR7643). This region from the spectrum obtained on 1980 September 18 (LWR8841) is similar but noisier because the image is underexposed. To compare the two spectra, their wavelengths were first corrected for earth and spacecraft motion (Harvel 1980) and for temperature-dependent shifts in the spectral format location (Thompson et al. 1981). These adjustments corresponded to +4.6 km/sec for LWR7643 and -19.1 km/sec for LWR8841. Next the fluxes during the minimum (LWR8841) were scaled up by a factor of 3.44 derived from the ratios of the low dispersion spectra at 2750 A and 2850 A. Finally, the spectrum from LWR7643 was subtracted from the scaled spectrum from LWR8841 to give the difference spectrum shown in Figure 4. We expect changes in line absorption or emission from development of a dense gas cloud to appear as features in this difference spectrum. Figure 4 appears to show emission in both Mg I and Mg II. This emission corresponds to features seen in the extinction curve in Figure 2. There may be other features in this difference spectrum that are real. However, we haven't identified them in this region of low signal-to-noise. Moreover, there is no systematic pattern of absorption that would account for a significant modification of the shape of the extinction curve shown in Figure 2.

Figure 5 shows another section of the 1980 April 30 spectrum. Figure 6 shows another difference spectrum that was generated in the same way as the one in Figure 4. The scaling factor was 3.08. The spectrum in Figure 6 has a better signal-to-noise ratio than that in Figure 4. It shows no evidence for line features that would significantly modify the extinction curve.

REFERENCES

Bohm-Vitense, E. 1981, in "The Universe at Ultraviolet Wavelengths", ed. R. Chapman, NASA Conference Publication 2171, p. 303.

Fernie, J.D. 1982, Publ. A.S.P., Feb. issue.

Harvel, C. 1980, NASA IUE Newsletter, No. 10, 32.

Holm, A., and Rice, G. 1981, NASA IUE Newsletter, No. 15, 74.

Holm, A.V., Wu, C.-C., and Doherty, L.R. 1982, Publ. A.S.P., June issue.

Kurucz, R.L. 1979, Ap.J. Suppl., 40, 1.

Kurucz, R.L., and Peytremann, E. 1975, Smithsonian Ap. Obs. Spec. Report, No. 362.

Savage, B.D., and Mathis, J.S. 1979, Ann. Rev. Astron. Astrophys., 17, 73.

Schonberner, D. 1975, Astron. Astrophys., 44, 383.

Thompson, R., Turnrose, B.E., and Bohlin, R.C. 1981, NASA IUE Newsletter, No. 15, 8.

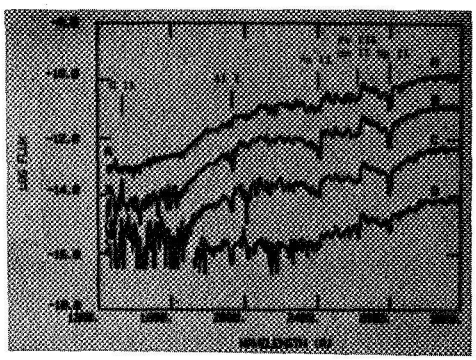

Fig. 1- IUE spectra of A) γ Cyg, F8 Ib, B) R CrB, C) RY Sgr, and D) XX Cam. Fluxes have been offset by small constants for visibility.

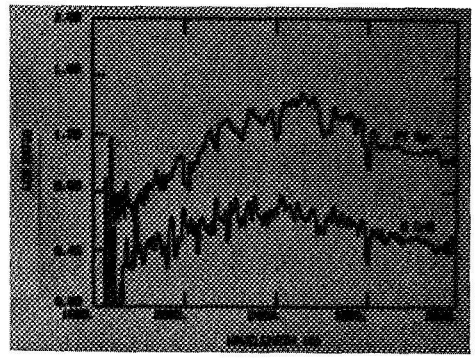

Fig. 2-Circumstellar extinction curves for RY Sgr and R CrB.

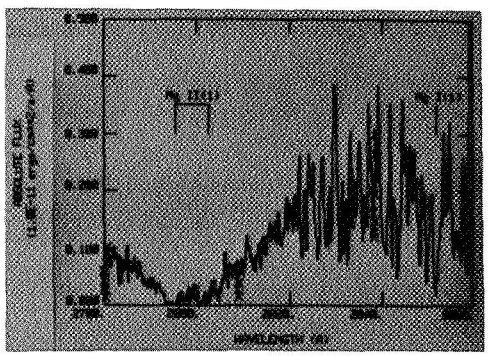

Fig. 3- The spectrum of R CrB at maximum, 1980 April 30.

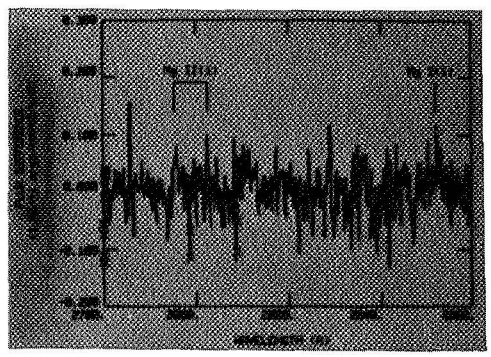

Fig. 4-R CrB's spectral changes between maximum and Sept. 1980 minimum.

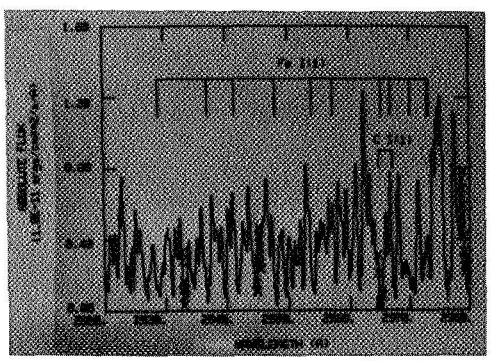

Fig. 5- The spectrum of R CrB at maximum, 1980 April 30.

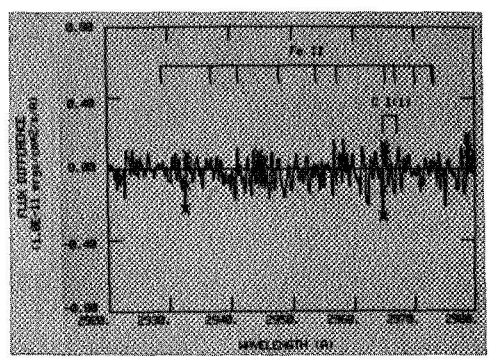

Fig. 6- R CrB's spectral changes between maximum and minimum. The Fe I(1) multiplet is mislabeled as "Fe II".

ULTRAVIOLET AND OPTICAL SPECTRA OF THE OUTER SHELL OF ETA CARINAE

Kris Davidson
University of Minnesota

Nolan R. Walborn and Theodore R. Gull
Laboratory for Astronomy and Solar Physics
Goddard Space Flight Center

ABSTRACT

Despite 150 years of studies, the fundamental nature of the underlying, explosively variable object within Eta Carinae has not yet been established beyond the attributes of high mass, high luminosity, and great instability. The basic cause of this uncertainty is the opaque, high-density ejected material which immediately surrounds the central object. Here we report spectroscopic observations from 1200Å to 6800Å of condensations in the more extended outer shell of Eta Carinae. These spectra show lower density, nebular characteristics. Furthermore, proper motion studies of these outer condensations have shown that they were also ejected from the central object within Eta Carinae. Hence, their spectra provide remarkable information about the central object. Five successive ionization stages of nitrogen (N I through N V) are strongly present, but no carbon or oxygen is detected above the noise level of these data. We interpret these spectra in terms of anomalous abundances caused by CNO-cycle processing within the progenitor star. These results imply that, 1) relatively pure processed material may be observable at low densities; 2) a massive star has transported processed material to its surface and ejected it; and 3) a pre-main sequence interpretation of Eta Carinae is essentially ruled out. (The paper appears in The Astrophysical Journal Letters, 254, L47, 1982.)

HYDROGEN TWO PHOTON EMISSION IN THE UV SPECTRUM OF TYPE II SUPERNOVAE

P. Benvenuti, ESA IUE Tracking Station, Madrid
M.A. Dopita, Mt Stromlo & Siding Spring Observatories, Canberra
S. D'Odorico, European Southern Observatory, Garching-bei-Munchen

Up to date, five Supernovae have been observed by IUE: two of them, SN 1979c in NGC 4321 and SN 1980k in NGC 6946, were classified as type II and were bright enough in the UV range to be observed by IUE during a few months. The relevant data collected at the European Ground Station, VILSPA, were first presented by the Team of experts especially set up by ESA and SERC (Panagia et al. 1980; Panagia et al., in preparation). Herewith we have limited the discussion to a particular aspect of the UV spectrum of the type II SNe: the continuum emission.

The UV continuum emission in type II SNe is rather smooth and extends along the whole range covered by IUE. At a first analysis it seems the natural continuation of the optical continuum, which is known to be satisfactorely fitted by Black-Body emission (Kirshner and Kwan, 1974). However, an attempt to fit also the UV range by Black-Body emission, failed due to an UV excess shortward of 1600 Å which remains present at all dates.

Without attempting to build a photospheric model for type II SNe, we intend to draw the attention to a mechanism, the hydrogen two photon emission, which provides a satisfactory explanation of the UV excess and should therefore be taken into account in any further modelling.

The two photon emission from hydrogen was theoretically investigated by Spitzer and Greenstein since 1951 and subsequentely by several authors (e.g. Brown and Mathews 1970, Gerola and Panagia 1968, 1970). Recently, after IUE, a number of papers presented detailed computations of the two photon emission, pointing out its importance even at high plasma densities (Gaskell 1980, Drake and Ulrich 1981).

The UV spectra of the two type II SNe, together with U,B,V photometric data, were fitted with the following function:

$$F_\nu = \theta^2 \left[\pi B_\nu(T) + F_\nu(2q) \right] e^{-\tau_\nu}$$

where: F_ν = Observed flux
θ = Angular photospheric radius = R_{ph}/D
πB = Black Body flux at the photosphere
$F_\nu(2q)$ = Two photon flux at the photosphere
τ_ν = Optical depth

The color excess $E_{(B-V)}$ was assumed 0.1 for sn 1979c and 0.32 for SN 1980k (Panagia et al. 1980; Panagia et al. in preparation). The Black Body tempe-

rature, the angular radius and the two photon flux were varied simultaneously to obtain a best fit to the data. The result is very satisfactory at all dates for both the SNe. In Fig. 1 and 2 we present a sample of these fits.

One of the interesting results which can be obtained from the parameters of the fits, is the angular velocity of expansion of the SN envelope $\dot{\theta}=\dot{R}_{ph}/D$. For both the SNe, $\dot{\theta}$ is linear, starting from the first observation up to at least 20 days. In the case of SN 1979c, $\dot{\theta}$ is decreasing at a later stage as the photosphere recedes in the expanding material due to the decrease of the optical depth. For the linear part we measure an angular velocity of expansion of 1.7 E-17 rad/s and 2.6 E-17 rad/s for SN 1979c and SN 1980k respectively. Assuming that the optical emission lines are formed at the photosphere we can derive from their blue wing the linear velocity of expansion and hence the distance of the parent galaxy.

For SN 1979c, $\dot{R}_{ph}$ = -9200 Km/s (Panagia et al. 1980), from which we derive a distance of 17.3 Mpc for NGC 4321. For SN 1980k, $\dot{R}_{ph}$ = -5600 Km/s (Ciatti private communication) and the distance of NGC 6946 becomes 7.1 Mpc.

In a forthcoming paper we will present additional proofs on the two photon nature of the observed UV excess and we will compare the above distances with previous determinations.

REFERENCES

Brown, R.L. and Mathews, W.G. 1970, Ap.J. 160, 939
Drake, S.A. and Ulrich, R.K. 1981, Ap.J. 248, 380
Gaskell, C.M. 1980, Observatory 100, 148
Gerola, H. and Panagia, N. 1968, Astrophys.&Space Sci. 2, 285
- - - 1970, Astrophys.&Space Sci. 8, 120
Kirshner, R.P. and Kwan, J. 1974, Ap.J. 193, 27
Panagia, N. et al. 1980, M.N.R.A.S. 192, 861
Panagia, N. at al. 1982, in preparation
Spitzer, L. and Greenstein, J.L. 1951, Ap.J. 114, 407

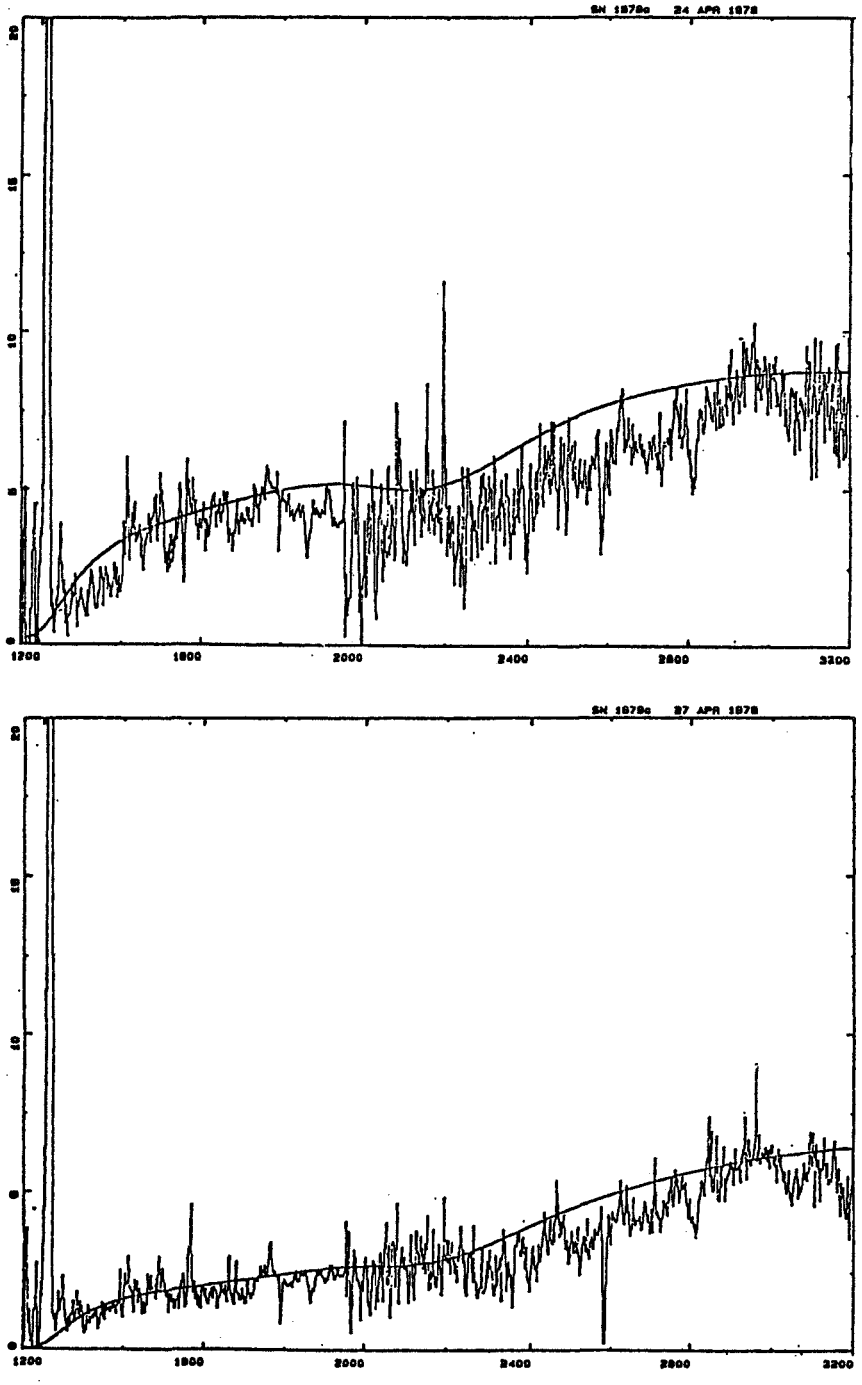

Fig. 1 - SN 1979c, IUE observations of april 24 and 27, 1979.

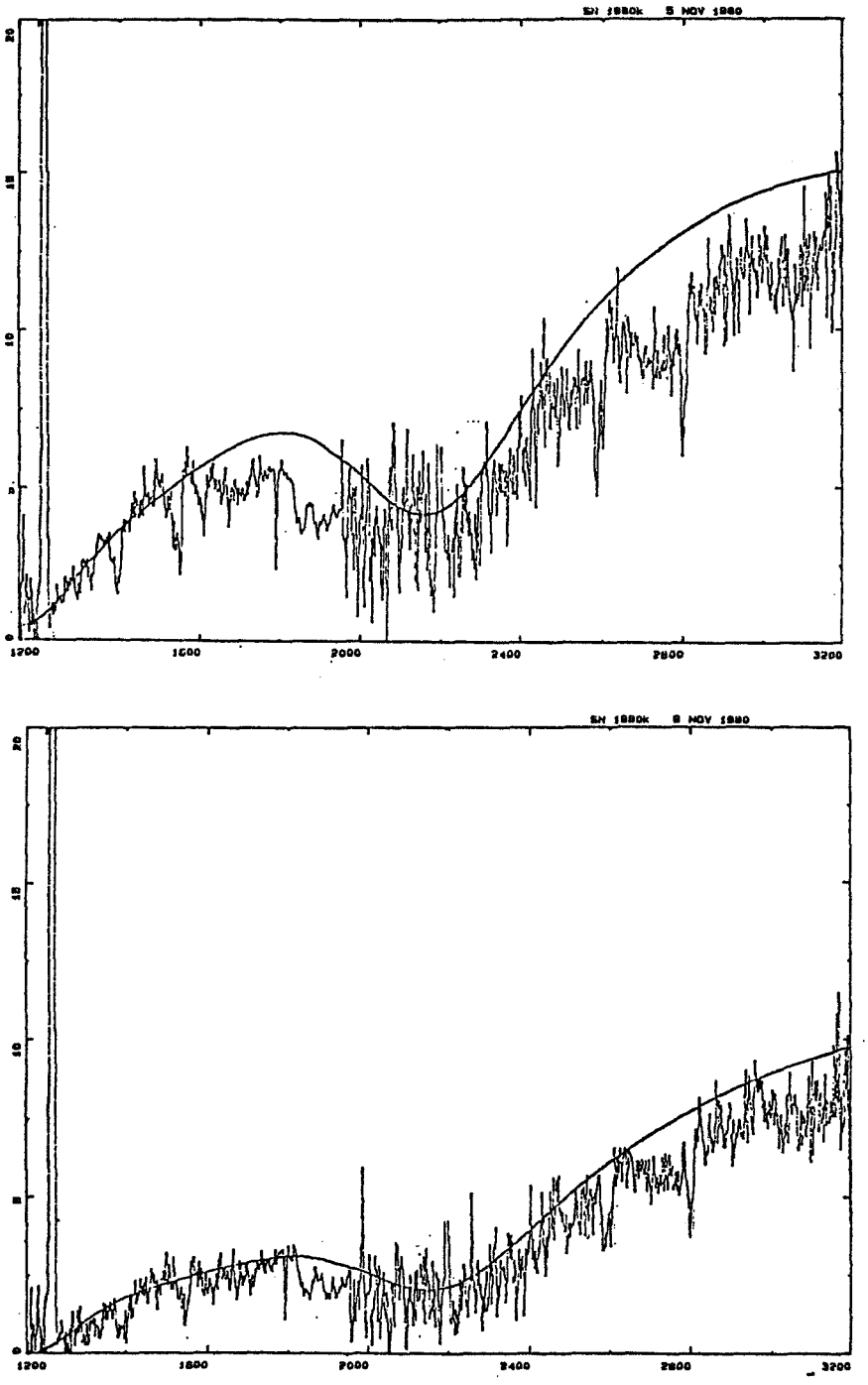

Fig. 2 - SN 1980k, IUE observations of november 5 and 9, 1980

AN ATLAS OF UV SPECTRA OF SUPERNOVAE

P. Benvenuti[1], L. Sanz Fernandez de Cordoba[2], W. Wamsteker[1]

1) Astronomy Division ESTEC, IUE Observatory, Madrid, Spain
2) Instituto Nacional de Técnica Aerospacial, Madrid, Spain

Three type I and two type II Supernovae have been observed with IUE up to date. The three type I are: SN 1980l in NGC 1316, SN 1981b in NGC 4536 and the one just exploded in NGC 2268. The type II are: SN 1979c in NGC 4321 and SN 1980k in NGC 6946.

A total of 25 short wavelength and 52 long wavelength low dispersion spectra were collected. Four additional spectra in high resolution (two SW and two LW) were obtained for SN 1980k.

These data, as they can be retrieved from the IUE Data Bank, are not homogeneous since different software and calibrations were used in the reduction process.

We have now completed the reprocessing of all the relevant images with the latest version of the Image Processing Software and we intend to publish these data as an Atlas of UV spectra of SNe. The Atlas, which will be edited by ESA as a Special Publication, will contain all the spectra in numerical and graphical formats. The Atlas will also be available on tape in standard IUE format.

CHROMOSPHERES OF CLASSICAL CEPHEIDS

Edward G. Schmidt
Department of Physics and Astronomy, University of Nebraska

and

Sidney B. Parsons[1]
Laboratory for Astronomy and Solar Physics, Goddard Space Flight Center
and McDonald Observatory, University of Texas at Austin

ABSTRACT

We have obtained IUE spectra of five classical Cepheids in both the short wavelength region and in the long wavelength region at low dispersion and in the long wavelength region at high resolution. Ultraviolet light curves and emission line strengths have been obtained from the low resolution spectra. The amplitudes of the light curves increase with decreasing wavelength except around 1550 Å where the amplitude is surprisingly small. The emission line fluxes behave differently in the various stars and it appears that bumps in the ultraviolet light curves are related to the behavior of the chromospheres. However, the strengths of the emission lines are roughly comparable to nonvariable stars of similar temperature and luminosity.

The high resolution spectra have been used to study the fluxes of the emission from the Mg II h and k lines. It is found that the emission components come and go during the cycles and the behaviour differs from one star to another, with generally stronger and more persistent emission at longer periods. This is compared with the times of appearance of the Ca II H and K emission features and gives us insight into the way in which the chromosphere reacts to shock waves generated by the pulsation of the star.

INTRODUCTION

Prior to space astronomy, there was an indication of transient chromospheres for the classical Cepheid pulsating stars through observations of emission in the core of the Ca II K line (summarized by Kraft 1957). The fraction of the pulsation cycle during which emission was evident tends to increase with increasing pulsational period but is not found to exceed 40% of the cycle. Observations with IUE of the bright Cepheids δ Cep (5.37d), η Aql (7.18d), β Dor (9.84d), ζ Gem (10.15d), and ℓ Car (35.5d) by Parsons (1980) and Schmidt and Parsons (1982) have greatly expanded our

---

[1] Senior NRC-NASA Research Associate

knowledge of the behavior of Cepheid chromospheres, which are more persistent and more complex than indicated by the Ca II observations.

LOW DISPERSION RESULTS

The recent paper of Schmidt and Parsons (1982) discusses results from the low dispersion LWR and SWP spectra obtained during the first three years of IUE, which cover many phases of four Cepheids and phases within a few days of maximum light for ℓ Car. Most of the results are summarized in the present abstract and the reader is referred to the published paper for further details, while a few items of note follow.

Except for some phases around 0.75 at which weak emission appears present, δ Cep does not normally show detectable emission at low dispersion in lines such as O I λ1304. The 10-day Cepheids, on the other hand, show definite emission at most phases. In β Dor, λ1304 emission builds to a pronounced maximum from phase 0.7 to 0.8 with a subsequent decline to almost undetectable strength around phase 0.65. The general emission strength is greater in ζ Gem although our phase coverage is less complete; it probably has a similar peak in strength around phase 0.7 to 0.8. The phase of rapid increase in O I emission strength corresponds with increased continuum flux seen as bumps in the mid- to far-UV light curves of these stars.

Mg II EMISSION

Many LWR high dispersion spectra were obtained in order to study the Mg II h and k lines. In addition, nearly simultaneous ground-based observations of the Ca II H and K lines were made in order to increase the phase coverage and sensitivity of previous work; Ca II emission was in fact found at a few phases not noted previously. Because of the greater abundance of Mg than of Ca and the smaller continuum radiation of cool stars in the UV, the Mg II resonance line profiles are more sensitive than Ca II as indicators of chromospheres. In fact we observe significant Mg II emission at all phases of the longer-period Cepheids, whereas the occasional Ca II emission must be sampling transient events near the base of the chromosphere. The optical thickness is much greater in Mg II, so these lines present conditions further from the stellar surface. In δ Cep, the only phase observed with strong Mg II emission is 0.89, delayed from the phases 0.84 - 0.88 of significant Ca II emission.

We have now analyzed the Mg II data for δ Cep in more detail by modelling the photospheric, interstellar, and emission components of the complex and low signal-to-noise profiles. This deconvolution allows much firmer estimates of emission strength than direct inspection. Plotting the results versus phase shows similar behavior to the O I emission of β Dor, but with a much steeper rise, occuring between phases 0.85 to 0.89.

It thus appears from all of the ultraviolet evidence obtained that in each Cepheid, a pulse of energy is delivered to the chromosphere at about the time of maximum outward acceleration of the atmosphere (as derived from the photospheric radial velocity curve). Thereafter the degree of excitation and ionization decreases apparently monotonically for the chromosphere as a whole until the next cycle, while a few "aftershocks" are felt near the surface and manifested as sporadic Ca II emission.

REFERENCES

Kraft, R. P. 1957, Ap. J., 125, 336.
Parsons, S. B. 1980, Ap. J., 239, 555.
Schmidt, E. G., and Parsons, S. B. 1982, Ap. J. Suppl., 48

INTENSITY CHANGES IN THE UV SPECTRUM OF BETA CEPHEI

Richard P. Fahey, David Fischel*, and Warren Sparks
Laboratory for Astronomy and Solar Physics
Goddard Space Flight Center
Greenbelt, Maryland 20771

ABSTRACT

Fifty eight short wavelength IUE spectra were taken over a 152 day period. Variations in the absorption lines of C IV (1550 Å), Si IV (1393 and 1404 Å) and N V (1239 and 1243 Å) and a Cr III feature (1208 to 1211 Å) were observed. A new data reduction technique was developed in order to compare the changes in the equivalent widths of these absorption lines.

Periods were determined by least-squares fit to a sinusoid using several combinations of the data. In one case eighteen spectra for each ion taken at approximately one day intervals were used; in another, all fifty-eight measurements of each were used; and in a third all measurements from all the ions were combined. Using both variable metric and interactive algorithms we have determined that for all combinations mentioned a period of 6.10 $\pm$ .06 days is the best fit to the vector of equivalent widths versus time. No other period, with or without the 6.10 day period removed from the data, was found.

Analysis of the Cr III feature near 1210 Å gives the same period as the others, but in antiphase.

1.0 Introduction

Beta Cephei stars are a small group of short-period, pulsating variables lying in a narrow region just above the upper main sequence. Beta Cephei itself is a B2 III star with a radial velocity variation of a few tens of km/sec^{-1} over a 4 hour 34 minute period.

A 1971 spectrum of Beta Cephei taken with OAO-2 showed variations in several absorption lines (Fischel and Sparks, 1980). Because of the limited resolution of the OAO-2 ($\sim$6 Å) about all that could be determined was that the C IV absorption doublet (1550 Å) disappeared and the Si IV absorption doublet (1400 Å) weakened in a periodic fashion. The period was found to be 6 days with an estimated uncertainty of $\pm$ 0.25 day.

(*) Information Extraction Division, GSFC, Greenbelt, MD. 20771

2.Ø Recent Observations

In October of 1978, eleven SWP spectra of Beta Cephei were obtained from IUE. They were taken at roughly half hour intervals and the higher resolution of IUE allowed a better study of the six day period. Forty-seven additional SWP spectra were obtained in February of 1979 covering an 18 day period. From this latter data set it is possible to select 18 spectra at approximately equal, one day intervals.

Significant variations were observed in the absorption lines C IV (155Ø Å), Si IV (1393 and 14Ø4 Å), N V (1239 and 1243 Å), and a Cr III feature (12Ø8 to 1211 Å). There equivalent widths were measured on all 58 spectra of Beta Cephei. No other significant variations were found in the lines of these spectra. The calculations were performed at the Goddard Space Flight Center using a PDP 11/44 computer at the Interactive Astronomical Data Analysis Facility (IADAF).

3.Ø Analysis Method

In order to measure the same absorption feature on many different spectra with maximum consistancy, the best method seems to be : a) normalize each spectrum to "the same" flux level and b) make the equivalent width measurement in exactly the same way on each spectrum. However, precisely because the features in question vary in intensity, this approach must be modified.

For the present analysis, the following procedure was used. First, the echelle order containing the line to be measured was displayed on the video screen such that 18 observations at one day intervals were superimposed. Visual inspection indicated, for each line analysed, a region of 1ØØ or more data points that showed little or no change from one day to the next. Each spectrum was next multiplied by a factor that left that unchanging region at the same level on each of the 58 spectra. Then it was possible to have the computer calculate the equivalent width between the same two wavelengths and with the same reference "continuum" on all 58 spectra as a single, one minute procedure.

4.Ø Period Determination

A least-squares fit to a sinusoid using the language APL on a IBM 36Ø/65 at GSFC was performed using both the variable metric Davidon-Fletcher-Powell algorithm (Fletcher and Powell, 1965) and a rapid, interactive program (Fahey, 198Ø) which searches the 4-dimensional hypersurface coarsely for minima. Both programs give the same results with essentially the same uncertainties.

5.Ø Results

Intensity variation in C IV, Si IV, N V, and Cr III all occur with the same period of 6.1Ø ± .Ø6 days, regardless of size of sample tested (e.g., Figure 1). From Figure 2 it is clear that, not only the equivalent width, but also the profile of C IV λ155Ø is variable. Profile changes are less obvious for Si IV 1393 and N V λ1243, but in both cases it appears that part of the change in equivalent width is due to the presence or lack of emission at the redward edge of the feature.

The Cr III λ12Ø8 line is in an area seen to vary strongly (Figure 3 and 4) in both flux and slope. Although the period for this variation is 6.1Ø ± .Ø6 days as with the other lines, the variation is in anti-phase. Similar behavior has been reported (Fahey, 1981) in the B2 V helium variable a Centauri. The Cr III line at 12Ø8 Å is the strongest Cr III line within the range of IUE sentivity, and lies very close to several Mn III lines as well as the Cr III λ121Ø. This line is part of the wing of the Si III λ12Ø5 double singlet. Earlier studies by Fischel and Sparks (1972, 1981) attributed the variations in this region to the Si III line.

6.Ø Conclusions

The strong changes of 6 day period in UV features of Beta Cephei reported here are not related to the four and a half hour, short-period variation. Rather, it appears to be a feature of the behavior of the outer atmosphere, and may indicate temperature or pressure inhomgeneities of non-radiative origin.

7.Ø References

Fahey, R. P. 198Ø, Ph. D. Thesis, Catholic University of America, Washington, D.C.

_____, 1981, "Variations in the UV Spectrum of a Centauri", in The Universe at Ultraviolet Wavelengths, ed. R. D. Chapman, pp. 177-184, NASA Conference Publication 2171.

Fischel, D. and Sparks, W. M. 1972, "Ultraviolet Observations of Beta Canis Majoris and Beta Cephei", in Scientific Results from the Orbiting Astronomical Observatory (OAO-2), pp.475-78, NASA SP-31Ø.

_____, 1981, "Line Strength Variations in Beta Cephei", in The Universe at Ultraviolet Wavelengths, ed. R. D. Chapman, pp. 217-244, NASA Conference Publication 2171.

Fletcher, D. and Powell, M. J. D. 1963, Computer Journal, 6, 163.

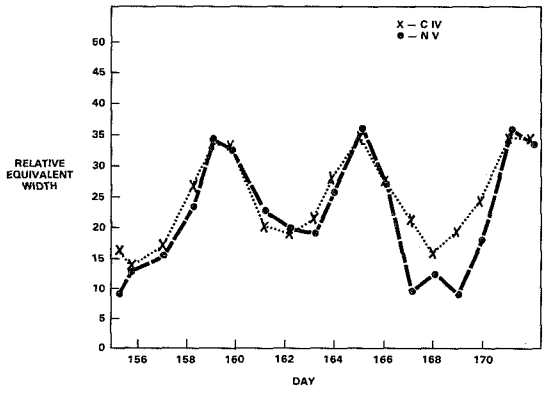

Fig. 1 Normalized equivalent widths of C IV 1550 A and N V 1239 A vs. time.

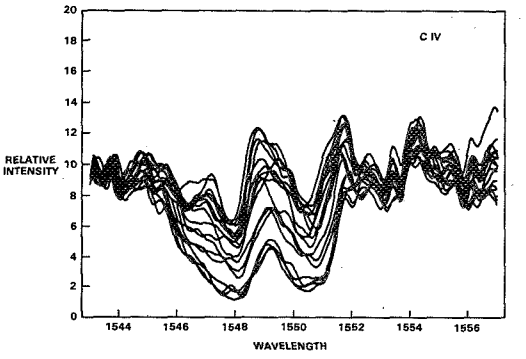

Fig. 2 Superposition of normalized intensitites of C IV 1550 A from 18 spectra of Beta Cephei taken at one day intervals.

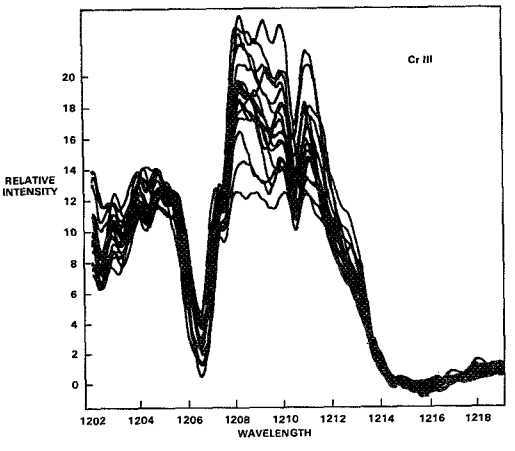

Fig. 3 Superposition of normalized intensities of Cr III 1208 A region from 18 spectra of Beta Cephei taken at one day intervals.

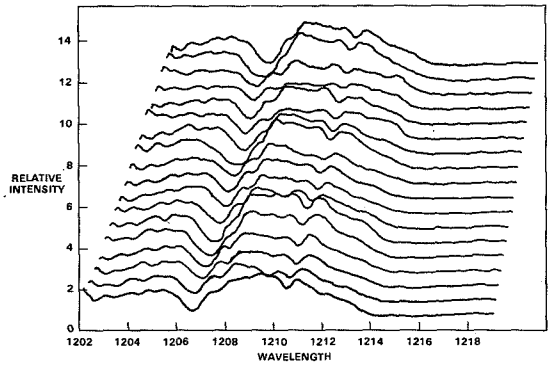

Fig. 4 Spectra from Fig. 3 displayed in time sequence with first at bottom.

THE HIGH VELOCITY SYMBIOTIC STAR AG DRACONIS AFTER ITS 1980 OUTBURST

R. Viotti[1], A. Altamore[2], G.B. Baratta[3], A. Cassatella[4], M. Friedjung[5], A. Giangrande[1], D. Ponz[6], O. Ricciardi[1]

1 Istituto Astrofisica Spaziale, CNR, Frascati, Italy
2 Istituto Astronomico, Universita di Roma, Italy
3 Osservatorio Astronomico, Roma, Italy
4 Astronomy Division, ESA, Villafranca, Spain
5 Institut d'Astrophysique, Paris, France
6 ESO, Garching Bei Munchen, West Germany

Extensive high and low resolution spectra of AG Dra (BD+67°922) were obtained in 1981 when the star was in an active phase, following a long period of relative quiescence. The variability of the UV energy distribution from 1979 to 1981 is shown in Fig. 1.

The UV spectrum of AG Dra is characterized by prominent high ionization emission lines superimposed on a strong continuum. At high resolution, several intense absorption lines of interstellar origin are seen, in spite of the low interstellar extinction (E(B-V)=0.06, as derived from the 2200 A feature and from the width of Lyα).A similar situation is displayed by the high galactic latitude sdO stars. The radial velocity difference between the emission lines and the i.s. lines is about -105 Km/sec in agreement with the optical observations. This is seen in Fig. 2 where the MgII emission lines appear strongly mutilated by the interstellar lines so simulating an inverse P Cygni profile.

The He II 1640 A line appears much stronger than in other symbiotic stars and suggests the presence of a hot (10^5°K) source which is variable according to the activity of the star. The line also exhibits broad emission wings which could be formed in a rotating disk.

The NV resonance doblet displays a P Cygni profile and is probably formed in a warm wind.

Two components can be identified in the UV continuum: a steep component dominating the far UV probably associated with the hot source, and a flatter continuum in the near UV which cannot be accounted for by f-f and f-b emission alone, but it is probably emitted by an optically thick region or disk.

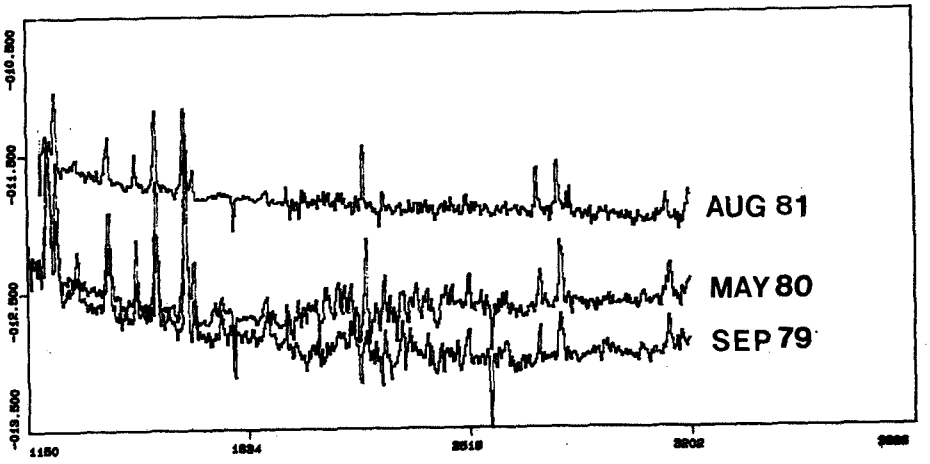
AUG 81
MAY 80
SEP 79

FIG. 1

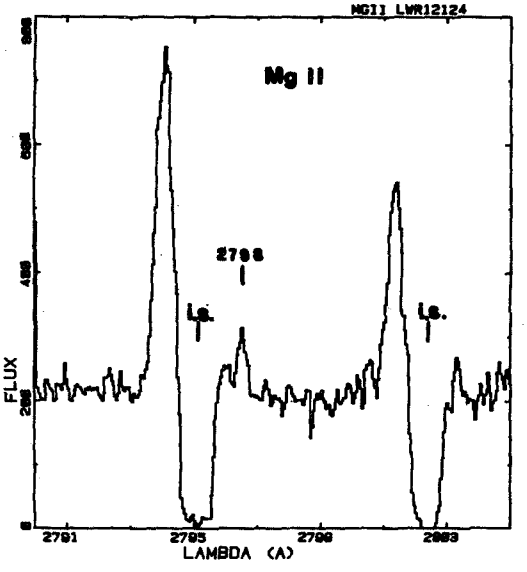
MGII LWR12124
Mg II
2798
Ls.
Ls.
FLUX
2791
2795
2799
LAMBDA (A)

FIG. 2

LOW RESOLUTION ULTRAVIOLET AND OPTICAL SPECTROPHOTOMETRY OF SYMBIOTIC STARS

Mark H. Slovak
Department of Astronomy
University of Wisconsin

ABSTRACT

Low resolution IUE spectra combined with optical spectrophotometry ($\Delta\lambda$ = 7.5 Å) provide absolute flux distributions for seven symbiotic variables from 1200 to 6450 Å. For five stars (EG And, BF Cyg, CI Cyg, AG Peg, and Z And) the data are representative of the quiescent/out-of-eclipse energy distributions; for CH Cyg and AX Per, the observations were obtained following their latest outbursts in 1977 and 1978, respectively. The de-reddened distributions reveal a remarkable diversity of both line spectra and continua. While the optical and near infrared regions ($\lambda > 5500$ Å) are well represented by single-component stellar models, multi-component flux distributions are required to reproduce the ultraviolet continua.

INTRODUCTION

A program of combined ultraviolet and optical spectrophotometry of a selected sample of symbiotic stars has been pursued over the past four years. Multiple low resolution IUE spectra have been obtained; these have been combined with comparable optical data taken with the cassegrain Digicon spectrograph (Tull, Vogt, and Kelton 1979) at the McDonald Observatory. The combined spectrophotometry for CH Cyg, CI Cyg, and AG Peg appear in Figure 1, illustrating the diverse extremes in both line emission and continuum appearance displayed by the symbiotics.

Since the ultraviolet and optical observations are not contemporaneous and as no overlap exists between them, the data were merged in the following fashion: (i) the optical fluxes were scaled so that they yielded the FES V magnitude at the time the IUE spectra were obtained, and (ii) continuity was demanded across the region where no overlap exists (at the end of the LWR bandpass at 3300 Å and the beginning of the optical data at 3400 Å). The combined data were then de-reddened using estimates of E(B-V) from the 2200 Å feature and the extinction curve of Code et al. (1976).

ANALYSIS

The attempt to interpret the continua of symbiotics poses a difficult deconvolution problem, as the individual components cannot be inferred from other observations (e.g. eclipses, orbital solutions) with any degree of certainty. For the S-type, or stellar, symbiotics (Allen 1979), the late-type component appears to be a relatively undisturbed giant, and as seen in Figure 2, the observations are well reproduced longward of 5500 Å by such distributions. CH Cyg shows the coolest continuum, approximated by an M6III star; CI Cyg and AG Peg are even better matched by the continuum for an M3III star.

In general, however, an analysis of the ultraviolet continuum apart from the emission line spectrum leads to specious results. Color temperatures of 30,000 - 40,000 K have been derived from OAO-2 as well as IUE data by Gallagher et al. (1979) and Keyes and Plavec (1980), respectively, for AG Peg: Figure 2(a) confirms these results, where good agreement is found upon comparing the observations to the flux distribution of an O9 star (T_{eff} = 30,000 K). Yet the Zanstra temperature estimated from the HeII (1640 Å) line indicates a hot source with T_{eff} = 90,000 K. Figure 2(b) shows the residual flux distribution that arises upon removing the combined contribution of a cool giant ($L/L_{\odot}$ = 426, T_{eff} = 3200 K) together with a hot star ($L/L_{\odot}$ = 366, T_{eff} = 90,000 K). Ignoring the U and B fluxes, contaminated by strong line emission, the distribution in Fig. 2(b) displays the characteristic rise and peak at 3650 Å of Balmer free-bound continuum radiation, and strongly suggests that the excess flux in this region has its origin from this process rather than from an accretion disk. A detailed model of this flux distribution is now being explored using the nebular code described in Harrington, Lutz, and Seaton (1981) and kindly provided by M. J. Seaton.

A similar analysis of AG Draconis can be further constrained using the X-ray observation of Anderson, Cassinelli, and Sanders (1981). Using only IUE continuum fluxes, a color temperature of T_{eff} = 15,500 K is indicated (Slovak 1982) for the hot component. Using all the data, and assuming the X-rays have a thermal origin, reveals that a best fit is obtained for a hot source having $L/L_{\odot}$ = 196 and T_{eff} = 200,000 K. Again, the residual flux distribution shows the defining features attributable to Balmer free-bound continuum radiation.

SUMMARY

Color temperatures inferred from the ultraviolet continua of symbiotics seriously underestimate the actual temperatures deduced from both Zanstra type estimates and from detailed modeling. The ultraviolet data alone, however, are insufficient to provide a unique solution and both EUV and additional X-ray observations are required.

REFERENCES

Allen, D.A., in IAU Colloq. No. 46, 125.
Anderson, C.M., Cassinelli, J.P., and Sanders, W.T. 1981, Ap.J.(Letters), 247, 127.
Code, A.D., Davis, J., Bless, R.C., and Brown, R.H. 1976, Ap.J., 203, 417.
Gallagher, J.S., Holm, A.V., Anderson, C.M., and Webbink, R.F. 1979, Ap.J., 229, 994.
Harrington, J.P., Lutz, J.H., and Seaton, M.J. 1981, M.N.R.A.S., 195, L21.
Keyes, C.D., and Plavec, M.J. 1980, in IAU Symp. No. 88, 535.
Slovak, M.H. 1982, Unpublished Ph.D. dissertation, Univ. of Texas.
Tull, R.G., Vogt, S.S., and Kelton, P.W. 1979, S.P.I.E., 172, 90.

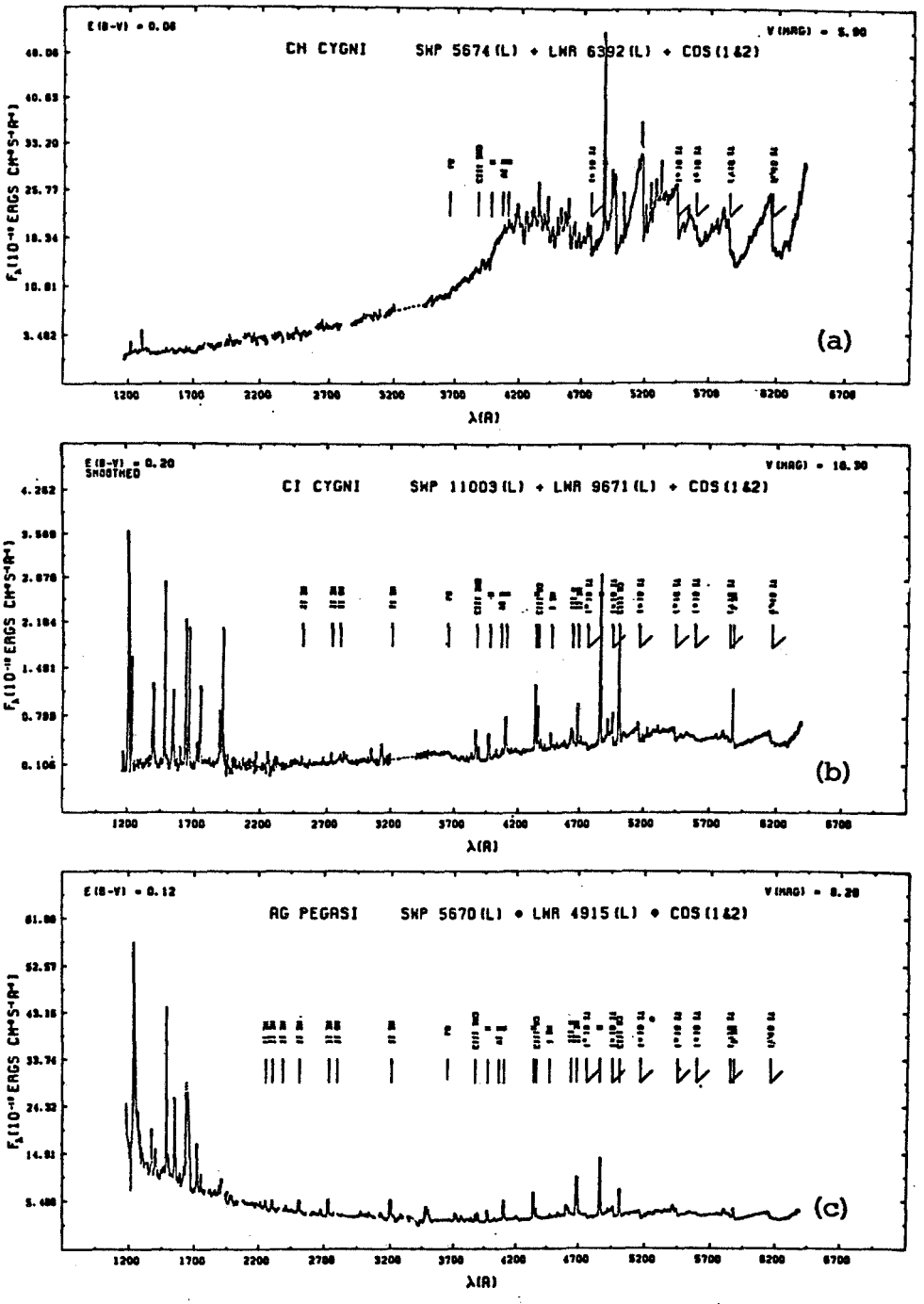

Figure 1 - Combined ultraviolet and optical spectrophotometry for three of the symbiotics in the survey: (a) CH Cygni following its 1977 outburst, (b) CI Cygni outside of primary eclipse, and (c) AG Pegasi in relative quiescence. The fluxes were dereddened using E(B-V) as estimated from the 2200 A feature. Dotted line near 3300 A indicates region where no overlap exists between the ultraviolet and optical data. Various emission lines are indicated as well as the strong TiO bandheads. Note emission "bump" in CI Cyg at 3650 A.

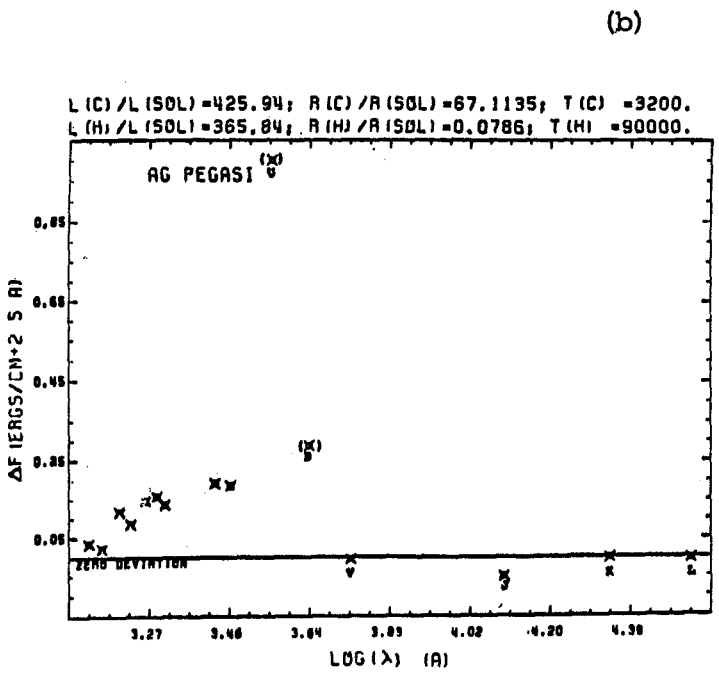

Fig. 2(b) - Residual flux distribution for AG Pegasi. Both a cool giant ($L/L_\odot$ = 426, T_{eff} = 3200 K) and a hot star ($L/L_\odot$ = 366, T_{eff} = 90,000 K) have been subtracted from the energy distribution in Fig. 2(a). The residual fluxes rise and peak near λ3650 Å, a signature of Balmer free-bound continuum radiation from the surrounding nebula.

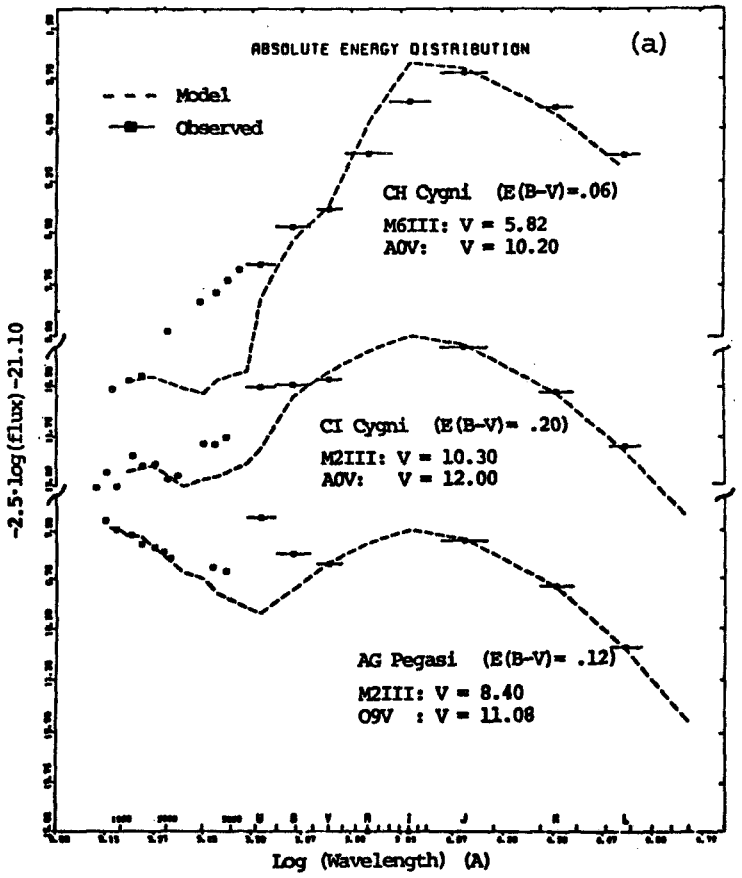

Fig. 2(a) - Mean continuum fluxes compared to composite stellar distributions. Note large excess flux between λ3000 - 3600 A. The broadband U and B fluxes are contaminated by emission lines in CI Cyg and AG Peg.

OBSERVATIONS AND ANALYSIS OF THE R AQUARII JET

Minas Kafatos
and
Andrew G. Michalitsianos
Laboratory for Astronomy and Solar Physics
NASA Goddard Space Flight Center
Greenbelt, Maryland

ABSTRACT

Ultraviolet, optical and radio observations of the symbiotic star R Aquarii are discussed in the light of the discovery of a bright radio and optical jet from this star. The star is probably a binary with a period of 44 years. The VLA maps of the jet reveal a protruding structure extending $\sim$10 arc sec from the central radio source with a position angle virtually identical to that of the optical jet observed at Lick. We interpret the observations of R Aqr as indicating the existence of an accretion disk around an unseen companion. The hot subdwarf has effective temperature $\lesssim$65,000 K. We believe that the Mira primary and the hot secondary are in orbit around each other with a high eccentricity. At periastron the hot subdwarf accretes at super critical rates and a jet forms. It is difficult to understand how an accretion disk would have eclipsed the Mira in 1928-1935 and 1974-1980. We prefer to interpret the suppression of maximum light in these two periods as due to a distortion of the Mira envelope at periastron by the tidal interaction with the secondary. The jet may help to explain the excitation of the R Aqr nebula. It is possible that R Aqr flared up as a nova $\sim$1000 years ago forming the nebula.

INTRODUCTION

R Aquarii is a symbiotic system which contains a Mira variable having a period of 387 days. The system has long been known to be surrounded by a complex emission nebulosity. Outward motion of this nebulosity was suspected by Hubble (1940 and 1943) and confirmed by Baade (1943, 1944) who estimated an ejection of the nebula about 600 years ago. There is also nebulosity much nearer the star, variable to some extent in both brightness and structure; it tends to be extended north and south of the star, at right angles to the outer arcs. A new feature of this inner nebulosity appeared between 1970 and 1977, in the form of a jet or spike extending approximately 10 arc sec toward position angle 24 degrees. It was observed by Wallerstein and Greenstein (1980) and by Herbig (see Sopka et al. 1982). The same jet has also been observed in radio waves at 6 cm and possibly at 2 cm (Sopka et al. 1982). At 6 cm its intensity is $\sim$ 25% of the primary source at R Aqr itself. Moreover, in a wider field a spatially unresol-

ved source has been detected approximately 3 arcmin from R Aqr close to the axis defined by the jet. The morphology of the jet at 6 cm is strikingly similar to that seen in the near ultraviolet direct plate obtained at the Lick Observatory. On the 1960 Lick plates obtained by Herbig (Sopka et al. 1982) the brightest features of the inner nebulosity are the three knots or condensations A, B, C, and a peculiar, horseshoe-shaped loop opened toward the star and extending about 8" south. The most recent plates were taken on October 18, 1980. Mrs.Janet Mattei has kindly informed us that AAVSO observations show that minimum light occured on October 21, 1980. In the 1980 Lick exposures a bright jet projecting slightly east of north is apparent. It extends about 10" in both the red and ultraviolet plates toward position angle 22^0 and it is an order of magnitude brighter than any other part of the inner or outer nebulosity. Wallerstein and Greenstein (1980) reported detecting a "spike" of emission nebulosity extending north of Aqr at the time of the deep minimum of September 1977. It is clear that the spike must have appeared between 1970 and 1977. A series of spectrograms taken of the spike at the Coudé focus of the 120-inch telescope reveal a mean spike velocity -71 $km_1 s^{-1}$ (heliocentric) in the mean, while knot B shows a mean velocity of -24 km s^{-1}.

The ultraviolet IUE observations of R Aqr by Michalitsianos, Kafatos and Hobbs (1980) have been re-interpreted in the light of the higher extinction, E_{B-V} = 0.65 (Wallerstein and Greenstein 1980). We find that the size of the inner, high density nebula responsible for the IUE lines and continuum has a radius of $\sim 2.5 \times 10^{14}$ cm and electron density $n_e \sim 5 \times 10^6$ cm^{-3}. If a hot subdwarf is responsible for the photo-excitation of this nebula its effective temperature has to be less than 65,000 K to account for the weakness or complete abscence of He II emission and most probably $T_{eff} \lesssim 35{,}000$ K. Its luminosity is 14 $L_\odot$ and it is located in the lower part on the H-R diagram occupied by central stars of planetary nebulae.

DISCUSSION

Merrill (1935, 1950) discussed the behavior of R Aqr in 1919 -1949. He finds from the radial velocities of the nebular lines in 1920-1950 that the eccentricity of the orbit is high (e = 0.5). Willson, Garnavich and Mattei (1981) have studied the light of the Mira in the last 100 years and find that the maximum of the Mira was suppressed in the late 20's-early 30's and again in the late 70's. They interpret this effect as an eclipse of the Mira by a cloud. From the duration of the "eclipse" of $\sim$8 years they conclude that the eclipse should have taken place at apoastron in a highly elliptical orbit. They find an orbital period of 44 years. We believe this period but we have difficulty in accepting the simple eclipse interpretation. If the eccentricity of the orbit is high (say e = 0.85, see below) then for a 44 year period and a combined mass of the two stars of 2.5 $M_\odot$ we find that the minimum size of the occulting disk or nebula is obtained if the line of sight to the earth is along the major axis of the ellipse and the eclipse takes place at apoastron. This size is $\sim$ 2 R_1 where the index "1" refers to the Mira. This value is similar for other masses of the system stars. What kind of gas (presumably disk) could eclipse a Mira? We find that the luminosity of the disk should be not more than $\sim$ 1/5 of the Mira luminosity and it should be spatially thick ($h/r \gtrsim \frac{1}{2}$). The disk temperature in the outer regions should then be appreciably less than

the effective temperature of the Mira, T_{eff} = 2800 K (Willson 1981). Such cool extended disks are difficult to envisage around a hot subdwarf. Moreover, the IR brightness of such a disk would be in excess of the Mira. We favor an interpretation where the suppression of the light of the Mira occurs near periastron and is due to the distortion of the Mira envelope by the compact secondary. Due to the extended shape of the Mira envelope, we can see further into the Mira atmosphere than normally and, therefore, the Mira appears smaller and less luminous. We emphasize that the radial curves of Merrill (1950) indicate that the timing of the suppression of the Mira light occured much closer to the periastron of 1940.

The extended nebula is still expanding with a velocity of 50 - 100 km s^{-1} (see Hubble 1940, 1943). From the densities of Wallerstein and Greenstein (1980) and using a filling factor of 0.1 for the nebula we find an average electron density in the nebula $\langle n_e \rangle \gtrsim 10^4$ cm^{-3}. The mass of the nebula is $\sim 0.2\ M_\odot$ and its kinetic energy greater than 2×10^{46} erg. We note that typical nova light outputs are in the range 10^{44} - 10^{45} erg (Payne-Gaposchkin 1964) while they are $\sim 10^{45}$ for slow novae, RR Tel and RT Ser which may be more closely associated to R Aqr. The nebula radiates more than 5×10^{44} erg every year in Balmer, Lyman continuum and lines! The cooling timescale of the nebula is $\sim$ 2 years and one may ask what powers the nebula at least 600 years after the outburst that produced it. A hot star would have to be much brighter than the Mira and would be radiating in excess of the Eddington limit for 1 $M_\odot$. We suspect that the jet may help to power the nebula. Taking a minimum size of the jet of 7", corresponding to a linear size of $\sim 2 \times 10^{16}$ cm, and assuming that it travelled that distance since 1970 we find a jet velocity of 700 km s^{-1}. If the mass of the jet is a few $\times 10^{-5}$ $M_\odot$-as result of supercritical accretion lasting a few years near periastron-we find a kinetic energy of the jet at present of a few $\times 10^{44}$ erg. Such jets forming approximately twice a century could deposit enough energy in the last hundreds of years to possibly explain the high excitation state of the nebula.

What is the origin of the jet? We attribute it to a supercritical accretion onto a compact secondary (cf. Bath 1977). We have modelled accretion disks around a 10^9 cm hot subdwarf and we find that the disk would be characterized by drift velocities of $\sim 6.5\ \alpha$ km s^{-1}, where α is the usual viscocity parameter (Shakura and Sunyaev 1973). For a reasonable value $\alpha \sim 0.1$ the disk would last about 10 years. From Willson (1981) we find that the radius of the Mira $R_1 \sim 300\ R_\odot$, its mass $M_1 \sim 1.5\ M_\odot$. It follows that the Mira fails to fill its Roche lobe by at least a factor of 5. The possibility remains, however, that the orbit is higly elliptical and the Mira fills its Roche lobe only at periastron, while during the rest of the orbit, the secondary accretes material from the cool stellar wind expelled from the Mira. The presence of the jet suggests the existence of a well developed accretion disk if R Aqr is similar to other stellar objects with jets such as SS 433 (cf. Margon 1982). The compact star would be accreting material from the disk at super-Eddington values if the mass accretion rate is larger than 4.3×10^{-5} $M_\odot$ yr^{-1}. Such large rates would occur if the orbit is highly elliptical ($e \gtrsim 0.84$) and the periastron is $\sim$ 1 to 2 times the radius of the Mira. The appearance of the jet $\sim$ 44 years after the outburst of 1928-1935 would then be indeed tied to the orbit of the two stars. Such a disk and jet would make an excellent Space Telescope target because of

the proximity of R Aqr. At B wavelengths the disk would be about 3 magn brighter than the Mira at minimum light.

The nebula must have been ejected about 550 - 1100 years ago for a distance of 200 pc and a radius of 1'. We find that the only recorded nova outburst in historical times from the Chinese and Japanese records was that of 930 A.D. (Hsi Tsê-tsung 1958; Pskovskii 1972). The outburst is described as "guest star entering Yŭlin". Yŭlin is a faint ancient Chinese asterism in Aquarius. The term "entering" could mean "at the edge of" (Clark, private communication). The approximate coordinates of the guest star of 930 A.D. are R.A.~ 23 h, Dec~ -20°, within 10° of R Aqr and near the edge of Yŭlin. The probability of finding a random nova inside Yŭlin-and near R Aqr-is extremely small (R Aqr is 70° below the galactic plane), less than 0.02 in the last 1000 years. It is, therefore, highly probable that the 930 outburst is associated with the R Aqr outburst that produced the extended nebula. If this is correct, it would be the first nova-like outburst that is tied to the Chinese records.

REFERENCES

Baade, W. 1943, Ann. Rep. Dir. Mt. Wilson Observ., 1942-43, 17.
_____. 1944, Ann. Rep. Dir. Mt. Wilson Observ., 1943-44, 12.
Bath, G.T. 1977, M.N.R.A.S., 178, 203.
Hsi, Tsê-tsung 1958, Smithson. Contr. Astrophys., 2, 109.
Hubble, E.P. 1940, Ann. Rep. Dir. Mt. Wilson Observ., 1939-40, 19.
_____. 1943, Ann. Rep. Dir. Mt. Wilson Observ., 1942-43, 17.
Margon, B. 1982, Science, 215, 247.
Merrill, P.W. 1935, Ap. J., 81, 312
_____. 1950, Ap. J., 112, 514.
Michalitsianos, A.G., Kafatos, M., and Hobbs, R.W. 1980, Ap. J., 237, 506.
Payne-Gaposchkin, C. 1964, The Galactic Novae (Dover Publications, New York).
Pskovskii, Yu.P. 1972, Soviet Astr., 16, 23.
Shakura, N.I., and Sunyaev, R.A. 1973, A.&A., 24, 337.
Wallerstein, G., and Greenstein, J.L. 1980, Pub. Astr. Soc. Pacific, 92, 275.
Willson, L.A. 1981, Physical Processes in Red Giants, edit. I. Iben and A. Renzini, Astrophys. and Space Sci. Library (D. Reidel Publ. Co., Holland), 88, 263.
Willson, L.A., Garnavich, P., and Mattei, J.A. 1981, I.B.V.S., 1961.
Sopka, R.J., Herbig, G., Kafatos, M., and Michalitsianos, A.G. 1982, Ap. J. (Lett.), in press.

CHROMOSPHERES AND CORONAE IN THE T TAURI STARS

Catherine L. Imhoff
Computer Sciences Corporation
Mark S. Giampapa
Harvard-Smithsonian Center for Astrophysics

ABSTRACT

The T Tauri stars exhibit strong far-ultraviolet emission lines of CII, III, IV, OI, SiII, III, IV, and sometimes NV and HeII. We have computed surface fluxes of the lines for several T Tauri stars, drawing upon both our IUE observations and published spectra. The surface fluxes are quite high, typically 10^6 - 10^7 erg cm^{-2} s^{-1}. The FUV lines together account for 0.1% of the stellar luminosity. These results indicate the presence of active, relatively dense chromospheres.

The T Tauri stars showing very strong visual emission spectra exhibit weakened high temperature FUV lines of CIV and NV, as well as HeII which may be produced by X-rays. In the same stars, no X-ray emission was detected with Einstein. Among all the T Tauri stars the X-ray luminosities are deficient by factors of 100-1000 compared to the FUV lines. We argue that the X-ray flux has not been heavily absorbed by circumstellar gas, as has been previously suggested, but that the X-rays are truly underluminous, perhaps due to the stellar wind. We suggest that we may be witnessing the birth and development of the chromosphere and corona during the T Tauri stage of protostellar evolution.

DISCUSSION

The T Tauri stars are pre-main sequence stars of roughly solar mass and ages of a few million years. It is thought that most if not all low- to intermediate-mass stars go through a "T Tauri" phase of evolution. Thus the properties and peculiarities of these stars are in all likelihood connected with their youthful nature.

We have employed IUE observations of the T Tauri stars to investigate the stars' nascent chromospheres, transition regions, and (indirectly) coronae. This paper is a brief summary of an extensive paper describing our results currently in preparation for publication.

Published spectra for eight T Tauri stars were compiled for this investigation (Appenzeller and Wolf 1979, Appenzeller et al. 1980, Brown et al. 1981, Gahm et al. 1979, Gondhalekar et al. 1979, Imhoff and Giampapa 1980, 1981). By appropriate choices of spectral types, luminosities, and extinction, surface fluxes for the FUV lines may be computed (see Table 1). We find that the surface fluxes of the stronger emission lines are typically 10^6 to 10^7 erg cm^{-2} s^{-1}, or several thousand times the solar values. These surface fluxes equal and exceed those found for other late-type stars. We note that if the emission originates in plages or active regions the local surface fluxes are even higher.

The proportion of the stellar luminosity contributed by the FUV lines is large, typically 0.1-0.2%. Giampapa et al. (1981) found a similar contribution by the very strong MgII h and k lines. If the CaII and Balmer lines are included, then as much as 1% of the stellar luminosity may be emitted in the chromospheric and transition-region lines. A very high degree of direct, non-radiative heating is thus required (Cram et al. 1980).

We find that the high temperature lines of CIV and NV are weakened relative to the other FUV lines in some of the T Tauri stars. In addition the HeII, FeII 1640 feature is weakened or absent in the same stars. These "strong emission" T Tauri stars are characterized by strong visual emission lines of HI, CaII, and FeII and, we note, by the lack of detectable X-ray emission. The "weak emission" T Tauri stars exhibit CIV, NV, and HeII emission lines in fairly normal relative strengths and were detected in the X-ray region with the Einstein satellite.

About four dozen T Tauri stars were observed with Einstein, of which about one third were detected (Feigelson and DeCampli 1981, Gahm 1980, Walter and Kuhi 1981). Typical X-ray luminosities of the detected stars are 10^{30}-10^{31} erg s^{-1}; L_x/L_{bol} is typically 10^{-4}. The X-ray emission appears to be a few orders of magnitude underluminous compared to other late-type stars if one scales by the strength of MgII or the FUV lines (compare Ayres et al. 1981).

It has been suggested that the X-ray flux from the T Tauri stars is heavily abosrbed by circumstellar gas (Gahm 1980, Walter and Kuhi 1981). If the HeII 1640 line is produced primarily by recombination after X-ray ionization, as indicated in some other late-type stars (e.g. Hartmann et al. 1980, Ayres et al. 1981), then the intrinsic X-ray luminosities must be on the order of 10^{32} erg s^{-1}. Thus 90 to 99% of the X-ray flux would be absorbed in the circumstellar envelope.

No reliable estimate of the gas column density has been made. But several lines of reasoning indicate that the X-ray luminosities are not so large: (1) The observed X-ray luminosities alone equal the highest values of L_x and L_x/L_{bol} found for active coronal late-type stars (Walter et al. 1980); (2) The observed correlation between vsini and L_x followed by late-type stars (Pallavicini et al. 1981) is met if the observed X-ray luminosities are correct but badly violated if the higher values are used; (3) The circumstellar envelope must be dust-free or high visual extinction results; (4) Simple computations indicate that the HeII line may be collisionally produced; and (5) The observed weakening of HeII, NV, and CIV in the "strong emission" T Tauri stars goes unexplained. Thus we conclude that the true X-ray luminosities are probably not much different from the observed luminosities.

Whether the HeII line is produced through recombination after X-ray ionization or collisionally, its disappearance from the ultraviolet spectra of the "strong emission" T Tauri stars , along with the weakening of NV and CIV, signals a reduction or absence of high temperature gas in the atmospheres of these stars. These same stars possess fairly massive winds ($\dot{M} \sim 10^{-9}$ to 10^{-8} $M_\odot$/yr) which may carry off the energy that normally produces a corona. Even in the "weak emission" T Tauri stars, the X-ray luminosities are reduced by 100 to 1000 times compared to what one would expect judging from the transition-region lines. Thus even in these stars the wind probably dominates the energy balance in the outer atmosphere. One might picture

the stars as surrounded by one huge "coronal hole".

It is tempting to associate these remarkable atmospheres with the pre-main sequence evolutionary status of the T Tauri stars. Could we be witnessing the birth and development of the chromosphere and corona during the T Tauri stage of evolution? This is an exciting possiblity that we will continue to explore.

REFERENCES

Appenzeller, I., Chavarria, C., Krautter, J., Mundt, R., and Wolf, B. 1980, Astron. Ap., 90, 184.

Appenzeller, I., and Wolf, B. 1979, Astron. Ap., 75, 164.

Ayres, T. R., Marstad, N. C., and Linsky, J. L. 1981, Ap. J., 247, 545.

Brown, A., Jordan, C., Millar, T. J., Gondhalekhar, P., and Wilson, R. 1981, Nature, 290, 34.

Cram, L. E., Giampapa, M. S., and Imhoff, C. L. 1980, Ap. J., 238, 905.

Feigelson, E. D., and DeCampli, W. M. 1981, Ap. J. (Letters), 243, L89.

Gahm, G. F., Kredga, K., Liseau, R., and Dravins, D. 1979, Astron. Ap., 73, L4.

Gahm, G. F. 1980, Ap. J. (Letters), 242, L163.

Giampapa, M. S., Calvet, N., Imhoff, C. L., and Kuhi, L. V. 1981, Ap. J., 251, 113.

Gondhalekar, P. M., Penston, M. V., and Wilson, R. 1979, in The First Year of IUE (ed. A. J. Willis), p. 109.

Hartmann, L., Dupree, A. K., and Raymond, J. C. 1980, Ap. J. (Letters), 236, L143.

Imhoff, C. L., and Giampapa, M. S. 1980, Ap. J. (Letters), 239, L115.

Imhoff, C. L., and Giampapa, M. S. 1981, in The Universe at Ultraviolet Wavelengths: The First Two Years of IUE (ed. R. D. Chapman), p. 185.

Pallavacini, R., Golub, L., Rosner, R., Vaiana, G. S., Ayres, T., and Linsky, J. L. 1981, Ap. J., 248, 279.

Walter, F. M., and Kuhi, L. V. 1981, Ap. J., 250, 254.

Walter, F. M., Linsky, J. L., Bowyer, S., and Garmine, G. 1980, Ap. J. (Letters), 236, L137.

TABLE 1

Far-Ultraviolet Emission Line Surface Fluxes for Eight T Tauri Stars

	Surface Fluxes[a]									
Line	T Tau	DR Tau	RW Aur (1978)	RW Aur (1979)	GW Ori	CoD-35° 10525	RU Lup	AS 205[c] (Case I)	AS 205[c] (Case II)	S CrA
NV 1240	46:			< 3.6	28:	43	3			
OI,SI 1304	110		< 4.7	39	55	98	38			
CII 1335	77		4.7	4.7	28	65	130			
SiIV 1400	120	62	9.4	33	83	43	120	350	2.9	60
CIV 1550	180	230	8.8	19	120	120	100	280	2.9	47
HeII,FeII 1640	40	35		< 2.1	37	29	< 11	85	1.0	< 10
SiII,SI 1813	100	140	19		24	36	120	480	4.8	90
SiIII 1892	25	150	12	62:	14	34	42	170	1.4	77
CIII 1909	57	140	1:		17	34	33	140	1.2	23
MgII 2800[b]	990	170:		1090	> 170	> 430	> 160	2200	54	> 560

Notes to Table 1 - (a) In units of 10^5 erg cm^{-2} s^{-1}. No data indicates low signal-to-noise or, in RW Aur (1979), saturated portion of the spectrum. (b) Taken from Giampapa et al. (1981). (c) Spectral type and extinction uncertain. Case I - K0 and A_v = 3.0 mag. Case II - M0 and A_v = 1.3 .

THE NOVA-LIKE VARIABLE KQ MON AND THE NATURE OF THE UX URSA MAJORIS STARS

Edward M. Sion and Edward F. Guinan

Astronomy Department, Villanova University

ABSTRACT

KQ Mon is a new UX UMa-type nova-like variable discovered by Howard Bond. Optical spectra taken by Bond in 1978 reveal very shallow Balmer absorption lines and He I (λ4471) absorption. Bond also did UBV and high speed photometry in 1978 and early 1981. There has been no evidence of orbital variations but the appearance of the optical spectrum and the presence of low amplitude flickering suggested a strong similarity to CD-42°14462 (=V3885 Sgr) and other members of the UX UMa class. KQ Mon was observed at low dispersion with the IUE satellite. Six spectra taken with the short wavelength prime (SWP) camera are dominated by strong broad absorption lines due to N V, O I, Si III, Si IV, C IV, He II, N IV, and Al III. There is little evidence of orbital phase modulation over the time baseline of our observations. Unlike UV observations of other UX UMa-type objects, KQ Mon exhibits no emission lines or P Cygni-type profiles and the velocity displacements appear to be smaller, suggesting the absence of a hot, high velocity wind characterizing other UX UMa stars. The relationship of KQ Mon to other UX UMa disk stars is discussed and a model is suggested to explain their observed properties and the lack of major outbursts.

INTRODUCTION

In a continuing investigation of the nature of nova-like variables, a new system, KQ Mon, recently discovered by H.E. Bond (1978) was added to our program of study with the International Ultraviolet Explorer Satellite. Bond's (1981) optical spectra revealed very shallow Balmer absorption lines and HeI (λ4471) absorption, while his UBV and high speed photometric observations in 1978 and again in early 1981 revealed no light variations due to possible orbital phase modulation nor was any brightness change expected given the absence of radial velocity variations in the optical spectra. However, Bond's high speed photometry revealed the presence of low amplitude flickering. This observation coupled with the appearance of the optical spectrum and its location near the old novae and white dwarfs in the two color diagram suggested a strong similarity of KQ Mon to the UX Ursa Majoris subset of the nova-like variables (Warner 1976). Analysis of our ultraviolet spectra confirm that KQ Mon shares the UV characteristics of the other UX Ursa Majoris stars.

OBSERVATIONS

KQ Mon has been observed at low dispersion with the IUE satellite on

December 5, 1981 and February 5, 1982. The instrumentation and spacecraft characteristics are described by Boggess et al (1978). We obtained four spectra with the short wavelength prime (SWP) camera, and four spectra with the long wavelength redundant (LWR) camera. The exposure times were 35 minutes and 40 minutes respectively, with the large and small aperture and two of the spectra were trailed.

Using the Fine Error Sensor (FES) photometer, visual magnitudes of +13.06 and +12.97 were obtained in December 1981 and February 1982 respectively while Bond obtained V=+13.06 in 1978, indicating that the light level appears reasonably constant. Broad band color indices for KQ Mon were measured by Bond (1982) to be B-V=+0.08, and U-B=-0.72. The U, B and V magnitudes were converted to absolute flux units using the absolute calibration of Hayes (1980). Since our data tapes from the February 1982 observing run were not available when we went to press, we cannot address here the question of whether line and continuum variations are present due to orbital phase modulation.

In figure 1 a single SWP spectrum typical of the others is shown together with labelled identification of the most important line features. The spectrum is dominated by strong broad absorption lines due to NV, OI + SiIII, SiIV, CIV, HeII and NIV. Possible Lya absorption is obscured by the strong geocoronal feature. The long wavelength (LWR) spectrum appears essentially featureless. No absorption dip is apparent at $\lambda 2200$ indicating that interstellar reddening for KQ Mon is probably small. In figure 2 we plot the unreddened satellite continuum fluxes on a log F_λ vs. logλ (Å) scale along with the broad band U B and V fluxes. On the same figure we show, for comparison, theoretical continuum fluxes from model steady state accretion disks calculated by Williams (1981b) assuming a disk inclination angle i=0 (pole-on). The models shown in figure 2 are normalized to the optical B band flux.

COMPARISON TO OTHER UX UMA STARS

The UV line spectrum of KQ Mon shows strong broad absorption lines of the resonance doublets and excited species but unlike other members of the UX UMa class (e.g. TT Ari LS I 55 8, V 3885 Sgr, RW Sex) they are not appreciably violet-displaced and P Cygni-type emission is entirely absent. Thus a hot wind from the disk driven by X-radiation from the inner disk may be weak or absent in KQ Mon. Moreover, the absorption lines of KQ Mon appear to be somewhat broader than those of LS I 55 8, V 3885 Sgr and RW Sex.

The estimates of mass loss rates due to wind outflow in the UX UMa stars give $\dot{M}_{wind} \simeq 10^{-2}$ to 10^{-4} $\dot{M}_{acc}$ where $\dot{M}_{acc}$ is the mass accretion rate (cf. Guinan and Sion 1982, Greenstein and Oke 1982). The weakness or absence of an outflowing wind in KQ Mon may be due either to (1) a somewhat lower $\dot{M}_{acc}$ than other UX UMa stars (2) accreting gas flowing above and/or below the disk plane or (3) a weak white dwarf magnetic field preventing disk gas from forming a high pressure zone at the equator which could drive the type of polar wind described by Greenstein and Oke (1982), also Witta (1982).

Like other UX UMa stars, the UV continuum is essentially flat from UV to the optical and can be fitted quite well with accretion disk fluxes (see fig. 2). Reddening corrections would shift the fluxes upward in figure 2 toward a higher accretion rate. The accretion rate of KQ Mon probably lies between $10^{-8} M_\odot$ yr^{-1} and $10^{-10} M_\odot$ yr^{-1}.

NATURE OF THE UX URSA MAJORIS STARS

Given the high ionization states of the UV absorption lines and the evidence for mass outflow in most of the UX UMa stars, the following tentative interpretation of the UV line and continuum spectra is suggested based in part on the wind models of Cassinelli Olson and Stalio (1978 cf. section IV, Guinan and Sion 1982). If we assume the X-radiation in these systems emerge from the hot inner disk boundary layer region rather than say a "hot spot" at the disk edge it is likely that the UV resonance doublets such as N V (λ1240), C IV (λ1550) and Si IV (λ1396) arise in an outflowing wind. These high ionization features, seen in combination with a relatively "cool" integrated disk continuum, are similar to the UV spectra of O and B stars with outflowing winds (Cassinelli, Olson, and Stalio). A thin hot corona ($\sim 10^6$K) at the base of the flow in the boundary layer region provides the X UV photon source needed for the high ion states. The high ionization stages can be produced by the Auger mechanism, whereby two electrons are removed from C, N and O following K shell absorption of X-rays. Greenstein and Oke (1982) have independently proposed for RW Sex that an outflowing wind from the disk is driven by X-radiation, with the gas in conical geometry at the poles of the degenerate dwarf. They propose a broad cone while Guinan and Sion (1982) did not specify the geometry. In either case the outflowing gas is seen silhouetted against a luminous disk for a large range of orbital inclinations which explains the appearance of the blue-shifted absorption lines and P Cygni-type features observed in a number of UX UMa stars. It is likely that when the accretion rate $\dot{M}$ is high, X UV quanta do not penetrate to the disk edge because the accretion flow is optically thick to that flux region. When the disk luminosity declines (i.e. $\dot{M}$ decreases), it is predicted that mass loss should cease, the absorption lines formed in the wind should disappear, the continuum should fade and the UV line spectrum should go into emission with the high excitation UV emission lines originating in a "chromosphere" surrounding the inner disk region (cf. TT Ari; Krautter et al 1981). The site of this "chromosphere" is predicted to be the upper parts of the disk atmosphere more than one scale height from the central plane of the disk. When $\dot{M}$ again increases, the boundary layers' luminosity goes up and the UV spectrum again goes into absorption and an outflowing wind may again be driven.

That UX UMa stars may have higher accretion rates than other types of cataclysmic variables is indicated directly or indirectly by (1) derived accretion rates from continuum fits (e.g. RW Sex, Greenstein and Oke 1982; V 3885 Sgr, Guinan and Sion 1982; TT Ari, Krautter et al 1982), (2) the flat continuum of a luminous, thick disk dominating light from the UV through the optical and IR, (3) the low ratio of L_X/L_{opt} for those UX UMa stars observed with the Einstein satellite (Cordova Mason and Nelson 1981) and (4) the outflowing winds from accretion disks which may manifest a higher boundary layer

luminosity or local super Eddington accretion. It is very likely that the accretion rate of UX UMa stars is higher than, for example, the dwarf novae during quiescence.

We suggest here that the higher accretion rates of UX UMa stars are responsible for their lack of major outbursts. The optical spectra of the UX UMa stars resemble the spectra of dwarf novae in outburst (e.g. Warner 1976) and the UV continuum distribution and line spectra of the UX UMa stars also resemble the UV spectra of dwarf novae in outburst (cf. Krautter et al, 1982). H.E. Bond (1978) described V 3885 Sgr as being in continuous outburst since at least 1899 with only very minor changes in brightness in the last eighty-three years. If the UX UMa stars are in a continuous outburst state, we are led to seek a cause of the extended outburst. There is excellent agreement between our observed fluxes and the disk continuum fluxes of Williams (1981b). Thus the disk physical parameters and accretion rates from Williams (1981a) model grid can be adopted with reasonable validity. The higher accretion rates of the UX UMa stars implies more massive thicker disks with a source of viscosity which allows gas to continually accrete onto the white dwarf photosphere. Vila (1982) has calculated steady disks with high mass fluxes which become convective in their central planes. In these models, convective instability increases as the mass accretion rate increases. We argue here that higher $\dot{M}$ in the UX UMa stars produces disk convection which allows gas to continually dump onto the degenerate dwarf with the release of gravitational potential energy. According to Starrfield (1982) a similar scenario based upon disk calculations in progress is proposed to explain dwarf novae outbursts as due to the transition from an optically thin to an optically thick disk with onset of convection. In summary, we propose that UX UMa stars have higher accretion rates than dwarf novae in quiescence and post-novae and thus are in an extended outburst state until accretion from the companion star ceases or declines to the point that steady disk structure with convection ends.

ACKNOWLEDGEMENTS

It is a pleasure to thank Dr. Robert E. Williams for kindly making available unpublished model accretion disk continuum fluxes for normal and helium-rich compositions. We are very grateful to Dr. Howard Bond for calling our attention to KQ Mon as a possible UX UMa star and providing a finding chart as well as unpublished optical photometry. Useful discussions with Drs. S.G. Starrfield, S.C. Vila and P. Wiita are gratefully acknowledged.

REFERENCES

Bond, H.E. 1978, PASP, 90, 216.
Bond, H.E. 1981, private communication.
Bond, H.E. 1982, unpublished observations.
Boggess, A., et al. 1978, Nature, 275, 372.
Cassinelli, J.P., Olson, G.L., and Stalio, R. 1978, Ap.J., 220, 573.
Cordova, F.A., Mason, K.O., and Nelson, J.E. 1981, Ap.J., 245, 609.
Greenstein, J.L., and Oke, J.B. 1982, Ap.J., in press.

Guinan, E.F., and Sion, E.M. 1982, Ap.J., in press.
Hayes, D.S. 1979, Dudley Obs. Report No.14, p. 297.
Krautter, J., Klare, G., Wolf, B., Duerbeck, H.W., Rahe, J., Vogt, N. and Wargau, W. 1982, Astr.Ap., in press.
Starrfield, S.G. 1982, private communication.
Warner, B. 1976, Observatory, 96, 49.
Williams, R.E. 1981a, Ap.J., 235, 939.
Williams, R.E. 1981b, unpublished models.
Vila, S.C. 1982, unpublished models.
Wiita, P. 1982, private communication.

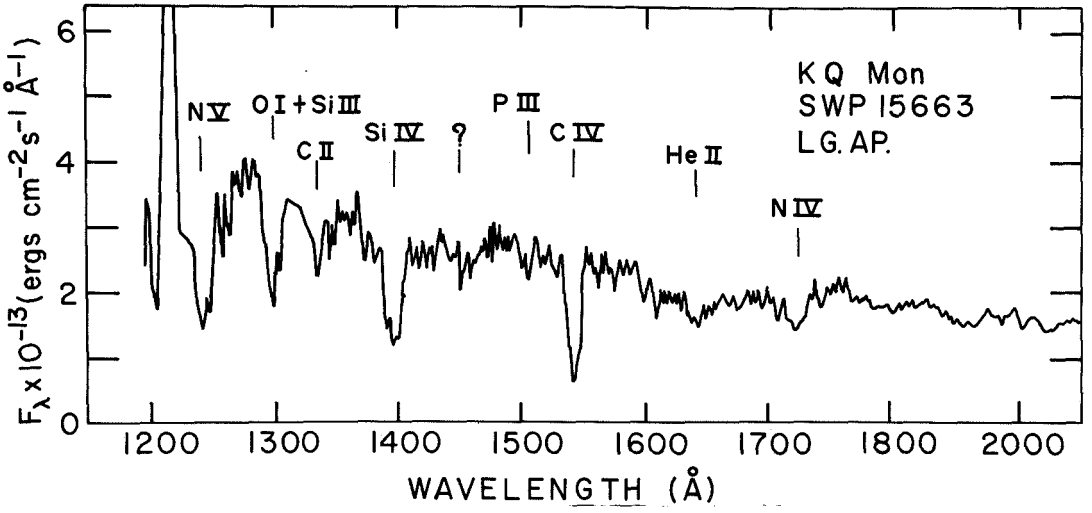

Figure 1: Short Wavelength Prime (SWP) low dispersion IUE spectrum of KQ Mon. The strong off-scale emission line at λ1216 Å is geocoronal Lyman Alpha. Strong absorption features are identified.

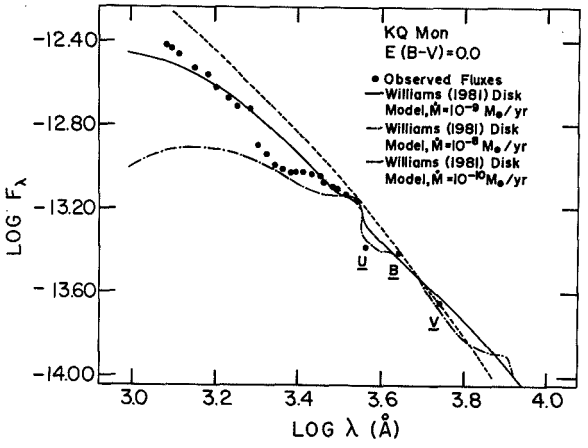

Figure 2: Flux plot log F_λ versus log λ compared with three accretion disk models of Williams (1981b) normalized at the optical V band flux. Optical fluxes are labelled with corresponding bandpass designations and all continuum fluxes are unreddened.

HIGH VELOCITY GAS OUTFLOW FROM THE NOVA-LIKE VARIABLE LSI 55°-8

Edward F. Guinan and Edward M. Sion
Astronomy Department, Villanova University

INTRODUCTION

LSI 55°-8 ($\alpha = 00^h18^m10^s$; $\delta = +55^\circ 26'.1$:1950) was identified as a possible subluminous, blue object by Haug (1970) from its unusual UBV colors during the Hamburg-Case Survey of Luminous Stars (Hardorp et al. 1959). Palomar spectra of LSI 55°-8 obtained by Greenstein, Sargent and Haug (1970; hereafter GSH) show a blue, nearly smooth continuum with weak, broad Balmer absorption lines having weak emission cores; other weak, broad emission lines of He II λ4686 and C III λ4647 were also reported. From its spectrum and UBV measures (V=+12.79; B-V=+0.07; U-B=-0.79), GSH suspected the object of being an old nova or a cataclysmic variable. High speed photometry was carried out during 1977 by Africano and Quigley (1978), where they monitored the star on 7 nights for a total of 20 hours and found rapid, nonperiodic light variations of up to 0.4 mag. Rapid light variability (flickering) is a common photometric characteristic of many cataclysmic variables and nova-like variables (Robinson 1976) and is believed to be associated either with a hot spot at the impact region of the gas with the accretion disk, or with non-radial oscillations of the disk, driven in the boundary layer region (Hesser, Lasker and Osmer 1972). Since LSI 55°-8 is not known to have undergone a large change in brightness with time like the dwarf novae, Quigley and Africano classified it (correctly) as a nova-like variable. It is generally believed that nova-like variables are either (a) old novae that have undergone outbursts that were unrecorded or (b) dwarf novae that are in very extended high states similar to those observed for the Z Cam systems, but of much longer duration (Warner 1976).

THE OBSERVATIONS

LSI 55°-8 was observed with the IUE satellite on 1981, December 05 as part of a continuing ultraviolet study of nova-like variables. Five low dispersion (~6A) SWP spectra ($\lambda\lambda$1175-1900) and two LWR spectra ($\lambda\lambda$2100-3100) were obtained over a 4 hour time interval. In addition, the optical brightness of the star was monitored between the UV exposures using the Fine Error Sensor (FES) onboard the satellite. The FES counts were converted to V-magnitudes using the calibration of Holm and Crabb (1979). During the observing interval the range of visual magnitudes was between $+12^m.63 \leq V(FES) \leq +12^m.78$. These values are close to the value of V=+12.79, measured earlier by Haug, and the short-term variability in light is similar to that found previously by Africano and Quigley.

RESULTS

The far UV spectrum of LSI 55°-8 (SWP 15659S) is shown in Fig.1 where the data reduction was by the standard IUESIPS routines. The identified spectral features are shown in the figure and also

are listed in Table I along with the rest and measured wavelengths, the residual intensities, the line widths at half maximum, and the corresponding Doppler displacement velocities. The LWR spectra of the star are essentially featureless. The UV spectrum of LSI 55°8 is strikingly similar to the nova-like binaries V3885 Sgr (Guinan and Sion 1982) and RW Sex (Greenstein and Oke 1982), which both show strong, blue-shifted absorption lines of such high temperature ions as C IV, NV, Si IV, and He II in their SWP spectra. As can be seen from the table, the high temperature ($\sim 10^5$K) ions of C III, C IV, He II, NV, and Si IV have relatively large negative Doppler shifts corresponding to radial velocities between -800km s^{-1} and -1400km s^{-1}. Much higher expansion velocities are associated with the broad absorption wings of the lines. The low temperature ($\sim 10^4$K) ions of H I (Lyα), O I, Si II, and Si I do not appear to show significant velocity displacements and probably originate from the outer accretion disk, with some contribution from the interstellar medium. In addition, the C IV (λ1549) resonance doublet shows a variable P Cygni-type profile with a blue-shifted absorption component. The presence of this feature, along with the blueshifted absorption features of the high temperature ions, indicate the existence of outflowing hot plasma (i.e. a wind). Using the method of Castor, Lutz and Seaton (1981), an upper limit of the mass outflow rate can be made from the short wavelength edge of the C IV absorption which yields $\dot{M}_{max} \gtrsim 10^{-9} M_\odot$/yr. Fig. 2 shows a plot of the normalized C IV profile as a function of time. As shown in this figure, the C IV profile is variable with the largest changes occurring in the relative strength and shape of the emission component. These changes appear to be systematic and may be associated with the changing projection of the outflowing hot plasma against the disk as a function of orbital motion. We have found similar behaviour for the C IV feature of TT Ari, in which the profile appears to change with its orbital motion (Guinan and Sion 1981). Fig.3 shows the residual line intensities of a few of the stronger spectral features as a function of time; in addition to the C IV variations, it appears that strength of the He II (λ1640) absorption feature is also time dependent. Although at low resolution it is difficult to be certain, it appears that the observed changes in the He II residual intensity are caused by broad emission filling in the bottom of the absorption feature. If this is the case, there appears to be correlation between the observed decrease in the C IV emission line strength with time and the decrease of the He II emission, inferred from the apparent strengthening of the He II absorption line feature with time.

Although LSI 55°8 is not definitely known to be a binary system, it has most of the characteristics (both spectral and photometric) exhibited by the nova-like, UX UMa-type variables, as well as with the dwarf novae in outburst or standstill. These systems are believed to be very short period, close binaries involved in active mass transfer and mass loss via Roche lobe overflow of gas from a low mass, cool star onto a white dwarf (Robinson 1976). An accretion disk is formed around the white dwarf compon-

ent as a result of the mass transfer mechanism and is predicted by Herter et al. (1979) to dominate the luminosity of the system at all but long wavelengths. Using the interstellar extinction law of Nandy et al. (1975), the data was de-reddened after several trials until no perceptable 'dip' (under-corrected for interstellar extinction) or 'hump' (overcorrected interstellar extinction) appeared at $\lambda 2200$. A value of $E_{B-V}=0.30$ was adopted and the observations were corrected for interstellar extinction and appear in Fig. 4 as $\log F_\nu$ vs. $\log \nu$. Various steady state, accretion disk model fluxes were tried (Herter et al.(1979); Pacharintanakul and Katz (1980); Williams(1981)) with the model fluxes of Williams yielding the best fit to observations. As shown in the figure, the steady-state accretion disk of Williams with accretion rate of $\dot{M}\sim 10^{-7} M_\odot$/yr and i=0 fits the data very well. The disk model fluxes of Herter et al. and Pacharintanakul and Katz produce higher than observed fluxes in the far UV relative to the optical wavelength fluxes. Unfortunately the Williams' fluxes are available only for the case in which the disk is seen face-on (i=0). The effect of viewing the disk at higher inclination has been investigated by Herter et al., and produces a decrease in the far UV flux relative to optical wavelengths, as the outer, cooler portion of the disk begins to dominate the observed radiation. From the appearance of its optical and UV spectrum (especially the presence of the blueshifted absorption features of the highly ionized species and C IV P Cygni-type profile), and the lack of significant periodic light variations, it appears that LSI 55-8 is being viewed at a low inclination ($i\sim 50^\circ$). The high accretion rate of $\dot{M}\sim 10^{-7} M_\odot$/yr, inferred from fitting the Williams disk model fluxes to our data, would appear to support the hypothesis that LSI 55-8 and related nova-like systems are in a state of prolonged outburst.

A ground-based radial velocity study of the star is needed to confirm the binary nature of the object and to determine its orbital period. The spectral changes observed in our study indicate a period $3^h<P<7^h$. We plan to publish a more thorough investigation of this interesting star in the near future. We wish at this time to thank Dr. Howard Bond for supplying us with an identification chart, and also to thank Dr. Robert Williams for sending unpublished theoretical disk model fluxes.

REFERENCES

Africano, J. and Quigley, R. 1978, P.A.S.P. 90, 191.
Castor, J.I., Lutz, J.H. and Seaton, M.J. 1981, M.N.R.A.S., 194, 547.
Greenstein, J.L., Sargent, A.I., and Haug, U. 1970, Astr. & Ap, 7, 1.
Greenstein, J.L. and Oke, J.B. 1982, Ap. J. (in press).
Guinan, E.F. and Sion, E.M. 1981, in The Universe at UV Wavelengths: The First Two Years of the IUE, NASA Conf. Publ. No.2171, p. 471.
Guinan, E.F. and Sion, E.M. 1982, Ap.J. (in press)
Hardorp, J., Rohlfs, K. Slettebak, A. and Stock, J 1959, Luminous Stars in the Northern Milky Way, vol.I Hamburger Sternwarte, Warner and Swasey Observatories.

Haug, U. 1970, Suppl. Astr. and Ap. 1, 35.
Herter, T., Lacasse, M.G. Wesemael,F. and Winget,D.E. 1979, Ap.J. Suppl., 39, 513.
Hesser, J.E. Lasker,B.M. and Osmer,P.S. 1972,Ap.J.Letters,176,L31.
Holm, A.V.and Crabb,W.G. 1979, IUE/NASA Newsletter No.7, p.40.
Kurucz, R.L. 1979, Ap. J. Suppl. 40, 1.
Nandy,K. Thompson, G.I. Jamar,C.Monfils,A. and Wilson,R. 1975, Astr. and Ap. 44, 195.
Pacharintanakul, P. and Katz, J.I. 1980, Ap. J., 238, 985.
Robinson, E.L. 1976, Ann.Rev. Astr. and Ap. 14, 119.
Warner, B. 1976, Observatory, 96, 49.
Williams, R.E. 1981, unpublished models.

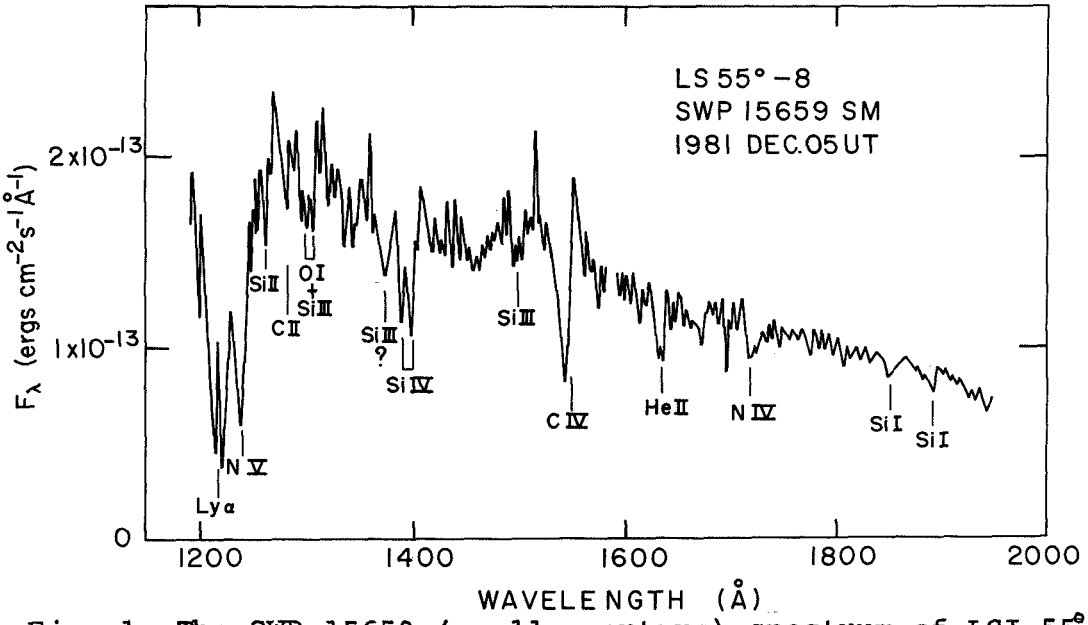

Fig. 1. The SWP 15659 (small aperture) spectrum of LSI 55°-8 with the stronger spectral features identified.

TABLE I

Measurements of Some of the Stronger Spectral Features of LS55 -8 (on SWP 15659S)

ION	λ_0(Å)	λ_{OBS}(Å)	$(F_C-F_L)/F_C$	W_λ(Å)	V_r(KMS^{-1})
CIII	1175.67*	1170	0.49	6	-1445
HI(Ly)	1215.67	1216	0.82	24	+81
HeII	1215.17				
NV	1240.15*	1237	0.77	11	-760
SiII	1262.6*	1263	0.17	3:	+100
OI+SiIII	1303*	1302	0.21	14:	-230
SiIV	1393.73	1390	0.28	6	-800
SiIV	1402.73	1399	0.32	7	-800
CIV	1549.05*	1542	0.44	10	-1365
		1553	-0.28	8	+785
HeII	1640.47	1633	0.23	10	-1365
SiI	1852.5*	1853	0.10	9	+80
SiI	1893.2S*	1893	0.12:	10	+120

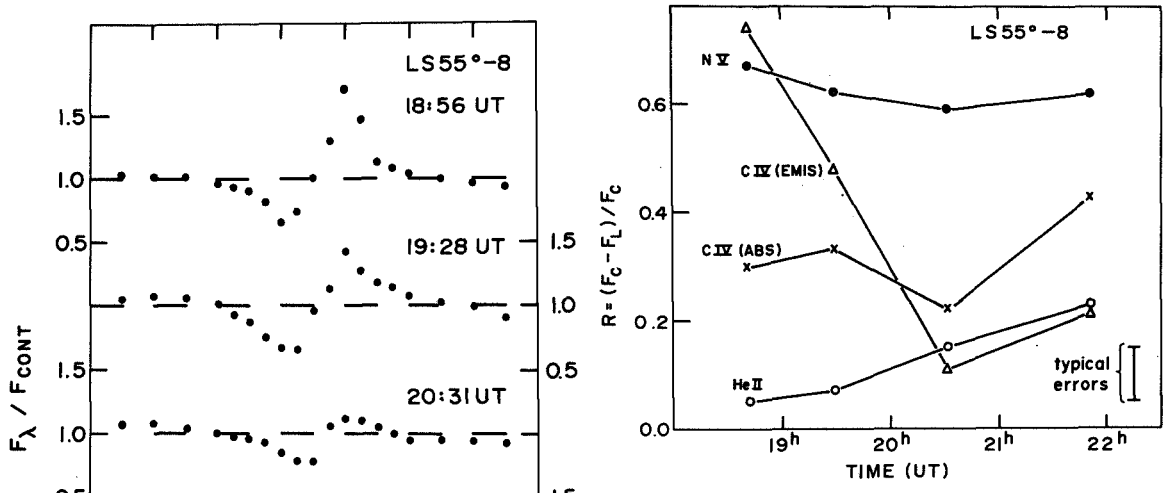

Fig. 3. The observed residual intensities of C IV (absorption and emission components), He II(λ1640), and N V(λ1240) as a function of time.

Fig. 2. The variation of the normalized C IV (λ1549) profiles of LSI 55°-8 with time.

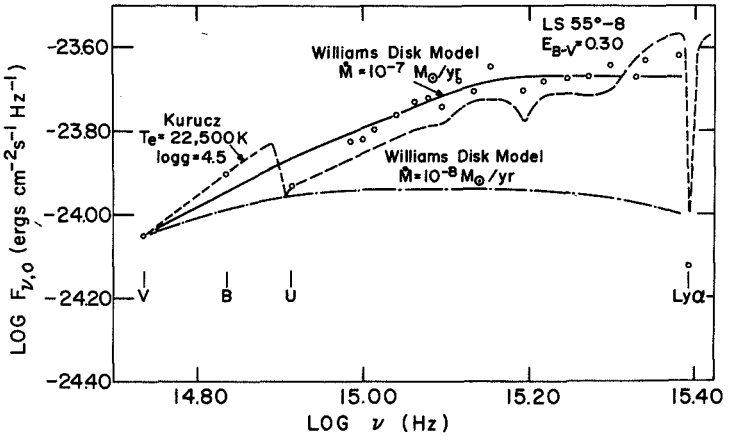

Fig. 4. The de-reddened continuum fluxes of LSI 55°-8 plotted along with the Williams' (1981) accretion disk fluxes. The stellar fluxes for T_{eff} = 22,500°K; log g=4.5 from Kurucz (1979) are also plotted for comparison. All of the model fluxes have been normalized to the observed flux near λ5500. (i.e. log F_ν=14.74).

A MODEL FOR THE 1979 OUTBURST OF THE RECURRENT NOVA U SCORPII

Sumner Starrfield
Dept. of Physics, Arizona State University

and

Theoretical Division, Los Alamos National Laboratory

Warren M. Sparks
Code 681, Laboratory for Astronomy and Solar Physics
NASA-Goddard Space Flight Center

and

R. E. Williams
Steward Observatory, University of Arizona

ABSTRACT

A series of ultraviolet spectra were obtained of the recurrent nova U Sco during its recent outburst with the IUE satellite. These spectra have been analyzed and found to consist primarily of emission lines although broad resonance absorption is present during the first week (Williams, et. al. (1981). These data, in combination with the optical data, show that the nova ejecta is very depleted in hydrogen relative to helium and is rich in nitrogen. An optical spectrum, obtained nine months after the outburst, shows predominantly HeII emission lines, indicating that the gas being transferred from the secondary is very helium rich and that the secondary is highly evolved. We interpret these data to imply that the outburst is associated with the accretion of helium rich material by a massive ($M \gtrsim 1.3M_{\odot}$) white dwarf in a close binary system. Neither the observational data nor the theoretical calculations, allow us to differentiate between a thermonuclear runaway or an accretion event as the cause of the outburst. In both cases, $\gtrsim 10^{-10}$ $M_{\odot}$ of material is ejected with speeds exceeding 8×10^3 km sec^{-1}.

In a recent paper (Williams, et.al 1981; hereafter W81) we reported on an analysis of the IUE observations of the most recent outburst of U Scorpii, a recurrent nova. These data combined with the optical study of Barlow et.al (1981) showed that this outburst was extremely rapid and much faster than either the outburst of Nova Cygni 1978 (Stickland, et.al 1981) or Nova Corona Austrina 1981 (Sparks, et.al 1982, this volume). Inasmuch as a detailed comparison of the differences between the outburst of U Sco and a more typical classical nova has already appeared in W81, we shall only discuss the major discrepancies in this paper and then discuss two possible models for the cause of the U Sco outburst.

The most puzzling aspect of U Sco is shown in the spectrum of the object taken $\sim$ 9 months after the outburst when it had presumably returned to minimum (Figure 1). It shows what we interpret as an accretion disc spectrum of a cataclysmic variable (c.f.; Robinson 1976) but there is no sign of any hydrogen. Since it is generally accepted that the accretion disc is formed from material being lost by the secondary, this spectrum implies that the secondary is very evolved. In addition, since it is the accreted material that(we assume) provides the fuel for the outburst, the fact that for U Sco it appears to be pure helium is surprising. In addition, the optical spectra taken during outburst did show that hydrogen is present in the ejected nebula. Since it seemed possible that the presence of hydrogen might not have been detected in the original spectrum, another recent optical spectrum was obtained at the MMT in February 1982. It also shows no evidence for hydrogen.

The outburst itself was also unusual in that the active phase was very short and the expansion velocities were quite large as compared to a classical nova. In addition, the amount of ejected mass was only $\sim 10^{-7}M_{\odot}$; about 10^3 times smaller than is ejected during the typical classical nova outburst. Moreover, the analysis of the IUE and optical data showed that the helium/hydrogen ratio was about 2 and that only nitrogen was enhanced (W81). If the outburst was caused by a CNO thermonuclear runaway in an accreted hydrogen envelope (Starrfield, Truran, Sparks 1978), then one would expect such behavior from an outburst on a very massive white dwarf.

We proceeded to simulate the observed outburst by evolving a thermonuclear runaway in an accreted envelope on a $1.38M_{\odot}$ white dwarf with a luminosity of $\sim 1L_{\odot}$. The high value of the luminosity was used to reduce the recurrence time (Starrfield, Sparks, Truran 1976). Here, we assumed that the abundances of the ejecta were characteristic of the accreted shell and deliberately ignored the apparent lack of hydrogen in the "accretion disc." We used a high helium mixture for the envelope (X=0.1, Y=0.88, Z=.02) obtaining the opacities from the Los Alamos computations kindly provided by A. N. Cox (Heubner, et.al 1977). We did <u>not</u> enhance the CNO nuclei.

We determined the mass of the accreted envelope necessary to produce a runaway by gradually increasing the mass of the envelope until a runaway occurred. For our $1.38M_{\odot}$ white dwarf and $L\sim 1.0L_{\odot}$, the critical mass is $\sim 2 \times 10^{-6}M_{\odot}$. We evolved this model to a peak envelope temperature of 4×10^8K and a peak luminosity of $\sim 5 \times 10^4 L_{\odot}$. This value is L_{edd} for a $1.38M_{\odot}$ white dwarf with a normal composition and a pure electron scattering opacity. However, the hydrogen in the envelope burns out just after this luminosity is attained and before the outer layers have expanded to 10^9cm. However, by this time, the high temperature in the shell source has ignited the triple-α reaction and the energy production from helium burning continues the expansion of the shell (at about constant luminosity) until it reaches 10^{12}cm. The rate of energy generation from the triple-α reaction reaches 10^{11} erg gm^{-1} s^{-1} and produces a helium burning front which moves inward into regions of higher density. The energy from helium burning causes about $10^{-9}M_{\odot}$ of the accreted envelope to be ejected over the first few days of the outburst. However, the outburst has now been proceeding for more than 100 days (much longer than the observed outburst) and we stopped the computations because of lack of computer time. At a time 50 days after maximum M_{Bol}, the visual

magnitude reached to only -4 and was still increasing. In addition, the entire amount of accreted hydrogen has been processed to helium so that the ejected nebula consists almost entirely of helium. It appears, therefore, that the most reasonable initial conditions for a thermonuclear runaway model for the outburst do not produce an evolutionary sequence in agreement with the observations.

Therefore, we have also considered a rapid accretion event as a possible explanation of the U Sco outburst. In this case we assume that a steady (or unsteady) flow of gas has accumulated in the accretion disc over the forty year interval since the last outburst and an instability (of unspecified nature) occurs which causes a short phase of rapid accretion onto the surface (c.f., Bath 1977; Webbink 1976). Recent studies of instabilities in accretion discs have indicated a possible physical mechanism (Lin 1982, private communication).

We again chose a $1.38M_\odot$ dwarf but now assumed that the accreting gas was pure helium in accordance with the post outburst spectra. Our opacities for this mixture were also provided by A. N. Cox and are abstracted from the Los Alamos Opacity Library (Heubner, et.al 1977). We simulated a rapid accretion event by allowing a blob of gas ($m \sim 2 \times 10^{-8} M_\odot$) to extend from the surface of the white dwarf ($R \sim 1.6 \times 10^8$cm) to a distance of 3×10^9cm. This material is initially at rest with respect to the white dwarf, is optically thick, and has a radial decrease in density. We begin the evolution by initiating a phase of infall at various speeds. The value of the accreting mass was chosen to be equal to the amount of helium that could have been transferred to an accretion disk in 40 years at $\dot{M} = 5 \times 10^{-10} M_\odot yr^{-1}$. We also studied evolutionary sequences with more massive envelopes but the results were not in agreement with the observations.

The initial model had a luminosity of $1.0L_\odot$ and the effective temperature was 1.7×10^4K. We adjusted the pressure support so that the infall would take about 10 days and reach maximum inward velocities of 10 km sec^{-1}. The light curve for this evolution is shown in Figure 2. This sequence reached a maximum luminosity of 2×10^{36} erg sec^{-1} and this occurred 1.4 days after the initiation of the infall. Because the radius had decreased to 2×10^8 cm, the effective temperature reached 5×10^5K so that $M_\odot$ at this time is only 8.7; much too faint to agree with the observations. This object stays bright, bolometrically, for another few days before beginning its decline. No material is ejected during the outburst and the peak luminosity never approaches L_{edd}.

We increased the envelope mass to $2 \times 10^{-6} M_\odot$ and allowed the material to reach free fall velocities. In this study an accretion shock forms and ejects $10^{-10} M_\odot$ of gas in the initial bounce and more later on in a slower phase of wind-type mass loss. Unfortunately, we do not envisage a mechanism for storing this great an amount of material in the accretion disc.

Our conclusions are, therefore, that the rapid accretion (disk instability) theory for the outburst of a recurrent nova such as U Sco does not fit the observations. The thermonuclear runaway theory is somewhat more successful but the length of the outburst was much too long to agree with the

observations. We are continuing our investigations of both these theories and shall report on those results in a later paper.

REFERENCES

Barlow, M.J. et.al 1981 M.N.R.A.S., 195, 61.

Bath, G.T. 1977, M.N.R.A.S., 178, 203.

Heubner, W.F., Merts, A.L., Magee, N.H., and Argo, M.F. 1977, (Los Alamos Scientific Report LA-6760-M).

Robinson, E.L. 1976, Ann.Rev. Astr.Ap, 14, 119.

Starrfield, S., Sparks, W.M., and Truran, J.W. 1976, in Structure and Evolution of Close Binary Systems, ed P. Eggleton, S. Mitton, and J. Whelan (Dordrecht: Reidel) p 155.

Starrfield, S., Truran, J.W., and Sparks, W.M. 1978, Ap.J., 226, 186.

Stickland, D.J., Penn, C.J., Seaton, M.J., Snijders, M.A.J., and Storey, P.J. 1981, M.N.R.A.S., 197, 107.

Webbink, R.F. 1976, Nature, 262, 271.

Williams, R.E., Sparks, W.M., Gallagher, J.S., Ney, E.P., Starrfield, S.G., and Truran, J.W. 1981, Ap.J., 251, 221.

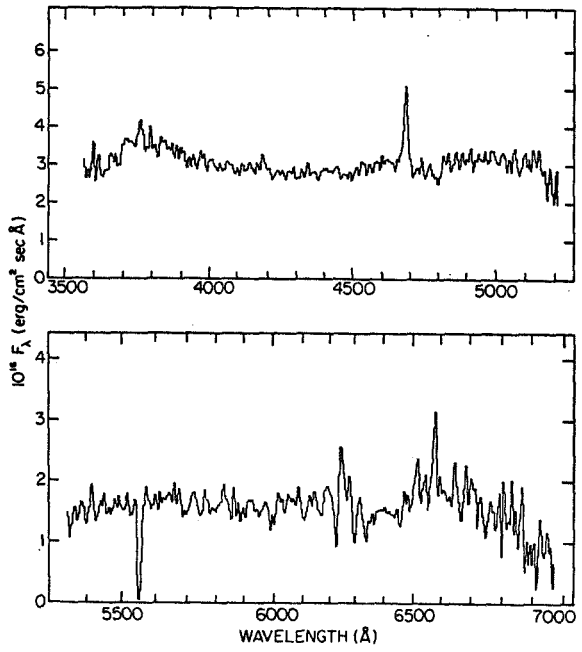

Figure 1

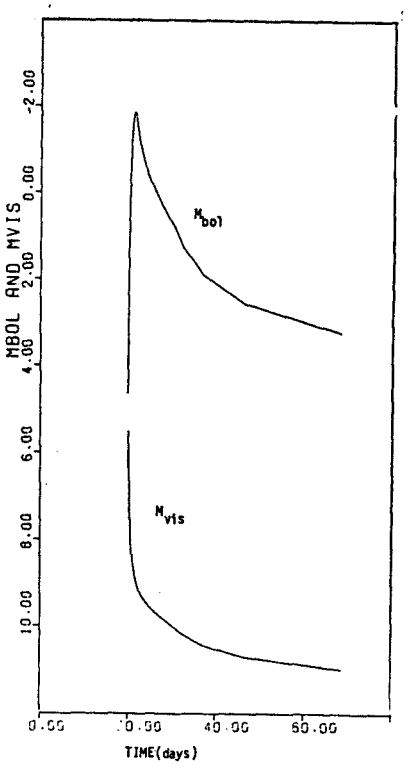

Figure 2

Figure 1 - Optical Spectrum of U Scorpii.
Figure 2 - Theoretical light curve for the rapid accretion simulation of the U Scorpii outburst.

CATACLYSMIC VARIABLES:DISK CHARACTERISTICS FROM UV OBSERVATIONS

Paula Szkody
Astronomy Department, University of Washington

ABSTRACT

Low dispersion IUE spectra of 3 cataclysmic variables (V442 Oph, V794 Aql and H2215-086) are discussed in terms of current disk models. The range of continuum fluxes, line emission and disk parameters ($\dot{M}$, T_{max}) of these three novalike systems are compared with past observations of dwarf novae at outburst and quiescence. Evidence of variability on orbital timescales is presented for V442 Oph and H2215-086.

INTRODUCTION

The cataclysmic variables consist of close binaries with a late type main sequence (or slightly evolved star) transferring mass to a white dwarf companion. Usually, the dominant source of light in the system is the accretion disk, which is the holding area for the transferred material before it accretes onto the white dwarf. The first attempts at modelling this disk have assumed a steady state viscous disk with a spectrum computed by assuming a given radius has a temperature T which is a function of the accretion rate $\dot{M}$ and emits a Planck function. The summation of the Planck functions over the entire disk gives the emerging flux (Bath, Pringle and Whelan 1980) which has an $F_\lambda \alpha \lambda^{-2.3}$ slope over a large wavelength range and a turndown of the flux at short and long wavelengths due to the inner and outer edges of the disk. Observation of the turnovers determines the temperatures of the inner and outer edges and $\dot{M}$. The ultraviolet is usually critical for this type of analysis to obtain the large wavelength coverage and the maximum temperature of the disk.

The available IUE observations of cataclysmic variables have shown a wide range of results with distributions ranging from $F_\lambda \propto \lambda^{\circ}$ to λ^{-4} (Bath, Pringle and Whelan 1980, Szkody 1981). Some improvement to the disk models has come about by including the optically thin outer regions which contribute line emission and create the Balmer jump, etc. (Williams and Ferguson 1981). This flattens the flux distribution from $F_\lambda \alpha \lambda^{-2.3}$ for $\dot{M} < 10^{-7}$ $M_\odot$/yr.

The accumulation of disk characteristics for a large variety of cataclysmics can provide clues as to why different types of systems (dwarf novae vs. novalikes) exist. Results are presented here for 3 recently discovered cataclysmic variables.

V442 Oph

Initial spectroscopy and photometry (Szkody and Wade 1980) showed this object to be a cataclysmic variable with strong HeII 4686 and Balmer line emission. Further high resolution spectra have showed an orbital period near 3 hours. The optical light curve shows flickering of 0.5 magnitude amplitude but no repeatable feature on orbital timescales. Six low dispersion IUE spectra (alternating between the short and long wavelength cameras) were obtained from 23^h on Oct. 13 to 5^h on Oct. 14, 1981. The short wavelength exposures

were 1 hour and the long wavelength were 50 minutes (a 35 minute LWR exposure was obtained on Oct. 17). With the extinction curve of Savage and Mathis (1979), E(B-V) = 0.25±.05.

The emission lines are abnormally weak for a cataclysmic variable (a typical SWP spectrum is shown in Fig. 1a) with SiIII in absorption and weak SiIV and CIV in emission. The FES magnitude during the IUE spectra ranged from 13.6 to 13.8 so that the system was near its high state (normal range V = 12.6->14.5). Combining the UV data with non-simultaneous optical and IR fluxes gives the distribution in Figure 1b. The 1000-4400Å slope is $F_\lambda \alpha \lambda^{-2}$, closest to the $\dot{M} = 10^{-8} M_\odot$/yr model of Williams and Ferguson (1981), (dashed line in Fig. 1b). The maximum disk temperature is 6×10^4K ($T_{max} = 2 \times 10^4 (\dot{M}/10^{16})^{1/4}$ for a $1 M_\odot$, R = 10^9 cm white dwarf (Bath, Pringle and Whelan (1980).

Phasing the data with the 3 hour period and selecting several continuum points throughout the UV provides evidence for variability (0.15 mag) at the short wavelengths which is surprisingly less than in the optical at a similar outburst state. This could mean that the hot spot does not contribute significantly in the UV.

V794 Aql

Bond (1978) first indicated that V794 Aql could be a cataclysmic variable. Einstein X-ray results and optical photometry and spectroscopy (Szkody et al. 1981) confirmed this identification. Short and long wavelength IUE spectra were obtained on October 15, 1981 when the FES magnitude was 15.6 (normal range of V794 Aql is V = 14-17th mag). The short wavelength exposure was 2 hours followed by a long wavelength of one hour duration. No reddening correction was needed. (Fig. 2a). The ultraviolet emission is typical of cataclysmics (Szkody 1981) showing strong CIV, followed by SiIV. The ultraviolet continuum is very flat ($F_\lambda \alpha \lambda^{-1}$) in the UV (Fig. 2b) and closest to the William and Ferguson $\dot{M} = 10^{-9} M_\odot$/yr. model with $T_{max} = 3 \times 10^4$ (dashed line in Fig. 2b). However, this type of model does not give enough flux to account for the FES magnitude or the IR fluxes taken when the system was at a similar optical magnitude. Either the disk is more extended than the model assumes or another component is contributing at wavelengths longer than 2500Å.

H2215

This X-ray emitting cataclysmic variable which is very similar to H2252-035 and V1223 Sgr was recently pointed out by Patterson and Steiner (1981). Optical data show a 4-4.85 hour (0.3 mag.) orbital period and a 21 min. (0.4 mag.) pulsation. Schafter and Targon (1982) argue that the 21 min. periodicity is due to radiation from the magnetic poles of the compact star (rotation P = 19.5 min) which is reprocessed in the rim of the accretion disk near the hot spot.

Seven IUE spectra (4 SWP and 3 LWR) were obtained on Oct. 4, 1981 from 5:32 - 11:34 UT. During this time, the FES magnitudes ranged from 13.4 to 14.0. The reddening is estimated to be E(B-V) = 0.05. A typical SWP spectrum is shown in Fig. 3a. The usual emission lines are apparent (CIV, SiIV, NV, HeII, MgII). The continuum fluxes joined with non-simultaneous optical and IR data are shown in Fig. 3b. The best Williams & Ferguson (1981) model match to the UV and optical data is with $\dot{M} = 10^{-10} M_\odot$/yr, (dashed line in

Fig. 3b) which gives $T_{max} = 2 \times 10^4$K. The IR points fall below the expected values which could mean a less extended disk than used by the model (or variability due to the non-simultaneous observations). For such a strong X-ray source with strong HeII 4686 emission, it is surprising that the disk has such a low temperature and accretion rate. The situation is explicable if the magnetic field in H2215 is stronger than in systems like V794 Aql and V442 Oph so that a thin outer disk exists and the material near the white dwarf is within the Alfven radius and so is accreted onto small polar areas of the star.

There is evidence of UV continuum variability but a more accurate period is needed to determine if a UV drop in the short wavelength fluxes coincides with any feature in the optical region. The largest variability (20% from the mean) is evident at the shortest wavelengths (1300 and 1500Å) while the 2700Å flux is constant. The NV, SiIV, CIV, HeII and MgII line fluxes are also variable (deviations of 10-20% from the mean) but do not appear correlated with the continuum variations. Better time resolution is required to detect if the UV continuum is pulsed with the 21 minute period. Since the UV continuum appears to arise from a disk and there is evidence for an orbital variation, the probable location is the hot spot area. The line ratios of NV, SiIV, CIV are consistent with a collisionally excited gas at $T > 10^5$K (Jameson, King and Sherrington 1980). Since the disk is relatively cool, the line emission probably originates closer to the compact object and might show the predicted 19.5 min rotation period.

This work was partially supported by NASA grant NSG-5395.

REFERENCES

Bath, G. T., Pringle, J. E. and Whelan, J. A. J. 1980, M.N.R.A.S. 190, 185.
Bond, H. E. 1978, Pub. A.S.P. 90, 526.
Jameson, R. F., King, A. R. and Sherrington, M. R. 1980, M.N.R.A.S. 191, 559.
Patterson, J. and Steiner, J. 1981, B.A.A.S. 13, 817.
Savage, B. D. and Mathis, J. S. 1979, Ann. Rev. 17, 73.
Schafter, A. W. and Targan, D. M. 1982, preprint.
Szkody, P. 1981, Ap.J. 247, 577.
Szkody, P. and Wade, R. A. 1980, Pub. A.S.P. 92, 806.
Szkody, P., Crosa, L., Bothun, G., Downes, R. and Schommer, R. 1981, Ap.J. Letters, 249, L61.
Williams, R. E. and Ferguson, D. H. 1981, preprint.

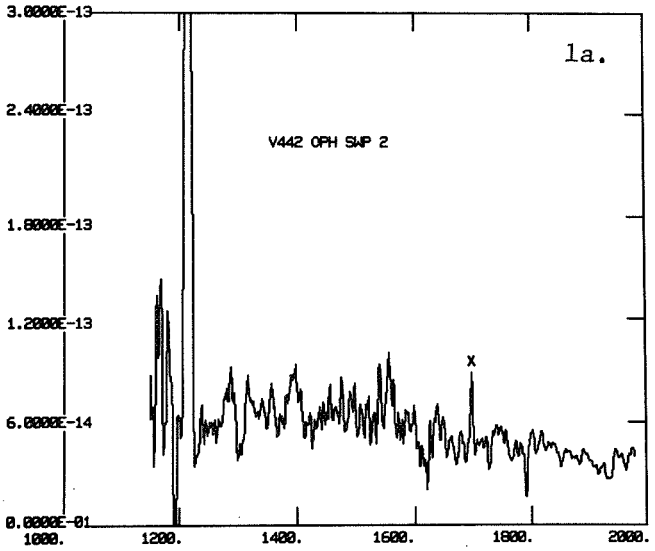
1a.
V442 OPH SWP 2
3.0000E-13
2.4000E-13
1.8000E-13
1.2000E-13
6.0000E-14
0.0000E-01
1000.
1200.
1400.
1600.
1800.
2000.

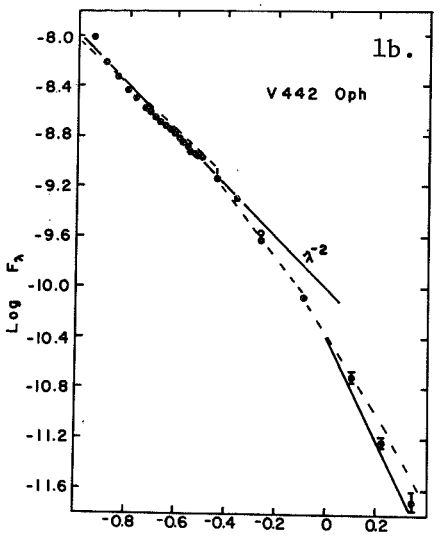
1b.
V442 Oph
Log F_λ
λ^-2
-8.0
-8.4
-8.8
-9.2
-9.6
-10.0
-10.4
-10.8
-11.2
-11.6
-0.8
-0.6
-0.4
-0.2
0
0.2

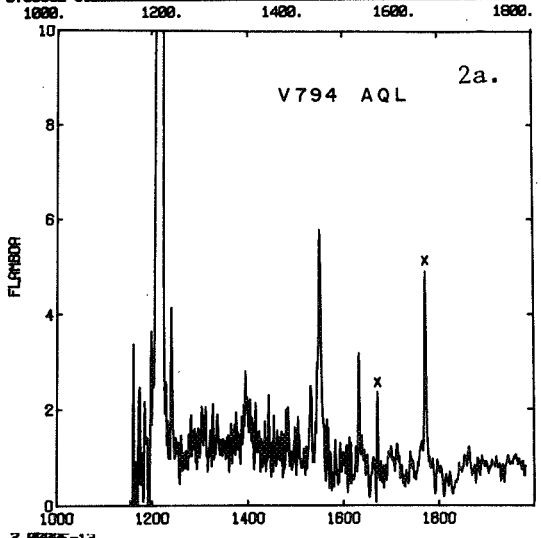
2a.
V794 AQL
FLAMBDA
10
8
6
4
2
0
1000
1200
1400
1600
1800

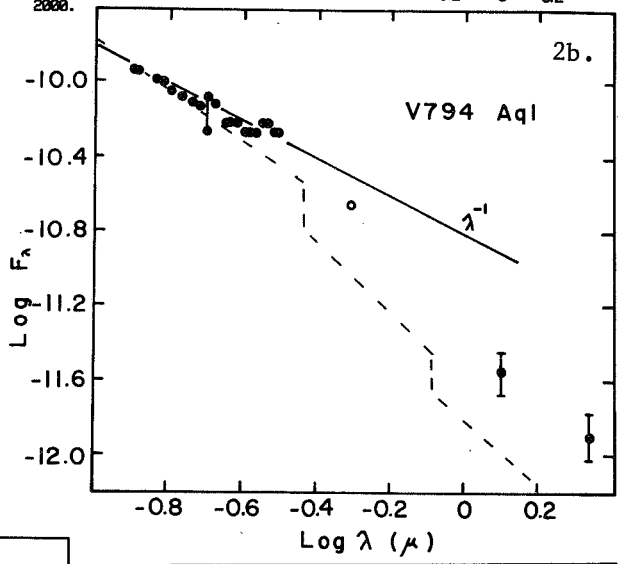
2b.
V794 Aql
Log F_λ
λ^-1
-10.0
-10.4
-10.8
-11.2
-11.6
-12.0
-0.8
-0.6
-0.4
-0.2
0
0.2
Log λ (μ)

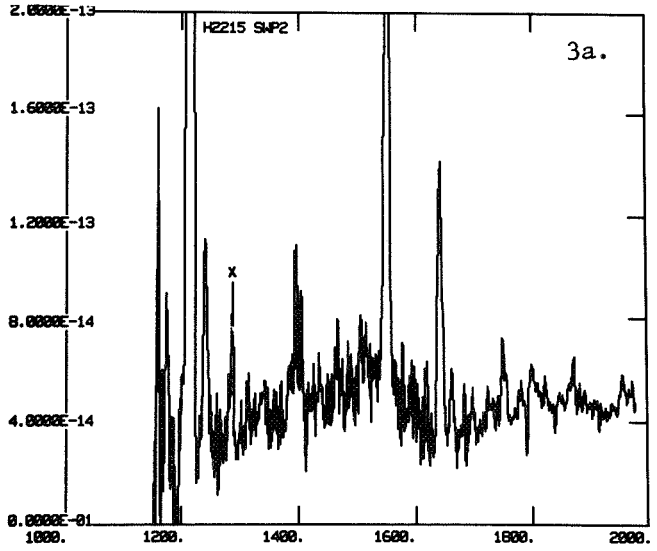
3a.
H2215 SWP2
2.0000E-13
1.6000E-13
1.2000E-13
8.0000E-14
4.0000E-14
0.0000E-01
1000.
1200.
1400.
1600.
1800.
2000.

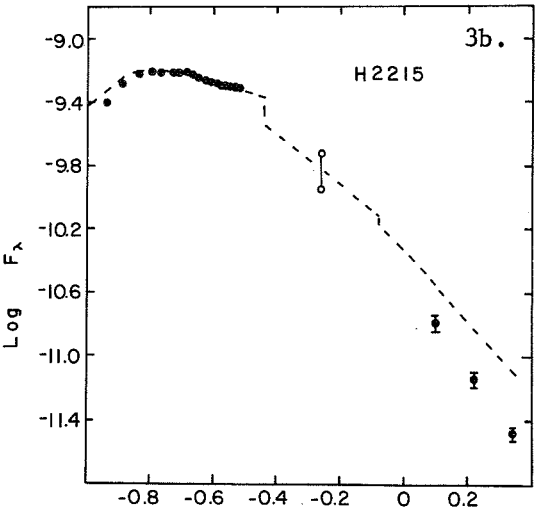
3b.
H2215
Log F_λ
-9.0
-9.4
-9.8
-10.2
-10.6
-11.0
-11.4
-0.8
-0.6
-0.4
-0.2
0
0.2

IUE OBSERVATIONS OF THE 1981 OUTBURST OF NOVA Cr A

Warren M. Sparks
Laboratory for Astronomy and Solar Physics
NASA/Goddard Space Flight Center

Sumner Starrfield and Susan Wyckoff
Department of Physics, Arizona State University

Robert E. Williams
Steward Observatory, University of Arizona

James W. Truran
Department of Astronomy, University of Illinois

Edward P. Ney
Department of Astronomy, University of Minnesota

ABSTRACT

IUE Spectra of Nova Cr A 1981 have been obtained on 11 dates from outburst in April 1981 through mid November 1981. These spectra cover the range 1150-3200 Å, and are mostly at low dispersion. The emission lines identified in the low dispersion spectra cover a range in ionization potential from ∿ 8 eV (Mg II) to ∿ 80 eV (N V). The strongest line in the first spectrum is OI at 1303 Å. Line emission fluxes and widths have been measured in all spectra. Results of a preliminary abundance analysis will be reported.

Nova Corona Austrina 1981 was discovered by Honda on April 2, 1981 at $7^{m}.0$ (I.A.U. Announcement card No. 3590). It was declared a target of opportunity by the IUE Observatory and we obtained our first spectrum on April 10, 1981. We continued to observe the nova until November 1981 at which time it entered the sun constraint of the IUE satellite.

The light curve of this nova is shown in Figure 1. It was obtained using magnitudes determined by the FES on the satellite. To our knowledge, no other optical data was obtained for this nova at late times of the outburst. The light curve indicates a moderately fast nova.

Inasmuch as its southern declination ($\delta = -37^{\circ}.5$) prevented us from obtaining optical spectra, we shall only report here on our initial analysis of the ultraviolet data obtained with the IUE satellite. Figure 2 shows a flux calibrated, merged spectrum of the nova taken on April 12, 1981. A similar spectrum obtained on September 13, 1981 is shown in Figure 3. These spectra are remarkable for the very strong lines of aluminum and silicon. In addition we have also identified very strong emission lines of carbon, nitrogen, oxygen, and neon. UV spectrograms (not shown) show that emission lines due to highly ionized species such as Mg VII and Aℓ VI were present for short times in May 1981 and June 1981.

The FWHM of the emission features such as C IV λ1549 was 4500 km sec^{-1} on May 25. This velocity is not unusual for a fast nova but seems somewhat excessive for a moderately fast nova such as Nova Cr A 1981 (Gallagher and Starrfield 1978).

Our analysis of the spectra obtained during this outburst has not yet reached the stage where we can make detailed and specific statements about either the physical conditions in the expanding nebula or the elemental abundances. One difficulty, is that preliminary analyses of our last spectrum, obtained some 200 days after maximum, indicate that the nebula is still in transition and has not yet reached the nebular stage. This means that we cannot assume that a steady-state has been reached which complicates the analysis. Nevertheless, the presence in the early spectra of the intercombination line of NII] λ2140, along with the plethora of other nitrogen lines, strongly suggests that nitrogen is overabundant in this nova. This agrees with the analyses for other novae (Williams 1982, in preparation). In addition, the presence of permitted Ne IV λ1602, λ2422 and forbidden [Ne III] λ1815 in the strengths observed also suggests that neon is overabundant in this nova (Snijders 1982, private communication). A more detailed analysis of these data is in progress.

REFERENCES

Gallagher, J.S. and Starrfield, S. 1978, Ann. Rev. Astron. Astro. Ap., 16, 171.

TABLE 1

Emission lines present in the spectrum of Nova Corona Austrinae 1981

Identification atom/ion	Wavelength λ (Å)	April 12, 1983 (present)	Sept 13, 1981 (present)
N V	1240	yes	yes
Si II	1263	yes	no
OI	1304 blend	yes	no
Si II	1308 blend		no
C II	1335 (?)	yes	no
O V	1370	yes	no
Si IV	1398 blend		no
O IV]	1402 blend	yes	yes
N IV]	1486	yes	yes
C IV	1549	yes	yes
Ne IV	1602	no	yes
He II	1640		yes
O III]	1663 blend	yes	no
Aℓ II	1671		no
N IV	1718 blend	yes	no
Aℓ II	1722 blend		no
N III]	1750	yes	yes
Si II	1808, 1817 blend	yes	no
[Ne III]	1815	no	yes
Aℓ III	1855, 1863	yes	no
Si II	1895	yes	no
C III]	1909	yes	yes
N II]	2140	yes	no
C II	2326	yes	no
Ne IV	2422	no	yes
Aℓ II	2669	yes	no
Mg II	2798	yes	yes

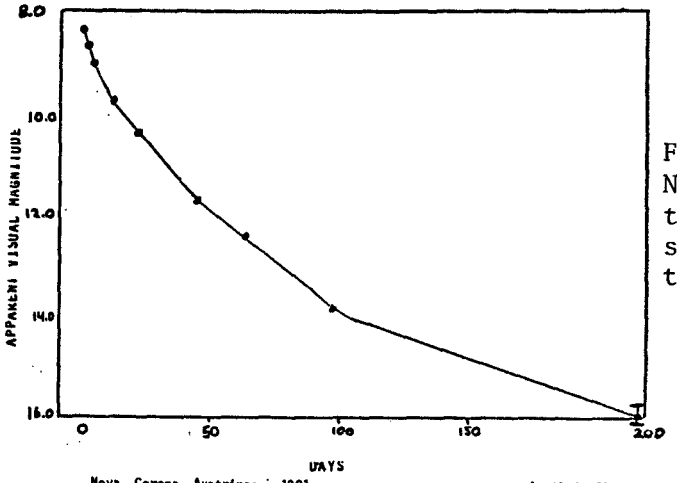

Figure 1. The light curve of Nova Corona Austrinae 1981 obtained from the FES on the IUE satellite. The error bars on the last point are an estimate.

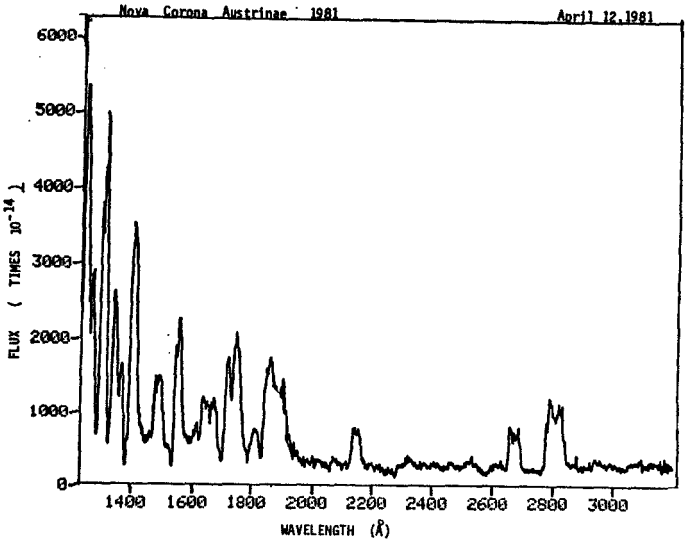

Figure 2. The spectrum of the nova obtained on April 12, 1981. A line list is given in Table 1.

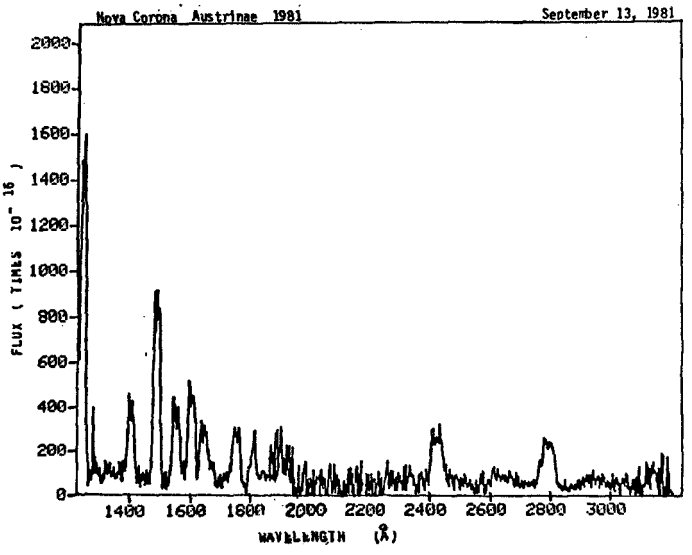

Figure 3. The spectrum of the nova obtained on September 13, 1981. A line list is also given in Table 1.

THE ULTRAVIOLET VARIABILITY OF T Cr B

A. Cassatella[1], P. Patriarchi[1], P.L. Selvelli[2], L. Bianchi[1], C. Cacciari[1], A. Heck[1], M. Perryman[3], W. Wamsteker[1]

1 ESA, Astronomy Division, Villafranca Satellite Tracking Station, Spain

2 Astronomical Observatory, Trieste, Italy

3 ESA, Astronomy Division, ESTEC, Holland

ABSTRACT

Preliminary results of the Ultraviolet variability monitoring of the recurrent nova T Cr B are presented. The star, since 1979 showed striking changes of the continuum (both shape and integrated luminosity) and of the emission lines, with a maximum activity in early 1981. In the same period the visual luminosity remained practically constant.

The data, which are under study suggest that the UV variability is due to changes in the physical structure of the accretion disk around the secondary.

INTRODUCTION

The recurrent nova T Cr B is a double line spectroscopic binary of period 227.6 d. In the optical region it appears as a M3 giant showing broad Balmer lines in emission as well as forbidden lines (Kraft, 1958). From the emission lines radial velocity variations and making use of the fact that no occultation effects were observed, Kraft (1958) derived lower limits for the masses of the primary cool star and the secondary hot component ($M_1 \geq 3.7$, $M_2 \geq 2.6$; see also Paczynsky, 1965).

Although the UV and optical spectrum of T Cr B has analogies with symbiotic stars spectra (Altamore et al., 1981) and with cataclismic variables (Bath et al., 1980; Webbink, 1976), its detailed model, also in view of the present UV observations and of its X-ray detection (Cordoba et al., 1981) has to be studied in more details.

OBSERVATIONS

IUE observations of T Cr B started in 1978 and continued through Dec. 1981. The low resolution mode was generally used, but a few spectra were also obtained at high resolution as to study the emission line profiles and the line ratios. In Table 1 the dates of some selected low resolution observations are listed together with other information as the corresponding visual flux (derived from the FES counts), the continuum flux at 1300 A and the slope, α, of the continuum ($F_\lambda \propto \lambda^{-\alpha}$).

RESULTS

The first interesting result obtained is that the interstellar absorption toward T Cr B is not negligible as generally believed. A careful analysis of the best exposed IUE spectra reveals that the interstellar feature around 2200 A is present and it is removed for E(B-V)= 0.15 .

The UV continuum is strongly variable in both shape and total flux. The dereddened low resolution spectra are fairly well represented by a power law $F_\lambda \propto \lambda^{-\alpha}$, with α varying from 0.2 in March 1979 to 1.2 in Feb. 1981. As shown in Table 1, the continuum flux at 1300 A also varied increasing almost linearily from March 1979 to Feb. 1981. At the date of the latest observations in Dec. 1981, the UV brightness of T Cr B faded down to the pre-maximum values and the spectrum appeared quite similar to that obtained in June 1980, but with a slightly different slope α = 1.0.

Fig. 1 shows the spectrum of T Cr B at two sample dates, together with the power law fit to the continuum. The figure shows as well that the emission line intensities were variable, appearing stronger as the continuum level increased. Particular interest deserves the line ratio SiIII] 1892/CIII] 1908 which indicates (assuming standard chemical composition and the same line formation region) that the electron density increased from 1.2 10^{10} cm^{-3} in June 1980 to about 2 10^{11} cm^{-3} in Feb. 1981 and decreased again in Dec. 1981. The electron density variations are confirmed by the NIII] 1750/CIII] 1908 line ratio. High resolution spectra obtained on June 9, 1980 and Jan., 17 1981 allow a careful electron density determination from the NIII] multiplet line intensities, which again agrees with the above estimates from low resolution spectra.

DISCUSSION

Although the UV spectra of T Cr B during activity phases could in principle be represented with black body emission at about T=27000 °K plus free-bound emission, the strong variability of the integrated UV fluxes as well as the variable slope of the continuum do not favor this representation. Our preliminary interpretation of the above phenomenology, is that the UV spectrum of T Cr B is not mainly contributed by the photosphere of a hot star, but rather by an accretion disk formed aroun it as a consequence of mass loss from the cool Roche lobe filling cool primary. The continuum variability would then imply a change of the physical structure of the disk. Note that the orbital inclination of T Cr B ($i \lesssim 68°$; Kraft, 1958) favors the detection of such changes.

REFERENCES

Altamore, A., Baratta, G.B., Cassatella, A.,Friedjung, M., Giangrande, A., Ricciardi, O., Viotti, R. 1981, Ap. J. 245,630

Bath, G.T., Pringle, J.E., Whelan, J.A.J. 1980,MNRAS 190,185

Cordoba, F.A., Mason, K.O., Nelson, J.E. 1981, Ap. J. 245, 609

Kraft, R.P. 1958, Ap. J., 127, 625

Paczynski, B. 1965, Acta Astron, 15, 197

Webbink, R.F. 1976, Nature 262, 271

TABLE 1

DATE	DAY NUMBER	VISUAL FLUX (erg $cm^{-2}s^{-1}A^{-1}$)	CONT. FLUX at 1300 A (erg $cm^{-2}s^{-1}A^{-1}$)	SLOPE
21 MAR 79	0	$4.9\ 10^{-13}$	$5.22\ 10^{-14}$	0.2
15 JUL 79	111	$5.2\ 10^{-13}$	$9.80\ 10^{-14}$	0.5
3 AUG 79	135	$4.5\ 10^{-13}$	$1.84\ 10^{-13}$	0.5
8 JUN 80	445	$5.0\ 10^{-13}$	$4.03\ 10^{-13}$	1.2
17 FEB 81	699	$4.8\ 10^{-13}$	$6.51\ 10^{-13}$	1.2
15 DEC 81	1000	$5.1\ 10^{-13}$	$3.80\ 10^{-13}$	1.0

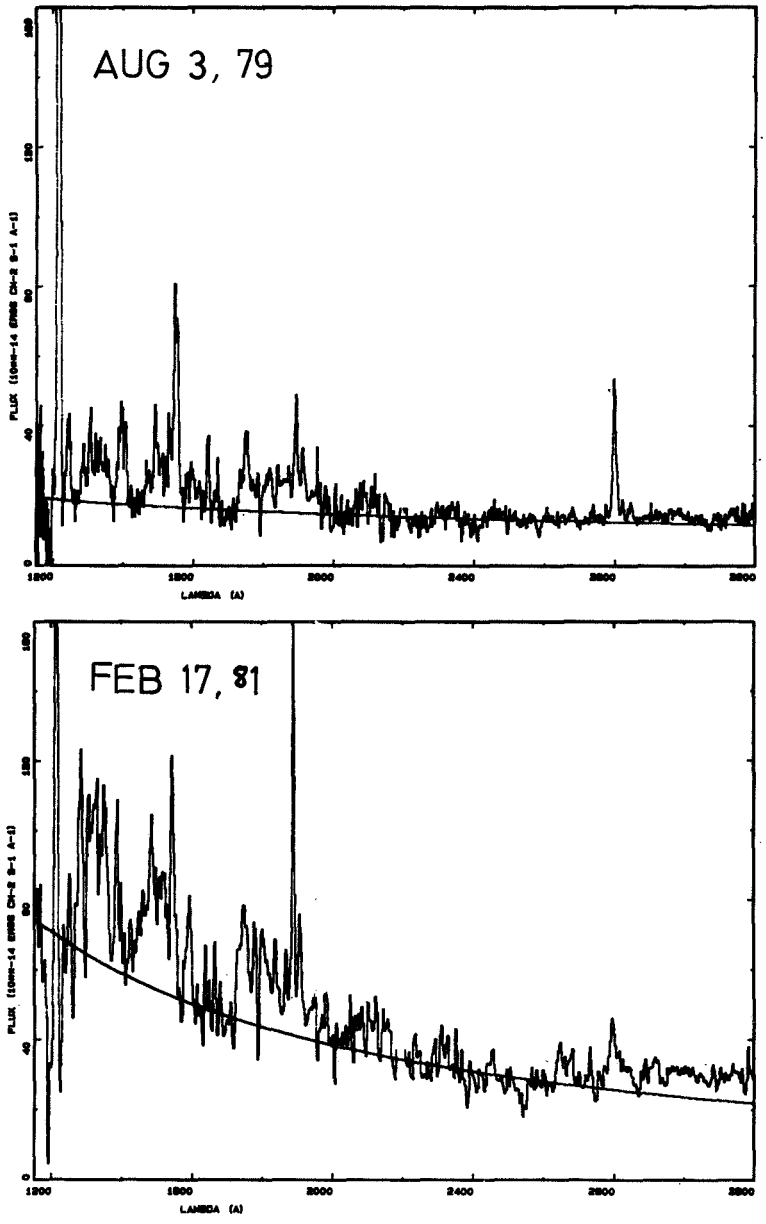

FIG 1

OPTICAL LIGHT CURVES OF SOME

CATACLYSMIC AND SYMBIOTIC VARIABLES

Janet A. Mattei
American Association of Variable Star Observers (AAVSO)

ABSTRACT

Observers of AAVSO have been involved in simultaneous monitoring of large number of cataclysmic and symbiotic variables in the observing program of several IUE guest observers. Our immediate alerts of the outbursts of cataclysmic variables and the behavior of these stars have helped astronomers in efficient use of telescope time.

Optical light curves of some of these IUE observing targets, listed below, will be exhibited in poster form.

Cataclysmic Variables	Symbiotic Stars
RX And	Z And
SS Aur	R Aqr
Z Cam	CH Cyg
SS Cyg	CI Cyg
U Gem	AG Dra
AH Her	AX Per
AY Lyr	

Copies of these and other AAVSO visual light curves may be obtained from AAVSO at 187 Concord Avenue, Cambridge, Massachusetts 02138.

DISCUSSION - VARIABLE STARS

Thomas: So it seems that these results put in their grave the discussion of "blobs", "puffs" and "shells", which traverse the atmosphere without affecting its quasi-steady state.

Jordan: What is the history of the visual data from 59 Cygni?

Doazan: 59 Cyg has been known as a Be star since the beginning of the century. It lost its emission after having undergone a spectacular episode of variation in 1977 and re-entered a new Be phase in 1978. The Hα emission increased slowly and irregularly and is still, 4 years later, at a low level. We have monitored the star with IUE during this period which was found to be a phase where the largest displacements of the superionized lines were observed. This suggests that the beginning of the formation of a cool envelope, which defines the Be phenomena, is an epoch of strong activity of the mass flux of the star.

Holm: At the symposium two years ago, you pointed out that the appearance of line profile variations was caused by image processing artifacts. Do you believe that you have managed to eliminate such artifacts from your spectra? An improved high dispersion processing system was instituted at Goddard in November 1981 so that only your most recent spectra were processed by it.

Grady: Yes, most of the artifacts I reported on two years ago can be eliminated in the spectra by thoroughly smoothing the interorder spectrum and then subtracting it from the gross spectrum. Use of improved echelle "ripple" correction algorithms also improve the quality of the data. Together with the most recent improvement in the high dispersion processing system, data artifacts can be largely removed.

Peters: I observe similar, though not identical, spectral variations in the Be stars W Ori, 66 Oph, and HR 4009 which will be discussed tomorrow. Although their C IV, Si III, Si IV profiles, variations, and velocities are very much alike, Hα is weak in W Ori and strong in 66 Oph and HR 4009. Hα strength and variations do not parallel changes in the UV features.

Thomas: Unless my memory is bad, a strongly puzzling feature of R CBr has been the appearance of λ4686 He II in emission at light minimum. Have you tried to compare your far-UV spectrum with visual observations that show such λ4686 emission, i.e., at epochs where 4686 is and is not present, to see what happens in the far-UV?

Holm: Most investigators (Payne-Gaposchkin, 1963, Ap. J., 138, 320; Alexander et al., 1972, MNRAS, 158, 305; Spite and Spite, 1979, A&A, 80, 61) have reported strong emission lines of Ca II, H and K, Na I D, and He I λ3888 and sharp lines of neutral and ionized metals. This is consistent with the IUE spectra. I do not see, in this set of observations, lines of C IV λ1550 or He II λ1640 and have not yet tried to put an upper limit on their fluxes. It is possible that He II emission might be associated with the pulsational variation. Schmidt and Parsons (1982, this symposium) find phase dependent C IV emission in the spectrum of the classical cepheid φCar.

Blair: Your optical spectra showed the N II] lines to be very strong. Have you used these lines to obtain a temperature?

Walborn: These lines are saturated on the photographic spectra and cannot be used to get a temperature. We do have some SIT spectra that are as yet unanalyzed.

Starrfield: What are the upper limits to the C/N and O/N ratios?

Walborn: If the excitation is due to shocks, the relevant temperatures are probably between 10^4 and 10^5K. The Hα luminosity and the [S II] lines independently suggest a density near 10^4 cm^{-3} in the condensation. Comparing similar ionization stages, one can then derive upper limits to the C/N and O/N abundance ratios ranging between 0.05 and 0.5.

Bell: Have you pursued this to the point of estimating the absolute magnitudes of the supernovae and obtaining a value of the Hubble constant?

Benvenuti: For the moment we have limited our estimates to the distance and therefore, absolute magnitudes of the two supernovae. Inthe future, for more distant supernovae, we might apply this method to obtain the Hubble constant.

Underhill: Does your 6.10 day period equal the rotation period of the star? One could conceive of the C IV and N V lines being formed in localized hot parts of the atmosphere which remain fixed, more or less on the face of the star, and rotate with the star. The period for rotation could be estimated by measuring $V_{rot} \sin i$ on visible spectra and using a radius typical for a star of the spectral type of βCep.

Peters: (1) Do you observe variation in the non-resonance lines such as the S III 1300 multiplet? (2) Were the Al III resonance lines variable?

Fahey: There were no significant changes in Si III at 1300 Å nor did there seem to be any for Al III at 1860 Å, though they may bear a second look.

Hack: Do the UV continua of your Cepheids agree with those expected from the visual spectral type?

Parsons: Probably so, although this has not been examined explicitly. Except for the bumps (the phases of excess flux), the UV light seems to just go up and down as expected from temperature variations.

Stencel: Is there in general a phase lag between Ca II K and Mg II 2800 Å emission in your sample of cepheids?

Parsons: Yes, to some degree. In δ Cep, for example, the Ca II emission is seen mainly from phase 0.84 to 0.88, while the Mg II peaks at 0.89

Underhill: Is the real bump due to Balmer continuum emission or to a general heating of the photosphere?

Parsons: My feeling is that the bump or excess flux is due to a general heating of the atmosphere. The bump is more pronounced at the shorter wavelengths. Radiation at longer wavelengths could be masked, however, by the stronger photospheric radiation.

Kafatos: How did you derive the ionic abundances needed for emission measurement determinations? Did you use a 100,000 UV continuum to do this?

Cassatella: Yes, we did.

Stencel: How does the N V emission component velocity compare with the velocities of Si IV, C IV or the intersystem lines?

Cassatella: On December 11, 1981, the N V 1239 A line was very slightly redshifted with respect to C IV and Si IV, and it is redshifted by about 18 km/sec with respect to the average of the intercombination lines. Naturally, we should remember that N V shows a P Cygni profile not seen in the other lines, and this clearly affects radial velocity determinations.

Slovak: Has the 554^{d} variation seen in the U light curve continued since AG Dra's 1980 outburst?

Cassatella: I would expect to find evidence for these variations also in the UV. Such a study is in progress.

Michalitsianos: Would you summarize again the line profile structure of the AG Dra outburst? He II 1640 Å shows evidence for a wind. Are there other emission lines which also show such features aside from N V?

Cassatella: No other lines except N V have ever shown P Cygni profiles since June 1980, not even He II 1640 Å, which is the strongest emission line in the UV and it is superimposed to a better detectable continuum than N V. We believe that the He II line does not form in the source region as N V, not only for their flux ratio, but also for their completely different shapes. While the observation in N V suggests the presence of an accelerating wind, the H II broad component (F_{α} HM$\sim$6 Å) is more suggestive for the presence of our accretion disk in AG Dra.

Mattei: Between March and October 1981, AG Dra faded by 1 magnitude and then recovered. Do you have any IR observations during this time? If yes, does IR emission show any increase?

Cassatella: (Reply unavailable.)

Hack: I have observed CH Cyg in the HR mode, both in the SW and LW ranges on November 29, 1981. A reliable continuum has been traced through several windows where no emission and absorption lines are present. This continuum fits very well a Kurucz model for T_e = 8500 and log g $\sim$ 1 or 2. Hence, it mimics a late A supergiant. If a real supergiant were there it would be at least 3 vis. mag. brighter than the M6 III star, thus, masking completely the visual spectrum which instead is well observable at $\lambda\cong$4600. From our HR spectra (of 1980 and 1981) no trace of λ1640 He II is visible, while a very sharp and strong emission of λ1641 OI] is present.

Stencel: What is the geometry of your 'generic' model, i.e., where does quiescent state emission arise in the : (a) resonance lines; (b) intersystem lines; (c) Balmer continuum, in such systems? In CI Cyg?

Slovak: The "generic model" posits a cool star (T$\sim$3000 °K; L/L$_{\odot}$ $\simeq$ 200-400) and a hot source (T$_{*}\sim$50,000-200,000 K; L/L$_{\odot}$ $\simeq$ 100-500) separated by order of 10^2-10^3 R$_{\odot}$. The late-type component does not fill its Roche lobe at quiescence. The resonance lines arise near the hot source or possibly in a shocked boundary layer formed by the interaction

of winds from both sources (e.g., AG Peg). The intersystem lines and Balmer continuum seemed to be formed over a larger volume. The behavior of these lines during the eclipse in CI Cyg suggests that the resonance lines arise from a shocked region (or bright accretion spot) further away from the central source than the intersystem lines.

Malkan: Can you determine, (1) the Balmer continuum flux; and (2) the Balmer continuum temperature, or are these parameters unconstrained by the data?

Slovak: In principle, the residual fluxes obtained upon subtracting the contributions of both the hot and cool components can be used to estimate the Balmer continuum flux and temperature. I am currently using a planetary nebulae code, kindly provided by M. J. Seaton, to model the residual fluxes in terms of Balmer free-bound and free-free radiation.

Hack: Maybe the presence of the nebula can explain the anomalous extinction law ($E_{B-V} \sim 0.70$) but no trace of $\lambda 2200$ feature, according to L. Johnson, (Ap.J., February 1982). According to Johnson this extinction law could be explained by the presence of olivine grains (which are oxygen rich).

Starrfield: What are the abundances in the outer shell?

Kafatos: Normal.

Devinney: Can you estimate the mass of the nebula?

Kafatos: Yes. About 0.2 $M_\odot$.

Slovak: Why a jet, and not a spherical shell, in R Aqr? σ Ceti is very similar in morphology to R Aqr, a binary system containing a regular Mira variable and a hot companion. Another R Aqr candidate?

Kafatos: (Reply unavailable.)

Cassatella: How do you explain the two lobes which appear in the photographic plates of R Aqr you just showed?

Kafatos: (Reply unavailable.)

Jordan: What range of v(sin i)do those T Tauri stars exhibit?

Imhoff: Early values measured by Herbig were very large, in the range 35-50 km s^{-1}. More recent values we have obtained with improved techniques, more sensitive to lower values, yield, typically, 20 km s^{-1}. This is still large for a late-type star.

Dupree: Are there any systematic physical differences between the weak and strong line emitters that suggest in which direction your proposed evolution is proceeding?

Imhoff: It is not clear. The fact that "post T Tauri stars" have even weaker visual emission could indicate that the "strong emission" T Tauri stars are relatively younger than the "weak emission" stars. But the differences among the T Tauri stars themselves could be due to other factors such as mass, v(sin i), etc. The major point is simply that whatever "peculiarities" we see in the T Tauri chromospheres and coronae are likely associated with their youth.

Simon: What allowance for extinction have you made in your analysis of the emission line strengths?

Imhoff: We have corrected the emission line fluxes for extinction using a "normal" extinction law (R = 3.3) and the values of A_V given by Cohen and Kuhi (1979, Ap. J. Suppl, 41, 743). If the extinction is peculiar or these estimates are incorrect, then these fluxes may be off by, say, a factor of 2. The relative fluxes of the lines, however, should change very little. We have drawn primarily on these relative fluxes for our analysis largely because of this problem.

Szkody: Some of the dwarf novae at outburst show accretion rates in the same range as the UX UMa group, i.e, 10^{-7} to 10^{-9} $M_\odot$/yr so the distinction might not be higher accretion rates but a longer sustained high accretion rate.

Sion: Thank you. I meant to compare the high derived mass accretion rates for UX UMa type nova-like variables with those of dwarf novae in quiescence. In that case, it may be correct to say the UX UMa type binaries have higher $\dot{M}$. I feel very strongly that the high $\dot{M}$ inferred for UX UMa systems explains why they do not exhibit dwarf novae-type outbursts.

Slovak: Care must be taken in using broadband UBV fluxes, if strong emission lines are present, in making continuum fits since large errors will be made in setting the true continuum level.

Guinan: The optical spectrum of LS 55°-8 was obtained by Greenstein, Sargent and Haug (1970), and this shows only weak, broad Balmer absorption features with weak central emissions. Thus, I do not think these features will seriously affect the UBV fluxes.

Hack: (1) Are those spectra corrected for reddening? In this case the more recent continuous spectrum seems to indicate a higher temperature than the previous one.

Cassatella: (1) Yes.

Kafatos: The temperature of ~25,000K for the hot subdwarf that you mentioned, is it obtained by fitting IUE continua with black body curves? How does the temperature change?

Cassatella: Yes. We obtained it with fits to IUE continua near maximum T_{eff} ~20,000K, and it does not change very much.

Kiplinger: In your last (disk) model what physical process drives the instability and how did you treat viscosity?

Starrfield: We assumed an instability, i.e., we assumed the velocity was very low until a subsequent instability produced an increase in viscosity.

Slovak: What (gross) effect would a large magnetic field produce on the Williams et al. accretion disk models?

Szkody: It would eliminate the inner areas of the disk because they would be within the Alfven radius and the disk would just be a thin outer ring. Thus, it would be a relatively cool disk with less extent than the values used by Williams. This type of situation might exist for AE Aqr also.

Guinan: In your recent measures of SU UMa, was the star at relatively constant low brightness or high brightness?

Mattei: SU UMa was at minimum, with brightness between $13.^{m}5$ and $14.^{m}5$. This inactivity in SU UMa is different than the stillstands of Z Cam type dwarf novae, where the inactivity there is halfway between maximum and minimum.

CLOSE BINARIES

UV OBSERVATIONS OF THE 1981 ECLIPSE OF 32 CYGNI

Robert E. Stencel
Joint Institute for Laboratory Astrophysics
University of Colorado and National Bureau of Standards

Robert D. Chapman
NASA-Headquarters

Yoji Kondo
NASA-Goddard Space Flight Center

and

Robert F. Wing
Dept. of Astronomy, Ohio State Univ.

ABSTRACT

Preliminary results of an extensive set of high dispersion UV spectra of the supergiant eclipsing system 32 Cyg are detailed and contrasted with spectroscopic studies of other ζ Aur systems.

INTRODUCTION

32 Cygni (K5 Ib+B6 V) is a member of the ζ Aur class of 'atmospheric' eclipsing binaries. This group includes ζ Aur, 31 Cyg, 32 Cyg, VV Cep and ε Aur, with orbital periods ranging from 972 to 9890 days (Wright 1970; Hack 1981). Historically, optical studies have used the B dwarf stars in such systems to probe the cool supergiant's outer atmosphere. Such data have formed a cornerstone in our knowledge of stellar chromospheres. We approached ultraviolet observations in this spirit and found that as a bonus, information concerning binary star interaction arises.

The archetype, ζ Aur, underwent eclipse in late 1979, and Chapman (1981) has reported that the mid-eclipse UV spectrum is dominated by numerous emission lines. Comparing line strengths at second contact and mid-eclipse allowed us to determine that the hot lines are formed in a shell/halo around the B star rather than in a cool star transition region (Stencel and Chapman 1981). Outside of eclipse, we also discovered pronounced redshifted absorption, in the resonance lines of Mg II and C IV, which occurs only near time of secondary minimum. Chapman (1981) has proposed an accretion shock structure to explain this. It was against this background of results that we examined the subsequent eclipse of 32 Cyg. Unlike the central eclipse of ζ Aur however, 32 Cyg experiences a grazing occultation.

OBSERVATIONS

As a result of our efforts in programs MF2YK, CBCRW and OD46B, we have achieved fair synoptic coverage of the 1147 day orbit of 32 Cyg since late 1978. As a fortunate consequence of time trades with T. R. Ayres who was monitoring Capella, we obtained 24 sets of LWR+SWP spectra during March and April 1981. These spectra very clearly show the gradual extinction of the B star continuum and the development of a rich emission line spectrum at mid-eclipse. We note good agreement between observed and predicted times of eclipse.

ANALYSIS

The large amount of data poses a challenge to efficient analysis strategies. Our efforts are focused along the following lines. First, we have selected the longwave end of the SWP images (1600-2000 Å) as a region optimized for absorption line curve-of-growth studies. We have measured equivalent widths for a thousand lines of Fe I and Fe II to examine the height dependence of excitation and density in the K supergiant's outer atmosphere. The results are shown in Figure 1, and argue for the existence of a chromosphere, much as did the optical work of Wright (1959), with two important distinctions: we can probe to much greater distances in the UV and we have evidence for a geometrically extended chromosphere. This latter point is of interest in current cool star research (cf. Stencel 1982).

Second, we have measured emission line and continuum fluxes and velocity shifts in an effort to correlate these with tidal distortions observed photometrically by E. Guinan (private communication). Although substantial flux variations occur in many emission lines, they appear uncorrelated with the optical variations. Monitoring the velocity shifts in the multiple absorption components in the Mg II lines reveals no substantive shifts during the 1981 eclipse interval. In fact, repeated observations during 8 hour intervals near first and fourth contacts place stringent limits on the scale size and filling factor of "prominence-like" structures in the K star atmosphere, because little profile variation was noted.

Third, our observations spanning the interval near secondary minimum show pronounced changes in Mg II absorption and Fe III emission features, suggesting accretion shock structure with a scale size comparable to the orbital separation (cf. Chapman 1981). With secondary minimum approaching in March 1983, it would be prudent to monitor this system during the fifth year of IUE operations.

Finally, progress is being made in realistic models for calculation of the emergent radiation from these systems. Hempe (1982) has developed a generalized Sobolev method for three-dimensional flows with local nonradiative coupling. With this escape probability approach, he has qualitatively reproduced the phase variations of line profile shapes in ζ Aur. It is hoped that this approach will lead to accurate supergiant mass loss rate determinations.

OUTLOOK

1. Our experience in monitoring the ζ Aur systems suggests to us that understanding the nature of the binary interaction will require careful observation of secondary minimum passage, particularly in the UV. This should reveal details of the proposed accretion shock structure. One immediate application may be in the case of ε Aur (eclipse 1982-84) where the "mysterious secondary" may be an extended shock structure around a B dwarf. This hypothesis suggests strong changes may be seen in UV and the Balmer lines (cf. Chapman *et al.* — this volume).

2. The ζ Aur system interpretation may prove useful in application to related types of binaries, particularly the symbiotics and Ba II binaries. In each instance, similarities of spectral details (P Cyg features, line velocities) support the suggestion that comparable interaction processes are involved.

3. The ζ Aur systems will continue to play an important role in cool star outer atmosphere research. Three ways in which this will occur include: (a) exploration of extended chromospheres; (b) discovery of new fluorescence mechanisms with a *known* source of excitation (viz. Fe II UV 191), and (c) improvements in stellar wind and mass loss rate data.

ACKNOWLEDGMENTS

We wish to thank NASA and the staff of the IUE Observatory for their support of this research.

REFERENCES

Chapman, R. 1981, *Ap. J.*, *248*, 1043.
Hack, M. 1981, *Astr. Ap.*, *99*, 185.
Hempe, K. 1982, *Astr. Ap.*, in press.
Stencel, R. 1982, in *Second Cambridge Workshop on Cool Stars*, ed. M. S. Giampapa, S.A.O. Spec. Report, in press.
Stencel, R. and Chapman, D. 1981, *Ap. J.*, *251*, 597.
Wright, K. O. 1959, *P.D.A.O.*, *11*, 77.
_____. 1970, *Vistas in Astr.*, *12*, 170.

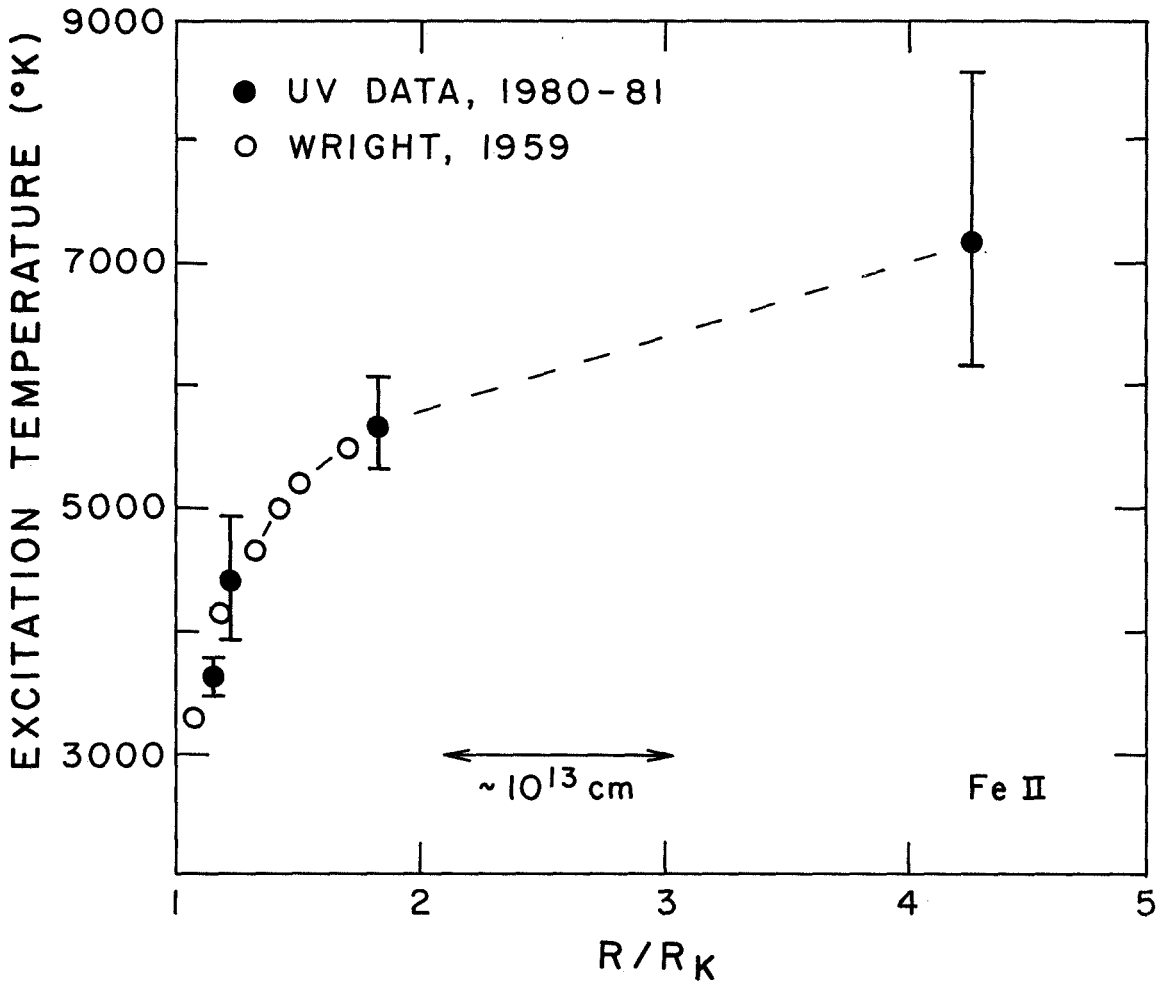

Fig. 1. Excitation temperature with height variation in the chromosphere of the K supergiant in 32 Cyg.

ANALYSIS OF NON-INTERACTING BINARIES WITH LUMINOUS COOL PRIMARIES

Sidney B. Parsons[1]
Laboratory for Astronomy and Solar Physics, Goddard Space Flight Center
and McDonald Observatory, University of Texas at Austin

ABSTRACT

High dispersion LWR spectra are being analyzed for the differential velocity between hot and cool components of heretofore single-lined spectroscopic binaries with late-type giant or supergiant primaries. Cross-correlation of a composite spectrum against early- and late-type standard stars yields relative velocities with an accuracy of 2 to 3 km s^{-1}. When the orbit of the primary is known, the differential measurement from IUE gives the mass ratio of the system.

Low dispersion SWP and LWR flux spectra are being used together with ground-based photometry to disentangle the composite energy distributions of the binaries. Temperatures of both components, their relative luminosities, and the reddening of the system are obtained. Assuming the hot secondaries to be main sequence stars, their probable luminosities and masses may be obtained from their temperatures. Then absolute magnitudes and masses may be obtained for the evolved primaries with more confidence than with existing techniques.

INTRODUCTION

The physical properties of luminous F and G stars are very poorly known, due to their rapid rate of evolution, hence low space density, and to the almost total lack of eclipsing binary systems containing such stars. The progenitor stars would have been of type O or early B, so we may expect a fair fraction to have companion stars of type early B to early A still near the main sequence. The visual magnitude difference is often considerable, and many hot companions have been detected unambiguously for the first time with IUE: the supergiants HR 4511 (Böhm-Vitense and Dettmann 1980) and HR 8752 (Stickland and Harmer 1978) and the Cepheids η Aql and T Mon (Mariska, Doschek, and Feldman 1980a, 80b) are examples. A new window has truly been opened with space ultraviolet instruments for the study of luminous cool stars by means of analysis of their UV-bright companion stars. When the systems are wide enough so that interaction is negligible, normal masses and luminosities may be assumed for the secondaries to derive estimates of these properties for the primaries.

---

[1] Senior NRC-NASA Research Associate

HIGH DISPERSION

For the known single-lined spectroscopic systems, for which ground-based work has provided the orbits of the cool components, the LWR high-dispersion mode now allows these to be studied as double-lined binaries, so that mass ratios may be obtained. Typically the crossover in dominance of the combined flux occurs between 2600 to 3000 Å, so that different portions of a single LWR spectrum may be analyzed for the separate velocities of the components.

An example is provided by HR 3080 (a Pup), which was noted by Parsons et al, (1976) to have a hot companion from its Skylab spectrum. An LWR exposure obtained in 1978 by Kondo shows absorption lines around 3000 Å that are typical of late G or K stars but diluted by about 50% by flux from the hot component. B stars have very little line absorption in this region, whereas around 2500 Å they have many lines primarily from Fe II. In this region the cool component contributes negligible flux, and the net spectrum correlates well with late B or early A stars.

For efficient analysis of the relatively low signal-to-noise data, a cross-correlation procedure was written in IDL for use at the Regional Data Analysis Facility. The procedure works best on about one spectral order at a time (after ripple correction). Standard velocity stars of types B7 V, A0 V, G0 Ib, and K0 III were selected from data available at the NSSDC, but each image is affected by the ± 2.7 km s^{-1} uncertainty in absolute wavelength scale (Thompson, Turnrose, and Bohlin 1981). Portions of synthetic spectra for A0 V and G0 Ib models by Dreiling and Bell (1980) and Bell and Parsons (1974) were cross-correlated against the standard star LWR spectra, and these stars against each other, resulting in self-consistent velocity zero-points with better than 1 km s^{-1} accuracy.

When applied to HR 3080, the cross-correlation results for $\lambda > 2850$ Å show very little scatter from order to order and give a well-defined mean for the cool component. For $\lambda < 2650$ Å the veolcities are definitely less positive than the longer wavelength mean but show more scatter, especially toward the shorter wavelengths where the exposure level is rather weak. A difference of 17.5 ± 2.5 km s^{-1} is obtained between the two wavelength domains. The orbit derived by Christie (1936) from 14 old observations predicts that the unseen star should have a more positive velocity in 1978 instead. New McDonald 2.1m coudé Reticon observations have been obtained and require a considerable revision in the period of the system, from 2660 to about 2555 days, and the IUE observation is now consistent. Since the absolute velocity is not dependably derived from IUE images, we shift the cool component value onto the orbital curve and find that a mass ratio $\mathcal{M}(\text{hot})/\mathcal{M}(\text{cool}) \approx \frac{1}{2}$ will fit the velocity differential. In collaboration with T. Ake, F. Fekel, C. Harvel, and Y. Kondo, IUE observations of several spectroscopic binaries are planned for this year, including one of HR 3080 near the revised time of periastron passage, when the velocity difference should be ≈ 40 km s^{-1}.

LOW DISPERSION

The fluxes obtained from IUE exposures are combined with Johnson system photometry for analysis by means of the plot program described by Parsons (1981). A grid of intrinsic colors is used to match the observations by trial and error combinations of two spectral types, two V magnitudes, and a reddening parameter E(B-V). The LWR spectra are particularly useful for determining the reddening of the system, while the SWP fluxes provide a rather good determination of the temperature class of the hot component. Several absorption line features in the low-dispersion SWP spectra are temperature sensitive and provide independently a classification of the hot component through use of the IUE standard star spectra (Wu et al. 1981).

Given the temperature class of the secondary and the probability that it is only moderately evolved, its absolute magnitude may be estimated with an uncertainty of around ±0.7 mag in general. The difference in V magnitude between the two components is inferred from the flux fitting to an accuracy of about ±0.3 mag. This combined uncertainty is still considerably less than that of spectroscopic absolute magnitudes for luminous cool stars, where the difference beween luminosity classes is 2 to 3 magnitudes. Quantitative techniques such as the O I 7774 strength (earlier than G2) and Ca II K-line emission width (G0 and later) promise greater accuracy but are not adequately calibrated for supergiants. The binary technique will provide several new calibration points of moderate reliability.

Table 1 lists those systems which have been examined so far. The UV spectral types given are obtained primarily by inspection of the SWP spectra. Most systems were known spectrum or spectroscopic binaries, while ν Her had no ground-based evidence of duplicity. Analysis of the fluxes is in progress, and visual absolute magnitudes have been estimated now for three of the primaries: HR 2786, -3.8; HR 2859, -4.0; and HR 3080, -2.0. It now appears unnecessary for the secondary of HR 3080 to be subluminous as was claimed by Parsons et al. (1976).

REFERENCES

Bell, R. A., and Parsons, S. B. 1974, M.N.R.A.S., 169, 71.
Böhm-Vitense, E., and Dettmann, T. 1980, Ap. J., 236, 560.
Christie, W. H. 1936, Ap. J., 83, 433.
Dreiling, L. A., and Bell, R. A. 1980, Ap. J., 241, 737.
Mariska, J. T., Doschek, G. A., and Feldman, U. 1980a, Ap. J., 238, L87.
------. 1980b, Ap. J., 242, 1083.
Parsons, S. B. 1981, Ap. J., 247, 560.
Parsons, S. B., Wray, J. D., Kondo, Y., Henize, K. G., and Benedict, G. F. 1976, Ap. J., 203, 435.
Stickland, D. J., and Harmer, D. L. 1978, Astr. Ap., 70, L53.
Thompson, R. W., Turnrose, B. E., and Bohlin, R. C. 1981, IUE NASA Newsletter No. 15, p. 8.
Wu, C.-C., Holm, A.V., Schiffer, F.H., and Turnrose, B.E. 1981, ibid., No. 14, p. 2.

Table 1

Luminous F and G Stars with Companions
Observed with IUE

Name	HD #	Ground Spectral Type	SB?	UV Sp. Type
HR 1129	23089	G0 III + A3 V F8 III-IV + A2:	220^{d}	B9 (-)
52 Per	26673	G2 I + B G5 Ib + A2 G8 III	1577^{d}	B9.5-A0
HR 2786	57146	†G1 Iab-b (H&K shallow) G2 Ib "	?	B9-9.5
HR 2859	59067	G8 I-II + B	no	B2
HR 3080	64440	G5 III K1/2 II + A	2555^{d}	A0
HR 4511	101947	F9 Ia v	?	B0.5-1 Iab-b
ν Her	164136	F2 II	no	B9.5
β Sct	173764	G4 II	832^{d}	B9.5 (-)
35 Cyg	193370	F5 Ib	2451^{d}	B8 (-)
HR 8157	203156	F3 II (v) + ?	prob.	B6-7
HR 8242	205114	G0 II + A G2 Ib + A-B G2 II + B9	?	B8 (+)

PRE-ECLIPSE ULTRAVIOLET SPECTRA OF EPSILON AURIGAE

Robert D. Chapman and Yoji Kondo
Laboratory for Astronomy and Solar Physics
NASA, Goddard Space Flight Center

and

Robert E. Stencel
Joint Institute for Laboratory Astrophysics
Boulder, Colorado

The enigmatic supergiant eclipsing binary system Epsilon Aurigae is predicted to enter eclipse beginning in 1982 July. The eclipse is very broad: ingress and egress partial phases last about six months, and totality lasts about one year. The system, one of the longest period eclipsing binaries known, is often classed as a Zeta Aurigae type system, (Wright 1970). However, in Zeta Aurigae the primary eclipse occurs when the K-type supergiant star eclipses a B-type main sequence star, while in Epsilon Aurigae the eclipse occurs when an unknown companion eclipses the F-type supergiant. Ground based observations during the 1955-56 eclipse have been interpreted to support a picture proposed by Struve (1956) and Huang (1965) in which an early-F type supergiant is losing mass through its inner Lagrangian point. The mass flow from the supergiant most probably occurs in all directions like a typical stellar wind, though there may be superposed on that flow an additional flow through the inner Lagrangian point. Some of the material forms a cloud around the supergiant and some forms an accretion disk around the secondary. The spectral type of the secondary is uncertain, though it is usually assumed to be an early type main sequence star. Hack and Sevelli (1978) observed the system with IUE at low resolution, and found evidence for a B-type spectrum in the far ultraviolet. Plavec (1981) asserts that the B-type spectrum could come from a hot spot at the center of an accretion disk. Chapman (1981) has suggested a model of Zeta Aurigae based on IUE data of the 1979-1980 eclipse, in which the high speed wind from the K-supergiant interacts with the B-star to produce an accretion bow shock around the B star. Stencel and Chapman (1981) have elaborated on the model. It is possible that the eclipse in Epsilon Aurigae could be caused by a structure like that bow shock.

The eclipse occurs when the supergiant is eclipsed by the mysterious secondary companion. Huang (1965) suggests that the eclipse is caused by a very large (800 solar radii) partially opaque disk. The idea that the disk is partially opaque is inferred from the fact that some late-A or early-F spectrum is

present at all times in the visible light spectrum. The possibility of an immense accretion disk that is capable of occulting the supergiant at an eclipse, but at the same time is undetected in the visible is an intriguing astrophysical problem. One possibility is that the temperature of some segments of the disk is so high that it is visible only in the ultraviolet. It is this possibility that has prompted our observing program to study the eclipse with IUE.

Castelli et al. (1982) have described a high-dispersion, long-wavelength IUE spectrum of Epsilon Aurigae made on 19 April 1978. The spectrum was well exposed longward of 2450 Angstroms. We obtained high-dispersion long- and short- wavelength spectra on 18 August 1981. In addition, a spectrum made in 1976 with the Balloon-borne Ultaviolet-Stellar Spectrograph (BUSS) is available, (Castelli et al. 1982). The Buss spectrum has an ample signal-to-noise ratio only in the wavelength range 2750 - 3170 A, thus the IUE and BUSS spectra can be intercompared only in the 2750 to 3000 A range. These spectra all provide a baseline measurement of the ultraviolet spectrum of the system before eclipse, and should be a valuable aid in the analysis of the data to be taken by several groups of investigators in the fifth year of IUE.

There is very little detail in the spectrum in the vicinity of the C IV resonance doublet, and it is questionable whether these lines are present in the August spectrum. We intend to take at least one very deep exposure in our fifth year program, which may help resolve this question. According to Castelli et al. (1982) the profiles of the Fe II lines of multiplets UV 1, 62 and 63 are peculiar. They point out that the strong cores of some of the lines are greatly weakened as if affected by a central emission, and an absorption peak shifted toward shorter wavelengths is present. In our spectrum, there also appears to be a weak emission in the cores of the lines. A similar emission is also visible in the cores of the lines of multiplet UV 161. There also appears to be a strong longward shifted, multiple absorption in the vicinity of Fe II (1), (Figure 1) perhaps indicating the presence of isolated, moving clouds of material in the circumstellar cloud.

The Mg II resonance lines sit within a depression of the continuum which is probably the broad photospheric lines from the F-supergiant photosphere. The strongest component of the absorption--which we believe to be interstellar--appears to be a single line in our IUE spectrum, but appears to be double in BUSS spectrum. Castelli et al.'s IUE spectrum is described (Castelli et al. 1982) as very similar to ours. Our spectrum shows clear evidence of multiple absorption, not unlike that in the Fe II lines. On the longer wavelength side of the interstellar component, there are three obvious red shifted absorptions. The situation in the BUSS spectrum is a bit more ambiguous, because of the lower signal-to-noise ratio. Nevertheless, there is a

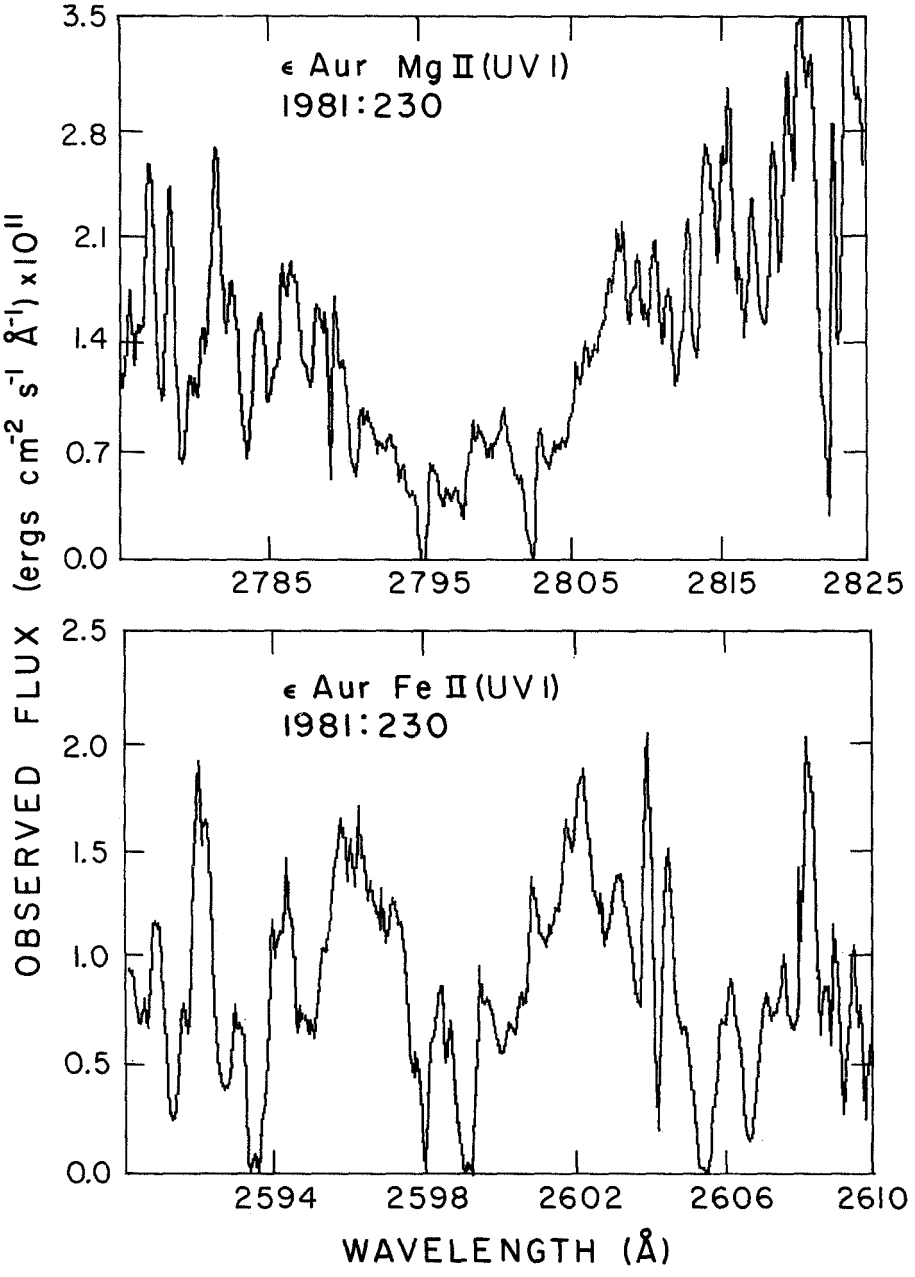
ε Aur Mg II (UV 1)
1981:230
ε Aur Fe II (UV 1)
1981:230
OBSERVED FLUX (ergs cm⁻² s⁻¹ Å⁻¹) x 10¹¹
WAVELENGTH (Å)
3.5
2.8
2.1
1.4
0.7
0.0
2785
2795
2805
2815
2825
2.5
2.0
1.5
1.0
0.5
0.0
2594
2598
2602
2606
2610

Figure 1

strong indication of an ill-resolved red-shifted absorption associated with both of the lines of the resonance doublet. It is premature to make any more detailed speculations on the nature of the absorbing volume in the Epsilon Aurigae system.

Epsilon Aurigae will be within the solar occultation limits of IUE for the three month period from early May to late July. So called hot betas--positions of the star relative to the sun that allow sunlight to heat critical portions of the spacecraft during observations--may limit lengthy exposures in the Sept.-Oct. 1982 and Jan.-Feb, 1983 time frames.

During the 1982-1984 eclipse of Epsilon Aurigae, there will be a campaign of observations in addition to the IUE programs that have been approved. The aim is to encourage photometry, spectroscopy and polarization studies in the visible and infrared to go along with the ultraviolet spectroscopy being done on IUE.

REFERENCES

Castelli, F. et al. 1982, Preprint, Astronomical Observatory of Trieste

Chapman, R. D. 1981, Ap.J. 248, 103.

Hack, M. and Sevelli, P. L. 1978, Nature, 276,376.

Huang, S-S. 1965, Ap.J. 141, 976.

Plavec, M. J. 1981, in "The Universe at Ultraviolet Wavelengths: The First Two Years of IUE," ed. R. D. Chapman, NASA CP-2171, p. 397.

Stencel, R. E. and Chapman, R. D. 1981, Ap.J. 251, 597.

Wright, K. O. 1970, Vistas In Astronomy, 12, 147.

CI CYGNI SINCE THE 1980 ECLIPSE

Robert E. Stencel
Joint Institute for Laboratory Astrophysics, University of Colorado
and National Bureau of Standards

Andrew G. Michalitsianos
NASA Goddard Space Flight Center

and

Minas Kafatos
Physics Department, George Mason University

ABSTRACT

Following the 1980 eclipse of the 855 day period symbiotic binary CI Cyg, we were confronted with a data set showing high excitation resonance lines which were largely uneclipsed but brightening on an orbital timescale, and intercombination lines exhibiting pronounced but nontotal eclipses and which were fading on an orbital timescale. Our model invoked a low density dissipating nebula surrounding the hot companion to explain the intercombination lines, and a shock between stellar winds to interpret the resonance lines. Subsequent synoptic observations have revealed continuing changes in the UV emission line fluxes, consistent with those described above, except for the brightening of Mg II and the emergence of strong, not previously seen [Mg V] emission. Post-outburst and phase dependent changes must be included in any interpretation of this system as the archetypal symbiotic binary. We anticipate that critical observations will be made during the 1982 October eclipse.

INTRODUCTION

CI Cygni (HV 3625) is relatively unique among symbiotic stars in that its complex but quasi-regular light variations are indicative of eclipses on an 855 day period (cf. Mattei 1978). Eclipsing symbiotics present not only an *a priori* argument for binarity, but can also be extremely useful in delimiting the physical interaction involved. Other eclipsing systems include AR Pav (Hutchings and Cowley 1982), possibly SY Mus (Michalitsianos and Kafatos 1982), and EG And (Stencel — this volume).

In the course of IUE programs ZACRS (1980) and ZADRS (1981) we have, with the addition of archival data from 1979, extended synoptic coverage of CI Cyg over more than one full orbital cycle, including the 1980 June eclipse. The results of the eclipse study are presented in detail elsewhere (Stencel *et al.* 1982). In this report we wish to detail striking recent changes in the UV spectrum of CI Cyg.

The light curve of CI Cyg can be characterized by outbursts on a many-orbit timescale, with a decay period between bursts, all punctuated by rapid, deep eclipses every 855 days (Bath 1981). Placing the IUE observations in this context indicates that the data were obtained during the later asymptotic decay phase following the 1975 outburst. To our surprise, we discovered that while the intermediate temperature intercombination lines (N III, Si III, O III) were becoming fainter, He II 1640Å, and other high temperature (100,000 K) resonance lines (N V, Si IV, C IV) were actually brightening. At the same time the intercombination lines showed substantial eclipse effects, while the resonance lines were largely unaffected. The Balmer continuum, measured at 3000Å showed a total eclipse but comparatively little secular change. He II also showed a deep eclipse.

THE MODEL

We suggested that the Balmer continuum originates in the exterior of a thick but aging accretion disk. From the integrated light and reddening, we can estimate a total disk luminosity of about 200 $L_\odot$. Scaling laws for accretion disks suggest that a 1 $M_\odot$ white dwarf and a mass transfer rate of 10^{-7} $M_\odot$ yr^{-1} would satisfy the observed luminosity. Using a model for the continuum distribution, Kenyon (1982) argued for a main sequence companion to the red giant in CI Cyg, and our results suggest that if such an object is present (inclination and reddening factors may allow this) a transfer of 10^{-5} $M_\odot$ yr^{-1} would be needed. This latter rate may lead to super-Eddington flows and these may be involved in the outbursts.

To explain the secular behavior, we also postulated a low density dissipating nebula surrounding the hot companion. This may help to understand the changes in the intercombination lines and the He II feature (assuming photoionization-recombination). To explain the behavior of the hot resonance lines requires substantial emissivity at distances large compared to the dimensions of the occulting red giant star. A shock between stellar winds might accomplish this, and may also represent the "steady state" configuration of the system between outbursts.

RECENT SPECTRA

Mg II 2800Å emission presented a puzzlement because throughout 1980 it was observed to decline essentially irrespective of the eclipse phenomena seen in other lines. However, in early 1981 the trend sudddenly reversed and Mg II emission has been steadily strengthening in CI Cyg (see Fig. 1a). One could interpret this behavior in terms of a phase dependent modulation by the binary: bright between phases 0.5-0.75; faint between phases 0.75-0.5. Perhaps this represents a bright spot on the disk where the stream of accreting matter arrives, or a bright quadrant on the red giant star. Either way, the asymmetry is puzzling. Critical observations in spring 1982 will reveal the degree to which the Mg II behavior is modulated in phase.

Contemporaneous with the increasing Mg II emission in the appearance of [Mg V] emission at 2783 Å. This high excitation forbidden feature has not

been detected in any of the UV spectra of CI Cyg preceding 1981, and it has brightened throughout the past year (see Fig. 1b). Although the change in low dispersion sampling procedure has helped to augment the visibility of the 2783Å feature, comparing photowrites leads us to believe that the pre-1982 upper limits are valid. A high dispersion observation in 1981 August showed the feature to be diffuse, with a base width of about 150 km s^{-1}. The Mg II emission in that same high dispersion image showed redshifts with respect to lab wavelengths, much as though only the emission portion of a P Cygni profile was detected. This is reminiscent of P Cyg Mg II features seen in other interacting binaries containing late type stars (Stencel 1981). The emergence of [Mg V] must hail a new density threshold for the expanding nebula, and suggests that other forbidden lines may strengthen prior to a new outburst. Again, continued observations are critical.

OUTLOOK

The next eclipse of CI Cyg is fast approaching (October 1982), with ingress in the UV lines likely to begin before July. In addition to the secular changes in Mg II and [Mg V], their eclipse variations are worthy of close study. Also the odd behavior of the Si IV 1393/O IV] 1402 ratio which decreases dramatically during eclipse, deserves reobservation, as does the peculiar mid-eclipse flare-like brightening which is present in the optical data and suggested in the UV line variations. Deeply exposed high dispersion observations will also prove of value.

ACKNOWLEDGMENTS

We wish to thank NASA and the staff of the IUE Observatory for valuable assistance in this research. We also express appreciation to A. A. Boyarchuk and the Crimean Astrophysical Observatory for optical photometry in support of this monitoring program.

REFERENCES

Bath, G. 1981, in Proceedings North American Workshop on Symbiotic Stars, ed. R. Stencel (Boulder: JILA), p. 20.

Hutchings, J. and Cowley, A. 1982, Publ. Astron. Soc. Pacific, in press.

Kenyon, S. 1982, Bull. A. A. S., 13, 804.

Mattei, J. 1978, J. Roy. Astron. Soc. Canada, 70, 325.

Michalitsianos, A. and Kafatos, M. 1982, in The Nature of Symbiotic Stars, IAU Colloq. No. 70, eds. M. Friedjung and R. Viotti (Dordrecht: Reidel), in press.

Stencel, R. 1981, in Proceedings North American Workshop on Symbiotic Stars, ed. R. Stencel (Boulder: JILA), p. 25.

Stencel, R., Michalitsianos, A., Kafatos, M. and Boyarchuk, A. 1982, Ap. J., 253, L77.

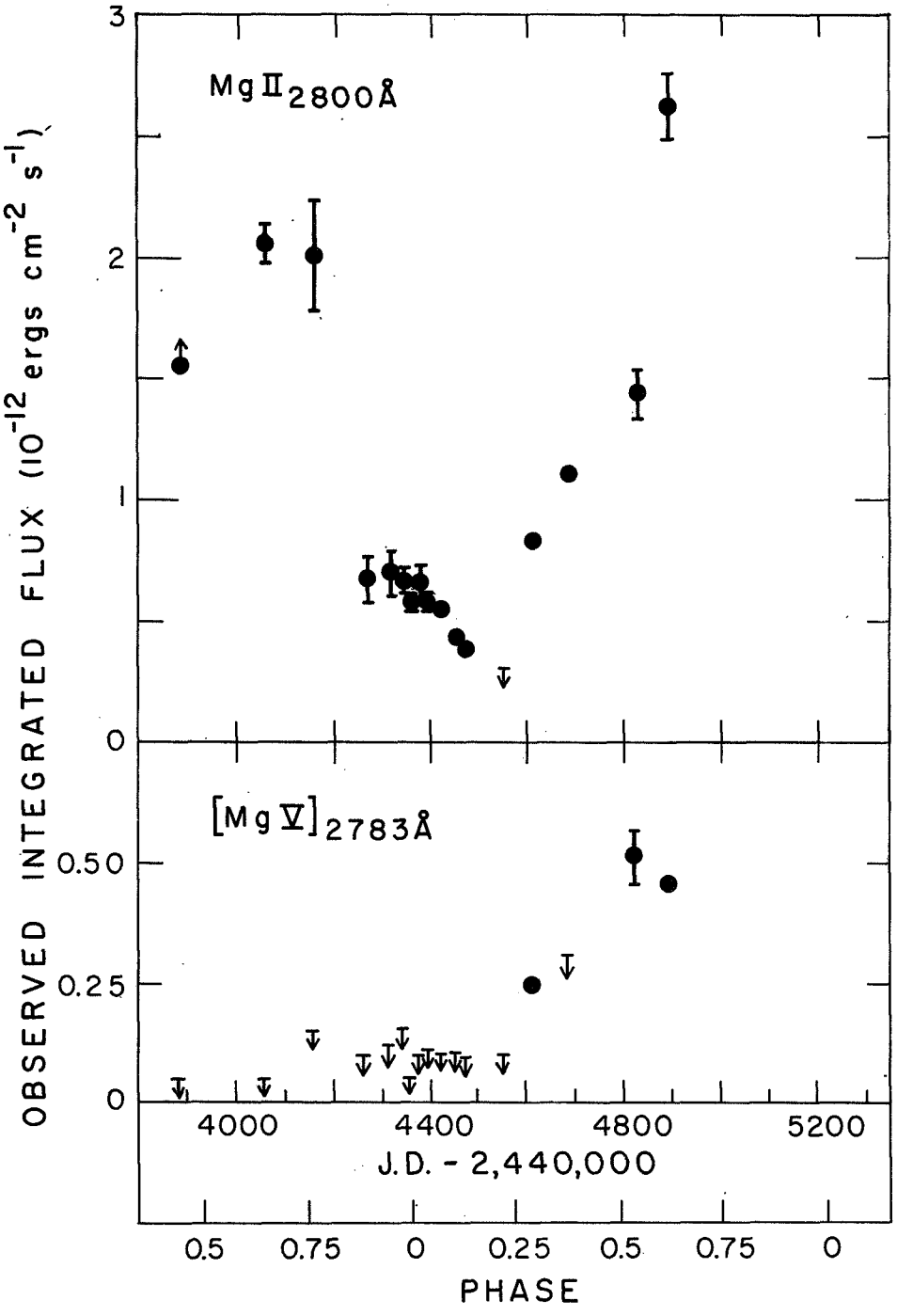

Figure 1. Temporal line variations in the spectrum of CI Cygni.

IUE SPECTROSCOPY, VISIBLE-BAND POLARIMETRY, and RADIOMETRY OF V641 Mon

R.H. Koch, B.J. Hrivnak, D.H. Bradstreet, and W. Blitzstein
Department of Astronomy & Astrophysics, University of Pennsylvania

R. J. Pfeiffer
Department of Physics, Trenton State College

P. M. Perry
Space Science Division, Computer Science Corporation

ABSTRACT

This hot, double line, ellipsoidal variable member of NGC2264 has been shown previously to be either a semi-detached or contact close binary. Low-resolution IUE spectra are best fitted to a Kurucz model atmosphere for very small (~ 0.08 mag) E(B-V). The familiar interstellar absorption dip near λ2200 is apparently absent. A suitable model atmosphere can be fitted to the IUE fluxes, but flux excesses (compared to the model) appear for all the published U- through L-magnitudes. The spectrum of the B- through L-excess appears to follow a λ^{-4} dependence. We show that this cannot be interpreted as arising from another star fortuitously observed in the visible band or IR. New ground based polarization measures indicate V641 Mon to be a polarization variable. Previous and new V light curves show the amplitude of light variability itself to be variable by about a factor of 2. It is suggested that all these observed characteristics are best explained by postulating "third light" and identifying part of it with Rayleigh scattered starlight very near to the stars. From this same region there arises circumstellar absorptions which give rise to non-theoretical strengths for Si II and Si III lines.

INTRODUCTION

According to Vasilevskis et al. (1965), V641 Mon (HD47732, vM37, W50) has a high probability of membership in the very young open cluster NGC2264. For a long time this star was known to show doubled absorption lines, and eventually Beardsley and Jacobsen (1978) collected and solved the radial velocity curves. Walker (1956) obtained the first modern photometry of the star and showed it to be the 6-th brightest cluster member. Subsequently, Koch et al. (1978) discovered ellipsoidal variability and presented limiting semi-detached and contact models for the binary system. The Keplerian period is close to 1.3 days.

Our group at the University of Pennsylvania monitored the light curve of V641 Mon for 4 consecutive observing seasons and found it to be intrinsically variable in amplitude and shape. In fact, during the 1978-1979 season no variability could be convincingly detected while in 1979-1980,

the peak-to-peak light amplitude was about 0.03 mag, i.e. nearly half the amplitude during the discovery season. Consequently, we decided to observe this relatively hot and massive system with the IUE spacecraft in order to see if any UV details could offer help in interpreting the visible band results. In the fall 1980, 8 SWP and 6 LWR spectra, all well exposed, were obtained. These are about equally divided between high and low resolution spectra.

THE STELLAR LINE SPECTRUM

Numerous double lines of C II, III and IV; Al III; Si II, III and IV and S II are seen on the IUE high dispersion spectra. Those which are not contaminated by reseaux or too badly blended by interstellar lines have been planimetered for equivalent widths and yield a light ratio, $(L_c/L_h)=0.46$ ($1\sigma=0.03$) which is consistent with either two limiting solutions of the light curve. The well-determined light ratio might be interpreted in the sense that the line spectrum is uncomplicated. However, this is not so for the Si lines. Compared to Kamp's (1978) theory, the Si IV absorptions are too weak and the Si II and III absorptions too strong for the stellar temperature (derived below). Another indication of complexity appears in the log (Si IV/C IV)-ratio. If one uses the calibration from S-019 and low resolution IUE data by Henize, Wray and Parsons (1981), the ratio for V641 Mon is too small. These complexities suggest that line-of-sight circumstellar gas adds shell or stream absorption to the photospheric strengths for the II and III ions while the Si IV absorptions are filled in by emission from a weak wind from the hot star for which $-5.5 < M_{bol} < -4.4$.

THE CONTINUUM

On the low resolution spectra smooth continua were drawn and the time-integrated flux values read at 50 Å-intervals. These were manipulated with the sensitivity calibration of Bohlin *et al.* (1980), corrected to the standard temperatures of the camera heads, and divided by the exposure times corrected for the camera rise and decay intervals.

These continua were then subjected to de-reddening for values of $E(B-V)$ from 0.04 to 0.12 using the extinction laws of Nandy *et al.* (1975) and Seaton (1979). From the beginning it was evident that the λ2200 "dip" was lacking in these spectra and therefore that any conventional de-reddening would introduce a "bump" into the spectra. The spectra, so de-reddened, were then tested against a wide range of model atmospheres by Kurucz (1979). Although it was difficult to choose between the two extinction laws, the best fit was attained with Seaton's law for $E(B-V)=0.08$ and a model atmosphere with ($T=22{,}500$K, log $g=4.0$, and log $A=0.00$). While this value of $E(B-B)$ is consistent with the value derived from UVB data alone and while the temperature for the model compares favorably with the weighted mean of the temperatures used for the light curve modelling, there remain two problems with acceptance of these results. The first of these - the intrusion of the "bump" near λ2200 - can only be explained if the grains which ordinarily give rise to the absorption feature do not exist or have not survived within the cluster medium. Presumably, these could not form or did not survive because

of the UV flux from the hot cluster members, but this is only a speculation. The second problem concerns the UBV photometry and IR radiometry observed by Walker (1956), Warner et al. (1977) and Mendoza and Gomez (1980). With the exception of the J-bandpass, the U- through L-magnitudes developed from these observations have been converted into absolute fluxes by the calibration of Hayes (1978). The calibration of the J-magnitude was simply a personal interpolation between Hayes's calibrations for I and H. The value of V determines, in part, the interpretation of the rest of the visible-band and IR radiometry. If V = +8.11 is accepted (this being the brightest value ever assigned to the star), all U- through L-magnitudes are brighter than the model atmosphere permits. If V = +8.22 is accepted (this having been derived from the FES-counts and being very close to the faintest observed value of V = +8.24), the U- and L-magnitudes are marginally fainter than required and all other magnitudes brighter than permitted by the model atmosphere.

We have considered several possible explanations for this effect. (1) Hayes's calibration could be systematically in error. However, Koch et al. (1981, unpublished) used this calibration successfully for the UBV-data of the hot binaries V Pup and HD 47755. (2) The reddening is really greater than E(B-V)=0.08. Because A/E increases with decreasing wavelength, a larger value of E will preferentially lift the IUE fluxes compared to the UBV- and IR-fluxes. A value of E(B-V) as large as 0.14 can be countenanced from Walker's photometry but, when it is used, it leads to a model atmosphere temperature significantly higher than can be justified from the spectral types and temperature scale of Code et al. (1976) employed for the light curve modelling. (3) The UBV- and IR-magnitudes are fallaciously bright because the observer measured background in dark parts of the NGC2264 nebulosity rather than in an offset field where the nebulosity has the distribution of brightness appropriate for the variable. It is true that this star appears amid some of the most complicated nebulosity in the cluster, and it inevitably happens that the papers relating the photometry and radiometry do not describe the locations where background was measured. Nonetheless, it seems most unlikely to us that 3 different teams working at different stations over a span of more than 20 years will fall into the same systematic error. (4) Since the V light curve is variable at least in shape and since the IUE spectra are not contemporaneous with any of the V-light curves or the U- through L-magnitudes, it is unreasonable to expect a unique fit. This objection cannot be denied but the correlation, described in (6) below, of the excess fluxes above the level of the model atmosphere suggests that only a minor contribution to the excess fluxes can be expected from this cause. (5) The excess flux arises from a third star that is fortuitously observed in the line of sight to the binary. The spectral continuum peak of the excess flux suggests a late-F spectral type and the absolute V flux level would be appropriate for a star of V ~ +10. No such star has ever been noted in the close vicinity of HD 47732. Even if the star were spatially unresolved, the excess flux has a λ^{-4} continuum, rather than a Rayleigh Jeans continuum, and therefore we reject the third star hypothesis. (6) The excess flux represents light from HD 47732 scattered toward the observer from circum-binary material, certainly gas but possibly dust as well. The scattered light hypothesis led us to monitor the

V-band polarization of V641 Mon with a photoelastic modulator instrument at Pennsylvania. By now, 51 measures have been accumulated and their mean is consistent with Breger and Dyck's (1972) value. Although phase coverage is not complete, there is indicated a low amplitude (peak-to-peak : $0.05\% < \Delta p < 0.10\%$) variability. At this time we have no knowledge of the intrinsic polarization spectrum and thus cannot firmly affiliate the polarization with the scattered light, but we offer the following speculations. Most stars which display intrinsic polarization have circumstellar densities between 10^{10} and 10^{16} scatterers cm^{-3}. The hypothesis that the visible and IR λ^{-4} excess continuum is the result of circumstellar Rayleigh scattering requires neutral but excited H. Furthermore, the variable light curve indicates circumstellar gas at least sometimes co-rotating with the stellar angular velocities and thus most likely within a few stellar radii of the systemic center of mass. All these properties of the circumstellar regime, when manipulated with Strömgren sphere theory, lead to $n_H n_e \gtrsim 10^{22}$ for 10^3 K < T < 10^4 K. If $n_H \cong 0.1\ n_e$, then $n_H \gtrsim 10^{11.5}$ cm^{-3}. This is sufficiently low to account for the general absence of H emission lines.

REFERENCES

Beardsley, W.R., and Jacobsen, T.S. 1978, Ap.J. 222, 570.
Bohlin, R.C., Holm, A.V., Savage, B.D., Snijders, M.A.J., and Sparks, W.M. 1980, A. and Ap.85, 1.
Breger, M. and Dyck, H.M. 1972, Ap.J. 175, 127.
Code, A.D., Davis, J., Bless, R.C., and Brown R.H. 1976, Ap.J. 203, 417.
Hayes, D.S. 1979, in Problems of Calibration of Multi-Color Photometric Systems, ed. A.G.D. Philip (Dudley Obs.), p. 297.
Henize, K.G., Wray, J.D., and Parsons, S.B. 1981, A.J. 86, 1658.
Kamp, L.W. 1978, Ap.J. Suppl. 36, 143.
Koch, R.H, Sutton, C.S., Choi, K.H., Kjer, D.E., and Arquilla, R. 1978, Ap.J. 222, 574.
Koch, R.H., Bradstreet, D.H., Perry, P.M., and Pfeiffer, R.J. 1981, Publ. A.S.P. 93, 621,
Kurucz, R.L. 1979, Ap.J. Suppl. 40, 1.
Mendoza, E.E., and Gomez, T. 1980, MNRAS 190, 623.
Nandy, K., Thompson, G.I., Jamar, C., Monfils, A., and Wilson, R. 1975, A. and Ap. 44, 195.
Seaton, M.J. 1979, MNRAS 187, 73P.
Vasilevskis, S., Sanders, W.L., and Balz, A.G.A. 1965, A.J. 70, 797.
Walker, M.F. 1956, Ap. J. Suppl. 2, 365.
Warner, J.W., Strom, S.E., and Strom, K.M. 1977, Ap. J. 213, 427.

AN ULTRAVIOLET INVESTIGATION OF THE UNUSUAL ECLIPSING BINARY SYSTEM FF AQR

J.D. DORREN[1], E.F. GUINAN[2] and E.M. SION[2]
(1) Department of Astronomy, University of Pennsylvania
(2) Department of Astronomy, Villanova University.

INTRODUCTION

FF Aqr (BD-3°5357) is an eclipsing binary which consists of a G8 III-IV star and a subdwarf in a $9^d.2$ orbit. IUE and optical observations of such a system provide a unique opportunity to extract information about the temperature, gravity and composition of the subdwarf as well as about the chromosphere of its giant companion, which is known to have strong Ca II H+K emission and may resemble members of the RS CVn group. A series of 7 low-dispersion IUE exposures in both wavelength regions was obtained on Dec. 6, 1981 during the eclipse of the subdwarf, during egress, and out of eclipse. In Fig. 1 these observations and the binary phase at which they were made are shown on a schematic representation of the V-band light curve obtained in 1975 by Dworetsky et al. (1977). The depth in V is 0.15 mag. The circles are IUE V- magnitudes from FES measures obtained during the observing run. They indicate an eclipse depth some 0.05 mag. lower than expected, possibly due to difficulties with the color term in the FES calibration. In our calculations we assumed the eclipse depths of Dworetsky et al. in U, B and V.

THE SUBDWARF COMPONENT

The smoothed continuum flux of the spectrum LWR 12086 (large aperture) taken during total eclipse was subtracted from the out-of eclipse spectrum LWR 12088 (large aperture) to yield the UV continuum flux longward of 1900 Å for the subdwarf alone. For the shortwave region, spectrum SWP 15662 yields the subdwarf flux directly since the continuum is essentially zero in the spectrum SWP 15660 taken in eclipse. The calibrated flux from these large-aperture exposures is shown in Fig. 2, and includes the Lyα line. The UV flux was de-reddened adopting $E_{B-V} = 0.10$, and the interstellar extinction law of Nandy et al. 1975, which is sufficient to fill in the shallow interstellar extinction feature near 2200Å. In principle log g and T_{eff} can now be determined. However suitable model atmospheres for subdwarfs are not readily available. We used the model atmospheres of Kurucz (1979) for stars of solar abundance, and the pure hydrogen models of Wesemael et al. (1979) for high gravity stars. Fits using both models are shown in Fig. 2. The Kurucz model provides a better fit to the UV continuum and the optical U, B, V fluxes, while the Wesemael model gives a much better fit to the Lyα line, and permits a more accurate determination of log g. A temperature near 35,000°K and log g ~ 6.0 are suggested. For $E_{B-V} = 0.10$ the intrinsic color of the giant component is $(B-V)_o = +1.00$ which corresponds to a spectral type near G8 III and T = 4800°K, hence $m_{bol} = +9.17$. A distance of 320 pc and a radius of 6.1 $R_\odot$ is consistent with the analysis of Dworetsky et al. and with an absolute magnitude $M_{bol} \sim +1.60$ derived from our own analysis of λ And, which is also a G8 III-IV star, but of known distance (Dorren and Guinan 1982). Masses of 0.5 $M_\odot$ and 2.0 $M_\odot$ for the subdwarf and giant respectively are consistent with the mass function of f(m) = 0.0188 and the inclination of 81° which, following

Dworetsky et al., we adopt. The eclipse duration implies that for i = 81°, $R_{sd} = 0.1\ R_{\odot}$ and log g ~ 6.1.

The subdwarf spectrum is shown in Fig. 3 for the short wavelength region, with the identification of the prominent absorption lines. It shows strong C II as well as C IV and Si IV. Note that He II λ1640 is relatively weak. Its presence is, however, confirmed by our other spectra. Its weakness can be understood as either representing a low surface abundance due to diffusion or as due to the lower effective temperature range of the subdwarf ($35{,}000K \leq T_e \leq 40{,}000$) especially in view of the absence of the middle ultraviolet He II ($3 \rightarrow n$) series in the LWR spectrum. Thus it is expected that HeII (λ4686) would be weak in the optical spectrum and the classification would probably be sdOB. Unfortunately the cool component dominates the light at optical wavelengths making a direct measurement of the He II λ4686 feature difficult. On a log g/log T_{eff} plot (Fig. 4, from Hunger and Kudritzki, 1981) the subdwarf in FF Aqr appears to the right of the subdwarf group. The approximate boundary between sdB and sdO subdwarfs lies at log $T_e \sim 4.6$. In the same figure we show for comparison a downward extension to higher gravity and temperature of the Strittmatter and Norris (1971) boundary between the domain of radiation pressure driven mass loss and surface diffusion. Stars to the right of the dashed boundary should generally be weak helium line/metal deficient objects due to downward diffusion. Neglecting the possible effects of accretion, the observed strength of the helium and metal lines in the subdwarf in FF Aquarii may shed light on the evolutionary status of the hot subdwarfs and in particular the possibility of an sdO/sdB evolutionary transition.

THE COOL COMPONENT

The SWP spectrum of the G8 star is shown in Fig. 5 in which the emission lines are identified. The spectrum is generally similar to that of λ And (Baliunas and Dupree 1982) with the hot transition region lines of NV, C IV and C II prominent and with weaker Si IV and He II as is found in stars with active chromospheres. In fig. 6 the ratio of line fluxes at Earth to apparent bolometric luminosity (Ayres et al. 1981) are plotted against the same ratio for Mg II (from LWR 12086) and compared with the fluxes from the most active RS CVn stars HR 1099 and UX Ari, with the similar giant component of the RS CVn system λ And, and with the unusual rapidly rotating G - giant FK Comae and another member of this interesting small group, HD 199178 (Bopp and Stencel 1981). Relative to Mg II, the star has greater emission in the hot lines in particular than the active RS CVn stars. We note that the observed distortions of the light curve (Dworetsky et al.) may be due to surface activity on the G star (spots?) rather than the reflection effect which should be negligible for this system.

In a separate paper we hope to analyze the subdwarf with more suitable model atmospheres and investigate its evolutionary status. Our own optical photometry from 1977-1978 will also be analyzed to obtain tighter constraints on the parameters of this important system.

REFERENCES

Ayres, T., Marstad, N. and Linsky, J.L. 1981, Ap. J. 247, 545.
Baliunas, S.L. and Dupree, A.K. 1982, Ap. J. 252, 668.
Bopp, B.W. and Stencel, R.E. 1981, Ap. J. (Letters) 247, L131.
Dorren, J.D. and Guinan, E.F. 1982, in preparation.
Dworetsky, M.M., Lanning, H.H., Etzel, P.B, and Patenaude, D.J. 1977, M.N.R.A.S. 181, 13P.
Hunger, K. and Kudritzki, R.P. 1981, ESO Messenger 24, 7.
Kurucz, R.L. 1979, Ap. J. Suppl. 40, 1.
Nandy, K., Thompson, G.I., Jamar, C., Monfils, A., and Wilson, R., 1975, Astr. Ap. 44, 195.
Strittmatter, P.A., and Norris, J. 1971, Astr. Ap. 15, 239.
Wesemael, F., Auer, L.H., Van Horn, H.M. and Savedoff, M.P., 1980, Ap. J. Suppl. 43, 159.

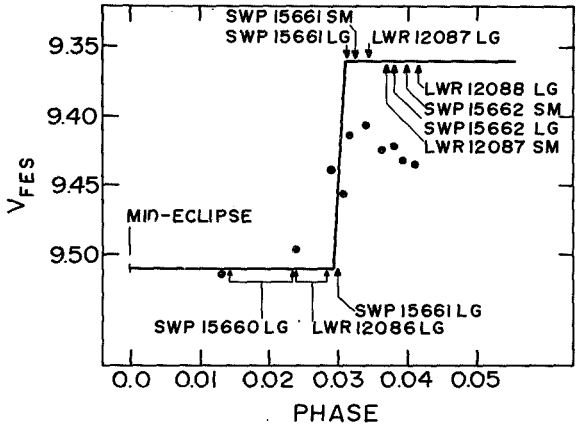

Fig.1-Orbital phase of the IUE exposures shown on a schematic light curve. The circles are the FES V-magnitudes.

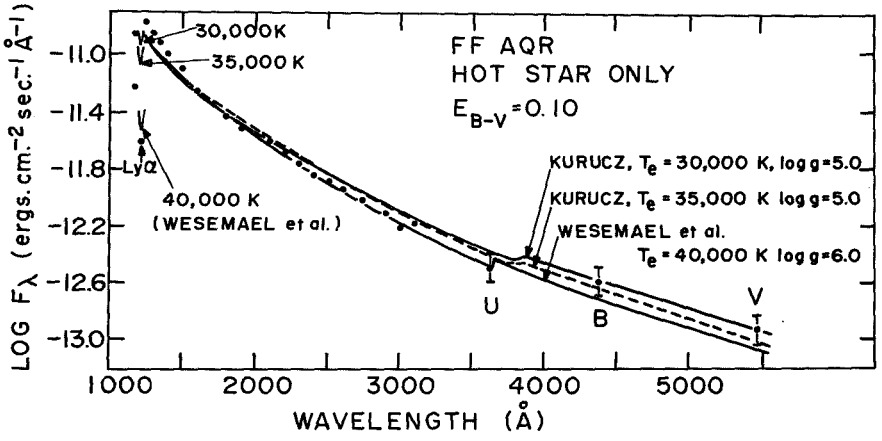

Fig.2-UV and optical fluxes for the hot subdwarf, assuming E_{B-V} = 0.10. Kurucz and Wesemael et al. fits are shown.

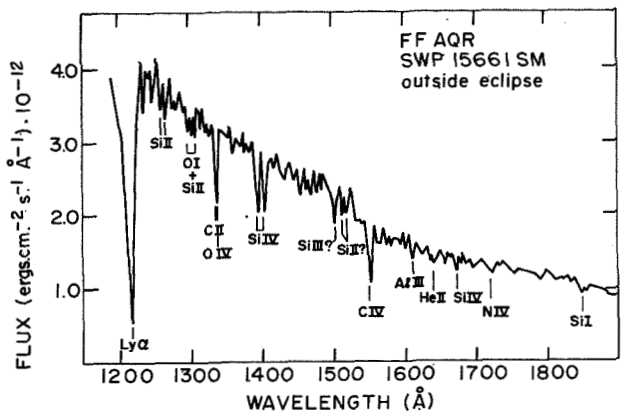

Fig.3-The subdwarf UV spectrum from 1200-1900 Å with prominent absorption lines identified.

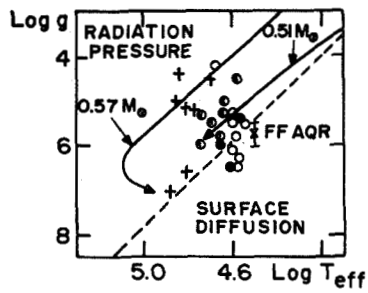

Fig.4-Position of the subdwarf on a log g / log T_{eff} plot. Evolutionary tracks for 0.51 and 0.57 $M_\odot$ stars are shown. The dashed line is discussed in the text. The positions of sdOB stars (o), extreme He-rich (•) and intermediate He-rich stars (•), and central stars of planetary nebulae (+) are shown. (From Hunger and Kudritzki 1981).

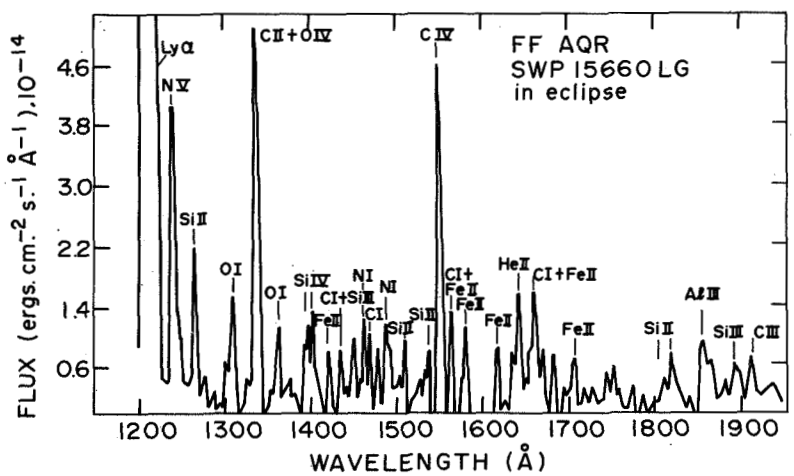

Fig.5-The spectrum of the G8 III-IV component with prominent emission lines identified.

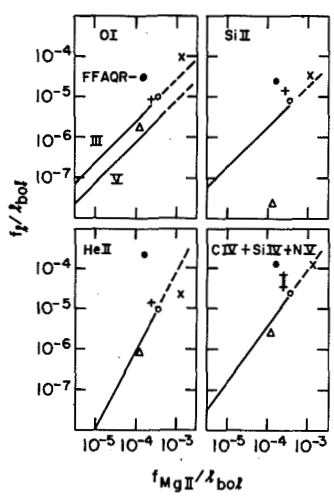

Fig.6-Correlation diagrams for chromospheric and transition region fluxes for late-type giants and dwarfs (solid lines: Ayres et al. 1981). The cool star in FF Aqr (•) compared with FK Com (x), HD 199178 (+), the mean of HR 1099 and UX Ari (o), and λ And (Δ) (Bopp and Stencel 1981).

LINE-PROFILE AND CONTINUUM VARIATIONS OF THE CONTACT BINARY SV CENTAURI

Jurgen Rahe
Laboratory for Astronomy and Solar Physics
NASA/Goddard Space Flight Center

Horst Drechsel
Walter Wargau
Remeis Observatory Bamberg
Astronomical Institute University Erlangen-Nuernberg, F.R.G.

ABSTRACT

A total of five high and ten low dispersion UV spectra of the interacting contact binary SV Centauri has been obtained between 1979 and 1982. The low resolution observations cover the whole phase range, while a few selected phases were observed in high dispersion. The UV data were complemented with optical photometric and spectroscopic observations, in order to determine the structure and absolute dimensions of the system.

The profiles of prominent UV resonance and metastable lines undergo drastic changes with phase angle and time. Their overall appearance indicates relatively strong mass loss from the system, exhibiting pronounced variations of the stellar wind.

The far UV continuum distribution suggests the presence of a luminous hot radiation source with maximum emission in the soft X-ray range, which is most apparently seen during the first quadrature phase, while it is weakest close to primary minimum. The mass exchange and mass loss process as well as the evolutionary stage of SV Centauri are discussed.

INTRODUCTION

The interacting early-type contact binary SV Centauri (= HD 102552 = CoD $-59^{o}3950$ - CPD $-59^{o}3809$) has a period of p = 1.6 days which is rapidly decreasing with an average rate of about $-2\ 10^{-5} yr^{-1}$. The spectral types of the two components are B 1 V (photometric primary; 7.7Mo, 6.8Ro; T= 23,000K; L(bolo) = 12,000 Lo, M(V) = $-3^{M}1$) and B 6.5 III (9.6 Mo, 7.4Ro; T=14,000K; L (bolo) = 2,000 Lo; M(V) = $2^{M}3$; separation 15.3 Ro; E (B-V) = 0.27; d = 1800 pc). The general properties of the system are discussed in Drechsel et al. (1982).

SV Cen has previously been regarded as a rare example of a binary that is presently observed during the early stage of evolution, prior to the reversal of the mass ratio. The period decrease was explained through conservative mass transfer from the more to the less massive component (e.g., Wilson and Starr, 1976). Recent IUE observations revealed instead the presence of an expanding circumbinary envelope.

OBSERVATIONS AND DISCUSSION

Between November 1979 and January 1982, SV Cen was repeatedly observed in the UV with the IUE satellite. Near orbital phases 0.25, 0.4, and 0.9, both high and low resolution spectra were taken with the SWP and LWR cameras. The UV data were complemented with optical photometric and spectroscopic observations, in order to determine the structure and absolute dimensions of the system. In all UV spectra, highly displaced envelope components of C II, C IV, Si IV, Al III, and Mg II were found. The central wavelengths are shifted by about $-1000\ kms^{-1}$, which exceeds the escape velocity of about $-750\ kms^{-1}$, and indicates the occurance of mass loss from the system. The observed strong period decrease is conceivably caused by the loss of angular momentum carried away by the ejected matter.

The main difference between the spectra obtained at various phases, is the presence of several sharp absorption components superimposed on the broad envelope absorption profiles of the resonance and metastable lines (see Figs. 1, 2). In a quantitative analysis of the observed profiles (Drechsel et al. 1982), local condensations forming radially expanding shells in the expanding envelope were found to explain the well-defined absorption components. The time scale for the ejection of material blobs producing these shells, was found to be of the order of a few hours.

Finally, the presence of a hot radiation source in SV Cen was detected. The strong UV excess has a maximum intensity which is below 1500A, and can be represented by a superposition of the contributions of the two stellar components and an additional hot area of about 2000K with an extension of about 1% of the projected area of the two stars.

CONCLUSION

The profiles of prominent UV resonance and metastable lines observed in SV Cen, undergo drastic changes with phase angle and time. Their overall appearance indicates relatively strong mass loss from the system, exhibiting pronounced variations of the stellar wind.

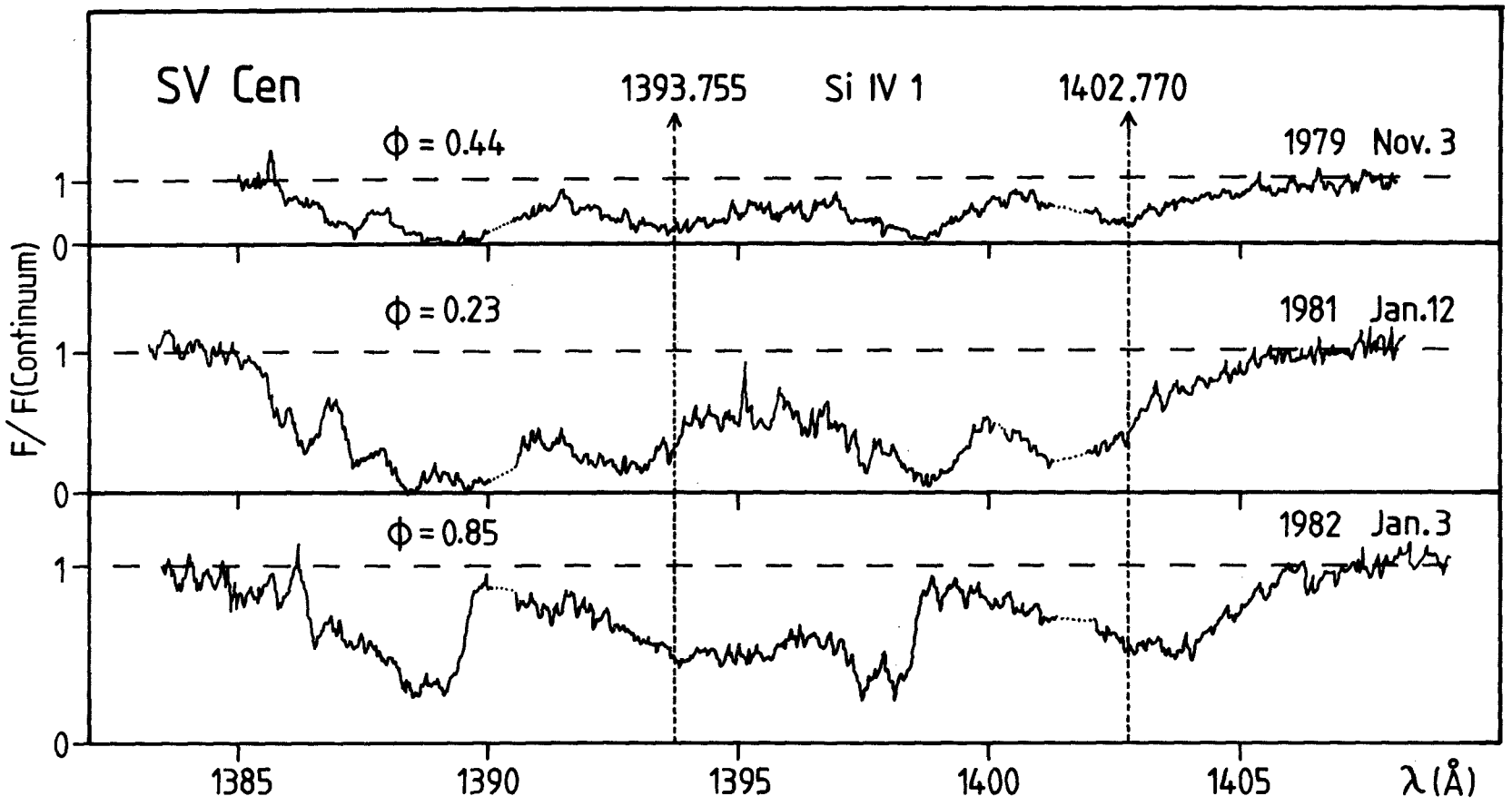

Fig. 1 IUE spectra of SV Cen, obtained in 1979, 1981, and 1982, covering the spectral range 1385-1405A.

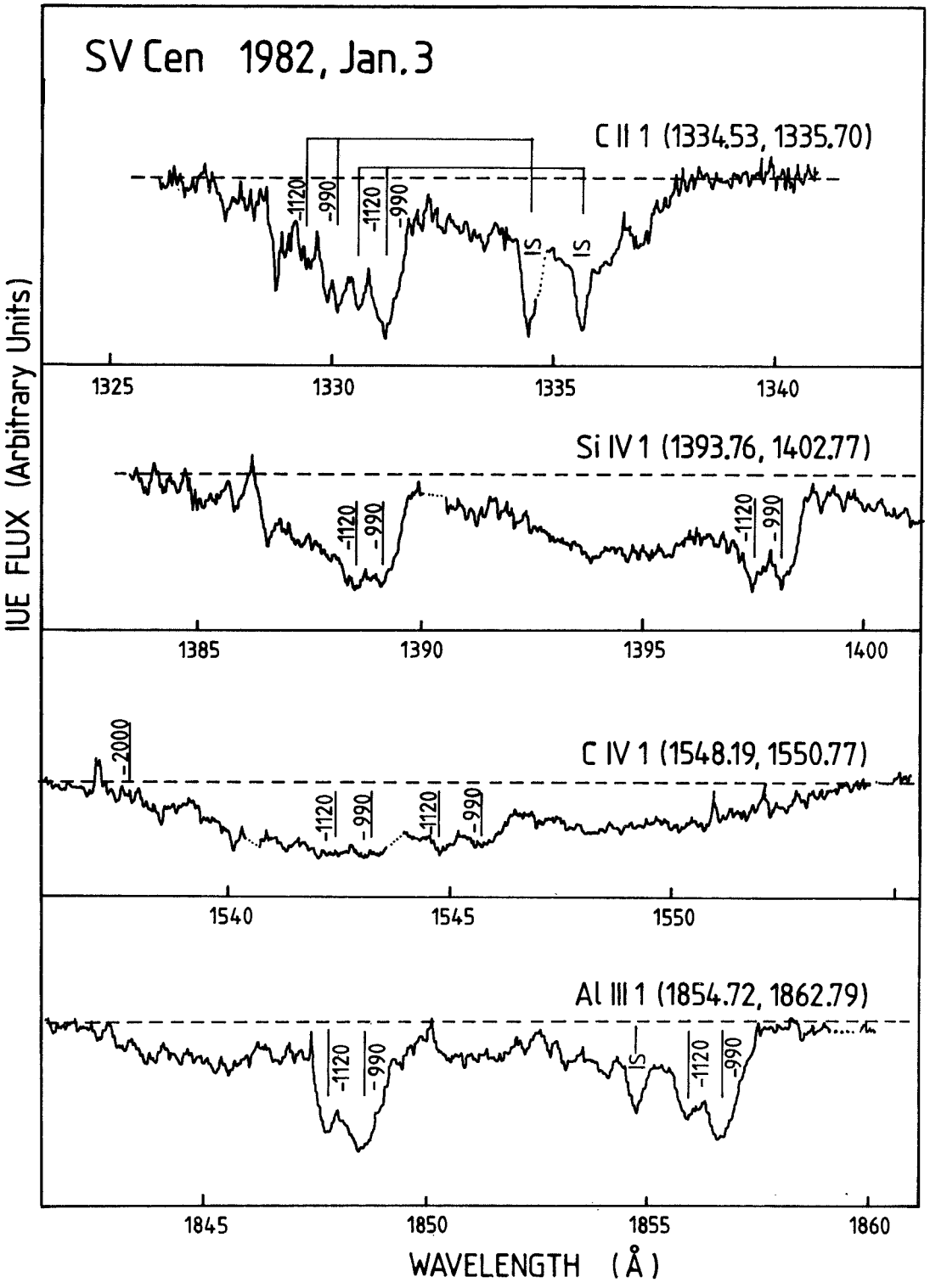

Fig. 2 Envelope components of C II, Si IV, C IV and Al III, showing narrow absorption dips at radial velocities of -990 and -1120 km^{-1}.

The far UV continuum distribution suggests the presence of luminous hot radiation source with maximum emission in the soft X-ray range, which is most apparently seen during the first quadrature phase, while it is weakest close to primary minimum.

The hot source is conceivably caused by the mass flow from the less massive component. Part of the matter will leave the system, carry away some of the angular momentum and thus cause the period decrease. The observed long and short term variations of the mass loss rate could be due to an unsteady Roche lobe overflow, as well as changes in the ratio of ejected to transferred matter.

REFERENCES

Drechsel, H., Rahe, J., Wargau, W., and Wolf, B.; 1982, Astron. Astrophys., in press

Wilson, R.E., Starr, T.C.; 1976, Monthly Not. Roy. Astron. Soc., 176, 625.

A PROGRESS REPORT ON THE W SERPENTIS BINARIES, WITH A FEW WORDS ON ε AURIGAE

Mirek J. Plavec

Department of Astronomy, University of California, Los Angeles

ABSTRACT

My recent observations show that two well-known Algol systems, U Cephei and V356 Sagittarii, should be included among the W Serpentis stars, characterized by strong ultraviolet emission lines. The spectra of the W Ser stars are similar to those of the T Tauri stars, and a similarity of physical conditions is indicated. A model of W Serpentis, namely a B star embedded in a thick disk, may be relevant to other "exotic" eclipsing systems, possibly even to ε Aurigae. In connection with ε Aur, the case of BM Orionis is reviewed; that system probably contains a pre-main-sequence star highly flattened by differential rotation.

EMISSION LINES IN THE SERPENTIDS

In 1978, collaborating with R. H. Koch, we have discovered that a group of eclipsing binaries display strong emission lines of C IV, N V, Si IV, Fe III etc. in the ultraviolet, although neither of the component stars is hot enough to supply the ionizing photons. The systems of this type (RX Cas, SX Cas, W Cru, V367 Cyg, β Lyr, and W Ser) had all been known before as "peculiar" or even "exotic" binaries because of many spectral and photometric peculiarities. These peculiarities are most likely due to the fact that mass transfer and/or mass loss occur at a higher rate in these systems than in ordinary Algols; larger emitting volumes probably help to enhance the emissions.

I believed at first that a necessary condition for a W Serpentis-type emission spectrum is a sufficiently long period of the system, ensuring a large volume available to the emitting material. Recent observations have pushed the limiting period (and therefore system dimensions) down, since similar emission lines were detected in V356 Sgr (P = 8.9 days) and in particular in U Cephei (P = 2.5 days). The character of the UV spectrum typical for the W Serpentis stars seems to be present in interacting binaries more often than we thought before. However, in U Cephei the emissions are visible only at and near the total eclipse, while in SX Cas and the rest of the W Serpentis stars enumerated above they appear to be visible at all phases. This behavior of the far ultraviolet emission lines is rather similar to what has long been known about the optical region: While in short-period systems such as U Cephei or RW Tauri, the Balmer line emission as a rule shows up only during the total eclipse of the hotter (B-type) component star, in the longer-period systems like β Lyr, SX Cas, RX Cas, etc., they remain visible in full light. However, other similar systems show little or no emission. So the important factors must be both the rate of mass transfer or mass outflow, and the volume available for emission.

The emission lines observed in the far UV spectrum of SX Cas are quite strong. The C IV resonance doublet itself emits a power of 0.17 L_o; compare this with 10^{-3} L_o in U Cep, and 4×10^{-5} L_o in the very active RS CVn star HR 1099. Interesting numbers result if we calculate the power emitted per unit surface area of either component of the binaries. The G8 III-IV star in U Cep is rather small with a radius of 4.7 R_o, therefore the surface flux in C IV is large: 3×10^7 ergs cm^{-2} s^{-1}. In SX Cas, the (much less accurately known) radius of the K3 III secondary is about 18 R_o, and, surprisingly, the surface flux for that star would turn out to be about the same as in U Cep, namely 3×10^7 ergs cm^{-2} s^{-1}. The surface fluxes referred to the (somewhat smaller) primary components will be of the order of 10^8 ergs cm^{-2} s^{-1}. It is noteworthy that Giampapa and Imhoff, in a paper presented at this meeting, found very similar surface fluxes for the T Tauri stars. This similarity indicates rather similar physical conditions at which the emission lines are formed. In both cases, we have a rather dense circumstellar envelope ultimately coming from accretion, in which the physical conditions are strongly affected by the interaction between the star and its environment; and both accretion as well as expulsion of matter are probably present.

THE CONTINUA

Observations of SX Cas showed that the far ultraviolet continuum is much higher than expected from the traditionally adopted spectral type of the hotter component, A6 III. At first, we thought that the UV continuum is the radiation coming from the transition zone between an accretion disk and the accreting star. An analysis of the optical scans at various phases led us to revise the spectral type of the primary component to about B7 (Plavec, Weiland and Koch, 1982). We now have an additional strong argument in favor of this solution, since the ultraviolet continuum of U Cep --no doubt stellar -- matches that of SX Cas very satisfactorily. This result in turn corroborates our opinion that the strong ultraviolet fluxes observed in some W Serpentis stars are of stellar origin. In particular, this appears to be the best explanation for W Serpentis itself. But if we accept this idea, how can we explain that the observed line and continuous spectrum of W Ser in the optical region indicates a spectral type of about F5 II ?

The most promising explanation is to assume that the F-type spectrum originates not in a star but in a surrounding accretion disk, more specifically that it comes from its outer edge. Madej and Paczynski (1977) advanced a similar idea for the dwarf nova U Gem. I believe that the primary eclipse of W Ser is due to an as yet undetected cool star partially eclipsing the disk, and, near mid-eclipse, also partially eclipsing a B star, which itself is partly obscured by its accretion disk.

ε AURIGAE, BM ORIONIS, AND ECLIPSES OF NON-SPHERICAL BODIES

I believe that a number of bizarre eclipsing binary systems will be better understood if we accept the idea that some eclipses are eclipses by or of non-spherical objects. Eclipses caused by non-sperical bodies have been proposed for ε Aurigae and BM Orionis; after reviewing them, I want to propose that we should also consider the other alternative: an eclipse of a disk.

The long-period eclipsing system of ε Aurigae is most interesting these days since we will be able to observe another eclipse starting in July 1982 --

after 27 years of waiting. The most puzzling problem of this system is that the eclipse appears to be total (since the light curve has an essentially flat bottom for about one year) while only one spectrum, that of a supergiant of spectral type about F0, remains visible at all times. Among several models proposed over the years, only three appear at all viable, but none is quite satisfactory: Huang (1965) proposed that the eclipsing body is a geometrically thick disk seen edge-on; Wilson (1971) advocated a geometrically thin disk, mildly tilted, and with a central semi-transparent opening; and Hack (1961) suggests that the eclipse is caused by an extremely large ionized shell surrounding a Be star which itself does not participate in the eclipse. IUE observations by Hack and Selvelli (1979) as well as by me do show additional flux in the far ultraviolet (visible shortward of about λ 150 nm) which may be interpreted as due to a B star; however, I am not sure if this rather weak source could provide the required ionization of hydrogen in a truly enormous shell.

The most conspicous peculiarity of ε Aurigae, namely the quasi-total character of the eclipse is not unique to ε Aur. In 1970, the same enigma was discovered in BM Orionis. This eclipsing binary is the faintest of the four stars forming the famous Trapezium in the Orion nebula. The system was studied photometrically by Hall and Garrison (1969). The bottom of the primary eclipse was found to be essentially flat for about 8.5 hours out of the 16 hours of the total duration of the primary eclipse. Hall and Garrison therefore concluded that the eclipse is total, and obtained a satisfactory solution assuming that the hotter star, about B3 V, is totally eclipsed by an A star with a rather peculiar ultraviolet excess.

The puzzle arose when Doremus (1970) obtained a spectrum at totality and found again only the spectral lines of the B star, which should have been totally eclipsed. An analogy with ε Aur was immediately invoked. It is indeed interesting that the depth of the eclipse in BM Ori, about 0.7 mag in V, is very similar , and so is also the ratio of the durations of the partial phase to the quasi-total phase of the eclipse. Consequently, Wilson (1972) and Huang (1975) attempted to adjust their ε Aur models to the case of BM Ori. Huang repeated his model of a geometrically thick disk seen edge-on; he only replaced the solid particles believed to form the disk in ε Aur by scattering electrons. The required ionization energy as well as at least part of the mass of the disk were supposed to be supplied by the B-type primary --a somewhat difficult assumption since that star is too small for a Roche-lobe overflow and of too low a luminosity for a powerful stellar wind. Wilson promoted his model of a geometrically thin disk mildly tilted to the orbital plane, with a central semi-transparent hole. Since no eclipse was seen to be caused by the central star of such a disk, Wilson's contention was that the star is most likely compact, and since it cannot be a white dwarf, a black hole was invoked --a precarious assumption about a very young stellar pair. In both models, the shallow secondary eclipse obvserved by Hall and Garrison is explained by an assumption that the disk reflects some light of the B star.

Popper and Plavec (1976) detected faint but unmistakable spectral lines of the secondary star and concluded that, although flattened, that object must be considered as a genuine star, of spectral type about A7 IV. This conclusion makes the models by Huang and by Wilson unlikely, and strongly favors the early suggestion by Hall (1971), namely that the secondary star is still con-

tracting to the main sequence, and is an object described by the Bodenheimer-Ostriker (1970) models of differentially rotating stars. These models are applicable to BM Ori if one assumes that we see the flattened, biconcave disk very nearly edge-on.

Is this result of any relevance for ε Aurigae? The equatorial radius of Hall's disk-shaped star, about 7 $R_{\odot}$, represents almost 25% of the separation of the two stars. The flat object in ε Aur actually has a smaller fractional radius, 0.171. But because of the enormous dimensions of the system, its absolute radius must be about 950 solar radii. It is hard to imagine that an object such as the secondary star in BM Ori could exist in the dimensions of ε Aur, but the same problem arises whether we consider a thick disk or a thin disk.

An important aspect of ε Aur is that the eclipse depth seems to be independent of the wavelength at which it is observed. We must postulate a "neutral" disk or a semi-transparent object with grey opacity. Wilson's model needs a semi-transparent hole so adjusted that it always exactly compensates light gains and losses to make the eclipse light curve flat. I think that an alternative explanation may be an eclipse of an extended, elongated disk; that is, I propose a model analogous to the one used above for W Serpentis. The disk would only simulate an F type supergiant. Actually, at its center there may be a hotter star, perhaps B. Wilson (1971) noticed that near mid-eclipse, one observes an eclipse-like drop in brightness by about 0.2 mag., lasting about 80 days. He interpreted it as a stellar eclipse, caused by the secondary star (at the center of the eclipsing disk) eclipsing the F supergiant. In my picture, this central eclipse could be the eclipse of the central star of the eclipsed disk; and this central star may be identified with the weak hot source found by Hack and Selvelli. If I am right, this source should be eclipsed; if it becomes more conspicuous instead, the model by Hack will be closer to the truth. My proposed model with an eclipsed disk seems to offer a good qualitative explanation of the observed asymmetries of the F-type spectral lines. The eclipsing body in my model may be a spherical star considerably cooler than spectral type F --just as the eclipses in W Serpentis are most likely caused by a cool giant component, which has not been detected yet, but may soon be discovered by means of the modern infrared techniques.

REFERENCES

Bodenheimer, P. and Ostriker, J.P.: 1970, Astrophys. J. 161, 1101.
Doremus, C.: 1970, Publ. Astron. Soc. Pacific 82, 745.
Hack, M.: 1961, Mem. Soc. Astron. Ital. 32, 3.
Hack, M. and Selvelli, P.L.: 1979, Astron. Astrophys. 75, 316.
Hall, D.S.: 1971, IAU Coll. No. 15 (Bamberg), 217.
Hall, D.S. and Garrison, L.M.: 1969, Publ. Astron. Soc. Pacif. 81, 771.
Huang, S.S.: 1965, Astrophys. J. 141, 976.
Huang, S.S.: 1975, Astrophys. J. 195, 127.
Madej, J. and Paczynski, B.: 1977, in The Interaction of Variable Stars with their Environment (ed. Kippenhahn, Rahe, Strohmeier), 313.
Plavec, M.J., Weiland, J.L., and Koch, R.H.: 1982, Ap.J. 255, May 1 issue.
Popper, D.M. and Plavec, M.J.: 1976, Astrophys. J. 205, 462.
Wilson, R.E.: 1971, Astrophys. J. 170, 529.
Wilson, R.E.: 1972, Astrophys. Space Sci. 19, 165.

A SEARCH FOR CATACLYSMIC BINARIES CONTAINING STRONGLY MAGNETIC WHITE DWARFS

Howard E. Bond and G. Chanmugam
Department of Physics and Astronomy
Louisiana State University, Baton Rouge

ABSTRACT

The AM Herculis-type binaries contain accreting white dwarfs with surface magnetic fields of a few times 10^7 gauss. If white dwarfs in cataclysmic binaries have a range of field strengths similar to that among single white dwarfs, AM Her-like systems should exist with fields as high as 3 x 10^8 gauss. Theoretical studies suggest that such objects will not have the strong optical polarization of the AM Her variables; however, they will exhibit high-harmonic cyclotron emission, making them spectacular UV sources. We made IUE observations of seven candidate cataclysmic variables selected for optical similarity to AM Her binaries. Although all seven objects were detected in the UV, none display unusually strong UV continua. We suggest therefore that the distribution of magnetic field strengths among single white dwarfs may be different from that among binaries.

INTRODUCTION

Cataclysmic variable stars are close binaries containing a white dwarf that accretes matter from a companion main-sequence star. About 5% of single white dwarfs are known to have magnetic fields, with the observed fields ranging from 3 x 10^6 to 3 x 10^8 gauss; over this range the field distribution is roughly a constant number per octave (Angel *et al.* 1981). It might therefore be expected that some cataclysmic binaries may have strongly magnetic white dwarfs.

The recently discovered AM Her-type systems indeed seem to contain magnetic white dwarfs. In these cataclysmic binaries, the magnetic field is sufficiently strong to prevent formation of an accretion disk; instead, the accreting matter is channeled directly onto the polar cap of the white dwarf (Chanmugam and Wagner 1977; Stockman *et al.* 1977). The accretion column that forms above the pole emits strongly polarized light, allowing such binaries to be recognized with optical polarimetry (Tapia 1977). About half a dozen AM Her binaries are now known.

Recent quantitative theoretical studies show that the optical polarization, especially the strong linear-polarization "pulses" exhibited by the AM Her binaries, can be understood only if the light is due to cyclotron emission at about the fifth to tenth harmonic of the fundamental cyclotron frequency $\omega_c = eB/mc$ (Chanmugam and Dulk 1981; Meggitt and Wickramasinghe 1982). Only fields of a few times 10^7 gauss place these high harmonics in the optical band. Such strengths are consistent with recent direct observational measurements of the fields in two of the AM Her variables, based on

cyclotron absorption lines or Zeeman splitting (Visvanathan and Wickramasinghe 1979; Stockman et al. 1979; Schmidt et al. 1981).

On the basis of the field-strength distribution among single white dwarfs, we would expect some cataclysmic binaries to contain white dwarfs with even stronger fields than in the AM Her variables. Such hypothetical binaries would not have measurable optical polarization (since the polarization would shift into the UV) and hence they would so far have gone undetected by ground-based observers. However, we expect that such systems will be spectacular UV sources, for the following reason. Just above the magnetic pole of the accreting white dwarf is a shock-heated region (kT ~ 20 keV) of the accretion column. Cyclotron radiation from this region is self-absorbed up to a frequency $m^*\omega_c$, where $m^* \sim 10$ (Chanmugam and Wagner 1979; Lamb and Masters 1979). The emitted spectrum therefore follows a Rayleigh-Jeans curve for $\omega < m^*\omega_c$, but for $\omega > m^*\omega_c$, the region becomes optically thin. Thus, for fields stronger than about 5×10^7 gauss, a blackbody curve extends well down into the UV, making the binary system a very strong UV source. The shock-heated region has a surface area of about 10^{16} cm^2 (Fabbiano et al. 1981); the UV flux observed at the Earth from this region (in erg cm^{-2} s^{-1} A^{-1}) is

$$F_\lambda \sim 4 \times 10^{-11} \, (d/100pc)^{-2} \, (kT/20keV) \, (\lambda/1500A)^{-4} \, ,$$

up to the frequency $m^*\omega_c$ at which the region becomes optically thin.

AM Her itself has been observed with IUE, and showed only weak UV radiation (Raymond et al. 1979), in accord with the subsequent direct determination of its magnetic field from Zeeman-split absorption lines. The UV radiation that was detected from AM Her and from the similar system AN UMa (Hartmann and Raymond 1981) probably corresponds to the UV tail of the soft X-ray flux from the surface of the white dwarf, due to blackbody radiation at kT ~ 30 eV.

IUE OBSERVATIONS

From the above considerations, we would expect cataclysmic binaries containing white dwarfs with extremely strong magnetic fields (> 5×10^7 gauss) to exhibit the following properties: (1) they will not show measurable optical polarization; (2) however, they will be very conspicuous UV sources because of high-harmonic cyclotron emission from the shock-heated region; (3) their optical spectra would presumably resemble those of the AM Her binaries, particularly in showing high-excitation emission-line spectra even at maximum light (rather than the continuous spectra exhibited by ordinary dwarf novae at maximum), since the magnetic field prevents formation of an optically thick accretion disk; (4) their long-term light curves might resemble those of the AM Her systems (which are normally at maximum light, but sometimes have occasional minima).

For the past few years, Bond has had underway an optical spectroscopic survey of cataclysmic variables, using the 2.1-m telescope at Kitt Peak National Observatory and the image-dissector scanner. To date, about 150 objects have been observed. From this survey, we selected for

low-resolution IUE observations seven objects that appear to satisfy the above criteria (1), (3), and (4). The stars chosen were V794 Aql, FS Aur, KR Aur, V425 Cas, CM Del, V380 Oph, and V442 Oph. The visual magnitudes of the variables at the time of observation ranged from 13 to 16. SWP exposures were made for all seven, and LWR exposures for KR Aur, CM Del, and V442 Oph.

All seven objects were detected with IUE (with exposure times of up to 115 min). However, none of the stars appeared to show the extremely strong UV continua expected from strongly magnetic accreting white dwarfs. Examples of our data are given in the figure, in which our SWP and LWR exposures of KR Aur and CM Del are combined with the optical scans obtained at Kitt Peak. Clearly, KR Aur and CM Del do not show Rayleigh-Jeans spectra in the UV, nor do their UV flux levels approach the high values expected for extremely high fields. Similar results were obtained for the other five targets. All seven stars resemble ordinary cataclysmic variables (or AM Her binaries) in the UV.

SUMMARY

The observed distribution of field strengths among single white dwarfs leads to the prediction that significant numbers of AM Her-like systems with fields stronger than 5 x 10^7 gauss should exist. However, our survey of seven strong candidates failed to reveal any examples of the very strong UV continua predicted for such binaries.

It may be that such hypothetical systems do not resemble ordinary cataclysmic variables or even AM Her systems in the optical region, and hence are still completely unknown objects. If this is not the case, the fact that half a dozen AM Her binaries are now known, but no binaries with stronger fields, suggests that the distribution of field strengths among white dwarfs in close binaries differs from that among single white dwarfs. Since single white dwarfs and white dwarfs in cataclysmic binaries undoubtedly have very different evolutionary histories, this difference in magnetic field strengths might not be surprising.

This research was supported by NASA (grant NAG 5-197) and NSF (grant AST 80-25250). The optical observations were made at Kitt Peak National Observatory, which is operated by AURA under contract with the National Science Foundation.

REFERENCES

Angel, J.R.P., Borra, E.F., and Landstreet, J.D. 1981, Ap. J. Suppl., 45, 457.

Chanmugam, G., and Dulk, G.A. 1981, Ap. J., 244, 569.

Chanmugam, G., and Wagner, R.L. 1977, Ap. J. (Letters), 213, L13.

_____. 1979, Ap. J., 232, 839.

Fabbiano, G., Hartmann, L., Raymond, J., Steiner, J., and Branduardi-Raymont, G. 1981, Ap. J., 243, 911.

Hartmann, L., and Raymond, J.C. 1981, in The Universe at Ultraviolet Wavelengths: The First Two Years of IUE, ed. R.D. Chapman (NASA), p. 495.
Lamb, D.Q., and Masters, A.R. 1979, Ap. J. (Letters), 234, L117.
Meggitt, S.M.A., and Wickramasinghe, D.T. 1982, M.N.R.A.S., in press.
Raymond, J.C., Black, J.H., Davis, R.J., Dupree, A.K., Hartmann, L., and Matilsky, T.A. 1979, Ap. J. (Letters), 230, L95.
Schmidt, G., Stockman, H.S., and Margon, B. 1981, Ap. J. (Letters), 243, L157.
Stockman, H.S., Schmidt, G.D., Angel, J.R.P., Liebert, J., Tapia, S., and Beaver, E.A. 1977, Ap. J., 217, 185.
Stockman, H.S., Liebert, J., and Bond, H.E. 1979, in White Dwarfs and Variable Degenerate Stars, IAU Colloq. No. 53, eds. H.M. Van Horn and V. Weidemann (Univ. of Rochester Press), p. 334.
Tapia, S. 1977, Ap. J. (Letters), 212, L125.
Visvanathan, N., and Wickramasinghe, D.T. 1979, Nature, 281, 47.

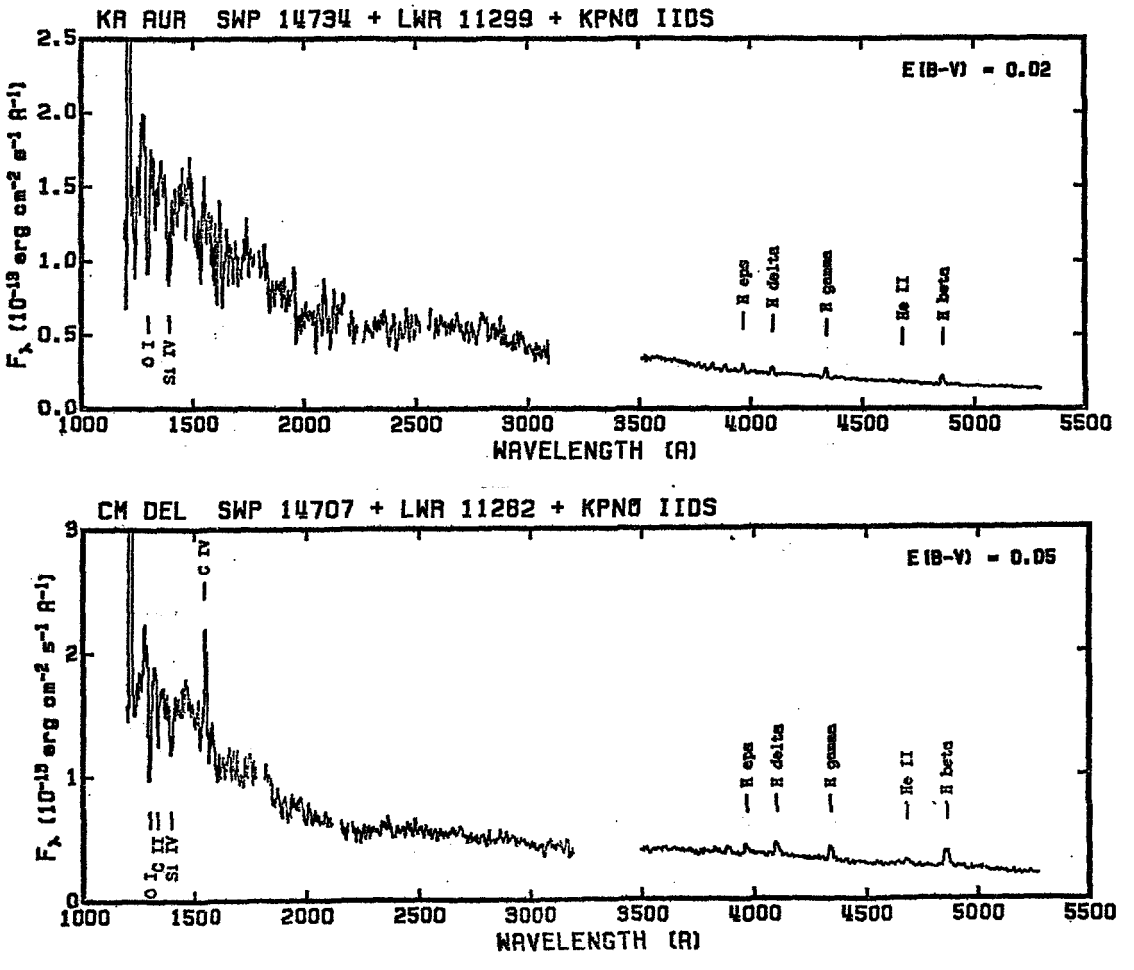

FIGURE 1
Low-resolution spectra of KR Aur and CM Del from IUE and KPNO observations. The fluxes have been corrected for assumed interstellar reddenings of E(B-V) = 0.02 and 0.05 respectively.

OBSERVATIONS OF MASS ACCRETION IN BINARY STARS

R. S. Polidan
Princeton University Observatory

G. J. Peters
Department of Astronomy
University of Southern California

ABSTRACT

Results from high resolution observations of eight close binary stars (TX UMa, U CrB, CX Dra, TT Hya, AU Mon, KX And, HR 2142, and ϕ Per) are presented. Variable absorption lines, indicative of mass flow, are observed in all systems except ϕ Per. Emission lines are seen in KX And and ϕ Per. Variable high ionization features (NV, SiIV, and CIV) are seen in TX UMa, UCrB, CX Dra, and AU Mon. The observations are modeled using the calculations of Lubow and Shu.

INTRODUCTION

Lubow and Shu (1975, 1976) in their discussion of gas dynamics in close binary stars defined three parameters that can be used to discuss gas streams and disks: A scale parameter ε = isothermal sound speed/angular velocity, the dense accretion disk radius ϖ_d, and the distance of closest approach to the detached component by a test particle released at L1 ϖ_{min}. The latter two parameters are functions only of the mass ratio $q = M_{contact}/M_{detached}$. It is useful to construct a diagram of fractional radius of the detached component r (R/A) versus mass ratio (q) with the loci of ϖ_d and ϖ_{min} marked (Figure 1). This divides the diagram into three zones. Stars in Zone I have $r > \varpi_d$, in Zone II $\varpi_{min} < r < \varpi_d$, and in Zone III $r < \varpi_{min}$. The location of a star in this diagram should generally specify the behavior of the mass flow in the system. Stars in Zone I should display evidence of the direct impact of a gas stream onto the stellar surface, whereas stars in Zone III should form dense accretion disk and show no impact. Stars in Zone II should show something intermediate. The parameter ε must also be considered. Typically stars in Zone I have ε small relative to r, in Zone II $\varepsilon < r$, and in Zone III $\varepsilon > r$. The parameter is important because it approximates the gas stream width.

OBSERVATIONS

Eight binary stars were observed with high resolution, four are eclipsing: TX UMa, U CrB, TT Hya, and AU Mon and four non-eclipsing: CX Dra, KX And, HR 2142, and ϕ Per. Periods range from 3^d to 127^d. The stars fall into all three zones of the rq diagram (Figure 1). All systems, except for TT Hya, were observed at three or more phases.

DISCUSSION

Two stars fall into Zone I: TX UMa (ϕ = .07, .40, .90) and U CrB (.32, .53, .62, .88). A model of U CrB is shown in Figure 2A. The behavior of both systems is similar. Evidence for a gas stream is weak (TX UMa in SiIV) or absent (U CrB). However, near the stream impact point unshifted absorption lines of NV and SiIV are seen in both stars. TX UMa also exhibits a sharp absorption line in FeIII and AlIII ($v_r \sim -50$ km s^{-1}) at phase 0.07. These observations can be understood from Figure 2A. The gas stream is weak or invisible because it is narrow and does not cover a significant portion of the stellar surface. The impact point is consistent with mass flow calculations.

Three stars fall into Zone II CX Dra (many phases between 0.40 and 1.0), AU Mon (.30, .48, .85, .93) and TT Hya (.40, .90). The details of these observations have been described elsewhere (Peters and Polidan 1982). Their general behavior is similar to the stars of Zone I except that the high ionization absorption is seen over a wider range of phase. This also is consistent with models (Figure 2B). In these systems the stream is larger and impacts a larger fraction of the stellar surface. Because ϖ_{min} is smaller than the stellar radius no dense disk forms.

The remaining three stars KX And, HR 2142, and ϕ Per lie in Zone III. These observations have also been discussed elsewhere (Peters and Polidan 1982). The key difference between these systems and the other systems discussed here is that a dense accretion disk forms and no impact occurs (Figure 2c). KX And and ϕ Per show shell absorption spectra and emission lines but they do not exhibit obvious phase dependent variations. HR 2142 on the other hand exhibits pronounced phase dependent variations (Peters and Polidan 1982). These variations are consistent with viewing the star through a gas stream structure that penetrates a low density (H emission) disk until it is stopped by the dense accretion disk. The stream is visible because the stream width, ε, is greater than the stellar radius.

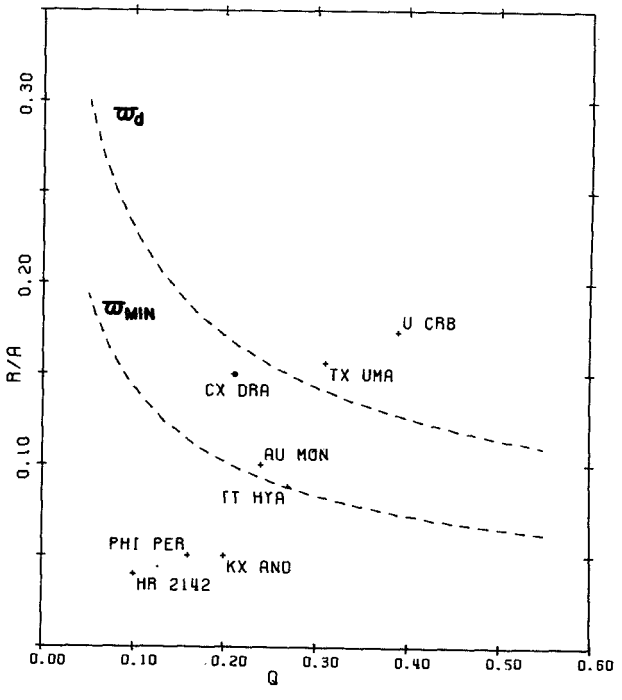

Figure 1. Fractional radius versus mass ratio diagram for program stars.

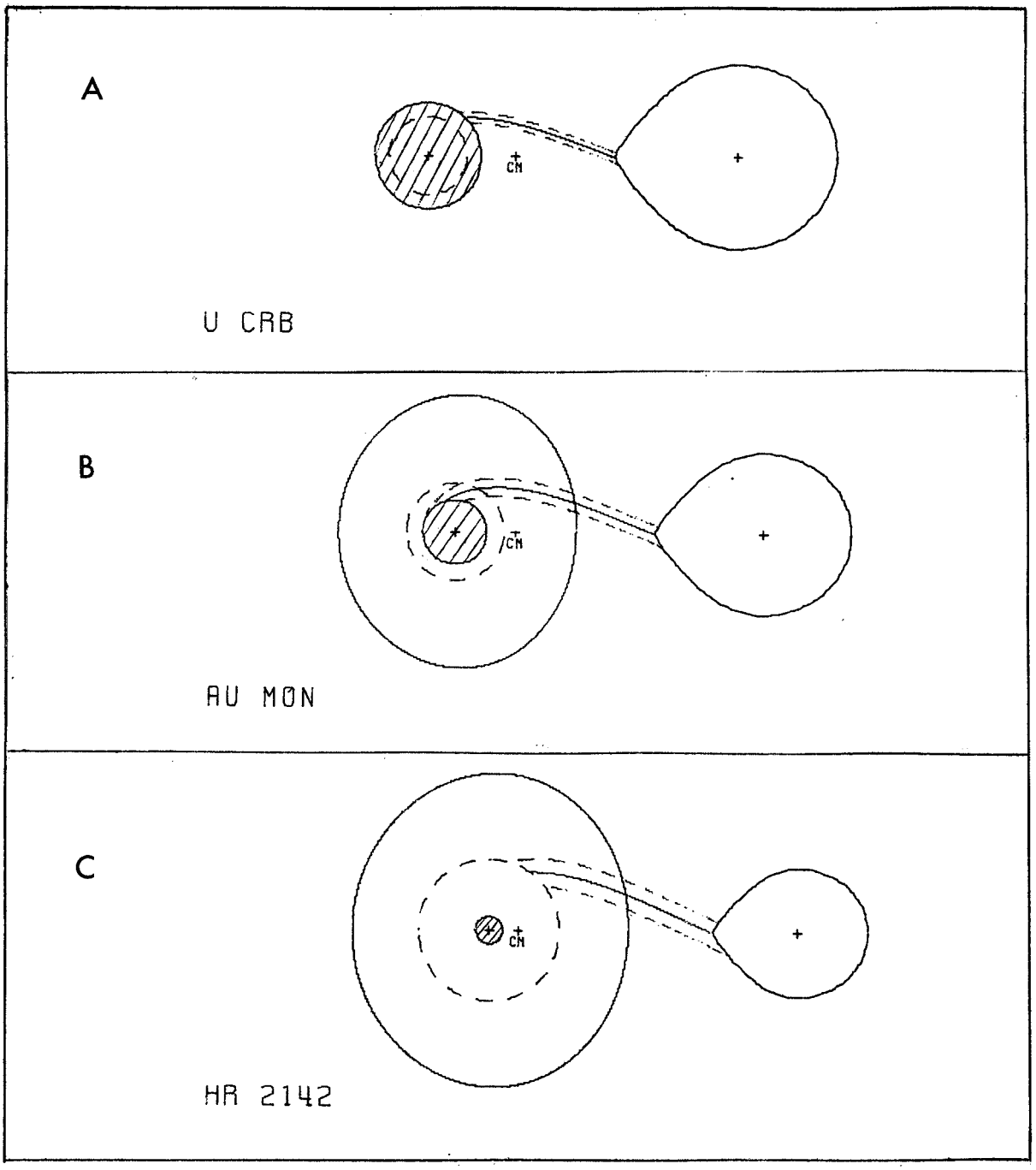

Figure 2. Models for three binary stars. Dashed circle drawn at ϖ_d, outer solid circle: maximum low density disk size. Dashed lines associated with stream indicate approximate stream width.

CONCLUSIONS

Observations of a wide variety of binary stars suggest general agreement with the calculations of Lubow and Shu. In particular no evidence is found for dense accretion disks in Zone I stars. The disks do, however, seem to be present in Zone III stars. Stars in Zone II do not appear to have dense disks. This supports Lubow and Shu's suggestion that if $r > \varpi_{min}$ no dense disk will form. While the observations generally agree differences are noted. Further work particularly on the stream/disk vertical structure and the motion and conditions in the lower density gas in the binary are needed before detailed comparisons can be made.

REFERENCES

Lubow, S.H., and Shu, F.H., 1975, Ap.J, 198, 383.

_____, 1976, ApJ, 207, L53.

Peters, G.J., and Polidan, R.S., 1982, in "Be Stars" (eds. M. Jaschek and H.-G. Groth), Reidel, p. 405.

MODEL FITTING OF THE ALGOL BINARIES

Jan J. Dobias and Mirek J. Plavec

Department of Astronomy, University of California, Los Angeles

ABSTRACT

Energy distributions of the component stars of the Algol-type semi-detached binaries are being studied by combining IUE low-dispersion spectra with optical scans made with about the same resolution. In most cases, the flux distributions can be very well matched by Kurucz model atmospheres with normal solar composition (Kurucz, 1979). A search is being made for deviations from normal atmospheres, which would probably indicate a higher level of activity and interaction in the binaries. So far, eclipse observations in U Cep and V356 Sgr revealed emission lines of the W Serpentis type.

OBSERVATIONS

The Algol binaries are semidetached close binary systems, in which the Roche lobe filling component is the less massive one, but by its position on the subgiant or giant branch of the evolutionary track, it appears to be more advanced in evolution than the more massive star. The more massive star is of an earlier spectral type, but (in all or most cases) still lies within the Main Sequence band. This combination of stars is supposed to be the result of mass transfer (as well as mass loss) from the now less massive component; although the most important phase of the process must have occurred in the past, some mass interaction still exists, and the degree of it apparently varies from system to system.

We have been studying systematically the energy distribution in the spectra of numerous Algols, combining the IUE spectra with optical scans made with the IDS scanners at Lick Observatory. The importance of using IUE observations lies in two directions: (1) In some systems, the late-type components are sufficiently faint and cool, and the ultraviolet spectrum is not affected by them. Then the UV observations provide a cleaner picture of the hotter component, although the spectrum still can be contaminated by circumstellar material. Indeed, we have encountered both simple as well as contaminated cases. In some systems, the hotter component can be easily fitted by a Kurucz model atmosphere and the parameters obtained agree well with the spectroscopically and photometrically derived spectral types from the optical region, obtained by other authors. Among such simple Algols are U Sge and U CrB.

(2) In other Algol systems, the flux from the later-type component is significant not only in the optical region but also in the ultraviolet; this group includes systems such as RZ Sct, V356 Sgr, etc. Here the UV observations broaden the observational basis for model fitting. Substantial progress can be achieved only if both eclipses are observed both in the UV and in the

optical regions. We managed to obtain such observations for several systems, but the work must be continued. Partially eclipsing systems with both components visible in the UV, such as RZ Sct, are the most difficult objects. Yet even for them, better solutions can be accomplished when IUE observations are used, since we can at least eliminate the additional unknown, namely the color excess. The color excess is obtained in our project by two independent ways: once from the bump at λ 220 nm, and again from an overall least-squares fit provided that a Kurucz atmosphere can be found to fit the data satisfactorily. Both methods have so far led to a very satisfactory agreement in all cases.

I must now point out one obvious shortcoming of our approach. For lack of time, it has not been possible to obtain sufficient phase coverage of the systems. Thus significant distortions of the light curve, such as ellipticity or gravitational darkening cannot be taken into account and may affect our solutions in an unknown way. We suggest that our results are considered as complementary to the determinations of spectral types and surface gravities published by Olson (1975).

RESULTS

A total of 14 Algols have so far been adequately observed. For RZ Eri, TT Hya, UX Mon, and RZ Sct, the reduction has not advanced enough. The other ten systems are listed in the following preliminary Table:

System	Primary	Secondary	E(B-V)
U Cep	B9 V	G8 III	0.03
RS Cep	A0 -A2 III	G8 III	0.03
U CrB	B6 V	-	0.03
RX Gem	A1 V	-	0.04
RY Gem	A1 - A2 V	-	0.03
AU Mon	B5 V	F:	0.00
AW Peg	A2 IV	G1 II-III	0.00
RY Per	B6 III	F6 - F7 III-IV	0.15
V356 Sgr	B1.5 V	A1 II	0.30
U Sge	B7 V	G4 III	0.06

The most difficult case encountered so far among the totally eclipsing systems was U Cephei. It is usually classified, from its UBV colors and optical line spectrum, as B7 V, although this classification is uncertain by at least one subclass. Batten (1974) in his comprehensive study of this system quotes B-V values ranging from -0.07 to -0.14 mag. The corresponding effective temperatures (denoted here simply T) for main-sequence stars lie between

11,000 °K and 14,000 °K according to the calibrations by Hayes (1978), Flower (1977), and Popper (1980). The optical flux distributiuon can be matched by a Kurucz model atmosphere for T = 13,000 °K, but the ultraviolet fluxes are decidedly too low for this kind of temperature. The only acceptable overall fit is for T = 11,000 °K, so that our results lie at the lower limit of the range defined by Batten.

ULTRAVIOLET EMISSION LINES IN ALGOLS

Our spectra were as a rule obtained at random phases outside eclipses. No spectra taken outside eclipse show any emission lines, with the possible exception of RS Cephei. This star was observed mainly because Hall (1969) suggested that its accreting component is a disk-like object; therefore we anticipated another W serpentis system. The spectrum taken on 14 December 1981 (phase 0.99, i.e. just prior the primary eclipse) shows one conspicuous emission line at λ 1492 A. The line is unusually narrow and may be spurious, athough there is no other evidence for a cosmic ray hit. Unless this line is actually the intercombination line of N IV] λ 1486 A, its identification is also a problem. Another spectrum is badly needed. Hall may be right in his prediction, since we suspect, from Lick scans, considerable amount of circumstellar hydrogen emission, which is rather typical for the W Serpentis stars.

Several systems were observed during eclipses: U Cephei in primary eclipse, V356 Sgr and RZ Scuti in both eclipses. A rich emission-line spectrum was seen twice in U Cephei, at and near totality. It resembles the spectra of the W Serpentis stars, with lines of C II, C IV, Si II - Si IV, N V, Al II, Al III, and Fe III. The C IV resonance doublet is by far the strongest line. Yet even this line is much weaker than the out-of-eclipse continuum of the B star; this limits its visibility only to phases very close to the total eclipse of the B star. The observed peak flux in C IV is 7×10^{-13} ergs cm^{-2} s^{-1}, while the out-of-eclipse continuum level near λ 155 nm is about 3×10^{-11} ergs cm^{-2} s^{-1}. Contrary to this, the peak flux in the same line in SX Cas (1.3×10^{-11} ergs cm^{-2} s^{-1}, observed but dereddened) is about 30 percent higher than the flux in the adjacent continuum, and the line remains easily visible at all phases.

Emission lines were also seen during the primary eclipse of V356 Sgr, when the B1.5 V star is totally eclipsed, but there still remains a fairly high ultraviolet continuous flux from the A1 II secondary. The emission line spectrum of V356 Sgr is much poorer and consists only of the lines of N V, Si III (λ 130 nm), Si IV (λ 140 nm), and C IV. However, contrary to U Cep, C IV in V356 Sgr is very much weaker than N V. The differences in intensity and absence of other lines cannot be fully accounted for by the A star continuum rising toward longer wavelengths. It is quite possible that the circumstellar material has been partly processed by the CNO bi-cycle. V356 Sgr has usually been considered to be an old, quiescent Algol. However, Wilson and Caldwell (1978) found photometric evidence for a circumstellar ring. We made an attempt to observe the total eclipse of V356 Sgr at high-dispersion, to see if the emission lines have the P-Cygni type profiles found in β Lyrae and KX Andromedae. The results are inconclusive. One spectrum was too faint, the other was completely obliterated by the background radiation. The weak spectrum

seems to show double-peaked profiles indicative of a rotating circumstellar ring rather than mass outflow. This problem must be decided soon.

The two succesful observations of emission lines in "classical" Algols indicate that they may be present rather often, although weakly, and could be detectable in totally eclipsing Algols. The emission lines suggest that there probably is a smooth transition to the stronger phenomena observed in the W Serpentis stars. The obvious importance of such observations for better understanding of the interaction between the components makes it imperative to continue this kind of work.

REFERENCES

Batten, A.H.: 1974, Publ. Domin. Astroph. Obs. Victoria 14, 191.

Flower, P.J.: 1977, Astron. Astrophys. 54, 31.

Hall, D.S.: 1969, Bull. Amer. Astron. Soc. 1, 345.

Hayes, D.S.: 1978, in The HR Diagram, IAU Symp. No. 80, (ed. A.G.D. Philip and D.S. Hayes), 65. Dordrecht: Reidel.

Kurucz, R.L.: 1979, Astrophys. J. Suppl. 40, 1.

Olson, E.C.: 1975, Astrophys. J. Suppl. 29, 43.

Popper, D.M.: 1980, Ann. Rev. Astron. Astrophys. 18, 115.

Wilson, R.E. and Caldwell, C.N.: 1978, Astrophys. J. 221, 917.

A RECENT TIME OF MINIMUM FOR AND ATMOSPHERIC-ECLIPSE EFFECTS IN THE ULTRAVIOLET SPECTRUM OF THE WOLF-RAYET ECLIPSING BINARY V444 CYGNI

Joel A. Eaton
Vanderbilt University

A. M. Cherepashchuk and Kh. F. Khaliullin
Shternberg State Astronomical Institute, Moscow University

ABSTRACT

We have used the IUE satellite to obtain continuum observations in the 1200-1900Å region and fine-error-sensor observations in the optical for V444 Cyg. More than half of a primary minimum and almost a complete secondary minimum were observed. They imply a time of primary minimum for their epoch of JD(Hel.) 2444913.424 ± 0.003 which is somewhat early (~0.027 days) when compared to the trend of recent times of minimum from ground-based observations. The time of minimum for the secondary eclipse seems to be consistent with that for primary eclipse, and the ultraviolet times of minimum are consistent with the optical ones. The spectrum shows a considerable amount of phase dependence. Most of this seems to result from the atmospheric eclipse of the O6 component by the WR component. NIV λ1718 has a deep absorption component of its P-Cyg profile around primary eclipse with the maximum degree of absorption at about phase 0.06, somewhat after mid-eclipse. HeII λ1640, likewise, has a P-Cyg profile during primary minimum, and the SiIV λ1400 absorption is strengthened at primary minimum. The general shapes and depths of the light curves for the FES siginal and the 1565-1900Å continuum are similar to those for the blue continuum. The FES, however, seems to have detected an atmospheric eclipse in line absorption at about the phase the NIV absorption was strongest. The continuum shortward of 1460Å, however, has a primary minimum much deeper than the optical eclipse. This suggests that there is a source of continuum absorption shortward of 1460Å which exists throughout a large part of the extended atmosphere and which, by implication, must redden considerably the ultraviolet continuua of WN stars. A preliminary value of the expansion velocity, determined for two spectra obtained outside eclipse, is 2500 ± 400 km/s. This implies a fairly high degree of ionization for the inner part of the WN star's atmosphere.

INTRODUCTION

The WN5+O6 eclipsing binary V444 Cygni (HD 193576) is nearly unique in that its deep eclipses and relatively uncomplicated light curve make it possible for one to analyze reliably the radial structure of the WN atmosphere. Likewise, its well documented period changes may be used to determine the mass-losss rate in the WR wind. Analyses of the shapes of the optical eclipses (Hartmann 1978, Cherepashchuk, Eaton, and Khaliullin 1982) have shown that the star has a dense expanding atmosphere which causes the intensityy of the WR star to be highly concentrated to the center of its disk and which gives atmospheric eclipses of the O6 component. Khaliullin (1974) found that the period of V444 Cyg is increasing at about the rate $\dot{P}/P = 2.88 \times 10^{-8}$/yr. A more

recent study of Kornilov and Cherepashchuk (1979) has refined the rate of period change and the mass loss rate derived from it, $\dot{M} = -1.11 \times 10^{-5}$ $M_\odot$/yr. The best explanation for the period change seems to be mass loss in a rapidly expanding wind which Hall and Kreiner (1980) used to explain the period increases of RS CVn binaries.

OBSERVATIONS

V444 Cyg was observed during both a primary and a secondary eclipse with the IUE satellite in early November 1981. Observations were also obtained during 7 other shifts in April and November 1981. The data consist of 64 spectra, 53 taken with the SWP camera and 11 with the LWR camera. For the most part, the spectra were exposed for the same length of time which was chosen not to saturate the prominent emission lines in the short-wavelength region. Figure 1 shows a representative spectrum, SWP13848, obtained in April 1981. Prominent emission lines are NV λ1240, NIV] λ1486, CIV λ1550, HeII λ1640, and NIV λ1718. The fine error sensor (FES) was used to estimate the brightness of the system in a broad optical band centered in the green (see Holm and Rice 1981). As part of our analysis the flux in the spectra was integrated over two relatively broad photometric bands in the short-wavelength region. The shorter, 1370, is a square band between 1270 and 1470Å. The longer, 1740, is a combinarion of four square bands (1565-1630, 1655-1698, 1730-1780, and 1800-1900Å) designed to avoid prominent lines and reseaux marks.

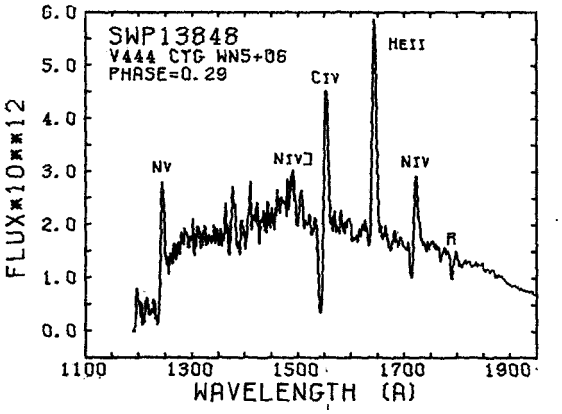

Fig. 1 -- The short-wavelength spectrum of V444 Cyg. Prominent emission lines are indicated. The R indicates the position of a reseaux mark.

The light curves in primary and secondary eclipses are plotted in Figures 2 and 3, respectively. Both eclipses were covered well only during the rising branch. The solid curves in the figures are 4244Å mean continuum light curve of Cherepashchuk and Khaliullin (1973).

TIME OF MINIMUM

We have determined the time of minimum light for each eclipse for both the FES and 1740 data. For the FES data we applied a procedure developed by G. W. Henry (see Sowell 1981) to 15 points for secondary minimum and 8 of the points in the deepest part of primary eclipse. For the 1740 data we found the time for which there was best agreement with the optical continuum light curve by comparing the optical and UV data graphically. The times of minimum for the FES and 1740 data agree to within their errors and combine to give the

following mean times of minimum, JD(Hel.) 2444915.5255 and JD(Hel.) 2444913.4244, respectively, for primary and secondary eclipse. The efective time of minimum for all the data, referred to primary eclipse, is JD(Hel.) 2444913.424 ± 0.003. As in the study of Kornilov and Cherepashchuk (1979) we will refer our time of minimum to the linear ephemeris:

$$\text{Min I} = \text{JD(Hel.)}2441164.337 + 4^{d}.212435E.$$

from which the deviation of our time of minimum is (O-C) = 0.0173 ± 0.004 days. This time is roughly 0.027 days early when compared to the parabolic trend in the (O-C)'s found by Khaliullin, Kornilov, and Cherepashchuk for all the photoelectric times of minimum. It may simply indicate a change in the asymmetry of the flow of the expanding atmosphere. Such a result means that it is now more important than ever to continue obtaining times of minimum for V444 Cyg to study the parabolic trend.

INTERPRETATION OF THE SPECTRA

The light curves point out in a striking manner some of the properties of the spectra. Generally, the FES and 1740 variation agree well with the blue continuum data. The 1370 light curve, however, has a markedly deeper primary minimum. Indeed, the (1370-1740) color is 0.56 mag bluer near secondary than at primary minimum. This increased eclipse depth results from what appears to be an ionization edge in the spectrum near 1460Å. Line absorption is likewise stronger during primary minimum. Much of this phase dependence results from atmospheric eclipse effects, although some of it likely is contributed by asymmetries produced by the binary system (cf. Dupree, Hartmann, and Raymond 1980 for Cyg X-1). UV lines obviously strengthened at primary minimum are SiIV λ1400, HeII, and NIV. The maximum absorption for these species seems to occur near phase 0.06 as if produced in a shell of radius ~15$R_{\odot}$. Two spectra have been analyzed for expansion velocity. The total widths of the CIV, HeII, and NIV P-Cyg profiles (blue edge of the absorption to red edge of the emission) imply a terminal velocity of around 2550 ± 400 km/s. These widths have been derived by assuming gaussian profiles and correcting for an instrumental width of 5Å. The blue edges of the the CIV profiles, similarly corrected for a 5A instrumental spreading, also give a terminal velocity of ~2500 km/s with respect to the WR component. When combined with the continuum solution of Cherepashchuk, Eaton, and Khaliullin (1982) this implies that helium is doubly ionized throughout the inner zone ($r \lesssim 10R_{\odot}$) in which most of the expansion occurs.

REFERENCES

Cherepashchuk, A. M., and Khaliullin, Kh. F. 1973, Soviet Astr.--AJ, 17, 330.
Cherepashchuk, A. M., Eaton, J. A., and Khaliullin, Kh. F. 1982, Ap. J., subm.
Dupree, A. K., Hartmann, L. W., and Raymond, J. C. 1980, in IAU Symposium No. 88, p. 39.
Hall, D. S., and Kreiner, J. M. 1980, Acta Astr., 30, 387.
Hartmann, L. 1978, Ap. J., 221, 193.
Holm, A., and Rice, G. 1981, IUE NASA Newletter, No. 15, p. 74.
Khaliullin, Kh. F. 1974, Sovier Astr.--AJ, 18, 229.
Kornilov, V. G., and Cherepashchuk, A. M. 1979, Pisma Astr. Zu., 5, 398.
Sowell, J. R. 1981, Masters thesis, Vanderbilt University.

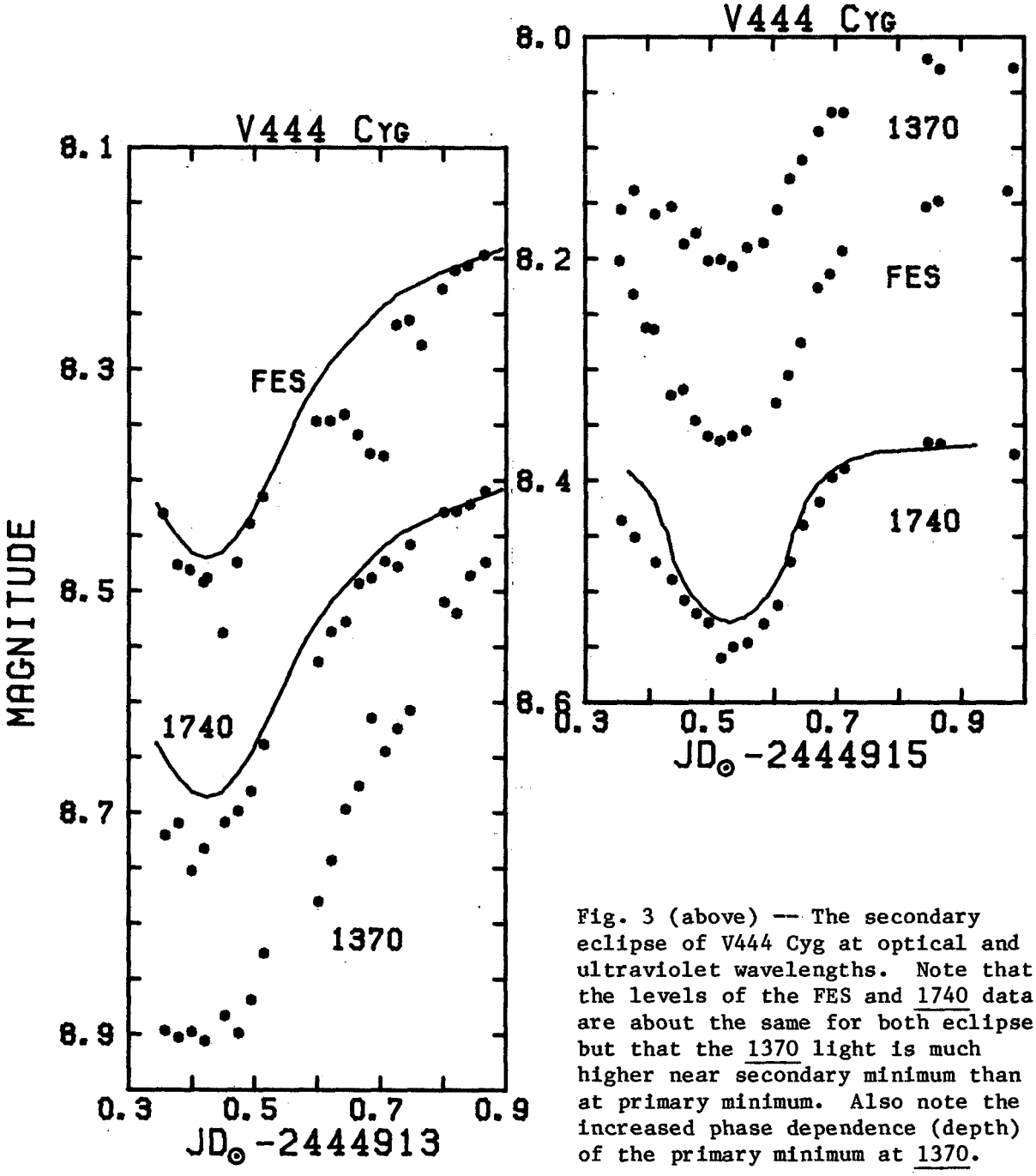

Fig. 3 (above) -- The secondary eclipse of V444 Cyg at optical and ultraviolet wavelengths. Note that the levels of the FES and 1740 data are about the same for both eclipses but that the 1370 light is much higher near secondary minimum than at primary minimum. Also note the increased phase dependence (depth) of the primary minimum at 1370.

Fig. 2 (above, left) -- The primary eclipse of V444 Cyg at optical and ultraviolet wavelengths. The shell absorption feature referred to in the abstract is evident in the FES data.

THE HOT COMPONENTS OF HYDROGEN-DEFICIENT BINARIES

J. S. Drilling and D. Schoenberner
Dept. of Physics and Astronomy, Louisiana State University

ABSTRACT

We compare low-resolution IUE observations of the hot components of three very similar but peculiar objects: LSS 4300, Upsilon Sgr, and KS Per. We discuss the possible evolutionary scenarios in view of these observations and the extremely low hydrogen contents of the visible stars.

Drilling (1981) has shown that the visible absorption-line spectrum of LSS 4300 (HDE 320156) is intermediate at low dispersion to those of the extreme helium stars Upsilon Sgr and HD 168476. These two stars have similar effective temperatures, but Upsilon Sgr is known to be a single-lined spectroscopic binary with a very high atmospheric abundance of nitrogen, whereas HD 168476 is carbon-rich and is apparently a single star. Upsilon Sgr also differs from HD 168476 in that it shows strong H-alpha emission, has an ultraviolet excess due to the flux contribution from the hotter component (Hack et al. 1980), and an infrared excess due to circumstellar dust (Treffers et al. 1976). LSS 4300 resembles Upsilon Sgr in that it too shows very strong H-alpha emission.

In order to see whether LSS 4300 resembles Upsilon Sgr in the other two respects mentioned above, infrared photometry has been carried out at Cerro Tololo, and low-resolution spectra have been obtained with IUE. The results are shown in Fig. 1, where the spectra of all three stars have been corrected for interstellar reddening according to the reddening law of Seaton (1979), using the reversal of the 2200 Å feature as the criterion for zero reddening. LSS 4300 is seen to have infrared and ultraviolet excesses very similar to those of Upsilon Sgr. We therefore conclude that LSS 4300 is a member of the class of hydrogen-deficient binaries, which contains only two other known members: Upsilon Sgr and KS Per (see Hack 1967).

The ultraviolet spectra of these three stars are shown in Fig. 2 along with two artificial spectra produced by adding the fluxes of pairs of stars selected from the atlas of Wu et al. (1981). All of these spectra have been corrected for interstellar reddening according to the method described above. The spectrum of Upsilon Sgr is best reproduced by adding to the flux of an F0Ib star the flux of a B2Ib star which is 5.2 magnitudes fainter in V. Those of LSS 4300 and KS Per, which are very similar, are best reproduced by adding to the flux of a star of spectral type A2Ia the flux of a B2Ib star which is 3.0 magnitudes fainter in V. The LWR spectra of all three stars can be matched even more closely with the spectrum of the hydrogen-deficient star LSS 3378, but this star does not give the proper contribution to the SWP spectrum because of very strong carbon absorption features. We attribute this to the fact that LSS 3378, like the other apparently single hydrogen-deficient stars, is carbon-rich, whereas the hydrogen-deficient

binaries have a much lower atmospheric abundance of carbon and are nitrogen-rich.

As first pointed out by Hack et al. (1980), the SWP continuum of Upsilon Sgr can be well matched with the spectrum of an 09.5V star or an early B-type supergiant. However, of all of the spectra in the atlas of Wu et al. (1981), only the B2Ib spectrum comes close to matching the observed strengths of the SiIII, SiIV, and CIV features in the spectra of the hydrogen-deficient binaries. The luminosities of the hot secondaries are, however, much too low in comparison to those of the primaries for them to be supergiants. Furthermore, Duvignau et al. (1980) estimate the mass of the secondary in Upsilon Sgr to be between 1.6 and 3.8 solar masses, which rules out even an early-type main sequence star. These problems are circumvented if the secondary is a star of lower mass with an extended spheroidal envelope produced by accretion of material from the primary.

Turning now to the visible spectra of these stars, we use the theoretical H-gamma profiles given by Wallerstein et al. (1967) to estimate the atmospheric hydrogen abundances for Upsilon Sgr and LSS 4300. These profiles were used by Wallerstein et al. (1967) to obtain n(H)/n(He) = 10E-4 for KS Per. The observed H-gamma profile given by Hack and Pasinetti (1963) also yields n(H)/n(He) = 10E-4 for Upsilon Sgr. This value is much lower than the value 1/40 found by Hack and Pasinetti (1963), and we attribute the discrepancy to the inappropriate use by these authors of a curve of growth analysis for the determination of the hydrogen abundance. Drilling (1981) finds the Balmer lines to be weaker in the spectrum of LSS 4300 than in the spectrum of Upsilon Sgr, even though the effective temperatures are similar, indicating that n(H)/n(He) is even less than 10E-4 in the atmosphere of this star.

What can we say about the evolution of the hydrogen-deficient binaries in the light of these new findings? We can rule out Case B and Case C evolution for a very simple reason: in both cases the radius of the region in which hydrogen has been totally depleted is much smaller than the Roche radius. In fact, both scenarios are able to produce hydrogen depletion down to only X = 0.2 (n(H)/n(He) = 1) in the envelope of the star which looses mass, contrary to the observation that n(H)/n(He) is around 10E-4 in the atmospheres of all three stars (for Case C see Lauterborn, 1970). The only scenario which is consistent with this observation appears to be the following: the system goes first through a Case B mass exchange in which most of the hydrogen envelope of a massive primary (5 - 14 solar masses) is lost. The remnant is then able to evolve like a massive helium star. If its mass is between 1 and 2 solar masses, it will expand to a (helium) supergiant and will reach low surface temperatures prior to the onset of core carbon burning (see de Greve and de Loore, 1977). This star (the original primary) will then fill its Roche lobe a second time, spilling its (helium) envelope over onto the secondary (Case BB, see Delgado and Thomas, 1981). This picture is consistent with all existing observations, and predicts that the hot secondaries in hydrogen-deficient binaries should also be hydrogen-deficient.

REFERENCES
Duvignau, H., Friedjung, M., Hack, M., 1980, Astron. Astrophys. 71, 310.
Delgado, A. J., Thomas, H.-C, 1981, Astron. Astrophys. 96, 142.
Drilling, J. S., 1981, Ap. J. 242, L43.
De Greve, J.-P. de Loore, C., 1977, Astrophys. Space Science 50, 75.
Hack, M., 1967, Modern Astrophysics: A Memorial to Otto Struve, ed. M. Hack (Paris: Gauthier-Villars), p. 163.
Hack, M., Flora, U., and Santin, P. 1980, Close Binary Stars: Observations and Interpretation, eds. M. J. Plavec, D. M. Popper, and R. K. Ulrich (Dordrecht: D. Reidel), p. 271.
Hack, M., and Pasinetti, L. 1963, Contr. Obs. Astr. Milano-Merate, Vol. 6, No. 215.
Lauterborn, D., 1970, Astron. Astrophys. 7, 150.
Seaton, M. J. 1979, M.N.R.A.S. 187, 73P.
Treffers, R., Woolf, N. J., Fink, U., and Larson, H. P. 1976, Ap. J. 207, 680.
Wallerstein, G., Greene, T. F., Tomley, L. J. 1967, Ap. J. 150, 245.
Wu, C. C.. Boggess, A., Holm, A. V., Schiffer, F. H., and Turnrose, B. E. 1981, IUE Newsletter No. 14, p. 2.

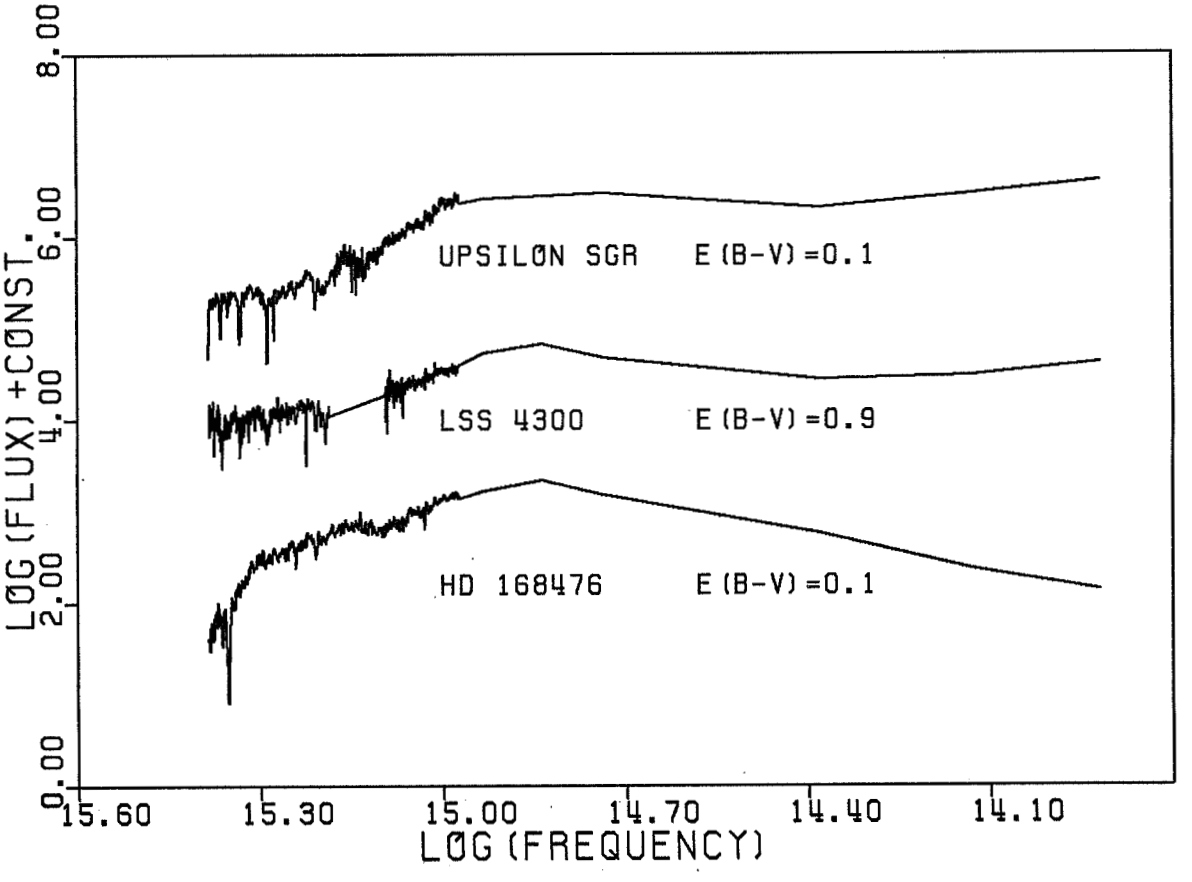

Fig. 1. Results of UV spectroscopy and UBVJHKL photometry for Upsilon Sgr, LSS 4300, and HD 168476

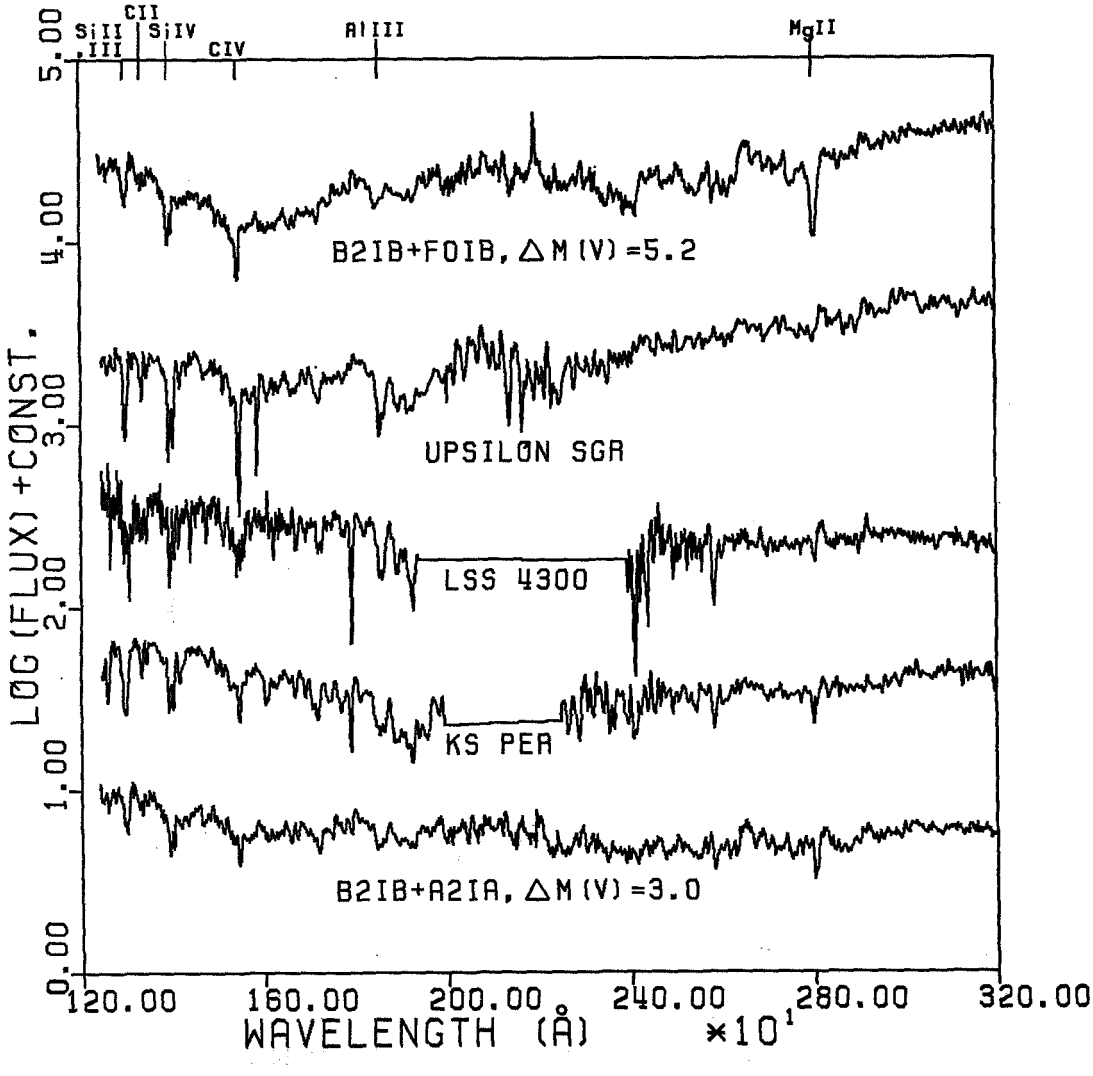

Fig. 2. Low-dispersion IUE spectra of the hydrogen-deficient binaries and two composite spectra made using the atlas of Wu et al. (1981)

CONTINUUM AND EMISSION LINES IN BETA LYRAE

Mirek J. Plavec, Janet L. Weiland, and Jan J. Dobias

Department of Astronomy, University of California, Los Angeles

ABSTRACT

Integral photometric characteristics of β Lyrae have been re-determined using its brightest visual companion, the star HD 174664. An attempt was made to separate the fluxes coming from the two components. The flux distributions are badly contaminated by the radiation of the circumstellar hydrogen. On top of that, peculiarities seem to be present in both components; in particular, the secondary star cannot be represented by an atmosphere with a unique effective temperature, and will probably be best represented by a thick disk.

GENERAL PROPERTIES OF THE SYSTEM

Beta Lyrae remains in the forefront of the interest in interacting close binaries. We have been conducting systematic studies aimed at better determining the photometric properties of the system over a wide range of wavelengths (110 -700 nm), combining IUE spectra and spectral scans obtained at the Lick Observatory. Photometric properties can now be expressed on an absolute scale more reliably, since we have used the brightest optical companion to Beta Lyrae, the star HD 174664, to redetermine the distance (350 pc) and color excess E(B-V), which is only 0.02 mag. This determination is quite reliable and should terminate a prolonged discussion, in which color excess values as high as E(B-V)= 0.13 mag were suggested. The spectrum of the eclipsing pair shows no λ 220 nm dip that would support such a high value, but it was possible to argue that the combined spectrum of the eclipsing pair is too complex to permit this assumption. The star HD 174664 is a quite normal B7 V star, and it was possible to fit it by a Kurucz model without difficulty; the small value of the color excess is a by-product of the least-squares fit.

THE CONTINUOUS RADIATION OF THE COMPONENTS

It is much more difficult to match the energy distributions of the two eclipsing components. We should describe here our technique by means of which we attempted to separate the fluxes from either component. Lack of observing time precludes the only really correct approach, i.e. obtaining well-covered light curves at all pertinent wavelengths, and then solve them for elements. Instead, we had to select one phase as representative of the situation when both components contribute unobscured, and then subtract the energy distribution at either eclipse from this "standard" distribution. The pitfalls of this approach are rather obvious. For one thing, we are unable to take into account photometric perturbations such as the varying projected shape of the components, or their gravitational darkening. Again, the eclipses most likely

are not total, so the fluxes we obtain by subtraction are to be multiplied by a constant greater than 1, in order to obtain the actual fluxes from either of the components. This constant can be derived only from a rigorous photometric solution. Thirdly, the region of space eclipsed at either mid-eclipse together with the eclipsed component contains luminous circumstellar gas which contaminates the energy distribution of the eclipsed components. Knowing all these troublesome facts, we decided to go ahead with the project, since it still provides us with valuable information on the system, not available to us before.

Neither star can be fitted by a simple Kurucz model atmosphere. The primary cause is the presence of circumstellar hydrogen clouds, which may surround each component and/or the whole system. When we tentatively subtract the optically thin hydrogen radiation, the primary component still does not match the flux distribution of a B8 II star, which is its usual spectral classification. In fact, there is a good match between a Kurucz model atmosphere for T_{eff} = 11,000 K and log g = 2 only within the wavelength interval usually covered by optical observations, namely between about λλ 380 -600 nm. At most other places within the observed wavelength range λλ 120 -680 nm, the flux from the primary component is higher than the model requires. It has long been known that there is excess radiation in the infrared, due to circumstellar hydrogen (see, e.g., Phillips et al., 1980). Our IUE observations show a similar very strong excess between 170 -290 nm, probably at least partly due to the same source. Unfortunately, we do not have good coverage of the vicinity of the Balmer jump, which makes it very difficult to find a good model representation for the radiation of the circumstellar hydrogen cloud.

Contrary to this excess flux at most wavelengths, the primary component shows a conspicuous flux deficiency (with respect to the above model flux for a B8 II star) at wavelengths shorter than λ 160 nm. This deficiency may be due to an incomplete line blanketing correction, and may be a more general phenomenon, common to stars of about this spectral type and this low surface gravity.

The secondary component (the one in front at primary eclipses) probably radiates as an optically thick disk. In the optical region, its radiation level is lower than that of the primary, but its color temperature is not much different, probably only slightly lower. In the far ultraviolet, the color temperature of the secondary star becomes higher than that of the primary. In fact, the secondary component radiates more than the primary star at wavelengths shorter than λ 160 nm; its eclipses become deeper. As already pointed out by Kondo et al. (1976), the role of the eclipses is interchanged in the far ultraviolet, and the eclipse with the B8 II star behind is now shallower than the other one.

According to our observations, the flux in the region λλ 185 -210 nm is practically the same at phases 0.181, 0.495, and 0.995. In other words, we found almost no eclipses for these wavelengths. Kondo et al. (1976) did not find the conditions so extreme, but even they noted that the eclipses are shallower at the wavelength of 191 nm. Clearly, the integral flux coming to us from the system at these wavelengths is dominated by luminous circumstellar material which is spread over a volume of space much larger than defined by the dimensions of the two components. It is quite possible that this circum-

stellar contribution is not constant in time, and may undergo significant secular variations.

The character of this circumstellar radiation at wavelengths around 200 nm is in our opinion still questionable. It was explained as a superposition of numerous weak emission lines of Fe III, for example by Viotti (1976). But the general presence of strong hydrogen radiation makes it possible to explain part -- and probably most -- of this "λ 200 nm bulge" by a suitable model of a circumstellar hydrogen cloud.

THE EMISSION LINES

The emission lines observed in the far ultraviolet are all of the P Cygni type, but they differ significantly from the emissions typically observed in early type stars with a pronounced stellar wind. The profile width indicates that the terminal velocity of the outflow is only some 480 km/s. This is much less than the terminal velocities observed in hot stars. However the same order of magnitude of the terminal velocity prevails among late B-type supergiants (Panagia and Macchetto, 1982).

The emission component of each emission line in β Lyrae is considerably stronger than the absorption component, which is probably due to a significant collisional contribution to the population of the upper levels. The absence of the intercombination lines indeed indicates that the electron density in the region of the emission line formation must be relatively quite high, about 5×10^{12} cm^{-3}. Another factor may also be present, namely the non-spherical character of the wind. We observe the system nearly edge-on, and one must anticipate the existence of fairly dense circumstellar or circumbinary disks in the orbital plane. The wind may be blowing predominantly towards the polar regions, and this orientation factor will also affect the relative strength of the absorption and emission components. An investigation into the physics and geometry of the emission lines is currently under way.

REFERENCES

Kondo, Y., McCluskey, G.E., and Eaton, J.A.: 1976, Astroph. Space Sci. 41, 121
Panagia, N. and Macchetto, F.: 1982, Astron. Astrophys. 106, 266.
Phillips, J.P., Selby, M.J., Wade, R., and Sanchez Magro, C.: 1980, Mon. Not. R. A. S. 190, 337.
Viotti, R.: 1976, Mon. Not. R. A. S. 177, 617.

FIGURE 1 ON NEXT PAGE:

Ultraviolet flux distribution in β Lyrae, at phases 0.181 and 0.495, respectively. Note the absence of change in flux at λ 200 nm.

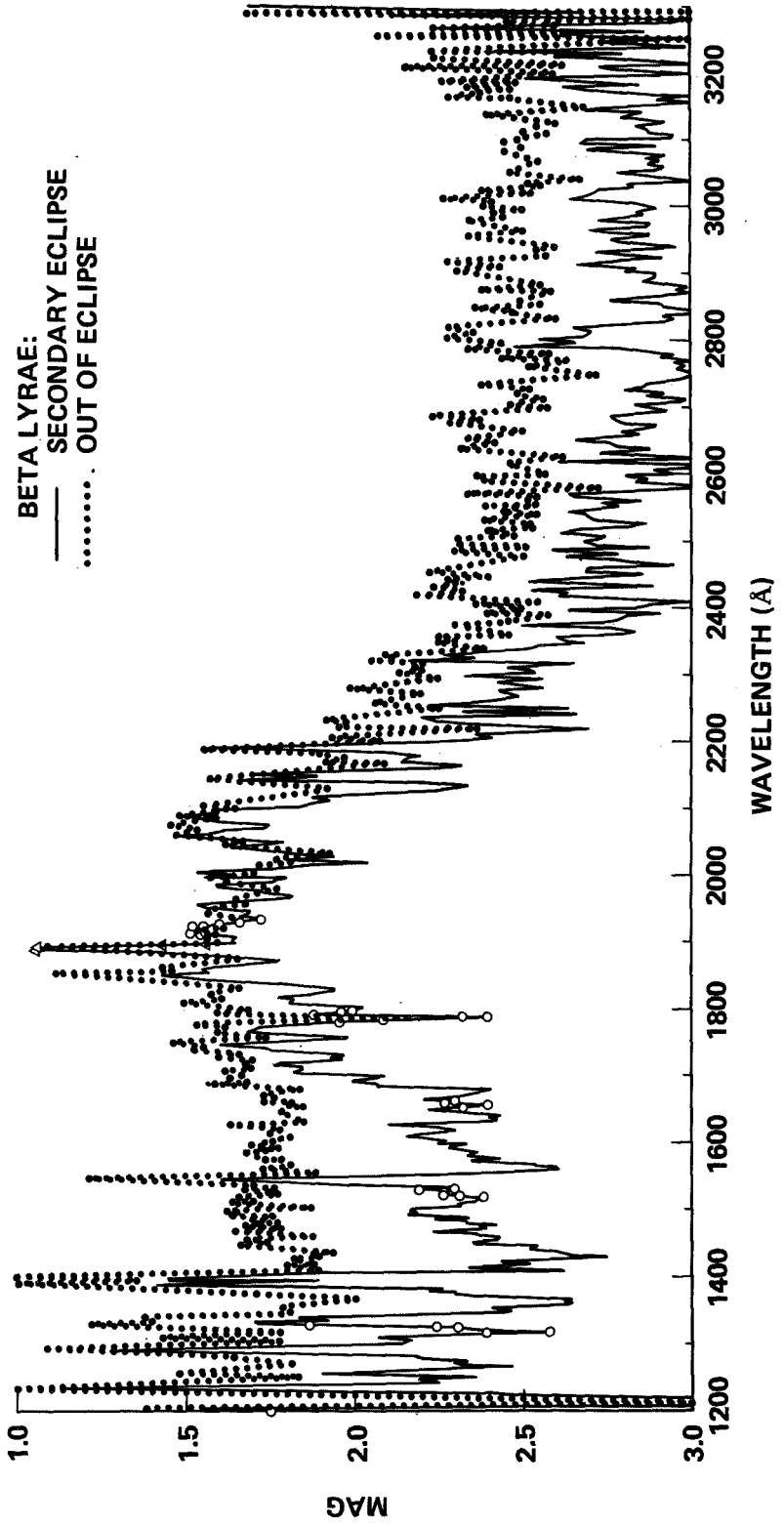
BETA LYRAE:
SECONDARY ECLIPSE
OUT OF ECLIPSE
MAG
1.0
1.5
2.0
2.5
3.0
1200
1400
1600
1800
2000
2200
2400
2600
2800
3000
3200
WAVELENGTH (Å)

RESULTS OF AN IUE PROGRAM OF MONITORING THE ULTRAVIOLET EMISSION LINE FLUXES OF FOUR BINARY SYSTEMS: HR 1099, II PEG, AR Lac, AND BY Dra

N. Marstad, J. L. Linsky,* and T. Simon
Joint Institute for Laboratory Astrophysics, National Bureau of Standards and University of Colorado, Boulder, Colorado 80309

M. Rodono, C. Blanco, S. Catalano, and E. Marilli
Osservatorio Astrofisico, Catania, Italy
and
A. D. Andrews, C. J. Butler, and P. B. Byrne
Armagh Observatory, Armagh, Northern Ireland

ABSTRACT

We present a preliminary report on a collaborative program to obtain IUE spectra and optical photometry and spectra of three RS CVn-type binaries (HR 1099, II Peg, and AR Lac) and the prototype BY Dra system. We monitored these systems for at least one orbital phase, and detected periodic variations in emission line flux from II Peg and HR 1099, indicative of rotational modulation of an active region on these stars. For II Peg the active region is in phase with photometric minimum as expected, but for HR 1099 ultraviolet emission maximum occurs at the time of photometric maximum.

I. INTRODUCTION

RS CVn-type binary systems are generally detached systems of 1-14 day periods that rotate synchronously due to tidal forces and generally consist of a K0 IV primary (typically the active star) and a G5 V secondary. Hall (1976) has reviewed the properties of these systems. The most striking peculiarity of RS CVn binary systems (Hall 1980; Rodonð 1980) — a migrating quasi-sinusoidal distortion in the light curve — was discovered in RS CVn itself by Catalano and Rodonð (1967). Among the different models that have been proposed, the spot model (Hall 1972; Eaton and Hall 1979) appears to be the most successful: the outside of eclipse sinusoidal variation being attributed to rotational modulation of an uneven distribution of photospheric spots.

During the last several years, observers have used IUE to study a number of these systems. These programs include: (1) a study of the nonsynchronous Capella system (G6 III+F9 III) by Ayres and Linsky (1980), (2) a study of HR 1099 (K0 IV+G5 IV) by Ayres and Linsky (1982), (3) a model chromosphere and transition region computed by Simon and Linsky (1980) that matches IUE spectra of HR 1099 and UX Ari, and (4) a study of λ And (G8 III-IV+?) by Baliunas and Dupree (1982) indicating that chromospheric and transition region emission lines are brighter at photometric minimum for this system.

Wide-band photometric monitoring of BY Draconis stars has led to the widely accepted theory that the nearly sinusoidal light variations, with periods of a few days, are also due to large, dark spotted regions whose visibility is modulated by the stellar rotation. The BY Dra systems are typically binary,

*Staff Member, Quantum Physics Division, National Bureau of Standards.

consisting of early M or late K-type dwarf stars with periods of a few days, but Bopp (1979) has shown that not all BY Draconis stars are binaries as EQ Vir (K7 Ve) appears to be single. Thus the spots and flares, and by implication strong magnetic fields, are not a direct consequence of duplicity, but rather of efficient dynamo processes in stars that are rapid rotators (due to tidally-induced synchronism or young age). Linsky et al. (1982) have discussed IUE observations of EQ Vir and AU Mic.

II. OBSERVING PROGRAM

In the Sun there is an excellent correlation of strong magnetic fields with bright emission in lines formed in the chromosphere, transition region, and corona. Plage regions generally overlie spots on the Sun, but the area of plages is several times the spot area. This is likely due to the spreading out of field lines above the photosphere. If, as expected, photometric wave and other phenomena, which Kunkel (1975) collectively referred to as the "BY Draconis syndrome," are magnetic in character, then we predict that the emission lines formed in the chromosphere and transition region should undergo cyclic changes anticorrelated with the photometric variability. To test this hypothesis and to obtain spectra of plage and quiescent regions separately for modeling purposes, we monitored three RS CVn-type binaries (HR 1099, II Peg, and AR Lac) and the prototype BY Dra binary system with IUE on 1-7 October 1981. These stars were observed by IUE 4-9 times each at regular intervals throughout their 2.0-6.7 day periods, together with ground-based photometry and radio observations. Each IUE observation consisted of several low dispersion SWP spectra and several high dispersion LWR spectra.

We found essentially no line flux variations for AR Lac above the noise. BY Dra does show variations in the C IV and C II lines up to 50%, but no evidence for dependence on phase. By contrast, II Peg shows two distinct spectra (see Figs. 1 and 2) — a quiescent spectrum between phases 0.95 and 0.35, and

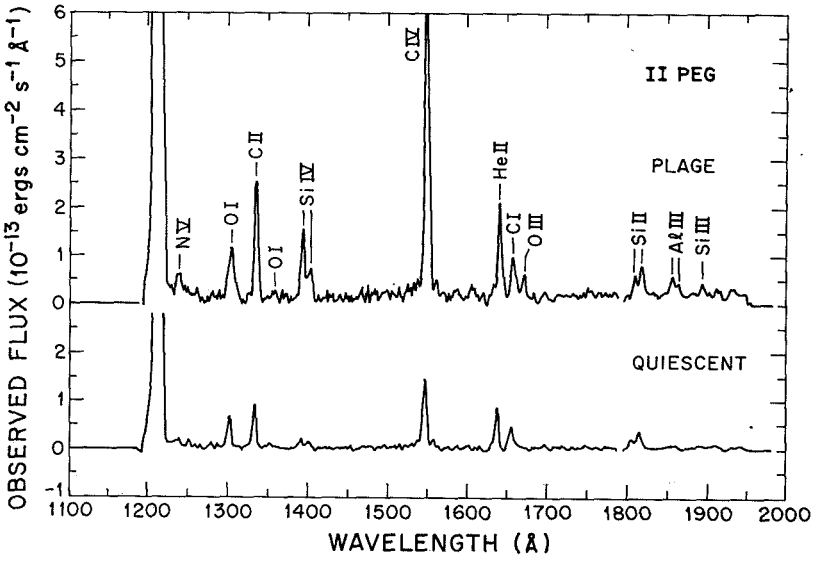

Fig. 1. Composite IUE spectra when the plage is present (sum of three spectra) and when the plage is not present (sum of five spectra).

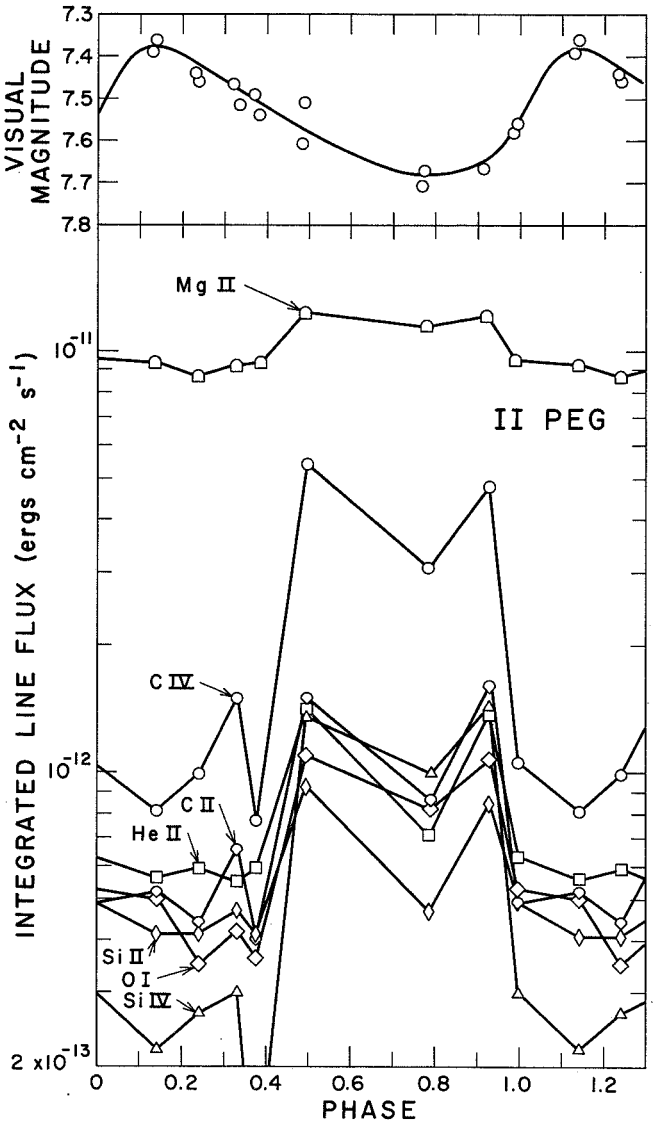

Fig. 2. Observed flux in the Mg II λ2800, C IV λ1550, He II λ1640, C II λ1335, Si II λ1812, O I λ1304, and Si IV λ1400 features as a function of phase using the parameters t_o = 2442316.29 and P = 6.69296 days. Also given are the FES visual magnitudes obtained simultaneously with the IUE spectra.

an active region spectrum between phases 0.40 and 0.90. The active region spectrum shows transition region emission lines a factor of 5 enhanced and chromospheric emission lines a factor of 2 enhanced compared to the quiescent spectrum. The active region appears centered on photometric minimum as determined using FES photometry and thus overlies dark star spots.

Our nine observations of HR 1099 show enhanced emission centered on phase 0.7 and a flare at phase 0.74. Flux enhancements near phase 0.7 and in the flare are also larger for transition region lines than for chromospheric lines. Observations during the second and third cycle are consistent with observations at similar phases during the first cycle. HR 1099 now exhibits a changing and complex photometric curve, but minimum now occurs at phase 0.20, out of phase with the ultraviolet emission line maximum.

III. DISCUSSION

This is only a preliminary discussion of a large data set that will be useful for many purposes, but several trends in the data appear very interesting. First, II Peg clearly shows the correlation of maximum chromospheric and transition region emission with photometric minimum, indicating as expected that stellar plages overlie star spots. Since the plage appears for 0.50 in phase, we are likely seeing the rotational modulation of a plage that is not very extensive in longitude. Second, the increasing enhancement of line flux with increasing temperature of formation is a phenomenon generally seen in solar plages and indicates that as the nonradiative heating rate increases in closed magnetic flux tubes, an increasingly large proportion of this heating goes into high temperature regions. Third, HR 1099 does not show a correlation of emission line maximum with photometric minimum either due to the presently complex photometric curve indicating spots on both hemispheres or the occurrence of a flare. Finally, the repeatability of ultraviolet emission line fluxes over three cycles indicates that the plages do not change appreciably on a time scale of one revolution.

We acknowledge the support of NASA through grant NAG5-82 to the University of Colorado, and thank the staffs of the IUE Observatory at Goddard and Vilspa for assistance in the acquisition and reduction of these data.

REFERENCES

Ayres, T. R. and Linsky, J. L. 1980, Ap. J., 241, 279.
_____. 1982, Ap. J., 254, 168.
Baliunas, S. L. and Dupree, A. K. 1982, Ap. J., 252, 668.
Bopp, B. M. 1979, IAU Joint Meeting on Close Binaries and Stellar Activity, Montreal 1979.
Catalano, S. and Rodonò, M. 1967, Mem. S. A. Ital., 38, 395.
Eaton, J. A. and Hall, D. S. 1979, Ap. J., 227, 907.
Hall, D. S. 1972, P.A.S.P., 84, 323.
_____. 1976, in Multiple Periodic Phenomena in Variable Stars, ed. W. S. Fitch (Dordrecht: Reidel), p. 287.
_____. 1980, in Solar Phenomena in Stars and Stellar Systems, eds. R. M. Bonnet and A. K. Dupree (Dordrecht: Reidel), p. 431.
Kunkel, W. E. 1975, in Variable Stars and Stellar Evolution, eds. V. E. Sherwood and L. Plaut, p. 15.
Linsky, J. L., Bornmann, P. L., Carpenter, K. G., Wing, R. F., Giampapa, M. S., Worden, S. P., and Hege, F. K. 1982, Ap. J., in press.
Rodonò, M. 1980, in Binary Stars, Maratea (Italy), in press.
Simon, T. and Linsky, J. L. 1980, Ap. J., 241, 759.

OBSERVATIONS OF THE MAY 1979 OUTBURST OF CENTAURUS X-4

William P. Blair, John C. Raymond and Andrea K. Dupree
Harvard-Smithsonian Center for Astrophysics
Cambridge, MA 02138

ABSTRACT

We have obtained IUE spectra of the X-ray transient/X-ray burst source Cen X-4 at three intervals during the peak and decline of the May 1979 transient event. The spectrum is characterized by a blue continuum ($F_\nu \propto \nu^{0.0}$) and strong emission lines of N V λ1240, Si IV λ1398 and C IV λ1550. We investigate the origin of these emission components in the context of an X-ray dwarf nova model. It appears that an accretion disk plays a prominent role in the generation of the continuum emission and that X-ray heating of the accretion disk and the companion star may be important in the formation of the emission lines.

INTRODUCTION

Centaurus X-4 is the first of the pre-Uhuru transient X-ray sources to undergo an additional observed X-ray outburst. It was first observed in July 1969 with the Vela 5 satellites in the 3-12 keV energy band (Conner, Evans and Belian 1969, Evans, Belian and Conner 1970). The source apparently remained dormant until early May 1979 when it was detected in 3-6 keV X-rays with the all-sky monitor (ASM) on Ariel 5 by Kaluzienski, Holt and Swank (1980; hereafter KHS). Monitoring of the object by Ariel 5 and later by the HAKUCHO satellite (Matsuoka *et al.* 1980) showed that it remained visible in X-rays for about one month. KHS have shown that, except for the timescale of the decay, the characteristics of the Cen X-4 outburst are very similar to those of other soft X-ray transients such as A0620-00 (Kaluzienski *et al.* 1977) and H1705-25 (Watson, Ricketts, and Griffiths 1978). They also found evidence for an 8.2 hour periodicity during the X-ray decay, although other observers have been unable to confirm this (Matsuoka *et al.* 1980).

Canizares, McClintock and Grindlay (1980) obtained plates of the region near the Ariel 5 position and found an object which had brightened by more than six magnitudes (from $m_V \gtrsim 19$ to $m_V \approx 13$) over its appearance on the Palomar Observatory Sky Survey. Their subsequent photometry and spectroscopy confirmed that the optical properties of the object were similar to those of other X-ray transient and burst sources.

Optical spectra of Cen X-4 were obtained by van Paradijs *et al.* (1980) about five weeks after X-ray maximum when the optical source had decayed to nearly pre-outburst magnitude ($m_V \approx 18.2$). Van Paradijs *et al.* were able to use their continuum measurements to demonstrate the presence of a cool dwarf star (K3 to K7) in addition to a blue component, thus directly establishing the binary nature of Cen X-4.

In addition to the transient X-ray event discussed above, an intense type 1 X-ray burst of about ten seconds duration was detected by the HAKUCHO satellite on May 31, 1979, during the decay phase of the transient event (Matsuoka *et al.* 1980). A burst was also seen during the 1969 flare-up, although it came before the main transient activity (Belian, Conner and Evans 1972). Thus, Cen X-4 is important not only because it demonstrates that X-ray transient and burst sources may be related (Fabbiano and Branduardi 1979) but also because it links X-ray bursters to binary systems.

In this paper, we report ultraviolet spectra of Cen X-4 obtained during the May 1979 X-ray outburst with the International Explorer (IUE) satellite and discuss these observations in relation to the X-ray and optical observations reported earlier.

OBSERVATIONS

Cen X-4 was observed in the low dispersion mode on three dates during the 1979 outburst with the IUE satellite as detailed in Table 1; three observations were made with the short wavelength prime (SWP) camera ($\lambda\lambda$ 1150-2000Å) and two were obtained with the long wavelength redundant (LWR) camera ($\lambda\lambda$1900-3200Å). All observations were obtained using the large aperture to maintain photometric accuracy. The spectra have been placed on an absolute energy scale using the updated IUE absolute energy calibration given by Bohlin and Holm (1980). After merging the SWP and LWR spectra for May 22 and May 23, we have used the UV extinction function of Nandy *et al.* (1975) to determine the reddening to Cen X-4; we find $E(B-V) = 0.10 \pm 0.05$.

The May 22 and May 23 spectra were obtained during the peak of the X-ray outburst while the June 2 spectrum was taken on the tail of the X-ray decline (*cf.* KHS). Figure 1 shows the May 22 SWP spectrum after smoothing and reddening correction (assuming $E(B-V) = 0.10$). This spectrum shows emission lines of N V, Si IV, C IV and other fainter lines emerging from a fairly smooth, blue continuum. No emission lines were seen in the LWR spectrum for this date. The May 23 and June 2 spectra are very similar in appearance to the spectrum shown in Figure 1. By June 2, the source had become fainter by about a factor of five. The continuum in the June 2 spectrum is quite noisy, but there is no clear evidence that the spectrum has changed substantially either in terms of the shape of the continuum or in the relative strengths of the emission lines to the continuum. Even the ratios of emission line intensities stayed nearly constant, with only a slight indication of a more rapid decay of N V relative to Si IV and C IV.

DISCUSSION

In one regard or another, Cen X-4 shows similarities to a wide range of related objects including novae, dwarf novae, X-ray binaries, X-ray transients and bursters. The X-ray and optical behavior is most similar to the classical soft X-ray transient A0620-00 (see Kaluzienski *et al.* 1977, Whelan *et al.* 1977, Oke 1977), which has been described by Avni, Fabian and Pringle (1976) using an "X-ray dwarf nova" model. Thus, a similar model has been developed for Cen X-4; assuming that the 8.2 hour X-ray period detected by (KHS) is the binary period, Cen X-4 consists of a neutron star with a K4 companion which fills its Roche lobe (van Paradijs *et al.* 1980) at a distance of roughly 1.8 kpc. Below we discuss the ultraviolet measurements in relation to this general model.

It has been shown that the continuum component of a theoretical steady state accretion disk would have a power law spectrum with $\alpha = 1/3$ ($F_\nu \propto \nu^\alpha$) over a large wavelength range (Lynden-Bell and Pringle 1974 and references therein). Such a spectrum is occasionally seen in accreting objects (*cf.* Kiplinger 1979), although it is more often the exception than the rule. This is because many parameters, such as accretion rate, viscosity and turbulence in the disk, inclination angle and X-ray reprocessing can alter the observed spectrum. Figure 2 shows that a power law with $\alpha = 0$ fits not only the UV continuum data for May 22, but also the interpolated U, B, V fluxes from Canizares *et al.* (1980) for this date. A similar spectrum has also been seen in a number of dwarf novae, including VW Hyi, EX Hya (Bath, Pringle and Whelan 1980), Z Cam and SY Cnc (Szkody 1981). An $F_\nu \propto$ constant power law is also reminiscent of optically thin bremsstrahlung radiation, and may indicate that this mechanism is important in Cen X-4. This shape is distinctly

different from the $\alpha = -1$ power law that would be expected if X-ray heating of the companion star's atmosphere was important (Milgrom and Salpeter 1975). We therefore conclude that the UV continuum radiation during this time was dominated by an accretion disk.

As can be seen from Figure 1, only emission lines of moderately high ionization are evident in the spectrum of Cen X-4. The relative intensities of the emission lines remain roughly constant during the decline, which is in contrast to what is seen in dwarf novae outbursts where the spectrum at maximum light generally shows absorption lines that change over to emission lines as the continuum subsides.

The strongest lines in the Cen X-4 spectrum are N V λ1240, C IV λ1550 and Si IV λ1398. These lines have been seen in a wide variety of sources observed with IUE, but C IV is most often seen to be several times stronger than either N V or Si IV. Using the reddening corrected line intensities for Cen X-4, we find N V:C IV:Si IV $\approx$ 3.5:1.2:1.0. These ratios are much higher than theoretically expected from optically thin, X-ray heated gas (*cf.* Hatchett, Buff and McCray 1976). However, similar peculiar line ratios have been detected in a variety of objects, including the recurrent nova U Sco (Williams *et al.* 1981), the X-ray binary Her X-1 (both in and out of eclipse; see Gursky *et al.* 1980), the peculiar dwarf nova AE Aqr (Jameson, King, and Sherrington 1980) and the X-ray transients Cyg X-2 (Maraschi, Tanzi and Treves 1980) and A0538-66 (Raymond 1982). The latter three objects are even more extreme cases than Cen X-4, showing strong N V and Si IV lines, but little or no C IV.

Comparison with these objects provides some insights into the origin of the emission lines in Cen X-4, the most probable mechanism being X-ray heating of the accretion disk or of the companion star's atmosphere. However, interpretation of the observed line ratios as coming from a collisionally ionized transition region is not straightforward. This is because Si IV is formed in a slightly cooler region than C IV, while N V is formed in a region which is hotter (*cf.* Raymond 1982). It would take a very peculiar temperature structure to enhance both N V and Si IV relative to C IV, although optical depth effects may also be important in such a transition zone (see London, McCray and Auer 1981). An analysis of the probable physical characteristics of the Cen X-4 system indicates that the companion star may be slightly evolved. Hence, peculiar abundances may also play a role in the eventual interpretation of the spectra of Cen X-4.

TABLE 1
IUE Observations of CEN X-4

Image Number	UT Date (1979)	Julian Date 2,444,000+	Exposure Time (sec)
SWP 5326	May 22.719	16.2396	3600
LWR 4566	May 22.764	16.2778	2400
SWP 5343	May 23.741	17.2549	2400
LWR 4575	May 23.772	17.2861	2400
SWP 5428	June 2.385	26.8986	2400

REFERENCES

Avni, Y., Fabian, A. C., and Pringle, J. E. 1976, *M.N.R.A.S.*, **175**, 297.
Bath, G. T., Pringle, J. E., and Whelan, J. A. J. 1980, *M.N.R.A.S.*, **190**, 185.
Belian, R. D., Conner, J. P., and Evans, W. D. 1972, *Ap. J. (Letters)*, **171**, L87.
Bohlin, G., and Holm, A. 1980, *IUE Newsletter No. 10*, 37.
Canizares, C., McClintock, J., and Grindlay, J. 1980, *Ap. J. (Letters)*, **236**, L55.
Conner, J. P., Evans, W. D., and Belian, R. D. 1969, *Ap. J. (Letters)*, **157**, L157.
Evans, W. D., Belian, R. D., and Conner, J. P. 1970, *Ap. J. (Letters)*, **159**, L57.
Fabbiano, G., and Branduardi, G. 1979, *Ap. J.*, **227**, 294.
Gursky, H., *et al.* 1980, *Ap. J.*, **237**, 163.
Hatchett, S., Buff, J., and McCray, R. 1976, *Ap. J.*, **206**, 847.
Jameson, R. F., King, A. R., and Sherrington, M. R. 1980, *M.N.R.A.S.*, **191**, 559.
Kaluzienski, L. J., Holt, S. S., Boldt, E. A., and Serlemitsos, P. J. 1977, *Ap. J.*, **212**, 203.
Kaluzienski, L. J., Holt, S. S., and Swank, J. H. 1980, *Ap. J.*, **241**, 779.
Kiplinger, A. L. 1979, *Ap. J.*, **234**, 997.
London, R., McCray, R., and Aner, L. H. 1981, *Ap. J.*, **243**, 970.
Lynden-Bell, D., and Pringle, J. E. 1974, *M.N.R.A.S.*, **168**, 603.
Maraschi, L., Tanzi, E. G., and Treves, A. 1980, *Ap. J. (Letters)*, **241**, L23.
Matsuoka, M., *et al.* 1980, *Ap. J. (Letters)*, **240**, L137.
Milgrom, M.. and Salpeter, E. E. 1975, *Ap. J.*, **196**, 589.
Nandy, K., Thompson, G. I., Jamar, C., Monfils, A., and Wilson, R. 1975, *Astr. Ap.*, **44**, 195.
Oke, J. B. 1977, *Ap. J.*, **217**, 181.
Raymond, J. C. 1982, *Ap. J.*, in press.
Szkody, P. 1981, *Ap. J.*, **247**, 577.
van Paradijs, J., Verbunt, F., van der Linden, T., Pederson, H., and Wamsteker, W. 1980, *Ap. J. (Letters)*, **241**, L161.
Watson, M. G., Ricketts, M. J., and Griffiths, R. E. 1978, *Ap. J. (Letters)*, **221**, L69.
Whelan, J. A. J. 1977, *M.N.R.A.S.*, **180**, 657.
Williams, R. E., Sparks, W. M., Gallagher, J. S., Ney, E. P., Starrfield, S. G., and Truran, J. W. 1981, *Ap. J.*, **251**, 221.

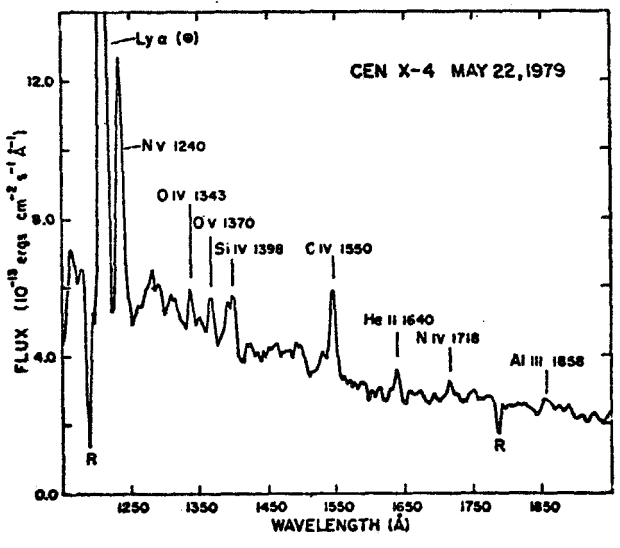

Figure 1

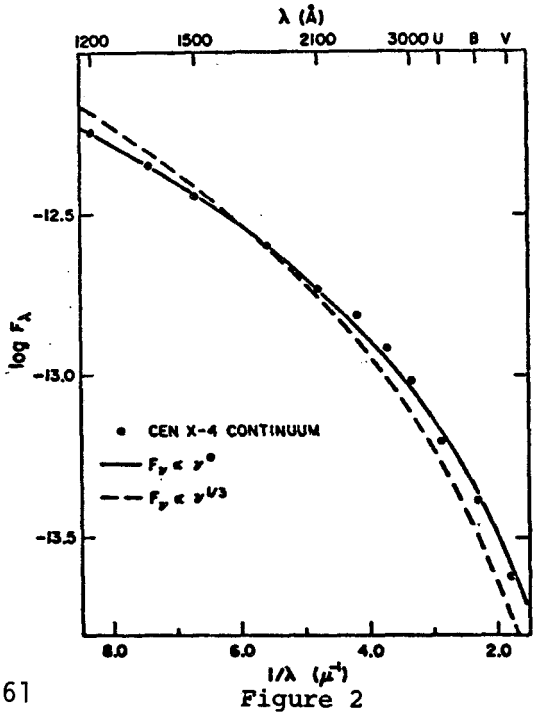

Figure 2

THE "X-RAY BINARY", UW CMa

Sara R. Heap
Laboratory for Astronomy and Solar Physics
Goddard Space Flight Center, NASA

UW CMa is a close, eclipsing binary composed of an O7f primary with a strong wind and a less luminous O-type companion. Recently, UW CMa was found to be a variable x-ray source, whose x-ray variations are in phase with its optical light curve (Snow et al. 1981). Since both components of the binary system are O stars, accretion by a compact object is ruled out as a mechanism for generating x-rays. Instead, it seems likely that UW CMa represents a new class of x-ray binaries, first predicted by Prilutskii and Usov (1976), in which x-rays result from the collision of a wind from one star -- in this case, the primary -- with the surface or wind of the other star. According to this hypothesis, the impact of a wind against a star generates a shock wave about 0.25 stellar radii above the stellar surface, and material behind the shock front, heated to about 10 million degrees, radiates the x-rays.

I don't think there is any question that some sort of continuing collision must occur in the UW CMa binary system: it is inevitable, given a demonstrably intense wind from the primary, and given the proximity of the secondary. The questions that remain concern the circumstances and consequences of the collision -- whether the collision is, in fact, the source of the observed, variable x-rays. These are questions on which IUE spectra have a direct bearing, because they contain certain ultraviolet lines that act as tracers of the wind. These lines allow you to sample the wind both as a function of aspect (phase) angle and as a function of radial distance from the primary. This possibility of building a two-dimensional picture of the wind derives from the fact that each IUE spectrogram of UW CMa may be associated with a particular aspect angle since the exposure time (about 2 minutes for a high-dispersion spectrum) is short compared to the 4.4-day orbital period. In addition, each IUE spectrogram contains a variety of lines that are formed in different regions of the wind -- from the photosphere, where the wind is just starting, to the outermost regions of the wind, far from the binary system.

IUE spectra reveal structure in the wind of the primary of UW CMa that supports the hypothesis of a colliding wind. They show (Figure 1) that like other O-type supergiants, the primary of UW CMa has an intense wind, but the wind becomes even more intense when coming from the tidal bulges. Material flowing from the outer bulge (the bulge pointing away from the secondary) develops into an identifiable stream that can be followed out to rather high velocities. Material from the inner bulge, however,

disappears from view soon after it leaves the stellar surface. The disappearance of the inner stream is due to photo-ionization by x-rays generated in the collision.

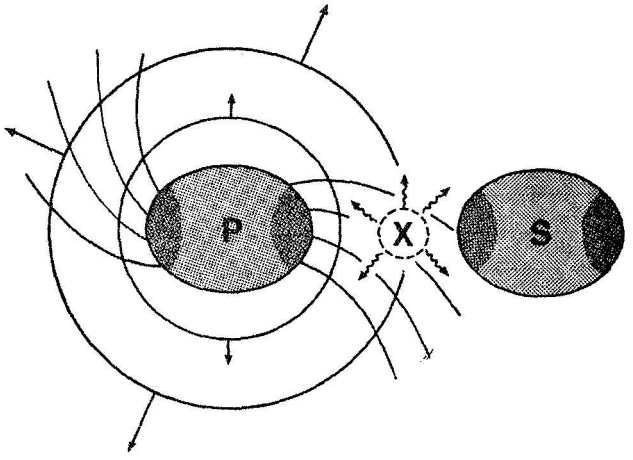

Figure 1. Schematic Model for UW CMa

Let me show you the evidence for structure in the wind by showing you how the profiles of three spectral features change with phase. I'll start with a photopheric feature, the N III 1750 doublet, then go on to the inner wind line, N IV 1718, and the saturated resonance doublet, Si IV 1400.

It is known from light curves for UW CMa (Eaton 1978) that the primary is a highly-distorted star with tidal bulges. Because the gravity is lowest at the tidal bulges, the rate of mass loss is enhanced from there. A tidally-induced enhancement has been shown theoretically by Friend and Castor (1982) to occur in close binaries in which an O-type primary is close to filling its Roche lobe (as is the case for the primary of UW CMa), and it is consistent with IUE observations of photospheric lines, like the N III doublet, that are formed just where the wind is starting. Figure 2 shows a series of spectra of the NIII 1750 doublet. The first thing to notice from this phase-history is that the doublet strengthens at conjunction, which is when the bulge of the primary is seen straight-on. This increase in strength is consistent with an enhanced rate of mass-loss from the tidal bulges: it is partly due to desaturation of the line by an increase in the velocity gradient and partly due to an increase in N ++ ions at the tidal bulge, which, by von Zeipel's theorem, is cooler than the rest of the star. The second thing to notice from this phase-history is that blue-shifted absorption components appear after secondary eclipse. A similar development in the profile of of He I 5876 was detected by Struve et al. (1958). The blue-shifted absorption component appearing after secondary eclipse has sometimes been attributed to the secondary, although Struve et al. cautioned that it disappears by

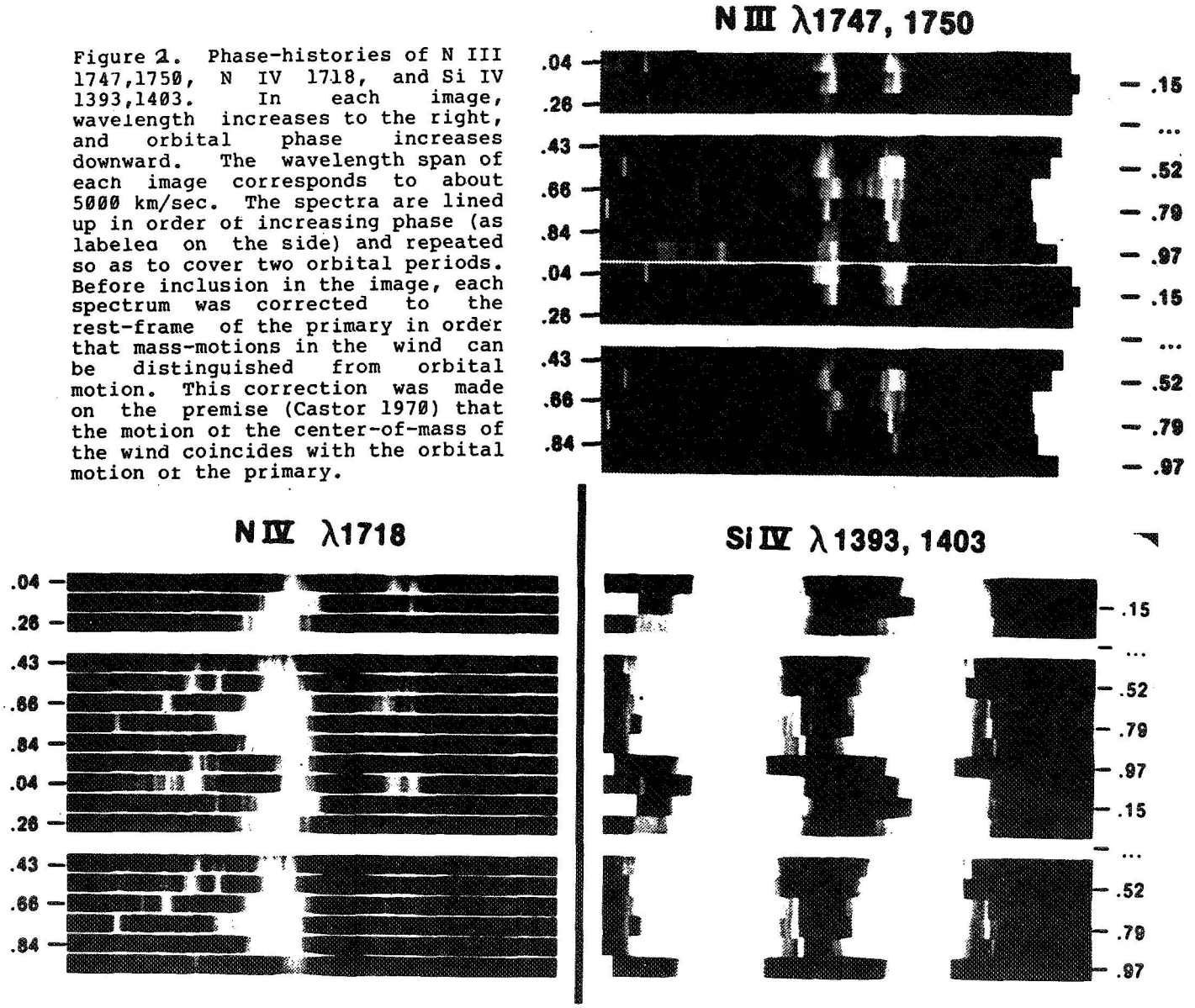

Figure 2. Phase-histories of N III 1747,1750, N IV 1718, and Si IV 1393,1403. In each image, wavelength increases to the right, and orbital phase increases downward. The wavelength span of each image corresponds to about 5000 km/sec. The spectra are lined up in order of increasing phase (as labeled on the side) and repeated so as to cover two orbital periods. Before inclusion in the image, each spectrum was corrected to the rest-frame of the primary in order that mass-motions in the wind can be distinguished from orbital motion. This correction was made on the premise (Castor 1970) that the motion of the center-of-mass of the wind coincides with the orbital motion of the primary.

quadrature, where, if it were due to the secondary, it should be most easily detected. I would identify the blue-shifted absorption component appearing after secondary eclipse as a condensation in the wind that originally left the stellar surface at its outer bulge.

A similar stream should be seen to leave the inner tidal bulge. However, phase changes in the wind line profiles around primary eclipse are completely different in character from those at secondary eclipse. First, the density concentration indicated by the N III doublet after secondary eclipse does not develope into an identifiable stream following primary eclipse. Secondly, P-Cygni lines, such as the N IV 1718 singlet or the Si IV doublet (Figure 2), lack absorption at high velocities around primary eclipse. I would interpret the disappearance of the N +2 stream following primary eclipse and the lack of high-velocity absorbing N +3 and Si +3 ions around primary eclipse as the effect of a depletion of these ions in a highly ionized region in between the two stars.

In conclusion, EINSTEIN photometry and IUE spectra support the hypothesis of a wind-star collision in UW CMa. The collision sets up a high-temperature region, which is the source of x-rays detected with EINSTEIN. Its apparent x-ray variability is due to its location between the two stars, where it undergoes eclipses. The high-temperature region maintains an ionization cavity in the wind, as detected with IUE. The ionization cavity is the source of depletion of absorbing ions in the wind between the two stars.

REFERENCES

Castor, J.I. (1970) Astrophys. J. 160, 1187.
Eaton,J. (1978) Astrophys. J. 220,582
Friend, D. and Castor, J.I. (1982) preprint
Prilutskii, O.F. and Usov, V.V. (1976) Soviet Astron. 20, No. 1.
Snow, T.P., Cash, W., and Grady, C.A. (1981) Astrophys. J. Lett. 244, L19.
Struve,O., Sahade, J., Zebergs, V., Lynds, B.T. (1958) Publ. ASP 170, 267.

THE CHROMOSPHERIC ROTATION-ACTIVITY RELATION IN LATE TYPE CLOSE BINARY SYSTEMS

Frederick M. Walter
Joint Institute for Laboratory Astrophysics
University of Colorado and National Bureau of Standards

Gibor S. Basri and Robert Laurent
Space Sciences Lab and Dept. of Astronomy
University of California at Berkeley

ABSTRACT

We present IUE data on 36 late-type close binary stars (F8-K0). We show that the chromospheric and TR line fluxes increase with decreasing stellar rotation period, though not as rapidly as does the X-ray flux. There is an increasing dependence upon rotation with increasing line temperature. We show that the data are consistent with the hypothesis that there exists a critical rotation rate, which depends on temperature, below which the emission flux is independent of rotation and above which it increases linearly with increasing angular velocity Ω.

I. INTRODUCTION

It is evident that rotation is an important parameter in determining the structure of the chromospheres and coronae in late type stars (e.g. Kraft 1967; Skumanich 1972; Walter and Bowyer 1981). Skumanich showed that the Ca II K emission flux from G dwarfs decayed as $T^{-1/2}$. Since stellar rotation also decays as $T^{-1/2}$, it follows that the chromospheric Ca II K emission flux increases linearly with stellar rotation in G dwarfs. Walter and Bowyer (1981) showed that in RS CVn systems, the coronal X-ray surface flux increases linearly with the stellar angular velocity, and Walter (1981, 1982) has shown that a similar relation holds for rapidly rotating G dwarfs and giants.

These data, upon cursory analysis, imply that all chromospheric and coronal emission should increase in the same manner with increasing stellar rotation, which is unexpected. By solar analogy the heating and confinement of the corona and TR are likely to be dominated by closed stellar magnetic fields, which are likely produced in a stellar dynamo which, in turn, is likely to be highly sensitive to the stellar rotation. However, the physics of the lower chromosphere may well be dominated by acoustic heating, and the existence of a cool chromosphere may not require closed magnetic loops. It is unclear why the two extremes should behave so similarly. Furthermore, the X-ray (Walter 1982) and chromospheric (Vaughan & Preston 1980) data indicate that there is a clear difference between the chromospheres and coronae of young and old (slowly rotating) G dwarfs. Consequently, it appears that one can create an artificially steep rotation-activity relation by considering too extensive a sample of stars (e.g. Walter 1982). Therefore we have decided to limit our investigation of this relation to rapidly rotating stars. These are the stars for which the linear f_X/f_{bol} vs. Ω relation holds. Most are close binaries, and many are RS CVn systems.

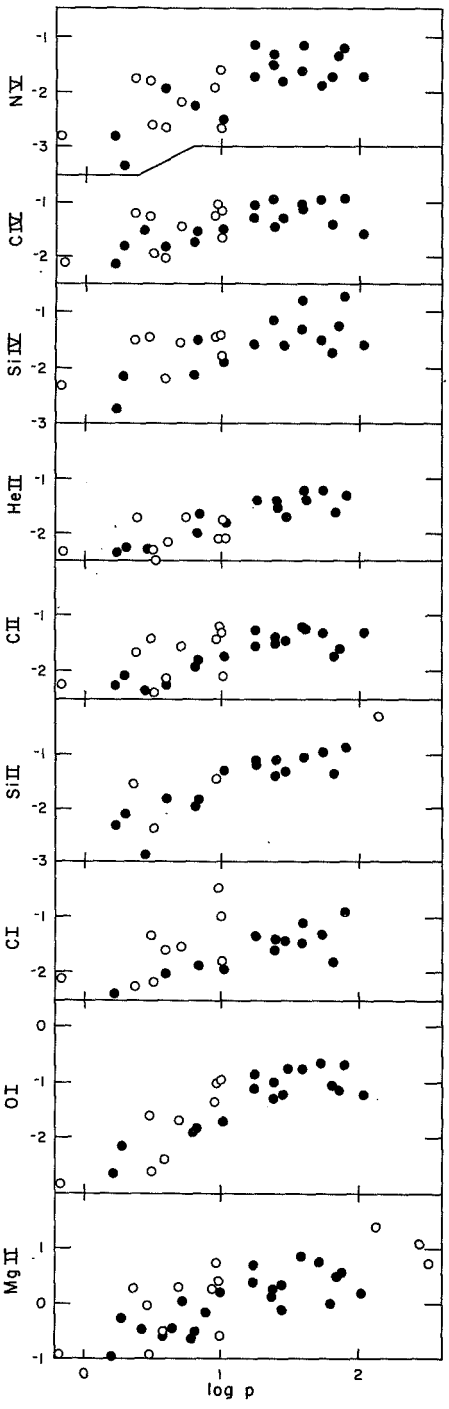

II. DATA

The data presented here (36 stars) were obtained using IUE over the past few years in a variety of programs investigating close binary and RS CVn systems. Mg II fluxes are derived from LWR-HI spectra; other line fluxes are from SWP-LO spectra. The X-ray data are from Walter and Bowyer (1981) or Walter (1981).

In examining the rotation-activity relation, we consider the ratio of the line flux to the X-ray flux as a function of rotation period (see Fig. 1). Since $f_X/f_{bol} \propto P^{-1}$, one can extract from the f_ℓ/f_X vs. P relation the slope of the mean f_ℓ/f_{bol} vs. P relation. Because there is a difference of a factor of four in the mean f_X/f_{bol} between G and K stars with the same rotational period (half of which is due to the T^4 term in f_{bol} and half of which may be due to the hot coronal component of K stars, cf. Walter et al. (1982)), we have corrected the G star data downward by 0.54 dex. The resultant plots are of f_ℓ normalized by the X-ray surface flux.

There is considerable scatter in the Mg II plot, with the G stars showing greater scatter than the K stars. The best fit relation for Mg II for the K stars alone is $f_{Mg\ II}/f_X \propto P^{0.70\pm0.15}$; inclusion of the G stars increases the uncertainty but does not significantly alter the relation. This implies that $f_{Mg}/f_{bol} \propto \Omega^{0.3\pm0.18}$, which is a considerably shallower relation than exhibited by the coronae of these stars. We have fit power laws to each of the line ratios, and find a general increase in β with temperature of line formation (where $f_\ell/f_{bol} \propto \Omega^\beta$), as shown in Figure 2. For the low temperature lines, $\bar{\beta} = 0.22\pm0.07$; for the high temperature lines, $\beta = 0.51\pm0.07$. These relations were derived for the K stars alone because of the additional scatter exhibited by the G stars. We note that certain lines, notably

Fig. 1. The ratio of the line to X-ray flux as a function of stellar rotation period. G stars are represented as open circles, K stars are solid. The G star data are corrected downwards to account for the greater X-ray surface flux in K stars. There is a general trend towards decreasing slope with increasing temperature of formation. Since f_X/f_{bol} decreases as P, f_ℓ/f_{bol} increases as $P^{1-\beta}$, where β is the slope of the data presented here.

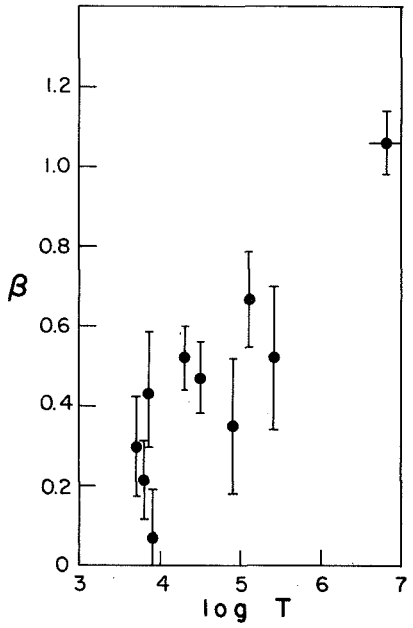

Fig. 2. Slopes of the rotation-activity relation as a function of line temperature.

C II, C IV, Si II, and He II, exhibit extremely tight relations, whereas the variance is comparatively large for Mg II, Si IV, and N V. Part of the scatter in N V may be due to the statistical errors in computing the line flux, the analysis of which is still incomplete. The He II/X flux ratio relation is particularly tight (for the G stars as well), and lends credence to the idea that He II may be a good indicator of the coronal X-ray flux (Hartmann et al. 1979). However, the slope of the relation is considerably different from zero ($f_{He\ II}/f_X \propto P^{0.53\pm0.09}$), which indicates that some mechanism other than coronal excitation may be important.

III. DISCUSSION

The rotation-activity relation shows a systematic increase in dependence upon rotation with increasing temperature, roughly as $f_\ell \propto \Omega^{(1/4 \log T - 3/4)}$. This supports the contention that the lower chromosphere is only weakly influenced by stellar rotation, that the TR is more affected, and that the corona is most dominated by stellar rotation.

The physical meaning of the slope of this relation is uncertain, other than indicating that the effect of the magnetic fields is strongest in the hottest regions of the stellar atmosphere. We hypothesize that the effect of the magnetic field, whether it be manifested through heating or confinement of the plasma, has the same dependence upon rotation for all lines, but perhaps fails to operate below some critical angular velocity Ω_c. Then a plot of f_ℓ/f_{bol} versus P will be flat up to Ω_c, and show an increasing flux at higher Ω. Since the coronal X-rays exhibit a linear relation, we adopt this relation for all lines, and hypothesize that

$$f_\ell/f_{bol} = A + B(\Omega-\Omega_c) \quad , \quad B = 0 \quad \text{when} \quad \Omega < \Omega_c \quad .$$

A is constant and may be determined by stellar (T_{eff}, R, g, M) or environmental (e.g. tides) parameters.

If we measure a mean slope β over the entire range of Ω for log f_ℓ/f_{bol} vs. log Ω (= -log P), then, for this range of 0 to -2 in log Ω, $\Omega_c = -2\beta$. A line showing a steep slope $\beta \sim 1$ has a low Ω_c; a line with a low β should be composed of a long constant flux section plus a short section increasing with unit slope. To test this hypothesis, we have examined the data for each line above and below Ω_c (as determined from β) to see if indeed the data at $\Omega < \Omega_c$ show little dependence upon rotation, and if the data at $\Omega > \Omega_c$ show a linear increase. The data are shown in Figure 3. Those data at $\Omega > \Omega_c$ clearly show a steeper relation, with a mean slope of 1.03±0.08; those data at $\Omega < \Omega_c$ show

a mean slope of -0.20±0.14, which is consistent with zero. Only He II does not display this change in slope between the lines with $\Omega > \Omega_c$ and the lines at $\Omega < \Omega_c$; this may be attributable to its dependence upon the coronal X-ray flux.

We caution the reader that this is a preliminary assessment of the data. We have not shown that the data warrant a fit more complex than a single line. Nonetheless, we conclude that our hypothesis, that the influence of magnetic fields in the stellar atmosphere occurs above some critical Ω, manifested as a linear increase in emission flux with Ω, is indeed tenable. The coronal X-rays show the linear relation for $\Omega > 100\ d^{-1}$; at lower levels in the chromosphere Ω_c increases with decreasing line temperature.

Further analysis may lead to a better understanding of the empirical response of the stellar chromosphere, TR, and corona to increased stellar rotation and to increased energy input. While it may not be possible from studies of this kind to elucidate the method of coronal or chromospheric heating, these correlations certainly are important probes of the basic physics of the atmospheres of convective stars.

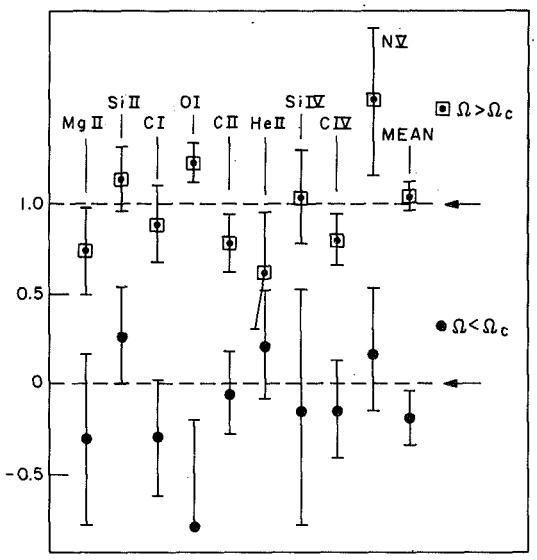

Fig. 3. Best fit slopes for data above or below Ω_c (see text). Rapidly rotating stars ($\Omega > \Omega_c$) have log f_ℓ/f_{bol} increasing linearly with log Ω, as is seen for the coronal X-rays. Slowly rotating stars ($\Omega < \Omega_c$) have roughly constant log f_ℓ/f_{bol} as a function of Ω. He II may be anomalous.

REFERENCES

Hartmann, L. et al. 1979, Ap. J. (Letters), 233, L69.
Kraft, R. P. 1967, Ap. J., 150, 551.
Skumanich, A. 1972, Ap. J., 171, 565.
Vaughan, A. and Preston, G. 1980, P.A.S.P., 92, 385.
Walter, F. 1981, Ap. J., 245, 677.
_____. 1982, Ap. J., 253, 745.
Walter, F. and Bowyer, S. 1981, Ap. J., 245, 671.
Walter, F., Gibson, D., Basri, G. and Feldman, P. 1982, in preparation.

DISCUSSION - CLOSE BINARIES

Shore: Do you have a large enough sample to be able to look at the mean mass ratio? If yes, how much different is it from unity?

Parsons: Only one system has been analyzed so far; the others are to be observed during the coming year. HR 3080 yields a preliminary mass ratio of about one-half.

Guinan: I noticed that some of your stars are bright and have long orbital periods. Can any of these objects be resolved using speckle interferometry?

Parsons: I believe that some of these stars are being attempted by McAlister. The separations should be of the order 0.01 to 0.1 arc see, but the magnitude differences may make it tough.

Guinan: In your polarization observations did you have any evidence of orbital modulation?

Koch: At the moment we have hints of phase-locked modulation but cannot say for sure.

Devinney: According to R. Wilson's model, there is a ring whose dimensions are well-determined. There is some evidence for Keplerian motion in the disk from spectra taken around first and fourth contacts. You might want to bear this in mind when analyzing the corresponding IUE spectra.

Chapman: Right.

Szkody: What are slopes of distributions of CM Del and KR Aur?

Chanmugam: On the order of $F\lambda \propto \lambda^{-2}$ at short wavelengths; however, the spectrum is noisy.

Aizenman: What makes fields of order 10^8 G difficult to detect in binaries as opposed to single white dwarf stars?

Chanmugam: Because of the emission from the accretion column it is difficult to detect Zeeman lines for magnetic white-dwarfs in binaries.

One needs to see the photosphere of the white dwarf which is difficult unless the system is in a low state. In fact, this is how the Zeeman lines in AM Her were discovered - many years after the detection of the optical polarization. The polarization mechanism for magnetic white-dwarfs is different from that of single magnetic white-dwarfs. If B is $\sim 10^8$ gauss, in the former, there would be little optical polarization since the accretion column is optically thick at low harmonics.

Thomas: How do your models compare with the non-LTE models of H-K-H?

Drilling: The differences become significant for effective temperatures greater than 25,000°K.

Ahmad: How do you determine the value of Ωc, the critical rotational velocity at which the linear relation between rotational velocity and line flux sets in? Quantitatively, how is it calculated?

Walter: (Reply unavailable.)

HOT STARS

MASS LOSS AT DISCRETE VELOCITIES IN Be STARS: EVIDENCE FOR A NON-RADIATIVELY DRIVEN WIND

Geraldine J. Peters
Department of Astronomy
University of Southern California

ABSTRACT

The temporal behavior of the high velocity (-250 to -850 km s^{-1}), relatively narrow (<200 km s^{-1})absorption components in C IV, Si III,IV observed in the "pole-on" Be stars ω Ori, 66 Oph, and HR 4009 and what these observations contribute toward our understanding of the Be phenomenon are discussed. Ground-based and X-ray data on the above mentioned stars are compared as well as their UV differences with similarly active Be stars with larger projected rotational velocities.

INTRODUCTION

The episodic nature of mass loss in Be stars combined with recent observations showing that binary mass transfer, non-radial pulsation, and chromospheric activity may be responsible for the emission line envelopes in certain stars have cast doubt on models for mass loss which require slow, orderly ejection of matter such as rapid rotation or radiatively driven winds (cf. Jaschek and Groth 1982). Perhaps one of the more intriguing observations has been the discovery of high velocity, relatively narrow absorption components in the resonance lines of C IV and Si III, IV in IUE spectra of the "pole-on" Be stars ω Ori and 66 Oph (Peters 1982a). Subsequent IUE observations were obtained of these objects and other pole-on Be stars to assess the stability of the line formation region and search for similar mass loss in other stars. One additional object, HR 4009, was discovered to display the phenomenon. Observations of these objects are discussed in this paper.

OBSERVATIONS

ω Ori (HD 37490, vsin i = 160 km s^{-1}) was the most extensively observed. As one can see from Fig. 1, the high velocity component at -800 km s^{-1}, originally observed in 1980 March, persisted through 1981 November. Subtle profile variations were observed but the region in which the high velocity features were formed remained remarkably stable. But with the 1982 January observations the component originally at -550 km s^{-1} suddenly became prominent while the higher velocity one virtually disappeared. Perhaps most significant is the short termed variability seen in the January observations. Evidence for daily profile variations can be seen in the latter three profile sets displayed in Fig. 1. However, observations taken 4 - 6 hours apart on 1982 January 5, 6 revealed clear evidence of even more rapid variability in the C IV line (Fig.2). Since the rotational period of ω Ori is about one day, this strongly suggests the presence of a non-symmetrical distribution of material in the line formation region.

66 Oph (HD 164284, 280) displayed long termed behavior similar to that observed in ω Ori. As seen in Fig. 3, when IUE observations resumed in 1981 July, the component observed at -700 km s^{-1} in 1980 March had considerably weakened. Instead, the component originally observed at -250 km s^{-1} dominated. This component persisted during the remaining 1981 observations.

HR 4009 (HD 88661, 280) showed weak high velocity C IV features when it was first observed for this program in 1980 March and Dachs (1980) reported such components shifted by -660 km s^{-1} in 1980 January. IUE observations from 1981 July to 1982 January reveal that this component reappeared in 1981 November (Fig. 4). A component was observed at -850 km s^{-1} in 1981 July, September and a sharp feature at -400 km s^{-1} appeared in 1982 January.

DISCUSSION

ω Ori, 66 Oph, and HR 4009 apparently share a common mass loss phenomenon which remains rare in pole-on Be stars since, of the 25 such objects observed with IUE, only three displayed the high velocity lines. It is presently unclear how this mass loss relates to such quantities as X-ray emission, polarization, or the emission lines observed in the visible. HR 4009 appears to be a weak hard X-ray source but 66 Oph does not (Peters 1982b). ω Ori and 66 Oph show variable polarization (Hayes 1980, Poeckert, Bastien, and Landstreet (1980) but, in 1981 September, 66 Oph was observed to have a large polarization of 1.3% while ω Ori showed only 0.2% (Hayes, personal communication). All three of the stars display variable Balmer line emission but so do many pole-on Be stars which do not show the high velocity mass loss. Presently, Hα is strong in 66 Oph and HR 4009 but weak in ω Ori and variations do not parallel changes in the profiles of the high velocity lines.

Similar high velocity lines have been observed in Be stars with larger values of vsin i (59 Cyg, γ Cas, HR 2855 - numerous papers in Jaschek and Groth 1982) except that the level of ionization tends to be higher in the latter objects (N V is observed but not Si III, IV). High velocity outflow in low ionization species (eg. Si II, C II) was not observed in either group of objects. Mass transfer binary Be stars such as CX Dra, AU Mon, and HR 2142 do not display the high velocity lines even though some show phase dependent N V.

Multiple components are commonplace, the pattern seems to be unique for each star, and the individual components are persistent but variable. The fact that the path lengths are small for reasonable densities (Peters 1982a), the plasma displays long term stability, and there appears to be azimuthal asymmetry in the line formation region suggest the possibility that we are observing a magnetohydrodynamical phenomenon. Since the mass loss rates are large (10^{-9} $M_\odot$ yr^{-1}), the mechanism producing the high velocity lines certainly qualifies as an important one in the establishment of some Be star envelopes.

REFERENCES

Dachs, J. 1980, Proc. Second European IUE Conference, ESA SP-157
Hayes, D. P. 1980, Pub.A.S.P., 92, 661.
Jaschek, M. and Groth, H.G. 1982, Be Stars (IAU Symposium 98),(Dordrecht:Reidel).
Peters, G. J. 1982a,Ap.J.(Letters), 253, L33.
Peters, G. J. 1982b, Be Stars, ed M. Jaschek and H. G. Groth(Dordrecht:Reidel),353.
Poeckert, R., Bastien, P., and Landstreet, J. D. 1979, A.J., 84, 812.

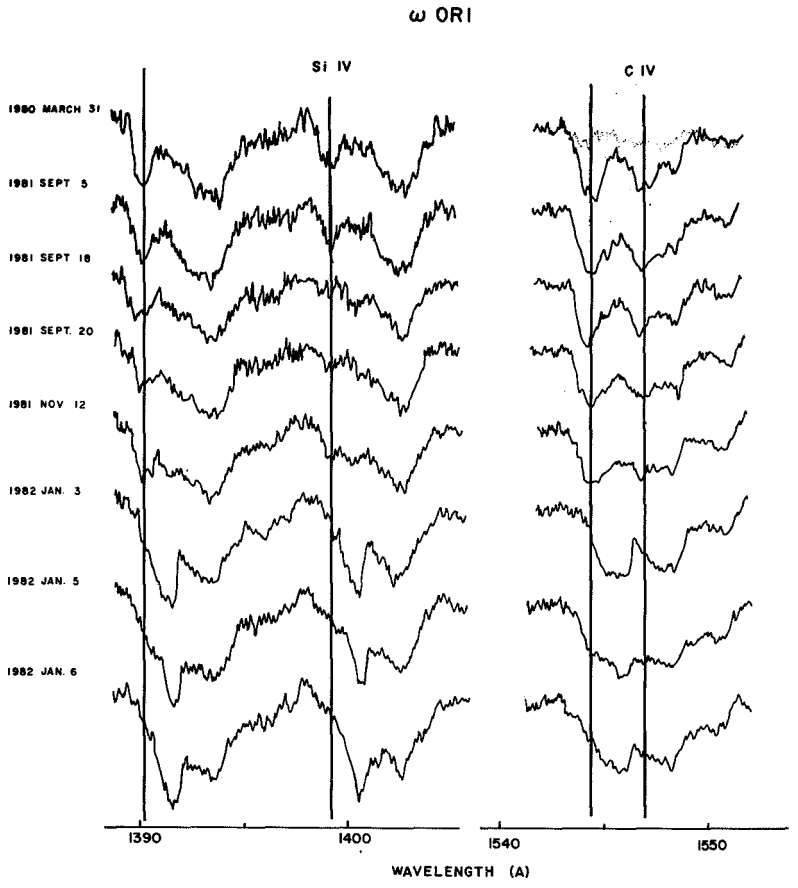

Fig. 1 - Si IV and C IV observed in ω Ori. Vertical lines show the position of the component at -800 km s^{-1}.

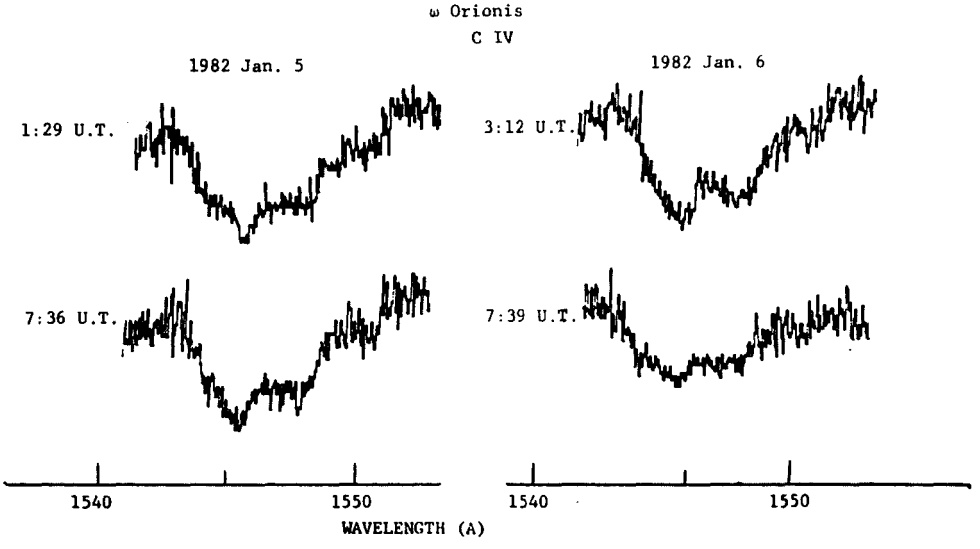

Fig. 2 - Observations of C IV in ω Ori in 1982 January reveal profile variations on the time scale of hours.

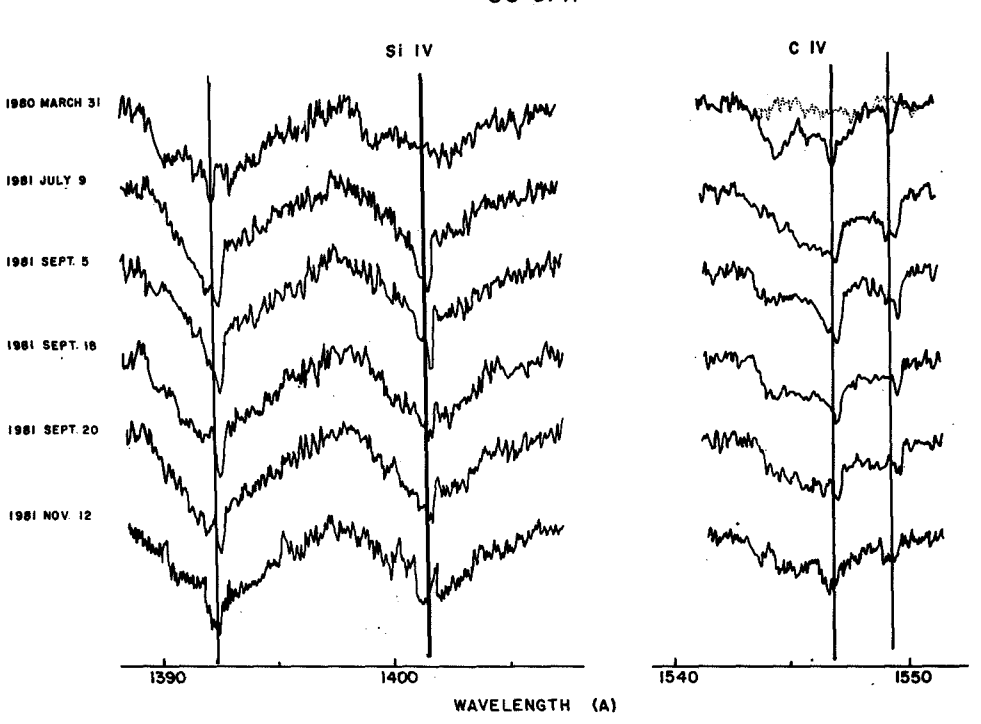

Fig. 3 - Same as Fig. 1 for 66 Oph. Components shifted by -250 km s^{-1} are noted.

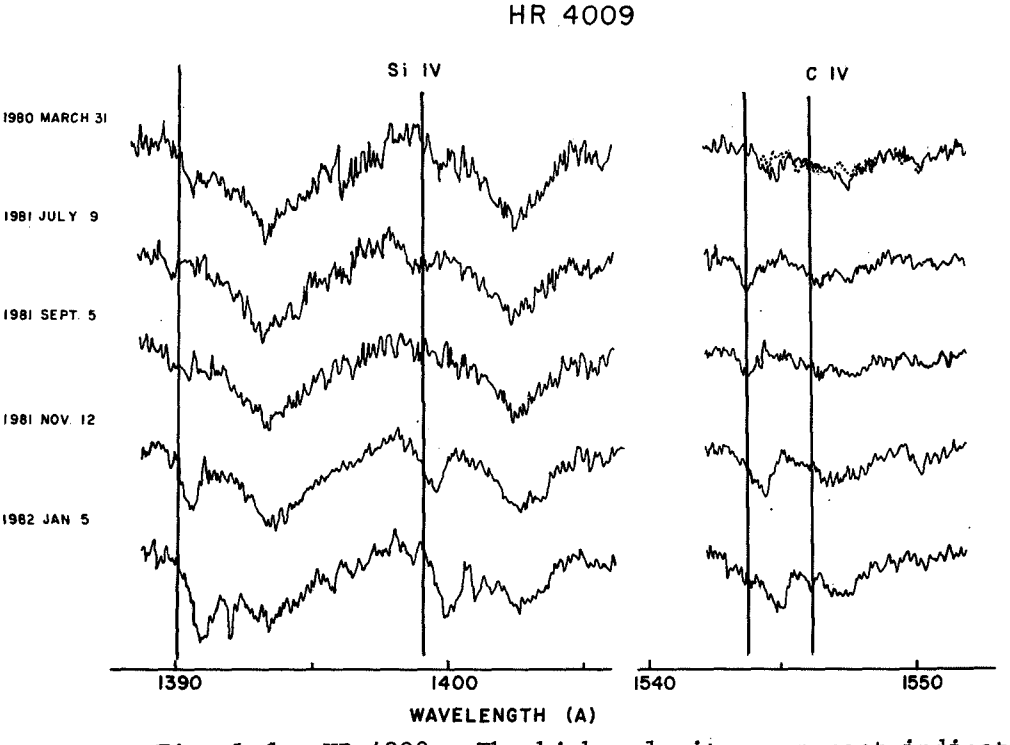

Fig. 4 - Same as Fig. 1 for HR 4009. The high velocity component indicated is the one shifted by -850 km s^{-1}.

ULTRAVIOLET SPECTRA OF SOME BRIGHT LATER-TYPE Be STARS AND A-F SHELL STARS

Arne Slettebak

Perkins Observatory
Ohio State and Ohio Wesleyan Universities

ABSTRACT

Anomalous ionization (C IV and Si IV) is seen in IUE spectra of Be stars as late as B8, and occurs also in standard stars of similar spectral type. Asymmetrical lines suggesting mass loss are present in all the Be stars and several of the standard stars as well, with no obvious correlation with v sin i. Emission shoulders are present in the Mg II lines of two B5e stars but not in Be stars of later type. Again there is no correlation with v sin i. The A-F shell stars show rich Fe II absorption spectra in the ultraviolet, in one case with velocity structure.

I. INTRODUCTION

Early ultraviolet spectroscopic observations of Be stars (e.g. Marlborough and Snow 1976) concentrated on the stars of early type, demonstrating mass-loss effects in their spectra. More recently, these investigations have been extended to cooler Be stars. Thus, Snow (1981) found mass-loss effects in the spectra of Be stars as late as B6, and Marlborough and Peters (1982) detected anomalous ionization (C IV and Si IV) in Be stars as late as B8. This investigation concentrates on the ultraviolet spectra of the later-type Be stars and A-F shell stars, with emphasis on mass-loss effects and anomalous ionization.

II. THE PROGRAM

High-dispersion IUE spectra of 13 bright later-type Be stars and A-F shell stars were obtained in both the short and long wavelength regions, plus 8 standard stars of corresponding spectral types. These are listed in Tables 1a and 1b, with spectral types and rotational velocities from a recent study of the brighter Be stars (Slettebak 1982). The program and standard stars were selected to include both sharp-lined and broad-lined stars of various spectral types between B3 and F0.

Special attention was paid to resonance lines, for possible mass-loss effects, and lines which indicated anomalous ionization in earlier investigations. These included Si II 1190.418, 1193.284, 1260.418, 1264.730; Si III 1206.510; C II 1334.532, 1335.708; Si IV 1393.755, 1402.769; C IV 1548.202, 1550.774; Al II 1670.787; Al III 1854.716, 1862.790; Fe II multiplets 1, 62, and 63; and Mg II 2795.523, 2802.698. Some of these are illustrated in Figures 1-4.

III. RESULTS AND DISCUSSION

A. The Be Stars of Later Type.

The approach taken in this investigation is that of spectral classification: standard non-emission-line stars with MK spectral types close to those of the program stars were observed along with the program stars for direct comparison purposes. Furthermore, both sharp-lined and broad-lined standard stars were included, to match as closely as possible the sharp-lined (interpreted as pole-on, according to the rotational model) Be stars and broad-lined (absorption-line shell-type) Be stars. An unexpected result is that the standard star ultraviolet spectra are almost as interesting as the Be spectra, from the point of view of mass loss and anomalous ionization.

1. Anomalous Ionization

According to Marlborough and Peters (1982), the coolest spectral type at which C IV or Si IV would be expected under radiative equilibrium conditions, either in the photosphere or in a cool circumstellar envelope, is B0 and B2, respectively. They observed both ions in IUE spectra of Be stars as late as B8, however. My results, obtained with different stars, confirm their conclusion: the B8e and B7e stars β Cyg B and η Tau have both C IV (see Fig. 1) and Si IV lines in their spectra. On the other hand, C IV seems not to be present in the spectrum of the B5e star β Psc nor in the B6.5e star φ And (see Fig. 1), though both are pole-on stars like η Tau. Si IV (see Fig. 2) is present in all the B5-6e stars as well as the later-type stars shown in Fig. 1.

Among the standard non-emission-line stars, anomalous ionization effects also exist. Thus, C IV is seen weakly in the B8 standard ι And (Fig. 1) but is very weak or not present in the B5 standards ρ Aur and ψ^2 Aqr. Si IV, on the hand, is visible in the spectra of all three standard stars.

2. Mass-Loss

Fig. 1 shows that the C IV doublet is asymmetrical and shifted toward shorter wavelengths in both η Tau and β Cyg B. The same is true for the shell stars 48 Lib, ψ Per, and o And. Fig. 2 shows that the Si IV doublet is present and asymmetrical for the B5-6e stars shown there. The lines are also asymmetrical for the B6.5-8e stars shown in Fig. 1. The Al III resonance doublet is also strongly asymmetrical in the spectrum of ψ Per. Thus, mass-loss effects appear to be present in the spectra of both shell and pole-on Be stars of spectral types B3 to B8.

Interestingly, the standard non-emission line stars also show asymmetrical lines, suggestive of mass-loss effects. Thus, Fig. 2 shows the Si IV lines in the sharp-lined B5 standard ρ Aur to be strongly asymmetrical, as are the Al III resonance lines in the broad-lined B5 standard ψ^2 Aqr. In Fig. 3, the Mg II resonance lines are clearly asymmetrical in the spectrum of ρ Aur.

3. Emission Lines

Emission wings in the Mg II and Fe II resonance lines were observed in nearly all the Be stars of earlier type studied with IUE by Dachs (1980). Fig. 3 shows the resonance doublet of Mg II in the spectrum of a number of Be and standard stars. Note that the lines have emission shoulders in the spectra of both β Psc and ψ Per. Both are of spectral type B5, but β Psc is a pole-on star and ψ Per a shell star. The only other emission lines detected in this investigation are the short-wavelength shoulders of the Fe I multiplet 1 lines in ψ Per, but this is not a certain identification.

B. The A-F Shell Stars

The four A-F shell stars in Table 1a are identified as shell stars in the optical wavelength region because of the simultaneous presence of rotationally-broadened lines, from the underlying star, and sharp absorption lines from ground states or low-lying metastable levels, presumably from some kind of shell. All four show rich Fe II absorption spectra in the ultraviolet (especially from multiplets 1, 62, and 63) which are considerably stronger than in the standard star of corresponding type. Fig. 4 shows a portion of the spectrum of one of the A-type shell stars, β Pic, with the A5 standard δ Cas. Note that the Fe II lines are not only stronger and deeper in the shell star, but asymmetrical, indicating velocity structure.

It is a pleasure to acknowledge the very kind hospitality shown to me during a stay at the Institute for Astronomy of the University of Vienna, where much of this work was done. I am grateful also to Ted Snow for very helpful discussions, Ken Carpenter for much help with computer aspects of this investigation, Bob Wing for permission to use his spectra of β Cyg B, Charlie Wu and Al Holm for their spectra of η U Ma, and the IUE team at Goddard for their help and cooperation.

REFERENCES

Dachs, J. 1980, Proc. of Second European IUE Conf. (ESA SP-157. April 1980), p.139.

Marlborough, J. M., and Peters, G. J. 1982, IAU Symp. 98, "Be Stars", ed. M. Jaschek and H.-G. Groth (Dordrecht-Reidel), p. 387.

Marlborough, J. M., and Snow, T. P. 1976, IAU Symp. 70, "Be and Shell Stars", ed. A. Slettebak (Dordrecht-Reidel), p. 179.

Slettebak, A. 1982, Ap. J. Suppl. (in press).

Snow, T. P., Jr. 1981, Ap. J. 251, 139.

TABLE 1a. PROGRAM STARS

Name	Sp. Type	v sin i ($km\ s^{-1}$)
48 Lib	B3:IV:e	400
ψ Per	B5 IIIe	280
β Psc	B5 Ve	100
o And	B6 IIIe	260
φ And	B6.5 IIIe	80
η Tau	B7 IIIe	140
β Cyg B	B8 Ve	250
28 Tau	B8 (V:)e	320
1 Del	B8-9e	280
β Pic	A5 IV-shell	120
21 Vul	A5 IV-shell	200
φ Leo	A7 IV-shell	230
14 Com	F0 III-shell	200

TABLE 1b. STANDARD STARS

Name	Sp. Type	v sin i ($km\ s^{-1}$)
η U Ma	B3 V	150
ρ Aur	B5 V	90
ψ^2 Aqr	B5 V	280
α Leo	B7 V	280
ι And	B8 V	90
α Lyr	A0 V	< 10
θ Leo	A2 V	15
δ Cas	A5 III-IV	100

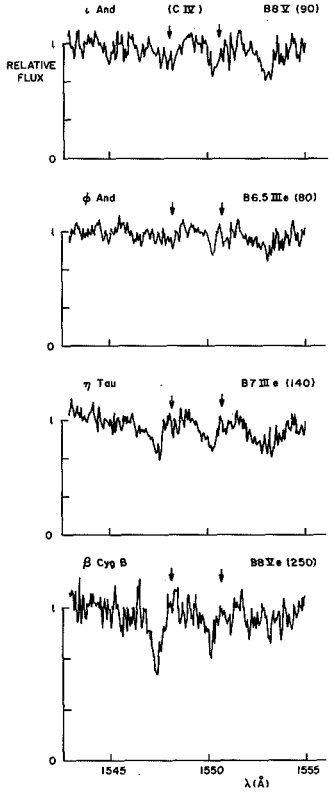

Fig. 1. The C IV resonance doublet in the spectra of B6.5-8 stars.

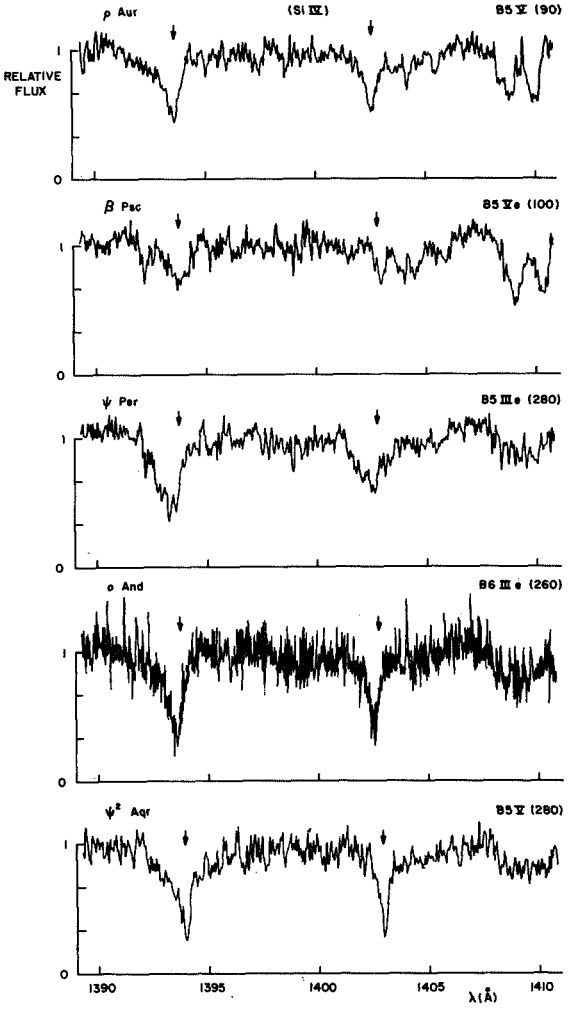

Fig. 2. The Si IV resonance doublet in the spectra of B5-6 stars.

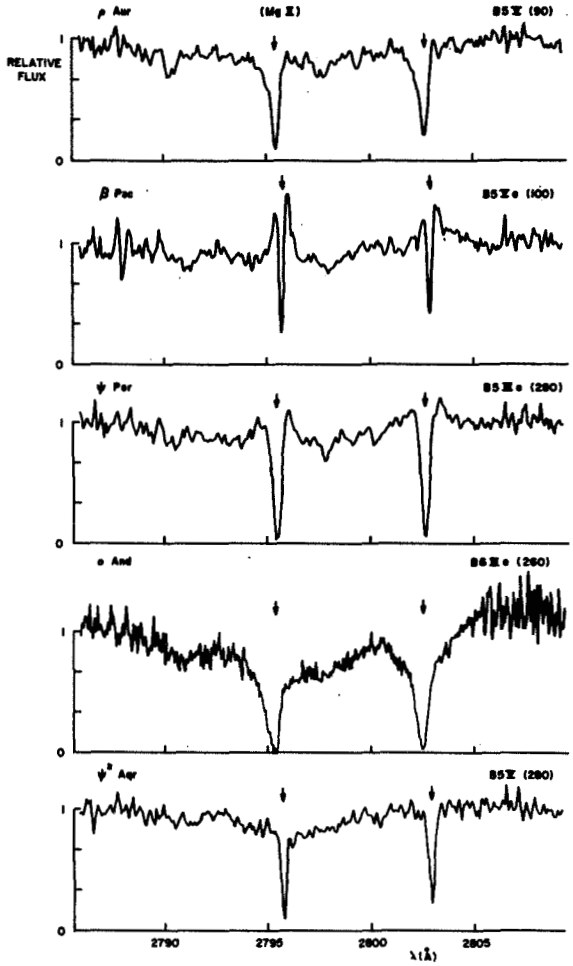

Fig. 3. (left). The Mg II resonance doublet in the spectra of B5-6 stars.

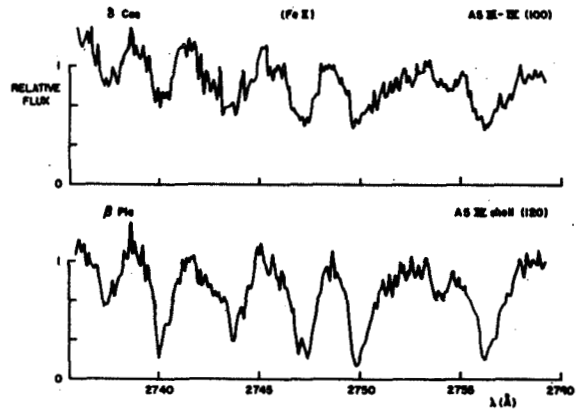

Fig. 4. Fe II multiplet 62 and 63 lines in the spectra of an A5 standard and an A5 shell star.

EMPIRICAL ATMOSPHERIC VELOCITY PATTERNS FROM COMBINED IUE AND VISUAL OBSERVATIONS : THE Be-SIMILAR STARS

V. DOAZAN, R. STALIO and R.N. THOMAS

Observatories of Paris and Trieste ; Institut d'Astrophysique,PARIS

ABSTRACT :

A summary of the velocity pattern which pan-spectral observations of the Be stars suggest, and an outline of its extension via similar pan-spectral observations of the Be-similar stars. An emphasis on the time-dependent interaction between the stellar mass flux and the local environment produced jointly by the star itself and its original environment.

INTRODUCTION

In modeling stellar atmospheres, basic nonEquilibrium thermodynamics and empirical studies show that at least three independent fluxes must be specified at the base of the atmosphere : radiative energy, nonradiative energy, and mass (Cannon and Thomas, 1977 ; Heidmann and Thomas 1980 ; Doazan and Thomas, 1982 ; Thomas, 1982). Possibly a magnetic flux is also necessary ; presently, we have insufficient observations to decide. Specifying an observational value of the radiative flux is directly possible for some stars, except in the XUV. Values of the nonradiative fluxes come only by inference from T_e and velocity distributions. Any value of the mass flux derived observationally is highly model-dependent, especially in the atmospheric distribution of ionization and excitation states for a given density distribution, but also for the coupled velocity, T_e, and density distributions. Presently-existing theories of mass flux do not aid in resolving the observational uncertainty coming from model-dependence. In addition to uncertainty in the validity of their basic assumptions : (i) coronal-origin theories require empirical specification of density and T_e distributions, because of the uncertainty in nonradiative flux; (ii) radiative-origin theories must be amended to produce chromospheres-coronas; (iii) neither kind of theory represents modern data on variability and individuality (Costero, Doazan, Stalio, Thomas, 1981 ; Doazan

and Thomas, 1982). Thus it is not possible to use these theories to provide even gross parametric patterns of velocity, T_e, and ionization/excitation distributions, on which patterns a variety of individual measures might be superposed to check their consistency.Lamers(1981)has tried such an approach, to reconcile a wide range of inferences on mass flux, showing large individual scatter, by assuming a common pattern of velocity distribution ---that of the radiative-origin model--- and the same asymptotic density distribution, for all stars in the sample. Again, the characteristics of variability and individuality negate this approach. In a parallel paper (Doazan and Thomas, 1982b), we exhibit the variability in velocity patterns across the Be and B-normal phases for some Be stars. A comparison of the behaviour of the farUV superionized, to that of the visual Hα, spectral lines during such phase changes in one star ; and comparison of variously inferred mass flux values to Hα luminosity in a number of stars, at random phases ; suggest that the velocity field carrying the mass flux is not a simple, monotonically-accelerating,flow. Lamers' suggestion (ibid) that such variability and individuality reflect the role of rotation is negated by Peters' observations of identical phenomena in pole-on and large vsini Be stars (1980). In the present paper, we make a tentative beginning to extend these kinds of conclusions on velocity field patterns from the Be to the Be-similar stars, following such categorization as proposed by Struve, Beals, McLaughlin and others in the 1930's and 1940's (cf discussion in Doazan, 1982). The visual data of that epoch can now be supplemented by spatial data in the x-ray, farUV, farIR and radio(Doazan,ibid)

Be-Star Velocity Patterns :

Several kinds of tests of a simple, monotonically-accelerating mass flow can be made by combining farUV and Hα observations. Far UV observations of displacements and profiles of spectral lines from superionized ions measure velocities, and mass fluxes, in the hot regions interior to the cool Hα envelope. The Hα emission measures the envelope's mass content which, for simple expansion,is determined by the density at its base under an r^{-2} distribution. Under the same simple flow, the base-density is given by photospheric model plus size of mass flux. Thus mass flux size, and Hα luminosity, should be correlated ; a plot of available data shows simply a scatter diagram (Doazan and Thoms, 1982b). Turning to an individual star for which we have data across a range of phases : 59 Cyg (B1.5Ve) was a strong emission-line star in 1972 ; it showed essentially no emission Hα in 1977 ; by 1982, it has recovered to only some 10% of its 1972 Hα luminosity. If the flow pattern during the increasing-Be phase were a simple,monotonically-accelerated outflow, then the 1978-observed velocities of some 1000km/s imply the flow traverses one photospheric radius in 2 hours. Classically, the Hα emission from a Be star is thought to originate within some 20 radii. Such a region should be filled within 2 days, at such flow velocities. In 1982, 5 years has elapsed since the B-normal phase, and some 3 years since the 1000 km/s velocities were first observed. A simple flow would have expanded to 10^4 photospheric radii ; but the region beyond some 20 radii would not contribute significantly to the Hα emission ; and this region would have been filled within a few days. So, we conclude the very gradual rise in Hα emission from 59 Cyg corresponds to "back-filling" from some barrier outside the Hα emission envelope. So, schematicized, the flow-configuration is that of Fig.1. The "hardness" of the schematic barrier determines whether the mass flow from the central star is completely stopped ---and reflected--- or partially transmitted ; and this

"hardness" is fixed by the mass concentration outside this particular episode of mass flux. That is, it is a combination of "primordial" ISM and the star-produced ISM from previous mass flow episodes. Thus the parameters of this schematicized picture are : U_r, unperturbed mass flow velocity, with n_r the corresponding concentration, at this particular radius and epoch ; S, the velocity of the shock-interface, propagating back toward the star ; V, the post-shock, decelerated, flow, which can be in either direction ; t, the time since the present mass flux episode began ; n_S, and T_{eS}, the immediate post-shock concentration and electron temperature ---these increase to n_V and decrease to T_{eV}, respectively, corresponding to post-shock cooling as ionization-excitation first increase,then decrease, and to radiativecooling. T_{eS} will not exceed, and n_S will not be less, than corresponding to shock-conditions with $\gamma = 5/3$. Since n_r decreases as $(U_r r^2)^{-1}$, the cooling will be more rapid, the smaller is r. $n(r_o)$ quits its chromospheric outward exponential decrease, and begins its coronal r^{-2} dependence, hence n_r in the post-corona is the larger, the larger is the mass flux, F_M. The Hα envelope begins at $r_{ev} > r_S = (U_r t_1 + S t_2)$ where $t_1 + t_2 = t$. $r_{ev} - r_s$ is fixed by the cooling rate ; hence depends on n_r, thence on F_M. Doazan and Thomas present a first approximation to the details for B_e stars ; here we consider the possible utility of the Be-similar stars.

Be-Similar Velocity Patterns :

The Struve-Beals-McLaughlin visually-inspired sequences of similar stars lead to our definition of Be-similar stars to be those characterized by hot-star visual continua,some Balmer emission lines, and cooler-star (Cyg type) metallic absorption lines. The Be stars are prototypes: McLaughlin characterized them as"little planetary nebulae" because their H envelopes occur much closer to the star than do the H emission regions of planetary nebulae; at their shell phases, FeII is strong and narrow,as in the supergiant Cyg.If one abstracts these characteristics, he describes a star which exhibits both hot and cool star, compact photosphere and extended reversing layer, characteristics; and which star passes through phases where one aspect dominates, then another phase where another aspect dominates. This is the classical description of a symbiotic star, to which the Bep stars are a bridge from the Be-shell phases. Today, the farUV+x-ray,and farIR+radio observations put such"hot/cool" symbiotic characteristics onto many stars. The Be-similar stars simply show these symbiotic features in a more pronounced way; and their strong variability brings successively the hot and cold,collapsed and extended,static and dynamic, features into predominance. Using 59 Cyg as an extensively-observed prototype,we suggested a "representative cycle" to be:a B-normal star when mass flux is small and not strongly variable;a "hibernating"Be phase when it has been a long interval since a phase of strong mass flux;a"beginning-Be"phase when the mass flow is very high;a"saturated"Be phase when the mass flow levels off to a value just sufficient to maintain the quasi-filled"balloon";the declining Be phase,entering a shell phase,when the mass flow greatly decreases. Each of these phases should have its distinctive velocity pattern,which we try to determine,empirically,by combined spatial and terrestrial studies of a given Be star,as 59 Cyg; and by comparing various B and Be stars, like Sco, Cas, Oph,and 59 Cyg at their different phases. In the same way, a study of the empirical velocity patterns among the Be-similar stars should extend our knowledge of the empirical range of velocity patterns,and possibly provide a kinematic pattern for constructing a dynamical representation, then a theory.

The extrème range among such Be-similar stars lies in the contrast of Be stars proper to the planetary nebulae.The classical models of each have been equally perturbed by the farUV observations showing o(1000km/s)velocities very close to the star;the classical visual observations of each show the o(30-100km/s) velocities far from the star---in the H emission envelope.The contrast between the two "Be-similar"objects lies in a variety of aspects:the regions close to the star;the regions where the decelerating shock occurs; the H envelopes of each; the regions of that quasi-static local environment manufactured by the star. The symbiotic stars probably lie somewhere intermediate.The WR stars exhibit the very high mass flux extreme;their variability seems smaller; the comparison of the "ordinary"WR stars and the WR-type spectra of the central stars of certain planetary nebulae may provide information on the effect of mass flux variability. Finally, the critical question is:"how broad is the meta-class of Be-similar stars"?We note that Struve included the Sun among them,as giving the prototype of his pattern of exo-photospheric atmospheric structure. In such an inclusion,one has problems with the photospheric continuum---not with the exo-photospheric regions,on which studies of non-thermal phenomena in stellar atmospheres focus.

References:

Cannon,C.J.,Thomas,R.N.1977,ApJ. 211,910

Costero,L.,Doazan,V.,Stalio,R.,Thomas,R.N.,1981:Proc.IAU Colloq.59,Trieste

Doazan,V.1982: B Stars With and Without Emission Lines;Vol.2,NASA-CNRS Monograph series:NonThermal Phenomena in Stellar Atmospheres: NASA pub. ed.A.B.Underhill,V.Doazan

Doazan,V.,Thomas,R.N. 1982; Chap.13 of preceeding reference

Doazan,V.and Thomas,R.N. 1982b in Madrid-ESA IVth Year of IUE Symposium

Heidmann,N.,Thomas,R.N.,1980; Astron.andAstrophys. 87,36

Lamers,H.1981 Proc.IAU Colloq.59; Trieste,Reidel pub.

Peters,G. 1980. Second JILA Workshop on Mass Loss;Boulder.cf also Proc. of Goddard-IUE Symposium on Four Years of IUE Research:Goddard,1982

Thomas,R.N. 1982, in publication

FIGURE 1

SCHEMATIC EXO-PHOTOSPHERIC VELOCITY PATTERN FOR A Be-SIMILAR STAR

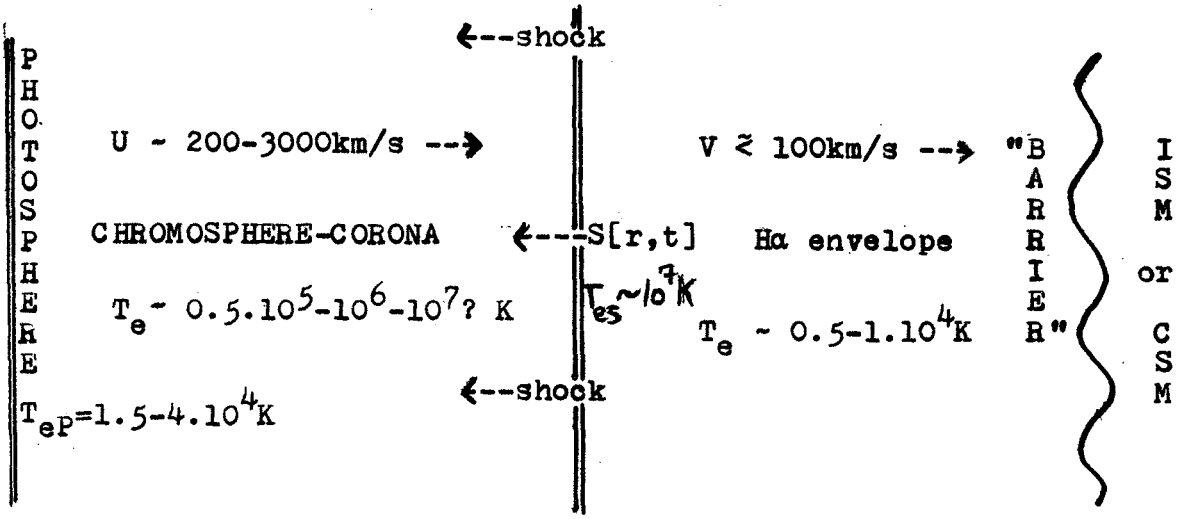

THE EFFECTIVE TEMPERATURES OF EARLY O AND WOLF-RAYET STARS

Anne B. Underhill
Laboratory for Astronomy and Solar Physics
NASA/Goddard Space Flight Center

ABSTRACT

Large-aperture, low-resolution spectra of 24 stars of types O5, O4, and O3 have been obtained, and from these the energy distribution between 1200 and 3200Å has been derived in absolute units. These energies have been combined with energies deduced from uvby and UBV photometry and corrected for interstellar extinction. Then angular diameters and effective temperatures were derived. The effective temperatures range from 24800K to 63000K. There is no correlation between effective temperature and spectral type or luminosity class for the early O stars. The size of the expected errors have been studied; typically $\Delta \log T_{eff}$ is ± 0.01 and $\Delta \log L/L_{\odot}$ is ± 0.12.

Energy distributions have been found for nine Wolf-Rayet stars from small-aperture, high-resolution IUE spectra and they have been put on an absolute energy scale by tying to energies measured with the ANS satellite. The energy distribution of HD 184378 (= BD+30°3639) has been measured from large-aperture high-resolution IUE spectra. These ultraviolet energies have been combined with energies deduced from photometry in the visible range, and corrected for interstellar extinction and for infrared excesses. They lead to effective temperatures ranging from 18000 for HD 184378 to 39900K for HD 192163. The effective temperatures of most of the WR stars lie in the bracket 25000 to 30000K, confirming earlier results.

The effective temperatures of Wolf-Rayet stars are like those of early B stars. In the case of B supergiants, O, and Wolf-Rayet stars, the terminal velocity, v_{∞}, correlates with T_{eff}. This correlation confirms that the effective temperatures of Wolf-Rayet stars are lower than those of most O stars.

The full text will be submitted for publication in the Astrophysical Journal as two papers.

(1) Angular Diameters, Effective Temperatures, Radii, and Luminosities of O3, O4, and O5 Stars;
(2) The Angular Diameters, Effective Temperatures Radii, and Luminosities of Ten Wolf-Rayet Stars.

MAGNETOSPHERES AND WINDS OF THE HELIUM STRONG STARS: DEPENDENCE ON ROTATION

Paul K. Barker
Department of Astronomy, University of Western Ontario

Douglas N. Brown
Department of Natural Sciences, University of Michigan-Dearborn

C.T. Bolton
David Dunlap Observatory, University of Toronto

J.D. Landstreet
Department of Astronomy, University of Western Ontario

ABSTRACT

Contemporaneous ultraviolet and optical spectroscopy and Zeeman polarimetry have been obtained of the B2V helium strong star HD 184927, a slow rotator newly discovered to be magnetic. The C IV and Si IV resonance doublets vary markedly on the rotation period; the phase dependence of extended violet absorption and redshifted emission at C IV reveals the existence of circumstellar material in a wind which is modulated by the global stellar magnetic field. The C IV profiles in HD 184927 and in other helium strong stars exhibit a complex dependence upon stellar rotation rate, magnetic geometry, and observer aspect. However, the strongest and most asymmetric C IV emission occurs in the stars which are either intrinsically the slowest rotators or which are observed pole-on; in sharp contrast, Hα emission is strongest in the most rapid rotators.

INTRODUCTION

The helium strong stars occur in the region of the H-R diagram near B2V and show abnormally strong lines of neutral helium for that spectral type. Many of the helium strong stars are spectrum variables, and many have strong magnetic fields which vary on the same period as the spectrum and photometric variations; thus, these objects are hot analogs of the Ap stars. In the oblique magnetic rotator model for such stars, the magnetic period is identified with the stellar rotation period; ultraviolet observations of three rapidly rotating magnetic helium strong stars in Orion (Shore and Adelman 1981) indicated the existence of weakly variable mass losing stellar winds. In this paper we present a few preliminary results from an ongoing extensive program of contemporaneous UV and optical spectroscopy and magnetic field measurements. Phase resolved observations have been (or will be) obtained for a variety of helium strong stars chosen to provide a wide-ranging sample in rotation rate and magnetic field strength, in order to investigate the interaction of magnetic, rotational,

and radiative forces in the winds from these stars.

THE SLOW ROTATOR HD 184927

This recently discovered helium strong star has a rotation period of 9.536 days as determined by Levato and Malaroda (1979). During a 9-day interval in 1981 July, 20 high dispersion images were obtained with IUE. In July and August magnetic field observations were made with a Balmer line Zeeman polarimeter on the 1.5 m telescope at Mt. Palomar; during the same months, 12 Å/mm optical spectra were also obtained with the 1.9 m telescope at David Dunlap Observatory.

Figure 1 shows the magnetic observations and the measured equivalent widths of selected features, phased on the adopted period 9.536 days, with arbitrary zero phase taken at J.D. 2444796.0. The star has a strong and variable magnetic field; the upper solid line in Figure 1 is a

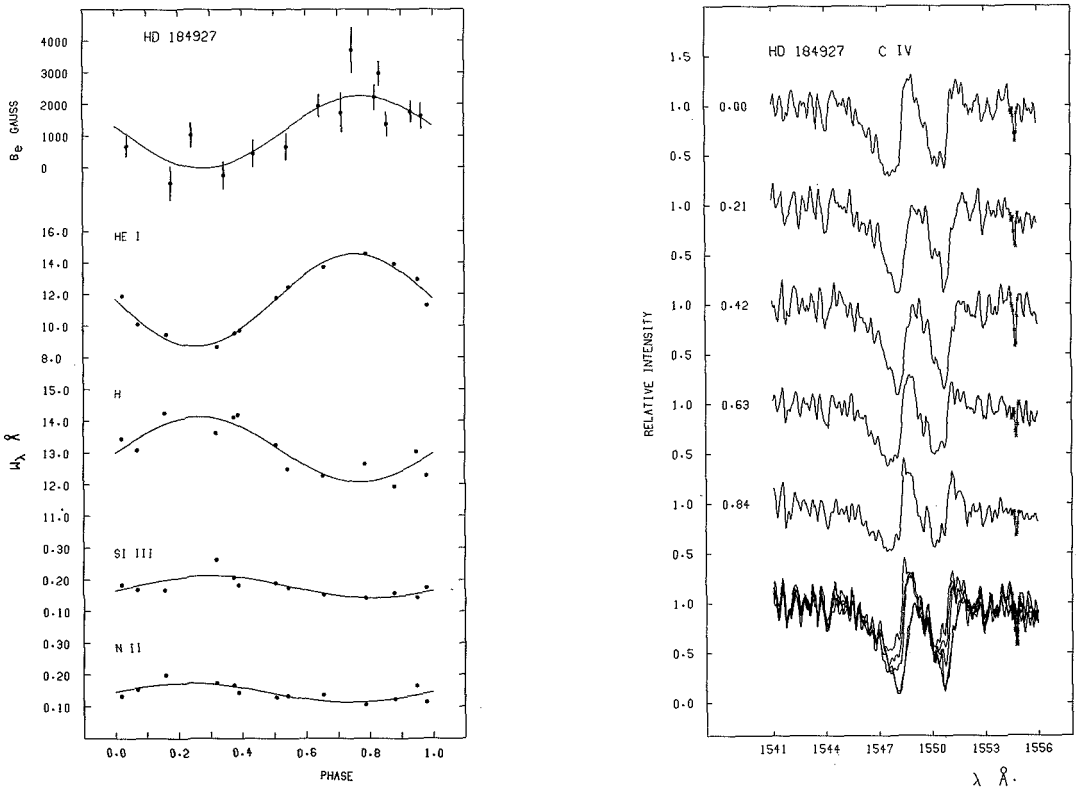

Figure 1.--Left panel: The mean longitudinal magnetic field, and equivalent widths of optical features, in HD 184927 phased on the ephemeris JD 2444796.0 + 9.536E. The smooth curves show least-squares sine wave fits to the data. Right panel: The top five profiles show the C IV resonance doublet in HD 184927 at the marked rotational phases; the same five spectra are shown superposed at the bottom.

sine wave fit to the data (1σ error bars). The field variation is sinusoidal, implying a strong dipolar field. Also shown is the variation in the total equivalent width of 8 He I lines, and the summed equivalent widths for H, Si III, and N II. The He I varies in phase with the field, but the other lines vary in antiphase; thus, there is a helium rich region near the positive magnetic pole.

The C IV resonance doublet (Figure 1) is highly variable on the stellar rotation period. When the positive magnetic pole is closest to the subsolar point, each component of the doublet displays strong redshifted emission, whereas when the magnetic equator traverses the line of sight, C IV is strongly in absorption. The steep blue edge to the redshifted emission occurs essentially at the rest wavelength. At all phases, there is an extended violet absorption to the shortward component, which extends out to 600 km/s from line center, and reveals the presence of a stellar wind. The rotational modulation of C IV shows that the wind is partly controlled by the magnetic field. Further, the amplitude of the modulation implies that a significant portion of the circumstellar material is contained in a highly compact magnetosphere.

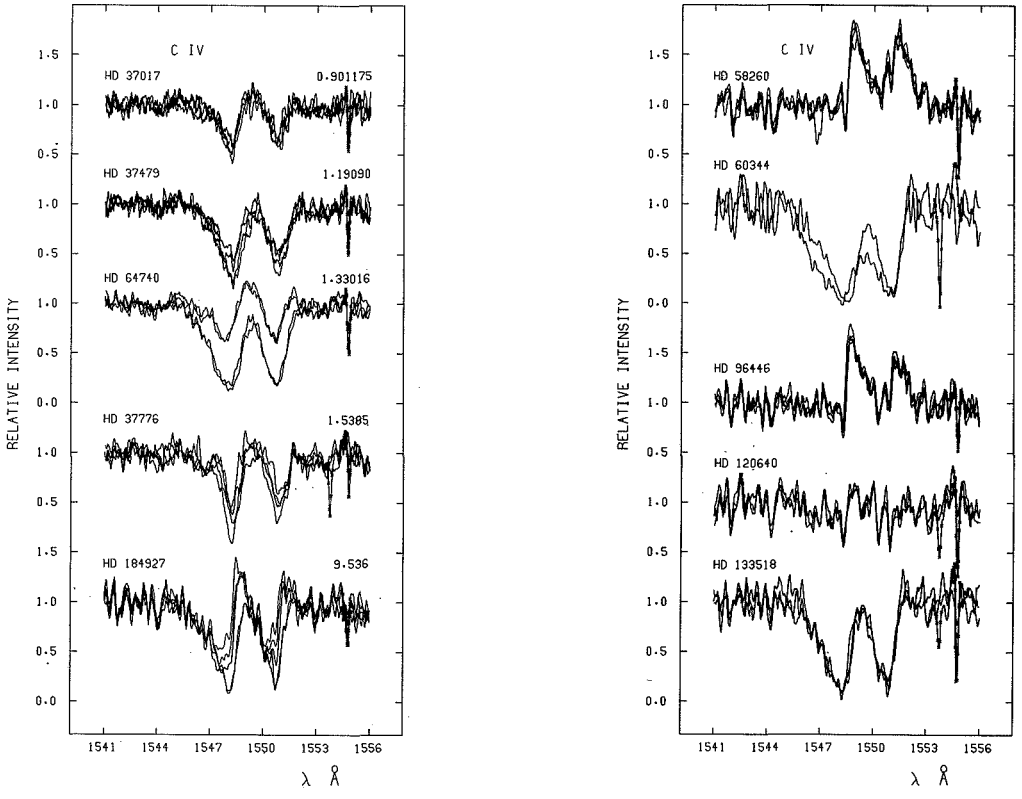

Figure 2.--IUE spectra are superposed here to show the characteristic variation of C IV in the helium strong stars observed at high dispersion. Left panel: The stars of known photometric period; the period in days is indicated for each object. Right panel: The stars of unknown rotation period.

ROTATION AND C IV EMISSION

Figure 2 shows C IV in all the helium strong stars observed at high dispersion with IUE; magnetic field data and relevant references are presented by Borra and Landstreet (1979). The variety in the C IV profile shape and in the amplitude of any variability for this sample of stars is overwhelming. The most common feature is the presence of extended violet absorption wings, indicating mass loss in a stellar wind, for those stars with C IV absorption.

The only cases of dominant C IV emission occur for stars in which the line of sight to the observer roughly corresponds to the magnetic axis: that is, at the maximum field phase of HD 184927, and also for HD 58260 and HD 96446, both of which have large and apparently constant fields. The lack of magnetic and spectral variations in HD 58260 and HD 96446 may arise either from their being viewed rotationally pole-on, or from intrinsic slow rotation; HD 184927 is a known slow rotator. These three stars are similar in that the C IV emission has a pronounced asymmetry, which is not true of the C IV emission in HD 64740, the star with next strongest emission. Walborn (1974) has reported weak broad emission wings to Hα in the rapid rotators HD 37017, HD 37479, and HD 64740--but not in HD 58260 or HD 96446. The present spectroscopic data show little or no Hα emission in HD 184927. Thus one arrives at the first taxonomic conclusion regarding this sample of helium strong stars: the strongest and most asymmetric C IV emission occurs in the stars which are either intrinsically the slowest rotators, or which are observed pole-on, whereas Hα emission is strongest in the most rapid rotators.

It is evident that these objects have winds and magnetospheres which are modulated by the stellar magnetic field. It is hoped that the complex phenomenology of the helium strong stars may be elucidated by the observational program, still in progress, designed to disentangle the effects of rotation rate, magnetic geometry, radiative forces, and observer aspect, upon the emergent line profiles.

We especially wish to thank all the IUE staff for their friendly and efficient operation of the spacecraft. We thank Dr. E.F. Borra for his generous loan of the polarimeter used at Mt. Palomar, and we also thank Dr. S.N. Shore for provocative discussions. This work was supported by the Natural Sciences and Engineering Research Council of Canada, and by the University of Michigan-Dearborn.

REFERENCES

Borra, E.F., and Landstreet, J.D. 1979, Ap.J., 228, 809.

Levato, H., and Malaroda, S. 1979, Pub. A.S.P., 91, 789.

Shore, S.N., and Adelman, S.J. 1981, Liège Symposium.

Walborn, N.R. 1974, Ap.J. (Letters), 191, L95.

UV FLUXES AND EFFECTIVE TEMPERATURES OF EXTREME HELIUM STARS

D. Schoenberner and J. S. Drilling
Dept. of Physics and Astronomy, Louisiana State University

A. E. Lynas-Gray
Dept. of Physics and Astronomy, University College London

U. Heber
Institut fuer Theoretische Physik und Sternwarte, Kiel

ABSTRACT

We present low-resolution IUE spectra of a complete ensemble of extreme helium stars and discuss their appearance in comparison with normal stars. We have determined effective temperatures from these observations by means of line-blanketed model atmospheres. The temperatures are in accordance with earlier results from ground-based observations.

We have obtained low-dispersion IUE spectra of all known extreme helium stars in both wavelength regions. The spectra were calibrated using the absolute calibration of Bohlin and Holm (1980), and were then corrected for interstellar reddening using the empirical reddening law of Seaton (1979). Our de-reddening procedure, which uses the reversal of the 2200 Å feature as the criterion for zero reddening, is illustrated in Fig. 1 for HD 124448 (E(B-V) = 0.08). The resulting color excesses for all of the stars are given in Table I. In general, we were able to determine E(B-V) to within $\pm$0.05 magnitudes, and our results are in reasonable agreement with the earlier work of Heber and Schoenberner (1981), where the color excesses were derived from a comparison of theoretical and observed UBV colors.

Effective temperatures have been determined by the so-called semi-empirical method (for a detailed description see Boehm-Vitense 1981). We have matched the de-reddened UV fluxes and UBVJHKL photometry (Drilling 1982) of each star with a newly computed grid of LTE model atmospheres. The computational details will be given elsewhere (Heber 1982, Schoenberner et al. 1982), but we want to mention that these models have a uniform composition (n(H)=0, n(He) = 0.99, n(C) = 0.01, other elements solar with respect to the total mass), and that they include line blanketing for about 800 ionic transitions in the UV. The procedure is illustrated in Fig. 2 for HD 124448, which is best matched with a 16,000 ^{o}K model. This match fixes the angular diameter of the star, which then yields the effective temperature via the Stefan-Boltzmann law if the total flux at the earth's surface is known. The latter quantity was determined by adding to the observed flux between 1239 Å and 3122 Å the fluxes predicted by the model

atmosphere at longer and shorter wavelengths. The observed spectrum shortward of 1239 Å was not used because of the effects of geocoronal L-alpha emission and interstellar L-alpha absorption. This method works very well for the extreme helium stars because a significant contribution to the total stellar flux emerges in the observable UV, even for the cooler objects. The method begins to break down for effective temperatures greater than 30,000 °K due to the increasing contribution to the flux from wavelengths shorter than 1239 Å.

The results are given in Table I, where they are seen to be in remarkably good agreement with earlier results obtained from ground-based observations using an older grid of unblanketed model atmospheres. We estimate the errors in the effective temperatures to be around ±500 °K due to the uncertainties of the IUE calibration (10%), the color excesses (±0.05), and the angular diameters (5%). The temperature differences between individual objects are, of course, much better determined.

In Fig. 3, a representative sample of the de-reddened spectra is arranged in the order of decreasing temperature and compared with the spectra of normal stars selected from the atlas of Wu et al. (1981). All of the extreme helium stars are seen to show the strong metallic lines characteristic of objects with low surface gravities, as expected from earlier fine analyses of ground-based observations. The extreme helium stars with effective temperatures lower than 12,000 °K show a remarkable depression of the far UV continuum due to the CI absorption edge at 1440 Å together with various CII absorption edges. We attribute this to the high carbon abundances of these stars as compared to normal stars. The same holds true for the very strong CII resonance absorption at 1335 Å in the intermediate temperature range and for the CIV resonance absorption at 1550 Å in the hotter stars.

REFERENCES

Boehm-Vitense, E., 1981, Ann. Rev. Astron. Astrophys. 19, 295.
Bohlin, R. C., and Holm, A. V., 1980, IUE Newsletter No. 10, p. 37.
Drilling, J. S., 1982, in preparation.
Heber, U. 1982, in preparation.
Heber, U., and Schoenberner, D., 1981, Astron. Astrophys. 102, 73.
Schoenberner, D., Drilling, J. S., Lynas-Gray, A. E., and Heber, U., 1982, in preparation.
Seaton, M. J., 1979, M.N.R.A.S. 187, 73P.
Wu, C.-C., Boggess, A., Holm, A. V., Schiffer, F. H., and Turnrose, B. E. 1981, IUE Newsletter No. 14, p. 2.

TABLE I. Color excesses and effective temperatures of extreme helium stars

Star	E(B-V)	T(eff) new	T(eff) old
HD 160641	0.40	34,000:	
BD $-9^{\circ}4395$	0.30	23,500	25,000
BD $+10^{\circ}2179$	0.00	17,300	16,800
HD 124448	0.08	15,600	16,000
LSII $+33^{\circ}5$	0.25	14,700	
LSE 78	0.13	14,000	
HD 168476	0.13	12,600	14,000
LSIV$-1^{\circ}2$	0.45	11,500	
LSS 1922	0.70	11,100	
BD $-1^{\circ}3438$	0.40	11,000:	
BD $+1^{\circ}4381$	0.15	9,500	
LSS 3378	0.35	9,200	
LSIV $-14^{\circ}109$	0.20	8,500	

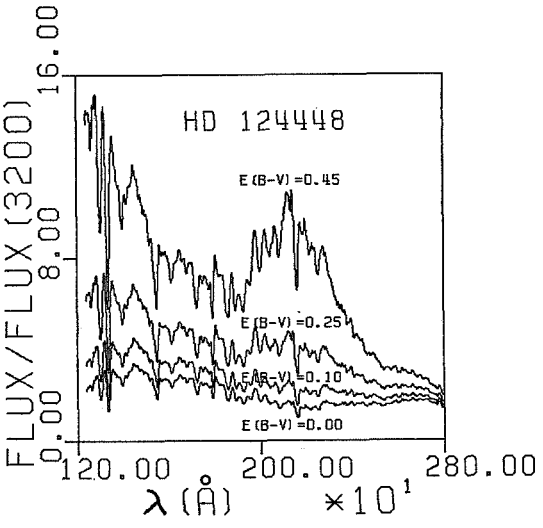

Fig. 1. IUE spectrum of HD124448 de-reddened by E(B-V) = 0.00, 0.10, 0.25, and 0.45 according to the reddening law of Seaton (1979).

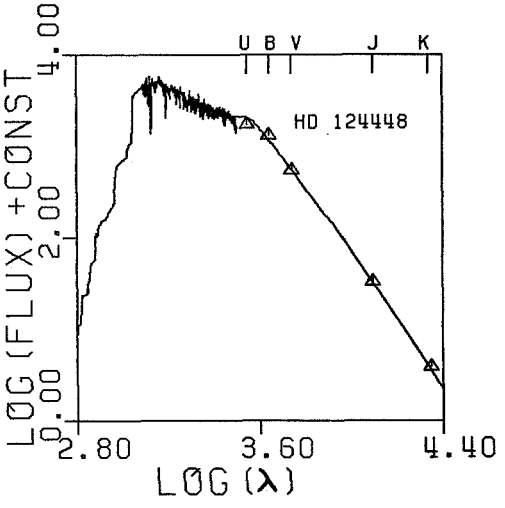

Fig. 2. De-reddened IUE spectrum of HD124448 and upper envelope of 16,000 $^{\circ}$K model atmosphere. Broad-band colors are from Drilling (1982).

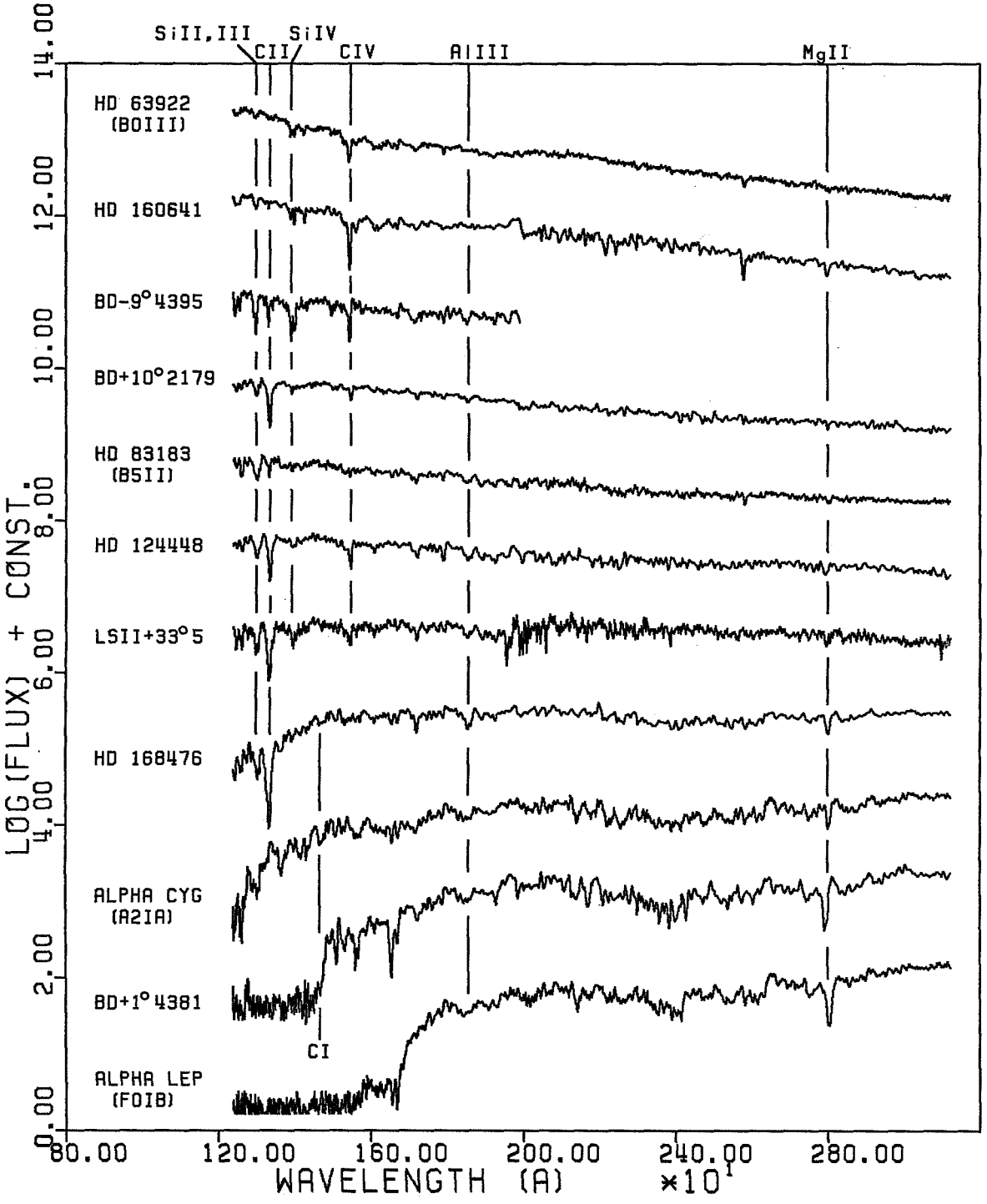

Fig. 3. Low-dispersion IUE spectra of extreme helium stars and of normal giants and supergiants selected from the atlas of Wu et al. (1981). The spectra have been corrected for interstellar reddening, and are arranged in the order of decreasing effective temperature.

ULTRAVIOLET PHOTOMETRY OF A-TYPE STARS AT HIGH GALACTIC LATITUDES

W. B. Landsman, R. C. Henry, and P. D. Feldman
Physics Department, The Johns Hopkins University

ABSTRACT

IUE has been used in a study of four stars located in one target (ℓ=179°, b=65°) of an earlier "diffuse background" sounding-rocket experiment. The resulting stellar correction is much smaller than that previously estimated, giving a higher diffuse background at this target.

INTRODUCTION

The sounding-rocket data are those of Anderson *et al.* (1979), who did warn that "until the far-ultraviolet brightness of HD 95934 has been directly measured, the residual intensity found for target 3 must be given relatively low weight". (The stellar correction for targets 1 and 2 was much smaller). Anderson *et al.* estimated the stellar flux from visible-light data, the models of Kurucz (1979), and the temperature scale of Morton and Adams (1968); here we directly measure the flux.

OBSERVATIONS

The observing sequence is given in Table 1. The stars were observed with the IUE large aperture, on 24 January 1979. The spectra were corrected using the 3 Agency 4th file method. Figure 1 shows the three observations of HD 95934 taken at different exposure levels (together with [dashed line] the spectrum of a standard IUE comparison star). Their close agreement indicates that non-linearities have been adequately corrected. Fluxes are based on the absolute calibration of May 1980.

In Table 2, we present the observed fluxes in a 100 Å bandpass about 1600 Å, a region free from reseaux marks and saturated pixels. Anderson *et al.* estimates are also given; clearly, the stellar contribution was over-estimated.

All four stars were also observed by the S2/68 instrument on the TD1 satellite in 1972-1974: Table 3 shows that agreement with our IUE results is good, with the possible exception of HD 95884. TD1 fluxes were corrected to IUE photometry using relations in Carnochan (1982).

DISCUSSION

To decide whether the observed stars show abnormalities, we compare photometry with "standard" stars from the IUE spectral atlas (Wu *et al.* 1981).

TABLE 1

IUE OBSERVING LOG

HD	IUE Image Number (SWP)	Exposure Time (minutes)	Saturated Wavelengths
95310	4009	25	> 1685 Å
95934	4010	5	> 1709 Å
	4011	15	> 1635 Å
	4012	45	> 1564 Å
94479	4013	60	> 1730 Å
95884	4014	60	> 1690 Å

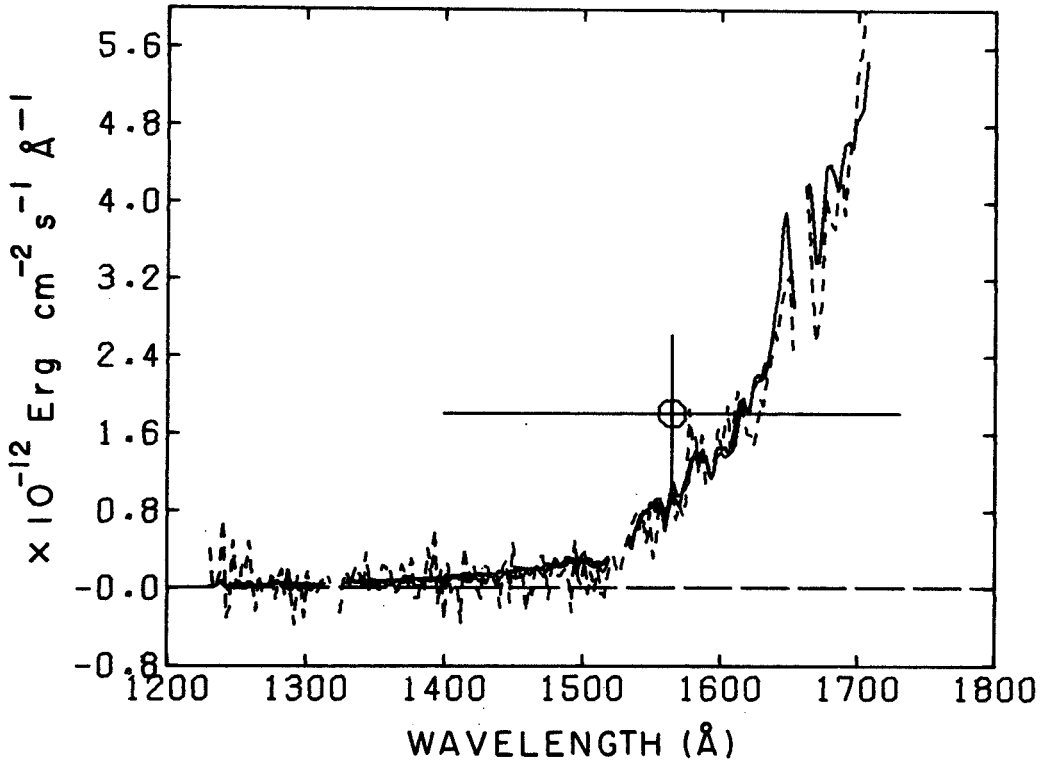

FIG. 1. - The three IUE observations of HD 95934 (solid lines), made with substantially different exposures, agree well with each other and with the TD1 observation at 1565 Å (bandwidth shown). The spectra ressemble that of the standard A5V star HD 116842 (dashed line), shown scaled down by a factor of 4.

TABLE 2

OBSERVATIONAL RESULTS

HD	V	Spectral Type	1600 Å Flux (10^{-14} Erg $cm^{-2}s^{-1}$ Å^{-1}) Observed (IUE)	Predicted (Anderson *et al.*)	$m_{1600} - m_{2740}$	$m_{1600} - V$
95310	5.07	FOm	48.6	67	3.61	4.54
95934	6.00	A3V	167.9	1025	1.93	2.26
94479	8.32	Am[1]	3.7	310[2]	3.47	4.08
95884	7.15	A7V	14.3	408[3]	3.15	3.79

[1] Balmer Line Type A7

[2] Used V=7.8, A2

[3] Used A3

TABLE 3

COMPARISON OF IUE AND TD1

HD	Wavelength (Bandpass)	Flux (10^{-14} Erg cm^{-2} s^{-1} Å^{-1}) IUE	TD1
95310	1455 A (110 A)	7.4	13 ± 18
	1565 A (110 A)	30.1	32 ± 36
95934	1565 A (330 A)	200.9	182 ± 24
94479	1565 A (330 A)	7.8	12 ± 21
95884	1455 A (110 A)	2.9	29 ± 23
	1565 A (110 A)	11.0	73 ± 48

TABLE 4

IUE STANDARD STARS

HD	V	Spectral Type	Derived T_{eff}	$m_{1600} - m_{2740}$	$m_{1600} - V$	$m_{1600} - V$ (Carnochan 1982)
80081	3.83	A2V	8680	0.07	0.23	0.18 ± 0.30
216956	1.16	A3V	8280	0.78	1.15	0.84 ± 0.35
116842	4.03	A5V	7860	2.46	2.88	2.10 ± 0.46
76644	3.15	A7IV	7670	3.27	3.76	3.23 ± 0.51
12311	2.86	FOV	7270	4.48	5.46	

Table 4 lists the m_{1600}-V and m_{1600}-m_{2740} colors for these stars. Fluxes are converted to magnitudes using the absolute calibration of Hayes and Latham (1975). The 2740 Å magnitudes are from the 320 Å-wide TD1 photometry. Also shown are the m_{1600}-V colors of Carnochan (1982), for the tabulated spectral type.

Comparison of observed ultraviolet fluxes of A-type stars with the model atmospheres of Kurucz is done by Wesselius *et al.* (1980) and Böhm-Vitense (1981). Each give an effective-temperature/spectral-type calibration cooler than that used by Anderson *et al.* Also, Wesselius *et al.* find temperatures derived from fluxes at 1550 Å to be 600 K too low for spectral types B9.5 V to A5V. We also see this inadequacy in the Kurucz models in Table 4, where temperatures derived from the observed m_{1600}-V for the IUE standard stars are lower than canonical values.

None of our four stars shows any indication of reddening. With these preliminaries completed, we now discuss each of our four stars:

a) HD 95310 (=HR 4288, B-V=0.25, β=2.793)

B-V and β both indicate a spectral type, if main sequence, near A8 (Fitzgerald 1970, Crawford 1979), in agreement with our ultraviolet flux measurements, which show its m_{1600}-V and m_{1600}-m_{2740} magnitudes to be somewhere between A7 and F0.

b) HD 95934 (=HR 4309, B-V=0.16, β=2.855)

Here again the observed ultraviolet magnitudes show better agreement with visible color indices than with spectral type. B-V, β, m_{1600}-V, and m_{1600}-m_{2740} all indicate an A4 or A5 star. The dashed line in Figure 1 is the standard A5V star HD 116842; agreement is good. Anderson *et al.* used V=5.98, A4V.

c) HD 94479

Anderson *et al.* used a spectral class of A2, from the SAO star catalog (Whipple 1966); Slettebak *et al.* (1968) give Balmer and CaII K-line types of A7, and a metallic-line type of F2. Am stars, in the ultraviolet (van't Veer-Menneret *et al.* 1980), are flux-deficient, but with a large scatter. Our flux is somewhat smaller than that of a normal A7 star, but it is not clear whether line-blanketing has played any role.

d) HD 95884

Anderson *et al.* used A3, from the SAO catalog, while Slettebak *et al.* give A7V. This star shows the same m_{1600}-V and m_{1600}-m_{2740} colors as does the standard A7 star.

CONCLUSION

None of our stars appears abnormal in the ultraviolet, although visible photometry does appear, for these essentially unreddened stars, to be a better indicator of ultraviolet flux than does spectral type. The discrepancy between previous predictions and the present observations can be explained in terms of 1) misclassification of two stars, 2) use of a spectral-type/effective-temperature calibration hotter than more recent determinations, and 3) inadequacy of the Kurucz (1979) models, in the far ultraviolet, for A-type stars. The revised target 3 spectrum, and its significance, will be discussed elsewhere (Landsman and Henry 1982).

We thank R. Wilson for making unpublished TD1 data available, and the IUE project, Goddard Space Flight Center, for making the Spectral Atlas data available. This work was supported by NASA.

REFERENCES

Anderson, R. C., Henry, R. C., Brune, W. H., Feldman, P. D., and Fastie W. G. 1979, *Ap.J.* 234, 415.
Böhm-Vitense, E. 1981, *Ann. Rev. Astron. Astrophys.* **19**, 295.
Carnochan, D. 1982, submitted to M.N.R.A.S.
Crawford, D. L. 1979, *A.J.* **84**, 1858.
Fitzgerald, M. P., 1970 *Astron. Astrophys.* 4, 234.
Hayes, D. S., and Latham, D. W. 1975, *Ap.J.*, **197**, 595.
Kurucz, R. L. 1979, *Ap. J. Suppl.* **40**, 1.
Landsman, W., and Henry, R. C. 1982, in preparation.
Morton, D. C., and Adams, T. F. 1968, *Ap.J.*, **151**, 611.
Slettebak, A., Wright, R. R., and Graham, J. A., 1968 *A.J.* **73**, 152.
van't Veer-Menneret, C., Faraggiana, R., and Burkhart, C. 1980, *Astron. Astrophys.* **92**, 13.
Wesselius, F. R., van Duinen, R. J., Aalders. J. W. G., and Kester, D. 1980, *Astron. Astrophys.* **85**, 221.
Whipple, F. L. 1966, *Smithsonian Astrophysical Observatory Star Catalog* (Washington: Smithsonian Institution Press).
Wu, C. C., Bogess, A., Bohlin, R. C., Holm, A. V., Schiffer, F. H., and Turnrose, B. E. 1981 *IUE Ultraviolet Spectral Atlas* (Greenbelt, GSFC).

THE PECULIAR, LUMINOUS EARLY-TYPE EMISSION LINE STARS OF THE MAGELLANIC CLOUDS: A PRELIMINARY TAXONOMY

Steven N. Shore and N. Sanduleak
Warner and Swasey Observatory
Case Western Reserve University

ABSTRACT

A sample of some 20 early-type emission supergiants in the Magellanic Clouds has been observed with both the SWP and LWR low resolution mode of IUE. The stars are chosen on the basis of their optical spectral morphology as follows: all have strong H emission, some showing P Cygni structure as well, with HeI, HeII, FeII and other ions also showing strong emission. We find that the stars fall into three convenient and somewhat distinct groups on the basis of the HeII/HeI and HeI/HI strengths -- HeII strong,HeI,HI; HeII absent,HeI,HI strong; HeI absent,HI,FeII,[FeII],etc.strong in addition to low excitation ions. We discuss some preliminary results from the more complete program now near completion on the UV spectra of this sample. We discuss in some detail the two most extreme emission line stars found in the Clouds -- S 134/LMC and S 18/SMC. Also discussed are some results for the 2200A feature in these supergiants, and evidence for shells around the most luminous stars in the Clouds.

INTRODUCTION

This study is based on a homogeneous sample of optical spectra covering λλ3550 - 6700 A, obtained with the CTIO 40 in. during 1974 and 1975. The details of the optical spectroscopy will be published elsewhere (Shore and Sanduleak 1982, in preparation). It is intended as a survey of all of the LMC supergiants with $M_V < -5$ with strong emission lines, in order to deyermine both temperature classes and other physical properties about these the most massive stars in the Local Group. Our IUE observations were initiated in the hope that the classifications thus obtained might allow for a qualitative grouping, and that we might be able to examine the effects of metallicity on the driving of stellar winds in early-type supergiants in the LMC and SMC. As luck would have it, this is perhaps the least interesting, and likely the last thing possibly addressed, question which is posed by our spectra.

CLASSIFICATIONS

Our program stars, all of which are listed in Henize (1954), fall into three rather broad groups, unimaginatively referred to subsequently as class A, B, and C. They are differentiated as follows.

Class A: S 9,30,61,83,91,128,131/LMC and S 18/SMC. These stars all show strong HeII 4686, very strong HeI and H emission, and sometimes P Cygni structure on the H lines (S 61,128). Two of these, S 18 and S 83 are known HeII spectrum variables (Sanduleak 1978, D.Allen 1978 private communication). The stars with P Cygni profiles do not differ from their

galactic counterparts, with velocities of 350 to 450 km s^{-1}. In the UV, they differ dramatically. S 9, 30, 83, and 131, and S 18, all display emission lines, with only the NIII] 1754 line in common. S 30 and 131 also have HeII 1640 strong, the line being quite complex in 131. There is no evidence for variability in either. S 18 is totally different! The HeII line is variable by 50% over the time of our observations: 120 A (7/13/81) to 71 A (3/22/82) in equivalent width. A similar decrease was observed in CIV 1550 and OIII] 1667. The FES magnitude during this time was constant (13.5). The spectrum is shown in fig.4 (SWP 16599). The amplitude of variation agrees with HeII 4686.

Class B: S 22,96,124,127,134/LMC and S 65/SMC. This class has strong HeI,no HeII4686, strong HI and other lower excitation ions. It includes S Dor = S 96. The UV observations show that S 65/SMC is also a member. The absorption spectra of S 22,65, and 96 are extraordinarily complex, and can only currently be understood qualitatively. S 96 has been found to be de - creasing steadily in brightness longward of 1400A (fig.3), a trend confirmed by LWR images taken recently (3/24/82). No variations of S 65 have been found yet. It looks like the earlier of the S 96 spectra, and may be in one phase of its variations. The most unusual freak in our sample, totally unexpected on the basis of the optical spectra, is S 134. The star has been studied carefully because of its deviance. It shows no obvious HeII4686, yet it has strong HeII1640 (4A). It shows a unique SiIII]1895/CIII]1909 ratio, characteristic of symbiotics(!) and η Car (Heap et al. 1978)-- there is no evidence for a red companion from the visual or red spectra. The CIV doublet shows P Cygni structure with v_∞ = 2400 km s^{-1}, and the same is true for the NV lines. The third spectrum ions are stronger in S 134 than in the other stars in Class B. It also displays an enhanced 2200A bump and some second spectrum absorption lines. The absolute bolometric magnitude is -9.5 using a derived T_{eff} of 3×10^4K and the B.C.'s from Kurucz (1979), and log g of about 3.5. It is the brightest member of NGC 2081, brighter than the WR stars in the cluster. From Maeder (1981) it is consistent with a 50 to 60 $M_\odot$ star; its $dM/dt \sim 10^{-5}$-$10^{-6} M_\odot$ yr^{-1}. The star is likely in a compact HII region. Indeed,the Barnes-Evans relation yields 90 solar radii from B-V and 1500 $R_\odot$ for V-R, perhaps due to an extensive dust shell. Our IUE data show this star to be a stectrum constant. It has a temperature similar to S 71, see below. A more detailed study is being completed. S 124 and 83 are similar, as is S 127 in T_{eff}. (See below). S 9 is like S 127.

Class C: S 12, 17, 71, 73, 86, 89, and 111/LMC. These stars show no HeI emission, strong HI and lower excitation lines primarily composed of FeII,[FeII] and OI. While one might anticipate that these are the coolest stars in our survey, they in fact span the greatest range in T_{eff}. For example, S 111 is as hot as the blue component in the VV Cep star S 91, a Class A star. On the other hand, S 17 is one of the coolest. There are no strong emission lines in the UV, and NIII] is notable by its absence; no strong FeII emission shows up in the LWR spectra. S 71 is similar to S 124, with perhaps a little lower local reddening.

CONCLUSIONS

The results of our study thus far show that the optical temperature classes are a potentially misleading guide to the ultraviolet properties of the hottest emission supergiants in the LMC and SMC. On the basis of

the stars we have so far examined in some detail, we present the following tentative ordering:

[S 91 (VV Cep analog)],[S 111, 71, 12],[S 83, 124, 128], [S 134], [S 9, 17, 89], [S 30]

and S 22, 65/SMC, and S 96 being somewhat separated. Here we have grouped stars with approximately the same continuum appearance. We do not claim to have definitivly characterized our taxa, but perhaps to have begun to locate them aright on the HR diagram. Using S 134 as a fiducial marker, the hottest of our sample should have $T_{eff} \geq 45000$ K, while the coolest may be nearer 17000 K. We have not reached the continuum of S 18 and can only say that on the basis of its emission spectrum, it is certainly one of the hottest stars in our survey. The stars S 83 and 128 are practically identical (fig.2), with nearly the same luminosities and effective temperatures. We have, though, a paucity of such coincidences. With these stars, the optical is still the blind mass describing the elephant by grasping its tail. This is a position we hope this data will begin to improve.

We wish to thank the staff of the International Ultraviolet Explorer Satellite, especially Skip Schiffer and Tom Ake, for all of their kind aid during the course of this study. This paper, containing as it does data only 6 days old (at the time of this writing) would have been impossible without the use of the RDAF at Goddard Space Flight Center.

REFERENCES

Henize, K. 1956, Ap.J.Suppl.,2, 315.
Heap, S. et al. 1978, Nature, 275, 385.
Sanduleak, N. 1978, IBVS Nr. 1389.

TABLE I -- Partial Listing

Henize Number	HD(HDE)	Cluster	Optical remarks	UV Remarks
9		N 11	HI PCyg,HeI/II,NIII	NIII],CIII] emission
12			HI PCyg,FeII	NIII]
17	268939	NGC1820	HI	no strong emission
22	34664	NGC1871	HI,HeI,[OI],FeII,[FeII]	S Dor-like,wk em.
30	269445		HI,HeI/II,NIII,[OII]	NIII],HeII 1640
61			HIPCyg,HeI/II,[OI]	No strong emission
71			HI,FeII,OI	no strong emission
73	268835		HI	
83	269582		HI,HeI/II(var!),NIII	NIII]
86	269128		HI	NIV?
89	269217		HI,[OI],FeII,[FeII]	
96	35343	NGC1910	S Dor	very complex abs.!
111	269599		HIPCyg,FeII	no strong emission
124	37836		HI,HeI,PCyg?,FeII	SiIII]
127	37974	NGC 2050	HI,HeI,FeII	no strong emission
134	38489	NGC2081	HI,HeI,[OIII],FeII	see text,very rich!
128	269858		HI,HeI/II,NIII,var!	no strong emission?
131			HI,HeI/II,noHeI5016	NIII/IV/V,CIV,HeII?

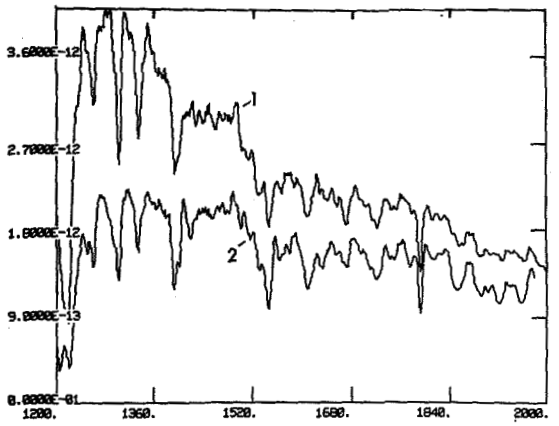

Fig 1.(1)S 111/LMC compared with (2) S 128/LMC. Both seem to show weak NIV emission at 1488. Unscaled data. 5 point smoothing.

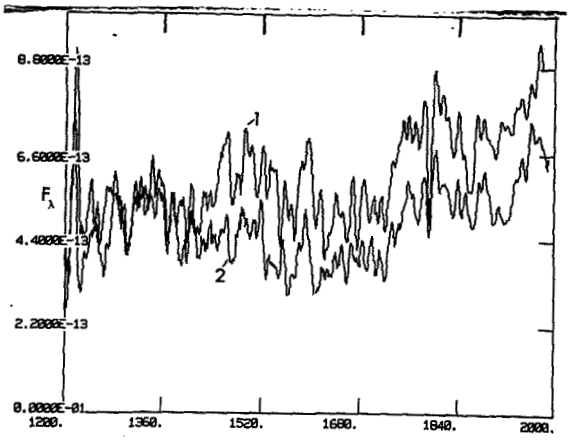

Fig.3.(S 96/LMC=S Dor. (1) SWP13519 (3/16/81);(2) SWP 14466(7/13/81). Note the wavelength dependence of the variations.

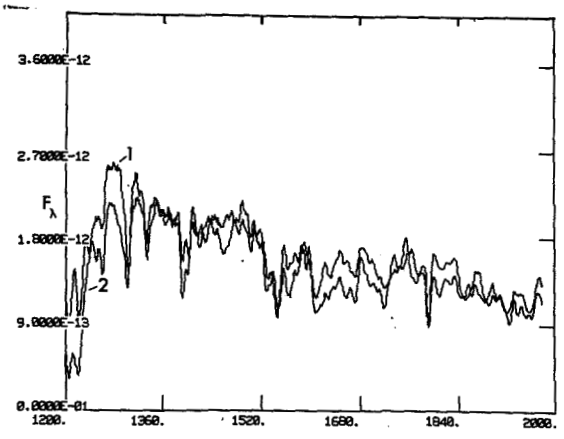

Fig.2. (1)S128 and (2) S 83/ LMC. Unscaled data, 5 point smoothing.

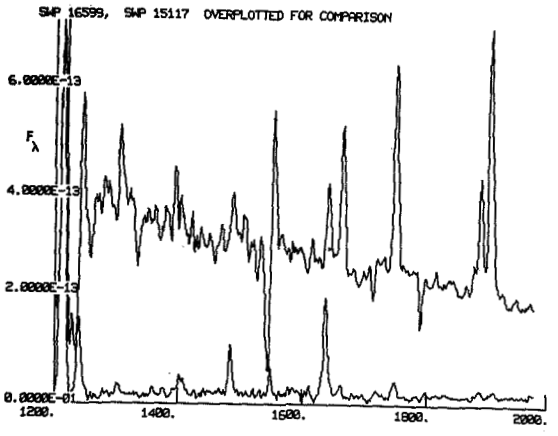

Fig.4. Top spectrum, S 134 (SWP15117) and S 18/SMC (SWP 16599) . Note the CIII]/SiIII] ratio in S 134 and the very strong HeII in S 18.

THE ORION NEBULA STAR CLUSTER

Robert J. Panek
Computer Sciences Corp.

INTRODUCTION

As discovered by Trumpler (1931), photography through filters which suppress nebular light reveal a clustering of faint red stars centered on the Trapezium. This is evidence for a distinct cluster within the larger OB1 Association. We consider stars within about 20' of the Trapezium as comprising the Orion Nebula Star Cluster. We will restrict ourselves to stars of type F and earlier. These have been quite completely studied by groundbased observers: - spectral classification: most recently Levato and Abt (1976). - broadband photometry: from Walker (1969), Penston (1973), Penston etal (1975), and Breger etal (1981) we have UBVRIJHKLM mags. -rotational velocities: from Abt etal (1970). - radial velocities: Johnson (1965). - linear polarization: Breger (1976). A number of topics of interest have arisen: A. Extinction by dust grains. Most stars have a mild color excess of 0.07 in (B-V). This is consistent with a general, uniform extinction in the intervening interstellar line of sight. For the stars which are heavily reddened, there is evidence of peculiar extinction in the form of anomalously high $R=A_V/E(B-V)$. Bohlin and Savage (1981) find that the UV extinction of the Trapezium stars is peculiar. B. Photometric peculiarities. The HR diagram has the classical form of a young cluster, in which the early type stars fit the ZAMS but stars redward of (B-V)= -0.09 lie in the region of pre-main sequence evolution. Many of the early type stars exhibit strong excess infrared flux. C. Spectroscopic peculiarities. The cluster contains several B and A type emission line and shell stars, and a few Am stars. However, the unique feature of the cluster is the peculiar broad hydrogen-lined stars (class Vb). This is a rare type which is found virtually only in this cluster. The spectra resemble ordinary main sequence stars except that the hydrogen lines are much broader than the class V stars. In a recent study, Abt (1979) concludes that the phenomenon is associated with extreme stellar youth. D. Young variables. Many of the stars are low amplitude variables. T Orionis, the prototype of a class of irregular variables, found among young stars, has a V range 9.5-12.5. Walborn (1981) finds that θ^1C Ori is a spectrum variable. E. The distribution and motion of gas within the cluster. An extensive mapping of the velocities of the nebular emission has been made by Wilson etal (1958).

IUE OBSERVATIONS

The above discussion argues for a systematic survey of the cluster, and this has been accomplished with 4 IUE observing shifts. Table 1 identifies the stars observed. The stars in θ^1 and θ^2 Ori were not included except θ^1C. An identification chart is available in the catalogue of Brun (1935). Positions are available from Strand (1958). The UV brightness of the Orion Nebula is a serious handicap for IUE study of the cluster stars. Four stars identified with * in Table 1 required correction for nebular background. This was accomplished using the spatially resolved spectral data for large aperture

observations. The flux for 5 "lines" centered on the stellar spectrum was extracted. This includes essentially all the stellar flux plus some nebular flux. A second extraction was made to include the full width of the large aperture (11 lines). Then the nebular flux in the 5-line-extracted spectrum was found as F(neb;5 lines)=(F(11 lines)-F(5 lines))/0.93. The factor 0.93 which applies to both the SWP and LWR, was determined from spectra of Orion nebular light which were kindly provided by Dr. F.H. Schiffer. One star, MR Ori, was deemed hopelessly overwhelmed by nebular background.

Extinction curves have been derived for the significantly reddened stars. Figure 1 shows normalized extinction curves $E(\lambda-V)/E(B-V)$. The solid line is the average interstellar extinction derived by Savage and Mathis (1979). We see that the weakness of the far UV extinction is a common characteristic as with the Trapezium stars (Bohlin and Savage 1981). Where the spectral type was uncertain the earliest possible type was adopted so that any error causes the weakness of the UV extinction to be underestimated. There is a variety in the strength of the feature at 2200A, from strong (B530) to weak (B655). The deviations at the infrared wavelengths reflect the infrared excesses. Since the distance to the cluster can be unambiguously determined by fitting the lightly reddened stars to the ZAMS, we can in principle determine absolute extinction curves. If R is greater than the average interstellar value of 3, say R=6, then the far UV extinction in Orion approaches the normal interstellar extinction while the visual extinction is abnormally high, for a given E(B-V).

Several spectroscopic peculiarities are obvious in the low dispersion spectra. In the A0 shell star V566 Ori, the MgII absorption is much weaker than expected for the spectral type and UV flux distribution. The F star NV Ori has MgII neither in absorption nor in emission. These observations indicate that a substantial MgII line emission must be present in these stars.

The stars of Table 1 include 6 of the 9 class Vb stars of the cluster (the other 3 are in θ^1 and θ^2 Ori, and spectra will be obtained from the IUE archives). A preliminary comparison of the flux distributions and spectral features with normal stars has not revealed any pronounced peculiarities. A more definitive study will be made with a finer grid of normal stars of various spectral types.

High dispersion spectra of V361 Ori show C IV absorption which is typical of B2V type, in contrast to the B5V spectral type. Repeat spectra have shown that this star is a radial velocity variable with a range in excess of 30 km/s. Also the profiles of the SiIV and the MgII resonance lines are strongly variable. It appears that this star may be a double-lined spectroscopic binary, although the interpretation of the spectra is not straightforward. The star B655 (B2V+shell) does not show shell features. The star HD37115 (B7eV+shell) shows sharp SiIV, C IV, and FeIII absorptions superimposed on the rotationally broadened photospheric spectrum. The SiIV and C IV absorptions are asymmetric, with blueshifted absorption extending out to several hundred km/s. MgII occurs in emission as a broad, roughly symmetric feature with a full width of 400 km/s. A quick survey of 3 new high resolution spectra of θ^1C Ori does not reveal any striking variability.

The variable T Ori was observed in low dispersion at V=10.3 (LWR only), and V=10.8, as determined by the IUE fine error sensor. The UV flux (2000-3000A) is found to have faded with the visual brightness, but by a larger factor of about 2.8. Recently, spectra were obtained at V=11.3, not yet analyzed. A definitive result awaits an SWP observation with the star bright (near V=10.0, which is the most common state).

A preliminary study of the absorption line spectrum of the interstellar gas shows that the C I column density is much higher toward LP Ori than toward any of the other stars in Table 1. Lines from the excited levels appear very strongly.

REFERENCES

Abt, H.A. 1979, Ap.J.,230,485.
Abt, H.A., Muncaster, G.W., and Thompson, L.A. 1970, A.J., 75,1095.
Bohlin, R.C., and Savage, B.D. 1981, Ap.J., 249,109.
Breger, M. 1976, Ap.J., 204,789.
Breger, M., Gehrz, R.D., and Hackwell, J.A. 1981, Ap.J., 248,963.
Brun, A. 1935, Pub. Obs. Lyon 1, Ser. 1, No.12.
Johnson, H.M. 1965, Ap.J., 142,964.
Levato, H. and Abt, H.A. 1976, PASP, 88,712.
Penston, M.V. 1973, Ap.J., 183,505.
Penston, M.V., Hunter, J.K., and O'Neill, A. 1975, M.N.R.A.S., 171, 219.
Savage, B.D., and Mathis, J.S. 1979, Ann. Rev. Astr. Ap., 17,73.
Strand, K. Aa. 1958, Ap.J., 128,14.
Walborn, N.R. 1981, Ap.J. Letters, 243,L37.
Walker, M.F. 1969, Ap.J., 155,447.
Wilson, O.C., Munch, G., Flather, E.M., and Coffeen, M.F. 1958, Ap.J. Suppl., 4,199.

Table 1 Stars Observed

Brun catalogue	HD/variable/BD	V	S.T.	E(B-V)	IUE Spectra
304	HD36866	9.3	A2Vb	.05	Low
388	V372 Ori	8.0	B9.5+A0.5	.16	Low
442	HD36939	9.0	B8.5Vb	.08	Low, High
502	HD36981	7.8	B4V	.10	Low, High
530	LP Ori	8.4	B2V	.38	Low, High
598	θ^1C/HD37022	5.1	O6:	.32	High(SWP)
608	HD37019	9.4	B9.5Vb	.05	Low
655*	BD-5°1318	9.7	B2:V+shell	.49	Low, High
734*	BD-5°1326	9.5	B9.5	.1	Low
747	HD37061/NU Ori	6.8	B0.5Vb	.57	Low, High
760*	HD37062/V361	8.2	B5Vb	.20	Low, High
767	NV Ori	9.9	F0-F6V	.07	Low
776	HD37060	9.4	A0Vb	.04	Low
786	V566 Ori	9.9	A0:V+shell	.09	Low
884*	T Ori	10.3-11.3	A3e	.4	Low
907	HD37115	7.1	B7eV+shell	.05	High

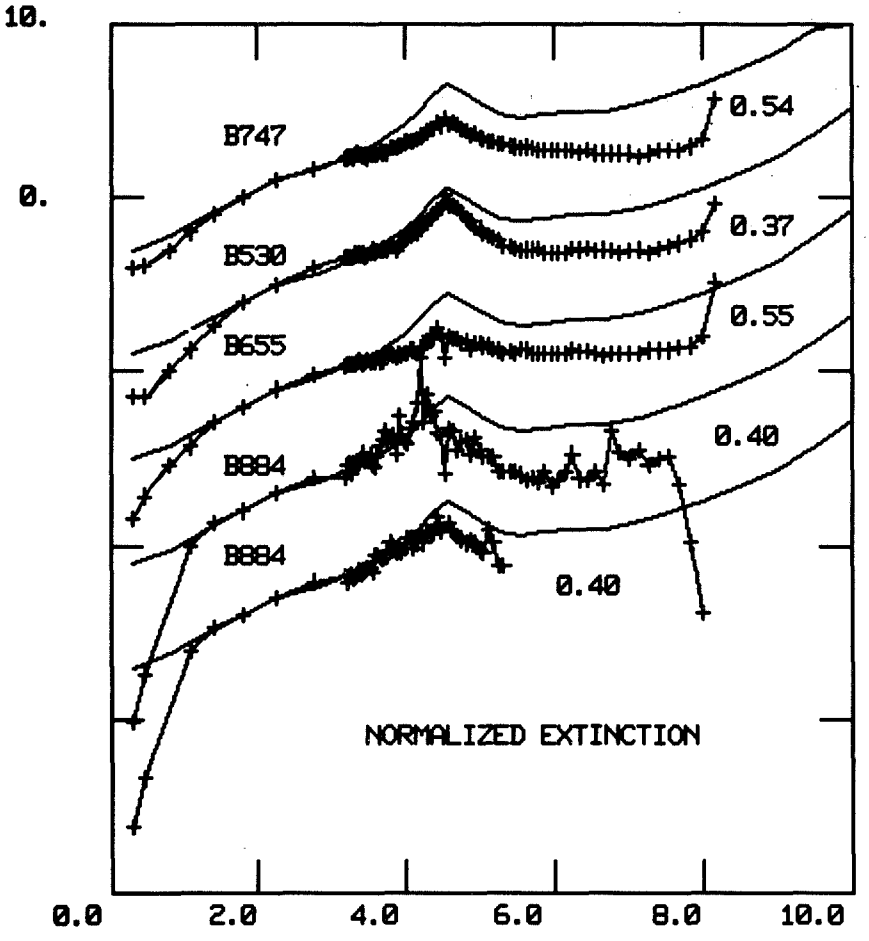

Figure 1. Normalized extinction curves for 4 stars from Table 1. The quantity $E(\lambda-V)/E(B-V)$ is plotted against $1/\lambda$. The observed curves (+) are identified by the Brun catalogue number and by the color excess relative to the unreddened standard star of the same spectral type. The solid curve is the average interstellar curve of Savage and Mathis. The curves have been shifted vertically to avoid overlapping between stars; the vertical scale is noted.

MASS LOSS FROM THE CENTRAL STAR OF THE PLANETARY NEBULA IC 3568

J. Patrick Harrington
University of Maryland

ABSTRACT

Low resolution IUE spectra of IC 3568 have shown several stellar P Cygni features. A high resolution spectrum has been obtained which shows a saturated N V λ1240 profile from which we find the terminal velocity of the stellar wind to be v_∞ = 1840 km/s. We also observe P Cygni features due to C IV λ1549, O V λ1371 and N IV λ1719.

The unsaturated O V λ1371 line seems best for determination of the mass loss rate. We obtain $\dot{M} \simeq 4 \cdot 10^{-9}$ $M_\odot$/yr. The level of ionization in the stellar wind appears to increase outwards.

We discuss the possible effects of such stellar winds from central stars on the surrounding nebulae.

INTRODUCTION

Because IC 3568 is a symmetric planetary nebula well suited for comparison with theoretical models, a number of low resolution IUE spectra of this object were obtained. The spectra showed that any C IV λ1549 emission - important for the nebular analysis - was masked by the strong stellar P Cygni feature. Thus we obtained a high dispersion spectrum (SWP 14868, 387 min) which clearly seperated the nebular and stellar components. Harrington and Feibelman (1982, hereafter HF) have made a detailed study of the nebula based on this data; here we consider the stellar features in the spectrum.

LINE PROFILES

Fig. 1 shows N V λ1240, the strongest stellar line. From its sharply defined blue edge we obtain the terminal velocity v_∞ = 1840 km/s. While the C IV λ1549 doublet (HF, Fig. 2) has a low residual intensity at intermediate velocities, the absorption rises gradually to the continuum level and does not extend as far as v_∞ defined by N V. The best line for evaluation of the mass loss is O V λ1371, which has a minimum residual intensity of 0.5 (Fig. 2). The N IV λ1719 line is weaker and noise makes its analysis less certain. The spectrum also shows weak lines of O IV λ1339, 1342 and Si λ1394, 1403. These are absorption features of less than 400 km/s in width, although there may be some emission in λ1342. They are presumably formed close to the photosphere and are not suitable for determination of the wind parameters.

Theoretical P Cygni profiles have been computed by Olson (1978) and by Castor and Lamers (1979, hereafter CL). We have used the latter because CL give tabular values useful for the computation of the overlapping doublets C IV λ1549 and N V λ1240. For these lines we used equation (25) of CL and for simplicity let both components of the doublet have the same f-value, which we set at half the total value.

CL consider velocity laws of the form $w(x) = (1 - 1/x)^{\beta}$, where $x = r/R_*$ and $w = v(r)/v_\infty$. We use $\beta = 1$ for all lines. Let F_i be the fraction of the element in the relevant stage of ionization, N_g the ground state population of the ion and N_ℓ that of the lower level of the P Cygni line. Then we assume there is a γ such that N_ℓ varies with distance as

$$(N_\ell/N_g)\ F_i = [(N_\ell/N_g)F_i]_{x=x_o}\ [x_o^\gamma/w(x_o)]\ w(x)\ x^{-\gamma}. \qquad (1)$$

This representation has its maximum value at $x_o = (\gamma + 1)/\gamma$. Then the corresponding optical depth is $\tau(w) = (\gamma + 1)\ (1 - w)^\gamma\ T$, where T is the total optical depth integrated over velocity. The profiles of CL are given as functions of β, γ and T.

The profiles of O V λ1371, C IV λ1549 and N IV λ1719 do not extend to v_∞ ($w = 1$), and we infer that N_ℓ drops rapidly with x for these lines. $\gamma = 4$ proved satisfactory. Fig. 2 shows the fit for the O V line.

For N V λ1240 we use $\gamma = 1$. Fig. 1 shows the fit for this case. A reasonable fit can also be obtained with higher optical depths, e.g., $\gamma = 2$ and $T = 100$. But in any case, the population of absorbers, N_ℓ, seems to persist further from the star for this ion.

The adopted parameters for the four lines considered are given in Table 1.

MASS LOSS RATE AND WIND IONIZATION

Equation (1) may be combined with the law of mass conservation to give the mass loss rate $\dot{M}$ as

$$F_i(x_o)\ \dot{M}(M_\odot/yr) = 8.68\cdot10^{-17}(R_*/R_\odot)[v_\infty(km/s)/1000]^2\ [\gamma/(\gamma + 1)]^\gamma$$
$$[\mu/f\ \lambda_o(\mu)\ A_E]\ T\ [N_\ell/N_g]^{-1}_{x=x_o}\ , \qquad (2)$$

where A_E is the abundance and μ the mean weight relative to hydrogen, λ_o the wavelength in microns and f the f-value. We use the nebular abundances as determined by HF: 2.9(-4), 5(-5) and 3.7(-4) for C, N and O, respectively. HF find that $R_*/R_\odot = 0.44\ d$, where d is the distance to the nebula in kpc, and $d = 1$ is adopted. Then for the N V and C IV lines, where ℓ is the ground state, $N_\ell/N_g = 1$ and we find $F_i\dot{M}$ as shown in Table 1.

O V λ1371 and N IV λ1719, however, arise from excited levels. We follow Castor, Lutz and Seaton (1981), and write N_ℓ as

$$[N_\ell/N_g]_{x_o} = (\omega_\ell/\omega_g)\ \exp\ [-E_{\ell g}/kT_r]\ D\ , \qquad (3)$$

where $E_{\ell g}$ is the energy difference between ℓ and the ground state and the quantity $D = [1 - (1 - x^{-2})^{1/2}]/2$ is the dilution factor. For $\gamma = 4$ ($x_o = 1.25$) $D = 0.2$. T_r is the brightness temperature of the photosphere at the wavelength of the $\ell \rightarrow g$ transition (λ630 for O V, λ765 for N IV). From the stellar atmosphere flux distribution adopted by HF, we obtain 47,700K for O V and 45,400K for N IV. Thus we obtain the values of $[N_\ell/N_g]$ and $F_i\dot{M}$ listed in Table 1.

If we assume $F_i(x_o) \simeq 1$ for O^{+4}, we obtain a minimum mass loss rate of $\dot{M} = 4\cdot10^{-9}\ M_\odot/yr$. In Table 1, "$F_i$" is the fractional ionization which is required if the other lines are to be consistent with this value of $\dot{M}$.

Table 1

λ(A)	Ion	γ	T	$E_{\ell g}$	$[N_\ell/N_g]_{x_o}$	$F_i \dot{M}(M_\odot/yr)$	"F_i"
1240	N V	1	10	0.0 eV	1	1.4(-9)	0.35
1371	O V	4	2	19.7	5.0(-3)	3.9(-9)	0.97
1549	C IV	4	30	0.0	1	3.5(-10)	0.09
1719	N IV	4	0.1	16.2	9.5(-3)	5.4(-10)	0.13

We note first of all that the higher stages of ionization, O V and N V, are more abundant than C IV and N IV. The weakness of the O IV and Si IV features are in line with this trend. We also observe that the smaller value of γ required to fit the N V line in comparison to C IV indicates that the level of ionization increases with distance from the star. The value γ = 4 required for the O V line is partly due to the dilution factor, an effect which does not apply to N V. Again, this is reinforced by the indications that O IV and Si IV are formed near the photosphere.

DISCUSSION

The mass loss rate we have obtained is comparable with, but somewhat smaller than, values found for the central stars of other planetary nebulae (e.g., Castor, Lutz and Seaton, 1981; Perinotto, Benvenuti and Cacciari, 1981). HF found that $L_* = 1100\ L_\odot$ for IC 3568, so that the "maximum" mass loss rate for a radiatively driven wind, $L_*/cv_\infty = 1.2 \cdot 10^{-8}\ M_\odot/yr$, is three times larger than $\dot{M}$.

The outward increase in ionization may be related to the results of HF with regard to the flux distribution of the central star. They found that the flux from an LTE model atmosphere with T_{eff} = 50,000K provides the necessary ionization and heating for the nebula except that the presence of a small amount of He^{+2} in the nebula requires the stellar flux to be 35 times greater than the model prediction for λ < 228A. As the density in the outflowing wind drops, this high frequency radiation may photoionize the gas. One possibility may be a wind model which has a corona at its base from which high frequency radiation could leak through the wind (e.g., Waldron, 1982).

EFFECT OF THE WIND ON THE NEBULA

From its size and expansion velocity, the age of this nebula is t_n = 2000 yrs. If the wind blows for t_n years, the mass lost is $\dot{M}t_n = 8(-6)\ M_\odot$, which is much less than the nebular mass $M_n = .005\ M_\odot$ (HF). The momentum deposited by the wind is $(\dot{M}t_n)v_\infty = .015\ M_\odot$ km/s, which is the same order as the present shell momentum, $M_n v_n = .04\ M_\odot$ km/s. Therefore the stellar wind will be of importance to the nebular dynamics.

The kenetic energy that the wind carries off each second is $L_w = \dot{M} v_\infty^2/2 = 1.4\ L_\odot$, much less than $L_* = 1100\ L_\odot$. However, the nebula is optically thin and converts only a fraction of the stellar radiation. For example, the luminosity radiated in the Hβ line is $L(H\beta) = 0.8\ L_\odot$. Thus there could be observable effects if a modest fraction of the wind energy were radiated at accessible wavelengths.

Pikel'ner (1968, 1973) has presented a theory for the interaction of stellar winds with planetary nebulae. The high velocity wind is stopped at the nebula by a strong collisionless shock, resulting in a thin ($n_H \simeq 1$ cm^{-3}) gas with a temperature of $5 \cdot 10^7$K. This gas cannot cool over the lifetime of the nebula. It approaches pressure equilibrium with the nebular shell, accelerating it outwards. Instabilities result, and as a consequence, globules of nebular gas ($n_H \simeq 10^4$ cm^{-3}) are detached and contained by the hot component. This would explain the small filling factors needed for many planetary nebulae.

This picture, however, may not be self-consistent. If we ask what will happen at the surface of the globules, we find that they must evaporate. Such evaporation has been discussed in detail by McKee and co-workers (Balbus and McKee, 1982, and references therein). Ordinary conduction will not apply; an elementary calculation (e.g., Spitzer, 1962) shows that the mean free path for stopping the hot electrons in the dense gas ($n_e = 10^4$ cm^{-3}) is of the order of 10^{15} cm, which is the expected size of the globules themselves. In the nomenclature of Balbus and McKee, the evaporation will be suprathermal. Such penetration of the nebular gas by the suprathermal electrons would lead to anomalous ionization and excitation effects. On the other hand, it provides a mechanism for cooling the hot gas which might completely alter the conditions postulated by Pikel'ner. This is clearly an area of inter--esting physics which has yet to be explored.

ACKNOWLEDGMENTS

This data was obtained as part of a program in collaboration with R. C. Bohlin, W. A. Feibelman and T. P. Stecher. I owe thanks to WAF for the data reduction and to S. R. Heap for some useful advice.

REFERENCES

Balbus, S.A. and McKee, C.F. 1982, Ap.J., 252, 529.
Castor, J.I. and Lamers, H.J.G.L.M. 1979, Ap.J. Supplement, 39, 481 (CL).
Castor, J.I., Lutz, J.H. and Seaton, M.J. 1981, M.N.R.A.S., 194, 547.
Harrington, J.P. and Feibelman, W.A. 1982, "The Planetary Nebula IC 3568: A Model Based on IUE Observations", Ap.J., submitted (HF).
Olson, G.L. 1978, Ap.J., 226, 124.
Perinotto, M., Benvenuti, P. and Cacciari, C. 1981, IAU Colloquium No. 59, "Effects of Mass Loss on Stellar Evolution", ed. C. Chiosi and R. Stalio, p 45 (D. Reidel Pub. Co.; Dordrecht, Holland).
Pikel'ner, S.B. 1968, Ap. Letters, 2, 97.
Pikel'ner, S.B. 1973, Ap. Letters, 15, 91.
Spitzer, L. 1962, "Physics of Fully Ionized Gases" (Interscience; New York).
Waldron, W.L. 1982, "Corona-Warm Wind Model for the X-ray Emission from Of Stars and OB Supergiants", U. of Wisconsin preprint No. 148.

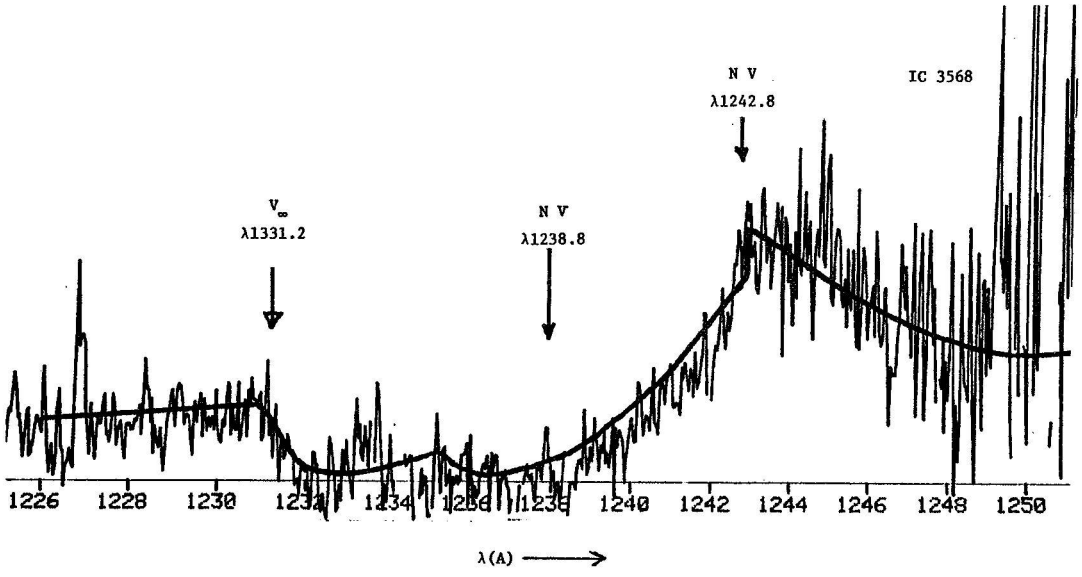

Fig. 1. The λ1240 N V duoblet in the spectrum of the central star of IC 3568. The data is from SWP 14868, orders 111 and 112. The heavy solid curve is a theoretical doublet profile computed according to equation (25) Castor & Lamers (1979), using their tabulated profile for $\beta = 1$, $\gamma = 1$ and $T = 10$.

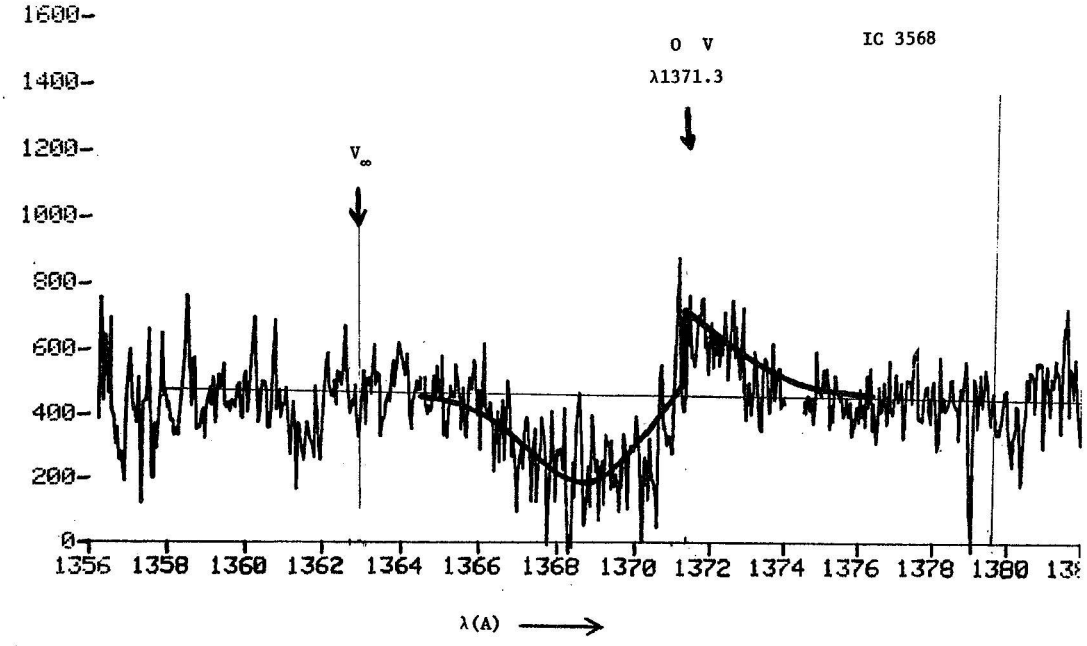

Fig. 2. The λ1371 O V line in the central star of IC 3568. Data from SWP 14868. The heavy curve is the theoretical profile of Castor and Lamers (1979) for $\beta = 1$, $\gamma = 4$ and $T = 2$.

ON THE UV VARIABILITY OF LSI+61°303 (≡ GT 0236)

E.G.Tanzi[1], G.F.Bignami[1], P.A.Caraveo[1], L.Maraschi[1,2], F.Sormani[2], A.Treves[1,2]
1) Istituto di Fisica Cosmica del CNR, Milano, Italy
2) Istituto di Fisica dell'Università, Milano, Italy

INTRODUCTION

LSI+61°303 is the optical counterpart (m_V=10.8) of the periodically variable radio source GT 0236+610 (P=26^d.52±.04; Gregory and Taylor, 1978; Taylor and Gregory, 1981). A binary interpretation of the period is supported by spectroscopic observations (Hutchings and Crampton, 1981). Soft X-ray emission has been detected with the Einstein Observatory with F(0.5-4.5 keV)=2.1x10^{-12} erg/cm^{2}s (Bignami et al. 1981). The object is located within the error box of the ∿100 MeV γ-ray source 2GC 135+01 (Swanenburg et al., 1981) and of the ∿MeV γ-ray source reported by Perotti et al. (1980).

Models invoking a young pulsar in a binary system or production of high energy particles in a magnetized accretion disk around a collapsed object have been proposed (Maraschi and Treves, 1981; Taylor and Gregory, 1981).

The optical-UV spectrum is complex. A fit to the continuum from 1200 to 5500 Å with Kurucz (1979) model atmospheres suggests a classification B1-2 Ib (Maraschi et al., 1981). However the line spectrum indicates rather a BOV star with equatorial disk (Gregory et al., 1979; Hutchings and Crampton, 1981). In order to account for the observed continuum, the emission contributed by the disk should be important at λ>2000 Å, and larger than in other Be stars. Because of the peculiar binary nature of the system, an accretion disk around a compact companion could also contribute to the optical-UV spectrum.

Since previous ultraviolet observations (Hutchings, 1979; Maraschi et al., 1981) indicated substantial variability of both the lines and the continuum, a program of observations with IUE was undertaken. The results obtained thus far are given here as a progress report; the observational program is continuing.

OBSERVATIONS

LSI+61°303 was observed by us in 1980 and 1981 in the low resolution mode (Δλ∿6Å) with both the short wavelength (SWP) and the long wavelength (LWR) camera of IUE. In addition, spectra SWP 2127 and SWP 2951 (Hutchings 1979) were retrieved from IUE archives. A journal of the observations is given in Table 1.

All data have been processed with the Interactive Processing System of the European Southern Observatory from the standard line-by-line extracted spectrum, with the calibration curve of Bohlin et al.(1980). Spectra SWP 2127 and SWP 2951 have been corrected for errors in the ITF function by applying a variant of the method of Cassatella and Ponz (1979).

In Fig.1, integral fluxes in six wavelength intervals are reported against the radio phase of Taylor and Gregory (1981). The scatter of the short wavelength points is compatible with the long term photometric accuracy of IUE (Bohlin, 1980; Bohlin and Holm, 1981). On the other hand, in the long wavelength range, the exposure LWR 8901, taken at phase 0.12, appears to be 20% weaker than all other spectra. This effect, which, as already noted in Maraschi et al, (1981) is more conspicuous at longer wavelenfths, seems real. The observed variation is comparable with that found in the optical historical light curve of Gregory et al., (1979).

In the X-rays, two observations taken 561 days apart with the Imaging Proportional Counter and with the High Resolution Imager respectively on board the Einstein satellite are consistent with the same flux from the source, within the $\sim$30% accuracy with which the two instruments can be compared. Within each exposure ($\sim$1 h) no evidence of rapid variability is apparent.

The UV line spectrum exhibits strong emission features; the most readly identificable being NV($\lambda\lambda$1238, 1242), SiIV ($\lambda\lambda$1393, 1402), CIV ($\lambda\lambda$1549, 1551) and Mg II ($\lambda\lambda$2795, 2802). Inspection of the line-by-line extracted spectrum reveals that the two strong emissions at λ1750 in SWP 2951 and at λ1920 in SWP 2127 (Hutchings, 1979) are most probably due to flaws. Variability is observed in the strength of NV and Si IV and in the strong P Cygni profile of C IV (Fig. 2) and Mg II.

DISCUSSION

Out of six long and six short wavelength observations, one spectrum exhibits a significant photometric variation: $\gtrsim$20%. Interpreting the continuum as due to superposition of an early B main sequence star plus a gaseous component contributing at λ>2000 Å, the wavelength dependence of the variation suggests that it derives from the latter component. The data (see Fig.1) indicate that if the observed variation is phase dependent, a minimum should occur between phases 0.8 and 0.2. However, since the variation is observed in only one spectrum, it may well be erratic. Extended observations from ultraviolet to infrared wavelengths are needed in order to clarify the phase and wavelength dependence of the variation.

ACKNOWLEDGEMENTS

We are grateful to the European Southern Observatory for the use of their Interactive Image Processing System.

REFERENCES

Bignami, G.F., et al., 1981, Ap.J.(Letters), 247, L85
Bohlin, R.C., et al., 1980, Astr.Ap. 85, 1
Bohlin, R.C., and Holm, A.V., 1981, ESA IUE Newsletter No.11, p.18
Cassatella, A. and Ponz, D., 1979, ESA IUE Newsletter No.4, p.5
Gregory, P.C. and Taylor, A.R., 1978, Nature 272, 704
Gregory, P.C. et al., 1979, A.J. 84, 1030
Hutchings, J.B., 1979, PASP 91, 657
Hutchings, J.B. and Crampton, D., 1981, PASP, 93, 486
Kurucz, R.L., 1979, Ap.J. Suppl., 40, 1
Maraschi, L. and Treves, A., 1981, M.N.R.A.S. 194, 1p
Maraschi, L., Tanzi, E.G. and Treves, A., 1981, Ap.J. 248, 1010
Perotti, F. et al., 1980, Ap.J. (Letters) 239, L49
Swanenburg, B.M., et al., 1981, Ap.J. (Letters) 243, L69
Taylor, A.R. and Gregory, P.C., 1981, preprint

TABLE 1.- Observations of LSI + 61°303

Image Number	Exp.Time (minute)	Date	Start	Julian Day 2,440,000+	Radio Phase	Ref.
SWP 2127	30	27.07.78	19:15	3717.30	.217	1
SWP 2951	90	13.10.78	13.17	3795.05	.149	1
LWR 8901	35	27.09.80	22:41	4510.40	.122	2
SWP 10249	120	29.09.80	19:27	4512.31	.195	2
LWR 8914	67	29.09.80	21:30	4512.40	.195	2
LWR 9582	45	26.12.80	13:53	4600.08	.505	3
SWP 10896*	120	26.12.80	14:43	4600.11	.505	3
LWR 9583	45	26.12.80	16:47	4600.20	.509	3
SWP 14807	106	25.08.81	00:02	4841.50	.608	3
LWR 11791	40	16.10.81	20:28	4894.35	.601	3
LWR 11811	45	20.10.81	18.34	4898.27	.749	3
SWP 15300	138	20.10.81	19.29	4898.31	.750	3

* microphonic noise in the range 1200-1500 Å
References to Table : 1) Hutchings, 1979
2) Maraschi et al., 1981
3) Present work

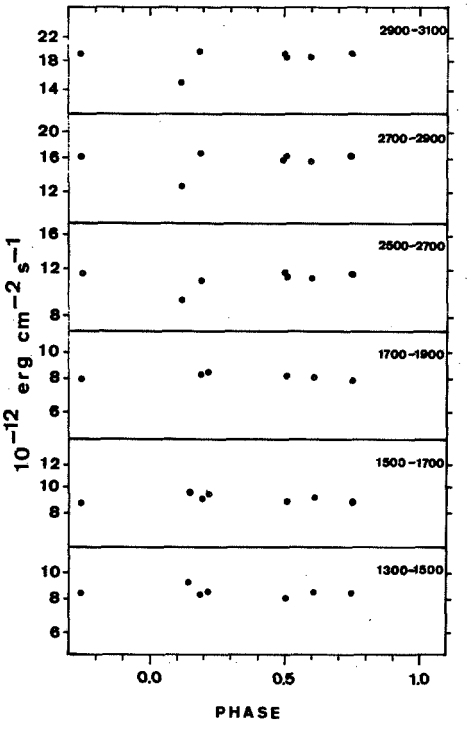

Fig. 1 Broad band fluxes as a function of radio phase of LSI +61.303. The wavelength intervals are indicated in each frame.

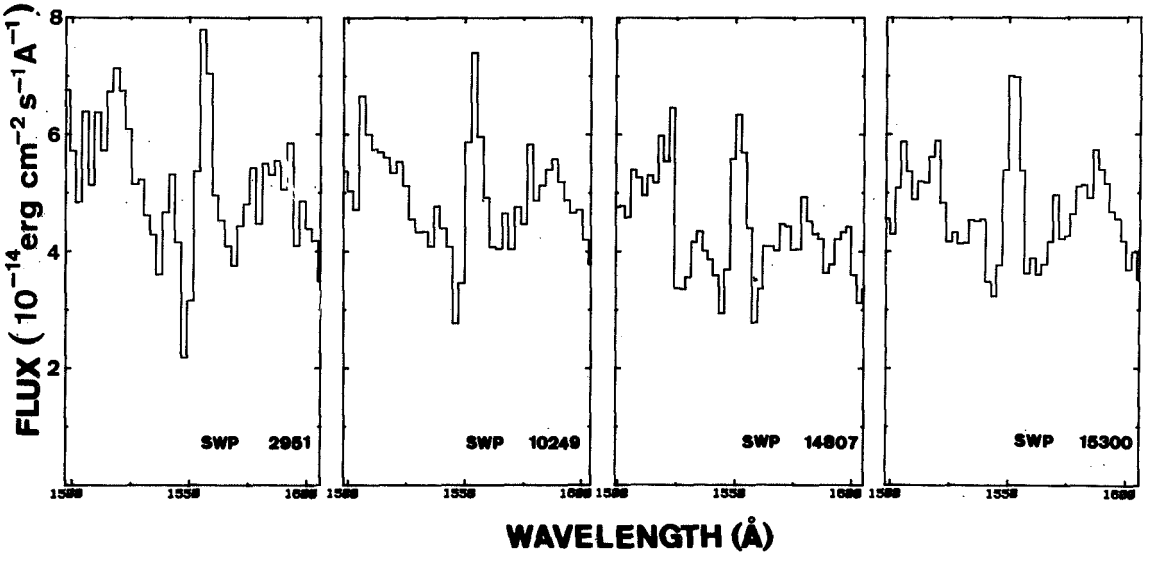

Fig. 2 Profiles of C IV (λ1550) at different epochs.

AN ALTERNATIVE MODEL FOR THE MANTLES OF HOT STARS

Anne B. Underhill
Laboratory for Astronomy and Solar Physics
NASA/Goddard Space Flight Center

ABSTRACT

The customary model of the mantle of a Wolf-Rayet star consists of a spherically symmetric wind which has a density large enough to give a rate of mass loss of the order of 3×10^{-5} solar masses per year. This model leads to three difficulties: (1) it requires 10 to 50 X the amount of outward directed momentum available in the radiation field of the star; (2) it implies the action of an efficient mechanism of unknown origin to supply a significant amount of outward momentum to layers of the wind which are opaque at all wavelengths; (3) it implies the action of an unknown force which is more efficient at causing mass loss from Wolf-Rayet stars than it is from O stars even though the effective temperatures, thus the radiation densities in the mantles of Wolf-Rayet stars, are smaller than those of O stars.

An alternative model, composed of magnetically supported loops and a low-density wind, it proposed. The properties of the model are derived and it is shown that the model is capable of explaining the observed radio fluxes from Wolf-Rayet stars and a Wolf-Rayet-type line spectrum. The alternative model implies a rate of mass loss typically less than 10^{-6} solar masses per year. Consequently, mass loss is of no significance for the evolution of Wolf-Rayet stars. The alternative model is also useful for interpreting the spectra of O stars and B-type supergiants. It implies low rates of mass loss from these types of star, suggesting that mass loss is of no significance for massive stars during their first stages of evolution.

The full text will be submitted for publication in the Astrophysical Journal as a paper entitled "An Alternative Model for the Atmospheres of Wolf-Rayet and O stars."

A SEARCH FOR UV LINE VARIABILITY IN R136a

Dennis C. Ebbets, Blair D. Savage and Marilyn R. Meade
Washburn Observatory, University of Wisconsin-Madison

INTRODUCTION

R136a is the brightest object in the central cluster of stars in the 30 Doradus nebula. Optical imaging and ultraviolet spectroscopy show that a luminosity $L_*/L_\odot \sim 10^8$ originates in a volume less than 0.1 pc across. A very tight cluster of ~30 luminous O and WR stars could produce this energy. An alternative interpretation is the possibility that a single supermassive ($200 < M_*/M_\odot < 3000$) object dominates the light (Feitzinger et al. 1980; Cassinelli, Mathis and Savage 1981). The visual spectrum can be classified as WN 4.5. A common characteristic of WN spectra is variability of the emission lines, especially He II λ4686. No convincing evidence for visual variability has been presented, although the literature is rather sparse. We have been observing R136a with IUE since 1978, and thought it worthwhile to search for variability in the ultraviolet lines. The detection of variability would favor the single star hypothesis. The addition of many spectra has produced a composite of high quality, from which line strengths and profiles can be accurately measured.

DATA

Five low and six high resolution SWP spectra were obtained during the course of several Wisconsin IUE programs. The low resolution spectra were processed using the Washburn Extraction Routine (Koornneef and de Boer 1979) which corrects for the early ITF error. Small adjustments to the wavelength scales were determined by aligning interstellar features. Shifts of up to ± 4 Å and ± 0.06 Å were applied to low and high dispersion observations, respectively. After resampling onto a uniform wavelength grid, coaddition produced the composite spectra. Separate mean spectra were formed from the small and large aperture low dispersion observations. A high resolution mean spectrum was also produced using the Goddard extracted data corrected for echelle ripple. Because the large aperture spectra are contaminated at about the 30% level by other sources in the crowded field, we have concentrated our attention on the low resolution small aperture data.

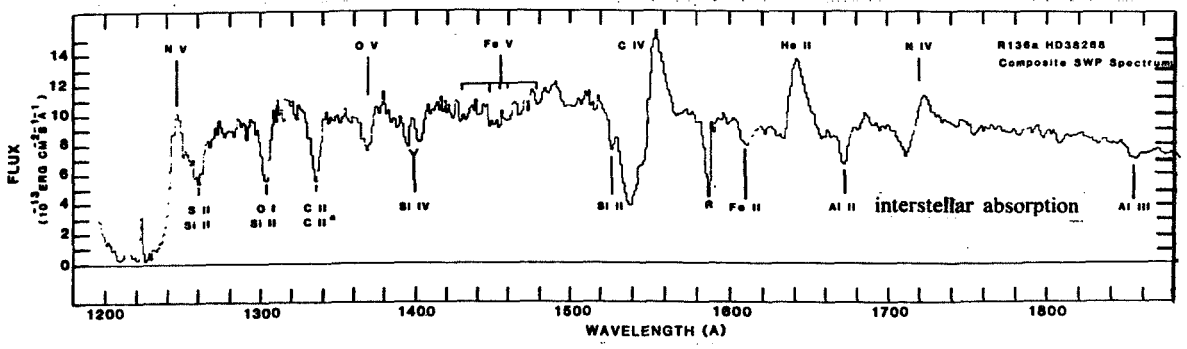

Figure 1. Coaddition of five low resolution, small aperture spectra. The indicated flux does not allow for the small aperture light loss, which usually amounts to a factor of 2.

THE STELLAR SPECTRUM

The prominant stellar features in Fig. 1 are lines of O V, C IV, He II and N IV. N V is blended with interstellar Ly α, and the weak stellar Si IV if present, is also obscured by interstellar absorption. The line profiles are shown in more detail in Figure 2, with equivalent widths and edge velocities listed in Table 1. The C IV resonance line, which shows the steepest edge presumably gives the best estimate of the terminal velocity of the stellar wind. This spectrum can be compared to that of other early WN type stars (Garmany and Conti 1982; Nussbaumer et al. 1982). In stars earlier that WN5, O V is a conspicuous P Cygni feature, Si IV is faint, and C IV is only weakly visible. N IV is faint at WN3, but strengthens in WN4 and later types. He II λ1640 is weaker than in most WN stars. Garmany and Conti have pointed out that the strength of this line is strongly correlated with λ4686, and inversely correlated with the abundance of hydrogen. In R136a both λ1640 and λ4686 are relatively weak, and hydrogen Balmer lines are present in absorption (Ebbets and Conti 1982). The strengths and ratio of He II emission lines are in good agreement with other WN stars in which H/He > 1. In general, the presence and strengths of lines in the UV spectrum of R136a are very similar to other Galactic and LMC early type Wolf Rayet stars, and in complete agreement with the visual classification of WN4.5. There are no features in the UV spectrum which suggest contributions from stars of other spectral types. There is apparently a significant abundance of hydrogen in the outer envelope of this object.

The line profiles are very well determined, and can be compared with theoretical P Cygni profiles (Klein and Castor, 1978; Castor and Lamers, 1979; Olson 1981). Although we cannot be certain about the abundances or ionization structure, we can assume that the same velocity law must apply to all of the lines. From the depths of the P Cygni absorption component, the radial optical depths (as defined by the above authors) are $\tau_{rad} \sim 1$ for O V and N IV, and $\tau_{rad} \sim 3$ for C IV. The velocity shift of the absorption minima, and the overall shape of the profiles suggest a steep velocity law. Profiles calculated from $v(r)/V_\infty \approx (1-1/x)^\beta$ where $x = r/R_*$ and $\beta = 1/2$ appear to give the best representation of the observations. In fact, a steeper velocity law ($\beta<1/2$) might give an even better fit. The He II λ1640 profile also suggests a steep law. He is almost entirely He^{++} in the winds of hot stars (Klein and Castor 1978), so that emission is produced mainly by recombination. Since the line emissivity is proportional to the density squared, the densest regions (closest to the star in spherical outflow) produce the most emission. Since the λ1640 emission is visible to $\sim 0.7\ V_\infty$, we infer that the wind accelerates very rapidly. Similar considerations apply to the O V and N IV lines. Their lower levels are populated by photoexcitation, which decreases rapidly with increasing distance from the star, due largely to geometrical dilution of the radiation field (Olson 1981). Since their absorption components are visible to over $\sim 0.7\ V_\infty$, large velocities must be reached close to the star.

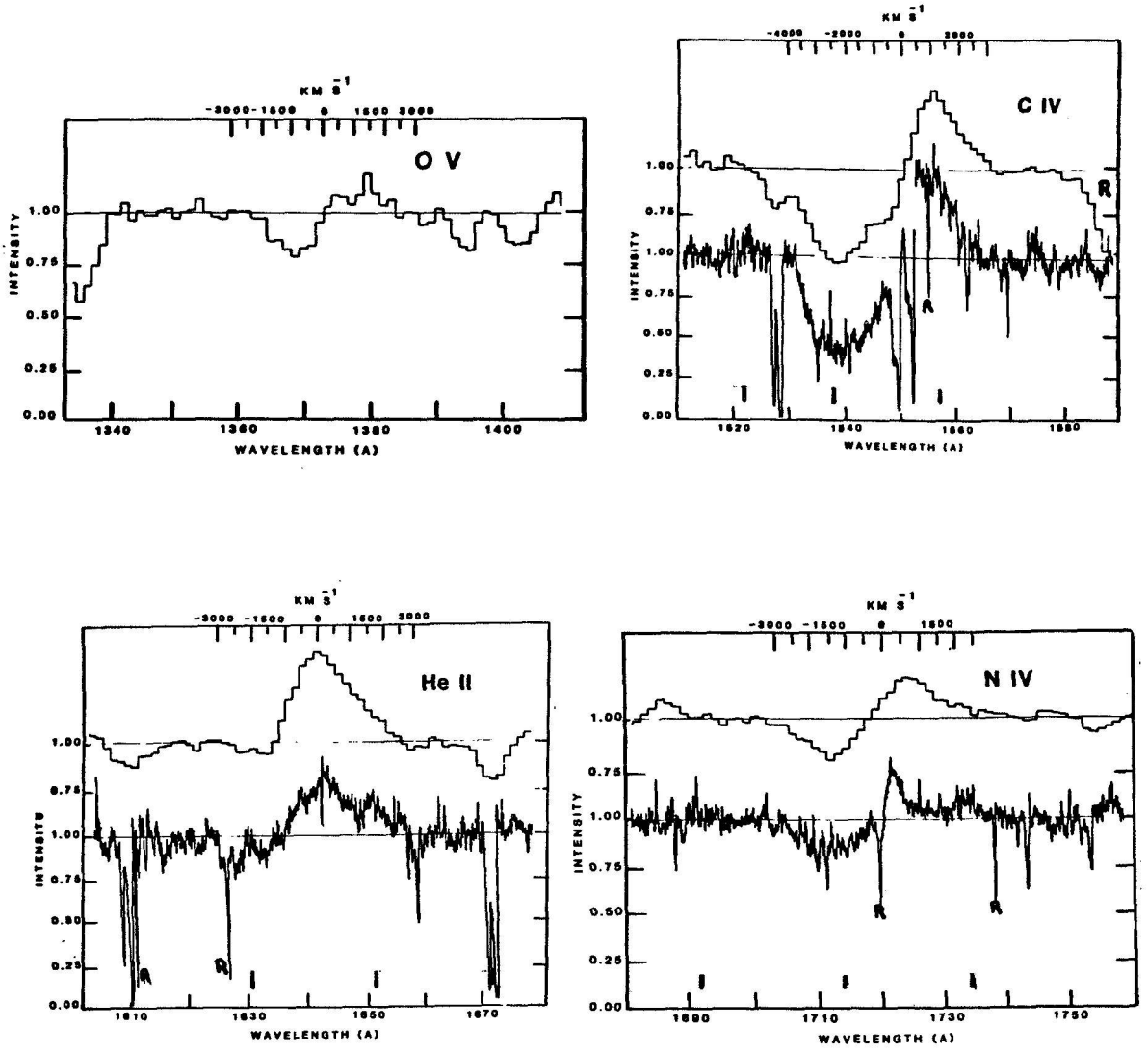

Figure 2. Line profiles from the composite spectra. The low resolution small aperture and high resolution large aperture data are plotted on the same scales. The zero point of the velocity scale is set at +280 km s^{-1} heliocentric. Nearby sources in the crowded field contaminate the high dispersion large aperture data with approximately 30% of the total light. This symbol "R" indicates a Reseau. The small tic marks locate transitions from one echelle order to the next.

TABLE 1: STELLAR LINE PARAMETERS

ION	λ_o(A)	$W_{\lambda ABS}$(A)	σ_{ABS}	$W_{\lambda EM}$(A)	σ_{EM}	V_∞(km s^{-1})
O V	1371.29	1.66	---	0.60	---	2100
C IV	1548.19	8.09	0.32	4.94	0.44	3600
	1550.76					
He II	1640.4	0.47	---	5.88	0.69	2200
N IV	1718.55	1.62	0.40	1.16	0.50	2720

Note: σ = standard deviation of the individual observations with respect to the mean.

POSSIBLE VARIABILITY

Visual inspection of the spectra did not reveal any gross changes in any of the emission or absorption lines. Superposition of the C IV and N IV profiles showed that no changes in the absorption depth, terminal velocity or emission strength had occurred. The He II line showed larger variations, so a more careful analysis was performed. Only the small aperture data was used, in order to minimize the problem of contamination by other stars in the field. The five independent profiles, and their composite are shown in figure 3. We computed ratio and variance spectra by comparing each observation to the composite at each wavelength. These procedures give a more objective indication of the noise in the spectrum, and the overall photometric reproducibility. The absence of variability is confirmed for C IV and N IV. The variance across the He II line was twice the value in the neighboring continuum, and clearly greater than that of the other spectral features. As seen in Table 1, the standard deviation of the He II equivalent width is the largest. Since this line lacks a strong absorption component, its emission is the broadest in the spectrum, and most sensitive to the continuum placement. A random error of $\pm$3% in the adopted continuum level would account fully for the range of equivalent widths of all lines. Even the higher quality of the composite spectrum does not allow the continuum to be unambigously located more precisely than this. We conclude that on the basis of the five small aperture observations there is some objective evidence that changes at about $\pm$10% in the strength and profile of He II λ1640 have occurred. Slight differences in satellite focus and pointing might introduce apparent variability due to changes in the amount of contamination from nearby sources. It is difficult to estimate the importance of this effect. We have not detected any variability in either the C IV or N IV lines.

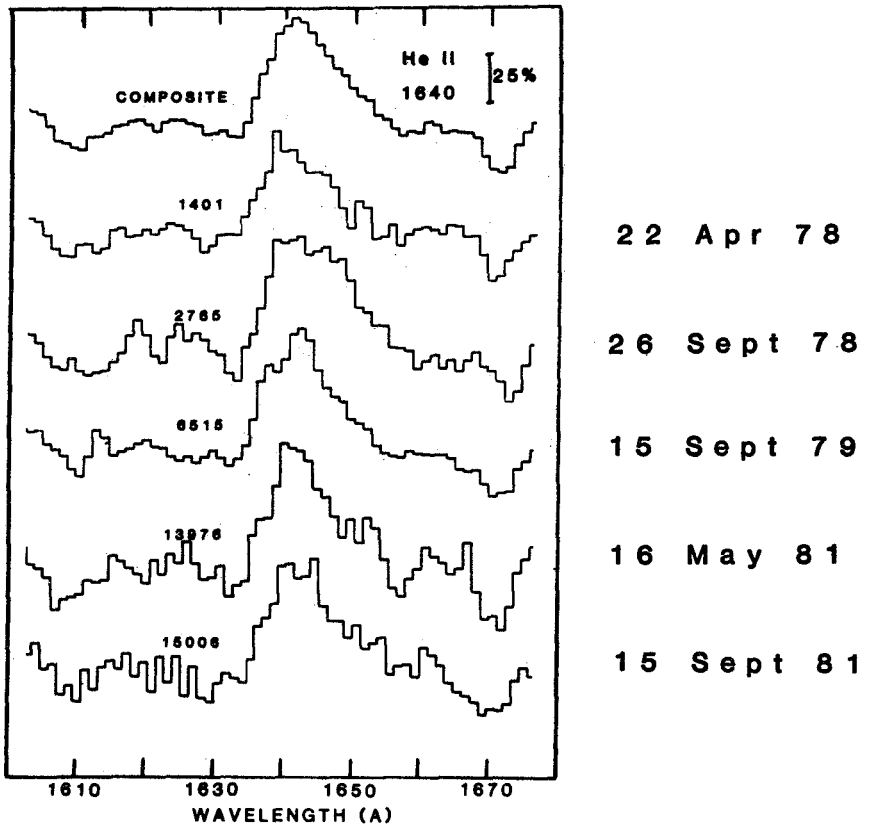

Figure 3. Individual profiles of He II λ1640 and their mean. The numbers to the left of the emission identify the SWP images. This was the only line that showed an indication of variability during the time interval April 1978-September 1981. The changes if real are in the width and total strength of the emission.

REFERENCES

Cassinelli, J.P., Mathis, J.S., and Savage, B.D. 1981, Science, 212, 1497.
Castor, J.I. and Lamers, H.J.G.L.M. 1979, Ap.J.Suppl.Ser., 39, 481.
Ebbets, D.C. and Conti, P.S. 1982, "The Optical Spectrum of R136a" submitted to Ap.J.
Feitzinger, J.V., Schlosser, W., Schmidt-Kaler, Th. and Winkler, C. 1980, Astron.Astrophys., 84, 50.
Garmany, C.D. and Conti, P.S. 1982 in Wolf-Rayet Stars: Observations, Physics, and Evolution, ed. C. de Loore and A.J. Willis, (Dordrecht: Reidel).
Klein, R.I. and Castor, J.I. 1978, Ap.J., 220, 902.
Koornneef, J. and de Boer, K.S. 1979, NASA IUE Newsletter #5.
Nussbaumer, H., Schmitz, W., Smith, L.J., and Willis, A.J. 1982, Astron. Astrophys.Suppl.Ser., 47, 257.
Olson, G.L. 1981, Ap.J., 245, 1054.

ULTRAVIOLET OBSERVATIONS OF NOVA AQUILA 1982.

M.A.J.Snijders[1], M.J. Seaton[1] and J.C. Blades[2]

1. Department of Physics & Astronomy, University College London, U.K.
2. Rutherford Appleton Laboratory, U.K.

ABSTRACT

A bright nova in Aquila was announced by Honda on 1982 Jan 27.85 UT, with a visual magnitude of 6 to 7 at discovery. It was declared a European Target-of-Opportunity and, as a result, we have obtained a number LWR and SWP spectra of the object with the IUE. Observations made during 24 Feb and Mar 2 show that the nova has a heavily reddened spectrum, $E(B-V) = 0.55 \pm 0.15$, and a complex short-wavelength spectrum with both narrow emission features and broad absorption troughs, indicating terminal velocities as high as 10000 km/s. Both the continuum flux and the absorption line profiles changed between the two observations. On Feb 24 short period variations were also present. Complementary ground-based and ultraviolet observations are planned for the future.

OBSERVATIONS

At discovery the nova was situated well inside the sun constraint of the IUE satellite and hence the important early decline could not be observed. Because the object was situated so close to the sun (28° at discovery) ground-based spectrographic observations were also very difficult at first. Indeed, the only monitoring we know of was that obtained by a few members of the American Association of Variable Star Observers (IAU telegrams and J.Mattei private communication). Their work shows that the nova initially had a fast decline in the visible (2.5 mag in the 8 days after discovery), which then slowed down to a 3.5 mag decline over the next 38 days. On Mar 21 the visual magnitude was about 13. A finding chart based on the IUE FES 5 kb field is shown in Fig. 1, along with the nova's approximate light curve (Fig. 2) which was derived from a number of observations from different sources.

The ultraviolet observations obtained sofar were made during Feb 24, Mar 2 and Mar 21, a detailed log of the observations will be published elsewhere. The object became again constrained for the IUE between the second and third observing shift. FES magnitudes were measured and gave on average, 10.8 (Feb 24.4) and 11.7 (Mar 2); on Feb 24 the FES measurements showed that the optical flux probably varied on a time scale of hours.

An astrographic plate of the nova field was obtained at the Royal Greenwich Observatory on Feb 22 by R.W. Argyle and R. Wood who reported the first accurate position of the nova, with a formal standard error of 0".4 in each coordinate. Accurate positions of nearby offset stars accompany Fig. 1.

PRELIMINARY RESULTS

The combined IUE spectra give a good continuum from which we have made an estimate of the extinction using the 2175 Å extinction feature. It yields E(B-V)=0.55 $\pm$ 0.15. The continuum after dereddening varied as $f_\lambda \sim \lambda^{-2}$ from atleast 1400 Å to 6000 Å.

The short wavelength region is quite remarkable (Fig. 3). It shows on Feb 24:

i. Fairly narrow emission features due to intercombination and permitted lines, typical FWHM 2000 km/s.

ii. Broad absorption between -340 and -4000 km/s in Al III λ1860, C IV λ1549, N V λ1240 and possibly Si IVλ1399. This component, system a, shows up only in permitted resonance lines.

iii. Broad absorption with velocities up to -10000 km/s, system b. It is definitly present in N IV λ1718, C IVλ1549 and Si IV λ1399, it is possibly present in the C II λ1335 and O Vλ1371 lines. The terminal velocity of system b varied during the observations of Feb 24 but system a showed no changes.

The FES magnitudes show strong evidence for variability on 24 Feb which is confirmed by the IUE spectra. The ultraviolet fluxes decreased between the beginning and end of the Feb 24 shift by up to 25% with the largest decrease at the longest wavelength. Between Feb 24 and Mar 2 the optical and ultraviolet fluxes decreased by a factor 2 to 4. Between both dates the system b aborption troughs showed rapid changes.

The velocities in the emission lines and system a are in line with those found in classical novae. However the very large velocities found in system b are unusual: up to 3000 km/s is normal for fast novae, and 4000 km/s has been observed occasionally. Other objects in the 10000 km/s class are type II supernovae! Unless the explosion happened long before the nova was detected (which is possible given its proximity to the sun) the object is simply too faint to be a supernova. Additionally, the presence of many strong Nitrogen lines suggest that this element could be over-abundant, a typical signature of classical novae.

We are grateful to the members of the American Association of Variable Star Observers who provided us with finding charts and magnitudes of the nova, to Drs. Argyle and Wood for their astrometric measurements, and to the co-chairmen of the joint European time allocation committee for providing the IUE time.

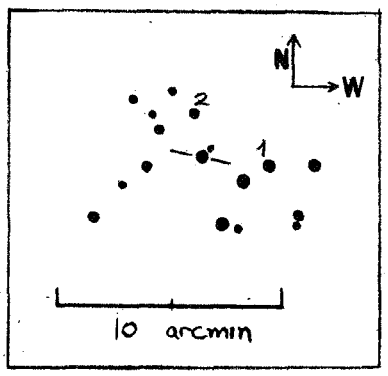

1950 coordinates for objects in the field are:

Nova α $19^h\,20^m\,50^s.15$, δ $+2^\circ\,23'\,35''.3$

Ref 1 $19^h\,20^m\,36^s.94$, δ $+2^\circ\,22'\,54''.8$

Ref 2 $19^h\,20^m\,51^s.21$, δ $+2^\circ\,25'\,26''.0$

from R. Wood (personal communication).

Figure 1. Finding chart for Nova Aquilae, 1982, based on the FES.

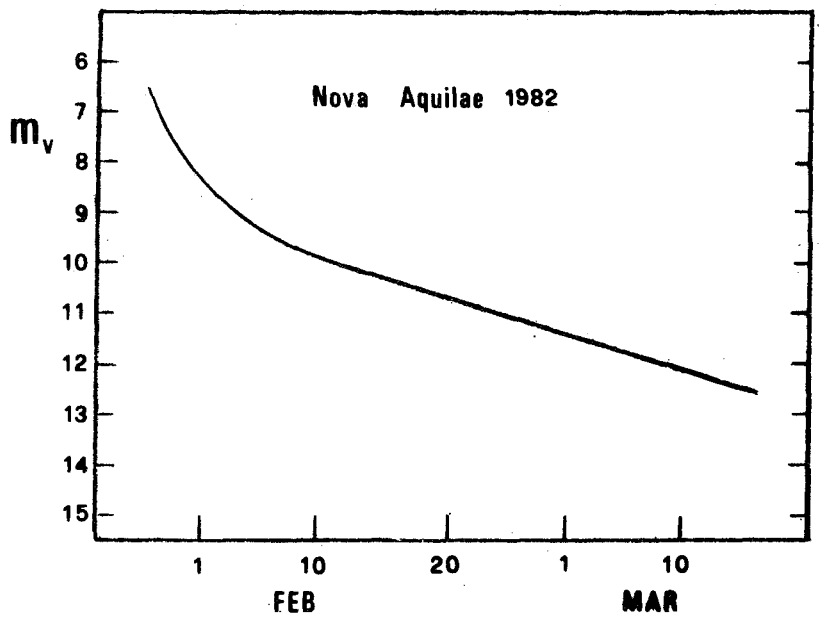

Figure 2. A light curve for the nova.

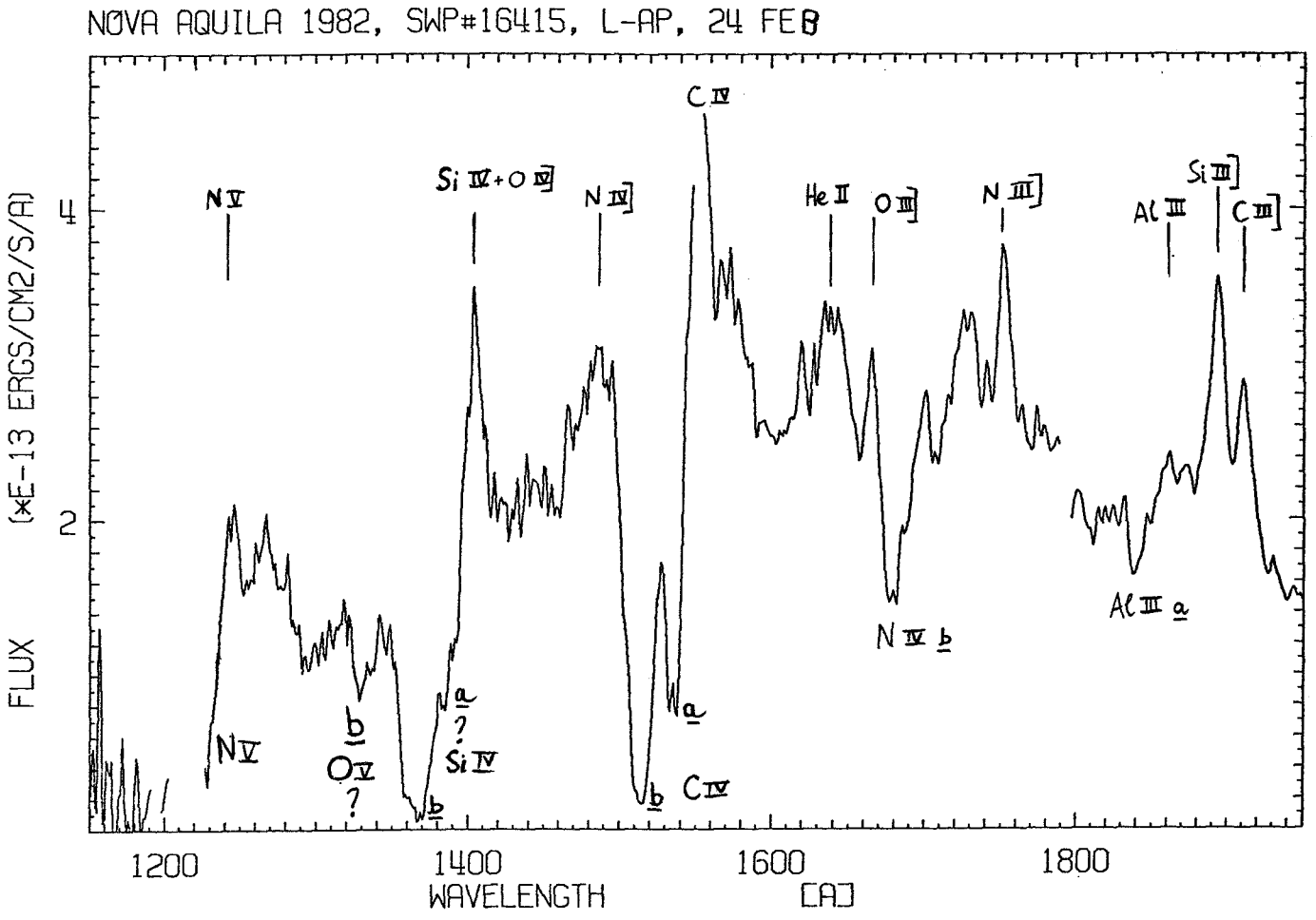

Figure 3. A SWP spectrum of Nova Aquilae, 1982 obtained on Feb 24.34 UT

THE IUE OBSERVATORY
A STATUS REPORT

A. Introduction

For the benefit of symposium participants interested in a review of the current status of the IUE, the observatory staff has compiled this summary discussing various aspects of our operation. In a word, the outlook for the IUE in the foreseeable future is excellent. The scientific program continues to span the breadth of ultraviolet astronomy. Record numbers of proposals for both U.S. and VILSPA observing time were received this year. NASA has approved a record 162 programs for the fifth year of U.S. operations, just begun. These programs will involve 107 different principal investigators from 55 institutions. Altogether some 266 scientists will participate in obtaining and reducing new IUE data in support of these programs. In 1981, observational papers dealing with IUE data and appearing in the principal refereed journals numbered 161. Since 1978, the IUE has contributed to nearly 1000 papers in both the refereed and unrefereed literature.

B. The Spacecraft

In spite of problems in a few areas, the spacecraft still performs very satisfactorily. A synopsis of subsystem health follows.

Hydrazine Subsystem: Approximately 50 years worth of fuel remains for orbit- maintaining maneuvers and momentum wheel unloads. Subsystem temperatures are a concern, but they are not expected to limit normal operations for the next two years or more.

Power Subsystem: The 25 percent degradation in solar array capacity over the last four years is significantly less than predicted. The performance of the spacecraft batteries is also exceeding design predictions. Operational restrictions imposed by power limitations are expected to remain fixed for the next couple of years.

On-Board Computer (OBC): The OBC is fully operational. Improvements to its software have largely eliminated computer crashes and the corresponding loss of observing time.

Attitude Control Subsystem: Of the initial set of six gyros, four continue to function normally. Three gyros are required for attitude control.

C. The Spectrographs and Detectors

With a few exceptions the spectrographs are in approximately the same condition they were in during their commissioning in April, 1978. There are no indications of imminent failure in any component.

The performance of the IUE detectors is monitored regularly by observatory personnel. The status of each detector is summarized as follows.

Long Wavelength Redundant (LWR) camera: The LWR camera functions without operational problems. An analysis of low dispersion LWR spectra, however,

shows that between mid-1980 and mid-1981 the camera's sensitivity dropped at some wavelengths by 4 to 5 percent from a previously stable value. An analysis of high dispersion spectra now in progress indicates a 10 to 20 percent loss of sensitivity at the long wavelength end of some orders.

Long Wavelength Prime (LWP) camera: The LWP camera has suffered from an occasional malfunction in the scan control logic that causes piecemeal readouts of the detector. Control software still under development has had some success in detecting these malfunctions and rendering them harmless. As a result, but with some risk of data loss, the camera is available for use by Guest Observers upon approval by the Project Scientist. The LWP camera's sensitivity is about 20 percent greater than that of the LWR camera near 2800 A, but the LWP is only about two-thirds as sensitive as the LWR near 2200 A. The camera's calibration, though progressing (at VILSPA), remains in a comparatively primitive state. There is a one hour penalty in observing time to change from the LWR camera to the LWP camera.

Short Wavelength Prime (SWP) camera: The SWP camera functions without operational problems. The camera experienced a 6 to 8 percent decrease in sensitivity in 1978 as indicated from analysis of low dispersion spectra. Its sensitivity has since remained stable.

Short Wavelength Redundant (SWR) camera: The SWR camera has suffered from intermittent and increasingly frequent failures in the grid voltage of its read section. There are no plans to use this camera.

Fine Error Sensors (FESs): The FES is the instrument used in target location and guiding. The prime FES suffers from an intermittent 1 to 5 arc second electronic offset. The frequency of occurrence of this offset is minimized by operational procedures. The backup FES, although believed to be functional, has about two magnitudes less sensitivity than the operational unit and is not available for use.

Improvements in software procedures and instrument calibrations continue to be made. A technique to suppress microphonics in the LWR camera has been tested. An improved procedure to correct for the echelle ripple is near completion. Progress is being made on a partial read capability which will reduce the overhead time associated with reading out a detector when it is used in the low dispersion mode.

The calibration program includes work to improve corrections for non-linearities in camera sensitivity and work to develop corrections for changes in the wavelength-dependent sensitivity of the LWR and SWP cameras. A number of other efforts are also underway. The details of developments are published in the IUE Newsletters as they become available.

D. Image Processing Software, Data Archives and User Services

In the past year and one-half the IUE Spectral Image Processing System software has experienced a major upgrade of its capabilities. New software now exists for extracting both low dispersion and high dispersion spectra from

camera images. Details of the changes are available in the NASA IUE Newsletters. Major features involve elimination of the explicit geometric correction and use of a greater data sampling frequency in performing the extraction of spectra from images, and application of explicit time and temperature corrections to reseau-position and dispersion-constant files. The latter increase the accuracy of both flux and wavelength measurements, particularly in high dispersion.

Improvements in the flow of data through the processing system and the IUE Data Management Center now permit Guest Observers to obtain most of their raw-image photowrites and their magnetic tapes of reduced data within 24 hours. When necessary, priority processing of newly obtained data is possible for users of the IUE Regional Data Analysis Facility located at the Goddard Space Flight Center (GSFC).

The IUE data archives at the National Space Science Data Center continue to grow and receive increased use. Some 22,000 images acquired at either IUE/GSFC or IUE/VILSPA have been archived. Each image enters the public domain six months after its processing, and the request rate for archival data now rivals the rate of acquisition of new data. Automated techniques for filling requests for archival data are expected to reduce dramatically the turnaround time associated with these requests.

E. The IUE Regional Data Analysis Facilities (RDAFs)

Two facilities have been established to aid astronomers wishing to reduce and analyze IUE spectra. The facilities are located at the GSFC and at the University of Colorado. The hardware and software at these two facilities allow users to reduce and display IUE spectra, to make astrophysically significant measurements (e.g., equivalent widths, radial velocities, emission line fluxes, etc.), to convert data to units appropriate for comparison with theory, and to produce wet-ink plots which are suitable for publication. Most of the software has been written in a high-level interactive language and is easily modified to suit the specific requirements of individual users.

The Goddard facility helps IUE observers to perform "quick-look" analyses of their data both during and immediately after their observing runs. In addition, it will assist users in obtaining within a few days archived IUE spectra. Both facilities are staffed by astronomers and assistants prepared to aid users in their data analyses.

DISCUSSION - HOT STARS

Doazan: Do you conclude that the large amplitude variations you observe occur during short-time scales?

Peters: Although the profiles of the C IV lines in μ Ori apparently vary during the course of a day, the radial velocities obtained from the centroids of the features remain fixed. Each of the three stars discussed in this paper appears to have a unique pattern of component lines but at a particular time, only one component dominates.

Hack: I wish to report about a late A shell star, HR 5999 (probably the companion of HR 6000; they have common proper motions). It shows rather strong emission lines at 1218 (OV?), N V, C IV. To my knowledge it is the only late A star showing far-UV emission. It may be a still contracting star, because it is in a T Tauri stage, and probably embedded in a dusty cloud as indicated by the variability of IS extinction (paper by The, Tjin van Drije, Hack and Selvelli, 1982, A and Ap.).

Doazan: I would like to mention that the B8e star HD 50138, which shows also the red [O I] emission lines in the visual, exhibits red emission wings in the lines of Fe II, Mg II in the range $\simeq$ 2500-3000 Å while in the 1200-2000 A, these emissions are not seen.

Underhill: When you compare the spectra of B stars and Be stars in the visible and in the ultraviolet range, you detect differences which are primarily due to the differing visibility of the mantle of each star. Cold parts of the mantle are seen best by spectroscopic criteria in the visible range, hot parts by spectroscopic criteria in the ultraviolet range. Your observations indicate that B and Be stars have closely similar hot parts in their mantles, but widely different cool parts.

Peters: (1) What do you suppose initiates the mass loss? (2) Would you admit that magnetic fields might be of some importance?

Thomas: (1) A nonthermal internal structure, i.e., subatmospheric structure, of the star. (2) Anytime there are two independent velocity fields in an ionized gas, you cannot avoid having a magnetic field. This does not require "admitting" anything. We observe mass-motion outward, rotation, pulsation, etc., so we expect magnetic fields in all such stars even though we have not yet measured them. The whole question, of course, is which influences what: do the several nonthermal velocities produce the fields; or does a primordial magnetic field condition the kind and details of nonthermal velocity fields which exist, and transport the mass flux, and the nonradiative energy fields that produce chromosphere-coronas?

Heap: I note that your sample of early O stars are heavily reddened. To what extent are your derived effective temperatures sensitive to uncertainties in the amount of interstellar extinction?

Underhill: The uncertainty in E(B-V) is about $\pm$0.03 mag. Changes in E(B-V) by this amount would generate changes in T_{eff} of the order of 1000-2000K at most. Changing E(B-V) also changes the deduced angular diameter. This change tends to counteract the change which occurs in the value for integrated flux.

Harrington: If you want to count most of the photons to find the effective temperatures of the O stars, the best way is to look at the size of the H II region, the Strömgren sphere, around them. Is there any information of this sort available for these stars?

Underhill: Very little quantitative information is available about the H II regions around my target stars. Pottasch, Wesselius, and van Duinen (1979 A. Ap., 77, 189) have attempted to use H II regions to measure the far-UV radiation of a few O stars. Possibly more stars could be studied in this way. I am not familiar with much of the literature on H II regions.

Bell: Is there any difference in the appearance of the UV spectrum between the hotter and the cooler of the O5 stars, for example, that you have studied?

Underhill: I have studied only the continuous spectrum of the stars. The amount of energy between 1200 and 5500 Å is more for a hot O5 star than for a cool one, when scaled by the angular diameter, and the continuous spectrum is steeper for a hot O5 star than for a cool O5 star. The observed energy distributions, when corrected for intersteller extinction, truly do fit the energy distributions from model atmospheres having temperatures in the range 25000 to 50000K. The UV line spectrum has not been compared yet. High-dispersion IUE spectra would be needed for that. I do have a few high-dispersion IUE spectra of some of my stars. However, most of the stars are too faint to be observed easily with IUE in the high-dispersion mode.

Aller: BD+30° 3639 is a planetary nebula which shows [) III] and I think some [Ne III]. There is no way you can get these lines with T_{eff} = 19000K. We required T > 30,000 with Kurucz models to reproduce spectra of objects such as Campbell's H-envelope star. Application of model atmospheres is very precarious for WR stars.

Underhill: The radiative continuous flux which comes from HD 184378 = BD+30°3639 corresponds to a star with T_{eff} = 18000 $\pm$ 2000K. On the

other hand, WR spectrum lines correspond to electron temperatures much higher than this; lines are excited as a result of the deposition of non-radiative energy. You have to have superheating in order to obtain a Wolf-Rayet type spectrum. This is shown by the theory of steller spectra. Very likely the passage of non-radiative energy form the star to the planetary nebula is what excites the high-energy nebular lines you mention. I do not know what form of non-radiative energy is heating the mantle of the star and giving a WR spectrum, nor do I know where the energy comes from. However, I suspect that it comes from local magnetic fields. I use model atmospheres only to represent the photosphere of the star. This is the region where the continuous spectrum is formed. The continuum is probably due chiefly to hydrogen opacity. The hot plasma giving the stellar emission lines lies outside of this photosphere. The source of continuous opacity in the hot line-forming region is electron scattering.

Walborn: I think it very unlikely the WN/WC sequences can be explained in terms of solar composition. To what extent does your basic model depend upon that assumption and could it be applied to the case of anomalous compositions?

Underhill: Wolf-Rayet spectral types are assigned according to the relative intensities of a few emission lines. The apparent intensities of emission lines depend upon the temperature of the plasma, its composition and density, and on how much plasma is projected in the sky in the immediate neighborhood of the star. There is evidence that with Wolf-Rayet stars we are seeing a combination of hot and cold plasmas. How much of each will determine the gross characteristic properties of the emission line spectrum which is seen. A WC spectral type is assigned when CIII is seen (mostly a dense, not too hot plasma, I think); a WN spectrum corresponds to hotter and denser plasma. Both types also show He I lines and often H lines which requires the presence of cool plasma. I have not made numerical models of Wolf-Rayet atmospheres and predicted spectra. To do so would be a complex and difficult job. However, I know enough about the temperature and density ranges favoring emission lines from different ions that it seems to me one could readily predict any sort of WR spectrum by simply varying the amount of plasma present at each of a few temperatures and allowing for non-LTE physics, all based on solar composition. You cannot think in terms of one uniform plasma at one temperature.

Jordan: To put things into perspective, would you give your views on these systematically lower effective temperatures for O stars than those obtained from selected spectral lines by Conti?

Underhill: The effective temperatures for O stars deduced by Conti from correlating the observed relative strengths of He I λ4471 and He II λ4541 with the calculated strengths predicted by Mihalag, using non-LTE model atmospheres in radiative equilibrium, are systematically higher than what I find by typically 10000 K. This happens because the line-

forming layers of O stars are superheated by non-radiative energy. I believe that the effective temperatures found by studying the continuous spectrum of O stars, in the way I have done, are quantities which correctly specify the total amount of energy coming from the center of the star as radiation. The study of spectral features formed in parts of the stellar atmosphere which have been superheated by the deposition of non-radiative energy leads to "effective temperatures" which are systematically too high. This systematic effect can be detected for Wolf-Rayet stars also and for B-type supergiants.

Barker: In the three Orion stars, HD 37017, 37776, and 37479, we find T_{eff} between 18,000K and 25,000K (37017 coolest, 37479 hottest); in other words B1-B3V. This was done from both optical He I, C II, and H I and NLTE Si II/III/IV. The C IV lines do not appear to differ drastically from ι Her and other standards provided by Dave Leckrone. They are clearly young main sequence stars.

Walborn: Are the C IV aborption strengths in these stars similar to or greater than those in normal B main sequence stars of the same effective temperatures? I believe there is some question whether HD 120640, which showed little or no C IV, is really helium-rich.

Barker: As far as I know there is no systematic difference in absorption strength between helium strong and "normal" B stars; the ten stars in this sample were selected on the basis of work by Osmer and Peterson, and on the basis of having been observed for magnetic fields. We have no independent optical spectra of HD 120640.

Aller: When I carried out a curve-of-growth analysis of HD 140641 using a Mt. Wilson Coude plate (kindly supplied to me by Münch), I had the impression that the abundances of N and O per gram of stellar material was about the same as those found for "normal" O and B stars. The method was very crude, however. What do you find for the O and N abundances?

Drilling: We have not derived N and O abundances from our IUE data. However, recent fine analyses of ground-based observations for a number of these stars indicate that N is over-abundant, and O under-abundant, compared to the sun.

Witt: You referred to enhanced 2200 Å bumps in some of your stars. With respect to which type of extinction curve do you call this feature enhanced?

Shore: With respect, to S111 or S127 - internal calibrators in the LMC. S131 has an E(B-V) $0.^{m}12$ or so, for example, S134 has E(B-V) = 0.10 or so.

Shore: Against LP Ori, do you see an anomalous 2200 A bump?

Panek: See Figure 1.

Shore: It is interesting that the radio behavior of this source reminds one of the other radio and x-ray "boomer" source Cir X-1. How do the other phenomenological aspects compare?

Caraveo: (Reply unavailable.)

Walborn: Given the probability of uncertainties in the model choices and extinction corrections, it seems worthwhile to consider either kinds of information as well in interpreting these objects, such as the regions in which they are found. Six of the ten known O3 stars are located at the tops of the color-magnitude diagrams for young clusters in the Carina Nebula, indicating that they are indeed all very similar and massive objects. Similarly, three WN-A stars, for which low effective temperatures are derived, are associated with and have closely related spectra and absolute magnitudes to an O3f star in the Carina Nebula, which has a high effective temperature. Rather than interpret the WN-A objects as BO stars, it seems preferable to me to hypothesize, for example, that they have similar high masses and energy generation to the O3f star, but that some of the energy is emerging in a form other than radiative and is producing the excitation of the WN envelope.

Underhill: The spectroscopic details by which you are recognizing the stars you mention and by means of which you are assigning them to separate bins, such as O3 or WN7, are representative of the physical state in the mantle of each star. For these spectral types, in particular, the spectral type gives no information about the size of the photosphere or the effective temperature of the star, i.e., total flux of radiation from the core of the star. Only if you know T_{eff} to within about 5 percent and $L/L_{\odot}$ to within about 20 percent, can you enter a theoretical HR diagram derived from stellar-evolution calculations and, using an estimate of the mass of the stars, derive conclusions about the stage of evolution of the stars. What I am saying is this: among the earliest spectral types, more than one spectral type is associated with each place in the HR diagram and also each spectral type is not associated with only one, fairly well-defined position in the HR diagram. Consequently, spectral type cannot be used as a key factor for inferring the stage of evolution of any of the stars you mention. It is essential to estimate T_{eff} and $L/L_{\odot}$ by the method I have used. If you can also find out the mass of the stars from other information, then you will know enough to make deductions of the sort you wish to make. It is impossible to use the physical state of the mantle (i.e., the spectral type) to find T_{eff} and $L/L_{\odot}$ until we understand the physics of how a mantle is heated and set in motion, and are able to relate this knowledge (action of some mechanism) uniquely and unambiguously to the state of evolution of a massive star.

Shore: Your star has a C IV line like our Sk188/SMC, an O VI star. We have looked carefully at the bottom of the line, and it is not saturated. Could R136a be a nursery of sorts, with agglomerating fragments heating a common envelope?

Ebbets: Unsaturated C IV aborption appears to be characteristic of objects with early WN type spectra. Whether this is an effect of ionization, anamolous carbon abundance, electron scattering, or something else is not clear. In any case, R136a is not unique in this regard. The possibility that R136a is a cluster of dozens to perhaps hundreds of individual objects is an interpretation that cannot be ruled out at this time. The main objection is the space density. The volume available appears to be less than 1 pc in diameter, but the total luminosity is on the order 0.5 - 1 x 10^8 $L_\odot$. Unless you want each object to be extremely luminous, a very large number of stars must be postulated to exist in a very crowded region of space.

INDEX TO AUTHORS

INDEX TO AUTHORS

☆U.S. GOVERNMENT PRINTING OFFICE: 1982 539-007/10 1-3

BIBLIOGRAPHIC DATA SHEET

1. Report No.	2. Government Accession No.	3. Recipient's Catalog No.
NASA CP-2238		

4. Title and Subtitle	5. Report Date
ADVANCES IN ULTRAVIOLET ASTRONOMY: FOUR YEARS OF IUE RESEARCH	July 1982
	6. Performing Organization Code
7. Author(s) Editors: Yoji Kondo, Jaylee M. Mead, Robert D. Chapman	8. Performing Organization Report No.
9. Performing Organization Name and Address Laboratory for Astronomy and Solar Physics NASA-Goddard Space Flight Center Greenbelt, MD 20771	10. Work Unit No.
	11. Contract or Grant No.
	13. Type of Report and Period Covered Conference Publication
12. Sponsoring Agency Name and Address National Aeronautics and Space Administration Washington, DC 20546	14. Sponsoring Agency Code

15. Supplementary Notes

16. Abstract

This volume contains the invited and contributed papers presented at a symposium held at the Goddard Space Flight Center March 30 through April 1 1982, to mark the beginning of the fifth year of guest observations with the International Ultraviolet Explorer (IUE) satellite. The program emphasized physical insights into the various astronomical objects which have been studied using the observatory. Topics covered at the symposium included galaxies, cool stars, hot stars, close binaries, variable stars, the interstellar medium, the solar system, data reduction, and possible IUE follow-on missions: FUSE (Far Ultraviolet Spectroscopic Explorer) and MAGELLAN.

17. Key Words (Selected by Author(s))	18. Distribution Statement
International Ultraviolet Explorer (IUE), ultraviolet astronomy, solar system, stars, binary stars, nebulae, interstellar medium, galaxies	Unclassified - Unlimited Subject Category 89

19. Security Classif. (of this report)	20. Security Classif. (of this page)	21. No. of Pages	22. Price*
Unclassified	Unclassified	659	A99

*For sale by the National Technical Information Service, Springfield, Virginia

GSFC 25-44 (10/77)